NASA Conference Publication 3220

Piloting Vertical Flight Aircraft:
A Conference on Flying Qualities and Human Factors

Proceedings of a workshop held at
San Francisco, California
January 20–22, 1993

NASA Conference Publication 3220

Piloting Vertical Flight Aircraft:
A Conference on Flying Qualities and Human Factors

Edited by
Christopher L. Blanken
and
Matthew S. Whalley
Aeroflightdynamics Directorate
U.S. Army Aviation and Troop Command
Ames Research Center
Moffett Field, California

Proceedings of a workshop held at
San Francisco, California
January 20–22, 1993

National Aeronautics and
Space Administration

Ames Research Center
Moffett Field, California 94035-1000

1993

PREFACE

This document contains papers from a specialists' meeting entitled "Piloting Vertical Flight Aircraft: A Conference on Flying Qualities and Human Factors". The conference was co-sponsored by the American Helicopter Society — San Francisco Bay Chapter, and the NASA Ames Research Center. It was held January 20-22, 1993 at the Sheraton Hotel Fisherman's Wharf, San Francisco, California.

Vertical flight aircraft, including helicopters and a variety of Vertical Takeoff and Landing (VTOL) concepts, place unique requirements on human perception, control, and performance for the conduct of their design missions. The intent of this conference was to examine, for these vehicles, advances in: (1) design of flight control systems for ADS-33C standards; (2) assessment of human factors influences of cockpit displays and operational procedures; (3) development of VTOL design and operational criteria; and (4) development of theoretical methods or models for predicting pilot-vehicle performance and mission suitability. Recognizing that human capabilities and limitations form an integral aspect of the operations for these classes of vehicles, a secondary goal of the conference was to provide an initial venue for enhanced interaction between human factors and handling qualities specialists.

The conference was divided into five sessions:

***Applying and Enhancing Criteria** — papers focusing specifically on developing design or assessment criteria for these aircraft*

***Assessing New Technologies** — papers that examine the impact of advanced technologies on the operation of these aircraft*

***Modeling and Analysis Techniques** — papers that present models or designs based on models of human-vehicle performance*

***Understanding Visual Cues** — papers, primarily from a human performance standpoint, defining display requirements for these aircraft*

***Aircraft Applications and Development** — papers that discuss piloting aspects of specific vehicles*

Special appreciation is due to the Session Chairpersons, who also doubled as session organizers: Mr. John Clark, Major Johnnie Ham, Dr. Gareth Padfield, Ms. Sandy Hart, and Mr. Jim Howlett; their efforts in organizing the program and directing discussion of the papers were excellent. Likewise, particular appreciation is extended to Mr. Chris Blanken, the conference General Chairman, for his tireless efforts and superb organization on behalf of the conference, as well as to Administrative Chairman Mr. Robert Stroub and Financial Chairman Mr. Matthew Whalley, and to the Technical Information Division for preparing and publishing the proceedings of the meeting.

Dr. J. Victor Lebacqz
Conference Technical Chairperson

CONTENTS

Session 3 – Modeling and Analysis Techniques

Session 4 – Understanding Visual Cues

Session 5 – Aircraft Applications and Development

Session 1

Applying and Enhancing Criteria

ADS-33C Related Handling Qualities Research Performed Using the NRC Bell 205 Airborne Simulator

J.Murray Morgan
Stewart W.Baillie

Flight Research Laboratory
Institute for Aerospace Research
National Research Council
Canada

ABSTRACT

Over 10 years ago a project was initiated by the US Army AVSCOM to update the military helicopter flying qualities specification MIL-8501-A. While not yet complete, the project reached a major milestone in 1989 with the publication of an Airworthiness Design Standard, ADS-33C. The 8501 update project initially set out to identify critical gaps in the requisite data base and then proceeded to fill them using a variety of directed research studies. The magnitude of the task required that it become an international effort: appropriate research studies were conducted in Germany, the UK and Canada as well as in the USA. Canadian participation was supported by the Department of National Defence (DND) through the Chief of Research and Development.

Both ground based and in-flight simulation were used to study the defined areas and the Canadian Bell 205-A1 variable stability helicopter was used extensively as one of the primary research tools available for this effort. This paper reviews the involvement of the Flight Research Laboratory of the National Research Council of Canada in the update project, it describes the various experiments conducted on the Airborne Simulator, it notes significant results obtained and describes ongoing research associated with the project.

Presented at Piloting Vertical Flight Aircraft: A Conference on Flying Qualities and Human Factors, San Francisco, California, January 1993

INTRODUCTION

For over 20 years, the Flight Research Laboratory (FRL) of the NRC has operated a Bell 205-A1 helicopter as a full authority fly-by-wire research aircraft. This aircraft has been used as a fundamental research tool for flight mechanics research at the laboratory, simulating a wide range of vehicle types (including fixed wing and lighter than air aircraft) but specialising in advanced rotorcraft topics. This long interest and the resulting expertise in the area of helicopter flight mechanics led to a natural symbiosis between the FRL and the US Army AVSCOM when it was required to update the US Military helicopter handling qualities specification, MIL-8501-A. The 8501 update program was announced by Key [1] in 1982 and while it has followed the general outline presented at that time, it has been affected by various changes in military emphasis and funding in the intervening years. A milestone in the process, but by no means the final one, was the publication of ADS-33C in 1989.

In cooperation with the US Army AVSCOM and NASA(Ames) the FRL, under the auspices of TTCP and with support and funding from DND, has been involved in the 8501 update process from the first. Not only have piloted experiments using the Bell 205 developed a considerable rotorcraft handling qualities data base, they have also served a significant role in 'ground truthing' the results obtained from experiments performed in the NASA(Ames) Vertical Motion Simulator (VMS). In addition to the independent experiments flown at the FRL, pilots from the laboratory participated as subjects in vari-

ous VMS experiments, thus ensuring a measure of continuity and direct comparison between the two facilities. This was felt to be such an important factor that, to the extent possible, US military and NASA pilots who had participated in the VMS experiments were also invited to fly in the FRL studies.

While the activity spawned by the 8501 update project provided new direction, purpose and thrust to the FRL research program on rotorcraft handling qualities, it was not the beginning of such studies at this laboratory. Prior to the start of the 8501 update project, the most recent area of research had concentrated on the use of integrated side-stick controllers of various types and in various configurations (References [2] to [4]). Reference [4] also reports some initial work on yaw axis response types.

It is important to note the contribution made to this work by Systems Technology Inc (STI). This company, as the prime contractor to AVSCOM for 8501 update activities was responsible for the initial VMS experiments, the philosophical approach to the structure of the ADS-33C objective criteria and the introduction of the concept of a Useable Cue Environment (UCE), a metric used to describe, numerically and objectively, flight in Degraded Visual Environments. The STI principal investigator, Mr.R.H.Hoh took a full and active part in the design and execution of the initial bandwidth experiments at the FRL and cooperated frequently in most of the remaining studies.

This paper will provide a thorough review of those portions of the ADS-33C
data base generated using the FRL Airborne Simulator. It will highlight the relationships between in-flight research and research conducted using ground based facilities. The specific studies to be discussed include:

- Control system bandwidth and sensitivity
- Vertical axis dynamics and installed thrust requirements
- Control system disturbance rejection requirements
- The effects of stick dynamics
- Useable Cue Environment (UCE) studies and flight in a Degraded Visual Environment
- The development of Part 4 flight test manoeuvres for use in a normal visual environment

Ongoing experiments concerning Part 4 manoeuvres in DVE and the potential of limited authority attitude SCAS in DVE will also be discussed.

The prime purpose of this paper is to provide a single reference point for the considerable Canadian contribution to the ADS-33C data base.

THE NRC AIRBORNE SIMULATOR

The Airborne Simulator operated by the FRL (Figure 1) is an extensively modified Bell 205-A1 single engine teetering rotor helicopter. It was acquired by the laboratory in 1969 and had been converted to the research configuration by early 1972. The modifications to enable this machine to operate in a fly-by-wire mode were extensive, the most significant being:

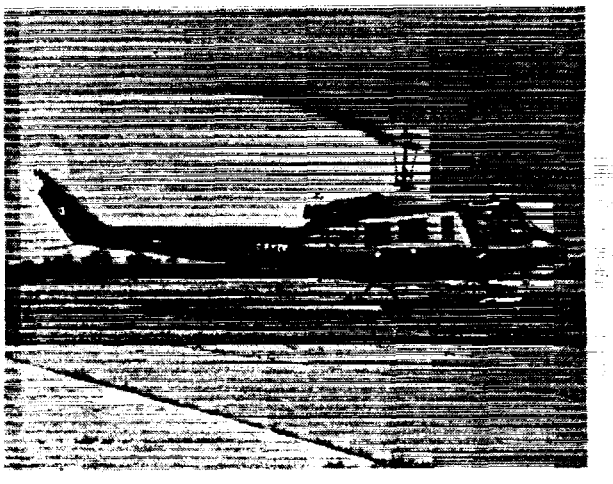

Figure 1: The IAR Airborne Simulator

- The normal 205 actuators were replaced by full authority dual mode (electrical or mechanically signalled) HR Textron HYDOMAT units. These actuators have approximately a 10 Hz bandwidth to small signals and a maximum rate of 100% per second under ground static conditions.
- The main rotor stabiliser bar was removed to improve dynamic response.
- The swash-plate to horizontal stabiliser linkage was removed and the stabiliser provided with

its own electrically signalled actuator. The stabiliser effectiveness was increased by sealing the fuselage/stabiliser gap with a faired-in plane surface.

- The pilot in command station was moved to the left side of the cockpit and the right station provided with a force feed-back control loading system with which to signal the flight computers. This system was provided with its own hydraulic system independent of the primary aircraft controls.
- A nose boom was added to carry airflow direction vanes and a swivelling static pressure sensor.

Fly-by-Wire System. The fly-by-wire (FBW) system in this aircraft is controlled by a hybrid digital/analogue general purpose computing system. This has been updated over the years to reflect changing computing technologies: it has changed in nature from a primarily analogue system to one in which all control functions are performed digitally, the analogue section being relegated to one or two display filtering or general purpose signal scaling functions.

The computer system reads a comprehensive suite of aircraft state sensors, the evaluation pilots control inputs (both primary inceptors and ancillary controls as required) and directly controls actuator commands and cockpit displays. Since very few constraints are placed on the control system logic and architecture, the project engineer has complete freedom in the design of feed-forward and feedback loops to attain the vehicle dynamics desired for a particular program

Safety of Flight Issues. The Bell 205 FBW system is both single string and experimental and therefore does not have adequate reliability to be permitted full time control of the aircraft. For safety of flight reasons, the aircraft operation revolves around a safety pilot. The safety pilot always remains in contact with all flight controls, even when an evaluator is in control of the vehicle. In the event of a system malfunction, the safety pilot has several methods available to him of disengaging the FBW system and reasserting full control of the aircraft. To assist the safety pilot there is a hardware monitoring system which will trip the FBW system in the event of power supply or hydraulic pressure failures and software monitoring of sensor consistency is also employed. The inherent 150 to 180 ms lags in the Bell 205 teetering rotor response coupled with over twenty years of experience in the aircraft make this approach to safety satisfactory for operations throughout the flight envelope and into the NOE environment. The experience of the laboratory in this aircraft indicates that there is greater danger from an evaluation pilot attempting to fly a poor model close to the ground than from any hardware or software errors that have ever been seen.

Performance and Limitations. The simulation flight performance envelope of an in-flight simulator is obviously subject to the performance limitations of the host aircraft, but the quality of the FBW system will determine the proportion of the overall flight envelope which is available to the experimenter. The FRL Bell 205 is routinely flown in the FBW mode throughout the entire envelope. Within the normal regime, the performance of the flight control systems depends primarily on available control power and inherent lags. By using fairly simple techniques to produce a compound feed-back signal comprising the aircraft's response at low frequency and that of a lag free model at high frequency, the effects of the natural aircraft lags can be nullified (See Figure 2), leaving the ultimate limitations on the dynamics available for a given experiment to those of control power versus the excitation of undesirable structural modes. The limited control power of a teetering rotor system plus the potential excitation of a fuselage/transmission oscillation (the Bell 205 mast rocking mode) limit the achievable

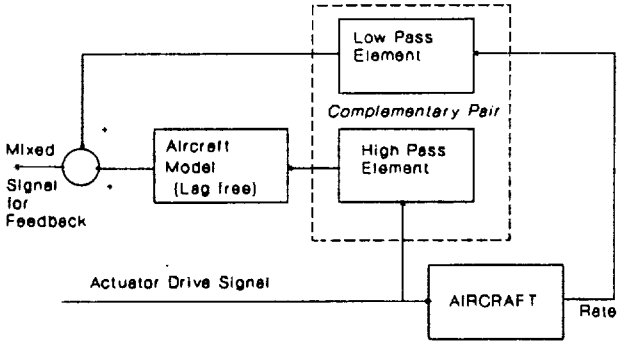

Figure 2: Compound Feedback Signal Arrangement

control bandwidths of the Airborne simulator to about 3.5 rad/sec laterally and 2.4 rad/sec in pitch. Yaw bandwidths of just over 2.5 rad/sec are also achievable.

A more complete, though somewhat dated in detail, description of the Airborne Simulator may be found at Reference [5].

RELATIONSHIPS BETWEEN IN-FLIGHT AND GROUND BASED SIMULATION

By its very nature, in-flight simulation is a difficult, costly and (compared to ground based simulation) of limited scope. The principle limitations to in-flight simulation arise from the nature of the task itself.

Without installing additional force and moment generators, the implementation of simulator models is restricted to those degrees of freedom over which the host aircraft offers direct control. The experimenter has to accept the aircraft's natural responses in the remaining freedoms. In the case of the FRL Airborne Simulator, it is impossible to modify the linear X and Y characteristics of the raw 205.

Secondly, since the evaluation is conducted in the real atmosphere, it is necessary to accept whatever disturbances exist at the time of flight. To an extent this problem can be overcome by choosing to fly only in very calm conditions and applying a known disturbing signal. While this is done for specific experiments which demand either no disturbances or a well understood disturbance pattern, it is far too restrictive a procedure for common use. The available research time would be very seriously depleted.

The final major limitation to in-flight simulation is the uncertainty which always exists regarding the nature of the plant under control and the current state of the host vehicle. What this means in practice is that, although quite precise design methods may be used to develop gain matrices for candidate control systems, the final outcome has to be identified by analysis of the vehicles's responses to a known exciting function. This is often an iterative process during the development stage of any study, consisting of control system design, measurement, adjustment and re-measurement.

The experimenter using ground based machines, on the other hand, has complete control over his model systems and the computed environment. However, he faces severe limitations on pilot cuing due to imperfect visual and motion systems, computer throughput times and other artifacts of the full simulation process. These deficiencies are very pronounced in the case of the helicopter simulations. It is generally accepted that helicopter pilots use very fine visual cues when operating at low speed near the surface, but whether these cues are primarily textural or kinematic is not well understood, nor are the mechanisms the brain uses to interpret them. To date it has not been possible to produce adequate visual cues for high precision tasks on any computer generated imaging system that this author has seen.

It is worth also considering another factor, the psychology of the pilot. In ground based simulation the pilot knows, albeit subconsciously, that he is ultimately not at risk whereas in the air that is not true: this may well have an effect on both the level of aggressiveness he is prepared to use in flying the tasks and the quality of control system he is prepared to accept.

By and large, experience has shown that handling qualities trends taken from ground based simulation are valid, but that the absolute values of the ratings achieved are *sometimes* not. Results from ground based simulation *often* tend to be conservative and this point will be emphasised later.

The remarks above suggest a natural complementary relationship between data from ground based and in-flight research. Although large matrix experiments can be conducted with relative ease in a ground based simulator, the results need to be examined closely for their validity due to lack of fidelity in the pilot's environment. In contrast, the smaller matrix experiments which lend themselves to in-flight testing have the advantage that the visual and motion cues are full scale and coherent, yet suffer from a range of uncertainties in implementation which are not a factor in ground based studies. It also follows that the in-flight simulator has a significant role in fundamental handling qualities

research both in its own right and in the important task of anchoring data from ground based experiments into the actual flight regime. It is in this role that the FRL Airborne Simulator was first employed in support of the ADS-33C data base generation.

BANDWIDTH AND RESPONSE TYPE EXPERIMENT

This was the first formal experiment designed to generate a data base for ADS-33C performed on the Airborne Simulator; it was also the largest single study carried out in this program.

A 1984 experiment conducted in VMS (Reference [6]) used bandwidth and response type as major variables, and it was desired to validate these studies in actual flight. A total of 14 control systems were programmed into the Airborne Simulator, representing Rate, Rate Command/Attitude Hold and Attitude Command response types. The responses with respect to attitude were tailored to provide bandwidths over the ranges 0.85 to 2.7 rad/sec in pitch and 1.0 to 3.1 rad/sec in roll. It has been argued that these bandwidths are inadequate to represent modern rotor systems, however during the development of ADS-33C criteria the critical *minimum* bandwidths for the vast majority of tasks were determined to be within these ranges. The control system architecture was identical to that used in VMS and a similar set of tasks was used.

Since this study followed recent FRL work in the area of integrated side-stick control, the opportunity was taken to fly the experiment using both conventional controllers (cyclic and collective levers with yaw pedals) and a four function integrated side-stick. The experiment was initially reported in Reference [7], while the same data with a rather deeper analysis is to be found at Reference [8].

This experiment served as the foundation for the small amplitude manoeuvre bandwidth criteria to be found in ADS-33C and served in measure to define the response type requirements in the same document, at least for operations in normal visual conditions. It also emphasised the relationship between ground based and in-flight simulation regarding the need to relate data from ground based experiments to those conducted in actual flight. Figures (3 and 4), which have appeared in several publications, show that in flight, not only were the spreads of pilot ratings less than in VMS, indicating greater pilot confidence in their ability to evaluate the systems, but that the bandwidth requirements to obtain Level 1 handling qualities were lower by up to 3 rad/sec. This is most noticeable in the plot relating to the evaluation of attitude response types. The implications of the significantly lower bandwidth requirements are very far reaching. Bandwidth costs money, weight, structural stiffness and control system complexity.

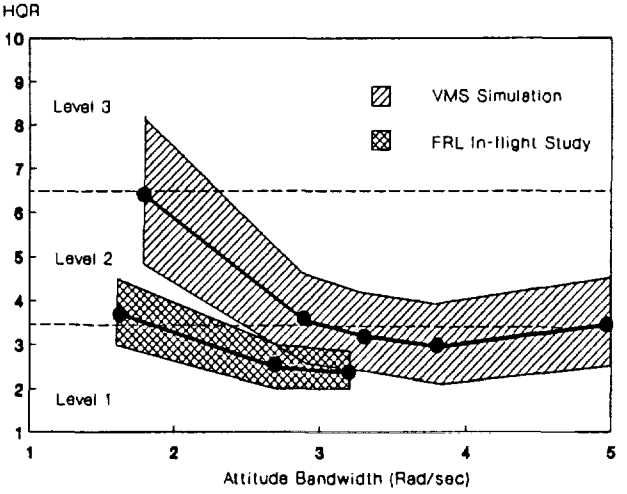

Figure 3: Flight/Ground Comparison, Attitude Command .

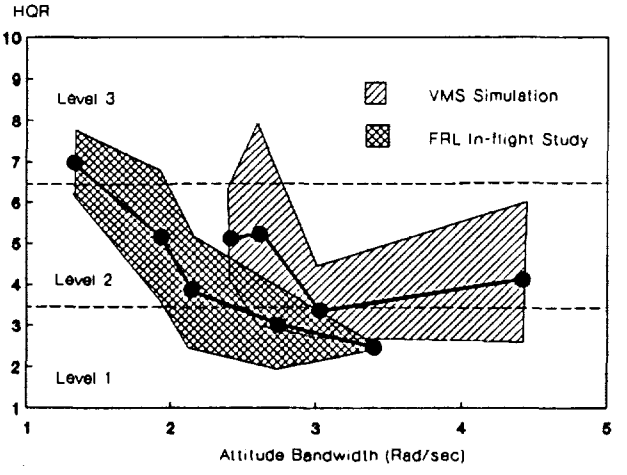

Figure 4: Flight/Ground Comparison, Rate Command

VERTICAL AXIS REQUIREMENTS

Two experiments in the 8501 update project concentrated on vertical axis requirements. The initial study concentrated on variations in heave damping and collective sensitivity (Reference [9]) while the second also considered the effects of thrust to weight ratio and the effects of engine/governor dynamics (Reference [10]). A more detailed analysis of data from these experiments can be found in Reference [11].

Again, following work already performed in VMS, these experiments were concerned with a topic already examined on the ground. The aircraft was configured with nominal pitch, roll and yaw control and airframe dynamics while the effective heave damping (Z_w), maximum thrust to weight ratio (T/W) and engine/governor/rotor dynamics parameters were varied.

Handling qualities ratings (HQR) of models which varied in Z_w and T/W showed that, in the airborne experiment, pilots were once again more tolerant of values which tended to degrade handling qualities than they were in VMS, however, the trends were the same. Figure (5), taken from Reference (10) demonstrates this point.

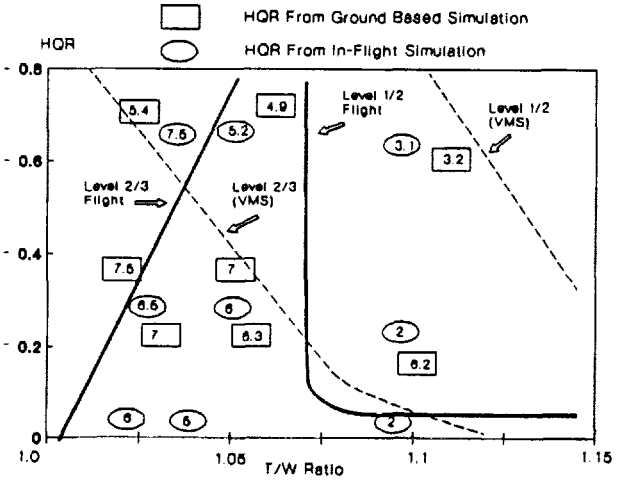

Figure 5: Suggested T/W v Zw Boundaries Ground and Flight

Led by the work of Corliss[12] and Hindson[13], typical engine/governor/rotor dynamic models were also evaluated on the Airborne Simulator. The sensitivity of HQR to torque monitoring workload became quite clear in this experiment. Analysis of the engine/governor/rotor models using the same criteria as those used by previous experimenters showed a significant discrepancy in predicted versus actual HQRs. Our own attempts to quantify a handling qualities boundary based on parameters related to the engine governor/rotor system dynamics was able to describe our observed trends in handling qualities ratings but overall the criterion was less than satisfactory. The authors of ADS-33C were able to coalesce handling qualities data from a variety of sources to develop an equivalent systems approach to defining the a more "satisfying" torque dynamics boundary. Each set of data, from VMS, the NASA CH-47 and the FRL 205 highlighted different areas of concern regarding the dynamics of torque in rotorcraft operations and all were reflected in the final specification.

FLIGHT IN DEGRADED VISUAL ENVIRONMENTS

It has long been recognised, if informally, that the helicopter pilot, unlike his fixed wing counterpart, has to operate for prolonged periods in visual conditions that are neither of the two traditional designations VMC or IMC. Whether it be night, fog, precipitation, dust, sand or snow, his problems are compounded in several ways, particularly in NOE flight. The task of stabilising today's helicopters when visual references are poor is known to be both difficult and dangerous. Every year the flight safety publications contain several reports of loss of control or inadvertent ground strike accidents caused by prolonged or inadvertent operations in such conditions. It has become important to the military philosophy that NOE operations should be possible under almost all conditions and within an acceptable risk envelope.

To facilitate the design of helicopters for which protracted operations in a degraded visual environment is a practical reality, it was necessary to examine the requirements for such flight. Following early work by Hoh [14], which resulted in the postulation of a system to quantify the level of visual cuing that the pilot had at his disposal from all sources, termed a useable cue environment rating

(UCE), experiments were performed in the Airborne Simulator to continue the research and further refine the concept. Since the primary concept of the UCE work was that the pilot stabilises the rotorcraft based on the full set of cues available to him, it was predicated that a degradation in the UCE was similar to a reduction in gains in or the order of a closed loop stabilisation system. To maintain overall system stability as the cue environment degrades, the obvious step is to augment the stability of the plant which the pilot is required to stabilise, in this case the uncommanded rotorcraft.

With this concept in mind a variety of configurations were developed for the Bell 205 ranging from the raw vehicle to a highly augmented vehicle possessing Translational Rate Command/Position Hold with Yaw Rate Command and Height Hold control systems (TRC/PH/HH). Night Vision Goggles, used in conjunction with day training filters and focus adjustments, were used to degrade the visual environment in which the pilot had to operate as were goggles with liquid crystal foggable lenses.

The handling qualities evaluations of a variety of low level tasks (Summarised in Figures 6 and 7) confirmed the tradeoff between uncommanded vehicle stabilisation and UCE. While rate response models were able to provide Level 1 handling qualities in good visual conditions (UCE=1), only highly augmented configurations such as ACAH or TRC/PH/HH were able to produce the same results in degraded visual environments (UCE 2 or 3). A description of this study may be found at Reference [15].

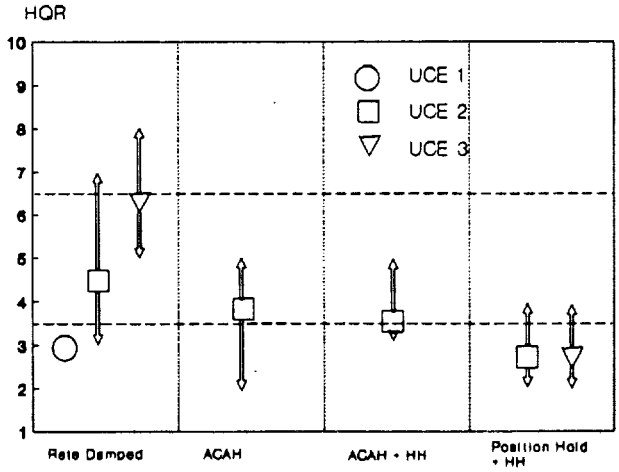

Figure 6: HQR v Augmentation, Stationary Tasks

Unlike previous examples mentioned in this paper, ground based simulation followed rather than led in-flight experimentation in this area. The associated VMS experiment (Reference [16]) corroborated the basic findings of the FRL study and was able to confirm some conclusions drawn from, but not fully justified by, the in-flight work. ADS-33C incorporates the UCE - augmentation tradeoff as the cornerstone for the entire handling qualities specification.

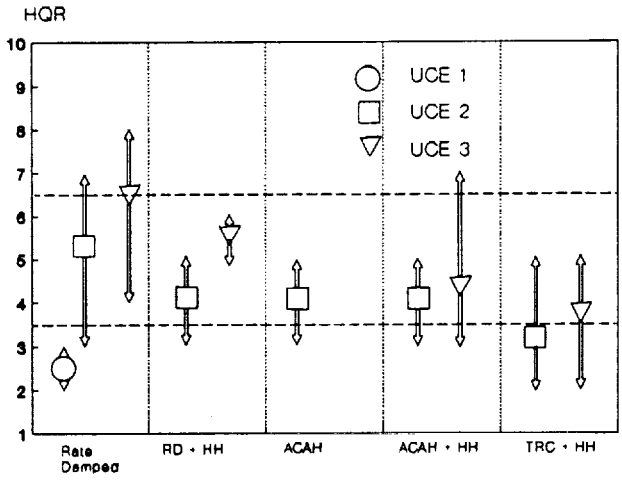

Figure 7: HQR v Augmentation, Manoeuvring Tasks

CONTROL SYSTEM DISTURBANCE REJECTION QUALITIES

In 1989 it became apparent that further in-flight data were required to confirm the bandwidth and, more importantly, the phase delay (τ_p) boundaries postulated after our previous experiments. There was a particular concern that the values of τ_p permitted for both Level 1 and level 2 boundaries were too high. Therefore, a second control bandwidth experiment was performed using the Airborne Simulator (References [17] and [18]). This differed from the first studies in that the elements of pilot selectable "optimum" sensitivity and the disturbance rejection characteristics of the control systems were considered in the evaluation matrix.

The previously determined bandwidth and phase delay handling qualities boundaries were confirmed

by the evaluation data gathered during this study and so this area will not be discussed further. On the other hand, the novel feature of considering disturbance rejection capability as a rotorcraft handling qualities determinant should receive further attention.

It is clear that a closed loop control system with specific bandwidth and phase delay characteristics can be produced by numerous combinations of forward path shaping and state error feedback, but that only the state error feedback loops will augment the vehicles disturbance rejection capability. The tradeoff between forward path manipulation and feedback can make a considerable difference to the control system design, especially when failure tolerance is considered, therefore the definition of a minimum level of disturbance rejection (conversely, a maximum response to defined disturbances) is desirable.

The handling qualities evaluations of disturbance rejection capability were conducted using a matrix of 24 control systems using different levels of feed forward and feedback to accomplish specific bandwidth and phase delay design constraints. To ensure that all systems were subjected to the same disturbance environment, the evaluations were performed in calm ambient conditions, the disturbances being provided by the superimposition of a time series of actuator commands on the control system control path.

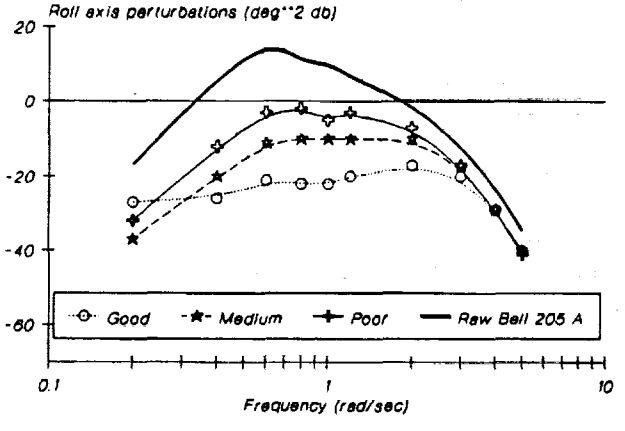

Figure 8: Model Responses to Disturbing Signal

The disturbance signal used had been developed by recording the motions of the unaugmented Bell 205 in a steady hover in very heavy turbulence - the lee side of a large obstruction in a strong wind. The aircraft response traces were processed through an inverse mathematical model of the Bell 205 to yield actuator commands which would produce similar motions. When empirically scaled and filtered, the data trace produced a 'turbulence model' considered to be the most realistic ever flown at the NRC. The responses of the subject models as well as the raw 205 to this disturbing signal is shown at Figure 8.

The result of this preliminary study was an envelope of attitude perturbations against frequency (Figure 9) which, for an otherwise Level 1 aircraft, seemed to cause degradation of its handling qualities to the Level 2 area. It is felt that further work in this area could be fruitful. A detailed documentation of this study can be found at Reference [19].

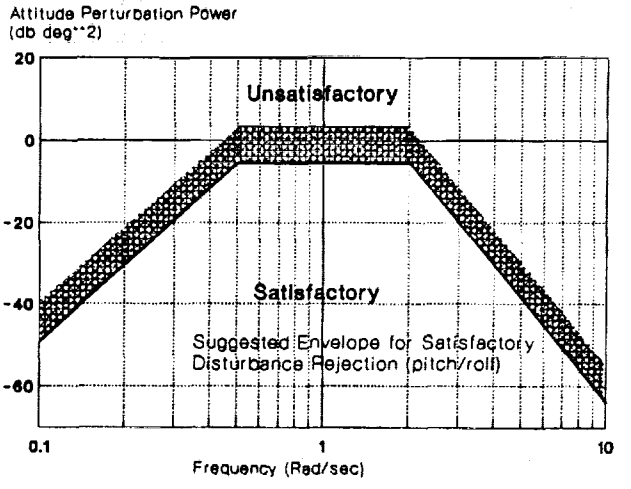

Figure 9: Suggested Disturbance Rejection Boundary

STICK DYNAMICS STUDIES

The ADS-33C bandwidth criteria section states that bandwidth should be measured from the transfer function relating the force applied to a given control to the aircraft attitude, but there have been suggestions that this is not necessarily correct for large displacement controls. In particular, research in the fixed wing world (Reference [20]) has suggested that a pilot can compensate more readily for control response lags due to the dynamics of a particular controller than he can for those due to forward path

signal manipulation. This particular result might be expected since the pilot can form a neuro-muscular closed loop control system around the parameters of stick force and position, thus reducing their overall effect while the pilot has no feedback parameter available regarding forward path computational lags except for the final aircraft response.

The experiment performed at FRL on this subject revolved around the evaluation of helicopter handling qualities when the aircraft was controlled through a cyclic controller which had a variety of dynamic characteristics. The cyclic dynamics evaluated could be grouped into two types, one in which frequency domain characteristics were varied by the choice of physical model parameters, and one having different physical characteristics while maintaining constant natural frequencies and damping. Unfortunately, the evaluations of the latter group were less than satisfactory due to deficiencies in the Airborne Simulator control loading system.

Results from this study confirmed that pilots are very tolerant of low bandwidth displacement controllers; the results also permitted boundaries for controller design to be postulated based on natural frequency and damping (Figure 9). The evaluation data gathered during this experiment also suggests that the control bandwidth criteria in ADS-33C should be measured from stick displacement rather than applied force, *especially* if the cyclic stick is of rather low natural frequency. A full description of the experiment can be found at Reference [21]. Numerous other studies on rotorcraft handling

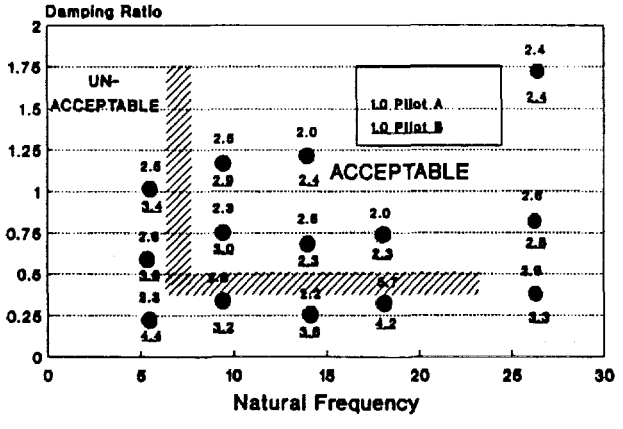

Figure 10: Suggest Cyclic Stick Dynamics Boundary

qualities variations due to control feel system dynamics have taken place in the last few years and a good survey of recent work can be found in Reference [22].

It is clear that the subject of how a pilot interacts with his vehicles control feel system dynamics has yet to be fully understood. With this in mind, work is currently in progress at FRL to replace the analogue control loading system in the Bell 205 with a more consistently repeatable digitally based system. When this system becomes operational, further studies in this area will be undertaken.

ADS-33C MANOEUVRES FOR PART 4

Although it was intended that the use of ADS-33C should rely heavily on the objective open loop criteria to be found in Part 3 of the document, specific flight test manoeuvres were written into Part 4 to supplement the objective criteria. These manoeuvres were designed to reveal handling qualities deficiencies that might be otherwise missed but were intended to be used for piloted checks of a candidate aircraft in a 'quick look' form of evaluation. When exercises were undertaken to evaluate the use of ADS-33C by flying existing aircraft against the criteria, the manoeuvres assumed a greater importance than was the original intention with evaluators wishing to apply them as aircraft acceptance criteria in their own right. This use of the manoeuvres required a further project at the FRL, to define the manoeuvres in a sufficiently rigorous way so that they could be used to evaluate handling qualities almost in lieu of the Part 3 criteria.

There were several significant constraints imposed on the manoeuvre designs by the US Army authorities, particularly:

- flight test costs should be kept as low as possible which implies very little special equipment could be required;
- performance limits should be such that achievement of them, or otherwise, should be readily obvious to the pilot or an external observer and;
- the manoeuvres should be applicable to any type of helicopter without significant changes.

While these constraints may seem trivial, in many ways they are not: the last constraint in particular legislates against using, for example, marked ground courses with target speed gates for the acceleration/stop manoeuvre as has been the standard practice at FRL for many years.

To insure that the intent of the Part 3 criteria would be met by the piloted evaluation of Part 4 manoeuvres only (that is, the manoeuvres should enable a pilot to distinguish between Levels 1,2 and 3 systems as defined in Part 3), the process of designing the manoeuvres had to include the evaluation of control systems which would pass and fail the criteria of Part 3. For this purpose, three control system models were incorporated in the Airborne Simulator. One of these was on the putative Level 1/Level 2 boundary, one well into the Level 2 region and the third just inside the Level 3 boundary. The evaluation pilots were asked to produce handling qualities ratings for each vehicle/manoeuvre combination and manoeuvres were varied to obtain a good correlation between pilot ratings and the system design handling qualities predictions. The necessity of producing models which would offer a range of handling qualities and the ability to record pilot performance numerically were the factors that legislated the use of the Airborne Simulator for this exercise, rather than an aircraft with greater performance capabilities.

The most difficult types of manoeuvre to design were those for which the aim was to determine handling qualities, but in which aircraft performance was a significant factor. An excellent example of this is the accelerate/stop manoeuvre. Traditionally the task has been defined at FRL by setting out a ground course marked by a start point, a 'gate' and an end zone and defining the task thus:

Establish a 10 foot hover at the start point, accelerate to achieve 40 kt groundspeed at the gate and return to the hover inside the end zone markers. Desired performance shall be ±10 feet laterally, ±10 feet vertically, ±10 degrees in heading and 2 knots at the gate. Adequate.....

For the evaluation of the Bell 205 models this defined manoeuvre was quite acceptable and the combination of speed and distance targets ensured that the pilot had to fly in a very aggressive manner. If, however, the test vehicle were not a Bell 205 but, say an Apache, these limits would not represent the same proportion of the aircraft's capability as they do with the Bell 205. The task would become too easy because of the performance margins the pilot had available to him. To make the task aircraft independent clearly requires a different approach to the manoeuvre. The final definition of this example task became, *somewhat abbreviated*:

Starting from a stabilised hover, rapidly increase power to approximately maximum and maintain altitude constant with pitch attitude. Hold collective constant during acceleration to an airspeed of 50 knots. Upon reaching the target airspeed, initiate a deceleration by aggressively reducing power and holding altitude constant with pitch attitude. The peak pitch attitude should occur just before reaching the final stabilised hover.

Desired Performance

Complete the manoeuvre over the reference point at the end of the course. The longitudinal tolerance is plus zero, minus a distance equal to one half the overall length of the helicopter (positive forward)

Maintain altitude below 50 feet.

Maintain lateral track within ±10 feet.

Maintain heading within ±10 degrees.

Achieve at least 95% of either maximum continuous power or the maximum transient limit, whichever is greater, within 1.5 seconds from initiation of the manoeuvre. If 95% power results in pitch attitudes that are deemed to be objectionable, use the maximum nose down pitch attitude that is felt to be acceptable. This pitch attitude will be considered as a limit of the operational flight envelope.

The power should be decreased to full down collective within 3 seconds to initiate the deceleration. Significant increases in power are not allowed until just before the stabilised hover.

The pitch attitude during the deceleration should be at least 30 degrees nose-up above the hover attitude, and should occur shortly before hover.

The rotor RPM shall remain within the limits of the Operational Flight Envelope without undue pilot compensation.

The greatly increased complexity in the second definition serves to produce a script which is easily interpreted by the pilot and gives him, or his observer, clear guidance as to whether the desired performance limits have been met. It meets the constraints on the manoeuvres mentioned initially, requiring no specific flight test instrumentation and being aircraft type independent. However, such a complex description of what is essentially a very simple piloting task raises questions as to the understandability of the definition and whether it would be interpreted by the pilot in such a way as to meet the intentions of the guide. This was checked by asking pilots who had not been party to the development process to fly the tasks, using only the draft definitions as a brief. This final stage in task development resulted in only minor changes in wording or emphasis.

This kind of re-working of task descriptions was necessary for most of the manoeuvres in ADS-33C Part 4 requiring large changes in attitude and power since these are the areas where individual aircraft capabilities are the most predominant.

The manoeuvre re-definition exercise was completed at FRL in two sessions in 1991, with the participation of US Army pilots from AQTD and was reported in Reference [23].

ONGOING RELATED STUDIES

The cooperative studies in support of ADS-33C at the FRL are continuing. Currently the laboratory is in the preparatory stage of a study on the potential benefits of modifying the typical rate feedback SAS found in current helicopters (eg, Bell 412,Blackhawk) to provide a limited authority attitude command mode to assist the pilot during operations in degraded visual environments. Again, this is a study which will complement a VMS experiment by repeating the evaluations of selected configurations in the cue rich environment of actual flight. The software development stage of this project is currently nearing completion and it is anticipated that piloted evaluations will commence early in February 1993.

In the longer term, the NRC is in the process of purchasing a replacement airframe to carry on the process of in-flight simulation. The decision to make this major capital investment was driven primarily by our acknowledgement that the agility of a teetering rotor helicopter will always be limited to levels far below those obtainable in most current helicopters and that it will be necessary to address that factor if the laboratory is to maintain the ability to conduct world class research in the area of helicopter flight dynamics.

The new aircraft, a Bell 412, is expected to be received at the laboratory in the late spring of 1993 and will be designated the Advanced Systems Research Aircraft (ASRA). It is anticipated that some 18 months will be required to convert the aircraft to a fly-by-wire capability, a process that will be primarily conducted in-house with the use of outside contractor assistance where necessary. The ASRA will be the fourth generation FBW helicopter at the FRL and will continue a nearly thirty year tradition of in-flight simulation activity with a machine capable of carrying out manoeuvres more appropriate to helicopters of the next decade.

CONCLUSIONS

The National Research Council's Airborne Simulator has played a large role in developing the data base against which the frequency domain criteria and the flight test manoeuvres incorporated in ADS-33C have been written. It has, as a part of this project, again highlighted the complementary nature of ground based and in-flight simulation, indicating that there would be quite severe cost and technological risk in specifying or designing radically new helicopters using data acquired purely from either source, ground-based simulation or in-flight simulation. As shown in this report, there have been occasions during the production of ADS-33C when data from several sources was necessary to formulate a given criterion.

The FRL, through its connection with TTCP, has renewed its intentions to continue its participation in the international effort in support of handling qualities criteria development and update.

ACKNOWLEDGEMENTS

The Canadian contribution to the development of a new military helicopter Airworthiness Design Standard was funded in part by the Canadian Department of National Defence through the Chief of Research and Development and in part by the National Research Council of Canada.

REFERENCES

1. Key, D.L.,**The Status of Military helicopter Handling Qualities Criteria**, Criteria for Handling Qualities of Military Aircraft, AGARD CP-333, June 1982

2. Morgan,J.M., Sinclair, S.R.M., **The Use of Integrated Side-Arm Controllers in Helicopters,** AGARD CP-425, October 1987

3. Morgan,J.M., **In-Flight Research into the Use of Integrated Side-Stick Controllers in a Variable Stability Helicopter,** Royal Aeronautical Society International Conference on Helicopter Handling Qualities and Control, London, UK, November 1988

4. Morgan, J.M.,**A Piloted Experiment in the Use of a Multi Function Force-Sensing Side-Arm Controller with an Automated Control System in a Helicopter,** Ninth European Rotorcraft Forum, Stresa, Italy,September 1983

5. Sattler,D.E.,**The National Aeronautical Establishment Airborne Simulation Facility,** NRC NAE Misc 58, May 984

6. Hoh,R.H., et al,**Proposed Revision to MIL-F-83300 V/STOL Flying Qualities Specification,** NADC-82146-60, January 1986

7. Morgan J.M., **Airborne Simulation at the National Aeronautical Establishment of Canada,**AGARD CP-408, September 1985

8. Mitchell,D.G.,Hoh, R.H. and Morgan, J.M., **Flight Investigation of Helicopter Low Speed Response Requirements**, Journal of Guidance, Control and Dynamics, Vol 12 No 5, Sep-Oct 1989

9. Baillie,S.W.,Hoh,R.H.,**The Effect of Heave Damping on Helicopter Handling Qualities,** AIAA-86-2129, August 1986

10. Baillie,S.W.,Morgan,J.M.,**Investigation of Vertical Axis Handling Qualities for Helicopter Hover and NOE Flight,** AGARD CP-423,October 1986

11., Baillie,S.W.,Morgan,J.M.,**The Impact of Vertical Axis Characteristics on Helicopter Handling Qualities,** NRC Aeronautical Report LR-619, August 1897

12. Corliss,L.D.,**The Effects of Engine and Height Control Characteristics on Helicopter Handling Qualities,** Journal of the American Helicopter Society, Vol.28,No.3, July 1983

13. Hindson,W.S. et al, **Flight Evaluation of Height Response Characteristics for Hover Bob-up Task and Comparison with Proposed Criteria,** 42nd National Forum of the American Helicopter Society, Washington, DC, June 1987

14.Hoh,R.H., **Handling Qualities Criterion for Very Low Visibility Rotorcraft NOE Operations,**AGARD CP-423, October 1986

15. Baillie,S.W., Hoh,R.H.,**The Effect of Reduced Useable Cue Environments on Helicopter Handling Qualities,** CASI Journal, Vol 34, No. 3, September 1988

16. Blanken,C.R.,Hart,D. and Hoh,R.H. **Helicopter Control Response Types for Hover and Low-speed Near-earth Tasks in Degraded Visual Conditions,** 47th Annual Forum of the American Helicopter Society, Phoenix, Ar. May,1991

17. Baillie,S.W.,Morgan,J.M.,**Control Sensitivity, Bandwidth and Disturbance Rejection Concerns for Advanced Rotorcraft,** Proceedings of the 45th Annual Forum of the American Helicopter Society, Boston,Mass,May 1989

18. Baillie,S.W.,Morgan,J.M., **An In-flight Investigation into the Relationships Amongst Control Sensitivity, Control Bandwidth and Disturbance Rejection Bandwidth using a Variable Stability Helicopter,** Proceedings of the 15th European Rotorcraft Forum, Amsterdam,September 1989

19. Baillie,S.W., Morgan,J.M.,**The Effects of Control Bandwidth, Control Sensitivity and Disturbance Rejection Ability on Rotorcraft Handling Qualities,** NRL Laboratory Technical Report LTR-FR-111, March 1990

20. Johnston,D.E., Aponso,B.L,**Design Considerations of Manipulator and Feel System Characteristics in Roll Tracking,** NASA CR-4111,1988

21. Morgan, J.M.,**An Initial Study into the Influence of Control Stick Characteristics on the Handling Qualities of a Fly-by-Wire Helicopter**,AGARD CP-508, October 1990

22. Mitchell,D.G.,Aponso,B.L. and Klyde,D.H., **Effects of Cockpit Lateral Stick Characteristics on Handling Qualities and Pilot Dynamics,** NASA CR-4443, June 1992

23. Morgan,J.M.,**The Design of Flight Test Manoeuvres in Support of ADS-33C,** CASI Symposium on Flight Test, May 1992

MIL-H-8501B: APPLICATION TO SHIPBOARD TERMINAL OPERATIONS

A. N. Cappetta
Aerospace Engineer, Flight Dynamics and Controls
Naval Air Warfare Center - Aircraft Division
Warminster, PA 18974-5000

J. B Johns
Chief, Research Support Division
U.S. Army Aeroflightdynamics Directorate
Moffett Field, CA 94035-1000

ABSTRACT

The philosophy and structure of the proposed U.S. Military Specification for Handling Qualities Requirements for Military Rotorcraft, MIL-H-8501B, are presented with emphasis on shipboard terminal operations. The impact of current and future naval operational requirements on the selection of appropriate combinations of basic vehicle dynamics and usable cue environment are identified. An example "walk through" of MIL-H-8501B is conducted from task identification to determination of stability and control requirements. For selected basic vehicle dynamics, criteria as a function of input/response magnitude are presented. Additionally, rotorcraft design development implications are discussed.

NOMENCLATURE

OFE - Operational Flight Envelope. The boundaries within which the rotorcraft must be capable of operating in order to accomplish the mission.

SFE - Service Flight Envelope. Boundaries defined by aircraft limits as distinguished from mission requirements.

MTE - Mission-Task-Element. An element of a mission that can be treated as a handling qualities task.

H/LS - Hover/Low Speed. Ground speeds from 0 to 45 knots.

F/F - Forward Flight. Ground speeds 45 knots and above.

UCE - Usable Cue Environment. The cue environment defined by the mission visual environment including both Outside world Visual Conditions (OVC) and the available displays and vision aids.

VMC - Visual Meteorological Conditions.

IMC - Instrument Meteorological Conditions. Meteorological conditions which require operation of the rotorcraft solely with reference to flight instruments. Occurs when rotorcraft is clear of all obstacles.

IFR - Instrument Flight Rules. Standard procedures which generally apply in IMC.

Near Earth Operations - Operations sufficiently close to the ground or fixed objects on the ground, or near water and in the vicinity of ships, etc., that near-field navigation is primarily accomplished with reference to outside objects.

Response-Type - The basic shape of the response in terms of dynamic parameters.

1.0 INTRODUCTION

The proposed U.S. Military Specification for Handling Qualities Requirements for Military Rotorcraft, MIL-H-8501B (reference 1), represents a radical new approach to the specification of air vehicle flying qualities. For the first time, flying qualities criteria are explicitly specified as a function of both flight task and usable cue environments. As a direct consequence, MIL-H-8501B has strong mission oriented design implications. Further, this flying qualities specification will have particular impact in the design of not only the airframe, rotor system and

Presented at Piloting Vertical Flight Aircraft: A Conference on Flying Qualities and Human Factors, San Francisco, California, 1993.

flight control system, but also the displays and vision aids.

Shipboard recovery is one of the more difficult flight tasks required of a pilot and his aircraft. This flight task even in the best environmental conditions is demanding. Mission requirements, however, force poor weather operations where launch and recovery in poor visual conditions and high sea states are routine. Under these conditions, the aircraft's flying qualities are a function of not only the vehicle's stability and control characteristics, but also the visual cues available to the pilot.

This paper presents the philosophy, structure and criteria of MIL-H-8501B with emphasis on shipboard terminal operations. The impact of current and future naval operational requirements on the selection of appropriate combinations of basic vehicle dynamics and usable cue environment are identified. An example "walk through" of MIL-H-8501B is conducted from task identification to determination of stability and control requirements. For selected basic vehicle dynamics, criteria as a function of input/response magnitude are presented. Additionally, rotorcraft design implications are discussed.

2.0 MIL-H-8501B BACKGROUND

It has long been recognized that the current U.S military specification of General Requirements for Helicopter Flying and Ground Handling Qualities, MIL-H-8501A (reference 2), is inadequate for application to modern rotorcraft. Several handling qualities specialists (references 3 through 6) have identified the inadequacies. Specific areas of concern lie with MIL-H-8501A's inability to specify technically sufficient requirements for performance of demanding tasks in severe environments, employment of high control augmentation systems, and the use of advanced displays and vision aids. Due to the combination of current day mission requirements and current rotorcraft design methodologies, MIL-H-8501A simply can no longer ensure satisfactory flying qualities.

The development of several recent rotorcraft weapon systems, including the U.S. Navy Light Airborne Multipurpose System (LAMPS) Mk III SH-60B, have required the use of flying qualities type specifications (reference 7). These type specifications, while incorporating several MIL-H-8501A requirements, have utilized many new requirements which are primarily mission performance oriented.

Beginning in 1982 the U.S. Army initiated a three phased effort to develop mission oriented handling qualities requirements for military rotorcraft. The objectives of the phase I effort were: the development of a new specification structure, the incorporation of existing criteria and data, the definition of critical gaps in the data base, and the formulation of a draft specification and background information and users guide (BIUG). Two major and distinctly different approaches evolved and were documented in references 8, 9 and 10.

The objectives of phase II were to fill in the critical data and criteria gaps and generally refine the specification. Continuing in 1984 with phase II, utilizing the approach of references 9 and 10, the U.S. Army shifted the development of the specification from general requirements to LHX oriented requirements. Once this effort was complete, they again sought, with the aid of the Navy and industry, to develop a generic specification. This was accomplished by generalizing the LH specification and BIUG for application to all types of modern rotorcraft. In this phase investigations were performed to generate data to fill the numerous data gaps. Through the last part of phase II, several government and industry reviews of the specification and BIUG (reference 11) were conducted in order to refine the criteria.

While currently in phase III, tri-service (Army, Navy, Air Force) review, adoption of the new specification is expected soon.

Through demonstration of MIL-H-8501B applicability to aircraft/ship operations, this paper represents part of the continuing effort by the U.S. Navy to assist in maturing the proposed specification.

3.0 MIL-H-8501B PHILOSOPHY

MIL-H-8501B incorporates several fundamental concepts in it's philosophy. The first of these concepts is the use of the Cooper-Harper Handling Qualities Rating (HQR) Scale (reference 12) and the associated handling qualities levels, defined in Figure 1, as a metric to quantify the acceptability of a vehicles flying qualities.

Many MIL-H-8501B criterion boundaries are based on both simulation and flight test HQR data. The primary use of the scale is to correlate pilot ratings

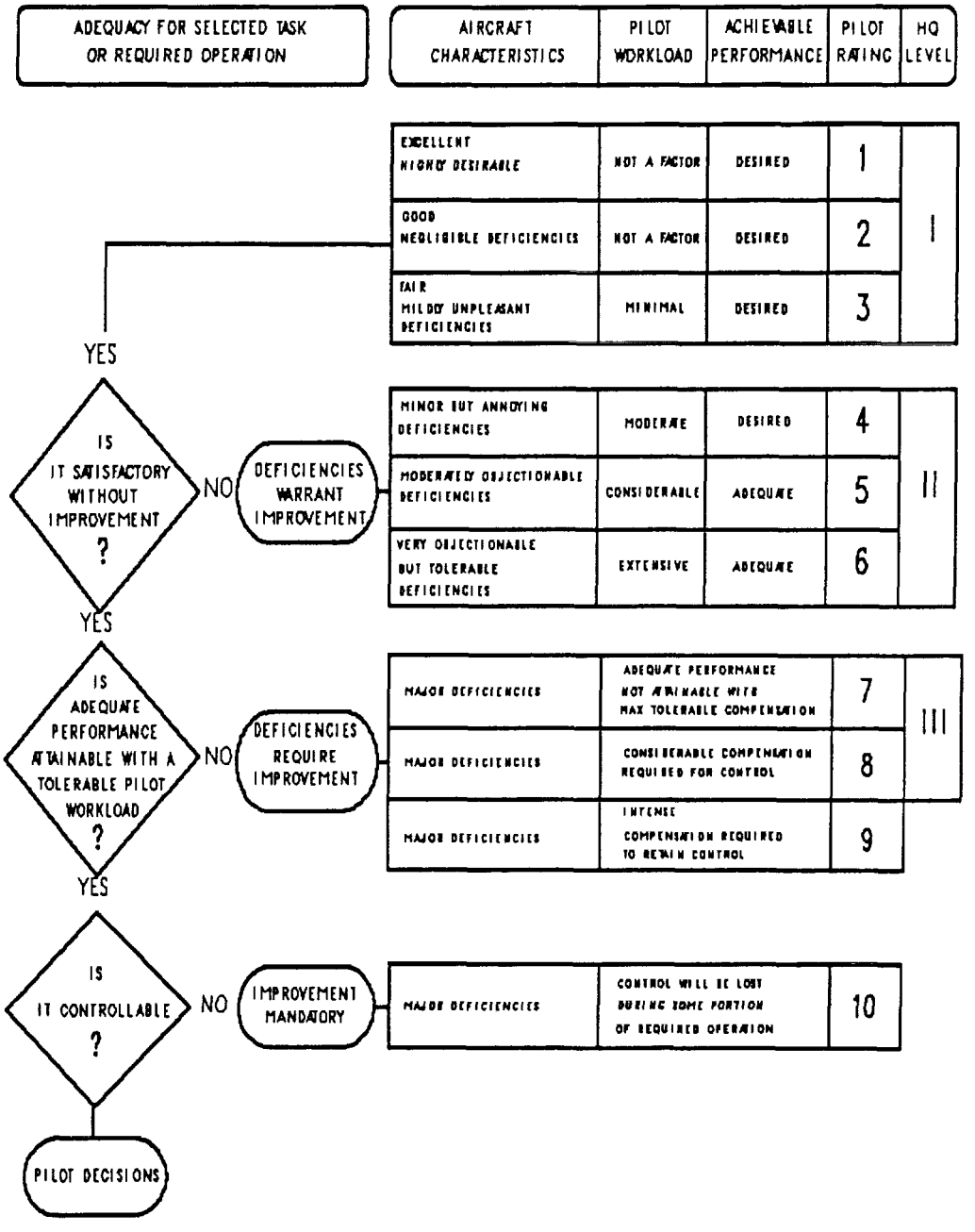

Figure 1 Handling Qualities Rating Scale.

from handling qualities experiments and compliance tests conducted in simulation or flight with parameters used in the specification. The requirements specify that the minimum handling qualities must be Level 1 within the OFE and Level 2 within the SFE. Further, the specification allows for degradation of flying qualities due to failures. One of the two methods describing the allowable degradations is given in Table 1.

Table 1 Levels For Rotorcraft Failure States

Probability of Encountering	Within Operational Flight Envelope	Within service Flight Envelope
Level 2 after failure	< 2.5 x 10-3 per flight hr	
Level 3 after failure	< 2.5 x 10-5 per flight hr	< 2.5 x 10-3 per flight hr

The U.S. Navy uses two other scales to determine the general acceptability of a helicopter - the Dynamic Interface Pilot Rating Scale (Table 2) (references 13 and 14), which is specifically used in the shipboard launch and recovery environment, and the Deficiencies Scale (Table 3) (reference 15). Neither scale, however, specifically addresses the acceptability of the vehicle's handling qualities. The former quantifies relative degrees of pilot effort required for conducting helicopter launches and recoveries during shipboard operations. The latter, quantifies the severity of aircraft deficiencies with regard to their impact on the vehicles ability to perform it's intended mission.

The second fundamental concept of MIL-H-8501B is the specification of a minimum required response type as a function of the Mission Task Element (MTE) and Usable Cue Environment (UCE). The intent of this concept is to establish a methodology which allows the specification to relate required vehicle dynamics to mission requirements and the operational visual environment. Implicit in this concept is a "trade-off" relationship between response type, displays and vision aids, and task difficulty. Essentially, as task difficulty increases, stability and control augmentation should be increased. As visual conditions degrade, stability and control augmentation or visual augmentation should be increased.

The complete procedure for determining the UCE is given in Section 3.2.2.1 of reference 1. In summary, the UCE is determined by taking an existing rotorcraft with a rate command response type and exhibiting Level 1 flying qualities in clear day negligible turbulence conditions, installing all the displays and vision aids proposed for use in the production rotorcraft, and flying test maneuvers in the actual operational environment. Three pilots perform this evaluation, quantifying the useable cues using the rating scale shown in Figures 2a and 2b. The test maneuvers consist of a basic set of MTE's including: hover, vertical landing, pirouette, acceleration and deceleration, sidestep, bob up and down.

Table 2 Dynamic Interface Pilot Rating Scale

Defining relative degrees of pilot effort required for conducting helicopter launches and recoveries during shipboard operations.

PRS	Pilot Effort	Description
1	Slight	No problems; minimal pilot effort required.
2	Moderate	Consistently safe launch and recovery operations under these conditions. These points define the fleet limits recommended by NAVAIRTESTCEN.
3	Maximum	Landings and takeoffs successfully conducted through maximum effort of experienced test pilots under controlled conditions. These evolutions could not be consistently repeated by fleet pilots under operational conditions. Loss of aircraft or ship system is likely to raise pilot effort beyond capabilities of average fleet pilot.
4	Unsat	Pilot effort and/or controllability reach critical levels, and repeated safe landings and takeoffs by experienced test pilots are not probable, even under controlled test conditions.

Both the minimum required control system types and the specific trade-off relationships with displays and vision aids for hover and low speed near earth operations are defined in Table 1(3.2) of reference 1. Similarly, Table 2(3.2) of reference 1 define these requirements/relationships for forward flight.

The third concept is the use of a combination of specific quantitative requirements, the "Section 3" criteria, and separate but equally important flight test requirements, the "Section 4" criteria, to completely determine the vehicle's handling qualities. The Section 3 criteria are a combination of frequency and time domain requirements to quantitatively define the required vehicle dynamics. The flight test requirements are included as an independent assessment of the overall vehicle handling qualities. The flight test requirements compliment the quantitative requirements and are intended to "smoke out" handling qualities deficiencies which may be undetermined by the Section 3 criteria. Section 4 is less comprehensive then Section 3 and is not intended as a substitute for Section 3.

Table 3 Definition of Deficiencies

Part I indicates a deficiency, the correction of which is necessary because it adversely affects: a. Airworthiness of the aircraft. b. The ability of the aircraft to accomplish its primary or secondary mission. c. The effectiveness of the crew as an essential subsystem. d. The safety of the crew or the integrity of an essential subsystem. In this regard, a real likelihood of injury or damage must exist. Remote possibilities or unlikely sequences of events shall not be used as a basis for safety items.
Part II indicates a deficiency of lesser severity than a Part I which does not substantially reduce the ability of the aircraft to accomplish its primary or secondary mission, but the correction of which will result in significant improvement in the effectiveness, maintainability, or safety of the aircraft.
Part III indicates a deficiency that appears too impractical or costly to correct in this model but which should be avoided in future designs. Included are violations of specifications for use by the contract negotiator in final settlement of the contract.

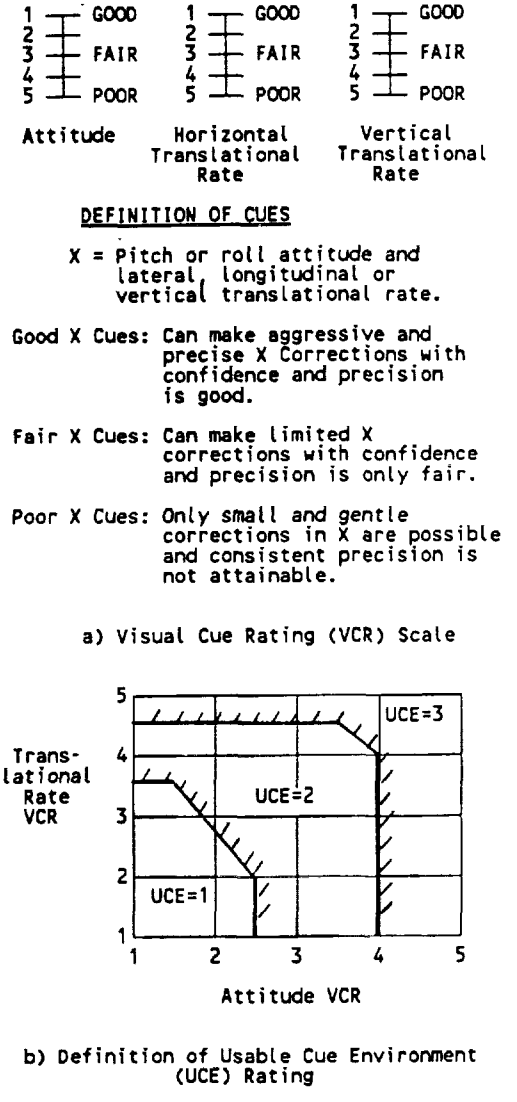

Figure 2 UCE Determination

The U.S. Navy currently uses developmental and operational testing (DT and OT respectively) for evaluation of a new or modified weapon system (reference 15). Bearing no relationship to the flight test requirements of MIL-H-8501B Section 4, these tests are performed to evaluate the airworthiness of the aircraft and the ability of the aircraft to accomplish it's primary or secondary mission. DT and OT, by design, evaluate the aircraft as a weapon system, and as such, involve a myriad of considerations. Handling qualities evaluations are typically conducted during and after full scale engineering development. Often faulty or non-optimum design characteristics are already part of the completed system and are difficult and/or expensive to fix.

Section 4.0 criteria of the proposed specification and the DT and OT evaluations seek to achieve related but distinctly different results. Therefore, there remains a necessity for both.

4.0 MIL-H-8501B STRUCTURE

The general structure of the proposed specification is illustrated in Figure 3. The Scope, Compliance, and Definitions blocks correspond to Sections 1 and 2,

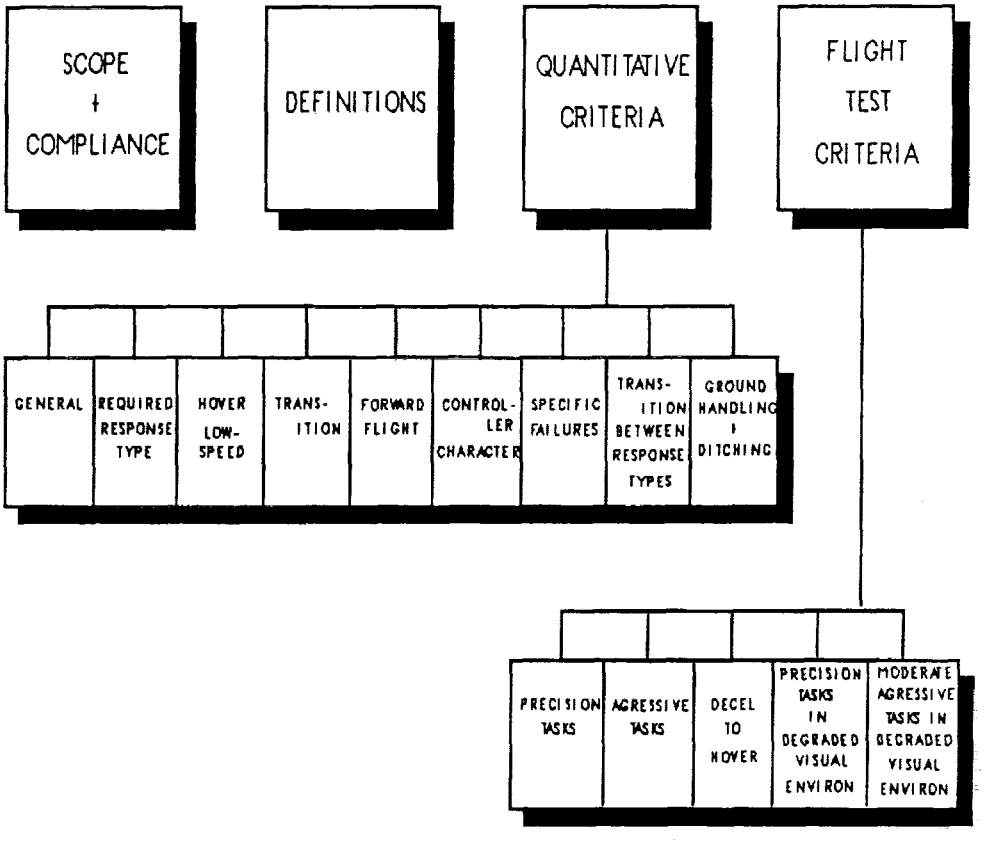

Figure 3 Specification Structure.

and the quantitative and flight test blocks to Sections 3 and 4, respectively.

5.0 MIL-H-8501B METHODOLOGY

The process by which the user and designer apply the specification is illustrated by Figure 4. Essentially, the user must first define the mission and mission environments. This includes definition of the mission task elements, degraded visual environments, requirements for divided attention, maximum winds in which the aircraft is expected to operate, and any other mission oriented requirements. From this the designer can determine the flight envelopes, usable cue environments, and required response types. Using the Section 3 criteria the designer can then determine the required dynamic characteristics for a given level of handling qualities. Trade-offs between visual and control augmentation can be made using the guidance provided in Section 3. These design trade-offs would be motivated by both the user's and manufacturer's design philosophies. With the application of MIL-H-8501B, handling qualities requirements will directly effect many areas of the

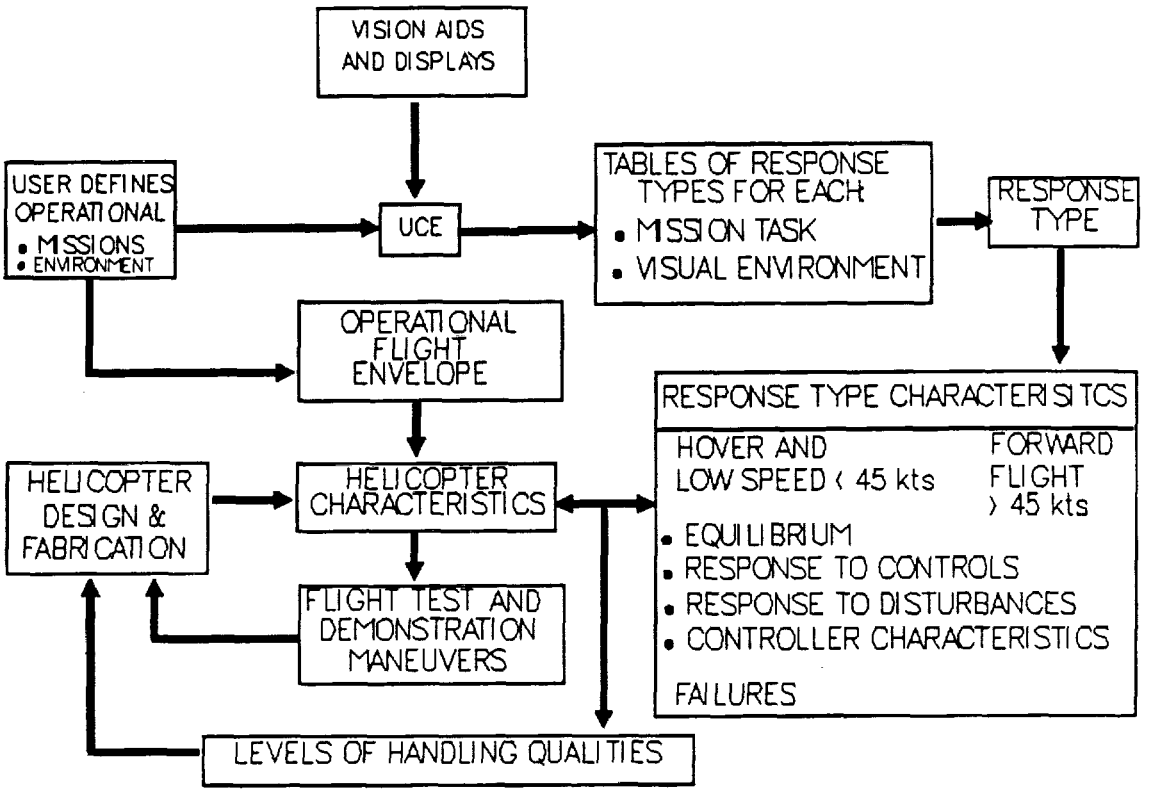

Figure 4 Schematic for Handling Qualities Specification and Assessment.

design, including the airframe, rotor system, control system, cockpit layout, and avionics, and, therefore must be considered early in the design process. Due to the timing of this process, handling qualities take on a renewed importance.

6.0 NAVAL OPERATIONS

6.1 Mission and Vehicles

The U.S. Navy's overall mission is to control the seas in wartime and project military power ashore. The tasks required to accomplish this mission include, among others, the acquisition and distribution of intelligence, surface ship and submarine attack, amphibious assault and deployment, and defense of related assets ashore in friendly or enemy territory. In support of these tasks, rotary wing aircraft operate from a wide variety of U.S. Navy ships ranging from the large deck carriers (CV) to smaller deck carriers for amphibious assault operations (LHA, LHD, LPH), to much smaller aviation capable ships such as destroyers (DD) and frigates (FFG). The associated missions include airborne mine countermeasures (AMCM), antisubmarine warfare (ASW), antiship surveillance and targeting (ASST), vertical on board delivery (VOD), naval gunfire support (NVG), amphibious assault, amphibious reconnaissance, and search and rescue (SAR).

The U.S. Navy currently operates several different multi-role rotorcraft. Among these are the SH-3D/H Sea King for shore and ship based ASW, logistical support and SAR, the SH-2F Sea Sprite LAMPS Mark I for ASW and ASST, the SH-60B Seahawk LAMPS Mark III for ASW and ASST, and the RH-53D Sea Stallion for ship or shore based AMCM. Vertical replenishment (VERTREP), medical evacuation (MEDEVAC) and passenger transfer operations are common alternate roles. Other rotorcraft include the AH-1W Cobra, UH-1N Iroquois, CH-46 Sea Night and CH-53E Sea Stallion.

Currently all naval rotorcraft are equipped with standard electro-mechanical instruments, e.g. clocks, radar and barometric altimeters, airspeed, vertical velocity, attitude, hover and torque indicators. There is extremely limited precision guidance instrumentation and no operational head-up or helmet-mounted displays.

6.2 Impact of Environmental Conditions

Even though it is desirable to have an all-weather capability, flight operations are often limited by environmental conditions. Reference 16, the Naval Air Training and Operating Procedures Standardization (NATOPS) General Flight Operating Instructions and the vehicle specific NATOPS manuals provide guidelines on, among other issues, the operational limitations related to environmental conditions. Further, these guidelines are often tailored by the organizational commanders of shore based operational commands, e.g. reference 17 and 18. For many shipboard operations, the vehicle NATOPS and the specific ship's standard operating procedures (SOP) provide the operational pilots with the necessary information on the environmental conditions within which they can operate.

The factors influencing helicopter flight operations include weather (sea state, winds, visibility and ceiling) at takeoff and forecasted for time of arrival, the pilot's rating, and the vehicle's rating (with regard to ability and qualification to operate in degraded visibility). Helicopter operations are not normally conducted with a ceiling below 500 feet and visibility less than 1 mile (reference 19). Moreover, recommended weather minimums for launching helicopters on SAR operations are 300 foot ceiling with 1 mile visibility.

Shipboard launch and recovery envelopes are limited by visibility, ship pitch and roll, physical obstructions, and ship airwake. All combine to make shipboard terminal operations hazardous. The compatibility of specific rotorcraft and ship combinations are determined by static interface tests to examine space and servicing issues and dynamic interface tests to determine operational flight envelope parameters. During the dynamic interface tests, aircraft performance and flying qualities are evaluated in the actual ship environment to establish the actual takeoff and landing limitations. Test results are published for operational use as launch/recovery envelopes expressed in terms of relative wind direction and magnitude for specified levels of ship motion (references 20, 21, 22). An example is illustrated in Figure 5.

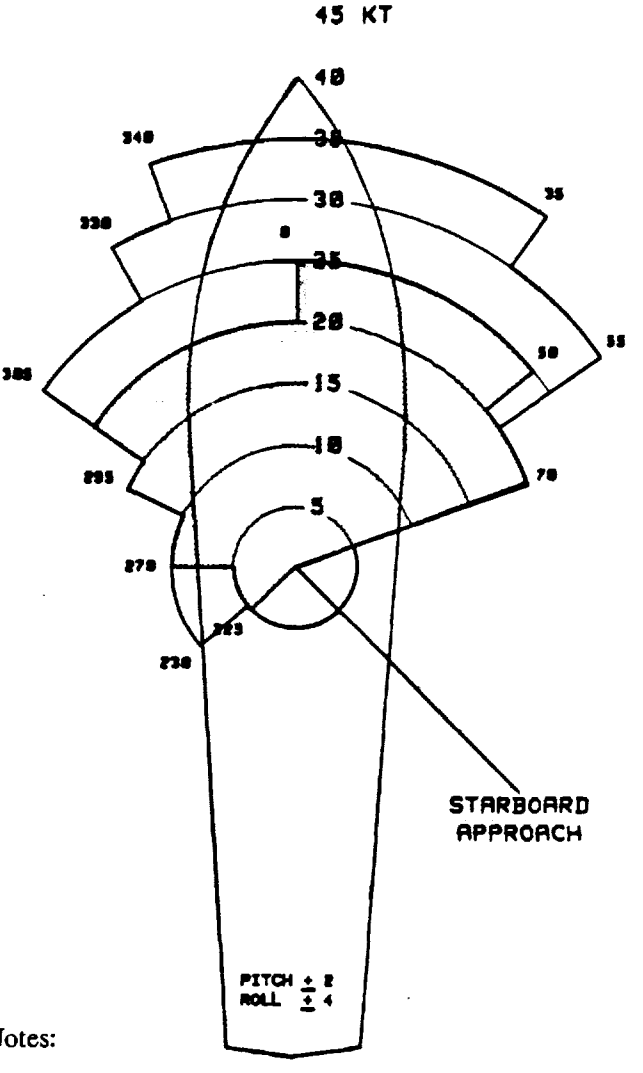

Notes:

Spot 1 Only

Entire Envelope:
Day Launch / Recovery

Shaded Area:
Night Launch / Recovery

Caution: Rotor downwash during landing flare may cause flight deck safety nets to bounce upright momentarily, reducing tail clearance, and possibly causing damage to aircraft or nets.

Figure 5 Sample DI Launch and Recovery Envelope.

During night operations, the U.S Marine Corps makes it common practice to launch and recover from ships using night vision goggles (NVGs). The Marines base their use of NVGs on ambient light conditions as measured by the Light Level Calender (reference 23). The minimum light level at which the Marines no longer use NVGs is approximately 0.0022 LUX. Although the use of NVGs by the Marines indicates the acceptability of NVGs as a vision aid for shipboard operations, the U.S Navy does not normally conduct night VFR shipboard terminal operations with NVGs.

A recent investigation of shipboard operations in degraded visual environments was conducted during the dynamic interface testing of the SH-60B LAMPS Mk III aboard the USS Cushing (DD 985) (reference 24). This investigation examined the feasibility of conducting reduced illumination helicopter night launch and recovery operations in conditions simulating wartime or emergency lighting situations. These tests were conducted under night VFR conditions, with a variety of degraded shipboard visual landing aids (VLA), and without the use of night vision devices. The evaluation further included emergency condition (EMCON) procedures, in which shipboard emissions, such as radio transmissions and guidance signals are secured.

The test results indicated that pilot workload and task difficulty are a clear inverse function of outside world visual cues and degree of aid provided by the ship. The results have strong implications with regard to on-board helicopter capabilities required for safe operation in emergency conditions. Specifically, there is an apparent need for improved displays and vision aids, as well as self contained terminal guidance systems.

Improved rotorcraft capabilities are necessary to satisfy future naval operational requirements. As an example, a recent U.S. Navy rotorcraft acquisition, the HH-60H, is representative of the future naval operation philosophy of establishing and exploiting a night/all-weather capability. The HH-60H, which can draw it's lineage from the SH-60F, was designed to perform the mission of combat search and rescue (CSAR) and special warfare support. The Navy plans to have the HH-60H's carry out CSAR in littoral missions operating off of small deck ships. Inherent in this mission is night/poor weather operational capability (reference 25). To insure adequate CSAR capability, the HH-60H is fitted with a host of mission enhancing avionics. The cockpit instrument panel includes a 10-inch multifunctional display for display of flight and navigation information. In addition, the HH-60H is fully night vision goggle compatible. The incorporation of NVGs demonstrates the recognition of the impact that visual augmentation has on operational capabilities. Using NVGs, HH-60H units are cleared to fly below the minimum light levels set for most other military units. This allows the unit to accomplish strike-rescue missions in two ways: immediate rescue in prevailing conditions or rescue within twenty-four hours under the cover of darkness. The later relies on a "stealthy" approach rather than the use of brute firepower to suppress enemy fire.

Another example of a recent acquisition which demonstrates the impact of future naval operational requirements on the design development of rotorcraft, is that of the upgrade from the Royal Navy's primary ASW helicopter, the Lynx Mk 3, to what is to be called the Lynx Mk 8. Operated from the flight decks of most Royal Navy frigates and destroyers, the Lynx Mk 3 HAS (helicopter antisubmarine), equipped with Sea Skua ASM and antisubmarine torpedoes, extends the effective range of its parent ship's sensors and weapons while operating as an integral part of the parent ship's tactical system. The Lynx Mk 8 is simply an enhanced version of the Lynx Mk 3 (reference 26).

The Lynx Mk 8 employs an upgraded Central Tactical System (CTS) which aids navigation and the Sea Owl Passive Identification Device (PID) for day, night, poor weather surveillance and automatic target cueing and tracking. These systems reduce pilot workload and enhance mission performance.

It is important, however, to recognize here that unlike the outfitting of the HH-60H with a NVG capability, the CTS and Sea Owl, although reducing pilot workload and improving mission performance, are not UCE related. The visual cue rating (VCR) scale (Figure 2a) used in determining the UCE measures the cues for stabilization and control, not navigation or mission related divided attention tasks.

6.4 Shipboard Terminal Operations (STOPS) Procedures

Although U.S. Navy rotorcraft may have different primary and secondary missions, there remains one element of these missions, two flight phases, that are rudimentary to all U.S Navy aircraft operations - shipboard launch and recovery.

Shipboard procedures for launch are described as follows (references 19, 27, 28 and 29). The pilot lifts the aircraft to a stable hover, performs checks on all performance indicators, and depending on ship size maneuvers the aircraft to the aft portion of the flight deck while maintaining gear mounts over the deck and again stabilizes a trimmed hover. If necessary, a pedal turn is executed to place the aircraft approximately 45 degrees off of the ships heading in the direction of the relative wind. The pilot then transitions the aircraft to forward flight by increasing collective to selected takeoff power establishing a positive vertical climb. The departure is complete when the prebriefed altitude and airspeed are attained. For IMC or night operations the helicopter typically does not deviate from the departure course until minimum altitude of approximately 300 feet is reached.

Approach conditions generally fall into three categories, day VMC, night VMC, and IMC. Further, there are three types of shipboard approaches. First, a visual glide path approach which utilizes the stabilized glide slope indicator (SGSI) on board the ship, second the standard instrument approach to minimums, and, finally, an emergency approach when the helicopter does not have adequate fuel to safely divert to an alternate airfield or aviation ship and the weather is below standard minimums. The visual and standard instrument approach are discussed below.

The visual approach glide path is used for both day and night VMC approaches as well as the visual final approach phase of the standard instrument approach in IMC. Beginning in cruise flight with an airspeed of approximately 80 knots, the pilot typically flies to intercept a 3 degree glide path from 1 to 1.2 nautical miles out at altitudes of 350 to 400 feet. Note this pattern (Figure 6) may, and is often, shortened during day/night VMC commensurate with pilot proficiency. In a general a descending, decelerating, constant glide slope angle approach is employed. The pilot routinely cross checks the visual cues from SGSI with the radar altimeter to ensure glide path control (altitude vs. range) is accurate. Rates of descent typically do not exceed approximately 500 ft/min throughout the approach.

During the day visual approach phase, the lineup is maintained using the lineup lines on the ships deck as well as visual cues from the ships structure. At night the approach line is maintained using a lighted lineup, vertical dropline lights and any other visual cues from the ships lighting (references 22). The final approach to amphibious class ships (Figure 7) is made at a 45 degree angle to the ship centerline toward designated the landing spot on the deck. Approaches to small deck ships are flown from either directly astern (Figure 8), or at an angle, typically 30 degrees, to the landing deck on the aft end of the ship (Figure 9).

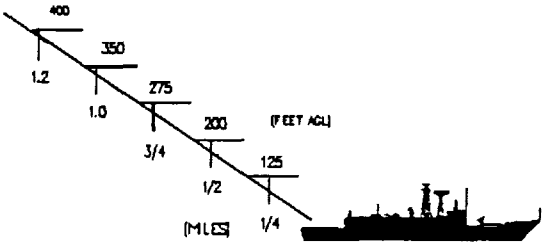

Figure 6 Typical VMC Approach path.

During the last portion of the flight phase, the pilot brings the aircraft to a stationkeeping position, depending on aircraft flying qualities and size, either just off the deck edge or over the deck for larger aircraft, waits for a lull in ship motion, transitions over the deck if necessary, and lands the aircraft. Throughout the process, the pilots are assisted by a landing signalman (LSO/LSE) who plays and advisory role, except in a wave off condition where the pilot must follow his direction.

The basic instrument approach is only utilized in a night/IFR environment. This approach is commenced from a position 2 miles astern on a heading within 30 degrees of the ships basic recovery course (BRC) at 200 feet above ground level (AGL) and 80 Knots airspeed. Upon crossing the 2 mile mark, a decent is made to 100 ft AGL, and altitude hold is then engaged. The approach is continued until visual contact is made or until a range of 1/2 mile from the ship is reached, whichever occurs first. Once visual contact is established, course and altitude are adjusted to arrive 15 ft above the flight deck. Airspeed is adjusted as required to establish a comfortable closure rate not to exceed 15 knots. The last segment of the basic instrument approach is accomplished as that of the VMC day/night approach.

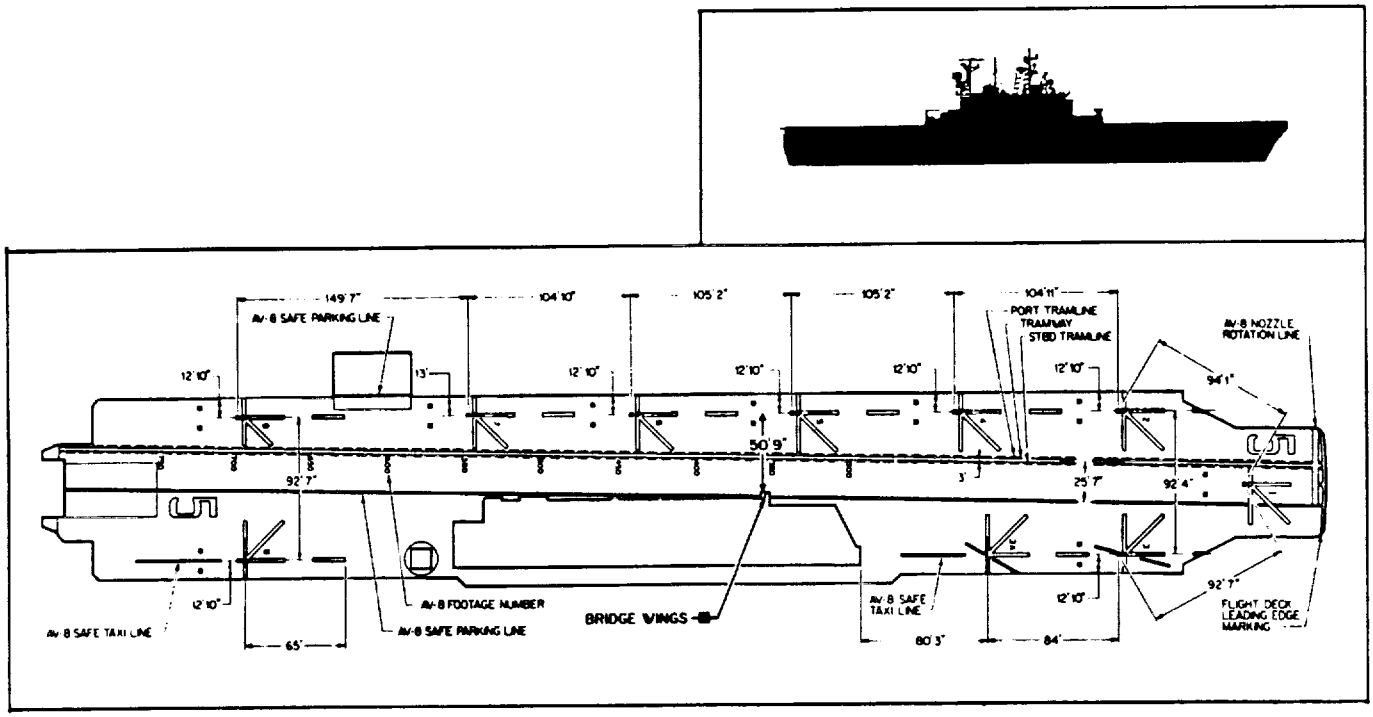

Figure 7 Amphibious (LHA) Landing Deck.

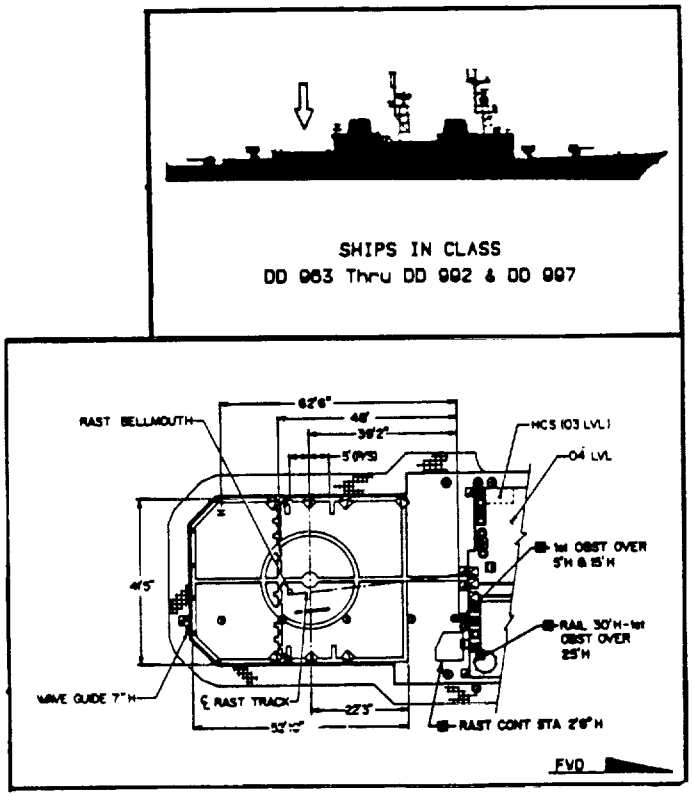

Figure 8 Small Deck Ship (DDG) Landing Area, Stern Approach Path.

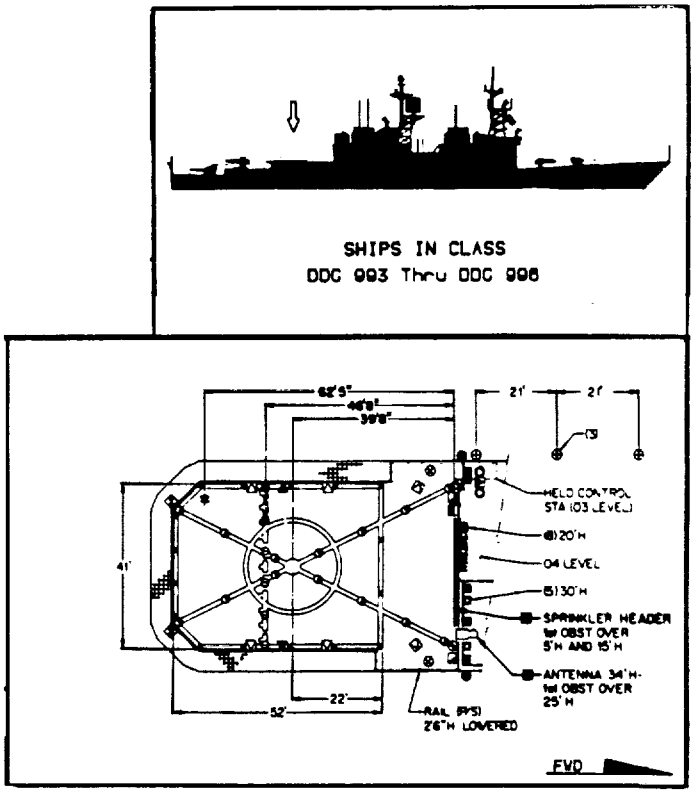

Figure 9 Small Deck Ship (DD) Landing Area, 30 Degree Approach Path.

In high sea states, the U.S. Navy SH-60B can be assisted in shipboard landing by a haul down system referred to as RAST (Recovery, Assist, Secure and Traverse). This recovery assist system is installed in the landing decks of certain guided missile frigates, guided missile cruisers, and destroyer class ships (reference 30).

During launch, approach and landing the pilot is not performing any additional tasks. There are no divided attention operations.

7.0 MIL-H-8501B AND STOPS

7.1 MTE / UCE / Response Type Relationship

Examining only the portion of STOPS in hover/low speed conditions, the number of specification requirements can be further reduced, as illustrated by Figures 10 and 11.

For shipboard terminal operations, several mission task elements (MTEs) can be identified. They include hovering, shipboard stationkeeping, takeoff and transition, and landing. Defining the applicable MTE/UCE/response type relationship, Tables 1(3.2) and 2(3.2) of reference 1 can be reduced to Tables 4 and 5.

To achieve Level 1 handling qualities during these MTEs, MIL-H-8501B requires at least a rate response type in pitch, roll and yaw for UCE=1. For UCE=2, required control augmentation increases to attitude command/attitude hold in pitch and roll, rate command/direction hold in yaw, and rate command/altitude hold in the vertical axis. For UCE=3, translational rate command and position hold are also required. In forward flight with degraded visual conditions, MIL-H-8501B requires rate command/attitude hold in pitch and roll and turn coordination in heading. Furthermore, in forward flight no specific response type for the vertical axis is specified. The requirements for required response types are minimums and can be upgraded if desired. If the mission and mission environment dictates the use of more than one response type, then the requirement on switching between response types, Section 3.8, also applies.

As can be seen from Table 6, many of the U.S Navy helicopters discussed earlier in Section 6.1, satisfy the requirements of MIL-H-8501B for STOPS MTEs conducted in UCEs 1 through 3. Moreover, it is interesting to note that the aircraft which does not possess the minimum required response type for shipboard operations, in visual cue conditions resulting in UCEs>1, is the AH-1W - a U.S Marine Corps aircraft. As discussed earlier, the Marines routinely operate in the shipboard environment with NVG's, effectively improving the UCE at night.

7.2 Sample Qualitative Requirements - Section 3 Criteria

Based on current and future operational environments, procedures and rotorcraft characteristics, a majority of the MIL-H-8501B section 3 hover/low speed criteria will apply to shipboard terminal operations. To convey the nature of these criteria, samples are presented below.

Section 3.3.2.1. Hover and Low Speed, Small Amplitude Pitch and Attitude Changes, Short Term Response to Control Inputs (Bandwidth).

> The pitch response to longitudinal cockpit control force or position inputs shall meet the limits specified in Figure 12.
>
> The small amplitude, short term response to control inputs, criteria is defined in terms of bandwidth and phase delay. These frequency domain parameters describe the system's short term transient response characteristics.

Section 3.3.3. Hover and Low Speed Moderate Amplitude Pitch Attitude Changes (Attitude Quickness).

> The ratio of peak pitch rate to change in pitch attitude shall exceed the limits specified in Figure 13. The required attitude changes shall be made as rapidly as possible from one steady attitude to another without significant reversals in the sign of the cockpit control input relative to the trim position. The initial attitudes, and attitude changes required for compliance with this requirement, shall be representative of those encountered while performing the required MTEs.
>
> The parameters that make up the moderate amplitude criteria are the ratio of the peak rate to peak attitude and the minimum change in attitude during the change from

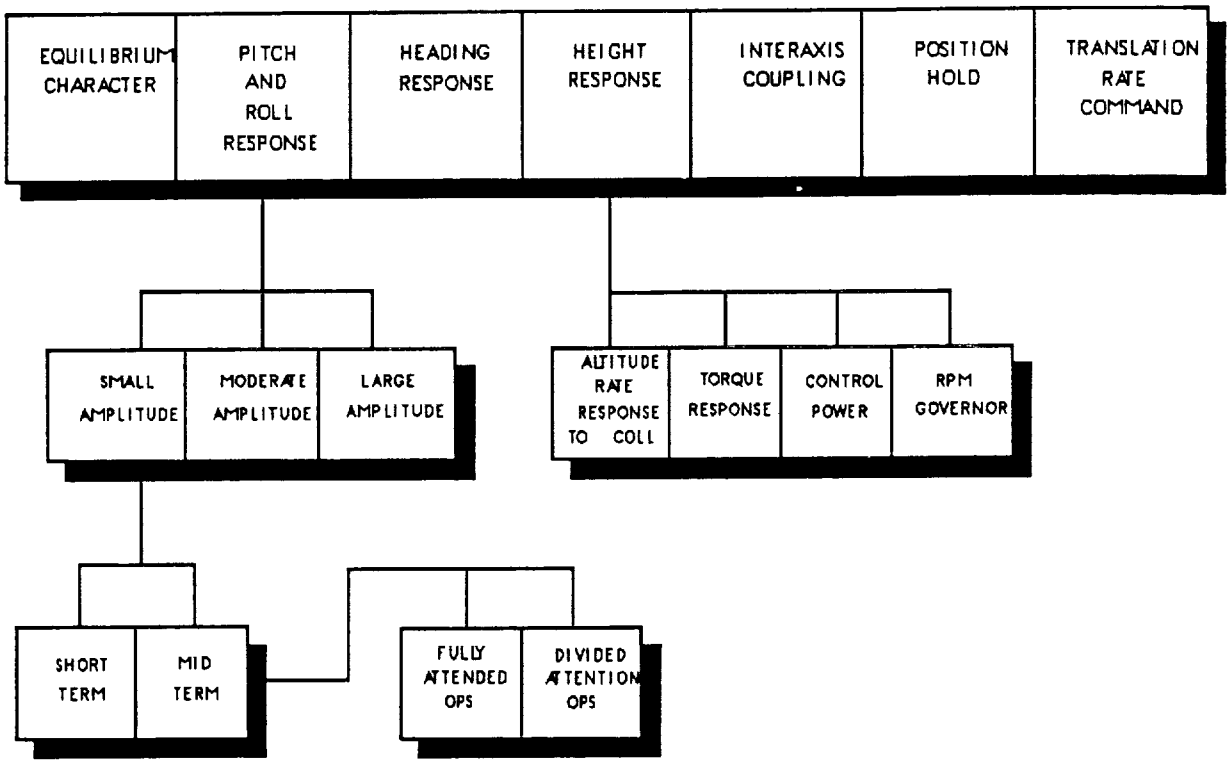

Figure 10 Specification Structure - Quantitative Requirements - Shipboard Terminal Operations.

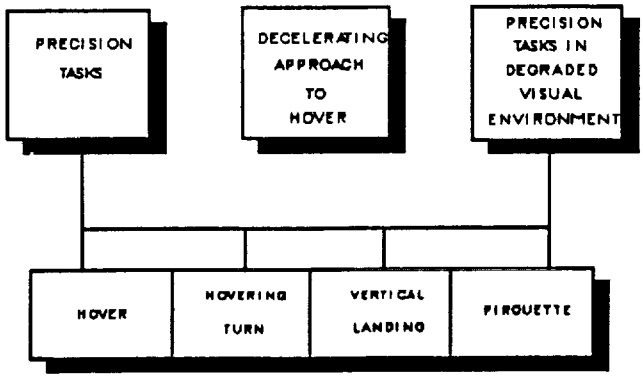

Figure 11 Specification Structure - Flight Test Requirements Relating to Shipboard Terminal Operations.

Table 4 Required Response-Type for Hover and Low Speed - Near Earth

	UCE=1		UCE=2		UCE=3	
	LV 1	LV 2	LV 1	LV 2	LV 1	LV 2
Vertical takeoff and transition to F/F - clear of earth.	Rate	Rate	Rate	Rate	Rate	Rate
Precision hover Shipboard landing including RAST Vertical takeoff and Transition to near earth flight Hover Taxi/NOE Traveling			ACAH + RCDH + RCHH	Rate + RCDH	TRC + RCDH + RCHH + PH	ACAH + RCDH + RCHH
Precision Vertical Landing			ACAH + RCDH			ACAH + RCDH

Notes:

1. A requirement for RCHH may be deleted if the Vertical Translational Rate Visual Cue Rating is 2 or better, and divided attention operation is not required. If RCHH is not specified, an Altitude-Rate Response Type is required (See Paragraph 3.2.9, reference 1).

2. Turn Coordination (TC) is always required as an available Response-Type for the slalom MTE in the Low Speed flight range as defined by Paragraph 2.6.2. However, TC is not required at airspeeds less than 15 knots.

3. For UCE =1, a specified Response-Type may be replaced with a higher rank of stabilization, providing that the moderate and Large Amplitude Attitude Change requirements are satisfied.

4. For UCE=2 or 3, a specified Response-Type may be replaced with a higher rank of stabilization.

5. The rank-ordering of combinations of Response-Type from least to most Stabilization is defined as:
   1. Rate
   2. ACAH+RCDH
   3. ACAH+RCDH+RCHH
   4. Rate+RCDH+RCHH+PH
   5. ACAH+RCDH+RCHH+PH
   6. TRC+RCDH+RCHH+PH

Rate => Rate or Rate Command Attitude Hold (RCAH) Response-Type (Paragraph 3.2.5 and 3.2.6, reference 1).

TC => Turn Coordination (Paragraph 3.2.10.1, reference 1)

ACAH => Attitude Command Attitude Hold Response-Type (Paragraph 3.2.6 and 3.2.7, reference 1).

RCHH => Vertical-Rate Command with Altitude (Height) Hold Response-Type (Paragraph 3.2.9.1, reference 1).

RCDH => Rate-Command with Heading (Direction) Hold Response-Type (Paragraph 3.2.5 and 3.2.6, reference 1).

PH => Position Hold Response-Type (Paragraph 3.3.11, reference 1)

TRC => Translational-Rate-Command Response-Type (Paragraph 3.2.8, reference 1)

Table 5 Required Response-Types in Forward Flight

Pitch and Roll Attitude	
Rate	Pitch - Rate or Attitude, Attitude Hold Required (RCAH or ACAH) Roll - Rate with Attitude Hold (RCAH)
VMC cruise/climb/decent	IMC cruise/climb/decent IMC departure IMC approach (constant speed) IMC decelerating approach (3-cue director required)
Heading -- All require Turn Coordination (see Paragraph 3.4.6.2)	
Height -- No specific Response-Type (see Paragraph 3.4.3)	

Table 6 Response Type of Current Fleet Helicopters

A/C	Pitch	Roll	Yaw	Heave	Other Modes
MH-53E	ACAH	ACAH	RCDH	RCHH	BARALT/RADALT Hold Cable Tension/Skew Hold Crew Hover (TRC) Hover Coupler (PH) Airspeed Hold (>60 Kts)
AH-1W	RC	RC	RC	RC	
SH-3G/H	ACAH	ACAH	RCDH	RCHH*	TRC W/Doppler Cable Angle Hold Crew Hover (TRC) Auto Depart/Approach
CH-46E (SR+M)	ACAH	ACAH	RCDH	RCHH*	
SH-2G/F	ACAH	ACAH	RCDH	RCHH*	TRC W/Doppler
SH-60B	ACAH	ACAH	RCDH	RCHH*	Hover Coupler Ground Speed Command/Hol

* Altitude Hold Pilot Selectable
Note: In all cases, Attitude Command authority is limited to 10-15% of control movement due to series actuation limits.

Table 7 MIL-H-8501B Requirements for Large Amplitude Attitude Changes with regard to Maneuvering Associated with Shipboard Operations

MISSION-TASK-ELEMENT	RATE RESPONSE-TYPES MINIMUM ACHIEVABLE ANGULAR RATE (DEG/SEC)						ATTITUDE RESPONSE-TYPES MINIMUM ACHIEVABLE ANGLE (DEG)			
	LEVEL I			LEVEL II+III			LEVEL I		LVLII+III	
	Q	P	R	Q	P	R	θ	φ	θ	φ
LIMITED MANEUVERING All MTEs not otherwise specified	± 6	± 21	±9.5	±3	± 15	±5	±15	±15	±7	±10
MODERATE MANEUVERING Rapid Transition to Hover Slope Landing Shipboard Landing	±13	± 50	±22	±6	± 21	+9.5 - 30	± 20	±60	±13	±30

one steady attitude to another. This requirement is a measure of the agility, or attitude quickness, of the system. Use of the peak rate/peak attitude ratio is based, in part, on the concept that for an ideal system, this ratio can be analytically related to the system bandwidth. Using this relationship, the lower end of the moderate amplitude requirement is anchored at the equivalent small amplitude requirements. Similarly, the upper boundary is anchored at the equivalent value of the large amplitude requirements.

Section 3.3.4. Hover and Low Speed, Large Amplitude Pitch Attitude Changes (Control Power).

The minimum achievable angular rate shall be no less than the values specified in Table 7. The specified rate must be achieved in each axis while limiting excursions in the other axis with the appropriate control inputs.

The large amplitude criteria is defined in terms of the maximum achievable rates or attitudes. As such, this criteria is a measure of the vehicle's control power.

Section 3.3.10.1 Height Response Characteristics.

The vertical rate response shall have a qualitative first-order appearance for at least 5 seconds following a step collective input. The limits on the parameters defined by the following equivalent first-order vertical rate to collective transfer function are given in Table 8.

Table 8 Maximum Values for Height Response to Collective Controller

LEVEL	$T\dot{h}_{eq}$ (sec)	$\tau\dot{h}_{eq}$ (sec)
I	5.0	0.20
II		0.30

$$\frac{\dot{h}}{\delta_c} = \frac{k\, e^{-\tau\dot{h}_{eq}\, s}}{T\dot{h}_{eq}\, s + 1}$$

The equivalent system parameters are to be obtained using the time domain fitting method defined in Figure 8(3.3) of reference 1. The coefficients of determination, r^2 shall be greater than 0.97 and less than 1.03 for compliance with this requirement.

The height response criteria is defined in terms of rise time and delay. Not unlike the bandwidth parameter in the frequency domain, rise time is a measure, in the time domain, of how rapidly the systems responds. Time delay simply measures how long the heave response lags the collective

Section 3.3.10.3 Vertical Axis Control Power.

While maintaining a spot hover with the wind from the most critical direction at a velocity of up to 35 knots, and with the most critical loading and altitude, it shall be possible to produce the vertical rates specified in Table 9, 1.5 seconds after initiation of a rapid displacement of the vertical axis controller from trim. Applicable engine and transmission limits shall not be exceeded.

Table 9 Vertical Axis Control Power

LEVEL	Achievable Vertical Rate in 1.5 Seconds m/s (ft/min)
I	0.81 (160)
II	0.28 (55)
III	0.20 (40)

An example evaluation of selected specification requirements utilizing the predicted and actual handling qualities of a naval rotorcraft may be found in reference 31.

8.0 GENERAL DESIGN IMPLICATIONS AND OPERATIONAL CAPABILITY

Application of MIL-H-8501B has vast design implications. These implications are driven by the MIL-H-8501B philosophy that the rotorcraft should be viewed as a whole system and not a collection of individual isolated systems. As such, MIL-H-8501B is designed to ensure the pilot is provided with a total system yielding superior flying qualities and allowing him to effectively and safely perform his mission. In this regard, MIL-H-8501B criteria will influence the design of every major aircraft component from the

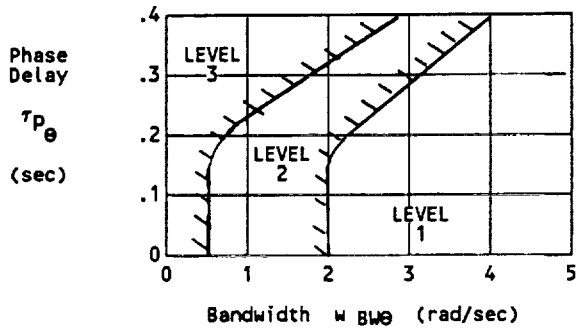

a) Target Acquisition and Tracking

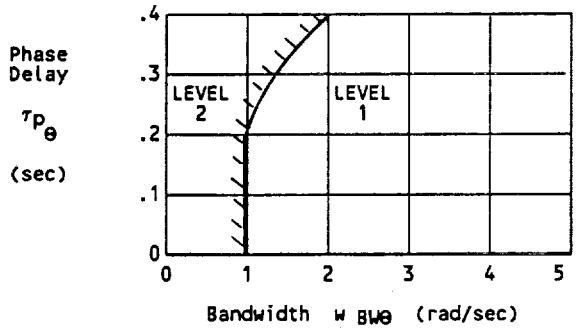

b) All Other MTEs - UCE =1 and Fully Attended Operations

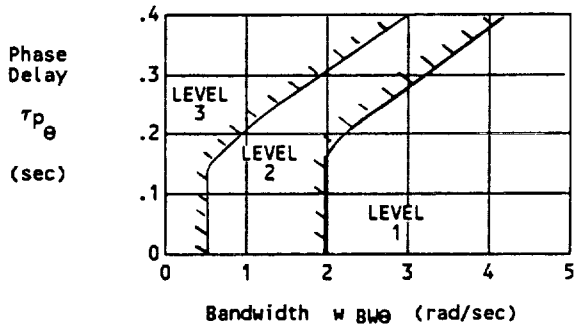

c) All Other MTEs - UCE>1 and/or Divided Attention Operations

Figure 12 Requirements for Small Amplitude Pitch Attitude Changes, Hover and Low Speed, STOP MTEs, and fully attended operations.

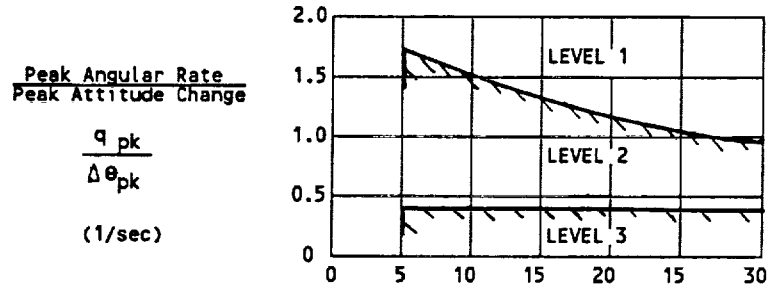

a) Target Acquisition and Tracking (pitch)

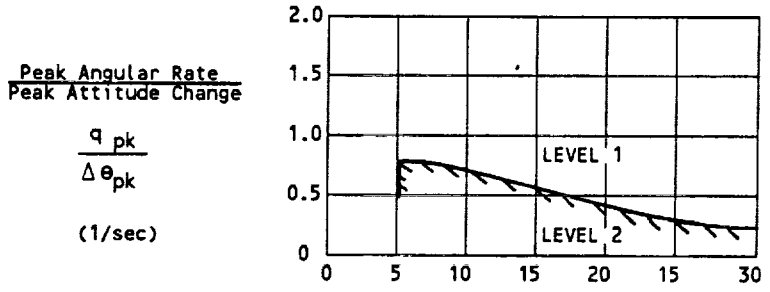

b) All Other MTEs

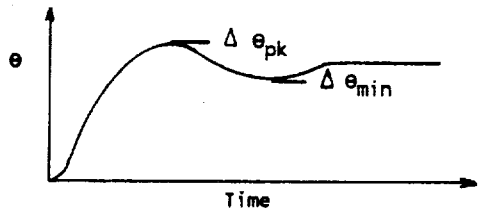

c) Definition of Moderate Amplitude Criterion Parameters

Figure 13 Requirements for Moderate Amplitude Pitch Attitude Changes, Hover and Low Speed, STOP MTEs, and Fully Attended Operations.

airframe and rotor to flight controls, displays, and vision aids.

The explicit relationship between the vehicle's dynamics, UCE and resultant flying qualities as defined in MIL-H-8501B, will force the designer to consider the displays and vision aids on an equal footing with the flight control system. For example, the reliability or redundancy of all flight control and avionics system components, that impact the vehicles dynamics as well as the UCE, must be considered. These components include, but are not limited to: gyros, flight control computers, mission computers, display processors, sensors, actuators, and display units. Furthermore, the dynamic response criteria will directly impact actuator, hub, blade, airframe, and flight control law design.

Both the philosophy of and the criteria specified in MIL-H-8501B are mission oriented. The philosophy is founded on a systems approach and involves a partitioning of criteria according to the fundamental characteristics necessary to satisfactorily perform the defined mission task elements. The dynamic response criteria have been derived from experimentation utilizing mission related evaluation tasks. As a result, compliance with MIL-H-8501B should insure flying qualities will not detract from an adequate operational capability. Likewise, non-compliance will most likely result in increased pilot workload and/or a reduction in operational capability.

9.0 CONCLUDING REMARKS

A complete understanding of the philosophy, structure, methodology, and application of the proposed U.S. military specification for Handling Qualities Requirements for Military Rotorcraft, MIL-H-8501B (reference 1), is a requisite for the proper specification of flying qualities design requirements. Proper selection of the flying qualities design requirements is critical to proper helicopter design and, in turn satisfactory operation. Satisfactory operation of all new helicopters, tiltrotors and V/STOLS, in the shipboard environment as well as all other mission environments, is critical to the U.S Navy.

10.0 ACKNOWLEDGMENTS

The authors would like to thank Mr. Kurt Long of the Dynamic Interface Branch at Naval Air Test Center, Mr. Bob Miller of United States Naval Test Pilot School, and MAJ. Doug Isleib USMC HMX-1, for sharing their knowledge and expertise.

REFERENCES

1. Anon., "Handling Qualities Requirements of Military Rotorcraft." U.S. Army ADS-33 (Proposed MIL-H-8501B), August 1989.

2. Anon., "Military Specification -- Helicopter Flying and Ground Handling Qualities; General Requirements for." MIL-H-8501A, w/amendment April 1962.

3. Goldstien K., "A Preliminary Assessment of Helicopter/VSTOL Handling Qualities Specifications." NADC Report No. 81023-60, November 1982.

4. Walton, R.P. and Ashkenas, I.L., "Analytical Review of Military Helicopter Flying Qualities." Systems Technology, Inc. Technical Report No. 143-1, August 1967.

5. Key, D.L., "A Critique of Handling Qualities Specifications for U.S. Military Helicopters." AIAA 80-1592, August 1980.

6. Hoh, R.H. and Mitchell, D.G, "Status of Several Ongoing Military Flying Qualities Specification Development Programs." AIAA 85-1785-CP, August 1985.

7. Anon., "Flying and Ground Handling Qualities Specification for Light Airborne Multipurpose System (LAMPS) Rotary Wing Aircraft." Appendix I Rev. No. R-4, SD-567, October 1979.

8. Chalk, C.R. and Radford, R.C, "Mission-Oriented Flying Qualities Requirements for Military Rotorcraft." Calspan Report No. 7097-F-1, January 1984.

9. Clement, W.F., Hoh, R.H, and Ferguson, S.W, et al., "Mission-Oriented Requirements for Updating MIL-H-8501A. Volume I: STI Proposed Structure." NASA CR-177331, Vol. I, January 1983.

10. Clement, W.F., Hoh, R.H, and Ferguson, S.W, et al., "Mission-Oriented Requirements for Updating MIL-H-8501A. Volume II: STI Background and Rationale." NASA CR-177331, Vol. I, January 1985.

11. Hoh, R.H, et al., "Background Information and User's Guide for Handling Qualities Requirements for Military Rotorcraft," USAAVSCOM TR-89-A-008, December 1989.

12. Cooper, G.E and Harper, R.P, "The Use of Pilot rating in the Evaluation of Aircraft Handling Qualities." NASA TN D-5153, April 1969.

13. Carico, D. and Maday, Cdr USN S. L. Jr., "Dynamic Interface, Conventional Flight Testing Plus A New Analytical Approach." American Helicopter Specialist Meeting, Williamsburg VA, September 1984.

14. Carico, D. et al. "Dynamic Interface Flight Test and Simulation Limitations." Eleventh European Rotorcraft Forum, Paper No. 100, September 1985.

15. United States Navy Board of Inspection and Survey Instruction, INSURVINST 13100.1D, April 1987.

16. NATOPS General Flight Operation Instructions, OPNAV 3710.7M, July 1987.

17. Air Operations Manual, Naval Air Station Patuxent River, NASPAXRIVINST 3710.5N, November 1987.

18. Air Operations Manual, Naval Air Station Oceana, NASOCEINST 3710.1M, February 1988.

19. Shipboard Helicopter Procedures, NWP-42 (Rev H), December 1988.

20. Trick, L., Hammond, LT USN A., et al., "SH-60B/DD 963 Dynamic Interface Tests Aboard the USS Moosbrugger (DD 980)." NAVAIRTESTCEN, Rep. No. RW-85R-85, April 1986.

21. Petz, J.C., and Madey, CDR USN S.L., "SH-60B/DD 993 USS Kidd Class Dynamic Interface Tests." NAVAIRTESTCEN, Rep. No. RW-65R-84, January 1985.

22. Long, K.R., Lescher, LCDR USN W.K., and Smith, LT USN P.D., "SH-60B Degraded Visual Landing Aids Evaluation aborad USS Cushing (DD 985)." NAVAIRTESTCEN, Rep. No. RW-14R-90, April 1990.

23. Anon., Light Level Calander, NOAH, January 1991.

24. Long, K.R., Storey, Lt Col USMC J., et al., "CH-53A, CH-46E Dynamic Interface Tests Aboard USS Whidbey Island (LSD 41) -- Quick Response Report." NAVAIRTESTCEN, Rep. No. RW-123R-88, November 1988.

25. Harvey, D., "The HH-60: Navy CSAR Gets A Shot in the Arm." Rotor & Wing International, August 1988.

26. Walters, B., "Lynx Mk8: More Capable with Less Pilot Workload." Rotor & Wing International, November 1990.

27. CV NATOPS Manual, NAVAIR 00-80T-105, December 1985.

28. NATOPS Flight Manual Navy Model SH-60B Aircraft, A1-H60BB-NFM-000; September 1987.

29. NATOPS Flight Manual Navy Model SH-3D/H Helicopters, NAVAIR 01-230HLH-1, September 1988.

30. Jewell, D.H., "Shipboard Aviation Facilities Resume." NAEC-ENG-7576, Revision AJ, January 1991.

31. Cappetta, A.N., and Johns, J.B, "An evaluation of the proposed specification for handling quailities of military rotorcraft, MIL-H-8501B, utilizing predicted and actual SH-60B handling qualities." American Helicopter Society's 46th Annual Forum, Washington D.C, May 1990.

DESIGN CRITERIA FOR INTEGRATED FLIGHT/PROPULSION CONTROL SYSTEMS FOR STOVL FIGHTER AIRCRAFT

James A. Franklin

Group Leader
V/STOL and High Speed Flight Dynamics
NASA Ames Research Center
Moffett Field, California

ABSTRACT

As part of NASA's program to develop technology for short takeoff and vertical landing (STOVL) fighter aircraft, control system designs have been developed for a conceptual STOVL aircraft. This aircraft is representative of the class of mixed-flow remote-lift concepts that was identified as the preferred design approach by the US/UK STOVL Joint Assessment and Ranking Team. The control system designs have been evaluated throughout the powered-lift flight envelope on Ames Research Center's Vertical Motion Simulator. Items assessed in the control system evaluation were: maximum control power used in transition and vertical flight, control system dynamic response associated with thrust transfer for attitude control, thrust margin in the presence of ground effect and hot gas ingestion, and dynamic thrust response for the engine core. Effects of wind, turbulence, and ship airwake disturbances are incorporated in the evaluation. Results provide the basis for a reassessment of existing flying qualities design criteria applied to STOVL aircraft.

NOMENCLATURE

AC	attitude command
F_G	gross thrust, lb
g	acceleration due to gravity, ft/sec^2
h	landing gear wheel height above ground, ft
HGI	hot gas ingestion
HUD	head-up display
IGE	in-ground effect
IMC	instrument meteorological conditions
LIDS	lift improvement devices
OGE	out-of-ground effect
PIO	pilot-induced oscillation
SCAS	stabilization and command augmentation system
T	propulsion system vertical thrust, lb
VC	velocity command
W	gross weight, lb
WOD	wind over deck
ΔL	lift increment referenced to out-of-ground effect conditions, lb
$\Delta L/T$	normalized jet-induced aerodynamic ground effect
$(\Delta L/T)'$	normalized lift increment due to ground effect and hot gas ingestion
θ	temperature ratio as a function of wheel height
σ	standard deviation

Presented at Piloting Vertical Flight Aircraft: A Conference on Flying Qualities and Human Factors, San Francisco, California, 20-23 January, 1993.

INTRODUCTION

NASA has been involved in a collaborative program with other government agencies in the United States and with the Ministry of Defence of the United Kingdom to develop technology for supersonic short takeoff and vertical landing (STOVL) aircraft. As a result of this effort, a wide variety of airframe and propulsion system concepts have been assessed through analytical studies, and critical technical issues have been identified for investigation (Ref. 1). The preferred design approach identified by the US/UK STOVL Joint Assessment and Ranking Team for the airframe and propulsion system is known as mixed-flow remote-lift, an example of which is illustrated in Figure 1. This configuration features mixed fan and core flows that can be directed forward or aft to generate the lift and thrust forces and to provide (partially or exclusively) control moments. The propulsion system will have forward thrust-producing device(s) that may deflect as well as modulate that thrust component, a variable area cruise nozzle that may provide thrust deflection for pitch and yaw control, and rear lift nozzle(s) that provide a thrust component for pitch control and which may also deflect about the vertical. Combined with these propulsion components are the aerodynamic surfaces that function during both wing-borne and jet-borne flight. These may include leading and trailing edge flaps on the wings, canards, ailerons, stabilators and rudders for lift and moment control.

Integration of these flight and propulsion controls has been identified as one of the critical technologies to be developed for these aircraft. A program has been conducted to define control concepts that combine the various aerodynamic and propulsion control effectors with control laws designed to achieve fully satisfactory (Level 1) flying qualities throughout the powered-lift flight envelope. Furthermore, criteria for the control authority and dynamic response of the individual effectors have been explored. The control system designs have been evaluated throughout the powered-lift flight envelope on Ames Research Center's Vertical Motion Simulator. Included in the control system evaluation were assessments of maximum control power used in transition and vertical flight, control system dynamic response associated with thrust transfer rates for attitude control, thrust margin in the presence of ground effect and hot gas ingestion, and dynamic thrust response for the engine core. Effects of wind and turbulence and airwake disturbances from a ship are incorporated in the assessment. The purpose of this paper is to review these assessments as a basis for possible revisions or extensions of flying qualities design criteria for this class of aircraft.

This paper includes a description of the aircraft, the simulation facility and the experiments which were conducted. A summary of the results of these experiments follows, including suggestions for revision or modification of existing criteria.

MIXED-FLOW REMOTE-LIFT AIRCRAFT

The design criteria presented in this paper are based on simulation experiments involving a mixed-flow remote-lift STOVL aircraft concept (Fig. 1). This concept is specifically referred to as mixed flow vectored thrust (MFVT) and is described in further detail in Reference 2. The aircraft is a single-place, single-engine fighter/attack aircraft with supersonic dash capability. It features a blended wing-body configuration with a canted empennage that provides longitudinal and directional control. The wing is characterized by a leading edge sweep of 50° and aspect ratio of 2.12. The propulsion system concept uses a turbofan engine where the mixed fan and core streams are either ducted forward to the lift nozzles or aft to a thrust deflecting cruise nozzle. A ventral nozzle diverts some of the mixed flow to provide pitching moment to counter that of the lift nozzles. Lift nozzle thrust can be deflected up to ±20° about a nominal rearward cant angle of 8°. The cruise nozzle can be deflected laterally or vertically ±20°. In conventional flight, the mixed flow is directed aft through the cruise nozzle, whereas in hover it is diverted from the cruise nozzle to the forward lift nozzles, with a small portion reserved for the ventral nozzle. During transition from hover to conventional flight, the flow is smoothly transferred from the lift to the cruise nozzle to provide acceleration.

The basic flight control system uses a variety of control effectors: ailerons, a fully deflecting empennage, reaction control system nozzles located in the tail, differential thrust transfer between the lift nozzles and ventral nozzle, longitudinal deflection of lift nozzle thrust, and vertical and lateral deflection of cruise nozzle thrust. Pitch control is achieved by a combination of symmetric empennage deflection, reaction controls, thrust transfer between the lift and ventral nozzles, and vertical deflection of the cruise nozzle. Roll control is produced by the ailerons and by lateral thrust transfer (differential lift nozzle thrust). Yaw control is derived from the combination of differential empennage deflection, reaction control, and lateral cruise nozzle deflection. Longitudinal acceleration is achieved through thrust transfer between the lift and cruise nozzles and by deflection of lift nozzle thrust.

To achieve the desired level of flying qualities during low-speed flight, stabilization and command augmentation modes were provided in the flight control system as noted in Table 1. During transition, either attitude or flightpath SCAS mode was available. Both modes offer rate-command/attitude hold for pitch and roll control and dutch roll damping and turn coordination for the yaw axis. When only the attitude SCAS is selected, the pilot must control thrust magnitude and deflection. When flightpath SCAS is engaged, the pilot commands flightpath angle and flightpath acceleration directly; the control system coordinates thrust magnitude and deflection to achieve the desired response. Either the attitude or velocity SCAS may be selected in hover. Both modes provide pitch and roll attitude command/attitude hold and yaw rate command. With attitude SCAS, the pilot controls longitudinal and lateral translation through changes in pitch attitude and bank angle. Thrust is used for height control. For the velocity SCAS, longitudinal, lateral, and vertical velocities are commanded directly. A thorough description of the control system is included in Reference 2.

A head-up display presented the primary flight information for these experiments. The display format was a flightpath centered, pursuit presentation in transition. In hover, the display switched to a format that superimposed vertical and horizontal command and situation information in a pursuit tracking presentation. A complete description of the display is included in Reference 3.

SIMULATION EXPERIMENT

Simulation Facility

The experiments on which these criteria are based were conducted on the Vertical Motion Simulator (Fig. 2) at NASA Ames Research Center. This simulator provides six degree-of-freedom motion, with large excursions in the vertical and longitudinal axes, and acceleration bandwidths in all axes that encompass the bandwidths of motion that are expected to be of primary importance to the pilot in vertical flight tasks. A three-window, computer generated image system presented the external view to the pilot, which consisted of either an airfield scene or a shipboard scene consisting of a Spruance-class destroyer. An overhead optical combining glass projected the HUD for the pilot. Control inceptors consisted of a center stick, rudder pedals, and a left-hand quadrant that contained throttle and thrust vector deflection handles.

Evaluation Tasks and Procedure

The pilot's tasks for evaluation during the simulation were those considered the most demanding for precision control of the aircraft—curved decelerating approaches to hover followed by a vertical landing. For evaluation purposes, the decelerating approach was initiated under instrument meteorological conditions (IMC) in level flight at 1100 ft and 200 knots in the landing configuration. Capture of a 3° glide slope ensued, followed by initiation of a 0.1 g deceleration, a turn to align with the final approach course, and acquisition of a stable hover over the hover point. Vertical landings were accomplished either on a 100 by 200 ft landing zone marked on the airfield's main runway or on a 40 by 70 ft pad on the ship's aft deck. Six pilots with V/STOL and powered-lift aircraft experience participated in the program.

Experiment Configurations

Experiment variables for the decelerating approach and vertical landing included the control system configuration, control system dynamics, thrust/weight ratio, jet-induced ground effect and hot-gas ingestion, and environmental conditions (wind, turbulence, and sea condition). Both the attitude SCAS and attitude-plus-flightpath SCAS were investigated for the decelerating approach; attitude SCAS and attitude-plus-velocity SCAS were evaluated for the vertical landing. System dynamics variations included control system authority, thrust transfer rates, engine core thrust response bandwidth and acceleration rate. Nine ground effect and ingestion profiles representative of a broad range of STOVL aircraft characteristics of lift and temperature profile as a function of height (four of which were representative of the YAV-8B Harrier with LIDS on and off) were included for both airfield and shipboard landings. Wind conditions for the approach and airfield landing were calm, 15 knots, and 34 knots, with crosswind components of 30° and 20°, respectively, for the latter two wind conditions. Turbulence of 0, 3, and 6 ft/sec rms accompanied the respective wind cases. Conditions for shipboard recovery included sea states of 0, 3, and 4 with wind over deck of 15, 27, and 46 knots from 30° to port.

CONTROL POWER

Existing design specifications and guidance for pitch, roll, and yaw control power for fixed-wing V/STOL aircraft are contained in References 4 and 5.

Additional information from STOL aircraft experience that would apply to the V/STOL transition is provided in Reference 6. Flight and simulation data on which these publications are based date back to the late 1960s. Given the present capability for achieving highly augmented stability and control characteristics and the necessity for operating in IMC, it is worthwhile to reassess the validity of the control power requirements derived from the earlier data. The results which follow relate to control power for maneuvering and for suppressing disturbances and have control required for trim removed. These results are presented to reflect the influence of flight phase, including effects of control augmentation and magnitude of atmospheric disturbance. The breakdown related to flight phase is important not only because of the difference in the pilot's tasks, but because of the demands placed on different control effectors (aerodynamic surfaces and propulsion system components) that, in turn, place different demands on the aircraft's design. Control power usage is presented in terms of individual maximum values (plus or minus about the mean value) for each run and an aggregate value of two standard deviations for the ensemble at that condition. For a Gaussian distribution of frequency of occurrence of control use, expected maximum values would be three to four times the standard deviation. Two standard deviations represents a level of control use that is exceeded 4.6% of the time over the ensemble of data runs. Aircraft response specifications of References 4 and 6 were translated to measures of control power for direct comparison with the current results. These criteria were converted from attitude change in 1 sec using an attitude control bandwidth of 2 rad/sec for an attitude command response that is critically damped, or using a first-order response with a time constant appropriate to the axis being controlled.

Maximum demands for pitch control during hover and vertical landing are pertinent to sizing requirements for the aircraft's reaction control system or for thrust transfer between components of the propulsion system. Demands for roll control generally size the amount of thrust transfer required between the lift nozzles. Yaw demands contribute to sizing of the reaction control system. During transition, the requirements on control sizing would incorporate both the propulsion system and the aerodynamic effectors.

Pitch Control

Effect of Flight Phase. A collection of results of pitch control usage for both attitude command and attitude-plus-flightpath command SCAS over a range of wind and turbulence for the tasks of transition, airfield vertical landing, and shipboard landing is presented in Figure 3. For the transition (Fig. 3a), results in calm air, which are indicative of maneuvering demands, show that, for attitude command SCAS, pitch control power maximums fall within the range considered to be satisfactory in Reference 5 for STOL operations (which can be related to the transition phase of this simulation). Two standard deviation levels are well below the Reference 5 maximum. Peak values generally equate to 3–4σ levels. The influence of turbulence on the additional control required for disturbance suppression is apparent. For rms turbulence of 6 ft/sec (Turb6), a few instances of control usage exceed the maximum recommended level of Reference 5. Thus, to cater for maneuvering and the effects of turbulence, a control power of 0.2–0.25 rad/sec^2 would provide for at least 99% of all demands encountered.

Results for the attitude-plus-flightpath SCAS are comparable to those for the attitude SCAS, reflecting the fact that the pilot's pitch control task is similar for the two systems during transition. The pilot uses pitch attitude changes for flightpath control during the early stages of the approach, where a frontside control technique is appropriate, as well as to regulate against disturbances arising from wind and turbulence.

Pitch control during the vertical landing with the attitude SCAS (Fig. 3b) shows levels of peak control usage that are less than the requirements of References 4 and 5. The maximum control required was 0.27 rad/sec^2 (3–4σ values of 0.14–0.18 rad/sec^2). Turbulence disturbances did not impose additional demands on control authority. Consequently, control authority of 0.14–0.27 rad/sec^2 would accommodate most of the demands for the attitude SCAS. By comparison, the 3° attitude change in 1 sec required by Reference 4 converts to a peak pitch control power of 0.29 rad/sec^2 for a 2 rad/sec attitude command bandwidth.

With the velocity command SCAS, even less pitch control is required, reflecting the difference in the pitch control task between the two SCAS configurations. With attitude SCAS alone, control of longitudinal position and velocity in hover is accomplished through modulation of pitch attitude. When the velocity command system is engaged, control of the longitudinal axis is achieved through deflection of the thrust vector with attitude fixed. In this case, the vertical landing can require a control authority of 0.17 rad/sec^2, independent of winds and turbulence.

Results for hover and vertical landing aboard ship with attitude command alone (Fig. 3c) are comparable to the criteria of Reference 5 and Level 1 handling values in Reference 4 (although neither criterion applies to shipboard operation, but rather to hover out-of-ground effect). Peak control usage is 0.38 rad/sec^2 or less, with 3–4σ levels being 0.12–0.16 rad/sec^2. For the attitude-plus-velocity command system, peak control use is approximately two-thirds of that for attitude command alone, reflecting, as in the airfield vertical landing, the different task required for the pitch axis. For neither system does wind over deck seem to influence the amount of control required for the landing. Thus, for shipboard operations, the control power requirement of References 4 and 5 appear appropriate with attitude SCAS alone, and a requirement for 0.2 rad/sec^2 should suffice for the attitude-plus-velocity command SCAS.

Summary of Pitch Control Requirements. A summary of the required pitch control authority determined from these STOVL aircraft simulation results, compared to (1) the Level 1 criteria of References 4, 5, and 6, (2) available control power for some relevant V/STOL fighter aircraft designs (Refs. 7–9), and (3) earlier fixed-base simulation results for the E-7A STOVL concept (Ref. 10), is presented in Table 2. For the transition phase, the pertinent criteria are those of References 5 and 6; no control power data are available for the individual aircraft. For the vertical landing, References 4 and 5 apply; the total available control power has been tabulated for the Harrier and VAK-191.

In the transition phase, the highest value of the criteria of Reference 5 does not quite accommodate the peak control use in turbulence noted for this experiment (MFVT STOVL). Maximum control experienced during the E-7A STOVL simulation was considerably greater, both for maneuvering and control in turbulence, and is more in line with the requirement of Reference 6. For the vertical landing, both References 4 and 5 appear to be too demanding. The current results indicate that less control power is used, especially with a velocity command system that employs thrust deflection for longitudinal control. No criteria are available for shipboard operations. Values shown for the Harrier and VAK-191 aircraft represent total control authority available for trim and maneuvering; actual control used by these aircraft is not available. By comparison, the total control available for the MFVT STOVL aircraft is 0.42 rad/sec^2 in hover, with 0.08 rad/sec^2 of that being used on the average for trim in winds up to 34 knots. Thus, the pitch control for this aircraft was adequate to handle the measured trim and maneuver demands in hover and vertical landing for the attitude SCAS and considerably more than adequate for control with the velocity command SCAS.

Roll Control

Effect of Flight Phase. Roll control use for the different flight phases, SCAS modes, and turbulence is shown in Figure 4. Maximum roll control use for maneuvering in calm air during transition (Fig. 4a) substantially exceeds that called for in Reference 5, with peaks of 0.4–0.9 rad/sec^2. However, the 3–4σ levels of 0.3–0.4 rad/sec^2 are more in line with the criteria. For control in the heaviest turbulence, demands for as much as 1.2 rad/sec^2 occur, although the range is more typically 0.6–0.9 rad/sec^2, which is consistent with 3–4σ values. As a further comparison, the Level 1 requirement of Reference 6 for maneuver control during STOL operations provides for 30° of bank angle change in 2.4 sec, which is satisfied by a control authority of 0.55 rad/sec^2 for a roll damping time constant of 0.5 sec. The latter requirement represents a more specific criterion for operation during transition, particularly where that phase consists of precision path tracking in forward flight during instrument flight conditions in adverse weather. Based on the results of this STOVL aircraft simulation, a roll control authority of 0.9–1.2 rad/sec^2 would be necessary to satisfy demands for maneuvering and control in turbulence.

Control use for the vertical landing, shown in Figure 4b, is consistently less than the Reference 4 requirement, and falls within the range suggested in Reference 5. Peak maneuvering demands for attitude command SCAS range from 0.1 to 0.3 rad/sec^2, and are comparable to 3–4σ values. The heaviest turbulence increases these levels modestly to 0.2–0.4 rad/sec^2. For the attitude-plus-velocity SCAS, which provides lateral velocity command through bank angle control, calm air maneuvering control use is somewhat less than for attitude SCAS alone; however, in turbulence the demands for the two systems are similar.

Results for shipboard recovery are generally in agreement with the criteria of References 4 and 5, except for high wind over deck conditions (Fig. 4c). In light winds, the peaks vary from 0.2 to 0.4 rad/sec^2. In the heaviest winds, maximum control of 0.9–1.1 rad/sec^2 was observed for the attitude command SCAS; for the lateral velocity command SCAS, maximums ranged from 1.3 up to 2.0 rad/sec^2. Based on pilot comments from the subject simulation experiments, operation aboard ship would be precluded at higher sea states because of the limit on capability to recover to a more actively moving

deck. If shipboard operations at these extreme conditions are anticipated, roll control authority in excess of that given in References 4 and 5 must be provided. Further, lateral velocity command capability will demand more control authority than that used for attitude command alone. The latter two conclusions are contingent both on the validity of the ship airwake model used in this experiment (Ref. 11) and on the aircraft's sensitivity to airwake disturbances and should be qualified accordingly.

Summary of Roll Control Requirements. Table 3 presents a summary of the required roll control authority determined from these simulation results, compared to the Level 1 criteria of References 4, 5, and 6, to available control power for the V/STOL fighters, and to the E-7A STOVL concept. For the transition phase, the pertinent criteria again are those of References 5 and 6. In the hover and vertical landing, References 4 and 5 are the applicable documents.

During transition, References 5 and 6 accommodate the level of roll control required for maneuvering in calm air, but call for an insufficient level of control to handle the current STOVL configuration in turbulence up to the level shown. Considering experience of the Harrier design evolution, the dominant requirement for roll control during transition may well be associated with countering sideslip excursions. The AV-8B has sufficient lateral control to trim with sideslip angles of 15° or more during transition. The current MFVT configuration can achieve lateral trim with sideslip of 10° or greater over the low speed flight envelope. Criteria of References 4 and 5 are about right for the vertical landing. No criteria are available for shipboard operations. Total control authority available for trim and maneuvering is shown for the Harrier and VAK-191. Total control available for the current STOVL aircraft in its basic configuration in hover is 1.1 rad/sec^2, which was adequate for disturbance suppression and more than adequate for control of the vertical landing. However, it was necessary to augment the baseline roll control system with reaction control to provide sufficient control power to handle the highest wind over deck for recovery to the ship. In the latter case, the total control power was 2.15 rad/sec^2. Control used for maneuvering in calm air and control needed in turbulence for the E-7A were less than those required for the MFVT STOVL and more in line with the criteria of References 5 and 6. It should be noted that for the MFVT STOVL design every 0.1 rad/sec^2 of additional roll control power would require an additional ±170 lb of differential thrust at the lift nozzles in the hover condition, or 2.4 lb/sec of reaction control bleed at the tail mounted reaction control nozzles. If wing tip reaction controls were employed for roll control, this increment of control power would demand 0.7 lb/sec of bleed flow. The bleed flow values are based on an assumption of 90 lb of reaction control thrust per pounds per second of bleed flow rate (Ref. 12), and on minimal nozzle flow losses or adverse jet interference. If the latter two influences are not optimized, bleed flow requirements would increase.

Yaw Control

Effect of Flight Phase. Yaw control use shown in Figure 5 is considerably less than the criteria of References 4 and 5 for any flight phase. For the transition (Fig. 5a), peak demands in calm air range from 0.02 to 0.04 rad/sec^2. In the heaviest turbulence, maximum control usage of 0.04–0.14 rad/sec^2 was observed, with most confined to the range of 0.05–0.07 rad/sec^2, within the 3–4σ band. In contrast, the recommended range is 0.15–0.25 rad/sec^2 from Reference 5. As a further example, the requirement of Reference 6 for a 15° heading change in 2.2 sec translates into a maximum yaw control power of 0.22 rad/sec^2 for a yaw damping time constant of 1 sec. The disparity between these two criteria for yaw control and the recent simulation experience is likely attributable to good yaw stability augmentation employed and the lower sensitivity to disturbances for the recent STOVL fighter concepts compared to the collection of aircraft on which the earlier criteria were based.

Maximum yaw control for the vertical landing (Fig. 5b) is comparable to that for the transition. Maximum maneuvering control in calm air varies from 0.015 to 0.065 rad/sec^2; control in turbulence increases somewhat with an occasional peak excursion as large as 0.1 rad/sec^2. The maximum range in turbulence corresponds to 3–4σ values. The Reference 4 requirement for a heading change of 6° in 1 sec converts to a maximum control power of 0.28 rad/sec^2 for a yaw time constant of 1 sec. For the shipboard landing (Fig. 5c), maximum control use is similar to that for the runway landing, with peaks to 0.1 rad/sec^2 for the highest wind over deck.

Summary of Yaw Control Requirements. Yaw control summaries of authority determined from these STOVL aircraft simulation results, compared to the Level 1 criteria of References 4, 5, and 6, to available control power for other V/STOL fighter designs, and to the E-7A, are provided in Table 4. For the transition phase, the pertinent criteria once more are those of References 5 and 6. For the vertical landing, References 4 and 5 are the pertinent criteria.

For the transition and vertical landing, the criteria of References 4, 5, and 6 all exceed the current experience for yaw control use to a significant degree. Based on the current experience, yaw control power for maneuvering and turbulence suppression could be considerably reduced. As before, shipboard operations are not covered by the existing criteria. Total control authority for the Harrier and VAK-191 are somewhat in excess of that for the current STOVL design (0.28 rad/sec^2). Control used by the E-7A in the fixed-base simulation experiment is comparable to that for the MFVT STOVL tested on the VMS. For this STOVL aircraft design, every 0.1 rad/sec^2 reduction in yaw control power would reduce the reaction control bleed at the tail mounted reaction control nozzles by 4.8 lb/sec.

THRUST TRANSFER RATES

Ability to achieve adequate rates of thrust transfer between propulsion system components for pitch and roll control is an important aspect of control system dynamic response. Maximum thrust transfer rates observed for the different tasks in the simulation program are documented in this section. Results are presented both as maximum rate of change of thrust and, more generally, as the rate of change of pitch and roll angular acceleration. Implications for thrust control bandwidth are also noted.

Pitch Control

Effect of Flight Phase. Thrust transfer rates for pitch control are documented in Figure 6. During the transition (Fig. 6a), maneuvering control in calm air produces peak rates ranging from 0.2 to 1.3 kilopounds (klb)/sec for the attitude command SCAS. Maximum rates of 1.5–3.3 klb/sec are reached under the highest wind and turbulence condition. This maximum range exceeds that for 3–4σ values. Results are independent of SCAS mode. Runway vertical landings appear to be more demanding on maneuver control rates than the previous flight phase, but with no influence of SCAS mode (Fig. 6b). Peak rates ranging from 1 to 2.6 klb/sec are observed in the data. Turbulence has no influence on the rate of control use. The most significant control rates appear for the shipboard landings (Fig. 6c). Maximum rates of 3–4 klb/sec with attitude command and 3–6 klb/sec with longitudinal velocity command SCAS occur at the highest wind over deck.

To generalize these results, thrust transfer rates can be expressed in time rate of change of control power for this aircraft configuration, where 4 klb/sec is equivalent to 1 rad/sec^3. In turn, the maximum rate of change of control power can be used to define the relationship between peak control usage and the effective bandwidth of control that can be achieved without encountering the control rate limit. For example, a maximum thrust transfer rate of 2 klb/sec (corresponding to a rate of change of angular acceleration of 0.5 rad/sec^3) and a peak control usage of 0.05 rad/sec^2 (representative of 1σ level of control use for closed-loop regulation) would imply a rate limit free control bandwidth of 10 rad/sec. Conversely, for the same thrust transfer rate and a representative control bandwidth of 5 rad/sec, rate limit free operation could be sustained up to a control authority of 0.1 rad/sec^2.

Roll Control

Effect of Flight Phase. In Figure 7, the rates of thrust transfer employed for roll control are indicated for the different flight phases. Throughout the transition (Fig. 7a), typical maximum rates for maneuver control ranged from 1 to 2 klb/sec with the exception of two cases which demanded 4.5–6.5 klb/sec. In the heaviest turbulence, rates of 3–4 klb/sec occur frequently, with occasional peaks from 5 to 8 klb/sec. For roll control, a thrust transfer rate of 10 klb/sec is equivalent to 3 rad/sec^3.

Maneuver control rates for the runway vertical landing (Fig. 7b) generally ranged from 2 to 4 klb/sec. Turbulence did not affect control rates up to the magnitude of disturbances evaluated. For shipboard landings (Fig. 7c), peak rates of 7–8 klb/sec are observed for the attitude SCAS with significant wind over deck and represent a substantial increase over other phases of operation. With the attitude-plus-velocity SCAS, wind over deck has a strong influence on thrust transfer rates, with peaks of 10 klb/sec (3 rad/sec^3) reached on occasion for the highest wind over deck. In lighter winds, transfer rates are comparable for the two SCAS modes.

As an example for roll control, a maximum thrust transfer rate of 5 klb/sec (corresponding to a rate of change of angular acceleration of 1.5 rad/sec^3) and a peak control usage of 0.2 rad/sec^2 would imply a rate limit free control bandwidth of 7.5 rad/sec. For the same thrust transfer rate and a bandwidth of 5 rad/sec, a peak control authority of 0.3 rad/sec^2 could be achieved without reaching the control rate limit.

THRUST CONTROL

Influence of Ground Effect and Ingestion

Vertical axis control power in vertical flight is associated with the margin of thrust in excess of that required to equilibrate the aircraft's weight. The requirements for thrust margin during vertical landing are influenced by the disturbances imposed by jet-induced aerodynamic forces in proximity to the ground and degradation in engine thrust that results from temperature rise at the engine inlet due to the recirculation of hot gas exhaust from the propulsion system. Experiments have been conducted on the VMS to evaluate in general the influence of ground effect and hot gas ingestion on thrust margin necessary to control height and sink rate during airfield vertical landings (Ref. 2). In turn, these results were validated with specific simulation assessments of vertical landings with the YAV-8B Harrier, an aircraft whose vertical landing characteristics are well known and have been related to the simulation experience. Results from these simulations are presented in Figure 8. The boundaries shown define acceptable and unacceptable regions for combinations of mean ground effect and ingestion and thrust/weight ratio. One boundary was extracted from the generalized evaluations reported in Reference 2. Data from the YAV-8B ground effect evaluation are also presented with an appropriate fairing to illustrate the trend. The YAV-8B data correspond to configurations with and without lift improvement devices (LIDS) and for two levels of hot gas ingestion, and span the range of mean ground effect covered in the previous generalized investigations. Thrust/weight ratio is determined out-of-ground effect. Mean ground effect and ingestion are defined here by the relationship

$$\frac{1}{43}\int_0^{43} (\Delta L/T)'dh$$

where $(\Delta L/T)'$ incorporates jet induced aerodynamic ground effect as well as thrust variations with inlet temperature and is defined as

$$(\Delta L/T)' = \{[1 + \Delta L/T][1 + (\Delta F_G/\Delta\theta)(\Delta\theta/W)] - 1\}$$

The altitude range over which the mean ground effect and ingestion are based is 43 ft and represents the range over which ground effect exists for the Harrier. For the earlier generalized ground effect simulation, the integral defining mean ground effect was based on an altitude range of 15 ft, where ground effect did not vary above that altitude. The mean ground effect that defined the boundary for that experiment (Ref. 2) was adjusted by the ratio 15:43 to bring it into conformity with the definition of mean ground effect used herein.

The shape of the boundaries is established by height control out-of-ground effect for positive ground effect, on abort capability at decision height for neutral to moderately negative ground effect and ingestion, and on control of sink rate and hover position to touchdown for larger negative ground effect. Results from simulation evaluation of the YAV-8B Harrier are somewhat less conservative than the boundary derived from the evaluation of generalized ground effect and are consistent with Harrier flight experience as described in the aircraft's operations manuals (Refs. 13 and 14). The boundary correlates over much of its range with an analytical prediction of the trend of thrust/weight with mean ground effect required to arrest a nominal sink rate of 4 ft/sec prior to touchdown with an application of maximum thrust at an altitude of 21 ft. This analytical relationship is expressed as

$$\left(\dot{h}_i^2 - \dot{h}_o^2\right)/2g = \int_0^{43} (\Delta L/T)'dh + \int_0^{h_i} (\Delta T/W)dh$$

and can be used in synthesis of new STOVL designs to determine the required thrust margin for anticipated levels of mean ground effect and ingestion. Finally, based on the results of Reference 2, it was noted that the employment of a vertical velocity command control did not shift the boundary shown in Figure 8, which was obtained for attitude SCAS alone. However, as noted in Reference 2, vertical velocity command does reduce the chance for abuse of sink rate control during the descent to landing and, hence, improves the control margin for vertical landing.

Influence of Engine Dynamics

Effects of thrust response dynamics on the pilot's assessment of control of the vertical landing are shown in Figure 9. These data come from Reference 2 and apply to manual control of thrust with only attitude SCAS available. It is apparent that bandwidth of thrust response of the engine core of 4–5 rad/sec is sufficient to achieve satisfactory ratings for height and sink rate control. For bandwidths below 3 rad/sec, the control task deteriorates rapidly. Both the transition and hover point acquisition tasks were less sensitive to variations in thrust control bandwidth than was the vertical landing (Ref. 2). Vertical velocity command in addition to attitude SCAS insulates the pilot from the dynamics of the propulsion system response and results in toleration of slower engine

response (providing the overall airframe response is not altered) than for attitude SCAS alone.

To a point, the vertical landing is insensitive to maximum rate of change of core thrust, which is associated with engine acceleration limits imposed by maximum allowable temperatures in the core. Thrust rates varying from 25% of maximum thrust/sec down to nearly 10%/sec were tolerable for height control. However, at about 10%/sec, thrust rate limiting and loss of control were encountered on occasion for such slow acceleration characteristics. These acceleration rate limits can be related to surge margin in design of the propulsion system control. Deceleration rate limits are important to the ability to rapidly reduce thrust at touchdown, as well as to the dynamic control of vertical velocity in the hover. Vertical velocity command does not seem to alter these results.

CONCLUSIONS

A program has been conducted to define and experimentally evaluate control system concepts for STOVL fighter aircraft in powered-lift flight. The control system designs have been evaluated in Ames Research Center's Vertical Motion Simulator. Items assessed in the program were maximum control power, control system dynamic response associated with thrust transfer for attitude control, thrust margin in the presence of ground effect and hot gas ingestion, and dynamic thrust response for the engine core. Results provide the basis for a reassessment of existing flying qualities design criteria for this class of aircraft.

This experience shows that pitch control power used in transition is in general accord with existing criteria, whereas that used for vertical landing is somewhat lower. When a translational velocity command system using deflected thrust for longitudinal force control is employed, pitch control use is considerably less than the criteria suggest. No criteria, except that for hover, exist for shipboard recovery.

In the roll axis, control power recommended by current design criteria is insufficient to cover demands for transition. Agreement is good with criteria for vertical landing. Again, no criteria are available for shipboard operations. For these operations, lateral velocity command through bank angle control typically used greater control power than did an attitude command system alone.

For the transition and vertical landing, the existing criteria all exceed the current experience for yaw control use. As before, shipboard operations are not covered by the existing criteria.

Thrust transfer rates for pitch and roll control were observed to be greatest for shipboard operations, with the decelerating transition placing the next greatest demand. Control mode did not have a strong influence on these results.

Thrust margins for vertical landing in the presence of ground effect and hot gas ingestion were defined based on results from simulation of the YAV-8B Harrier. The shape of the boundaries is established by height control out-of-ground effect for positive ground effect, on abort capability at decision height for neutral to moderately negative ground effect and ingestion, and on control of sink rate and hover position to touchdown for larger negative ground effect. The boundary correlates with an analytical prediction of the trend of thrust/weight with mean ground effect required to arrest a nominal sink rate with an application of maximum thrust at decision height. The employment of a vertical velocity command control does not alter the thrust margin requirement.

Bandwidth of thrust response of the engine core of 4–5 rad/sec is sufficient to achieve satisfactory ratings for height and sink rate control. For bandwidths below 3 rad/sec, the control task deteriorates rapidly. Vertical velocity command systems can tolerate somewhat slower engine response (providing the overall airframe response is not altered) than can be accepted by the pilot for manual control of thrust. To a point, the vertical landing is insensitive to maximum rate of change of core thrust; however, loss of control appears at the lowest thrust transfer rates. Vertical velocity command does not seem to alter these results.

REFERENCES

1. Levine, J. and Inglis, M., "US/UK Advanced Short Takeoff and Vertical Landing Program," AIAA Paper 89-2039, July 1989.

2. Franklin, J. A., Stortz, M. W., Engelland, S. A., Hardy, G. H., and Martin, J. L., "Moving Base Simulation Evaluation of Control System Concepts and Design Criteria for STOVL Aircraft," NASA TM-103843, June 1991.

3. Merrick, V. K., Farris, G. G., and Vanags, A. A., "A Head-Up Display Format for Application to V/STOL Approach and Landing," NASA TM-102262, Sept. 1989.

4. Chalk, C. R., Key, D. L., Kroll, J. Jr., Wasserman, R., and Radford, R. C., "Background Information and User Guide for MIL-F-83300 – Military Specifications – Flying Qualities for Piloted V/STOL Aircraft," AFFDL-TR-70-88, Nov. 1971.

5. "V/STOL Handling, I – Criteria and Discussion," AGARD R-577-70, Dec. 1970.

6. Innis, R. C., Holzhauser, C. A., and Quigley, H. C., "Airworthiness Considerations for STOL Aircraft," NASA TN D-5594, Jan. 1970.

7 Anon., "AV-8B Aircraft Stability, Control and Flying Qualities," McDonnell Douglas Corporation Report MDC A5192, Aug. 1981.

8. Lacey, T. R., "MIL-F-83300, View from an Aircraft Designer," Proceedings of the Navy/NASA VSTOL Flying Qualities Workshop, April 1977.

9. Fortenbaugh, R., Hutchins, D., Miller, D., Schweinfurth, R., Traskos, R., and Tumilowicz, R.,"USN/FMOD FRG VAK-191B Joint Flight Test Program – Stability and Control," Final Report, Vol. 4, NAVAIR-4R-76, Aug. 1976.

10. Franklin, J. A., Stortz, M. W., Gerdes, R. M., Hardy, G. H., Martin, J. L., and Engelland, S. A., "Simulation Evaluation of Transition and Hover Flying Qualities of the E-7A STOVL Aircraft," NASA TM-101015, Aug. 1988.

11. Fortenbaugh, R. L., "Mathematical Models for the Aircraft Operational Environment of DD-963 Class Ships," Vought Corp. Rep. 2-55800/8R-3500, Sept. 1978.

12. Hange, C. and Gelhausen, P., "An Investigation Into Sizing the Reaction Control System in Conceptual STOVL Aircraft," NASA TM-103990, 1993.

13. Anon., "NATOPS Flight Manual Navy Model AV-8B," A1-AV8B-NFM-000, Dec. 1984.

14. Anon., "NATOPS Flight Manual Navy Model AV-8A and TAV-8A," NAVAIR 01-AV8A-1, June 1978.

Table 1. Flight Control Modes

	Transition		Hover	
Control axis	Attitude SCAS	Flightpath SCAS	Attitude SCAS	Velocity SCAS
Pitch/roll	Rate command-attitude hold	Rate command-attitude hold	Attitude command-attitude hold	Attitude command-attitude hold
Yaw	Turn coordination	Turn coordination	Yaw rate command	Yaw rate command
Vertical	Thrust magnitude	Flightpath command	Thrust magnitude	Velocity command
Longitudinal	Thrust deflection	Acceleration command-velocity hold	Thrust deflection	Velocity command
Lateral				Velocity command

Table 2. Comparison of Pitch Control Power Criteria with STOVL Aircraft Designs

Flight phase	MIL-F 83300 Ref. 4	AGARD R-577 Ref. 5	NASA TN 5594 Ref. 6	AV-8B Ref. 7	AV-8A Ref. 8	VAK-191 Ref. 9	Recent STOVL Concepts MFVT Maneuver	MFVT Turb6	E-7A (Ref. 10) Maneuver	E-7A (Ref. 10) Turb6
Transition		0.05–0.2	0.5				0.15–0.19	0.2–0.25	0.6	0.6
Vertical landing	0.29	0.1–0.3		0.53 –0.83	0.8 –0.75	1.0	0.16–0.27 0.17	0.16–0.27 (AC) 0.17 (VC)		
							WOD 15	WOD 46	WOD 15	WOD 34
Shipboard landing				0.53 –0.83	0.8 –0.75		0.31 0.22	0.37 0.22 (VC)	0.3	0.4

Notes: (1) All values expressed in terms of control power in rad/sec^2.
(2) Reference 7 and 9 requirements converted from attitude response based on a time constant of 0.5 sec for rate command systems or a natural frequency of 2 rad/sec for a critically damped attitude command system.
(3) Control power for actual aircraft represent total available in hover; transition values not available.
(4) Control power for MFVT and E-7A represent maximum used.

Table 3. Comparison of Roll Control Power Criteria with STOVL Aircraft Designs

Flight phase	MIL-F 83300 Ref. 4	AGARD R-577 Ref. 5	NASA TN 5594 Ref. 6	AV-8B Ref. 7	AV-8A Ref. 8	VAK-191 Ref. 9	Recent STOVL Concepts MFVT Maneuver	MFVT Turb6	E-7A (Ref. 10) Maneuver	E-7A (Ref. 10) Turb6
Transition		0.1–0.6	0.55				0.3–0.4	0.9–1.2	0.25	0.6
Vertical landing	0.38	0.2–0.4		2.2	1.73	1.4	0.1–0.3	0.2–0.4		
							WOD 15	WOD 46	WOD 15	WOD 34
Shipboard landing				2.2	1.73		0.2–0.4	0.9–1.1 (AC) 1.3–2.0 (VC)	0.55	1.8

Notes: (1) All values expressed in terms of control power in rad/sec^2.
(2) Reference 7 and 9 requirements converted from attitude response based on a time constant of 0.5 sec for rate command systems or a natural frequency of 2 rad/sec for a critically damped attitude command system. .
(3) Control power for actual aircraft represent total available in hover; transition values not available.
(4) Control power for MFVT and E-7A represent maximum used.

Table 4. Comparison of Yaw Control Power Criteria with STOVL Aircraft Designs

Flight phase	MIL-F 83300 Ref. 4	AGARD R-577 Ref. 5	NASA TN 5594 Ref. 6	AV-8B Ref. 7	AV-8A Ref. 8	VAK-191 Ref. 9	Recent STOVL Concepts MFVT Maneuver	MFVT Turb6	E-7A (Ref. 10) Maneuver	E-7A (Ref. 10) Turb6
Transition		0.15–0.25	0.22				0.02–0.04	0.05–0.07	0.04	0.04
Vertical landing	0.28	0.1–0.5		0.43	0.46	0.4	0.15–0.065	0.1		
							WOD 15	WOD 46	WOD 15	WOD 34
Shipboard landing				0.43	0.46		0.065	0.1	0.05	0.12

Notes: (1) All values expressed in terms of control power in rad/sec^2.
(2) Reference 7 and 9 requirements converted from attitude response based on a time constant of 1 sec for rate command systems.
(3) Control power for actual aircraft represent total available in hover; transition values not available.
(4) Control power for MFVT and E-7A represent maximum used.

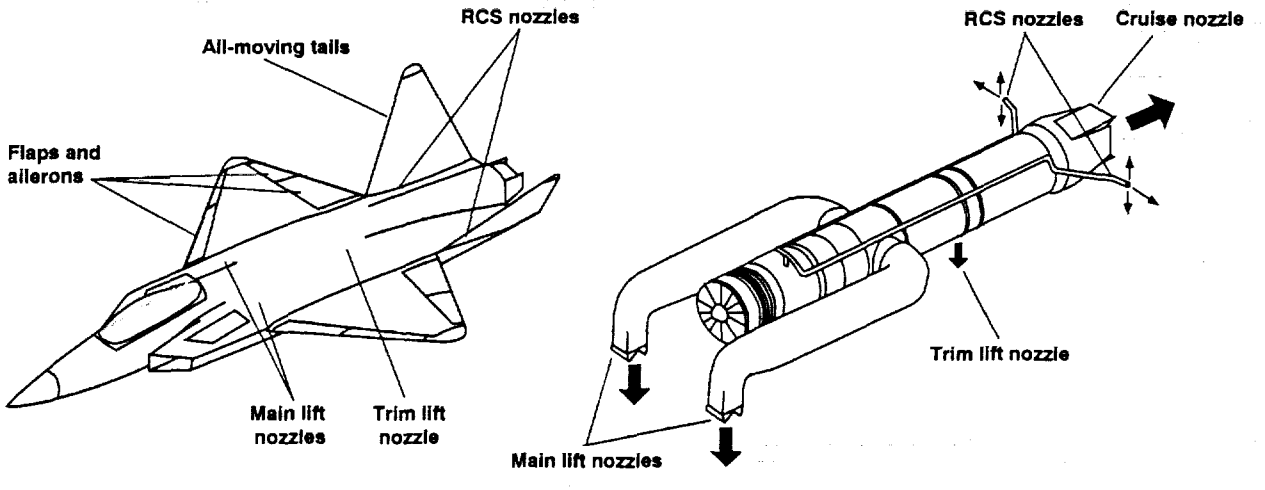

Figure 1. Mixed-Flow Remote Lift STOVL Aircraft

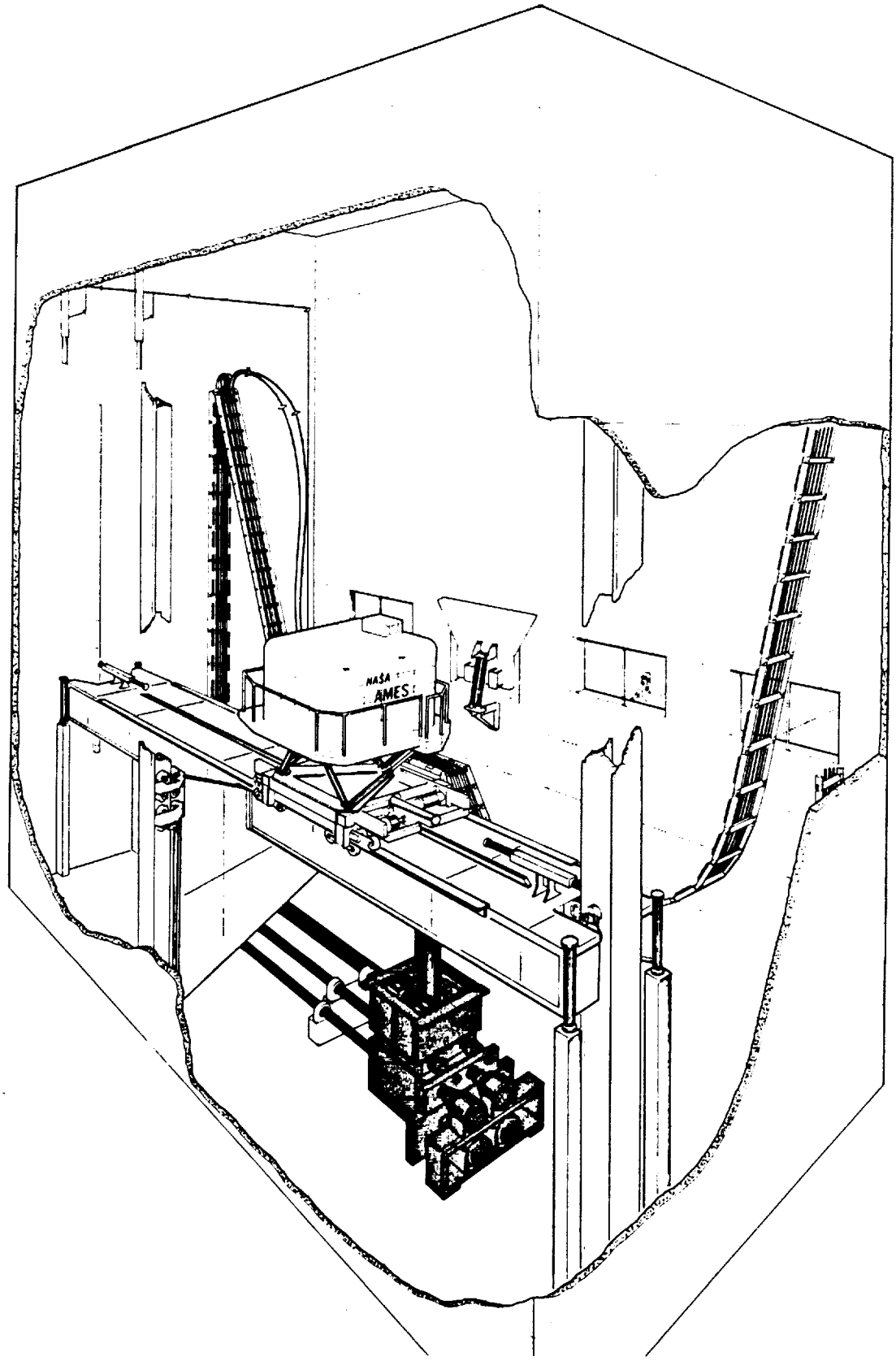

Figure 2. Vertical Motion Simulator

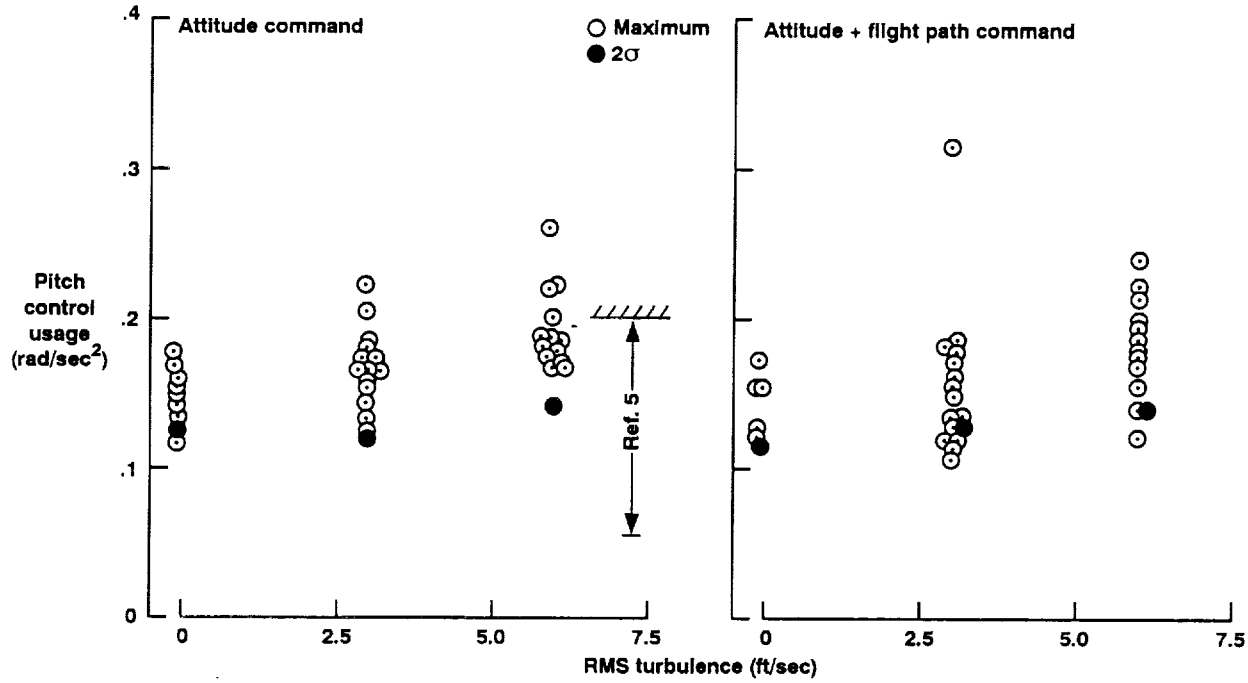

(a) Transition

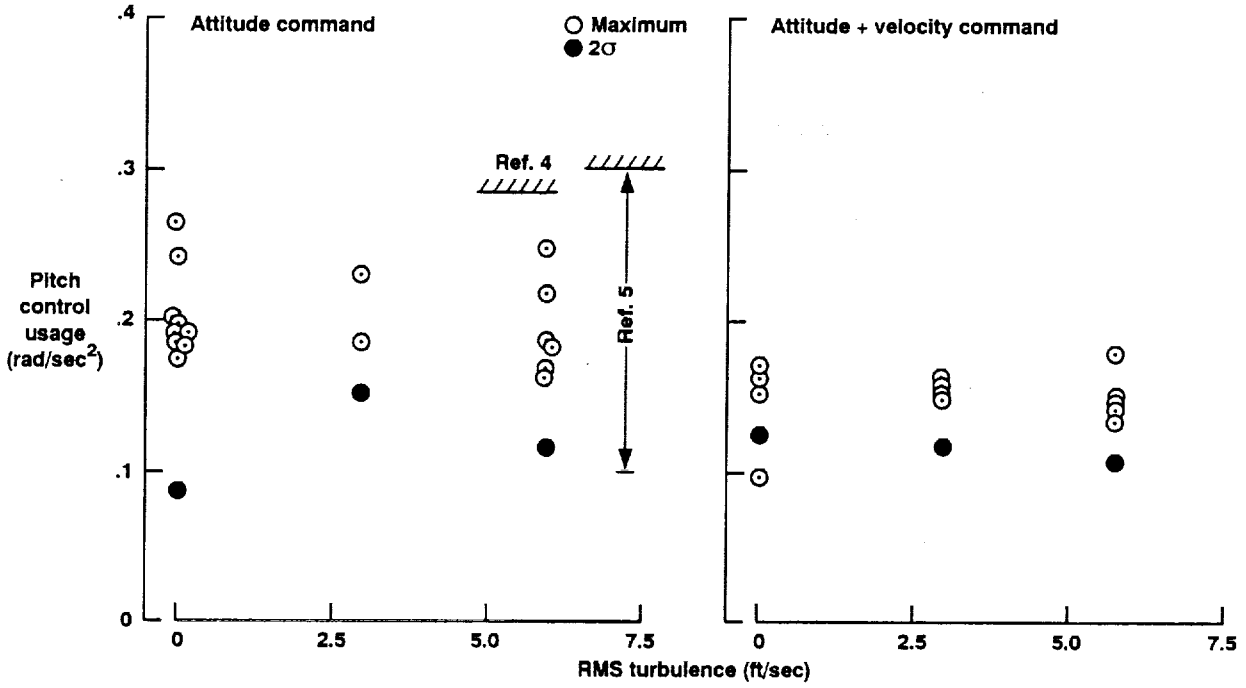

(b) Vertical Landing

Figure 3. Influence of SCAS Configuration and Wind Environment on Pitch Control Use.

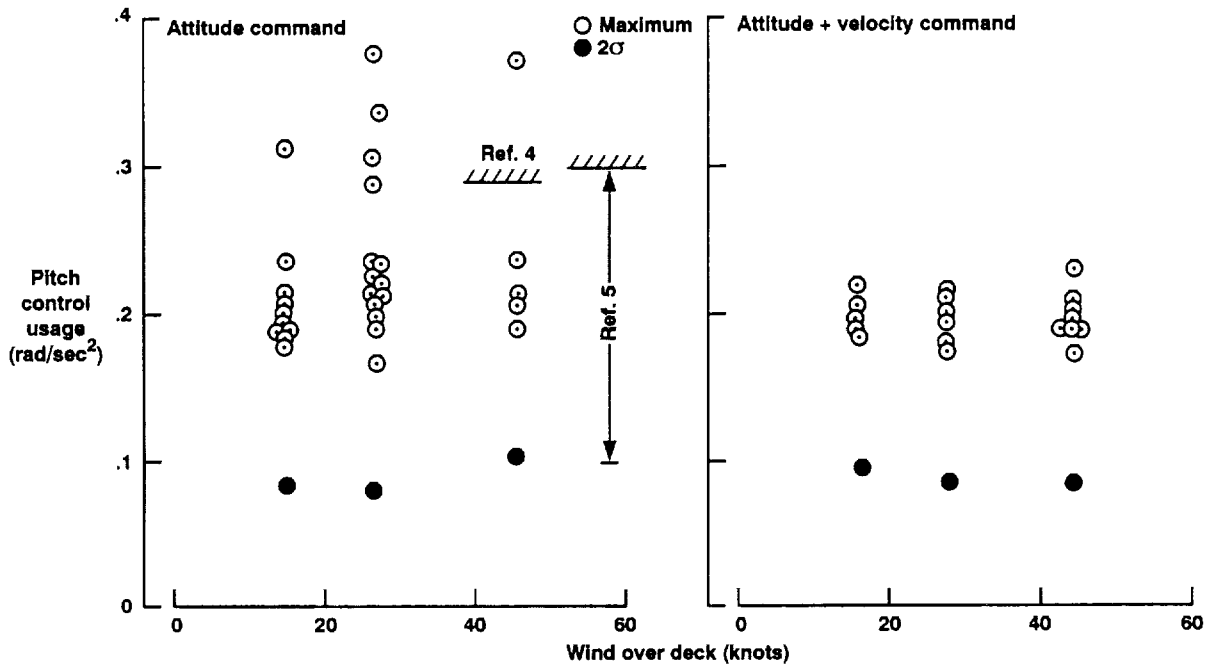

(c) Shipboard Landing

Figure 3. Concluded.

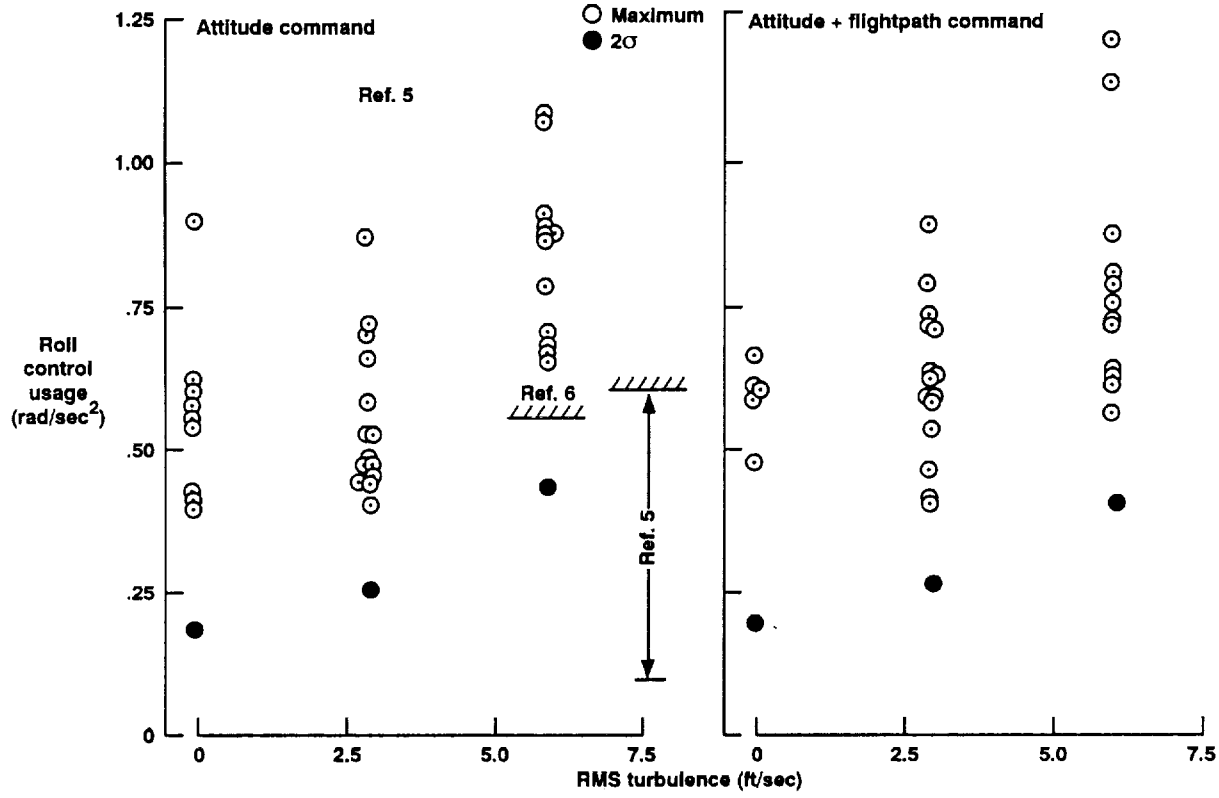

(a) Transition

Figure 4. Influence of SCAS Configuration and Wind Environment on Roll Control Use.

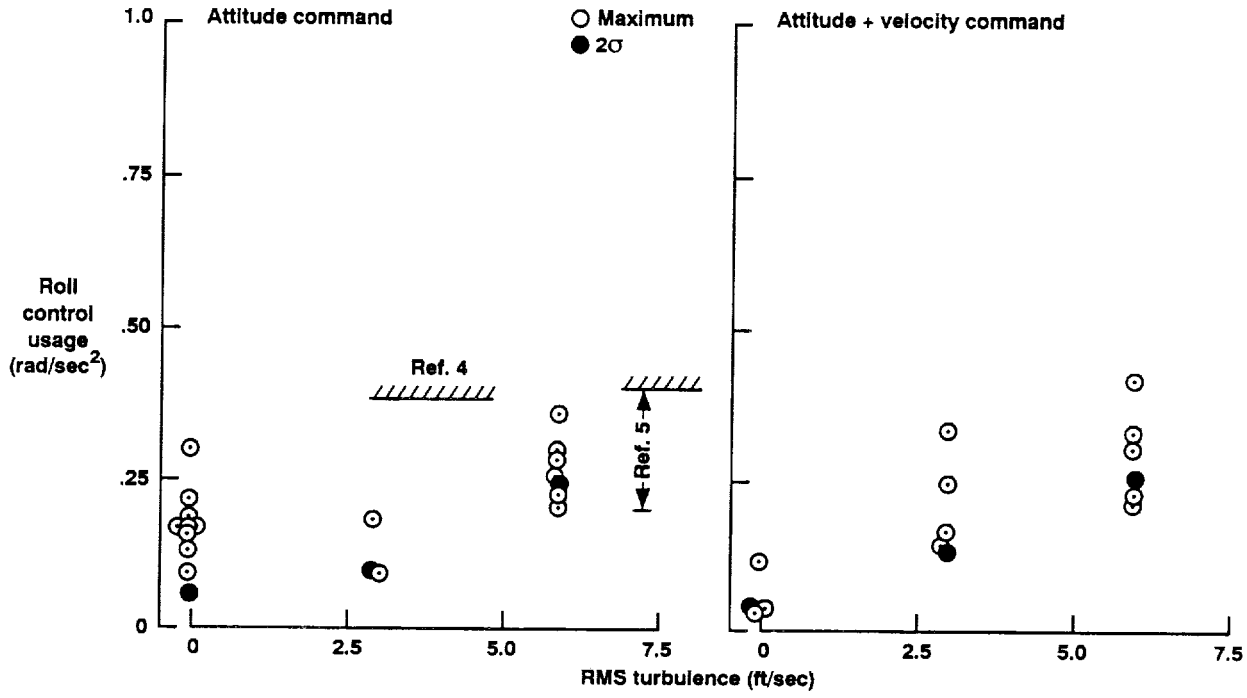

(b) Vertical Landing

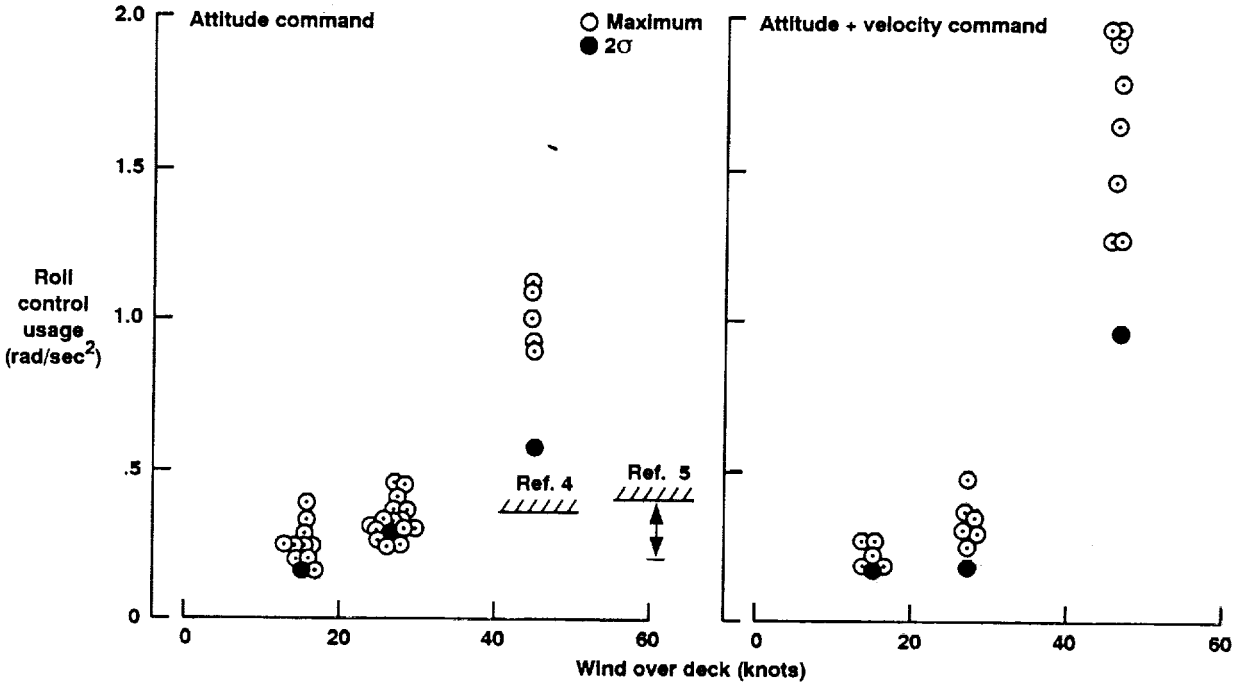

(c) Shipboard Landing

Figure 4. Concluded.

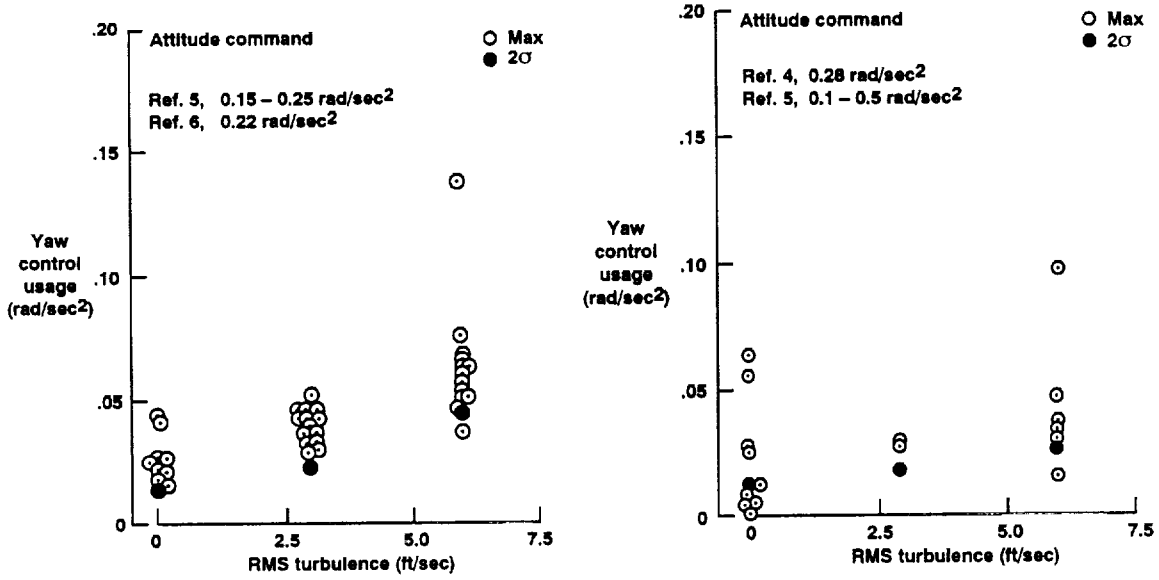

(a) Transition

(b) Vertical Landing

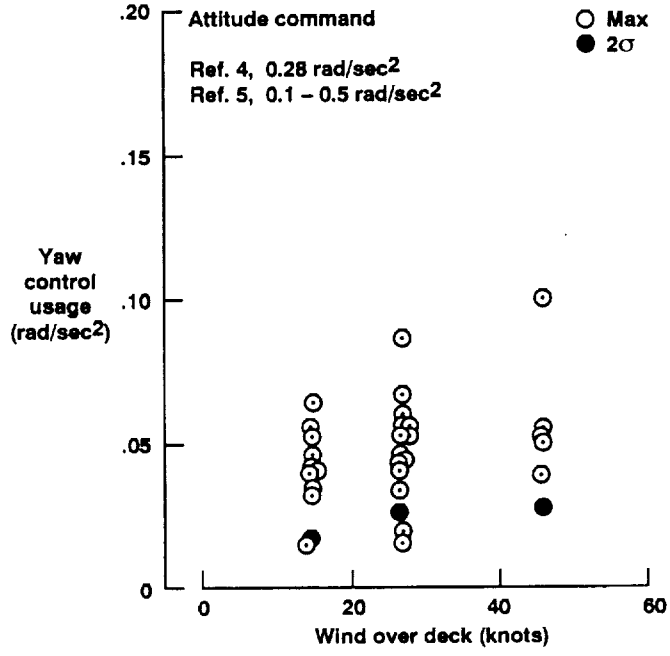

(c) Shipboard Landing

Figure 5. Influence of Wind Environment on Yaw Control Use.

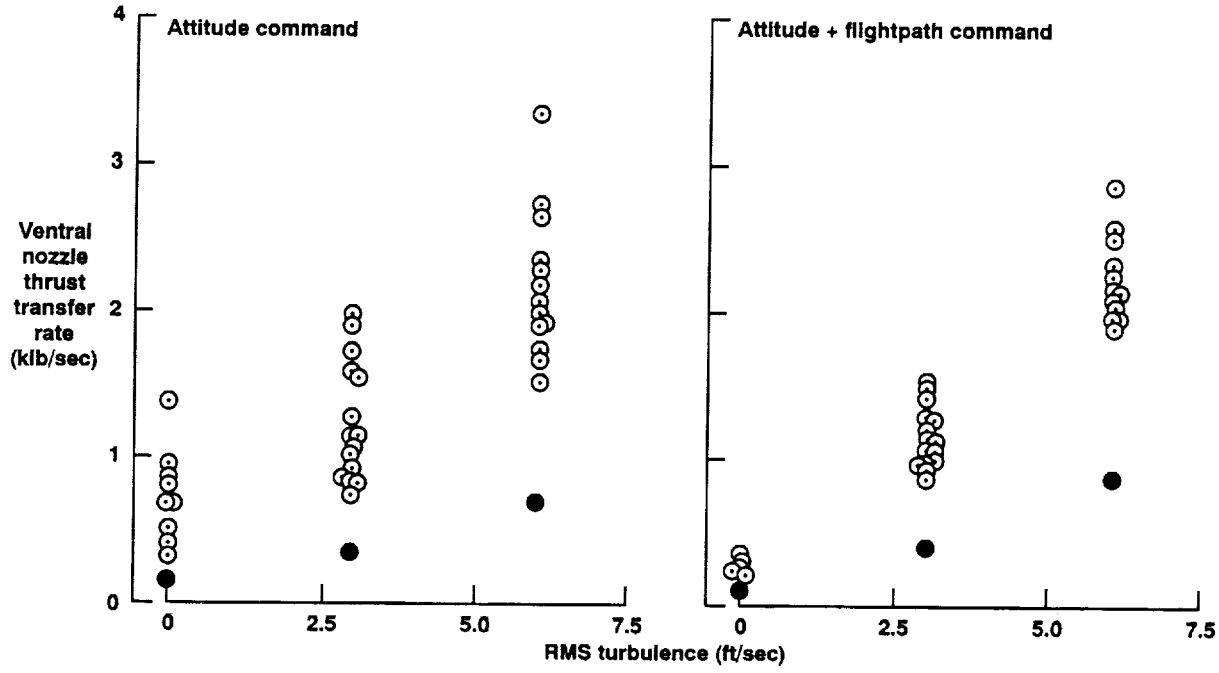

(a) Transition

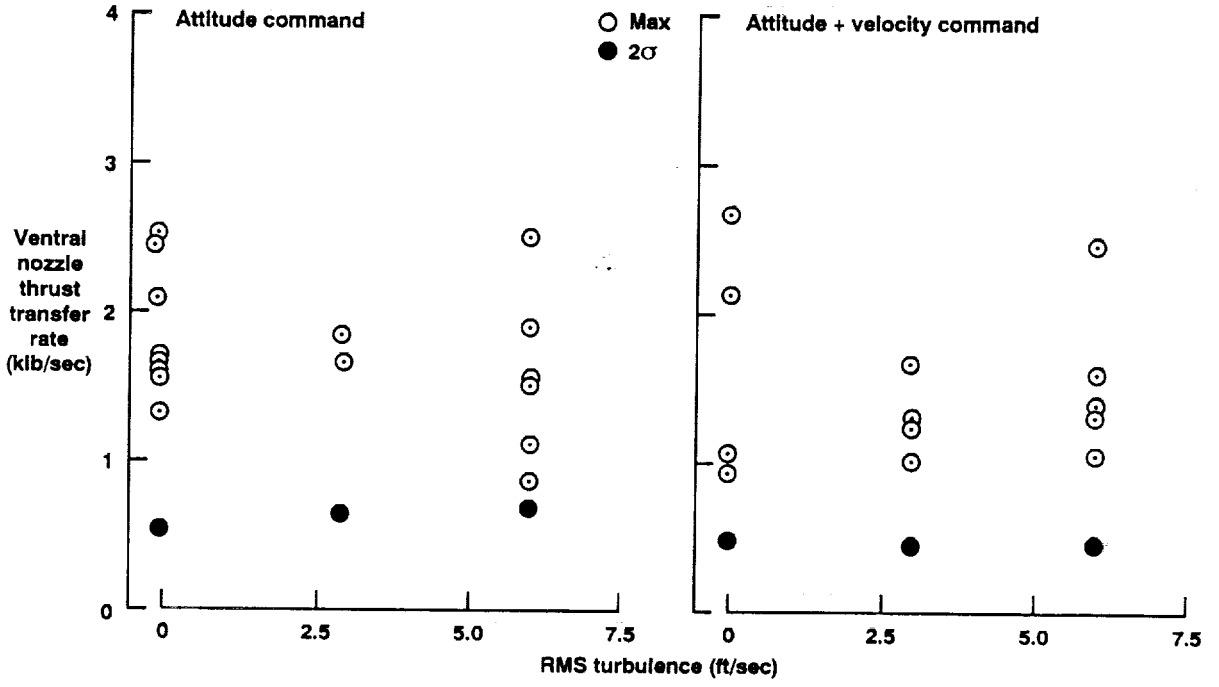

(b) Vertical Landing

Figure 6. Influence of SCAS Configuration and Wind Environment on Thrust Transfer Rate for Pitch Control.

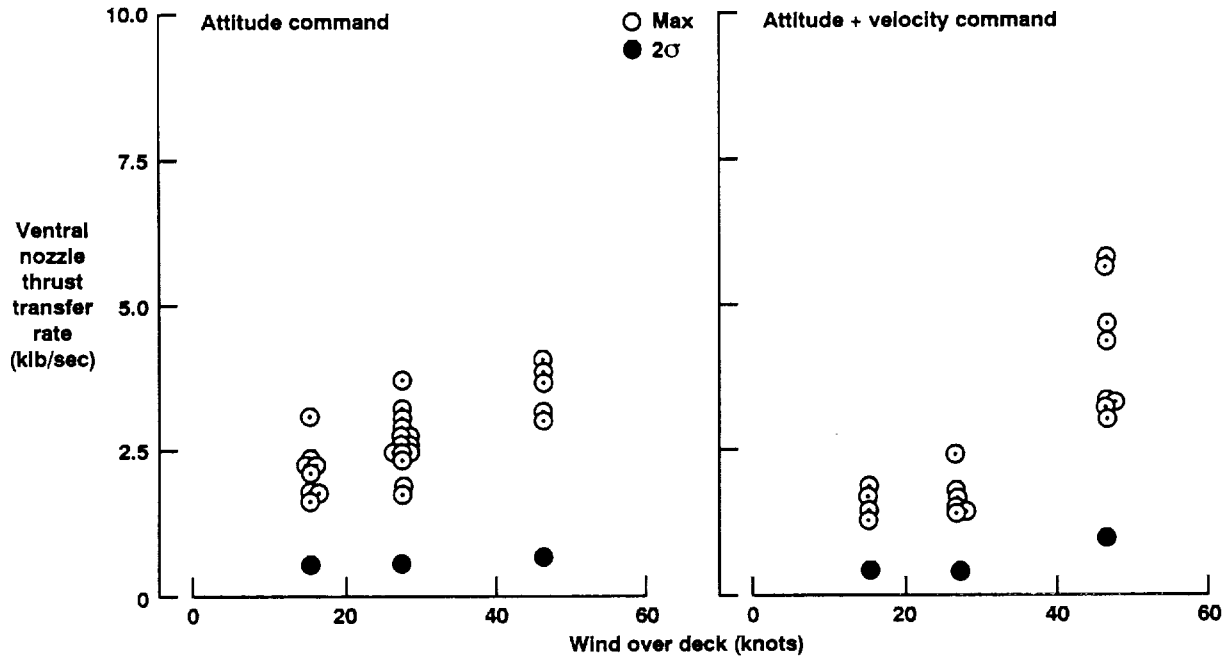

(c) Shipboard Landing

Figure 6. Concluded.

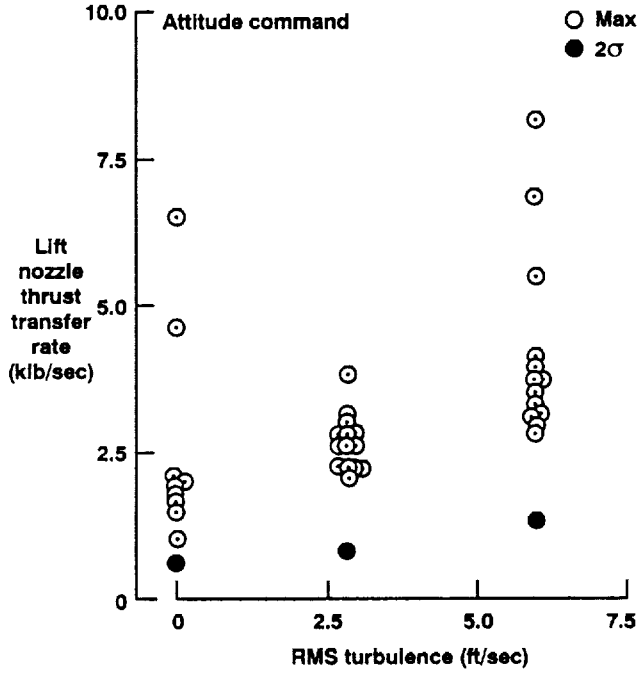

(a) Transition

Figure 7. Influence of SCAS Configuration and Wind Environment on Thrust Transfer Rates for Roll Control.

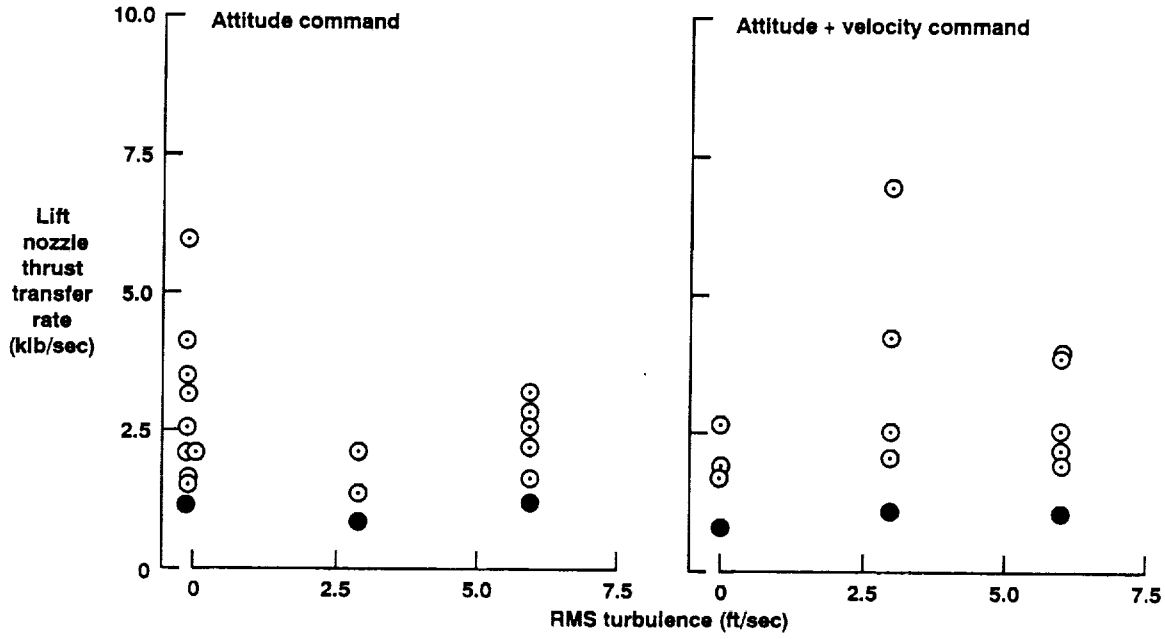

(b) Vertical Landing

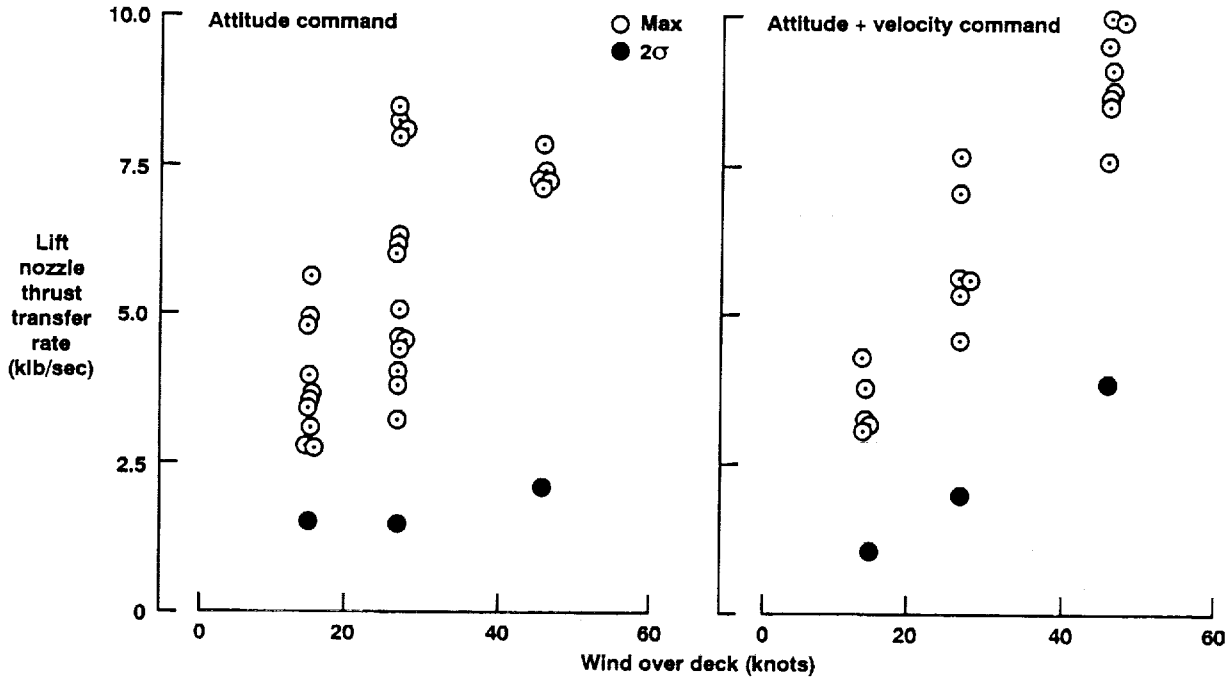

(c) Shipboard Landing

Figure 7. Concluded.

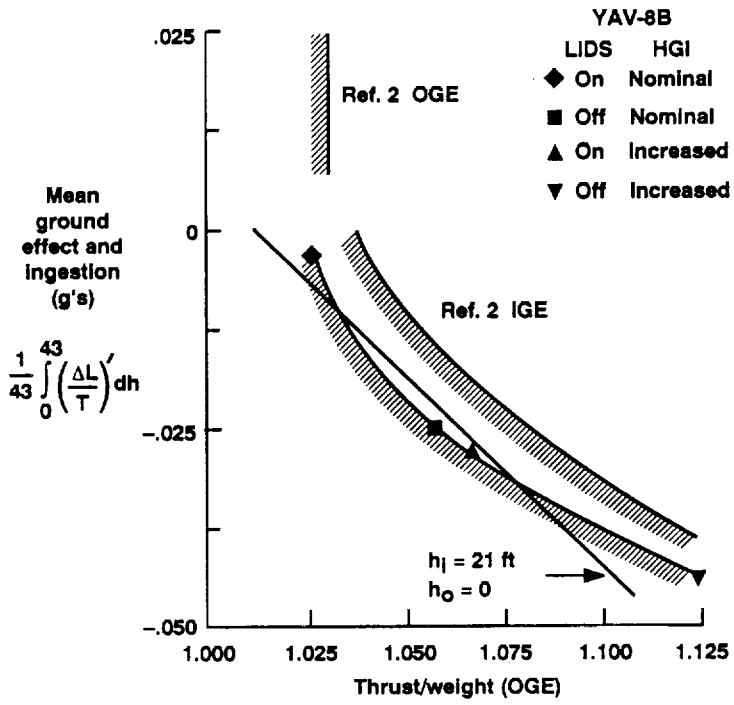

Figure 8. Influence of Ground Effect and Hot Gas Ingestion on Thrust Margin for Vertical Landing

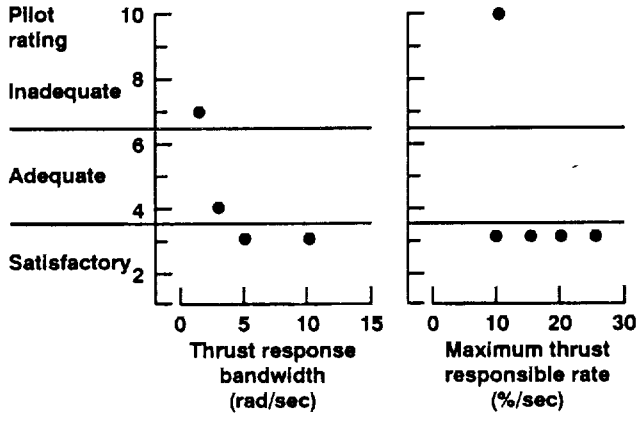

Figure 9. Effect of Thrust Response Bandwidth and Response Rate on Control of Vertical Landing

A PERSPECTIVE ON THE FAA APPROVAL PROCESS: INTEGRATING ROTORCRAFT DISPLAYS, CONTROLS AND WORKLOAD

David L. Green
President
Starmark Corporation
Arlington, Virginia

Jake Hart
Director, Flight Operations & Standardization
American Eurocopter Corporation
Grand Prairie, Texas

Peter Hwoschinsky
Technical Manager, Vertical Flight Program Office
Federal Administration Agency
Washington, D.C.

ABSTRACT

The FAA is responsible for making the determination that a helicopter is safe for IFR operations in the National Airspace System (NAS). This involves objective and subjective evaluations of cockpit displays, flying qualities, procedures and human factors as they affect performance and workload. After all of the objective evaluations are completed, and all Federal Regulations have been met, FAA pilots make the final subjective judgement as to suitability for use by civil pilots in the NAS. The paper uses the flying qualities and pilot workload characteristics of a small helicopter to help examine the FAA pilot's involvement in this process. The result highlights the strengths of the process and its importance to the approval of new aircraft and equipments for civil IFR helicopter applications. The paper also identifies opportunities for improvement.

NOMENCLATURE

AFCS	Automatic Flight Control System
CAS	Calibrated Airspeed
c.g.	Center of Gravity
FAR	Federal Aviation Regulations
IFR	Instrument Flight Rules
IMC	Instrument Meteorological Conditions
MCP	Maximum Continuous Power
NAS	National Airspace System
OEI	One Engine Inoperative
PRs	Pilot Ratings
T&E	Test and Evaluation
VFR	Visual Flight Rules
VMC	Visual Meteorological Conditions
V_{MINI}	Instrument Flight Mininum Speed
V_{NE}	Never Exceed Speed
V_{NEI}	Instrument Flight Never Exceed Speed
V_Y	Climb Speed
V_{YI}	Instrument Climb Speed

Presented at Piloting Vertical Flight Aircraft:
A Conference on Flying Qualities and Human Factors,
San Francisco, California, 1993

INTRODUCTION

The engineering and operational criteria contained within the Federal Aviation Regulations (FARs) have evolved as the result of operational experience and flight research. Yet these regulations alone can not absolutely guarantee the suitability of an aircraft, principally because the quantitative criteria do not address the integrated aircraft system. So as the final check, FAA pilots are assigned to fly the aircraft and make a determination as to the suitability of the total system.

More than any other measures, suitability is determined by gauging the performance which is achieved in return for the spectrum of workload required to achieve this performance. In short, the workload that the pilot is required to accept must never exceed the capability of the minimum qualified pilot. In addition, the performance should never fall below an acceptable level during periods when the pilot is required to operate at the maximum tolerable workload.

The role of the FAA pilot during flight evaluations is similar to the role of the military T&E pilot. That is, while a civil helicopter may meet all of the FARs (References 1 and 2) for IFR flight (or meet Military specifications in the case of a military aircraft), the FAA pilot may find that the aggregate of performance and workload is not good enough to recommend the aircraft for approval. As a result, an unsatisfactory evaluation often includes a finding that the workload is too high.

It is also possible for both civil and military helicopters to fail to meet the demonstration requirements of the relevant specifications (FARs) yet still be found suitable for normal operations. This highlights the uncertainty of the preliminary design specification process. The manufacturer needs design guidance (criteria) but the Government can only provide its best estimate of what is required. It can only provide best estimate because: (1) technology and changing missions often change faster than the criteria can be updated, and (2) it is extremely difficult to predict the performance of the resultant system.

Finally, while the intent of the criteria or regulations is rarely in error, it is often difficult to demonstrate compliance of new automatic flight control systems (AFCS), workload relief equipment, and displays to existing objective criteria. In some cases, there are no objective criteria. In the case of helicopter approvals for civil use, Advisory Circulars 27-1 and 29-2 (References 3 and 4) recognize this situation and provide the applicant with the opportunity to use a variety of means to demonstrate compliance. Never-the-less, it is the FAA pilot team that determines the suitability of the aircraft for operations in the NAS. This is as it should be.

This paper focuses on the aggregate of workload and pilot-aircraft performance. It presents a joint perspective to examine the process which is used by the FAA to insure that only safe aircraft are approved for operations in the National Airspace System (NAS). It explores the alternative approaches available to applicants and strives to increase the rotorcraft community's understanding of how the FAA defines adequacy, and how adequacy can be predicted by the applicant with confidence.

RELIABILITY

Before considering the impact of displays, flying qualities, control characteristics, and various workload relief equipment, one must appreciate the need for reliability of function. If the quality (or correctness) of a function is not sufficiently reliable, the FAA pilot will often evaluate the aircraft as though the function is never available.

Suffice it to say that if the helicopter incorporates a workload relief feature which is not extremely reliable (or does not include redundant elements), the FAA pilots will treat the feature as a "nice to have". Such "nice to have" features will not normally figure prominently in the determination of suitability for IFR operations in the National Airspace System (NAS).

The same constraints apply to displays. If the attitude display and its power supply are not adequately reliable, a standby display is required to insure the availability of an attitude display under the most adverse failure mode condition. In such a case, the standby attitude indicator will often be evaluated as the primary attitude reference during evaluation of cockpit management workload and flying qualities.

FAILURE MODES

The failure modes of components of the total system are also extremely important. The transient condition associated with the introduction of a failure must not introduce an "upset" condition which will require unusual pilot skill to avoid a dangerous situation during the period subsequent to the failure.

The multi-layered systems available in the more expensive aircraft generally exhibit fail-operate or fail-passive characteristics (sometimes accompanied by a modest but very acceptable degradation in capability). Smaller, less expensive aircraft are typically less able to afford the same degree of redundancy and the transient introduced by a flight control or related sub-system failure can be very significant to the suitability of the aircraft in the eyes of the FAA evaluation pilot.

THE MINIMUM QUALIFIED PILOT

Unless otherwise stipulated by the applicant, FAA pilots must evaluate the suitability of a helicopter for IFR operations based upon their personal perception of the capabilities of the least qualified pilot that can legally be expected to fly the aircraft. This recognizes the fact that FAA approves pilots with as little as 150 hours of first pilot time in helicopters and airplanes. That is, the "worst case crew" could involve one or two pilots with these minimal qualifications. This suggests that every helicopter approved for instrument flight must be suitable for operation by a pilot with immature piloting skills and an under developed appreciation for the potential hazards of instrument flight in the NAS.

PILOT TECHNIQUE AND PROCEDURES

The FAA recognizes that tandem helicopters and single rotor helicopters do not fly alike, nor will a 3000 pound and a 30,000 pound helicopter fly alike. The FAA's evaluation pilots recognize that these configuration and size differences dictate unique operating procedures and techniques. The addition of series and parallel automatic flight control systems can also dictate configuration unique procedures and piloting techniques. These equipment and related techniques may make the direct comparison of an aircraft to the objective requirements of the FARs difficult if not irrelevant. The installation of a sidearm control stick is a case in point.

Regardless of the configuration, the evaluation pilots understand the intent of all of these requirements and they understand that they have a responsibility to evaluate existing flight control characteristics against the intent of the requirements, as explained in Advisory Circulars 27-1 and 29-2A. As noted earlier, this means that some issues are resolved during the inflight determination of the overall suitability.

While the FAA pilot has a responsibility to understand the techniques developed by the applicant, the evaluation pilot(s) may not find all of the procedures acceptable. Some may be found to be too difficult and require special training or a periodic demonstration of proficiency, or both to obtain approval for operations in the NAS. The applicant has the option either to accept such findings or to alter the aircraft in ways which improve the aircraft and eliminate the need for special skills.

EVALUATION ENVIRONMENT

Implied in any FAA evaluation of a helicopter for IFR operations is the need to evaluate the aircraft in an adverse environment. An extensive evaluation in a variety of adverse environments is most likely to be

conducted if: (1) the margin of suitability is perceived to be small, or (2) innovative control techniques or equipments are incorporated which introduce uncertainties because of the lack of precedent or the lack of hands on experience on the part of the FAA pilot(s).
In the case of an IFR application, the FAA pilot is likely to include an evaluation flight in a building cumulus cloud formation and, or a night flight profile in frontal weather. If this is not a practical choice, other evaluation tasks are executed to build an understanding of the aircraft which is sufficient to accurately predict its suitability in bad weather. The duration of flights in adverse weather is also important to the determination of suitability. The evaluation pilot must deal with the workload for an appropriate period to be able to answer the question: does a pilot at the controls need either a co-pilot or a highly reliable workload relief system to make it through the flight?

ONE PILOTS VS. TWO PILOT

The applicant must request approval of an aircraft with a crew of one or a crew of two.

SINGLE PILOT FLYING QUALITIES

A helicopter is said to exhibit single pilot flying qualities, when one pilot is able to fly the aircraft for a period of time equal to the endurance of the aircraft without being relieved by a second pilot. Implicit in this definition, is the concomitant ability of the pilot to accomplish essential non-piloting, cockpit management duties such as communication, navigation and typical emergencies.

AUTO PILOT VS. CO-PILOT

If an auto pilot is employed, the pilot is free to perform the co-pilot's duties. This is an acceptable alternative if the auto pilot never fails, but what if it does fail? If the auto pilot fails, the flying qualities and the non-flying workload must be managed by one pilot.... on a bad night.

DUAL PILOT FLYING QUALITIES

A helicopter is said to exhibit dual pilot flying qualities, when the pilot in command is unable to fly the entire flight (for a period equal to the endurance of the aircraft) without being relieved from time to time by a second pilot. The pilot who is not at the controls normally handles the cockpit duties attendant to the flight. This includes tasks which the pilot at the controls does not desire to perform or can not perform.

WORKLOAD

Workload during instrument flight is the result of one or a combination of the following: (1) task complexity including the cockpit management tasks and the control required to accomplish the maneuvers which in turn produce the desired flight trajectory, (2) residual flight path errors and the time dependent growth of these errors due to the control and flying qualities characteristics of the aircraft (including the AFCS), (3) the volume and quality of the flight instrumentation situational awareness displays. The display equipment either facilitates the control of the aircraft (and aids the pilot in efforts to eliminate errors), or the displays are inadequate; degrading situational awareness and, or frustrating the pilot's efforts to trim, suppress gust responses, and accomplish a variety of compensatory control inputs, and (4) the pilot's experience and familiarity with similar equipment, vehicle responses, and environmental conditions, as well as proficiency in any given situation.

EXCESSIVE WORKLOAD

When a single pilot can fly the aircraft for the duration of the flight without relief, but can not accomplish all of the cockpit management duties in a timely fashion, the aircraft is exhibiting an excessive workload characteristic. When an excessive workload situation exists, the flying qualities can be improved to make more time available to accomplish cockpit management duties, or the cockpit management workload can be decreased, or a combination of ameliorating changes can be incorporated. For example: (1) A crew of two can be substituted for the desired single pilot crew, or (2) An extremely reliable flying workload relief system (auto pilot) can be incorporated, or (3) The flying qualities of a helicopter can be augmented through electro-mechanical or electro-hydraulic means, or (4) The display system can be improved, or (5) Workload intensive equipment can be eliminated or replaced, or (6) The flight envelope of the aircraft can be tailored to include only that portion of the flight envelope which is suitable for the desired flight operations.

FLYING QUALITIES BOUNDARIES

Figure 1 provides a characterization of a hypothetical helicopter which has been evaluated for IFR flight using the Cooper Harper pilot rating scale. Such scales are not utilized by FAA pilots during the evaluation-approval-reporting process, but since all FAA pilots use the Cooper-Harper scale during research evaluations, it seems appropriate to use this scale here. Assume, for the sake of this discussion, that the pilot ratings in Figure 1 were developed as the result of conducting precision standard rate turns during level, climbing and descending flight. In addition, precision approaches were conducted at a number of airspeeds on each of the three glide slopes. Precision performance criteria was also established and observed in the normal way provided for in the associated literature (Reference 5).

This figure reflects the fact that there is a band of airspeed within which a helicopter will fly best (each helicopter has its own set of boundaries). It also illustrates the gradual degradation in flying qualities which occurs if the aircraft slows down, or if power is added and the aircraft climbs. Also note that the typical single rotor helicopter becomes easier to fly as the aircraft descends. But at some speed, an acceleration will also cause a degradation in flying qualities.

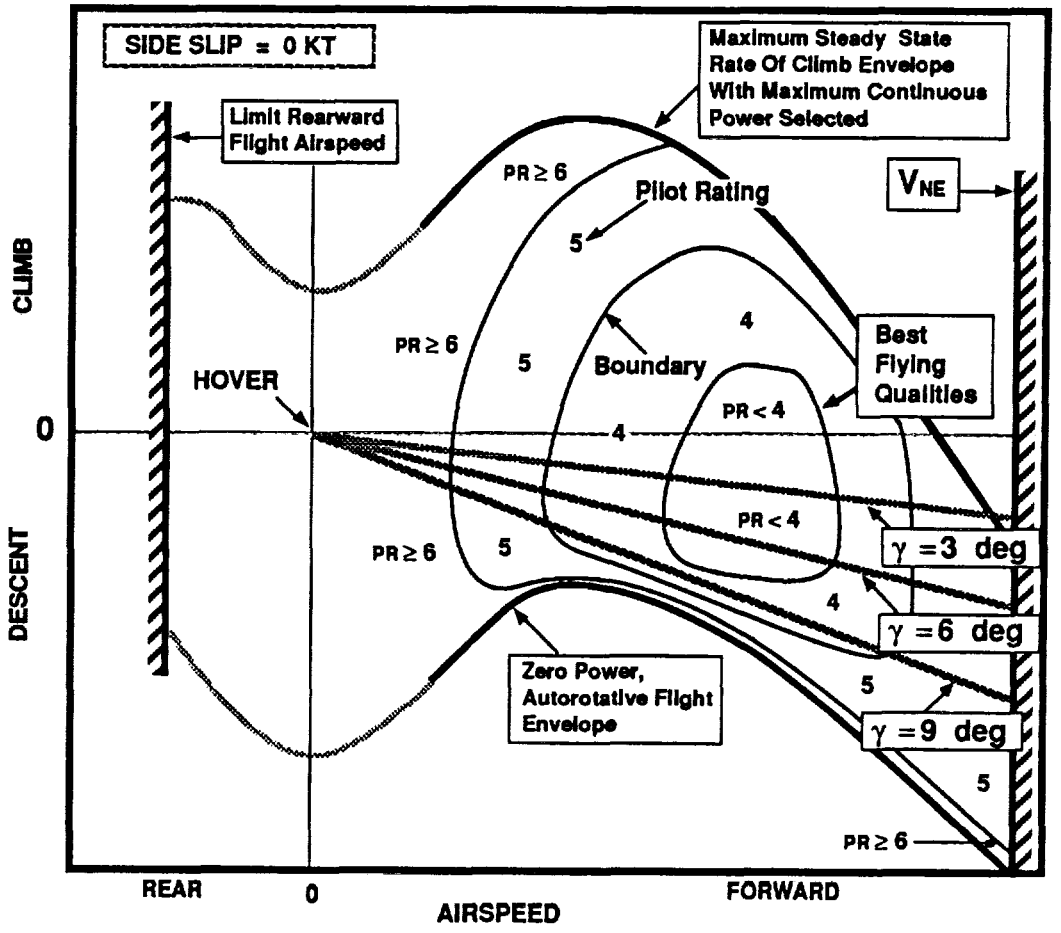

Figure 1: A Generalization of the Flying Qualities Of A Small Modern Unaugmented Helicopter Evaluated During Level Flight, Climbs, Descents and Precision Approaches Under Night IMC-IFR Conditions

It is important to realize that the pilot comments associated with a given pilot rating change as the flight conditions change from slow-level to slow-climb to fast-climb to fast-level to fast-descent to slow-descent. That is, while the rating of "5" may be assigned to many different flight conditions, the pilot's comments which explain the rating "5" may differ substantially throughout the envelope.

THE BASIC FLIGHT ENVELOPE

The flight evaluations conducted by the FAA are accomplished within the bounds of a proposed IFR envelope. The boundaries of this envelope coincide with, or fall within the boundaries of, the previously approved VFR envelope. The VFR envelope is determined by the performance capability of the aircraft and the limitations established due to structural considerations (component fatigue lives), stability and controllability (see boundaries in Figure 1).

All of today's civil IFR operations assume that pilots will utilize Visual Meteorological Conditions (VMC) to accelerate to some minimum airspeed which is approved for Instrument Meteorological Condition (IMC), before entering IMC. That is, the low speed end of the IFR approved flight envelope must support climbing, level and descending transitions into an IMC airmass during day and night operations. The minimum airspeed approved for instrument flight is referred to as V_{MINI}. This is an extremely important airspeed limit for it typically precludes helicopter unique IFR flight, constraining helicopter IFR operations to "airplane like" flight.

Typically, V_{MINI} is equal to or less than V_Y, the speed for best rate of climb. Alternately, an applicant can establish a best climb speed for instrument flight V_{YI} in which case V_{MINI} is equal to or less then V_{YI}.

In principle, V_{MINI} defines the speed above which the pilot will not encounter any troublesome non-linearity, dynamic instability, or strong adverse collective control coupling. These are characteristics that can cause the aircraft to become difficult or even unsafe to fly during IMC. For this reason, inadvertent flight substantially below V_{MINI} can be expected to require the pilot to concentrate on the retention of attitude control and flight path management to the exclusion of other tasks.

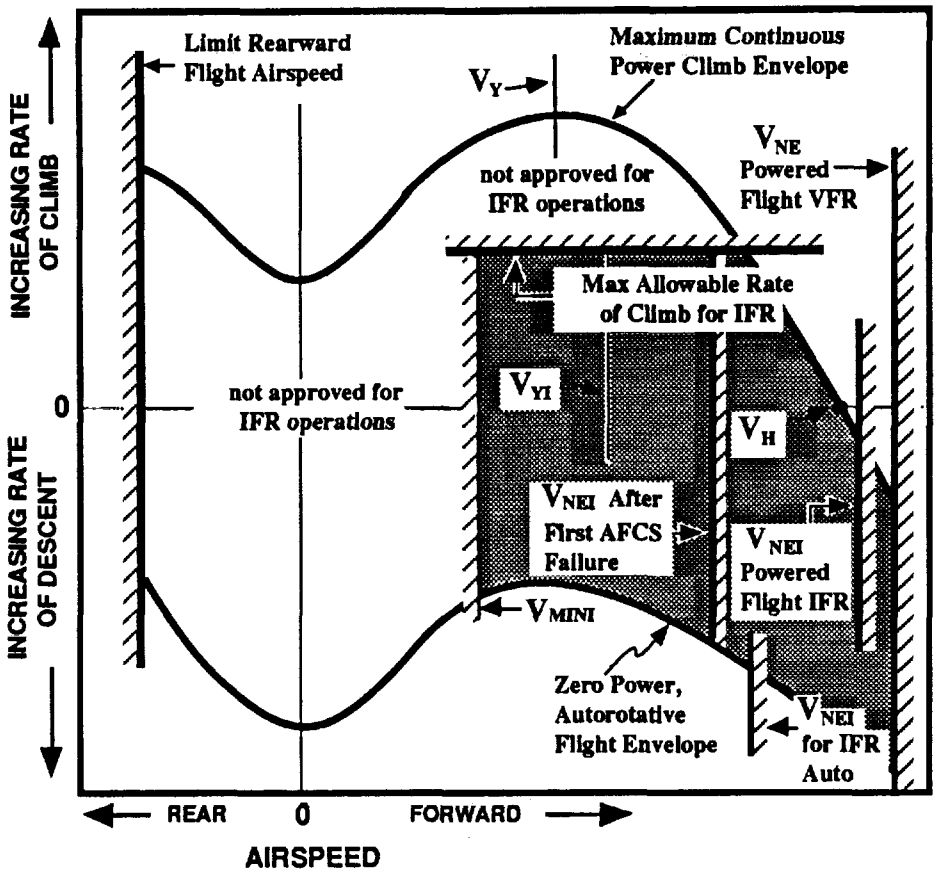

Figure 2: Typical Flying Qualities Envelopes Of A Small To Medium Size Helicopter

The applicant may also chose a speed for V_{MINI} which is based on considerations other than the flying qualities of the aircraft. For example, the low limit of an airspeed transducer in the AFCS may define V_{MINI}. In general, V_{MINI} can be established at a speed which is as high or as low as the applicant desires, as long as the aircraft exhibits adequate flying qualities, is capable of adequate climb performance, and has a practical operating speed envelope.

BASIC CONFIGURATION FOR EVALUATION

As mentioned earlier, the approval of an IFR envelope is based on the characteristics exhibited by the aircraft while it is being operated at the most adverse combinations of c.g., gross weight, etc., for which an approval is sought by the applicant. These adverse configurations will include the disengagement of all workload relief systems which have not met the requirements of the FAA for reliability. In some cases, a failure mode is acceptable if the pilot can be reasonably expected to observe the limits of a smaller envelope after a failure occurs.

TAILORING THE ENVELOPE

Typically there is an airspeed below which any given helicopter can no longer be easily flown under IMC, on airways. The actual airspeed defining the lower limit of the suitable flight envelope typically varies as a function of climb rate. For example, the boundary between the PRs of 5 and PRs of 6 in Figure 1 could define the minimum safe airspeed for IMC operations. Note that such an approach would produce a limit which varies as the function of rate of climb. Since a variable minimum limit speed would be relatively difficult to observe, the FAA has adapted the practice of selecting a single airspeed for all allowable climb rates (see Figure 2).

Typically a minimum airspeed for IFR operations (V_{MINI}) is proposed by the applicant and the flying qualities are investigated at the limit climb capability of the aircraft, or the maximum rate of climb proposed by the applicant (the FARs stipulate a minimum climb of 1000 ft/min, or a climb at maximum continuous power, whichever is less, while trimed at V_{YI}). The shape and location of the boundary between PRs of 5 and PRs of 6, as depicted in Figure 1, provides the reader with an insight into the alternative combinations of minimum airspeed (V_{MINI}) and the maximum allowable rate of climb for instrument flight which the applicant can choose from. In most past cases, the applicant has had an opportunity to increase V_{MINI} to obtain approval of a higher maximum allowable climb rate. Alternately, the applicant might agree to decrease the maximum

allowable climb rate to gain approval of a lower V_{MINI}. In the latter case, the resultant limit climb rate must provide a practical capability on airways.

In a similar way, the IFR operational envelope of a civil helicopter is often reduced to insure the availability of good flying qualities by limiting the maximum gross weight or minimum gross weight, and/or by limiting the range of the center of gravity (c.g.). Sometimes the envelope is limited in autorotative flight, and sometimes it is limited after a failure. For example, in Figure 2, the maximum forward speed has been limited after an AFCS failure (the speed is limited to protect the crew against a second failure). These are now limitations to the scope of the FAA evaluation and the envelope available for operational use. Any time an envelope is reduced in this way, it is said to have been tailored. The FAA now investigates the objective or the subjective requirements of the FARs within the envelope defined by these new boundaries.

STEEP APPROACHES AND V_{MINI}

The authors realize that there is current interest in the potential of reducing V_{MINI} to facilitate low speed, steep approaches into metropolitan vertiports. Such approaches will require the applicant to propose a relatively low V_{MINI} in combination with an indication of airspeed which is reliable at (and below) V_{MINI}, and the minimum airspeed for a Category A approach -- to insure the ability to execute a one engine inoperative (OEI) balked landing. (Note: The definition of V_{MINI} will need to be revised to accommodate instrument approach and balked landings under instrument conditions.)

FLIGHT DISPLAYS, FLYING QUALITIES, WORKLOAD

A search of past explanations of the relationships between displays, controls, task, performance and workload produced the AGARD Advisory Report No. 51 on "Displays for Approach and Landing of V/STOL Aircraft" (Reference 6). Figures 3 through 5 have been adapted from this reference to help us examine the complex but long recognized relationships which are an integral part of the FAA's evaluation-approval process. These figures illustrate the interdependence between display capability, aircraft handling qualities, automated flight control systems and well designed or automated cockpit management functions.

The adapted AGARD graphic presented in Figure 3, tells us that it is possible to trade-off display sophistication (capability) with control sophistication (capability) in a way which produces about the same performance for the same crew effort (pilot rating). This common capability is depicted as a single curved line in Figure 3. Each line is referred to here as a continuum of capability. To improve the pilots evaluation or pilot rating of an aircraft, the display-control combinations must improve. In Figure 3, this incremental improvement is illustrated by the inclusion of three lines representing three individual continua of capability.

Two continuum lines have been drawn in Figure 4 to consider the issue of workload. Lines (a) and (b) both represent acceptable performance and workload during the execution of an identical task. Observe that the pilot ratings are the same for the two lines but the distribution of the workload is different.

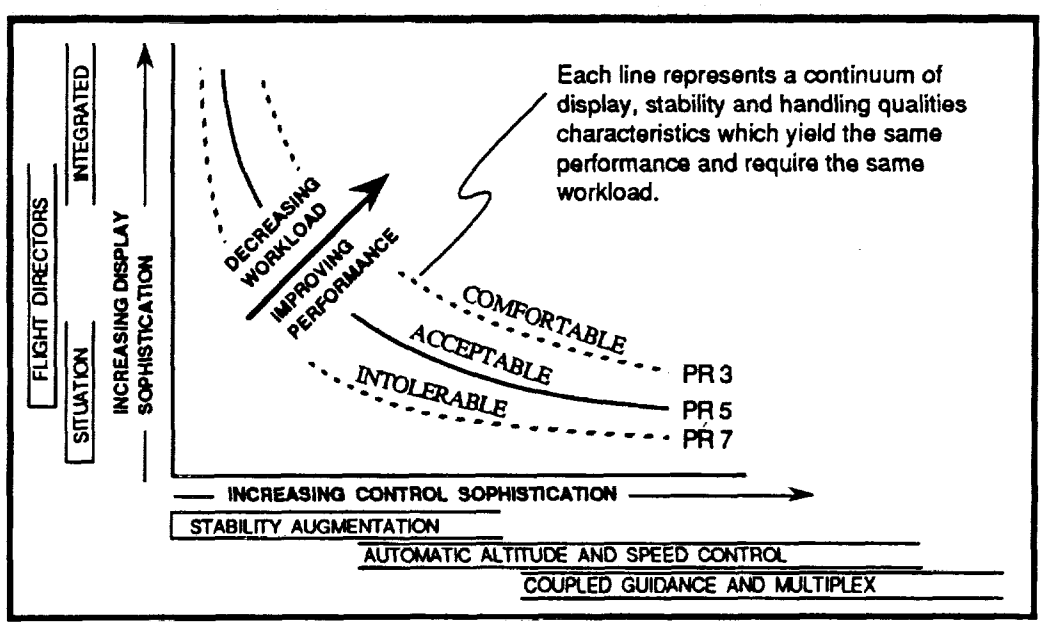

Figure 3: Tradeoff Between Display And AFCS Sophistication For An Instrument Approach

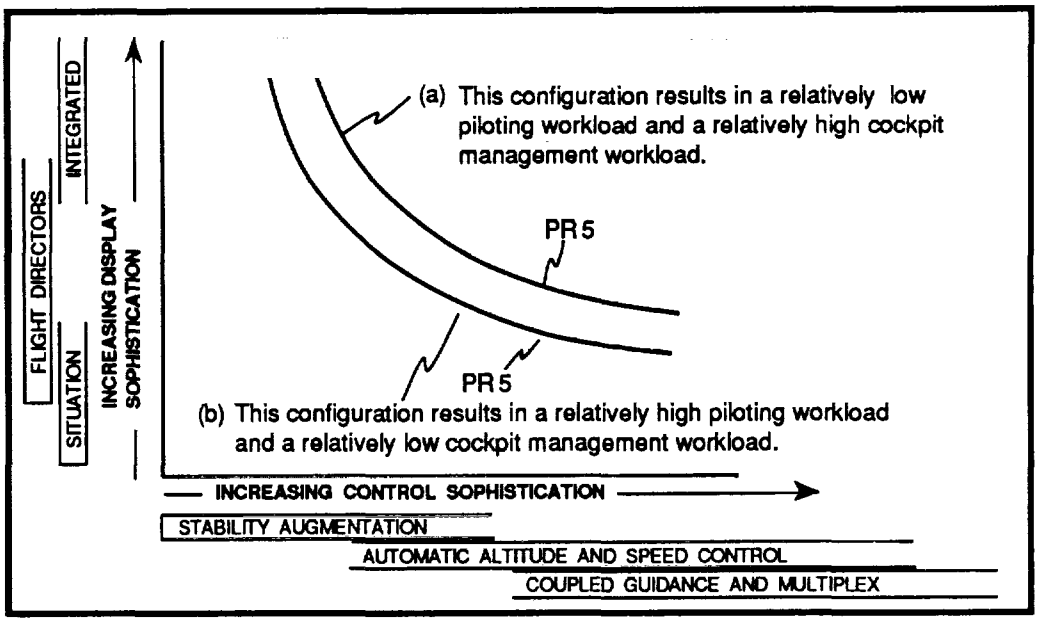

Figure 4: Enhanced Display And Control Sophistication Required For An Instrument Approach

The pilot's task to fly the aircraft is the least difficult when the display-control combinations of (a) are selected. When any of the combinations of displays and controls represented by continuum (b) are selected, the pilot effort to fly the aircraft is the greatest. The fact that the same pilot rating is assigned to both ofthese lines is explained by the fact that the pilot-aircraft performance (combined flight path management and cockpit management performance) is more or less equal and the total workload is more or less equal. Restated, while the total performance and workload are approximately the same for the two cases, the ratio of piloting workload to cockpit management workload are reversed. Once a satisfactory continuum of capability has been identified, the applicant is free to trade-off displays to find the most affordable and reliable combination of equipment.

MINIMUM EQUIPMENTS AND FLYING QUALITIES

An understanding of the workload relationships is very important when trying to understand the FAA's approval methodology. First, as a design guide, minimum display and flying qualities guidance is provided in the FARs and related Advisory Circulars. This guidance has been characterized by the VFR and the IFR limits included in Figure 5. That is, a minimum set of flight instruments (and related equipment) are stipulated by horizontal lines, and a minimum set of stability and handling qualities characteristics (vertical lines) are provided for the control side of the equation.

For the sake of discussion, assume the IFR limits in Figure 5 define the minimum stability, handling qualities and display requirements which will support approval of a helicopter for non-precision approaches with a crew of two. The limits also include consideration of the workload which can be accepted by two pilots. If the crew is reduced to a single pilot, it follows that workload must be reduced by incorporating either improved cockpit displays or an improved flight control system (or both).

For example, an improvement in the flight control system and/or AFCS should reduce the flight path control workload and yield a more desirable aircraft. The resultant operating point, "b" in Figure 5 represents a significant handling qualities improvement over "a". Such a change should make the aircraft easier to fly and improve pilot-aircraft performance as well as reduce workload. Similarly, an improvement in the display configuration is illustrated in Figure 5 as operating point (c). This should also help reduce the workload as well as help a pilot achieve the objective performance.

When the combined effect of the display and AFCS improvements are considered, a new operating point (d) is defined. If both point (b) and point (c) produced an adequate single pilot IFR capability, then theoretically a failure of either addition would be acceptable. This inferred redundancy once again briefly illustrates the potential connectivity between displays and controls.

PROVISIONS FOR FAILURES

The FAA process also insures that no failure of the displays or controls will result in an operating condition where the workload is inappropriate for continued IFR operations, or the pilot-aircraft performance is unsatisfactory. For example, this need for redundancy typically requires a second attitude indicator

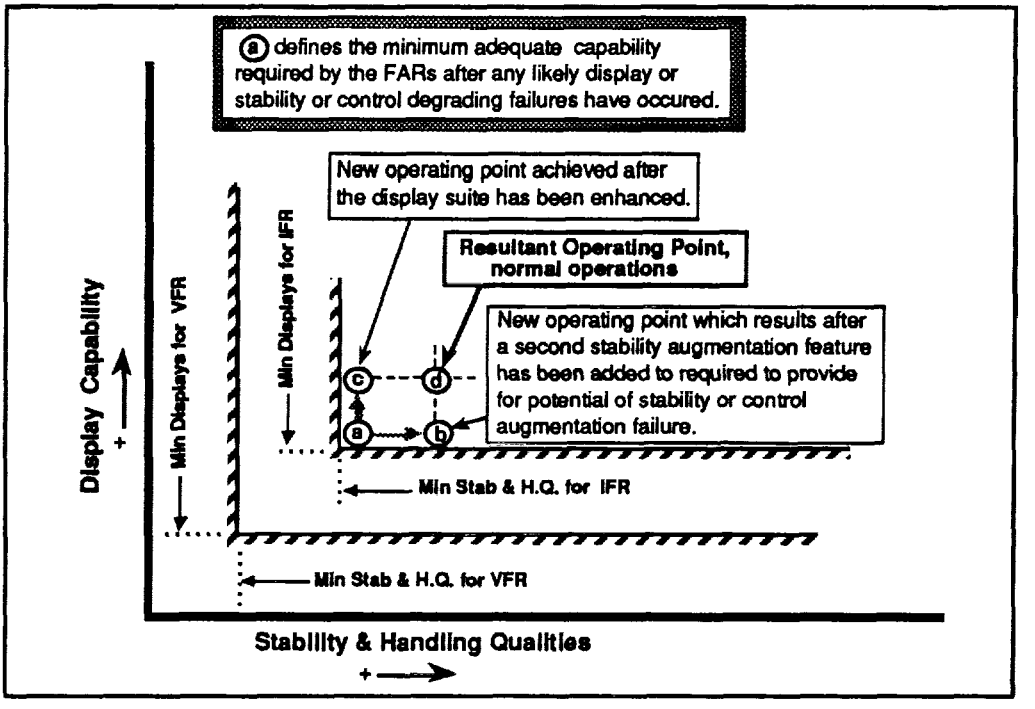

Figure 5: An Incremental Increase In Display Capability (or Redundancy) And Stability And Handling Qualities (or Redundancy)

to be installed in "single pilot" instrument panels. The addition of the redundant attitude indicator insures that the capability of the aircraft will not fall below that defined by operating point (a) in Figure 5.

Redundancy is also required to accommodate AFCS failures which degrade the stability or handling qualities of the aircraft. Sometimes, the addition of redundant AFCS channels allows the design to be altered in a way which simultaneously improves the flight characteristics of the aircraft (see path (a) to (b) in Figure 5) and provides the needed redundancy.

DISPLAYS COULD BECOME MORE IMPORTANT

Some argue that the (IFR enabling) credit assigned to displays and control system features of IFR helicopter systems tends to favor the use of AFCS. It can be argued that the development of display rich cockpits would be facilitated if the FAA allocated more credit to advanced electronic sensor-display systems with rotorcraft unique features. Such cockpits should decrease the need for multi-layers of stability and flight control augmentation. This might be especially true during a steep approach to a high pre-landing hover under IMC. Other less revolutionary yet equally important additions, such as display of ground speed and omni-directional low airspeed may substantially enable steep approaches to hovering flight. A powerful indication of yaw rate could also simplify pilot control of heading during slow speed flight without heading hold (subsequent to an AFCS failure).

A careful review of lessons learned during basic rotorcraft display research may be sufficient to justify greater specificity in the allocation of credit to existing conventional displays such as large turn and slip indicators, and large attitude indicators, with less credit allocated to very small attitude indicators, and turn and slip indicators that have been integrated into attitude indicators (ADI). For example, the work reported in Reference 7 found the large turn and slip display was the preferred display for IFR helicopter operations on airways, while the small integrated turn and slip dispalys were judged inferior.

In addition, a review of past flight director projects suggests that fight directors are substantially under valued, especially in the small helicopter application. This data has been overcome by the widely held belief that flight directors can be expected to improve performance, but typically at the cost of an increase in workload. As a point in fact, there is little rotorcraft data which suggest that a mature flight director design increases workload when the performance objective is held constant.

Counter to conventional wisdom, Reference 8 presents data which seems to establish the fact that a good flight director will lower workload and improve performance when: (1) the flight director is installed in a helicopter with poor inherent flying qualities and, (2) no AFCS is operating. That is, the inclusion of a proper flight director should cause the operating point to move from (a) to (c) in Figure 5.

It is the opinion of the authors that early flight director successes which involved the use of simple contact analog displays were pursued on the military side but abandon (by the civil community) in favor of the electronic reproductions of the current electro-

mechanical displays. In short, the perceived risk associated with customer acceptance and FAA acceptance of advanced electronic display formats has retarded advances in this area.

Similarly, most commercially available flight directors do not incorporate flight director laws which command the pilot to use the collective to maintain glideslope. The longitudinal control is used instead. This of course is not an acceptable solution for operations on the back side of the power required curve. The most important fact here is that this mechanization reflects a lack of concern for display techniques which could allow the pilot to enter the control loop in a way which might lead to the effective exploitation of the slow speed portion of the helicopter flight envelope. In summary, few seem to appreciate the display priority which should be allocated to the collective during operations on the back side of the power required curve, especially during steep approaches.

A future cockpit might incorporate an extremely powerful vertical situation display, with flight director capabilities which could enable the pilot to quickly and precisely trim the aircraft. The ability to trim precisely and quickly should do two things. It should significantly speed up the trimming process and delay the unattended departure from trim. This would allow a single pilot to spend more time with other flying and cockpit management tasks. This capability might prove to be most important as a safety enhancement feature subsequent to a stability augmentation failure or the failure of a work load relief system. Other improvements might include: airspeed displays, heading reference displays, and power management displays as suggested by Reference 9.

RISK AND AFFORDABILITY

The more affordable an IFR system is, the greater the applicant's monetary risk during the approval cycle. A precedent setting expansion of the operational utility of a helicopter model, such as the first configuration offered for Category III B instrument approaches also has an associated high risk relative to the cost to obtain approval of an aircraft of interest to a very small initial customer base. The risk at both ends of the sophistication spectrum involves concern for the calendar time to achieve approval and the cost of the effort (including the improvements which may be inferred by the FAA). The larger the anticipated investment and the greater the uncertainty associated with approval, the greater must be the potential return on investment. The fact that demand for IFR helicopters appears to be low seems to exacerbate the potential applicants worst fears.

The key to progress seems to reside in the development of an improved vertical flight infrastructure, and an aggressive effort to integrate more small helicopters into the IFR portion of the NAS. This effort should probably focus on the large potential fleet of helicopters in the 3000 to 5000 pound class.

Such an effort would require a number of demonstration programs to evaluate the alternative display-AFCS-cockpit workload design improvements. The resultant alternative configurations must be both clearly safe and affordable. It seems logical that the FAA approval process should be used as the format for these demonstrations. Finally, none of the resultant data should be proprietary.

SPECIAL OPPORTUNITIES

The following areas are identified as providing important enhanced capability to the rotorcraft community and the public it serves:

Partitioned-Independent Systems

Stability and control augmentation, autopilot and other workload relief systems should be designed so that the probability of total loss of a single system is unlikely and the loss of a partial system is not disabling. Failures could cause the pilot to retreat to the best portion of the flight envelope for the remainder of the flight.

Velocity Sensors and Displays

Doppler, airspeed and other speed measurement-display systems (not now in civil helicopters) will be required to allow approval of approaches to extremely low airspeeds or hovers during steep instrument approaches. A new family of logic can be developed which responds to the need to observe V_{MINI} and single engine minimum airspeed constraints (Cat A operations) while conducting steep approaches to a hover. Such a logic would be expected to address the practical attributes of currently available airspeed and ground speed sensor-display equipment in context with the air crew's need for the data under normal and failure mode operations.

Special Flight Director Functions

On the complex system end, flight director computers are required which incorporate relatively brilliant laws which in turn are able to provide steep approach guidance and hover or vertical descent/assent guidance. This might even respond to the need for flight directed Cat A takeoffs, rejected takeoffs, landings, and rejected landings.

On the low end, a new application of flight director logic could be used to direct the pilot to put the pitch attitude in the right place and the flight controls in the right place to steady the aircraft on trim in the shortest possible time, providing the pilot with more time to spend on navigation, communications, etc. In addition, there seems to be an opportunity for an improved display of commanded collective position.

Attitude Indicators

Attitude indicators come in a variety of sizes. Some are electro-mechanical, some are electronic. But what is their relative value? What is the benefit obtained with the largest practical display and the smallest emergency (two inch) display? The potential (or relative) advantage of the large display needs better definition.

Enhanced Vision Systems

There is clearly a need for affordable first step applications of vision enhancing sensor-display systems. The need exists all across the spectrum of aircraft size and capability. The potential is virtually unexploited in the civil helicopter community.

Helicopter Unique Displays

The slow and vertical modes of the helicopter are its principal attributes. Displays which facilitate pilot in the loop activity during slow and steep helicopter operations could make the helicopter more affordable and help the industry realize its potential. The current flight director, miniture turn needle, typical engine torque indicators, horizontal situation display (HSI) and pitot static airspeed indicator are five excellent examples of instruments which are not well suited to the helicopter during slow speed helicopter unique flight.

OBSERVATIONS

The FAA pilot has the authority and responsibility to evaluate and approve the aggregate suitability of combinations of controls, displays and workload relief equipment to facilitate and expedite the expanded application of large numbers of IFR helicopters in the NAS.

Innovation is required to demonstrate: (1) Partitioning between the axes of an AFCS to provide a form of graceful degradation which can be applied to low cost stability augmentation and workload relief equipment suitable for IFR operations of small helicopters. (2) The relative value of robust displays and concepts for granting credit in the FAA IFR approval process. Such displays will help pilots compensate for some of the weaker flying qualities of some small helicopters. (3) The advantages and limitations of vision systems for credit during approaches to metropolitan vertiports.

In addition, there is a continuing need to better articulate the way modern helicopters fly and are flown in the civil environment. This is required to support a broader understanding of the issues and opportunities for improvement, so as to facilitate the development of and garner FAA approval of, affordable equipment sets with accommodating flight envelopes.

SUGGESTIONS

Research and development should be encouraged to develop background data which will enable expeditious approval and encourage the intelligent applications of technology to develop affordable IFR equipment for a wide range of single and multi-engine helicopters.

The insight developed through R&D and FAA evaluations of aircraft offered for approval, should be used to enhance the guidance contained in Advisory Circulars 27-1 and 29-2.

REFERENCES

1. "Airworthiness Standards: Normal Category Rotorcraft," Code of Federal Regulations #14, Aeronautics and Space, Part 27, U.S. Department of Transportation, Federal Aviation Administration, revised 1 January 1991

2. "Airworthiness Standards: Transport Category Rotorcraft," Code of Federal Regulations #14, Aeronautics and Space, Part 29, U.S. Department of Transportation, Federal Aviation Administration, revised 1 January 1991

3. "Certification of Normal Category Rotorcraft," Advisory Circular 27-1, U.S. Department of Transportation, Federal Aviation Administration, 29 August 1985

4. "Certification of Transport Category Rotorcraft," Advisory Circular 29-2, U.S. Department of Transportation, Federal Aviation Administration, 28 May 1985

5. Cooper, George E., and Harper, Robert P., Jr., "The Use of Pilot Rating in the Evaluation of Aircraft Handling Qualities," NASA TN D-5153, National Aeronautics and Space Administration, Washington, D.C., April 1969

6. "Displays for Approach and Landing of V/STOL Aircraft," AGARD AR-51, AGARD Advisory Group for Aerospace Research & Development, November 1972

7. Armstrong, Gerald C., et. al., "Pilot Factors for Helicopter Refined ADI/HSI and Supporting Displays Evaluation," IFC-TR-74-5, Final Report, USAF Instrument Flight Center, Randolph AFB, Texas, June 1975

8. Griffith, Warren E., II., et. al., "Flight Evaluation OH-6A Helicopter Kaiser FP-50B Flight Director System," Part II, USAASTA Project No. 72-06, Final Report, U.S. Army Aviation Systems Test Activity, Edwards Air Force Base, California, February 1973

9. Green, David L., "Cockpit Integration From A Pilot's Point Of View," NASA Conference Publication 2219, Proceedings of a Specialists Meeting on Helicopter Handling Qualities, NASA Ames Research Center, Moffett Field, CA., 14-15 April 1982

Some Lessons Learned in Three Years with ADS-33C

David L. Key and Chris L. Blanken
Aeroflightdynamics Directorate
U.S. Army Aviation and Troop Command
Ames Research Center
Moffett Field, CA

and

Roger H. Hoh
Hoh Aeronautics, Inc.
Lomita, CA

ABSTRACT

Three years of using the U.S. Army's rotorcraft handling qualities specification, Aeronautical Design Standard – 33, has shown it to be surprisingly robust. It appears to provide an excellent basis for design and for assessment, however, as the subtleties become more well understood, several areas needing refinement became apparent. Three responses to these needs have been document in this paper: (a) The yaw-axis attitude quickness for hover target acquisition and tracking can be relaxed slightly. (b) Understanding and application of criteria for degraded visual environments needed elaboration. This and some guidelines for testing to obtain visual cue ratings have been documented. (c) The flight test maneuvers were an innovation that turned out to be very valuable. Their extensive use has made it necessary to tighten definitions and testing guidance. This was accomplished for a good visual environment and is underway for degraded visual environments.

INTRODUCTION

Aeronautical Design Standard – 33 (ADS-33C) (Ref. 1) was adopted in August 1989. Since that time, it has been used in several programs which cover the spectrum of possible applications. These include a full flight test evaluation of a current Army helicopter (Apache), full design application and simulator assessment of the competing designs for LHX, which later evolved into Comanche, analytical evaluations using high fidelity math models for the Black Hawk and Sea Hawk, and flight tests of several aircraft including the OH-58D and the BO-105. Such application early in its lifetime is a specification writer's dream. We can already see the influence modern handling qualities concepts are having on new design and assessment methods and we also get feedback on criteria which need more work, or topics which need more guidance to enable users to understand and apply the methodologies. This paper describes some of the results of efforts to resolve questions on three topics that have arisen during the last three years.

The first topic covered is attitude quickness. The evolution of this new requirement is outlined. Several experiments were performed to enhance the database, and a proposed revision to a yaw-axis boundary in hover has been developed.

The second topic treated is related to Degraded Visual Environment (DVE). To handle the Army's need to fight at night, as well as, or perhaps even more than during the day, a new concept was introduced into ADS-33C which relates the required helicopter flying qualities to degradations in the visual cuing. A definition of DVE is provided and the methodology of obtaining Visual Cue Ratings (VCR's) and relating these to required Response-Types through the concept of Usable Cue Environment (UCE) is described. Particular guidance is presented for pilot briefing notes and questionnaires to help in obtaining consistent VCR's.

Since degraded visual cuing is usually encountered on ground-based simulators even when trying to simulate day, the basic concept of UCE has been extrapo-

Presented at *Piloting Vertical Flight Aircraft: A Conference on Flying Qualities and Human Factors*, San Francisco, California, January 1993.

lated to calibrate simulators; the methodology, called SIMulated Day UCE (SIMDUCE), is described.

The last topic described is refinement of the flight test maneuvers. These were introduced into the handling qualities specification to provide guidelines for an overall assessment of the design. They have turned out to be a major item used by the test and assessment community, and also as a primary goal for the designer. In applying these tests, it was realized that they needed to be defined more precisely for repeatability, and also the standards needed to be well-justified. In addition, guidance was clearly needed on how elaborate the test maneuver cuing and test performance documentation had to be. The progress made for both the day and the DVE maneuvers is described.

ATTITUDE QUICKNESS

The ADS-33C is a mission-oriented specification, based upon mission task elements (MTE's) and the cuing available to the pilot. Minimum requirements are established for control Response-Types and their characteristics. These requirements are categorized into terms of small, moderate, and large amplitude changes. The moderate amplitude requirements include the attitude quickness criteria, where attitude quickness is defined as the ratio of peak angular rate to the change in angular attitude. ADS-33C establishes minimum Levels of attitude quickness for pitch, roll, and yaw depending upon the speed range and MTE (see Fig. 1).

Criteria Development

Most of the background and the initial supporting data for the attitude quickness requirement came from a helicopter roll control study (Ref. 2). The basis for the requirement was extracted from "maneuver performance" diagrams that were constructed from a number of discrete lateral maneuvering tasks. For a maneuver that requires discrete control inputs, the ratio of peak angular rate to change in attitude for the entire maneuver describes a "task signature" related to the pilot's demands on the vehicle. For small attitude changes, the value of attitude quickness is dominated by the bandwidth criteria. For large attitude changes, the attitude quickness is dominated by the large amplitude requirements. The attitude quickness requirements effectively connect the frequency-domain bandwidth limits at small amplitudes with the time-domain peak angular rate limits at large amplitudes.

Since Reference 2 was specifically a roll control study, there was no information for setting the pitch limits, and therefore, some assumptions were made for the pitch requirements. The extrapolation to the pitch axis was fairly well justified given the well-substantiated small and large amplitude pitch requirements and the attitude quickness formulation technique based upon the roll axis.

Initially the yaw-axis attitude quickness boundaries were based upon the same procedure as pitch. Recently, an in-depth piloted simulation study was performed by the Aeroflightdynamics Directorate (AFDD) at Ames Research Center to provide an improved basis for the yaw-axis boundaries. The simulation, performed on the NASA-Ames Vertical Motion Simulator (VMS), examined the yaw attitude quickness in hover while performing a target acquisition task and a 180 degree turn task. Configuration bandwidth and attitude quickness were varied via the yaw damping derivative and the tail rotor collective pitch actuator rate limit.

The results from the target acquisition in hover task suggest that the current ADS-33C yaw-axis attitude quickness boundaries might be relaxed without sacrificing Level 1 handling qualities (see Fig. 2). The results from the 180 degree turn in hover task indicate that relaxation of the attitude quickness requirement indicated by the target acquisition in hover task would not adversely impact the pilot's ability to perform large, aggressive heading changes. These refined yaw attitude quickness boundaries will be included the new version of ADS-33C.

Compliance Testing

The attitude quickness requirement states that the attitude changes must be made as rapidly as possible from one steady attitude to another without significant reversals in the sign of the cockpit control input relative to the trim position. The initial attitudes and the attitude changes required for compliance shall be representative of those encountered while performing the required mission task elements. It should be noted that the attitude changes should be made "open-loop," i.e., without a specific target attitude and as rapidly as possible.

The recommended control input for a Rate command Response-Type is to utilize spike (or very short duration pulse-like) inputs of varying magnitude to produce the necessary range of attitude changes. For the larger attitude changes it is acceptable to initiate the changes from a non-level equilibrium, e.g., a large roll attitude change may be initiated from a positive or a negative bank angle.

The recommended control input for an Attitude command Response-Type is to initially overdrive the commanded attitude followed by an essentially steady value of the stick consistent with the commanded attitude. The purpose of this control strategy is not to provide lead equalization, but simply to overcome the inherent stability of the attitude command response. On the other hand misleading results can be obtained if significant control reversals from the trim position are allowed. This technique is not representative of rotorcraft alone dynamics and is more a measure of the pilot skill in timing the inputs. In fact, using significant control reversals to quicken the response and arrive at a steady attitude change is like having the pilot closing the angular rate and attitude loops just like a Stability Control Augmentation System (SCAS), and of course, paying the penalty in terms of workload. The purpose of this requirement is to specify the rotorcraft dynamics without pilot equalization, and hence, significant control reversals are not allowed during compliance demonstration. In general, control reversals are not considered significant if the control reversals are significantly less than the initial input.

DEGRADED VISUAL ENVIRONMENT (DVE)

Helicopters are inherently unstable. The flight control system can change this, but current-generation aircraft typically only enhance rate damping so the pilot is still left with the task of constant manipulation of the controls to maintain attitude. It must be realized that this is primarily a visual task. Unlike riding a bicycle, it is not possible to balance the helicopter solely using vestibular cues. This means that the pilot needs good visual cues, not only for guidance, that is, to see where he is going and avoid obstacles, but also for control and stabilization. It has been found that the stabilization needs can be reduced or almost eliminated if the appropriate stability is build into the helicopter. Such a flight control system is, of course, more elaborate and expensive than a simple rate damping system, and hence the handling qualities specification had to devise a scheme for informing the designer when he had to change to the more elaborate system. The process involves defining the Degraded Visual Environment (DVE), obtaining a Visual Cue Rating (VCR), and hence, defining the Usable Cue Environment (UCE), and this in turn is related to the flight control system Response-Type. Some of the questions that have arisen in applying this methodology will be addressed in this section.

DVE is an environment in which the pilot of a Level 1 Rate response helicopter cannot get adequate visual cues to perform maneuvers aggressively and precisely. This can occur because there are reduced or few cues for him to see, such as over desert, snow, or water, or because he cannot see the features that are there because of a lack of illumination, such as at night, or because of obscuration, such as in smoke, dust, fog, or restricted cockpit field of view. Vision aids such as night vision goggles (light intensification) or infrared devices such as the helmet mounted FLIR help compensate for some of these deficiencies, but can introduce deficiencies of their own such as reduced resolution, remotely located eye point, slow tracking dynamics, and vibration of the scene image.

Visual Cue Rating (VCR)

The VCR scale was developed as a basis for quantifying the UCE. It is a subjective pilot rating scale intended to quantify the usability of the visual cue environment for stabilization and control during low-speed and hover operations near the ground. The basis for this scale is discussed in detail in Reference 3. It has been in use for over six years, and experience has shown that certain procedures must be followed to achieve repeatable and valid pilot ratings. These procedures are still being developed and refined as the scale is used for new applications. This evolution is similar to the Cooper-Harper subjective pilot rating scale (Ref. 4). Early use of that scale resulted in significant pilot rating scatter because the importance of certain procedures were not understood. When the established procedures are carefully adhered to (see Ref. 5) this subjective rating scale is reliable and repeatable. This experience emphasizes the importance of identifying and implementing proper procedures in the use of subjective pilot rating scales.

The cues required for aggressive and precise low-speed and hover operations are not well understood by pilots or engineers. Therefore, it is not possible to assess them directly. The VCR scale is an attempt to circumvent this gap in the knowledge base by making an assessment of the cuing environment in terms of the pilot's ability to accomplish aggressive and precise maneuvers with an aircraft that would be Level 1 in a good visual environment (GVE). The scale is shown in Figure 3. Factors to be considered to ensure that the test aircraft is Level 1 are discussed under SIMDUCE in this paper.

The descriptions in Figure 3 have been slightly modified from those shown in the current version of ADS-33C to eliminate any reference to the word "cues." This is based on experience that has shown that pilots are tempted to evaluate their perception of the cues rather than their ability to achieve the noted aggressiveness and precision. That experience has shown that pilot perceptions of visual cues are usually excessively optimistic. For example, essentially all pilots feel that hovering will be no problem when sitting in the cockpit of a modern ground-based simulator and visual system before it is put into operate. They are surprised to find that a simple hover task requires extreme concentration, or may not even be possible without considerable practice. Experiments have resulted in evidence that pilots rely heavily on fine-grained texture to hover and maneuver in low-speed flight (Ref. 3). Such "micro-texture" is not available in most digital image generators, and in cockpit vision aids in marginal conditions (e.g., night vision goggles on a moonless night).

To get a measure of the UCE, ADS-33C specifies that the following Flight Test Maneuvers be performed, and VCR's be assigned: Hover (4.4.1), Vertical Landing (4.4.3), Pirouette (4.4.4), Acceleration and Deceleration (4.5.1), Sidestep (4.5.2), and Bob-up and Bob-down (4.5.3). The VCR's are to be assigned while attempting to achieve desirable performance in the DVE where the DVE is to be specified by the procuring activity. The following guidelines have been established for assigning the VCR's and should be a part of any pilot briefing where such ratings are to be given.

Pilot Briefing Notes

Assign the ratings based only on the ability to be precise and aggressive.

Use the precision hover and vertical landing tasks as primary measures of precision.

Aggressiveness should be considered in the context of mission performance and may not require large aircraft attitudes. Consider the ability to stabilize quickly at the end of the pirouette, sidestep, and acceleration/deceleration maneuvers as a good measure of aggressiveness. Any tendency to "back out of the loop" to avoid undesirable oscillations should be considered as in inability to be aggressive.

Do not try to make a distinction between the aircraft dynamics and the visual cuing environment that is being evaluated.

Try to meet the desired performance standards for most of the maneuver. Small deviations from the desired performance limits should not be a primary factor in the evaluation. However, an inability to aggressively correct back to the desired region without exciting undesirable aircraft excursions or oscillations should be cause to consider the fair-to-poor region of the scales.

If the evaluation is being made on a ground-based simulator, do not try to extrapolate to the "real world"; rate what you see.

It is a good idea to assign Cooper-Harper handling qualities ratings (HQR's) during the UCE testing. There should not be a significant discrepancy between the VCR's and the HQR's. For example, if the VCR's are between good and fair (1 to 3) it would be expected that the HQR's would be no worse than five. If the VCR's are in the fair-to-poor range (3 to 5), HQR's of five or worse would be expected.

The UCE testing should be accomplished in an environment where the cues for desired and adequate performance are reasonable and consistent with purpose of performing the task. For example, testing the precision hover task in a large field, with minimal cues for position, bears no relationship to the task that established the requirement in the first place. Such requirements are driven by mission-related tasks, such as hovering in confined areas where the cues representing obstructions are not subtle. This aspect is treated in more detail in the section discussing the flight test maneuvers. The purpose of the UCE testing is to establish the ability to be precise and aggressive with respect to realistically sized and located objects.

The inability to achieve good VCR's can usually be traced to a lack of visible details, and should not be related to the inability to see obstructions soon enough, such as when driving a car too fast in fog. Such issues cannot be resolved with improved handling qualities and should be evaluated separately.

A separate set of VCR's should be assigned for each task. It is recommended that the pilot practice the task at least twice before conducting the evaluation run. The VCR's may be averaged across pilots, but may not be averaged across tasks.

One final point, it has been observed that there are a very select group of pilots who can hover and precisely maneuver with poor visual cues when most pilots cannot. Ideally, they should be aware of their unusual capabilities and give ratings accordingly.

SIMULATED DAY UCE (SIMDUCE)

During the evolution of the design process and evaluation of new rotorcraft designed for compliance with ADS-33C, ground-based simulation will likely occur. Visual systems with computer generated imagery (CGI) and their associated presentation device(s) are typical for ground-based flight simulators. Initially, these visual systems lacked field of view, resolution, and detail, and their dynamic response was sometimes less than optimum. For example, the poor resolution in an early visual system is illustrated in Figure 4 from Reference 6. Although the quality of visual cues has improved as the technology has advanced, simulated day scenes still do not compare with the real-world day scene. This observation is illustrated by the fact that good Rate command Response-Types continue to receive Level 2 handling qualities on ground-based simulators whereas, in-flight they typically receive solid Level 1 ratings.

To quantify the quality of the simulated day visual cues for handling qualities work, a technique of using the VCR-UCE concept has been applied. We call this SIMulated Day UCE (SIMDUCE). With a Level 1 Rate response model, if the cues are as good as they would be during the daytime, SIMDUCE = 1. If the SIMDUCE = 2 or 3, it is roughly equivalent to having Level 2 or Level 3 handling qualities. The procedure for determining the SIMDUCE follows the same approach as the UCE evaluation with the exception that the day maneuvers and performance standards are used for the evaluation instead of the DVE maneuvers and standards. So to obtain an overall assessment of the simulator, the following Flight Test Maneuvers of ADS-33C should be flown: Hover (4.1.1), Vertical Landing (4.1.3), Pirouette (4.1.4), Rapid Acceleration and Deceleration (4.2.1), Rapid Sidestep (4.2.2), and Rapid Bob-up and Bob-down (4.2.3). While performing these maneuvers, VCR's are collected from which a SIMDUCE is determined. The VCR collection and consolidation procedures for SIMDUCE are the same as for the UCE determination.

Level 1 Rate Response Hellcopter

In performing the UCE determination, the ADS-33C states that the test rotorcraft must meet the requirements for a Rate Response-Type and must have a Level 1 mean pilot rating by at least three pilots operating without any vision aids in good visual conditions (UCE=1) and negligible turbulence. This concept was established with the idea of performing this test in-flight and not necessarily on a ground-based simulator. The potential hitch in the process when using a ground-based simulator is the establishment and documentation of the Level 1 aircraft. Implementing a Rate Response-Type is not difficult, but even if all the ADS-33C requirements are met there are additional parameters which can result in poor handling qualities such as control sensitivity and inceptor force-displacement characteristics. The ADS-33C guidance for conventional controls force-displacement characteristics are quite comprehensive, and if met, the handling qualities are likely to be good if tests are conducted to optimize the sensitivity. Unfortunately, the same cannot be said of multi-axis side sticks where many unspecified characteristics could cause a degradation. This another topic which needs elaborating in ADS-33C.

FLIGHT TEST MANEUVERS

Motivation for Flight Test Maneuvers

A selection of maneuvers is specified to provide an overall assessment of the rotorcraft's ability to perform certain critical tasks. It is recognized that although quite comprehensive, the state of knowledge is such that the quantitative criteria in Section 3 are not sufficient to guarantee that the handling qualities will be Level 1. Some important characteristics, such as control sensitivity are not specified, and a poor choice could easily result in poor handling qualities. The requirements have been formulated with the philosophy that each one is necessary, and not meeting any one will be sufficient to result in a degradation in the handling qualities. Hence, it was decided that some overall "proof of the pudding" should be applied to ensure that the combination of characteristics result in good handling qualities for some tasks important to that aircraft's role.

The flight test maneuvers are not comprehensive in terms of tasks or flight conditions. However, they do include critical task elements which could be encountered in many applicable missions. They include single-axis and multi-axis tasks for each direction, and for different levels of aggression. In addition, sets of maneuvers are provided for Day and for DVE.

Experience in Application

Significant experience has now been gathered on the application of the maneuvers in ADS-33C. The two primary examples are the LHX assessments performed on

each of the competing teams' simulators during the Demonstration Validation (Dem Val) program, and the flight test evaluation of the AH-64 Apache. References 7 and 8 describe these efforts in some detail, so only a few of the topics which influenced the evolution of the criteria will be mentioned here.

LHX Dem Val – As part of ADS-33C, the flight test maneuvers were included in the contract so they became benchmarks which had to be met. As such, they became design drivers, but for nearly all of the maneuvers the only way they could be assessed was subjectively in piloted simulation. This put considerable pressure on simulation fidelity/validity assessment. It also showed-up any ambiguities or vagueness in the criteria. Some of the reactions were as follows: Systematic application required specifying adequate standards, not just desired. The precision with which some of the maneuvers were defined allowed the pilots to adopt different levels of aggressiveness, thus resulting in different pilot ratings. With insufficient cuing, the pilots did not know if they had met the performance standards. Such a lack of cues was clearly unrealistic since the need for precision would usually mean that there were constraints nearby which would be providing the cues. The defined performance standards had a big effect on pilot rating, so the chosen standards must be meaningful. Accuracy of performance standards suggested that the eventual flight test program would involve some very expensive test equipment to demonstrate compliance.

Apache flight tests – Flight testing reinforced most of the overall impressions developed on the simulators during LHX Dem Val. However, the simulation related issues went away, and new issues related to flight testing became apparent. For example: Some of the aggressive maneuvers (Fig. 5), especially in DVE, were quite thrilling and resulted in much philosophical debate. Though perhaps not universally accepted yet, it is the authors' opinion that if these stylized maneuvers are representative of maneuvers which will be performed by the Army in operational use, then the flight test community must be willing to test them. Certainly, if they are too dangerous for a skilled test pilot to perform in a tightly controlled environment, it is unreasonable to expect the user to fly such maneuvers in an unfamiliar, unfriendly environment in the fog of war.

The need for simple solutions to cuing and compliance issues was re-emphasized. Some solutions were developed which served to achieve the desired intent, but clearly more work was required.

Overall, these results showed that the flight test maneuvers were important. Not only were they well accepted by the test community, but they were given even more influence than initially intended. In view of this, it was decided to make an effort to refine the maneuvers and resolve the questions that had been raised.

Objectives of Refinement

The objectives of the maneuver refinement effort were focused in the following four areas:

Maneuver Definition – To refine and standardize the definition of the maneuvers so that the written descriptions can be easily understood, and will be repeatable by different pilots in different organizations.

Performance Standards – To ensure that the level of precision and aggressiveness for Level 1 (desired performance) was appropriate, and to generate a valid set of standards for Level 2 (adequate performance).

Cuing Requirements – To define test courses and suitable cuing. The important characteristics here were that there should be sufficient cuing, but that it should be kept simple and therefore cheap and easy to reproduce. Also, to allow considerable flexibility for the flight test organization to make modifications as needed to accommodate their own particular capabilities or limitations.

Compliance Methods and Documentation – An additional constraint on the cuing was that it must be useful for showing compliance. In particular, to provide guidance on the type and scope of instrumentation to be used so that it was clear to the flight test organization that they did not need multi-million dollar laser tracking or GPS systems.

New Maneuvers- Good Visual Environment

This section describes the maneuver refinement effort approach, lists the new maneuvers, and describes one of them in detail.

Approach – Flight tests were performed by the Flight Research Laboratory of the Institute for Aerospace Research, National Research Council of Canada, using their variable-stability Bell 205 airborne simulator (Fig.

6). In addition, help and expertise was provided by engineers and test pilots from the U.S. Army's Airworthiness Qualification Test Directorate (AQTD). Each of these pilots and engineers had experience in the LHX or Apache tests so their inputs were extremely valuable.

The approach was to discuss the aim of each task and the possible approach for meeting it. The tasks were then flown and pilot comments and performance data reviewed. If necessary the tasks were revised and re-flown. Finally two pilots who had not been part of the task development were asked to perform the maneuvers working only from the written description.

The tasks were performed using three configurations: one which just met the Level 1 quantitative requirements of ADS-33C, one well within the Level 2 region, and one just inside the Level 3 boundary. The pilots gave Cooper-Harper HQR's and these were expected to correspond with the configuration "Levels" inferred from the quantitative standards. Further details are described in Reference 9.

Since the Bell 205 is limited in maneuverability, it was necessary to develop the aggressive and high speed maneuvers in a different aircraft. Such tests were performed using similar techniques, only without any changes to the basic flying qualities, by AQTD on a UH-60, and a T-34. The T-34, a fixed wing training aircraft was particularly useful for evolving the air-to-air maneuvers.

New Maneuvers – Table 1 summarizes the major revisions made to the maneuvers. In addition to refinements to the existing maneuvers, several new maneuvers were added. These primarily addressed aggressive maneuvering tasks, both in hover and forward flight.

The Precision Hover task illustrates many of the factors treated. The Appendix shows the current and revised versions of the maneuver, and Figure A-1 in the Appendix is a sketch of the suggested cuing devices in the test course.

In the original maneuver definition, it was found that although the task of achieving the desired hover point was quite likely to cause higher pilot workload than the actual hover, it was not part of the task that was evaluated. To rectify this, the maneuver was modified to start some distance from the desired hover point and a 45-degree crabbing translation made to the hover point.

To force some uniformity in the task aggressiveness, the time to reach hover, and the nature of the deceleration are defined.

Other details changed were: The maneuver is to be performed in calm (< 5 knots) and moderate (20 to 35 knots) winds; To change the hover target from a circle to a square since this would be easier to cue the pilot and for observers to check; The use of any available hover assists was allowed if they were available and consistent with operational use; Adequate standards were generated with looser tolerances and less aggressive time requirements; The simple cuing props, illustrated in Figure A-1 of the Appendix, gave sufficient guidance for the pilot to be able to tell if the required standards were being achieved. The same cues could be used by outside observers and onboard video recording to document the performance for compliance demonstration purposes.

New Maneuvers- Degraded Visual Environment (DVE)

The day maneuvers have now been reviewed and revised several times and are now considered to provide excellent benchmarks. The maneuvers for Degraded Visual Environment (DVE) are less refined, but two efforts are underway to refine them.

The first effort involves a simulation performed by AFDD on the NASA Ames Vertical Motion Simulator (VMS). The CGI representation of the proposed cuing for DVE was set up with a UCE=2. The various tasks were flown with a Level 1 and Level 2 Attitude Command Attitude Hold (ACAH) Response-Types, and also with a Level 1 Rate command. The pilot performance and pilot commentary was obtained in much the same way as done at the National Research Council of Canada for day. The results are still being analyzed, but Figures 7-10 shows some preliminary data for the Hover task.

As would be expected, the Level 1 rate configuration shows frequent excursions into the adequate region (Fig. 7) and the Cooper-Harper HQR was Level 2.

With a Level 1 ACAH response (Fig. 8), the pilots were essentially within desired standards and the rating was 2.8, clearly Level 1. Figure 9 shows all of the runs for pilot 6 whereas, the other figures only show the last three runs for each pilot. It is interesting to note that the pilot took several runs to achieve the desired performance. It appears as though he first increased the aggressiveness to achieve the desired time and then worked on maintaining his longitudinal precision.

Figure 10 shows what happens with a Level 2 ACAH response. Aggressiveness is only adequate, longitudinal precision frequently is worse than desired, and the

spread for lateral error increases noticeably though it is generally in the desired range.

Overall it would appear that the standards chosen for this task are compatible with the Level achieved. The reduction in aggressiveness for night operations does not seem unwarranted; the precision standards were the same as day in the horizontal plane, but loosened very slightly for altitude ($\pm$ 2 ft became $\pm$ 3 for desired and $\pm$ 4 ft became $\pm$ 5 ft for adequate.)

The second effort at refinement is a joint Army/NASA project to actually fly the tasks in a real DVE, that is, at night. An Army AH-1G Cobra helicopter (Fig. 11) equipped with the Apache Integrated Helmet and Display Sight System (IHADSS) is operated at the NASA Ames Research Center in various joint Army/NASA research tasks. This is not a variable-stability helicopter so it will not be possible to assess the Level 1 standards in the DVE. The Cobra is a Rate Response-Type with essentially Level 1 ratings for day; it would be expected to be Level 2 in a UCE=2. The aircraft will be used to evaluate the other aspects of trying to perform these evaluations at night. Topics of concern are the details of cuing when using night vision goggles or FLIR, how to calibrate the degraded visual environment, and how to perform the necessary compliance assessment and documentation. These efforts are currently underway and the flight test program is expected to be performed by about March 1993.

CONCLUSIONS

Three years of using the U.S. Army's rotorcraft handling qualities specification, Aeronautical Design Standard – 33 (ADS-33C) has shown it to be surprisingly robust. It appears to provide an excellent basis for design and for assessment, however, as the subtleties become more well understood, several areas needing refinement became apparent. Three responses to these needs have been documented in this paper:

(a) the yaw-axis attitude quickness for hover target acquisition and tracking can be relaxed slightly.

(b) understanding and application of criteria for degraded visual environments needed elaboration. This and some guidelines for testing to obtain visual cue ratings have been documented.

(c) the flight test maneuvers were an innovation which turned out to be very valuable. Their extensive use has made it necessary to tighten definitions and testing guidance. This has been done for good visual environment and is underway for degraded visual environments.

REFERENCES

[1] "Handling Qualities Requirements for Military Rotorcraft," Aeronautical Design Standard – 33 (ADS-33C), August 1989.

[2] Heffley, R.K., Bourne, S.M., Curtiss, H.C., Jr., Hindson, W.S., and Hess, R.A., "Study of Helicopter Roll Control Effectiveness Criteria," NASA Contractor Report 177404, USAAVSCOM TR-85-A-5, April 1986.

[3] Hoh, Roger H., "Investigation of Outside Visual Cues Required for Hover," AIAA Paper No. 85-1808, August 1985.

[4] Cooper, G.E., and Harper, R.P., "The Use of Pilot Rating in the Evaluation of Aircraft Handling Qualities," NASA TN D-5153, April 1969.

[5] Hoh, Roger H., "Lessons Learned Concerning the Interpretation of Subjective Handling Qualities Pilot Rating Data," AIAA-90-2824, August 1990.

[6] Blanken, C.L., Hart, D.C., and Hoh, R.H., "Helicopter Control Response Types for Hover and Low-Speed Near-Earth Tasks in Degraded Visual Conditions," American Helicopter Society 47th Annual Forum, Phoenix, AZ, May 1991.

[7] Ham, J.A. and Metzger, M., "Handling Qualities Testing using the Mission Oriented Requirements of ADS-33C," American Helicopter Society 48th Annual Forum, Washington, D.C., June 1992.

[8] Ham, J.A. and Butler, C.P., "Flight Testing the Handling Qualities Requirements of ADS-33C - Lessons Learned at ATTC," American Helicopter Society 47th Annual Forum, Phoenix, AZ, May 1991.

[9] Morgan, J.M., "The Development of Flight Test Maneuvers in Support of ADS-33C," Annual CASI Meeting, Ottawa, Canada, May 1992.

Table 1. Overview of Major Revisions to ADS-33C Section 4 Flight Test Maneuvers

ADS-33C	MAJOR REVISIONS
4.1 Precision Tasks	
1. Hover 2. Hovering Turn 3. Vertical Landing 4. Pirouette 5. Slope Landing	Hovering Turn ~ changed to a precision maneuver tighter position stds and longer time to complete Vertical Ldg. ~ renamed Precision Landing ~ decreased position tolerance and vertical displacement ~ increased time to complete
4.2 Aggressive Tasks	
1. Rapid Acceleration and Deceleration 2. Rapid Sidestep 3. Rapid Bob-up and Bob-down 4. Pull-up/Push-over 5. Rapid Slalom 6. Transient Turn 7. Roll Reversal at Reduced and Elevated Load Factor	Accel/Decel ~ relaxed pos'n and altitude tolerance Bob-up/dn ~ increase req'd height change and time to complete Pull-up/Push-over ~ increase req'd "g's" to OFE ADDED New Maneuvers: Vertical Remask Deceleration to Dash Aggressive Turn to Target (old HT) High and Low Yo-Yo
4.3 Decelerating Approach to Hover	
4.4 Precision Tasks in DVE	
1. Hover 2. Hovering Turn 3. Vertical Landing 4. Pirouette	
4.5 Moderately Aggressive Task in the DVE	
1. Acceleration and Deceleration 2. Sidestep 3. Bob-up and Bob-down 4. Slalom	Accel/Decel ~ relaxed pos'n and altitude tolerance Bob-up/dn ~ increase req'd height change and time to complete

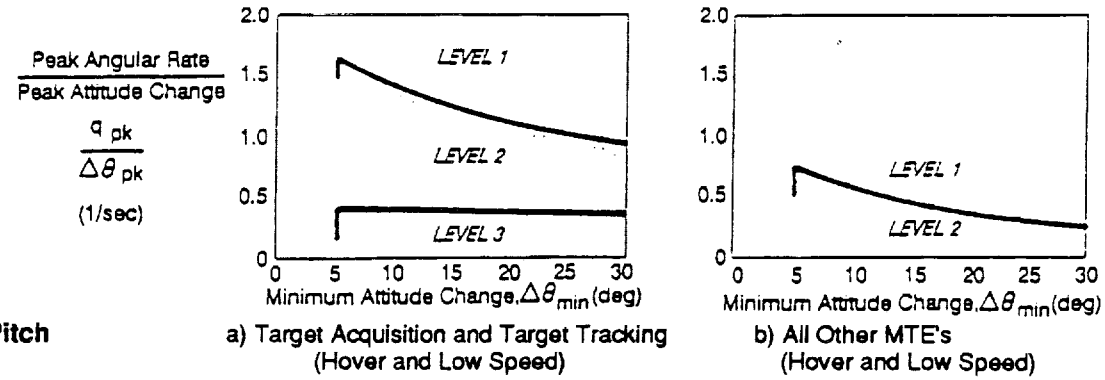

Pitch

a) Target Acquisition and Target Tracking (Hover and Low Speed)

b) All Other MTE's (Hover and Low Speed)

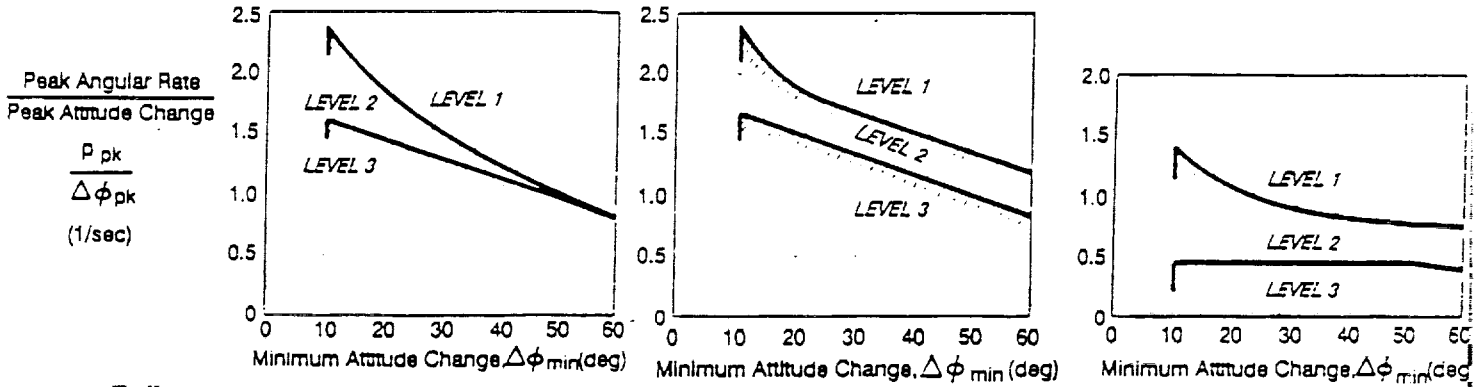

Roll

c) Target Acquisition and Target Tracking (Hover and Low Speed)

d) Air Combat (Forward Flight)

e) All Other MTE's (Hover / Low Speed and Forward Flight)

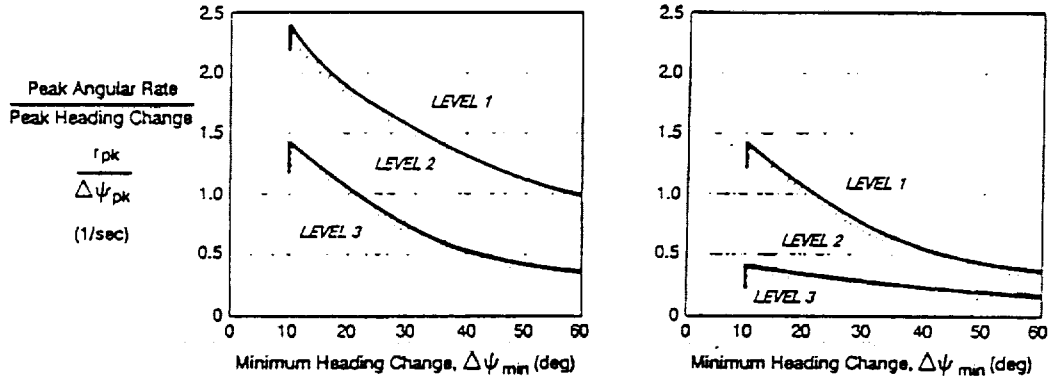

Heading

f) Target Acquisition and Target Tracking (Hover and Low Speed)

g) All Other MTE's (Hover and Low Speed)

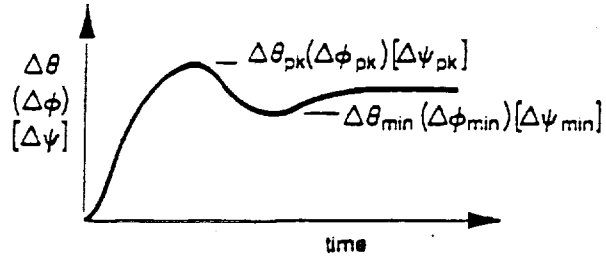

h) Definition of Moderate -Amplitude Criterion Parameters

Figure 1. Requirements for Moderate Amplitude Attitude Changes (Attitude Quickness)

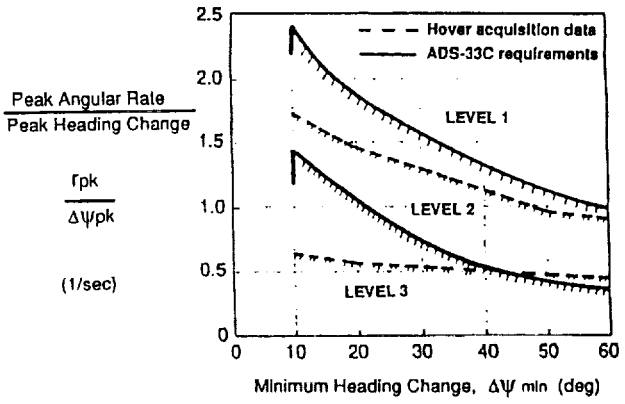

Figure 2. Refined Heading Attitude Quickness Boundaries for Target Acquisition and Tracking (hover/low speed).

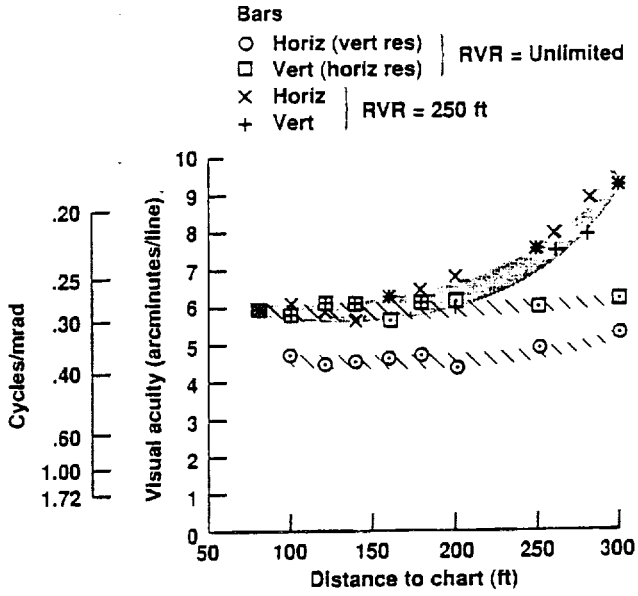

Figure 4. Resolution Results from the VMS Singer-Link DIG 1 (from Ref. 6).

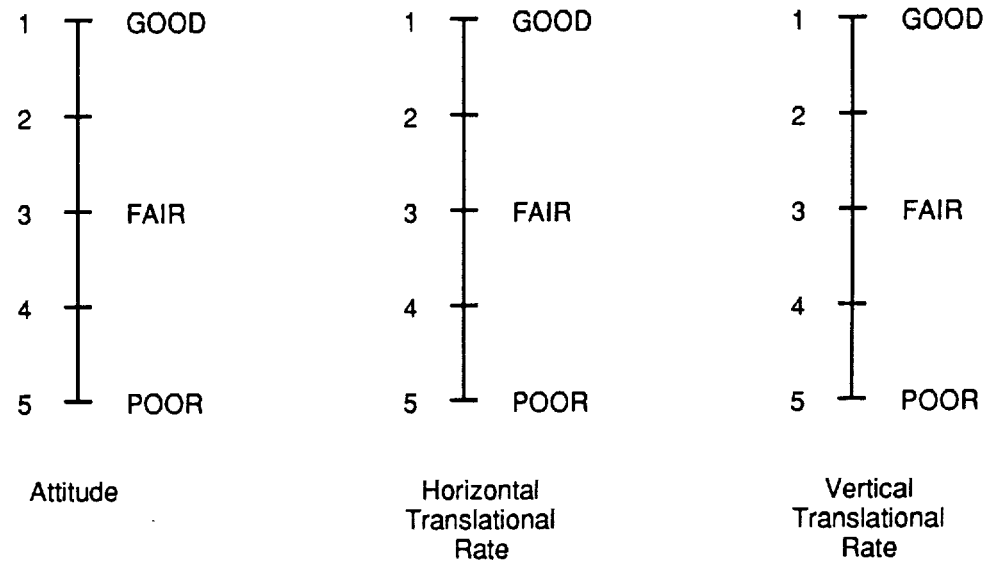

Pitch, roll, and yaw attitudes, and lateral-longitudinal and vertical translational rate shall be evaluated for effectiveness for stabilization and control according to the following definitions:

GOOD: Can make aggressive and precise corrections with confidence and precision is good.

FAIR: Can make limited corrections with confidence and precision is only fair.

POOR: Only small and gentle corrections are possible and consistent precision is not attainable.

Figure 3. Modified Visual Cue Rating (VCR) Scale to be Used When Making UCE Determinations.

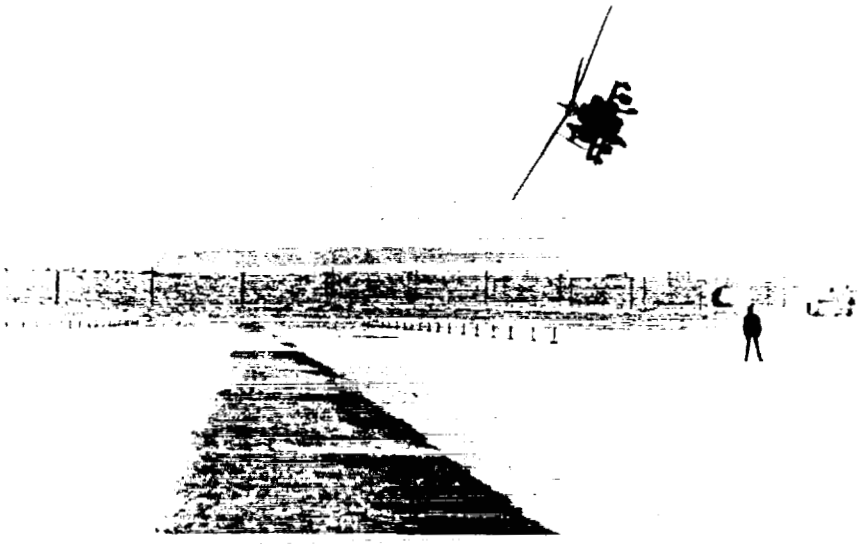

Figure 5. AH-64 Apache Performing ADS-33C Rapid Slalom.

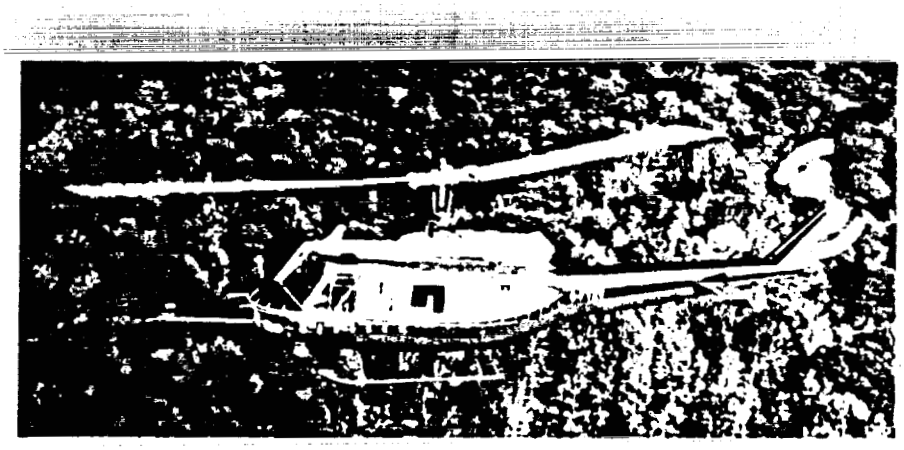

Figure 6. IAR Variable-Stability Bell 205 Airborne Simulator

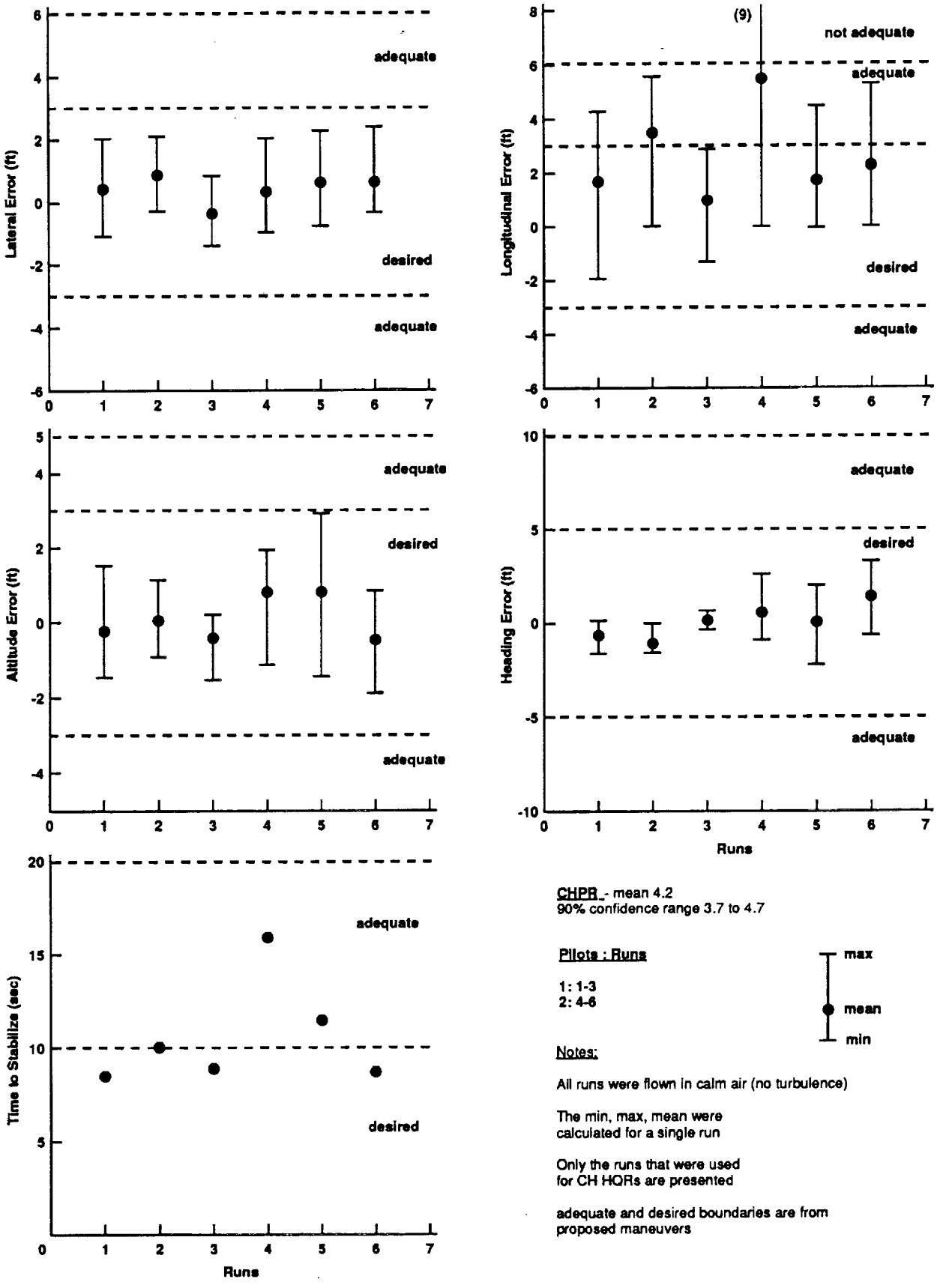

Figure 7. Hover task, Level 1 Rate Command Response-Type

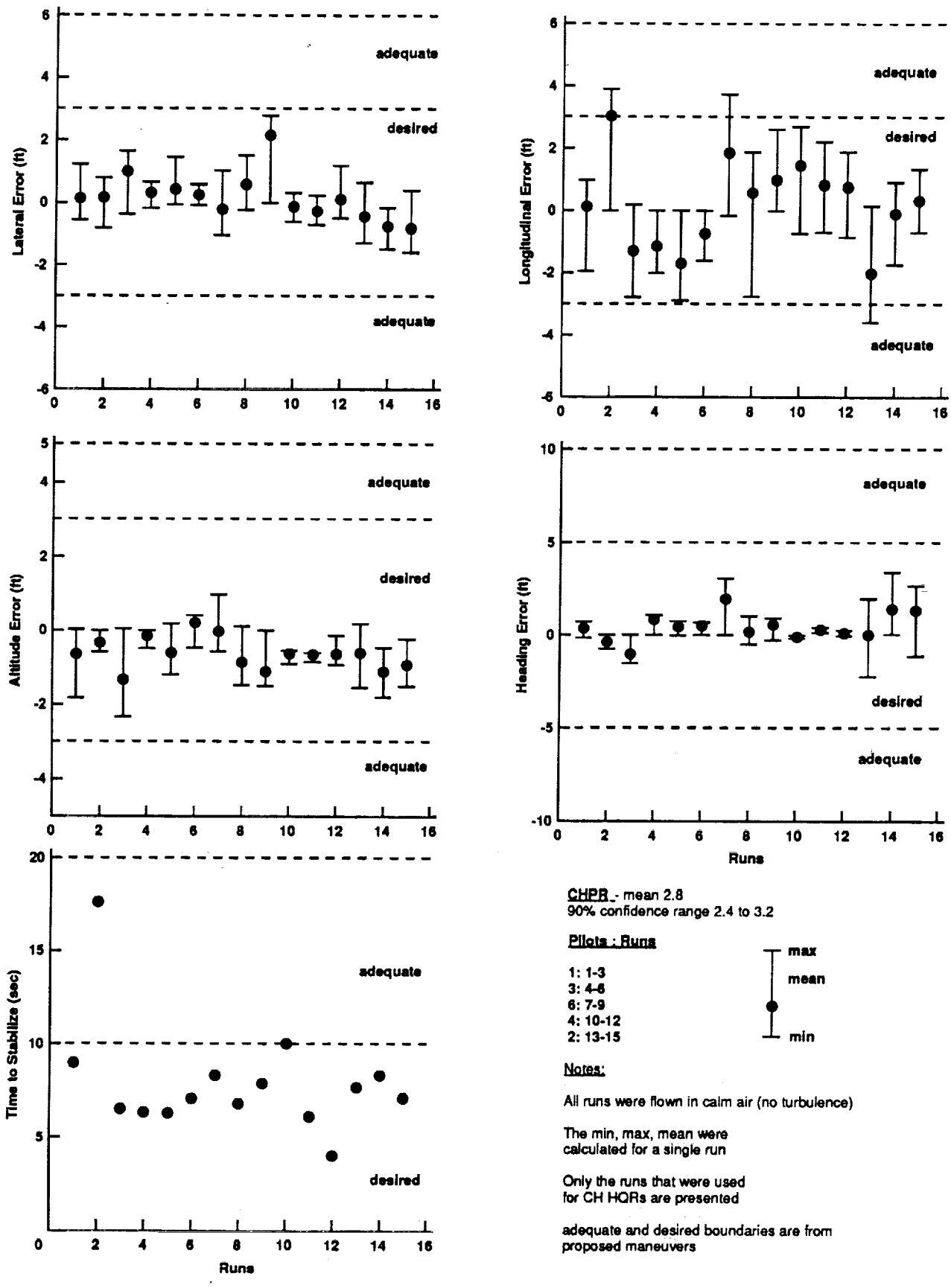

Figure 8. Hover task, Level 1 Attitude Command Attitude Hold (ACAH) Response-Type

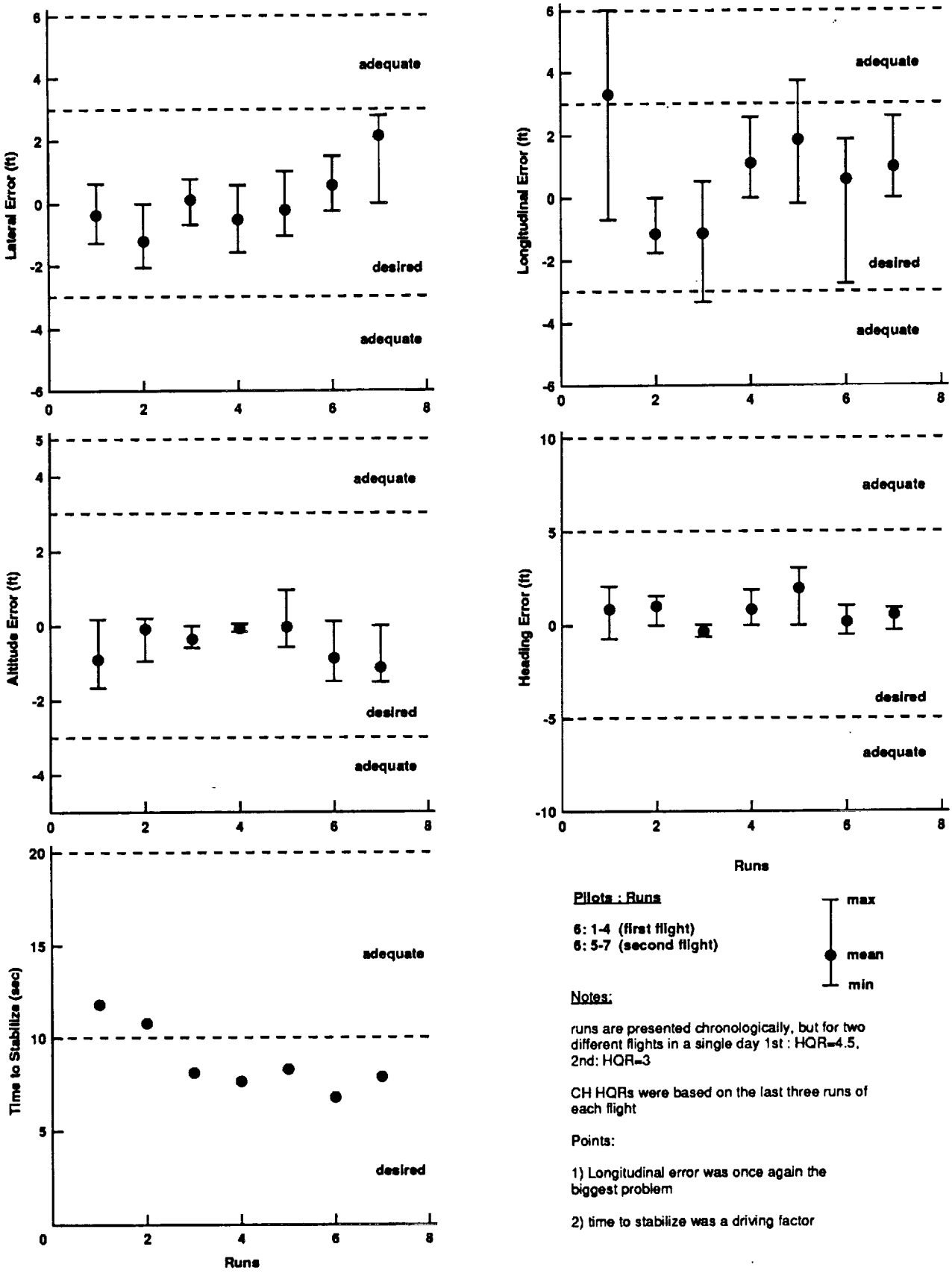

Figure 9. Hover task, Level 1 ACAH Response-Type – Effect of Training

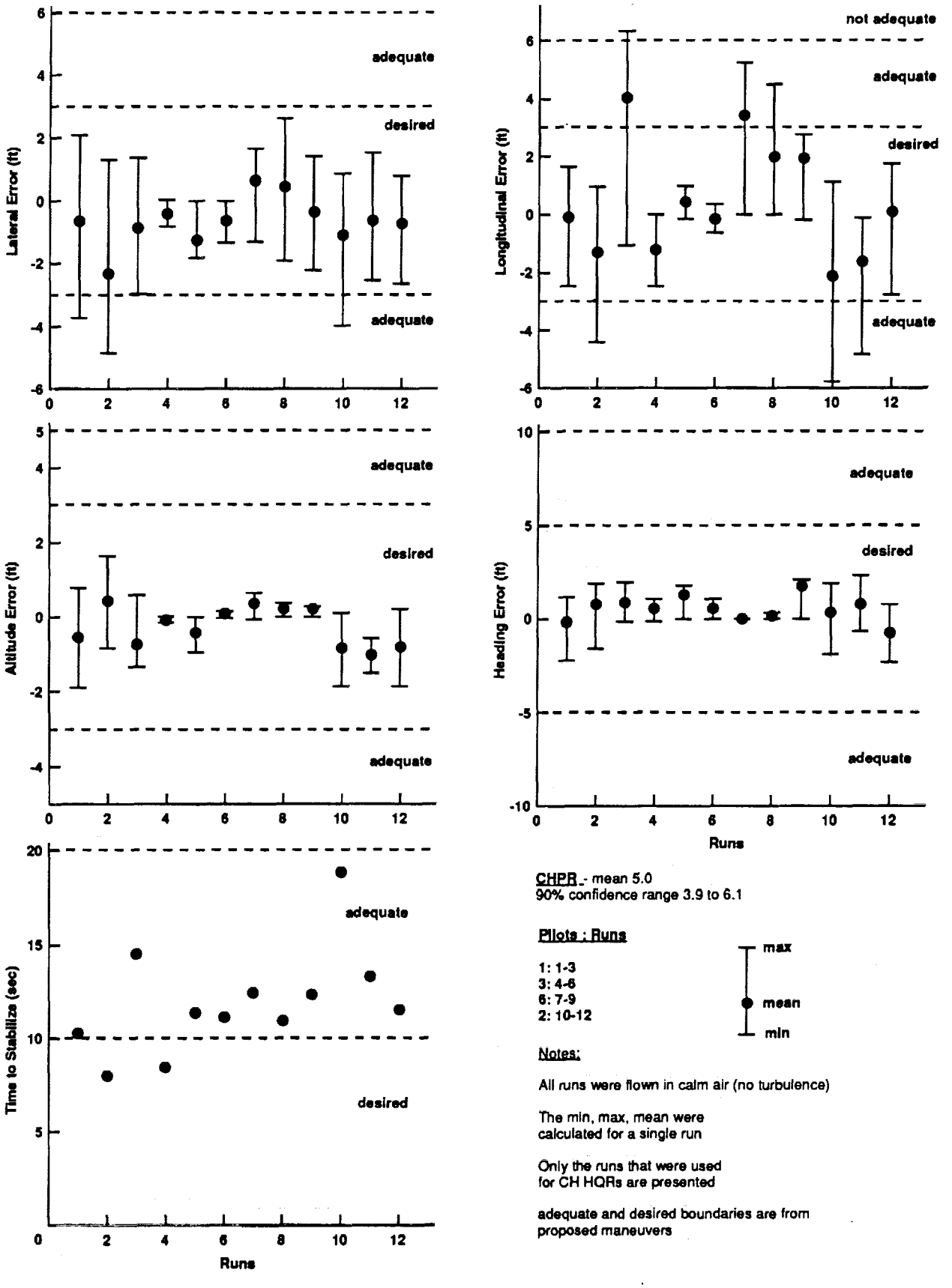

Figure 10. Hover task, Level 2 ACAH Response-Type

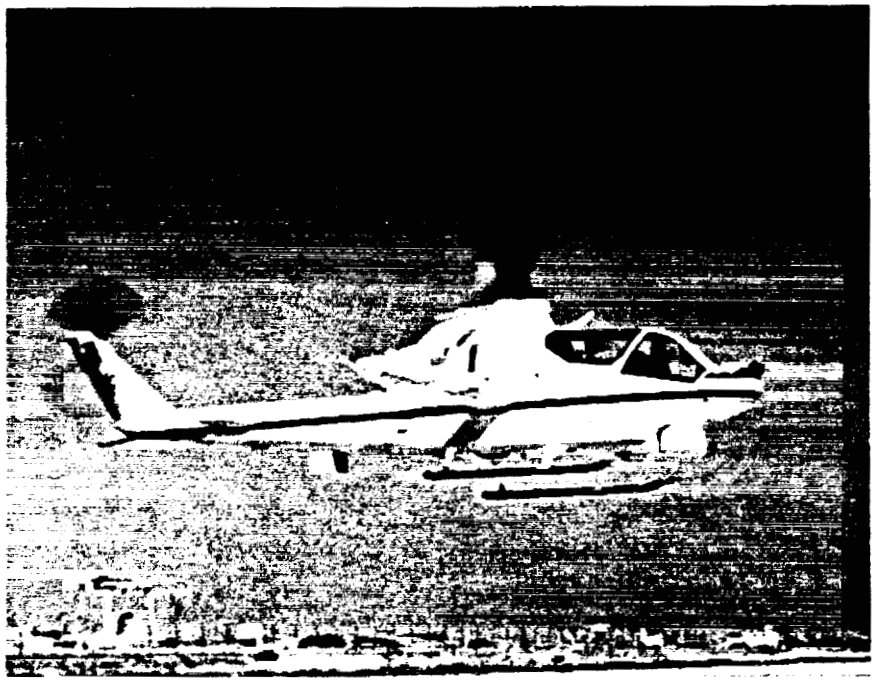

Figure 11. Army/NASA AH-1G Cobra Equipped with Apache IHADSS

APPENDIX

4.1 PRECISION TASKS (DAY)

ADS-33C TASK DEFINITION

4.1.1 Hover. Maintain a precision hover for at least 30 sec in winds of at least 20 knots from the most critical direction. If a critical direction has not been defined, the hover shall be accomplished with the wind blowing directly from the rear of the rotorcraft. The hover altitude shall be equal to or less than 6.1m (20 ft).

Desired Performance

- Maintain horizontal position of the pilot's station within 0.91m (3 ft) of a reference point on the ground.
- Maintain altitude within ± 0.61m (2 ft).
- Maintain heading within ± 5 degrees.
- There shall be no objectionable oscillations in any axis. In particular, oscillations which interfere with precision control, or with operation of controls or switches, would be deemed objectionable.

NEW PRECISION TASK DEFINITION

4.1.1 Hover.

Objectives

Check ability to transition from translating flight to a stabilized hover with precision and a reasonable amount of aggressiveness.

Check ability to maintain precise position, heading, and altitude in the presence of a moderate wind from the most critical direction.

Description of Maneuver

Initiate the maneuver at a ground speed of between 6 and 10 knots, at an altitude less than 6.1m (20 ft). The desired hover point shall be oriented approximately 45 degrees relative to the heading of the aircraft. The ground track should be such that the aircraft will arrive over the target hover point (see illustration in "description of test course"). The maneuver is to be accomplished in calm and moderate winds from the most critical direction. If a critical direction has not been defined, the hover shall be accomplished with the wind blowing directly from the rear of the rotorcraft. This maneuver is to be performed with any available hover or position hold functions turned on.

Description of Test Course

The suggested test course for this maneuver is shown in Figure A-1. Note that the hover altitude depends on the height of the reference symbol, and the distance between that symbol, the hover-board, and the helicopter. These dimensions may be adjusted to achieve a desired hover altitude.

Desired Performance

- -- The transition to hover should be accomplished in one smooth maneuver. It is not acceptable to accomplish most of the deceleration well before the hover point and then to creep up to the final position. The time from the initiation of deceleration to a stabilized hover must not exceed 3 seconds.
- -- Transition to the stabilized hover should be such that once the rotorcraft is within the hover box (see Fig. A-1), it should remain within that volume for at least 30 seconds.
- -- Maintain the longitudinal and lateral position within ± 0.91m (± 3 ft) of a point on the ground and altitude within ± 0.61m (± 2 ft). Keeping the hover reference symbol within the desired box on the hover board (Fig. A-1) will insure desired lateral and vertical performance.
- -- Maintain heading within ± 5 degrees.
- -- There shall be no objectionable oscillations in any axis either during the stabilized hover, or the transition to hover.

Adequate Performance

- -- The transition to the stabilized hover should be accomplished in one smooth maneuver. It is not acceptable to accomplish most of the deceleration well before the hover point and then to "creep up to" the final position. The time from the initiation of deceleration to a stabilized hover must not exceed 8 seconds.
- -- Transition to the stabilized hover should be such that once the rotorcraft is within the hover box (see Fig. A-1), it should remain within that volume for at least 30 seconds.
- -- Maintain longitudinal and lateral position within ± 1.83 m (± 6 ft); see test course description.
- -- Maintain altitude within ± 1.22 m (± 4 ft).
- -- Maintain heading within ± 10 degrees.

4.4 PRECISION TASKS IN THE DEGRADED VISUAL ENVIRONMENT

The following precision maneuvers shall be flown in the Degraded Visual Environment (DVE) specified in Paragraph 3.1.1, and using the displays and vision aids which will be available to the pilot. The wind conditions may be calm, but it would be desirable to demonstrate the maneuvers in stronger winds.

ADS-33C TASK DEFINITION (DVE)

4.4.1 Hover. Maintain a steady hover at an altitude of not more than 6.1 m (20 ft) above the ground.

Desired Performance

- -- Maintain horizontal position of the pilot station within 0.9 m (3 ft) of a reference point on the ground.
- -- Maintain altitude within ±0.91 m (3 ft).
- -- Maintain heading with ±5 degrees.
- -- There shall be no objectionable oscillation in attitude or position.

NEW TASK DEFINITION

4.4.1 Hover.

Objectives

Check ability to transition from translating flight to a stabilized hover with precision and a reasonable amount of aggressiveness in the DVE.

Check ability to maintain precise position, heading, and altitude in the DVE.

Description of Maneuver

Initiate the maneuver at a ground speed of between 6 and 10 knots with the desired hover point oriented approximately 45 degrees relative to the heading of the aircraft. The ground track should be such that the aircraft will arrive over the target hover point (see illustration in "description of test course").

Description of Test Course

The suggested test course for this maneuver is shown in Figure A-1. Note that the hover altitude depends on the height of the reference symbol, and the distance between that symbol, the hover-board, and the helicopter. These dimensions may be adjusted to achieve a desired hover altitude. The hover board will have to be modified from Figure 4.1 to reflect the increased altitude tolerances allowed for the DVE.

Desired Performance

- -- The transition to hover should be accomplished in one smooth maneuver. It is not acceptable to accomplish most of the deceleration well before the hover point and then to creep up to the final position. The time from the initiation of deceleration to a stabilized hover must not exceed 10 seconds.
- -- Transition to the stabilized hover should be such that once the rotorcraft is within the modified hover box (see Fig. A-1), it should remain within that volume for at least 30 seconds.
- -- Maintain the longitudinal and lateral position within $\pm$ 0.9 m ($\pm$ 3 ft) of a point on the ground and altitude within $\pm$ 0.91 m ($\pm$ 3 ft). Keeping the hover reference symbol within the desired box on the modified hover board (Fig. A-1) will insure desired lateral and vertical performance.
- -- Maintain heading with $\pm$ 5 degrees.
- -- There shall be no objectionable oscillations in any axis either during the stabilized hover, or the transition to hover.

Adequate Performance

- -- The transition to the stabilized hover should be accomplished in one smooth maneuver. It is not acceptable to accomplish most of the deceleration well before the hover point and then to "creep up to" the final position. The time from the initiation of deceleration to a stabilized hover must not exceed 20 seconds.
- -- Transition to the stabilized hover should be such that once the rotorcraft is within the modified hover box, it should remain within that volume for at least 30 seconds.
- -- Maintain longitudinal and lateral position within $\pm$ 1.83 m ($\pm$ 6 ft); see test course description.
- -- Maintain altitude within $\pm$ 1.53 m ($\pm$ 5 ft).
- -- Maintain heading within $\pm$ 10 degrees.

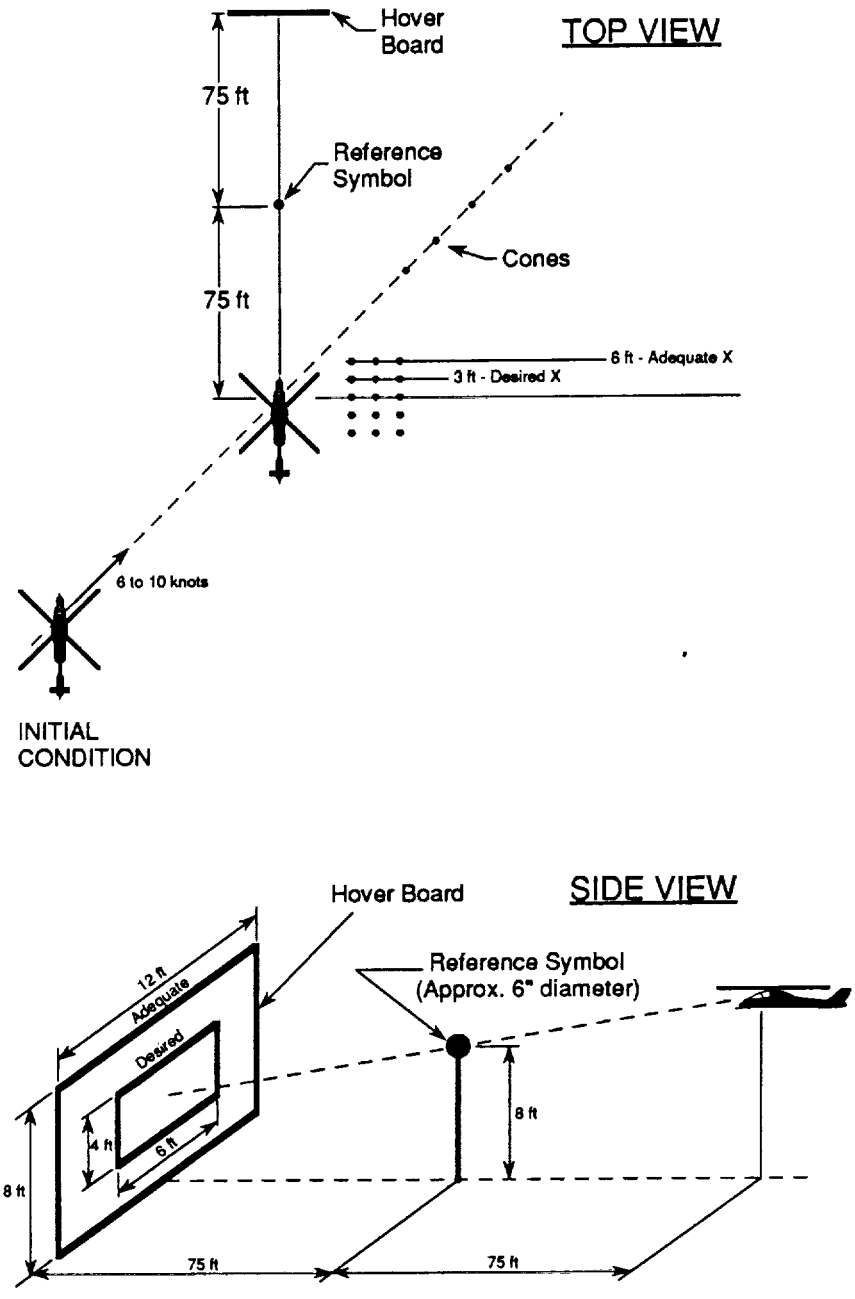

Figure A-1. Suggested Precision Hover Task Cuing and Standards.

Investigation of the Effects of Bandwidth and Time Delay on Helicopter Roll-Axis Handling Qualities

Heinz-Jürgen Pausder
Deutsche Forschungsanstalt für
Luft- und Raumfahrt e.V. (DLR)
Institut für Flugmechanik
D-3300 Braunschweig, FRG

and

Chris L. Blanken
Aeroflightdynamics Directorate
US Army Aviation and Troop Command
Ames Research Center
Moffett Field, California, USA

ABSTRACT

Several years of cooperative research conducted under the U.S./German Memorandum of Understanding (MOU) in helicopter flight control has recently resulted in a successful handling qualities study. The focus of this cooperative research has been the effects on handling qualities due to time delays in combination with a high bandwidth vehicle. The jointly performed study included the use of U.S. ground-based simulation and German in-flight simulation facilities. The NASA-Ames Vertical Motion Simulator (VMS) was used to develop a high bandwidth slalom tracking task which took into consideration the constraints of the facilities. The VMS was also used to define a range of the test parameters and to perform initial handling qualities evaluations. The flight tests were conducted using DLR's variable-stability BO 105 S3 Advanced Technology Testing Helicopter System (ATTHeS). Configurations included a rate command and an attitude command response system with added time delays up to 160 milliseconds over the baseline and bandwidth values between 1.5 and 4.5 rad/sec. Sixty-six evaluations were performed in about 25 hours of flight time during ten days of testing. The results indicate a need to more tightly constrain the allowable roll axis phase delay for the Level 1 and Level 2 requirements in the U.S. Army's specification for helicopter handling qualities, ADS-33C.

Presented at the *18th European Rotorcraft Forum*, Avignon, France, September 1992, and at *Piloting Vertical Flight Aircraft: A Conference on Flying Qualities and Human Factors*, San Francisco, California, January 1993.

INTRODUCTION

An updated military rotorcraft handling qualities specification has been published and adopted by the U.S. Army Aviation and Troop Command as Aeronautical Design Standard (ADS-33) (Ref. 1). Although the ADS-33 is a U.S. specification at present, the ADS-33 is of international interest and some international studies have contributed to the data bases for the definition of the requirements. The overall philosophy follows that of the fixed-wing aircraft specification, MIL-F-8785C, although specific requirements have been generated to cover helicopter characteristics and modern military helicopter missions. The ADS-33 is a mission-oriented specification, based upon the mission task elements and the cueing available to the pilot. Minimum requirements are established for control response types and their characteristics. These requirements are categorized into terms of small, moderate, and large amplitude attitude changes and are defined for comparison with the rotorcraft characteristics. This provides a quantitative assessment of the Level of rotorcraft handling qualities. These Levels are related to the Cooper-Harper handling qualities rating scale (Ref. 2), Figure 1. The small amplitude response requirements include both short-term and mid-term responses where the short-term response refers to the rotorcraft characteristics in pilot tasks such as closed-loop, compensatory tracking and the mid-term response criteria are intended to ensure good flying qualities when less precise maneuvering is required.

The requirements for the short-term response are specified in terms of a frequency based criterion called bandwidth. The frequency response data required to mea-

sure the bandwidth parameters are defined in Figure 2. The bandwidth, ω_{BW}, is measured from a frequency response (Bode) plot of the rotorcraft angular attitude response to the cockpit controller input and must include all the elements in the flight control system. Generally, a good system will have a high bandwidth and a poor system will have a low bandwidth. The bandwidth criterion is an application of the crossover model concept (Ref. 3). It is based on the premise that the maximum crossover frequency that a pure gain pilot can achieve, without threatening the stability, is a valid figure-of-merit of the controlled element. Physically, low values of bandwidth indicate a need for pilot lead equalization to achieve the required mission performance. Excessive demands for pilot lead equalization have been shown to result in degraded handling qualities ratings. The efforts to develop bandwidth as a generalized criterion for highly augmented aircraft have shown that the pilots were also sensitive to the shape of the phase curve at frequencies beyond the neutral stability frequency, ω_{180}. This is addressed by the phase delay parameter, τ_p, as defined in Figure 2. Large values of phase delay can arise from many sources, among which are the high order rotor response, control actuator dynamics, filters, and computational time delays. An aircraft with a large phase delay may be prone to pilot induced oscillations (PIO).

As previously stated, ADS-33 is a mission-oriented handling qualities specification and hence, the control response requirements are a function of the degree of divided attention, the visual environment, and the agressiveness demanded in the mission task element (MTE). The forward flight (> 45 knots) bandwidth criteria for the roll axis are shown in the Figure 3. Three sets of limits are specified: the more stingent limits apply to the air combat MTEs and the more relaxed boundaries cover all other MTEs. For divided attention operations (specifically IMC flight), the more relaxed bandwidth values are combined with the more stringent phase delay requirements.

The air combat boundaries are mainly based on a ground-based simulation study. The boundaries for all other MTEs were primarily established from flight tests with helicopters having relatively low inherent roll and pitch damping which result in low bandwidth. Also, the evaluation tasks appear to have been low-precision and moderate or large amplitude tasks. Some recent, but limited data, has indicated that some refinement in these boundaries may be necessary in the region of high bandwidth and high phase delay. Helicopters having a large flapping hinge offset and full authority digital control systems have this potential.

Under the U.S./German Memorandum of Understanding (MOU) for cooperative research in helicopter flight control, the U.S. Army Aviation and Troop Command's Aeroflightdynamics Directorate and the German's DLR Institute for Flight Mechanics have been performing research in handling qualities. The most recent task has been to study the effects on handling qualities due to time delays in combination with a high bandwidth response vehicle. Specifically, the effect of time delay in roll axis tasks in forward flight (around 60 knots) has been investigated. The technical approach has been to use the U.S. ground-based simulator to define the piloting task and to explore the scope of the variation of system configurations and then use the German helicopter in-flight simulator ATTHeS for the evaluation flight tests while covering a more finely meshed set of configurations.

This paper will discuss the existing data base, the approach used to develop a task specifically adapted for the in-flight simulation, the complementary use of the NASA-Ames ground-based Vertical Motion Simulator (VMS) and the DLR Advanced Technology Testing Helicopter System (ATTHeS) in-flight simulator, and the handling qualities results.

DISCUSSION OF EXISTING DATA

The ADS-33 forward flight roll axis bandwidth criteria in Figure 3 are divided into three sets of limits covering the effects of task bandwidth and pilot attention. The requirements are applied for rate command and attitude command response types. Figure 4 illustrates the influences of response parameters. For a first order rate command and a second order attitude command response type, the bandwidth and phase delay values are mapped by varying the damping or frequency and time delay parameters. The discussion of the existing data will focus on the air combat limits, the limits for all other MTE's - VMC and fully attended operations, some miscellaneous helicopter data, and related fixed wing requirements.

Air Combat Requirements

As previously stated, the roll-axis air combat bandwidth limits were established from a ground-based simulation study of yaw axis requirements for air combat (Ref. 4). More recently, the roll-axis air combat limits

were specifically investigated in a piloted simulation of pitch and roll requirements for air combat (Ref. 5). This simulation verified the 3.5 rad/sec Level 1 boundary but suggested the Level 2 boundary should be raised to 1 rad/sec. In all these aforementioned investigations the effect of time delay variation was not included. Hence the data from these studies is only pertinent in establishing where the portion of the boundaries intersect the abscissa. The shape of the boundaries above the vertical portion, i.e., the curved portion for phase delays above 0.15 sec, has been established from data applicable to the hover and low speed requirements. In fact, the shape of the roll-axis air combat boundaries are identical to the hover and low speed pitch and roll target acquisition and tracking boundaries. The supporting data for the curvature in these boundaries comes from two experiments: an in-flight pitch tracking study (Ref. 6); and a ground-based pitch tracking study (Ref. 7). Based on these two studies, supporting data for curving the boundaries over for high phase delays and bandwidths is somewhat questionable.

All Other MTE's - VMC and Fully Attended Operations

The forward flight All Other MTE bandwidth limits were established from two flight test experiments (Refs. 8,9). In these experiments the primary variable was roll damping. The effects of time delay were not included and hence the data from these studies is also only pertinent in establishing where the vertical portion of the boundaries intersect the abscissa. The curved portion of the boundaries for the forward flight All Other MTE's are identical to those in the hover and low speed requirements. The hover and low speed roll-axis bandwidth supporting data comes from an in-flight experiment (Ref. 10) using the Canadian Institute for Aerospace Research variable-stability Bell 205 helicopter. This experiment included rate command and attitude command control response types. A variety of hover and low speed tasks were performed but the boundaries were drawn based on the handling qualities ratings from a sidestep task. The criteria boundaries are primarily based on data which does not cover the area of high bandwidth and high phase delay configurations. In addition, there may be some questions concerning the applicability of the evaluation task related to small amplitude precision tracking.

Miscellaneous Helicopter Data

Singular data points achieved in previous tests by the U.S. Army (Ref. 11) and DLR (Ref. 12) are marked in Figure 5. Recognizing the discrepancies between the pilot ratings for these data points and the criteria boundaries, a discussion was started about the need to extend the data base and to verify the Level boundaries. Additional tests were performed with a BO 105 fly-by-wire helicopter using an open loop technique to vary the bandwidth and phase delay. The achieved data points (Fig. 6) underline the request to extend the data base.

Related Fixed Wing Requirements

In the fixed-wing standard (Ref. 13), a bandwidth criterion is only defined for the pitch axis. Although the requirements for the pitch axis are not directly comparable with the roll-axis requirements, the fixed-wing criteria show a fundamental difference in the slopes of the boundaries. The requirements specify a limitation of the phase delay for high bandwith and an upper bandwidth limit whereas, the helicopter requirements allow a higher phase delay with higher bandwidth values without any upper limit for the bandwidth. An interesting aspect can be shown by superimposing the fixed wing requirements for equivalent roll-axis time delays to the phase delay and bandwidth parameters by using a first-order rate and a second-order attitude command system with pure time delay. The requirements for the equivalent time delays in this rough approximation correlate with a limitation on the phase delay (Fig. 7).

The above discussion highlights the need to verify and to extend the existing data and, if necessary, to refine the rotorcraft bandwidth boundaries.

GROUND BASED AND AIRBORNE SIMULATOR

This section will describe the ground-based and in-flight simulation facilities that were used for the pretests and the formal evaluations.

Ground-Based Flight Simulator

The piloted ground-based simulation was conducted on the NASA Ames 6-degree-of-freedom Vertical Motion Simulator (VMS). Figure 8 illustrates the VMS and lists the operational limits of the motion system. The cockpit had a single pilot seat mounted in the center of the cab and four image presentation "windows" to provide outside imagery. The visual imagery was generated using a Singer Link DIG 1 Computer Image Generator (CIG). The CIG data base was carefully tailored to con-

tain adequate macro-texture (i.e., large objects and lines on the ground) for the determination of the rotorcraft position and heading with a reasonable precision. A seat shaker provided vibration cueing to the pilot, with frequency and amplitude programmed as functions of airspeed, collective position, and lateral acceleration. Aural cueing was provided to the pilot by a WaveTech sound generator and cab-mounted speakers. Airspeed and rotor thrust were used to model aural fluctuations. Standard helicopter instruments and controllers were installed in the cockpit.

Mathematical models of the following items were programmed in the simulation host computer: (1) filters for the cockpit controller commands, (2) trim capability, (3) stability command and augmentation system (SCAS), (4) dynamics of the helicopter, and (5) ground effects. The SCAS was a stability-derivative model with known dynamics and no coupling (Ref. 14), and the character of its response was easily manipulated by changing the stability derivatives. A buffer between the pilot's controls and the SCAS enabled setting the desired amounts of pure time delay. The baseline stick-to-visual delay was 70 msec.

Airborne Flight Simulator ATTHeS

The DLR Institute for Flight Mechanics has developed a helicopter in-flight simulator. The Advanced Technology Testing Helicopter System (ATTHeS) is based on a BO 105 helicopter (Fig. 9). The testbed is equipped with a full authority nonredundant fly-by-wire (FBW) control system for the main rotor and fly-by-light (FBL) system for the tail rotor. The testbed requires a two-person crew consisting of a simulation pilot and a safety pilot. The safety pilot is equipped with the standard mechanical link to the rotor controls whereas, the simulation pilot's controllers are linked electrically/optically to the rotor controls. The FBW/L actuator inputs, which are commanded by the simulation pilot and/or the control system, are mechanically fed back to the safety pilot's controllers. With this mechanization, the safety pilot is enabled to monitor the rotor control inputs. The testbed can be flown in three modes: (1) the FBW/L disengaged mode, where the safety pilot has the exclusive control, (2) the 1:1 mode, where the simulation pilot has the full authority to fly the baseline helicopter, and (3) the simulation mode, where the simulation pilot is flying a simulated helicopter command model with full authority. In the 1:1 and the simulation modes the flight envelope of the testbed is restricted to not lower than 50 ft above the ground in hover and 100 ft in forward flight.

For in-flight simulation purposes, the most promising method of a control system design is to force the host helicopter to respond on the pilot's inputs as an explicitly calculated command model. The ATTHeS explicit model following control system (MFCS) design provides the airborne simulator with the demanded level of simulation flexibility. A detailed description of the ATTHeS in-flight simulation system is given in References 15,16. The capability of the ATTHeS simulator is described by a high quality of simulation fidelity up to a frequency of about 10 rad/sec in the roll axis. The level of decoupling which can be achieved with a decoupled command model is significantly lower than 10 percent of the on-axis response. For these tests, a control computer cycle time of 40 msec was realized. A generated subcycle one-fifth of the frame time allowed refreshing of the FBW/L actuator inputs in a lower time frame than the main cycle which was 16 msec for this bandwidth study. The equivalent time delay for the overall system due to high order rotor effects, actuators dynamics, computational time and pilot input shaping was 100 to 110 msec in the roll axis and 150 to 160 msec in the pitch axis related to first-order rate command responses.

DEVELOPMENT OF SLALOM TRACKING TASK

The objective of this study was to investigate the effects of time delay on the small amplitude (< 10 deg) roll attitude response to control inputs, i.e., the bandwidth criteria. This criteria is applicable to continuous precision tracking with aircraft attitude. A key to the success of this study was to develop an appropriate small amplitude precision tracking task that could be implemented both on the ground-based and on the in-flight simulator while considering the constraints of each. For the ground-based simulator, some of these constraints include a reduced field of view and visual resolution whereas, for the flight tests these include 100 feet minimum altitude. In adition, it was desired to keep the complexity of the task cueing to a reasonable level to minimize the building of exotic and expensive task cues. Based on previous slalom testing experience (Refs. 8,18), a modified slalom task with precise tracking phases through a set of gates was proposed (Fig. 10). This course layout included transition and precision tracking phases. The transition phases were intended to be a lower frequency disturbance with the main emphasis of the task being the higher frequency tracking

phases just prior to and through the gates. The relative spacing between successive gates was established through the use of an inverse modelling technique (Ref. 19) that considered the aircraft response, speed, bank angle, and the time to travel between the gates. The width of a gate (desired performance) was three meters. In pre-tests on the VMS and with an operational BO 105 helicopter, the adequacy of the task was evaluated. It should be noted that due to the relative poor visual resolution in the VMS (approximately 0.35 cycles per milliradians (Ref. 20)), the task had to be flown at 50 feet instead of 100 feet.

Figure 11 shows a typical time history based upon flying through the VMS course. Also shown is a frequency domain plot of the lateral control input. From these one can see the lower frequency large amplitude inputs used in the transition between the gates and the higher frequency small amplitude control inputs that occur during the final acquisition and tracking through the gates. The flight test data show a very similar tendency with low frequency inputs between the gates and an additional peak in the power or amplitude spectrum, which is 1 Hz and higher, for the acquisition and tracking phases.

CONDUCTION OF TESTS

For the pilot evaluatios, a first-order rate command (RC) and a second-order attitude command (AC) response system was defined for both the roll and pitch axes. Table 1 shows the form of these command responses. A rate of climb response and a sideslip command were implemented for the vertical and the directional axes respectively. The response to the pilot's inputs were decoupled except for the terms formulating the turn coordination and the pseudo altitude hold. A feedforward to the collective was implemented as a function of the roll attitude. For the RC response, the primary experimental variables were the roll damping, L_p, and the time delay, τ. For the AC response, the primary variables were the narural frequency, ω_n, and the time delay, τ. The relative damping was held constant at 0.7. The pitch axis parameters were varied in harmony with the roll axis parameters. A variation and selection of the optimal control sensitivity (L_δ) values were defined in the VMS simulations. This selection process covered a range of natural frequencies and dampings for the attitude and rate command response types. Initial in-flight evaluations confirmed these sensitivities.

To gain an initial impression of the task and the sensitivity to the experimental variables, piloted simulation tests were conducted on the VMS. The studied configurations together with pilot ratings are shown in Figure 12. The configurations are summarized in Table 2. The VMS results demonstrate the consistency between the RC and AC ratings and support the premise that the bandwidth criteria is independent of the response type. These results also supported the selection of the flight test configuration matrices which are shown in Table 3.

The flight tests were conducted at the German Forces Flight Test Center (WTD 61) in Manching. Twenty-eight flight hours were performed within 10 days. Four test pilots, one each from DLR, U.S. Army, WTD 61, and DRA-Bedford were involved in the tests. All pilots were experienced test pilots. The U.S. Army pilot also performed the VMS evaluations.

The following signals were measured in the flight tests: (1) position of the helicopter in relation to the ground track course, (2) pilot control inputs, (3) angular attitudes and rates, (4) accelerations, (5) airspeed, and (6) MFCS internal signals like command to the actuators. Because of the limited space in the test helicopter, the tests had to be observed from the ground station. On two quicklook terminals selected onboard signals were displayed. Additionally, the helicopter position data was displayed online in relation to the tracking gates. The individually achieved task performance in the tests were computed using the helicopter track in relation to an idealized ground track. With this performance parameter, the effects of training and task performance could be checked. When the test pilot had obtained a nearly constant task performance in the training phase for a given test configuration, two evaluation runs were performed. This test technique was used to ensure the pilot ratings and comments were based on a pilot that was well trained for the task and the configuration. For each configuration, the pilot had to fill out a questionnaire and had to summarize his evaluation in a Cooper Harper handling qualities rating. The questions were related to task performance, pilot workload, and system response characteristics. At least two test pilots flew each configuration but when the difference in the two ratings was higher than one rating point an evaluation with a third pilot was conducted. This technique allowed the coverage of a high number of configurations.

In Figure 13, a comparison of measured ground tracks for a Level 1 and a Level 2 rated rate command system is shown. The track of the Level 2 configuration shows that problems occured in the acquisition and track-

ing phases where the tracking performance was especially degraded through the second and the fourth gate. This change in the task performance correlates with the Cooper Harper rating scale and underlines the consistency of the ratings. In the Cooper Harper rating scale, a rating from 1 to 4 implies that a desired task performance can be achieved with increasing pilot compensation and ratings of 5 and 6 imply only adequate task performance can be achieved. A similar effect can also be seen in Figure 14 which shows time histories of selected attitute command system configurations to compare the rating consistency. In the measured pilot input and roll attitude signals of the Level 2 rated configuration, a slight tendency of pilot induced oscillation can be recognized. This Level 2 configuration had a natural frequency of 1.7 rad/sec and an additional time delay of 120 msec.

DISCUSSION OF RESULTS

To examine the bandwidth and phase delay values for the test configurations, a verification analysis was performed using the measured flight test data. Figure 15 demonstrates the high level of accuracy achieved in selected configurations with ATTHeS. For both rate command and attitude command responses the overall ATTHeS response tends to have an only slightly increased bandwidth value of about 0.1 rad/sec compared with the values calculated with the commanded models. The phase delays are approximated accurately within a spread of about 0.01sec which is within the accuracy of the phase delay assessment method. Summing up the verification results, it can be stated that ATTHeS met the commanded response configurations very well and that the flight test data are credible for an evaluation of the bandwidth requirements.

Figure 16 shows all the flight test Cooper-Harper handling qualities ratings for both response systems, rate and attitude command. A clear consistency of the required bandwidth and phase delay parameters for rate and attitude command systems is demonstrated. This consistency in the rate and attitude command ratings not only demonstrate the premise that the bandwidth criteria is independent of the response type but that the task was appropriate for investigating this criteria. Due to the technique to give the pilots sufficient flight time to familiarize themselves with the task and the configuration, the spread in the ratings for most configurations is not higher than one rating point which underlines the validity for the generated data.

In Figure 17 the averaged ratings of the flight tests and the VMS tests are presented together with recommended Level boundaries. There are several obvious observations. First and foremost, the shape of these recommended Level boundaries is dramatically different than those in the current ADS-33 requirements (see Fig. 3). In particular, these results suggest that there needs to be some upper limits on the phase delay parameter. These results also seem to agree, in concept, with the fixed-wing requirements. Specifically, considering only the flight test data for mid bandwidth configurations a limitation on the phase delay (lower than 0.1 sec for Level 1 and about 0.17 sec for Level 2) seems warranted. As the bandwidth increases, the flight data suggests even less amounts of phase delay are acceptable. Typical pilots' comments include: "I feel that time delay is more an effect" and "Low predictability due to time delay and rapid initial response." These comments are reflected in the degraded pilot ratings. The VMS data does not show this sensitivity in the phase delay as the bandwidth is increased and allows higher phase delays for the Level 2 mid bandwidth region. In the comparison of VMS and flight test data it should be taken into consideration that the VMS tests were performed with only a reduced number of configurations and one test pilot with the objective of evaluating the sensitivity of parameter variations for the definition of the flight test martrices.

Another observation from Figure 17 is that the vertical portions of the boundaries from the VMS and the flight data do not coincide which each other nor with those from the ADS-33C presented in Figure 3. For Level 1, the VMS data recommend at least a bandwidth value of about 3 rad/sec and the flight test data a value of 2.5 rad/sec. The ADS-33 Level 1 requirement is at least 3.5 rad/sec for air combat and 2.0 rad/sec for All Other MTE's - VMC and fully attended operations. For Level 2, the VMS data recommend at least a bandwidth of 2 rad/sec and the flight test data a value of 1.5 rad/sec. ADS-33 Level 2 requires at least 2.0 rad/sec for air combat and 0.5 rad/sec for All Other MTE's. It is speculated that the primary reason for these differences is related to the task bandwidth. It is very difficult to obtain a repeatable yet simple representative air target tracking task. This led to the development of the slalom ground tracking task used for this study. Based upon the pilots' comments, this task, in terms of task bandwidth, is probably somewhere between the air tracking and the All Other MTEs, as defined in the

ADS-33. The aforementioned bandwidth differences between the flight data and the VMS data are also attributable to slight differences in the task bandwidth manifested through differences in cueing. The VMS task was performed from a height of 50 feet whereas, the flight task had to be performed at 100 feet. After the flight tests, the two attitude command configurations with a bandwidth of 2.48 and 3.08 rad/sec and no added time delay were re-evaluated on the VMS at three different altitudes (25, 50, 75 ft) to get more insight on the impact of altitude on task cueing using a computer generated visual system. The test data demonstrate that the altitude was an influencing factor. The pilot ratings were significantly degraded with increasing altitude and the best consistency in the ratings with the flight test ratings was achieved in the 25 foot cases. These data and the variation in the vertical portion of the bandwidth boundaries points out the sensitivity to task differences and the fact that further work is needed which should address a systematical evaluation of the dependency between task bandwidth and Level boundaries and a refinement of the task categorization.

An analysis of control activity was performed to gain additional insight into the effects of changes in the aircraft bandwidth on the pilot's control strategy relative to performing the slalom tracking task. If the aircraft bandwidth is sufficiently higher than the task demands, then the pilot can act as a pure gain (i.e., not apply lead compensation) to satisfactorily perform the task. As the aircraft bandwidth decreases, to maintain desired task performance the pilot must increase his compensation. This increased compensation, which equates to an increase in workload, can cause a degradation in handling qualities. If the aircraft bandwidth is further decreased, then even larger amounts of pilot comsenpation are not sufficient to achieve desired task performance standards. These relations are also considered in the Cooper Harper rating scale. For a rating up to 4, the pilot can achieve desired task performance levels with increasing pilot compensation. Ratings of 5 and 6 mean that only adequate performance can be achieved. The pilot's lateral cyclic input power versus frequency (input auto-spectrum) was used to quantify the pilot's control activity and the effect of aircraft and task bandwidth.

The "pilot cut-off frequency," ω_{co}, was defined as a measure of the pilot's control activity bandwidth. The approach to determining the pilot cut-off frequency was to generate a ratio of root mean square (RMS) values expressed as $\sigma_{co}/\sigma_{total}$, where σ_{co} is the RMS value at the cut-off frequency. The value determined for this ratio was 0.707.

$$[\sigma_{co}/\sigma_{total}]^2 = 0.707^2 = 1/\pi \int_0^{\omega_{co}} G_{\delta\delta} d\omega$$

where; ω_{co} = pilot cut-off frequency
$G_{\delta\delta}$ = auto spectrum of the lateral cyclic control, δ_{lat}
σ_{total} = total RMS of δ_{lat}
σ_{co} = (0.707) σtotal

When the aircraft's bandwidth exceeds the task bandwidth, this pilot cut-off frequency, ω_{co}, approaches the pilot crossover frequency, ω_c, and gives a good approximation of the task bandwidth. The pilot cut-off frequency is just the frequency at which 70.7% of the control input is accounted for, which is also the classic -3dB bandwidth for servomechanisms. An analysis program, CIFER (Ref. 21), developed at AFDD was used to analyze the VMS data. A similar analysis program, DIVA (Ref. 22), was used to analyze the flight data at DLR.

Figure 18 shows the cut-off frequency versus the aircraft control response bandwidth from the VMS simulation. For the high aircraft bandwidth cases, the pilot's cut-off frequency levels off to around 1.5 rad/sec which is representative of the task bandwidth. It's clear that for these high aircraft bandwidths the pilot is not using all of the aircraft capability. As the aircraft bandwidth drops below about 3.0 rad/sec, the pilot's cut-off frequency starts to increase as the pilot trys to maintain task performance. Interestingly, the Level 1-2 boundary for the VMS task was about 3.0 rad/sec. Finally, as the bandwidth drops below about 2.2 rad/sec the pilot can no longer or will not increase his cut-off frequencey to attain even adequate task performance (Level 3 ratings). In other words, there was insufficient margin between excess aircraft control bandwidth and the task demand. Reference 23 implies a positive margin must exist for desired or adequate task performance to be acheived.

Figure 19 shows the pilot cut-off frequency versus the aircraft control response bandwidth from the flight test results for the same pilot who flew the VMS cases. Shown are the rate and attitude command cases with no additional time delay and with additional delays of 40, 80, 120, 160 msec. In general, the flight test results show a trend similar to the VMS results, i.e., as the aircraft bandwidth decreases the pilot cut-off frequency increases.

Based upon this data, the high aircraft bandwidth configurations indicate that the flight test task bandwidth may be around 2.1 rad/sec. It should be pointed out the apparent scatter in the pilot's handling quality rating data on this plot has been manifested by the effects of large phase delay. In some Level 2 attitude command configurations, the pilot used relatively low cut-off frequencies to avoid the pilot induced oscillations (PIO's) that can occur with attitude command response types with time delay. The results of an analysis of the pilot control activity suggest that the slalom tracking task bandwidth was somewhere around two radians per second, maybe a little lower for the VMS and a little higher for the flight tests. Hence with the large excess aircraft bandwidth over the task bandwidth, as provided by the capability of ATTHeS, a very thorough and valid investigation could be conducted into the effects of bandwidth and time delay on helicopter roll-axis handling qualities.

CONCLUSIONS

A helicopter handling qualities study has been conducted to investigate the effect due to time delay. This roll-axis investigation was conducted as a collaborative effort between the U.S. Army's Aeroflightdynamics Directorate (ATCOM) and the German Institute for Flight Mechanics of DLR. A U.S. ground-based flight simulator was used to develop and refine a slalom ground tracking task and to perform preliminary handling quality evaluations. The German in-flight simulator, ATTHeS, a variable stability BO 105 helicopter was used to conduct the flight tests while covering a more complete set of configuration dynamics. In the flight tests rate and attitude command control response configurations were evaluated which included bandwidths between 1.5 and 4.5 rad/sec and additional time delays up to 160 msec. The results of this cooperative research indicate:

1) the individual benefits of both ground-based and in-flight simulation can be used in a complementary and time efficient manner,

2) the developed slalom ground tracking task provided a relatively high gain compensatory tracking task that was sensitive to changes in the bandwidth and phase delay parameters,

3) for the task evaluated, the consistency in the ratings between rate and attitude command response systems verify the independence of the bandwidth parameters to control response type,

4) for the task evaluated, the shape of the Level boundaries for the bandwidth criteria in the U.S. Army's helicopter specification for handling qualities (ADS-33C) needs to be refined by placing upper limits on the phase delay parameter; 0.1 sec for Level 1 and about 0.17 sec for the Level 2 boundary, and

5) the variation in the vertical portion of the bandwidth Level boundaries between the ground-based simulation, the in-flight simulation, and the ADS-33 requirements points out the sensitivity to task bandwidth and the need for further research.

REFERENCES

[1] "Handling Qualities Requirements for Military Rotorcraft," Aeronautical Design Standard – 33 (ADS-33C), August 1989.

[2] Cooper, G.E. and Harper, R.P., " The Use of Pilot Rating in the Evaluation of Aircraft Handling Qualities," NASA TN D-5153, April 1969.

[3] McRuer, D.T. and Krendel, E.S., "Mathematical Models in Human Pilot Behavior," AGARD AG-188, January 1974.

[4] Decker, W.A., Morris, P.M., and Williams, J.N. " A Piloted Simulation Investigation of Yaw Dynamics Requirements for Turreted Gun Use in Low-Level Helicopter Air Combat," American Helicopter Society 44th Annual Forum, Washington, DC, June 1988.

[5] Whalley, M.S. and Carpenter, W.R., " A Piloted Simulation Investigation of Pitch and Roll Handling Qualities Requirements for Air-to-Air Combat," American Helicopter Society 48th Annual Forum , Washington, DC, June 1992.

[6] Houston, S.S. and Horton, R.I., " The Identification of Reduced Order Models of Helicopter Behaviour for Handling Qualities Studies," 13th European Rotorcraft Forum, Arles, France, September 1987.

[7] Aponso, B.L., Mitchell, D.G., and Hoh, R.H., "Simulation Investigation of the Effects of Helicopter Hovering Dynamics on Pilot Performance," Journal of Guidance, Control, and Dynamics, Vol. 13, No. 1, Jan.-Feb. 1990.

[8] Corliss, L.D. and Carico, D.G., "A Flight Investigation of Roll Control Sensitivity, Damping, and Cross-Coupling in a Low-Altitude Lateral Maneuvering Task," NASA TM-84376, Dec. 1983.

[9] Pausder, H.-J. and Gerdes, R.M., " The Effects of Pilot Stress Factors on Handling Qualities Assessments During U.S./German Helicopter Agility Flight Tests," 8th European Rotorcraft Forum, Aix-en-Provence, France, September 1982.

[10] Mitchell, D.G., Hoh, R.H., and Morgan, J.M., "Flight Investigation of Helicopter Low-Speed Response Requirements," Journal of Guidance, Control, and Dynamics, Vol. 12, No. 5, Sept.-Oct. 1989.

[11] Tischler, M. et al., " Application of Flight Control System Methods to an Advanced Combat Rotorcraft," Royal Aeronautical Society International Conference on Helicopter Handling Qualities and Control, London, UK, November 1988.

[12] Pausder, H.-J. and von Grünhagen, W., "Handling Qualities Evaluation for Highly Augmented Helicopters," AGARD-CP-508, Paper No. 26, 1990.

[13] Hoh, R.H. et al., "Proposed MIL Standard and Handbook - Flying Qualities of Air Vehicles, Volume II: Proposed MIL Handbook," AFWAL-TR-82-3081, November 1982.

[14] Lewis, M.S., Mansur, M.H., and Chen, R.T.N., "A Piloted Simulation of Helicopter Air Combat to Investigate Effects of Variations in Selected Performance and Control Response Characteristics," NASA TM-89438, April 1987.

[15] Pausder, H.-J., Bouwer, G., and von Grünhagen, W., "ATTHeS In-Flight Simulator for Flying Qualities Research," DLR International Symposium on In-Flight Simulation for the 90's, Braunschweig, FRG, July 1991

[16] Bouwer G., Pausder, H.-J., and von Grünhagen, W. "ATTHeS-A Helicopter In-Flight Simulator with High Bandwidth Capability," American Helicopter Society 48th Annual Forum, Washington, DC, June 1992.

[17] Kaletka, J. and von Grünhagen, W., "Identification of Mathematical Derivative Models for the Design of a Model Following Control System," American Helicopter Society 45th Annual Forum, Boston, MA., June 1989.

[18] Pausder, H.-J., "A Study of Roll Response Required in a low Altitude Slalom Task," 11th European Rotorcraft Forum, London, UK, September 1985.

[19] Whalley, M.S., "Development and Evaluation of an Inverse Solution Technique for Studying Helicopter Maneuverability and Agility," NASA TM-102889, USAAVSCOM TR 90-A-008, July 1991.

[20] Blanken, C.L., Hart, D.C., and Hoh, R.H., " Helicopter Control Response Types for Hover and Low-Speed Near-Earth Tasks in Degraded Visual Conditions," American Helicopter Society 47th Annual Forum, Phoenix, AZ, May 1991.

[21] Tischler, M.T. and Cauffman, M.G., "Frequency-Response Method for Rotorcraft System Identification: Flight Application to BO 105 Coupled Rotor/Fuselage Dynamics," Journal of the American Helicopter Society, Volume 37, Number 3, July 1992.

[22] Wulff, G., "DIVA on VAX-Computers: Handbook Part 1 - Analysis of Time Dependent Data," DLR IB 111-90/30, June 1990.

[23] Heffley, R.K., Bourne, S.M., Curtiss , H.C., Jr., Hindson, W.S., and Hess, R.A., "Study of Helicopter Roll Control Effectiveness Criteria," NASA Contractor Report 177404, USAAVSCOM TR-85-A-5, April 1986.

Table 1. Form of command responses

Axis	Rate Command	Attitude Command
Pitch	$\frac{q}{\delta_x} = \frac{M_{\delta x}\, e^{-\tau s}}{(s + M_q)}$	$\frac{\theta}{\delta_x} = \frac{M_{\delta x}\, e^{-\tau s}}{(s^2 + 2\zeta\omega_\theta s + \omega_\theta^2)}$
Roll	$\frac{p}{\delta_y} = \frac{L_{\delta y}\, e^{-\tau s}}{(s + L_p)}$	$\frac{\phi}{\delta_y} = \frac{L_{\delta x}\, e^{-\tau s}}{(s^2 + 2\zeta\omega_\phi s + \omega_\phi^2)}$

Table 2. VMS commanded roll-axis configurations

Command Response	Sensitivity (rad/sec^2 / inch)	Added Delay (msec)	Damping - Frequency	Bandwidth (rad/sec)	Phase Delay (sec)
Rate			L_p, sec^{-1}		
	1.0	0	4.0	2.71	0.047
	1.0	100	4.0	1.91	0.119
	1.5	0	8.0	3.88	0.054
	1.5	100	8.0	2.68	0.115
	1.5	200	8.0	1.95	0.176
Attitude			ω_ϕ, rad/sec		
	0.4	0	1.5	2.48	0.056
	0.4	100	1.5	2.07	0.132
	0.7	0	2.0	3.08	0.052
	0.7	100	2.0	2.55	0.126
	0.7	200	2.0	2.20	0.211
	0.7	300	2.0	2.03	0.274
	1.8	0	4.0	5.29	0.046
	1.8	100	4.0	4.11	0.133
	1.8	200	4.0	3.53	0.212
	1.8	300	4.0	3.05	0.286
	1.8	350	4.0	2.85	0.329

Table 3. ATTHeS commanded roll-axis configurations

Command Response	Sensitivity (rad/sec^2 / inch)	Added Delay (msec)	Damping - Frequency	Bandwidth (rad/sec)	Phase Delay (sec)
Rate			L_p, sec^{-1}		
	0.085	0	2.0	1.45	0.081
	0.093	0	3.0	1.93	0.081
	0.093	40	3.0	1.74	0.109
	0.100	0	4.0	2.34	0.080
	0.100	40	4.0	2.06	0.107
	0.100	80	4.0	1.85	0.134
	0.115	0	6.0	2.97	0.078
	0.115	40	6.0	2.55	0.105
	0.115	80	6.0	2.25	0.131
	0.130	0	8.0	3.44	0.077
	0.130	40	8.0	2.91	0.103
	0.130	80	8.0	2.52	0.127
	0.130	120	8.0	2.23	0.151
	0.145	0	10.0	3.82	0.076
	0.145	40	10.0	3.18	0.101
	0.145	80	10.0	2.73	0.125
Attitude			ω_ϕ, rad/sec		
	0.060	0	1.7	2.49	0.083
	0.060	40	1.7	2.34	0.114
	0.060	80	1.7	2.20	0.145
	0.060	120	1.7	2.11	0.175
	0.060	160	1.7	2.02	0.206
	0.100	0	2.3	3.17	0.084
($\zeta = 0.7$)	0.100	40	2.3	2.95	0.114
	0.100	80	2.3	2.77	0.145
	0.180	0	3.0	3.89	0.084
	0.180	40	3.0	3.58	0.115
	0.180	80	3.0	3.34	0.145
	0.180	120	3.0	3.14	0.176
	0.180	160	3.0	2.97	0.207
	0.300	0	4.0	4.80	0.084
	0.300	40	4.0	4.38	0.115

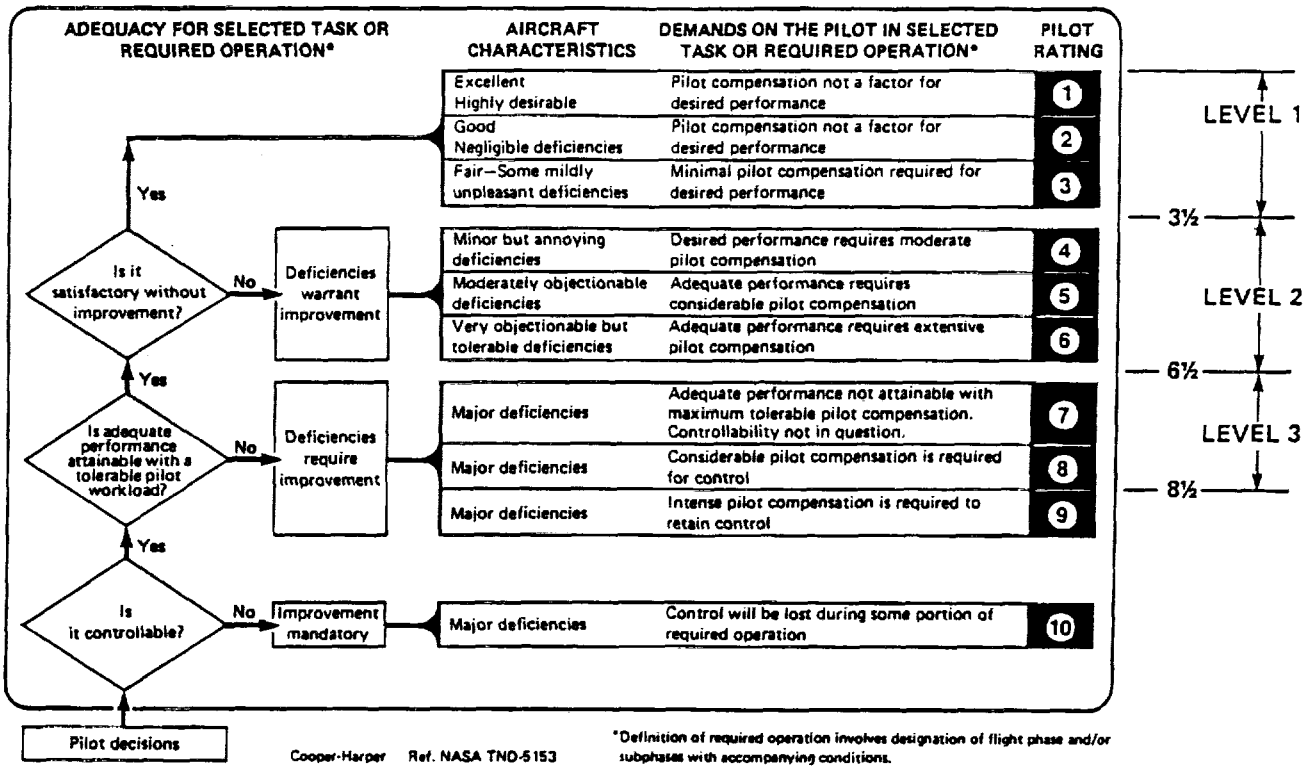

Figure 1. Definition of handling qualities Levels (from Ref. 1).

BANDWIDTH

- **RATE**

ω_{BW} is lesser of $\omega_{BW_{gain}}$ and $\omega_{BW_{phase}}$

- **ATTITUDE COMMAND/ATTITUDE HOLD**

$\omega_{BW} \equiv \omega_{BW_{phase}}$

PHASE DELAY

$$\tau_p = \frac{\Delta\Phi\, 2\omega_{180}}{57.3\,(2\omega_{180})}$$

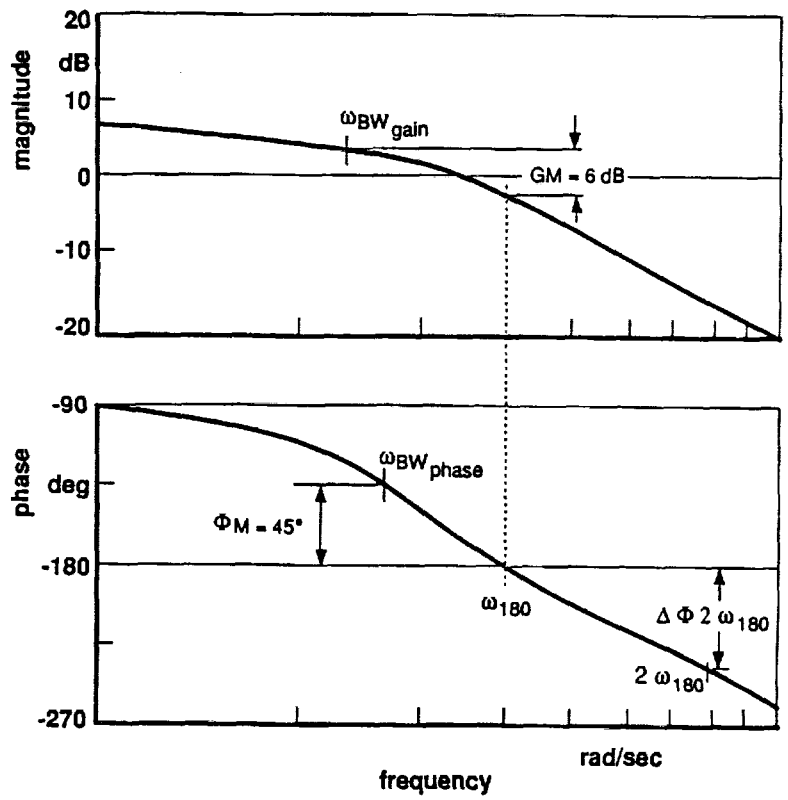

Figure 2. Definition of bandwidth and phase delay.

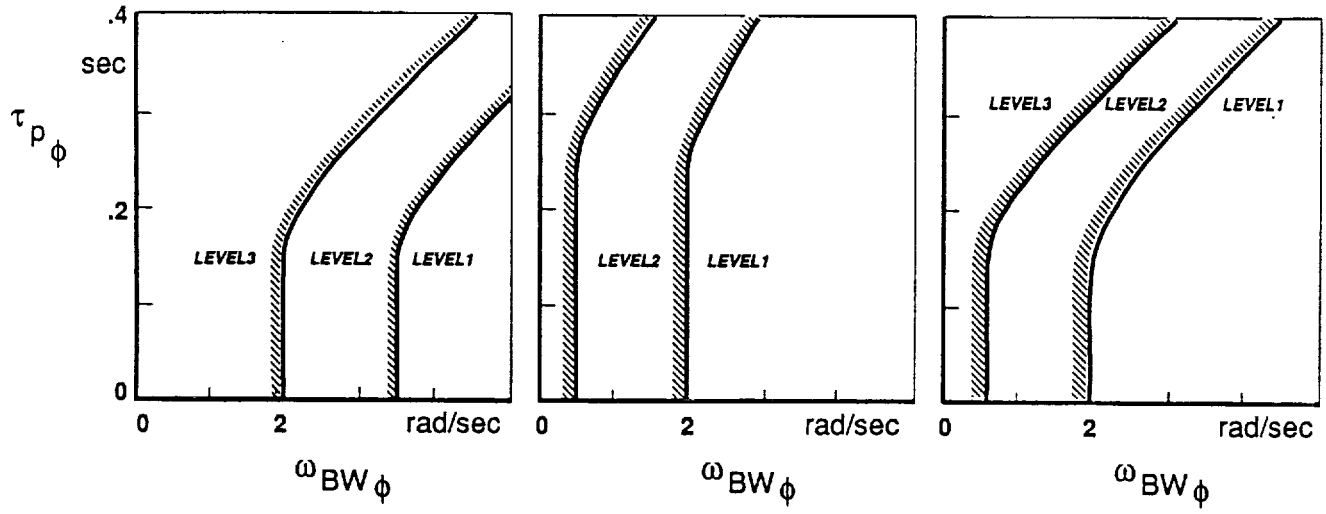

a) Air Combat

b) All Other MTE's - VMC and full attended operations

c) All Other MTE's - IMC and/or divided attention operations

Figure 3. ADS-33C requirements for small-amplitude attitude changes (roll-axis forward flight).

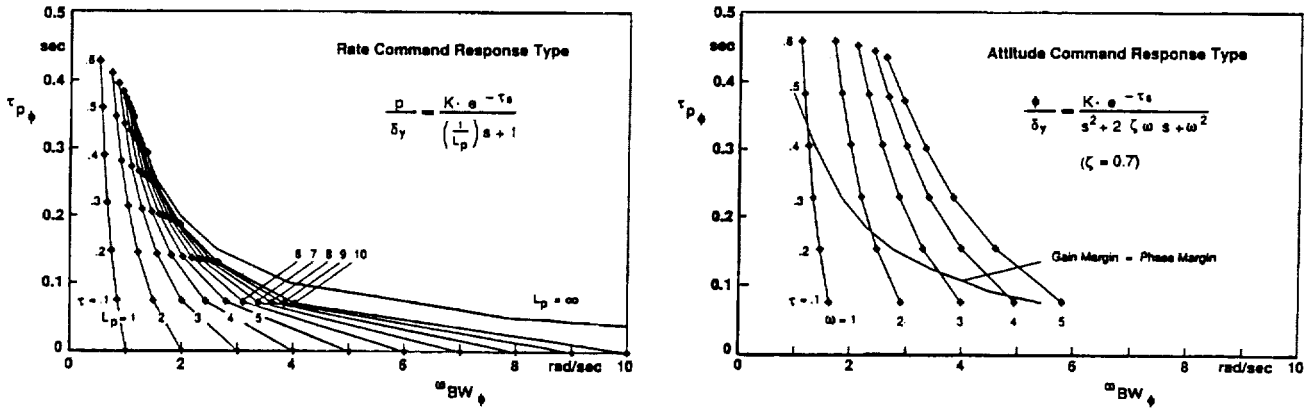

a) Rate command

b) Attitude command

Figure 4. Effect of time delay on bandwidth and phase delay.

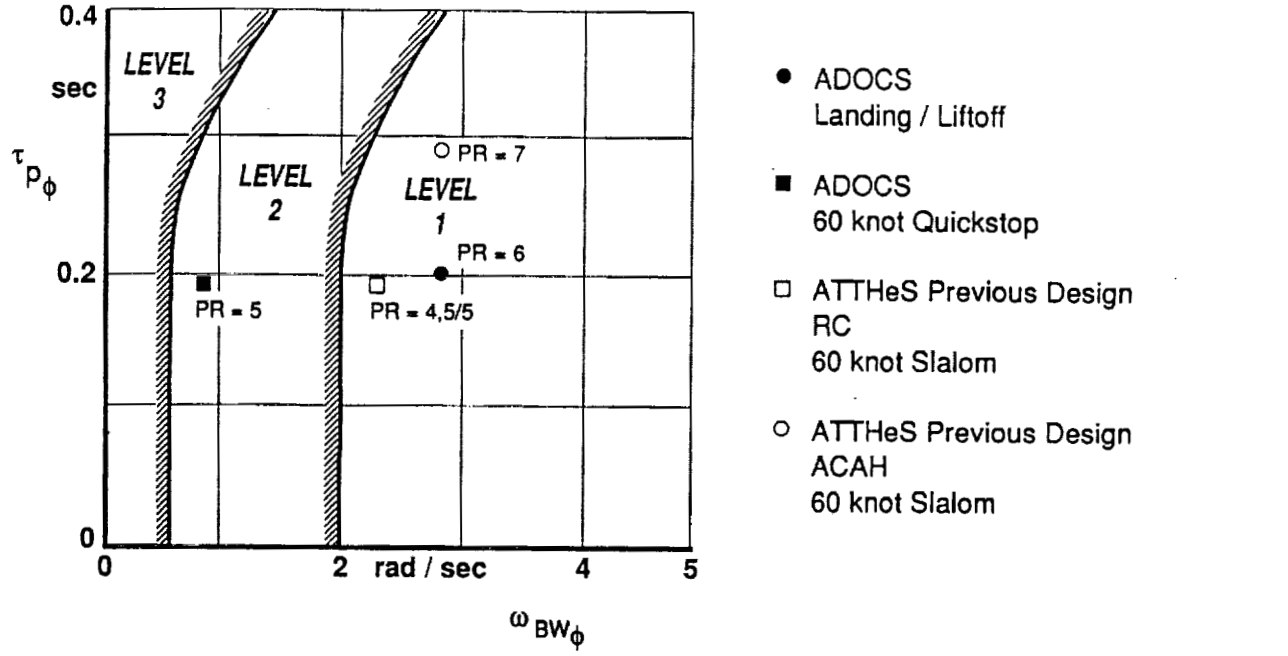

Figure 5. ADOCS (Ref. 11) and ATTHeS (Ref. 12) data points.

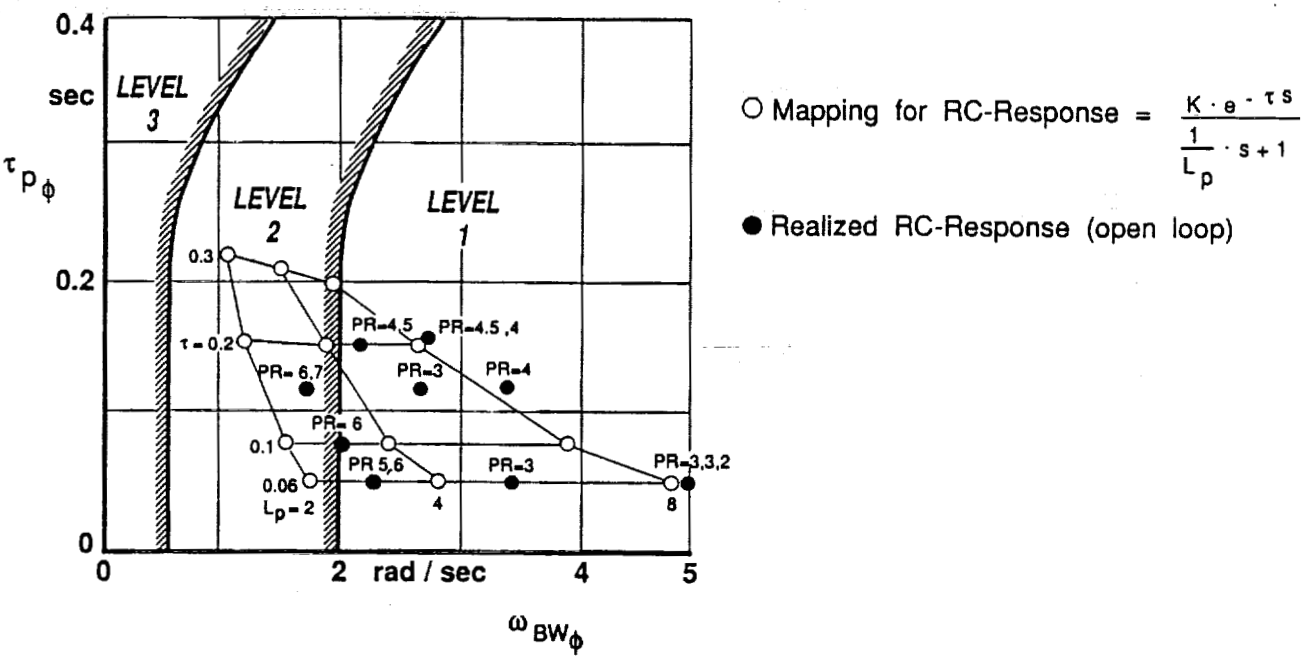

Figure 6. Slalom evaluation data (BO 105 FBW/L open-loop).

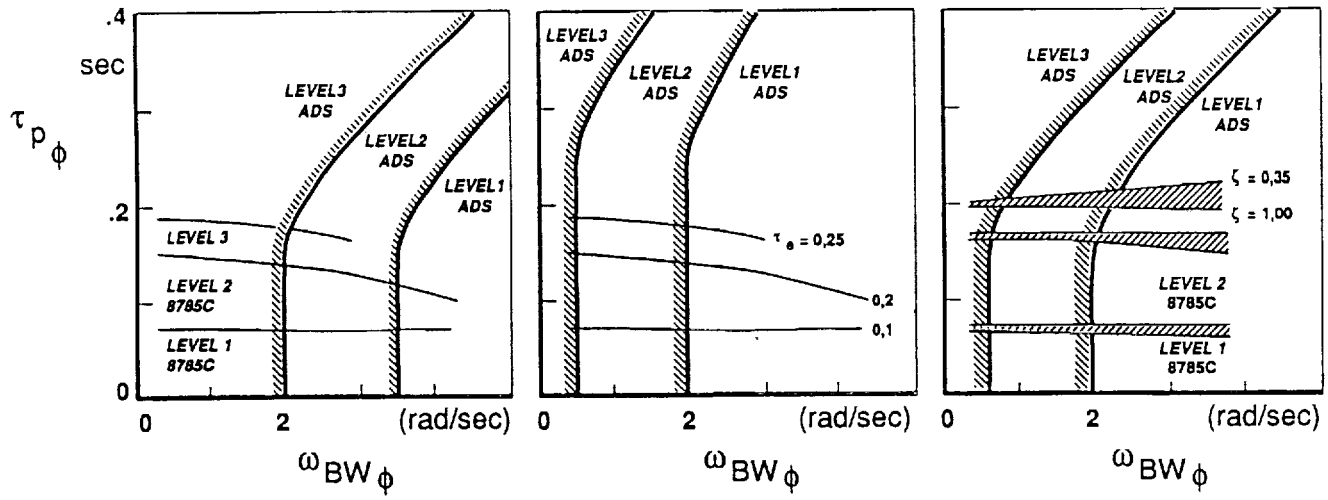

a) Air Combat

b) All Other MTE's - VMC and full attended operations

c) All Other MTE's - IMC and/or divided attention operations

Figure 7. Fixed-wing equivalent time delay requirements mapped onto the rotorcraft bandwidth requirements (assumes: first-order Rate command response and second-order Attitude command response).

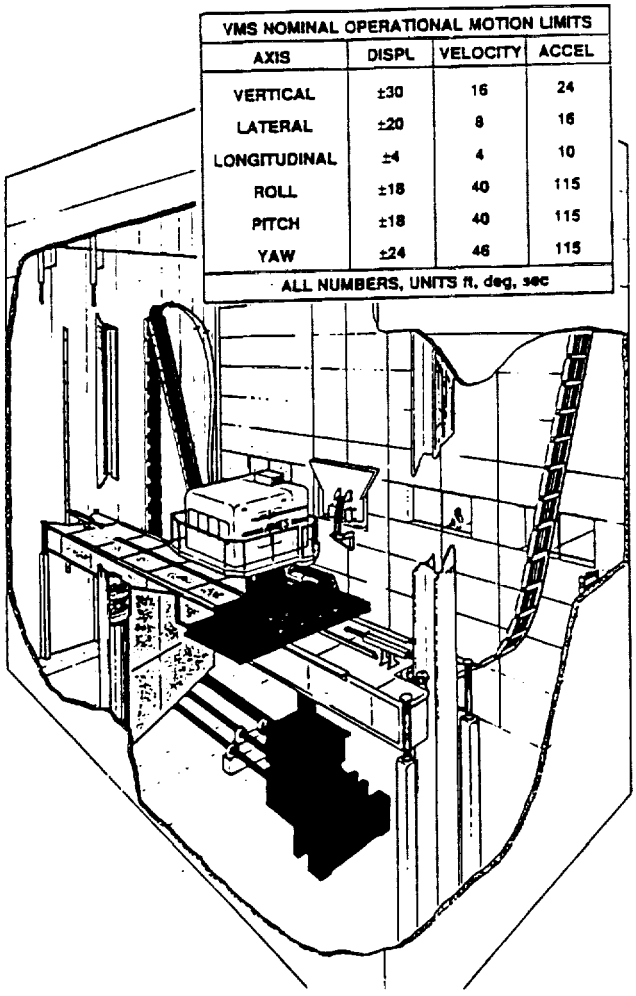

VMS NOMINAL OPERATIONAL MOTION LIMITS			
AXIS	DISPL	VELOCITY	ACCEL
VERTICAL	±30	16	24
LATERAL	±20	8	16
LONGITUDINAL	±4	4	10
ROLL	±18	40	115
PITCH	±18	40	115
YAW	±24	46	115
ALL NUMBERS, UNITS ft, deg, sec			

Figure 8. NASA Ames Research Center Vertical Motion Simulator (VMS).

Figure 9. DLR in-flight simulator ATTHeS.

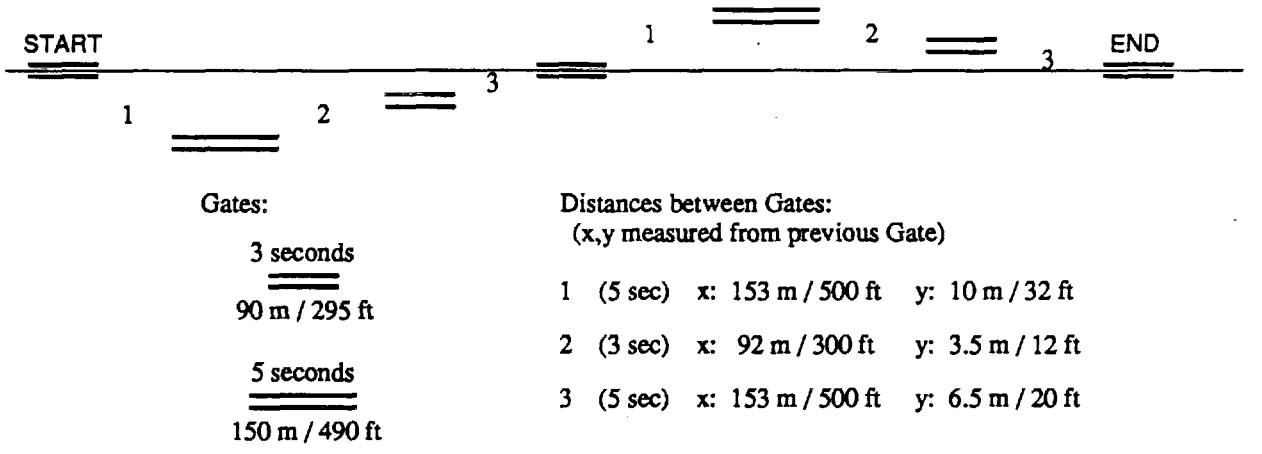

Figure 10. Slalom tracking course (times shown for 60 knots).

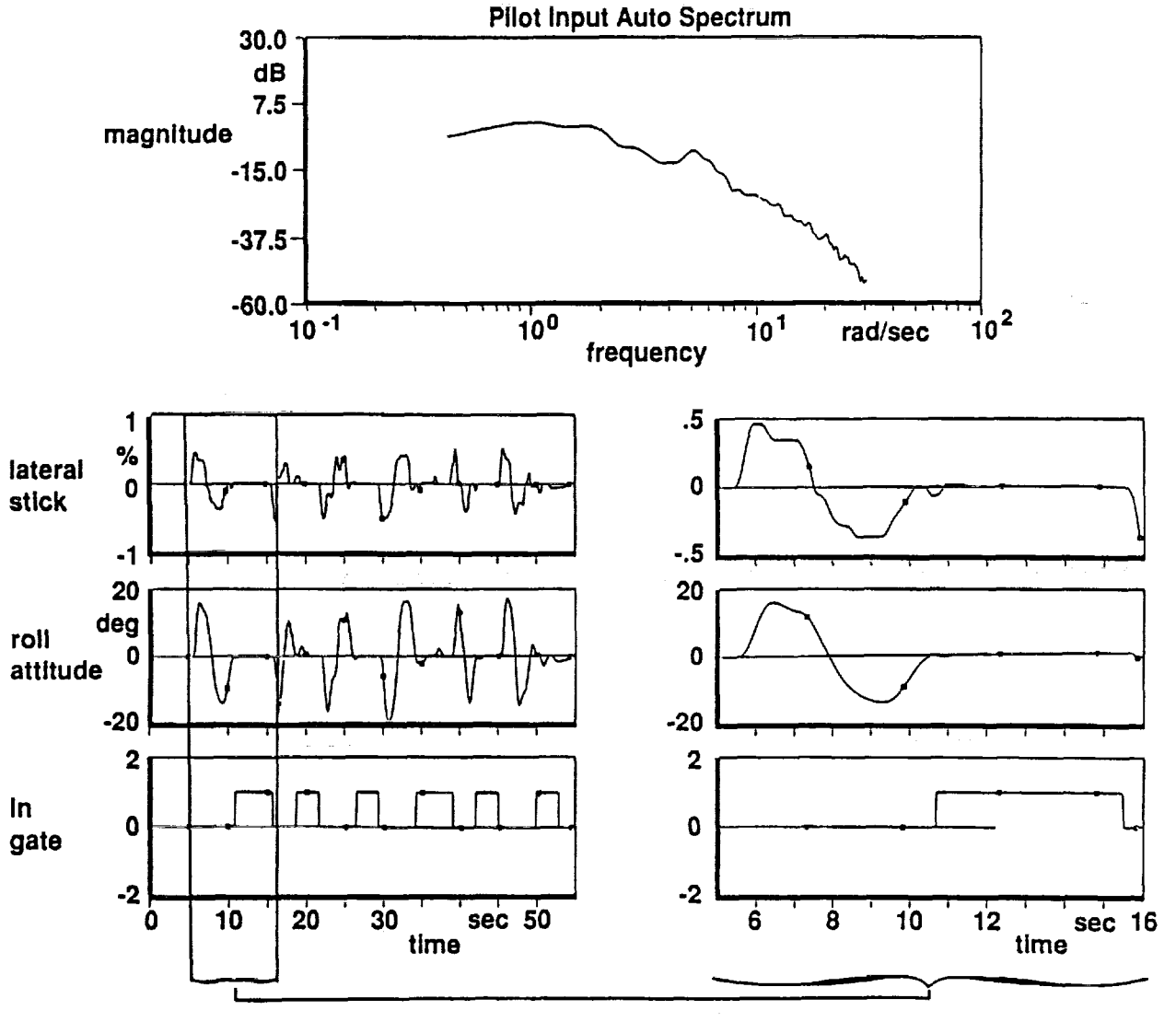

Figure 11. Time history and frequency plot from VMS test.

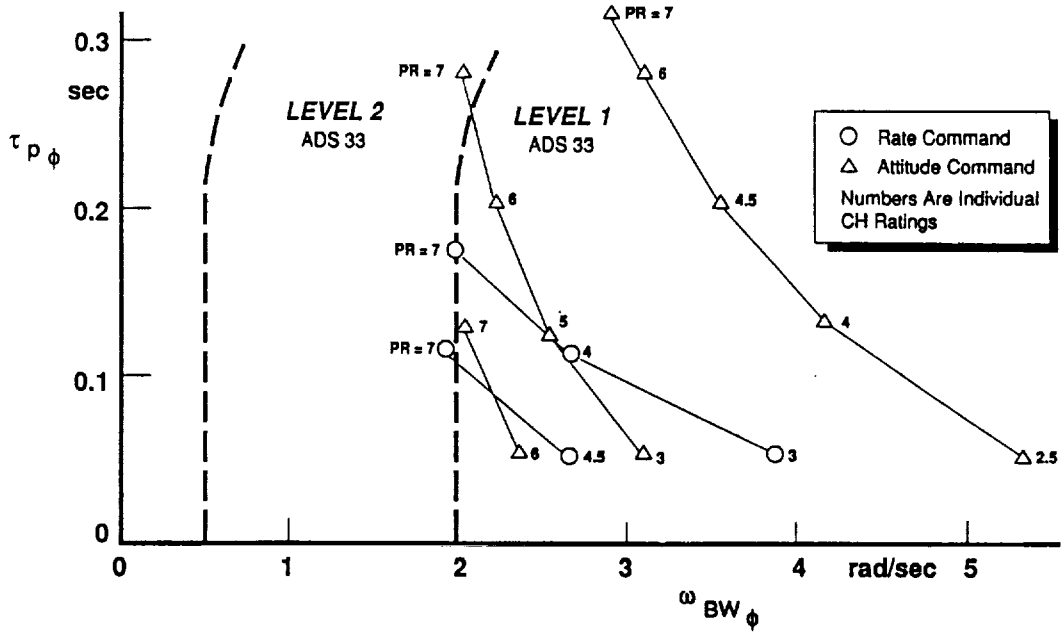

Figure 12. VMS data points.

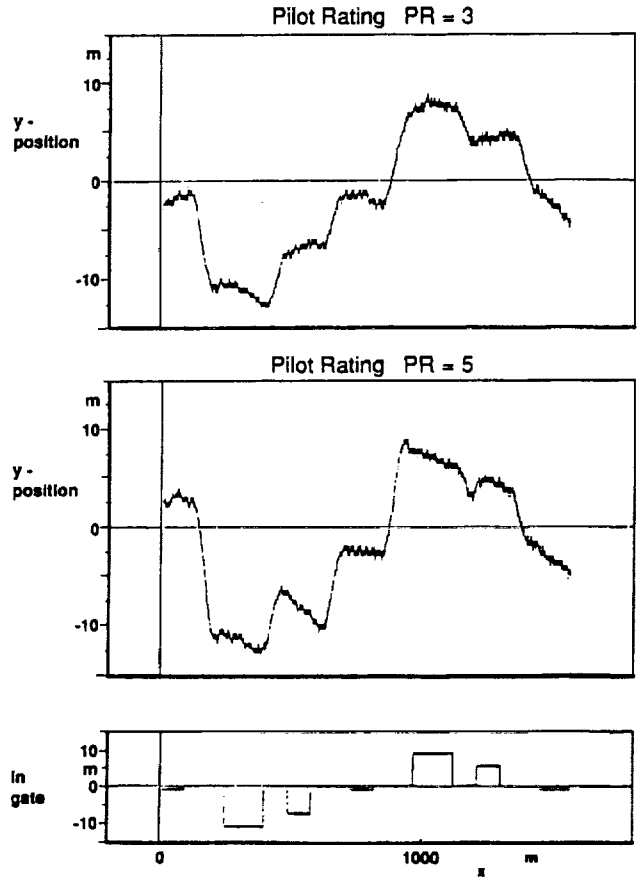

Figure 13. Comparison of ground tracks (RC in-flight).

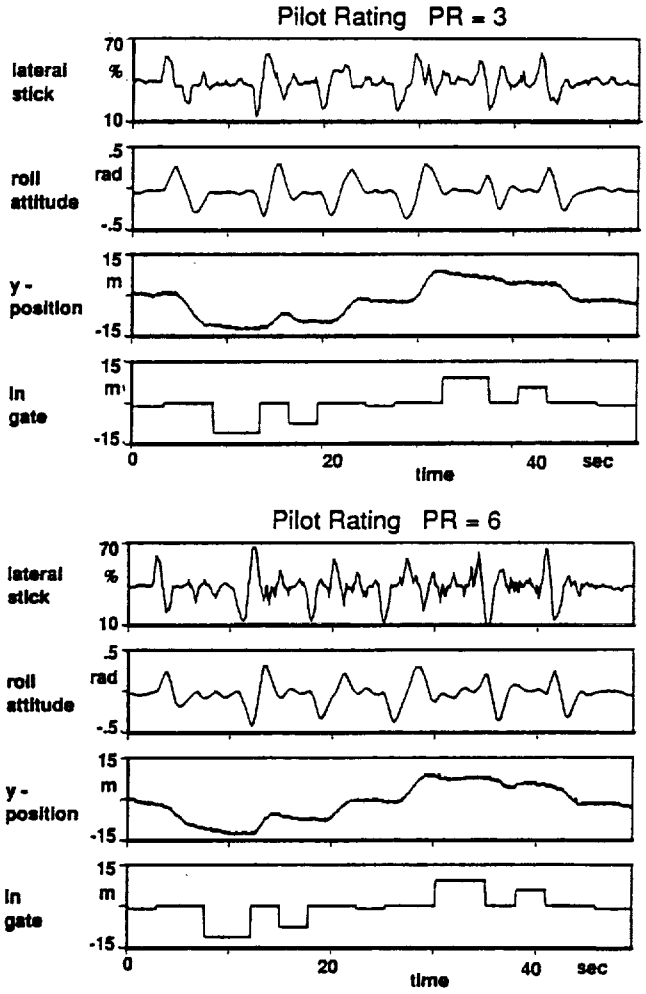

Figure 14. Comparison of time histories (AC in-flight).

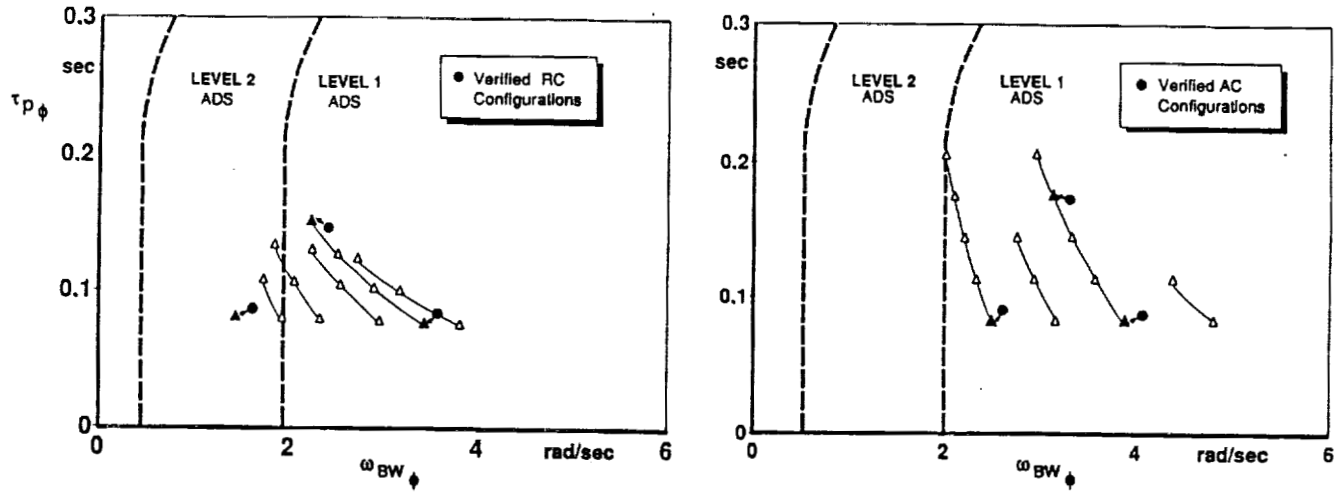

Figure 15. Verification of flight test configurations.

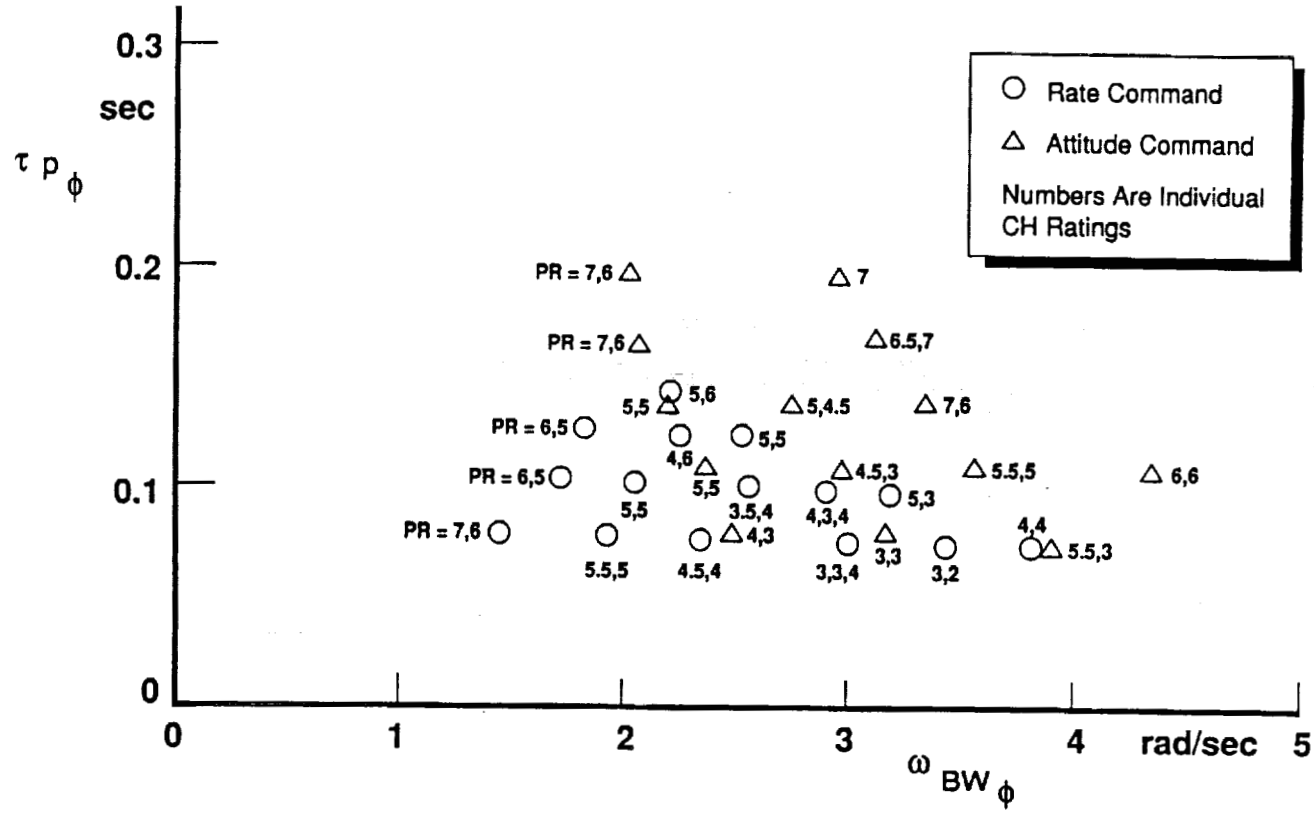

Figure 16. Flight test data points.

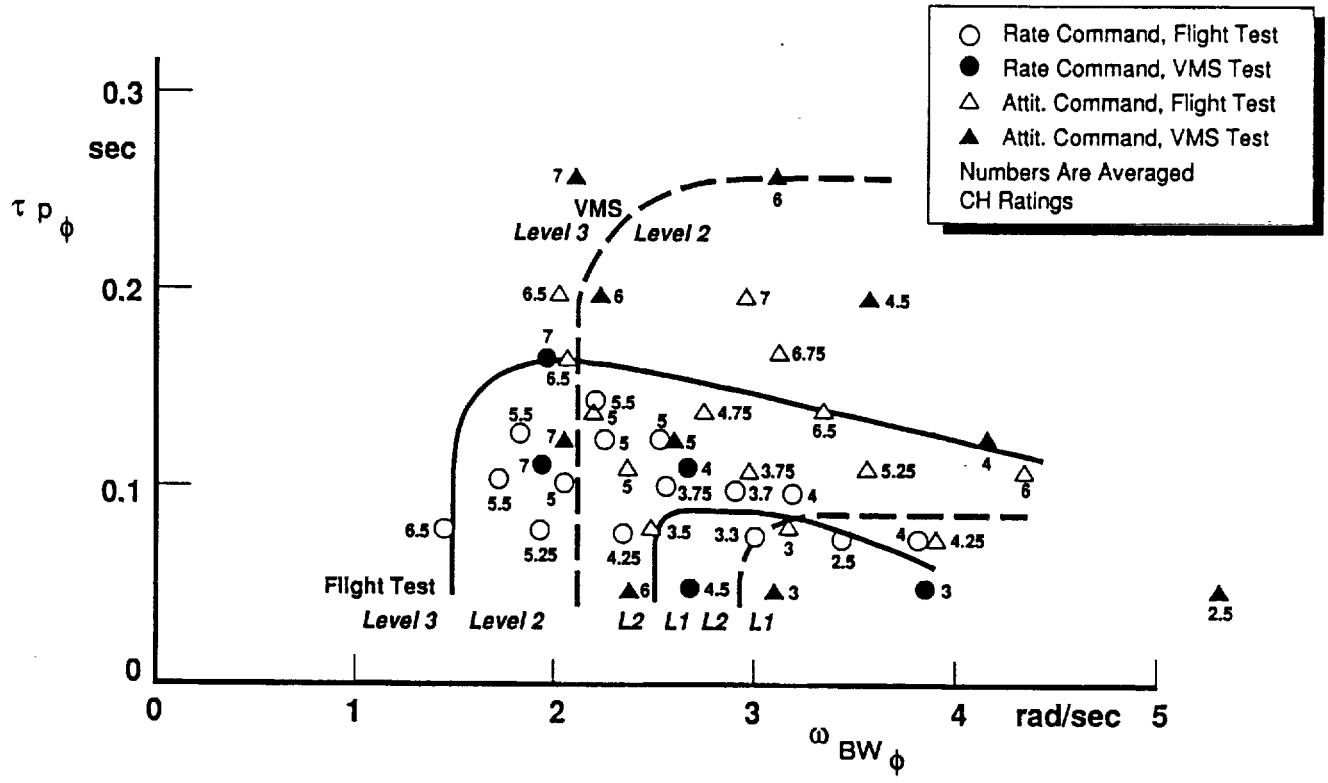

Figure 17. Summarized evaluations.

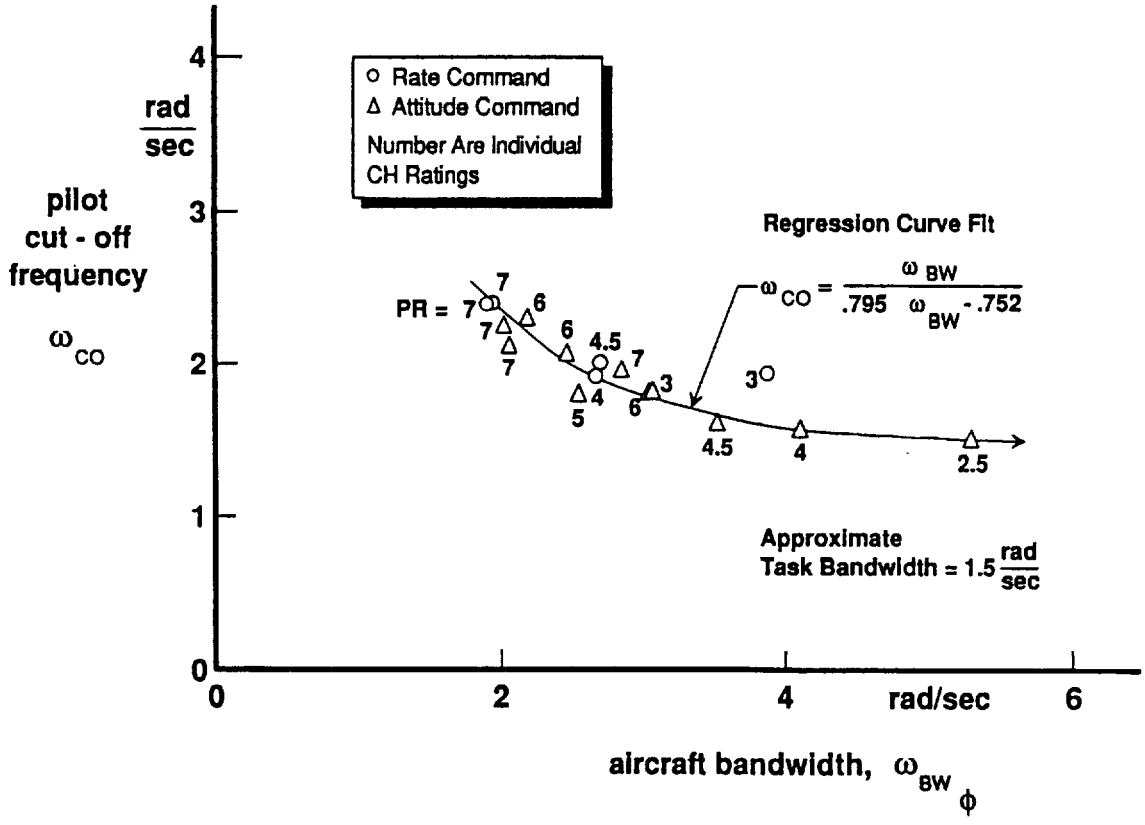

Figure 18. Pilot cut-off frequency data from VMS tests.

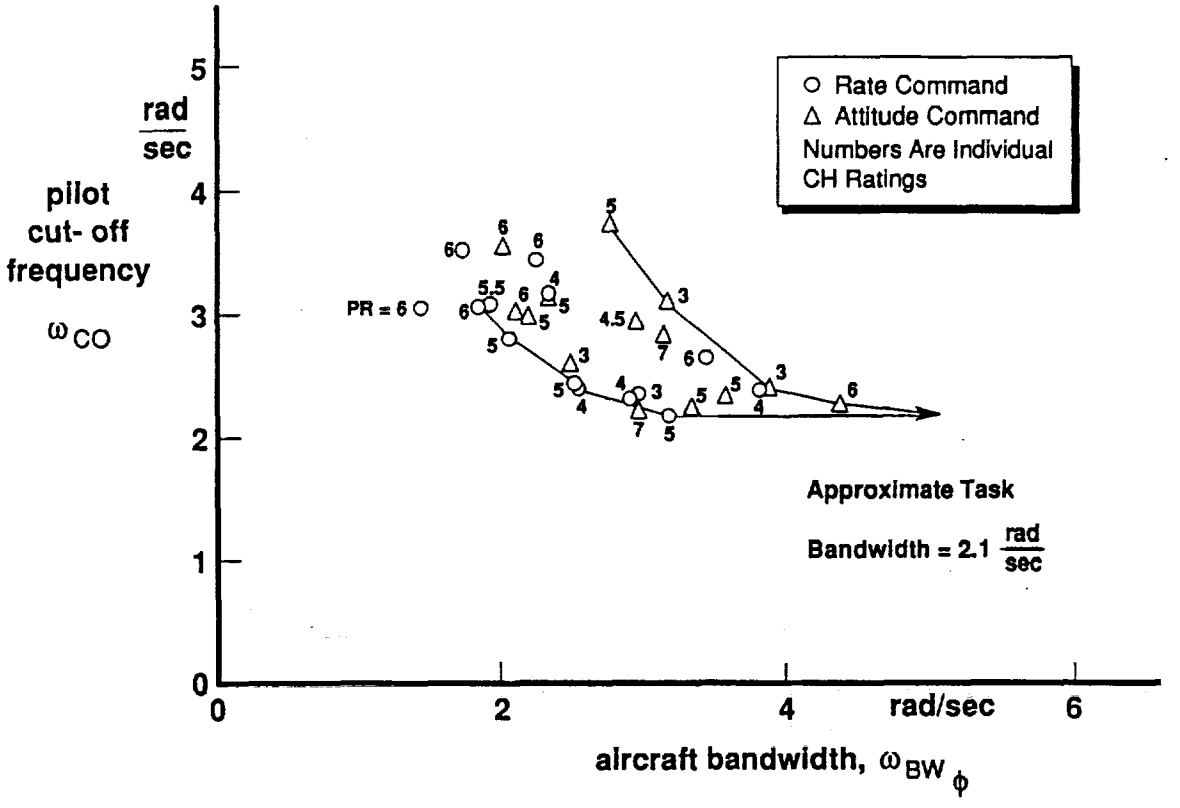

Figure 19. Pilot cut-off frequency data from flight tests (one pilot).

Session 2

Assessing New Technologies

A Piloted Simulation Investigation of the Normal Load Factor and Longitudinal Thrust Required for Air-to-Air Acquisition and Tracking

Matthew S. Whalley
Aerospace Engineer
U.S. Army Aeroflightdynamics Directorate
Moffett Field, California

ABSTRACT

A piloted simulation study was performed by the U.S. Army Aeroflightdynamics Directorate to develop insight into the maneuverability requirements for aggressive helicopter maneuvering tasks such as air-to-air combat. Both a conventional helicopter and a helicopter with auxiliary thrust were examined. The aircraft parameters of interest were the normal and longitudinal load factor envelopes. Of particular interest were the mission performance and handling qualities tradeoffs with the parameters of interest. Two air-to-air acquisition and tracking tasks and a return-to-cover task were performed to assess mission performance. Results indicate that without auxiliary thrust, the ownship normal load factor capability needs to match that of the adversary in order to provide satisfactory handling qualities. Auxiliary thrust provides significant handling qualities advantages and can be substituted to some extent for normal load factor capability. Auxiliary thrust levels as low as 0.2 thrust/weight can provide significant handling qualities advantages.

NOTATION

L_p	roll damping coefficient, 1/sec
M_q	pitch damping coefficient, 1/sec
N_x	longitudinal load factor, g
N_z	normal load factor, g
u_{body}	longitudinal airspeed, ft/sec
V	total airspeed ft/sec
x	inertial position, ft
y	inertial position, ft
z	vertical position, ft (+down)
γ	climb angle, rad
ϕ	roll attitude, rad
ψ	heading, rad

Presented at *Piloting Vertical Flight Aircraft: A Conference on Flying Qualities and Human Factors*, San Francisco, California, January 1993.

INTRODUCTION

The primary objective of this simulation experiment was to develop insight into the maneuverability requirements for aggressive helicopter maneuvering tasks such as air-to-air combat. Maneuverability and agility (MA) has been a topic of research for many years in both the fixed and rotary wing communities (Refs. 1-18). It is generally agreed that maneuverability is some measure of the maximum achievable time-rate-of-change of the velocity vector and that agility is the measure of the maximum achievable time-rate-of-change of the acceleration vector. It is also agreed that good MA is a key requirement for success in highly dynamic missions such as air-to-air combat. Unfortunately, that's where the agreement stops. A precise definition of MA and a quantification of the amount required have never been agreed upon. Regrettably, this author believes it unlikely that there will be agreement at any time in the near future.

To change the magnitude and direction of the velocity vector one has to apply a force. Obviously, then, the major contributor to good maneuverability is the ability to generate normal, longitudinal, and lateral load factor. In a conventional helicopter, acceleration is generated by changing the magnitude and direction of the main rotor thrust. In a compound helicopter, acceleration is generated by using a combination of the magnitude and/or the direction of the main rotor thrust and the magnitude of the auxiliary thrust. Maneuverability was examined in the context of these facts during this experiment. Namely, the effects that variations in the load factor envelope have on handling qualities and mission performance for some representative "aggressive" tasks were investigated. By taking this approach, it was expected that a set of data would be generated from which information regarding the relationship between maneuverability, mission performance, and handling qualities could be obtained.

DESIGN AND CONDUCT OF THE EXPERIMENT

To accomplish the stated objectives, a five week piloted simulation investigation was conducted on the NASA Ames Research Center (ARC) Vertical Motion Simulator (VMS) (Refs. 19, 20). This section contains a detailed description of the experiment, including the experimental facility, ownship and adversary aircraft, experimental variables, evaluation tasks, evaluation pilots, and collection of experimental data.

Facility Description

The investigation was conducted using the six-degree-of-freedom VMS with the NCAB cockpit (Fig. 1). The VMS is unique among flight simulators in its large range of motion (Table 1). This large motion capability provides cues to the pilot that are critical to the study of handling qualities.

The primary inputs to the motion base are the translational and rotational accelerations calculated by the math model for the pilot position. These signals are

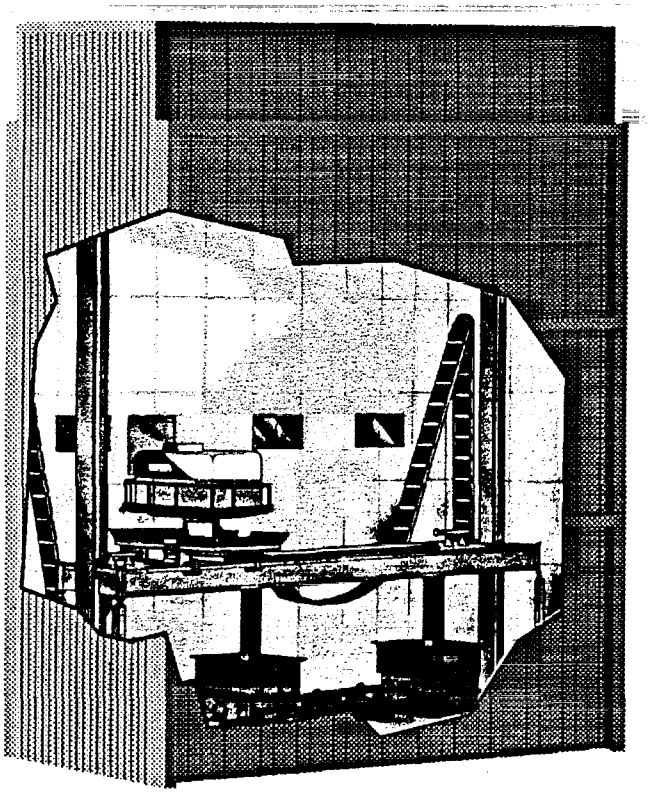

Figure 1. NASA Ames Research Center Vertical Motion Simulator.

Table 1. Vertical Motion Simulator motion limits.

	Displ. (ft)	Rate (ft/sec)	Accel. (ft/sec^2)
Long.	±4	±4	±10
Lat.	±20	±8	±16
Vert.	±30	±16	±24
	(deg)	(deg/sec)	(deg/sec^2)
Pitch	±18	±40	±115
Roll	±18	±40	±115
Yaw	±24	±46	±115

filtered by second-order washout filters characterized by a gain and a washout frequency. The motion system parameters used for this experiment were tuned to minimize the phase error between the accelerations generated by the model and those generated by the motion base while at the same time providing the largest possible motion envelope within the software limits.

The NCAB was configured as a single pilot cockpit with a three window computer generated imagery (CGI) display. The field of view is shown in Figure 2. The CGI database used for this experiment contained an 8-kilometer-by-16-kilometer gaming area consisting of mountains, rivers, and roadways. There was a ground pattern but no ground texturing.

Conventional helicopter controllers were used. A summary of the force characteristics of the controllers is contained in Table 2. Stick force per g was provided by scaling the cyclic pitch stick gradient with load factor:

$$\text{pitch gradient (lb/in.)} = 2.0\,N_z - 0.5.$$

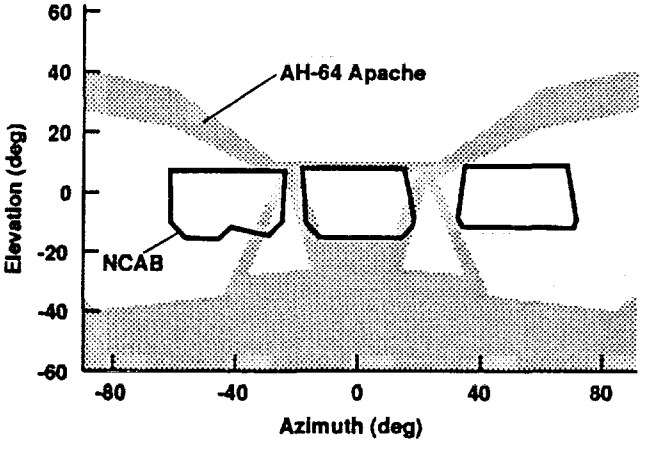

Figure 2. NCAB field of view.

Table 2. Controller characteristics.

	Pitch	Roll	Yaw	Heave
Range (in.)	±6.15	±6.10	±3.40	0 - 10.0
Deadzone (in.)	±0.15	±0.10	±0.15	0
Breakout (lb)	1.5	1.0	4.0	0
Gradient (lb/in.)	1.5[a]	1.0	2.5	0
Damp. (lb/in./sec)	0.8	0.5	1.0	0
Friction (lb)	1.0	1.0	2.0	3.0

[a] at 1.0 g

Four inceptors for the control of the auxiliary thruster were examined during the early stages of the simulation (Fig. 3). The four were: 1) a thumbwheel on the cyclic grip that contained a center detent but no spring gradient; 2) a thumb joystick on top of the cyclic grip; 3) a twist grip on the collective that contained only friction; and 4) a beep switch on the collective head. The thumbwheel and the collective twist grip were used as either direct X-force-command or u_{body}-command. The collective beep switch and the cyclic thumb joystick were used as either X-force-rate-command or u_{body}-rate-command. This gave eight auxiliary thruster control possibilities.

The instrument panel included a horizontal situation indicator (HSI), an airspeed indicator, a barometric altimeter, a vertical speed indicator, a turn and slip indicator, a torque meter, and a load factor meter. Also included was a moving map display which showed the relative position, altitude, and heading of the ownship and adversary.

Figure 4 shows the heads-up display (HUD) symbology. Included on the HUD were a torque meter, a radar altitude tape, a horizon bar, a heading tape, a sideslip ball, and digital readouts of torque, load factor, airspeed, radar altitude, and range to target. In the center of the display was a vector indicating the horizontal direction and range to the adversary, relative to the ownship nose. On the bottom of the display was an adversary position display that showed the azimuth and elevation of the adversary relative to the ownship nose. A floating pipper was used to track the target during the air-to-air task. The azimuth and elevation offset of the pipper from the boresight was computed in order to provide the proper lead angle required for a hypothetical fixed-forward-firing gun. Specifically, when the pipper was

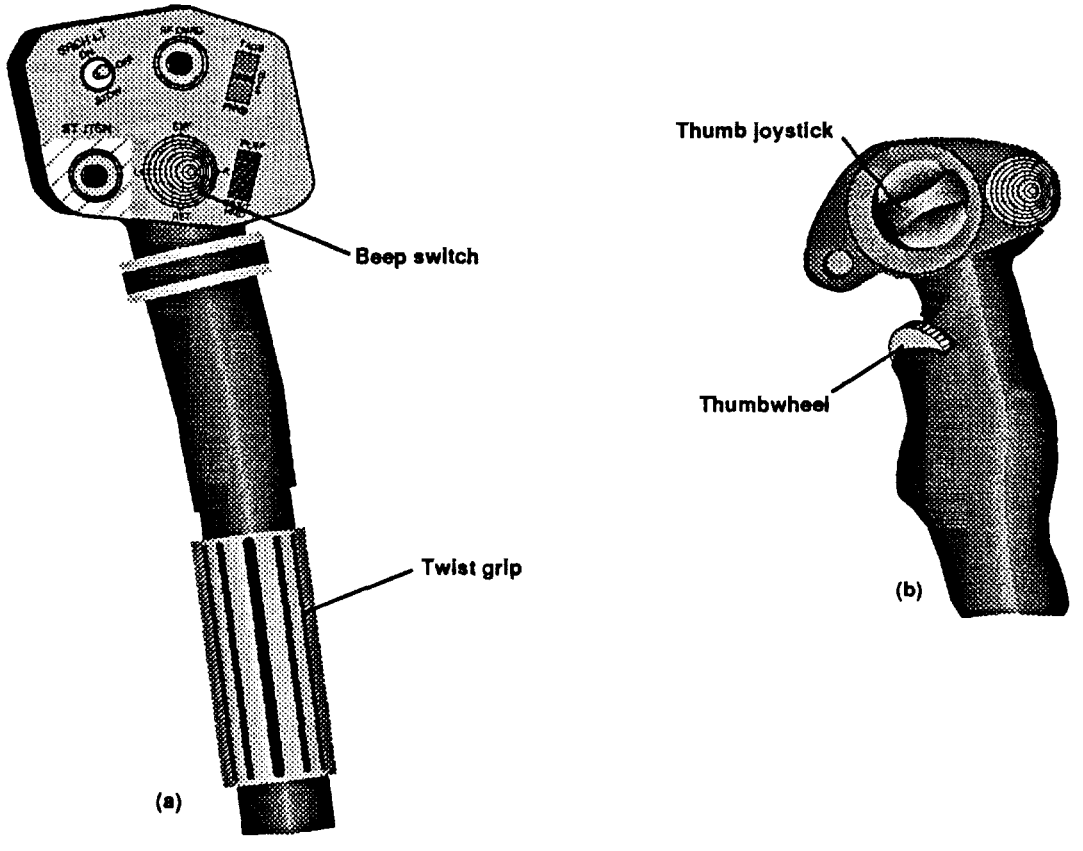

Figure 3. Location of auxiliary thrust control inceptors. (a) collective grip; (b) cyclic grip

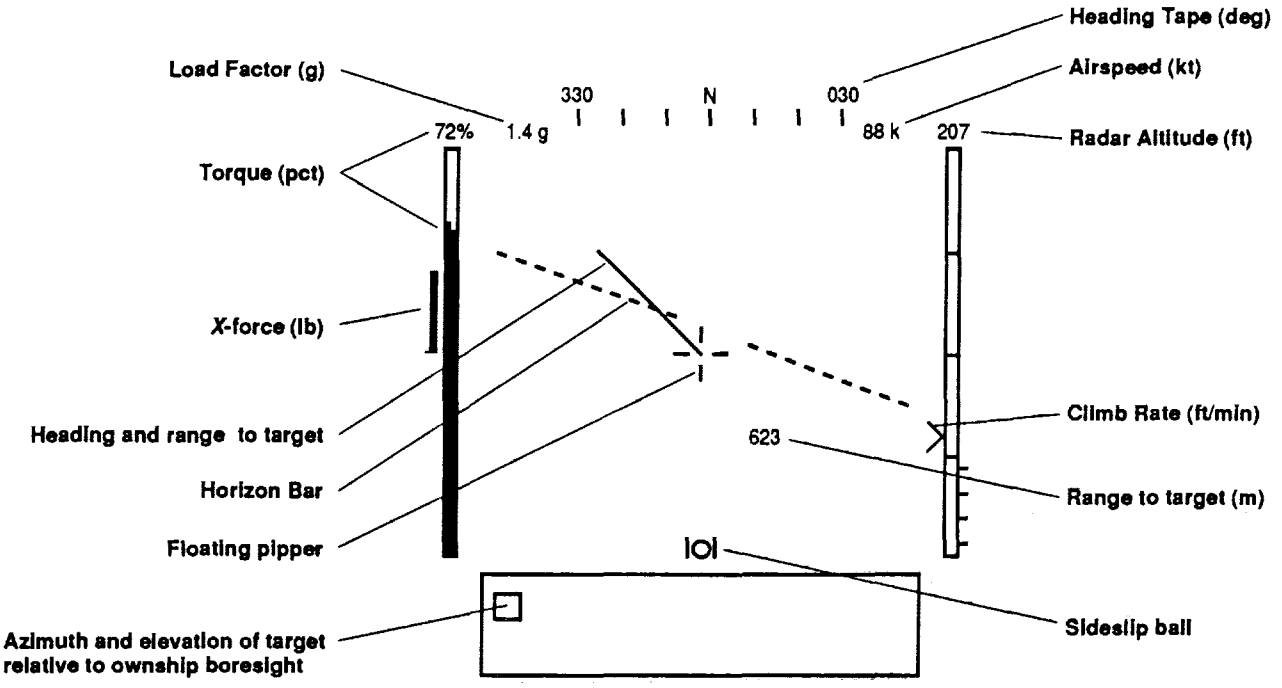

Figure 4. Heads-up display symbology

overlaid on the target, the boresight of the aircraft was pointing at the predicted target location one bullet time-of-flight into the future.

Rotor, engine, and transmission noises were simulated using a Wavetek Helicopter Sound Simulation System. Warning tones and weapon noises were simulated using a Mirage sound system generator.

A seat shaker simulated aircraft vibration. The vibration math model was based on the vibration model developed for a high-fidelity UH-60A Blackhawk simulation (Ref. 21). The amplitude and frequency of vibration were calculated as functions of rotor speed, collective stick position, load factor, and airspeed.

The stick-to-visual throughput time delay was 74.5 milliseconds. No visual time delay compensation was used because the stick-to-visual time delay already closely matched the stick-to-motion time delay in the pitch and roll axes.

AUTOMAN

The air-to-air adversary used during this experiment was the AUTOmated MANeuvering (AUTOMAN) opponent developed by Grumman Corporation under contract to the U.S. Army Aeroflightdynamics Directorate (Refs. 22, 23). In the past, air-to-air simulation experiments have relied on either a second pilot flying the adversary aircraft, or simple pre-programmed flight paths for the adversary aircraft. Both of these approaches can have drawbacks. Using a piloted target can lead to undesirable variations in the aggressiveness of the engagements, because the target pilot cannot always employ consistent maneuvering logic. In addition, a piloted target requires the use of one of the CGI channels, thus degrading the visual presentation to the ownship pilot. Preprogrammed flight paths can lead to skewed results because the pilot is able to memorize the flight path of the target and anticipate its movement. The AUTOMAN program was therefore developed to alleviate these problems.

The AUTOMAN computer program generates automated maneuvering decisions for helicopters during air-to-air combat at low altitude in hilly terrain. Maneuvers are selected by employing simple game theory (Ref. 24). Capabilities of AUTOMAN include a guidance law for target acquisition when a firing opportunity arises; fire-control sequence logic; low-flying capabilities; line-of-sight computations for the cockpit field-of-view; air-to-air collision avoidance maneuvers; decisions on and adjustable levels of simulated pilot experience.

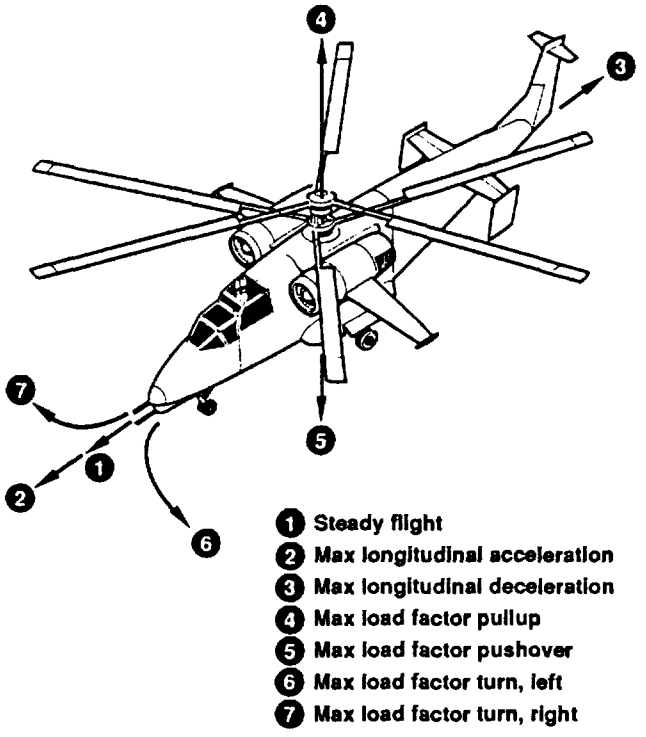

Figure 5. AUTOMAN elemental maneuvers

To determine the best maneuver choice, the consequences of performing various maneuvers are evaluated. It is assumed that each aircraft selects one of the seven elemental maneuvers shown in Figure 5. While the maneuvers shown are maximum-performance turns, climbs, etc., there are first-order lags, typical of the actual responses of the aircraft, between the command and control variables; consequently, the maneuvers are achieved gradually. Since maneuver choices are updated frequently, moderate maneuvers can occur as the average of a sequence of short-duration, maximum-performance maneuvers.

The helicopter math model used by AUTOMAN is a simple point mass model which performs coordinated turns. The equations of motion are as follows:

$$\dot{x} = V\cos\gamma\cos\psi$$
$$\dot{y} = V\cos\gamma\sin\psi$$
$$\dot{z} = -V\sin\gamma$$
$$\dot{V} = g(N_x - \sin\gamma)$$
$$\dot{\gamma} = \frac{g}{V}(N_z\cos\phi - \cos\gamma)$$
$$\dot{\psi} = \frac{gN_z\sin\phi}{V\cos\gamma}$$

Table 3. AUTOMAN time constants and angular rate constraints

N_x time constant	1.0 sec
N_z time constant	0.2 sec
ϕ time constant	.2375 sec
maximum $\dot{\phi}$	57.3 deg/sec
maximum $\dot{\gamma}$	120 deg/sec
maximum $\dot{\psi}$	40 deg/sec

The control variables are the roll rate $\dot{\phi}$ and the longitudinal and normal load factors, N_x and N_z, and the corresponding commands are ϕ_c, N_{xc}, and N_{zc}. A first order lag is assumed between the commanded values and the response. A summary of the time constants and angular rate constraints used in AUTOMAN for this experiment is given in Table 3. Figure 6 shows the AUTOMAN load factor, longitudinal acceleration, and turn rate capabilities.

Ownship Math Model

A stability derivative helicopter math model termed the Enhanced Stability Derivative Model (ESD) was used as the ownship. The ESD model is a derivative

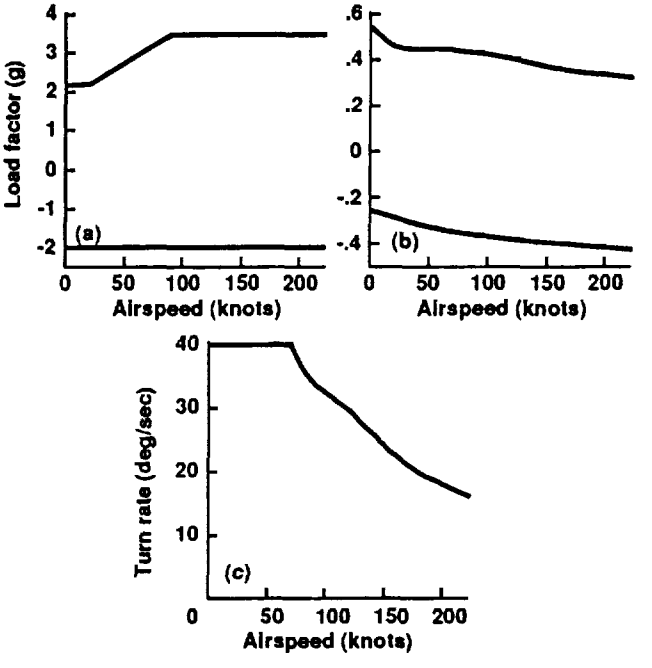

Figure 6. Performance capabilities of AUTOMAN (from Reference 22). (a) maximum and minimum normal load factor; (b) maximum and minimum longitudinal load factor; (c) maximum turn rate.

of the TMAN model developed for the Helicopter Air Combat (HAC) simulation experiments (Refs. 25-27). Earlier versions of the ESD model have been used for other handling qualities experiments (Refs. 28,29). The ESD model is a simple, non-linear, generic helicopter math model intended for use as a handling qualities research tool. The response dynamics are easily modified thus allowing a wide range of handling qualities to be studied. It includes the effect of load factor on the pitch and roll rate damping derivatives, the effect of forward speed on the force derivatives, a collective trim curve, and a ground effect model. The attitude response is rate-type in pitch, roll, and yaw with automatic turn coordination above fifty knots. The total aerodynamic forces and moments required for the six-degree-of-freedom equations of motion are generated as the summation of reference and first-order terms of a Taylor series expansion about a reference trajectory. The model does not include control or response coupling.

Auxiliary Thruster — An auxiliary thruster with a selectable force or u_{body} command system was added for this experiment. Table 4 shows a summary of the various control-inceptor/control-response types. The math model assumed axial flow through a 10 ft diameter propeller and included the effects of both power and stall limitations. Figure 7 shows a pitch trim sweep for a configuration with a 3.5 g normal load factor capability and auxiliary thrust/weight ratios of 0.1, 0.2, and 0.33. The solid lines indicate the maximum nose-up and nose-down attitudes that the configuration can trim at in level flight. The dashed line indicates the trim pitch attitude for the same configuration with no auxiliary thruster.

Experimental Variables

Normal and longitudinal load factor envelope were varied during this experiment. Maximum

Table 4. Auxiliary thruster control system gains.

Inceptor	Response Type
cyclic joystick	force rate
cyclic joystick	u_{body} rate
cyclic thumbwheel	force
cyclic thumbwheel	u_{body}
collective beep switch	force rate
collective beep switch	u_{body} rate
collective twist grip	force
collective twist grip	u_{body}

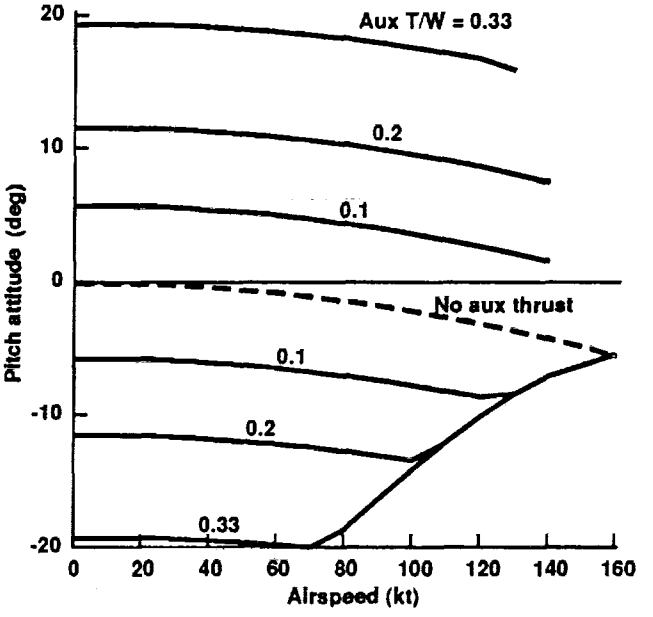

Figure 7. Pitch trim sweep of configuration with auxiliary thruster

continuous normal load factor capability was varied from 1.5 to 5.0 g (at 80 kt). Maximum longitudinal load factor capability was varied only for the thrust augmented cases and was varied from 0.1 to 1.0 auxiliary thrust/weight ratio. The transient load factor limit was set equal to 1.33 times the maximum continuous load factor capability at 80 kt. Table 5 shows the configurations matrix.

Tasks

Three tasks were flown during the experiment — the abeam air-to-air task, the mountain air-to-air task, and the return-to-cover task. The intent was to obtain handling qualities and mission performance data with respect to variations in the load factor envelope and auxiliary thrust level.

Air-to-air tasks — Both of the air-to-air tasks were taken from the RATAC experiment (Ref. 29). The objective of both tasks was the same; to track the AUTOMAN for as long as possible using the ownship pipper on the HUD. The position of the pipper on the HUD was driven by a set of equations such that the proper lead angle for a fixed-forward-firing gun was displayed. As mentioned earlier, when the pilot overlaid the pipper on the target, the nose of the ownship was pointed at the estimated location of the target one bullet-time-of-flight into the future. In addition, the pilot was required to

Table 5. Configuration test matrix

N_z (g)[a]	Auxiliary thrust/weight 0	0.1	0.2	0.33[b]	0.6	1.0
1.5	AMM_2R			AM		
1.75	AMR			AM		
2.0	AMM_2R	A		AM		
2.5	AMR			AM		
3.0	AMR	AM	AM	AMR	AMR	AR
3.5	AMM_2	M	M	AM		
4.0	AMR			AM		AM
5.0	AMR			AM		

A - Abeam air-to-air task

M - Mountain air-to-air task

M_2 - Mountain air-to-air task, low capability adversary

R - Return-to-cover task

[a] Maximum continuous capability at 80 knots.

[b] This level of thrust/weight represents the average value of several compound helicopters surveyed.

maintain less than 0.2 g lateral acceleration, two ball widths, while tracking. Pilots were encouraged to maintain airspeed above forty-five knots. Each run was limited to 25 seconds.

The initial conditions for the abeam air-to-air task are shown in Figure 8. The target was positioned 2000 feet in front of, and 100 feet below the ownship with a heading 135 degrees away to the left or right. The ownship was initialized at its maximum maneuvering speed, 80 knots, while the target was initialized at 120 knots. Line-of-sight existed for both aircraft over hilly terrain. The initial target heading was randomly set to either the left or right before each run to introduce some variability to the task. A typical run of the abeam task is shown in Figure 9.

The initial conditions for the mountain air-to-air task are shown in Figure 10. This task began with a mountain preventing line of sight between the two aircraft. The ownship was initialized at its maximum maneuvering speed, 80 knots, while the target was initialized at 140 knots. The initial target heading was randomly set to either the left or right before each run. A typical run of the mountain task is shown in Figure 11.

Task performance standards were based on the longest continuous tracking period measured during the run. Tracking time accumulated whenever the AUTOMAN cg was within 30 feet of a vector defined by the ownship pipper, azimuth and elevation < $\tan^{-1}$(30/range), and the ownship lateral acceleration was less than 0.2 g. Performance for the longest tracking period was categorized as unsatisfactory (< 2.0 seconds), adequate (>= 2.0, < 4.0 seconds), or desired (>= 4.0 seconds). These levels ensured a baseline level of aggression among the pilots. Task performance was indicated to the pilot via audio tones in the headset; i.e., a low, continuous tone meant that he was within the tracking constraints, a high continuous tone meant that he had met the constraints for 2.0 seconds, and a high, intermittent tone meant that he had met the constraints for

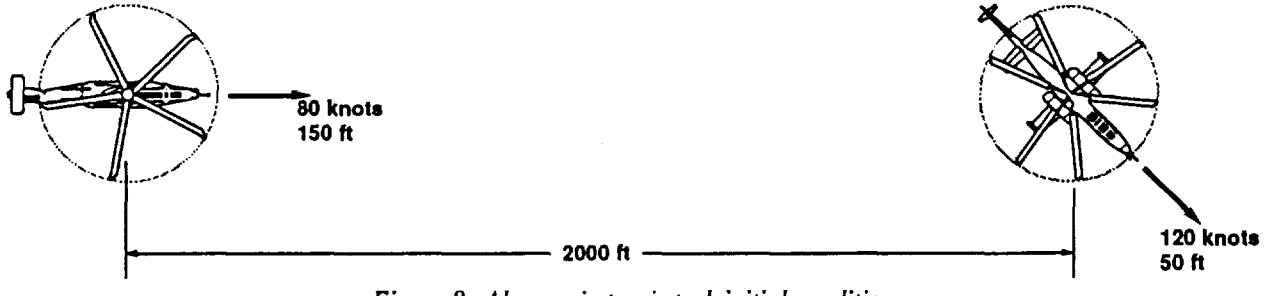

Figure 8. Abeam air-to-air task initial conditions.

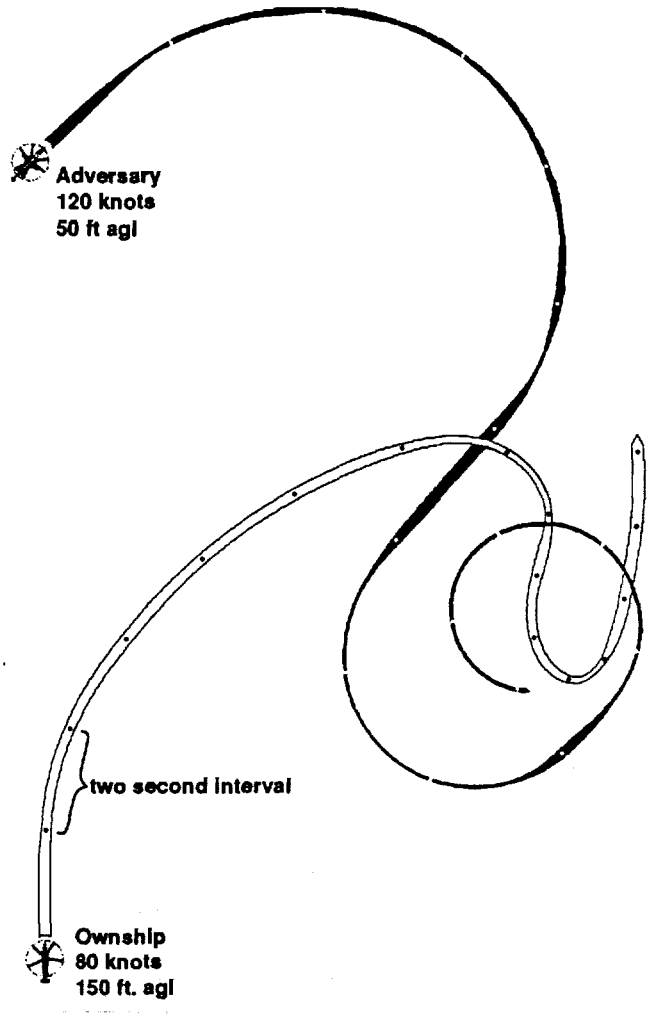

Figure 9. Typical run of the abeam air-to-air task

4.0 seconds. Pilots were encouraged not to assign CHR's based solely on their performance relative to these standards, but to assess the overall handling qualities of the vehicle.

To prevent the pilots from employing the stand-off techniques characteristic of missile engagements, the tracking cone was configured to only allow tracking within a thirty foot radius circle at the target range. This made distant engagements more difficult than close ones, resulting in more dynamic close-in maneuvering.

The run length was limited to twenty-five seconds because that was the point at which the engagements typically degraded into a "furball." Under those conditions, the generation of useful handling qualities data was difficult.

During the experiment, similar tactics for the air-to-air task emerged for all of the pilots. Task initial conditions created the opportunity for the ownship pilot to immediately begin tracking by using an aggressive lateral input. As the engagement progressed, tracking opportunities became clustered at ranges of less than 1000 feet. Given the dimensions and orientation of the tracking cone, a close-in, tail chase position provided the greatest performance potential, making it the tactical objective. A tail chase position also offered an advantage in maintaining situational awareness. Pilots found that it was essential to keep the target in sight, to maintain airspeed, and to establish a slight altitude advantage if they expected to perform well and to remain oriented.

During the experiment, the AUTOMAN usually tried to overcome the initial tactical disadvantage by performing a maximum performance turn towards the ownship culminating in a head-on engagement. Once the AUTOMAN had closed in on the ownship, it would continue to perform turns and roll reversals in an attempt to achieve a gun solution. Occasionally, the AUTOMAN

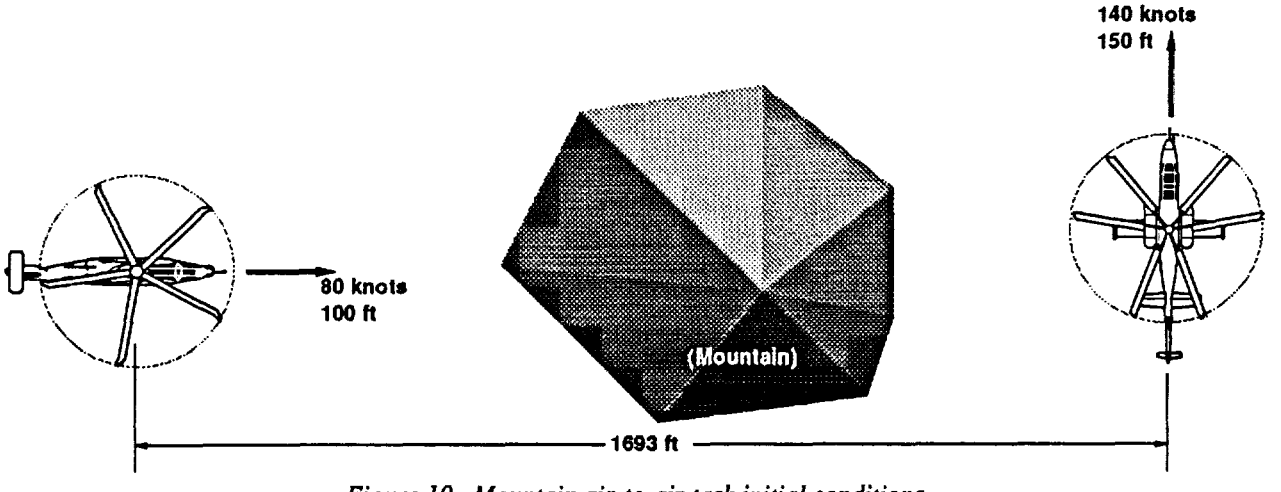

Figure 10. Mountain air-to-air task initial conditions

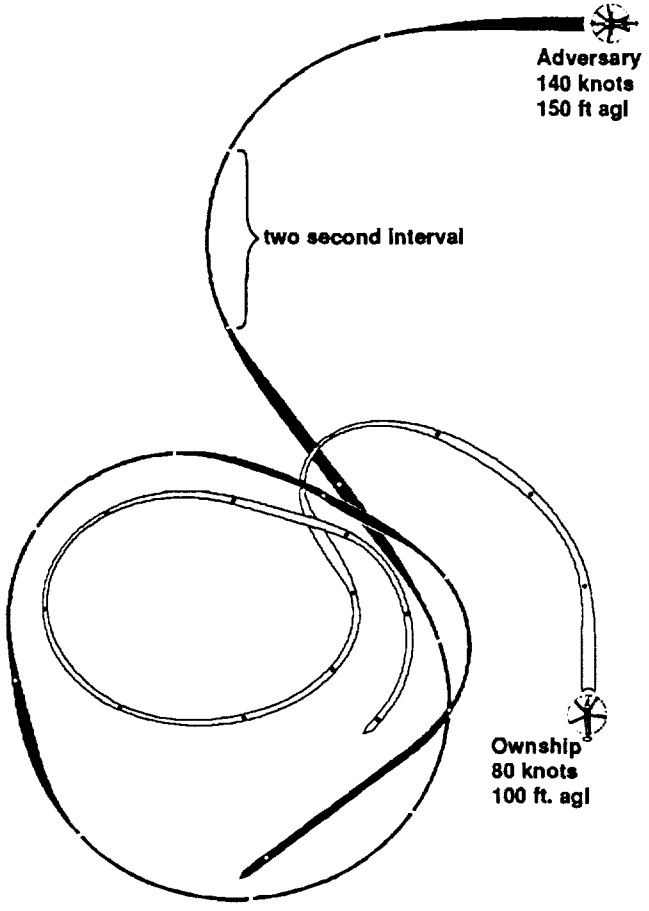

Figure 11. Typical run of the mountain air-to-air task

would turn away from the ownship in what appeared to be an attempt to disengage. Engagements usually concluded with the ownship having either improved or lost the advantage enjoyed at the outset. On rare occasions, the AUTOMAN had enough time to reverse its tactical disadvantage and place the ownship on the defensive.

Return-to-cover task — Figure 12 shows the return-to-cover task. The objective of the task was to return to the cover of the treeline as quickly as possible. The task was initialized with the ownship flying 80 kt at 100 ft above ground level (AGL). After the ownship passed over the treeline and the tank, the pilot was signaled to initiate a maneuver and return to the cover of the treeline as soon as possible.

Pilots

One U.S. Army/Ames test pilot, two NASA/Ames test pilots and one U.S. Army/AQTD test pilot participated in the experiment. All four pilots have had extensive handling qualities evaluation experience in a wide range of fixed and rotary wing aircraft.

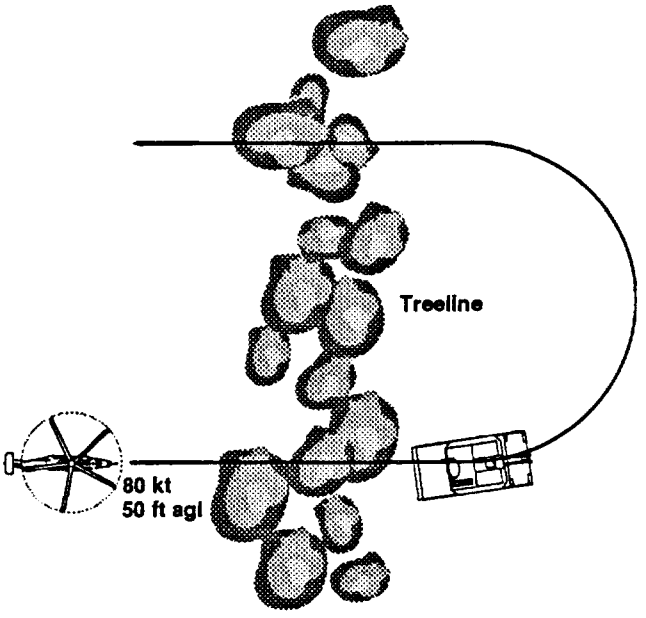

Figure 12. Return-to-cover task initial conditions.

Data Collection

Four types of data were collected during this experiment. Real time variables of interest such as position, attitude, and rates were digitally recorded. Performance measures such as time-on-target were recorded and printed out at the end of each run. Qualitative pilot opinion was gathered for each configuration in the form of commentary and a Cooper-Harper rating (CHR) (Ref. 31).

To minimize the effects of training, each pilot was given several hours to practice the tasks. During this time, task performance was communicated to the pilot at the end of each run. Data were not collected until both the pilot and the investigator were convinced that the pilot had achieved the necessary skill level.

Collection of data proceeded as follows. The helicopter was initialized in the test configuration and task. The pilot was not informed of which configuration he was flying. The pilot was allowed to practice the task until he was satisfied that his performance would not improve substantially with additional practice. At that point, the data collection equipment was turned on and the pilot proceeded to perform the task. After a minimum of three representative runs were completed, the pilot gave commentary and assigned a CHR.

RESULTS

This section contains the qualitative and quantitative data gathered during the experiment. The results from variations in load factor capability and auxiliary thrust level are presented in the form of task performance, CHRs, and pilot commentary. The data shown are a summary of the data gathered for all four pilots who participated unless otherwise noted.

The level of confidence in the data was measured. The range within which the true mean will occur with a ninety percent probability has been calculated using the *t*-test (Ref. 32). This confidence interval is indicated using error bars on the task performance plots and CHR summary plots. More simply stated, the true mean of the entire pilot population has a ninety percent chance of occurring within the error bars shown. This type of deviation calculation is useful in that it reflects both the spread and quantity of data collected.

Load Factor

Figure 13 shows a summary of the CHR data plotted versus load factor capability for the air-to-air task versus the 3.5 g adversary. Figure 14 shows a summary of the task performance data plotted versus load factor capability. The error bars indicate the ninety percent confidence interval for the data. The CHR data have been averaged together for the two air-to-air tasks because of the great similarity in tactics, control strategy, and workload. The performance data have been separated because the different initial conditions for the two tasks led to slightly different time-on-target results. The performance data for the abeam task do not include the first ten seconds of each run because the pilots found the tracking task to be relatively easy during this portion of the task and did not feel it was relevant to their evaluation of the configuration.

The CHR summary data indicate that a minimum load factor capability of 2 g is required for Level 2 handling qualities and a load factor capability of 3.5 g is required for Level 1 handling qualities. The performance data support the CHR data. There is a general improvement in performance out to 3.5 g and then a tapering off.

The pilot commentary strongly indicates that the Level 3 configurations lacked adequate maneuvering capability. For a 1.5 g configuration, pilot A states,

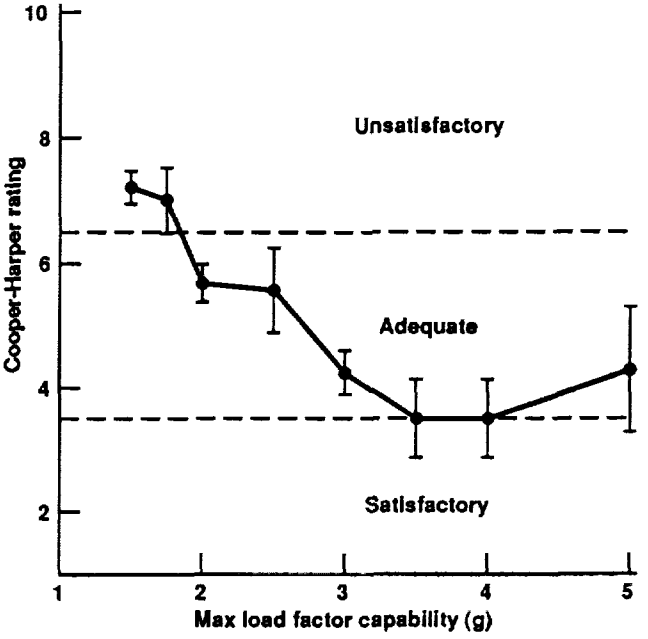

Figure 13. Cooper-Harper pilot ratings versus load factor capability.

"I think there was an inability to meet adequate performance standards. It was almost an inability to remain in flight. The primary reason was that you just didn't have anything to maneuver with. There was just no performance to gain out of the helicopter."

For a 1.75 g configuration, pilot A states,

"You just can't turn. You find yourself sinking down to the ground into the trees or into the hillside. It seemed like when you did get on the target you could stabilize pretty well, but it didn't stay on the target very long and it was difficult to track the target with the pipper. ... I would give this major deficiencies in that you can't achieve adequate performance, and there may even be a question of considerable pilot compensation to retain control."

Pilot comments for the Level 2 configurations indicate some improvement in the overall handling qualities but still not enough maneuverability to perform the task satisfactorily. Pilot C states that with the 2.0 g configuration,

"I think that it is shown that given this set of tactics and this level of capability on the aggressors part, that you can, in fact, get some reasonable tracking time on the guy But you can't expect to have immediate gratification. If you have to keep flying the aircraft and keep working it

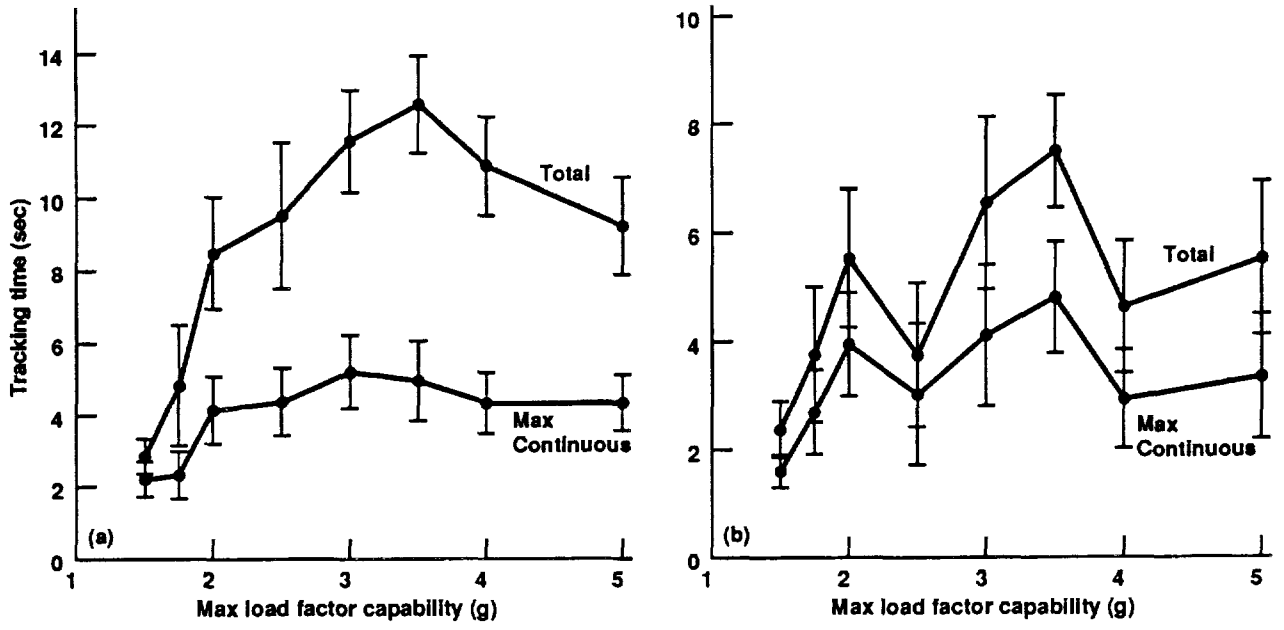

Figure 14. Task performance versus load factor capability. (a) mountain task; (b) abeam task.

into a position, you can not just pull the aircraft into position and expect to be able to ride there. The load factor does not allow that. ... You really do have to look at the load factor and the airspeed, make sure that you have the power all the way in, and be very careful with the controls. You keep telling yourself, 'don't pull any harder,' and see what happens."

The commentary for the Level 1 configurations indicate satisfaction with the maneuver capability. For a 3.5 g configuration Pilot E states,

"I would say that we definitely got desired performance for the most part. ... It was a pretty aggressive run, I didn't feel like I was limited in the aircraft in any way."

It is interesting to note the degradation in CHRs which occurred when the load factor capability was increased to 5.0 g. The pilot commentary indicated that the pitch and roll axes became more "ratchety" and "oscillatory." Pilot A stated,

"It seemed like it was a little bit more difficult to stabilize on the target with the high g load. It had a tendency to oscillate back and forth off the target and out of the cone. ... I'd say that there is a slightly objectionable control oscillation and slightly objectionable number of control reversals."

Pilot E stated,

"I found the oscillations to be something that is actually kind of interesting. I don't know why it is that I should be walking the target as badly — but it happened over and over again. I'm not sure if that is from trying too hard, or if there is some artifact of having a lot of power on the rotor system. Something makes it a little bit more goosey than I would expect from past experience."

What the pilots were probably experiencing was a result of the way the pitch and roll damping derivatives were scheduled with load factor. Figure 15 shows a plot of pitch and roll damping versus load factor as was implemented in the math model for this experiment. It can be seen that at 5.0 g the damping derivatives were approximately -12.0 and -14.0 1/sec in pitch and roll respectively. At this level, the pitch and roll response of the math model may have excited CGI and motion system dynamics that could be characterized as objectionably abrupt or ratchety as was seen during the RATAC experiment (Ref. 29).

Figure 16 shows a histogram of load factor usage for each of the eight different load factor configurations examined. The data shown are a summary of all runs flown of both air-to-air tasks by all of the pilots. It can be seen that for the configurations which had less than 3.0 g capability, the pilots were using all of the continuous load factor capability available and encountering the transient limit a significant amount of the time. For the configurations at or above 3.0 g capability the pilots were

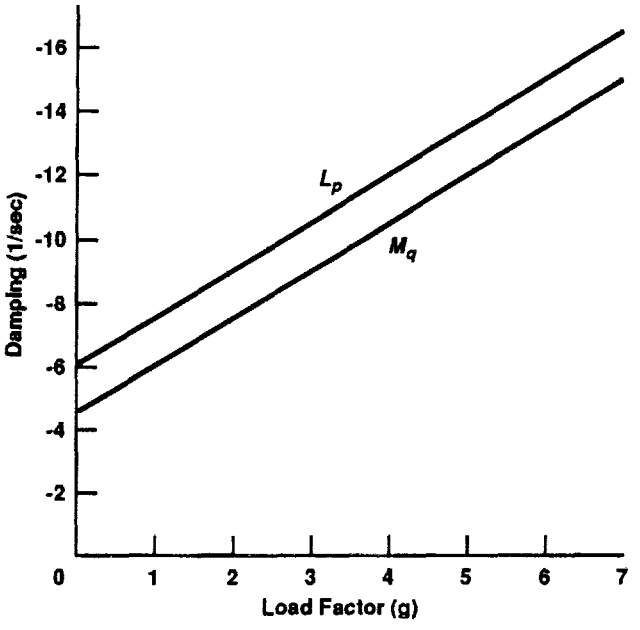

Figure 15. Variation of pitch and roll damping with load factor.

not encountering the transient limit at all. For the 4.0 and 5.0 g cases the pilots were rarely making use of the continuous capabilities of the configuration, if at all. These data support the previous commentary which indicated the pilots dissatisfaction with the maneuver capability of the Level 2 and Level 3 configurations.

It is important to note that all of the data presented so far are from air-to-air engagements against an adversary which had a continuous load factor capability of 3.5 g (Fig. 6). It is reasonable to expect that an adversary with a different maneuvering capability would change the maneuverability required of the ownship to successfully engage him air-to-air combat. Figure 17 shows CHR and performance data that was gathered for the same air-to-air tasks but against a low-capability adversary (only 2.0 g continuous load factor capability). Only two pilots participated in this portion of the experiment and only the 1.5, 2.0, and 3.5 g configurations were evaluated.

As one would expect, the 2.0 g adversary did not demand as much maneuvering capability from the ownship. The CHRs indicate that the pilots required a load factor capability only comparable to that of the adversary in order to successfully engage him. The performance data supports the CHR results. Pilot B states that for the 2.0 g ownship configuration,

"It was fairly easy to meet desired performance standards both in getting on to his tail and staying on his tail. ... You didn't have to perform the task too aggressively, because the target aircraft wasn't very aggressive. ... Minimal pilot compensation required for desired performance."

Figure 18 shows a plot of the mean time that was required during the return-to-cover task versus the load

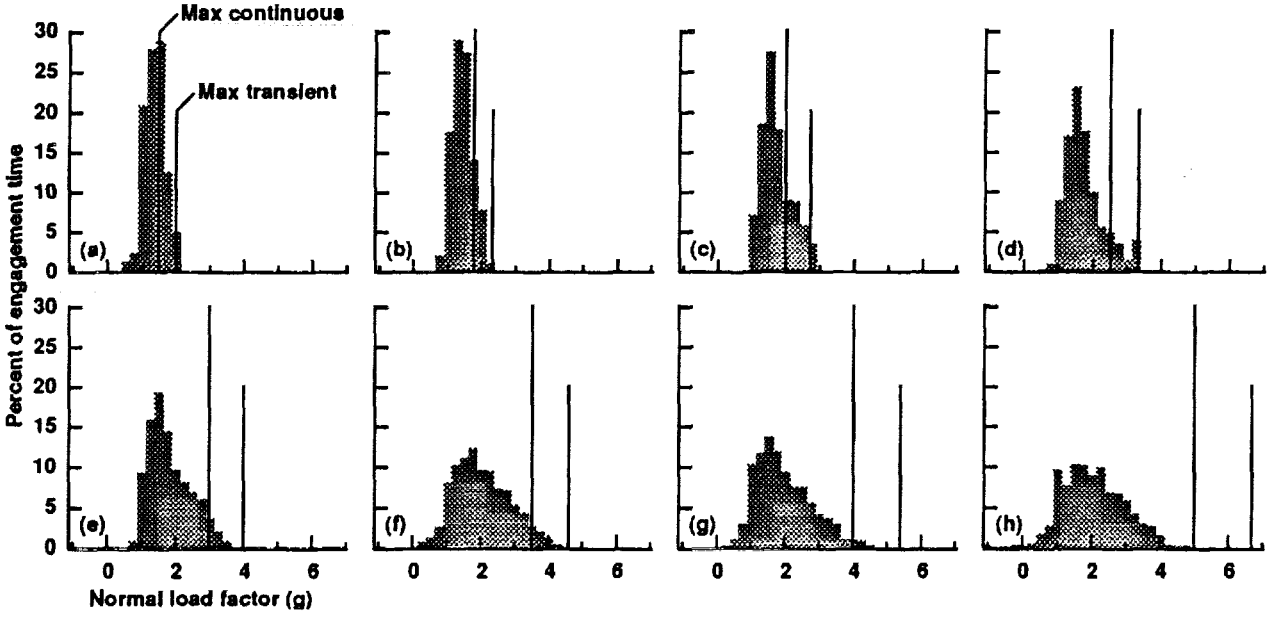

Figure 16. Load factor histogram for the mountain task. (a) 1.5 g config.; (b) 1.75 g config.; (c) 2.0 g config.; (d) 2.5 g config.; (e) 3.0 g config.; (f) 3.5 g config.; (g) 4.0 g config.; (h) 5.0 g config.

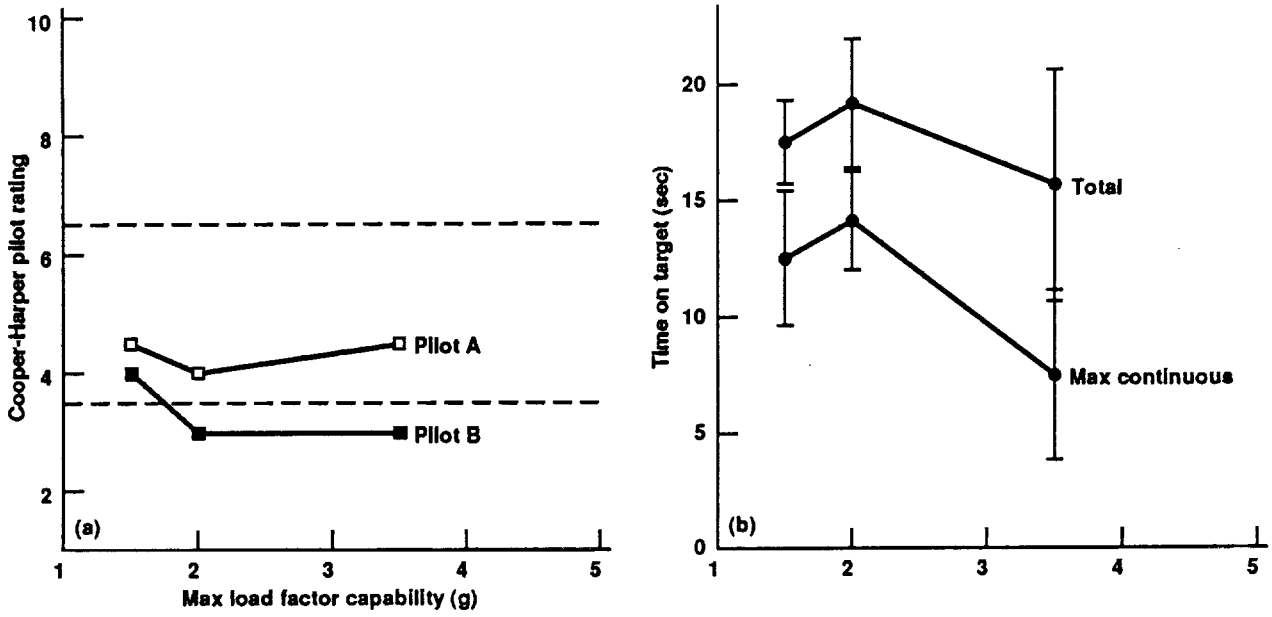

Figure 17. Results from abeam air-to-air engagements against low capability (2.0 g) adversary. (a) Cooper-Harper pilot ratings; (b) task performance.

factor configuration. The error bars indicate the ninety percent confidence interval. The dashed line on the plot shows the ideal time to turn 180 degrees in a steady turn versus load factor. No CHR data or pilot comments were gathered for this task

The trend of decreased time to regain cover with increased load factor capability is clearly shown. The trend neatly parallels that of the optimum time to turn 180 degrees with only a small time offset associated with rolling in to and out of the maneuver. This information might be useful to the designer or specification writer who has some estimate of the acceptable length of time an aircraft could be safely exposed.

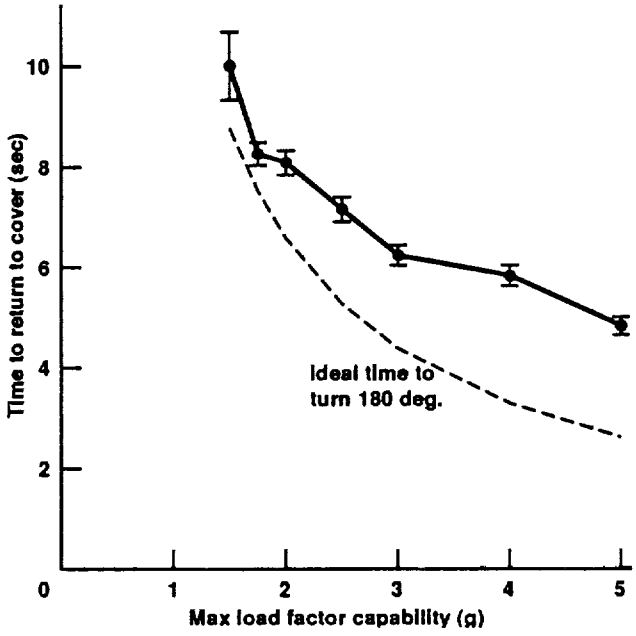

Figure 18. Time to return to cover versus maximum load factor capability.

Auxiliary Thrust

This section contains a discussion of the results from the auxiliary thruster.

Initially, the eight different auxiliary thruster inceptor/control response types were examined to determine the best candidate for the remainder of the experiment. The mean CHRs from the abeam air-to-air task for each of the eight different combinations are shown in Table 6. The pilots expressed a preference for

Table 6. Mean CHRs for auxiliary thrust inceptors.

Inceptor	Response force	Response u_{body}
cyclic joystick	5.5	2.9
cyclic thumbwheel	5.0	5.8
collective beep switch	4.8	3.5
collective twist grip	6.0	5.5

[a] Maximum N_z capability = 3.0, auxiliary thrust/weight = 0.33

the cyclic joystick with the u_{body}-rate command system. It is interesting to note though that one pilot favored the collective beep switch because of its location on the left side. He said he felt that the auxiliary thruster was a "power-type" control and should therefore be grouped with the collective. The cyclic joystick with the u_{body}-rate command system was used to generate the rest of the data presented in this section.

Figure 19 shows the CHRs and task performance results for the air-to-air tasks with and without the auxiliary thruster. Figure 19a shows the mean CHRs from both the air-to-air task and the abeam task. Figure 19b shows the task performance results for the mountain task only. The data shown for the auxiliary thruster were for a thruster which had a maximum thrust/weight capability of 0.33. The results shown for no auxiliary thruster are the same as those shown in Figures 13 and 14a.

The results indicate a significant improvement in both handling qualities and task performance when the auxiliary thruster was added. In general, there was 1.0 to 1.5 CHR improvement with the auxiliary thruster. The CHRs also indicate that the pilots were satisfied with an approximately 3.0 g configuration with the auxiliary thruster as compared to a 3.5 to 4.0 g configuration without the auxiliary thruster.

The pilot commentary indicates that the improved speed control that the auxiliary thruster afforded was a major factor in the improved CHRs. Pilot B stated,

"You could use [the auxiliary thruster] quite easily to slow yourself down, increase your turn rate or to speed yourself up to get into a better position without having to sort of lower the collective and bring the nose up so that your tracking has gone to worms."

Pilot A commented,

"During the initial part of this run, it looks like since the target is so far away from you that you can go ahead and use positive x-force to increase your speed quickly to get it up to a desired velocity for rate of closure. Once the adversary started turning, you could increase your rate of turn in an attempt to track him by using the negative X-force."

Figure 20 shows a summary of the mean CHRs given for all of the auxiliary thrust configurations. The data shown represent the average of both air-to-air tasks. The data have been shaded to indicate the CHR Level: Level 3 ratings are black, Level 2 rating are gray, and Level 1 ratings are unshaded.

The data indicate that some load factor capability can be traded for auxiliary thrust capability without significantly degrading handling qualities. It can be seen that a 3.0 g configuration with an auxiliary thrust/weight

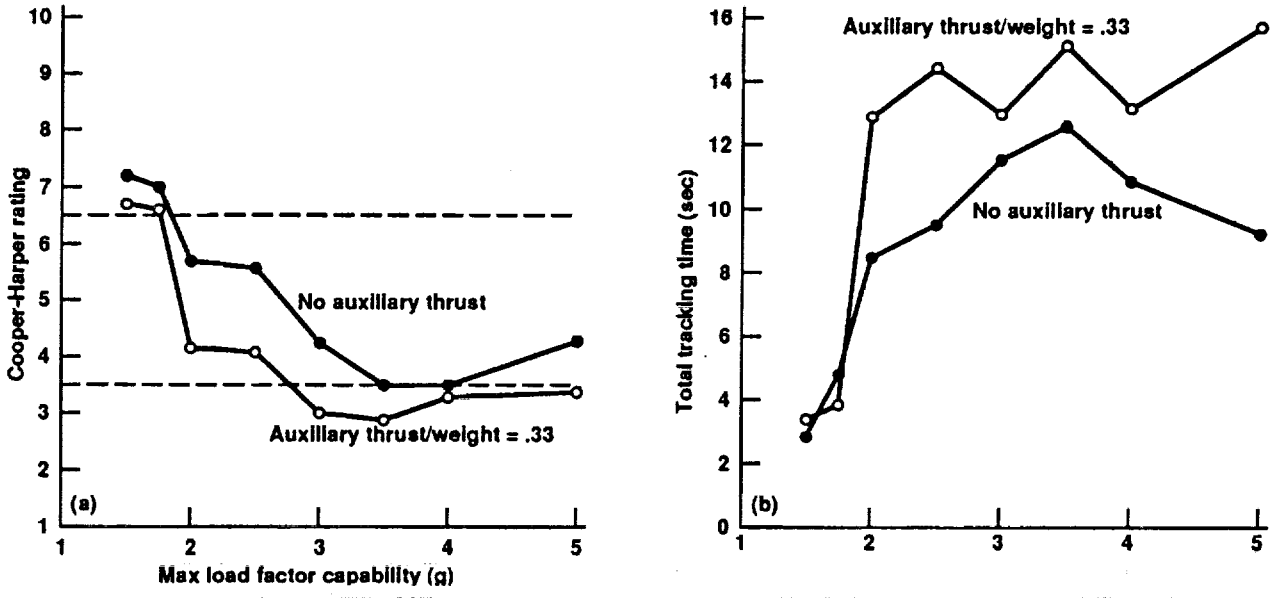

Figure 19. Air-to-air task results with and without auxiliary thrust. (a) mean CHRs for both tasks; (b) task performance for the mountain air-to-air task.

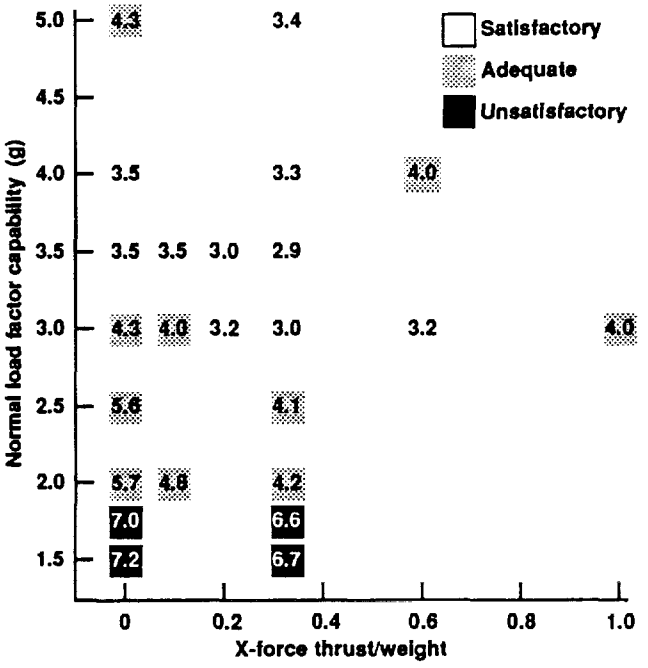

Figure 20. Mean CHRs versus load factor capability versus auxiliary thrust capability.

of 0.33 achieved better CHRs than a 4.0 g configuration without auxiliary thrust. Configurations with auxiliary thrust/weight levels as low as 0.2 are seen to possess significant handling qualities advantages over those without.

The data in Figure 20 indicate that the configurations with auxiliary thrust/weight levels of 0.6 and 1.0 did not have significant handling qualities advantages over those with 0.33 thrust/weight levels. This can be seen even more clearly in Figure 21 which shows a histogram of auxiliary thrust usage. The data in Figures 21a, b, and c show the pilots using all of the auxiliary thrust available as compared to Figures 21d and e where they do not.

Figure 22 shows a plot of the mean times that were required during the return-to-cover task versus the auxiliary thrust/weight configuration. The error bars indicate the ninety percent confidence interval. No CHR data or pilot comments were gathered for this task.

The data in Figure 22 can be compared to the data shown in Figure 18. The effect on time-to-turn of auxiliary thrust is not nearly as significant as the effect of load factor.

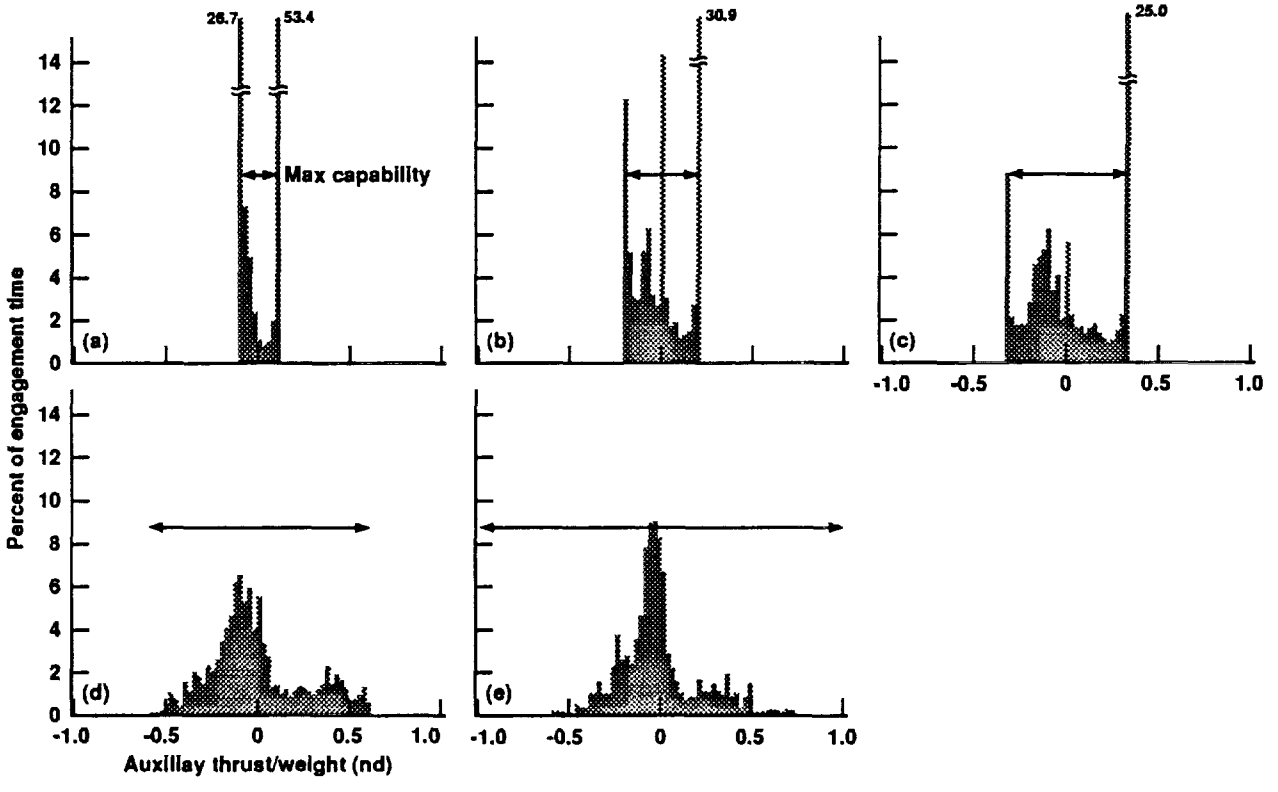

Figure 21. Auxiliary thrust histogram. (a) 0.1 thrust/weight config.; (b) 0.2 thrust/weight config.; (c) 0.33 thrust/weight config.; (d) 0.6 thrust/weight config.; (e) 1.0 thrust/weight config.

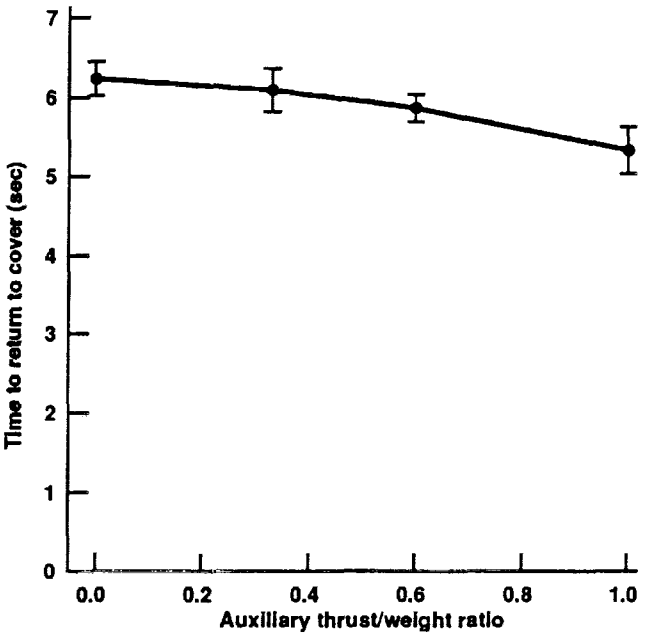

Figure 22. Time to return to cover versus auxiliary thrust capability (3.0 g maximum load factor capability).

CONCLUDING REMARKS

The U.S. Army Aeroflightdynamics Directorate performed a piloted simulation study on the NASA Ames Research Center's Vertical Motion Simulator to develop insight into the maneuverability requirements for aggressive helicopter maneuvering tasks such as air-to-air combat. Both a conventional helicopter and a helicopter with auxiliary thrust were examined. The aircraft parameters of interest were the normal and longitudinal load factor envelopes. Of particular interest were the effects of these load factor envelopes on mission performance and handling qualities. Two air-to-air acquisition and tracking tasks and a return-to-cover task were performed to assess these effects.

In general, CHRs, task performance, and pilot commentary indicated that without auxiliary thrust, the ownship normal load factor capability needed only to match that of the adversary in order to provide satisfactory handling qualities. This meant that against a 3.5 g adversary, the ownship needed 3.5 g normal load factor capability for Level 1 handling qualities and against a 2.0 g adversary, the ownship needed 2.0 g normal load factor capability.

At high levels of normal load factor capability (5.0 g) the CHR data and pilot commentary indicated some problem with pitch axis oscillations in tracking. This was probably due to the higher levels of pitch and roll damping generated by the math model at higher load factors.

The data gathered for the return-to-cover task show a clear improvement in task performance with increased load factor capability.

Of the auxiliary thruster/control systems examined, a u_{body}-rate command/u_{body}-hold system with a cyclic joystick inceptor was found to provide the best handling qualities. This system was successfully demonstrated to provide significant handling qualities advantages over configurations without auxiliary thrust.

Auxiliary thrust levels as low as 0.2 thrust/weight were shown to have significant handling qualities and mission performance advantages over those configurations without auxiliary thrust. Some normal load factor capability could be traded for auxiliary thrust capability without sacrificing satisfactory handling qualities. Increasing auxiliary thrust levels to 0.6 thrust/weight and higher did not yield further improvement.

REFERENCES

[1] Wells, C. D. and Wood, T. L., "Maneuverability — Theory and Application." Proceedings of the 28th Annual Forum of the American Helicopter Society, May 1972.

[2] Merkley, "An Analytical Investigation of the Effects of Increased Installed Horsepower on Helicopter Agility in the Nap-of-the-Earth Environment." USAAMRDL-TN-21, Dec. 1975.

[3] Attlfellner, S. and Sardanowsky, W., "Meeting the Maneuverability Requirements of Military Helicopters." Proceedings of the 2nd Annual European Rotorcraft Forum, Bückeburg, Germany, Sep. 1976.

[4] Tomlinson, B. N. and Padfield, G. D., "Piloted Simulation Studies of Helicopter Agility." Proceedings of the 5th European Rotorcraft Forum, Amsterdam, Sep. 1979.

[5] Vause, R., Harris, M., Falco, M., Shaw, D. and McDaniel, R., "The Utility of Speed, Agility, and Maneuverability for an LHX Type Mission." Proceedings

of the 39th Annual Forum of the American Helicopter Society, May 1983.

[6] Lappos, N. D., "Insights into Helicopter Air Combat Maneuverability." Proceedings of the 40th Annual Forum of the American Helicopter Society, May 1984.

[7] Curtiss, H. C. Jr. and Price, G., "Studies of Rotorcraft Agility and Maneuverability." Proceedings of the 10th Annual European Rotorcraft Forum, Aug. 1984.

[8] Houston, S. and Caldwell, A. E., "A Computer-Based Study of Helicopter Agility, Including the Influence of an Active Tailplane." Proceedings of the 10th Annual European Rotorcraft Forum, Aug. 1984.

[9] Levine, L. S., Wharburton, F. W. and Curtiss, H. C. Jr., "Assessment of Rotorcraft Agility and Maneuverability with a Pilot-in-the-Loop Simulation." Proceedings of the 41st Annual Forum of the American Helicopter Society, Fort Worth, Texas, May 1985.

[10] Thomson, D. G., "An Analytical Method of Quantifying Helicopter Agility." Proceedings of the 12th European Rotorcraft Forum, Garmisch-Parteenkirchen, Germany, Sep. 1986.

[11] Thomson, D. G., "Evaluation of Helicopter Agility through Inverse Solutions of the Equations of Motion." PhD dissertation, University of Glasgow, Nov. 1986

[12] Olson, J. R. and Scott, M. W., "Helicopter Design Optimization for Maneuverability and Agility." Proceedings of the 45th Annual Forum of the American Helicopter Society, Boston, Mass., May 1989.

[13] Scott, W. B., "Air Force, NASA Conduct Tests to Define Fighter Aircraft Agility." Aviation Week & Space Technology, Jan. 9, 1989.

[14] Bitten, R., "Qualitative and Quantitative Comparisons of Government and Industry Agility Metrics." Proceeding of the AIAA Atmospheric Flight Mechanics Conference, Boston, Mass., Aug. 1989.

[15] Drajeske, M. H. and Riley, D. R., "An Experimental Investigation of Roll Agility in Air-to-Air Combat." AIAA-90-2809-CP, 1990.

[16] Cliff, E. M., Lutze, F. H., Thompson, B. G. and Well, K. H., "Toward a Theory of Aircraft Agility." AIAA-90-2808-CP, 1990.

[17] Liefer, R. K., Valasek, J., Eggold, D. P. and Downing, D. R., "Assessment of Proposed Fighter Agility Metrics." AIAA-90-2807-CP, 1990.

[18] Schaefer, C. G. and Lutze, F. H., "Enhanced Energy Maneuverability for Attack Helicopters using Continuous, Variable (C-V) Rotor Speed Control." Proceedings of the 47th Annual Forum of the American Helicopter Society, May 1991.

[19] Danek, G., "Vertical Motion Simulator Familiarization Guide." NASA TM-103923, Jan. 1993.

[20] Jones, A. D., "Operations Manual, Vertical Motion Simulator (VMS) S.08." NASA TM-81180, May 1980.

[21] Plonsky, J. G., "Development of Equations to Improve Deficiencies in the GENHEL UH-60A Math Model." Aircraft Division, United Technologies Corporation, NAS2-11058, 1989.

[22] Austin, F. and George, D., "Automated Control of an Adversary Aircraft for Real-Time Simulation of Air-to-Air Combat." Grumman Corp. Report RE-786, Aug. 1991

[23] Austin, F., George, D. and Bivens, C., "Real-Time Simulation of Helicopter Air-to-Air Combat." Proceedings of the 47th Annual Forum of the American Helicopter Society, Phoenix, Arizona, May 1991.

[24] Von Neumann, J. and Morgenstern, O., Theory of Games and Economic Behavior, Princeton University Press, 1944, p 112.

[25] Lewis, M. S. and Aiken, E. W., "Piloted Simulation of One-on-One Helicopter Air Combat at NOE Flight Levels." NASA TM-86686, Apr. 1985.

[26] Lewis, M. S., Mansur, M. H. and Chen, R. T. N., "A Piloted Simulation of Helicopter Air Combat to Investigate Effects of Variations in Selected Performance and Control Response Characteristics." NASA TM-89438, Aug. 1987.

[27] Lewis, M. S., "A Piloted Simulation of One-on-One Helicopter Air Combat in Low Level Flight." J. AHS, Volume 31, No. 2, pp. 19—26, Apr. 1986.

[28] Whalley, M. S., "Development and Evaluation of an Inverse Solution Technique for Studying Helicopter Maneuverability and Agility." NASA TM-102889, USAAVSCOM TR 90-A-008, Jul. 1991.

[29] Whalley, M. S. and Carpenter, W. R., "A Piloted Simulation Investigation of Pitch and Roll Handling Qualities Requirements for Air-to-Air Combat." Proceedings of the 48th Annual Forum of the American Helicopter Society, Jun. 1992.

[30] Anon., "Handling Qualities Requirements for Military Rotorcraft, U. S. Army AVSCOM Aeronautical Design Standard, ADS-33C." Aug. 1989.

[31] Cooper, G. E. and Harper, R. P., "The Use of Pilot Rating in the Evaluation of Aircraft Handling Qualities." NASA TN-5153, Apr. 1969.

[32] Bethea, R. M. and Rhinehart, R. R., Applied Engineering Statistics. Marcel Dekker, Inc., New York, 1991, pp 63-65.

The Application of Active Side Arm Controllers in Helicopters

R. Knorr, C. Melz, A. Faulkner, M. Obermayer
Eurocopter Deutschland GmbH
Dept. Guidance and Control
P.O. Box 80 11 40
8000 München 80
Germany

ABSTRACT

Eurocopter Deutschland (ECD) started simulation trials to investigate the particular problems of Side Arm Controllers (SAC) applied to helicopters.

Two simulation trials have been performed. In the first trial, the handling characteristics of a "passive" SAC and the basic requirements for the application of an "active" SAC were evaluated in pilot-in-the-loop simulations, performing the tasks in a realistic scenario representing typical phases of a transport mission. The second simulation trial investigated the general control characteristics of the "active" in comparison to the "passive" control principle.

A description of the SACs developed by ECD and the principle of the "passive" and "active" control concept is given, as well as specific ratings for the investigated dynamic and ergonomic parameters affecting SAC characteristics. The experimental arrangements, as well as the trials procedures of both simulation phases, are described and the results achieved are discussed emphasizing the advantages of the "active" as opposed to the "passive" SAC concept. This also includes the presentation of some critical aspects still to be improved and proposals to solve them.

Presented at Piloting Vertical Flight Aircraft: A Conference on Flying Qualities and Human Factors, San Francisco, California, 1993

NOMENCLATURE

AC	Attitude Command
ACAH	Attitude Command/Attitude Hold
ACT	Active Control Technology
CHR	Cooper Harper Rating
ECD	Eurocopter Deutschland GmbH
FCC	Flight Control Computer
FRP	Finger Reference Point
IC	Inceptor
MTE	Mission Task Element
NSRP	Neutral Seat Reference Point
PIO	Pilot Induced Oscillations
RC	Rate Command
RCAH	Rate Command/Attitude Hold
SAC	Side Arm Controller
e_θ	rms tracking error pitch axis
e_ϕ	rms tracking error roll axis
rms	root mean square

INTRODUCTION

With the increase of requirements in both civil and military operations, conventional control technologies using mechanical linkages and automatic flight control systems with limited authority cannot relieve the pilot from higher mental and manual control activity. To alleviate pilot workload, today's high performance fixed wing aircraft as well as some transport aircraft use Active Control Technology (ACT) employing Fly-By-Wire, Fly-By-Light and full authority AFCS.

These technologies also enable the

employment of advanced primary controllers which present the aircraft designer with a great deal of freedom to produce an ergonomically more attractive cockpit. Different types and configurations of Side Arm Controller (SAC) have been investigated in several programs [1, 2, 7]. With the SAC employed in production aircraft new problems have been encountered as in particular Pilot Induced Oscillations (PIO), roll ratched, bio-dynamic interactions, command priority within the cockpit, etc.

Within the definition phase of a future FBW medium transport helicopter, Eurocopter Deutschland (ECD) performed a number of experiments to investigate the particular problems of SAC applied to helicopters. To this end, a 2-axis "active" cyclic and 1-axis "active" collective SAC had to be developed. Active inceptors (ICs) were choosen for the study because they gave the greatest flexibility of investigating different force gradients. But more important, was the aspect to asses the application of "active" SACs. Another main interest lay in the design of SAC devices, which should be able to be integrated into existing helicopters to perform inflight-simulation tests. As this aim excluded the design of an electro-hydraulic position servo system, the position servo system was realised by direct current linear motors.

Since the application of "active" SAC is an advanced concept, extensive simulator evaluations are necessary to optimise their ergonomics and dynamic characteristics together with the Flight Control Systems. To reach this goal, the simulation trials have been divided into three phases.The first phase consisted of pilot-in-the loop ground simulation trials where the SACs have been used as "passive" devices to concentrate on ergonomic aspects when assessing the handling characteristics of the SACs in a realistic scenario. The second phase represents off-line-simulations to investigate the general characteristics of "active" in comparison to "passive" controllers and to evaluate the dynamic characteristics of the "active" SACs with respect to the recommendations made in the first phase. In the third phase the "active" SACs will be tested in flight trials with a wide range of flight tasks from transport mission elements up to aggressive MTEs.

The report gives an overview of the experimental arrangements, the trials procedures and the results of the simulation trials of Phase I and II.

PASSIVE AND ACTIVE INCEPTORS

In the last 15 years several investigations at a number of research institutes have been undertaken dealing with the design of "active" controllers [3, 4, 5, 6]. Since the definition of "active" controllers sometimes vary between the different publications, it seems appropriate to stress the distinction between the "passive" and the "active" control principle (Fig. 1, 2).

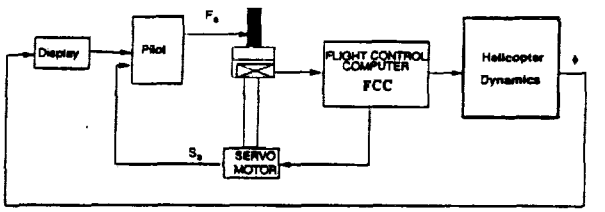

Fig. 1: Control Loop with "passive" Side Arm Controller

In the "passive" SAC the pilot feels spring forces according to the applied stick deflection which is the control input to the Flight Control Computer (FCC). These forces are realised either by a spring and damper package or by a servo controlled position system. In the first case the pilot's controller forces are usually fixed but a servo controlled position system can be used to vary the spring stiffness, damping, breakout forces, zero position easily to a pre-defined force deflection control law. In the second case the pilot "feels" a simulated control force via the sensor package and the position via the servo mechanism. A drawback of this "passive" control concept, as opposed to conventional controllers, is that the pilot looses the contact with the control surfaces of the aircraft. This means that the pilot looses tactile information and can only use peripheral cues (visual and vestibular) to inform him about his actual flight state and the available control power. Disastrous events could be the consequence if the pilot inadvertently tries to exceed the flight envelope.

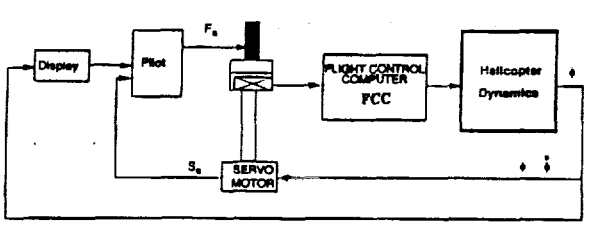

Fig. 2: Control Loop with "active" Side Arm Controller

In contrast to the "active" control concept, the applied stick force is the control input to the FCC and the responding control response (attitude or rate) of the aircraft is fed back as the command input to the position

servo system. In this approach, the pilot receives tactile information of the actual flight state of his aircraft on his SAC and with this he retains indications of his actual flight states as well as his control limitations.

The servo controlled SAC ("passive" and "active") of both pilot and copilot gives each crew member a tactical and optical feedback of the command input of the other one. In contrast to the "passive" concept, with the "active" concept there is no more need to nominate a pilot command priority since the commanded grip forces of the two controllers can be summed to obtain one control signal. Fully transparent transfer of command control can be made between the crew and the stick positions synchronised. This important aspect could be demonstrated in phase I.

INCEPTOR PRINCIPLE AND CHARACTERISTICS

As the report aims to stress the general characteristics of an "active" SAC, only the cyclic controller will be considered.

A schematic of the realised cyclic SAC is presented in Fig. 3. It consists of two axis providing a deflection of -18 deg, +12deg in the pitch axis and +/- 14 deg in the roll axis. The SAC has a force sensor at the pilot's hand grip together with a servo-actuator used to position the stick and provide artificial force feel. Since the actuation of the SAC is of secondary importance, it does not have to be included in the flight safety critical path and need hence only be simplex. On the other hand, the force sensing is the primary command input to the FCC and must be quadruplex redundant. In the event of a failure, both pilot and copilot can fly the helicopter without requiring a priority switch. The question of inceptor failure characteristics was one of the objectives of the simulation trials phase I.

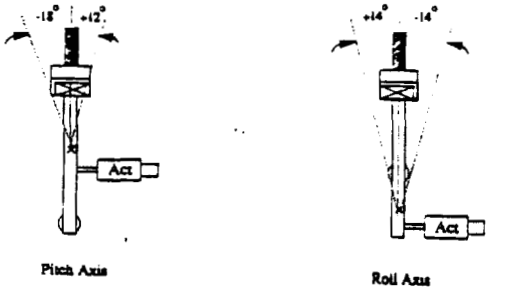

Fig. 3: Schematic of the cyclic Side Arm Controller

The integration of the inceptors in the flight control system with the FCC is shown in the functional block diagram (Fig. 4). The pilot's grip force is measured by an LVDT which is demodulated and sent to the FCC within which scaling, signal conditioning and filtering occurs. Parallel to the grip force, the primary "hands-on" flight state, the pilot is provided with a "beep" trim button on the top of the grip. The "beep" rate is also dependent on the pilots grip force so that if the pilot simultaneously puts a force on the grip and "beeps", the stick will move at a faster speed. An FTR switch is provided to synchronise and zero stick forces if desired. The final output signal of the inceptor position block is used to actuate the stick servo and provide the force feel.

Since the motion of the stick is designed to give the pilot tactile feedback of the helicopter response, the actuation bandwidth specification is dependent on the closed loop bandwidth of the helicopter and flight control system. Analyses of the closed loop bandwidth for the defined helicopter indicated a bandwidth requirement for the actuator of at least 1 Hz for both longitudinal and lateral since the differences in the corner frequency for the axes was only marginal.

SIMULATION TRIALS PHASE I

SIMULATON FACILITY

For pilot-in-the loop simulation trials both ECD and the Military Aircraft Divisions of DASA share a common simulation facility located in the Military Aircraft Division. The main features of the simulation facility at the time of the simulation trials Phase I shows Fig. 5, Fig.6:

- Denelcor HEP (Heterogenous Element processor) Simulation Computer with parallel processor architecture (A), (The HEP simulation computer has meanwhile been replaced by a more powerful HARRIS Nighthawk computer, together with a new interface computer)
- GE Compu-Scene IV computer image generator (B)
- fixed base with provisions for buffeting and g-seat
- 6 channel dome projectionsystem (C)
- Interface computer between cockpit and simulation computer (D)
- Hydraulic buffeting platform with

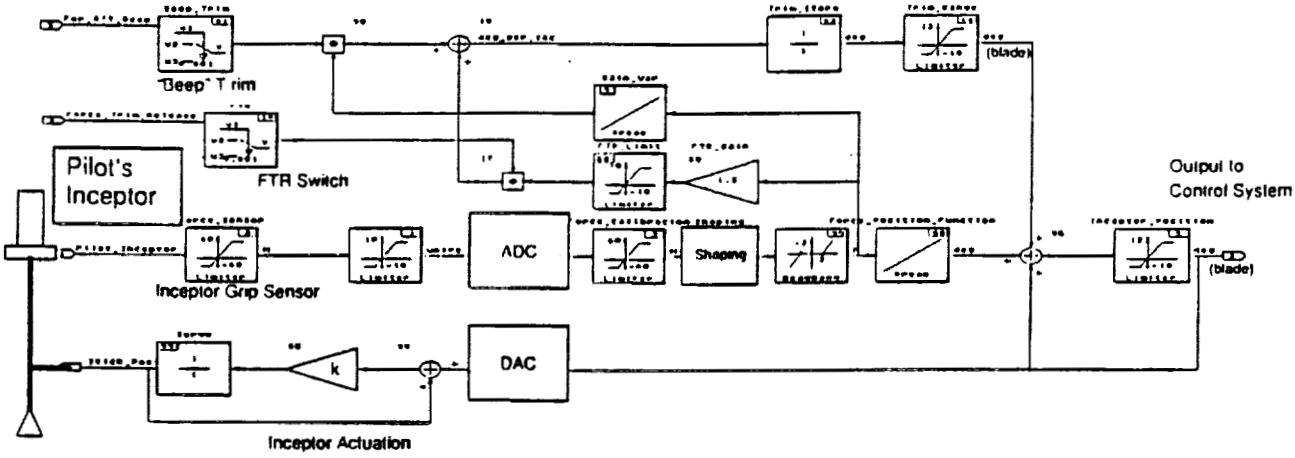

Fig. 4: Passive Inceptor Simulation Set-up

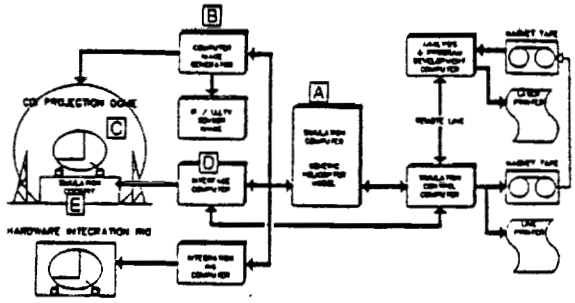

Fig. 5: ECD Helicopter Simulation Facility

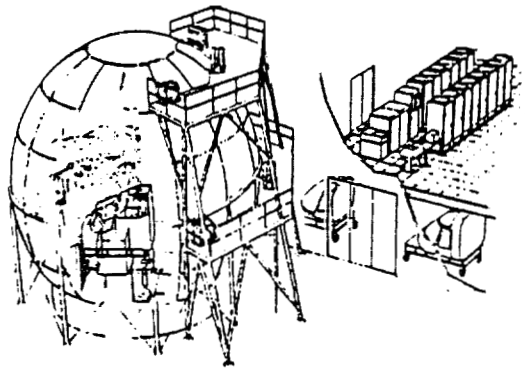

Fig. 6: Compu-Scene IV Dome Projection System

exchangeable cockpits

- large field of view (+/-70 deg horizontal, +70/-40 deg vertical)

ERGONOMIC ASPECTS

The right hand inceptor was installed horizontally with a slight (15°) tilt inward which was found to be a more ergonomic position than a purely vertical grip (Fig. 7, 8). Provision was made to adjust the position of the inceptor relative to the seat. The left hand inceptor was installed sloping downward with adjustment provision in the vertical and horizontal directions (Fig. 9). An overview of the choosen inceptor/seat geometry is given in Fig. 10.

A total number of 15 pilots, plus several other persons, were requested for evaluation of the flight controls and seat ergonomics. As published in [6] measurements as per Fig. 11 were made, which covered a significant range of percentiles. The flight experience of the pilots ranged from several hundred hours (private pilot) to nearly 10000 hours (test pilot) with different combinations of IFR and VFR time (civil/military) and varying levels of simulator experience and aptitude.

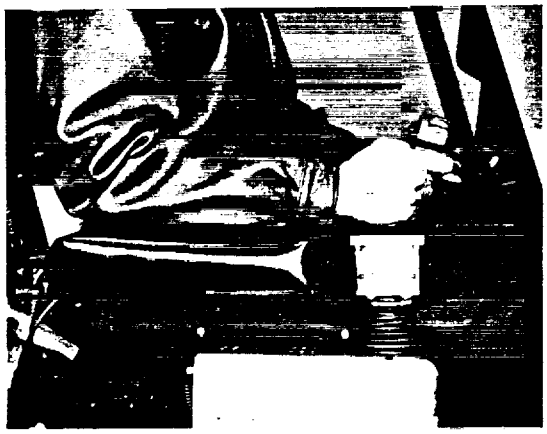

Fig. 7: Cockpit View of the Cyclic Controller (side view)

Fig. 8: Cockpit View of the Cyclic Controller (front view)

Fig. 9: Cockpit View of the Cyclic and Collective Controller

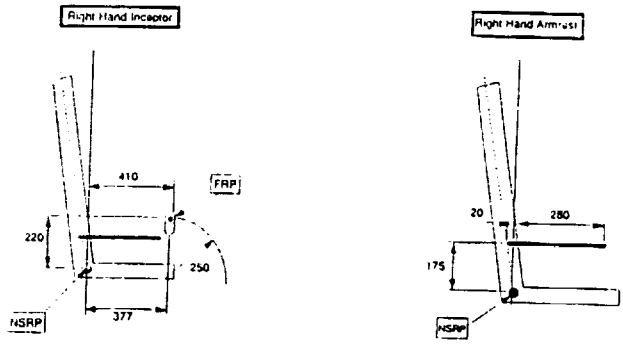

Fig. 10: Inceptor/Seat Geometry, dimensions in [mm]

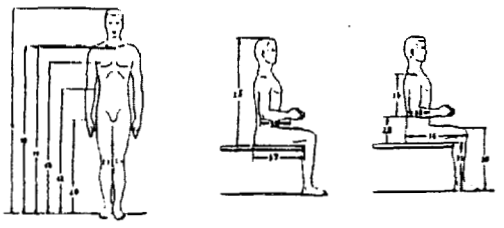

Fig. 11: AGARD-AG-205 Standard Definitions

FLIGHT MECHANICS MODEL

The helicopter flight characteristics are simulated by a non-linear simulation program calculating all external forces and moments of the individual components (e.g. main rotor, tail rotor, fuselage, empenage) based on non-linear aerodynamic coefficients from windtunnel data. The sum of these forces and moments including external influences like wind and ground effects yield the helicopter motion which is presented to the pilot on cockpit instruments and in the computer generated image.

FLIGHT CONTROL SYSTEM CONCEPT

Analysis of the defined helicopter dynamic characteristics showed a classic poorly damped phygoid mode and a better damped roll mode as well as a poorly damped "Dutch Roll" mode. For the simulation trials, a simple stabilisation system was realised with a quasi attitude hold

SIMULATION TASKS

To get as many results as possible concerning the influence of ergonomics and appropriate SAC characteristics under most realistic conditions, it was decided to perform the tasks in a realistic scenario representing typical phases of a tactical transport mission. The task elements were arranged so that they cover the full range of control input types between small/slow (IFR-cruise) and large/fast (VFR-NOE). The pilots were requested to asses their performance and workload for each task element with special emphasis on the SAC characteristics.

ASSESMENT METHOD

The basis for assessment was the Cooper Harper Rating (CHR) scale. Though not easy to differentiate, the pilots were requested to give specific ratings for the parameters like force levels, and gradients in all axes, controls travel and sensitivity, trim speeds, trim release function as well as the position of seat and controls.

PASSIVE SAC CONFIGURATION VARIATION

Experiments were performed prior to the trials, to initially determine the range of force displacement characteristics. These showed that at least 3 gradients were required, an initial steep gradient to provide a smooth breakout characteristic followed by a shallow gradient and finally a steeper gradient (Fig. 12, 13).

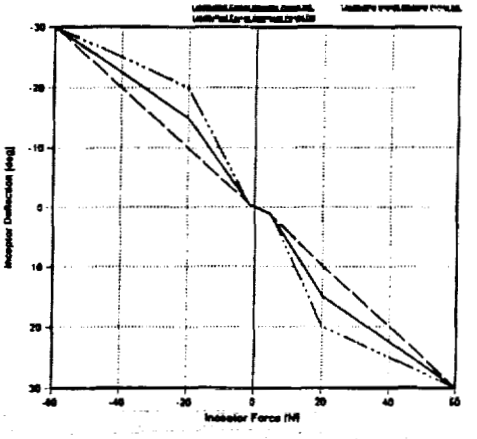

Fig. 12: Longitudinal Cyclic Inceptor Force /Deflection Charact.

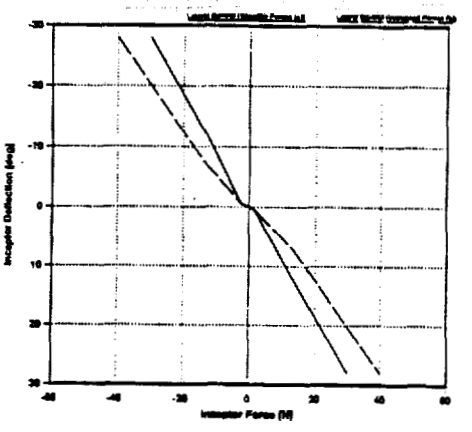

Fig. 13: Lateral Cyclic Inceptor Force /Deflection Charact.

Various combinations were prepared for the simulation trials consisting of:

(a) Basic data set: Cyclic large displacement controller with force gradients

(b) Increased cyclic force gradients

(c) Reduced cyclic force gradients

(d) No cyclic gradients

(e) Controller actuation failure

(f) 50% reduction in inceptor motion

RESULTS

Selected Seat And Control Position

To satisfy all test subjects which covered a wide range of percentiles a seat range of 8 cm in height variation and 18 cm in for/aft position were required. All pilots, however were able to accept the nominal SAC positions without adjustment.

SAC Ergonomics

The shape, position and inclination of the SAC in combination with the armrests were commented very favourably. The stick travels were found adequate. There was, however, a preference by some pilots for reduced forward controller travel. Firstly to prevent the pilot from having to stretch his arm to an uncomfortable position and secondly to minimise the "sliding action" required between the forearm and seat armrest.

There was a good tendency for lower force deflection gradients and in particular for asymmetric left/right gradients to compensate for asymmetric arm muscular characteristics.

SAC functions

The dynamic SAC characteristics were commented by all pilots as being acceptable in the lateral axis but as too "heavy" in longitudinal. The pilots needed too much effort for fast control inputs as in NOE manoeuvres. During high gain manoeuvres, the pilot had to be careful not to "block" the SAC by rigidly hold the grip as this tended to lead to small oscillations. This limitations could be removed later by increasing bandwidth and decreasing the simulator computer delays.

Spot checks confirmed that in the event of a blockage of the SAC actuators flight could be continued, including a safe landing, using beep trim which continues to operate but without stick position changes and pure force control.

RESULTING IMPROVEMENTS FOR PHASE II

Based on the pilot's assessments the following improvements were introduced.

- increase of bandwidth to 4 Hz at 25% control amplitudes
- lower force gradients to the right

SIMULATION TRIALS PHASE II

As the results from the simulation phase I showed mainly the control handling under ergonomic aspects, the prime objective in this phase was to investigate the improvements achievable when employing the "active" control characteristics to the SAC.

The simulation phase II was divided into 2 steps:

In the first step, only engineer-in-the loop simulations were performed, since evaluation of the general characteristics of the "passive"/"active" control characteristics at this stage did not need any pilot involvement.

In the second step, still to be performed, the dynamic characteristics of the cyclic controller will be optimised and fixed through pilot-in-the loop simulations in preparation for the later flight trials

SIMULATON TEST CONFIGURATIONS

Since the first step had not been the objective to evaluate an optimal dynamic characteristic for the "active" SAC, a test facility with a simplified control task was set up to investigate the control handling of the two control concepts in parallel.

The tests were performed in a realistic cockpit mock-up in which the ergonomic aspects like ingress/egress, armrest/seat/SAC configuration could be taken into account.

HELICOPTER MODEL AND SAC DYNAMICS

System dynamics represented a stabilised, decoupled helicopter with pitch and roll dynamics and a selectable RCAH or ACAH response type. This was realised by a simple lag filter (ACAH) or a lag plus additional integral filter (RCAH). For the first approach the time constants for the control modes were, up to for AC: T_θ = 2s, T_ϕ= 1s, and for RC: T_q = 1s, T_p = 0.5s, which covers a wide range of light to medium weight class helicopters.

The values for the force deflection characteristics for the investigation of the "passive" characteristics were taken as they were recommended from phase I.

EXPERIMENTS

To evaluate the control handling, a target tracking task in one control axis for, both pitch and roll, was established consisting of a randomly moving target circle, which the operator was required to maintain within the centre of a computer generated image of a simplified ADI. The simplified ADI gave the subject additional information about its actual flight attitude during the task. The simulation test arrangement is

shown in Fig. 14.

A number of 5 test person, all engineers, 4 of them with flight experience on different simulators, volunteered for the experiment. The trial consisted of a set of 4 different combinations for the tracking task in each axis and per subject with two runs recorded and analysed. Before the test runs were recorded each subject was given unlimited time until he felt familiar with the task, as well as one test run. Two runs were recorded where each run lasted 60s. To determine the tracking performance of each subject the rms value for the tracking error in the pitch axis $e_\theta = (\theta\_target - \theta\_heli)$ was calculated (in the pitch axis as well as in the roll axis).

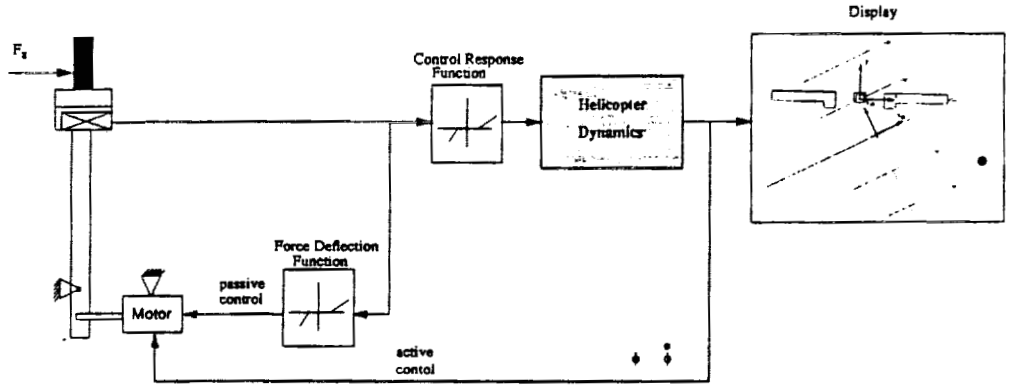

Fig. 14: Simulation Test Arrangement for Simulation Trials Phase II

TEST RESULTS

The rms tracking error e_θ for the different task configurations are presented in Fig. 15, 16. The different values for the rms value of the tracking error in the pitch and roll axis occurred because of different geometric definitions of the pitch and roll attitude for the simplified ADI.

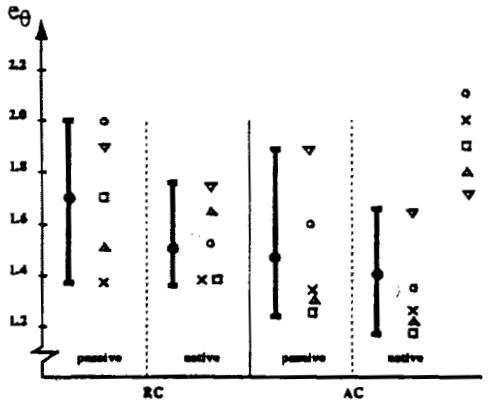

Fig. 15: RMS Tracking Error in the Pitch Axis

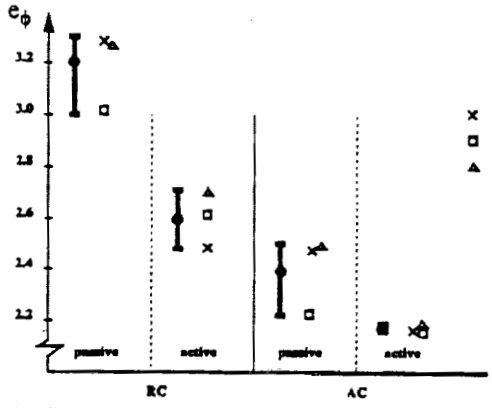

Fig. 16: RMS Tracking Error in the Roll Axis

Passive Mode:

As was expected, in the passive mode, the AC control strategy in both axes showed a lower tracking error as opposed to the RC control strategy. According to the defined control task the pilot is forced to perform precise control inputs to minimize the deviation from the target position. With the AC the pilot directly controls the attitude so he is able to perform attitude changes more precise. With a RC the pilot controls the rate. This provides him a quicker helicopter response but also forces him to integrate the rate to estimate when to counter control to stop the rate. In high aggression manoeuvres with a demand for large but not precise control inputs this control strategy gives him a quick aircraft response. However, in precision manoeuvres, like the target tracking task, this results in higher control activity to achieve a particular attitude and higher deviations from the track.

Active Mode:

Figures 15, 16 show that the rms value for e_θ and e_ϕ for both the RCAH and ACAH control strategy could be reduced with "active" feedback of the rate (RCAH) and attitude for (ACAH) respectively.

In the "active" mode with the RC control strategy, where the actual rate is fed back to the controller, the control behaviour for commanding a rate was totally different. At the moment the pilot applies a force to the hand grip he commands a particular rate which moves the stick in the direction of the applied force. This means that to hold a constant grip force the pilot has to push the stick forwards with the same speed as the stick is controlled by the servo motor. Otherwise the force decreases which consequences in a lower commanded rate. If the grip force is allowed to return to zero the stick stops at a new displaced position and the helicopter at a new attitude. This characteristic can be interpreted as a form of Follow-Up Trim. At the beginning, the subjects criticised the control behaviour of the stick as being too sluggish since the rate feedback did not allow the pilot to perform high frequent control inputs. But, after a short time when he became more familiar with this control characteristic he realised that he needed much less control activity to track the target and found it much more comfortable in comparison to the RC with "passive" characteristic. The improvement tracking error measurements for the "active" configuration confirmed this subjective comment. The advantages of the "active" characteristic were especially noted in the roll axis where the subjects were given a more difficult task with higher control effort as opposed to the pitch axis.

The comparison of the rms value e_θ for the AC control strategy shows once again a further decrease of the tracking error when the "active" mode was employed. This can be attributed to the additional attitude information the pilot receives from the SAC where the position is proportional to the actual attitude of the aircraft and correlated to the visual attitude information on his artificial horizontal display. Together, the subject gains a remarkable lead in his control activities reducing both amplitude and frequency of the control inputs. Furthermore, it is noticeably that in both axes the majority of the subjects achieved nearly identical rms tracking error values for the AC with the "active" feedback. Since all subjects had the same induction phase it would appear that it was more easy to adapt to the "active" controller than the "passive".

CONCLUSIONS

- The SAC concept tested received mostly very positive comments on the ergonomics. A cross-section of pilots were able to use the inceptor without necessitating adjustment relative to the seat. The pilot should be made as comfortable as possible; small points like including the grip inwards give a more natural sitting position.
- A 3-gradient force deflection curve was found adequate for the inceptor in the "passive" mode; asymmetric force/deflection gradients are desirable to compensate for the different bio-mechanical force characteristics of the arm.
- The control ranges of the SAC tested were acceptable, represented the upper limit; where possible a smaller longitudinal range would be desirable to prevent inter-axis coupling in large manoeuvres.
- In both AC and RC control modes the "active" control concept could significantly reduce the tracking error for all subjects.
- The "active" control concept provided the subjects tactile information of their actual flight state helping them to coordinate with the visual attitude information. This was found to make the tracking task easier to learn and to increase subject performance.
- A servo bandwidth of 4Hz as tested was found to be adequate for both "passive" and "active" activation modes.

REFERENCES

1. Landis, K. H.; Glusman, S. I., "Development of ADOCS (Advanced Digital/Optical Control System) Controllers and Control Laws. Vol. 1,2,3, Boeing Vertol Co., Philadelphia.*National Aeronautics and Space Administration, Washington, DC, 1984.

2. Aiken, E.W., "Effects on Side-Stick Controllers on Rotorcraft Handling Qualities for Terrain Flight", NAE Report No: NAS 1.15:86688, A-85141, 1985.

3. Doetsch, K.H.; Röger,W., "The Transfer of Control and Guidance Information to the Pilot through the Manipulator Forces", Sonderforschungsbereich Flugführung, TU Braunschweig, 3300 Braunschweig, P.O. Box 3329, Germany

4. Hosman, R.J.A.W.; van der Vaart, J.C., "Active and Passive Side Stick Controllers: Tracking Task Performance and Pilot Control Behaviour", Faculty of Aerospace Engineering, Delft University of Technology, Delft, The Netherlands.

5. Repperger, D, W.*; McCollor D.**; "Active Sticks - A New Dimension in Controller Design", *Air Force Aerospace Medical Research Laboratory, Wright Patterson Air Force Base, Ohio,45433, ** Raytheon Service Company

6. "A Review of Anthropometric Data of German Air Force and United States Air Force Flying Personnel, AGARD-AG-205, 1974.

7. Kissel, G.; "Steering Mechanism With An Active Force Feedback, Especially For Aircraft", United States Patent, Assignee: MBB GmbH, Germany, 1979.

Rotorcraft Flying Qualities Improvement Using Advanced Control

D.Walker[1], I.Postlethwaite[1], J.Howitt[2] and N.Foster[1]

1 Control Systems Research Group
Department of Engineering
University of Leicester
Leicester LE1 7RH U.K.

2 Flight Systems Department
Defence Research Agency
Bedford MK41 6AE U.K.

ABSTRACT

We report on recent experience gained when a multivariable helicopter flight control law was tested on the Large Motion Simulator (LMS) at DRA Bedford. This was part of a study into the application of multivariable control theory to the design of full-authority flight control systems for high-performance helicopters. In this paper, we present some of the results that were obtained during the piloted simulation trial and from subsequent off-line simulation and analysis. The performance provided by the control law led to level 1 handling quality ratings for almost all of the mission task elements assessed, both during the real-time and off-line analysis.

INTRODUCTION

The continuing drive to extend the operational capabilities of combat helicopters is demanding advanced flight control systems with handling qualities tailored appropriately for the mission task. By reducing pilot workload and allowing full use of the whole performance envelope, there is significant potential for improved mission effectiveness and survivability, particularly when required to manoeuvre at low level in bad weather and/or at night.

Leicester University has for the past three years been working on a research contract funded by the Defence Research Agency (DRA) Bedford, the primary aim of which has been to investigate the role of advanced multivariable frequency domain control theory to the design of helicopter flight control laws. The multivariable frequency domain approach is seen as essential if satisfactory decoupled performance is to be maintained in the presence of uncertain high frequency dynamics and disturbances. Here we report on the piloted simulation and off-line assessment of a controller designed by the first two authors under the terms of that agreement. The main purpose of the agreement was to enable an in-depth computer simulation study, backed up by periods of piloted simulation, that would help to assess further the role that advanced control theory might play in improving the handling qualities of future military helicopters. Our latest work follows on from earlier collaboration dating back to the mid 1980's between DRA Bedford and the second author [1,2,3], perhaps the most notable achievement of which was the piloted helicopter simulation of a multivariable control system designed using H-infinity optimal control theory [3].

The main achievement of the last three years work has been the significant improvements that have been obtained in relation to earlier

results [3,4], particularly during the last twelve months, in terms of wide-envelope decoupled performance, robust stability and compliance with ADS-33C [5]. This paper focuses on some of these latest results.

Description of the mathematical model

The mathematical model of the Lynx used for this study was the DRA Bedford Rationalised Helicopter Model (RHM) [6] which was used for both analysis and piloted simulation. The RHM models the separate aerodynamic force and moment contributions of the main rotor, tail rotor, fuselage, fin and horizontal stabilizer with the main rotor model consisting of rigid constant chord blades hinged with stiffness in flap at the centre of rotation. A constant lift slope and uniform induced flow are assumed and unsteady aerodynamic effects are ignored. A third order engine model defines torque and rotor speed degrees of freedom. Correlation with flight data is, in general, satisfactory and qualitative pilot comment has been favourable. Research is continuing to further improve the modelling fidelity of the rotor dynamics.

The same model was used for real-time piloted simulation and off-line handling qualities assessment.

Robustness

The equations governing the motion of the helicopter are complex and impossible to formulate with absolute precision. Consequently any mathematical model used for control synthesis will inevitably be inaccurate to some degree. Robustness means in essence the insensitivity of a feedback system to model error, parameter variations and non-linearities. Robust control theory provides methods of designing controllers that are insensitive to the errors and approximations present in the models that are available to the designer. Numerous design methods have been proposed over the last three decades which can to varying degrees accommodate robustness constraints. Here, a method based on H-infinity optimization was used.

The starting point for our designs was a set of five eighth-order linear differential equations modelling the small-perturbation rigid body motion of the aircraft about five trimmed conditions of straight-and-level flight in the range 0 to 80 knots. The controller designs were first evaluated on the eighth-order models used in the design, then on twenty-one state linear models, and finally using the full nonlinear model. The robust design methodology used in the controller design did turn out to provide excellent robustness with respect to nonlinearities and time delays simulated although not explicitly included in the linear design process.

OBJECTIVES AND DESIGN METHOD

The main design objectives were:

- Robust stabilization of the aircraft with respect to changes in flight condition, and model uncertainty and non-linearity.
- High levels of decoupling between primary controlled variables.
- Compliance with the ADS-33C Level 1 criteria.

Design method

The method that was used to synthesize the control law was based on the H-infinity open loop methods that have been widely documented recently [7]. It is not intended to discuss the design techniques in detail here, but it is worth noting that the procedure adopted led to a two degree-of-freedom multivariable controller that robustly stabilized the aircraft over a wide range of flight conditions, whilst simultaneously

forcing the closed loop system to approximate the behaviour of a specified transfer function model. It has also been found that the ADS-33C bandwidth requirements impact directly on the cross-over frequency of the loop shape weighting functions used in the design process. The overall control law was actually comprised of five controllers, designed at a range of flight conditions between 0 and 80 knots, each one having a Kalman filter-like structure. As the dynamics of the open-loop aircraft vary with speed, so too did the controllers obtained at each operating point. Therefore, these controllers could be scheduled with forward speed if required, to give wide-envelope performance.

Response type

The basic aim of the design was to synthesize a full-authority controller that robustly stabilized the aircraft and provided a decoupled Attitude-Command/Attitude Hold (ACAH) response type that closely approximated the behaviour of a simple transfer-function model.

The outputs to be directly controlled were:

- Heave velocity
- Pitch attitude
- Roll attitude
- Heading rate

With a full authority control law such as that proposed here, the controller has total control over the blade angles, and is interposed between the pilot and the actuation system. The pilot flies the aircraft by issuing appropriate demands to the controller. These demands, together with the sensor feedback signals, are fed to the flight control computer which generates appropriate blade angle demands. Other than that we make no assumptions about the implementational details.

The controller was designed to operate on six feedback measurements: the four controlled outputs listed above and the body-axis pitch and roll rate signals. The other inputs to the controller consisted of the 4 pilot inceptor inputs.

The control law output consisted of four blade-angle demands:

- Main rotor collective
- Longitudinal cyclic
- Lateral cyclic
- Tail rotor collective

These demands were passed directly to the actuator model.

Controller scheduling

The controller was designed to run in either of two modes: (i) fixed gain, (ii) interpolated. In fixed gain mode, the closest controller for the given flight condition would be switched in and provide control. This controller would remain operative until the mode was de-selected. If the interpolated mode was engaged, the controllers would be interpolated smoothly as a function of airspeed to compensate for variation in dynamics. To implement for real would require an accurate measurement (or estimate) of forward airspeed.

Outer-loop modes

To enhance the handling qualities provided by the basic ACAH response of the inner loop H-Infinity controller, three outer loop modes were also implemented:

- Turn coordination: this was provided by augmenting the heading rate demand as a function of bank angle at moderate/high speed. This enabled a coordinated turn to be effected as a single axis task

- Automatic trimming: this was achieved using a trim-map to offset the linear inner loop controller with the appropriate trim attitude.

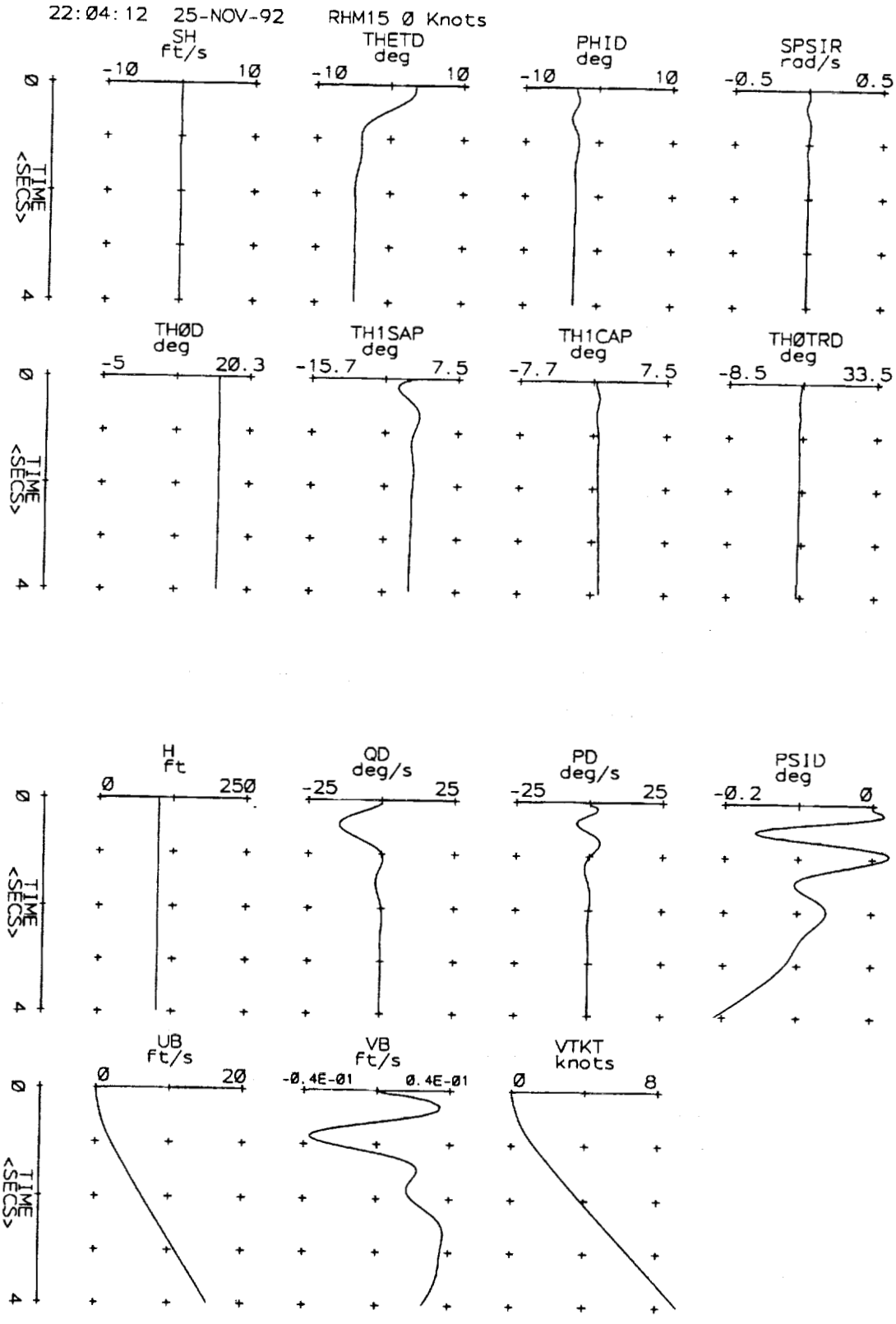

Figure 1 - Pitch axis step response

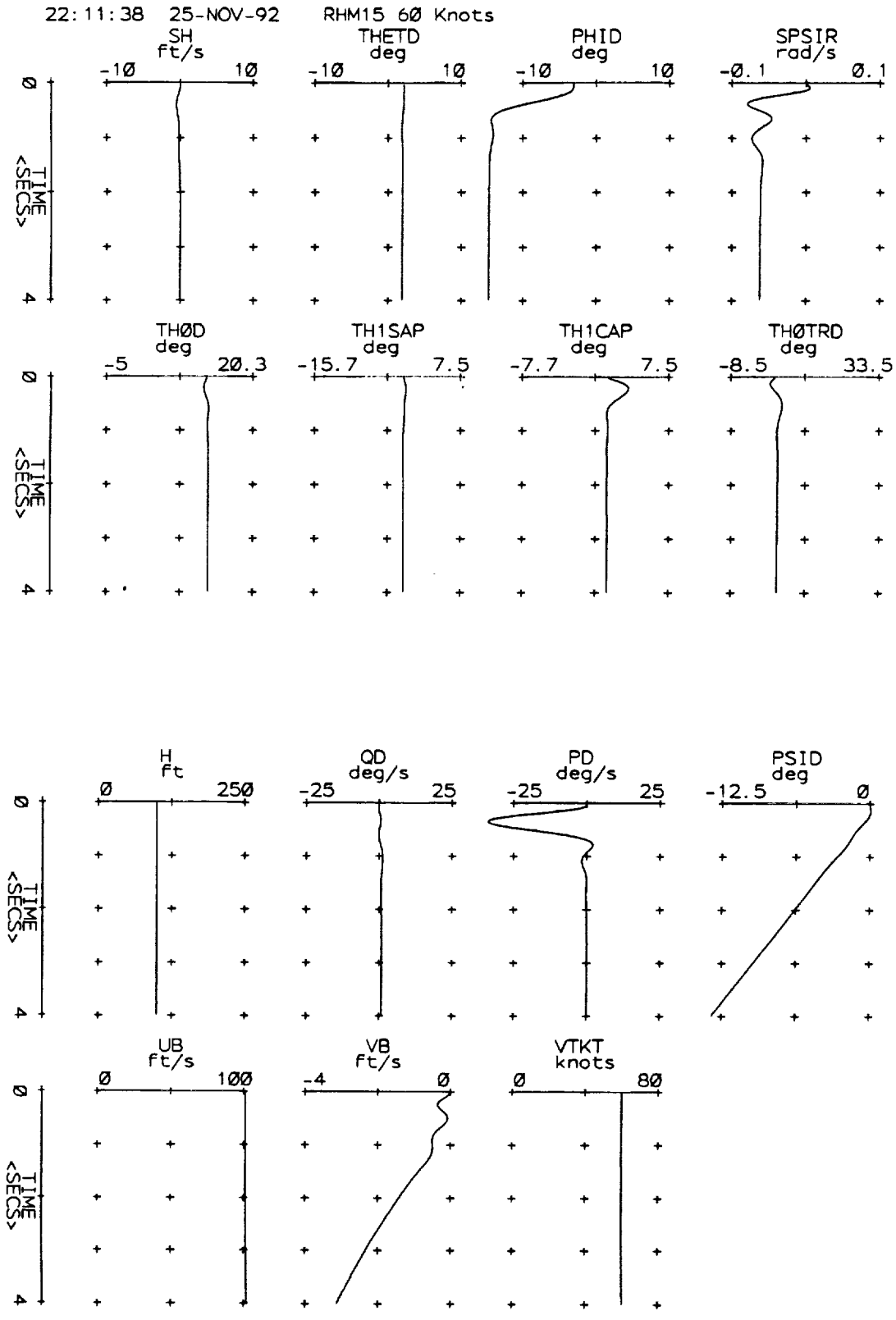

Figure 2 - Roll axis step response

• Hover acquisition/hold: this mode enabled the pilot to acquire and hold hover automatically. Longitudinal and lateral velocity state estimates were needed to achieve this.

During the piloted trials, the first two modes were used continuously, but insufficient time was available to evaluate the hover acquisition utility.

Step response analysis

The response of the closed loop system (comprising controller and full nonlinear model) to step input demands on pitch and roll channels are shown in Figures 1 and 2. These show, respectively, an acceleration from hover and the commencement of a co-ordinated turn at 60 knots. In both cases there is seen to be minimal cross-coupling.

HANDLING QUALITIES ANALYSES

Reference [5] details the latest requirements specification for combat helicopters which is intended to ensure that mission effectiveness will not be compromised by deficient handling qualities. The requirements are stated in terms of three limiting "levels" of acceptability of one or more given parameters. The levels indicate performance attributes that equate with pilot ratings on the Cooper-Harper scale. A MATLAB Handling Qualities Toolbox [8] was used as a supplement to existing computer aided control system design packages in order to integrate handling qualities assessment into the complete design and analysis cycle. The dynamics of the closed loop vehicle were assessed against the dynamic response requirements specified in sections 3.3 and 3.4 of [5] using the off-line simulation model. A selection of the results are reproduced here.

Short term response

The bandwidth (ω_{bw}) and phase delay (τ_p) parameters were calculated using frequency sweep inputs on pitch, roll and yaw axes to determine the frequency responses of the closed loop system. The values obtained at 0 and 50 knots are given below.

Table I - Bandwidth and phase delay (hover)

	ω_{bw} (rad/sec)	τ_p (sec)	Level
Pitch	4.88	0.1156	1
Roll	6.44	0.1211	1
Yaw	2.60	0.1002	2

Table II - Bandwidth and phase delay (50 knots)

	ω_{bw}	τ_p	Level
Pitch	4.93	0.1223	1
Roll	6.53	0.1220	1
Yaw	2.35	0.0936	2

These values are plotted for pitch and yaw axes in Figures 3 and 4, with the level 1, 2, and 3 boundaries superimposed. The high roll-axis bandwidth parameters fell outside the plotting range.

Mid-term response

To satisfy level 1 handling qualities criteria, a damping factor of at least 0.35 is required in pitch and roll axes. The following values were calculated by analysing the transient responses to pulse attitude demands in pitch and roll channels.

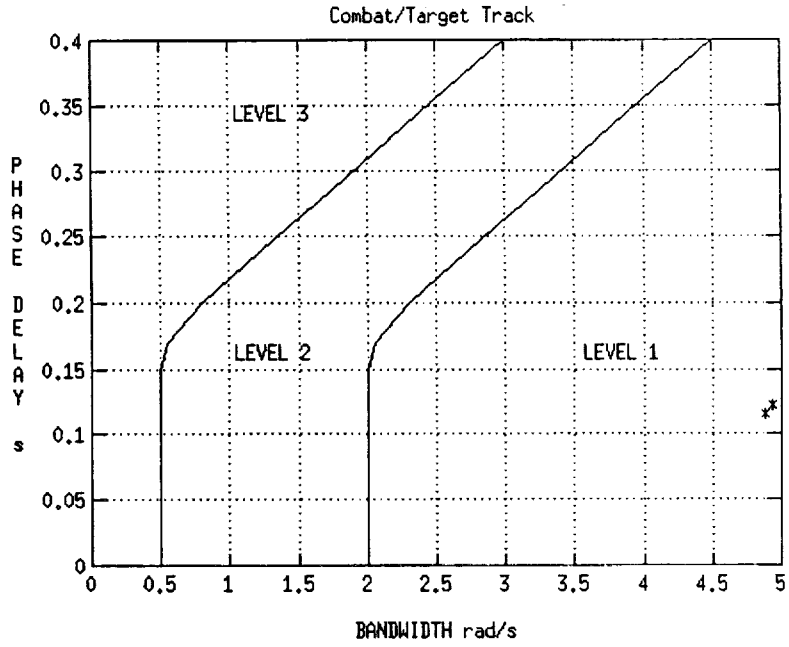

Figure 3 - Pitch axis short-term response

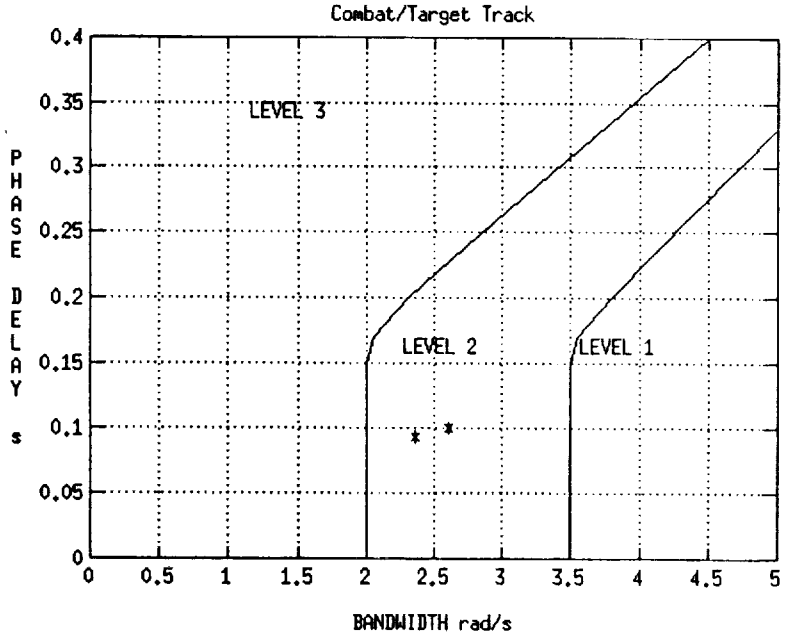

Figure 4 - Yaw axis short-term response

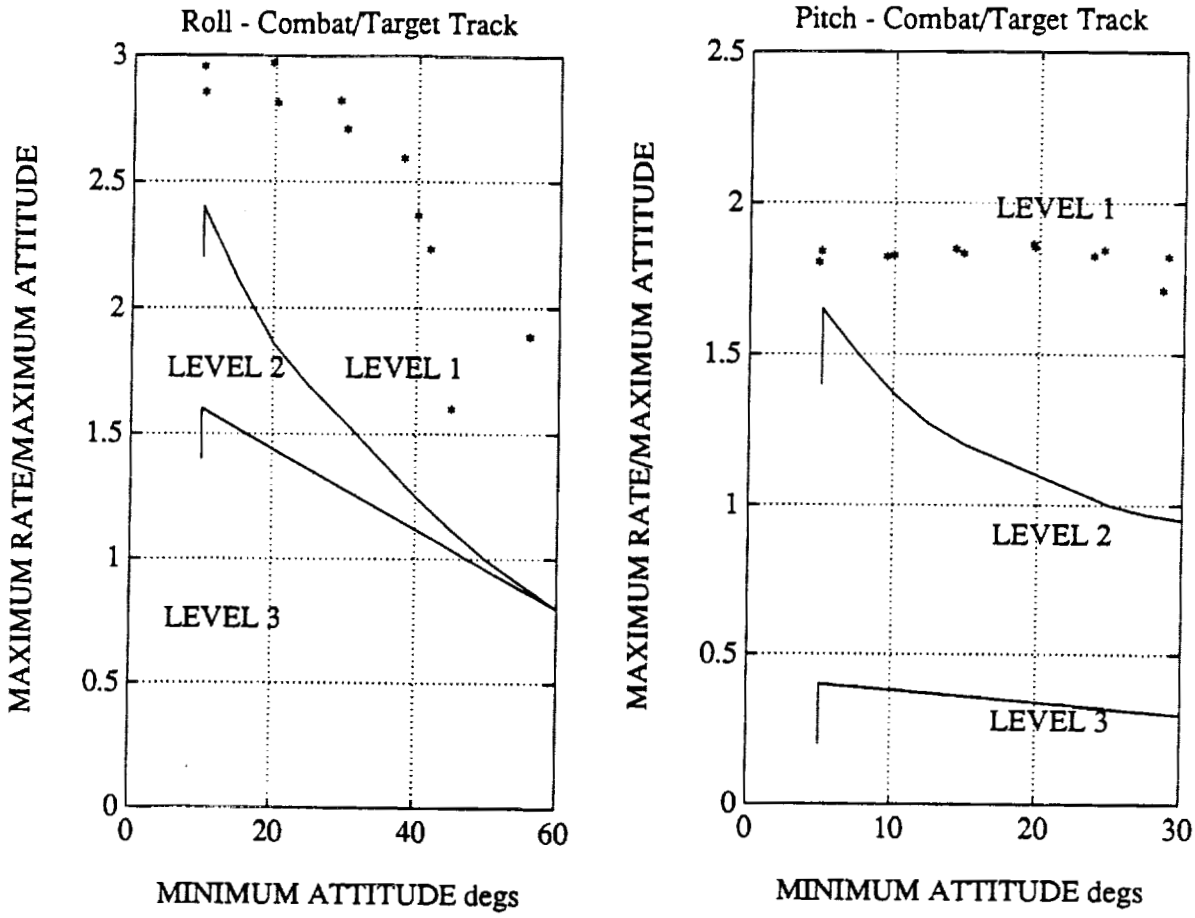

Figure 5 - Agility parameter (0 and 50 knots)

(Moderate amplitude response)

Table III - Damping Factor

	0 knots	50 knots
Pitch	0.75	0.81
Roll	0.94	0.98

These values comfortably satisfy level one requirements.

Moderate amplitude response

Using step inputs of varying sizes, compliance with the moderate amplitude criteria was assessed. Again, level 1 requirements were easily satisfied on pitch and roll axes. Figure 5 displays this information for both channels. The figure shows the agility parameter ($q_{max}/\Delta\theta$ versus $\Delta\theta$ and $p_{max}/\Delta\phi$ versus $\Delta\phi$) for a range of pitch and roll attitude changes at hover and 50 knots, with the boundaries which demarcate levels 1, 2 and 3 superimposed.

Inter-axis coupling

The ADS-33C level 1 requirement is that pitch-to-roll and roll-to-pitch coupling be less than 25%. The hover interaction levels are given in Tables IV and V.

Table IV - Pitch to roll coupling (Hover)

θmax	ϕmax	ϕmax/θmax (%)
9.99°	0.77°	7.9
19.74°	1.58°	8.1
31.24°	2.03°	6.9

Table V - Roll to pitch coupling (Hover)

θmax(deg)	ϕmax(deg)	θmax/ϕmax (%)
0.41°	10.07°	4.1
0.99°	20.32°	4.9
1.90°	30.48°	6.2

PILOTED SIMULATION ON THE DRA BEDFORD LARGE MOTION SIMULATOR

The simulation model was written in FORTRAN and run on an Encore Concept-32 computer with an integration step of 20 mS. A Lynx-like single seat cockpit was used, mounted on the AFS large motion system which provides ± 30 degrees of pitch, roll and yaw, ± 4 metres of sway and ± 5 metres of heave motion. Also, the pilot's seat was dynamically driven to give vibration and sustained normal acceleration cues. The visual display was generated by a Link-Miles IMAGE IV CGI system and gave approximately 48 degrees field of view (FOV) in pitch and 120 degrees FOV in azimuth with full daylight texturing. A three axis side-stick was used to control pitch, roll and yaw together with a conventional collective for heave.

Handling qualities were assessed for three hover/low speed mission task elements (sidestep, quick-hop, bob-up) and three moderate/high speed tasks (lateral jinking, hurdles, yaw pointing) using CGI databases developed by DRA [9] for the Euro-ACT programme [10]. The pitch and roll tasks were originally developed in flight trials and to maintain correspondingly representative control strategy, task aggression and task performance, the simulation visual databases are enhanced with additional artificial cues.

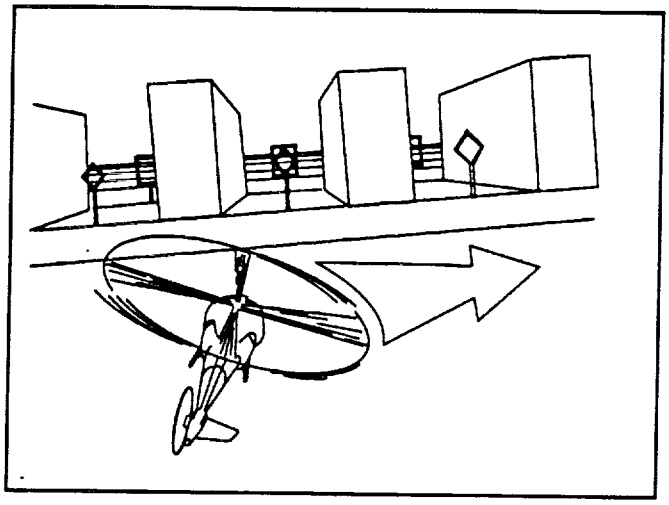

(a) Sidestep task

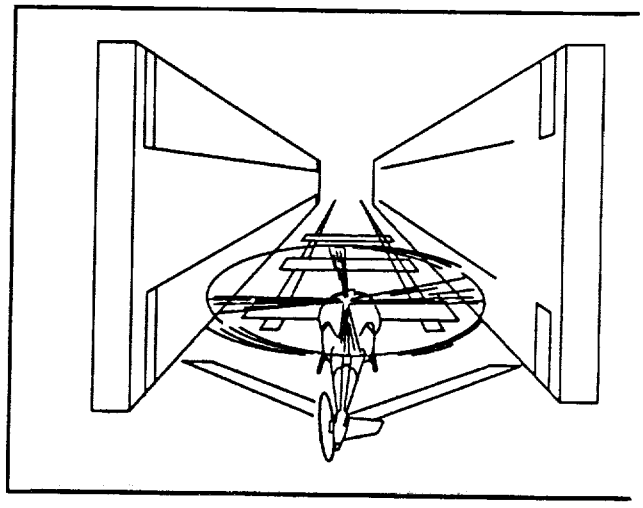

(b) Quick-hop task

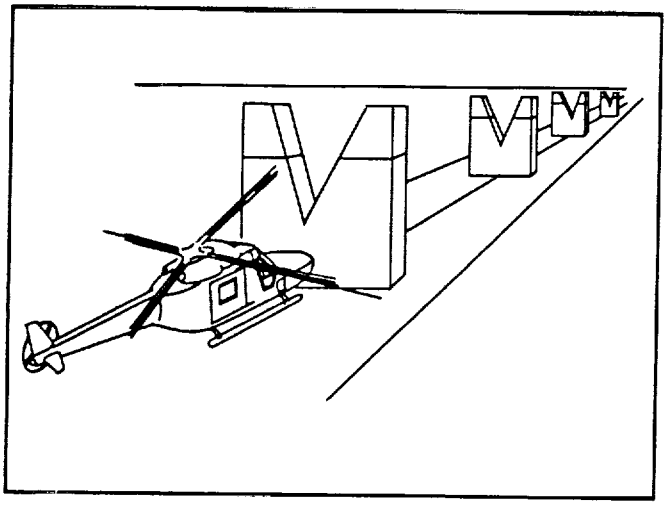

(c) Hurdles / Bob-up task

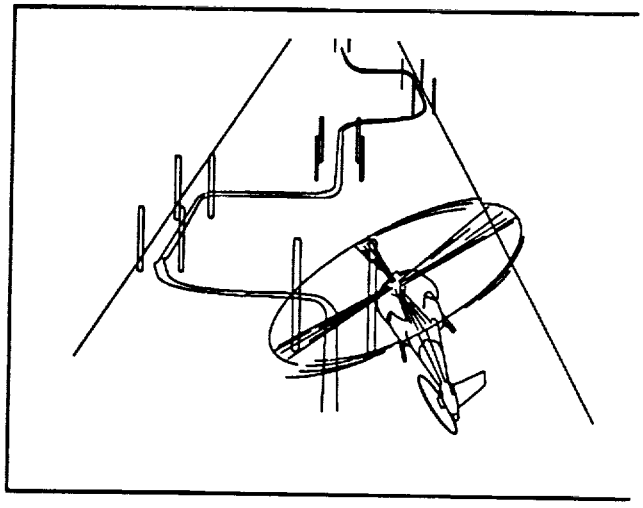

(d) Lateral jinking task

Figure 6

Two DRA test pilots took part in the trial, both with significant experience of Lynx and the AFS. For each task in turn, the pilot performed two or three familiarisation runs before performing a definitive evaluation run, at the end of which the simulation was paused so that comments and handling qualities ratings could be recorded.

Sidestep task description

With reference to Figure 6a, the objective was to translate sideways through 150' from a hover at a height of 30' above ground level in front of one diamond and square sighting arrangement, to acquire and maintain a stable hover in front of the next sighting system. Maintaining any two of the diamond points within the square satisfied the desired ±10' lateral position and height tolerances. Task aggression was determined via initial bank angle, with 10°, 20° and 30° corresponding to low, moderate and high levels of aggression. Figure 7 shows a time history of one particular sidestep manoeuvre.

Quick-hop task description

The quick-hop task (Figure 6b) is the corresponding longitudinal task to the sidestep, requiring a re-position from hover over a distance of 500'. Again, similar levels of initial pitch attitude were used to determine the task aggression. The task was flown down a walled alley to give suitable height and lateral position cues and the terminal position tolerance was increased to ±30' to allow for the reduced FOV over the nose.

Bob-up task description

The bob-up task was performed in front of one of the V-notch hurdles (Figure 6c). From a hover aligned with the bottom of the V-notch, the pilot had to acquire and maintain a new height denoted by the bottom of the black tips. Task aggression was determined subjectively by the pilot based on magnitude of collective displacement.

Lateral jinking task description

The lateral jinking task concerned a series of 'S' turns through slalom gates followed by a corresponding line tracking phase (Figure 6d). The task had to be flown whilst maintaining a speed of 60 knots and a height of 25' AGL. Once more, bank angle was used to determine task aggression with 15, 30 and 45 denoting low, moderate and high levels of aggression. Figure 8 shows the time history of one particular manoeuvre.

Hurdles task description

Using the same V-notch hurdles as seen for the bob-up task, a collective-only flight path re-positioning task was flown at 60, 75 and 90 knots to represent increasing task aggression. From an initial height aligned with the bottom of the V-notch, the pilot had to pass through each hurdle at the height denoted by the bottom of the black tips and then regain the original speed and height as quickly as possible.

Yaw pointing task description

Whilst translating down the runway centre line at 60 knots, the pilot was required to yaw to acquire and track one of a number of offset posts. Task aggression was determined by the magnitude of the initial offset.

Table VI is a compilation of one of the pilot's questionnaires.

Table VI - Pilot comment

Task	Level of aggression	Pilot comment	HQR	Level
Side-step	Low	Loads of spare capacity	2	1
	Moderate	Task workload still minimal, response perfect.	2	1
	High	Increased level of aggression does not increase workload. Very easy.	2 (low)	1
Quick-hop	Low	Desired performance easily achieved. Slight right drift. 3-axis task. A lot of model inertia. Control law good.	2	1
	Moderate	Easier at higher aggression because less anticipation required. No problems.	2	1
Hurdles	Low	Desired performance achieved satisfactorily. Yaw coupling only problem, but some spare capacity.	3	1
	High	At top of hurdle, control activity high and little spare capacity. > 10° coupling into heading.	5	2
Lateral jinking	Low	Stacks of spare capacity. Minimal control activity. Single axis task. No cross-coupling.	2	1
	Moderate	"	2	1
	High	"	3 (low)	1
Yaw pointing	V. low	Adequate performance achieved with difficulty. Control activity high. Not much spare capacity. Precision difficult.	5	2
	Low	PIO problems. Very high yaw inertia. Low sensitivity, possibly some lag. Maximum rate O.K. but needs to be tighter.	7	3

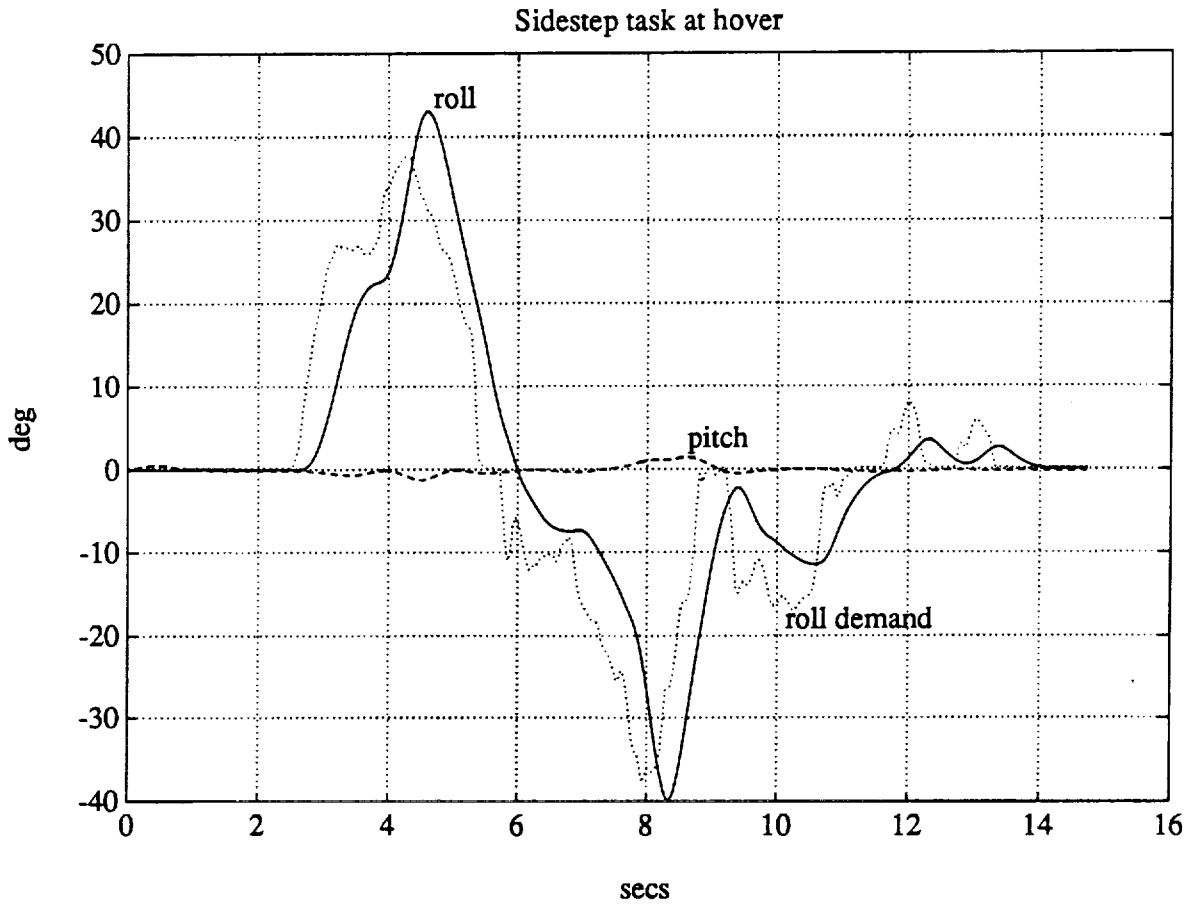

Figure 7 - Sidestep task data

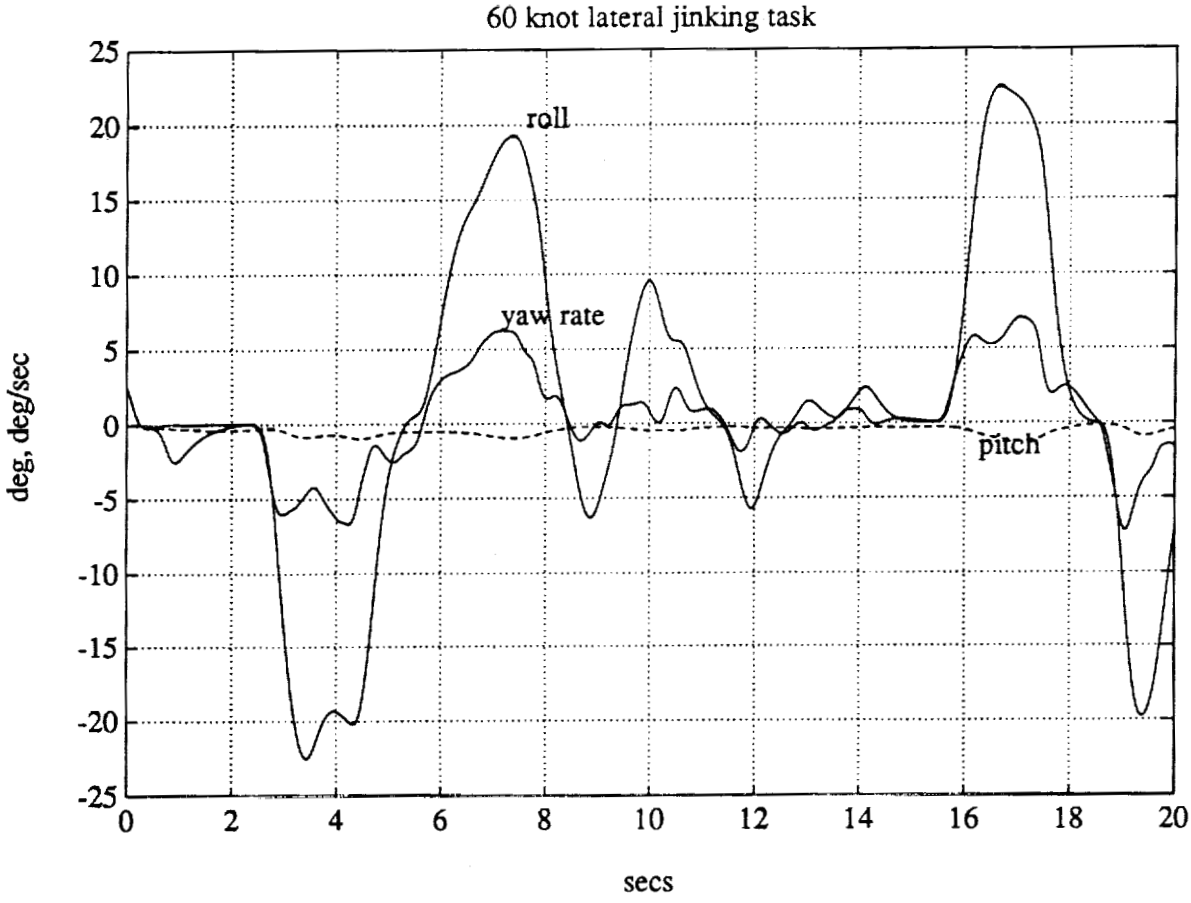

Figure 8 - Lateral jinking task data

CONCLUSIONS

Results have been presented for the piloted simulation and handling qualities analysis of a multivariable control law design for a typical combat helicopter. Through this study we have been able to demonstrate:

- Assimilation of handling qualities requirement specifications into control law design parameters.
- Robust stabilization of the aircraft with respect to changes in flight condition, model uncertainty and non-linearity.
- High bandwidth attitude command response with almost total decoupling between primary controlled outputs.
- Level 1 Cooper-Harper pilot ratings for a number of aggressively performed mission task elements.
- Compliance with many ADS-33C Level 1 requirements.

The controller has been subjected to significant and challenging tests that have shown that multivariable synthesis techniques offer considerable potential in the rotorcraft field.

ACKNOWLEDGEMENT

This work has been conducted with the support of the UK Ministry of Defence through Extramural Research Agreement No. 2206/32/RAE(B).

REFERENCES

1. Tombs, M., "Robust control system design with application to high-performance helicopters." D.Phil thesis, University of Oxford. 1987.

2. Yue, A., "H-infinity design and the improvement of helicopter handling qualities." D.Phil thesis, University of Oxford. 1988.

3. Yue, A. and Postlethwaite, I., "Improvement of helicopter handling qualities using H$^{\infty}$ optimization.", IEE Proc., vol. 137 Part D, No. 3, May 1990.

4. Walker, D. and Postlethwaite, I., "Full authority active control system design for a high performance helicopter." 16th European Rotorcraft Forum, Glasgow, 16-18 Sept 1990.

5. Anon, "Handling Qualities Requirements for Military Rotorcraft, Aeronautical Design Standard ADS-33C." US Army AVSCOM, August 1989.

6. Padfield, G.D., "Theoretical Model of Helicopter Flight Mechanics for Application to Piloted Simulation." RAE TR 81048, 1981.

7. McFarlane and Glover, K., "Robust control system design using normalized coprime factor plant descriptions." Springer Verlag. Lecture notes in control and information sciences.

8. Howitt, J., "MATLAB Toolbox for Handling Qualities Assessment of Flight Control Laws." Proc. IEE Control '91, Scotland 1991.

9. Padfield. G.D., Charlton, M.T., and Kimberley, A.M., "Helicopter Flying Qualities in Critical Mission Task Elements - Initial Experience with the DRA Bedford Large Motion Simulator." 18th European Rotorcraft Forum, 1992.

10. Schimke D., *et al*, "The European ACT Programme: Complimentary Use of Ground Based Simulation Facilities and Experimental Fly-by-Wire/Light Helicopters." 18th European Rotorcraft Forum, 1992.

The Impact of Flying Qualities on Helicopter Operational Agility

Gareth D Padfield
Defence Research Agency
Bedford, UK

Nick Lappos
Sikorsky Aircraft
Stratford, Ct, US

John Hodgkinson
McDonnell Douglas Aircraft
Long Beach, Ca, US

Abstract

Flying Qualities standards are formally set to ensure safe flight and therefore reflect minimum, rather than optimum, requirements. Agility is a flying quality but relates to operations at high, if not maximum, performance. While the quality metrics and test procedures for flying, as covered for example in ADS33C, may provide an adequate **structure** to encompass agility, they do not currently address flight at high performance. This is also true in the fixed-wing world and a current concern in both communities is the absence of sustantiated agility criteria and possible conflicts between flying qualities and high performance. AGARD is sponsoring a working group (WG19) titled 'Operational Agility' that deals with these and a range of related issues. This paper is condensed from contributions by the three authors to WG19, relating to flying qualities. Novel perspectives on the subject are presented including the agility factor, that quantifies performance margins in flying qualities terms; a new parameter, based on manoeuvre acceleration is introduced as a potential candidate for defining upper limits to flying qualities. Finally, a probabalistic analysis of pilot handling qualities ratings is presented that suggests a powerful relationship between inherent airframe flying qualities and operational agility.

Introduction

Good flying qualities are conferred to ensure that safe flight is guaranteed throughout the Operational Flight Envelope (OFE). Goodness, or quality, in flying can be measured on a scale spanning three Levels (Ref 1). Aircraft are normally required to be Level 1 throughout the OFE (Ref 2); Level 2 is acceptable in failed and emergency situations but Level 3 is considered unacceptable. Level 1 quality signifies that a minimum required standard has been met or exceeded in design and can be expected to be achieved regularly in operational use, measured in terms of task performance and pilot workload. Compliance flight testing involves both clinical open loop measurements and closed loop mission task elements (MTE). The emphasis on *minimum requirements* is important and is made to ensure that manufacturers are not unduly constrained when conducting their design trade studies.

Two issues arise out of this quality scale and assessment. First, the minimum requirements reflect and exercise only moderate levels of the dynamic OFE, rather than high or extreme levels. Second, the assessments are usually made in 'clean' conditions, uncluttered by secondary tasks or the stress of real combat. Beyond the minimum quality levels there remains the question of the value of good flying qualities to the overall mission effectiveness. For example, how much more effective is an aircraft that has, say, double the minimum required (Level 1) roll control power? More generally, how much more mission effective is a Level 1 than a Level 2 aircraft when the pilot is stressed? The answers to these questions cannot be found in flying qualities criteria. At higher performance levels, very little data are available on helicopter flying qualities and, consequently, there are no defined upper limits on handling parameters. Regular and safe (carefree) use of high levels of transient performance has come to be synonymous with the attribute **agility**. The relationship between flying qualities and agility is important because it potentially quantifies the value of flying qualities to effectiveness. This is the subject of the paper.

The issues that this paper addresses then, concern the flying qualities that are important for agility, in both an enabling and limiting context, and how far existing flying qualities requirements go, or can be extended to embrace agility itself. The answers are developed within a framework of deterministic flying qualities criteria coupled with the probabilistic analysis of success and failure. The definition of flying qualities by Cooper & Harper (Ref 1) provides a convenient starting point,

'those qualities or characteristics of an aircraft that govern the ease and precision with which a pilot is able to perform the tasks required in support of an aircraft role'.

The pilot subjective rating scale and associated flying qualities Levels introduced by Cooper & Harper (Fig 1) will be used in this paper in the familiar context of quality discernment and will be developed to make the link with agility and mission effectiveness.

Flying 'Quality' can be further interpretted as the **synergy** between the **internal attributes** of the air vehicle and the **external environment** in which it operates (Fig 2). The internals consist typically of the air vehicle (airframe, powerplant and flight control system) response characteristics to pilot inputs (handling qualities) and disturbances (ride qualities) and the key elements at the pilot/vehicle interface eg cockpit controls and displays. The key factors in the external environment which influence the flying qualities requirements are;

i) the mission, including individual mission task elements (MTE) and the required levels of task urgency and

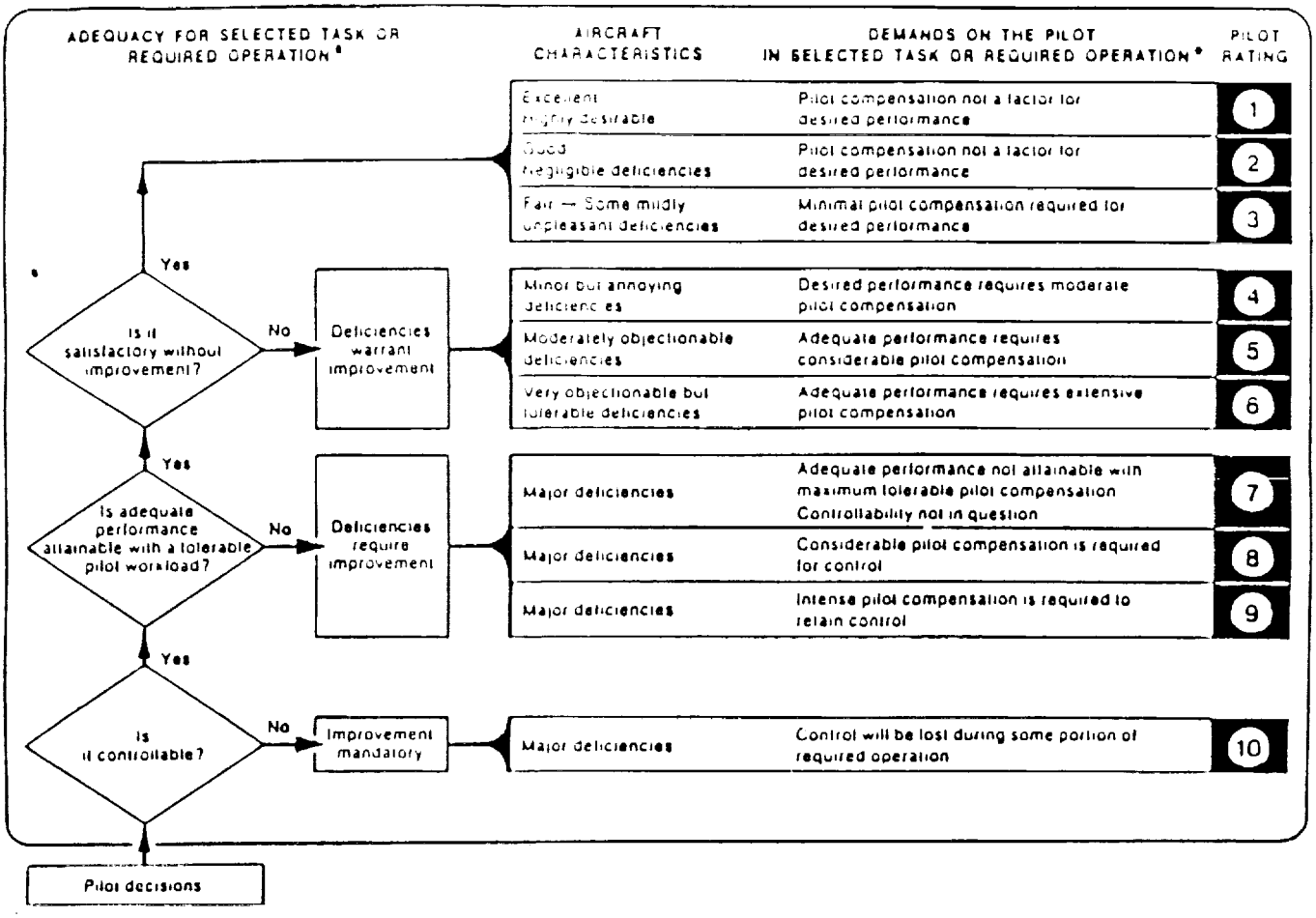

Fig 1 The Cooper-Harper Handling Qualities Rating Scale

Mission-Oriented Flying Qualities make the Link

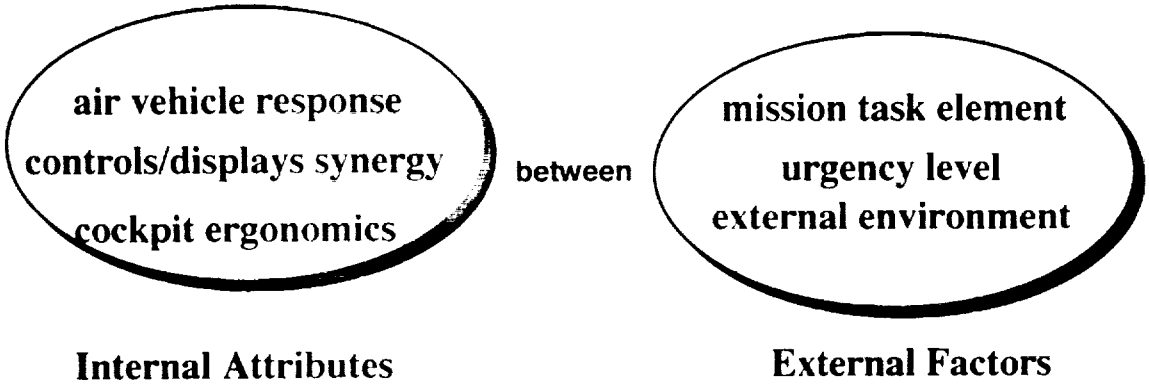

Fig 2 The Synergy of Flying Qualities

divided attention dictated by the circumstances governing individual situations, eg threat level.

ii) the external environment, including the usable cue environment (UCE) and level of atmospheric disturbance.

Flying qualities, as seen by the pilot who is ultimately the judge of quality, therefore change as the external world changes, for example, with weather conditions and flight path constraints and other task demands. Mission oriented flying qualities requirements, like those for fixed-wing aircraft, MIL STD 1797 (Ref 3), and, more particularly, helicopters, ADS33C (Ref 2), try to set quality standards by addressing the synergy of these internal attributes and external factors. ADS33C defines the response types required to achieve Level 1 and 2 handling qualities for a wide variety of different mission task elements, in different usable cue environments for normal and failed states, with full and divided pilot attention. At a deeper level, the response characteristics are broken down in terms of amplitude and frequency range, from the small amplitude, higher frequency requirements set by criteria like equivalent low order system response or bandwidth, to the large amplitude manoeuvre requirements set by control power. With these developments now mature, one would expect that any 'special' flying characteristics, like agility, could be embraced by the flying qualities requirements, or at least that the flying qualities criteria should be an appropriate format for quantifying agility.

The Flight Mechanics Panel of AGARD (Adviary Group for Aeronautical Research and Development) is currently sponsoring a working group (WG19) under the title 'Operational Agility', tasked with reporting the status of requirements and design capabilities for operational agility for aeroplanes and rotorcraft. The authors of this paper are members of WG19 and the work reported here is developed from their contribution to this group; the association and debate with fixed wing engineers and pilots has provided much fruitful discussion and comparison with the rotary wing world and some of this is embodied in the paper. While speed and manoeuvre envelopes and associated limits for aeroplanes and rotorcraft are quite different, often paradoxically so, they share the essence of agility and operational effectiveness. Agility requirements for the two vehicle types have traditionally stemmed from two quite different drivers; close combat of air-superiority fighters in the open skies contrasting with stealth of anti-armour helicopters in the nap-of-the-earth. While both still feature large in the two worlds, it is now recognised that agility is relevent to a wider range of roles including aircraft recovering to ships, transport refuelling, support helicopters delivering loads into restricted areas and, more recently, helicopter air-to-air combat.

AGARD WG19 is considering operational agility in the broader context of the total weapon system, encompassing sensors, mission systems, pilot, airframe/engine, flight control system and weapon; the concept is that the total system can only be as agile as the slowest element and that all elements need to work concurrently to be effective. AGARD will report on this activity in 1993. This paper focusses on the vehicle and the pilot centred agility requirements of the airframe, engine and flight control system elements. The next Section discusses the nature of operational agility, outlining some of the WG19 background and motivation and setting the scene for the following Section which addresses the relationship between flying qualities and agility. The principal innovations of this paper are contained here where the agility factor is introduced and related to quantitative handling criteria; the subjective quality scale (Cooper Harper) for pilot-perceived handling qualities is interprettted in a probabilistic fashion to indicate the likelihood of mission success or failure with a given level of flying qualities. Techniques for including flying qualities attributes in combat models are also discussed.

The Nature of Operational Agility

Operational agility is a primary attribute for effectiveness. Within the broader context of the total weapon system, the Mission Task naturally extends to include the actions of the different cooperating (and non-cooperating) sub-systems, each having its own associated time delay (Ref 4). We can imagine the sequence of actions for an air-to-air engagement - threat detection, engagement, combat and disengagement; the pilot initiates the action and stays in command throughout, but a key to operational agility is to automate the integration of the subsystems - the sensors, mission systems, airframe/engine/control system and weapon, to maximise the concurrency in the process. Concurrency is one of the keys to Operational Agility. Another key relates to minimising the time delays of the subsystems to reach full operational capability and hence effectiveness in the MTE. Extensions to the MTE concept are required that encompass the functions and operations of the subsystems, providing an approach to assessing system operational agility. WG19 is addressing this issue. Minimising time delays is crucial for the airframe, but flying qualities can suffer if the accelerations are too high or time constants too short, leading to jerky motion.

Later in this paper we examine how well existing flying qualities requirements address agility; to set the scene for this, we first consider a generalised definition of agility;

"the ability to adapt and respond rapidly and precisely with safety and with poise, to maximise mission effectiveness"

Agility requirements for helicopters falls into four areas - stealthy flying to avoid detection, threat avoidance once detected, the primary mission engagement (eg threat engagement) and recovery and launch from confined area; MTEs can be defined within each category. The key attributes of airframe agility, as contained in the above definition are,

i) rapid - emphasising speed of response, including any transient or steady state phases in the manoeuvre change; the pilot is concerned to complete the manoeuvre change in the **shortest possible time;** what is possible will be bounded by a number of different aspects.

ii) precise - accuracy is the driver here, with the motivation that the greater task precision eg pointing, flight path achievable, the greater the chance of a successful outcome.

iii) safety - this reflects the need to reduce piloting workload, making the flying easy and to free the pilot from unnecessary concerns relating to safety of flight, eg respecting flight envelope limits.

iv) poise - this relates to the ability of the pilot to establish new steady state conditions quickly and to be free to attend to the next task; it relates to precision in the last moments of the manoeuvre change but is also a key driver for ride qualities that enhance steadyness in the presence of disturbances.

v) adapt - the special emphasis here relates to the requirements on the pilot and aircraft systems to be continuously updating awareness of the operational situation; the possibility of rapid changes in the external factors discussed above (eg threats, UCE, wind shear/vortex wakes) or the internals, through failed or damaged systems, make it important that agility is considered, not just in relation to set piece manoeuvres and classical engagements, but also for initial conditions of low energy and/or high vulnerability or uncertainty.

Flying qualities requirements address some of the agility attributes implicitly, through the use of the handling qualities ratings (HQR), that relate the pilot workload to task performance achieved, and explicitly through criteria on response performance, eg control power, bandwidth, stability etc. The relationship has been fairly tenuous however, and the rotorcraft community can learn from fixed-wing experience in this context.

Flying Qualities - the Relationship with Agility

Fixed-Wing Perspectives

The original concern sprang from the notion that flying qualities specifications, as guardians of transient response, should embrace agility, since it too resides by definition in the transient domain. Initial thoughts on this theme appeared in Refs 5 and 6. Reference 5 indicated the interactions between agility, operational capability and flying qualities and listed some of the flying qualities requirements that, because of their treatment of the transient response, clearly crossed into the realm of agility. At that time, it was hypothesized that simply increasing the available agility, in terms of accelerations, rates etc, would lead to diminishing operational returns, since an over-responsive vehicle would not be controllable. That point was considered worth making because some combat analyses were being performed using computer tools that approximated the transient response only in a gross fashion. These models resulted in aircraft which had unquestionably high agility but did not account for the interaction of the vehicle with the pilot and, in fact, due to the approximations made in the interests of computational tractability, did not obey the laws of motion in their transient responses. In Ref 6, the Control Anticipation Parameter, CAP from the USAF Flying Qualities requirements (Ref 3), was quoted as an example of a criterion defining over-responsiveness, since an upper limit is specified for it. Artificially high pitch agility could, according to CAP, correspond to excessive pitch acceleration relative to the normal load factor capability of the aircraft. Performance constraints are also suggested by the tentative upper limits set on pitch bandwidth in Reference 3, although it is suspected that this is a reflection of the adverse acceleration effects associated with high bandwidth/control power combinations.

About that time, Riley et al at McAIR began a series of experiments on fighter agility. In Ref 7 it was emphasised that the definition of the categories in the Cooper-Harper pilot rating scale precluded the idea of an operationally useful vehicle with a rating worse than Level 2, using the US Military Specifications and Standard for flying qualities. In Level 3, the operational effectiveness of the vehicle is compromised, so increasing performance would add little as the pilot could not use it safely. In Refs 7, 8 and 9, Riley and Drajeske describe a fixed-base simulation in which the maximum available roll rate and roll mode time constant were independently varied and the pilot's time to bank 90 degrees and stop was measured. Care was taken in the experiment to allow sufficient time for learning and to generate large numbers (10 to 15) of captures for analysis. The start of the maneuver was when the stick deflection began, and the end was defined as when the roll rate was arrested to less than 5 degrees/second, or 5% of the maximum rate used, whichever was greater. Therefore a realistic element of precision was introduced into the protocol. The results from that experiment, in which the aircraft banked from -45 degrees to +45 degrees, are shown in Figure 3. The lower curved surface summarizes calculated time responses for a step lateral input and shows the expected steady increase in agility, ie a decrease in the time to bank with increasing roll rate. The upper surface in the plot summarizes the bank - to - bank and stop data obtained in the piloted cases. The references to controllability on that surface are from the pilot ratings and comments that were collected. The time to complete the maneuver actually increases for the higher available roll rates because the pilot could not adequately control the maneuver. The data therefore show that flying qualities considerations do limit agility. Though the data are from fixed-base simulation, we can speculate that in - flight results might show still more dramatic results. In Ref 9 the authors suggest that the effects of motion would in fact change the shape of Figure 3 to look like Figure 4.

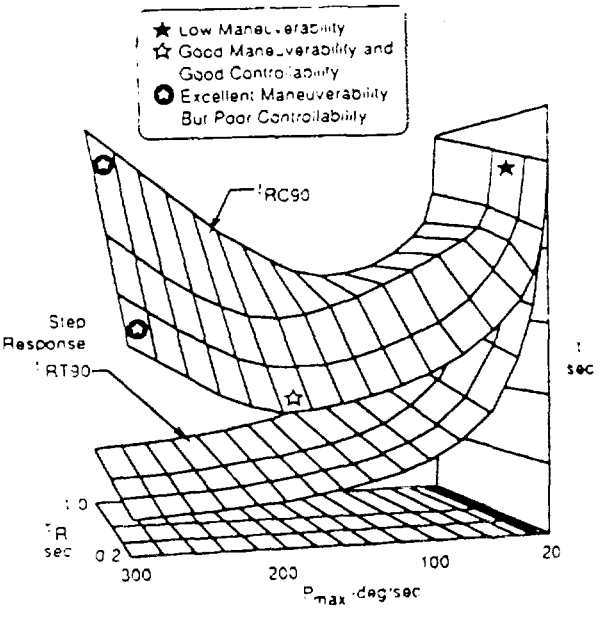

Fig 3 Agility in a Roll Manoeuvre (Ref 7)

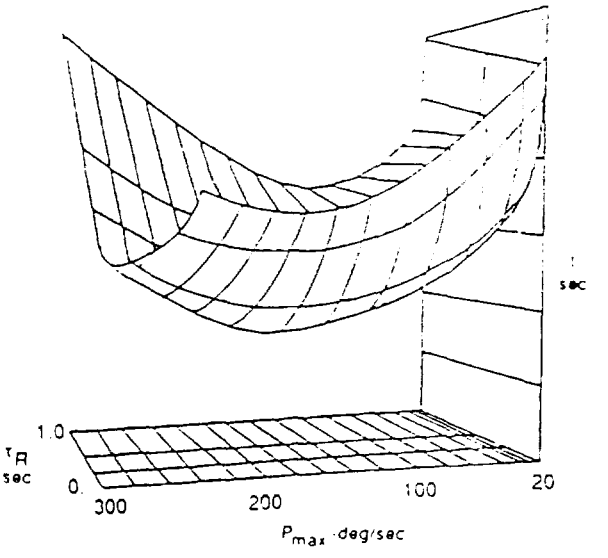

Fig 4 Effects of Motion on Agility

In MIL STD 1797, upper limits on lateral flying qualities are almost exclusively set by tolerable levels of acceleration at the pilot station, in the form of lateral g per control power; the Level 1 boundary at about 2g for a typical fighter seems extraordinarily high, but Reference 3 does state that "in order to achieve the needed roll performance it may be necessary to accept some uncomfortable lateral accelerations". There is considerable discussion on lateral control sensitivity in Reference 3, but as with helicopters, the criteria are strongly dependent on controller type and only guidance is given. Clearly there will always be upper limits to sensitivity but it seems a desirable goal to design the pilot/vehicle interface so that agility is not inhibited by this parameter.

The Agility Factor

One of the most common causes of dispersion in pilot HQRs stems from poor or imprecise definition of the performance requirements in a mission task element, leading to variations in interpretation and hence perception of achieved task performance and associated workload. In operational situations this translates into the variability and uncertainty of task drivers, commonly expressed in terms of precision but the temporal demands are equally important. The effects of task time constraints on perceived handling have been well documented (Refs 10, 11, 12), and represent one of the key external factors that impact pilot workload. Flight results gathered on Puma and Lynx test aircraft at DRA (Refs 12, 13) showed that a critical parameter was the ratio of the task performance achieved to the maximum available from the aircraft; this ratio gives an indirect measure of the spare capacity or performance margin and was consequently named the agility factor. The notion developed that if a pilot could use the full performance safely, while achieving desired task precision requirements, then the aircraft could be described as agile. If not, then no matter how much performance margin was built into the helicopter, it could not be described as agile. The Bedford agility trials were conducted with Lynx and Puma operating at light weights to simulate the higher levels of performance margin expected in future types (eg up to 20-30% hover thrust margin). A convenient method of computing the agility factor was developed as the ratio of ideal task time to actual task time. The task was deemed to commence at the first pilot control input and complete when the aircraft motion decayed to within prescribed limits (eg position within a prescribed cube, rates < 5 deg/s) for re-positioning tasks or the accuracy/time requirements met for tracking or pursuit tasks. The ideal task time is calculated by assuming that the maximum acceleration is achieved instantaneously, in much the same way that aircraft models work in combat games. So, for example, in a sidestep re-positioning manoeuvre the ideal task time is derived with the assumption that the maximum ***translational*** acceleration (hence aircraft roll angle) is achieved instantaneously and sustained for half the manoeuvre, when it is reversed and sustained until the velocity is again zero.

The ideal task time is then simply given by

$$T_i = \sqrt{(4S/a_{max})} \qquad 1$$

where S is the sidestep length and a_{max} is the maximum translational acceleration. With a 15% hover thrust margin, the corresponding maximum bank angle is about 30deg, with a_{max} equal to 0.58g. For a 100ft sidestep, T_i

then equals 4.6 seconds. Factors that increase the achieved task time beyond the ideal include,

i) delays in achieving the maximum acceleration (eg due to low roll attitude bandwidth/control power)

ii) pilot reluctance to use the max performance (eg no carefree handling capability, fear of hitting ground)

iii) inability to sustain the maximum acceleration due to drag effects and sideways velocity limits

iv) pilot errors of judgement leading to terminal re-positioning problems (eg caused by poor task cues, strong cross coupling)

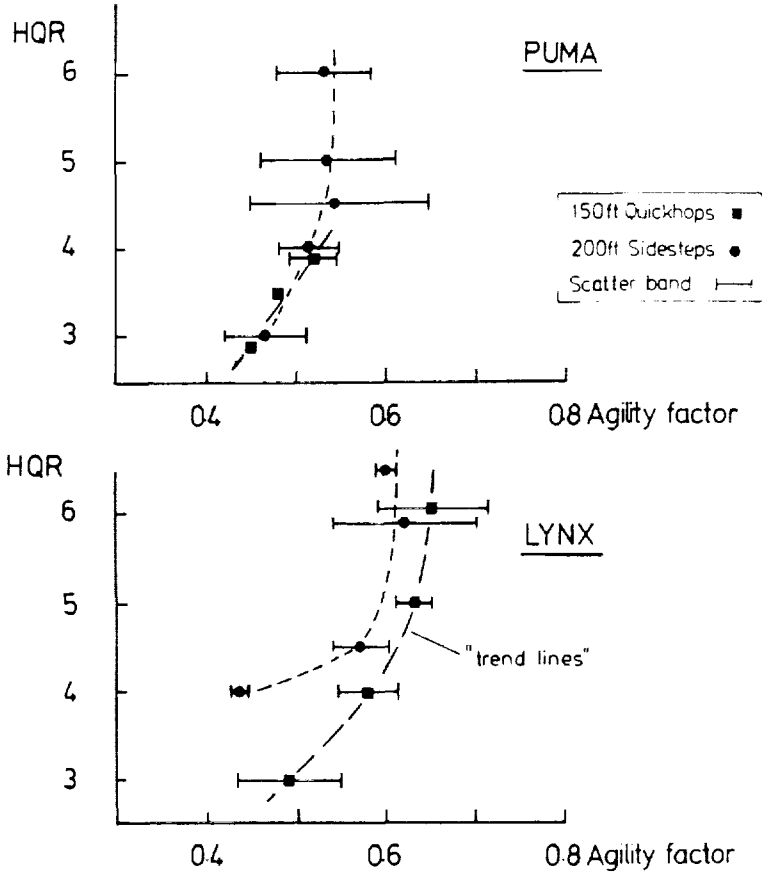

Fig 5 Variation of HQR with A_f showing the Cliff-Edge of Handling Deficiencies

To establish the kinds of agility factors that could be achieved in flight test, pilots were required to fly the Lynx and Puma with various levels of aggression, defined by the maximum attitude angles used and rate of control application. For the low speed re-positioning Sidestep and Quickhop MTEs, data were gathered at roll and pitch angles of 10, 20 and 30 degs corresponding to low, moderate and high levels of aggression respectively. Fig 5 illustrates the variation of HQRs with agility factor.

The higher agility factors achieved with Lynx are principally attributed to the hingeless rotor system and faster engine/governor response. Even so, maximum values of only 0.6 to 0.7 were recorded compared with 0.5 to 0.6 for the Puma. For both aircraft, the highest agility factors were achieved at marginal Level 2/3 handling; in these conditions, the pilot is either working with little or no spare capacity or not able to achieve the flight path precision requirements. According to Fig 5, the situation rapidly deteriorates from Level 1 to Level 3 as the pilot attempts to exploit the full performance, emphasising the 'cliff edge' nature of the effects of handling deficiences. The Lynx and Puma are typical of current operational types with low authority stability and control augmentation; while they may be adequate for their current roles, flying qualities deficiencies emerge when simulating the higher performance required in future combat helicopters.

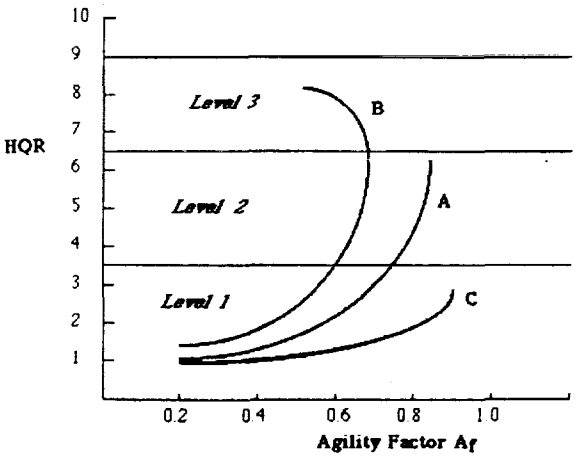

Fig 6 Variation of HQR with A_f for Different Notional Configurations

The different possibilities are illustrated in Fig 6. All three configurations are assumed to have the same performance margin and hence ideal task time. Configuration A can achieve the task performance requirements at high agility factors but only at the expense of maximum pilot effort (poor level 2 HQR); the aircraft cannot be described as agile. Configuration B cannot achieve the task performance when the pilot increases his aggression and Level 3 ratings are returned; in addition, the attempts to improve task performance by increasing aggression have led to a decrease in agility factor, hence a waste of performance. This situation can arise when an aircraft is PIO prone, is difficult to re-trim or when control or airframe limits are easily exceeded in the transient response. Configuration B is certainly not agile and the proverb 'more haste, less speed' sums the situation up. With configuration C, the pilot is able to exploit the full performance at low workload; he has spare capacity for situation awareness and being prepared for the unexpected.

Configuration C can be described as truly agile. The inclusion of such attributes as safeness and poise within the concept of agility emphasises its nature as a flying quality and suggests a correspondance with the quality Levels. These conceptual findings are significant because the flying qualities boundaries, that separate different quality levels, now become boundaries of available agility. Although good flying qualities are sometimes thought to be merely "nice to have", with this interpretation they can actually delineate a vehicle's agility. This lends a much greater urgency to defining where those boundaries should be. Put simply, if high performance is dangerous to use, then most pilots will avoid using it.

Conferring operational agility on future helicopters, emulating configuration C above, requires significant improvements in handling, but research into criteria at high performance levels and innovations in active control are needed to lead the way. There are two remaining links to be connected to assist in this process. First, between the agility factor and the operational agility or mission effectiveness and second between the agility factor and the flying qualities metrics themselves. If these links can be coherently established, then the way is open for combat analysts to incorporate prescribed flying qualities into their pseudo-physical models through a performance scaling effect using the agility factor. These links will now be developed.

Quality - Objective Measurement

Figure 7 provides a framework for discussing the influence of an aircraft's clinical flying qualities on agility.

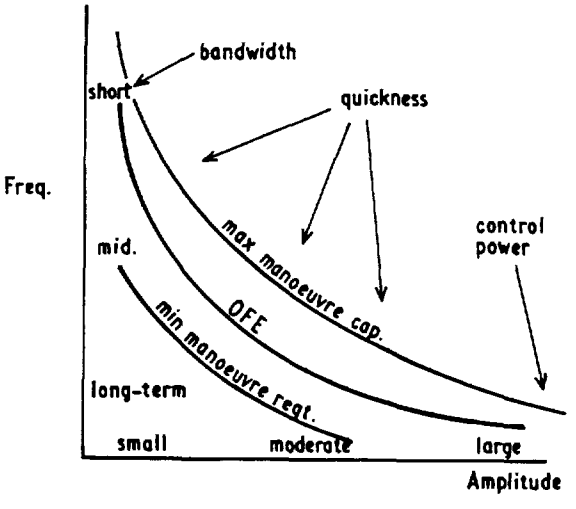

Fig 7 Response Characteristics on the Frequency-Amplitude Plane

The concept is that an aircraft's response characteristics can be described in terms of frequency and amplitude. The three lines refer to the minimum manoeuvre requirements, the normal OFE requirements and some notional upper boundary reflecting a maximum capability. Response criteria are required for the different areas on this plane - from high frequency/small amplitude characterised by bandwidth to low frequency/large amplitude motions characterised by control power. The region between is catered for by an ADS33 innovation, the Quickness parameter (Ref 2), and is particularly germane to agility. For a given manoeuvre amplitude change (eg bank angle, speed change), the pilot can exercise more of the aircraft's inherent agility by increasing the speed of the manoeuvre change, and hence the frequency content of his control input and the manoeuvre quickness. Likewise, the pilot can increase the manoeuvre size for a given level of attack or aggression. Increasing the manoeuvre quickness will theoretically lead to an increase in agility factor. But the maximum manoeuvre quickness is a strong function of bandwidth and control power. In ADS33C the quickness parameter is only defined for attitude response (ϕ, θ, ψ) and is given by the ratio of peak attitude rate (p_{pk}, q_{pk}, r_{pk}) to attitude change,

$$p_{pk}/\Delta\phi, \qquad q_{pk}/\Delta\theta, \qquad r_{pk}/\Delta\psi$$

Figure 8 shows derived quickness parameters for a sidestep MTE gathered on the DRA Lynx (Ref 13) and configuration T509 flown on the DRA Advanced Flight Simulator (AFS) (Ref 14).

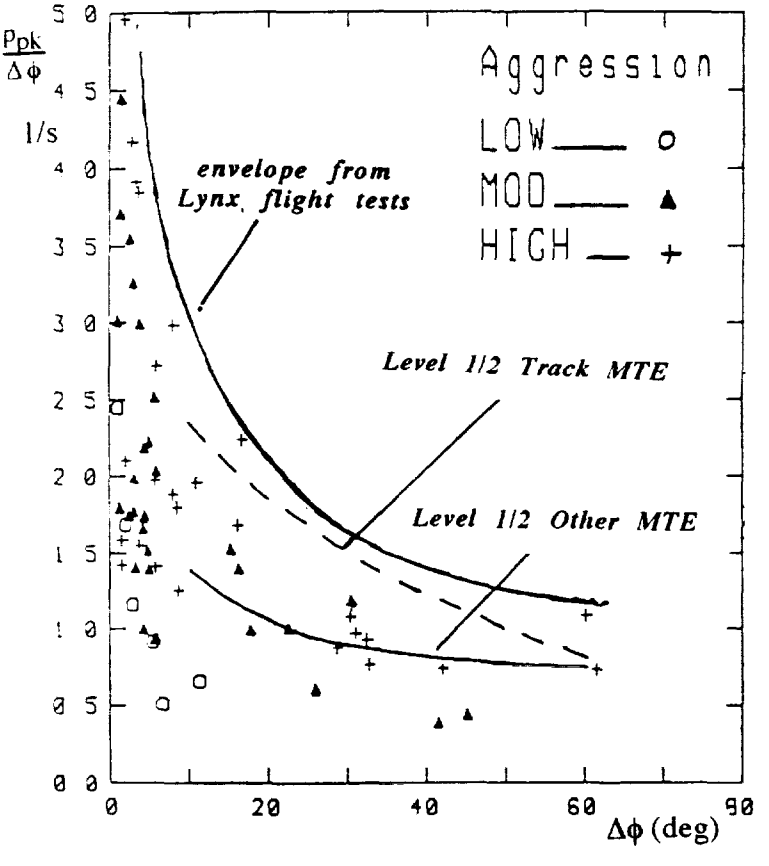

Fig 8 Roll Attitude Quickness from Sidestep Test Data in Flight (Lynx) and Ground-Based Simulation (AFS)

A quickness is calculated for every rate peak in the attitude time histories. The Lynx line on Fig 8 represents the upper boundary of all data gathered for a range of aggressiveness and sidestep sizes. The data includes the cases plotted in Figure 5 showing that at the highest agility factors/quickness, poor Level 2 ratings were awarded. The AFS data corresponds to a 150ft sidestep flown at the three levels of aggression shown; although the roll bandwidth of the AFS configuration T509 was less than the Lynx (~ 3 rad/s compared with ~ 5rad/s for the Lynx), the control power was similar (~ 100deg/s) and similar levels of quickness were achieved by the pilots across the full amplitude range. Also shown on Figure 8 are the Level 1/2 boundaries for tracking and other MTEs from ADS33C. There are several points worth making about this data that impact on agility.

1) the shape of the quickness boundaries reflect the shape of the response capability limits on Fig 7. The quickness has generic value and forms the link between the bandwidth and control power but is not, in general, uniquely determined by them.

2) the result of increased aggressiveness is to increase the achieved quickness across the amplitude range.

3) the cluster of quickness at small amplitude correspond with the pilot applying closed loop control in the terminal re-positioning phase and attitude corrections during the accel/decel phases.

4) at low amplitude, the quickness corresponds to the open loop bandwidth except when a pure time delay is present (as with the AFS configuration) when the bandwidth is lower than the quickness.

5) the lower ADS33C quickness boundaries at high amplitude correspond to the lower minimum control power requirements (50deg/s) of Ref 2.

From considerations of control power, quickness and bandwidth alone, Lynx and T509 are Level 1 aircraft. In practice, at the higher aggressiveness when the highest quickness is recorded, both are Level 2. Some of this degradation can be accounted for by simulated visual cue deficienies with T509 and severe cross couplings with the unaugmented Lynx. The data in Figure 8 is a useful benchmark for the kind of quickness required to achieve high agility factors in low speed MTEs, but it does not provide strong evidence for an upper boundary on quickness (or bandwidth and control power). The AFS rate response configuration T509 was implemented in the DRA's Conceptual Simulation Model (Ref 15) as a simple low order equivalent system of the form;

$$\frac{p}{\eta_{1c}} = K \frac{e^{-\tau s}}{(\frac{s}{\omega_m} - 1)(\frac{s}{\omega_a} - 1)} \qquad 2$$

where p is the body axis roll rate (rad/s), and η_{1c} is the pilot's lateral cyclic stick displacement($\pm$ 1). ω_m is the fundamental first-order break frequency or roll damping (rad/s) and ω_a is a psuedo-actuator break frequency (rad/s). K is the steady state gain or control power (rad/s, unit η_{1c}) and τ is a pure time delay.

Figure 9 illustrates the effects of the various parameters in the CSM on the maximum achievable quickness. In particular the actuator bandwidth has a powerful effect on quickness in the low to moderate amplitude range. Maximising the actuation bandwidth and minimising delays in the achievement of maximum acceleration is in accordance with maximising the agility factor.

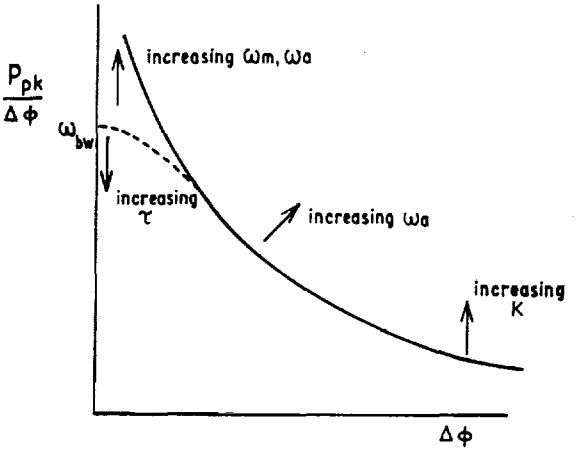

Fig 9 Effect of CSM Parameters on Roll Quickness

The sensitivity of agility factor with the parameters of the CSM is relatively easy to establish. If we consider the same bank and stop MTE discussed in the fixed-wing context earlier, some useful insight can be gained. A pulse type control input will be assumed, although in practice pilots would adopt a more complex strategy to increase the agility factor. To illustrate the primary effect we consider the case where the 'secondary' time delays are set to zero (ie $\tau = 0$, $\omega_a = \infty$). For a roll angle change of $\Delta\phi$, the ideal time is then given by assuming the time to achieve maximum rate is zero,

$$T_i = \Delta\phi / K = \Delta t \qquad 3$$

where Δt is the control pulse duration.

The time to reduce the bank angle to within 5% of the peak value achieved is given by,

$$T_a = \Delta t - \ln(0.05) / \omega_m \qquad 4$$

The agility factor is then given by,

$$A_f = T_i / T_a = \frac{\omega_m \Delta t}{\omega_m \Delta t - \ln(0.05)} \qquad 5$$

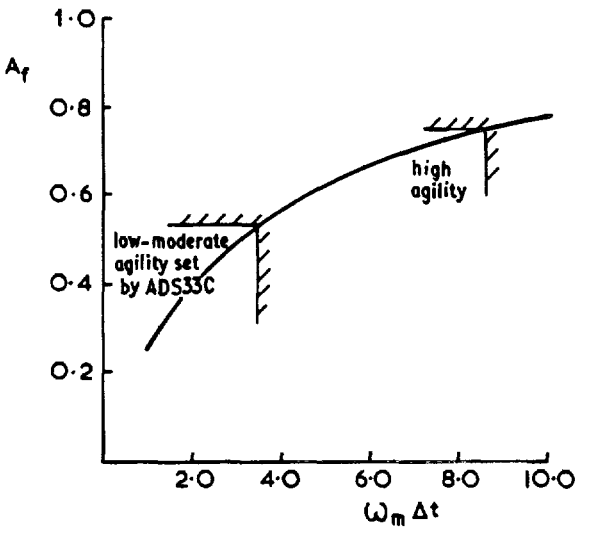

Fig 10 Variation of A_f with Normalised Bandwidth

Figure 10 illustrates the variation of A_f with $\omega_m \Delta t$. The bandwidth ω_m is the maximum achievable value of quickness for this simple case and hence the function shows the sensitivity of A_f with both bandwidth and quickness. The normalised bandwidth is a useful parameter as it represents the ratio of aircraft to control input bandwidth, albeit rather crudely. For short, sharp control inputs, typical in tracking corrections, high aircraft bandwidths are required to achieve reasonable agility factors. For example, at the ADS33C minimum required value of 3.5 rad/s and with 1 second pulses, the pilot can expect to achieve agility factors of 0.5 using simple control strategies in the bank and stop manoeuvre. To achieve the same agility factor with a half second pulse would require double the bandwidth. This is entirely consistent with the argument that the ADS33C boundaries are set for low to moderate levels of aggression. If values of agility factor up to 0.75 are to be achieved, Fig 10 suggests that bandwidths up to 8 rad/sec will be required; whether this is worth the 30% reduction in task time can only be judged in an overall operational context.

This simple example has many questionable assumptions but the underlying point, that increasing key flying qualities parameters above the ADS33C boundaries has a first order effect on task performance, still holds. But it provides no clues to possible upper performance boundaries set by flying qualities considerations. As stated earlier, ADS33C does not address upper limits directly. Also, practically all the upper boundaries in Mil Stan 1797 are related to the acceleration capability of the aircraft. As noted earlier, there are tentative upper limits on pitch attitude bandwidth, but it is suspected that these are actually a reflection of the high control sensitivity required to maintain the minimum level of control power required, rather than the high values of bandwidth per se. Control sensitivity itself (rad/s2.inch) is a fundamental flying qualities parameter and is closely related to the pilot's controller type; while some data exists for helicopter centre and side sticks, more research is required to establish the optimum characteristics including shaping functions. Mil Stan 1797 provides a comprehesive coverage of this topic for fixed-wing aircraft, rather more as guidance than firm requirements.

Another fruitful avenue appears to lie in the extension of the quickness parameter to the acceleration phase of an MTE. The fixed wing CAP already suggests this as the ratio of pitch acceleration to achieved normal 'g' (effectively, pitch rate). The DRA CSM used in the AFS trials offers a good example to explore and develop the concept of rate quickness. Setting the pure delay term in the CSM to zero for this study, the magnitude and time constant of the peak roll acceleration, for a step control input, can be written in the form;

$$\dot{p}_{pk} = \frac{K\omega_m}{\gamma} e^{-\omega_a t} \eta_{1c} \qquad 6$$

$$\omega_a t = \frac{\log\gamma}{1-\gamma}, \qquad \gamma = \omega_m/\omega_a \qquad 7$$

The rate quickness can then be written in the form,

$$\frac{\dot{p}_{pk}}{\Delta p} = \frac{\omega_m}{\gamma} e^{\frac{\log\gamma}{1-\gamma}} \qquad 8$$

and this is plotted in normalised form in Figure 11. During the AFS handling qualities trial described in Ref 14, the lag bandwidth ω_a was set at 20 rad/s to satisfy the pilot's criticism of jerky motion. This gave a γ of 0.5 at the highest bandwidth flown (T509). Corresponding values of rate quickness and time to peak acceleration were 0.5 and 0.7, both relative to the damping ω_m. Intuitively there will be upper and lower flying qualities bounds on both of these parameters. Hard and fast may be as unacceptable as soft and slow, both leading to low agility factors; the opposite extremes may be equally acceptable when referred to the maximum quickness. This suggests closed boundaries delineating the quality levels on the Figure 11 format. More systematic research is required to test and develop this hypothesis further.

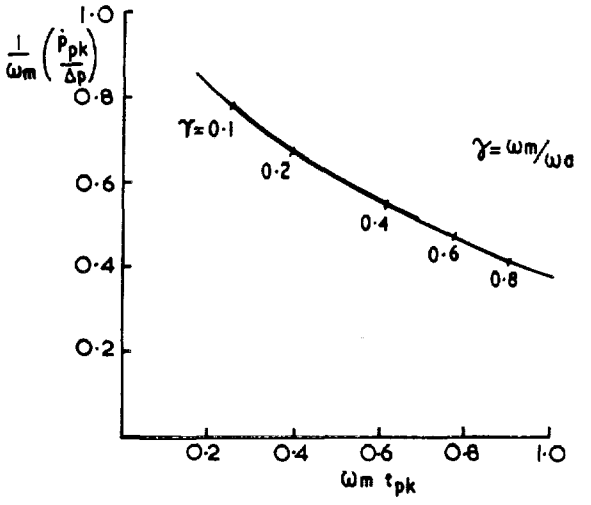

Fig 11 Variation of Rate Quickness with Acceleration Time Constant

Quality - Subjective Measurement

Flying quality is ultimately determined by pilot subjective opinion. The 'measurement scale' and understanding for this continue to stimulate vigorous debate but the Cooper-Harper handling qualities rating (HQR or CHR) provides the most widely accepted standard. The operational benefit of good flying qualities has never really been properly quantified using the CHR approach, however. The benefits to safety have been addressed in References 16 and 17, using the Cooper-Harper pilot rating scale as a metric (Fig 1). These references consider the pilot as a vital system component who can fail (be stressed to failure) in an operational context. The authors point out that if a normal distribution of ratings is assumed, then the probability of control loss, P_{loc}, can be calculated for various mean ratings and dispersions (Fig 12). P_{loc} is the probability of obtaining a rating greater/worse than 9.5, which in turn is simply proportional to the area under the distribution to the right of the 9.5 rating. Thus the probability of **flight**, and hence mission failure, due to flying qualities can be estimated. For the case studied in Ref 16 and depicted in Fig 12, operating a Level 1 aircraft can be seen to reduce the probability of a crash by an order of magnitude relative to a Level 2 aircraft. This result immediately raises the question - what is the probability of **mission** success or failure and can the same comparisons be made between aircraft with different mean flying qualities?

Figure 13 shows a notional distribution of ratings, with the regions of desired, adequate and inadequate performance clearly identified. The desired and adequate levels can be considered as reflecting varying degrees of mission (task element) success while the inadequate level corresponds to mission (task element) failure. Effectively the mission is composed of a number of contiguous MTEs, each having a virtual HQR assigned on the basis of performance and workload that the situation demands and allows respectively. If a particular MTE was assigned a Level 3 rating, then the pilot would either have to try again or give up on the particular MTE. Loss of control has obvious ramifications on mission success. The probability of obtaining a rating in one of the regions is proportional to the area under the distribution in that region. Note that, as discussed in Refs 16 an 17, we include ratings greater than 10 and less than 1 in the analysis. The rationale is that there are especially good and bad aircraft or situations, whose qualities correspond to ratings like 13 or minus 2. However, the scale enforces recording them as 10 or 1.

Note too, that the scatter produces, even with a good mean rating, a large probability of merely adequate performance and even a finite probability of total loss of control and crash. We have said in the Introduction to this paper that flying qualities are determined by the synergy between internal attributes and external influences. It follows then that sources of scatter originate both internally and externally. Internals include divided attention, stress and fatigue, pilot skill and experience. Externals include atmospheric disturbances, changing operational requirements and timelines, threats etc. The flying qualities community has done much to minimise scatter by careful attention to experimental protocol (Ref 18) but, in operational environments, the effective pilot rating scatter is omnipresent .

Fig 14 shows the probability of obtaining ratings in the various regions when the standard deviation of the ratings is unity. This curve, which we have labelled as preliminary, has some interesting characteristics. First, the intersections of the lines fall close to, or exactly at, the ratings 4.5, 6.5 and 9.5, as expected. Also it turns out that for a mean rating of 7, the probability of achieving inadequate performance is, of course, high, and we can also see that the probability of achieving desired performance is about the same as that for loss of control - about one in a hundred. Improving that rating to 2, lowers the probability of loss to 10^{-13} (for our purposes zero) and ensures that performance is mostly at desired levels. Degrading the mean rating from 2 to 5 will increase the chances of mission failure by three orders of magnitude.

We describe these results as preliminary because we assume that there is a rational continuum between desired performance, adequate performance and control loss. For example, desired and adequate performance may be represented by discrete touchdown zones/velocities on the back of a ship and loss of control might be represented by, say, the edge of the ship or hanger door. On a smaller ship (or bigger helicopter), the desired and adequate zones may be the same size, which puts the deck-edge closer to the adequate boundary, or represent a similar fraction of the deck size, hence tightening up the whole continuum. This raises some fundamental questions about the underlying linearity of the scale.

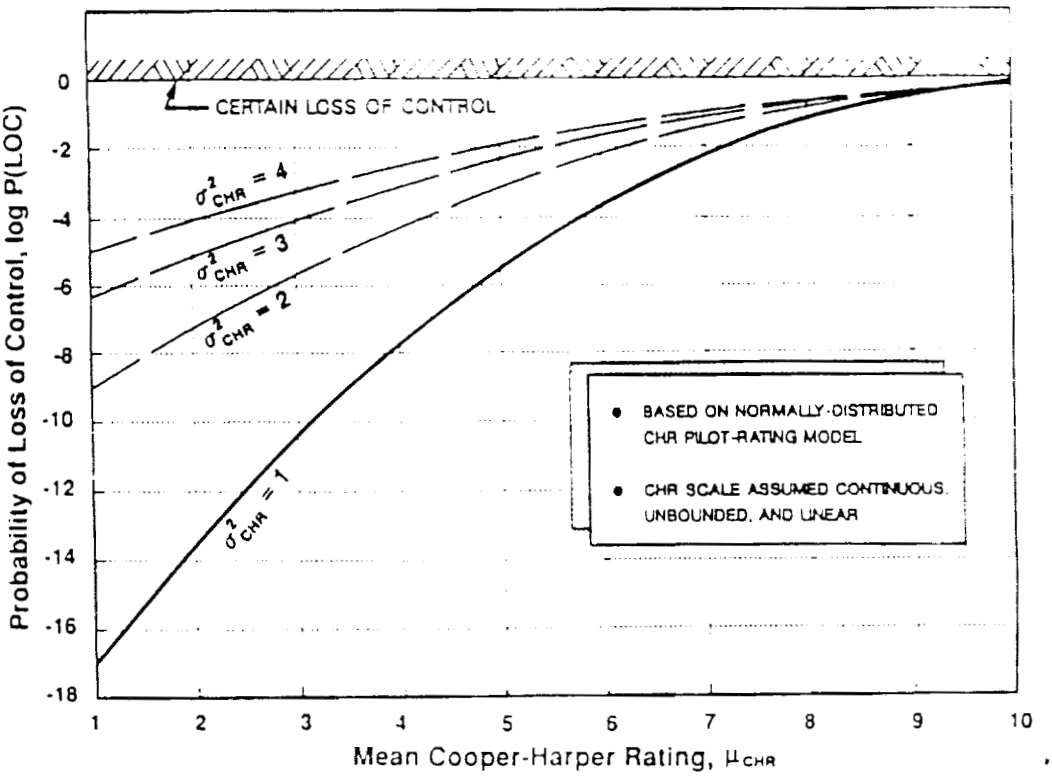

Fig 12 Relationship Between Mean CHR (HQR) and P_{loc}

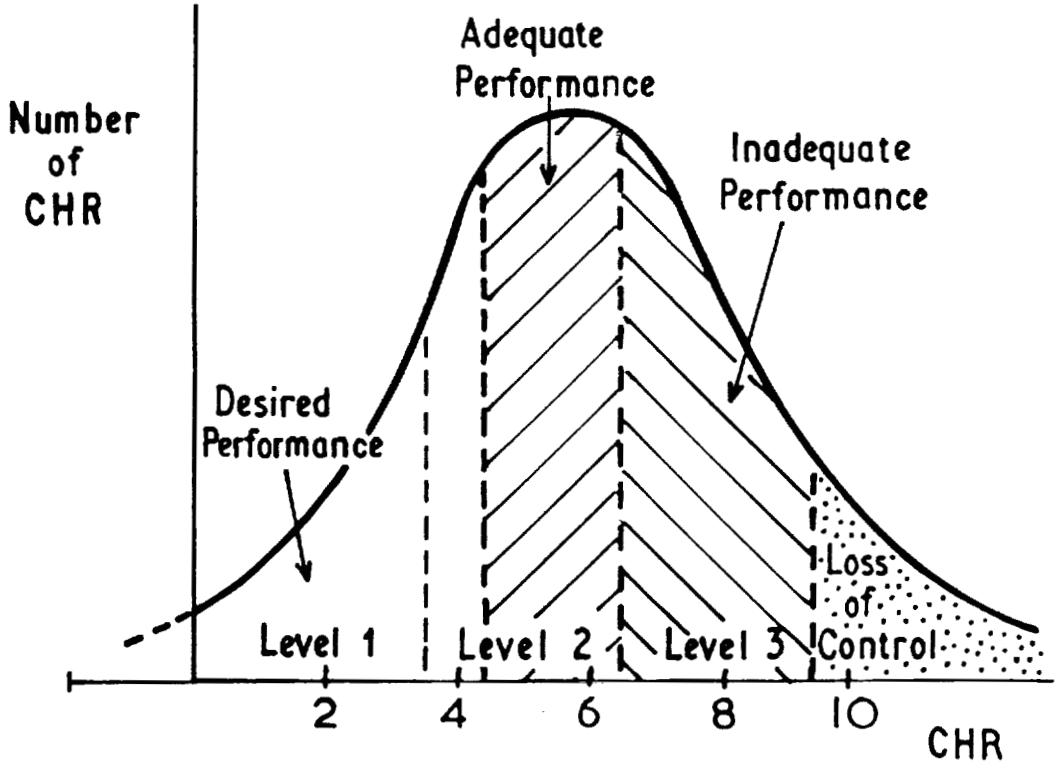

Fig 13 Notional Distribution of Pilot Handling Qualities Ratings for a Given Aircraft

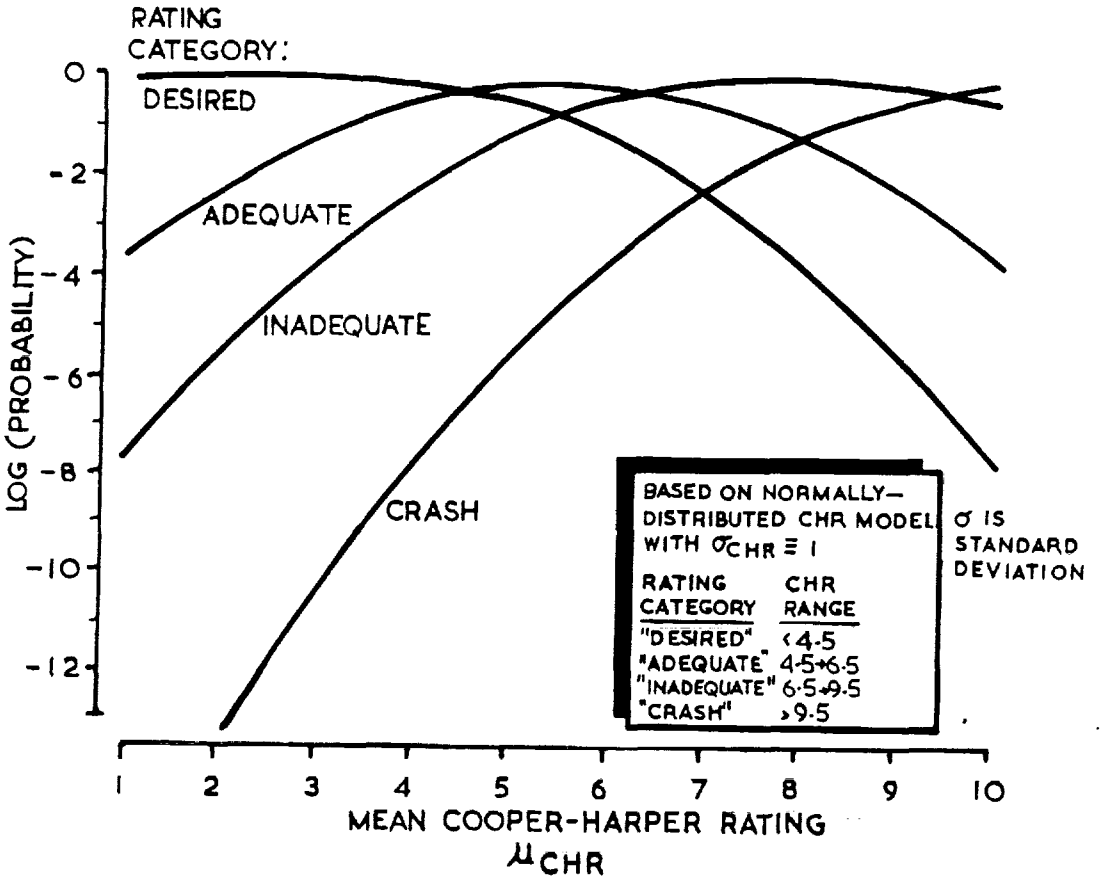

Fig 14 Relationship Between Mean CHR (HQR) and Probability of Mission Success, Failure or Crash - Preliminary Results

With the servo-model of piloting behaviour, for example, we can always define a desired level of flight path task performance so demanding that, whatever the aircraft attitude bandwidth, pilot induced oscillations will result.

Though these questions remain, pilot rating and mission success or failure are powerfully related through the preliminary data in Fig 14. Flying qualities alone can determine whether operational agility is flawless or whether control is lost.

Flying Qualities Effects in Combat Models

The results highlighted in this paper suggest ways by which the effects of flying qualities can be incorporated into unmanned combat mission simulations. Such models are regularly used to establish the effectiveness of different weapon system attributes or tactics, but the human element is usually absent for obvious reasons. The aircraft are therefore assumed to have perfect flying qualities and the models are often configured to ignore the transient responses, effectively assigning an agility factor of unity to each manoeuvre change or MTE. The impact of these assumptions is twofold; first, that there is no way that flying qualities or their enabling technologies can be included in the trade studies conducted with such models. Second, the implied perfect flying qualities may give a false impression of the importance or the value of mission performance enhancements. The key steps to embodying the key flying qualities effects are suggested as follows;

1) through objective design and assessment establish the level of flying quality and hence the effective mean HQR

2) describe the mission in terms a series of contiguous MTEs, selectable in the same way that set manoeuvres are in combat models

3) establish a MTE hazard weighting on the basis of threat, divided attention and other internal/external factors, that will define the effective HQR for the MTE. This will vary as the mission develops.

4) establish a time scaling for each MTE, on the basis of the maximum achievable agility factor

5) overlay the time scaling on the mission profile; there will be an option for each MTE to fly at reduced agility factor with level 1 HQR or to fly at the higher agility factor at a poorer HQR.

Improvements or degradations in flying qualities can then explored through variations in the achievable agility factors and mean HQR for the aircraft and can be linked directly to the enabling control technologies. There are, of course, some fundamental questions associated with this approach. How can we assign the mean rating and the standard deviation? How do we classify the hazards resulting from the various degrading influences? How are the maximum agility factors derived? These and others will need to be addressed if this approach is to be taken further; the benefits are potentially high however, both in terms of clarifying the value of active control to effectiveness and, conversely, establishing the cost of flying qualities limitations to operational agility.

Conclusions and Recommendations

Operational agility is a key attribute of any weapon system and its subsystems from sensors, through the airframe elements, to the primary mission element, eg weapon. The total system can only be as agile as its slowest element and maximising the concurrency within the subsystems is a key method for enhancing agility. AGARD Working Group 19 is currently examining this topic and will report in 1993; the present paper is assembled from material reviewed and developed within this activity. The focus of the paper is the airframe and its primary enabling attribute - its flying qualities. The adequacy of existing flying qualities criteria for providing agility is addressed along with the benefits to agility of good flying qualities and the penalties of poor flying qualities. The following principal conclusions can be drawn.

1) Existing flying qualities criteria provide a useful framework for describing and quantifying agility; however, the quality boundaries are only minimum standards and do not reflect or quantify the desirable characteristics at high performance levels. Indeed, there are no boundaries defined that set upper limits on usable performance.

2) The agility factor provides a measure of usable performance and can be used to quantify the effects of flying qualities on agility; agility factors up to 0.7 can be achieved with current aircraft types operated with high performance margins, but handling deficiencies typically lead to HQRs in the poor level 2/level 3 region. Moreover, the degradation from Level 1 to 3 is rapid. High agility factors achievable with Level 1 flying qualities should be a goal for future operational types.

3) Extensions of the ADS33C innovation, the quickness, into the acceleration response is suggested as a potentially useful parameter for setting flying qualities limits on performance. Flight and simulation data needs to be gathered and analysed systematically to test this hypothesis.

4) It is argued that even a Level 1 aircraft will degrade to level 2 and 3 in unfavourable situations. In this context, a probabalistic analysis can be used to highlight the benefits of improved flying qualities on operational agility and mission effectiveness. Operating a Level 2 aircraft is shown to increase the chances of mission failure by three orders of magnitude, compared with a Level 1 aircraft. The results are preliminary and dependent on a number of underlying assumptions, but indicate a powerful relationship. Experimental results are needed to substantiate the results; these could include learning runs and trials with varying degrees of external influences.

5) Considering the mission as a series of contiguous mission task elements enables the agility factor and probability of success/failure to be overlayed on non-piloted combat mission simulations. This should allow flying qualities to be included in such exercises and flight control technologies to be integrated into mission effectiveness trade studies.

6) The key to ensuring that future projects are not susceptable to performance shortcomings from flying quality deficiencies would appear to be in the development of a unified specification for flying qualities and performance, with a clear mission orientation in the style of ADS33C.

Acknowledgements

Many colleagues at the three agencies have aided the preparation and production of this paper; particular thanks go to Darrell Gillette at McDonnell Douglas for deriving the results shown in Figure 14. The authors acknowledge AGARD for enabling them to work together on WG19. The DRA contribution to this paper is funded through the UK MoD Strategic Research Programme.

References

1 Cooper, G.E., Harper, R.P.Jr.; "The Use of Pilot Ratings in the Evaluation of Aircraft Handling Qualities", NASA TM D-5133 (1969)

2 AVSCOM; Aeronautical Design Standard (ADS) 33C - Handling Qualities for Military Helicopters, US Army AVSCOM (1989)

3 USAF; Flying Qualities of Piloted Vehicles; Mil Std - 1797 (USAF) (1987)

4 Skow, A.M.; "Agility as a Contribution to Design Balance", AIAA 90-1305, 5th bi-annual Flight Test Conference, Ontario Ca., May 1990

5 Hodgkinson, J. and Hodgkinson, R.K.; "Fighter Transient Agility and Flying Qualities", AIAA Conference on Atmospheric Flight Mechanics, Flying Qualities Workshop, Monterey, California, August 1987

6 Hodgkinson, J. et al; "Relationships Between Flying Qualities, Transient Agility, and Operational Effectiveness of Fighter Aircraft", AIAA Paper 88-4329, AIAA Conference on Atmospheric Flight Mechanics, Minneapolis, Minn., August 1988.

7 Riley, D.R., and Drajeske, M.H.; "An Experimental Investigation of Torsional Agility in Air-to-Air Combat" AIAA Paper 89-3388, Conference on Atmospheric Flight Mechanics, Boston, Mass, August 1989

8 Riley, D.R, and Drajeske, M.H.; "Status of Agility Research at McDonnell Aircraft Company and Major Findings and Conclusions to Date". ICAS Paper 90-5.9.4, 1990a.

9 Riley, D.R. and Drajeske, M.H.; "Relationships Between Agility Metrics and Flying Qualities" Paper 901003, SAE Aerospace Atlantic, April 1990b

10 Brotherhood, P., Charlton, M. T.; "An assessment of helicopter turning performance during NOE flight"; RAE TM FS(B) 534, January 1984

11 Heffley, Robert E.; "Study of Helicopter Roll Control Effectiveness", NASA CR 177404, April 1986

12 Padfield, G. D., Charlton, M. T.; "Aspects of RAE flight research into helicopter agility and pilot control strategy"; paper presented at a Handling Qualities (Mil Spec 8501) specialists meeting, NASA Ames June 1986

13 Charlton, M. T., Padfield, G. D., Horton, R. I.; "Helicopter Agility in Low Speed Manoeuvres"; Proceedings of the 13th European Rotorcraft Forum, Arles, France, Sept 1987 (also RAE TM FM 22, April 1989)

14 Padfield, G. D., et al; "Helicopter Flying Qualities in Critical Mission Task Elements"; Paper F2, 18th European Rotorcraft Forum, Avignon, Sept 1992

15 Buckingham, S. L., Padfield, G. D., "Piloted Simulations to Explore Helicopter Advanced Control Systems"; RAE Tech Report 86022, April 1986

16 Hodgkinson, J., Page, M., Preston, J., Gillette, D.; "Continuous flying quality improvement - the measure and the payoff"; AIAA Paper 92-4327, 1992 Guidance, Navigation and Control Conference, Hilton Head Island, S. Carolina, August 1992

17 Page, M., Gillette, D., Hodgkinson, J., Preston, J.; "Quantifying the pilot's contribution to flight safety"; International Air Safety Seminar, Flight Safety Foundation, Long Beach, California, November 1992, MDC Paper 92K0377

18 Wilson, D., Riley, D.; "Cooper-Harper pilot rating variability"; AIAA Paper 89-3358, Atmospheric Flight Mechanics Conference, Boston, Massachusetts, August 1989

A Four-Axis Hand Controller for Helicopter Flight Control

Joe De Maio[1,2]
Max Bishop
McDonnell Douglas Helicopter Co.
Mesa, AZ

ABSTRACT

A proof-of-concept hand controller for controlling lateral and longitudinal cyclic pitch, collective pitch and tail rotor thrust was developed. The purpose of the work was to address problems of operator fatigue, poor proprioceptive feedback and cross-coupling of axes associated with many four-axis controller designs. The present design is an attempt to reduce cross-coupling to a level that can be controlled with breakout force, rather than to eliminate it entirely. The cascaded design placed lateral and longitudinal cyclic in their normal configuration. Tail rotor thrust was placed atop the cyclic controller. A left/right twisting motion with the wrist made the control input. The axis of rotation was canted outboard (clockwise) to minimize cross-coupling with the cyclic pitch axis. The collective control was a twist grip, like a motorcycle throttle. Measurement of the amount of cross-coupling involved in pure, single-axis inputs showed cross-coupling under 10% of full deflection for all axes. This small amount of cross-coupling could be further reduced with better damping and force gradient control. Fatigue was not found to be a problem, and proprioceptive feedback was adequate for all flight tasks executed.

[1] Dr. De Maio is currently Research Manager at the U.S. Army Aeroflightdynamics Directorate Ames Research Center Moffett Field, CA

[2] Opinions expressed herein are soley those of the authors and do not reflect those of the U.S. Army nor of McDonnell Douglas Helicopter Co.

INTRODUCTION

A major factor in the design of conventional helicopter controls was the need to provide the pilot sufficient mechanical advantage to overcome aerodynamic and mechanical forces that resist the movement of control surfaces. The conventional control design uses long, large displacement levers as control manipulanda. Cyclic pitch and roll control are on a lever between the pilot's legs. Collective pitch control is on a lever on the pilot's left side, along with a twist grip throttle. Anti-torque control is on pedals.

New technology has provided an impetus to change the conventional control arrangement. Increased pilot tasking associated with new mission equipment requires greater use of the pilot's hands for tasks other than flight control. The development of new flight control technologies has allowed redesign of the flight controls to support this need. For example an automatic throttle can eliminate or greatly reduce the need for the pilot to make inputs through the mechanical throttle twist grip.

The development of servo-actuated control surfaces has permitted significant change in the pilot-control interface. In fly-by-wire systems the pilot's control input consists of a change in line voltage which is interpreted by a logic circuit or computer in order to drive a control surface servo. Fly-by-wire systems offer a number of advantages over mechanical systems. These advantages include more sophisticated input schedules (e.g., variable gain, automatic coordination) and reduction in the size and travel of the control manipulanda, themselves.

The improvements that come from fly-by-wire allow a number of changes in the control manipulanda in the cockpit. Fly-by-wire control systems can support compact, small displacement controllers. They also permit the combining of control axes on a single manipulandum. Three- and four-axis controller configurations have been implemented with varying degrees of success. Common designs have been cascaded, that is, the multiple axes have been placed one atop the other (see Figure 1). In the most usual designs cyclic pitch and roll have been placed at the bottom of the controller in a configuration analogous to the conventional cyclic controller. Yaw, or anti-torque, control has been placed on a rotational axis of the grip. In four-axis designs collective input has been made through a translational movement of the grip.

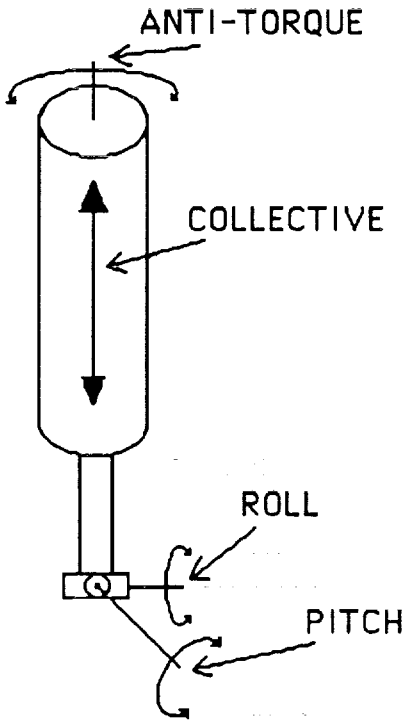

Figure 1. Cascaded Multi-axis Controller

Multi-axis controllers have had a number of problems with interface to the pilot. The quality of feedback on the size and direction of inputs has been poor. A related problem has been fatigue associated with sustained use. Also cross-coupling between axes has led to inadvertent control inputs (Prouty, 1992).

The usual approach to addressing these problems has been to attempt to minimize them by adjusting breakout force and force/input schedules. This approach has had limited success. The RAH-66 Comanche program has proposed 4-axis controller (Harvey, 1992), but this approach is now questionable.

Another approach to minimizing the negative characteristics of multi-axis controllers has been to alter the flight control laws to reduce the need for the pilot to make cross-coupled or fatiguing inputs. This approach has also been used to some extent on helicopters with conventional or hybrid control systems. Examples are the AH-64 Apache, command trim switch, and the OH-58 Kiowa, intermixing bell crank. The command trim switch allows the pilot to "center" the cyclic and pedals at the current position at the time of switch depression. This reduces pilot fatigue by eliminating the need for the pilot hold inputs. The intermixing bell crank is a mechanical system that trims cyclic pitch to compensate for the pitch up moment induced by increasing collective pitch, again reducing pilot fatigue.

Fly-by-wire allows even greater adjustment of the flight control laws because the flight control computer can interpret a single pilot input to command coordinated movement of several control surfaces. For example the Advanced Digital Optical Control System (ADOCS, Landis and Glusman, 1986) interprets a "cyclic roll" input to mean either commanded side slip rate or commanded coordinated turn rate, depending upon airspeed. This approach does not directly address the controller design problem, but it could reduce their effects by reducing the need to

make or sustain certain inputs. In practice this approach has experienced difficulty in defining control laws that are comfortable and intuitive to pilots and that support the full aircraft performance envelop.

THE TEST CONTROLLER

The problems of fatigue, poor precision and cross-coupling associated with cascaded multi-axis arise because the geometry of the controller is incompatible with that of the wrist. This incompatibility can cause cross-coupling within the wrist during multi-axis movements. The twisting anti-torque input is particularly prone to cross-coupling. Also certain input motions can place an excessive load on muscle groups that are easily fatigued. The lifting collective input is particularly fatiguing.

The design objective for the test controller was to minimize the negative characteristics of a cascaded, multi-axis controller design by orienting the axes in a way more compatible with the geometry of the wrist. Two aspects of the design supported this goal. The first aspect was a change in the orientation of the grip to place the hand in a more relaxed and natural position. The second aspect was to allow the hand to be positioned on the grip in a way that would facilitate isolated inputs.

A design drawing for the controller is shown in Figure 2. The cyclic pitch and roll were placed in the usual configuration on a universal joint at the base. Anti-torque ("pedals") is on a pivot atop the cyclic control. Two adjustments were provided at this point to allow for optimum ergonomic configuration. A rotational adjustment (not shown) allowed the grip to pivot in the plane of cyclic roll. This adjustment changed the position of the hand and wrist from horizontal to 45 deg. from horizontal. The second adjustment let the grip translate relative to the anti-torque pivot. This adjustment positioned hand over the roll/pitch pivot. The thrust (collective pitch) control was a motorcycle-type twist grip. Twisting the grip forward increased thrust. There was no separate throttle control.

The actual device was both simple and inexpensive. Centering was accomplished by means of opposite acting coil springs. Force gradient could be adjusted by replacing the springs. No damping was provided. A friction lock on the thrust control could be adjusted so that an input could be held or the control would return to the null position. The thrust control adjusted both forward and aft from the null, so that inputs could be either commanded thrust (forward only) or deltas from the current value (fore and aft).

CONTROLLER EVALUATION

Two evaluations were performed. One evaluation consisted of making full deflection inputs on one axis and measuring the cross-coupled output on the other axes. The second evaluation consisted of installing the controller in a limited fidelity flight simulator and evaluating it subjectively.

The controller was installed in a limited fidelity flight simulator at McDonnell Douglas Helicopter Company for both evaluations. For evaluation of cross-coupling the virtual prototyping computer system for generating flight instrumentation was programmed to simulate a four-channel oscillograph. The display in the cockpit was masked to prevent the subject's seeing his input. After data collection began, the subject made a full deflection input on one control axis. This input consisted of a movement from the null position to one stop back to the other stop and finally to the null position. Output of all four axes was recorded.

Typical controller output is shown in Figures A1 through A8. Two recordings are shown for each control axis. One shows an example of a small cross-

coupled controller response, and one shows a relatively large cross-coupled response. In the worst cases cross-coupling is about 10% of full deflection output. Typically it is under 5%, and in the best cases it is around 1% or less. The worst cross-coupling appears in cyclic pitch response to thrust inputs.

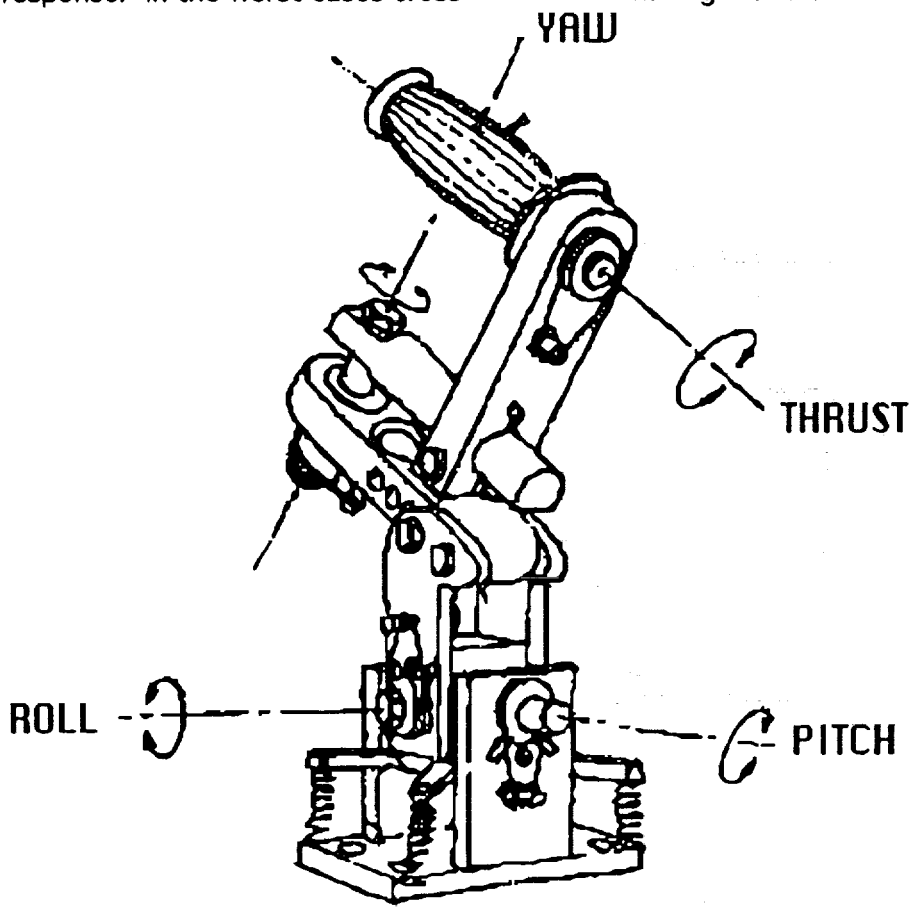

Figure 2. Test Controller

Interestingly, cross-coupling between roll and pitch axes is of about the same size as other cross-couplings. Roll and pitch are not problem axes in this type of controller configuration. The observed cross-coupling was very likely a result of the limited engineering design of the proof-of-concept device. Centering, control of breakout force and force displacement schedule were imprecise and the was no control of damping. Improvements in these areas should greatly reduce cross-coupling.

The simulator used for the subjective evaluation was a limited fidelity device having a two channel Sogitec computer generated out-the-window visual scene and a 9 inch CRT panel instrument display. In addition to the test controller, it contained conventional controls from an SH-53. Two aircraft models were used. The AH-64 model had stability augmentation as in the Apache. The MD-500 model had no stability augmentation. Both models had an autothrottle.

Simulation engineers, familiar with both the AH-64 and MD-500 simulated flight characteristics, performed a variety of flight tasks using both the conventional and test controls. These tasks included high speed flight, low speed flight, hover and hovering flight and "pedal" turns. Based on the

subjective opinions of the engineer/pilots the test controller was found to be comparable to the conventional controls in all modes of flight.

The most demanding task for the test controller was high speed flight with the MD-500 aircraft model. This model had no stability augmentation, coordination or command trim. Therefore the pilot had to make and hold anti-torque and anti-pitch inputs. The pilots were able to make the inputs as accurately with the test controller as with the conventional controls, but they found them more fatiguing due to the higher force gradients and lack of trim control in the proof-of-concept device.

CONCLUSIONS

The proof-of-concept, cascaded, four-axis controller showed cross-coupling between control axes that was small enough to be potentially applicable for helicopter applications.

While cross-coupling was intrinsic to the cascaded design, the quality of design and fabrication contributed significantly to the amount of cross-coupling. Improvements in breakout, force gradient and damping could greatly reduce cross-coupling.

The device was found to be accurate and easy to use in simulation. Control of the simulated helicopter was subjectively comparable to conventional controls.

ACKNOWLEDGMENTS

The authors wish to thank Mr. Robert Bunker for his help in supporting the handcontroller development and Mr. Lou Kildall for building the device.

REFERENCES

Harvey, D.S., "Can a computer Fly a Helicopter?", Rotor & Wing International, Aug. 1992.

Landis, K.H. and Glusman, S.I., Development of the ADOCS Controllers and Control Laws, Vol I-II, USAVSCOM Technical Report Number TR-84-A-7, St Louis, MO, Mar 1987.

Prouty, R.W., "The Sidearm Controller: a Few Considerations," Rotor & Wing International, Sep. 1992.

In-Flight Simulation of High Agility through Active Control
-Taming Complexity by Design-

Gareth D Padfield
Defence Research Agency
Bedford, England

Roy Bradley
The Caledonian University
Glasgow, Scotland

Abstract

The motivation for research into helicopter agility stems from the realisation that marked improvements relative to current operational types are possible, yet there is a dearth of useful criteria for flying qualities at high performance levels. Several research laboratories are currently investing resources in developing second generation airborne rotorcraft simulators. The UK's focus has been the exploitation of agility through active control technology (ACT); this paper reviews the results of studies conducted to date. The conflict between safety and performance in flight research is highlighted and the various forms of safety net to protect against system failures are described. The role of the safety pilot, and the use of actuator and flight envelope limiting are discussed. It is argued that the deep complextity of a research ACT system can only be tamed through a requirement specification assembled using design principles and cast in an operational simulation form. Work along these lines conducted at DRA is described, including the use of the Jackson System Development method and associated Ada simulation.

Introduction

The central issue when setting requirements for in-flight simulation involves the trade-off between performance and safety. The integrity of the experiment, from the very concept being tested through to its implementation in software and hardware, determines the achievable flight performance level. The greater the uncertainty in the behaviour of the simulated aircraft, then the greater the risk of misbehaviour; likewise, the lower the reliability of the experimental system, then the greater the risk of failure and consequent misbehaviour. It follows that the higher the inherent performance of the aircraft and its experimental system, the higher is the risk that misbehaviour will lead to an accident. Operational constraints and regulations usually dictate that this dilemma is resolved in favour of safety, hence compromising performance, or making it very expensive to achieve. These ideas are not new of course, and have featured large in the aircraft systems field for many years; the disciplines of modern design, test and implementation methods now ensure a degree of confidence in solutions to well defined problems. The compounding dilemma is that research into new and improved flying qualities contains the problem definition itself, and defining the flying qualities boundaries requires gathering data with Level 2 and 3 configurations.

The development of full authority, flight critical, active control technology (ACT) for helicopters has been proceeding apace for more than ten years with nine experimental aircraft in the form of research and technology demonstrators having flown in the western world. In the search for the quantum change in helicopter flying quality, a variety of solutions to the performance/safety tradeoff have been employed, including constrained experimental flight envelopes, multiple redundant hardware and limited performance actuation systems. All experimental systems have employed a Safety Pilot whose cockpit controls are back-driven, providing the primary cue on the behaviour of the system; experience has shown that the Safety Pilot is the most critical safety element. Along with ground-based simulators, these first generation variable-stability, active control helicopters have been used extensively to explore novel control methods and to build the database from which the ADS33C flying qualities criteria have been developed and substantiated.

Several Nations are now looking forward and planning the development of second generation ACT helicopters with a range of new research objectives in mind, centred on the need for greater levels of automation;

i) to extend operations in degraded visual cue environments,

ii) through the provision of carefree handling, enabling safe exploitation of the full operational flight envelope (OFE),

iii) through the integration of flight with fire control, engine control and mission systems to provide greater concurrency and hence operational effectiveness.

Research into these aspects of helicopter ACT needs to deliver solutions that will increase performance and safety in harmony. Ironically, as noted above, when exploring a new idea in flight, performance and safety attributes can conflict, and there is a potential problem that development of ACT and its operational benefits will be hindered by this dilemma. Recognition that a certain level of risk is inevitable is the first step towards resolving this problem; establishing well formulated operating procedures that contain the risks during the exploration of new concepts is the second. Adopting an approach to specification and design, that tames the complexity of the integration of the flight control system with the vehicle, its subsystems and

the pilot, is the important third step in this process and will feature as one of the key themes of this paper.

The paper reviews the UK DRA (formerly RAE) programme to define the requirements for and to build a high performance flight research system, designated ACT Lynx. Taking the performance/safety tradeoff as a starting point, a number of topics are addressed.

1) The performance requirements and the driving research objectives will be outlined; the emphasis from the outset has been to achieve high agility at low pilot workload.

2) The safety constraints and how they reflect on system architecture and airframe health will be addressed. The role of the safety pilot will be described and issues surrounding intervention times following failures will be addressed, drawing on results from an exploratory ground-based simulation conducted at DRA. Experience with other experimental ACT helicopters are discussed and (non-attributed) examples of the kind of failures that safety pilots have had to cope with in the past will be highlighted.

3) A vital key to confidence that an experimental flight control system will perform as required lies in the development of the functional requirements as an integral part of the system design. This has been achieved in the ACT Lynx project by the incremental development of an Ada simulation of the triplex redundant system using the Jackson System Development (JSD) methodology. The approach focusses attention on the interface of the experimental system with the outside world, eg operations at the pilot vehicle interface (PVI), the actuation system, sensor system etc. The behaviour of the system is considered from a constructional/design, rather than a hierarchical/descriptive, viewpoint. This distinction is crucial at an early stage to capture all the nuances of the intended behaviour. In addition, many of the human factors issues at the pilot/vehicle interface can be examined in detail through simulation. This approach is described.

4) The methodology for control law design and assessment is described. An important concern is the validation of the behaviour of the implemented control law; early in its life it will be immature and made up of several, limited flight-envelope, un-integrated functions. The development towards continuous, full flight envelope, agility enhancing control functions involves a gradual expansion of the envelope and actuator authority, using ground based simulation to pave the way for the flight tests. The philosophy will be described, including the role of the curtain limiter, a device for moderating the control inputs to the experimental actuators.

The UK programme is currently at a hiatus due to funding limitations, but sufficient ground has been covered to provide some clear messages for others striving for similar goals. The UK continues to collaborate with the key players in the research field - US Army/NASA, NRC and DLR - and this paper presents the opportunity to stimulate discussion, with the wider manufacturing and research community, on some of the trade-offs in this important area.

Harmonising Safety and Performance

Research Objectives

A companion paper at this Conference (Ref 1) has highlighted situations where current operational helicopters lack agility, such that when operated at high performance levels, flying qualities deteriorate and lead to high piloting workload. Figure 1 reflects this through the variation in pilot handling qualities ratings (HQR) with Agility Factor - the ratio of ideal task time to actual task time in a mission task element (MTE). As the pilot increases performance, the degradation from level 1 to poor level 2/level 3 ratings is rapid, making the use of high performance potentially quite dangerous.

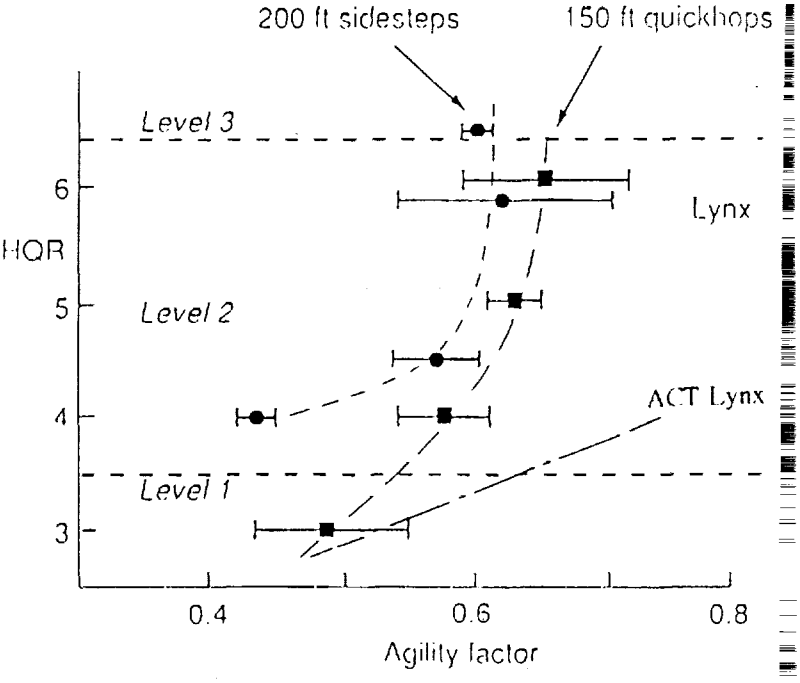

Fig 1 Pilot Handling Qualities Ratings vs Agility Factor for Lynx

The results shown in Figure 1 were gathered on the research Lynx at DRA Bedford, flown at much lighter weights than in normal operational Service, to simulate the higher performance margins expected of future types; the results are considered to be typical of all current Service aircraft and indicate a clear goal for research into improved flying qualities. A primary objective of ACT Lynx was therefore aimed at demonstrating the achievement of Level 1/2 flying qualities at high agility factors as shown in Fig 1. This and other key research objectives are summarised in question form as follows;

1) Can level 1 flying qualities be achieved at high agility factors? Research to answer this question would produce a database from which carefree handling functions could be defined and potential upper flying qualities boundaries identified.

2) Can multi-axis sidesticks be used effectively in such circumstances and what level of automation is required to facilitate their use? This research would address the ergonomic aspects of sidesticks and define the optimum feel characteristics and sensitivities; it would also address the use of such controllers with reversionary, less well augmented, modes.

3) Can high performance be achieved in the presence of strong disturbances? Disturbance rejection and ride-control functions can be designed to operate effectively at considerably higher bandwidths than handling-control functions and this research would define those control functions and associated sensor requirements.

4) What are the critical control augmentation/display trade-offs in degraded visual conditions? Research would address the integration aspects of displays and response types for different usable cue environments (UCE), blending issues and identify critical parameters in the controls/displays trade-off.

5) How can ACT be exploited to enhance functional integration between the flight control system and mission systems eg fire, engine, navigation? This question would direct research towards maximising concurrency between the flight and mission management systems, leading ultimately to the potential for fully automated flight.

Objectives 1, 2 and 3 require the high-fidelity environment of an in-flight simulator, able to operate in realistic scenarios close to the visual-cue-rich environment of natural terrain and cover, whereas considerable progress towards Objectives 4 and 5 can be made with ground-based simulation. In addition, the displays and integration research require considerably more on-board equipment. Hence the initial foci of ACT Lynx were to be the three high performance objectives.

Performance & Safety - The Conflict

The operational flight envelope for the Lynx Mk 7 represents the baseline ACT Lynx envelope. Key features are given in Table 1. The high values of attitude quickness and bandwidth stem from the hingeless rotor on the Lynx with its 13% effective flap hinge offset. The rotor provides a high natural damping and control moment capability enabling higher levels of agility to be exploited than with articulated rotor helicopters. Figure 2 illustrates the envelopes of roll and pitch quickness achieved in the Lynx for Sidestep and Quickhop re-positioning MTEs (Ref 2). The envelope covers the full attitude range to illustrate the high bandwidth (low amplitude) and control powers (high amplitude) achieved even in these, non-tracking, MTEs.

Table 1 ACT Lynx Performance Characteristics

Performance Aspect	Lynx Mk 7 Flight Envelope for ACT Lynx
hover thrust margin	> 20% (sea level, 20 deg C)
roll, pitch, yaw control power	> 100deg/s, 60deg/s, 60deg/s
quickness for 10deg attitude change	> 4 rad/s (roll), 2 rad/s (pitch)
attitude bandwidth in hover	> 5 rad/s (roll), 3 rad/s (pitch)
low speed side velocity envelope	30 kn
load factor	> 2 g, 0 g
Vmax	> 140 kn (sea level, 20 deg C)

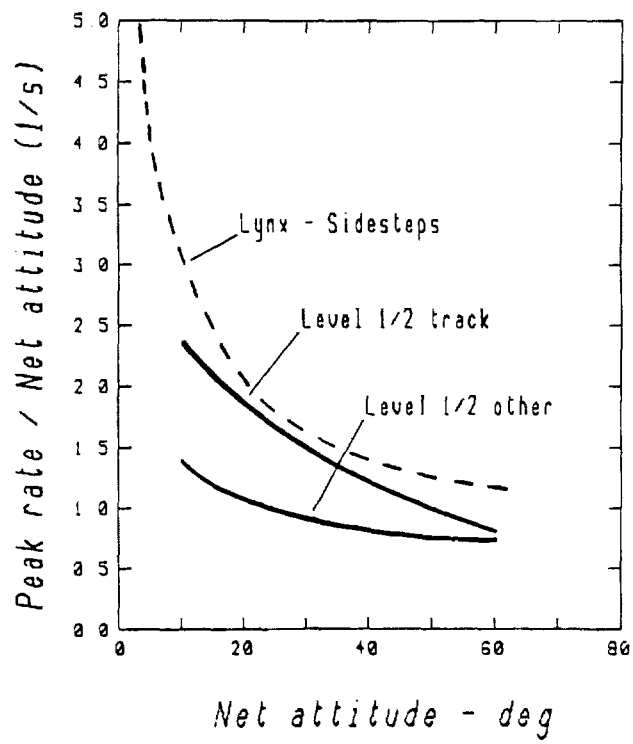

Fig 2a Roll Attitude Quickness

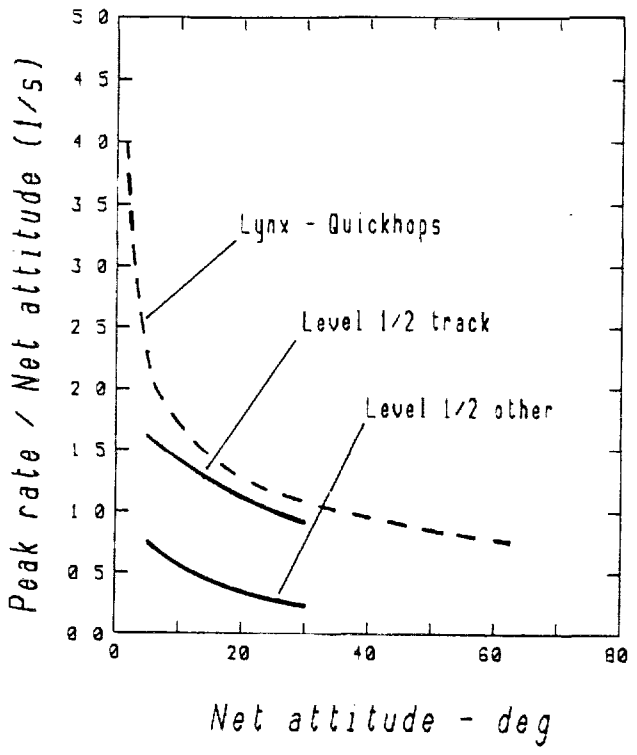

Fig 2b Pitch Attitude Quickness

The quickness is a direct measure of agility, closely related to the time to achieve an attitude change. At the two amplitude extremes the achieved quickness values are well above the ADS33C Level 1 requirements for bandwidth and control power and there is a generous margin in the moderate amplitude range, even relative to the tracking MTE boundary. Combined with a moderate hover thrust margin, maximum 'g' capability and wide speed envelope, these performance characteristics make Lynx well suited as an ACT testbed. But the performance is only useful if control laws are able to exploit fully the OFE and this raises fundamental safety issues concerning the aircraft behaviour following ACT system failures.

System failure can be loosely classified under two categories;

i) hardware failures; these are usually assumed to be random in nature, hence only predictable in a statistical sense, eg one failure expected within 10^n operating hours. The usual method of protecting against such failures is to build in hardware redundancy together with comparators and monitors, effectively to increase n.

ii) software failures; two ways that a software implementation can '***fail***' or misbehave follow from either the correct programming of the wrong reaction or failure to take certain situations into account. It is sometimes claimed that the probability of a software error occuring can be related statistically to the degree of testing carried out, but this does not appear to have a sound theoretical foundation. In reality, both the above software failures are deterministic and context dependent and unless the testing happens to include the particular conditions, the error is likely be missed.

The Safety Pilot

Failures in both categories can be expected to occur throughout the life of an ACT research vehicle and give rise to a variety of different behaviour including fast/slow hardover, oscillatory or frozen actuator demands. Acknowledging this, the next set of questions relate to the integrity of the system, the related tolerance to failures and the means of protection. All ACT research helicopters operated over the last ten years have included one principal element in common in this regard - they have all had a **Safety Pilot,** whose controls are back driven by the research actuators. The latter have either been special purpose, dual mode (electro-mechanical) type (Refs 3, 4, 5) or connected in parallel with existing power control units (Refs 6, 7, 8). All types have been full authority, high rate actuators. The safety pilot, with his backdriven controls providing an immediate and instinctive cue as to the health of the system and the experiment, is generally regarded as the most important and vital safety element. A well trained safety pilot will be able to identify misbehaviour through the motions of his backdriven controls, and can take rapid action to preserve flight safety. However, very special skills are required to make a good safety pilot, among which is the ability to judge when, and when not, to disengage and how to recover to a safe flight condition. It is a very demanding role and any help that the system can provide will reduce the workload and lessen the risk of a loss of control.

Help can be provided in the form of a fail-safe or fail-operate system configuration. Fail-safe normally relies on a monitor system running concurrently with the flight control system, either sampling and comparing dual channels or comparing the signals in a single lane with that from a model. If the comparator detects a difference, outside a defined threshold, the system will be tripped out and control will be returned to the safety pilot with appropriate alert signals. Fail-operate signifies that the system can continue operation following one or more failure; through monitoring and voting, faults can be detected and isolated. The remaining healthy system components continue to function as normal, but the crew is alerted to the fault. For a single fail-operate system, the system degrades to fail-safe following a failure. Operational fly-by-wire fixed wing aircraft are normally designed with a two fail-safe capability with respect to hardware failures to achieve the necessary overall system integrity. This requires a triplex-monitored or quadraplex system architecture. The research helicopters operated over the last ten years have a variety of different solutions implemented. The NRC's Bell 205 (Ref 3) and DLR's BO105 (Ref 6) are both single string systems with a limited fail-safe capability centred on the fly-by-wire actuator input/output relationship. Rotor flapping is monitored in the 205 and hub moment in the 105 with

both having limits which, if exceeded, trips the systems out. The ADOCS demonstrator (Ref 4) included a triplex fly-by-light hardware configuration and an independent (analogue) monitor. The latter was designed to model the behaviour of the primary flight control system (PFCS), hence automatic flight control system (AFCS) inputs were signalled as errors by the comparator; the thresholds were set to allow moderately aggressive flying. This, so-called DOCS monitor, was designed to catch software and other common mode 'failures'. The AV05 research aircraft (Ref 8) comprised a dual-duplex architecture providing, in principal, a two-fail operate capability. The concept included flight envelope limiting features within the control system. Most of these aircraft also featured a trip when the engine/rotor system torque exceeded a prescribed value.

From this very brief review of some of the current designs it is clear that help can be provided to the safety pilot in a multitude of ways; it is also clear that current wisdom suggests that he does need help, particularly in the detection of rapid, potentially rotor damaging, control inputs. The dilemma comes from trying to distinguish between a system failure and a genuine ACT system command; both can look very similar at the actuation stage. Failures from hardware faults can be detected and isolated through fail-safe or fail-operate architectures; software failures are considerably more difficult to detect. As noted above, software errors in both the categories discussed above are likely to be a regular occurance in the development of a control law. Examples (non-attributed) of software failures that have occured on ACT helicopters include,

1) 3-axis hardover caused by divide by zero - excursions of 20 deg pitch, 35 deg roll and 20 ft height loss during recovery,

2) control modes not referencing to correct flight condition, leading to position error and roll into turn,

3) integrators not inhibited at control stops, leading to time delay in response to following input,

4) no priority given when engage/disengage pressed simultaneously

All led to a transfer of control to the safety pilot, although there was inevitably some delay in recovery due to failure recognition problems. It should be stressed that no accidents have occured on ACT research helicopters to date.

Safety Pilot Simulation

To gain a better understanding of the kind of behaviour that Lynx would exhibit in response to failures and the resulting safety pilot reaction, an exploratory simulation trial was carried out on the Advanced Flight Simulator at DRA (Ref 9), using the small motion system. A Lynx, augmented with an ACT system, providing Level 1 flying qualities, was flown through a range of mission task elements. The safety pilot occupied the cockpit on the motion base, with the 'evaluation' pilot flying from the control desk.

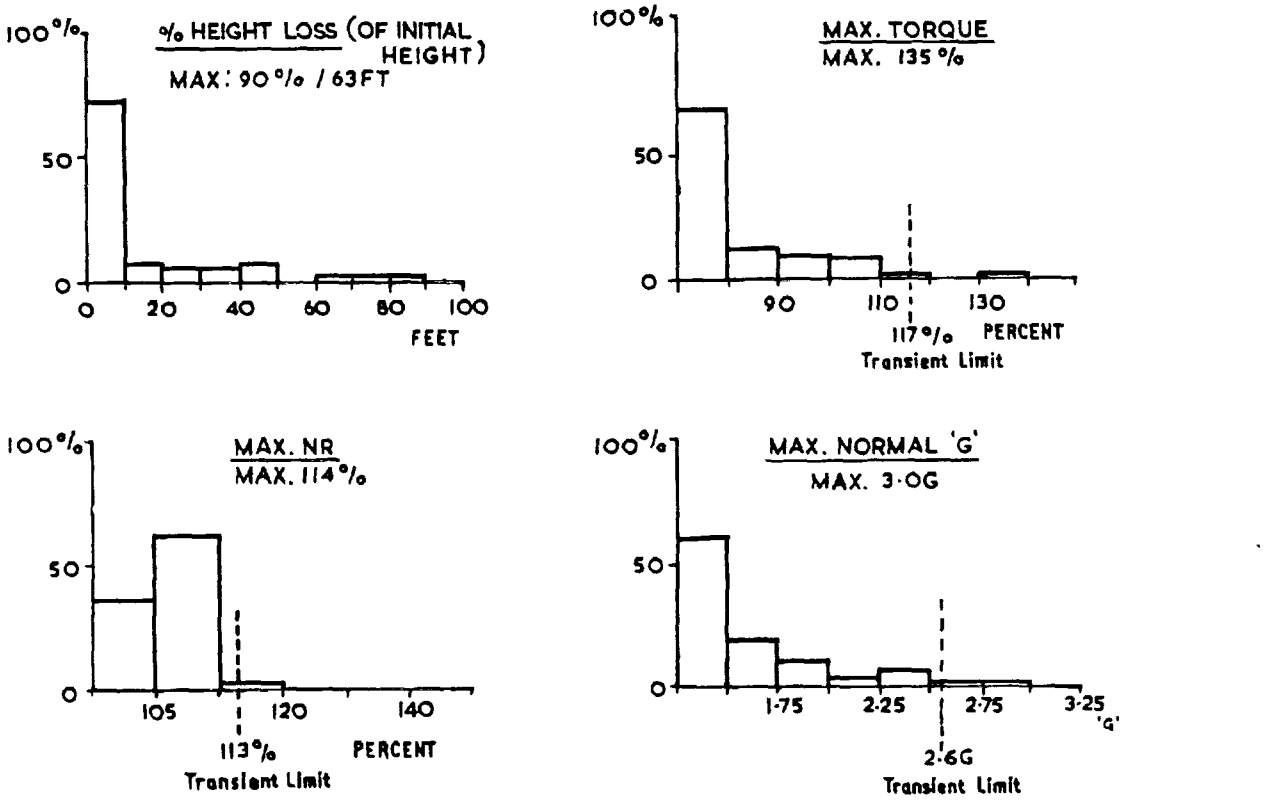

Fig 3 Statistical Summary of Excursions During Failures and Safety Pilot Recovery

Hardover failures were injected in combinations of axes at various points during the flying, and the safety pilot's task was to disengage the ACT system and recover the aircraft without exceeding limits and, of course, avoid the ground and obstacles. Following disengage, the aircraft configuration was Lynx with limited authority stability augmentation, as envisaged for ACT Lynx. This initial investigation had several related objectives including an evaluation of alternate disengage and alert mechanisms. A total of 61 failure events were flown with three evaluation pilots. With the preferred 'force' disconnect system, all disconnects were achieved in less than 0.3 second; 'button' disconnects resulted in longer times, up to 1 second. Figure 3 shows a statistical summary of the peak values of critical aircraft states recorded during recovery relative to the flight envelope limitations, including the height loss. The 3g peak occurred following a right cyclic/pedal runaway in a right turn, when a height loss of 63 feet was also recorded. The load factor limit was exceeded on this occasion to avoid hitting the ground. The main rotor torque and rotorspeed limits were both exceeded once, the former following a sympathetic positive collective failure in a bob-up. The results of the work reported in Reference 9 are tentative. The AFS simulation cues were limited and the Lynx aircraft model has known deficiencies particularly in the off-axis responses and in hard turns. Also, worst cases may not have been evaluated and instinctive, trigger disengage mechanisms were not evaluated. Nevertheless, the potential for very rapid flight envelope exceedances during failures, when operating close to limits, was demonstrated and the dangers of vertical flight-path excursions during recovery were highlighted.

Protection Devices

Protection against such occurrances needs to take into account that responses to failures can be similar to the response to an aggressive pilot-input applied to maximise agility. An approach used in the past has been to restrict the inputs to the rotor through employing both limited authority series actuators (as normally found in a conventional SCAS) and parallel actuators with reduced rates. Figure 4 illustrates the roll kinematics and pilot's lateral cyclic command during a sidestep manoeuvre on a phase plane. The shaded areas correspond to the excluded region if series/parallel, frequency-splitting, actuation had been used with typical 20% (20%/s) authority. The manoeuvre would have been severely compromised. Fig 5 illustrates the control/actuation quickness or 'attack' for the Lynx sidesteps showing values up to the PFCU bandwidth of 15 rad/s at small amplitude and quite high values extending out to large control inputs. The superimposed lines correspond to boundaries set by different actuation rates. The Lynx actuation system is able to achieve values greater than 200%.sec in single lanes. Any actuation rate limiting below this would clearly deprive the pilot of performance, but no systematic investigation of this aspect was carried out. Actuation limiting in such a crude manner can be effective but needs to be implemented in software if the limits are to be extended as confidence grows in the behaviour of a control law. This is effectively what happens with ADOCS, although in that implementation (Ref 4) the DOCS monitor tripped the ACT system out if rates and amplitudes from the AFCS were too high. For ACT Lynx, a scheme based on this approach was suggested, illustrated conceptually in Fig 6. The so-called 'Curtain Functions' would be defined in the software that limited the actuator inputs as shown in Fig 6. Initially, for a new control law, the curtain would be well closed, offering maximum protection following failures. As the control law developed and confidence grew in its behaviour, the curtains would be opened incrementally, until full performance was available. The concept has yet to be evaluated in simulation but potentially offers a safe route through to high agility.

As noted earlier, the ACT helicopters that have been operated over the last 10 years have adopted many different approaches to this protection question. It is believed that three main factors contribute to the 100% safety record in the operation of research ACT helicopters.

a) the reliance on an experienced, well trained and highly skilled safety pilot

b) the adoption of operating procedures that emphasise flight safety

c) the use of flight envelope monitors or restrictions that inhibit agility, particularly in low level trials.

For ACT Lynx, it was always considered that the practices in categories a) and b) developed by organisations like DLR, NRC and NASA would be fully adopted. The focus on agility research, however, meant that issues associated with c) had to be faced squarely and an alternate strategy developed that enabled a way forward. A fail-operate/fail safe (FOFS) architecture was selected to provide full protection against hardware failures, with the argument that in safety critical situations, even the safety pilot may not have sufficient time to recover with only a fail-safe system. Methodologies that ensure comprehensive verification and validation of the software system elements would be vigorously pursued. It was recognised that there would be two components to the embedded software, a high integrity 'core', including consolidation, monitoring, voting and actuator drive functions that would remain essentially fixed during the development of a control law, and the control law itself and its attendant curtain function, that would regularly change in structure and data input. The control law was envisaged as the most appropriate place for the envelope limiting to be incorporated, in the form of carefree handling functions. Ultimately, the control law would need to function without independent monitoring, to enable the high agility testing to be realised. For both kinds of software it was considered that a high investment in the requirements capture and definition process would pay off in high system integrity; these issues are developed further in later sections.

Airframe Fatigue Usage

Before discussing these aspects, there is one additional consideration regarding safety that was addressed with ACT

Lynx - the question of the impact of ACT flying on airframe fatigue. It was always recognised that an agility research aircraft would spend a greater proportion of flight time in high fatigue-usage manoeuvres, than its operational counterparts. Also, the effects of the ACT control functions on control linkage and rotor loads was relatively unknown. A third issue stemmed from the recognition that the existing aircraft's OFE was defined with a margin relative to the safe flight envelope and that carefree handling functions would, in principle, allow some of this additional performance to be used with safety. Some form of load monitoring in this regime would be essential. The critical structural areas were identified by the manufacturer and comprised components on the main/tail rotor hub and blades, control links, fuselage frame and gearbox, tail cone and fin. These components have since been strain-gauged for non-ACT purposes and are undergoing in-flight calibrations at the time of writing. The data from the strain gauges are processed in two different ways. First, via a telemetry link to a ground station to enable real-time monitoring of loads and, second, to the on-board recorder system for post-flight analysis and fatigue usage calculations. From a safety standpoint, the fatigue usage monitoring task was seen as an integral part of the comprehensive approach taken with the ACT Lynx concept.

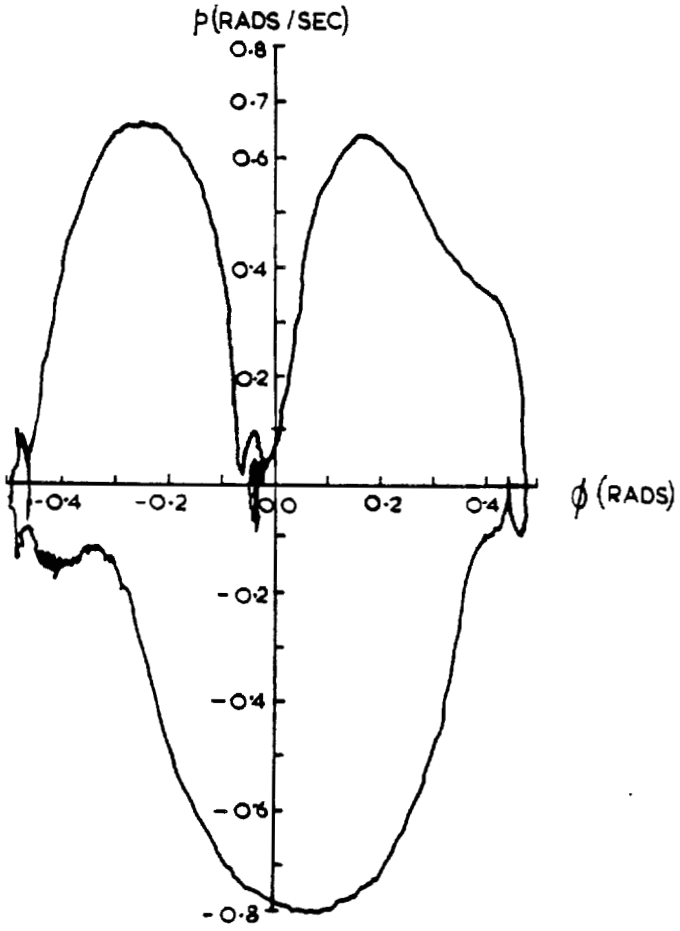

Fig 4a Lynx Roll Attitude Phase Plane Portrait in a Sidestep MTE

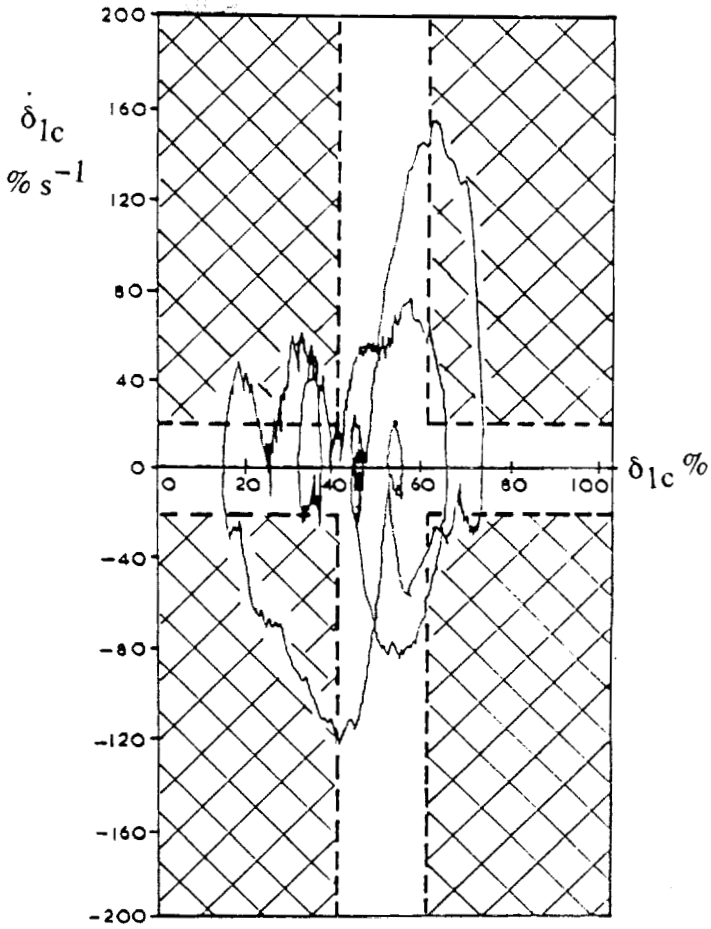

Fig 4b Lynx Roll Actuator Phase Plane Portrait in a Sidestep with Frequency Splitting

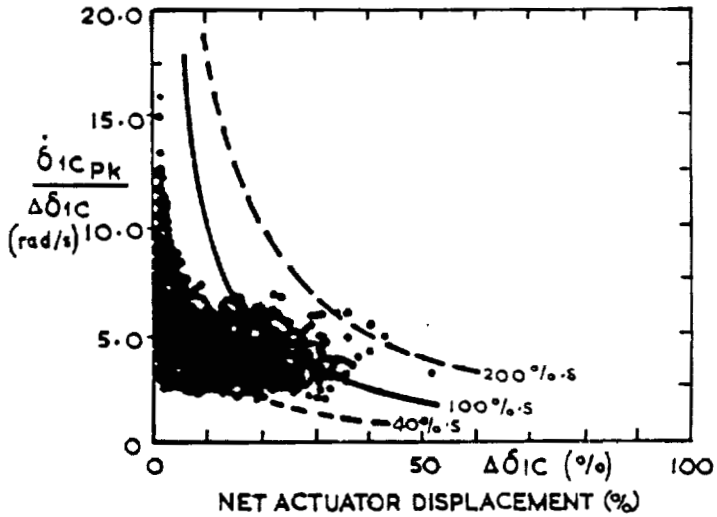

Fig 5 Lynx Control Quickness in Sidestep MTEs Showing Effects of Rate Limits

C-3

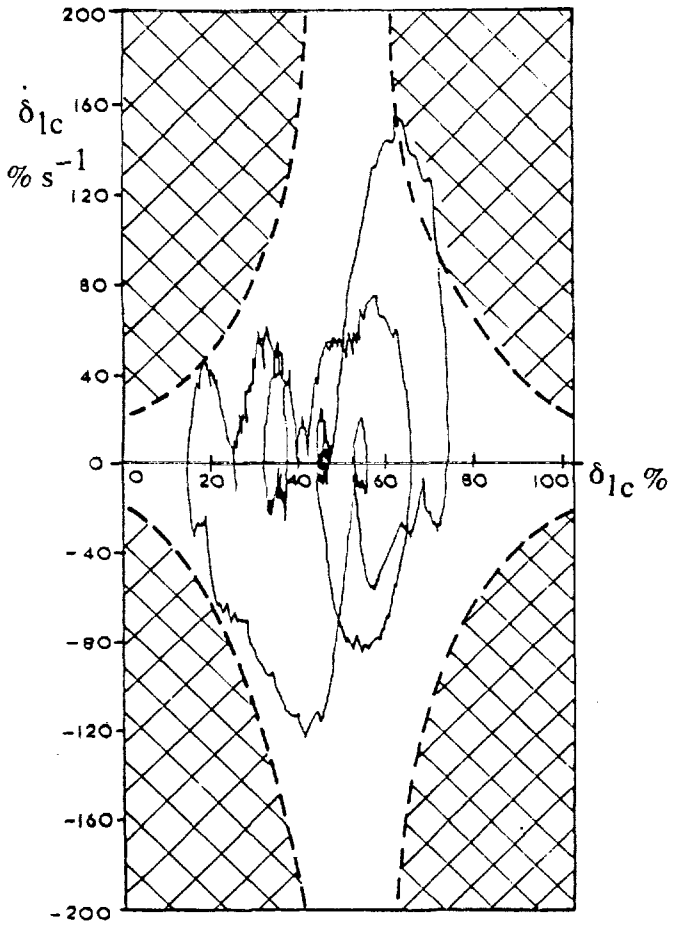

Fig 6 Actuator Phase Plane Portrait with Curtain Function

As a bonus, much valuable data on the different airframe load spectra experienced with the ACT system would be gathered and, ultimately, the load measurements would be available to the ACT system itself in the pursuit of envelope-expanding carefree handling functions.

In summary, the achievement of high performance with ACT Lynx was to be enabled through the incorporation of several layers of '**safety net**'. The hardware would be designed to exhibit fail-operate/fail safe reliability. The 'fixed' software would be designed and tested to be fault free. The control law software would operate within the constraints of the actuator curtain and be developed to a fault free state for testing in flight critical regimes. The safety pilot would be the ultimate protection against damaging flight path excursions and limit exceedances. Fatigue monitoring and accounting would protect against the consequences on airframe health of unconventional manoeuvres and control activity and provide a check for greater than usual fatigue life consumption. These safety nets were autonomous by design, yet it was recognised that only through their proper integration into the ACT Lynx concept would the performance targets be achievable. A comprehensive requirement specification was needed for the total system, developed through simulation, that defined the range of interacting functions and their operations.

Requirement Specification & Incremental Simulation

Preliminary Design Evaluation

The ACT Lynx design concept evolved from a number of preliminary studies which carefully explored the feasibility of modifying the DRA Research Lynx into a variable stability, active control, research helicopter.

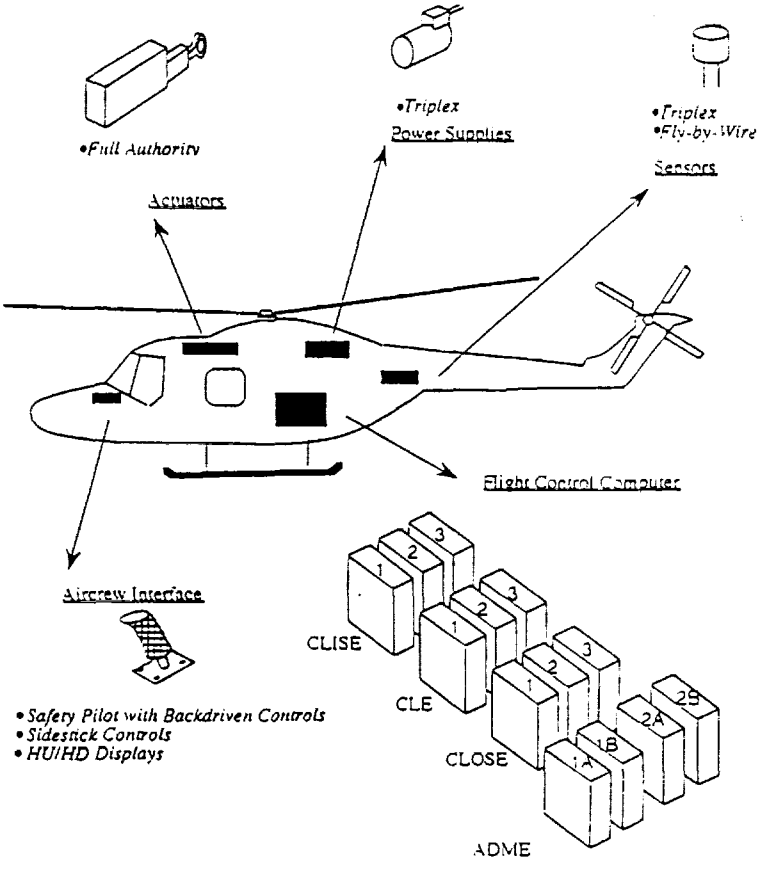

Fig 7 The ACT Lynx Concept

Practical issues addressed in these initial studies included a confirmation that the installed power and actuator system were sufficient to test to the limits of the desired ACT Lynx flight envelope, and that the mechanical linkages could be modified to allow backdriving by a set of high performance parallel actuators. Additional equipment such as sidestick controllers and advanced sensors were specified and an outline of the system architecture proposed in terms of a triplex flight control computer and a dual duplex actuator drive and monitoring unit. An entirely triplex architecture would have satisfied the fail-operate/fail-safe

requirement but, in the case of the ACT Lynx, a final component having a dual duplex arrangement was deemed to be more appropriate to connect harmoniously with the duplex hydraulic systems and primary flight control units (PFCUs). The ACT Lynx concept is illustrated in Figure 7.

A further aspect that received some preliminary design consideration was the nature of the pilot interface - that is, the displays, switches, buttons etc, that the pilot would require in order to engage and operate the facilities of the new system. These items were analysed and their likely functionality and appearance described in outline. When, in the light of these preliminary studies, the prospects for the ACT Lynx project seemed favourable, attention turned to developing a high quality specification (Refs 10, 11).

Specification Structure

In the design team there was a genuine commitment to avoid the pitfalls of many other projects and leave nothing to chance in the specification of the new system. In particular, there was a determination that the requirements specification must solve all of the significant design issues. That is, it must be correct, it must be complete, and it must be validated.

Such considerations placed a considerable challenge upon the team in the preparation of the requirements specification since there had to be sufficient detail to be totally unambiguous; that is, the implementation had to be clear, while at the same time there had to remain a high level of visibility of the design concepts and what the system was trying to do and why. These requirements are often incompatible since the very accumulation of a morass of detail imparts a complexity that militates against understanding. It is such complexity which needed to be tamed by an appropriate design and specification method, and which led to the decision to use modern software design methods for application to the whole diverse system. It was also recognised that hierarchically organised descriptions could be an effective technique for reducing complexity and in this case a decomposition of the system into its major functional elements seemed to be the most natural. This decomposition was the only one that was imposed on the system *a priori*. The outcome is shown in Figure 8, where the square and rectangular components are those relevant to the specification exercise. The bold rectangles are referred to as processing elements to be embodied in a Flight Control Computer (FCC), although such terminology was not used in the written specification. The elements of the system are described in the order of the primary flow of the signal information as illustrated by the arrows in Fig 8.

(i) Sensor Element (SE). This leading element contains the aircraft motion sensors - attitude and rate gyros and accelerometers, and also the air data units for obtaining velocity components, pressure and temperature information.

(ii) Crew Station Element (CSE). The other leading element incorporates the conventional controls for the safety pilot and a versatile sidestick controller facility for the evaluation pilot. For convenience these inceptor components were grouped together as an Inceptor Element (IE). The CSE also contains the various interfaces for the pilot to engage, operate and be cued by the ACT system as follows:

(a) Pilots Control Panel (PCP) - used by the Evaluation Pilot for engagement and disengagement and also for conducting the system-test sequence. Engage and Disengage operations would normally be performed using switches on the pilot's controls.

(b) Repeater Panel (RP) - provides a copy of the displays for the Safety Pilot.

(c) Menu Panel (MP) - provides other ACT interactions, such as selecting one of the available control laws and sets of parameter values. The same panel provides the interface for injecting preprogrammed disturbances into the system, as part of a flight-test facility used, for example, in gathering data for the validation of the helicopter simulation models and in demonstrating compliance with flying qualities requirements of new control laws.

(d) Mode Select Panel (MSP) - available for in-flight selection of control modes, for example, height-hold, speed-hold, hover hold.

(iii) Control Law Input Support Element (CLISE). This element has the main purpose of processing and managing the information from the Crew Station and Sensor Elements. It also contains the function for scheduling of a comprehensive system test.

(iv) Control Law Element (CLE). This element is supplied with inceptor, sensor, mode selection and related information by the CLISE. The CLE is the raison d'etre of the ACT Lynx since it hosts the experimental control laws which are to be evaluated. It is this element that the user of the ACT Lynx, the flying qualities engineer, will interact with. Carefully verified and validated control law software will be plugged into and unplugged from this element. Typically, six control laws will be selectable by the experimental pilot with an additional choice of up to six sets of parameters within each law.

(v) Control Law Output Support Element (CLOSE). The element following the CLE interfaces the demands produced to the remainder of the system. It also provides a selectable limiter on the demands produced by the control law as additional protection against immature software.

(vi) Actuator Drive and Monitoring Element (ADME). The final element to provide processing takes the demands from the CLOSE and produces drive signals for the parallel actuators resident in the Actuator Element, and the series actuators in the PFCU. The ADME also manages the

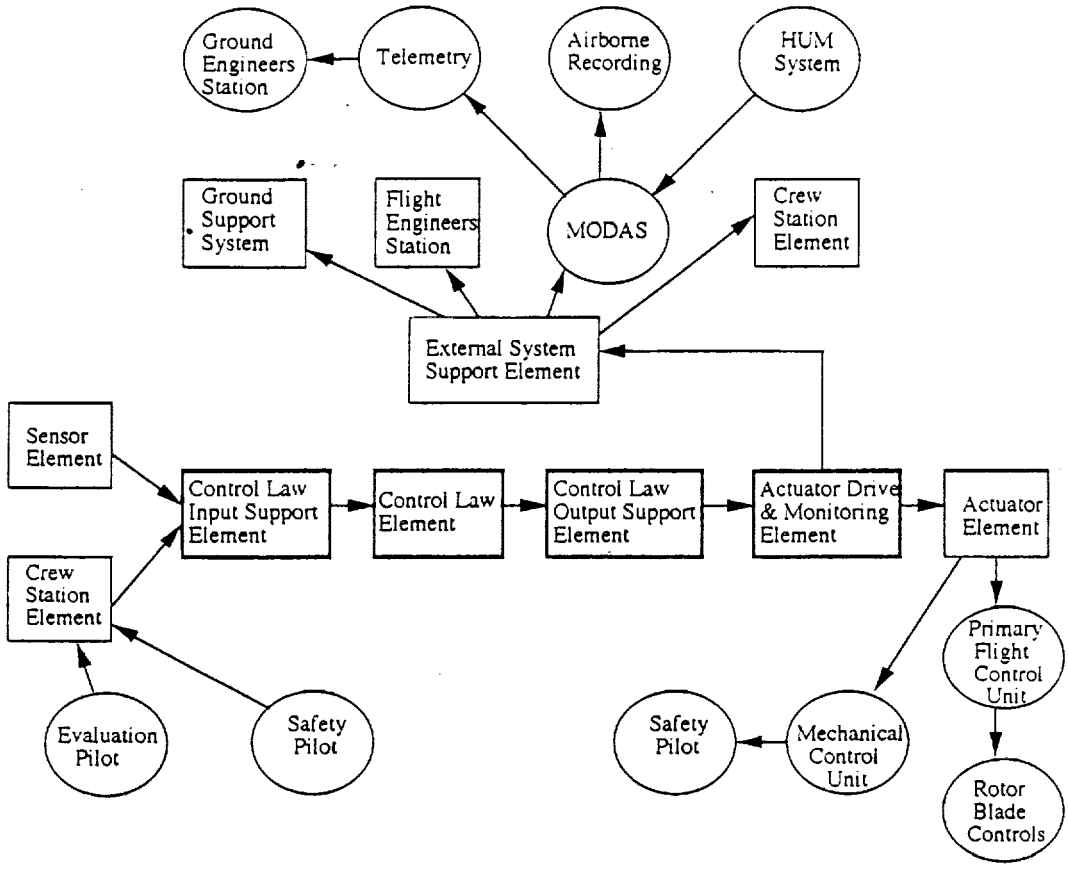

Fig 8 The ACT Lynx Logical Elements

engagement of the ACT system through the energising of the parallel actuators, and supplies a normal autostabilisation function when the ACT system is not engaged.

(vii) Actuator Element. The parallel actuator system is last in the sequence. The parallel actuators are connected to the conventional control runs from the safety pilot; when the actuators are engaged (hydraulically powered), the controls are back driven to provide the safety pilot with essential control position cues and to aid in recoveries, and forward driven to the Lynx PFCUs.

(viii) External System Support Element (ESSE). In support of the above network of elements is an element which essentially provides a catchment for all of the significant data in the system. It interfaces with the on-board data acquisition system and also with the experimental helmet mounted or head down displays. A record of all system related events such as engagement, disengagement and diagnostic messages is retained in a System Journal.

The specification takes each of the elements identified above and provides a detailed description. Each element is described in detail under the headings Type, Function, Operation, Performance, Inputs & outputs, Interfaces, Testing and Failure reporting & recovery. Where a particular element is composed of replicated units, so that several **units** together comprise an **element**, the replication of units in the element is stated and the unit itself is described under the same headings. For example, the CLISE is a triplex element composed of three identical CLISUs (Control Law Input Support Units).

In the event, this primary decomposition harmonised with the subsequently developed techniques for coping with the system's complexity. Hierarchies can lose their simplifying property if the structures become too deep; for the ACT Lynx project only three levels were employed, with quite different specification techniques and associated tools at each level:

(i) The top level is the written, structured text. It is manipulated and maintained by commercial text processing software.

(ii) The middle level is the capture of the specification in a Jackson System Development (JSD - Refs 12, 13) design, using CASE tools such as Speedbuilder (Refs 14, 15).

(iii) The lowest level is the Ada code. It is generated automatically from the JSD design using a CASE tool such as Adacode, and is acted on by a conventional compiler. The simulation so produced is an ideal vehicle for validation of the specification.

Thus each level has its own formalism and there is no decomposition from one level to another. The first consideration, as in many design problems, is deciding where to start; one advantage of the Jackson JSD approach is that the starting point is well defined: one must use the narrative text of the specification to begin the *modelling* phase.

Jackson System Development

Jackson System Development is a method of analysing a written specification for a computer system to produce a formally executable specification. The method was jointly developed by Michael Jackson and John Cameron in the early 1980s (Refs 12, 13). It consists of three stages: modelling, network and implementation. There is considerable emphasis placed on the modelling stage in order to establish, unequivocally, the information available from the world outside the system being designed, with which the system interacts.

Modelling and Entities: A model, in JSD, is a description of the real world as it appears to the system. Entities are objects in the real world which have to be modelled by the system, and of particular interest in the modelling activity are those entities which perform discrete actions. For example, a press of the ARM button by the evaluation pilot is an action to which the system must respond. The modelling phase requires that the actions be allocated to specific entities, and the main task is to identify viable entities and allocate the relevant actions to them. For each entity, the time ordering of the actions must be then be specified and, conventionally, a tree diagram is used for this purpose. As an example, consider the truncated list of actions from the ACT Lynx system shown in Figure 9. Some of these are related to the pilot entity in his role of engaging the ACT System; they may be identified and their time-ordering expressed as a tree diagram using Jackson Structured Programming (JSP) notation (Ref 13). The diagram is shown in Figure 10 where the root is named after the entity which performs the actions, and the leaves (the lowest level boxes which are named rather than numbered) hold the names of the individual actions. The intermediate nodes or boxes describe the possible types of behaviour: sequence, selection (o) and iteration (*), as denoted by the symbol in the top right hand corner of the box. The numbers in the lowest level boxes refer to changes in the state of the object (entity) as shown in the table in Figure 10.

Thus Figure 10 expresses a model of the Pilot Engagement entity as a repetition of occurrences of Engagement Cycles. An Engagement Cycle can either be a Normal Cycle, composed of a sequence of Arm, Armed, Engage, Disengage, or alternatively an Early Disengage, composed of only part of the normal sequence followed by a Disengage. The appropriate changes of state are indicated by the numbered operations for each action, and it can be seen that, prior to any action, the engagement state is initialised to DISENGAGED by operation 13.

Action	Summary	Attributes
ARM	The pilot requests that the system be armed.	
ARMED	The actuator positions and the control law demands are in harmony	
ARM_DEFAULT_MODE	The initial arming of a default control mode.	ID: MODE_ID_TYPE
CANCEL_SYSTEM_TEST	A request to cancel the system test	
CAPTURE	This is the signal to mode to go from ARM to ARM_AND_IN_CAP	ID: MODE_ID_TYPE
COMPLETED_SYSTEM_TEST	All tests of the system test have been successfully completed	
CONTINUE_SYSTEM_TEST	Indication that the current test of the system test has been successfully completed.	
DISENGAGE	The system has been disengaged. This may happen before engagement (1) by the pilot pressing the disengage button or (2) by the system failing to get into the ARMED or ENGAGED state. It may happen whilst ENGAGED on receipt of a signal from an actuator relaying the fact that it has become disengaged	
DOWN_DISTURBANCE_REQUEST	The pilot wishes to be offered the previous valid disturbance, that is the first disturbance with a lower index number (ID) This is equivalent to the pilot presssing the DOWN button	
ENGAGE	The pilot requests (successfully) that the system be engaged.	
FAIL_TEST_STAGE	The current 'automatic' stage of the system test has not been successfully completed.	

Fig 9 Typical List of Actions

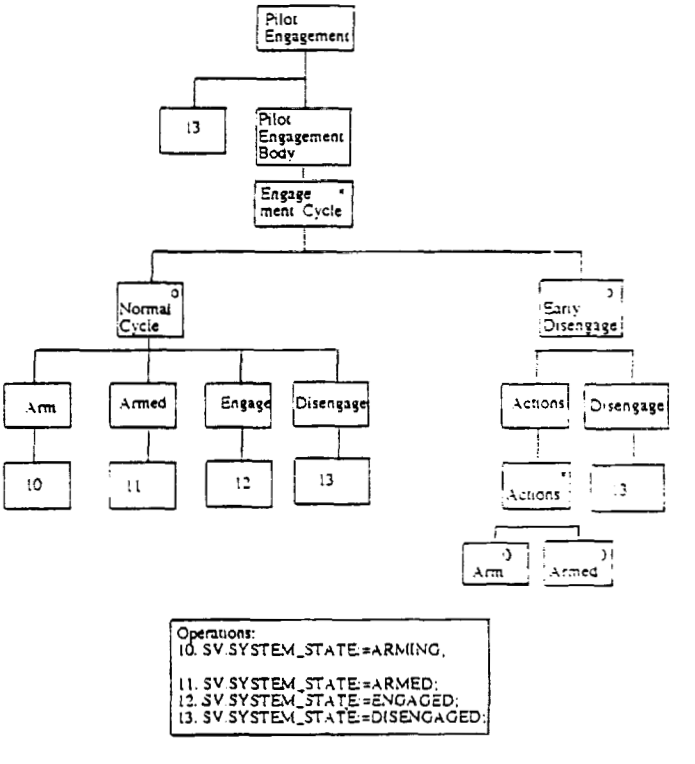

Fig 10 Pilot Engagement Cycle in JSP Form

The same type of modelling is applied to the other components of the CSE such as the activities associated with the Menu Panel and the Mode Control Panel, to obtain the full complement of model descriptions. In a completed modelling exercise, the total set of tree diagrams describes all of the time orderings of the actions plus the changes in system state. In real-time systems it is often only the activities at the man-machine interface which require this type of modelling and much of the real world is modelled simply by polling sensor information. In the ACT Lynx application, for example, the Lynx helicopter is modelled kinematically by polling data from inertial and air motion sensors. The tree diagrams in these cases are simply iterations of polling actions. The inceptor displacements are conveniently treated in this manner too.

It is fundamental to the JSD method that the model structure in Figure 10 can be used as a program structure for a process to control the engagement of the ACT system. Once operations have been added to read incoming action-messages then all that is required is for the operations to be expressed in the required language. The iterations can be expressed as loops and the selections as conditional statements with appropriate conditions. The result is that the tree diagram can be converted to code mechanically either by hand or, as in the current work, automatically.

Network and Implementation Following on from the modelling stage is the development of the *network* . Processes derived from the entities defined in the modelling stage are called model processes. Other processes are needed to make use of the data stored by the model processes in order to generate the outputs which provide the required functionality of the system. More details can be found in Reference 11.

JSD Summary The principal aim of the JSD method is to create a specification which can be usefully viewed from both above and below. The modelling stage is an object oriented analysis of the real world which produces a description which users can readily grasp, because the result is described in terms of objects familiar to the user. The tree diagrams of the method also provide important detail about the model of the real world. The network stage uses two descriptions: (a) Data flows, which can be presented to the user to indicate the architecture of the system and (b) Tree diagrams, which the analyst can use to express the design of a particular function. The resulting specification can be viewed by the user from above in terms of the interface with the real world and, simultaneously, the specification contains enough detail for the implementers below to perform their task. It is this general property that makes JSD particularly attractive and encouraged a determined assault on the difficulties associated with the application of JSD to the complete ACT Lynx System.

Specification Structure

Even with the brief review of the JSD method contained above, it should be clear that the envisaged application to the ACT Lynx presented substantial technical challenges. The primary difficulty was how to adapt the method to a system which had a diversity of types of component. For example, how was a hydraulic actuator to be specified using JSD and, in this context, what was the interpretation of data streams and state vector inspections - the JSD inter-process communication methods? A further complication was how to include the replication associated with the embedded redundancy without the occurrence of a comensurate increase in complexity. It was clear that the JSD method itself, although offering a desirable development route, did not, on its own, offer the reduction of complexity which was considered essential for the ACT Lynx requirements specification. As a compositional method, JSD eschews a top-down approach to system development. The rationale is argued at length by its proponents and a convincing case can be made for it in software development; however for more general systems, the physical architecture can impose a natural decomposition. This decomposition may then be harnessed and used to guide the development of those enhancements to JSD which are necessary to reduce the complexity of the system specification. This recourse to a decomposition based on the underlying hardware was adopted for the ACT Lynx system and led directly to a significant conceptual and practical reduction in the descriptive complexity.

JSD enhancements The next step in resolving the complexity of the system is to recognise that each identifiable element can be viewed as an independent system communicating in a limited way with other elements. For elements which are composed of replicated units, each unit is treated as independent.

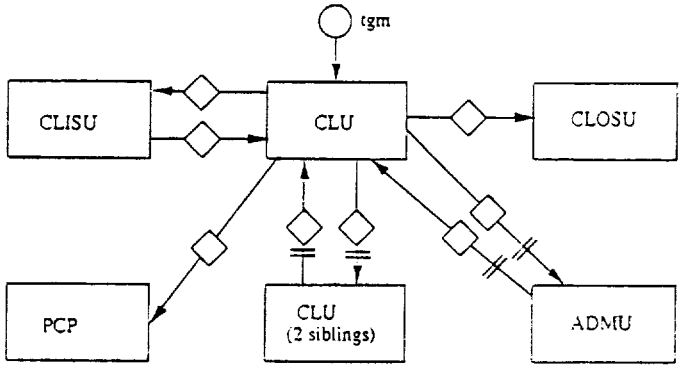

Fig 11 Top Down View of Control Law Unit

Figure 11 shows an example of such a top down view. The datastream into the CLU is a frame time-grain-marker, and the only inter-unit connections are state vector inspections. Each box represents a unit and JSD is applied in a conventional manner to that unit. The limitation of inter-unit communication to state vector inspections is crucial to the exploitation of the decomposition into elements. The absence of data-stream connections means that there are no inter-unit messages and consequently there

is no requirement to design complex process structures to handle the incoming and outgoing messages. Therefore, the complexity of a unit is determined solely by its internal functionality and, moreover, the effects of any redesign has limited impact on the rest of the system. The simplification which results from this is so significant that it justifies additional terminology, and the term *JSD unit* has been adopted.

The problem of the diversity of the system is resolved by transferring the specification to the software context. For those aspects of the system which are not expected to be digital, such as the actuator element, a simulation of that element is specified using the methods described above. Naturally, care has to taken to ensure that all of the relevant functional properties of the real element are included in the simulation specification with due authenticity. The integrity of replacing the real element in a specification by a simulation depends not only on an authentic duplication of its relevant functions, but also on ensuring that the remainder of the system only has access to that data which the real system can provide. In the case of the actuator element, for example, the actuator positions are not directly available to the ADMUs; one of the four simulated position pick-off signals for each control lane which must be used. Another example is the engagement state of the actuator; signals corresponding to appropriate sensors mounted on the actuator must be used to determine whether the actuator is hydraulically energised or not. As a consequence, the actuator entity must be modelled within the ADMU using JSD principles. The need for modelling one element within another is a natural consequence of the imposed decomposition into elements (Ref 16).

When system elements consist of replicated units, for example triplex or dual duplex, it is clearly undesirable to compose a JSD network diagram for each unit individually. At best, it duplicates effort, and at worst introduces errors caused by accidental differences in the individual networks. What is needed is to reflect the written specification and to describe a single unit in detail through a network diagram in the normal manner, supplemented by a formal description of the element in terms of its component units. Such a formal description is shown in Figure 12 (a) and (b) which depict descriptions of units of the Inceptor and Control Law Elements respectively as held on the CASE database. After some standard information (STD-INFO), consisting of its identifier and optional background detail, the MAIN-PART of the description includes a number of options such as:

(i) the type of unit - whether the unit is analogue or digital.

(ii) the number of units - here both are simplex units replicated three times.

(iii) Whether the units run synchronously or not.

To complete the description a list is required of all the JSD processes which belong to that unit, and thus need to be replicated; the final entry (UNIT-SID), being blank, shows that the name of the list on the database defaults to the name of the unit.

A similar format is provided for the description of the connections between elements as shown by the example in Figure 12 (c). The relevant fields are the source, destination and whether the connection is unit to unit individually (ONE-TO-ONE), or completely cross connected (BROADCAST). The connection description also holds some information relating to the fault tolerance implementation.

```
UNIT IE
   STD-INFO
      LONGNAME
      REFERENCE IE
      [*]CLASSIFICATION-SET
      [*]SUMMARY
      This unit is connected to the
      inceptors of the evaluation
      pilot.
      [o]NARRATIVE
         NO
MAIN-PART
   [o]TYPE
      ANALOGUE
   [o]BASE-REDUNDANCY
      SIMPLEX
   REPLICATION 3
   [o]UNIT-LVL-SYNCHRONISATION
      ASYNCHRONOUS
         FRAME-LAG
   [*]INTRA-UNIT-CONNECTIONS
UNIT-SID
```

(a) unit description (analogue)

```
UNIT CLE
   STD-INFO
      LONGNAME
      REFERENCE CLE
      [*]CLASSIFICATION-SET
      [*]SUMMARY
      This unit houses the control
      law algorithm and associated
      processing. It is the middle processor
      in a three processor "lane".
      [o]NARRATIVE
         NO
MAIN-PART
   [o]TYPE
      DIGITAL
   [o]BASE-REDUNDANCY
      SIMPLEX
   REPLICATION 3
   [o]UNIT-LVL-SYNCHRONISATION
      ASYNCHRONOUS
         FRAME-LAG 10
   [*]INTRA-UNIT-CONNECTIONS
   UNIT-SID
```

(b) unit description (digital)

```
CONNECTION IE_CLISE
   STD-INFO
      LONGNAME
      REFERENCE IECLIS
      [*]CLASSIFICATION-SET
      [*]SUMMARY
      [o]NARRATIVE
         NO
   MAIN-PART
      SOURCE IE
      DESTINATION CLISE
      [o]DATA-TRANSMISSION
         BROADCAST
      [o]SPEC-INTERFACE
         NO
      [o]CONSOLIDATION
         YES
            HISTORY_LENGTH 3
      [o]SIBLING_ERROR_MONITORING
         YES
            HISTORY_LENGTH 3
```

(c) connection description

Fig 12 CASE Database Formal Descriptions

Incremental Implementation

The compositional, or "middle out", nature of the JSD method has the property that once a model has been built, every new function added to it provides a, potentially deliverable, working system. In fact, at any stage of the development of the network, it can be implemented. Incremental development takes advantage of this natural property of JSD and phases development of a system over a number of increments. The added functionality required from each increment is defined initially in outline and, as each increment is completed, it is reviewed and the contents of future increments re-examined in the light of any modifications or additions that have been found to be necessary. The development of a system is thus responsive to an evolving specification but at the same time allows the project to be managed on the basis of milestones actually achieved.

The ACT Lynx simulation was developed over six increments distributed as follows:

> Increment 1: A model of the pilot/system interaction including engagement of the ACT system and inceptor movement, the Repeater Panel and a display of the control run position.
>
> Increment 2: A model of the pilot/system interaction as regards System Test, Control Law Selection, Disturbance Selection, Mode Selection, Parameter Set Selection, the Menu Panel, Mode Control Panel and Pilot's Control Panel.
>
> Increment 3: A definition of a hardware description language for units and connections, and development of associated tools. The functionality of Increments 1 and 2 is based on the specified hardware, including fault tolerance. Provision for injection of errors.
>
> Increment 4: Completion of the Control Law Input Support Element, including the development of a tool for building a System Test process from a non-procedural definition. The Aircraft Motion Sensor and the Air Data Elements
>
> Increment 5: Completion of the Control Law Element and the Control Law Ouput Support Element.
>
> Increment 6: Completion of the Actuator Drive and Monitoring Element and the Actuator Element. Further development of the System Test Builder.

The simulation also includes a simple model of a Lynx helicopter to provide sensor data and the actuator displacements.

From the distribution of material in the six increments it can be seen that the primary concern was to establish an acceptable model of the pilot's interface. One of the early lessons was that different readers of a specification can place different meanings on the same words, and, for example, the sequencing of the lamps relating to engagement and system test on the Repeater Panel needed to be revised. The reference to system test in Increment 6 is indicative of the difficulties encountered in specifying a comprehensive test. The contribution from Increment 4 was not sufficient and more work had to be included in the final increment.

During the development of the simulation no fundamental flaw or omission has been discovered in the written specification. Nevertheless, a wealth of additional detail has been accumulated mainly to reinforce inadequate descriptions or to compensate for minor omissions. The most significant inadequacy was the omission of a description about how to apply the consolidation algorithm of Reference 17 to replicated units in a fault tolerant manner (additional voting was included).

Implementation of the Simulation

Ada was selected as the implementation language; its selection was determined by a number of considerations. First, Ada is a US DoD mandated language, and was also "highly recommended" by the UK MOD, which has resulted in a number of very high quality compilers being available. In addition, packages and tasks are language features which have been very important in implementing the system. Finally, the code generation tool Adacode, described below, was already available in prototype form to serve as a basis for the project.

Complexity Overview

The question of complexity has been addressed from several viewpoints. The JSD method incorporates in its modelling phase a powerful technique for grasping the fundamentals of system development and provides a solid platform for subsequent work. On its own, however, it is not sufficient for resolving the complexity of a diverse system which has inbuilt redundancies. It is necessary to introduce additional features, JSD units and connections, to reduce the complexity of whole system to a manageable size. These conceptual advances are of little practical use without associated support from CASE tools. A database must be able to accept and manipulate the unit definitions, and code generation tools must be able to access this information in order to build the final system. The whole JSD-unit based approach gives rise to a management of the complexity of the system to the extent that it may be considered tamed. The verification which is embedded in the various stages of the development of the specification, and its resultant validation through operation of the simulation ensure that any *rogue* aspects of the specification have been eliminated.

At the heart of this complex specification, the detailed requirement for the control law element was left blank; for initial clearance this would be a unity transfer function followed by a digital representation of the Lynx analogue

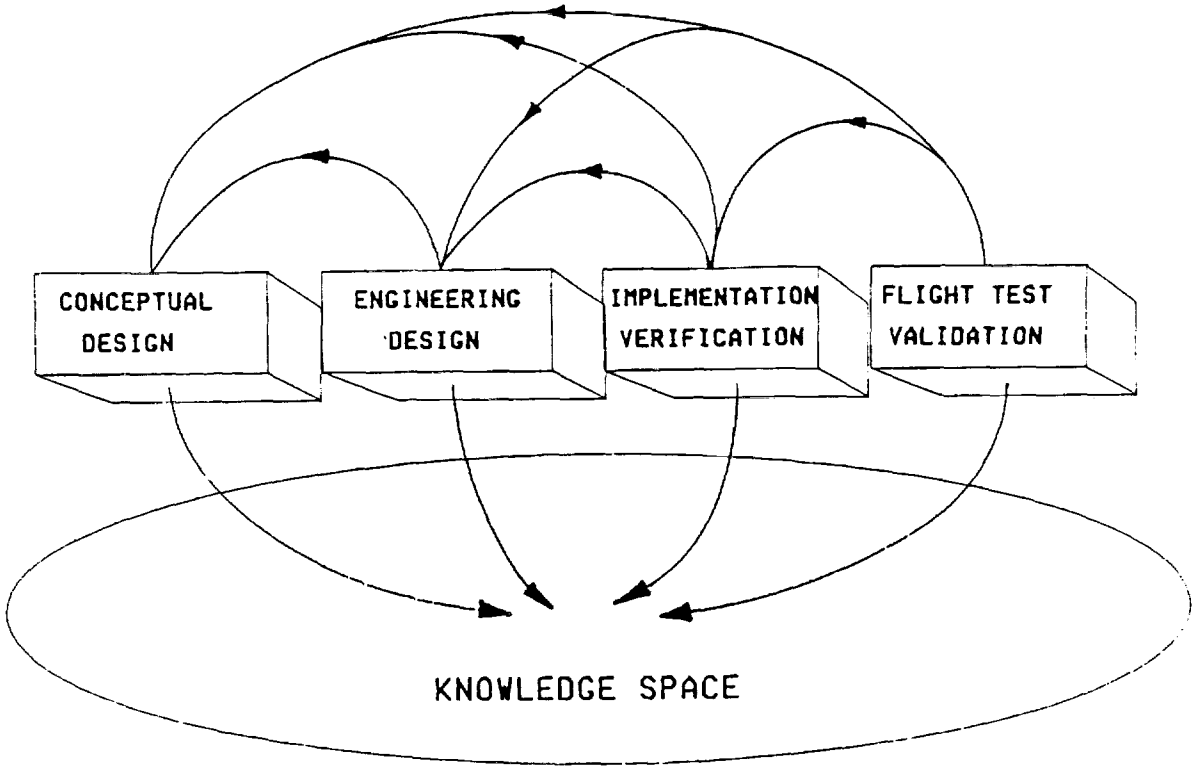

Fig 13 The Four Phases in a Control Law Life Cycle

AFCS. But the experimental control laws were the *raison d'etre* for the ACT Lynx project, and needed a different approach to their development.

Control Law/Concept Evaluation - Envelope Expansion

Recognising that immaturity would be a normal part of the development of ACT Lynx laws, a Control Law Life Cycle Model and associated working practices and procedures were developed at DRA to ensure a disciplined path to full control law validation (Ref 18, 19). The development cycle was formalised to ensure that when control laws were ultimately exercised in safety critical areas, there would be no possibility of them failing. Thus, along with the hardware redundancy, the system would have a truly comprehensive fail-operate capability. The cycle comprises four phases (Fig 13);

i) The Conceptual Phase (CP) evaluates basic concepts in a form that can capture the operational requirements. It includes simple modelling, design and analysis activities and pilot-in-the-loop simulation. Outputs from this phase include knowledge of the response types and system characteristics required to achieve the various Levels of flying quality.

ii) The Engineering Design Phase (EDP) takes results from the CP and involves full control law design with a representative vehicle model and includes refinements to control system architectures via detailed modelling and extensive piloted simulation.

iii) The Flight Clearance Phase (FCP) consolidates results from earlier stages and achieves a verified implementation for the target flight control computer. Validation of the design, including a loads and stability analysis, is a key activity in the Clearance phase. The techniques of 'Inverse Simulation' (Ref 20), with prescribed MTEs, offer a convenient and efficient method for exercising the control law in a wide range range of representative conditions prior to flight.

iv) The Flight Test Phase (FTP) evaluates the control system in full scale flight and appropriate operational MTEs. Experiments in this phase will be 'replicas' of tests conducted in ground-based simulation and changes to control laws would cover only those regimes mapped out in the Conceptual and Engineering Design phases. An incremental approach to safety critical, high risk, flight conditions would be normal practice.

The phases are sequential but also iterative, acknowledging that growth in knowledge can lead to a change in the requirement or criteria format, often the objective of the research itself. At all stages, the discovery of a fault, design error or uncertainty will generally require the return to a previous phase. Special care needs to be taken when 'imposing' a procedural discipline on research, that creativity is not inhibited, but the discipline needs to cut even deeper with well defined working practices and activities, if it is to have any real meaning as a safeguard against errors or faults being designed in. Fig 14, taken from Ref 18, illustrates a process structure diagram for the CP with the three principal tasks - problem expression,

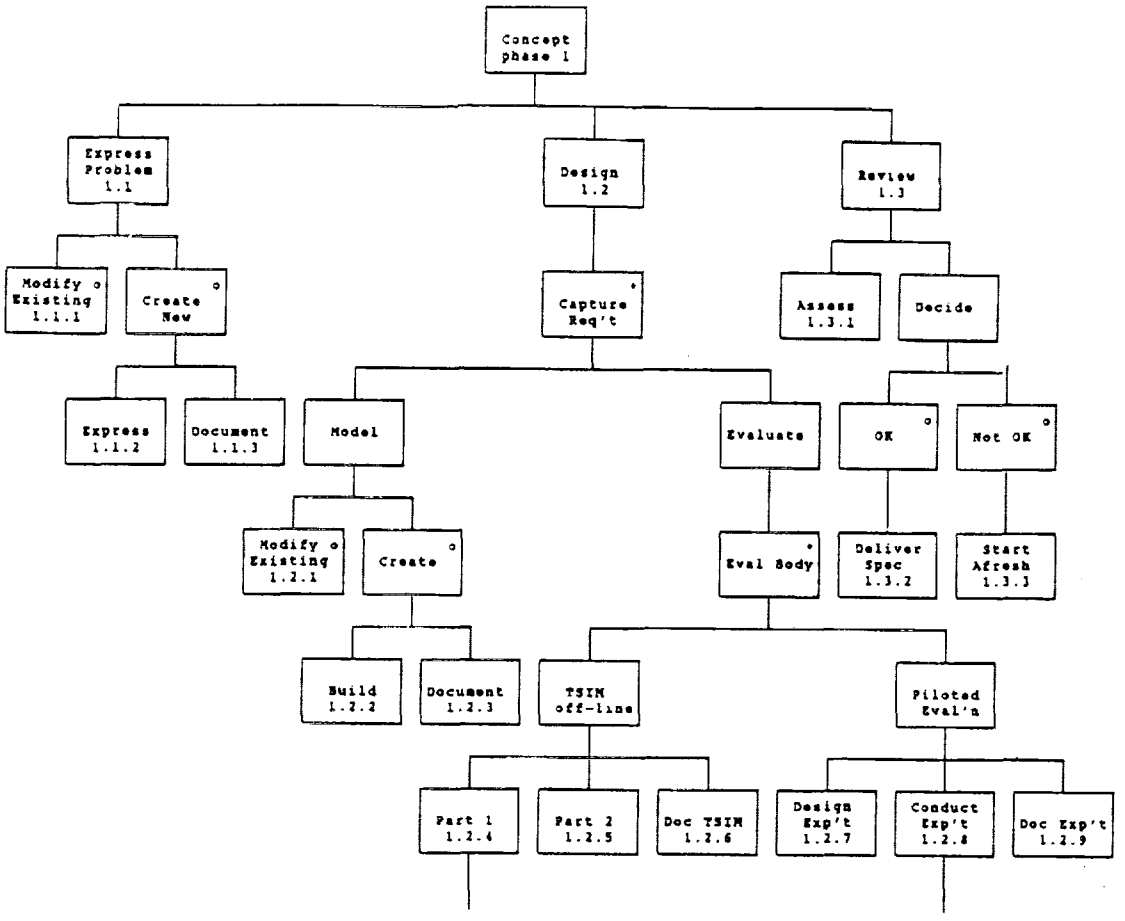

Fig 14 Structure Diagram for the Conceptual Phase

design and review. The JSD notation is again used, ie sequence, iteration (*) and selection (o), with the *activities* corresponding to the lowest level 'leaves' on each branch. Typically, documentation is required as each new piece of knowledge is accumulated and this is reflected in the right hand leaf of the branches.

Conceptual Phase

Examples of research in the Conceptual Phase can be found in References 21, 22 and 23. The archetypal DRA conceptual simulation model (CSM) was developed in Reference 21, which reported comparative results with different response types and autopilot modes. In Reference 22, the first conceptual results from the DRA/Westland research into carefree handling systems were published, indicating the significant benefits of direct intervention control laws. More recently, the first helicopter trials on the DRA Large Motion Simulator reported the achievement of Level 1 handling qualities for rate response types (Ref 23). Fig 15 shows one set of results from Reference 23, with pilot handling qualities ratings plotted against roll attitude bandwidth for a slalom task. The wide spread of ratings with each configuration illustrate the change in perceived handling as performance is increased, the poorest ratings generally corresponding to the highest levels of pilot aggressiveness.

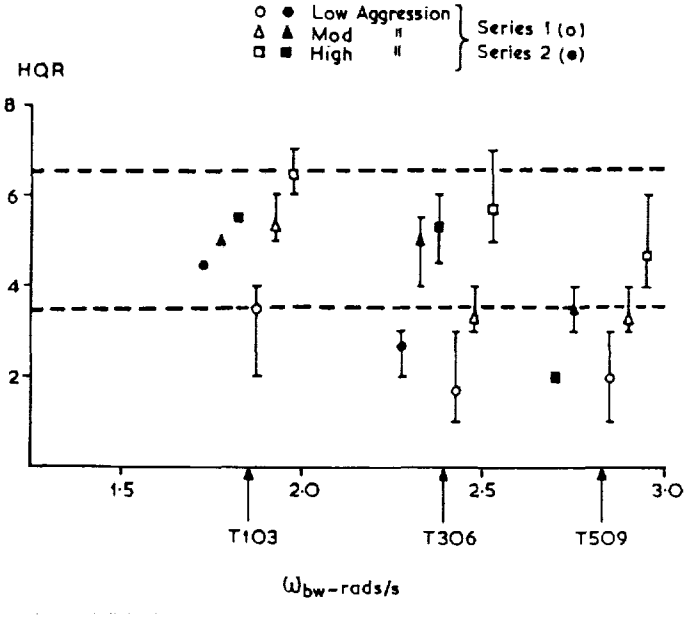

Fig 15 HQRs for Slalom MTE Flown With DRA Conceptual Simulation Model

The ADS33C Level1/2 bandwidth boundary for non-tracking tasks is 2 rad/s, corresponding with the lowest level of aggressiveness flown in the AFS trials. The degradation at higher performance levels is consistent with flight results (Ref 2), but pilots tend to be more senstitive to task cues and critical of simulator deficiencies as aggressiveness increases. Flying at large attitude angles near the ground is particularly demanding on the fidelity of the simulated visual cues; the limited vertical field of view and texture on the current AFS visual system must be a major factor in the inability to achieve Level 1 at high performance. This deficiency, along with modelling uncertainties, common to all ground-based simulators, is, of course, a primary reason for the vigorous pursuit of high performance in-flight simulators.

Engineering Design Phase

This phase consists of mapping the required characteristics from the CP onto the simulated target aircraft. As in the CP, problem expression, design and review cover activities in the Engineering Design phase. However, the level of detail will be considerably greater, including environmental constraints and robustness criteria. Internal control system loop performance requirements and stability of uncontrolled airframe modes will form parts of the problem expression. The design sub-phase contains the modelling and evaluation activities, as in the CP, but also includes significant new activities under the synthesis label (Ref 18). The desired flying qualities requirements, embodied in handling and ride quality functions, will be cast in functional form and the associated 'error' cost functions minimised with respect to control system gains and filter frequencies. This is the essence of the synthesis at the centre of control law design and a number of different techniques are available for working the optimisation, involving craft-like skills and trading performance and robustness to achieve the best controller. Examples of results from the Engineering Design phase are reported in Refs 24, 25 and 26.

Clearance and Flight Test Phases

Activities within this phase have not been well developed at DRA for the helicopter application. The clearance activities will include software verification and a degree of validation using more comprehensive models than in earlier 'real-time' evaluations, with the control law now embedded in the target hardware. Flight tests represent the ultimate research evaluation, although ironically, here there is little scope for design innovation and creativity. Flight test is essentially a knowledge gathering exercise, but there is considerable scope for innovation in experimental design. A procedure sequence in the evaluation of a control law might take the form;

i) engage ACT system when in required flight condition,

ii) build up task complexity and aggressiveness incrementally

iii) curtain function cleared for minimum flight envelope initially (low aggressiveness)

iv) open curtain incrementally as aggressiveness increased

v) test control law at safe altitude initially with representative task gain (eg using helmet display)

vi) test control law at low altitude with representative natural task cues

Throughout this process, regular reviews of the documented results with results from previous phases will be required. A fully developed control law, enabling Level 1 flying qualities at high agility levels, should never experience a software 'failure'. Hardware failures will be protected against to a high reliability through redundancy. Inadvertent excursions beyond flight envelope limits will be protected against with built-in carefree handling functions, working as an integral part of the control law.

Conclusions and Recommendations

With the aim of developing a high performance ACT research helicopter, the DRA has developed the ACT Lynx concept; focus has been on research at high agility levels to explore carefree handling concepts and the expansion of the helicopter's usable flight envelope. The inherent high agility of the Lynx, with its hingeless rotor, makes it an excellent airframe for establishing requirements for future types. This paper has reviewed this project from the standpoint of the conflict between safety and performance; we can see a way through but a number of concurrent safety nets need to be combined.

1) A highly skilled and motivated safety pilot with backdriven conventional controls is the most important safety net; exploratory simulation studies conducted at DRA have focussed on recoveries to common mode hardover failures. The results have highlighted recovery times generally consistent with past flight experience although torque, rotorspeed and 'g' limits can easily be exceeded.

2) System redundancy providing a fail-operate/fail-safe capability provides the strongest and most effective safety net against hardware failures.

3) A comprehensive requirement specification developed through simulation ensures that the integrated system is well understood and all functions and their operations are fully defined; this approach ensures that the 'fixed' software is coherent and fully validated, hence providing the most effective protection against common mode software failures.

4) Control laws developed within the framework of an iterative life-cycle, including ground based simulation, ensures protection against software errors during the early development stages of this critical element of the system. The four phases - conceptual, engineering, clearance and flight - have been briefly described.

5) Curtain functions, limiting the actuator drive signals, can also be used to protect against immaturity in the control laws and can be opened incrementally to allow more agility to be exploited.

6) A committment to carefree handling functions embedded within the control laws is considered to be an essential ingredient to ACT research if full agility is to be realised. Ultimately, together with the safety pilot and FOFS hardware, this should complete the triad of safety nets necessary for the synergy of performance and safety.

At the time of writing, the UK programme is at a hiaitus due to funding limitations. In this paper the authors have attempted to provide a candid exposure of some of the issues sorrounding the safety/performance conflict, to stimulate a continuing debate with collaborative partners pursuing similar goals. It is believed that flight research at high agility levels will only be possible, with acceptable risk, if these issues are squarely faced.

Acknowledgement

The research reported in this paper was conducted as part of the UK MoD's Applied Research Programme - Package 3D (Tri-Service Helicopters).

References

1 Padfield, G.D., Lappos, N., Hodgkinson, J.; "The Impact of Flying Qualities on Helicopter Operational Agility"; AHS/NASA Conference on Flying Qualities and Human Factors of Vertical Flight Aircraft; San Fransisco, Jan 1993

2 Charlton, M. T., Padfield, G. D., Horton, R. I.; "Helicopter Agility in Low Speed Manoeuvres"; Proceedings of the 13th European Rotorcraft Forum, Arles, France, Sept 1987 (also RAE TM FM 22, April 1989)

3 Morgan, M.; "Airborne Simulation at the National Aeronautical Establishment of Canada", AGARD CP 408 'Flight Simulation', 1985

4 Hartman, L.J. et al; "Testing of the Advanced Digital Optical Control System" 43rd AHS Forum, St Louis, May 1987

5 Damotte, S. et al; "Evaluation of Advanced Control Laws with a Sidestick Controller on the Experimental Fly-by-Wire Dauphin Helicopter"; 18th European Rotorcraft Forum, Avignon, France, Sept 1992

6 Bouwer, G. et al; "ATTHeS - A Helicopter In-Flight Simulator with High Bandwidth Capability", 48th AHS Forum, Washington, June 1992

7 Hindson, William S.; "Past Applications and Future Potential of Variable Stability Research Helicopters", Helicopter Handling Qualities, NASA CP 2219, April 1982

8 Gupta, B.P. et al; "Design, Development and Flight Evaluation of an Advanced Digital Flight Control System", 43rd AHS Forum, St Louis, May 1987

9 Kimberley, A.M., Charlton, M.T.; "ACT Lynx Safety Pilot Simulation - Trial Runaway"; RAE Working Paper WP(89) 031, June 1989

10 Padfield, G.D., Bradley, R., Moore, A.; "The Development of a Requirement Specification for an Experimental Active Flight Control System for a Variable Stability Helicopter - an Ada Simulation in JSD"; AGARD CP 503, 'Software for Guidance and Control', Sept 1991

11 Padfield, G.D., Bradley, R.; "Creation of a Living Specification for an Experimental Helicopter Active Control System Through Incremental Simulation"; Proceedings of the 17th European Rotorcraft Forum, Berlin, Sept 1991

12 Jackson, M.; System Development. Prentice Hall, 1983.

13 Cameron, J. R.; JSP & JSD: The Jackson Approach to System Development. IEEE Computer Society Press, 1983.

14 Michael Jackson Systems Ltd., Version 3 of Speedbuilder for IBM PC/Compatibles: Installation Guide, MJSL, 1989.

15 Lawton J R & France N. "The Transformations of JSD Specifications in Ada". Ada User, Jan 1988.

16 Bradley, R., "A Method for Specifying Complex Systems with Application to an Experimental Variable Stability Helicopter", Ph.D. Thesis, Glasgow University, 1992.

17 Silva, A.; "Mode Synchronisation Algorithm for Asynchronous Autopilot", Fourteenth European Rotorcraft Forum, Milan, 1988.

18 Tomlinson, B.N., Padfield, G.D., Smith, P.R.; "Computer Aided Control Law Research - from Concept to Flight Test"; AGARD CP 473 'Computer Aided System Design and Simulation', August 1990

19 Padfield, G.D., Tomlinson, B.N., Smith, P.R.; "Management of Computer Aided Control System Design from Concept to Flight Test"; 'Safecomp'90', Safety of Computer Control Systems, IFAC Symposia Series, 1990, No 17

20 Bradley, R., Thomson, D.; "The Development and Potential of Inverse Simulation for the Quantitative Assessment of Helicopter Handling Qualities", AHS/NASA Conference on Flying Qualities and Human Factors of Vertical Flight Aircraft, San Fransisco, Jan 1993

21 Buckingham, S. L., Padfield, G. D., "Piloted Simulations to Explore Helicopter Advanced Control Systems"; RAE Tech Report 86022, April 1986

22 Massey, C., Wells, P.M.; "Helicopter Carefree Handling Systems"; Proceedings of RAeSoc Conference on Helicopter Handling Qualities and Control, London, Nov 1988

23 Padfield, G.D. et al, "Helicopter Flying Qualities in Critical Mission Task Elements"; 18th European Rotorcraft Forum, Avignon, France, Sept 1992

24 Yue, A., Postlethwaite, I., Padfield, G.D.; "H^{∞} Design and the Improvement of Helicopter Handling Qualities"; Proceedings of the 13th European Rotorcraft Forum, Arles, France, Sept 1987, Also Vertica, Vol 13 No 2, 1989

25 Manness, M.A., Murray-Smith, D.J.; "Aspects of Multi-Variable Flight Control Law Design for Helicopters using Eigenstructure Assignment", J. AHS, Vol 37, No 3, July 1992

26 Walker, D. et al; "Rotorcraft Flying Qualities Improvement Using Advanced Control"; AHS/NASA Conference on Flying Qualities and Human Factors of Vertical Flight Aircraft, San Fransisco, Jan 1993

Session 3

Modeling and Analysis Techniques

COMPATIBILITY OF INFORMATION AND MODE OF CONTROL: THE CASE FOR NATURAL CONTROL SYSTEMS

Dean H. Owen

Department of Psychology
University of Canterbury
Christchurch, New Zealand

The operation of control systems has been determined largely by mechanical constraints. Compatibility with the characteristics of the operator is a secondary consideration, with the result that control may never be optimal, control workload may interfere with performance of secondary tasks, and learning may be more difficult and protracted than necessary. With the introduction of a computer in the control loop, the mode of operation can be adapted to the operator, rather than vice versa. The concept of **natural control** is introduced to describe a system that supports control of the information used by the operator in achieving an intended goal. As an example, control of speed during simulated approach to a pad by helicopter pilots is used to contrast path-speed control with direct control of global optical flow-pattern information. Differences are evidenced in the performance domains of control activity, speed, and global optical flow velocity.

"Smart" mechanisms for perception and control. It might be supposed that other flying animals have "smart" perceptual mechanisms (Runeson, 1977) for acquiring information that maps directly onto an action system specialized for controlling flight. In contrast, human flight must be mediated by a vehicle. Whereas the human's perceptual mechanisms may be sufficiently smart to pick up the relevant information, manipulation of the control surfaces is apt to be quite foreign to an animal whose effectivities (ways of being effective) and prior experiences involve adaptation to terrestrial locomotion. Smart action systems can evolve to support flight control by other flying animals, but for human control of flight they must be developed and tested. The flight environment demands that the principles be the same.

Accordingly, human guidance of flight can be described (a) in terms of the manipulation of controls, control surfaces, and power, (b) control of the path, speed, and orientation of the aircraft, or (c) control of the information which specifies where one is headed, at what speed and orientation, and the consequences of continuing without change. The last description has advantages for the development and evaluation of control systems because it keeps the variables to which the pilot is sensitive and the variables to be controlled in the same currency, i.e., in the domain of visual information. In performing a maneuver, the pilot cycles between sampling the information available and performing control adjustments to reduce deviations from desired optical conditions, repeating the perception-action cycle until satisfactory visual conditions have been achieved. As a consequence, the information

acquired by perceiving and the information controlled by acting must be the same. The compatibility between control adjustments and visual guidance of flight could be maximized by giving the pilot direct control of the informative variables.

The nature of information to be controlled. A canonical assumption of the direct theory of visual perception (Gibson, 1979) is that detection and control of any property of self motion must be supported by information. This holds for selecting and modulating a control action, timing the initiation and termination of the action, and observing the consequences of the action. In the case of visual guidance, the information is assumed to be one or more invariants in the surrounding, transforming optic array along the path of motion. Applications have been extended to rotocraft flight (Owen, 1991), simulation research (Owen & Johnson, 1992; Warren & Owen, 1982), and transfer of training (Lintern (1991).

The research approach first isolates variables in the optic array between the eye and environmental surfaces mathematically and operationally (through manipulation of scene-content and flight parameters). Second, experiments are conducted to determine which of the potential sources of visual information are functional, i.e., useful for detecting changes in speed and direction and for selecting and guiding a control action. To date, functional variables have been exclusively fractional rates of change characterized by higher-order ratios of such lower-order variables as speed, acceleration, altitude, climb or sink rate, and ground-texture-element size and spacing. The **eyeheight** of the observer above the ground is an optically privileged scaler for size, distance, and speed, and therefore fundamental to the perception and control of visual information. See Owen & Warren (1987) and Owen (1990) for summaries of the experiments.

Control of optical variables. If the criterion for skillful behavior is taken to be effective **control** of the informative structure of stimulation, then its study requires an **active** psychophysics that treats transformations and invariants in the ambient array as **dependent** variables (Owen & Warren, 1982; Warren & McMillan, 1984; Flach, 1990). Controlling self motion involves maintaining intended conditions of speed and direction of flight, as well as self orientation, relative to environmental surfaces. In the process, variables are linked and unlinked as speed, direction, and orientation change. With knowledge of the relevance of the different kinds of information to different kinds of flight tasks, the variables and their linkages can be controlled to achieve intended goals. The same ambient array properties which were independent variables in passive judgment experiments can be recorded as dependent variables in the study of active control.

Direct or natural control. Using the cyclic and collective, helicopter pilots currently make an average of 50 control adjustments per minute during an approach to hover above a place on the ground. Pilots are instructed to keep "visual streaming" constant at the rate of a brisk walk during an approach to hover. Control systems for helicopters and other

aircraft have been designed primarily around mechanical constraints, including those of cables, levers, and hydraulic systems. The development of electronic and optical systems communicating between controls and control subsystems, including power, allows for the implementation of "smart" control systems designed to provide a match between the sensitivity of the human perceptual system and the effectivities of the human-vehicle action system. Thus, a computer in the control loop can allow a hybrid between manual and supervisory control: The pilot maintains higher-order control (e.g., over path slope), while the computer manages the lower-order control tasks (power, rotor variables).

The logic is similar to that employed by Roscoe and Bergman (1980) in developing a control system that reduced higher-order control loops for bank angle and vertical velocity to first-order control of heading and vertical position (altitude). Compared to normal flight control, their system reduced pilot errors by a factor of ten. Ratio control differs in providing direct control of the higher-order variables to which the pilot is sensitive. (A simple example is the Vernier log scale for acoustic volume control.) The computer can take inputs from the controls and sensors (e.g., radar altimeter, forward-looking radar, a signal transmitted from the ground or a ship) and make adjustments in speed and direction to match the informational properties of the event that the pilot intended to produce. For approach to the ground or to surfaces with vertical extent, a fractional rate controller can reduce speed in the same proportion as distance to the surface is decreased. The pilot selects a fractional rate which matches the task demands, e.g., a high rate when time is critical, a low rate when accuracy is important. A second mode of control is appropriate for path angle. Whereas magnitude controllers vary the numerator or denominator of the ratio of vertical speed to ground speed, a path-slope controller varies the ratio directly. Since path slope equals the "dip" angle of the point of optical expansion below the horizon, the path-slope controller gives the pilot control over what he intends to achieve visually. Similar ratio modes could be developed for rotational control.

Advantages of natural control. A control system designed around perception-action compatibility should reduce flight-control demands, freeing the pilot's attention for other workload. Maneuvers under difficult conditions should be simplified. Given that control is scaled in units of distance to the ground, fractional-rate control is particularly appropriate to approach, hover, and low-level contour and terrain following. Modes of control compatible with information acquisition should greatly simplify training and increase safety at low altitudes in cluttered environments and under difficult conditions, e.g., high work load or stress. Although experienced helicopter pilots have shown no sign of negative transfer when using ratio controllers, having a computer in the control loop means that traditional modes of control could be programmed and selected, if desired, by a pilot more comfortable with those modes.

A design criterion for some new aircraft is that "trainability" be taken into account during development of

the aircraft itself. Ratio controllers are relevant to this criterion, since training should be considerably simplified with a high compatibility system having independent modes of control, as compared to the current system involving complicated and sometimes arbitrary relationships between control adjustments and visual stimulation as well as interdependent relationships between the controls themselves. Lintern (1991) has discussed the role of optical information in manual control and transfer of training.

Kurlik (1991) proposed that experts make a task easier because they constrain the task in ways that make the variables controlled much simpler to skillfully control. One reason that the novice may have difficulty learning what to attend to and control is that information **emerges** during an event. The information which the skilled pilot uses to select, initiate, and terminate control actions may not come into existence until the environment is **skillfully** controlled (Kurlik, 1991). Ratio controllers should give novices an advantage in that they automatically isolate task-relevant optical variables that are transforming in a specificity relationship with the flight event. In this way, they embed a dimension of skillful performance in the control system itself. Automatic braking systems on automobiles perform a similar function by pulsing the brakes in an optimal fashion to achieve deceleration while avoiding locking up the wheels. Braking performance of a novice driver using the automatic pulsing system should be better than without it, even though the driver is unaware of the mode of operation. Just as information is ordinarily transparent to the perceiver of an event, the means by which control of an event is achieved via the direct control of information can be transparent to the controller of the event. The test is whether direct control of the variable an operator is sensitive to results in better performance than control of a task-relevant property of the self-motion event itself.

Experimental tests. Two experiments will be used to illustrate direct control of optical flow-pattern information. Experienced pilots with an average of 1,500 hours helicopter flight time participated. In the first experiment, each pilot controlled speed for 25 seconds during 136 simulated approaches to a pad along a linear flight path. In one session the pilot controlled path speed, and in the other he controlled global optical flow velocity (path speed/ eyeheight). The approaches were made in 68 different environments designed to determine the relative influences of flow velocity and edge rate on speed control. In the second experiment, each pilot controlled vertical speed on a vertical path to maintain hover at 10 meters for 30 seconds, then descended to the ground while attempting to minimize vertical speed at touchdown. A total of 54 events were produced by combinations of disturbances in the three translational axes crossed with environments that isolated three types of information for change in altitude: change in the horizon ratio of a vertical surface, change in perspective angle of runway edges perpendicular to the horizon, and optical expansion and contraction of fields running parallel to the horizon. In one session, the pilot controlled path speed (sink and climb rate) and in the other he controlled global

optical flow velocity (vertical speed/eyeheight, or fractional change in altitude). Comparisons of the two control modes were made in three performance domains: control activity, speed, and global optical flow velocity.

Acknowledgements. The preparation of this paper and the research exploring the approach described were supported by the National Aeronautics and Space Administration Grant No. NAGW-2170. The author has benefitted from encouragement by and interaction with the scientific monitor for the grant, Walter W. Johnson, NASA Ames Research Center.

REFERENCES

Flach, J. M. (1990). Control with an eye for perception: Precursors to an active psychophysics. Ecological Psychology, 2, 83-111

Gibson, J. J. (1979). The ecological approach to visual perception. Boston: Houghton Mifflin.

Kurlik, A. (1991). Why does the skilled actor make it look easy? Because it is! Proceedings of the Sixth International Conference on Event Perception and Action (p. 61). Amsterdam, The Netherlands.

Lintern, G. (1991). An informational perspective on skill transfer in human-machine systems. Human Factors, 33, 251-266.

Owen, D. H. (1990). Perception and control of changes in self motion: A functional approach to the study of information and skill. In R. Warren & A. H. Wertheim (Eds.), Perception & control of self-motion (pp. 289-326). Hillsdale, NJ: Erlbaum.

Owen, D. H. (1991). Perception and control of rotocraft flight. In W. W. Johnson & M. K. Kaiser (Eds.), Visually Guided Control of Movement (NASA Conference Publication 3118) (pp. 87-97). NASA Ames Research Center, Moffett Field, California.

Owen, D. H., & Johnson, W. W. (1992). An information-based approach to simulation research. In Feik, R. A. (Ed.), Proceedings of the Future Directions in Simulation Workshop. Melbourne, Australia: Defence Science and Technology Organisation, Aeronautical Research Laboratory, Aircraft Systems Division.

Owen, D. H., & Warren, R. (1982). Optical variables as measures of performance during simulated flight. Proceedings of the Human Factors Society - 26th Annual Meeting, 1, 312-315.

Owen, D. H., & Warren, R. (1987). Perception and control of self motion: Implications for visual simulation of vehicular control. In L. S. Mark, J. S. Warm, & R. L. Huston (Eds.), Ergonomics and human factors: Recent research and advances (pp. 40-70). New York:Springer-Verlag.

Runeson, S. (1977). On the possibility of "smart" perceptual mechanisms. Scandanavian Journal of Psychology, 18, 172-179.

Warren, R., & Owen, D. H. (1982). Functional optical invariants: A new methodology for aviation research. Journal of Aviation, Space, and Environmental Medicine , 53, 977-983.

A Model for Rotorcraft Flying Qualities Studies *

Manoj Mittal
Post–Doctoral Fellow
School of Aerospace Engineering

Mark F. Costello
Research Engineer
Aerospace Laboratory, GTRI

Georgia Institute of Technology
Atlanta, Georgia

Abstract

This paper outlines the development of a mathematical model that is expected to be useful for rotorcraft flying qualities research. A computer model is presented that can be applied to a range of different rotorcraft configurations. The algorithm computes vehicle trim and a linear state-space model of the aircraft. The trim algorithm uses non linear optimization theory to solve the non linear algebraic trim equations. The linear aircraft equations consist of an airframe model and a flight control system dynamic model. The airframe model includes coupled rotor and fuselage rigid body dynamics and aerodynamics. The aerodynamic model for the rotors utilizes blade element theory and a three state dynamic inflow model. Aerodynamics of the fuselage and fuselage empennages are included. The linear state-space description for the flight control system is developed using standard block diagram data.

Introduction

In the past, rotorcraft flight control system preliminary design used mathematical models which assumed the fuselage to possess six degrees of freedom. The rotor dynamics were assumed to be substantially faster than the fuselage dynamics and were subsequently approximated as quasi-static. The process of fine tuning the flight control system was accomplished through an extensive flight test program comprised of a matrix of control system parameter variations. While fine tuning of the flight control system is still accomplished through flight testing the vehicle, significant improvements in the optimization process have been realized when high order dynamic rotorcraft models are utilized during the preliminary flight control system design stage.

Rotorcraft are now being designed with sophisticated electronic flight control systems. These complex control systems are utilized not only to satisfy standard flying qualities specifications but also to meet aerodynamic performance, vibration, and structural loads criteria. The design of modern rotorcraft flight control systems now stretches across many different individual disciplines and is indeed interdisciplinary. The general trend toward increased reliance on the flight control system for improving overall system performance has lead designers to consider higher bandwidth systems which rely on high levels of sensor feedback to yield desired aircraft stability. The main drawback of this approach is that increased levels of feedback, which in general improve the low frequency fuselage dynamic behavior, can destabilize higher frequency rotor blade motion. In order to make meaningful estimates of the impact of a particular flight control configuration on system requirements it has been found that a mathematical model which includes fuselage and rotor rigid body dynamics and rotor dynamic inflow is necessary [1].

The business of rotorcraft modeling for flight control system design and analysis support has been an active research area for many years. Deriving the equations of motion of a fully coupled fuselage and rotor system for a reasonably general configuration quickly becomes unwieldy due to complicated geometry including many matrix transformations and intricate logic branching. These complexities have lead engineers to develop digital computer programs which more or less relegate model computation to the computer and free the engineer to focus on analysis results.

Talbot, Tinling, Decker, and Chen [2] formulated a helicopter flying qualities model that includes fuselage dynamics and a three degree of freedom tip-path-plane representation for the main rotor flapping dynamics. Some simplifications are made in the analysis in order to formulate compact, analytical force

*Presented at Piloting Vertical Flight Aircraft: A Conference on Flying Qualities and Human Factors, San Francisco, California, January 1993.

and moment expressions for the rotor forces and moments. Gibbons and Done [3] derived a numerical method to automatically generate rotorcraft equations of motion. The method uses Lagrange's equations and relies on expressing inertial position vectors of the rotor blades as a matrix multiplied by the position vector in blade coordinates plus a term that is a function of the modal coordinates, time, and spanwise position. The required differentiations of the position vector to form the equations of motion are performed numerically. Miller and White [1] used concepts from Lytwyn [4] and Gibbons and Done [3] to automate generation of the equations of motion for rotorcraft handling qualities analysis. Miller and White [1] expressed all transformation matrices in complex variable form and were able to develop a compact algorithm to analytically obtain long strings of orthogonal transformation matrices along with all necessary derivatives to form nonlinear and linearized dynamic equations. Lagrange's equations were used in the formulation. Zhao and Curtiss [5] derived a set of linearized equations by analytic linearization of a nonlinear model formulated using Lagrange's equations. The symbolic manipulation computer program MACSYMA was used in forming the equations. Subsequent work by McKillip and Curtiss [6] has improved and extended the work by Zhao and Curtiss [5].

The work discussed in this paper derives a rotorcraft flying qualities model which has been implemented into a FORTRAN computer program. A fairly generic rotorcraft configuration, consisting of a rigid fuselage, two rotors, and an arbitrary number of fuselage fixed external surfaces has been assumed, as shown in Figure 1. It is important to note that the type of analysis carried out in this work can accommodate any arbitrary number of rotors in the configuration. The number of rotors has been chosen to be two since the majority of rotorcraft fall under this category. The fuselage possesses six degrees of freedom and the rotor blades have flap, lag, and pitch degrees of freedom. The rotor aerodynamic models are based on blade element theory and include three degree of freedom dynamic inflow. The equations of motion are formulated using Kane's equations [7]. More importantly, derivatives of transformation matrices are formed using angular velocity expressions as opposed to numerical or direct differentiation. The rotor dynamic inflow equations are based on the Pitt and Peters model [8] and include hub motion perturbations. The residual of the equations of motion and the residual gradient expressions are derived analytically and trim is calculated using the residual and residual gradients in concert with a modified Newton's method. The rotor trim variables are the rotor multiblade coordinates. A linear constant coefficient model of the composite airframe is formulated using a multiblade coordinate transformation with a subsequent constant coefficient approximation. The linear constant coefficient airframe model is coupled to the linear control system dynamic model to form the overall linear model. Linear analysis tools such as eigen values, eigen vectors, transfer functions, frequency response, and linear simulation are directly contained within the computer program.

Airframe Dynamic Model

As pictured in Figure 1, the airframe dynamic model consists of a rigid fuselage with the standard six degrees of freedom and two fully articulated rotor systems, each with dynamic inflow. The fuselage aerodynamic force and moment components are obtained in the wind axis from a two dimensional data table as functions of fuselage angle of attack and sideslip. The aerodynamic forces exerted on the external surfaces are obtained using standard lifting line theory. The rotor geometry details are shown in Figure 2. Provisions are made in the model to accommodate any of the six possible sequences of flap, lag, and pitch hinges for the rotor blades. Each hinge is accompanied by a linear torsional spring and damper. Each blade also has a non linear translational damper which is attached to the rotor blade from the rotor hub. Hingeless rotor systems can be approximately modeled using a virtual hinge representation. The aerodynamic forces exerted on the rotor blades are calculated using blade element theory. The blades on a rotor have identical yet arbitrary geometric and inertial properties.

The airframe nonlinear dynamic model is obtained using the flat and non-rotating earth assumption. Kane's Equations are then written for each degree of freedom by taking into account the contributions of the generalized inertia forces, the generalized gravity forces, the generalized aerodynamic forces, and the generalized spring-damper forces.

$$f_r(t) = f_{I_r}(t) + f_{G_r}(t) + f_{A_r}(t) + f_{SD_r}(t),$$

$$r = 1, \ldots, n_{RB} \qquad (1)$$

In equation 1, t denotes time and n_{RB} is the number of generalized speeds. The origin of each term on the right hand side of Equation 1 is discussed below.

The following nomenclature is introduced for deriving the generalized inertia forces. Let n_{R1} and n_{R2} denote the number of blades on rotor 1 and rotor

2, respectively. Let m_F and I_F, $m_{R1,i}$ and $I_{R1,i}$ ($i = 1,\ldots,n_{R1}$), and $m_{R2,j}$ and $I_{R2,j}$ ($j = 1,\ldots,n_{R2}$), respectively, denote the masses and inertia matrices for the fuselage, rotor 1 blades, and rotor 2 blades. Let ω_F, $\omega_{R1,i}$ ($i = 1,\ldots,n_{R1}$), and $\omega_{R2,j}$ ($j = 1,\ldots,n_{R2}$) represent the individual body axis components of the angular velocities of the fuselage, rotor 1 blades, and rotor 2 blades, respectively. Let v_{F^*} and a_{F^*}, v_{R1,i^*} and a_{R1,i^*} ($i = 1,\ldots,n_{R1}$), and v_{R2,j^*} and a_{R2,j^*} ($j = 1,\ldots,n_{R2}$) represent the inertial axis components of the c.g. (center of gravity) velocities and accelerations of the fuselage, rotor 1 blades, and rotor 2 blades, respectively. Then the generalized inertia forces acting on the configuration can be written as,

$$
\begin{aligned}
f_{I_r}(t) \;=\;& m_F \left(\frac{\partial v_{F^*}}{\partial u_r}\right)^T a_{F^*} + \\
& \sum_{i=1}^{n_{R1}} m_{R1,i} \left(\frac{\partial v_{R1,i^*}}{\partial u_r}\right)^T a_{R1,i^*} + \\
& \sum_{i=1}^{n_{R2}} m_{R2,i} \left(\frac{\partial v_{R2,i^*}}{\partial u_r}\right)^T a_{R2,i^*} + \\
& \left(\frac{\partial \omega_F}{\partial u_r}\right)^T \{I_F \dot{\omega}_F + S(\omega_F) I_F \omega_F\} + \\
& \sum_{i=1}^{n_{R1}} \left(\frac{\partial \omega_{R1,i}}{\partial u_r}\right)^T \{I_{R1,i} \dot{\omega}_{R1,i} + S(\omega_{R1,i}) I_{R1,i} \omega_{R1,i}\} + \\
& \sum_{i=1}^{n_{R2}} \left(\frac{\partial \omega_{R2,i}}{\partial u_r}\right)^T \{I_{R2,i} \dot{\omega}_{R2,i} + S(\omega_{R2,i}) I_{R2,i} \omega_{R2,i}\}, \\
& r = 1,\ldots,n_{RB} \qquad (2)
\end{aligned}
$$

where an overdot denotes differentiation with respect to time and $S(\cdot)$ is the standard cross product skew-symmetric matrix operator (Appendix). u is the vector of generalized speeds. Letting g be the acceleration due to gravity, the generalized gravity forces can be written as,

$$
\begin{aligned}
f_{G_r}(t) \;=\;& -m_F g \frac{\partial (v_{F^*})_3}{\partial u_r} \\
& - \sum_{i=1}^{n_{R1}} m_{R1,i} g \frac{\partial (v_{R1,i^*})_3}{\partial u_r} \\
& - \sum_{i=1}^{n_{R2}} m_{R2,i} g \frac{\partial (v_{R2,i^*})_3}{\partial u_r}, \\
& r = 1,\ldots,n_{RB} \qquad (3)
\end{aligned}
$$

The generalized aerodynamic forces are discussed next. Let v_F, and F_F and M_F be respectively the body axis components of the velocity and the aerodynamic force and moment acting on the fuselage aerodynamic center. Let b_{R1}, b_{R2}, and b_{S_i} ($i = 1,\ldots,n_S$) denote the number of elements or sections on any rotor 1 blade, any rotor 2 blade, and the ith external surface. Let $v_{R1,i,j}$ and $F_{R1,i,j}$ ($i = 1,\ldots,n_{R1}, j = 1,\ldots,b_{R1}$), and $v_{R2,k,l}$ and $F_{R2,k,l}$ ($k = 1,\ldots,n_{R2}, l = 1,\ldots,b_{R2}$) be the individual body axis components of the section velocity and the aerodynamic force acting on rotor 1 blades and rotor 2 blades, respectively. Let $v_{S_i,j}$ and $F_{S_i,j}$ ($i = 1,\ldots,n_S, j = 1,\ldots,b_{S_i}$) be the respective body axis components of the section velocity and the aerodynamic force acting on the external surfaces. The generalized aerodynamic forces acting on the configuration can then be written as,

$$
\begin{aligned}
f_{A_r}(t) \;=\;& -\left\{\left(\frac{\partial v_F}{\partial u_r}\right)^T F_F + \left(\frac{\partial \omega_F}{\partial u_r}\right)^T M_F\right\} \\
& - \sum_{i=1}^{n_{R1}} \sum_{j=1}^{b_{R1}} \left(\frac{\partial v_{R1,i,j}}{\partial u_r}\right)^T F_{R1,i,j} \\
& - \sum_{i=1}^{n_{R2}} \sum_{j=1}^{b_{R2}} \left(\frac{\partial v_{R2,i,j}}{\partial u_r}\right)^T F_{R2,i,j} \\
& - \sum_{i=1}^{n_S} \sum_{j=1}^{b_{S_i}} \left(\frac{\partial v_{S_i,j}}{\partial u_r}\right)^T F_{S_i,j}, \\
& r = 1,\ldots,n_{RB} \qquad (4)
\end{aligned}
$$

The generalized spring-damper forces are discussed next. Figure 2 shows the typical spring-damper attachment geometry for a typical blade. Let $v^D_{R1,i,j}$ and $F^D_{R1,i,j}$ ($i = 1,\ldots,n_{R1}, j = 1,2$), and $v^D_{R2,k,l}$ and $F^D_{R2,k,l}$ ($k = 1,\ldots,n_{R2}, l = 1,2$) be the individual rotor hub axis components of the velocities and the forces acting on the translational damper attachment points for rotor 1 blades and rotor 2 blades, respectively. Let $\omega^D_{R1,i,j}$ and $M^D_{R1,i,j}$ ($i = 1,\ldots,n_{R1}, j = 1,\ldots,4$), and $\omega^D_{R2,k,l}$ and $M^D_{R2,k,l}$ ($k = 1,\ldots,n_{R2}, l = 1,\ldots,4$) denote the individual body axis components of the angular velocities and the torsional spring-damper moments acting on the hub, link 1, link 2, and the blade for rotor 1 blades and rotor 2 blades, respectively. Then the generalized spring-damper forces can be expressed as,

$$
\begin{aligned}
f_{SD_r}(t) \;=\;& -\sum_{i=1}^{n_{R1}} \sum_{j=1}^{2} \left(\frac{\partial v^D_{R1,i,j}}{\partial u_r}\right)^T F^D_{R1,i,j} \\
& - \sum_{i=1}^{n_{R2}} \sum_{j=1}^{2} \left(\frac{\partial v^D_{R2,i,j}}{\partial u_r}\right)^T F^D_{R2,i,j}
\end{aligned}
$$

$$-\sum_{i=1}^{n_{R1}}\sum_{j=1}^{4}\left(\frac{\partial\omega^D_{R1,i,j}}{\partial u_r}\right)^T M^D_{R1,i,j}$$
$$-\sum_{i=1}^{n_{R2}}\sum_{j=1}^{4}\left(\frac{\partial\omega^D_{R2,i,j}}{\partial u_r}\right)^T M^D_{R2,i,j},$$
$$r = 1,\ldots,n_{RB} \quad (5)$$

The partial derivatives $\frac{\partial v}{\partial u_r}$ and $\frac{\partial \omega}{\partial u_r}$ in Equations 2 through 5 are known as partial velocities and partial angular velocities, respectively. The generalized coordinate vector q and the generalized speed vector u are defined as follows:

$$q = \{(q_F)^T,(q_{R1,1})^T,(q_{R1,2})^T,\ldots,(q_{R1,n_{R1}})^T, (q_{R2,1})^T,(q_{R2,2})^T,\ldots,(q_{R2,n_{R2}})^T\}^T \quad (6)$$

$$u = \{(u_F)^T,(u_{R1,1})^T,(u_{R1,2})^T,\ldots,(u_{R1,n_{R1}})^T, (u_{R2,1})^T,(u_{R2,2})^T,\ldots,(u_{R2,n_{R2}})^T\}^T \quad (7)$$

The subscripts F, $R1$, and $R2$ refer to fuselage, rotor 1, and rotor 2 variables, respectively. Further,

$$q_F = \{x,y,z,\phi,\theta,\psi\}^T \quad (8)$$

$$q_{R1,i} = \{\alpha^{(1)}_{R1,i},\alpha^{(2)}_{R1,i},\alpha^{(3)}_{R1,i}\}^T, \quad i = 1,\ldots,n_{R1} \quad (9)$$

$$q_{R2,i} = \{\alpha^{(1)}_{R2,i},\alpha^{(2)}_{21,i},\alpha^{(3)}_{R2,i}\}^T, \quad i = 1,\ldots,n_{R2} \quad (10)$$

$$u_F = \{u,v,w,p,q,r\}^T \quad (11)$$

$$u_{R1,i} = \{\dot\alpha^{(1)}_{R1,i},\dot\alpha^{(2)}_{R1,i},\dot\alpha^{(3)}_{R1,i}\}^T, \quad i = 1,\ldots,n_{R1} \quad (12)$$

$$u_{R2,i} = \{\dot\alpha^{(1)}_{R2,i},\dot\alpha^{(2)}_{R2,i},\dot\alpha^{(3)}_{R2,i}\}^T, \quad i = 1,\ldots,n_{R2} \quad (13)$$

The quantities $\alpha^{(1)}$, $\alpha^{(2)}$, and $\alpha^{(3)}$ are one of lag, flap, and pitch angles, depending on the rotor blade hinge sequence.

A brief description of the analysis involved in calculating the terms on the right hand sides of Equations 2 through 5 is given in the following. For simplicity, the analysis for the rotor terms will be restricted to rotor 1; the analysis for rotor 2 terms is analogous.

Generalized Inertia Forces

The six terms comprising the generalized inertia forces, Equation 2, are discussed here. The orientation of the fuselage with respect to inertial axes and the orientation of the rotors with respect to the fuselage can be described using transformation matrices. Each transformation matrix is composed of one, two, or three single axis transformation matrices. Referring to Figure 2, let T_F be the matrix of transformations from the fuselage axes to inertial axes. The following five matrices are defined for rotor 1. T_{S1} is the matrix of transformations from shaft axes to fuselage axes, $T_{H1,i}$ $(i = 1,\ldots,n_{R1})$ is the matrix of transformations from rotating hub axes to shaft axes, $T^{(1)}_{R1,i}$ $(i = 1,\ldots,n_{R1})$ is the matrix of transformations from link 1 axes to rotating hub axes, $T^{(2)}_{R1,i}$ $(i = 1,\ldots,n_{R1})$ is the matrix of transformations from link 2 axes to link 1 axes, and $T^{(3)}_{R1,i}$ $(i = 1,\ldots,n_{R1})$ is the matrix of transformations from blade axes to link 2 axes. The transformation matrices are expressed as follows:

$$T_F = [E_1(\phi)E_2(\theta)E_3(\psi)]^T \quad (14)$$

$$T_{S1} = [T_{S1,b}(\Gamma_{S1,b})T_{S1,a}(\Gamma_{S1,a})]^T \quad (15)$$

$$T_{H1,i} = [E_3(\pi - \psi_{R1,i})]^T \quad (16)$$

$$T^{(1)}_{R1,i} = T^{(1)}_{R1,i}(\alpha^{(1)}_{R1,i}) \quad (17)$$

$$T^{(2)}_{R1,i} = T^{(2)}_{R1,i}(\alpha^{(2)}_{R1,i}) \quad (18)$$

$$T^{(3)}_{R1,i} = T^{(3)}_{R1,i}(\alpha^{(3)}_{R1,i}) \quad (19)$$

In Equation 16, $\psi_{R1,i} = \Omega_{R1}t + \frac{2\pi}{n_{R1}}(i-1)$, where Ω_{R1} is the rotor 1 hub rotational speed. It is assumed that the shaft is inclined with respect to the fuselage by first a rotation with the angle $\Gamma_{S1,a}$ and then a rotation with the angle $\Gamma_{S1,b}$. Depending on the sequence of rotation, $T_{S1,a}$ and $T_{S1,b}$ are one each among E_1 and E_2. E_1, E_2, and E_3 are single axis transformation matrices about x, y, and z axes, respectively (Appendix). Clearly, $T^{(1)}$, $T^{(2)}$, and $T^{(3)}$ are one each among E_1, E_2, and E_3, depending on the rotor blade hinge sequence.

The body axis components of the angular velocity of the fuselage, ω_F, can be written as,

$$\omega_F = \{p,q,r\}^T \quad (20)$$

Using the transformation matrices defined above, the body axis components of the angular velocity of the ith rotor 1 blade can be written as,

$$\omega_{R1,i} = \left[T_{S1}T_{H1,i}T^{(1)}_{R1,i}T^{(2)}_{R1,i}T^{(3)}_{R1,i}\right]^T\omega_F + \left[T^{(1)}_{R1,i}T^{(2)}_{R1,i}T^{(3)}_{R1,i}\right]^T\{0,0,-\Omega_{R1}\}^T + \left[T^{(2)}_{R1,i}T^{(3)}_{R1,i}\right]^T b^{(1)}_{R1}\dot\alpha^{(1)}_{R1,i} + \left[T^{(3)}_{R1,i}\right]^T b^{(2)}_{R1}\dot\alpha^{(2)}_{R1,i} + b^{(3)}_{R1}\dot\alpha^{(3)}_{R1,i} \quad (21)$$

The unit vectors $b^{(1)}_{R1}$, $b^{(2)}_{R1}$, and $b^{(3)}_{R1}$ have been introduced to allow a general rotor blade hinge sequence. For example, if rotor 1 blades undergo a lag, flap, and pitch rotation sequence, then $b^{(1)}_{R1} = \{0,0,1\}^T$, $b^{(2)}_{R1} = \{0,1,0\}^T$, and $b^{(3)}_{R1} = \{1,0,0\}^T$. Equation 21

has been obtained using the concept of simple angular velocities [7].

The body axis components of the fuselage c.g. velocity are given as,

$$v_B = \{u, v, w\}^T \tag{22}$$

The inertial axis components of the fuselage and blade c.g. velocities can be written as,

$$v_{F^\bullet} = T_F v_B \tag{23}$$

$$\begin{aligned} v_{R1,i^\bullet} = {} & v_{F^\bullet} + \\ & T_F S(\omega_F)\bar{r}_{F1} + \\ & T_F T_{S1} S(\omega_{S1})\bar{r}_{H1} + \\ & T_F T_{S1} T_{H1,i} S(\omega_{H1,i})\bar{r}^{(1)}_{R1} + \\ & T_F T_{S1} T_{H1,i} T^{(1)}_{R1,i} S(\omega^{(1)}_{R1,i})\bar{r}^{(2)}_{R1} + \\ & T_F T_{S1} T_{H1,i} T^{(1)}_{R1,i} T^{(2)}_{R1,i} S(\omega^{(2)}_{R1,i})\bar{r}^{(3)}_{R1} + \\ & T_F T_{S1} T_{H1,i} T^{(1)}_{R1,i} T^{(2)}_{R1,i} T^{(3)}_{R1,i} S(\omega_{R1,i})\bar{r}^{*}_{R1} \end{aligned} \tag{24}$$

In Equation 24, ω_{S1} represents the body axis components of the angular velocity of rotor 1 shaft. $\omega_{H1,i}$, $\omega^{(1)}_{R1,i}$, and $\omega^{(2)}_{R1,i}$ are the individual body axis components of the angular velocities of the rotating hub, link 1, and link 2, respectively. The expressions for these angular velocities are given as follows:

$$\omega_{S1} = [T_{S1}]^T \omega_F \tag{25}$$

$$\omega_{H1,i} = [T_{H1,i}]^T \omega_{S1} + \{0, 0, -\Omega_{R1}\}^T \tag{26}$$

$$\omega^{(1)}_{R1,i} = \left[T^{(1)}_{R1,i}\right]^T \omega_{H1,i} + b^{(1)}_{R1}\dot{\alpha}^{(1)}_{R1,i} \tag{27}$$

$$\omega^{(2)}_{R1,i} = \left[T^{(2)}_{R1,i}\right]^T \omega^{(1)}_{R1,i} + b^{(2)}_{R1}\dot{\alpha}^{(2)}_{R1,i} \tag{28}$$

In Equation 24, the vectors $\bar{r}_{F1}$, $\bar{r}_{H1}$, $\bar{r}^{(1)}_{R1}$, $\bar{r}^{(2)}_{R1}$, $\bar{r}^{(3)}_{R1}$, and $\bar{r}^{*}_{R1}$ are defined as follows. $\bar{r}_{F1}$ is the position vector from fuselage c.g. to a point on shaft 1, expressed in fuselage axes. $\bar{r}_{H1}$ is the position vector from the point on shaft 1 to the center of hub 1, expressed in shaft 1 axes. For any rotor 1 blade, $\bar{r}^{(1)}_{R1}$ is the position vector from the center of hub 1 to the first hinge, expressed in rotating hub 1 axes; $\bar{r}^{(2)}_{R1}$ is the position vector from the first hinge to the second hinge, expressed in link 1 axes; $\bar{r}^{(3)}_{R1}$ is the position vector from the second hinge to the third hinge, expressed in link 2 axes; and $\bar{r}^{*}_{R1}$ is the position vector from the third hinge to the blade c.g., expressed in blade axes. Equations 20 through 24 are used to compute the partial velocities and partial angular velocities needed in Equation 2.

The angular acceleration vectors $\dot{\omega}_F$ and $\dot{\omega}_{R1,i}$ appearing in Equation 2 are obtained by a time-differentiation of the right hand sides of Equations 20 and 21, respectively. Similarly, the translational acceleration vectors $a_{F^\bullet}$ and $a_{R1,i^\bullet}$ appearing in Equation 2 are obtained by a time-differentiation of the right hand sides of Equations 23 and 24, respectively. While the equations for the rotor blade acceleration vectors are lengthy and omitted here, it is noticed from an inspection of Equations 20 through 24 that obtaining these equations is straight forward once the expressions for the time-derivatives of the transformation matrices has been obtained. The Appendix gives the derivation of a formula for calculating the time-derivative of a matrix in terms of a matrix product. Using this formula, the following are obtained:

$$\dot{T}_F = T_F S(\omega_F) \tag{29}$$

$$\dot{T}_{S1} = 0 \tag{30}$$

$$\dot{T}_{H1,i} = T_{H1,i} S\left(\{0, 0, -\Omega_{R1}\}^T\right) \tag{31}$$

$$\dot{T}^{(1)}_{R1,i} = T^{(1)}_{R1,i} S\left(b^{(1)}_{R1}\dot{\alpha}^{(1)}_{R1,i}\right) \tag{32}$$

$$\dot{T}^{(2)}_{R1,i} = T^{(2)}_{R1,i} S\left(b^{(2)}_{R1}\dot{\alpha}^{(2)}_{R1,i}\right) \tag{33}$$

$$\dot{T}^{(3)}_{R1,i} = T^{(3)}_{R1,i} S\left(b^{(3)}_{R1}\dot{\alpha}^{(3)}_{R1,i}\right) \tag{34}$$

Generalized Gravity Forces

The partial velocities $\frac{\partial v_{F^\bullet}}{\partial u_r}$, $\frac{\partial v_{R1,i^\bullet}}{\partial u_r}$, and $\frac{\partial v_{R2,i^\bullet}}{\partial u_r}$ obtained in the computation of generalized inertia forces are used to compute the generalized gravity forces given by Equation 3.

Generalized Aerodynamic Forces Due to Fuselage

The first term in Equation 4 represents the generalized aerodynamic forces due to the fuselage. The quantities comprising this term are obtained as follows. The body axis components of the velocity of the fuselage aerodynamic center (a.c.) can be written as,

$$v_F = v_B + S(\omega_F)\bar{r}_{AC} \tag{35}$$

where $\bar{r}_{AC}$ is the position vector from the fuselage c.g. to the fuselage a.c., expressed in body axes. Equation 35 is used to compute the partial velocity $\frac{\partial v_F}{\partial u_r}$.

For a rotorcraft, the wind-axis components of the aerodynamic force and moment acting at the fuselage a.c. are usually given as a function of fuselage angles of attack and sideslip:

$$L = L_1(\alpha) + L_2(\beta) \tag{36}$$

$$D = D_1(\alpha) + D_2(\beta) \tag{37}$$

$$M = M_1(\alpha) + M_2(\beta) \tag{38}$$

$$Y = Y_1(\alpha) + Y_2(\beta) \quad (39)$$
$$l = l_1(\alpha) + l_2(\beta) \quad (40)$$
$$N = N_1(\alpha) + N_2(\beta) \quad (41)$$

These forces and moments are scaled with respect to the local dynamic pressure and can be in the form of a two dimensional data table or fitted analytical expressions to wind-tunnel data. The force and moment components in the body axes are given as,

$$F_F = \bar{q}E_2(\alpha)E_3(-\beta)\{-D, Y, -L\}^T \quad (42)$$
$$M_F = \bar{q}E_2(\alpha)E_3(-\beta)\{l, M, N\}^T \quad (43)$$

The fuselage velocities, for purposes of calculating the aerodynamic variables α, β, and $\bar{q}$, include the effect of rotor 1 downwash:

$$\bar{v} = v_F - w_{R1,0} f_{R1}(\chi_{R1}) \quad (44)$$

where $w_{R1,0}$ is the rotor 1 collective inflow, and χ_{R1} is the rotor 1 wake skew angle. In absence of more sophisticated data, f_{R1} assumes the value $\{0,0,1\}^T$ or $\{0,0,0\}^T$, depending on whether the a.c. is within or outside of rotor 1 wake. χ_{R1} is given as,

$$\chi_{R1} = \tan^{-1}\left(\frac{\mu_{R1}}{-\lambda_{R1}}\right) \quad (45)$$

where μ_{R1} and λ_{R1} are, respectively, the rotor 1 advance ratio and rotor 1 inflow ratio. These quantities can be determined by computing the relative air velocity components at the rotor hub. Using Equation 44, the aerodynamic variables α, β, and $\bar{q}$ can be readily computed:

$$\alpha = \tan^{-1}\left(\frac{\bar{v}_3}{\bar{v}_1}\right), \quad \beta = \sin^{-1}\left(\frac{\bar{v}_2}{|\bar{v}|}\right) \quad (46)$$

$$\bar{q} = \frac{1}{2}\rho |\bar{v}|^2 \quad (47)$$

Generalized Aerodynamic Forces Due to Rotors

The second term in Equation 4 represents the generalized aerodynamic forces due to rotor 1. Blade element analysis is used to calculate this term. As mentioned earlier, the rotor blades are allowed to have any arbitrary variation of twist, chord length, and airfoil characteristics along the span. The body axis components of the blade element velocity are given as,

$$\begin{aligned} v_{R1,i,j} = {} & \left[T_F T_{S1} T_{H1,i} T^{(1)}_{R1,i} T^{(2)}_{R1,i} T^{(3)}_{R1,i}\right]^T v_{F^\bullet} + \\ & \left[T_{S1} T_{H1,i} T^{(1)}_{R1,i} T^{(2)}_{R1,i} T^{(3)}_{R1,i}\right]^T S(\omega_F)\bar{r}_{F1} + \\ & \left[T_{H1,i} T^{(1)}_{R1,i} T^{(2)}_{R1,i} T^{(3)}_{R1,i}\right]^T S(\omega_{S1})\bar{r}_{H1} + \\ & \left[T^{(1)}_{R1,i} T^{(2)}_{R1,i} T^{(3)}_{R1,i}\right]^T S(\omega_{H1,i})\bar{r}^{(1)}_{R1} + \\ & \left[T^{(2)}_{R1,i} T^{(3)}_{R1,i}\right]^T S(\omega^{(1)}_{R1,i})\bar{r}^{(2)}_{R1} + \\ & \left[T^{(3)}_{R1,i}\right]^T S(\omega^{(2)}_{R1,i})\bar{r}^{(3)}_{R1} + \\ & S(\omega_{R1,i})\bar{r}_{R1,j} \end{aligned} \quad (48)$$

The only new quantity introduced in the preceding Equation is $\bar{r}_{R1,j}$ $(j = 1, \ldots, b_{R1})$, which is the position vector from the root of the blade to the jth aerodynamic element, expressed in blade body axes. Equation 48 is used to obtain the partial velocity $\frac{\partial v_{R1,i,j}}{\partial u_r}$.

Figure 3 shows a typical jth element on the ith blade, and the lift and drag forces acting on it. $(y_{R1,i}, z_{R1,i})$ are the body axes of the blade. $\theta_{R1,j}$ is the blade twist angle at the jth section. $u^s_{R1,i,j}$ and $u^p_{R1,i,j}$ are the components of the relative air velocity parallel and perpendicular to the zero lift line. The variables $\alpha_{R1,i,j}$, $L_{R1,i,j}$, and $D_{R1,i,j}$ have obvious meanings. The velocity of the (i,j)th element with respect to air is given by the following equation,

$$\bar{v}_{R1,i,j} = v_{R1,i,j} + \left[T_{H1,i} T^{(1)}_{R1,i} T^{(2)}_{R1,i} T^{(3)}_{R1,i}\right]^T v^A_{R1,i,j} \quad (49)$$

The term $v^A_{R1,i,j}$ arises due to rotor inflow and can be approximately evaluated as,

$$\begin{aligned} (v^A_{R1,i,j})_1 &= 0 \\ (v^A_{R1,i,j})_2 &= 0 \\ (v^A_{R1,i,j})_3 &= -w_{R1,0} - [h_{R1} + (\bar{r}_{R1,j})_1/R_{R1}] \cdot \\ &\quad (w_{R1,1s}\sin\psi_{R1,i} + w_{R1,1c}\cos\psi_{R1,i}) \end{aligned} \quad (50)$$

where

$$h_{R1} = \frac{(\bar{r}^{(1)}_{R1})_1 + (\bar{r}^{(2)}_{R1})_1 + (\bar{r}^{(3)}_{R1})_1}{R_{R1}} \quad (51)$$

$w_{R1,1s}$ and $w_{R1,1c}$ are the sin and cos components of the rotor inflow and R_{R1} is the rotor radius. The radial, tangential, and perpendicular components of the air velocity at the airfoil can be computed as,

$$\{u^r_{R1,i,j}, -u^s_{R1,i,j}, u^p_{R1,i,j}\}^T = E_1(\theta_{R1,j})\bar{v}_{R1,i,j} \quad (52)$$

Using the air velocity components, the section angle of attack and Mach Number can be calculated as follows:

$$\alpha_{R1,i,j} = \tan^{-1}\left(\frac{u^p_{R1,i,j}}{u^s_{R1,i,j}}\right) \quad (53)$$

$$\mathcal{M}_{R1,i,j} = \frac{\sqrt{(u^s_{R1,i,j})^2 + (u^p_{R1,i,j})^2}}{c} \quad (54)$$

where c is the speed of sound at the altitude where the aircraft is operating. Airfoil lift and drag coefficients are usually specified as a function of the angle of attack and Mach Number. Thus,

$$c^l_{R1,i,j} = c^l_{R1,i,j}(\alpha_{R1,i,j}, \mathcal{M}_{R1,i,j}) \quad (55)$$

$$c^d_{R1,i,j} = c^d_{R1,i,j}(\alpha_{R1,i,j}, \mathcal{M}_{R1,i,j}) \quad (56)$$

The above data can be either in the form of a two dimensional data table or in the form of fitted analytical expressions to experimental data. However, in the absence of any data, simple analytical lift and drag models can be used. Based on reference [9], equations were generated for two simple models, one that ignored stall and compressibility effects and another that included the same. The section lift and drag forces are computed next:

$$L_{R1,i,j} = \bar{q}_{R1,i,j} c^l_{R1,i,j} c_{R1,j} (\Delta \bar{r}_{R1,j})_1 \eta_{R1,j} \quad (57)$$

$$D_{R1,i,j} = \bar{q}_{R1,i,j} c^d_{R1,i,j} c_{R1,j} (\Delta \bar{r}_{R1,j})_1 \quad (58)$$

where

$$\bar{q}_{R1,i,j} = \frac{1}{2}\rho[(u^s_{R1,i,j})^2 + (u^p_{R1,i,j})^2] \quad (59)$$

and $c_{R1,j}$ and $\eta_{R1,j}$ are, respectively, the chord length and lift efficiency factors at the jth section. The body axis components of the section aerodynamic force are given by:

$$F_{R1,i,j} = E_1(\alpha_{R1,i,j} - \theta_{R1,j})\{0, D_{R1,i,j}, -L_{R1,i,j}\}^T \quad (60)$$

Generalized Aerodynamic Forces Due to Surfaces

The generalized aerodynamic forces due to the external surfaces are derived in much the same way as those due to the rotors. One difference, however, is that the radial drag force due to radial flow is considered here. It is assumed that every surface has a fixed (invariant with time) orientation with respect to the fuselage. The orientation can be specified uniquely in terms of rotation angles about three mutually perpendicular axes. In order to have consistency in describing surfaces with different orientations, the body axes for any surface are defined as follows. The x axis coincides with the zero lift line of the root section and is directed from the trailing edge of the surface to the leading edge of the surface (see Figure 4). The y axis is perpendicular to the x axis, passes through the aerodynamic center of the root section and is directed outboard. z axis completes the right handed set.

The objective is to evaluate the last term in Equation 4. For illustration purposes, the mathematical analysis involved is outlined for surface 1. Let the surface be oriented with respect to the fuselage by three successive rotations of angles γ_{S_1}, δ_{S_1} and ϵ_{S_1} about mutually perpendicular axes. The sequence of rotations can be any of the possible six sequences. Let the matrices associated with the above transformations be $T^{(1)}_{S_1}$, $T^{(2)}_{S_1}$, and $T^{(3)}_{S_1}$, respectively. The matrix $T_{ES_1} = T^{(3)}_{S_1}(\epsilon_{S_1}) T^{(2)}_{S_1}(\delta_{S_1}) T^{(1)}_{S_1}(\gamma_{S_1})$ transforms components of a vector from fuselage axes to surface 1 axes. Let $\bar{r}_{S_1}$ be the position vector from the fuselage c.g. to the surface 1 reference point, expressed in fuselage axes. Let $\bar{r}_{S_1,j}$ be the position vector from the surface reference point to the aerodynamic center of the jth section, expressed in surface axes. Then the velocity of the jth section can be expressed as,

$$v_{S_1,j} = T_{ES_1}\left[v_B + S(\omega_F)\bar{r}_{S_1} + S(\omega_F)[T_{ES_1}]^T \bar{r}_{S_1,j}\right] \quad (61)$$

This expression is used to obtain the partial velocity $\frac{\partial v_{S_1,j}}{\partial u_r}$, which is needed for evaluating the generalized aerodynamic force contribution from surface 1.

For purposes of computing the aerodynamic force, the resultant section velocity with respect to air includes the effect of rotor 1 downwash:

$$\bar{v}_{S_1,j} = v_{S_1,j} - T_{ES_1} w_{R1,0} f_{S_1}(\chi_{R1}) \quad (62)$$

Similar to the case of the fuselage, in a simple analysis, f_{S_1} can be taken to be equal to $\{0,0,1\}^T$ or $\{0,0,0\}^T$, depending on whether the surface is within or outside of rotor 1 wake.

The effect of radial flow on a surface section is included in the same way as described in reference [10], where profile power is computed due to radial flow at blade sections. Let the free stream velocity at the jth section be yawed, as shown in Figure 5. An estimate of the normal and radial drag forces is desired, preferably in terms of the two dimensional sectional aerodynamic coefficients. It is assumed that the total viscous drag on the yawed section acts in the same direction as the free stream velocity. It is also assumed that the yawed section drag coefficient is given by the two dimensional unyawed airfoil characteristics. The normal section lift coefficient is assumed not to be influenced by yawed flow. The angle of attack and Mach Number for the unyawed and yawed sections are,

$$\alpha_{S_1,j} = \tan^{-1}\left(\frac{(\bar{v}_{S_1,j})_3}{(\bar{v}_{S_1,j})_1}\right) \quad (63)$$

$$\mathcal{M}_{S_1,j} = \frac{\sqrt{(\bar{v}_{S_1,j})_1^2 + (\bar{v}_{S_1,j})_3^2}}{c} \quad (64)$$

$$\hat{\alpha}_{S_1,j} = \tan^{-1}\left(\frac{(\bar{v}_{S_1,j})_3}{\sqrt{(\bar{v}_{S_1,j})_1^2 + (\bar{v}_{S_1,j})_2^2}}\right) \quad (65)$$

$$\hat{\mathcal{M}}_{S_{1},j} = \frac{\sqrt{(\bar{v}_{S_{1},j})_1^2 + (\bar{v}_{S_{1},j})_2^2 + (\bar{v}_{S_{1},j})_3^2}}{c} \quad (66)$$

The section lift and drag coefficients are given by:

$$c^l_{S_{1},j} = c^l_{S_{1},j}(\alpha_{S_{1},j}, \mathcal{M}_{S_{1},j}) \quad (67)$$

$$c^d_{S_{1},j} = c^d_{S_{1},j}(\hat{\alpha}_{S_{1},j}, \hat{\mathcal{M}}_{S_{1},j}) \quad (68)$$

As mentioned for the case of rotor aerodynamics, in the absence of lift and drag coefficient data, simple analytical models for the coefficients can be used. The section lift and drag forces are given as,

$$L_{S_{1},j} = \bar{q}_{S_{1},j} c^l_{S_{1},j} c_{S_{1},j} (\Delta\bar{r}_{S_{1},j})_2 \eta_{S_{1},j} \quad (69)$$

$$D_{S_{1},j} = \hat{q}_{S_{1},j} c^d_{S_{1},j} c_{S_{1},j} (\Delta\bar{r}_{S_{1},j})_2 \quad (70)$$

where

$$\bar{q}_{S_{1},j} = \frac{1}{2}\rho[(\bar{v}_{S_{1},j})_1^2 + (\bar{v}_{S_{1},j})_3^2] \quad (71)$$

$$\hat{q}_{S_{1},j} = \frac{1}{2}\rho[(\bar{v}_{S_{1},j})_1^2 + (\bar{v}_{S_{1},j})_2^2 + (\bar{v}_{S_{1},j})_3^2] \quad (72)$$

and $\eta_{S_{1},j}$ is the section lift efficiency factor. Finally, the body axis components of the section aerodynamic force are given as,

$$\begin{aligned} R_{S_{1},j} = & \left(L_{S_{1},j}/\sqrt{(\bar{v}_{S_{1},j})_1^2 + (\bar{v}_{S_{1},j})_3^2}\right) \cdot \\ & \{(\bar{v}_{S_{1},j})_3, 0, -(\bar{v}_{S_{1},j})_1\}^T + \\ & \left(D_{S_{1},j}/\sqrt{(\bar{v}_{S_{1},j})_1^2 + (\bar{v}_{S_{1},j})_2^2 + (\bar{v}_{S_{1},j})_3^2}\right) \cdot \\ & \{-(\bar{v}_{S_{1},j})_1, -(\bar{v}_{S_{1},j})_2, -(\bar{v}_{S_{1},j})_3\}^T \end{aligned} \quad (73)$$

Generalized Damping Forces Due to Translational Dampers

As shown in Figure 2, one end of the blade translational damper is attached to the rotating hub while the other end is attached to the blade itself. The damper force is assumed to be given as a function of the relative speed between it's two ends. The analysis associated with the first term in Equation 5, which is due to rotor 1, is developed in the following. The position vector from attachment point 1 to attachment point 2, expressed in the rotating hub axes, is given as,

$$\begin{aligned} d_{R1,i} = & \left(\bar{r}^{(1)}_{R1} - \bar{s}_{R1}\right) + \\ & T^{(1)}_{R1,i}\bar{r}^{(2)}_{R1} + \\ & T^{(1)}_{R1,i}T^{(2)}_{R1,i}\bar{r}^{(3)}_{R1} + \\ & T^{(1)}_{R1,i}T^{(2)}_{R1,i}T^{(3)}_{R1,i}\bar{t}_{R1} \end{aligned} \quad (74)$$

$\bar{s}_{R1}$ is the position vector from the center of the hub to attachment point 1, expressed in hub axes. $\bar{t}_{R1}$ is the position vector from the blade root to attachment point 2, expressed in blade axes. The preceding equation is used to determine the velocity of attachment point 2 relative to that of attachment point 1, expressed in hub axes:

$$\begin{aligned} \tilde{v}_{R1,i} = & S(\omega_{H1,i})\left(\bar{r}^{(1)}_{R1} - \bar{s}_{R1}\right) + \\ & T^{(1)}_{R1,i}S(\omega^{(1)}_{R1,i})\bar{r}^{(2)}_{R1} + \\ & T^{(1)}_{R1,i}T^{(2)}_{R1,i}S(\omega^{(2)}_{R1,i})\bar{r}^{(3)}_{R1} + \\ & T^{(1)}_{R1,i}T^{(2)}_{R1,i}T^{(3)}_{R1,i}S(\omega_{R1,i})\bar{t}_{R1} \end{aligned} \quad (75)$$

The component of this relative velocity along the damper arm can be written as,

$$\hat{v}_{R1,i} = (1/\mid d_{R1,i} \mid)(d_{R1,i})^T\tilde{v}_{R1,i} \quad (76)$$

The damper force $F_{R1,i}$ is assumed to be specified as a function of the above speed. Hence,

$$F_{R1,i} = F_{R1,i}(\hat{v}_{R1,i}) \quad (77)$$

The hub axis components of the forces acting at the attachment points are given as,

$$F^D_{R1,i,1} = -(F_{R1,i}/\mid d_{R1,i} \mid)d_{R1,i} \quad (78)$$

$$F^D_{R1,i,2} = (F_{R1,i}/\mid d_{R1,i} \mid)d_{R1,i} \quad (79)$$

The velocities at the attachment points, expressed in the hub axes, are:

$$\begin{aligned} v^D_{R1,i,1} = & [T_{S1}T_{H1,i}]^T(v_B + S(\omega_F)\bar{r}_{F1}) + \\ & [T_{H1,i}]^T S(\omega_{S1})\bar{r}_{H1} + \\ & S(\omega_{H1,i})\bar{s}_{R1} \end{aligned} \quad (80)$$

$$v^D_{R1,i,2} = v^D_{R1,i,1} + \tilde{v}_{R1,i} \quad (81)$$

The above two equations are used to calculate the required partial velocities, $\frac{\partial v^D_{R1,i,1}}{\partial u_r}$ and $\frac{\partial v^D_{R1,i,2}}{\partial u_r}$.

Generalized Spring-Damper Forces Due to Torsional Spring-Dampers

The torsional springs and dampers mounted on the blade hinges are assumed to possess linear stiffness and damping properties. They give rise to the third and fourth terms in Equation 5. The third term in this equation is due to rotor 1 and is discussed below. Referring to Figure 2, the following quantities are defined for the ith blade. $M_{R1,i,1}$ denotes the body axis components of the moment on acting link 1 due to the spring-damper at hinge 1. $M_{R1,i,2}$ denotes the body axis components of the moment on acting link 2 due to the spring-damper at hinge 2. $M_{R1,i,3}$ denotes the body axis components of the moment on acting on

the blade due to the spring-damper at hinge 3. These moments can be expressed as,

$$M_{R1,i,1} = -b_{R1}^{(1)}\left(k_{P_{R1}}^{(1)}\alpha_{R1,i}^{(1)} + k_{D_{R1}}^{(1)}\dot{\alpha}_{R1,i}^{(1)}\right) \quad (82)$$

$$M_{R1,i,2} = -b_{R1}^{(2)}\left(k_{P_{R1}}^{(2)}\alpha_{R1,i}^{(2)} + k_{D_{R1}}^{(2)}\dot{\alpha}_{R1,i}^{(2)}\right) \quad (83)$$

$$M_{R1,i,3} = -b_{R1}^{(3)}\left(k_{P_{R1}}^{(3)}\alpha_{R1,i}^{(3)} + k_{D_{R1}}^{(3)}\dot{\alpha}_{R1,i}^{(3)}\right) \quad (84)$$

where k_P and k_D denote sttifness and damping constants. The torsional spring-damper moments acting on the hub, link 1, link 2, and the blade, expressed in their individual body axes, are respectively given as,

$$M_{R1,i,1}^{D} = -M_{R1,i,1} \quad (85)$$

$$M_{R1,i,2}^{D} = M_{R1,i,1} - M_{R1,i,2} \quad (86)$$

$$M_{R1,i,3}^{D} = M_{R1,i,2} - M_{R1,i,3} \quad (87)$$

$$M_{R1,i,4}^{D} = M_{R1,i,3} \quad (88)$$

The individual body axis components of the angular velocities of the hub, link 1, link 2, and the blade, are respectively given as,

$$\omega_{R1,i,1}^{D} = \omega_{H1,i} \quad (89)$$

$$\omega_{R1,i,2}^{D} = \omega_{R1,i}^{(1)} \quad (90)$$

$$\omega_{R1,i,3}^{D} = \omega_{R1,i}^{(2)} \quad (91)$$

$$\omega_{R1,i,4}^{D} = \omega_{R1,i} \quad (92)$$

The preceding four equations are used to compute the four partial velocities needed for evaluating the third term in Equation 5.

Airframe Kinematics

To complete the description of the airframe dynamic model, the kinematic relationship between the vectors q, $\dot{q}$, and u needs to be stipulated. Let the airframe kinematic equations be given as,

$$f_{K_i}(q, \dot{q}, u) = 0, \quad i = 1, \ldots, n_{RB} \quad (93)$$

The elements of the vector f_{K_i} are given in detail as follows:

$$\begin{Bmatrix} f_{K_1} \\ \vdots \\ f_{K_6} \end{Bmatrix} = u_F - \begin{bmatrix} [T_F]^T & 0 \\ 0 & W_B \end{bmatrix} \dot{q}_F \quad (94)$$

$$\begin{Bmatrix} f_{K_7} \\ \vdots \\ \vdots \\ f_{K_{n_{RB}}} \end{Bmatrix} = \begin{Bmatrix} u_{R1,1} \\ \vdots \\ u_{R1,n_{R1}} \\ u_{R2,1} \\ \vdots \\ u_{R2,n_{R2}} \end{Bmatrix} - \begin{Bmatrix} \dot{q}_{R1,1} \\ \vdots \\ \dot{q}_{R1,n_{R1}} \\ \dot{q}_{R2,1} \\ \vdots \\ \dot{q}_{R2,n_{R2}} \end{Bmatrix} \quad (95)$$

The matrix W_B is given as,

$$W_B = \begin{bmatrix} 1 & 0 & -\sin\theta \\ 0 & \cos\phi & \sin\phi\cos\theta \\ 0 & -\sin\phi & \cos\phi\cos\theta \end{bmatrix} \quad (96)$$

Multiblade Coordinate Transformation

The airframe dynamic and kinematic models, given by Equations 1 and 93, respectively, are derived in the rotating system, with the rotor degrees of freedom describing the motion of individual rotor blades. However, the rotor usually responds as a whole to excitation and for physical insight it is desirable to work with the degrees of freedom which model the entire rotor system rather than the individual blades. To transform the equations of motion with respect to individual blade coordinates to rotor system coordinates, the method of multiblade coordinates is used [11]. Considering the example of rotor 1, for like degrees of freedom, the kth ($k = 1, \ldots, n_{R1}$) individual rotor blade degree of freedom is expressed as,

$$\alpha_{R1,k} = \alpha_{R1,0} + \sum_{i=1}^{(n_{R1}-1)/2} (\alpha_{R1,ic}\cos i\psi_k + \alpha_{R1,is}\sin i\psi_k) \quad (97)$$

for rotors with an odd number of blades and

$$\alpha_{R1,k} = \alpha_{R1,0} + \sum_{i=1}^{(n_{R1}-2)/2} (\alpha_{R1,ic}\cos i\psi_k + \alpha_{R1,is}\sin i\psi_k) + \alpha_{R1,d}(-1)^k \quad (98)$$

for rotors with an even number of rotor blades.

Let the generalized coordinate and generalized speed vectors in the multiblade or non-rotating coordinate system be represented by q' and u'. Then the following substitutions are made in the airframe kinematic and dynamic model descriptions, given by Equations 93 and 1, respectively.

$$q = T(t)q' \quad (99)$$

$$u = \dot{T}(t)q' + T(t)u' \quad (100)$$

$$\dot{u} = \ddot{T}(t)q' + 2\dot{T}(t)u' + T(t)\dot{u}' \quad (101)$$

Then the resulting airframe kinematic and dynamic equations can be written as,

$$f_{K_i}(q', \dot{q}', u') = 0, \quad i = 1, \ldots, n_{RB} \quad (102)$$

$$f_i(q', u', w, \dot{u}', t) = 0, \quad i = 1, \ldots, n_{RB} \quad (103)$$

where the vector w consists of the inflow coordinates of the two rotors:

$$w = \{w_{R1,0}, w_{R1,1s}, w_{R1,1c}, w_{R2,0}, w_{R2,1s}, w_{R2,1c}\}^T \tag{104}$$

Rotor Dynamic Inflow Model

The rotor dynamic inflow model used in this work is based on the Peters and HaQuang [12] model which is in turn based on the work of Pitt and Peters [8]. The model includes three inflow degrees of freedom that yield the time-varying induced flow parallel to the rotor shaft. Based on the small perturbation potential flow equations, the model accounts for dynamic changes in collective inflow and first harmonic inflow azimuthally. Inflow along the blades varies linearly. The inflow distribution is given by Equation 50. For simplicity only the dynamic inflow model for rotor 1 will be described. The dynamic inflow model for rotor 2 is similar with obvious changes.

The basic model formulation is carried out in the rotor wind axis system and is later transformed to the rotor shaft axis system. The dynamic inflow equations are forced by the averaged (over rotor revolution) rotor thrust, rolling moment, and pitching moment in the shaft axes. The resulting equations can be written in the form,

$$\begin{Bmatrix} \dot{w}_{R1,0} \\ w_{R1,1s} \\ w_{R1,1c} \end{Bmatrix} + [\mathcal{A}_{R1}] \begin{Bmatrix} w_{R1,0} \\ w_{R1,1s} \\ w_{R1,1c} \end{Bmatrix} = \begin{Bmatrix} \frac{-T_{R1}}{\rho \pi R_1^3} \\ \frac{-L_{R1}}{\rho \pi R_1^4} \\ \frac{M_{R1}}{\rho \pi R_1^4} \end{Bmatrix} \tag{105}$$

where,

$$\mathcal{A}_{R1} = \mathcal{A}_{R1}(q', u') \tag{106}$$

The blade element forces, given by Equation 60, are vectorially summed over all rotor blades to obtain the shaft axis components of the rotor thrust, rolling moment and pitching moment. These forces and moments are then averaged over the period of revolution of the rotor and used in Equation 105.

The complete set of dynamic inflow equations for the two rotors can be functionally represented as,

$$g_i(q', u', w, \dot{w}) = 0, \quad i = 1, \ldots, n_{DI} \tag{107}$$

where $n_{DI} = 6$ since three state inflow models are being used for each rotor. It should be noted that Equation 107 is written using the multiblade or nonrotating coordinate system.

Trim Algorithm

Trim of an aircraft is defined as an equilibrium condition where the translational and rotational accelerations of the fuselage are zero. Hence in trim, $\dot{p} = \dot{q} = \dot{r} = \dot{u} = \dot{v} = \dot{w} = 0$. For straight and level flight, $p = q = r = v = 0$ as well. For a fixed wing airplane this definition is sufficient since one can generally regard an airplane as a single rigid body with six degrees of freedom. For rotorcraft the concept of trim is more complicated because the vehicle is represented as a multibody system consisting of a fuselage, many rotor blades, and a drive system. By virtue of the rotor rotational motion, the blades are always accelerating. For the rotor blade degrees of freedom, trim is considered to be an operating condition such that the individual rotor blades follow a periodic path. This implies that all the first and second derivatives of the rotor multiblade coordinates must be zero in trim. This will force individual blades to track the same periodic path each rotor revolution. However, it should be noted that for even bladed rotors this condition will not force every blade on a rotor to follow the same path. This is due to the warping multiblade coordinate mode for even bladed rotors.

There are many different methods for obtaining the trim condition of a coupled rotor and fuselage combination. Included in these methods are iterative fuselage trim and rotor trim, fully coupled autopilot trim, finite elements in time trim, nonlinear optimization trim, and Galerkin method trim. While no one method for trim is superior in all settings, all the methods are sufficiently different to have qualities which make them more or less attractive in different settings. In this work a nonlinear optimization trim technique is used.

In nonlinear optimization, one seeks to minimize or maximize a certain nonlinear function by iterating on the independent variables of the problem. Here the sum of the squares of the dynamic equation residuals will be minimized and the independent variables will be the system states and controls. A modified Newton's method, sometimes called a damped Newton's method or a quasi Newton method, is used as the nonlinear optimization algorithm to compute the trim state of the vehicle.

The trim algorithm begins by noting that in trim, $\dot{u}' = 0$ and $\dot{w} = 0$ necessarily. Hence in trim, the airframe dynamic equations (Equation 1) and the dynamic inflow equations (Equation 107) can be written as,

$$f_i(x, t) = 0, \quad i = 1, \ldots, n_{RB} \tag{108}$$

$$g_i(x) = 0, \quad i = 1, \ldots, n_{DI} \tag{109}$$

where

$$x = \{(q')^T, (u')^T, (w)^T\}^T \tag{110}$$

Clearly, x is the state vector of the airframe dynamic model. Equation 108 contains a set of algebraic nonlinear equations which are periodic in time, with a period of τ. τ is the period of revolution common to rotor 1 blades and rotor 2 blades. The goal of the trim algorithm is to minimize the residual of each equation in Equations 108 and 109 for all values of time.

A natural scalar function to minimize for trim is,

$$\begin{aligned} J &= \frac{1}{\tau}\int_0^\tau \sum_{i=1}^{n_{RB}} f_i(t)^2 dt + \sum_{i=1}^{n_{DI}} g_i^2 \\ &\approx \frac{\Delta t}{\tau}\sum_{k=1}^{n_T}\sum_{i=1}^{n_{RB}} f_i(t_k)^2 + \sum_{i=1}^{n_{DI}} g_i^2 \end{aligned} \tag{111}$$

where n_T is the number of time points chosen for discretization. The function J is termed the cost function. Using the discretized form of the cost function, the gradient and hessian of the cost function can be formed.

$$\frac{\partial J}{\partial x_j} = 2\frac{\Delta t}{\tau}\sum_{k=1}^{n_T}\sum_{i=1}^{n_{RB}} f_i(t_k)\frac{\partial f_i(t_k)}{\partial x_j} + 2\sum_{i=1}^{n_{DI}} g_i\frac{\partial g_i}{\partial x_j} \tag{112}$$

$$\begin{aligned} &\frac{\partial}{\partial x_l}\left(\frac{\partial J}{\partial x_j}\right) \approx \\ &2\frac{\Delta t}{\tau}\sum_{k=1}^{n_T}\sum_{i=1}^{n_{RB}}\left[\frac{\partial f_i(t_k)}{\partial x_l}\frac{\partial f_i(t_k)}{\partial x_j} + f_i(t_k)\frac{\partial^2 f_i(t_k)}{\partial x_l \partial x_j}\right] \\ &+ 2\sum_{i=1}^{n_{DI}}\left[\frac{\partial g_i}{\partial x_l}\frac{\partial g_i}{\partial x_j} + g_i\frac{\partial^2 g_i}{\partial x_l \partial x_j}\right] \end{aligned} \tag{113}$$

The minimization problem described above is essentially a least squares problem. It is known that for least square minimization problems, where the cost function is small at the solution, the second derivative terms in the above equations are relatively small and can be neglected [13]. By definition, this assumption is valid in the trim problem.

In a modified Newton's method, a local optimization problem is solved iteratively. A flow chart for the iteration procedure is given in Figure 6. Using an initial condition or guess for the trim variables, a local quadratic model of the cost function is formed,

$$J(x + \Delta x) = J(x) + \frac{\partial J}{\partial x}\Delta x + \frac{1}{2}\Delta x^T \frac{\partial^2 J}{\partial x^2}\Delta x \tag{114}$$

At the local minimum of this approximation to the actual cost function one must have,

$$\frac{\partial J}{\partial \Delta x} = 0 \tag{115}$$

For a local minimum of a quadratic function to exist, hessian matrix of the cost function must be positive definite. Assuming this is the case,

$$\Delta x = -\left[\frac{\partial^2 J}{\partial x^2}\right]^{-1}\left\{\frac{\partial J}{\partial x}\right\} \tag{116}$$

The vector Δx is called the search direction because based on this direction a search to reduce the cost function shall be undertaken. For the local quadratic model of the cost function, the minimum is given by $x+\Delta x$, of course if a minimum exists. A new iteration on the minimum of the actual cost function can now be made by with the equation,

$$x_{new} = x_{old} + \alpha \Delta x \tag{117}$$

The parameter, α, is the step length. It is used because the local model is only an approximation to the actual cost. $\alpha = 1$ corresponds to a full Newton's method while $\alpha < 1$ implies a damped or modified Newton's method. The parameter α is determined at each trim iteration and is based on satisfying criteria for tracking sufficient decrease in the cost function at each iteration in the overall minimization problem. The process of determining the step length is called a step length procedure or line search strategy.

There are many criteria for determining sufficient decrease in the cost function at each iteration. Armijo's rule is used here which can be stated as,

$$J_0 - J_\alpha \geq -\mu\alpha\frac{\partial J}{\partial x}\Delta x \tag{118}$$

where the constant μ is a positive number. A back tracking strategy is used in the line search strategy. In this method, one always starts with $\alpha = 1$ and tries to use the full Newton's method if possible. If the current α does not fulfill the Armijo condition, then α is divided by a factor and retried. Once an appropriate value for α is obtained, new values for x are computed. Then a new local quadratic model is formed and the optimization procedure is again formed. It should be noted that in solving for the search direction a linear system must be solved. It is solved using a modified Choleski decomposition algorithm as described in reference [13].

Linear Model of Airframe Dynamics

Linearized rotorcraft dynamic models are extremely useful for flying qualities analyses. To this end, the composite airframe dynamic model consisting of the kinematic, dynamic, and dynamic inflow

models, given by Equations 102, 103, and 107, respectively, is linearized about an arbitrary trim state, x_0. The linear model can be written as,

$$C_p(x_0,t)\delta\dot{x} = D_p(x_0,t)\delta x \tag{119}$$

The $(2n_{RB}+n_{DI}) \times (2n_{RB}+n_{DI})$ square matrices C_p and D_p are given as,

$$C_P = \begin{bmatrix} \frac{\partial f_K}{\partial \dot{q}'} & 0 & 0 \\ 0 & \frac{\partial f}{\partial \dot{u}'} & 0 \\ 0 & 0 & \frac{\partial g}{\partial \dot{w}} \end{bmatrix} \tag{120}$$

$$D_p = -\begin{bmatrix} \frac{\partial f_K}{\partial q'} & \frac{\partial f_K}{\partial u'} & 0 \\ \frac{\partial f}{\partial q'} & \frac{\partial f}{\partial u'} & \frac{\partial f}{\partial w} \\ \frac{\partial g}{\partial q'} & \frac{\partial g}{\partial u'} & \frac{\partial g}{\partial w} \end{bmatrix} \tag{121}$$

where

$$f_K = \{f_{K_1}, \ldots, f_{K_{n_{RB}}}\}^T \tag{122}$$

$$f = \{f_1, \ldots, f_{n_{RB}}\}^T \tag{123}$$

$$g = \{g_1, \ldots, g_{n_{DI}}\}^T \tag{124}$$

In the ensuing analysis, the δ's in Equation 119 will be dropped and the perturbation state of the aircraft will be simply denoted as x_{ac}.

Transformation of the Airframe Linear Dynamic Equations

The multiblade coordinate transformation should be accompanied by a transformation of the equations of motion to the non-rotating coordinate system. This step is accomplished by taking linear combinations of the equations of motion given by Equation 119. The operations can be performed by premultiplying the dynamic equations by a transformation matrix, $\bar{T}(t)$. The fully transformed linear equations are,

$$\bar{T}(t)C_p(t)\dot{x}_{ac} = \bar{T}(t)D_p(t)x_{ac} \tag{125}$$

In rotorcraft handling qualities analysis, a linear time invariant system is most convenient to work with due to the powerful linear system analysis tools available. A standard approximation used in rotorcraft handling qualities work is to neglect the harmonic content in Equation 125 and hence obtain a linear time invariant system. This approximation is known as the constant coefficient approximation and it is used in the current effort.

The blade pitch control terms can be separated from the above equations by assuming that the multiblade coordinate blade pitch degrees of freedom do not possess dynamics. Appropriate rows of the dynamics matrix are deleted and the associated columns form the controls matrix. The final form of the airframe linear dynamic equations is,

$$\dot{x}_{ac} = Ax_{ac} + B\vartheta \tag{126}$$

$$y_{ac} = Cx_{ac} + D\vartheta \tag{127}$$

where the vector ϑ consists of individual rotor pitch control variables. This system can now be coupled to the flight control system to form the complete system.

Linear Control System Model

Most aircraft flight control systems are given in block diagram form and there is no standard structure. Although for modeling purposes, a generic flight control system structure could be assumed such that all or at least a majority of current aircraft flight control systems could be accommodated, it is felt this approach may be too restrictive in some cases and far too general, hence inefficient, in other cases. It is desirable to have a flight control system modeling capability which does not assume a structure aprior but uses the input data deck to generate the model. This approach allows for greater flexibility and increased utility of the control system model. With these considerations in mind, a linear state-space flight control system modeling capability was developed that takes the basic block diagram data as input.

The flight control system is assumed to be comprised of an arbitrary number of filters, given in polynomial form. Each filter is a multi input and single output filter as shown in Figure 7.

The inputs to each filter can consist of pilot stick inputs, outputs of other individual filters, aircraft states, and derivatives of aircraft states. A state-space realization is computed for each individual filter in phase variable canonical form. The filters are then assembled into an overll state-space realization. The realization can be written as,

$$\dot{x}_{cs} = A_u x_{cs} + B_u v_u \tag{128}$$

$$y_u = C_u x_{cs} + D_u v_u \tag{129}$$

The subscript u signifies that the state-space matrices do not account for the filter coupling. A filter coupling matrix can be computed in the form,

$$v_u = \zeta_u y_u + \beta_u \delta + \gamma_u x_{ac} + \sigma_u \dot{x}_{ac} \tag{130}$$

It should be noted that Equations 128, 129 and 130 can be constructed in a straight forward manner from the input block diagram data. Substituting Equation

130 into Equations 128 and 129, the coupled state-space model of the control system can be formed.

$$\dot{x}_{cs} = Fx_{cs} + G\delta + Hx_{ac} + E\dot{x}_{ac} \quad (131)$$

$$\vartheta = Px_{cs} + Q\delta + Rx_{ac} + Z\dot{x}_{ac} \quad (132)$$

where,

$$F = A_u + B_u\zeta_u S_u \quad (133)$$

$$G = B_u\zeta_u U_u + B_u\beta_u \quad (134)$$

$$H = B_u\zeta_u V_u + B_u\gamma_u \quad (135)$$

$$E = B_u\zeta_u W_u + B_u\sigma_u \quad (136)$$

$$P = X[C_u + D_u\zeta_u S_u] \quad (137)$$

$$Q = X[D_u\zeta_u U_u + D_u\beta_u] \quad (138)$$

$$R = X[D_u\zeta_u V_u + D_u\gamma_u] \quad (139)$$

$$Z = X[D_u\zeta_u W_u + D_u\sigma_u] \quad (140)$$

$$S_u = [I - D_u\zeta_u]^{-1} C_u \quad (141)$$

$$U_u = [I - D_u\zeta_u]^{-1} D_u\beta_u \quad (142)$$

$$V_u = [I - D_u\zeta_u]^{-1} D_u\gamma_u \quad (143)$$

$$W_u = [I - D_u\zeta_u]^{-1} D_u\sigma_u \quad (144)$$

The matrix X restricts the overall control system outputs to be the aircraft blade pitch angles. It should be noted that if the matrix $[I - D_u\zeta_u]$ is singular, then there is not a valid state-space model for the system and the system is non-causal. This is due to the fact that the flight control system output can be written as,

$$[I - D_u\zeta_u]\, y = C_u x_{cs} + D_u\beta_u\delta + D_u\gamma_u x_{ac} + D_u\sigma_u\dot{x}_{ac} \quad (145)$$

For a valid state-space realization the output must be uniquely determined from the state and control. Clearly when $[I - D_u\zeta_u]$ is singular this is not possible. This observation can be used for detecting input data errors.

Airframe and Control System Coupling

The linear airframe model which describes the rigid body aircraft motion and rotor dynamic inflow is given by Equations 126 and 127. The inputs to the airframe linear equations are blade pitch angles of the two rotor systems. The linear flight control system model is given by Equations 131 and 132. The outputs of the flight control system model are also the blade pitch angles of the two rotors. The linear airframe and control system models are coupled by noting that the output of the flight control system model is the input to the airframe model.

$$\begin{Bmatrix} \dot{x}_{ac} \\ \dot{x}_{cs} \end{Bmatrix} = \begin{bmatrix} A_{11} & A_{12} \\ A_{21} & A_{22} \end{bmatrix} \begin{Bmatrix} x_{ac} \\ x_{cs} \end{Bmatrix} + \begin{bmatrix} B_1 \\ B_2 \end{bmatrix} \{\delta\} \quad (146)$$

$$\{y_{ac}\} = \begin{bmatrix} C_1 & C_2 \end{bmatrix} \begin{Bmatrix} x_{ac} \\ x_{cs} \end{Bmatrix} + [D_1]\{\delta\} \quad (147)$$

where,

$$A_{11} = A + B\Pi \quad (148)$$

$$A_{12} = B\Upsilon \quad (149)$$

$$A_{21} = H + E(A + B\Pi) \quad (150)$$

$$A_{22} = F + EB\Upsilon \quad (151)$$

$$B_1 = B\Xi \quad (152)$$

$$B_2 = G + EB\Xi \quad (153)$$

$$C_1 = C + D\Pi \quad (154)$$

$$C_2 = D\Upsilon \quad (155)$$

$$D_1 = D\Xi \quad (156)$$

$$\Pi = [I - ZB]^{-1}(R + ZA) \quad (157)$$

$$\Upsilon = [I - ZB]^{-1} P \quad (158)$$

$$\Xi = [I - ZB]^{-1} Q \quad (159)$$

Concluding Remarks

A linear coupled rotor-fuselage-control system dynamic model is presented in this paper. The model is expected to be useful for flying qualities studies, stability and control investigations, and control design parametric studies. Efforts are underway to produce numerical results for the validation of the model.

References

[1] Miller, D.G., and White, F., "A Treatment of the Impact of Rotor-Fuselage Coupling on Helicopter Handling Qualities," Proceedings of the 43rd Annual Forum of the American Helicopter Society, St. Louis, MO, May 1987.

[2] Talbot, P.D., Tinling, B.E., Decker, W.A., and Chen, R.T.N., "A Mathematical Model of a Single Main Rotor Helicopter for Piloted Simulation," NASA TM 84281, September 1982.

[3] Gibbons, M.P., and Done, G.T.S., "Automatic Generation of Helicopter Rotor Aeroelastic Equations of Motion," *Vertica*, Vol. 8, No. 3, pp. 229-241, 1984.

[4] Lytwyn, R.T., "Aeroelastic Stability Analysis of Hingeless Rotor Helicopters in Forward Flight Using Blade and Airframe Normal Modes," Proceedings of the 36th Annual Forum of the American Helicopter Society, Washington DC, May 1980.

[5] Zhao X., and Curtiss H.C., "A Linearized Model of Helicopter Dynamics Including Correlation with Flight Test," Proceedings of the Second International Conference on Rotorcraft Basic Research, University of Maryland, College Park, Maryland, 1988.

[6] McKillip R., Curtiss H.C., "Approximations for Inclusion of Rotor Lag Dynamics in Helicopter Flight Dynamics Models," Proceedings of the Seventeenth European Rotorcraft Forum, Berlin, Germany, September 1991.

[7] Kane, T.R., and Levinson, D.A., *Dynamics: Theory and Applications*, McGraw Hill Book Company, 1985.

[8] Pitt, D.M., and Peters, D.A., "Theoretical Prediction of Dynamic Inflow Derivatives," *Vertica* Vol. 5, pp. 21-34, 1981.

[9] Prouty, R.W., *Helicopter Performance, Stability, and Control*, PWS Publishers, 1986, pp. 379-441.

[10] Johnson, W., *Helicopter Theory*, Princeton University Press, 1980, pp. 213-216.

[11] Hohenemser K.H., and Yin, S.K., "Some Applications of the Method of Multiblade Coordinates," *Journal of the American Helicopter Society*, Vol. 17, No. 3, July 1972, pp. 3-12.

[12] Peters, D.A., HaQuang N., "Dynamic Inflow for Practical Applications," *Journal of the American Helicopter Society*, Volume 33, Number 4, October 1988.

[13] Gill, P.E., Murray, W., and Wright, M.H., *Practical Optimization*, Academic Press, 1989, pp. 105-115.

Appendix

Skew-Symmetric Matrix Operator

For a vector $a = \{a_1, a_2, a_3\}^T$, the matrix $S(a)$ is defined as,

$$S(a) = \begin{bmatrix} 0 & -a_3 & a_2 \\ a_3 & 0 & -a_1 \\ -a_2 & a_1 & 0 \end{bmatrix}$$

Single Axis Transformation Matrices

The matrices E_1, E_2, and E_3 represent single axis transformations about x, y, and z axes, respectively, and are defined as follows:

$$E_1(\kappa) = \begin{bmatrix} 1 & 0 & 0 \\ 0 & \cos\kappa & \sin\kappa \\ 0 & -\sin\kappa & \cos\kappa \end{bmatrix}$$

$$E_2(\kappa) = \begin{bmatrix} \cos\kappa & 0 & -\sin\kappa \\ 0 & 1 & 0 \\ \sin\kappa & 0 & \cos\kappa \end{bmatrix}$$

$$E_3(\kappa) = \begin{bmatrix} \cos\kappa & \sin\kappa & 0 \\ -\sin\kappa & \cos\kappa & 0 \\ 0 & 0 & 1 \end{bmatrix}$$

Time-Derivative of a Transformation Matrix

Consider the time-derivative of a vector v in two reference frames denoted by A and B. Let the components of v in Frame A be denoted by v_A and those in Frame B be denoted by v_B. Let the angular velocity of Frame B with respect to Frame A be ω and let the components of ω in Frame B be denoted by ω_B. Let T represent the transformation matrix that transforms vector components from Frame B axes to components in Frame A axes. The time-derivatives of v in Frame A and Frame B are related by the following vectorial equation:

$$^A\frac{dv}{dt} = {}^B\frac{dv}{dt} + \omega \times v$$

In matrix-vector format, the preceding equation can be written as,

$$\dot{v}_A = T\dot{v}_B + TS(\omega_B)v_B$$

Also, since $v_A = Tv_B$, one gets for $\dot{v}_A$ the following expression:

$$\dot{v}_A = T\dot{v}_B + \dot{T}v_B$$

Comparing the two equations for $\dot{v}_A$, the following formula is obtained for $\dot{T}$:

$$\dot{T} = TS(\omega_B)$$

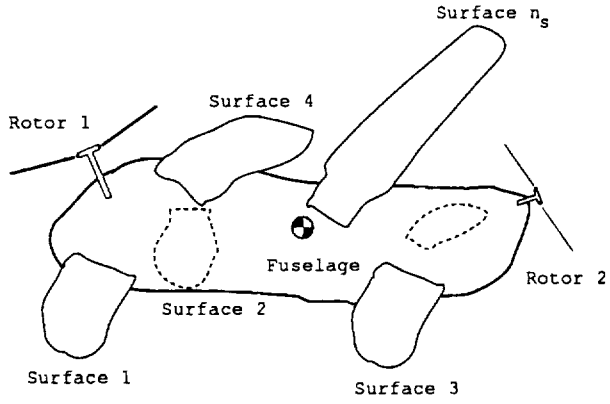

Figure 1: Generic Rotorcraft Configuration

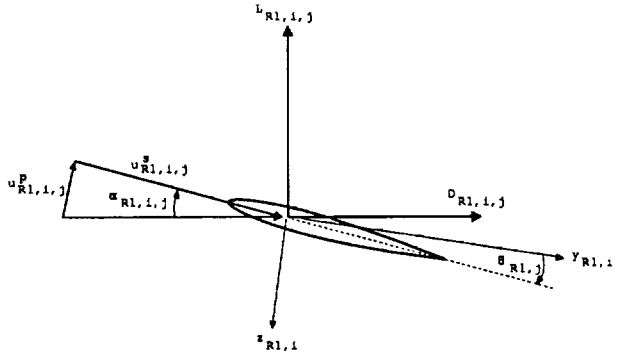

Figure 3: jth Aerodynamic Element of the ith Rotor 1 Blade

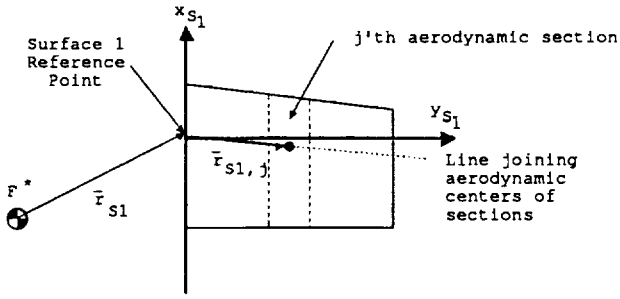

Figure 4: External Surface Aerodynamic Sections

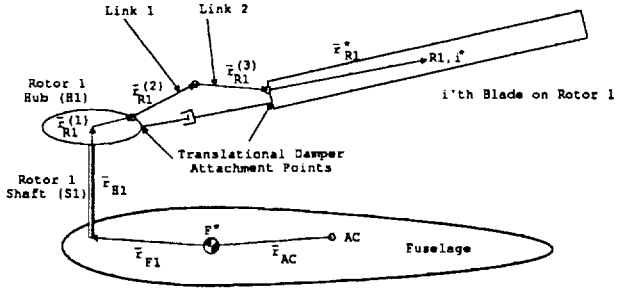

Figure 2: Rotor Blade Geometry

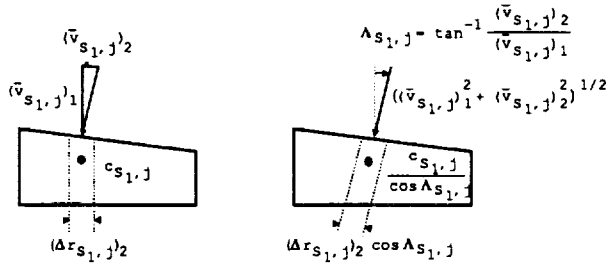

Figure 5: jth Aerodynamic Section of Surface 1 in Yawed Free Stream

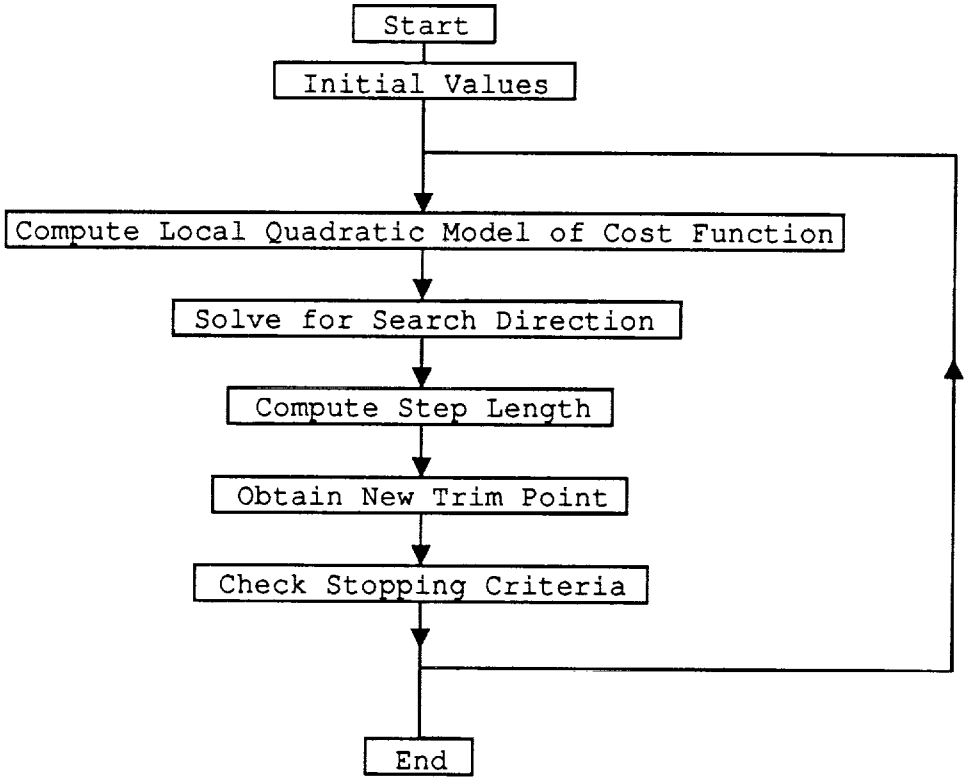

Figure 6: Trim Procedure Flowchart

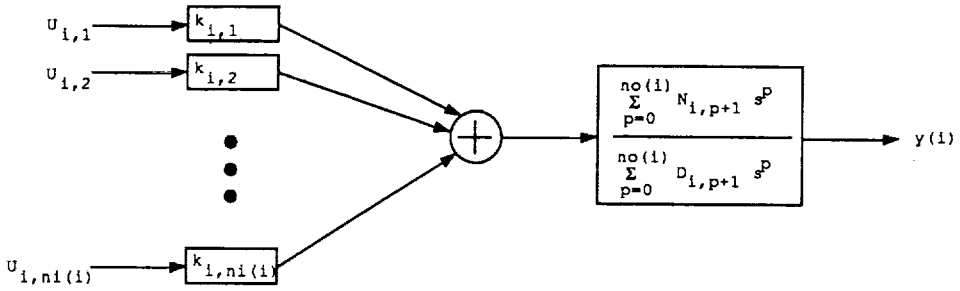

ni(i) = Number of Inputs to i'th Filter

no(i) = Order of i'th Filter

y(i) = Output of i'th Filter

$k_{i,j}$ = Gain Multiplying j'th input of i'th Filter

Figure 7: ith Flight Control System Filter

INTERPRETED COOPER-HARPER FOR BROADER USE

David L. Green
President, Starmark Corporation
Arlington, Virginia

Hal Andrews (retired)
Technical Director, Research and Technology
Naval Air Systems Command

Donald W. Gallagher
Night Vision Operations Project Manager
FAA Technical Center, Atlantic City International Airport, New Jersey

ABSTRACT

The current aircraft assessment process typically makes extensive use of operational personnel during simulations and operational evaluations, with increased emphasis on evaluating the many pilot and/or operator/aircraft control loops. The need for a crew assessment in this broader arena has produced a variety of rating scales. The Cooper-Harper Rating Scale is frequently misused and routinely overlooked in the process, for these applications often extend the scale's use beyond its originally intended application. This paper agrees with the broader application of the Cooper-Harper Rating Scale and presents a concept for the development of a "use unique" Interpreted Cooper-Harper Scale to help achieve this objective. This interpreted scale concept was conceived during efforts to support an FAA evaluation of a night vision enhancement system. It includes descriptive extensions, which are faithful to the intent of the current Cooper-Harper Scale and should provide the kind of detail that has historically been provided by trained test pilots in their explanatory comments.

NOMENCLATURE

CHPRS	Cooper-Harper Pilot Rating Scale
CM	Cockpit Management
DI	Deck Interface
EMS	Emergency Medical Service
FAA	Federal Aviation Administration
HQR	Handling Quality Rating
ICHRS	Interpreted Cooper-Harper Rating Scale
IFR	Instrument Flight Rules
IMC	Instrument Meteorological Conditions
IPR	Interpreted Pilot Rating
LFE	Limit Flight Envelope
MCHRS	Modified Cooper-Harper Rating Scale
NAS	National Airspace System
NFE	Normal Flight Envelope
NOE	Nap-of-the-Earth
OFE	Operational Flight Envelope
PR	Pilot Rating
VMC	Visual Meteorological Conditions

Presented at Piloting Vertical Flight Aircraft:
A Conference on Flying Qualities and Human Factors,
San Francisco, California, 1993

INTRODUCTION

The Cooper-Harper Pilot Rating Scale (CHPRS) has been very effective in handling qualities research and development applications, serving as an evaluation tool and communications medium in a community of trained experimental and R&D test pilots and engineers. The success of CHPRS has in some measure been due to the discipline involved in its use. This discipline has been instilled thorough training at test pilot schools, use of the scale in the military acquisition process, and because of adherence to the asterisk note which appears on the scale: "Definition of required operation involves designation of flight phase and sub-phases with accompanying conditions".

In Reference 1, Harper and Cooper emphasize the need to follow this stricture. While recognizing the difficulties in doing so, they also recognize the adverse impact of failure to treat this instruction in a comprehensive way.

Currently, the assessment process in new product development for aircraft has taken on a greater operational flavor. This is found both at the project initiation stage, where extensive simulations using operational personnel are becoming the rule, and at the final approval stage where operational personnel hold the final stamp. At the same time, the greatly increased integrated complexity of the pilot machine interface systems increases the emphasis on evaluating the many in-flight dynamic components of the pilot and/or operator/aircraft control loop. This complexity is amplified for rotorcraft, where the total flight regime includes the widest variety of flight path tasks.

The need for a rating scale in this broader arena has required the use of evaluation scales of some sort, and perhaps because piloting considerations are generally involved --- but not always --- the Cooper-Harper scale is frequently used. Sometimes it is misused in this broader context. Sometimes it is not applied because of concern for misuse, or a bureaucratic constraint or because it is simply not understood.

To those who have been trained in the use of the scale, it is clear and provides a concise and useful way for members of the handling qualities community to communicate. To many outside the handling qualities community, a reluctance to apply the scale is evoked by a lack of confidence in the use of subjective pilot evaluations. This group typically desires to use a pass fail criteria pilot (crew) evaluation or alternately base

decisions on quantitative measures alone. It appears that the reservations of some are reinforced by their unsuccessful attempts to use the scale. These attempts may have failed to observe the asterisked stricture of the CHPRS (see Figure 1).

A case can be made for using some other scale, or using the CHPRS with a second overlapping workload scale, or using no subjective scale at all. But because handling qualities are major components of all aircraft pilot/operator assessments, and because the scale has always included consideration of workload, it seems most appropriate to improve our understanding of the existing CHPRS and broaden its applications. To this end, this paper proposes that a well understood, expanded and interpreted version of the CHPRS would:

(1) Help the aviation community define the factors which respond to the asterisk note on the CHPRS, minimizing variance in pilot ratings.
(2) Include a concept which involves developing "application unique" extensions to the descriptive content of the scale to enhance its use by both trained engineering test pilots and by operational evaluation pilots. These expanded definitions will allow pilots to:
    (a) Select a correct rating which may be a whole number or a half pilot rating (PR), and
    (b) provide additional comments which will help others understand the experience underlying the selected rating (in terms which include flying qualities, flying workload, cockpit management (CM) workload and relevant performance measures).
(3) Better explain how experienced subject pilots can predict the suitability of an aircraft for operations in environments not specifically evaluated.

In summary, paper supports the broader application of the current CHPRS and it offers a concept for achieving this objective through the introduction of an use-specific, Interpreted Cooper-Harper Pilot Rating Scale.

COOPER-HARPER RATINGS

Background

The first widely used pilot rating scale was introduced in 1957 and known as the Cooper Scale (Reference 2). This was followed by an interim scale in 1966 (Reference 3) and finally in 1969 the Cooper-Harper rating scale, presented here as Figure 1, was published in NASA TN D-5153 (Reference 4).

The key to effective use of this scale lies in strict adherence to the guidelines contained in References 1 and 4, and in the thorough understanding of the scale's origins, strengths and limitations. In this regard, Harper and Cooper reported in Reference 1 that the "nearly universal use of the Cooper-Harper rating scale for handling qualities assessments is not commensurate with the general lack of access to and familiarity with NASA TN D-5153 (which gives background guidance, definition of terms, and recommended use)". In other words, everybody uses the scale, but few have studied Reference 4 and/or observe the counsel of Reference 4.

It is important to understand that most of the ideas and suggestions in this paper are not new. For the most part, they are over 30 years old and alluded to in the above references. This paper does provide suggested ways to implement the guidance of References 1 and 4 as well as expanding the application of the scale to address the current needs of the industry. In this regard, the following paragraphs quote, paraphrase, and amplify a number of key concepts and instructions contained in the primary references:

A Communication Enhancement Tool

There are two parts to the rating process: "The pilot's commentary on the observations he made, and the rating he assigned. ---- They are the most important data on the closed-loop pilot-airplane combination which the engineer has." (Reference 1). The rating numbers themselves are an aeronautical short hand developed for recording, quantifying and analyzing subjective data. These ratings are a means to an end. They are not the end of the process.

Engineering Test Pilots

The scale in Figure 1 was developed for use by experimental and engineering test pilots. These test pilots typically have an operational background and have been trained to communicate with the engineering community. The military pilot becomes a test pilot after acquiring a personal understanding of the environment, threat and related friendly weapons systems which will define the total combat environment. They then learn (civil or military) to evaluate flying qualities in context with the cockpit workload with a readiness to deal with the environment and the adversity introduced by equipment failures.

Pilot Comments

Engineering test pilots are expected to know how to provide task ratings and comments which are useful in the analysis of the flights they conduct. It is not enough to provide a rating. The pilot must provide comments as to what the pilot experienced. The pilot must report what did and (sometimes) what did not influence the assignment of a given rating. For example, one pilot may use one technique to compensate for a lateral directional oscillation and be very successful, while a second pilot may not understand the best compensatory technique, have a great deal more trouble and assign a poor rating.

Operational Pilots

There are three probable situations where the operational pilots (unschooled in the methods of the engineering test pilots) could be expected to utilize the CHPRS. --- In the ground based and inflight

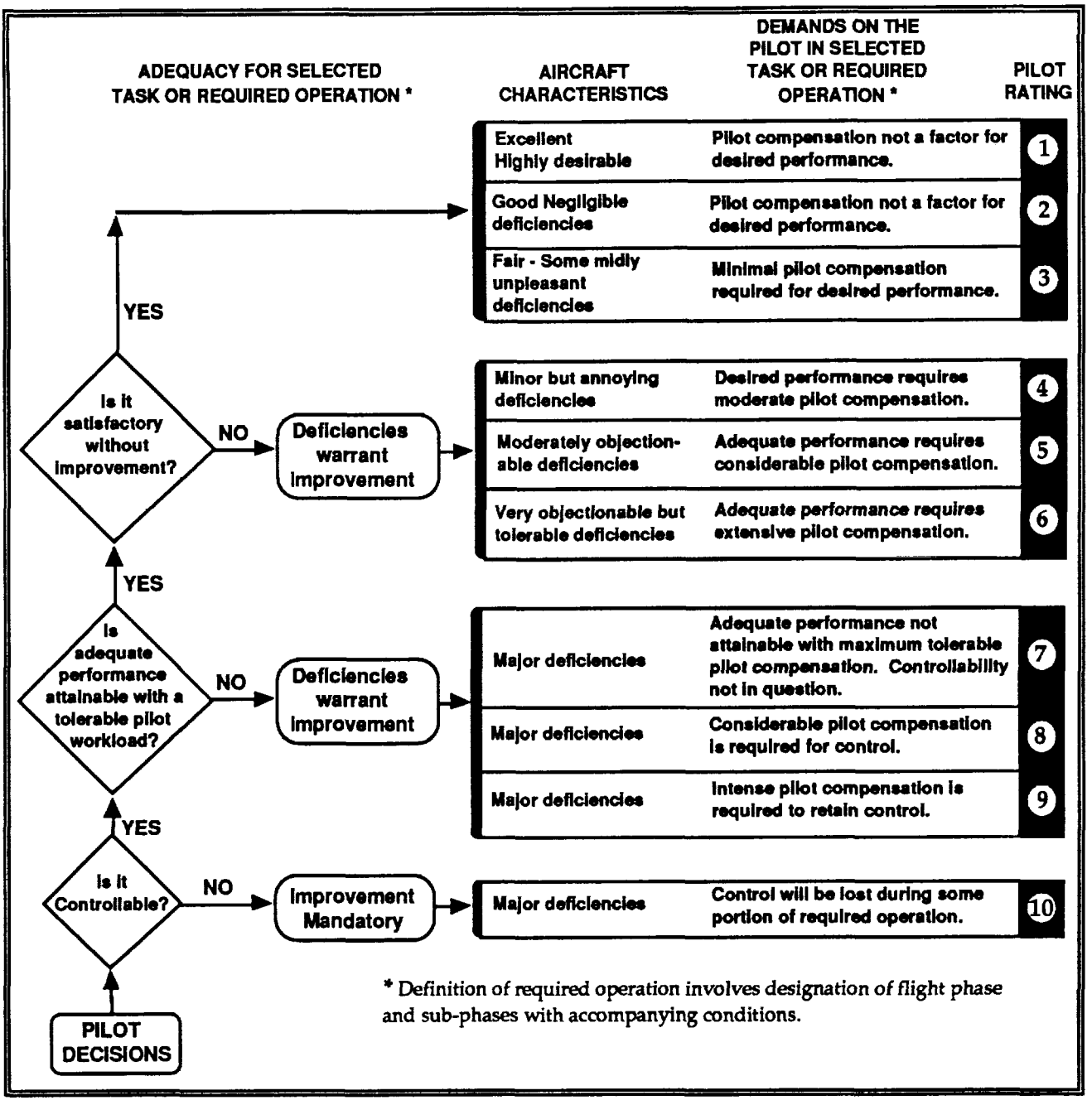

Figure 1: The Cooper-Harper Pilot Rating Scale

simulations cases, the resident simulation staff is very familiar with the use of the CHPRS and they are inclined to attempt to have the operational pilot use the CHPRS. The results of this application are potentially flawed because the operational pilots may not understand the proper use of the scale. --- The scale looks simple, and these otherwise very capable pilots understate their lack of comprehension in an effort to be accommodating.

In the operational evaluation venue, the resident engineers and analysts are much less familiar with the CHPRS and often hesitate to employ it. Here an opportunity for broader use is missed.

In brief, the CHPRS is not sufficiently user friendly for many operational pilot applications unless the pilots and engineers are diligently trained in its use.

The Scale

The scale presented in Figure 1 incorporates 10 ratings. Cooper and Harper feel that these ratings should be adequate for most evaluations (Reference 4). While they also recognize that the use of half rating gradation is appropriate for some applications (e.g. 3.5 and 4.5), they discourage the practice. One reason for this reluctance is obvious. There are no definitions of half ratings.

Another argument against the use of half ratings asserts that ability of pilots to discriminate between flying qualities (workload and performance) is not sufficient to empower them to assign half ratings. The data in Figure 2 argues against this last assertion, for it contains a family of boundaries which separate areas of the flight envelope which were judged by an engineering test pilot to contain flying qualities that differ by one half of one PR. Boundaries of this sort were first identified in Reference 5, and later defined in flight with a small, modern helicopter. Over 60 pilot ratings were recorded during stabilized, standard rate turning flight, while observing error limits of ± 5 knots and ± 50 ft/min. The actual ratings assigned to each area of the flight envelope vary as a function of the accompanying conditions (e.g., turbulence, lighting, visibility, etc.).

Pilot Compensation/Workload Factors

The level of pilot compensation necessary to achieve "adequate" or "desired" performance (see Figure 1) is integral to the use of CHPRS. Implicitly, this compensation is directly translatable to workload. Furthermore, the phrase "definition of required operation" (included in the asterisk note of the CHPRS) serves to include both direct flight control and other flight management functions which the pilot must perform to achieve satisfactory task performance.

In the real world, the pilot approaches a flight task with the expectation that the task is doable. That is, pilots look at all of the sources of workload and attempt to cope with each source in the way which produces the best performance with a minimum of effort. As Harper and Cooper observe in Reference 1, "the pilot adapts". From the view of the systems engineer, the pilot learns how to achieve the desired performance while optimally distributing the piloting (handling qualities) workload and cockpit management (CM) workload. In military combat aircraft, mission equipment monitoring and task execution workload is also involved.

The engineer understands that tasks are distributed by the crew in a natural attempt to avoid spikes in workload which are likely to be accompanied by an unwanted dip in performance. It is this effective search for adaptive techniques which exemplifies the pilot's contribution to crew-machine performance.

As the total workload builds, the pilot may have reason to periodically (albeit very briefly) allocate a high priority to CM tasks and allow errors in the flight path to build during a period of deferred attention. The performance during such unattended periods is therefore judged differently. The pilot who is prepared to allow an aircraft to drift off speed, or roll away from level flight, has substituted new (temporary) limits on

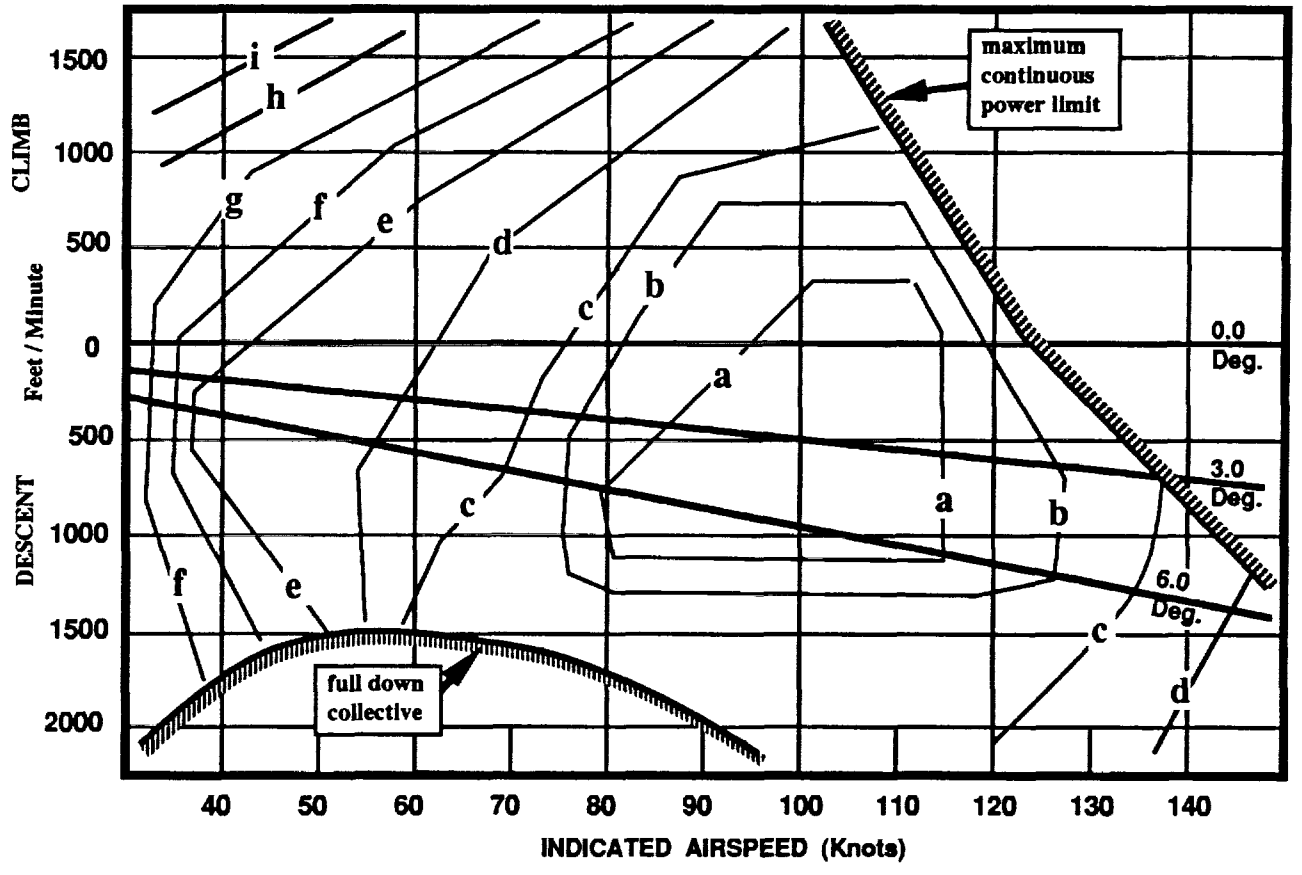

Figure 2: Boundaries of Flying Qualities Which Represent A Change of 0.5 Pilot Rating

the allowable flight path errors. These larger allowable errors apply only during the performance of the priority CM task. Typically, the pilot monitors the aircraft's departure from trim, and if every thing goes well, the CM task is completed during one period of unattended flight. If the aircraft departs too quickly, or is difficult to return to trim, several periods of unattended or deferred flight control activity may be utilized to complete the CM task. Pilots evaluate such shared attention requirements and make a determination as to suitability.

Pilots also develop CM techniques which minimize the time required to accomplish CM tasks. For example, they learn how to identify switches by location, shape and mode of operation. This allows them to find a switch while focusing their eyes on a flight control task. The mind is obviously able to share its attention more rapidly than the eyes, especially when head movement is required.

In addition, pilots who are faced with the need to use the right hand to conduct a CM task may use the left hand to control pitch and roll during the CM event. A pilot may also use a knee to hold a collective in position, or use both feet on the directional controls to keep the aircraft level in roll. Such techniques may result in substantially less deviation from the desired flight path with little or no increase in total workload. This is the way pilots learn to get the job done in the real world. Test pilots know these techniques and engineers need to report which ones they use.

When pilots encounter a task which is not doable, many will attribute the failure to a personal inability. But, the more experienced the pilot, the less likely this will occur. Never-the-less, this is one more reason why it is very important for the analyst to understand the attitudes of subject pilots.

In the vein of doable tasking, the "unexpected" typically places the ultimate stress on crew performance. The occurrence of unplanned events such as equipment malfunctions, unexpected route changes and unforecast weather are all a part of the equation. A totally correct evaluation of these events typically requires a concomitant engineering analysis to determine the probability of a given event.

Defining The Task

The CHPRS (Figure 1) contains a note which is often given less than adequate consideration. The note refers to the "task" or "operation" and alerts us to the effect: "Definition of required operation involves designation of flight phases and sub-phases with accompanying conditions."

Flight Phases and Sub-Phases. If we translate the definitions of flight phase and sub phases as stated in Reference 4, we find that hovering flight and cruise flight are two typical flight phases. Activities associated with achieving a 40 ft hover is a sub phase. Maintaining a steady 40 ft hover is also a sub phase.

Accompanying Conditions. The factors which collectively define "accompanying conditions" substantially influence the assignment and analysis of pilot ratings. Typically, the project engineer must define accompanying conditions prior to the flight for they at least partially define the test objective or "scope of test". The pilot needs this guidance to accomplish the desired evaluation. The actual accompanying conditions, observed during the execution phase, must be recorded to support the best possible analysis and avoid unexplainable variance in the data.

The factors which define some rotorcraft tasks can normally be selected from a list like the partial one presented below:

(1) VMC or IMC task
- type of cue field and display augmentation
- display system

(2) Performance Objectives
- altitude (absolute or as measured by radar altimeter)
- horizontal position error (X and Y)
- heading variation limits
- main transmission torque limits
- engine operating limits
- attitude variation limits during corrections ($\pm$ degrees)
- attitude variation allowed as the result of a gust or turbulence
- time available to conduct non flight control cockpit tasks (schedule of shared time)

(3) Environmental Factors
- underlying surface
- near field visual screen
- far field visual screen
- near hazards-obstructions to hover
- lighting
- visual range
- obstructions to visibility
- precipitation
- smoke, fog. dust, snow, sun.
- glare, sun, moon, reflections

While most of the flying qualities community clearly understands the importance of the items listed under (1) and (2) above, the environmental factors under (3) seem to be less appreciated and are more often than not treated in too general a way. For example, limit environmental conditions are sometimes established by as few as one or two parameters (e.g., visibility). Such an abbreviated treatment is often inadequate, especially in the case of helicopters required to operate to and from a variety of fixed and moving platforms, in a rapidly changing air mass, day and night. Figure 3 was adapted from Reference 5 to expand on the list above and to illustrate the variety of conditions which

may be of interest during rotorcraft evaluations. While this figure is admittedly incomplete, figures like this should be provided so that pilots and engineers can accurately define sets of conditions for evaluation. In the real world, we find that rotorcraft pilots are interested in a variety of environmental conditions, any or all of which can represent a limit condition.

Before leaving this subject, it is important to recognize that the introduction of "usable cue environments" in Reference 6 is an important contribution and a significant step in the right direction, as is the Navy's deck interface (DI) testing methodology which recognizes ship motion, lighting, wind, and other factors identified in Figure 3.

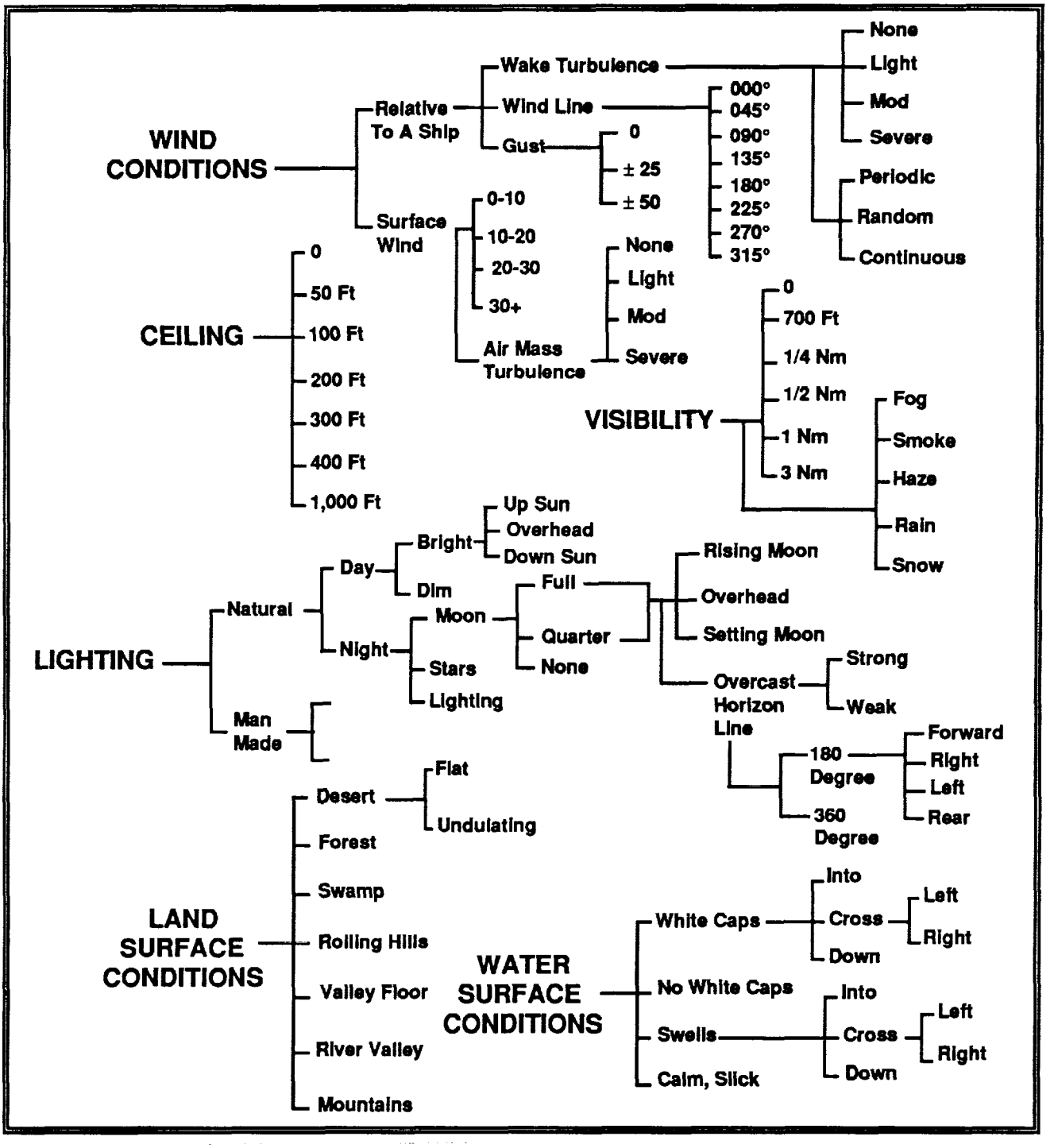

Figure 3: Characteristics Defining Operational Environment

FLIGHT CONDITION	ATMOSPHERIC DISTURBANCE								
	LIGHT			MODERATE			SEVERE		
	FLIGHT ENVELOPE								
	NFE	OFE	LFE	NFE	OFE	LFE	NFE	OFE	LFE
PROBABLE CONDITION	S	S	A	A	C	C	C	C	C
IMPROBABLE CONDITION	A	A	C	C	C		C		

S = SATISFACTORY A = ADEQUATE C = CONTROLLABLE

NFE: Normal Flight Envelope OFE: Operational Flight Envelope LFE: Limit Flight Envelope

Figure 4: Probability Guidelines and Minimum HQ Requirements

Probability of Encounter

The probability of encountering adverse environmental factors is another important consideration when evaluating the suitability of flying qualities and workload of a real aircraft. It would appear that the probability of encountering certain environments can be treated in a way that is similar to the treatment of failure modes as addressed in References 6, 7, 8 and 9.

In this regard, McElroy does an excellent job in Reference 10 of addressing and the probability of simultaneously encountering specific levels of atmospheric disturbance and failure states in context with flight envelopes. Figure 4 has been reproduced from Reference 10 as it is an excellent summary of the author's concept. In support of this figure, the author observes that the FAA could use subjective pilot ratings (from a scale like that in Figure 1) to determine compliance with the criteria "satisfactory," "adequate," and "controllable" (Figure 4), an idea which is still new to much of the FAA.

Analyzing Environmental Effects

Plotting pilot rating data as a function of one or more variables will often help the analyst develop the highest degree of confidence in the data. This concept is demonstrated in Reference 11 which presents a family of six data plots (one each for 5, 10, 15, 20, 25, 30 knots of wind), two of which are characterized in Figure 5. Observe that pilot ratings are plotted as a function of azimuth for two wind speeds.

Note that pilot ratings vary as a function of both wind speed and azimuth. Although not shown, the ratings can also vary as a function of gross weight, power available, center of gravity, rotor RPM, turbulence, visibility, lighting, and a host of other variables. If you inspect the 5 and 15 knot data for the wind azimuth of 300°, you will note that the pilot rating changes from a respectable PR 3 at 5 knots of wind to a relatively poor rating of PR 5 at 15 knots. But why? The pilots comments should provide the best insight. This is a clear demonstration of the need for pilot comments.

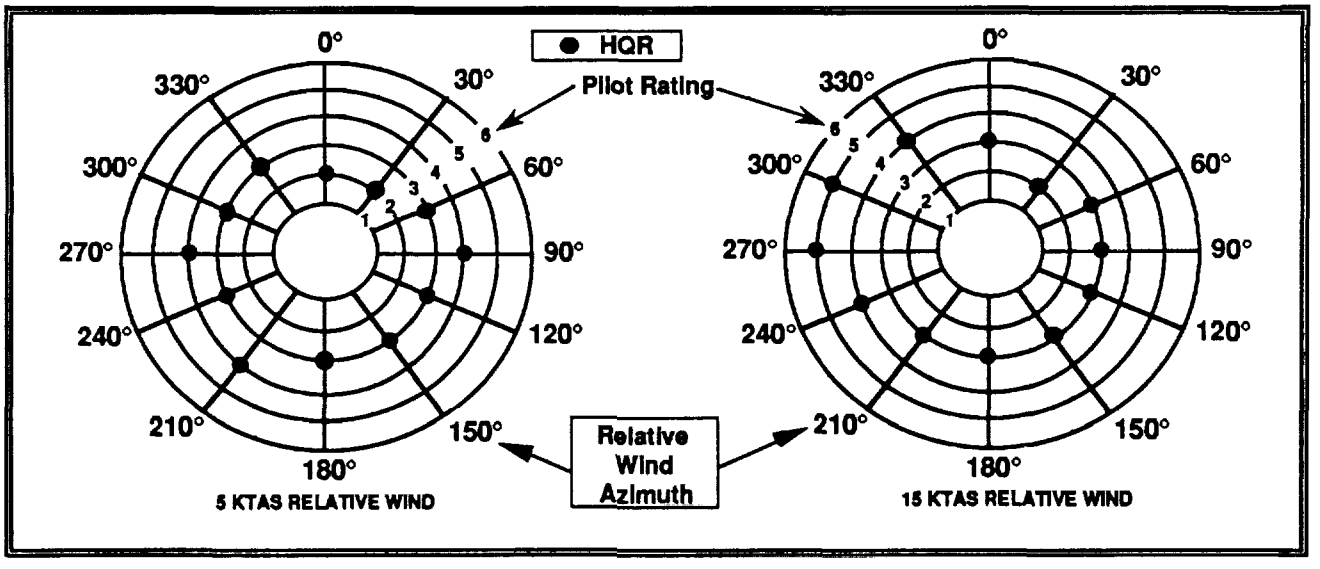

Figure 5: Handling Qualities For Various Wind Azimuth Angles (Pre-landing hover) Over Deck of Small Ships

Evaluating Simulation Facilities

Pilot ratings can also be used to evaluate the authenticity of a simulator. One way to check the authenticity of the simulation is to ask the crews to evaluate (or interpret) the simulator visual and motion systems while simulating an aircraft with which they are familiar.

To illustrate this application, the results of a hypothetical simulator evaluation are presented here as Figure 6. This figure contains the possible result of a day flight and a night flight in an existing helicopter followed by an attempt to replicate the real world test conditions in a ground based simulator. The data shown for "Bright Day - Actual Flight" in this figure is taken directly from Figure 5. In this illustration, the pilot's "actual flight" PRs and "simulated flight" PRs are approximately equal for the dark night case, but the data for the bright day case reveals a significant disagreement. The comments accompanying the pilot's ratings should confirm the ratings and provide insight into the probable cause. Depending upon the comparative evaluation of the pilot's control activity and overall performance, the findings would seem to suggest that the visual representation lacked adequate authenticity in the "bright day" case. In contrast, the dim, night scene was adequate. This is an important finding in and of itself.

The results of a second hypothetical evaluation are presented in Figure 7 which illustrates an alternative format for evaluating the authenticity of a simulator. In this case, the pilot first uses a real helicopter to conduct a demanding task in seven different, real world environments. The seven combinations have been plotted in ascending order for convenience.

When the same pilot attempts the identical task in the simulated environments (duplicated in the simulator), the pilot ratings should agree. If they do not agree, the pilots comments associated with each rating should provide useful data as to the cause of the difficulty. That is, an analyses of pilot control activity, attitude error, flight path error, etc., should include an equally exhaustive analysis of pilot comments.

Minimizing Variability In Ratings

Variance in PR data feeds the argument that the subjective rating approach can produce erroneous results. Cooper-Harper tell us to expect a limited amount of variability in ratings. Disparity in pilot background can produce variation in the pilot ratings. In addition, Cooper-Harper tell us that some pilots may be predisposed for or against a given configuration. In addition, some variability in PRs may simply reflect the presence of one or more factor(s) which were not accounted for in the definition of the experiment. That is, an important factor may not have been recorded.

Most of these sources of variability can be minimized through diligent planning. In particular, pilots and engineers are urged develop a table such as that included as Figure 3. Once the data are collected, presentations formats such as those suggested by Figures 5, 6 and 7 can help the analyst develop the best possible understanding of PR data and at the same time minimize the possibility of scatter in the data.

Extrapolations

The CHPRS authors recognize that some would have pilots evaluate only the situation experienced (first hand) by the subject pilot. Others would have pilots use a simulator evaluation experience to predict/-extrapolate to the real world. For example, assume that during a landing experiment, employing an inflight simulator, the pilot evaluates the test configuration only on a clear, bright sunny day. The pilot could then be asked to rate only the situation flown, (clear day to a runway), or alternately, the pilot could be asked to extrapolate the clear day observations into a dark, wet night environment.

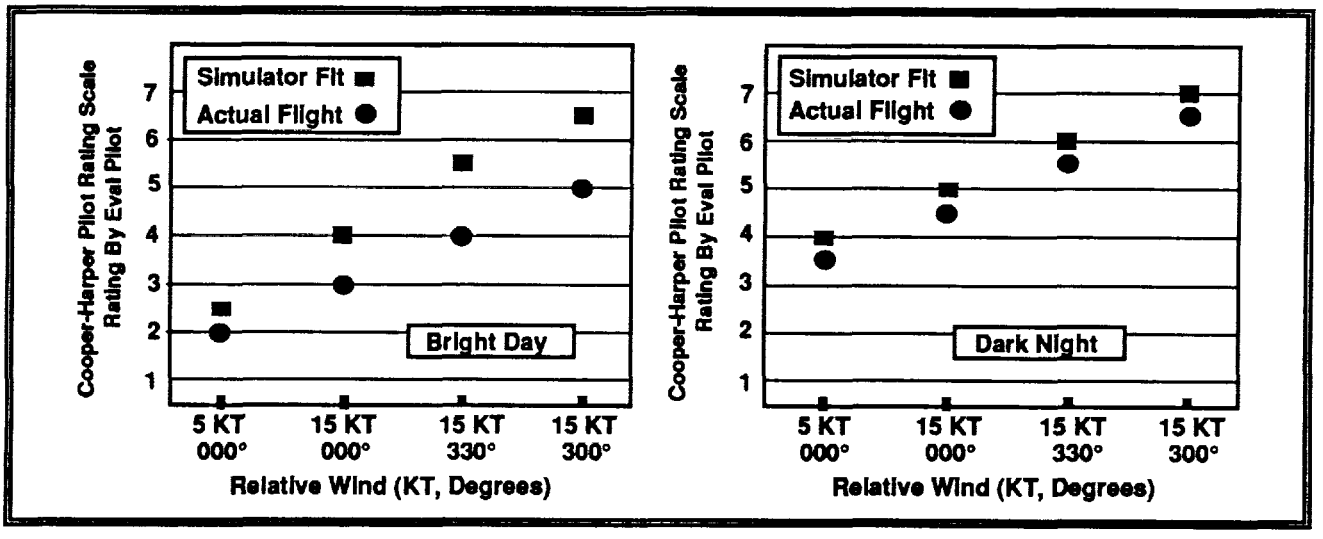

Figure 6: Comparison Of Pilot Ratings To Evaluate A Simulation Facility

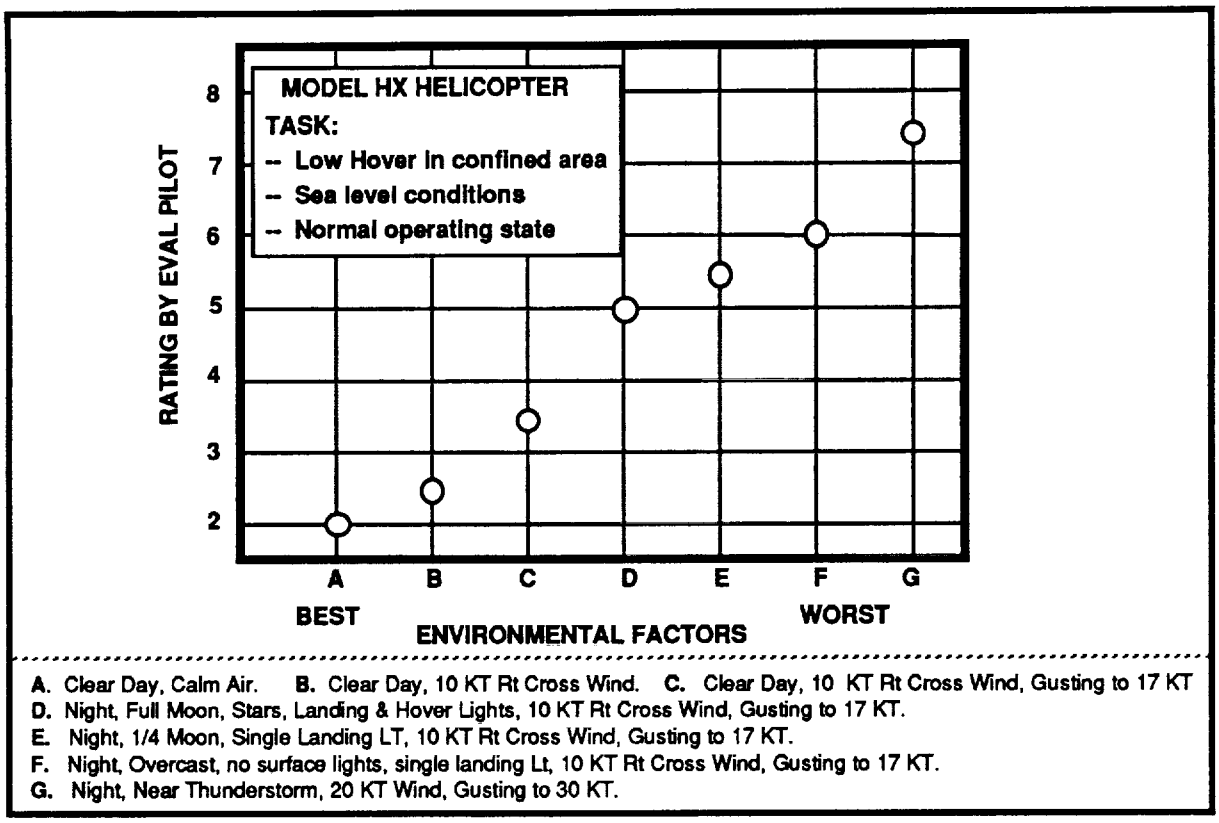

Figure 7: An Example Set of Progressively More Difficult Environmental Conditions Which Can be Evaluated in the Real World and Replicated in a Simulator to Collect Pilot Ratings for Evaluation of a Simulation Facility

Cooper-Harper agree that a pilot can extrapolate this experience and provide a rating for an environment worse than that observed in a hands-on evaluation. This of course assumes that the pilot has acquired an adequate understanding of the aircraft and is familiar with the operational environment of interest. Cooper-Harper go on to ask the question "... if the pilot doesn't do it, who will?". They also go on to conclude that an experienced pilot is probably the best qualified to extrapolate simulator experience into the real world.

The same ability to extrapolate has been recognized and utilized in the military and FAA evaluations of aircraft for at least forty years. That is, an experienced pilot is often asked to conclude in a few flights, that a given aircraft is, or is not, suitable for flight into instrument conditions without ever flying into instrument conditions. Regardless of the approach taken, the pilot and engineer should agree on which approach they will use and this selection should be reported with the data. This note of caution is supported by Harper and Cooper in Reference 1.

WORKLOAD AND INTEGRATED EVALUATIONS

With the increased use of computer based systems, the pilot's task has shifted more and more towards the overall flight management function. In minimum crew (one or two place) military combat aircraft, these system advances have added to the mission system functions over which the pilot has direct control. For military aircraft, the same technology advances have greatly expanded the functions of non-pilot air crew mission system operators - and increased the thrust towards the use of a minimum crew.

On the civil side, there is the potential of single pilot IFR helicopter operations, including approaches to busy airports and slow speed steep approaches into confined landing sites. These operations bring a similar concern for increased cockpit complexity and higher workload.

Workload

These developments have increased the attention of specialists in human task performance to the measurement of pilot and air crew workload, with recognition that in-flight measurement is needed to fully characterize the actual experience. Issues of objective vs. subjective measurement have received continuing attention in this field as elaborated in References 12 and 13. Due to the complexity of the total in-flight workload and the intrusiveness of available objective measurement techniques, there has been increasing acceptance of and support for subjective measurement.

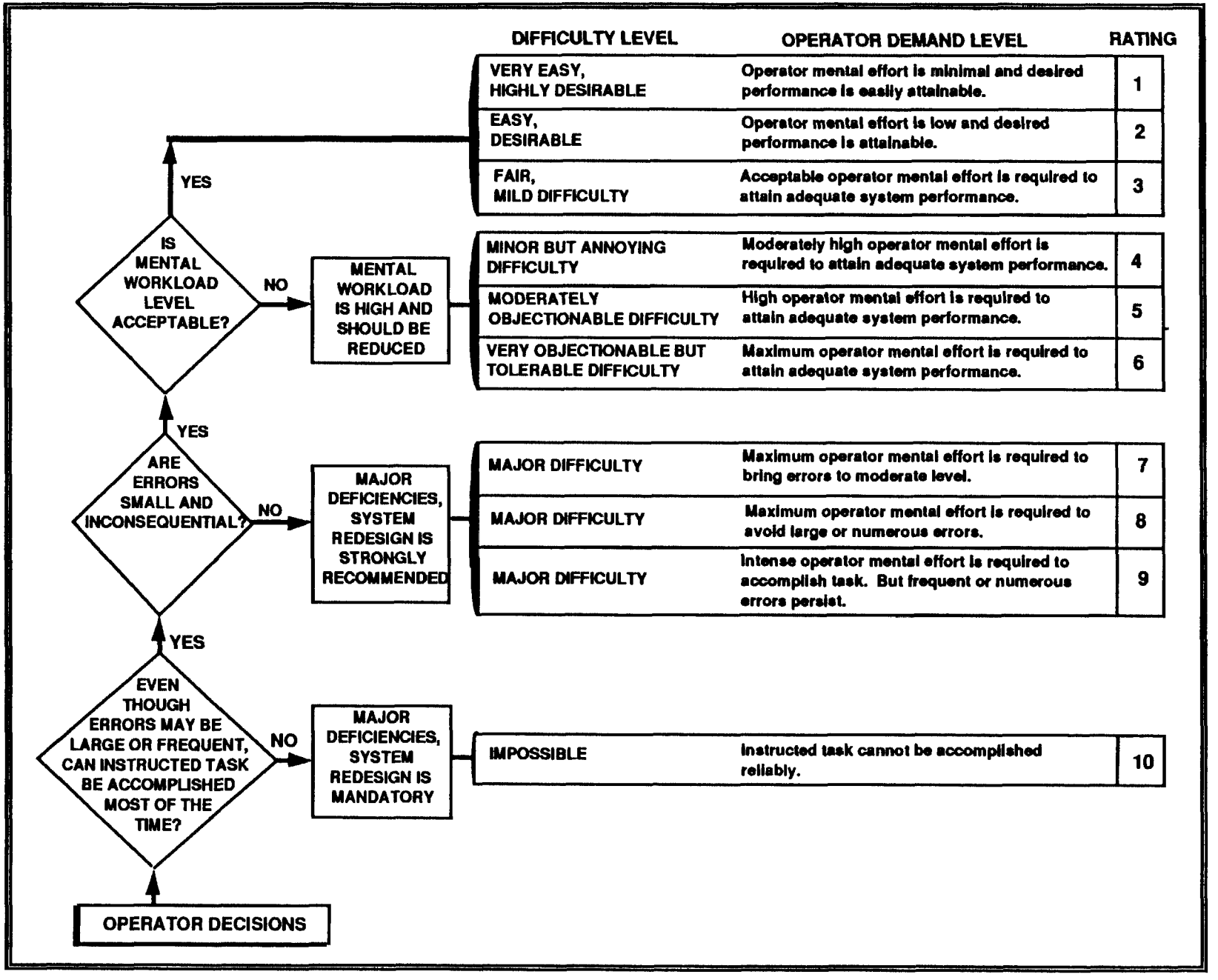

Figure 8: Modified Cooper-Harper Scale

Subjective measurements schemes that have been evaluated (Reference 14) indicate that some of them, while useful in laboratory investigations of pilot or operator workload, are quite cumbersome and too time consuming in ground based flight simulator or in-flight use. Chambers and Hilmer in Reference 14 clearly show the advantages of Weirwille's proposed Modified Cooper-Harper Rating Scale (MCHRS) (Figure 8) for workload assessment in both piloting and non-piloting tasks in these applications. The brief treatment in that paper, however, does not go on to point out other benefits of its use for these applications.

For example, the familiarity of engineering test pilots, simulation staff and flight test engineering personnel with the CHPRS provides a direct carry over to use of the MCHRS. This should allow its use in both workload measurement per se and in the evaluation of non-piloting flight management and mission systems, either individually or as part of the integrated overall pilot/pilot and mission specialist task. In the case of these applications, strictures similar to those which accompany the CHPRS would have to be developed. This would including the need for subject comments similar to those provided by pilots in the CHPRS.

Need For Single Integrated Rating

While separate assessments of handling qualities and workload can be useful in research investigations, for example Reference 15 contains the results of one such effort, this approach fails to give the decision maker a readily usable answer regarding operational suitability.

Decision makers need an overall rating which reflects the total suitability of the aircraft to accomplish its mission when operated by the typical air crew for which the aircraft was designed. For civil aircraft, FAA certification is the final go/no go decision. For military aircraft, the formal Operational Evaluation is the final stamp. But the use of the CHPRS to primarily evaluate flying qualities (with consideration of flying and CM workload inferred) and the use of the MCHRS as a sub-set to the CHPRS to evaluate workload, does not provide the desired single rating. It also fails to deal with comparative priorities (e.g., the flying task vs. the CM task). Another approach is needed.

INTERPRETED COOPER-HARPER PILOT RATING SCALE

Introduction

The preceding discussion has suggested that there is a need to apply the CHPRS more broadly while observing the strictures more diligently. This includes the need for a scale which is easier for operational pilots to use and which treats workload a bit more directly. This need includes both flying and the non-flying, cockpit management workload and the related priorities. In addition, there is the need to define half pilot ratings.

An example of how all of this might be accomplished is presented in Figure 9. The Interpreted Cooper-Harper Pilot Rating Scale (ICHPRS), as addressed here, is meant to have the same meaning as the original CHPRS of References 1 and 4. The concept also applies to the entire scale, but a complete treatment is beyond the scope of this paper. When compared to the CHPRS in Figure 1, it is quickly obvious that the first "pilot decision" steps are not included in Figure 9. In military version of this scale, these pilot decisions steps would be retained. In the civil version, they might not be retained (as suggested in Reference 16).

Half PRs

As discussed earlier, half PRs accomplish two objectives. First, they allow pilots to evaluate a condition or situation which does not meet the definition of a whole number in the CHPRS. Second, the half ratings allow the pilot or analyst to build a higher degree of confidence as to where the boundaries of interest are located. But the CHPRS does not provide definitions and, depending upon the application, this can represent a serious problem.

In contrast, the ICHPRS does include definitions for half ratings. These half ratings relate to the preceding whole integer rating and not to the subsequent rating. The logic of this approach is more apparent when one considers the transition between PRs of 3 and 4, and the PRs of 6 and 7 (especially when considering many of the military applications). Civil evaluators may draw the lines of suitability elsewhere with the same concern.

"Use Unique" Interpretative Narrative

The narrative in Figure 9 is meant to suggest an approach, not "the only" or "the recommended" approach. In most cases, the narrative in the ICHPRS should be developed by one or more engineering test pilot(s) and engineer(s) familiar with the test aircraft, its operational characteristics, and its operational requirements. This should produce one or more aircraft-mission unique scale(s), depending upon the scope of the evaluation.

The added descriptors might evolve during the initial shake down of an aircraft or during a familiarization period in the aircraft or in a simulator (if a real aircraft is not available). In any event, the use of a trained engineering test pilot, familiar with the Cooper-Harper scale, is strongly recommended.

Note that the descriptions under "Aircraft Characteristics" in Figure 9 are identical to those found in the CHPRS presented in Figure 1. The narrative under "To Achieve the best attainable performance" has two parts. The first part (left column) repeats the descriptions found in the CHPRS. The second part (right column) is split into two horizontal boxes. These two boxes contain the interpretive narrative for one whole PR and the associated

half pilot rating. Note that this second column contains comments relating to both flight control and CM tasking, including indications of priority and performance.

The final column (under Representative Observations) amplifies the preceding descriptions of the pilot effort required by characterizing performance in terms of operational suitability. Here, examples are provided to aid the pilot in efforts to discriminate. As described in References 1 and 4, failure to meet the intent of any specific rating forces the pilot to assign the next higher rating.

Performance. Performance objectives must be defined prior to commencing an evaluation. These objectives must relate to tasks for which the pilot expects to achieve minimum error, or for situations where the pilot desires to maximize time out of the loop to rest or to conduct a CM task during which some amount of flight path error is acceptable. For example, this might characterize the shared monitoring of the aircraft's flight path and a mission equipment display.

In this regard, CM tasking could to be evaluated to determine the critical tasks and the procedures which apply. What CM tasks must be accomplished during high gain flight control events? This includes consideration of failure modes. For example, if an engine fails, is the pilot expected to continue the task and deal with the emergency procedures, or does the pilot first transition to a new flight phase?

The interpretative narrative can include detailed references to performance expectations or objectives for both the flying and the CM tasks. That is, there is no reason why performance objectives should not be inserted in the narrative. It seems likely that this approach would reduce the potential for variance, but in some situations, this level of detail would probably not be necessary.

Definitions. Once the performance objectives have been defined, and the narrative has been drafted, definitions should be developed and supported with examples where required.

Performance Priority. The narrative in Figure 9 was developed with the idea that the flight path performance of the aircraft was the primary or critical objective. It is also possible to have situations where CM is of paramount concern. The narrative would be written appropriately for such flight phases to reflect these changing priorities. For example, it may be important accomplish an electronic warfare task in a very precise and timely way, while operating at altitudes and speeds which minimize concern for flight path error.

AIRCRAFT CHARACTERISTICS	DEMANDS ON THE PILOT IN SELECTED TASK OR REQUIRED OPERATION *		PILOT ** RATING
	To Achieve the best attainable performance.	Representative Observations	
Minor, But Annoying Characteristics	Desired performance requires moderate pilot compensation	Pilot must concentrate on flight path errors. CM tasks are accomplished following standard procedures.	Occasional relaxed control is possible, but workload sometimes results in unwanted deviation. Pilot is impatient and fatigued during extended operations.	4
		Pilot must concentrate on flight path errors. CM procedures are altered to accommodate reducted pilot capacity to monitor cockpit status.	Relaxed control is unachievable. Considerable compensation sometimes required. Pilot quickly impatient, quickly fatigued. Not accepted as the norm for the duration of routine or probable flight.	4.5
Moderately Objectionable Characteristics	Adequate performance requires considerable pilot compensation.	Pilot attention is fully focused on early error detection. Pilot is often unable to effectively plan and execute cockpit management tasking in accordance with standard procedures.	Performance is marginal for a precision task and is not acceptable for routine or probable operations. Pilot does not have the time to adequately monitor status of CM tasking.	5
		Concentration on error detection and compensation is intense, and approaching limit. Many cockpit management tasks are deferred, some are precluded.	Maximum acceptable compensation is required. Unusual attitude may develop while accomplishing CM task. Pilot is confident of success during 15 min precision and 120 min of improbable operations pursuing a non-precision.	5.5
Very Objectionable But Tolerable Characteristics	Adequate performance requires extensive pilot compensation.	Concentration on flying task is at limit. Critical CM activities are accomplished randomly, as opportunities arise during momentary improvement in flying task performance.	Excessive pilot compensation is required to continue marginally safe operations for 5 min in precision task and 30 to 60 min in non-precision tasks. Pilot is occasionally alarmed at combinations of error, error buildup rate and total workload.	6
		Concentration on flying task is at limit. Adequate flight performance can not be attained if any CM tasking is undertaken.	Compensation is at limit. Acceptable performance will probably only be achieved during very brief periods ranging from seconds to a minute. Pilot will persist only if there is no safer alternative. Aircraft will probably not be damaged is pilot persists. If pilot attempts CM task, aircraft may incur minor damage.	6.5

* Definition of required operation involves designation of flight phase and sub-phases with accompanying conditions.

** If a mission-flight critical cockpit management task can not be accomplished in a timely and effective way, the PR = 7.

Figure 9: An Example of Interpretive Narrative Added to a Portion of the Cooper-Harper Pilot Rating Scale

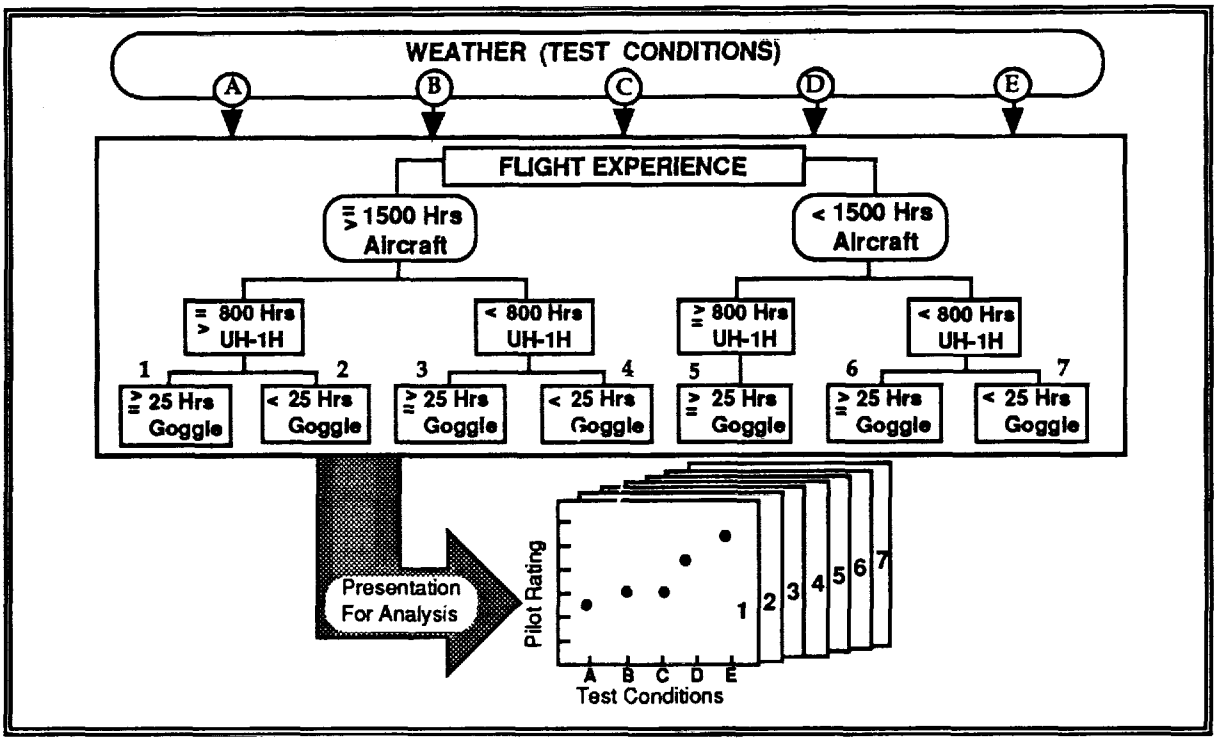

Figure 10: NVG Pilot Rating Analysis Classifications

NIGHT VISION TESTING BY FAA

This paper was in part made possible as the result of work funded by the FAA Rotorcraft Research Program Office in Washington, D.C., and accomplished in support of flight evaluations of night vision devices conducted by the Flight Test Division of the FAA Technical Center, Atlantic City International Airport, New Jersey. The objective of the evaluation was to provide an opportunity for a large number of civil and FAA pilots to fly with night vision goggles (NVGs) to determine their suitability for use by EMS operators.

This evaluation was chartered to use a group of civil helicopter pilots with dissimilar flying backgrounds to examine the safety of flight issues associated with the use of NVGs while operating in a variety of environments. For example, a variety of lighting environments and obstructions to visibility were of interest. --- None of the evaluation tasks involved Nap of the Earth (NOE) flying techniques.

As a result, a set of evaluation guides (booklets) were developed to help introduce pilots to the evaluation, and to help them understand an early ICHPRS. (References 17, 18, and 19). The interpreted pilot rating scale was meant to be faithful to the intent of the CHPRS. This project is currently underway and the results are yet to be documented. ---- The current plan is to sort the pilot rating assessment data and compile the results for each task in a way which is characterized above in Figure 10. This should provide decision makers with data they need to determine suitability in terms of pilot experience and environmental factors.

CONCLUSIONS AND OBSERVATIONS

Cooper-Harper is an effective subjective assessment tool when applied in accordance with its creators full instructions. Extensive successful use in the past, and the evolving "test and approval decision processes" are areas where its effectiveness can be enhanced for current and future applications.

The ability of pilots to extrapolate pilot ratings is a well proven capability which is essential to safe, affordable and timely evaluation of aircraft and simulations of proposed aircraft designs.

A suitably tailored Interpreted Cooper-Harper Rating Scale as proposed will provide pilots not having an engineering test pilot background with an effective rating system for use in simulations and final operational evaluations.

The effectiveness of using Cooper-Harper in handling qualities evaluations, where workload is a factor in the assessment, strongly supports the use of a proposed Modified Cooper-Harper, appropriately adapted, in specific subjective workload assessment and non-pilot airborne system evaluations.

REFERENCES

1. Harper, Robert P., Jr., and Cooper, George E., *"Handling Qualities and Pilot Evaluation,"* J. Guidance, Control and Dynamics, Vol. 9, No. 5, Sept-Oct 1986
2. Cooper, George E., *"Understanding and Interpreting Pilot Opinion,"* Presented at the 25th Annual Meeting, Institute of the Aeronautical Sciences, 28-31 January 1957
3. Cooper, George E., et al, *"The Revised Pilot Rating Scale for the Evaluation of Handling Qualities,"* CAL Report No. 153, The AGARD Specialist's Meeting on Stability and Control, Cambridge, England, 20-23 September 1966
4. Cooper, George E., and Harper, Robert P., Jr., *"The Use of Pilot Rating in the Evaluation of Aircraft Handling Qualities,"* NASA TN D-5153, National Aeronautics and Space Administration, Washington, D.C., April 1969
5. Green, David L., *"Collecting Rotorcraft and Flight Simulator Data for the Purpose of Determining Transferability of Flight Simulator Experience,"* presented at the Helicopter Simulator Technology Workshop, NASA Ames Research Center, Moffett Field, CA., 24-26 April 1991
6. *"Handling Qualities Requirements for Military Rotorcraft,"* ADS-33C, U.S. Army Aviation Systems Command, St. Louis, MO., Aug '89
7. Code of Federal Regulation Part 27, Appendix B, 1 January 1985
8. Code of Federal Regulation Part 29, Appendix B, 1 January 1985
9. Anon, Military Specification, Flying Qualities of Piloted Airplanes, MIL-F-8685B (ASG), Aug '69
10. McElroy, Collet E., *"FAA Handling Qualities Assessment - Methodology in Transition,"* Thirty-Second Symposium Proceedings, Oct '88
11. Kolwey, Herman G., *"Analysis Tools Derived from Investigating Aerodynamic Loss of Tail Rotor Effectiveness (LTE),"* presented at the Society of Flight Test Engineers 22nd Annual Symposium, August 1990
12. *"Assessing Pilot Workload,"* AGARD-AG-233, Advisory Group for Aerospace Research and Development, Paris/NATO, 1978
13. *"Survey of Methods to Assess Workload,"* AGARD-AG-246, Advisory Group for Aerospace Research and Development, Paris/NATO, 1979
14. Chambers, Randall M., Ph.D., and Kilmer, Kevin J., MA., *"Choosing A Pilot Subjective Workload Scale To Fit Flight Operational Requirements,"* IAR 89-21 (N90-26493), The Wichita State University Institute for Aviation Research, Wichita, KS., October 1989
15. Baillie, S., Kereliuk, S., and Hoh, R., *"An Investigation of Lateral Tracking Techniques, Flight Directors and Automatic Control Coupling on Decelerating IFR Approaches for Rotorcraft,"* NAE-AN-55, NRC No. 29604, National Research Council, Canada, Oct '88
16. Hoh, Roger H., and Mitchell, David G., *"Flying Qualities of Relaxed Static Stability Aircraft - Volume 1,"* DOT/FAA/CT-82/130-I, Final Report, U.S. Department of Transportation, Federal Aviation Administration, Sept '82
17. Green, David L., *"FAA Flight Test Engineer's Guide for Collecting and Evaluating Pilot Assessments of Workload and Performance While Operating with NVGs,"* First Draft, 10 June 1991
18. Green, David L., *"Evaluation Pilot's Guide (Part 1) for Collecting Civil Helicopter Pilot Assessments of VFR En Route Operations Involving the Use of Helmet Mounted, Night Vision Devices,"* Second Draft, corrected 18 June 1991
19. Green, David L., *"Evaluation Pilot's Guide (Part II) for Collecting Civil Helicopter Pilot Assessments of VFR Approach and Departure Operations Involving the use of Helmet Mounted, Night Vision Devices,"* Second Draft, corrected 29 October 1991

IMPROVEMENTS IN HOVER DISPLAY DYNAMICS FOR A COMBAT HELICOPTER

Jeffery A. Schroeder
Aerospace Engineer
NASA Ames Research Center
Moffett Field, California

Michelle M. Eshow
Aerospace Engineer
Aeroflightdynamics Directorate
U.S. Army ATCOM
Moffett Field, California

ABSTRACT

This paper describes a piloted simulation conducted on the NASA Ames Vertical Motion Simulator. The objective of the experiment was to investigate the handling qualities benefits attainable using new display law design methods for hover displays. The new display laws provide improved methods to specify the behavior of the display symbol that predicts the vehicle's ground velocity in the horizontal plane; it is the primary symbol that the pilot uses to control aircraft horizontal position. The display law design was applied to the Apache helmet-mounted display format, using the Apache vehicle dynamics to tailor the dynamics of the velocity predictor symbol. The representations of the Apache vehicle used in the display design process and in the simulation were derived from flight data. During the simulation, the new symbol dynamics were seen to improve the pilots' ability to maneuver about hover in poor visual cuing environments. The improvements were manifested in pilot handling qualities ratings and in measured task performance. The paper details the display design techniques, the experiment design and conduct, and the results.

NOTATION

A_x	acceleration cue longitudinal position, deg (degrees refer to angle subtended at pilot's eye)
A_y	acceleration cue lateral position, deg
$Error_{north}$	vehicle earth-axis position error northward, ft
$Error_{east}$	vehicle earth-axis position error eastward, ft
$f_i(s)$	sensor equalization filter on signal i
g	gravity constant, ft/sec^2
K_x	display longitudinal conversion factor for hover box, deg/ft
K_y	display lateral conversion factor for hover box, deg/ft
$K_{\dot{x}}$	display longitudinal conversion factor for velocity vector, deg/ft/sec
$K_{\dot{y}}$	display lateral conversion factor for velocity vector, deg/ft/sec
L_{δ_a}	vehicle derivative of applied specific rolling moment due to lateral cyclic, rad/sec^2/in.
M_{δ_b}	vehicle derivative of applied specific pitching moment due to longitudinal cyclic, rad/sec^2/in.
P_x	hover box longitudinal position, deg
P_y	hover box lateral position, deg
p	vehicle body-axis roll rate, rad/sec
q	vehicle body-axis pitch rate, rad/sec
s	Laplace operator
V_{north}	northward component of vehicle groundspeed, ft/sec
V_{east}	eastward component of vehicle groundspeed, ft/sec
V_x	velocity vector longitudinal position, deg
V_y	velocity vector lateral position, deg
x	vehicle longitudinal position, ft
x_{cmd}	commanded vehicle longitudinal position, ft
$\dot{x}$	longitudinal heading referenced groundspeed, ft/sec
$\dot{x}_{filt}$	filtered longitudinal groundspeed, ft/sec
$\ddot{x}_{comp}$	complementary filtered longitudinal acceleration, ft/sec^2
$\ddot{x}_{filt}$	estimated longitudinal acceleration, ft/sec^2
X_u	vehicle longitudinal velocity damping, 1/sec
$\dot{y}$	lateral heading referenced groundspeed, ft/sec
$\dot{y}_{filt}$	filtered lateral groundspeed, ft/sec
$\ddot{y}_{comp}$	complementary filtered lateral acceleration, ft/sec^2
$\ddot{y}_{filt}$	estimated lateral acceleration, ft/sec^2
Y_v	vehicle lateral velocity damping, 1/sec
δ_a	pilot lateral cyclic control position, in.

Presented at Piloting Vertical Flight Aircraft: A Conference on Flying Qualities and Human Factors, San Francisco, California, 1993. Originally published as an alternate paper of the 48th Annual Forum of the American Helicopter Society, Washington, D.C., 1992.

δ_b pilot longitudinal cyclic control position, in.
ζ damping ratio
θ vehicle Euler pitch angle, rad
$\dot{\theta}$ vehicle Euler pitch rate, rad/sec
ϕ vehicle Euler roll angle, rad
$\dot{\phi}$ vehicle Euler roll rate, rad/sec
ψ vehicle heading angle, rad
ω natural frequency, rad/sec

INTRODUCTION

A significant effort at Ames Research Center has aimed at developing and flight testing display law design methods for the hover flight regime. The flight experiment of Ref. 1 documented the influence of display dynamics on handling qualities for near-hover maneuvering; the Ref. 2 flight experiment examined the relative merits of two pilot-oriented design goals for the display dynamic response. Both experiments employed a cockpit panel-mounted representation of the AH-64 Pilot Night Vision System (PNVS) symbology (Ref. 3), which is shown in Figure 1. The flight experiment of Ref. 4, following many years of simulation research, examined control and display requirements for VTOL translation, hover, and landing, using an Ames-designed symbology format.

The common theme for all the experiments was the use of a velocity predictor symbol (called the acceleration cue in Figure 1). The emphasis of the research was placed on the specification of that symbol's dynamics. When used with the hover position symbol and the velocity vector, the acceleration cue is the pilot's primary controlled element for regulation of vehicle horizontal position. Although the acceleration cue predicts future horizontal velocities, it is used primarily in combination with another symbol that indicates a desired vehicle horizontal position, to control vehicle horizontal position. For helicopters with angular rate stabilization only, the resulting aircraft position dynamics are difficult to control, as there are approximately three integrations from pilot input to aircraft position response. This separation of the pilot from the vehicle state of interest presents a handling qualities challenge to the display designer. As will be described subsequently, the acceleration cue response to pilot control input must be designed considering the vehicle dynamics and the task requirements to maximize handling qualities and mission effectiveness.

The lessons learned from the three flight experiments provided the foundation for the flight investigation of Ref. 5, whose objectives were 1) to design new display laws tailored specifically to the Apache vehicle dynamics and 2) to compare the resulting handling qualities with those of the existing Apache display laws. While the first objective was achieved, the second was not because the documented representation of the existing Apache display laws used in the flight comparison was not correct. The correct display laws were obtained subsequently, and potential improvements were then shown analytically.

Since that experiment, as will be described, flight data documenting the Apache vehicle response characteristics were obtained that permitted the identification of high-quality design and simulation models. The nature of the identified vehicle response necessitated an extension of the display law design methods described in Ref. 2 and Ref. 4. Thus, the motivation for the simulation experiment described here was to examine the potential benefits of the extended design methods using an improved representation of the Apache vehicle and of its baseline display responses. The following sections detail the display law design methods, the simulation design and conduct, and the results.

DISPLAY LAW DESIGNS

The term "display laws" refers to the equations and scaling that determine the position of the central symbology, namely the acceleration cue, velocity vector, and hover position box (Figure 1). During hover maneuvering using primarily the symbology, the acceleration cue becomes the pilot's primary controlled element. To achieve a hover over the position box, he moves his stick to place the cue on the box, and he maintains it there as the box converges to the display center. The pilot workload to maintain the cue on the box, and the nature of the resulting vehicle trajectory, are the two issues that most impact the design of the acceleration cue dynamics.

These considerations are illustrated in Figure 2, which presents a block diagram of the pilot-vehicle-display system for the case where the pilot is attempting to zero the longitudinal displayed error between the hover box and acceleration cue. The ease of controlling the acceleration cue's position on the display is determined by the transfer function A_x/δ_b, which in turn is determined by the cue's response to each of the aircraft states that drive it.

Given any particular set of dynamics for the cue response to control, the trajectory that the aircraft follows while the pilot maintains the cue on the hover box is determined by the closed loop response x/x_{cmd}. This response must be tailored so that the trajectory is well-damped, with a bandwidth, or "aggressiveness," appropriate for the aircraft mission.

There is a tradeoff between the cue controllability, which affects the pilot workload, and the aircraft position response. In one extreme, the easiest cue to control would be one driven only by pilot control position; however, this would result in poor hovering performance. This problem has been referred to as poor "face validity" (Ref. 6). In the other extreme, the cue position could be driven to show the pilot control inputs required for a quick, well-behaved trajectory, probably resulting in complex control motions and high workload. Finally, the tradeoffs become more critical as the level of vehicle augmentation decreases, since stability margins deteriorate quickly.

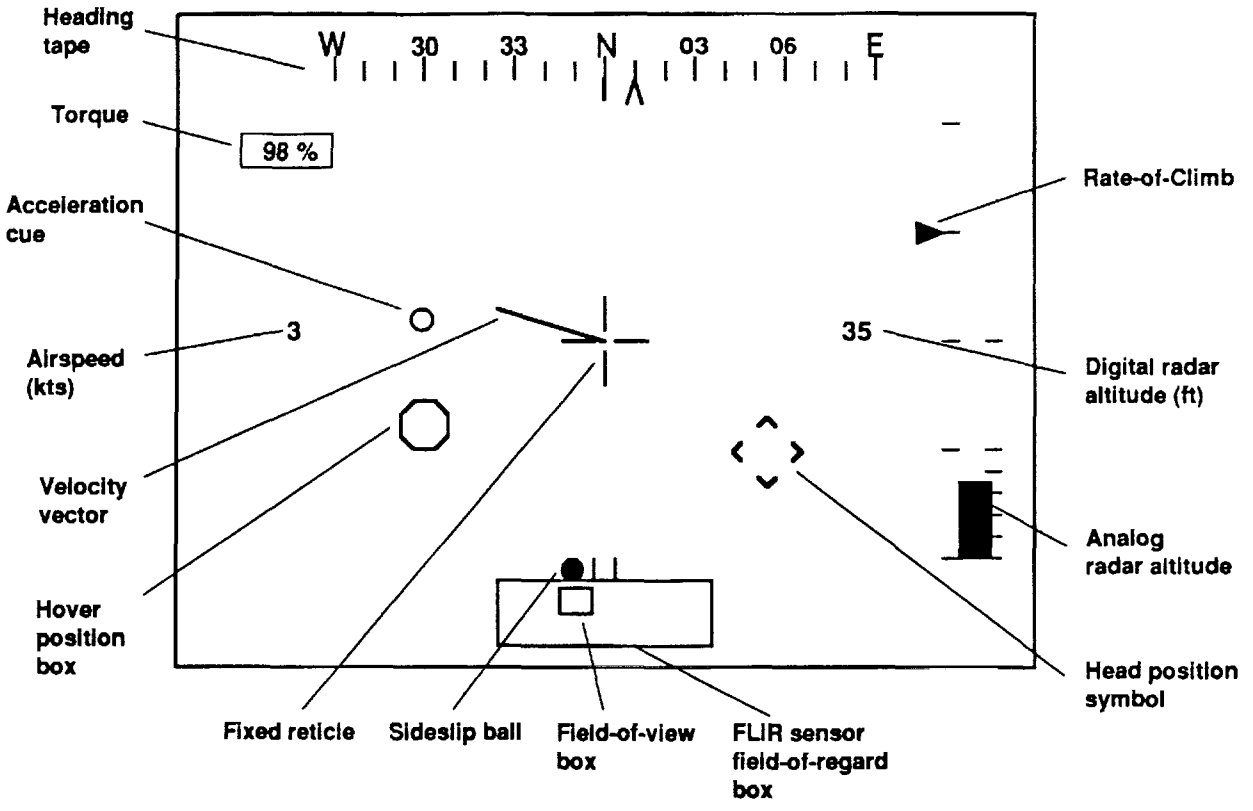

Fig. 1 AH-64 Pilot Night Vision System symbology.

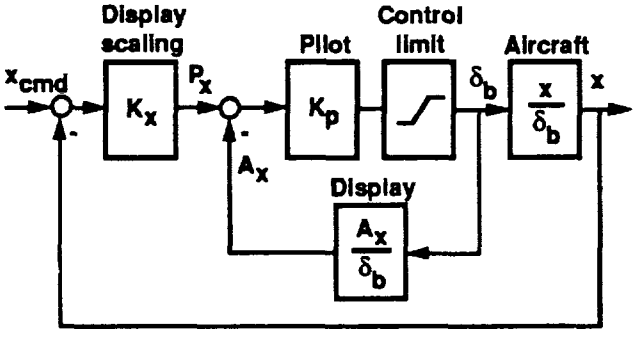

Fig. 2 Pilot-vehicle-display block diagram.

With these guidelines in mind, three methodologies for specifying display laws were examined for the experiment. After brief discussions of the vehicle dynamics model used for the display designs and of the baseline production display laws, a description of each design method is presented. Finally, all the display laws are compared analytically.

Vehicle Design Model

To support the display law design, a mathematical model was needed of the AH-64 Apache (Figure 3) with its Digital Automatic Stabilization Equipment (DASE) on. Parameter identification techniques described in Ref. 7 were used to identify from flight data a low-order model for the DASE-on vehicle near hover. The flight data were part of a larger AH-64 database generated by the Army at the Airworthiness Qualification Test Directorate (AQTD); the flight tests are described in Ref. 8.

The DASE-on design model has decoupled transfer functions with associated equivalent time delays for the longitudinal and lateral responses to pilot input. These were the only responses required for the display design. The following models were identified from flight data that exhibited

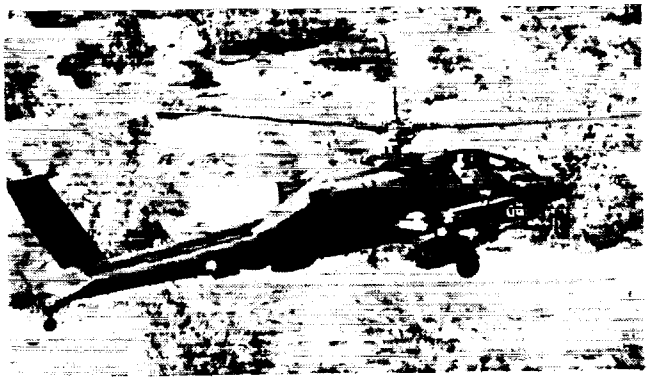

Fig. 3 AH-64 Apache.

excellent coherence in the frequency range of interest (0.2 to 10 rad/sec):

$$\frac{q}{\delta_b}(s) = \frac{-2.49(s+0.262)}{(s+0.399)[0.805;3.46]}e^{-0.103s} \quad (1)$$

$$\frac{p}{\delta_a}(s) = \frac{6.32}{[0.582;4.29]}e^{-0.0425s} \quad (2)$$

where the shorthand notation indicates the second order system $[\zeta;\omega] = s^2 + 2\zeta\omega s + \omega^2$. Note that these high-order rate responses approximate, over the fitted frequency range, the combined dynamic effects of the unaugmented vehicle and its limited-authority augmentation system. Previously, two of the display design methods had been applied to only first-order rate responses; those methods had to be extended to accommodate these high-order identified responses.

Production Display Laws

The PNVS display mode of interest for this study is the Bob-Up mode, which includes the velocity vector, acceleration cue, and hover box symbols. The symbol deflection definitions are shown in Figure 4. Based on unpublished documentation provided by the manufacturer and by the Army's program management office, the equations governing the movement of each symbol are next described.

Hover Position Box

In the current production version of the PNVS software, the hover box is an octagon drawn and scaled to have an edge-to-edge width of 8 ft. It is driven relative to the fixed reticle by the heading-referenced, Earth-axis position error to a pilot-selected point:

$$P_x = K_x(Error_{north}cos\psi + Error_{east}sin\psi) \quad (3)$$

$$P_y = K_y(-Error_{north}sin\psi + Error_{east}cos\psi) \quad (4)$$

Here, the errors equal the desired position minus the current position, and the desired position is the one existing when the Bob-Up mode was selected. The hover box moves opposite to the aircraft motion to show the relative location of the desired position. To re-initialize the box to the current vehicle position, centered on the fixed reticle, the pilot deselects then reselects the Bob-Up mode. The scale factors K_x and K_y are required to convert feet to display displacement, such that full-scale deflection of the center of the box is ±44 ft. The full-scale deflection point is such that the outer edge of the box is just below the heading tape. The values of K_x and K_y were 0.241 deg/ft, where the degrees refer to the angle of display displacement subtended, on the PNVS monacle, at the pilot's eye.

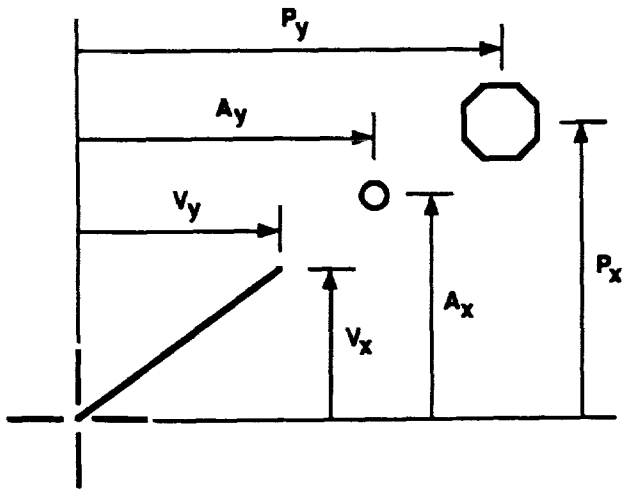

Fig. 4 Definitions of central symbology deflections.

Velocity Vector

The velocity vector tip location relative to the fixed reticle is calculated as follows:

$$\dot{x} = V_{north}cos\psi + V_{east}sin\psi \quad (5)$$

$$\dot{y} = -V_{north}sin\psi + V_{east}cos\psi \quad (6)$$

$$\dot{x}_{filt}(s) = \frac{1}{(s+1)}\dot{x}(s) \quad (7)$$

$$\dot{y}_{filt}(s) = \frac{1}{(s+1)}\dot{y}(s) \quad (8)$$

$$V_x = K_{\dot{x}}\dot{x}_{filt} \quad (9)$$

$$V_y = K_{\dot{y}}\dot{y}_{filt} \quad (10)$$

Where $K_{\dot{x}}$ and $K_{\dot{y}}$ are again scale factors to convert ft/sec to degrees of display displacement. They have the value of 1.03 deg/ft/sec so that the full scale deflection of the vector represents 12.0 ft/sec (7.13 knots). The velocity vector's full-scale deflection point on the display is 15% beyond that of the hover box, or midway into the heading tape.

Acceleration Cue

The acceleration cue center relative to the fixed reticle is calculated as follows:

$$\ddot{x}_{filt}(s) = \frac{s}{s^2+2s+1}\dot{x}(s) - \frac{32.2(s+2)}{s^2+2s+1}\dot{\theta}(s) \quad (11)$$

$$\ddot{y}_{filt}(s) = \frac{s}{s^2+2s+1}\dot{y}(s) + \frac{32.2(s+2)}{s^2+2s+1}\dot{\phi}(s) \quad (12)$$

$$A_x = K_{\dot{x}}(\dot{x}_{filt} + 1.507\ddot{x}_{filt} - 3.013\dot{\theta}) \quad (13)$$

$$A_y = K_{\dot{y}}(\dot{y}_{filt} + 1.507\ddot{y}_{filt} + 3.013\dot{\phi}) \quad (14)$$

Thus the acceleration cue is driven relative to the tip of the velocity vector with an estimate of linear acceleration plus some lead compensation generated by the attitude rate terms.

The three new display design methods applied to the PNVS will next be described. It should be noted that for these new display laws, the display scalings of the three symbols remained invariant and equal to those of the production laws to preserve their operational significance and to provide a consistent basis of comparison among all the laws.

Modified Production Display Laws

The first display law design method did not fully apply the techniques described in the introduction. Rather, it consisted of simply adjusting the gains on the acceleration and attitude rate terms in the production cue equations and the time constants of the velocity vector filter. The motivation for this design was to investigate whether simple changes in the existing equations, requiring no additional sensor information, would favorably impact handling qualities on AH-64's in the current fleet. The adjustments were made empirically based on a goal of improving the vehicle position trajectory response when the pilot is adopting the guidance strategy of placing the cue on the position box during the capture.

The transfer function of the controlled element, $A_x(s)/\delta_b(s)$, that results for the production display laws has an underdamped complex pair of zeros in its numerator (at -0.48±j0.66 rad/sec). These underdamped zeros result from the interaction of the display feedbacks with the heavily filtered groundspeed signal. If the velocity filter breakpoint is moved from 1 rad/sec to 10 rad/sec, the underdamped complex zeros are eliminated. This modification to the sensor filtering alone would likely result in increased cue noise in flight. So in combination with the above filtering change, the gains on high-frequency inputs (accelerations and attitude rates) were lowered. The lowering of these gains was accomplished while trying to achieve vehicle-display dynamics having an integrator-like response to pilot input in the crossover frequency range (Ref. 9). This design was developed during the simulation, and the authors recognize that depending on sensor signal quality in the AH-64, increased gains could improve this cue's response. The final equations for the modified production design were as follows:

$$\dot{x}_{filt}(s) = \frac{1}{(0.1s+1)}\dot{x}(s) \tag{15}$$

$$\dot{y}_{filt}(s) = \frac{1}{(0.1s+1)}\dot{y}(s) \tag{16}$$

$$V_x = K_{\dot{x}}\dot{x}_{filt} \tag{17}$$

$$V_y = K_{\dot{y}}\dot{y}_{filt} \tag{18}$$

$$A_x = K_{\dot{x}}(\dot{x}_{filt} + 1.290\ddot{x}_{filt} - 0.286\dot{\theta}) \tag{19}$$

$$A_y = K_{\dot{y}}(\dot{y}_{filt} + 0.800\ddot{y}_{filt} + 0.160\dot{\phi}) \tag{20}$$

with $\ddot{x}_{filt}$ and $\ddot{y}_{filt}$ defined in eqn. 11 and eqn. 12.

Display Laws Based on Workload Design

The second design employed the philosophy developed in Ref. 2 with an extension of that methodology to treat the identified AH-64 aircraft dynamics. Entitled the "workload" design, this method seeks to reduce pilot workload by providing high-frequency proportional, or gain-like, response of the acceleration cue to pilot input while also assuring desirable trajectory response. The handling qualities benefits of the gain-like response goal were established in the flight experiment of Ref. 2, which compared gain-like responses with integrator-like responses for hover maneuvering using the same display format.

In this method, a display law is specified for the cue in terms of a sum of compensated aircraft states and controls. The aircraft dynamics are then considered in order to define a desirable and achievable cue response to pilot control. This desired transfer function is next adjusted if necessary to achieve acceptable trajectory response. Then, the sensor compensation is determined that provides the desired cue response. The details of this approach are now described for the longitudinal and lateral axes.

Longitudinal Axis Design

The general display law for this method, as extended for this application, is:

$$A_x(s) = f_{\dot{x}}(s)\dot{x}(s) + f_\theta(s)\theta(s) + f_q(s)q(s) + f_{\delta_b}(s)\delta_b(s) \tag{21}$$

Where the f_i's represent the sensor signal compensation required to provide the desired cue response. Dividing by δ_b yields:

$$\frac{A_x}{\delta_b}(s) = f_{\dot{x}}(s)\frac{\dot{x}}{\delta_b}(s) + f_\theta(s)\frac{\theta}{\delta_b}(s) + f_q(s)\frac{q}{\delta_b}(s) + f_{\delta_b}(s) \tag{22}$$

For the desired gain-like cue response to pilot input above some frequency, this transfer function's numerator and denominator must be of equal order. The objective is to determine the order and parameter values for each filter to yield this gain-like cue response. The choices are also constrained by the requirement to provide good trajectory response dynamics. The relationship between the two can be seen by referring to Figure 2, where for high values of pilot gain, K_p, the open-loop position transfer function may be approximated by:

$$\frac{x}{x_{cmd} - x}(s) \approx K_x\frac{x/\delta_b}{A_x/\delta_b} \tag{23}$$

Thus, for fixed display position and velocity scalings and vehicle response, tailoring the cue response is the only means of assuring an acceptable closed-loop position response. The cue transfer function can be used, for example, to cancel unwanted dynamics in the vehicle position response to control input. Of course, this must be accomplished while still maintaining good cue controllability.

Next recall that the aircraft longitudinal response has the form (neglecting the transport delay):

$$\frac{\theta}{\delta_b}(s) = \frac{M_{\delta_b}(s+a)}{s(s+b)[\zeta;\omega]} \tag{24}$$

Substituting the aircraft responses into eqn. 22 with the approximations:

$$\frac{\dot{x}}{\theta}(s) = \frac{-g}{s - X_u} \tag{25}$$

$$q = \dot{\theta} \tag{26}$$

yields

$$\frac{A_x}{\delta_b}(s) = [terms\ in\ (f_i)]\frac{-gM_{\delta_b}(s+a)}{s(s+b)(s-X_u)[\zeta;\omega]} \tag{27}$$

This relation is simply the unaugmented vehicle velocity response with added zeros (in the terms in f_i) that can be used to provide lead to the cue position dynamics.

For the overall transfer function to be proper, the transfer function in the brackets must have an excess of four zeros. In addition, it is desirable to cancel the attitude response's lead-lag pair from the trajectory response, to eliminate position overshoot. For these reasons, the following form is chosen for the cue response transfer function:

$$\frac{A_x}{\delta_b}(s) = \frac{K_{\delta_b}(s+z_1)(s+z_2)(s+a)[\zeta;\omega]}{s(s+b)(s-X_u)[\zeta;\omega]} \tag{28}$$

where K_{δ_b} is a total gain that represents the high frequency cue sensitivity to control input. Note that two zeros are chosen to cancel the complex poles from the cue response, in order to simplify it. However, this means that they will be present in the trajectory response. This choice of zeros may not be appropriate for very poorly damped vehicles and should therefore be considered for each case. The placement of the zeros z_1 and z_2 determines the frequency at which the cue response becomes gain-like.

The numerator of eqn. 28 represents a fifth-order polynomial. Each of its terms must be taken with the denominator and considered separately to determine compensation terms f_i that are realizable, that is, they must not result in pure differentiation of any sensor signal. Defining the denominator of eqn. 28 as Δ for convenience and rewriting the numerator as a fifth-order polynomial gives:

$$\frac{A_x}{\delta_b}(s) = \frac{K_{\delta_b}(a_1 s + a_0)}{\Delta} + \frac{K_{\delta_b}(a_2 s^2)}{\Delta} + \frac{K_{\delta_b}(a_3 s^3)}{\Delta} + \frac{K_{\delta_b}(s^5 + a_4 s^4)}{\Delta} \tag{29}$$

Now each of these terms can be equated respectively with the terms of eqn. 22 to determine the filters f_i. For example, for the pitch rate term:

$$f_q(s) = \frac{K_{\delta_b}(a_3 s^3)}{s(s+b)(s-X_u)[\zeta;\omega]}\left(\frac{q}{\delta_b}(s)\right)^{-1} \tag{30}$$

$$\approx \frac{K_{\delta_b} a_3 s}{M_{\delta_b}(s+a)} \tag{31}$$

X_u was included for completeness until eqn. 31, where it has been approximated as zero. This is reasonable since for the Apache it was flight identified to be -0.02 sec^{-1}. Thus, the pitch rate filter is a first-order washout. Repeating the process for each sensor input, the total cue drive law is then:

$$A_x(s) = \frac{K_{\delta_b}(a_1 s + a_0)}{-M_{\delta_b} g(s+a)}\dot{x}(s) + \frac{K_{\delta_b} a_2 s}{M_{\delta_b}(s+a)}\theta(s) + \frac{K_{\delta_b} a_3 s}{M_{\delta_b}(s+a)}q(s) + \frac{K_{\delta_b} s^2(s+a_4)}{(s+b)[\zeta;\omega]}\delta_b(s) \tag{32}$$

Based on iterative examination of the cue controllability and the resulting trajectory response and on preliminary piloted evaluations, the zeros z_1 and z_2 were chosen to be equal at -1.765 rad/sec. Once these were selected, the numerator polynomial could be computed. Finally, the gain K_{δ_b} was chosen such that $f_{\dot{x}}(s)$ has a steady state value of $K_{\dot{x}}$, so that in the steady state the cue would rest at the tip of the velocity vector. Thus, the cue response transfer function was:

$$\frac{A_x}{\delta_b}(s) = \frac{-2.21(s+1.765)(s+1.765)(s+0.262)}{s(s+.399)(s+0.02)} \tag{33}$$

The following represents the corresponding display law that was evaluated in the simulation:

$$A_x(s) = K_{\dot{x}}\left[\frac{1.42s + 0.262}{s+0.262}\dot{x}(s) - 59.3\frac{s}{s+0.262}\theta(s) - 32.1\frac{s}{s+0.262}q(s) - 2.15\frac{s^2(s+9.36)}{(s+0.399)[0.805;3.46]}\delta_b(s)\right] \tag{34}$$

where now the display gain $K_{\dot{x}}$ has been factored out so that the terms in brackets are in physical units of ft/sec.

Lateral Axis Design

A similar design procedure is followed for the lateral axis, but it is less complex because of the simpler vehicle response in this axis:

$$\frac{\phi}{\delta_a}(s) = \frac{L_{\delta_a}}{s[\zeta;\omega]} \tag{35}$$

This leads to a fourth-order numerator for the cue response transfer function:

$$\frac{A_y}{\delta_a}(s) = \frac{K_{\delta_a}(s+z_1)(s+z_2)[\zeta;\omega]}{s(s-Y_v)[\zeta;\omega]} \tag{36}$$

which is then distributed among the sensor signals. Unlike X_u, the derivative Y_v cannot be cancelled with a numerator

free s, since it was flight identified to be -0.279 sec^{-1}. The resulting form for the lateral cue law is then:

$$A_y(s) = \frac{K_{\delta_a} a_0}{L_{\delta_a} g}\dot{y}(s) + \frac{K_{\delta_a} a_1 s}{L_{\delta_a}(s - Y_v)}\phi(s) + \frac{K_{\delta_a} a_2 s}{L_{\delta_a}(s - Y_v)}p(s) + \frac{K_{\delta_a} s^2(s + a_3)}{(s - Y_v)[\zeta;\omega]}\delta_a(s) \quad (37)$$

Again, after iterative examination to optimize the trajectory response, the two zeros and the gain K_{δ_a} were set such that the cue response transfer function for piloted evaluation was:

$$\frac{A_y}{\delta_a}(s) = \frac{2.77(s + 2.026)(s + 2.026)}{s(s + 0.279)} \quad (38)$$

and the drive equation was:

$$A_y(s) = K_{\dot{y}}\left[\dot{y}(s) + 40.5\frac{s}{s + 0.279}\phi(s) + 18.2\frac{s}{s + 0.279}p(s) + 2.69\frac{s^2(s + 9.05)}{(s + 0.279)[0.582; 4.29]}\delta_a(s)\right] \quad (39)$$

Display Laws Based on Performance Design

The third design, based on a methodology developed in Ref. 4, is referred to as the "performance" design. It seeks to ensure good task performance but is balanced by pilot workload considerations. Besides this difference in emphasis, the workload and performance designs differ in the sensor signal distribution used to achieve the desired frequency response characteristics of the cue.

This method begins by selecting a desired transfer function of the vehicle's velocity response to be achieved when the pilot closes the control loop via the display. These dynamics represent how the velocity vector on the display would respond to the pilot maintaining the cue position at a fixed distance from the reticle (i.e., when the pilot is trying to establish a desired horizontal velocity). From Figure 2, if the pilot raises his gain high enough in the inner loop, then

$$\frac{\delta_b}{P_x}(s) \approx \frac{\delta_b}{A_x}(s) \quad (40)$$

Consequently, the inverse of the cue-to-stick dynamics may be used as series equalization with the open-loop, potentially poor vehicle velocity and position dynamics. If a desired vehicle velocity transfer function is selected, the cue-to-stick transfer function is

$$\frac{A_x}{\delta_b}(s) = K_{\dot{x}}\frac{\dot{x}}{\delta_b}(s)\Big|_{Aircraft} \times \left(\frac{\dot{x}}{\dot{x}_c}(s)\right)^{-1}\Big|_{Desired} \quad (41)$$

since A_x is the pilot commanded velocity. The denominator of the cue-to-stick transfer function contains the dynamics of the open-loop aircraft so that when it is inverted by the pilot's high gain, the open-loop dynamics are effectively cancelled. These cancelled dynamics are replaced by the desired closed-loop velocity dynamics that are achieved when the pilot is controlling the vehicle in response to cue position errors.

For the AH-64, the velocity dynamics are (neglecting the identified delay from eqn. 1 and using eqn. 25)

$$\frac{\dot{x}}{\delta_b}(s) = \frac{-2.49g(s + 0.262)}{s(s + 0.02)(s + 0.399)[0.805; 3.46]} \quad (42)$$

In order for A_x/δ_b to have a gain-like response at high frequencies, its numerator and denominator should be of the same order. Thus, the desired $\dot{x}_c/\dot{x}$ transfer function should be 4th over a 0th order. To prevent any velocity overshoot in the desired response, all of the roots in the desired velocity transfer function were placed on the real axis in the complex plane. The four equal roots were selected at -2.5 rad/sec. The selection of these roots is empirical but is based on some important points. First, the roots should be selected such that the high frequency gain of the cue to pilot inputs (of eqn. 41) is within a desired sensitivity range. If the roots of the desired velocity transfer function are all at low frequency, the high-frequency gain will be too high for a given velocity vector scaling gain. Second, the roots should be at a low enough frequency so that some immediate response to stick input occurs in the 1-10 rad/sec range. Third, as the roots move lower in frequency, the gains on the feedback signals in the display laws tend to increase.

For the design in this experiment,

$$\frac{A_x}{\delta_b}(s) = K_{\dot{x}}\frac{\dot{x}}{\delta_b}(s)\Big|_{Aircraft} \times \frac{(s + 2.5)^4}{(2.5)^4} \quad (43)$$

This controlled-element transfer function then needs to be distributed among the aircraft states rather than depending solely on pilot input. If the cue position is treated as the commanded velocity, $K_{\dot{x}}\dot{x}_c$, then

$$A_x(s) = K_{\dot{x}}\frac{\dot{x}_c}{\dot{x}}(s)\Big|_{desired}\dot{x}(s) \quad (44)$$

$$= K_{\dot{x}}\dot{x} + K_{\dot{x}}\left[\frac{(s + 2.5)^4}{(2.5)^4} - 1\right]\dot{x} \quad (45)$$

$$= K_{\dot{x}}\dot{x} + 1.6K_{\dot{x}}\ddot{x}_{comp} + K_{\dot{x}}\left[\frac{s(s^2 + 10s + 37.5)}{(2.5)^4}\right]\ddot{x} \quad (46)$$

$$= K_{\dot{x}}\left[\dot{x} + 1.6\ddot{x}_{comp} + \frac{-2.49gs(s+0.262)}{(2.5)^4(s+0.02)} \times \frac{(s^2+10s+37.5)}{(s+0.399)[.805;3.46]}\delta_b\right] \quad (47)$$

In the steady state, the cue indicates the scaled velocity $K_{\dot{x}}\dot{x}$. A gained acceleration term and a 4th over a 4th order washout filter is on the stick. This high order filter indicates that a large portion of the cue response is generated from stick input, which is pure prediction based upon the known open-loop helicopter velocity response and a distributed portion of the desired velocity response. The simulation showed that the sensitivity of this stick term in the cue response for aircraft changes (across the vehicle operational weight and inertia envelope) was acceptable.

The development in the lateral axis is identical. Here the desired velocity roots are -2,-2, and [0.582;4.29]. The complex zeros were chosen to cancel the high frequency lightly damped roll axis natural response in the A_y/δ_a transfer function. Otherwise, a slight oscillation at the underdamped roll mode would appear in the cue response to pilot input. This jitter was a problem early in the simulation, and the proper placement of the zeros eliminated it. Using the same development as in the longitudinal axis, the lateral axis cue response is

$$A_y(s) = K_{\dot{y}}\left[\dot{y} + 1.25\ddot{y}_{comp} + \frac{6.32gs}{(2)^2(4.29)^2(s+0.279)} \times \frac{(s^2+9.07s+42.9)}{[0.582;4.29]}\delta_a\right] \quad (48)$$

The quantities $\ddot{x}_{comp}$ and $\ddot{y}_{comp}$ are complementary filtered values. They are comprised of low frequency accelerometer measurements and high-frequency attitude-rate inputs. This filtering attenuates vibratory accelerometer measurements and cuts off the immediate accelerations due to rotor flapping from stick inputs. These immediate accelerations contribute to noise and are not useful in the pilot-vehicle-display crossover frequency range. The filters are

$$\ddot{x}_{comp} = \frac{1}{s+1}\ddot{x} - \frac{gs}{(s+1)(s+0.02)}\dot{\theta} \quad (49)$$

$$\ddot{y}_{comp} = \frac{1}{s+1}\ddot{y} + \frac{gs}{(s+1)(s+0.279)}\dot{\phi} \quad (50)$$

Comparison of Display Laws and Task Performance Prediction

The analytical frequency responses for the four longitudinal-axis acceleration cues are presented in Figure 5. First, it is seen that the performance and workload designs are nearly identical, though they were developed independently. The gain-like characteristics are apparent above about 2 rad/sec. The other two designs roll off rapidly above this frequency. In the mid-frequency range around 1 rad/sec, the performance and workload designs have roughly K/s characteristics. The modified production design has more phase lag than the production design in the mid-frequency region, but has better damping characteristics as discussed in the design section. The lateral axis frequency responses, when plotted, show similar trends.

The effect of these differences on task performance can be shown analytically by again referring to Figure 2. The pilot gain was set to 0.3 in/deg, and the control limit was set to ±5 in. The selected pilot gain resulted in crossover frequencies in the inner loop of Figure 2 to be between 2 and 3 rad/sec for each display cue law. The position loop was closed for each design and then driven with a step position command of 10 feet. The resulting vehicle trajectory and the control inputs required to achieve those trajectories are shown in Figure 6 for all four cue designs. It is seen that the position trajectories for the workload and performance designs are well-damped and relatively smooth. The modified production design is damped but not as smooth, while the production design is oscillatory with undershoot. Regarding the control inputs, the workload and performance traces

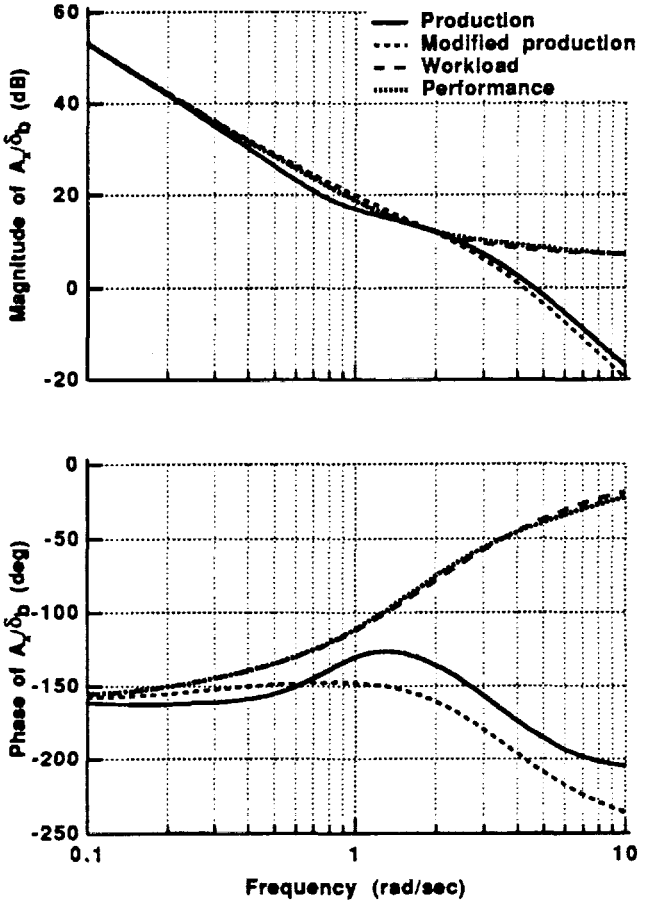

Fig. 5 Analytical frequency responses of four longitudinal cues.

show one control reversal, the modified production design shows significant oscillation, and the production design has some oscillation and is generally complex.

Based on these analyses, it could be predicted that the workload and performance designs would yield both the best performance and lowest workload, the modified production design the third best performance and the production design the poorest performance. The piloted assessments of relative workload for the modified production and production designs is difficult to predict from the traces.

The Bode plots for the workload and performance designs show the gain-like characteristics extending indefinitely to high frequency. Although noise is generally not a factor in simulation, in a flight environment the cue response must be attenuated to prevent sensor and pilot control-induced noise from passing through to the cue, causing it to jitter on the display. Therefore, for completeness of the experiment, a first-order 10 rad/sec filter was placed on the total cue displacements A_x and A_y before they were sent to the display. This was done for the performance and workload designs only, since the other designs already have high-frequency attenuation. While the filter adds phase lag to the cue response, for these hover maneuvering tasks it does not appear to significantly degrade stability margins. The flight data analyzed in Ref. 2 exhibited measured crossover frequencies of 1-4 rad/sec with the same noise attenuation filter. Other display laws with similar high-frequency gains and the same noise attenuation filters have also been flown successfully (Refs. 1, 4, and 5).

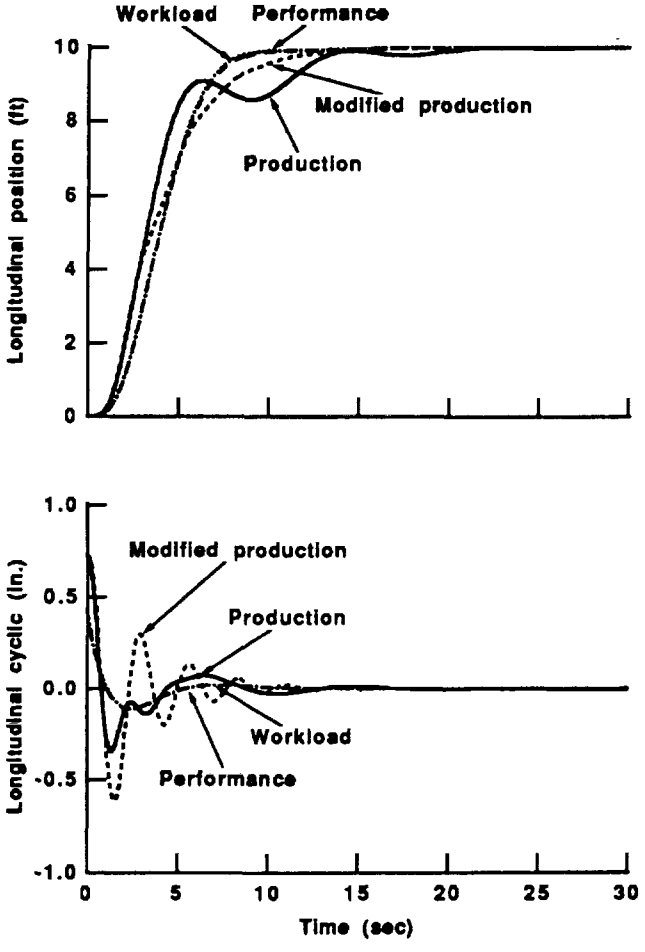

Fig. 6 Analytical position responses and control traces for four longitudinal cues.

EXPERIMENT CONDUCT

Simulator Configuration

The experiment was conducted on the NASA Ames Vertical Motion Simulator (VMS). The main objective was to perform piloted evaluations of the existing production display laws and the three new display designs to assess their impact on handling qualities, using both Apache-rated and non-Apache-rated test pilots. It was recognized that the validity of the results would be highly dependent on the simulation fidelity. Therefore, much attention was devoted to represent accurately the Apache using the simulator elements shown in Figure 7. This effort is described in detail in Ref. 10. To summarize, a nine-state (8 rigid body plus dynamic inflow) linear math model valid for the unaugmented AH-64 near hover was identified from flight data. A verified software representation of the AH-64 DASE was then added to the linear model. The aircraft rotorspeed and torque responses to collective were identified from flight data, to drive the cockpit and helmet-mounted displays. Significant effort was expended to identify also the static and dynamic characteristics of the AH-64's centerstick controller and pedals. These controller characteristics were used to tune the simulator's programmable control loaders. For added fidelity, a sound generator was matched qualitatively to an audio recording made within an Apache cockpit.

Because of the small displacements involved in the hover maneuvers, nearly the full potential of the VMS motion system could be used. At mid-to-high frequencies, 1:1 motion of the simulator with respect to the aircraft was achieved in all axes. In addition, the AH-64 Integrated Helmet and Display Sighting System (IHADSS) flight hardware was used (Figure 8). A simulated forward looking infrared (FLIR) image was shown on the helmet monacle, and the Apache Bob-Up mode symbology was superimposed on it. The FLIR and symbology images were made to match the written specifications and a video record from an AH-64 in terms of symbology placement, size, scaling, and display field-of-view. The total throughput time delay from control input to motion and visual response was matched as closely as possible to the flight-identified values for each axis. Pilot acceptance of the simulator as representative of an AH-64 was generally positive, as described in Ref. 10.

Piloted Tasks

Two tasks were developed to compare the display laws. In each, the pilot was advised to perform the task using the strategy of minimizing the acceleration cue error from the

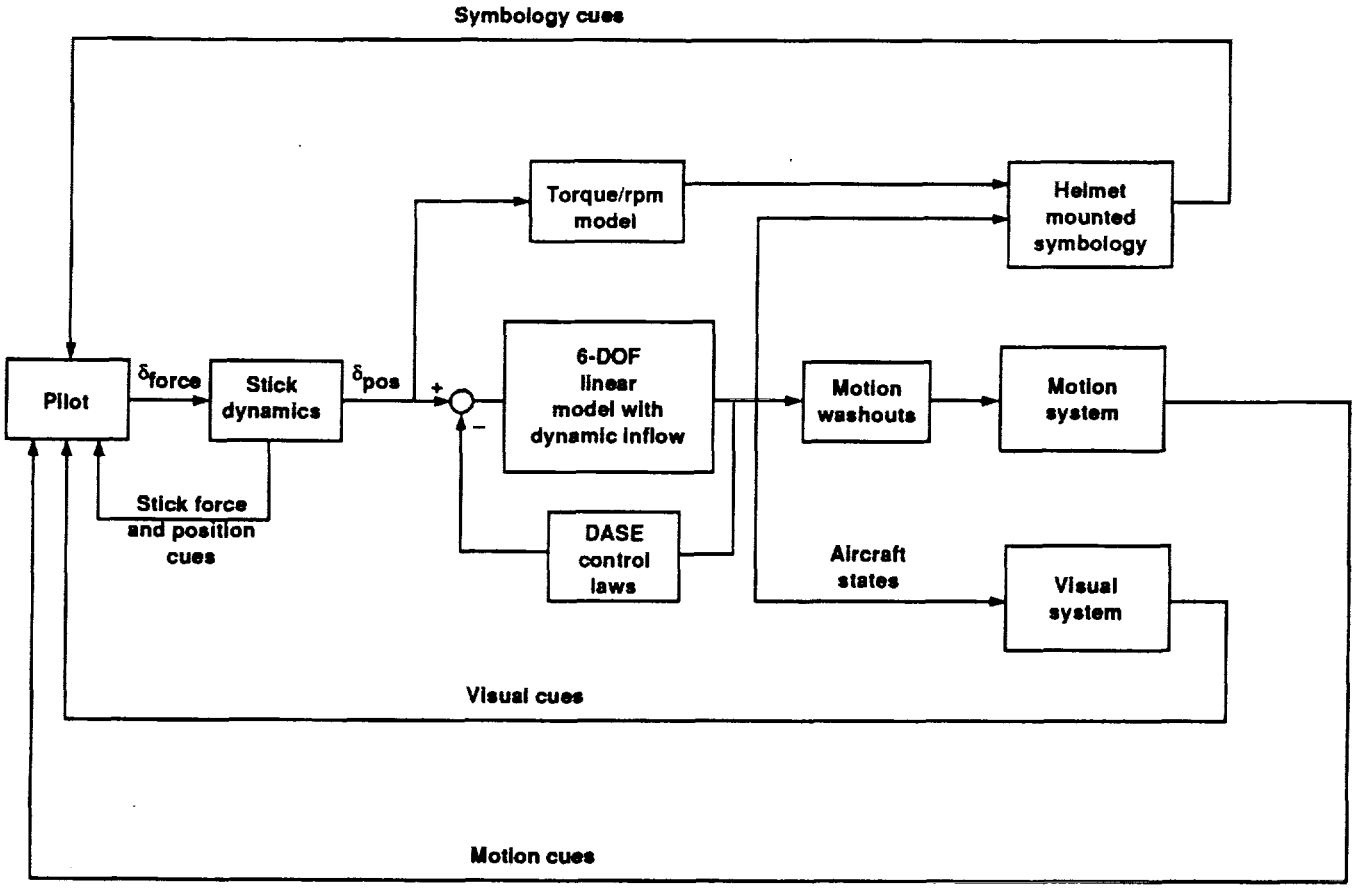

Fig. 7 AH-64 simulation components.

hover box. This strategy is the one taught to operational pilots. The first task, known as the pad capture, was to acquire the hover box from a diagonal 56 ft offset (40 ft each laterally and longitudinally) within 15 secs. In each run, the task was repeated four times; every 15 secs, the hover box was repositioned in earth axes 56 ft diagonally forward or rearward of its last position. The objective of the task was to achieve a stable hover over the box before it was moved to the new position. The standards for desired performance were: 1) achieve position over/undershoot of less than one hover box width; 2) maintain altitude at 40±10 ft; 3) maintain initial heading ±10 deg. The standards for adequate performance were twice those for desired. This task was meant to expose issues associated with the cue controllability and the position trajectories.

The second task was a Bob-Up/Bob-Down maneuver, in which the pilot began in a hover at 40 ft, ascended to a 70 ft target altitude, then immediately descended to 40 ft again. The objective was to perform the task in 15 secs while maintaining position over the hover box. The standards for desired performance were: 1) achieve target altitudes with over/undershoot less than 10 ft; 2) maintain heading ±5 deg; 3) maintain position within the hover box. The standards for adequate performance were twice those for desired. This task was designed to compare the regulation capabilities of each cue during off-axis inputs.

The tasks were conducted using a baseline level of Dryden turbulence that was termed very light. Its root-mean-square (rms) magnitude was 0.3 ft/sec. Three pilots evaluated the display laws in the pad capture task under a light-to-moderate turbulence level (rms of 1.5 ft/sec) to investigate potential disturbance rejection differences among the laws.

Outside Visual Scene

The pilot's visual information was presented using the AH-64 IHADSS monacle, which displayed the symbology superimposed on a simulated FLIR image of the outside world. The outside view was a head-tracked computer-generated scene. The offset of the FLIR turret from the pilot station was represented. The scene objects were adjusted in color to present a nighttime FLIR-like image once they were sent to the monacle display. Both white-hot and black-hot FLIR modes were available to the pilot. The monacle field of view was 40 Horiz. x 30 Vert. degrees, while the simulated sensor field-of-regard was 240 Horiz. x 90 Vert. degrees.

The pad capture task was flown over a flat area with grid lines at ten foot intervals. The grid lines provided strong heading cues and some position cueing. The bob-up task was

Fig. 8 AH-64 Integrated Helmet and Display Sighting System.

flown over a hover pad area with trees in the near field that provided some altitude cues.

While the simulated FLIR imagery was judged by the pilots to be reasonable in terms of object light intensity, all the pilots felt that the lack of texture and other fine detail made the outside cues far less useful than those of an actual FLIR. This, in combination with the symbology-oriented nature of the tasks and the nominal altitude used (40 ft), forced the pilots to rely more on the symbology than normally would be the case in reality. Some pilots estimated that they used the symbology for 90% of the cuing. Consequently, they were prevented from compensating for poor symbology drive laws by using outside cues, thus perhaps more clearly exposing the differences among the laws. Several Apache pilots stated that this poor-FLIR environment was similar to using the IHADSS at night during high hover operations, where significant ground cues are lost.

Off-Nominal Configurations

The new display laws were designed for a nominal aircraft configuration, namely the one used for the parameter identification flight tests that yielded the simple DASE-on transfer function models. The laws were then evaluated in the piloted simulation using the nine-state model with the DASE programmed explicitly. The simulation model had been identified for the same nominal aircraft weight and stores configuration as the display design model. To assure that the new display laws were not overly tuned to one aircraft configuration, the nine-state simulation model's parameters were varied to represent a light and a heavy stores configuration about the nominal. The pad capture task was performed by several pilots at these off-nominal conditions.

Test Pilot Participants

A total of ten experienced test pilots participated in the simulation as evaluators. Among them were four Apache-qualified pilots, including: one instructor pilot from AQTD with over 700 hrs in the Apache and over 400 hours using the PNVS; one from the AQTD with 150 PNVS hours; one from the Aeroflightdynamics Directorate (AFDD) with 25 PNVS hours; and one from the manufacturer, McDonnell Douglas Helicopter Co., with 200 PNVS hours. The non-Apache rated pilots included two from NASA Ames, one from AFDD (with 30 PNVS hours), one from Sikorsky Aircraft (with helmet-mounted display experience), one from Boeing Helicopters, and one from the Navy Test Pilot School.

Piloted Evaluations

Each pilot was allowed to practice the tasks with all four of the cues until he felt that his performance had stabilized. Several training sessions were generally required. He then completed formal evaluations of all the cues for one task with one aircraft and turbulence configuration. He was not informed of which cue he was evaluating. The order that the cues were presented was varied for each evaluation session. For any one task, the procedure was to finish a session with a re-evaluation of the cue flown first, to see if learning effects were a factor.

Data Collection

Data collected during evaluations comprised statistical and time history data to document task performance, verbal answers to a questionnaire, and Cooper-Harper pilot ratings (Ref. 11).

RESULTS

Task Performance Results

Figure 9 presents positioning performance crossplots for all pilots conducting four pad captures each for each acceleration cue. In terms of deviation from a 45° horizontal path, the trajectories are seen to be more accurate and more consistent for the workload and performance designs in comparison with both the production and modified production designs.

Figure 10 presents the acceleration cue error from the hover box for the same runs. Since the pilot was advised to place and keep the cue on the box during the acquisition,

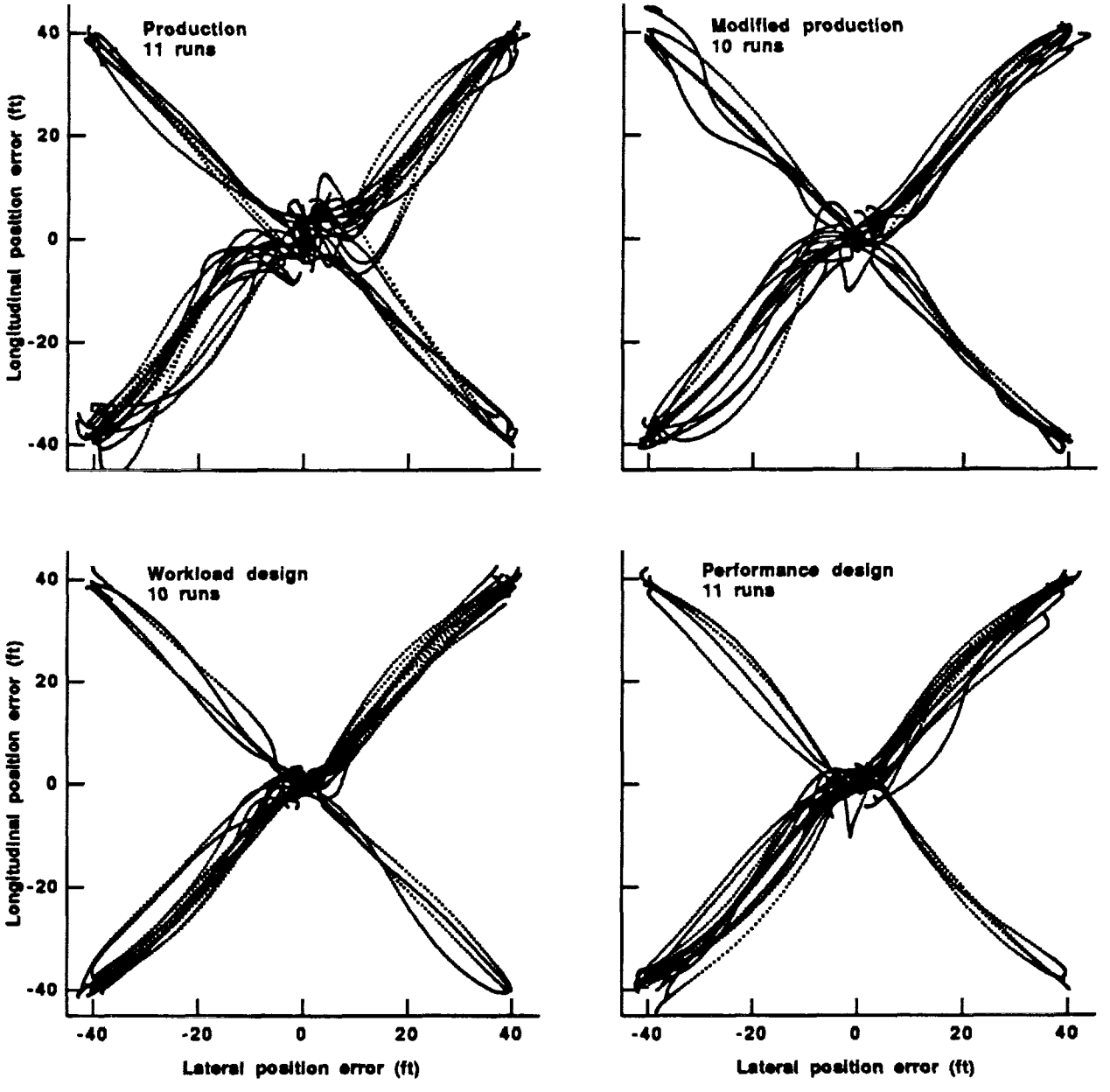

Fig. 9 Position crossplots for four cues, pad capture task.

these plots indicate cue controllability and are thus a measure of workload. The workload and performance designs show a narrower concentration of points along a 45° path and at the origin, indicating lower workload in comparison with the other two.

The altitude performance for four evaluation runs by one pilot is presented in Figure 11. While all the traces remain in the desired performance region, the production and modified production traces exhibit large oscillations that appear nearly divergent compared with the more damped traces for the workload and performance designs. The differences suggest that the improved controllability of the workload and performance cues allowed the pilot to devote more attention to scanning the altitude tape, thus better controlling the altitude.

As a check of the analytical performance predictions described earlier, Figure 12 presents longitudinal trajectory and control input time histories from analysis and from simulation for a 20 ft longitudinal capture using the performance design. The position trajectories are in good agreement except for pilot and system time delays that were not modeled in the analysis. The simulation control input trace shows a higher frequency component superimposed on a trend that generally matches the analysis. This "dither" may result from the pilot's uncertainty about how much control is required to move the cue to the box.

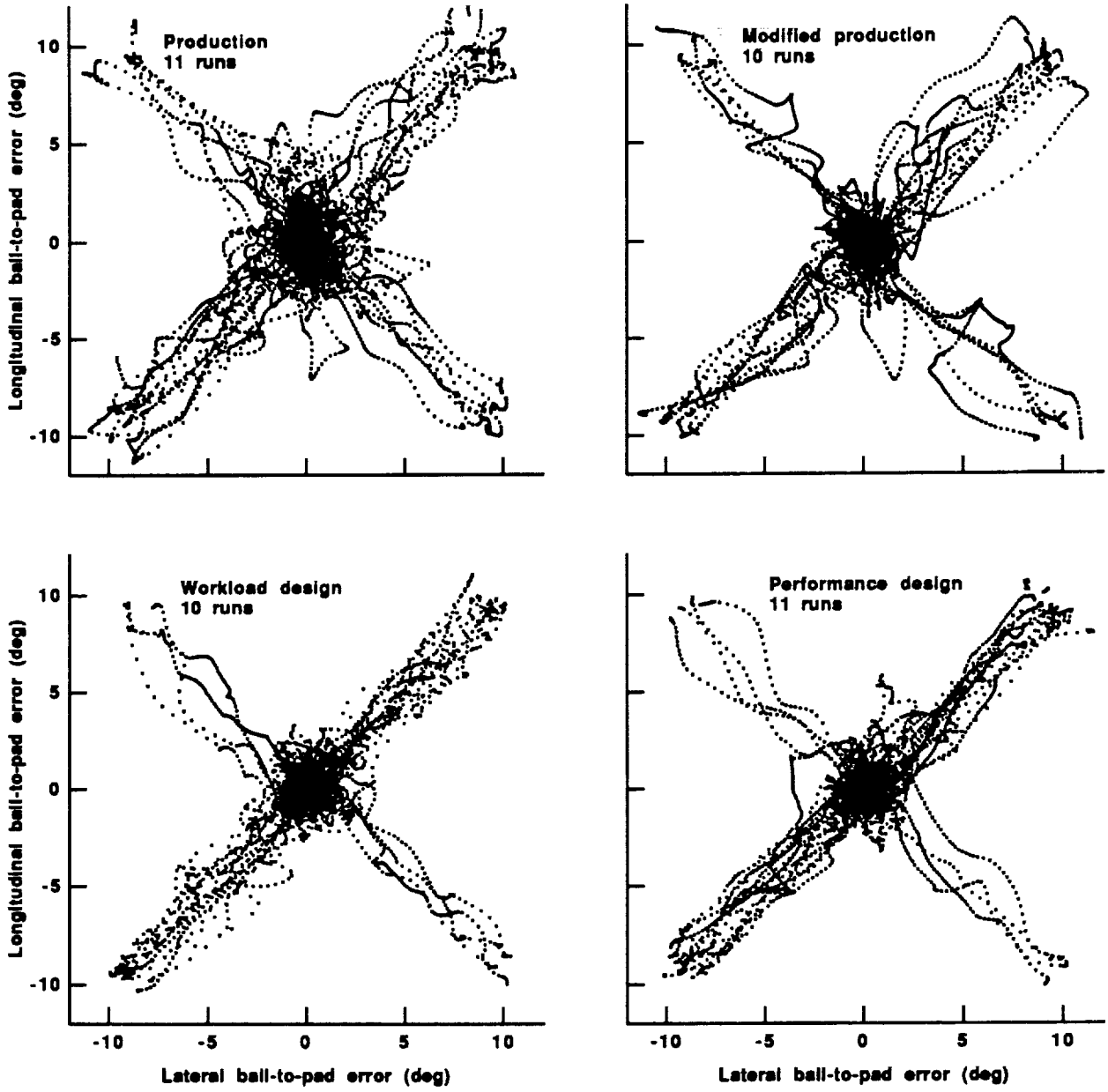

Fig. 10 Cue-to-box error crossplots for four cues, pad capture task.

The performance measure of interest for the bob-up task is the horizontal position error during the vertical maneuver. Figure 13 presents the root-mean-square position errors seen for the bob-up task as a function of cue drive law. Each point represents an individual bob-up maneuver. The modified production law has the lowest position error, followed by the workload, performance, and production laws. The most likely reason for this trend is that since the performance and workload laws use pilot input as one sensor for the cue, the high-frequency part of the cue motion is due to the control rather than to any actual aircraft movement. Thus, less aircraft motion is required to keep the cue on the box than for the production and modified production laws. While the pilot workload is reduced, for these small inputs the positioning performance may be slightly degraded.

Pilot Rating Results

Figure 14 presents a compilation of all the pilot ratings for the pad capture task in the baseline turbulence, nominal weight configuration. All the rating means fall in the Level 2 region. According to pilot comments given during the rating procedure, the workload associated with flying the rate-damped aircraft using a narrow field-of-view display with simulated FLIR imagery made the vehicle-display system unsatisfactory without improvement. The workload associated with control of the vertical axis, which required frequent

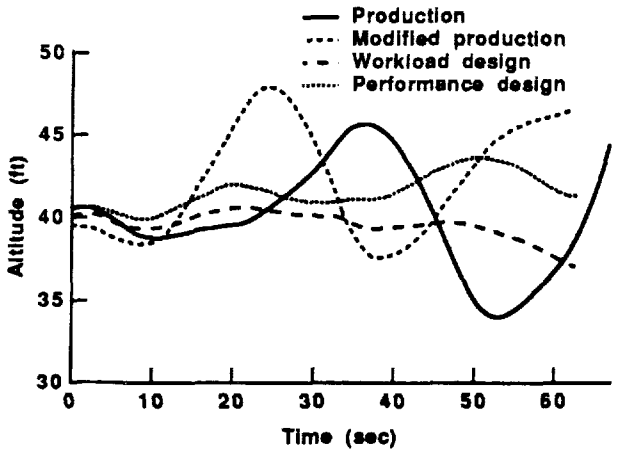

Fig. 11 Altitude performance for four cues during four pad captures.

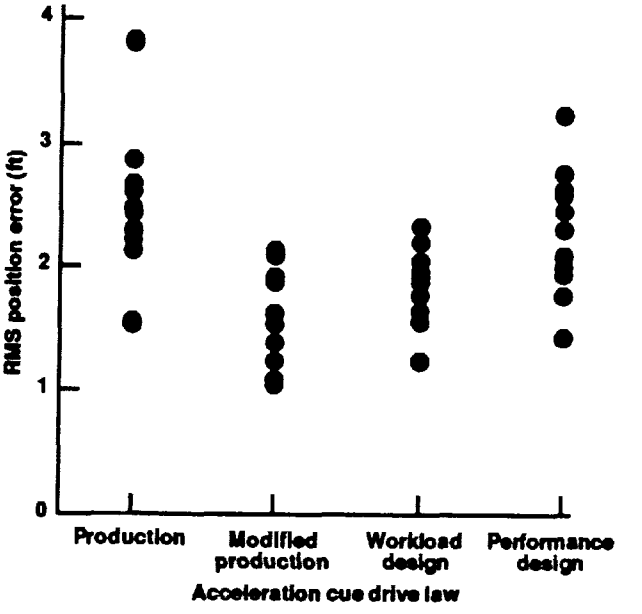

Fig. 13 Positioning performance for four cues, bob-up task, all runs.

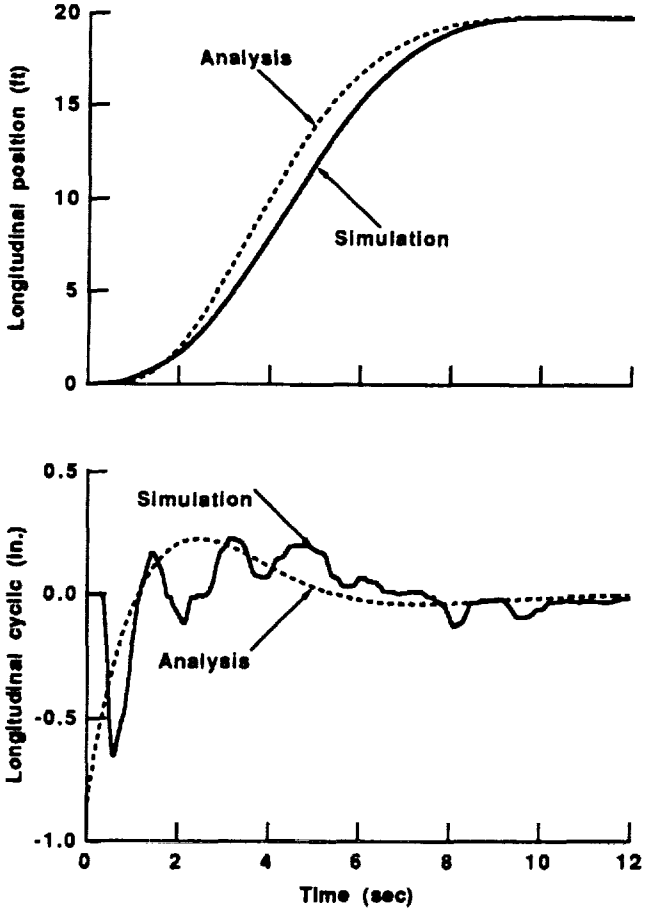

Fig. 12 Evaluation of pilot-vehicle-display model for performance design.

scanning away from the central symbology to the altitude tape, also was frequently sighted as a factor contributing to the Level 2 ratings.

However, there are significant differences among the cue drive laws. The mean rating improves from 5.9 for the production law to 4.3 for the workload design, which had a slightly better mean than the performance design. This improvement reflects a reduction in pilot compensation requirements from "extensive" to "moderate" to perform the task. It is important to note that the 90% confidence bars (Ref. 12) do not overlap for the best versus the worst display configurations. Moreover, each of the ten pilots assigned a better rating to the workload and performance designs than to the production laws.

Figure 15 presents the rating data for the the bob-up task at nominal weight and baseline turbulence. Again, the workload design received the best ratings, followed by the performance and then the production and modified production designs.

Summary of Pilot Comments

Following is a summary of the pilot comments for all the cue laws tested. They are extracted from answers given verbally in response to a questionnaire after every evaluation run.

Pilot comments concerning the production law indicated that the cue was unpredictable and difficult to control. A large amount of effort was required to keep the cue within the hover box. In the pad capture task, the cue was said to cause pilot-induced oscillations (PIO's) unless the task aggressiveness was reduced. Over- and undershoots in position were seen with the cue. The workload to control the cue

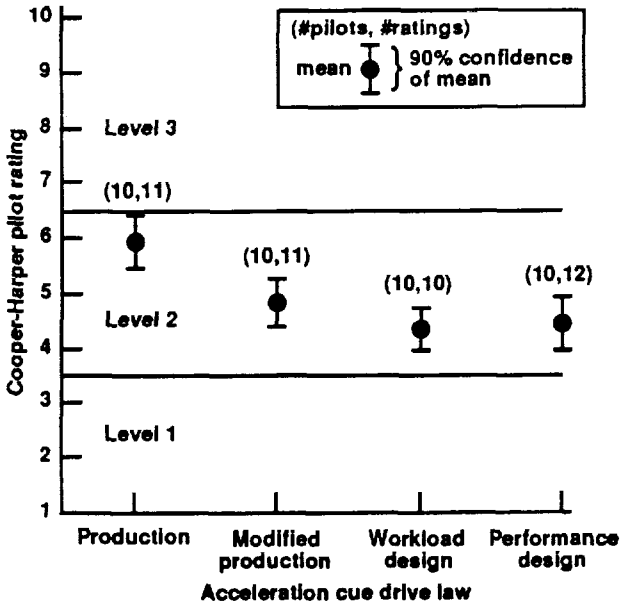

Fig. 14 Mean and 90% confidence values for all ratings, pad capture task.

allowed less time for crosschecking the altitude and heading, degrading performance in those axes. For the bob-up task, the attention required to maintain the cue on the box detracted from the altitude performance.

The modified production law was considered an improvement over the production law in controllability and positioning performance. It was still judged unpredictable, sluggish, and slightly prone to PIO. However, more attention was available to scan the altitude and heading for both tasks.

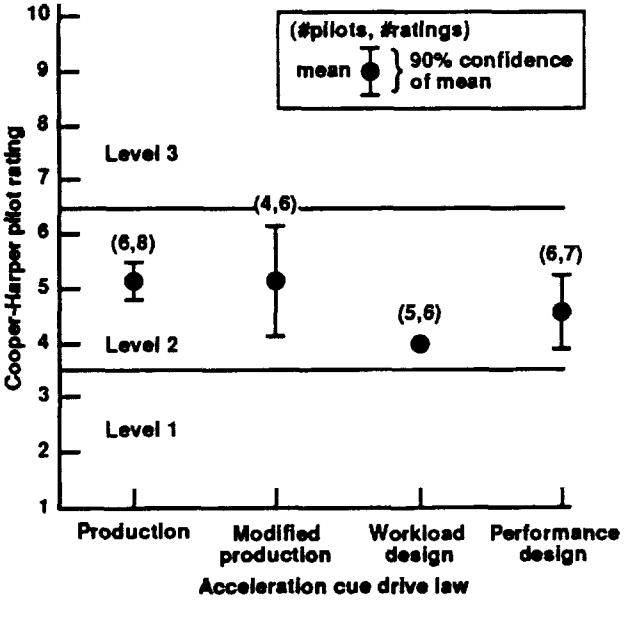

Fig. 15 Mean and 90% confidence values for all ratings, bob-up task.

The workload design was described as very predictable and easily controllable. It allowed more aggressiveness and was felt by the pilots to allow much improved position and velocity performance. There were no PIO tendencies, and the workload was reduced significantly. Thus, there was substantially more attention available for scanning and control of the altitude and heading. These improvements were apparent for both tasks. Pilots noted that the cue sometimes appeared to have a slight overshoot in response to a quick control input, which they referred to as jitter. However, the effect was not judged objectionable. All the AH-64 rated pilots noted that they had no trouble adjusting to the characteristics of this new law.

Comments on the performance design were very similar to those for the workload design, except that no cue jitter was noted. The position trajectories for the pad capture task were described as nicely convergent. There was a wider dispersion of ratings and a slightly worse mean rating with this design for both tasks. The difference in ratings for the bob-up task seems to correlate with the task positioning performance presented in Figure 13. Recall that the performance design assigns more of the cue response to the control input than does the workload design, which may degrade its regulation performance.

CONCLUSIONS

A piloted simulation was conducted to investigate handling qualities improvements attainable through the application of improved display laws for hover maneuvering, using FLIR imagery with superimposed symbology. Three new display law methods were applied to the AH-64 Apache and compared with its existing display laws. The new laws, termed the modified production, performance, and workload designs, were compared analytically, and then tested using a pilot-in-the-loop simulation that was extensively validated and well accepted by the pilots. The analytical comparisons showed an improvement in both performance and workload for the new laws. These analytical improvements were confirmed in the piloted evaluations by ten test pilots, four of whom were AH-64 rated. The new performance and workload laws, which use stick position to achieve an immediate response of the acceleration cue to pilot input, were determined to benefit significantly handling qualities in comparison with the production and modified production laws. First, the new laws yielded improved performance for the horizontal positioning primary task, while allowing more attention for improved performance in secondary tasks such as altitude regulation. Second, the new laws elicited favorable pilot comments; all ten pilots said they preferred the new laws over the existing laws. Finally, all ten pilots assigned a better pilot rating to each of the new laws than to the existing laws.

REFERENCES

[1]Eshow, M. M., Aiken, E. W., and Hindson, W. S.,"Preliminary Results of a Flight Investigation of Rotorcraft Control and Display Laws for Hover," American Helicopter Society National Specialists' Meeting in Flight Controls and Avionics, Cherry Hill, New Jersey, October 1987.

[2]Eshow, M. M., "Flight Investigation of Variations in Rotorcraft Control and Display Dynamics for Hover," *Journal of Guidance, Control, and Dynamics*, Vol. 15, No., 2, 1992, pp. 482-490.

[3]Tsoubanos, C. M., and Kelley, M. B., "Pilot Night Vision System (PNVS) for Advanced Attack Helicopter (AAH)," *Proceedings of the 34th Annual National Forum of the American Helicopter Society*, Washington, D. C., 1978.

[4]Schroeder, J. A., and Merrick, V. K., "Flight Evaluations of Several Hover Control and Display Combinations for Precise Blind Vertical Landings," *Journal of Guidance, Control, and Dynamics*, Vol. 15, No. 3, 1992, pp. 751-760.

[5]Schroeder, J. A., Eshow, M. M., and Hindson, W. S., "An In-Flight Investigation of Display Drive Law Improvements to an Operational Attack Helicopter," *Proceedings of the 46th Annual National Forum of the American Helicopter Society*, Washington, D. C., 1990.

[6]Weir, D. H., Klein, R. H., and McRuer, D. T., "Principles for the Design of Advanced Flight Director Systems Based on the Theory of Manual Control Displays," NASA CR-1748, 1971.

[7]Tischler, M. B., and Cauffman, M. G., "Frequency-Response Method for Rotorcraft System Identification with Applications to the BO-105 Helicopter," *Proceedings of the 46th Annual National Forum of the American Helicopter Society*, Washington, D. C., 1990.

[8]Ham, J. A., Butler, C. P., "Flight Testing the Handling Qualities Requirements of ADS-33C - Lessons Learned at ATTC," *Proceedings of the 47th Annual National Forum of the American Helicopter Society*, Phoenix, AZ, 1991.

[9]McRuer, D. T., and Krendel, E. S., "Mathematical Models of Human Pilot Behavior," AGARDograph No. 188, Jan. 1974.

[10]Schroeder, J. A., Tischler, M. B., Watson, D. C., and Eshow, M. M., "Identification and Simulation Evaluation of an AH-64 Helicopter Hover Math Model," AIAA Paper 91-2877, August 1991.

[11]Cooper, G. E., and Harper, R. P., "The Use of Pilot Rating in the Evaluation of Aircraft Handling Qualities," NASA TN D-5153, 1969.

[12]Mack, C., *Essentials of Statistics for Scientists and Technologists*, Plenum Press, New York, New York, 1967, pp. 65-66.

The Development and Potential of Inverse Simulation for the Quantitative Assessment of Helicopter Handling Qualities

Professor Roy Bradley

Department of Mathematics
Glasgow Polytechnic
Glasgow, U.K.

Dr Douglas G. Thomson

Department of Aerospace Engineering
University of Glasgow
Glasgow, U.K.

Abstract

In this paper it is proposed that inverse simulation can make a positive contribution to the study of handling qualities. It is shown that mathematical descriptions of the MTEs defined in ADS-33C may be used to drive an inverse simulation thereby generating, from an appropriate mathematical model, the controls and states of a subject helicopter flying it. By presenting the results of such simulations it is shown that, in the context of inverse simulation, the attitude quickness parameters given in ADS-33C are independent of vehicle configuration. An alternative quickness parameter, associated with the control displacements required to fly the MTE is proposed, and some preliminary results are presented.

Nomenclature

API	Agility Performance Index
n_s, n_c	number of states and controls in API function
p, q, r	components of aircraft angular velocity in body axes
q_i, r_j	weighting constants for API
t_a	time to reach maximum acceleration in Rapid Sidestep MTE
t_d	time to reach maximum deceleration in Rapid Sidestep MTE
t_l	time in acceleration phase of Rapid Sidestep MTE
t_m	time taken to complete manoeuvre
u	control vector
u, v, w	components of aircraft velocity in body axes
V_f	airspeed
V_{max}	maximum airspeed reached in manoeuvre
$\dot{V}_{max}$	maximum acceleration during Rapid Sidestep MTE
$\dot{V}_{min}$	maximum deceleration during Rapid Sidestep MTE
x	state vector
y	output vector
$\dot{\chi}$	turn rate
ϕ, θ, ψ	aircraft attitude angles
θ_0	main rotor collective pitch angle
$\theta_{1_s}, \theta_{1_c}$	longitudinal and lateral cyclic pitch angles
$\theta_{0_{tr}}$	tailrotor collective pitch angle

1. Introduction

The need to assess the overall handling qualities of a helicopter by its performance and handling characteristics in a range of typical manoeuvres has been recognised by the authors of the U.S. Handling Qualities for Military Rotorcraft [1]. As part of demonstrating compliance with these requirements, a set of standard manoeuvres, or Mission Task Elements (MTEs) has been defined and criteria for performance and handling have been specified. In addition, the authors of this document have indicated that mathematical models are an appropriate basis for evaluation and analysis at the design stage. By its nature, inverse simulation encapsulates this combination of precisely defined manoeuvre and mathematical modelling. With inverse simulation, a mathematical representation of a MTE is used to drive a helicopter model in such a way that the vehicle's response and control displacements may be derived. In effect, a flight trial of the modelled helicopter flying a given MTE is performed, and the information collected from such simulations is

as extensive as that recorded in a real trial. It follows that inverse simulation has the potential of being a useful validation tool for manoeuvring flight, [2], but the question arises as to whether the data collected can be analysed for the evaluation of handling qualities in the same manner as that from a flight test of the real aircraft. The two conditions:

i) The mathematical model of the helicopter must have a suitably high level of fidelity for the flight conditions encountered in the MTE;

ii) The mathematical model of the MTE must be representative, in some sense, of the real manoeuvre;

might reasonably be considered as necessary before a positive response can be made but whether these conditions are, in addition, sufficient is the subject of current research at Glasgow.

This paper describes the rationale behind the belief that inverse simulation has an important contribution to make in the evaluation of helicopter handling qualities. A number initial studies have been performed using the helicopter inverse simulation package Helinv, [3] and some preliminary results will be presented in later sections of this paper. In the section that follows some of the main features of inverse simulation and manoeuvre description are discussed. Next, in section 3, a number of exploratory studies are described. These studies involve three methods of extracting information from the results of inverse simulation: performance comparisons, handling qualities indices and quickness parameters. It will be argued that the first two methods are likely to be limited both in their potential and in their applicability, while the quickness parameter approach shows particular promise since it goes some way towards resolving the question of the sufficiency of the two conditions listed above.

2. Inverse Simulation of Mission Task Elements

It is convenient to begin the discussion relating to the assessment of handling qualities by clarifying the term 'inverse simulation' as it is employed in relation to the work at Glasgow. Other authors [4, 5] have different interpretations related to the context in which it is employed. Also, the technique is not universally familiar, so that the feasibility of deriving a unique set of control responses from a given flight path is often questioned. The general problem is a good starting point for the discussion.

2.1 Inverse Simulation - The General Problem

The simulation exercise of calculating a system's response to a particular sequence of control inputs is well known. It is conveniently expressed as the initial value problem:

$$\dot{\mathbf{x}} = \mathbf{f}(\mathbf{x},\mathbf{u}); \quad \mathbf{x}(0) = \mathbf{x}_0 \tag{1}$$

$$\mathbf{y} = \mathbf{g}(\mathbf{x}) \tag{2}$$

where $\mathbf{x}$ is the state vector of the system and $\mathbf{u}$ is the control vector. Equation (1) is a statement of the mathematical model which describes the time-evolution of the state vector in response to an imposed time history for the control vector $\mathbf{u}$. The output equation, (2), is a statement of how the observed output vector $\mathbf{y}$ is obtained from the state vector.

Inverse simulation is so called because, from a pre-determined output vector $\mathbf{y}$ it calculates the control time-histories required to produce $\mathbf{y}$. Consequently, equations (1) and (2) are used in an implicit manner and, just as conventional simulation attaches importance to careful selection of the input $\mathbf{u}$, inverse simulation places emphasis on the careful definition of the required output $\mathbf{y}$.

2.2 Application to the Helicopter

In the helicopter application discussed here, the state vector is $\mathbf{x} = [u\ v\ w\ p\ q\ r\ \phi\ \theta\ \psi]^T$ and the control vector is $\mathbf{u} = [\theta_0\ \theta_{1_s}\ \theta_{1_c}\ \theta_{0_{tr}}]^T$. The focus of the work at Glasgow is on manoeuvres that are defined in terms of motion relative to an Earth-fixed frame of reference so that the output equation is the transformation of the body-fixed velocity components into Earth axes. For a unique solution to the inverse problem it is necessary to add a further output, a prescribed heading or sideslip profile being the most appropriate choice. The four scalar constraints - three velocity components and one attitude angle - serve to define uniquely the four control axes of the helicopter.

The sophistication of the modelling implied by the form of $\mathbf{f}$ in equation (1) is of central importance since the more complex the basic formulation, the more difficult it is to cast into a useful inverse form. The mathematical model used for this early work was Helistab [6]; Thomson and Bradley [3] have described a method for the unique solution of the inverse problem in this case. Current work at Glasgow University employs an enhanced model, Helicopter Generic Simulation (HGS), [7] which is accessed by the inverse algorithm, Helinv. The main features of HGS include a multiblade description of main rotor flapping, dynamic inflow, an engine model, and look-up tables for fuselage aerodynamic forces and

moments. The host package, Helinv, incorporates several sets of pre-programmed manoeuvre descriptions which are required as system outputs from the simulation. In fact, the manoeuvres are essentially the input into the simulation and much of the value of Helinv lies in the scope and validity of the library of manoeuvre descriptions which have been accumulated. They include those relating to Nap of the Earth [8], Air-to-air Combat, Off-shore Operations [9], and of particular interest in this study, Mission Task Elements [10]. There is also a facility for accessing flight test data. Some examples of these manoeuvres are discussed in the following section below.

2.3 Mathematical Representation of Mission Task Elements for Use with Inverse Simulation

The need for careful attention to the modelling of the required output - here the flight-path - has been emphasised in 2.1 above. It might appear, at first sight, that for a given general description of a manoeuvre that there is a wide choice of possible definitions of the trajectory. This turns out not to be the case, however, because given such freedom, the obvious starting point is to choose the simplest option but, as is discussed below, the simplest option appears to omit key qualitative features and, subsequently, in section 3 it will be argued that this view can be confirmed by applying quantitative criteria to the manoeuvre definition. However, the simplest case is a useful entry point for the discussion.

2.3.1 Mathematical Representation of Manoeuvres Using Global Polynomial Functions

Part of the early work on inverse simulation at Glasgow involved creating a library of models on helicopter nap-of-the-earth manoeuvres. The approach used was to fit simple polynomial functions to the known profiles of the primary manoeuvre parameters; velocity, acceleration, turn rate, or simply the helicopter's position. For example, an acceleration from a trimmed hover state to some maximum velocity, followed by a deceleration back to the hover is one of the most basic forms of manoeuvre which might be encountered. Consequently the approach used to derive a model of it is fairly simple. As the vehicle is to be in a trimmed hover state at both entry and exit, implying both zero velocity and acceleration at these points, and applying the condition that the maximum velocity, V_{max} should be reached half way through the manoeuvre, it is possible to fit a sixth order polynomial to these conditions to give the velocity profile

$$V(t) = V_{max}\left[-64\left(\frac{t}{t_m}\right)^6 + 192\left(\frac{t}{t_m}\right)^5 - 192\left(\frac{t}{t_m}\right)^4 + 64\left(\frac{t}{t_m}\right)^3\right] \quad (3)$$

where t_m is the time taken to complete the manoeuvre.

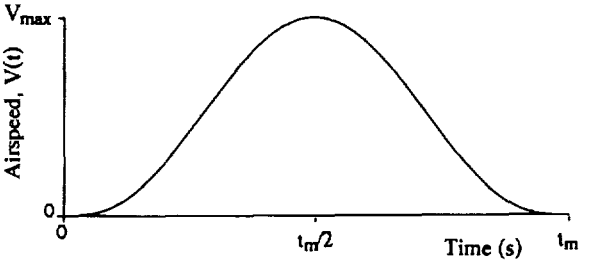

Figure 1 Velocity Profile for Acceleration and Deceleration Manoeuvre Using a 6th Order Polynomial

This velocity profile, shown in Figure 1, can be applied to any of the three component axes of the helicopter to give quick-hop (x), sidestep (y) and bob-up (z) manoeuvres, Figure 2.

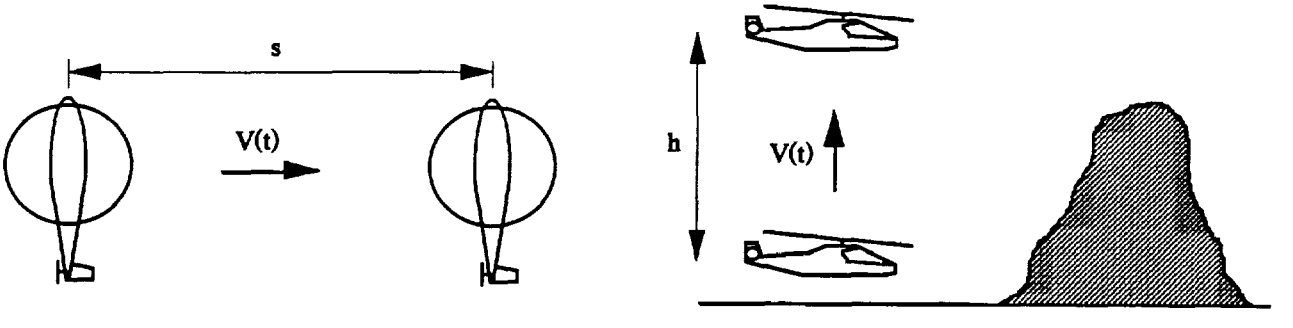

a) The Sidestep

b) The Bob-up

Figure 2 Acceleration and Deceleration Manoeuvres

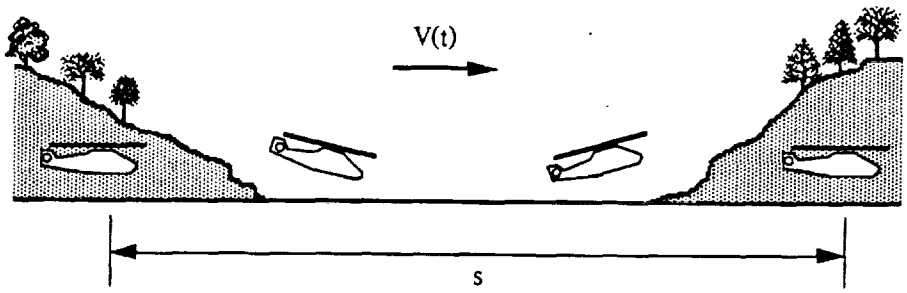

c) The Quick-hop

Figure 2 Continued

To establish the validity of the mathematical representation of a manoeuvre it is necessary to have a sufficient quantity of appropriate data from flight testing to allow comparison to be made. In the context of inverse simulation this data should consist of vehicle component velocities and accelerations as well as its position throughout the manoeuvre. When a comprehensive set of vehicle data, including ground based tracking measurements, was made available, it was clear that these simple functions compared well with the measured data [11]. However, subsequent analysis, reported below in section 3.3, has revealed that a direct comparison of velocities does not provide the appropriate measure of discrimination between candidate profiles and that the profile of equation (3) is not sufficiently aggressive to represent a MTE. Because of the smoothness of the global approximation described earlier in this section it is termed a ' non-aggressive' profile.

2.3.2 Mathematical Representation of Manoeuvres Using Piecewise Polynomial Functions

For the current work a series of models of the Mission Task Elements detailed in the ADS-33C document have been used. When these models were first created, [10] there was little published data on which to base the functions representing the geometry, or indeed the velocity or acceleration profiles, of the MTEs. The ADS-33C document itself gives clear descriptions of the MTEs in terms of performance levels which must be reached in key phases of the MTEs, but stops short of presenting an additional definitive geometry or positional time history. This is of course necessary, as imposing a rigid flight profile on top of a series of performance related targets will lead to a task with intolerable pilot workload. Thus, although the MTEs are described in sufficient detail for piloting purposes, further information is needed to describe the MTE in mathematical terms.

Care was taken when creating the mathematical models of the MTEs to encompass all of the features described in the ADS-33C document. For example, the key elements of the Rapid Sidestep MTE are described as follows

"Starting from a stabilised hover, ... initiate a rapid and aggressive lateral translation at approximately constant heading up to a speed of between 30 and 45 knots. Maintain 30 to 45 knots for approximately 5 seconds followed by an aggressive lateral deceleration back to the hover."

The following performance is also required

maintain the cockpit station within ±3m of the ground reference line,

altitude is to be maintained within ±3m,

maintain heading within ±10 degrees,

attain maximum achievable lateral acceleration within 1.5 seconds of initiating the manoeuvre,

attain maximum achievable deceleration within 3 seconds of initiating the deceleration phase.

It is quite clear from this description that the non-aggressive profile given by equation (3) will not meet all of these requirements. Instead, an alternative approach has been adopted where the MTE is considered as a sequence of polynomial sections where each section is chosen to represent one or more primary manoeuvre parameters of the MTE. A piecewise smooth function, involving one or more of the manoeuvre parameters for the whole MTE, can then be constructed. For the Rapid Sidestep described above there are five distinct sections, and after consideration of the ADS-33C description, it was decided that the most appropriate variable to specify was the vehicle's flight acceleration. This acceleration profile is shown in Figure 3, and the five sections consist of :

i) a rapid increase of lateral acceleration to a maximum value of $\dot{V}_{max}$ after a time of t_a seconds,
ii) a constant acceleration section to allow the flight velocity to approach its required maximum value, V_{max},
iii) a rapid transition from maximum acceleration to maximum deceleration $\dot{V}_{min}$ in a time of t_d seconds,
iv) a constant deceleration to allow the flight velocity to be reduced towards zero,
v) a rapid decrease in deceleration bringing the helicopter back to the hover.

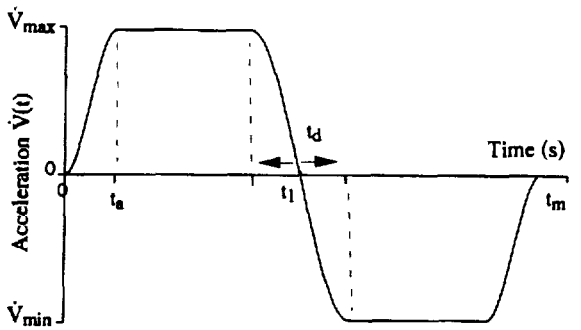

Figure 3 Piecewise Polynomial Representation of an Acceleration Profile for a Rapid Sidestep MTE

The control strategy and state time histories which this profile produces will be discussed in section 3.3. The values of $\dot{V}_{max}$ and $\dot{V}_{min}$ are inputs (effectively dependent on the vehicle being simulated) whilst in order to ensure that the performance limits are met, the values of t_a and t_d are set such that

$$t_a < 1.5s \quad \text{and} \quad t_d < 3.0\ s$$

Referring to Figure 3, the times t_1 and t_m are calculated to give

$$\int_0^{t_1} \dot{V}(t)\,dt = V_{max} \qquad \text{and} \qquad \int_{t_1}^{t_m} \dot{V}(t)\,dt = 0$$

where V_{max} is the maximum velocity reached during the manoeuvre and from Reference 1 is required to be such that $30 < V_{max} < 45$ knots. The transient acceleration profiles are expressed a cubic functions of time so that, for example in the range $t < t_a$,

$$\dot{V}(t) = [-2(\frac{t}{t_m})^3 + 3(\frac{t}{t_m})^2]\,\dot{V}_{max} \qquad (4)$$

The other performance requirements are readily incorporated into an inverse simulation. For example, heading can be constrained to be constant, whilst constant altitude flight along a reference line is guaranteed by ensuring that the off-axis components of velocity are set to zero. The only feature of the Rapid Sidestep MTE as given in ADS-33C which has been disregarded is the necessity to maintain the maximum velocity, lateral flight state between the acceleration and deceleration phases of the manoeuvre for approximately 5 seconds. For the purposes of flight trials this 5 second period may yield useful information on the handling characteristics of the vehicle - for example, poor handling might be indicated if any transient motions present in the vehicle's response do not diminish rapidly once the steady flight state had been attained. For inverse simulation this 5 second period would be modelled as a constant velocity, straight line flight path, and the calculated vehicle response would consist simply of a series of identical trim states. This will yield little useful information, and this phase of the MTE has therefore been ignored.

Developed in this way, in order to capture the aggressive nature of the MTE, the piecewise representation is termed an 'aggressive profile'. A comparison of sidestep manoeuvres generated by both aggressive and non-aggressive profiles can be obtained by differentiating equation (4) to obtain the acceleration for the global polynomial definition. This comparison is shown in Figure 4 from which it is apparent that if the manoeuvre is to be performed in the same time for both cases, then the peak acceleration encountered will be significantly greater in the global polynomial case. This effect is discussed further in section 3.3.1.

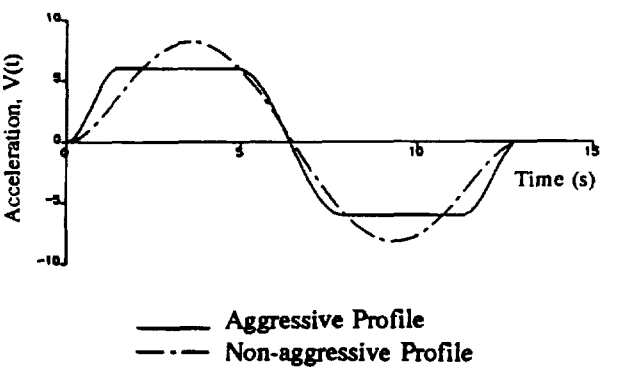

Figure 4 Comparison of Acceleration Profiles for Rapid Sidestep MTE

Not all of the MTEs described in Reference 1 can be converted in quite such a straightforward manner as the Rapid Sidestep described above. For

example, the Pull-up/push-over which is described only in terms of the load factor profile requires the imposition of additional criteria to complete the flight-path definition. In creating the mathematical representations of the MTEs used here, certain assumptions have been made based mainly on the experience gained modelling the earlier NOE manoeuvres. As further information on flight testing using MTEs becomes available it will be possible to validate these models, and improve them as necessary.

3. Inverse Simulation as a Tool for Handling Qualities Assessment

In this section several approaches to handling qualities assessment through inverse simulation are discussed, and some examples are presented to illustrate their effectiveness. Comparisons are made between the results obtained for two configurations of the same helicopter, a battlefield/utility type (based on the Westland Lynx). The baseline configuration, Helicopter 1, has a mass of 3500 kg, and a rotor which is rigid in flap. The second configuration, Helicopter 2, differs from Helicopter 1 in that it has a fully articulated rotor and is 500 kg heavier, the increase in mass causing the centre of gravity to shift approximately 7.5cm aft of a position directly below the rotor hub. The aim here was to create two configurations with a high degree of similarity (both have identical fuselage and rotor aerodynamic characteristics, for example), but with differing performance and agility characteristics.

3.1 Confirmation of Helicopter Performance when Flying Mission Task Elements

Although ADS-33C [1], is directed towards handling qualities, it is unavoidable that the Mission Task Elements that form part of the aggressive task requirements contain a significant element of performance related criteria which refer to the particular configuration being flown. Therefore, the ability to confirm that an existing or projected design can satisfy the criteria, in a performance sense, over the full range of MTEs is of some significance. Section 2.3 discussed how the descriptions of MTEs given in Reference 1 may be converted to a flight path trajectory definition. When the definition is complete, the availability of an inverse simulation enables a range of performance criteria of candidate helicopters to be investigated against configuration parameters - such as control limits, rotor stiffness and installed power. While it is recognised that these criteria may not be the primary considerations which drive the design of the helicopter, inverse simulation can quickly establish the performance limitations of a given design over the full range of MTEs. The following example has been chosen to illustrate this facility.

3.1.1 Comparison of Performance in the Transient Turn MTE

This particular MTE is of interest as, in order to fly it, high roll rates and large roll angles are inevitable, and the parametric differences between the two configurations will have a marked effect on the control time histories generated by inverse simulation.

a) Mathematical Description of the Transient Turn MTE

The main features of this MTE, as described in Reference 1, are that a 180 degree heading change should be completed within 10 seconds of initiating the manoeuvre at a flight velocity of 120 knots. Previous experience of creating models of turning manoeuvres [10] has indicated that the most appropriate parameter to specify is the vehicle turn rate. Following the technique used to model the Rapid Sidestep MTE discussed in section 2.3, the transient turn is assumed to be composed of three distinct sections, as shown in Figure 5 and described below :

i) from a rectilinear flight trajectory, the turn rate is increased rapidly to some maximum value, $\dot{\chi}_{max}$,
ii) the turn rate is maintained at the maximum value until the heading approaches 180 degrees,
iii) the turn rate is rapidly decreased to zero thereby returning the vehicle to straight line flight.

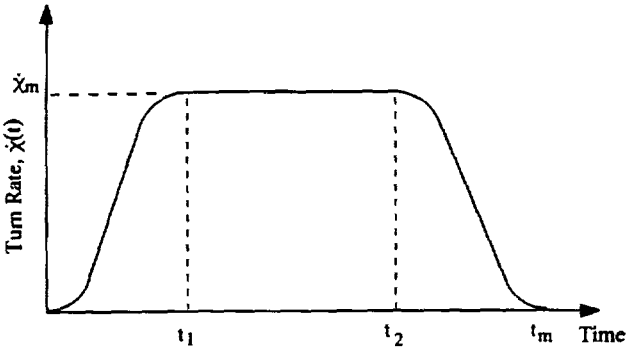

Figure 5 Turn Rate Profile for a Transient Turn MTE

This turn rate profile will force the simulated helicopter to roll to an appropriate bank angle, then hold this angle until the 180 degree heading change is approached, at which point the aircraft will be rolled in the opposite direction to return to straight line flight. If it is further assumed that constant altitude is desirable, and that to perform the task as quickly as possible, the entry speed of 120 knots is maintained

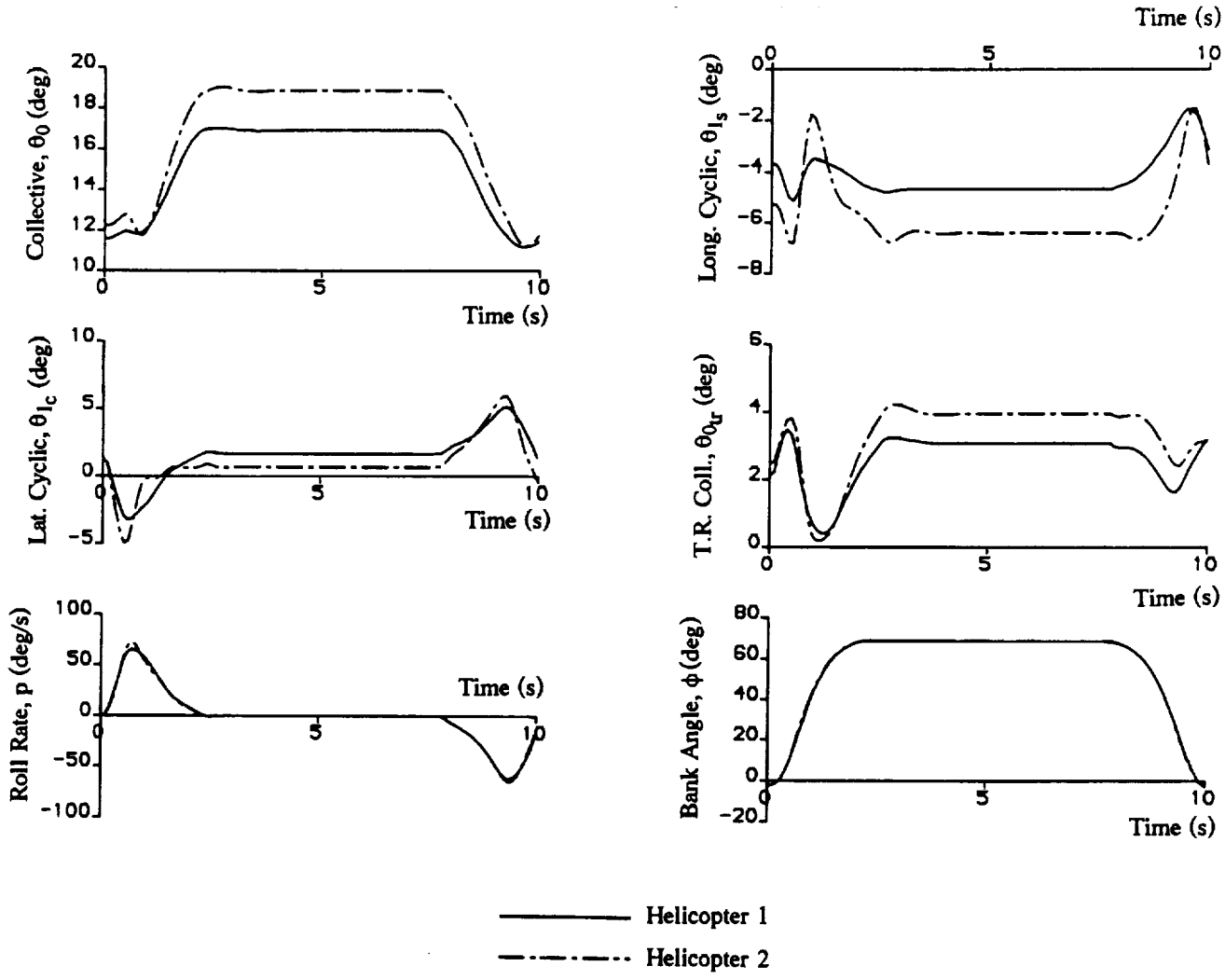

Figure 6 State and Control Time Histories from Inverse Simulation of a Transient Turn MTE

throughout, then the turn rate profile shown in Figure 5 is sufficient to obtain the required mathematical representation. A full description of how the flight path can be obtained from the turn rate profile and airspeed is given by Thomson and Bradley, [10], but the basic principle involves varying the maximum turn rate, $\dot{\chi}_{max}$, until the manoeuvre is completed within 10 seconds, and the heading change (effectively the area under the turn rate profile in Figure 5) is 180 degrees. This situation is reached when the turn radius is 155m and the resulting maximum normal load factor is 2.75. Note that the fraction of the manoeuvre spent in the entry and exit transients must also be specified and in this case a value of 15% was chosen after examination of flight test data from similar manoeuvres [8].

b) Inverse Simulation of Two Configurations Flying Transient Turn MTE - Control Strategy

Having defined the helicopter configurations and specified the manoeuvre, it is possible to perform inverse simulations of the two configurations flying it. The control time histories generated are shown in Figure 6, from which the overall control strategy can be deduced. The manoeuvre is initiated by a pulse in lateral cyclic to roll the aircraft, note that there is little difference in the amount required between the two configurations. As the aircraft rolls, also shown in Figure 6, collective (and hence thrust) must be added to maintain altitude. There is also a forward motion of the longitudinal stick (denoted by negative longitudinal cyclic) to maintain constant forward speed. The manoeuvre is performed without sideslip and tail rotor collective is used to ensure this condition is met. The initial pulse in lateral cyclic is opposed by a similar pulse in tailrotor collective

which then increases beyond its level flight trim position to offset the extra torque produced by increased main rotor collective. The main differences between the time histories of the two aircraft lie in the collective and longitudinal plots. The baseline configuration, Helicopter 1, requires less collective firstly because it is lighter, but one must also consider the effect of shifting the centre of gravity aft of the rotor hub. This produces a nose up pitching moment which must be countered by forward stick if velocity is to be maintained, which explains the 2 degrees of extra forward longitudinal cyclic required by the less agile configuration, Helicopter 2. The longitudinal tilt of the thrust vector is in addition to the lateral tilt required for rolling, and hence is a contributory factory in the 2.5 degrees of extra collective required by Helicopter 2. Examination of Figure 6 shows that the roll angle history which was suggested by the manoeuvre definition is obtained, and the maximum bank angle reached was approximately 70 degrees, with roll rates of approximately 70 degrees/second encountered in the transients.

c) Inverse Simulation of Two Configurations Flying Transient Turn MTE - Confirmation of Performance

The advantage of using inverse simulation becomes apparent when it is realised that the collective limit of this configuration is 20 degrees. Consequently, on examination of the collective time history in Figure 6, it is clear that Helicopter 2 is close to the limiting case for this manoeuvre. It then follows that the limiting case for various aircraft masses and centre of gravity positions could be obtained by repeated inverse simulation of the manoeuvre thereby allowing the aircraft configuration envelope for this MTE to be derived. This type of investigation may be extended to include a range of MTEs and configurational parameters.

For performance comparisons the application of inverse simulation is clear cut. Given the availability of a helicopter model of appropriate validity, it is straightforward to measure comparative control margins and control activity for a given set of manoeuvres. Experience has shown that the facilities offered by flight mechanics models such as HGS are adequate for such investigations. Therefore the remaining task is to compile a suite of validated manoeuvre definitions - and although several of the descriptions of Reference 10 have been validated against flight data there are several manoeuvres for which flight tests are required to provide practical validation. The conclusion to be drawn is that while performance comparisons of this kind are straightforward to conduct, the handling qualities information that it can provide is limited and likely to remain so.

3.2 The Handling Qualities Index

One of the earliest applications of inverse simulation was an attempt to quantify the agility of a given helicopter configuration through an Agility Performance Index (API) [12]. The difficulty of producing a general definition of the term agility is well known [4] but the API was based on the concept of installed agility, that is, it was dependant on the particular configuration of the helicopter and independent of any pilot model. This independence of a pilot model is a feature of the inverse formulation since it generates a precise piloting task and leaves no scope for other than ideal piloting of the helicopter. The API of a helicopter for a given manoeuvre was determined from the formula:

$$API = \sum_{i=1}^{n_s} q_i \int_0^{t_m} f(x_i(t))\, dt + \sum_{j=1}^{n_c} r_j \int_0^{t_m} g(u_j(t))\, dt \qquad (5)$$

where t_m is the time taken to complete the manoeuvre, q_i and r_j are weighting constants related to state i and control j. The integers n_s and n_c are the number of states and controls to be included in the performance index. The functions $f(x_i(t))$ and $g(u_j(t))$ were selected to penalise large state and control deviations during the manoeuvre: for example,

$$f(x_i(t)) = \left[\frac{x_i(t) - x_{i_{trim}}}{x_{i_{max}} - x_{i_{trim}}} \right]^2$$

where $x_{i_{trim}}$ is the value of state i, in the steady flight condition at the entry to the manoeuvre, and $x_{i_{max}}$ is the maximum value of the state encountered during the manoeuvre. Using this definition low values of API (i.e. small control and state displacements) will imply good agility. The obvious difficulty with such an approach is the appropriate choice of the weights q_i and r_j and, in practice, zero or unity were commonly employed in comparative studies of different helicopter configurations on the basis of whether it was felt that those quantities were significant or not in a particular manoeuvre. Nevertheless, despite this simplified approach, the work established the principle whereby different helicopters could be comparatively assessed for their agility over a range of standard manoeuvres by a reproducible simulation study.

Having established the principle for agility studies, it is attractive to consider a similar approach for handling qualities and define a Handling Qualities

Index (HQI) using a similar form to that in equation (5). It may be necessary to include other terms such as auto- and cross-correlations of the control responses but from the whole of the attitude, rate, velocity, acceleration and control information, it should not be unreasonable to expect that an appropriate balance of the coefficients in the formulation of the HQI could produce a formula which reflects, in large measure, an assessment of handling qualities. Unfortunately, the question of finding the values of the coefficients necessary to achieve the appropriate balance is impracticable - just as in the case of the API. Therefore, although conceptually attractive and demonstrable in principle, the HQI falls at the present time because of the lack of essential knowledge about the coefficient values, and if it were to be seriously considered for development in the future then an extensive validation programme would be needed to establish its credibility.

3.3 Quickness Parameters

In addition to the calculation of the time responses of the control displacements, inverse simulation of a given manoeuvre calculates the responses of the full range of kinematic variables. Included in this information, are the time-histories of roll rate p and roll angle ϕ, so that when a Rapid Sidestep manoeuvre is simulated according to the translation velocity profile defined by Figure 3 it is a straight forward matter to calculate the quickness parameter chart $p_{pk}/\Delta\phi_{pk}$ against $\Delta\phi_{min}$ in a manner described by the ADS-33C document, section 3.3. The time histories of p and ϕ shown in Figure 7 for the sidestep manoeuvre with t_a = 1.5s, t_d = 3s, V_{max} = 35 Knots, $\dot{V}_{max}$ = 5m/s^2 and $\dot{V}_{min}$ = -5 m/s^2, are obtained from the inverse simulation of Helicopter 1 for the Rapid Sidestep using the aggressive profile defined by Figure 3. They are annotated to show the calculations of the quickness parameters of the main pulses of roll rate. First there is the roll into the manoeuvre then, at about the midpoint, there is a roll in the opposite direction to bring the rotor into a position to decelerate the helicopter, and finally there is a roll back to the level, trim, position. The attitude quickness parameters corresponding to this data and data from a variety of similar manoeuvres (obtained by varying the parameters used to define the MTE model) are shown in Figure 8 and it can be seen that the values mainly lie in the Level 1 region.

The corresponding control displacement time-histories are shown in Figure 9 but it should be borne in mind that the attitude quickness parameters have been calculated solely as a result of a defined manoeuvre so are not, in the context of inverse simulation, necessarily an appropriate measure of the

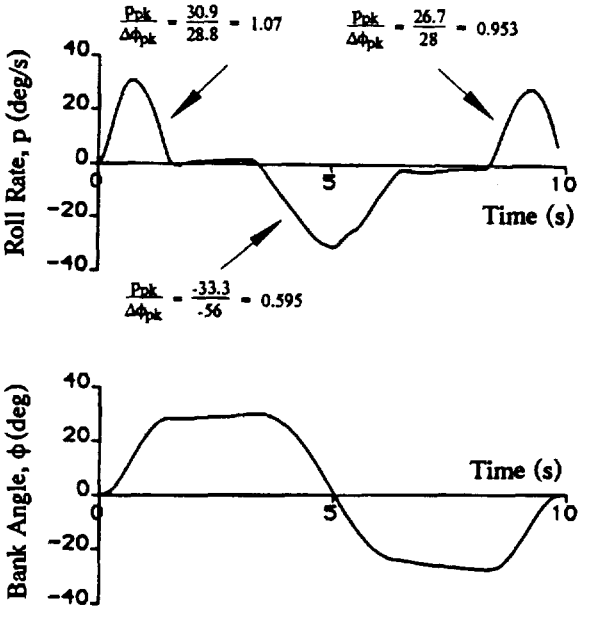

Figure 7 Calculation of Roll Quickness from Inverse Simulation of Helicopter 1 Flying a Rapid Sidestep MTE

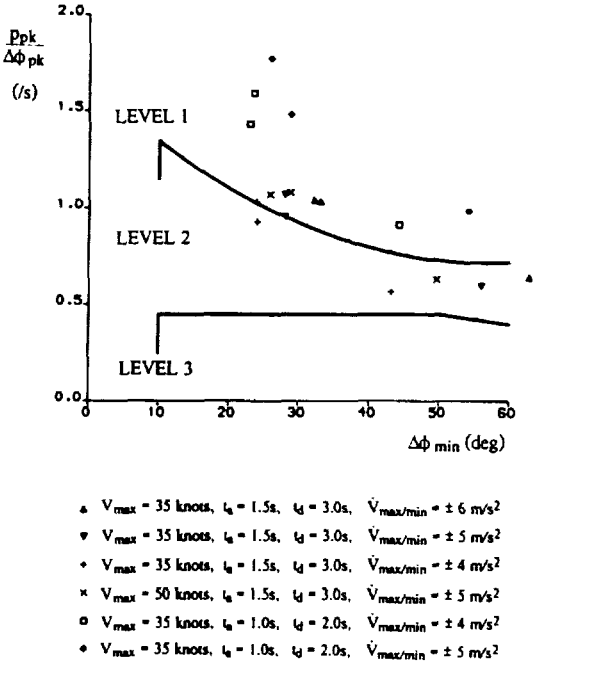

Figure 8 Roll Quickness Chart for Helicopter 1 from Inverse Simulation of Rapid Sidesteps

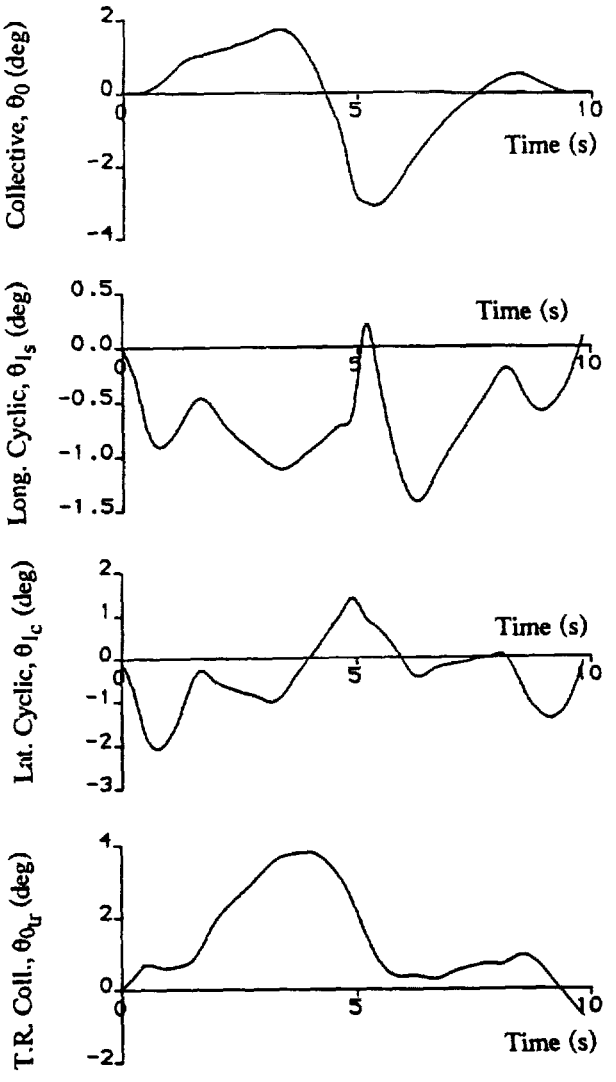

Figure 9 Control Displacements for Helicopter 1 Flying a Rapid Sidestep MTE

handling qualities of a particular configuration. These issues are further elaborated in sections 3.3.1 and 3.3.2 but before leaving the current discussion it is opportune to give some initial attention to the output of the inverse analysis - that is the set of control time histories - and pose the question of how to process it to afford some measure of handling quality or pilot workload. The lateral cyclic control displacement, θ_{1_c}, certainly does not have the characteristics of the bank angle so that the parameter $\dot{\theta}_{1_{cpk}}/\Delta\theta_{1_{cpk}}$ is unlikely to be useful - and indeed experimentation has shown this to be the case. In fact, it may be observed that the pulses of lateral cyclic away from the trim position are of a similar character to the pulses of roll rate, p, and this similarity suggests that Θ_{1_c}, the integral of θ_{1_c}:

$$\Theta_{1_c} = \int^{t} \theta_{1_c}(t)\, dt$$

relates to the value of the bank angle so that a control quickness parameter $\theta_{1_{cpk}}/\Delta\Theta_{1_{cpk}}$ may be the equivalent parameter, and when plotted against $\Delta\Theta_{1_c}$, would give a chart equivalent to that used to plot attitude quickness. The manner of calculation is identical to that of the attitude quickness as illustrated in Figure 10. That this quantity is a useful measure to invoke from the inverse simulation method is discussed in more depth in section to follow.

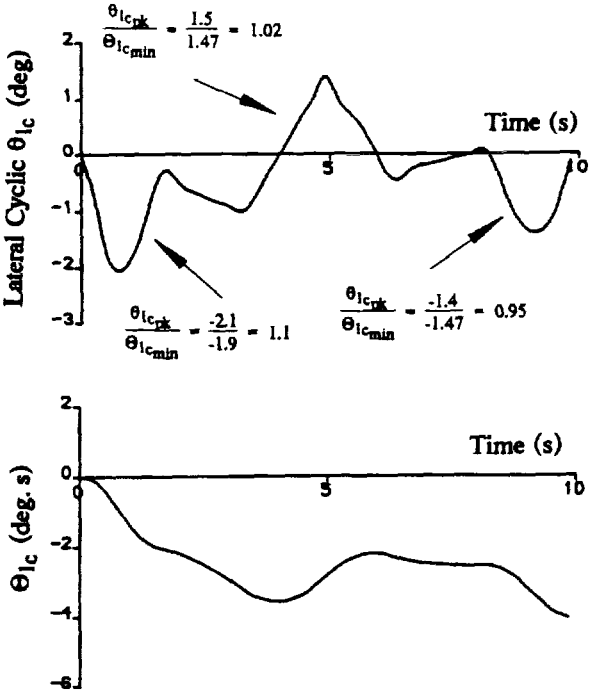

Figure 10 Calculation of Lateral Cyclic Quickness Parameter from Inverse Simulation of Helicopter 1 Flying Rapid Sidestep MTE

3.3.1 Influence of MTE Model

In this section we return to the issues raised above regarding the calculation of quickness parameters for predefined manoeuvres. The first aim of this discussion is to qualify the observations made on previous occasions that the details of the manoeuvre profile definition have not appeared to be significant. When faced with the requirement to specify the velocity profile of a sidestep MTE, for

example, it is natural, as described in section 2.3.1 above, to write down in the first instance the non-aggressive profile, since it is the computationally simplest description. It gives a smoother change in acceleration than the aggressive profile described in section 2.3.2 as has been illustrated in Figure 4. When this manoeuvre is simulated using the Helicopter1 configuration, the attitude quickness parameters vary significantly from those derived from the more sharply executed aggressive manoeuvre and lie mainly in the Level 2 region as is shown in Figure 11. Here then is a further criterion by which to select a manoeuvre description:- if it is to be used for handling qualities studies within the ambit of ADS-33C then a description must be employed which sets the manoeuvre in the Level 1 region. The attitude quickness parameters have discriminated quantitatively between the aggressive and non-aggressive profiles, confirming the quantitative discrimination noted earlier.

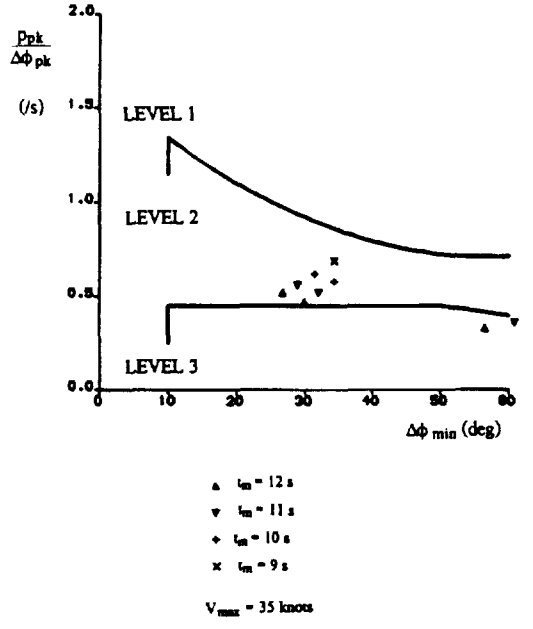

Figure 11 Roll Quickness Chart for Helicopter 1 from Inverse Simulation Using Non-aggressive Sidestep Profile

3.3.2 Influence of Configuration

Now consider the effect of altering the helicopter's configuration to a less agile version. The Helicopter 2 configuration of the vehicle has more weight and significantly reduced rotor stiffness. Applying the same manoeuvre to it produces, as seen in Figure 12, almost identical attitude quickness values - in fact occurring in closely positioned pairs. This result is typical of many simulations which have been conducted and which lead to the initially surprising conclusion that the attitude quickness parameters are largely independent of the configuration used in the inverse simulation. A little reflection will show that this effect is not unusual since the roll rates and attitude angles through a manoeuvre are largely dictated by the manoeuvre profile itself and one should expect some agreement for other than gross configurational changes.

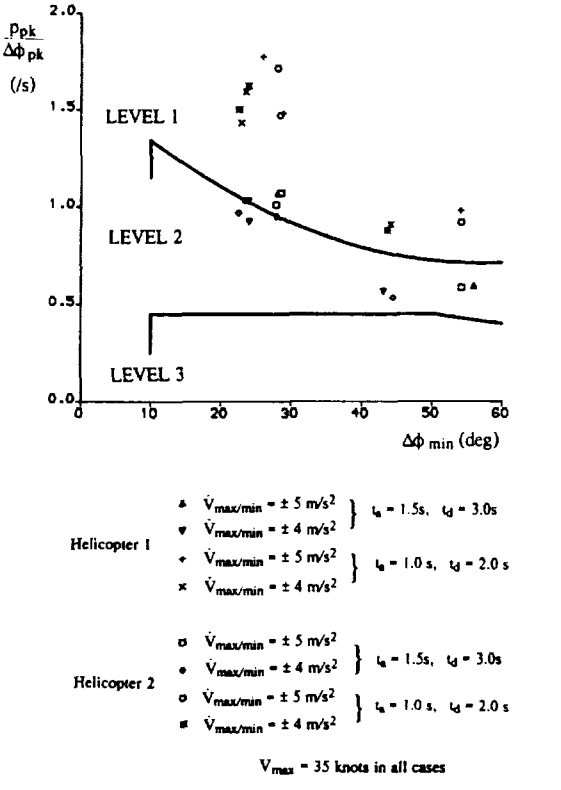

Figure 12 Roll Quickness Chart for 2 Configurations from Inverse Simulation of Rapid Sidestep MTE

However, the control quickness *is* influenced by the variation in configuration. Figure 13 shows quite clearly that it increases significantly for the Helicopter 2 configuration, representing the additional effort required by the pilot to drive the inferior configuration through the same manoeuvre. The control quickness parameter, as defined in Section 3.3, is remarkably effective in discriminating between different configurations.

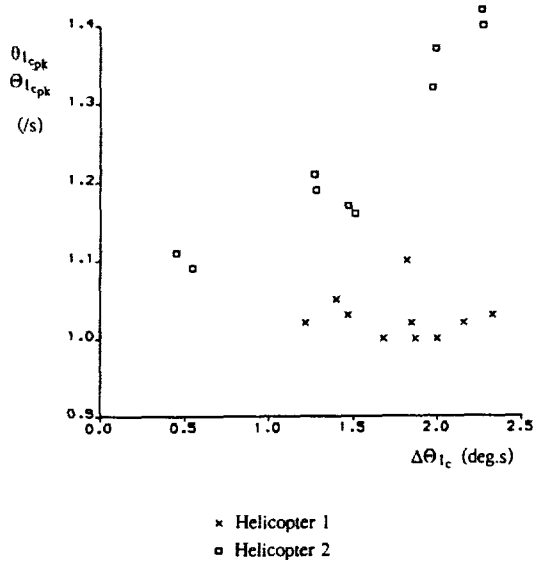

Figure 13 Lateral Cyclic Quickness Chart for 2 Configurations from Inverse Simulation of Rapid Sidestep MTE

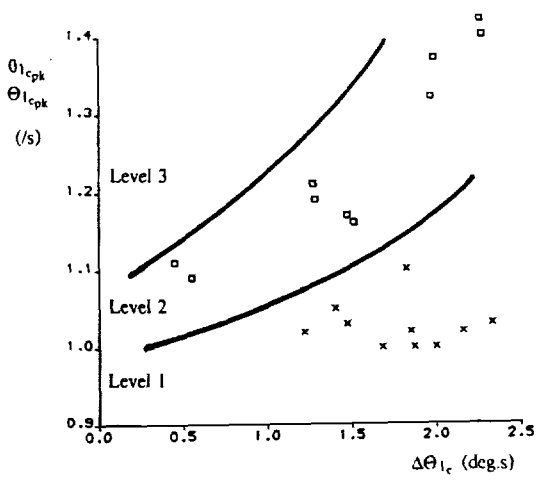

Figure 14 Lateral Cyclic Quickness Chart with Suggested Workload/Handling Qualities Boundaries

3.4 Handling Criteria

These simple illustrations suggest a procedure to be followed when using inverse simulation for handling qualities studies. One must use the requirements, such as ADS-33C, in an inverse manner. First the manoeuvre must be refined until it satisfies the level of handling demanded by the requirements regarding attitude quickness, then various configurational changes can be compared by examining the corresponding control quickness values. An increase in the value of the control quickness indicates an increased work load and hence a worsening of the handling qualities. In addition to there being a relative measure it may be possible, as indicated speculatively on Figure 14 to identify regions in the control quickness chart which correspond to particular levels of pilot workload or handling rating.

4. Conclusions

The potential of three approaches for employing inverse simulation to assess handling qualities have been discussed. Two of them, the Handling Qualities Index and the performance comparisons have been shown to have limited potential while the third, the use of attitude and control quickness parameters in a dual relationship, promises useful exploitation.

Two general conclusions may be made about the current state of inverse simulation:

(a) Current mathematical models, such as HGS, are adequate for basing inverse flight mechanics studies on.

(b) Flight tests should be made to validate the flight-path models currently being developed.

The main conclusion of this work resides in the significance of the quickness parameters in association with inverse simulation.

It is important to emphasise that these investigations have indicated a practical criterion for deciding on the appropriate modelling of an MTE for inverse simulation. That is, the model must generate attitude quickness parameters which lie in the Level 1 region. Moreover, the choice of manoeuvre model is practically independent of helicopter configuration. Therefore, referring to the conditions set out in the introduction, this is the sense in which manoeuvres must be representative.

The approach has been taken further and it has been shown to be possible to define a control quickness parameter which can discriminate between different helicopter configurations flying the same manoeuvre. While it is acknowledged that the choice of definition for the control quickness may require future development, it is clear from the work done so far that this general approach can potentially extend the scope of simulation in demonstrating compliance with handling qualities requirements. It does appear from this work that in using quickness parameters the conditions are sufficient for the successful use of inverse simulation providing that it is realised that it is the control quickness that is the determining factor in the assessment.

Acknowledgements

The authors wish to thank The Royal Society for their continued support of this work. The co-operation Dr Gareth Padfield of the Defence Research Agency, RAE Bedford, is also appreciated, with particular reference to the use of look-up tables and helicopter configurational data.

References

1. Anon, "Aeronautical Design Standard, Handling Qualities Requirements for Military Rotorcraft." ADS-33C, August 1989.

2. Bradley, R., Padfield, G.D., Murray-Smith, D.J., Thomson, D.G., "Validation of Helicopter Mathematical Models." Transactions of the Institute of Measurement and Control, Vol. 12, No. 4, 1990.

3. Thomson, D.G., Bradley, R., "Development and Verification of an Algorithm for Helicopter Inverse Simulation." Vertica, Vol. 14, No. 2, May 1990.

4. Whalley, M.S., "Development and Evaluation of an Inverse Solution Technique for Studying Helicopter Maneuverability and Agility." NASA TM 102889, July 1991.

5. McKillip, R.M., Perri, T.A., "Helicopter Flight Control System Design and Evaluation for NOE Operations Using Controller Inversion Techniques." 45th Annual Forum of the American Helicopter Society, Boston, May 1989.

6. Padfield, G.D., "A Theoretical Model for Helicopter Flight Mechanics for Application to Piloted Simulation." Royal Aircraft Establishment, TR 81048, April 1981.

7. Thomson, D.G., "Development of a Generic Helicopter Mathematical Model for Application to Inverse Simulation." University of Glasgow, Department of Aerospace Engineering, Internal Report No. 9216, June 1992.

8. Thomson, D.G., Bradley, R., "Modelling and Classification of Helicopter Combat Manoeuvres." Proceedings of ICAS Congress, Stockholm, Sweden, September 1990.

9. Taylor, C.D., Thomson, D.G., Bradley, R., "The Mathematical Definition of Helicopter Take-off and Landing Manoeuvres for Offshore Operations." University of Glasgow, Department of Aerospace Engineering, Internal Report No. 9243, October 1992.

10. Thomson, D.G., Bradley, R., "The Use of Inverse Simulation for Conceptual Design." 16th European Rotorcraft Forum, Glasgow, September 1990.

11. Thomson, D.G., Bradley, R., "Validation of Helicopter Mathematical Models by Comparison of Data from Nap-of-the-Earth Flight Tests and Inverse Simulations." Paper No. 78, Proceedings of the 14th European Rotorcraft Forum, Milan, Italy, September 1988.

12. Thomson, D.G., "An Analytical Method of Quantifying Helicopter Agility." Paper 45, Proceedings of the 12th European Rotorcraft Forum, Garmisch-Partenkirchen, Federal Republic of Germany, September 1986.

An Analytic Modeling And System Identification Study of Rotor/Fuselage Dynamics At Hover

Steven W. Hong
United Technologies Research Center
East Hartford, Connecticut

H. C. Curtiss, Jr., Professor
Princeton University
Princeton, New Jersey

Abstract

A combination of analytic modeling and system identification methods have been used to develop an improved dynamic model describing the response of articulated rotor helicopters to control inputs. A high-order linearized model of coupled rotor/body dynamics including flap and lag degrees of freedom and inflow dynamics with literal coefficients is compared to flight test data from single rotor helicopters in the near hover trim condition. The identification problem was formulated using the maximum likelihood function in the time domain. The dynamic model with literal coefficients was used to generate the model states, and the model was parametrized in terms of physical constants of the aircraft rather than the stability derivatives, resulting in a significant reduction in the number of quantities to be identified. The likelihood function was optimized using the genetic algorithm approach. This method proved highly effective in producing an estimated model from flight test data which included coupled fuselage/rotor dynamics. Using this approach it has been shown that blade flexibility is a significant contributing factor to the discrepancies between theory and experiment shown in previous studies. Addition of flexible modes, properly incorporating the constraint due to the lag dampers, results in excellent agreement between flight test and theory, especially in the high frequency range.

Presented at Piloting Vertical Flight Aircraft: A Conference On Flying Qualities and Human Factors, San Francisco, California, 1993.

Introduction

The investigation of rotorcraft dynamics, and specifically the coupled fuselage/rotor dynamics, is motivated by increasing sophistication in rotorcraft stability analyses and by the emergence of high-performance flight control system design requirements. The past few years have seen a concentrated effort directed toward providing an analytic simulation model of coupled fuselage/rotor dynamics and model validation against flight test data.

Helicopter dynamics include the rigid-body responses demonstrated by fixed-wing aircraft, plus higher-frequency modes generated by the interactions of the rotor system with the fuselage. For earlier flight control system designs with lower bandwidth requirements, it was satisfactory to use low-order analytic models which did not accurately model the high-frequency rotor dynamics; with the recent introduction of high-performance, high-bandwidth control system specifications, it has become increasingly necessary to correctly model the coupled fuselage/rotor dynamic modes. It has long been known that flap dynamics introduce significant time delays into the rotor system, and more recently, Curtiss has shown that inclusion of the lag dynamics is important in the design of high performance control systems (Curtiss, 1986). Recent studies have explored the possibility of using rotor state feedback designs to damp blade motion (Ham, 1983). An accurate understanding of the coupled fuselage/rotor dynamics is therefore important in rotorcraft control system design and stability analyses.

Recent flight test experiments have shown that existing simulation models do not accurately

predict these high-frequency modes (Ballin et. al, 1991, Kaplita et. al, 1989, and Kim et. al, 1990). These studies show significant differences between theory and experiment associated with the coupled rotor/body dynamics, especially in the frequency region dominated by the rotor lag motion. This research is therefore directed toward providing an improved understanding of the aeroelastic and aeromechanical phenomena which determine the coupled rotor/body dynamics at hover.

In order to gain physical insight into helicopter dynamics, development of linear models incorporating coupled rotor/fuselage dynamics has long been a research objective. Past approaches to linear model development have included direct numerical perturbation of nonlinear simulations (Diftler, 1988), identification of state-space stability and control matrix elements (Tischler, 1987), and analytic derivation of linear equations of motion (Zhao and Curtiss, 1988). This study uniquely combines system identification methods with analytic modeling techniques in order to investigate helicopter hover dynamics and to arrive at an improved linear model. The emphasis is on the high-frequency dynamics of the coupled rotor/body motion.

The identification study is carried out on flight test data from a Sikorsky H-53E helicopter at hover, using previously published data (Kaplita et. al, 1987, and Mayo et. al, 1990).

Research Objectives

This paper describes an investigation into the response of articulated rotor helicopters to control inputs in hover. The goal is an improved understanding of the coupled rotor/fuselage dynamics in hover directed toward a validated analytic simulation model including high-frequency rotor/fuselage dynamics for use in stability analyses and high-performance control system design studies.

Identification of linear, time-invariant state-space models representing high-order helicopter dynamics including main rotor degrees of freedom has long been an objective of engineers involved in rotorcraft simulation and control system design. The state and control matrix elements in an identified state-space model can provide physical insight into system dynamics and can be used in combination with mathematical modeling techniques to analyze differences between theory and experiment.

State-space identification techniques have been applied to conventional fixed-wing aircraft with useful results. Since identification of state-space models using directly parametrized state and control matrix elements requires the estimation of a large number of parameters, a reduced order model is often used, assuming six degree-of-freedom rigid body dynamics and decoupling between the longitudinal and lateral axes.

Identification of reduced order state-space models for rotorcraft have generally produced unsatisfactory results. The presence of the rotor produces significant rotor/body coupling, requiring additional states to describe the high-frequency dynamics, and also introduces significant interaxis coupling. The complete rotorcraft identification problem is therefore required to use a high-order, multi-input, multi-output model with as many as 18 or more states.

In order to avoid the inevitable problem of overparametrization which results when attempting to identify a directly parametrized high-order helicopter model, this study uses an analytic model to generate state time histories. The model used in this study has been developed at Princeton using the Lagrangian formulation. It includes the coupled fuselage/rotor dynamics, main rotor inflow, tail rotor thrust, and provides for tail rotor inflow dynamics. It was analytically linearized about hover. This model provides a state-space description of the helicopter at hover which is completely analytic and dependent only on an input set of physical parameters. A subset of these inputs are considered uncertain, and are to be estimated from flight test data. The flight-test derived parameter estimates can be used in combination with the mathematical formulation to trace various physical aspects of coupled rotor/body dynamics and thereby obtain physical insight. The complete high-order model including rotor dynamics can be reasonably parametrized by 15 or fewer physically meaningful input coefficients, resulting in a substantial reduction in the number of parameters to be estimated.

The framework of the identification approach is the time-domain maximum likelihood methodology. The likelihood function is formulated assuming the presence of Gaussian measurement and process noise. The process noise may be nonwhite. The noise covariances as well as process noise dynamics may be parametrized. With Gaussian noise assumptions, the likelihood function becomes the weighted least-square of the residual errors. The Kalman filter is the natural way to produce these residuals for state-space dynamic systems.

The maximum likelihood estimate is obtained by finding the global maximum of the likelihood function. The parameters are nonlinearly related to the cost function and the resulting parameter space is highly multimodal. Traditional function optimization techniques based on gradient methods generally become trapped in local optima.

The genetic algorithm is an alternative function optimization approach which does not rely on the use of local gradient information. The genetic algorithm is an adaptive scheme, based on the analogy with natural evolution, which efficiently searches a large parameter space for the 'fittest' solution to a given objective. This method has been demonstrated to be highly effective in obtaining the global maximum in a multimodal parameter space.

The formulation of the system identification problem in the maximum likelihood framework leads to estimates of physical coefficients which have attractive statistical optimality properties and represent the best possible combination of physical coefficients necessary to match the given test data set.

This identification methodology allows an assessment of model assumptions inherent in the mathematical model used to generate the state time histories. In this study, emphasis is placed on the frequency region associated with coupled rotor/fuselage dynamics. In the frequency domain, the dominant feature in the rotor magnitude response is a notch characteristic produced by the presence of the in-plane blade degree of freedom. Using rotor blade constants derived through the identification procedure, rotor blade modeling assumptions may be examined, resulting in analytic model improvements. This study examines in detail the blade structural modeling assumption and investigates the effect of accounting for blade flexibility effects generated by the presence of a large mechanical damper at the blade hinge.

Analytic Model Description

Research at Princeton has resulted in the development of a linearized rotor/body helicopter dynamic model. The dynamic equations are formulated using a Lagrangian approach in order to capture all the important inertial coupling terms. The model includes rigid-body translation and rotation (pitch, roll, and yaw rates, longitudinal and lateral velocities), rigid blade lag and flap multimodal coordinates, and main rotor cyclic dynamic inflow. The controls are main rotor cyclic and pedals. The version of the model used in this study was analytically linearized about the hover trim condition and does not include the collective degree of freedom.

Rotorcraft dynamics includes coupling between the motion of the fuselage which is in rotational and translational motion relative to inertial space, and the motion of individual rotor blades. The final set of equations of motion are referenced to the body-fixed axis system which has its origin at the fuselage center of gravity. In the Newtonian approach to modeling coupled rotor/fuselage equations of motion, blade acceleration terms are first written referenced to the hub axis which is rotating at constant velocity; coordinate transformations are then used to obtain acceleration terms in the body-fixed frame. The complexity of the resulting acceleration terms, combined with the number of degrees of freedom necessary to model rotor dynamics properly, has led to the use of Lagrange's equations for the derivation of the coupled rotor/body model.

The development of Lagrange's equations proceeds from the evaluation of the Lagrangian, which requires only position and velocity terms in order to relate the system generalized forces to changes in the system kinetic and potential energies. The generalized coordinates in Lagrange's approach represent the degrees of freedom in the system and are chosen to correspond to the system

states. The kinetic energy term includes the motion of the fuselage and rotor blades, and the potential energy includes the gravitational potential energy of the fuselage and stored energy in the mechanical springs in the rotor system. Mechanical dampers are accounted for by use of the dissipation function. The generalized forces include aerodynamic forces due to fuselage and blade aerodynamics. Evaluation of the time and partial derivatives in the Lagrangian can be time consuming for a high-order model and can be assigned to a symbolic manipulation program such as MACSYMA.

Identification Methodology

This paper describes an approach for identification of a coupled fuselage/rotor model for rotorcraft hover dynamics from flight test measurements. The identified model includes flap and lag degrees of freedom, main rotor inflow, and process and measurement noise disturbances. The process noise may be colored. The approach uses an analytically derived, linear time-invariant state-space model with literal coefficients which is parametrized in terms of aeromechanical input coefficients. The model order and structure may therefore be assumed to be determined by this approach, and the system parameters are to be estimated from observations. The parameter estimation problem is formulated using the statistical framework of maximum likelihood (ML) estimation theory, thereby benefitting from known optimality properties of ML estimators. This discussion first presents the parametrized dynamic model to be used in the identification methodology, and then describes the application of the maximum likelihood estimation approach to dynamic systems.

Model Parametrization

The helicopter is modeled as a continuous-time dynamic system whose measurements are discretely sampled as sensor outputs. Thus the identification algorithm is required to estimate continuous-time model parameters from discrete sensor measurements. This continuous/discrete formulation is well known and is discussed by Ljung (1987). The linear time-invariant state equations are derived using the Lagrangian approach, and are given by

$$\dot{x}(t) = A_c(\theta)x(t) + B_c(\theta)u(t) + F_c(\theta)w(t) \qquad (1)$$

The model form accounts for the presence of process noise, where $w(t)$ is assumed to be zero-mean white noise with unity spectral density. The continuous-time matrices, $A_c(\theta)$, $B_c(\theta)$, and $F_c(\theta)$, are parametrized by a vector of parameters, θ, which are to be estimated from observations.

The observations are sampled at discrete time intervals, where

$$y(kT) = C(\theta)x(kT) + G(\theta)v_T(kT)$$
$$t = kT, \quad k = 0, 1, 2, \ldots \qquad (2)$$

and $v_T(kT)$ are the disturbance effects at the sampled time intervals.

For digital implementation of the identification algorithm, the continuous-time state equation given in Equation (1) is discretized using zero-order hold. The input is assumed to be held constant over the sampling time interval, and the continuous-time state equation can then be integrated analytically over the interval in order to obtain the discrete-time state equation. The zero-order hold discretization introduces a phase lag equivalent to one-half sample interval, which is taken into account by advancing the control input by the corresponding one-half time interval.

Eliminating time subscripts for simplicity, the discrete-time state-space equations are given by

$$x(t+1) = A(\theta)x(t) + B(\theta)u(t) + F(\theta)w(t)$$
$$y(t) = C(\theta)x(t) + G(\theta)v(t) \qquad (3)$$

This equation is now understood to be a discrete-time equation. Here, $w(t)$ and $v(t)$ are sequences of independent random variables with zero mean and unit covariance.

Maximum Likelihood Formulation

Let Y^N be a vector of observations which are supposed to be realizations of stochastic variables,

and let $y(t)$ be a multi-dimensional observation taken at time t:

$$Y^N = [y(1), y(2), \ldots y(N)]$$

The observations, Y^N, depend on a vector of parameters, θ, which are also considered to be random variables. The conditional probability density function for θ, given the observations, Y^N, is then given by

$$p(\theta|Y^N) = \frac{p(Y^N|\theta) \cdot p(\theta)}{p(Y^N)} \qquad (4)$$

where $p(\theta)$ is the prior distribution of the random parameter vector. A reasonable estimate for θ can then be obtained by finding the value of θ which maximizes the conditional density function given by Equation (4). With no prior knowledge of the distribution of θ, $p(\theta)$ may be assumed to be uniform. The best estimate for θ is then obtained by maximizing the likelihood of obtaining the observations. This leads to the ML, or maximum likelihood, estimator, given by

$$\hat{\theta}_{ML} = \arg\max_{\theta} p(Y^N|\theta) \qquad (5)$$

For parametrized dynamical systems, with Gaussian noise assumptions, the maximum likelihood estimator has the form

$$\begin{aligned}\hat{\theta}_{ML} &= \arg\max_{\theta} p(Y^N|\theta) \\ &= \arg\max_{\theta} -\frac{1}{2}\sum_{t=1}^{N} \varepsilon^T(t,\theta)\Lambda^{-1}(\theta)\varepsilon(t,\theta) - \\ &\qquad \frac{N}{2}\log|\Lambda(\theta)| - \frac{Nm}{2}\log 2\pi \qquad (6)\end{aligned}$$

where

m = *number of measurements*

$\varepsilon(t,\theta) = y(t) - \hat{y}(t,\theta)$

$\Lambda(\theta) = E\varepsilon(\theta)\varepsilon^T(\theta)$

and $\hat{y}(t,\theta)$ is generated using Equation (3) with the discrete-time Kalman filter formulation.

The Genetic Algorithm

The evaluation of the likelihood function as presented in Equation (6) requires a search for the global maximum of the likelihood function over a multimodal parameter space whose contours are not known. Specifically, the identification methodology has led to a function optimization problem where the performance measure is a highly nonlinear function of many parameters. The principal challenge facing the identification problem is the very large set of possible solutions and the presence of many local optima. Hill-climbing methods for function optimization based on finding local gradients become trapped in local optima and are inadequate for this problem. Genetic algorithms overcome these difficulties by efficiently searching the parameter space while preserving and incorporating the best characteristics as the search progresses.

The problem of function optimization can be addressed using the paradigm of adaptive systems, where some objective performance measure (the cost function) is to be maximized (i.e., adaptation occurs) in a partially known and perhaps changing environment. The idea of artificial adaptive plans, based on an analogy with genetic evolution, was formally described by John Holland in the seventies and have recently become an important tool in function optimization and machine learning (Holland, 1975, and Goldberg, 1989). Holland's artificial adaptive plans have come to be known in recent literature as genetic algorithms.

Genetic algorithms are based on ideas underlying the process of evolution; i.e., natural selection and survival of the fittest. Using biological evolution as an analogy, genetic algorithms maintain a population of candidate solutions, or 'individuals,' whose characteristics evolve according to specific genetic operations in order to solve a given task in an optimal way.

As a general overview, genetic algorithms have the following attributes which distinguish them from traditional hill-climbing optimization methods (Goldberg, 1989):

1. GA's work with a representation of the parameter values rather than with the parameters themselves.

2. GA's search from a population of points, not from a single point.

3. GA's use objective function information, not gradient information.

4. GA's use probabilistic transition rules, not deterministic ones.

The genetic algorithm maintains a population of 'individuals'; i.e., possible solutions to the function optimization problem. In the context of the identification problem, each individual corresponds to a vector of parameters. The population of individuals 'evolves' according to the rules of reproduction and mutation analogous to those found in natural evolutionary processes, with the result that the population preserves those characteristics favoring the best solution to the cost function.

The following steps were described by Holland (Holland, 1975) and contain the essentials properties of the the basic genetic algorithm.

1. Select one individual from the initial population probabilistically, after assigning each individual a probability proportional to its observed performance.

2. Copy the selected individual, then apply genetic operators to the copy to produce a new individual.

3. Select a second individual from the population at random (all elements equally likely) and replace it by the new individual produced in step 2.

4. Observe and record the performance of the new structure.

5. Return to step 1.

This deceptively simple set of instructions contains the ability to test large numbers of new combinations of individual characteristics and the ability to progressively exploit the best observed characteristics. It does so through the use of genetic operators.

Genetic Operators

Parent selection based on fitness, and the subsequent application of genetic operators to produce new individuals are the steps by which the algorithm modifies the initial population and continually tests new combinations while maintaining those parameter sets which give high fitness. Each of these operations are performed probabilistically.

The initial population of individuals is selected randomly with a uniform distribution over the defined parameter space. After one generation, parent individuals are selected randomly, with a probability which is proportional to the fitness assigned to that individual. The selection procedure resembles spinning a roulette wheel whose circumference is divided into as many segments as there are individuals. The arc length of each segment is made proportional to the fitness value of the corresponding individual. Thus, the chance of choosing a given individual is uniformly random and yet proportional to its fitness.

The genetic operations of crossover and mutation are then applied to the selected parent individuals in order to introduce new characteristics into the population, enabling an efficient search for the optimal combination of parameters.

The crossover operation involves a recombination of two selected individuals at a randomly selected point. Thus the crossover operation produces two new individuals, each of whom inherit characteristics from both parents.

The mutation operation involves a random alternation of an individual's characteristic with a very low probability. This serves to introduce new information into the pool of structures and serves to guard against the possibility of becoming trapped in local optima.

Genetic Coding

Each individual is a candidate parameter set and is represented as a concatenation of individual parameters:

$$\theta = [\theta_1\ \theta_2\ ,\ \ldots\ ,\ \theta_N]$$

In a digital implementation, each parameter θ_i is encoded using a binary alphabet, and the individual is thus represented by a binary-valued string. The following specific coding scheme was suggested by Starer (Starer, 1990).

Let each parameter θ_i be bounded by $\theta_{i_{max}}$ and $\theta_{i_{min}}$. If each parameter is coded in binary with a word length of l, then the interval $\left[\theta_{i_{max}}, \theta_{i_{min}}\right]$ is discretized by 2^l values. A representation of the parameter θ_i can be obtained from the *l-bit* binary coding of

$$\mathrm{mod}\left\{\frac{\left(\theta_i - \theta_{i_{min}}\right)(2^l - 1)}{\theta_{i_{max}} - \theta_{i_{min}}}\right\}$$

To illustrate, let an individual represent a candidate parametrization where

$$\theta = [\theta_1\ \theta_2] = [3\ \ 4.5]$$

and bounds are given as

$$1 < \theta_1 < 4\ ,\ 2 < \theta_2 < 7\ ,\ l = 6$$

The binary-valued string representing this candidate vector is then

$$\theta_{binary} = [101010\ 011111]$$

The genetic algorithm is illustrated in Figure 1.

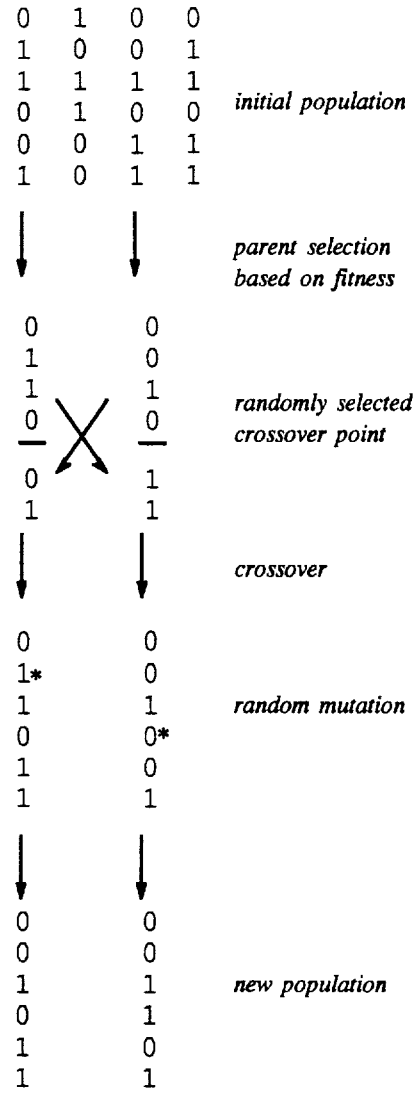

Figure 1 The Genetic Algorithm

Implicit Parallelism

Genetic algorithms efficiently conduct a search over a defined parameter space, converging

to a near-optimal solution. The basic unit of processed information in this genetic search is the schema, defined by Holland (1975). In the context of a digital implementation of genetic algorithms, a schema is a template specifying similarities at certain string positions.

Thus, an individual is a string of binary digits, and the alphabet is composed of $\{0, 1, \#\}$, where # denotes 'don't care' (i.e., the value at this position has no effect on the performance measurement). As an example, an individual may be represented as

[0 0 1 1 1 0 1 1 0 0 0 1 0]

A schema is a similarity template within this individual; so that this individual contains the schemata given by

[0 0 # # 1 0 1 1 0 0 0 1 0]

Given l positions, a single individual is an instance of 2^l distinct combinations, and an instance of 3^l distinct schemata. Further, a population of size N contains between 3^l and $N3^l$ distinct schemata. Holland has shown that each schemata are evaluated and processed independently of the others, providing a tremendous computational leverage on the number of function evaluations. Therefore, the use of genetic operators in the reproductive plan provides i) intrinsic parallelism in the testing and use of many schemata, and ii) compact storage and use of large amounts of information resulting from prior observations of schemata.

The concept of implicit parallelism is fundamental to the efficiency of genetic algorithms. Each schemata is processed and evaluated independently of other schema in the population; this provides a tremendous computational leverage. A very weak lower bound states that for a population of (n) individuals, more than $o(n^3)$ useful 'pieces' of information is processed in each iteration (Goldberg, 1989).

An Example

As an illustration of the genetic algorithm, consider the following example.

$$f(x,y) = 3(1-y)^2 e^{-y^2-(x+1)^2} - 10\left(\frac{y}{5} - y^3 - x^5\right)e^{-y^2-x^2} - \frac{1}{3}e^{-(y+1)^2-x^2}$$

The function surface is shown in Figure 2, along with the contour lines. This multimodal function has a global maximum at $(1.5814, -0.0093)$.

A genetic algorithm was run on this function with a population size of 20. The initial guesses were chosen randomly, and were bounded as $-3 < x < 3$, $-3 < y < 3$. A binary code with wordlength of 8 was used, which means that both x and y were discretized by 256 points. An exhaustive grid search under these conditions would involve evaluating 65536 possible points to find the global maximum.

Snapshots of the population distribution up to 7 generations are shown in Figure 2. The snapshots show the population converging upon the global maximum; by the 7^{th} generation, most of the individuals have converged on the maximum. The genetic algorithm in this case converges on $(1.5412, -0.0353)$ as the global optimum.

This convergence has occurred after 7 generations. With a population size of 20 individuals, this is 140 function evaluations as compared to the 65536 necessary for the grid search.

This relatively simple example serves to illustrate the ability of the genetic algorithm to find the optimum of a given function , *using no gradient information.*

Analytic Model Validation

The mathematical model is correlated with flight test data using nominal values for input coefficients. The correlation plots in Figure 3 show transfer function comparisons for pitch and roll axes. The data represent separate flights. In each

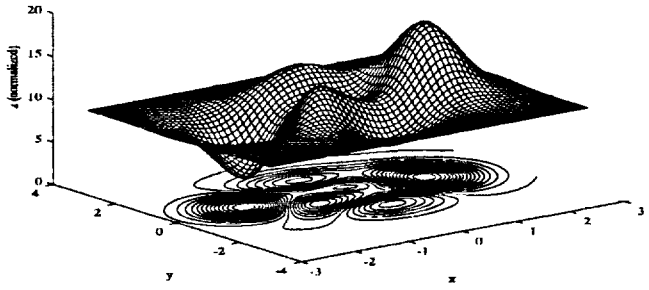

Sample Function

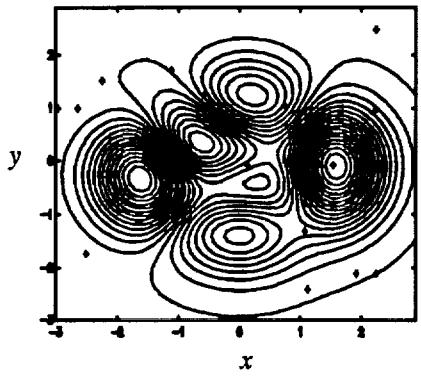

Generation 1

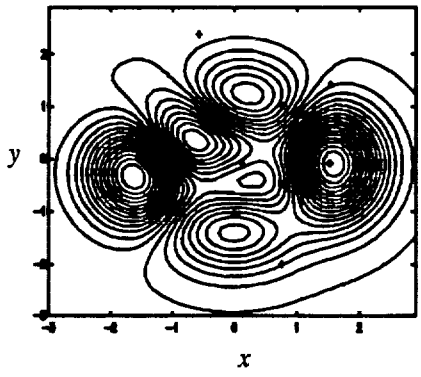

Generation 3

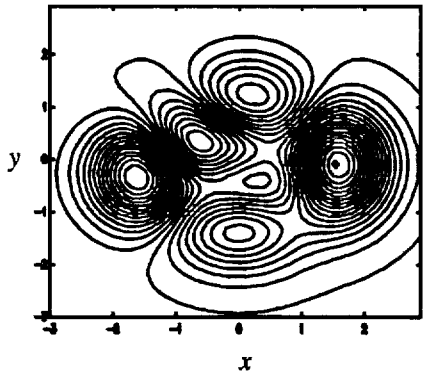

Generation 5

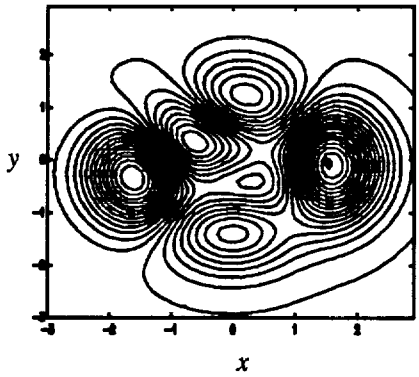

Generation 7

Figure 2 Genetic Algorithm Example

case, the comparison is between the flight test rate gyro output and the model state. The comparison is made between 0.5 Hz (3.14 rad/sec) and 6 Hz (37.7 rad/sec) since the input signal was designed to cover this frequency range. The fuselage structural bending modes are lightly damped and dominate the frequency above ~20 rad/sec. Therefore the identification procedure uses a bandpass filter with the upper cutoff frequency at 15.7 rad/sec. The frequency range of interest is therefore between 0.5 Hz to 2.5 Hz (3.14 rad/sec to 15.7 rad/sec).

The choice of physical coefficients used to parametrized dynamic model must allow adjustments to account for differences between test and theoretical responses using nominal physical input values. The gain differences at low frequencies, implying a mismatch in rigid body response, requires parametrization of the rigid body acceleration. The coupled fuselage/lagwise modes are a lightly damped pole-zero pair and create a notch-filter effect in the frequency response between 10 - 15 rad/sec. This frequency is near the -180 degree crossover, and a mismatch in this region adversely impacts the gain and phase margin calculations. Modeling the dynamics of this mode is important for control system design and stability analysis and will be the primary focus of modeling in this study.

Validation Of Identification Procedure Using Simulated Data

The maximum likelihood identification methodology for parametrized dynamic systems is validated first on a simulation with known parameters. These results demonstrate the feasibility of using genetic algorithms to estimate physical coefficients from noisy data, and establish the population size and crossover and mutation rates for this application.

The simulation model is driven by flight test control inputs from the hovering condition. Main rotor pitch and roll cyclic and tail rotor pedals are all active, with primary excitation into roll cyclic. The output states used to form the cost function are pitch, roll, and yaw rates, and pitch and roll attitudes. No velocity information is necessary.

Simulation Model Parametrization

The model structure and parametrization was presented in Equations (1) through (3). The continuous-time state space model is analytically derived using the Lagrangian approach and using a vector of physical input coefficients, θ. For the purposes of this simulation study, the model structure has been augmented to include a first order time constant on process noise. The process noise dynamics are to be parametrized and estimated from output data.

The simulation model was parametrized as follows:

aerodynamic coefficients:

- lift curve slope, a
- inflow equivalent cylinder height, *hhnd*
- inflow wake rigidity factor, *wrf*

hover trim values:

- trim flap angle, β_o
- trim main rotor pitch angle, t_o
- trim inflow velocity, v_o

main rotor blade constants:

- lag damper constant, $\overline{C}_\zeta$
- lag spring constant, $\overline{K}_\zeta$
- flap spring constant, $\overline{K}_\beta$

inertias:

- fuselage cross-moment, I_{xz}

tail rotor:

- tail rotor thrust scale factor, K_{TR}

noise parameters:

- noise covariance ratio, *NR*
- process noise time constant, τ

Kalman filter theory allows optimal state estimates to be obtained in the presence of state and measurement noise, where the Kalman gain is uniquely determined up to the ratio of process to measurement noise. The noise covariance estimate is therefore parametrized by the ratio of process to measurement noise.

Genetic Algorithm Procedure

The genetic algorithm was implemented using a population size of 500 individuals; a crossover

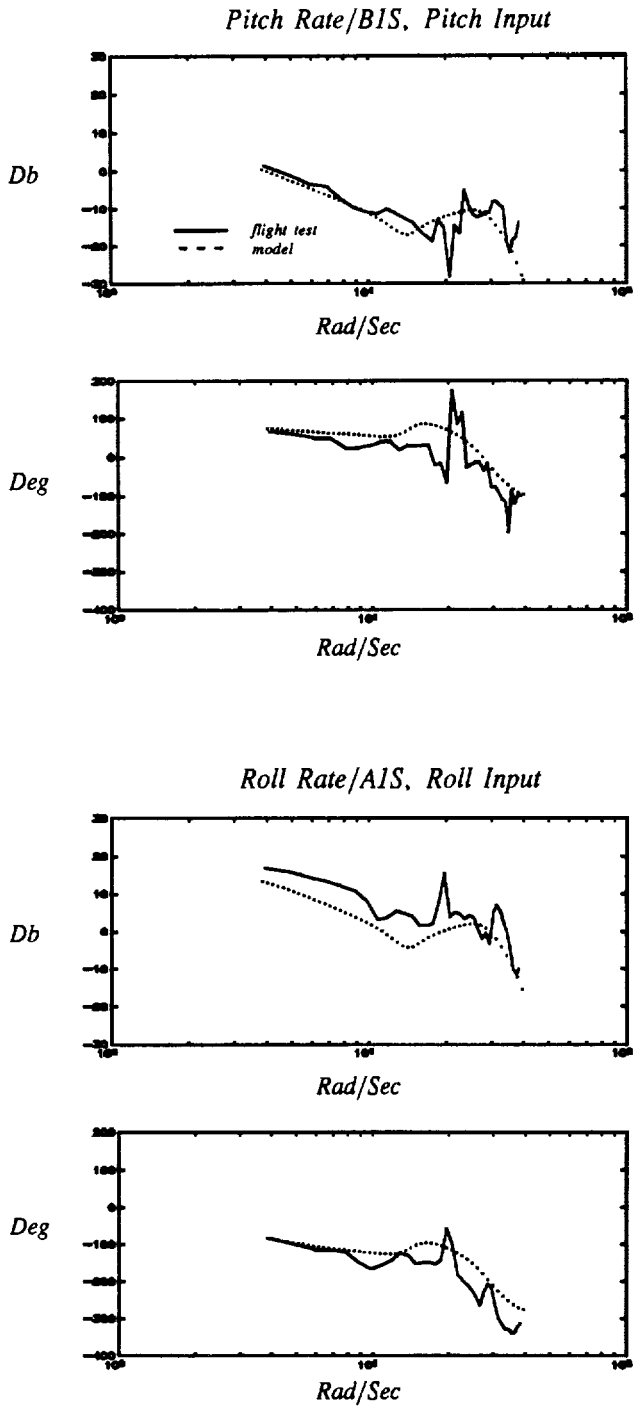

Figure 3 Model Validation

rate of 2/3; and a mutation rate of 1/1000. The parameters were allowed to vary within 50 percent of the known simulation values.

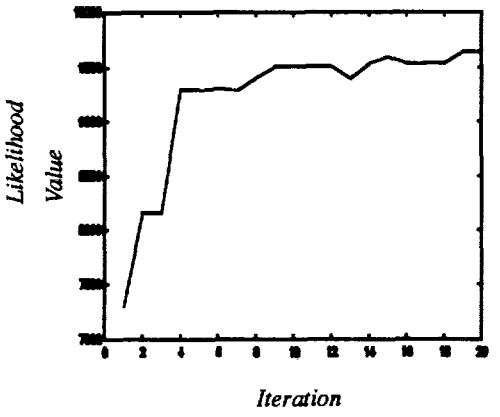

Figure 4 Best Likelihood Values

The sensitivity of the cost function to the parameter values vary widely. Therefore, as parameters begin to show convergence, the range of allowable values is progressively narrowed in order to demonstrate convergence for all parameters.

The identification proceeds by running 10–12 separate genetic algorithms simultaneously, where each algorithm begins with a new random number generator seed to select the initial guesses. Each set of runs therefore produces a scatter band of near optimal guesses for each parameter. The parameters which influence the cost function most are identified most tightly.

Figure 4 shows the progression of the best fitness values out of the population at each generation. The results are shown in Figure 5. The solid line in each figure denotes the true value.

The noise covariance ratio parameter couples only very weakly to the cost function and displays an almost random distribution until the physical coefficient estimates sufficiently converge. Therefore a two–step estimation procedure is required, where the noise ratio is allowed to remain free until physical coefficients have converged. The physical coefficients are then fixed while the noise ratio is estimated.

This methodology clearly demonstrates convergence. Twenty iterations of the genetic algorithm were run. Table 1 tabulates the parameter estimates.

Table 1 Estimated Parameters, Simulation Study

Parameters	θ_o	$\hat{\theta}_o$	std
lift curve slope, a	5.73	5.72	3.98e-4
inflow equivalent cylinder height, *hhnd*	0.46	0.46	2.23e-4
inflow wake rigidity factor, *wrf*	2.0	2.0	1.34e-4
trim flap angle, β_o	0.02	0.02	4.99e-7
trim main rotor pitch angle, t_o	0.05	0.0497	9.75e-6
trim inflow velocity, ν_o	0.02	0.0196	2.61e-6
lag damper constant, $\overline{C}_\zeta$	5.0	4.978	7.7e-3
lag spring constant, $\overline{K}_\zeta$	75.0	75.0	7.06e-2
flap spring constant, $\overline{K}_\beta$	45.0	44.92	6.3e-3
fuselage cross-moment of inertia, I_{xz}	30,000	30,035	4.98
tail rotor thrust factor, K_{TR}	1.0	0.99	9.35e-4
covariance ratio, process/measurement, *NR*	1.0	0.97	0.11
process noise time constant, τ	-1.0	-0.99	1.8e-3

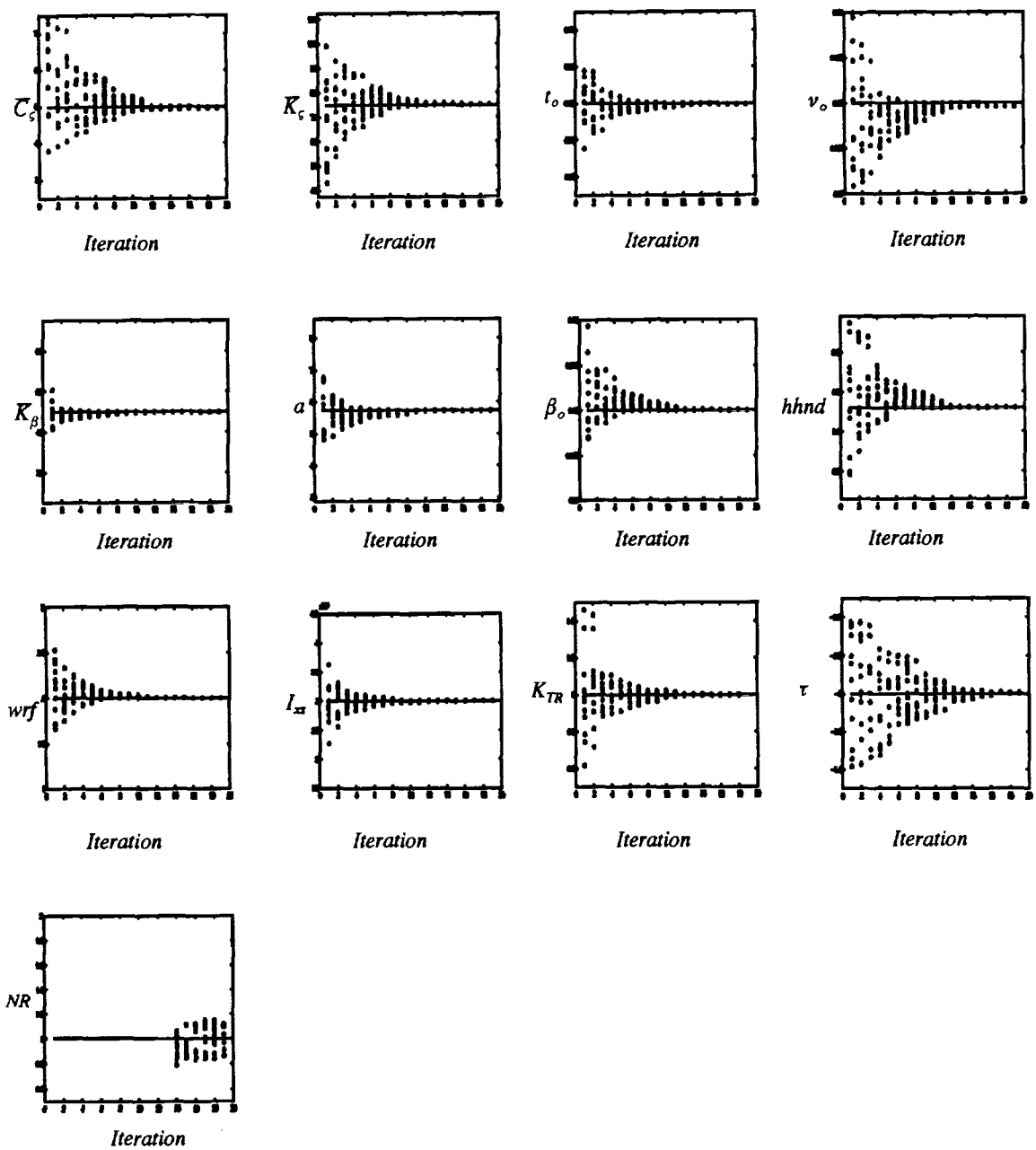

Figure 5 Simulation Identification Results

C-4

Flight Test Identification Results

Data consistency checks ensure that errors in data collection do not interfere with the estimation procedure. The requirements for this step were minimal in this study, since this estimation methodology requires only rate and attitude information. Consistency was checked by integrating accelerations and rates, and ensuring that sensor attitudes and rates match the integrated rates and attitudes.

The flight test data was processed by 1) applying a bandpass filter, and 2) decimating the data from 80 Hz to 8 Hz. The filter passband was from 0.5 to 2.5 Hz (3.1416 to 15.708 rad/sec). The lower bound corresponds to the beginning frequency of the frequency sweep input used to drive the system, and the upper bound is imposed to exclude the first fuselage bending mode at 3.4 Hz.

The flight test identification parametrization was modified to reflect information available from comparison between test and theoretical responses generated from the analytic model using nominal parameter values. The parameter list used in flight test identification runs is shown in Table 2. The modifications are explained below.

The parametrization of body inertias accounts for significant differences between theory and test in rigid body response, especially in the roll axis. Further, due to significant differences in cross-axis predictions, the roll and yaw rigid body responses could not be simultaneously satisfied. Therefore, yaw axis parameters were eliminated, and the identification scheme therefore attempts to fit pitch and roll responses only. This is permissible since for small motions about hover, yaw rate does not couple with main rotor cyclic multiblade coordinates and has no effect on pitch and roll responses in the rotor/body frequency region.

The inflow equivalent cylinder height (*hhnd*) is related to the main rotor dynamic inflow time constant. This parameter had no effect on the cost function in the bandpass frequency region used in this study. Therefore a quasistatic main rotor inflow formulation was used and this parameter was dropped.

The process noise dynamics, parametrized by a first order time constant, was also eliminated. This parameter is uniquely identifiable apart from the noise power ratio only if the time constant falls within the bandpass frequency range, and was found to have no effect on the cost function.

The identification run was carried out using flight test data from hover, with primary excitation into roll cyclic. The analytic model, parametrized as given in Table 2, was driven by main rotor pitch and roll cyclic and tail rotor pedal. The likelihood function was formed using pitch and roll rates only.

Table 2 Estimated Parameters, Flight Test

Parameters	$\hat{\theta}_o$	std	bounds	nominal
scale factor, fuselage roll moment of inertia, I_x	0.44	0.011	0.35-1.0	1.0
scale factor, fuselage pitch moment of inertia, I_y	1.15	0.033	0.7-1.3	1.0
lift curve slope, a	8.4	0.066	5-10	5.73
inflow wake rigidity factor, wrf	8.0	0.23	2-11	2.0
trim flap angle, β_o	0.162	0.0013	0.05-0.25	0.0848
trim main rotor pitch angle, t_0	0.0172	0.00016	0.005-0.15	0.1304
trim inflow velocity, v_o	0.048	0.0007	0.01-0.1	0.0613
lag damper constant, $\overline{C}_\zeta$	5.5	0.10	4-10	9.5
lag spring constant, $\overline{K}_\zeta$	85.0	0.735	0-100	0
flap spring constant, $\overline{K}_\beta$	16	1.34	0-20	0
noise covariance ratio, NR	-	-	0.001-0.1	-

The initial choice of boundary limits on each parameter defines the parameter space to be searched in the identification algorithm. The bounds applied to each parameter are shown in Table 2; in each case, the bounds are chosen to include the nominal value.

Table 2 shows the identification results for flight test data. It was found that the noise ratio parameter did not converge while the remaining physical coefficients did, indicating that relative to the aeromechanical coefficients, noise powers affect the cost function only very weakly.

The correlation with flight test data using the identified parameters is shown in Figure 6, where the roll axis response is correlated with the data set used in the identification, and the pitch axis response is an independent check. The roll axis correlation shows clear improvement in model correlation using identified coefficients. The low frequency gain prediction has been corrected through the inertia adjustment, and the notch in gain response due to the coupled lag/body response has been corrected.

The differences between identified and nominal parameters can provide physical insight into rotor phenomena when analytic explanations can be found for parameter differences. The identified parameters for lift curve slope, a, and wake rigidity factor, wrf, have produced significant improvement in model response, indicating a possible requirement for refinement of the aerodynamic theory used in the model. The identified parameters for main rotor spring and damping constants indicate necessary refinements in the prediction of frequency and damping of blade motion. A model improvement for blade in-plane dynamics is now presented.

Modeling Blade Elasticity

The identification procedure has resulted in estimated values for rotor blade spring and damping parameters which are different from nominal values. The nominal mechanical damper value may be assumed to be known since it can be independently verified through available data.

A procedure for modeling blade elasticity is presented which accurately accounts for differences between nominal and estimated values for in-plane motion frequency and damping. The method of assumed modes is used to model the case of a flexible beam with damper and spring constraints. This procedure is first demonstrated on a nonrotating beam, for which an exact solution can be obtained. The method of assumed modes will be shown to be a good approximation of the exact solution. This approximate solution can then be used in the flexible beam analysis in the analytic hover helicopter model. The beam formulations for both rotating and nonrotating blades with both spring and damper constraints at the root is given in detail in Appendices A and B.

Approximate solution methods such as the method of assumed modes display convergence toward the analytic solution as more assumed mode shapes are added to the set of basis functions. The first approach to the lagwise bending problem was to use increasing numbers of mode shapes that fulfilled the boundary conditions for a hinged beam. However, with this approach, convergence was not achieved after even after using 5 assumed modes. In order to avoid using an unacceptably large number of basis polynomials in the model, an alternative approach using a combination of modes that satisfy hinged and cantilever boundary conditions was used.

Figure 7 illustrates the assumed modes solution method using both the nonrotating and rotating beam formulations. For a nonrotating beam with spring and damper constraints, an exact expression for the beam eigenvalues is available and is given in detail in Appendix B. The analytic eigenvalue equation is solved numerically. In this case, the root finding problem was converted into a function optimization problem and solved using the genetic algorithm. This solution to the exact formulation is shown against approximate solutions in Figure 7. The approximate solution using the Lagrangian approach, when using only basis functions which fulfill hinged beam boundary conditions, approach the exact solution slowly. With 4 hinged basis polynomials, the solution has not yet converged. However, the assumed modes approach with only one hinged plus one cantilever mode shapes matches

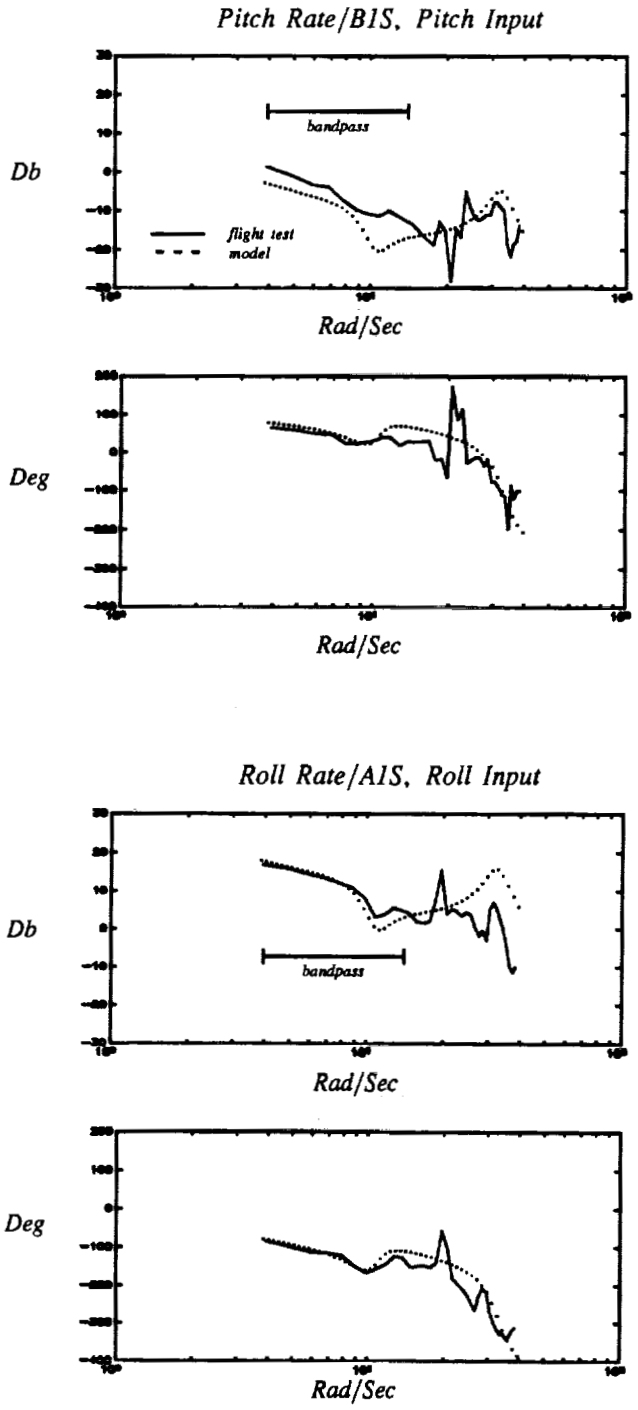

Figure 6 Identified Model Validation

Nonrotating Beam

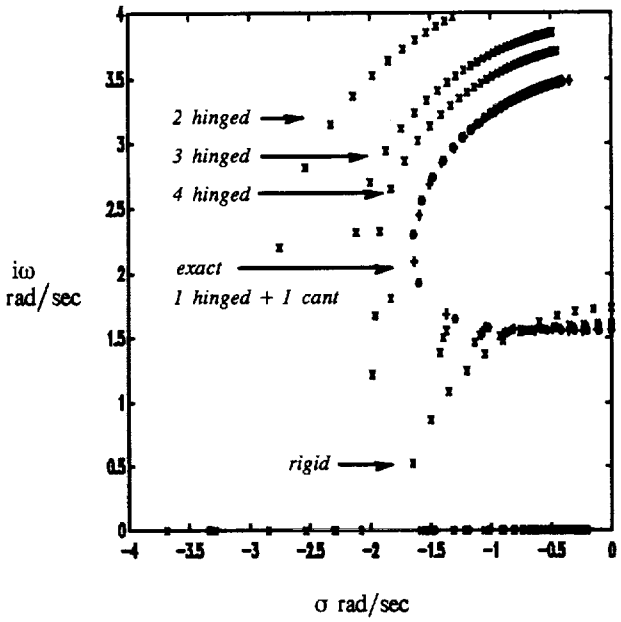

Rotating Beam

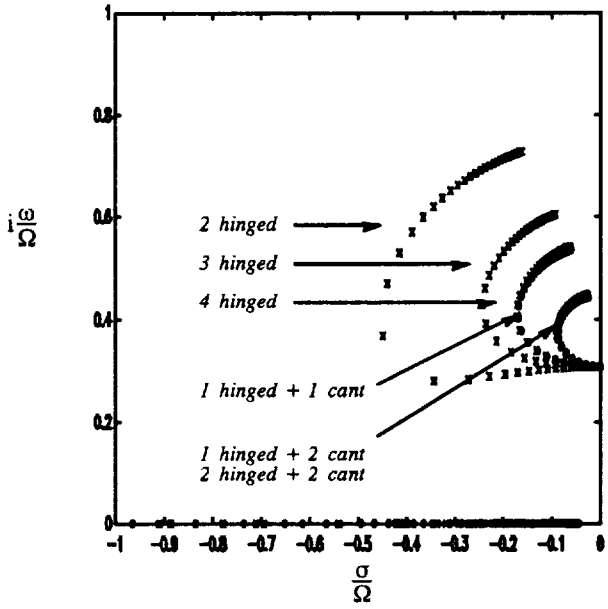

Figure 7 Modal Solutions For Beam Equations

the analytic solution exactly. Convergence is demonstrated by the fact that addition of either hinged or cantilever mode shapes do not further change the eigenvalue solution.

Figure 7 then shows the convergence of the approximate solution for the rotating beam, for which there exists no known exact solution. Here, the sum of 2 hinged plus 2 cantilever modes is near convergence. The addition of either one more hinged or one more cantilever mode does not change the solution appreciably. The combination of 2 hinged plus 2 cantilever modes is chosen for model development as a good compromise between model order and accuracy of solution.

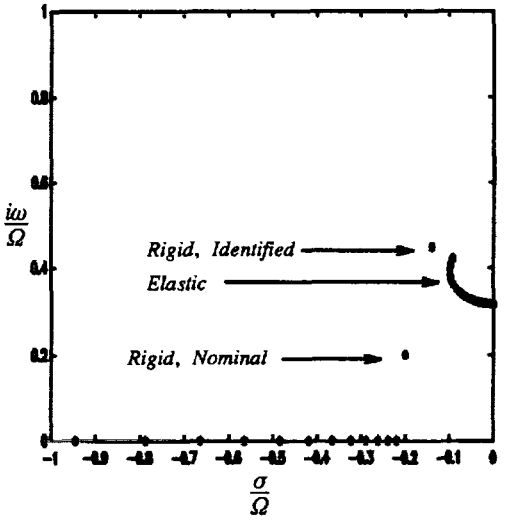

Figure 8 Rotating Frame Lag Roots

Figure 8 shows the location of the rotating frame lag mode eigenvalues. The elastic blade model using two hinged and two cantilever mode shapes is used to show the progression of the root location as damper value is increased from zero to the nominal value. The predicted root location for the elastic model with the nominal damper constant agrees reasonably well with the predicted location for the rigid blade model using a fictitious spring and using identified spring and damper constants. The rigid blade model using nominal damper constant only (no spring) predicts a much higher damping and lower frequency than is indicated by test data.

Conclusions

An analytically derived linear model of coupled rotor/body dynamics at hover has been validated against flight test data.

The analytic model with literal coefficients has been parametrized using 11 physically meaningful coefficients, including noise covariances. This model has been used to formulate a multi-input, multi-output likelihood function in the time domain. The analytic model is used to generate the state time histories. Only body rates are necessary in the cost function.

The likelihood function is globally maximized using the genetic algorithm approach, resulting in statistically optimal maximum likelihood parameter estimates.

The estimated parameters indicate that lag mode damping in flight is approximately one-half of the value expected from rigid blades.

The correct analytic prediction for lagwise motion is obtained using an elastic blade formulation. The flexible blade model was formulated using a normal mode approach and checked using the closed form solution for a nonrotating beam. The convergence results using assumed mode shapes indicate that the correct lagwise bending mode shapes are obtained using a combination of cantilever and hinged assumed modes.

Acknowledgement

One of the authors (S. Hong) would like to thank Mr. Bill Twomey in the Dynamics Section at Sikorsky Aircraft for key discussions on the effect of blade flexibility on blade motion, Professor P. M. Schultheiss at Yale University for insights into the identification framework, and Dr. Richard Williams at the United Technologies Research Center for generously supporting this research effort.

Part of this work was carried out at Princeton University under NASA Ames grant NAG2-561.

Appendix A. Modeling Blade Elasticity

Equation (A.1) gives the in-plane bending equation for a rotating beam. The derivation can be

found in Bramwell (1976), and in Johnson (1980). This partial differential equation relates the moments due to the inertial, centrifugal, and aerodynamic forces to the moment expression from engineering beam theory.

$$\frac{\partial^2}{\partial r^2}\left[EI\frac{\partial^2 Y}{\partial r^2}\right] - \frac{\partial}{\partial r}\left[G(r)\frac{\partial Y}{\partial r}\right] + m\left[\frac{\partial^2 Y}{\partial t^2} - \Omega^2 Y\right] = 0 \qquad (A.1)$$

All quantities are understood to refer to lagwise bending motion. Here, $G(r)$ is the centrifugal tension force at a point at a distance r from the hub center, E is the modulus of elasticity, I is the lagwise area moment, and Ω is the rotor rotational velocity.

The boundary conditions for a hinged blade are:

At the hinge:

$$Y(e) = 0$$

$$EI\frac{\partial^2 Y}{\partial r^2} = moment = 0$$

At the tip:

$$EI\frac{\partial^2 Y}{\partial r^2} = 0$$

$$\frac{\partial^3 Y}{\partial r^3} = shear\ force = 0$$

There is no known analytic solution for Equation (A.1) due to the presence of the centrifugal term. A solution based on the method of assumed modes is presented.

Let the lagwise displacement be of the form

$$Y(x,t) = R\sum_n \phi_n(x)q_n(t) \qquad (A.2)$$

where R = blade length. This solution method follows the method of separation of variables. $\phi_n(x)$ are a sequence of functions, not necessarily orthogonal, which approximate the expected blade shape and which satisfy the blade boundary conditions.

Substituting into Equation (A.1),

$$\frac{\partial^2}{\partial x^2}EI\sum_n q_n\frac{\partial^2}{\partial x^2}\phi_n - R^2\frac{\partial}{\partial x}G\sum_n q_n\frac{\partial}{\partial x}\phi_n + \sum_n(\ddot{q}_n - \Omega^2 q_n)\phi_n R^4 m = 0 \qquad (A.3)$$

Multiply Equation (A.3) by ϕ_m and integrate from $\frac{e}{R} < x < R$, or $\bar{e} < x < 1$ where $\bar{e}$ is understood to be a nondimensional offset value.

This gives

$$\sum_n q_n\int_{\bar{e}}^1 \phi_m\frac{\partial^2}{\partial x^2}EI\phi_n''dx - R^2\sum_n q_n\int_{\bar{e}}^1 \phi_m\frac{\partial}{\partial x}G\phi_n'dx + R^4\sum_n(\ddot{q}_n - \Omega^2 q_n)\int_{\bar{e}}^1 m\phi_m\phi_n dx = 0 \qquad (A.4)$$

Integrating each term by parts, the first term gives

$$\sum_n q_n\int_{\bar{e}}^1 \phi_m\frac{\partial^2}{\partial x^2}EI\phi_n''dx = \left[\sum_n q_n\phi_m\frac{\partial}{\partial x}EI\phi_n''\right]_{\bar{e}}^1 - \left[\sum_n q_n\phi_M' EI\phi_n''\right]_{\bar{e}}^1 + \int_{\bar{e}}^1\sum_n q_n EI\phi_n''\phi_m''dx = RD\sum_n \phi_n'\phi_m'\dot{q}_n + \int_{\bar{e}}^1\sum_n q_n EI\phi_n''\phi_m''dx \qquad (A.5)$$

Equation (A.4) was obtained using the boundary conditions for the hinged blade, along with the end constraint imposed by the damper, which is given by

$$EI\frac{\partial^2 Y}{\partial r^2}\Big|_{r=e} = -D\frac{\partial^2 Y}{\partial t\partial r}\Big|_{r=e} = -DR\sum_n\frac{\partial\phi_n}{\partial x}\frac{\partial q_n}{\partial t}\Big|_{x=\frac{e}{R}}$$

where D = damping constant.

Similarly, the second term gives

$$R^2\sum_n q_n\int_{\bar{e}}^1 \phi_m\frac{\partial}{\partial x}G\phi_n'dx =$$

$$- R^2 \sum_n q_n \int_{\bar{e}}^1 G\phi_n'\phi_m' dx \qquad (A.6)$$

Using Equations (A.4) through (A.6),

$$\int_{\bar{e}}^1 \sum_n q_n EI\phi_n''\phi_m'' dx + RD \sum_n \phi_n'\phi_m' \dot{q}_n + R^2 \sum_n q_n \int_{\bar{e}}^1 G\phi_n'\phi_m' dx + R^4 \sum_n (\ddot{q}_n - \Omega^2 q_n) \int_{\bar{e}}^1 m\phi_m\phi_n dx = 0$$

To evaluate this, nondimensionalize by $m\Omega^2R^4$ and collect terms, which results in

$$A_{nm}\ddot{q}_n + D_{nm}\dot{q}_n + B_{nm}q_n = 0$$

where

$$A_{nm} = \int_{\bar{e}}^1 \left[\frac{R^4 m}{m\Omega^2R^4}\phi_n\phi_m\right] dx$$

$$D_{nm} = \frac{RD\Omega}{m\Omega^2R^4}\phi_n'\phi_m'\Big|_{\bar{e}}$$

$$B_{nm} = \int_{\bar{e}}^1 \left[\frac{EI}{m\Omega^2R^4}\phi_n''\phi_m'' + \frac{R^2G}{m\Omega^2R^4}\phi_n'\phi_m' - \phi_n\phi_m\right] dx$$

Basis Functions For Assumed Mode Shapes

Polynomials are used as the basis functions, $\phi_n(x)$. Two sets of polynomials, meeting the necessary boundary conditions for hinged-free and cantilever-free beams, were used in this study. They are:

hinged-free:

$$\phi(x) = x$$

$$\phi(x) = x^6 - 2x^5 - \frac{5}{6}x^4 + \frac{10}{3}x^3 + x$$

cantilever-free:

$$\phi(x) = x^4 - 4x^3 + 6x^2$$

$$\phi(x) = x^5 - 10x^3 + 20x^2$$

Since these polynomials meet boundary conditions at $x=0$ and at $x=1$, and the blade formulation is integrated from $x = \bar{e}$ to $x=1$, the basis polynomials are transformed to new coordinates, where

$$x' = (1 - \bar{e})x + \bar{e}.$$

With this coordinate transformation, the new set of polynomials, which now fulfill the necessary boundary conditions at the hinge offset and at the blade tip, are now

hinged-free:

$$\phi(x) = x - \bar{e}$$

$$\phi(x) = 1.48x^6 - 3.33x^5 - 0.12x^4 + 4.2x^3 - 0.79x^2 + 1.12x - 0.07$$

cantilever-free:

$$\phi(x) = 1.3x^4 - 5.2x^3 + 7.8x^2 - 0.92x + 0.03$$

$$\phi(x) = 1.39x^5 - 0.44x^4 - 12.11x^3 + 25.10x^2 - 3.03x + 0.09$$

Appendix B. Exact Equations Of Motion For A Nonrotating Beam

The modal analysis assumes that the beam displacement is written as a sum of modal displacements:

$$Y(x,t) = R\sum_n \phi_n(x)q_n(t)$$

To find the exact analytic solution in the case of root constraint with both spring and damper, note that the boundary conditions are given by

$$\phi(0) = 0$$
$$\phi''(0) = \left[\frac{KR}{EI} + i\lambda\frac{DR}{EI}\right]\phi'(0)$$
$$\phi''(1) = 0$$
$$\phi'''(1) = 0$$

where K and D are spring and damper constants and all quantities are understood to refer to lagwise motion and are defined as in Appendix A.

These boundary conditions are satisfied by writing the mode summation equation as

$$\phi(x) = \phi_F(x) + \left[\frac{KR}{EI} + i\lambda\frac{DR}{EI}\right]\frac{\phi_F'(0)}{\phi_C''(0)}\phi_C(x)$$

where $\phi_F(x)$ and $\phi_C(x)$ refer to hinged and cantilever mode shapes.

The hinged end mode shape solutions are given by

$$\phi_F(x) = \cos(A)\sinh(Ax) + \cosh(A)\sin(Ax)$$
$$\phi_F(0) = 0$$
$$\phi_F'(0) = A\,[\cos(A) + \cosh(A)]$$
$$\phi_F''(0) = 0$$
$$\phi_F''(1) = A^2\,[\cos(A)\sinh(A) - \cosh(A)\sin(A)]$$
$$\phi_F'''(1) = A^3\,[\cos(A)\cosh(A) - \cosh(A)\cos(A)]]$$

The cantilever mode shape solutions are given by

$$\phi_C(x) = (\sin(A) - \sinh(A))(\sin(Ax) - \sinh(Ax)) + (\cos(A) + \cosh(A))(\cos(Ax) - \cosh(Ax))$$
$$\phi_C(0) = 0$$
$$\phi_C'(0) = 0$$
$$\phi_C''(0) = -2A^2\,[\cos(A) + \cosh(A)]$$
$$\phi_C''(1) = -A^2\,[1 + \cosh(A)\cos(A)]$$
$$\phi_C'''(1) = A^3[(\sin(A) - \sinh(A))(-\cos(A) - \cosh(A)) + (\cos(A) + \cosh(A))(\sin(A) - \sinh(A))\ ]$$

Now use these known solutions for hinged and cantilever mode shapes in the combined solution given above:

$$\phi(0) = 0$$
$$\phi'(0) = \phi_F'(0)$$
$$\phi''(0) = [K + i\lambda D]\left[-\frac{1}{2A}\right]\phi_C''(0)$$
$$\phi''(1) = \phi_F''(1) + [K + i\lambda D]\left[-\frac{1}{2A}\right]\phi_C''(1)$$
$$\phi''(1) = A^2\,[\cos(A)\sinh(A) - \cosh(A)\sin(A) + [K + i\lambda D]\left[-\frac{1}{2A}\right][-2A^2\,[1 + \cosh(A)\cos(A)]]$$
$$\phi'''(1) = 0$$

where

$$K = \frac{KR}{EI}$$

and

$$D = \frac{DR}{EI}$$

The boundary condition at the tip gives the eigenvalue equation:

$$\phi''(1) = 0$$

or

$$A^2\,[\cos(A)\sinh(A) - \cosh(A)\sin(A)] + A\,[K + i\lambda D][\,1 + \cosh(A)\cos(A)\,] = 0$$

References

Ballin, M. G., and Dalang-Secretan, M. (1991). *Validation Of The Dynamic Response Of A Blade-Element UH-60 Simulation Model In Hovering Flight.* J. of the American Helicopter Society, Vol. 36, no. 4.

Bramwell, A.R.S. (1976). Helicopter Dynamics. Edward Arnold Ltd., London, U.K.

Curtiss, H.C. (1986). *Stability and Control Modeling*. Proceedings 12th European Rotorcraft Forum, Garmish Partenkirchen, Germany.

Curtiss, H.C. and Zhao, X. (1988). *A Linearized Model of Helicopter Dynamics Including Correlation With Flight Test*. Paper presented at the 2nd International Conference on Rotorcraft Basic Research, College Park, MD.

Diftler, M. A. (1988). *UH-60A Helicopter Stability Augmentation Study*. Paper presented at the 14th European Rotorcraft Forum, Milan, Italy.

Goldberg, David E. (1989). Genetic Algorithms in Search, Optimization, and Machine Learning. Addison-Wesley Publishing Co., Reading, MA.

Ham, N. D., Behal, B., and McKillip, R. M., Jr. (1983). *Lag Damping Augmentation Using Individual Blade Control*. Vertica, Vol. 7, No. 4.

Holland, John H. (1975). Adaptation in Natural and Artificial Systems. The University of Michigan Press, Ann Arbor, Michigan.

Johnson, W. (1980). Helicopter Theory. Princeton University Press, Princeton, New Jersey.

Kaplita, T.K., Driscoll, J.T., Diftler, M.A., and Hong, S.W. (1989). *Helicopter Simulation Development By Correlation With Frequency Sweep Flight Test Data*. AHS 45th Annual National Forum, Boston, MA.

Kim, F. D., Celi, R., and Tischler, M. B. (1990). *High-Order State Space Simulation Models Of Helicopter Flight Mechanics*. 16th European Rotorcraft Forum, Glasgow, Scotland.

Ljung, L. System Identification: Theory for the User. (1987). Prentice-Hall, Inc., Englewood Cliffs, NJ.

Maine, R. E. and Iliff, K. W. (1985). *Identification of Dynamic Systems - Theory and Formulation*. NASA Reference Publication 1138.

Mayo, J. R., Occhiato, J. J., and Hong, S. W. (1990). *Helicopter Modeling Requirements For Full Mission Simulation And Handling Qualities*. AHS 47th Annual National Forum.

Milne, G. W. (1986). *Identification of a Dynamic Model of a Helicopter from Flight Tests*. Ph.D. Thesis, Stanford University.

Starer, David (1990). *Algorithms for Polynomial-Based Signal Processing*. Ph.D. Thesis, Center For System Science, Yale University.

Tischler, Mark B. (1987). *Frequency-Response Identification of XV-15 Tilt-Rotor Aircraft Dynamics*. Ph.D. Thesis, Stanford University.

Session 4

Understanding Visual Cues

Visual Cueing Aids for Rotorcraft Landings

Walter W. Johnson
Rotorcraft Human Factors Research Branch
NASA Ames Research Center
Moffett Field, CA

Anthony D. Andre
Western Aerospace Laboratories, Inc.
NASA Ames Research Center
Moffett Field, CA

ABSTRACT

The present study used a rotorcraft simulator to examine descents-to-hover at landing pads with one of three approach lighting configurations. The impact of simulator platform motion upon descents to hover was also examined. The results showed that the configuration with the most useful optical information led to the slowest final approach speeds, and that pilots found this configuration, together with the presence of simulator platform motion, most desirable. The results also showed that platform motion led to higher rates of approach to the landing pad in some cases. Implications of the results for the design of vertiport approach paths are discussed.

INTRODUCTION

Rotorcraft landings in physically constrained environments, such as urban vertiports, present potential hazards not commonly faced by fixed-wing or rotorcraft landings at conventional airports. One major hazard is the presence of buildings or other obstructions beneath their glideslope and directly behind the landing pad. In such environments it is necessary for pilots to accurately maintain their assigned glideslope and to reliably regulate their speed so as to achieve zero velocity at the landing pad.

The present study examined the effect of different combinations of visual and motion information upon simulated descents to hover. Specifically, the study was designed to determine the effects upon performance and subjective ratings of 1) three approach lighting configurations, and 2) the presence/absence of simulator motion. It was also designed to explore how theoretically significant types of optical and motion information combine to yield different deceleration and glideslope profiles.

Presented at *Piloting Vertical Flight Aircraft: A Conference on Flying Qualities and Human Factors*, San Francisco, California, 1993.

Optical Cues For Speed Control

Pilots in aircraft and aircraft simulators require information in order to accomplish their tasks. However, selecting what information to supply the pilot is not easy, especially since many potential information sources are costly (e.g., simulator motion) and/or may not provide much benefit in terms of training effectiveness, performance or flight safety (Andre and Johnson, 1992). Understanding the pilots' reactions to optical information in the environment during flight and in piloted flight simulation can lead to improved visual approach training procedures and may have an impact on the design of heliport approach paths.

There are three important optical variables that a pilot could use to control speed during the descent to hover. Optical Expansion Rate is the relative rate of growth in the optical size of the landing pad, and is proportional to the vehicle velocity divided by distance to the pad (i.e., physical closure rate). This optical variable provides information useful for deceleration since maintaining its value at or below some critical positive value will ensure that the vehicle arrives at the landing pad with zero touchdown velocity, with lower values yielding more gradual decelerations. Further, this cue is insensitive to altitude deviations. Figure 1a shows how constancy of optical expansion rate requires speed to be proportional to distance-to-go.

Optical Flow Rate is the angular velocity of surface elements in any one area of the field of view. This velocity in turn is proportional to vehicle velocity divided by the distance to the viewed surface, and is typically scaled in units of eye heights per second (Owen, Wolpert, and Warren, 1984). This is different from Optical Expansion Rate since that variable is defined with respect to contour expansion rate, while Optical Flow Rate is simply optical (angular) speed. When descending over a ground surface, deceleration can be governed by maintaining optical speed, at some locus in the field of view, at or below some critical positive value. (US Army training manuals instruct rotorcraft trainees to "make it look like a brisk walk" during landings. This is an explicit instruction to maintain a constant Optical Flow Rate). Figure 1b shows how constancy of angular flow rate requires speed to be proportional to altitude.

Finally, there is Optical Edge Rate, the frequency at which optical elements pass through some visual locale (e.g., the lower portion of the windscreen). For descents over a surface this is proportional to vehicle velocity divided by the spacing between the elements on that surface. When the elements are spaced apart evenly, this yields a frequency that is directly proportional to speed. To the extent that information about true speed is important in managing decelerations, this variable may prove valuable for speed regulation. Figure 1c shows how constancy of edge rate requires texture elements and speed to be proportional to distance-to-go.

Previous research by Moen, DiCarlo and Yenni (1976) examined altitude, ground-speed and deceleration profiles of visual approaches for helicopters. One goal of their research was to define the mathematical relationships describing nominal visual deceleration profiles. However, the effects of visual cues in the environment were not examined. More recent research has specifically addressed the influence of visual environmental cues on vehicle deceleration control.

For example, Denton (1980), in a somewhat related context, examined the influence of ground texture spacing (i.e., optical edge rate information) on driver's control of forward speed. Using an automobile simulator, he found that gradually reducing the spacing between horizontal stripes on a simulated roadway surface resulted in drivers reducing their speed. He then applied this finding in a field study where he placed horizontal stripes with gradually reduced spacing across the roadway at a highway exit ramp. This resulted in a reduction of a previously high accident rated caused by excessive speeding upon exiting the highway to lower speed roads. Other research has shown edge rate and flow rate to have roughly equal impact on the perception of self-speed (Larish and Flach, 1990; Owen et al., 1984).

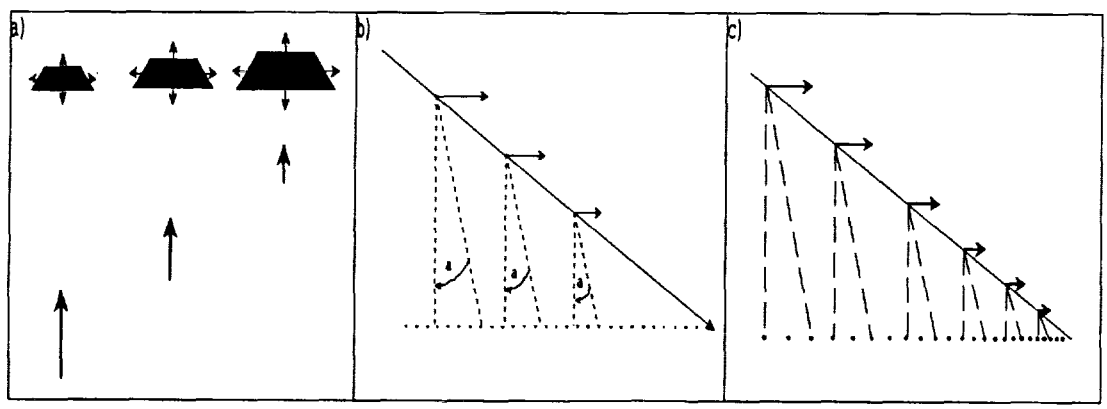

Figure 1. Optical variables useful for controlling deceleration. a) constancy of optical expansion rate requires speed to be proportional to distance-to-go; b) constancy of angular flow rate requires speed to be proportional to altitude; c) constancy of edge rate requires texture elements and speed to be proportional to distance-to-go.

Optical Cues for Glideslope Control

There are two important optical variables potentially useful for glideslope control: 1) Form Ratio, the angular optical height of the pad divided by its optical width, and 2) aim point Declination Angle, the optical angle subtended between the center of the landing pad and the horizon. If the pilot acts to keep either of these constant after the glideslope intercept, then he will still be on the initial glideslope (see Lintern and Liu, 1991 and Mertens, 1981, for a more complete discussion of these variables). Similarly, pilots can maintain a constant glideslope by simply keeping the image of the landing pad at a fixed point below the horizon.

THE PRESENT STUDY

The present study examined visual approaches in a rotorcraft simulator with various approach lighting configurations, under platform motion and non-motion conditions. These configurations were designed to highlight the utility of one or more of the three types of optical information about vehicle speed discussed above.

In one condition, only the landing pad itself, together with the horizon line, was visible. For control of speed, this makes available closure rate information in the form of the relative rate of the optical expansion of the landing pad surface itself. The reciprocal of this value, called *tau*, is the time to arrival at the landing pad if present vehicle speed is kept constant. By either maintaining relative closure rate information at a constant value, or by not allowing it to exceed some critical value, a pilot would be ensured of arriving at the pad with zero velocity.

A second condition added two rows of regularly spaced approach lights extending out from the edges of the landing pad. Now, in addition to the closure rate information mentioned above, the optical motion of the lights passing beneath the simulated vehicle provide information, in the form of optical flow rate and optical edge rate, about vehicle speed. For descents along a given glideslope, flow rate will be proportional to speed divided by altitude. By maintaining flow rate at a constant value, or not allowing it to exceed some critical value, one will ensure arrival at the landing pad with zero velocity. For descents over regularly spaced ground elements, optical edge rate is proportional to speed, but does not afford the pilot any simple available optical strategy for ensuring arrival at the pad with zero velocity. Similarly, there is no simple or obvious optical cue associated with the approach lights that a pilot can use to judge glideslope.

Finally, a third condition added a middle row of lights to the second condition configuration. This middle row light spacing was proportional to distance from the pad, so that the lights were spaced half as far apart when the distance to the pad was decreased in half (i.e., exponential). Here, the pilot could hold the edge rate associated with this middle exponential light string at or below some fixed value, and thus ensure arrival at the landing pad with zero velocity.

The impact of simulator platform motion upon descents to hover was also examined in the present study. Previous research has shown that the presence of flight simulator motion appears to help performance, but not transfer to the aircraft (Koonce, 1979; Lintern, 1987). Our interest here was in assessing if simulator motion interacted with the utility of the approach light patterns under investigation.

METHOD

Design

Five factors were manipulated in the present study: 1) Flight Control Instruction (undirected and directed), 2) Simulator Motion (moving and fixed), 3) Approach Lighting Pattern (no lights, linear lights, and exponential +linear lights), 4) Initial Closure Rate (slow vs. fast--see Figure 2), and 5) Initial Range (near vs. far--see Figure 2). These variables were factorial crossed in a 2x2x3x2x2 within-subjects design. Pilots performed 2 repetitions of each of the 48 unique factorial combinations for a total of 96 landing trials. An overview of the experimental design is shown in the top panel of Figure 2.

Simulation Apparatus

All trials were performed in the Vertical Motion Simulator (VMS) at the NASA Ames Research Center. The VMS, shown in Figure 3, is a large motion-base simulator which utilizes a four-window computer-

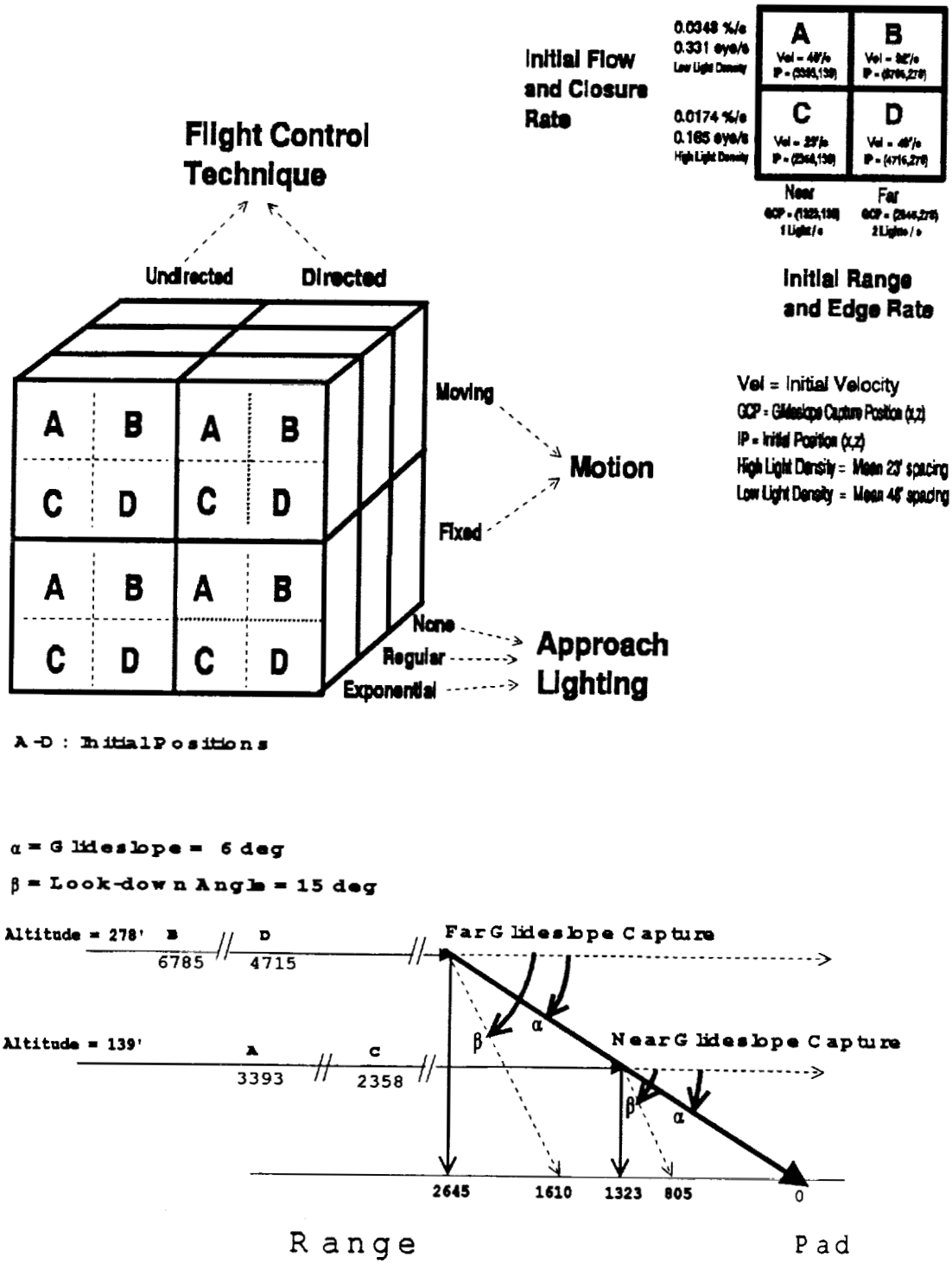

Figure 2. Experimental Design. Description of Factorial Structure (top panel) and of Flight Profiles (bottom panel).

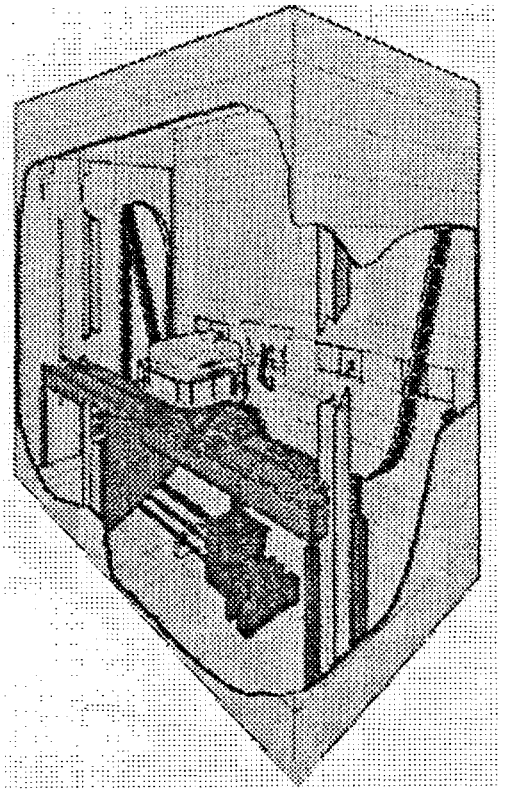

Figure 3. NASA's Vertical Motion Simulator

generated image system for displaying visual scenes to the pilot. The simulator was outfitted with a rotorcraft cab with conventional controls.

Vehicle Model. The experiment utilized a modified rotorcraft model with only two degrees of freedom: longitudinal and vertical. The three angles that describe the orientation of the vehicle and the lateral position were fixed at zero. Thus longitudinal velocity changes were achieved without pitching the aircraft. Physically, this situation would be realized with a helicopter that had an auxiliary x-force device to control longitudinal acceleration.

This simplification was made for several experimental reasons. First, since straight-in, decelerating approaches were of interest, the three lateral-directional degrees of freedom were unnecessary. Second, since the vertical field-of-view in the simulator was substantially less than in a typical helicopter, pitch-up maneuvers in simulation would result in a drastic loss of visual ground cues. Accordingly, to ensure that the approach lights were always in view during the approach, pitch attitude and rate was held constant. The pilots had acceleration command in the longitudinal axis. Acceleration command was proportional to longitudinal center stick position, with a sensitivity of 5 ft/sec^2/in. The longitudinal travel of the center stick was +/- 5 in.

The vertical axis dynamics were more complicated than the longitudinal axis. The collective sensitivity and the aircraft's vertical damping depended upon airspeed. The aircraft was also given a steep power required curve, so that as the helicopter slowed, increased collective was required. The combination of these dynamics made the vehicle sufficiently challenging to fly, thereby inhibiting the pilots from flying the task open-loop (i.e., essentially flying the vehicle without regard to the visual cues). Pilot comments indicated that while the vertical axis exhibited helicopter-like qualities, the longitudinal axis did not (due to the lack of pitching required to change speed).

Visual Landing Configurations

As shown in Figure 4, Three visual landing scenes were examined: 1) no approach lights with only a landing pad present (None); 2) the landing pad plus two linear strings of equally spaced lights leading up to the landing pad (Regular); and 3) the landing pad, the two linear strings, and an exponentially spaced string of lights (Exponential).

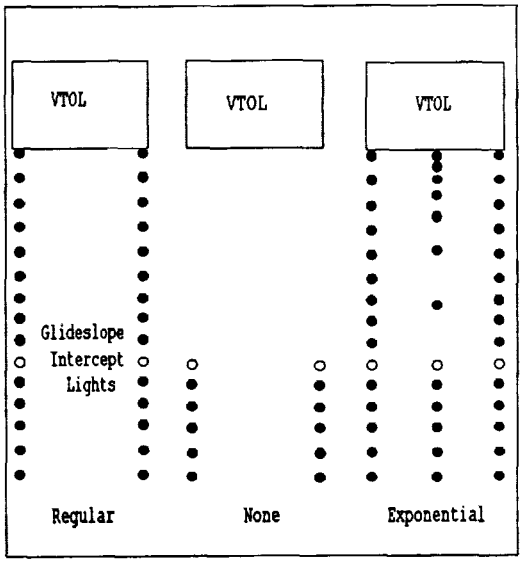

Figure 4. Approach light configurations.

Regular. The Regular configuration presented two rows of white approach lights in addition to a 100 ft x 100 ft landing pad and the horizon. These lights were aligned with the sides of the landing pad, spaced either 23 ft or 46 ft apart (a manipulation of light density used to affect initial edge rate), and extended out 5000 ft from the landing pad. The lights at 1610 and 805 ft out were green, while the rest of the lights were white, and the pilots were instructed to intercept the glideslope when these lights passed out of view at the bottom of their windscreen. They were instructed to use the first set of green lights when flying at the higher altitude (278 ft) and the second set of green lights when flying at the lower altitude (139 ft). The left panel of Figure 4 depicts this lighting configuration. The bottom panel of Figure 2 shows how the combination of intitial altitiude and positions of the intercept lights combined to yield a 6^0 glideslope capture.

None. This configuration was similar to the Regular configuration, but the approach lights were truncated at 805 ft from the pad for the 139 ft initial altitude, and 1610 ft from the pad for the 238 ft initial altitude. The pilots were told to intercept the glideslope when the last approach light passed out of view, and thus during the descent to hover only the landing pad and the horizon were visible. This configuration, depicted in the middle panel of Figure 4, does not provide either Optical Flow Rate or Edge Rate information, but provides all of the other information contained in the Regular configuration.

Exponential. This configuration was similar to the Regular configuration with the addition of a third row of lights aligned with the center of the landing pad. These extended out either 816 ft or 1609 ft (depending on initial altitude), and were exponentially spaced such that the inter-light spacing was 0 at the threshold of the landing pad, 53.9 ft at 816 ft, and 106 ft at 1609 ft for conditions using the high-density light spacing, and 106.9 ft and 212 ft for the low-density light spacing (inter-light separation divided by distance to the landing pad was approximately 0.066). (For the low-density spacing every other light in the Exponential light array was removed, so that inter-light spacing divided by distance to the landing pad was approximately 0.132). In both cases the lights in the center row were continued, using the final spacing found at 816 or 1609 ft so that the pilots would already be using the lights when they intercepted the glideslope. The pilots were again instructed to intercept the glideslope when the appropriate set of green lights passed from view. This configuration, depicted in the right panel of Figure 4, provides all of the information contained in the regular configuration, plus the exponential string of lights makes it possible to reach zero velocity by maintaining an edge rate for this middle row at or below some critical value. As in the other examples, the lower this critical value the milder the deceleration.

Procedure

Each landing trial consisted of a cruise phase and an approach phase. The cruise phase, which lasted approximately 10 seconds, did not require manual control as the vehicle maintained its initial level attitude. During this phase, a set of linear lights was present extending from the initial position to the glideslope intercept lights, regardless of the approach light condition (see Figure 4 above). This was done to allow the pilots to determine any altitude deviations due to the collective trim.

The approach phase began when the pilot crossed the glideslope capture position. This is the point where the green glideslope intercept lights just passed out of the lower field-of- view. At this point, the pilot was instructed to intercept the 6 deg glideslope down towards the center of the landing pad. The trial ended when the pilots reached a point approximately 15 ft AGL with the VTOL sign in their view.

The 96 experimental trials were completed over 4-6 sessions. Simulator motion and flight control instruction conditions were blocked between groups of 12 trials, while initial position and approach light pattern were counterbalanced and randomized within each block of 12 trials.

Following each trial, pilots were given feedback on their glideslope variation only.

Instruction. This task was performed under two sets of flight control instructions. In the undirected trials, the pilots were instructed to perform the approach in a way that was "comfortable" or "normal" for them. In the directed trials, the pilots were instructed to maintain a velocity profile that was proportional to their distance from the pad.

Subjective Ratings. Test pilots are trained to fly to some specified degree of performance and then judge difficulty in terms of the effort necessary to attain that degree of performance (e.g., Cooper-Harper Ratings). To this end test pilots generally want that level of performance to be made explicit (e.g., do not deviate more than ± 10 ft in altitude). However, when exploring flight performance on tasks where no standardized measure of goodness exists, or even where it may be presumed to vary across pilots, this is a difficult method to implement.

In this situation we can only try to use the inverse method, and require pilots to fly to some fixed level of effort, and then have them judge difficulty in terms of what they see as good flight performance. This is what we required in this study, defining the level of effort as "flying as well as possible". Thus difficulty (which we called "doability" to focus the pilots on task constraints) was judged in terms of performance variations relative to this fixed high level of effort. In addition we also asked pilots to judge their own performance in terms that took into account the "doability" of the task. Thus, average performance on a difficult task should get the same performance rating as good performance on a more simple task. If the pilots could truly distinguish these ratings, then the performance ratings should not vary as a function of the doability ratings (i.e., task condition).

Pilots were asked to provide the two subjective ratings, each on a 7-point scale, following each trial. For the doability (difficulty) rating, we asked, "how difficult was the task, independent of how well you performed?" The performance rating was to be considered relative to the doability rating. Here we asked, "given the doability of the task, how well did you perform?"

Practice. Each pilot received a practice session of 12 landing trials under motion, undirected conditions. Before the practice session, each pilot was given a set of instructions which explained the various approach conditions and experimental procedures. In addition, the visual information afforded by each approach light pattern, in the form of edge rate and closure information, was described.

Subjects

Six NASA helicopter test pilots participated in the experiment. Each had previous experience in the VMS.

RESULTS

Dependent Measures

Only the data from the undirected trials (where the pilots were free to choose their own approach speed) were analyzed to date.

Subjective Ratings. Prior to analysis normalized subjective difficulty and performance ratings (NR_i's) were computed for each subject using the equation

$$NR_i = \frac{R_i - M_R}{SD_R}$$

where R_i is the rating given by the subject, M_R is the mean difficulty or performance rating given by that subject, and SD_R is the standard deviation of the ratings given by the subject. This transformation was used to adjust for individual differences in the amount of the rating scale used by the pilots to make their judgments.

Performance Data. For each trial the descent trajectory was divided into 100 foot segments beginning 2600 ft from the pad for the far initial range trials, and at 1300 ft from the pad for the near initial range trials. This yielded 26 segments in the first case and 13 segments in the latter case. Since no approach lights would have been within view, and final adjustments to hover position were not of immediate interest, data in the final segment was not included beyond the point at which the front of the landing pad was not visible. Within each

segment, mean velocity, glideslope, and closure rate were calculated.

Subjective Ratings Analysis

A 2 (Replication) x 2 (Initial Closure Rate) x 2 (Initial Range) x 2 (Motion) x 3 (Approach Lighting) repeated measures analysis of variance (ANOVA) was used to analyze the Normalized Difficulty and Performance ratings.

The analysis of the Difficulty ratings yielded statistically significant main effects for Initial Range ($F(1,4) = 21.221$, $p = .01$) and for Motion ($F(1,4) = 35.144$, $p = .004$), and a statistically significant Range x Approach Lighting interaction ($F(2,8) = 10.533$, $p = .006$). Figure 5 shows that the presence of approach lighting also led to the task being judged as easier, although follow-up tests showed that the differences between ratings of the Exponential and Regular lighting configurations were not statistically significant. It also shows that trials with longer Initial Ranges were judged as more difficult, particularly when approach lights were absent. This pattern is not surprising since, at longer ranges to the pad, the absolute (not relative) rates of optical expansion are lower, and therefore probably less discernible. Figure 6 shows that trials with a moving platform were reliably rated as being less difficult, although this was not a very large effect.

The analysis of the Normalized Performance ratings yielded a statistically significant main effect for Initial Closure Rate ($F(1,4) = 9.97$, $p = .034$) and a statistically significant Trial x Initial Closure Rate x Initial Range x Approach Lighting interaction ($F(2,8) = 7.924$, $p = .013$). The effect of initial closure rate (not depicted) showed that the pilots rated their performance as lower on trials with high initial closure rates. The four way interaction is difficult to interpret.

Squared correlations of the Performance and Difficulty ratings yielded r^2 measures of .43, .43, .15, .10, and .003, showing that three of the five pilots succeeded well in keeping the estimates independent, while the other two had some problems in doing this. Together, these show that the pilots were moderately successful in separating task difficulty and performance contributions in making their judgements.

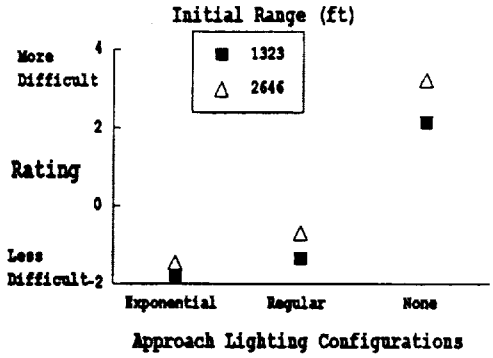

Figure 5. Average normalized difficulty ratings as a function of approach lighting and initial range for undirected descents to hover.

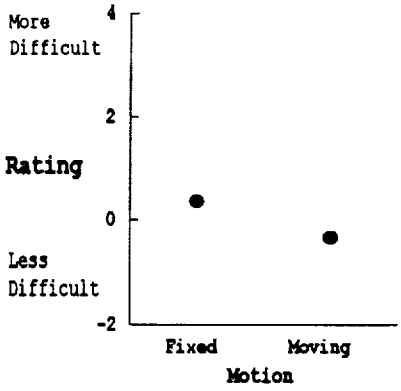

Figure 6. Average normalized difficulty ratings as a function of simulator platform motion for undirected descents to hover.

Performance Analysis

2 (Replication) x 2 (Motion) x 3 (Approach Lighting) x 13 (Segment) repeated measures multivariate analyses of variance (MANOVAs) were used to analyze glideslope and relative closure rate (i.e., ground approach velocity divided by distance-to-go) for the self-directed descents for each of the two initial closure rates in the near initial range condition. Similar analyses using 26 segments were conducted for the two initial closure rates in the far initial range condition. Where appropriate, Huynh-Feldt adjusted degrees of freedom were used to compensate for correlated data in the repeated measures (due primarily to the correlation of measures between adjacent trajectory segments).

Glideslope Analysis. Table 1 shows all statistically significant ($p < .05$) effects on glideslope. In addition to significant variations in glideslope across Segments for all four types of descents (refer to Figure 2, top panel), there were also significant effects involving the Approach Lighting factor in all four types of descents, and significant effects of Motion in all but the Type C descent.

Figures 7-10 show the glideslope profiles as a function of Motion (left panels) and Approach Lighting (right panels) for all four initial conditions. All figures also show an increase in glideslope with proximity to the landing pad (where distance-to-go approaches 0). This is not unexpected since an approach to hover at some distance above the landing pad will, necessarily, lead to increasing glideslopes as measured from the center of the landing pad. All four show the presence of motion yielded a higher glideslope during the final portions of the descent (upper panels), although this is not easily seen in the figures plotting height as a function of distance-to-go (lower panels). In addition, only the approaches from the farther range (types "B" and "D" descents--Figures 8 and 10) yielded statistically significant Motion x Segment interactions.

The absence of approach lighting ("None" condition) led to consistently higher glideslopes in all four conditions, with no consistent direction to the difference in average glideslope of the Regular and Exponential Approach Lighting patterns (i.e., the Regular pattern led to a higher average glideslopes in conditions A and C, and a lower average glideslope in condition B, with the glideslopes for the two being about equal in condition D).

Finally, there were two statistically significant interactions involving both Approach Lighting and Motion in Type B descents. These were an Approach Lighting x Motion interaction, and an Approach Lighting x Motion x Segment interaction. Figure 11 shows that the two-way interaction was due primarily to motion leading to an increased glideslope in the presence of the Exponential pattern, and to a decreased glideslope without approach lighting. The three way interaction (not shown) was due to high variance across segments in the no lights condition.

Table 1. Statistically Significant Effects Upon Glideslope by Descent Type

EFFECTS	Type A Descents	Type B Descents	Type C Descents	Type D Descents
Replication		$F(1,4) = 14.2$ $p = .0197$		
Lights	$F(2,8) = 10.5$ $p = .0058$	$F(2,8) = 6.06$ $p = .025$	$F(2,8) = 10.4$ $p = .0059$	
Path Segment	$F(2,15,8.59) = 69.7$ $p < .0001$	$F(1.58,6.3) = 23.9$ $p = .0015$	$F(5.84, 23.6) = 120.3$ $p = < .0001$	$F(2.16,8.62) = 37.8$ $p < .0001$
Motion x Lights		$F(2,8) = 5.1$ $p = .0374$		
Motion x Segment		$F(3.75,14.98) = 3.7$ $p = .0293$		$F(5.96,23.84) = 3.8$ $p = .008$
Lights x Segment	$F(3.8,15.21) = 3.97$ $p = .0224$			$F(10.79,43.17) = 2.4$ $p = .021$
Motion x Lights x Segment		$F(6.51,26.06) = 3.3$ $p = .0129$		

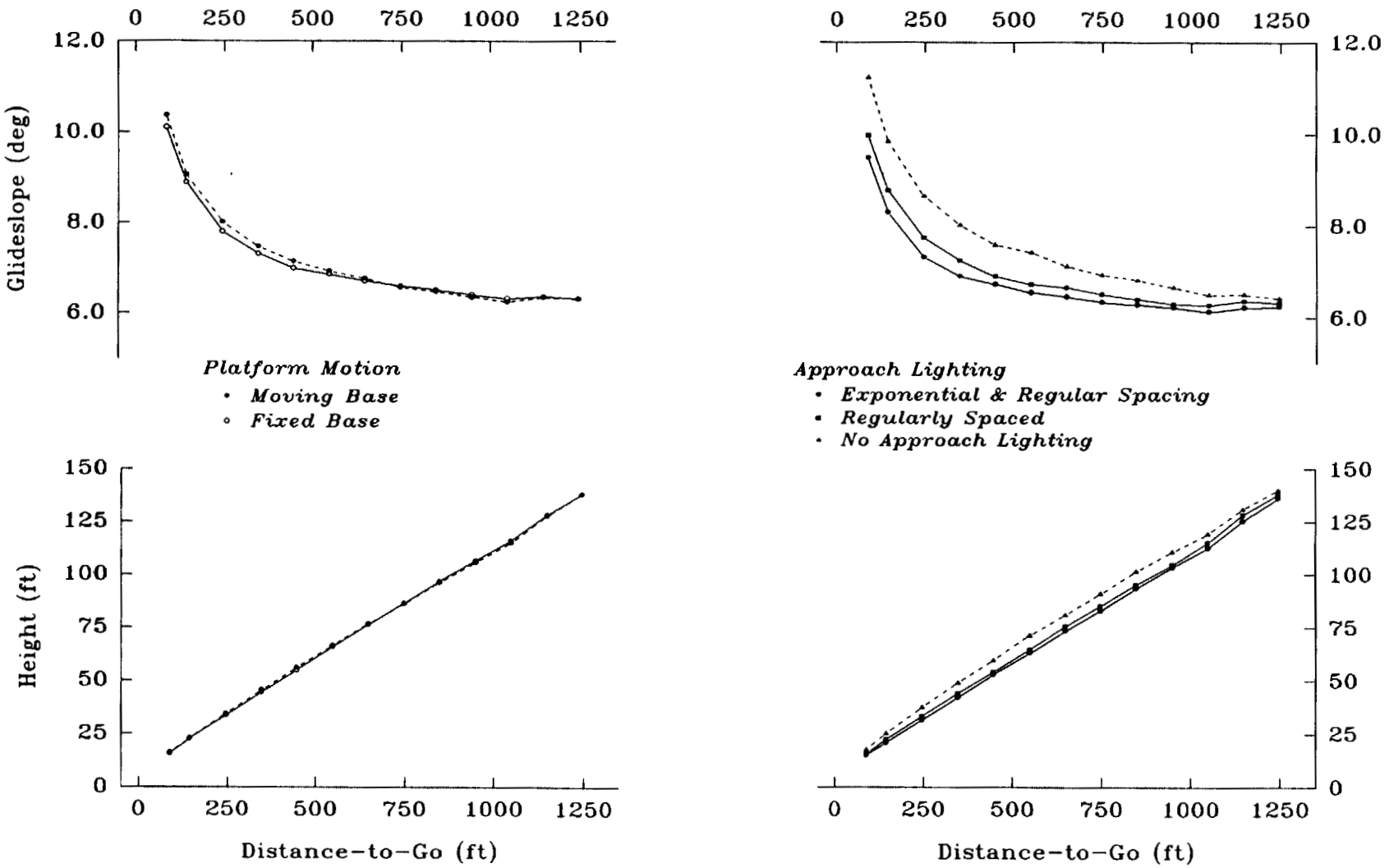

Figure 7. Average Glideslope as a Function of Motion and Lighting Configuration During Undirected Type 'A' Descents to Hover.

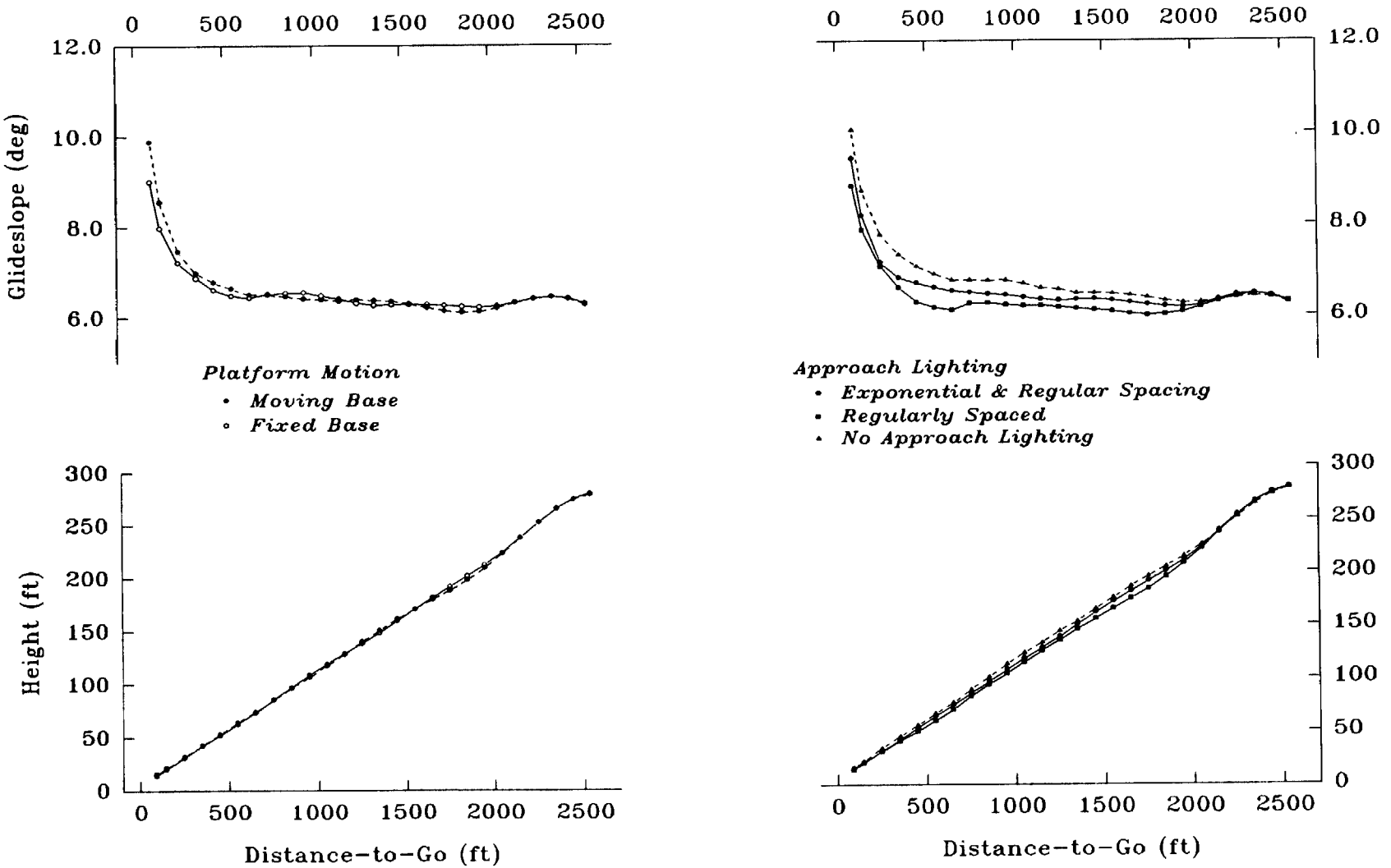

Figure 8. Average Glideslope as a Function of Motion and Approach Lighting During Undirected Type 'B' Descents to Hover.

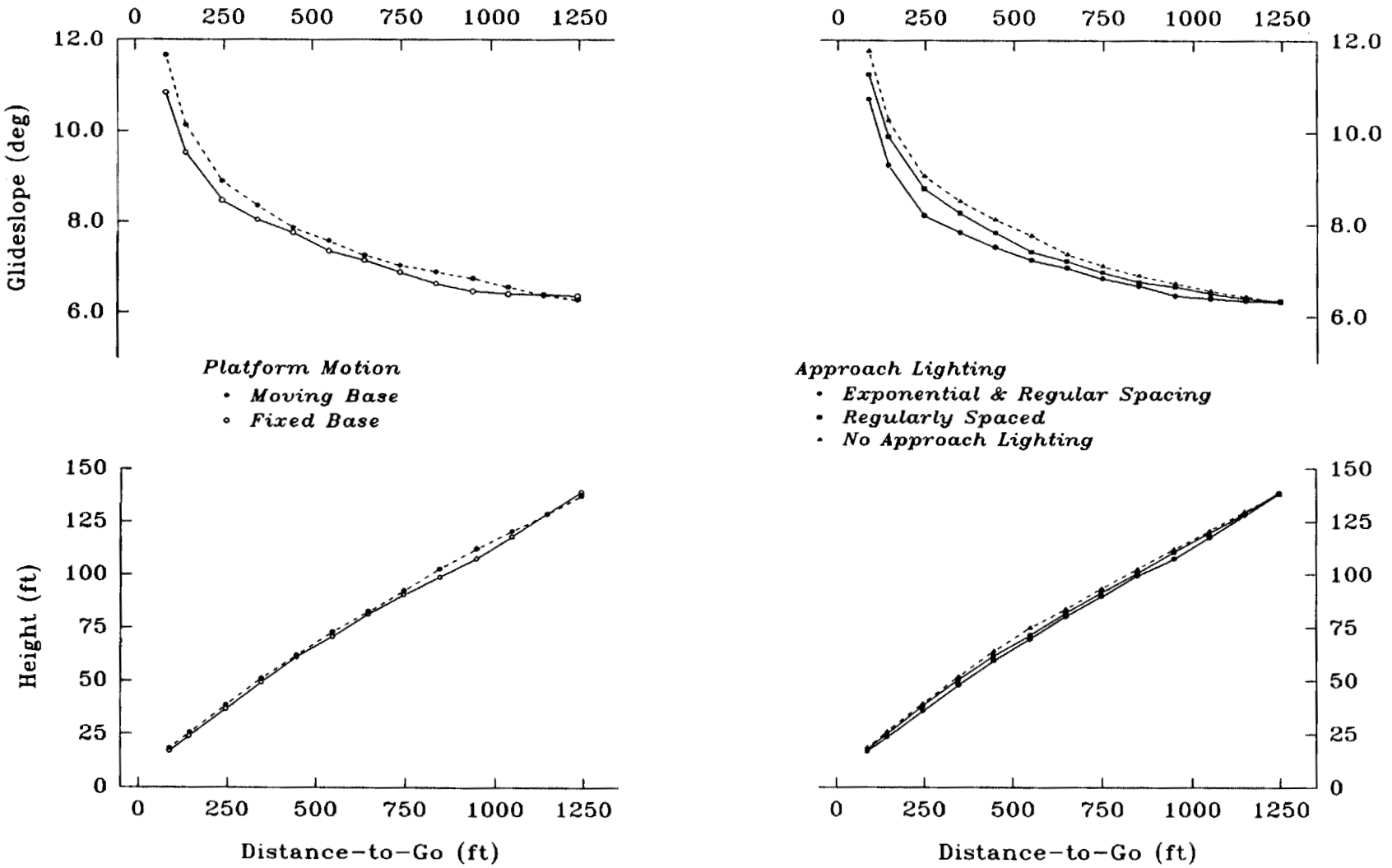

Figure 9. Average Glideslope as a Function of Motion and Approach Lighting During Undirected Type 'C' Descents to Hover.

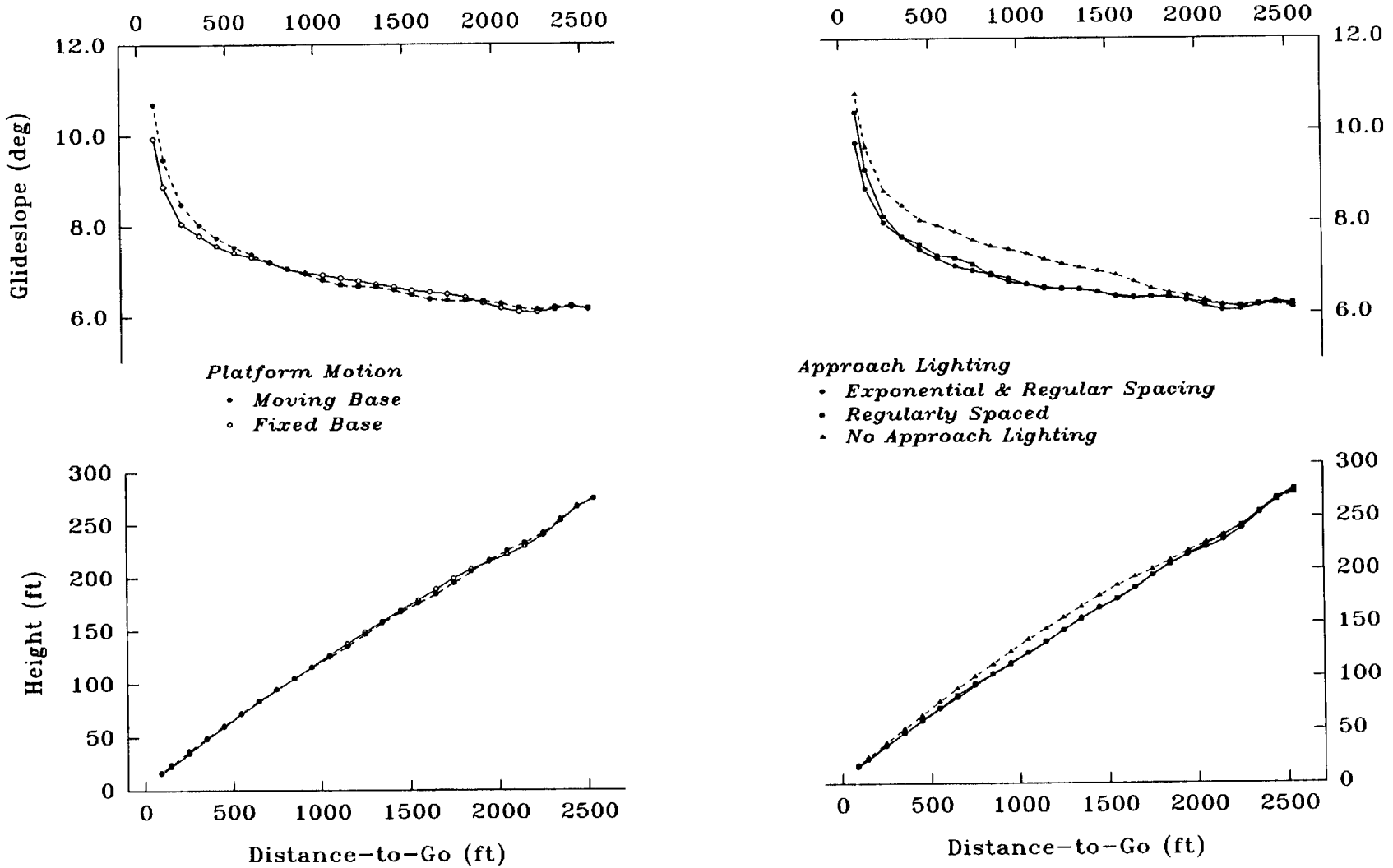

Figure 10. Average Glideslope as a Function of Motion and Approach Lighting During Undirected Type 'D' Descents to Hover.

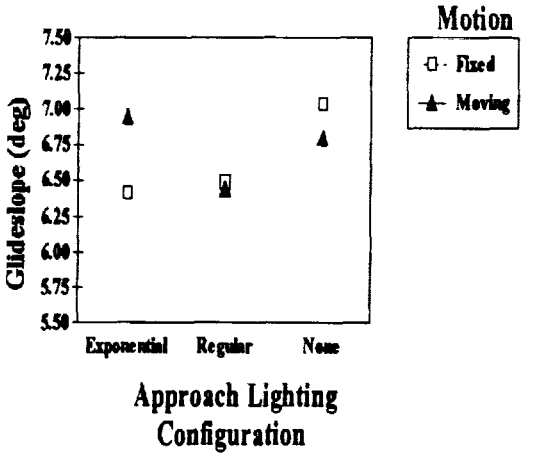

Figure 11. Glideslope as a function of approach lighting and platform motion for undirected Type B descents.

Closure Rate Analysis. Table 2 shows all statistically significant ($p<.05$) closure rate effects. Approach Lighting had a significant affect on closure rate for the Type A and Type D Descents, while Motion affected closure rate for both the Type B and Type D descents.

Figures 12-15 depict velocity (top panels) and closure rate (bottom panels) profiles as a function of Motion (left panels) and Approach Lighting (right panels) for all four descent types (refer to Figure 2, top panel). Similar to the findings for glideslope control, the Motion x Segment interactions were statistically significant only for the descents from the longer initial ranges (Type B and D descents), although Figures 12-15 show that the presence of motion tended to yield higher closure rates towards the end of all descents. This dependence of closure rate upon initial range may be due to reasons similar to those suggested for the glideslope effects. That is, at the more extreme initial ranges, the pilots may have been more strongly influenced by the vestibular cues provided by motion and therefore responded less vigorously.

Only Type A and Type D descents yielded significant effects of lighting configuration upon closure rate, but the average final closure rate was lowest in the Exponential light configuration for all four initial conditions. Since the most critical impact of the Approach Lighting factor is upon closure rates closest to the landing pad, a follow-up 2 (Replication) x 2 (Initial Closure Rate) x 2 (Initial Range) x 2 (Motion) x 3 (Approach Lighting) repeated measures ANOVA was conducted using just the closure rate from the final segment. This yielded statistically significant interactions of Initial Closure Rate x Initial Range ($F(1,4) = 0.04$), Initial Closure Rate x Motion ($F(1,4) = 9.61$, $p = .036$), and Replication x Approach Lighting ($F(2,8) = 6.346$, $p = .022$).

Table 2. Statistically Significant Effects Upon Closure Rate

EFFECTS	Type A Descents	Type B Descents	Type C Descents	Type D Descents
Lights	F(1.67,6.69) = 7.09 p = .0249			
Path Segment	F(1.58, 6.31) = 17.5 p = .0033	F(1.76,7.05) = 14.47 p = .0037	F(1.34,5.34) = 50.06 p = .0005	F(1.42,5.68) = 33.37 p = .001
Motion x Segment		F(5.43,21.73) = 2.95 p = .0324		F(2.23,8.92) = 4.99 p = .0327
Lights x Segment	F(9.63,38.54) = 3.88 p = .0012			F(7.19,28.78) = 4.40 p = .0019

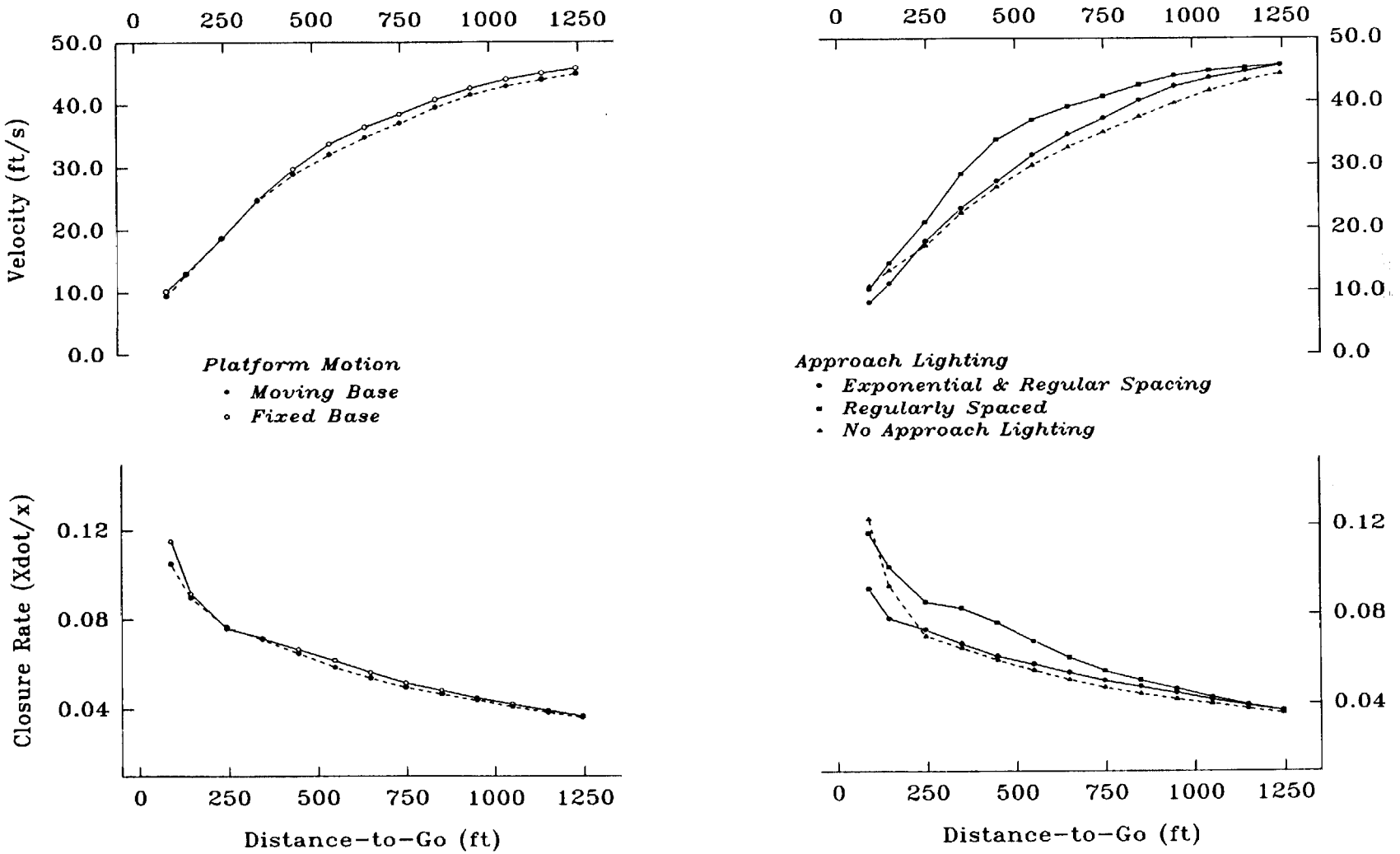

Figure 12. Average Velocity and Closure Rate as a Function of Motion and Approach Lighting During Undirected Type 'A' Descents to Hover.

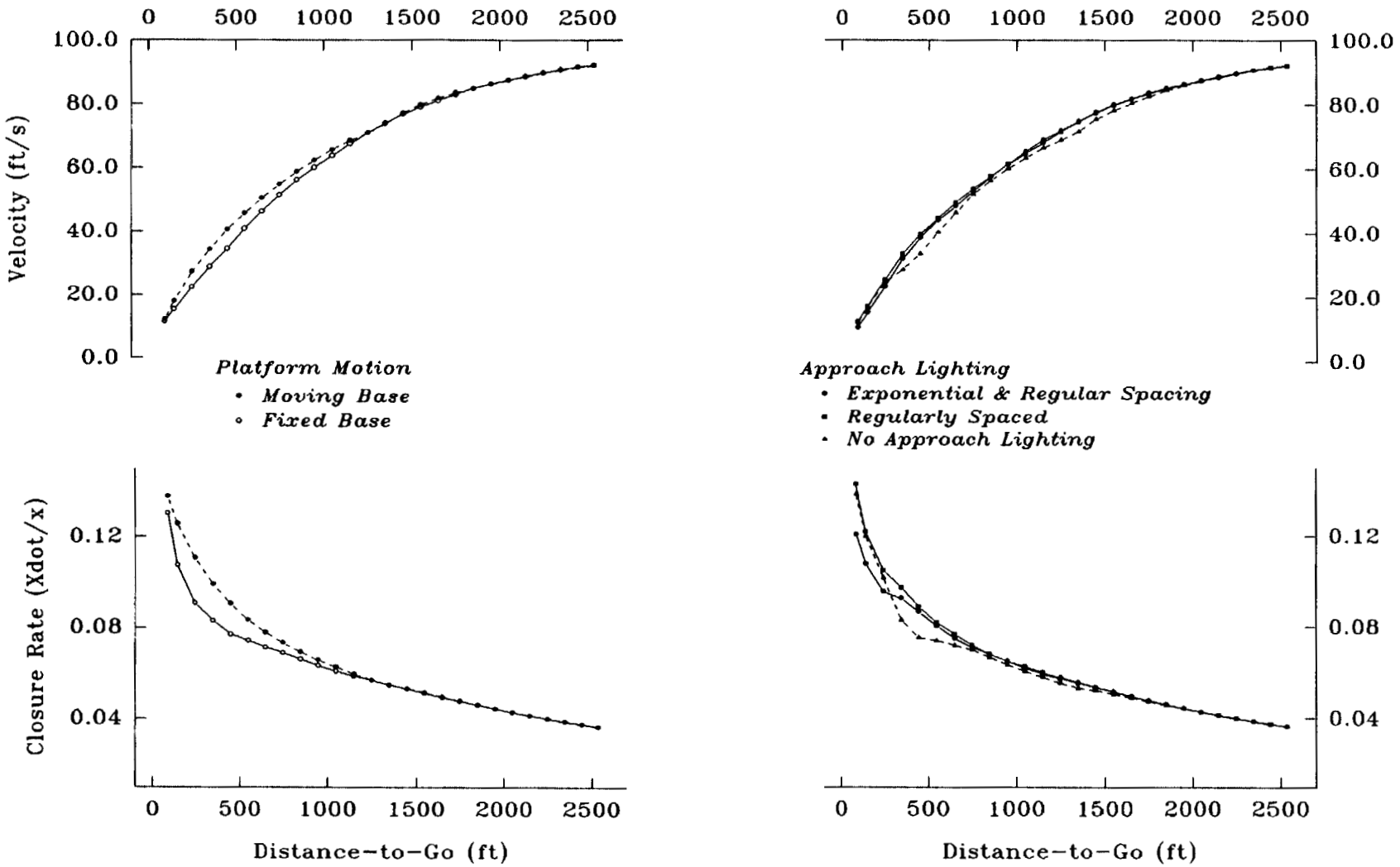

Figure 13. Average Velocity and Closure Rate as a Function of Motion and Approach Lighting During Undirected Type 'B' Descents to Hover.

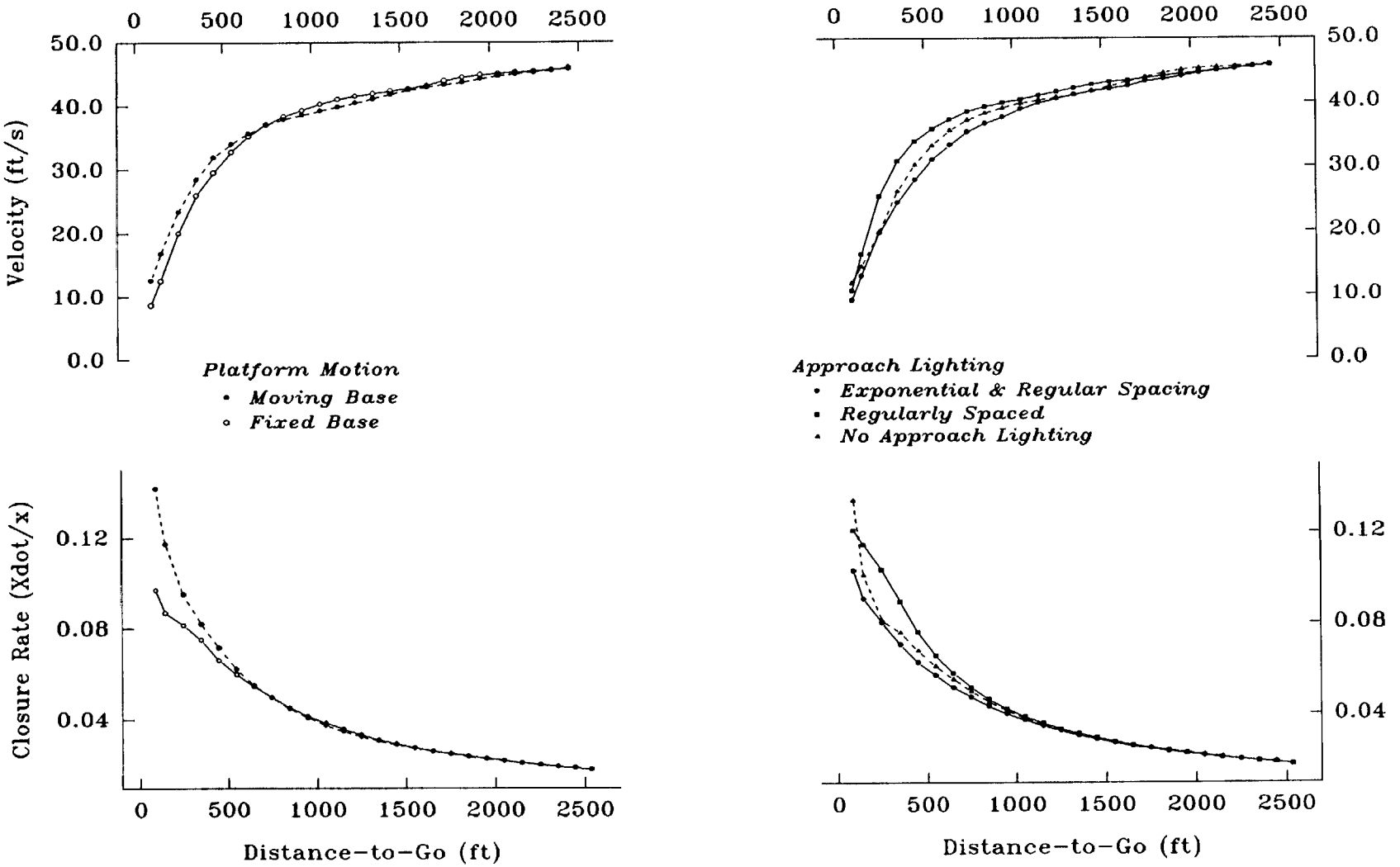

Figure 14. Average Velocity and Closure Rate as a Function of Motion and Approach Lighting During Undirected Type 'C' Descents to Hover.

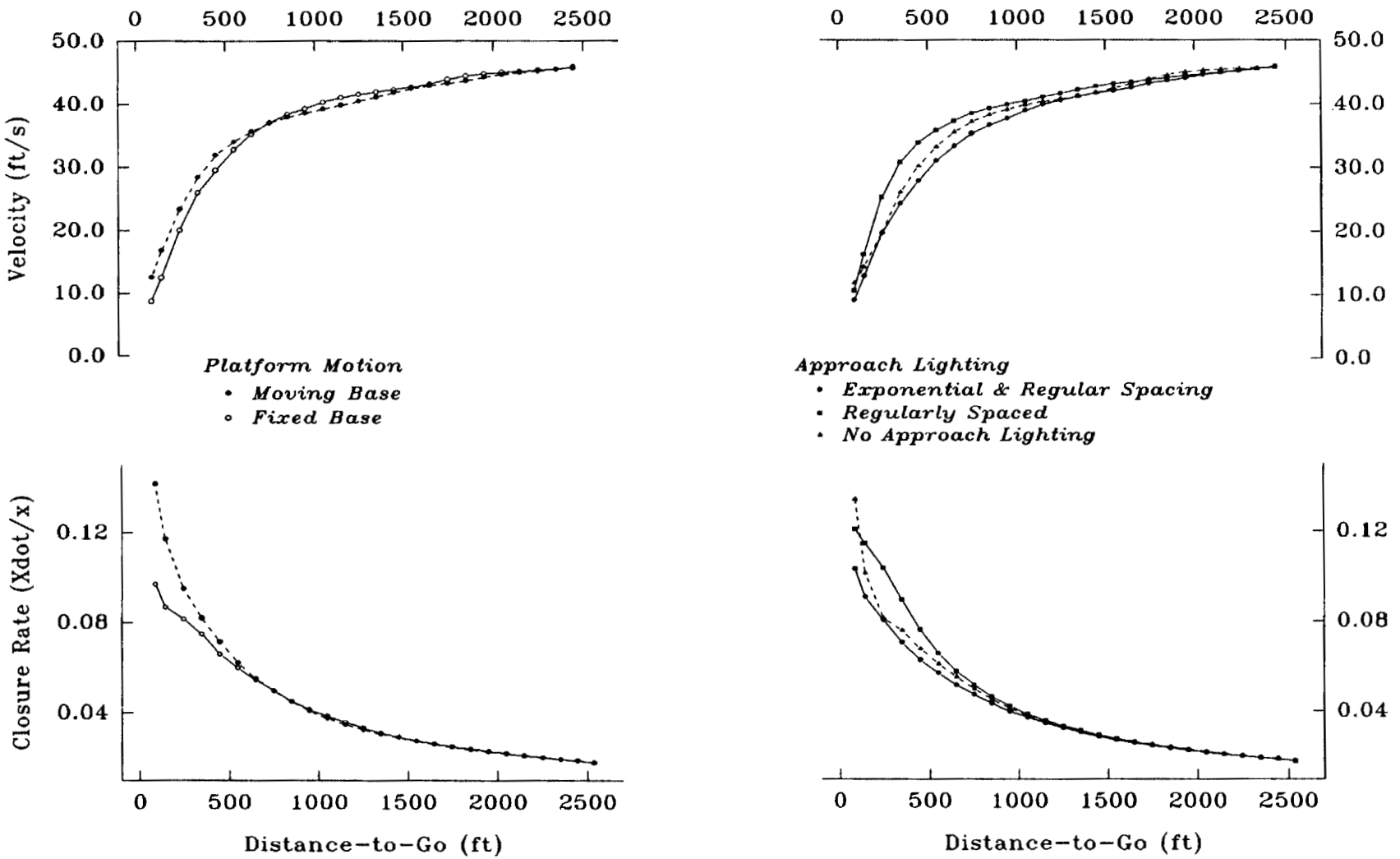

Figure 15. Average Velocity and Closure Rate as a Function of Motion and Approach Lighting During Undirected Type 'D' Descents to Hover.

The top panel of Figure 16 shows that descents over shorter ranges led to smaller final closure rates that were unaffected by Initial Closure Rate, but that higher Initial Closure Rates led to higher final closure rates, especially for the descents from the farther Initial Range. The middle panel of Figure 16 shows that the presence of platform motion led to lower final closure rates for the lower Initial Closure Rate, but not for the higher Initial Closure Rate. Finally, the bottom panel of Figure 16 shows that the advantage of the exponential lighting configuration strongly increased in the second replication, suggesting that the pilots were still learning to use the information afforded by this configuration.

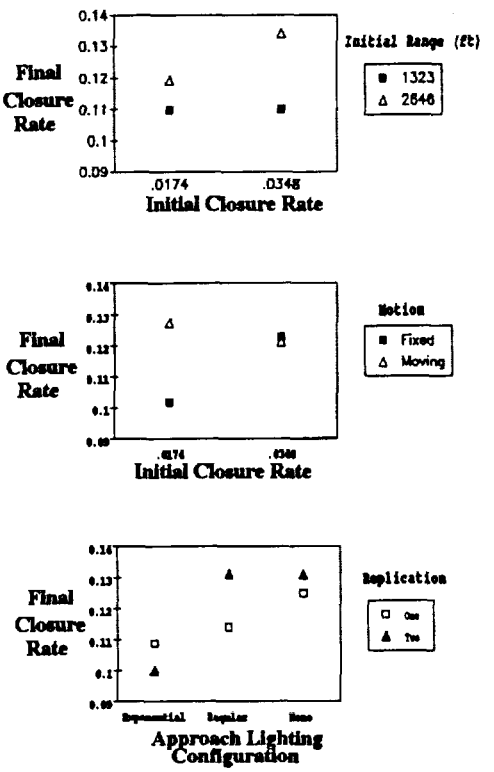

Figure 16. Final Closure Rate as a Function of Initial Closure Rate and Initial Range (top panel), Initial Closure Rate and Motion (middle panel), and Replication and Approach Lighting (bottom panel).

DISCUSSION

Collectively, these results have shown that glideslope and speed control can both be affected by the pattern of approach lights to helipads, as well as the presence of platform motion.

Approach Lights

The proposed impact of additional optical information afforded by the linear, and. to a greater degree, the exponential approach light configuration on control of deceleration was generally supported, although its effects tended to be confined to the most close in segments. This suggests that the effects of edge rate are most consequential during the final, and slowest, phase of the deceleration to hover. This may reflect an increased perceptual salience of this information in this phase, or perhaps more likely, a shift in relative emphasis, with pilots using the exponential pattern edge rate more during this phase.

The absence of approach lights also led to higher glideslopes, showing the influence of optical information in the linear and exponential approach light configurations other than form ratio and declination angle, since only these information sources were available in the no-light configuration. The specific nature of this beneficial information needs to be determined, but may reflect sensitivity to sink rate, since this will be heightened by having approach lights passing under the vehicle.

Finally, and perhaps not surprisingly, the pilots generally rated the linear and exponential + linear configurations as less difficult than the no lights configuration.

Simulator Motion

Generally, the presence of platform motion led to slightly higher closure rates and glideslopes, although the pilots rated motion trials as less difficult than non-motion trials.

The effects of motion on glideslope performance suggest that, for longer ranges, motion may have led to an initial descent with an aimpoint substantially beyond the landing pad. At these longer ranges, vertical displacements lead to smaller changes in glideslope and thus to the visual information specifying glideslope. However, the detectibility of sink rate, as given by platform motion, is not as strongly affected by range to the pad. Thus, increased reliance on the vestibular cues may have led to these results.

The impact of Approach Lighting and Motion appears to be generally additive, except

for glideslope control during the Type B Descents. There, motion appeared to help most when visual cues were weakest (i.e., in the no lights configuration).

Applications to Vertiport Design

The present findings may have important implications for the design of vertiport approach paths and other physically constrained landing sites. Specifically, they suggest that approach lights, or similar markings, that afford the pilot accurate edge rate information, might aid in regulating speed (and perhaps glideslope as well), especially as the pilot approaches the landing pad. An added and important benefit of such information is that it is a "natural" optical cue rather than an artificial information display. As such, abstracting the optical information should not require the attention of the pilot, leaving his/her attention to other aspects of the approach task.

CONCLUSION

The present study used a rotorcraft simulator to examine descents-to-hover at landing pads with one of three approach lighting configurations. The impact of simulator platform motion upon descents to hover was also examined. The results showed that the configuration with the most useful optical information led to the slowest final approach speeds, and that pilots found this configuration, together with the presence of simulator platform motion, most desirable.

Future research should aim to generalize the current findings to actual flight conditions or to more complex simulated approaches.

ACKNOWLEDGMENTS

The authors gratefully acknowledge Mr. Jeffrey Schroeder for his assistance with, and support of, this project. Thanks also to the staff of the NASA Ames Vertical Motion Simulator for providing the technical support for this project. The second author was supported by Cooperative Agreement No. NCC 2-486 from the NASA Ames Research Center. Sandra Hart was the technical monitor.

REFERENCES

Andre, A.D., and Johnson, W.W., Stereo effectiveness evaluation for precision hover tasks in a helmet-mounted display simulator. In Proceedings of the IEEE International Symposium on Systems, Man and Cybernetics, Vol. 2, Chicago, IL: IEEE, 1992

Denton, G.G., The influence of visual pattern on perceived speed, Perception, Vol. 9, 1980.

Koonce, J.M., Predictive validity of flight simulators as a function of simulator motion. Human Factors, Vol. 21, 1979.

Larish, J.F., and Flach, J.M., Sources of optical information useful for the perception of speed of rectilinear self-motion, Journal of Experimental Psychology: Human Perception and Performance, Vol. 16, 1990.

Lintern, G. and Liu, Y-T., Explicit and implicit horizons for simulated landing approaches, Human Factors, Vol. 33 (4), Aug. 1991.

Mertens, H.W., Perception of runway image shape and approach angle magnitude by pilots in simulated night landing approaches, Aviation, Space, and Environmental Medicine, Vol. 52, 1981.

Moen, G.C., DiCarlo, D.J., and Yenni, K.R., A parametric analysis of visual approaches for helicopters. NASA Technical Note TN D-8275, 1976.

Owen, D.H., Wolpert, L., and Warren, R. Effects of optical flow acceleration, edge acceleration, and viewing time on the perception of ego speed acceleration. NASA Scientific and Technical Information Facility, 1984.

Visual Information for Judging Temporal Range

Mary K. Kaiser
Principal Scientist
NASA Ames Research Center
Moffett Field, California

Lyn Mowafy
Research Scientist
University of Dayton Research Institute
Higley, Arizona

ABSTRACT

Work in our laboratory suggests that pilots can extract temporal range information (i.e., the time to pass a given waypoint) directly from out-the-window motion information. This extraction does not require the use of velocity or distance, but rather operates solely on a 2-D motion cue. In this paper, we present the mathematical derivation of this information, psychophysical evidence of human observers' sensitivity, and possible advantages and limitations of basing vehicle control on this parameter.

INTRODUCTION

Helicopter control and navigation require the pilot to orchestrate a complex set of control inputs in response to visual information gleaned from the external scene and cockpit instruments. We suggest that a temporal scaling of the external environment, i.e., gauging the time to reach a chosen way-point at current vehicle speed, is a highly useful metric for the pilot. And, in fact, there is sufficient information in the optical flow to support such temporal metrics.

In this paper, we delineate the visual information that specifies temporal range, describe laboratory research demonstrating people's sensitivity to this information, discuss how this information can be used in vehicular control, and consider specific situations in which this information leads to errors in perceived range.

TEMPORAL RANGE INFORMATION

In the mid-1950s, astrophysicist and novelist Fred Hoyle allowed one of the more clever characters in his book, The Black Cloud, to develop a proof showing that the time to impact of an approaching body can be calculated from the size of the object's image and its rate of expansion. Specifically, the time to contact (TTC) is approximated as:

$$TTC \equiv \phi_t / \delta\phi/\delta_t \qquad (1)$$

where ϕ_t is the angle subtended by the object at time t and $\delta\phi/\delta_t$ is that angle's temporal derivative (i.e., expansion rate). This equation is an approximation in that it assumes the Law of Small Angles (i.e., $\tan\phi = \phi$). The derivation of this equation can be found in Ref. 1.

This elegant observation that TTC can be derived without knowing either target distance or velocity was "rediscovered" by perceptual psychologists, most notably David Lee (Ref. 1), who recognized its significance for perception and control, and derived general formulations for such visual-temporal (or tau) variables. The one most relevant for our discussion describes a moving observer and a target not directly on the observer's motion track, i.e., the passage situation. In this case, an analogous approximation can be made for when the target will pass the observer (i.e., intersect the eye-plane perpendicular to the track vector, as shown in Figure 1):

$$TTP \equiv \theta_t / \delta\theta/\delta_t \qquad (2)$$

where TTP is time to passage, θ_t is the angle between the observer's track vector and the proximal edge of the target, and $\delta\theta/\delta_t$ is that angle's temporal derivative. As before, this equation requires the tangent approximation.

Presented at Piloting Vertical Flight Aircraft: A Conference on Flying Qualities and Human Factors, San Francisco, California, 1993.

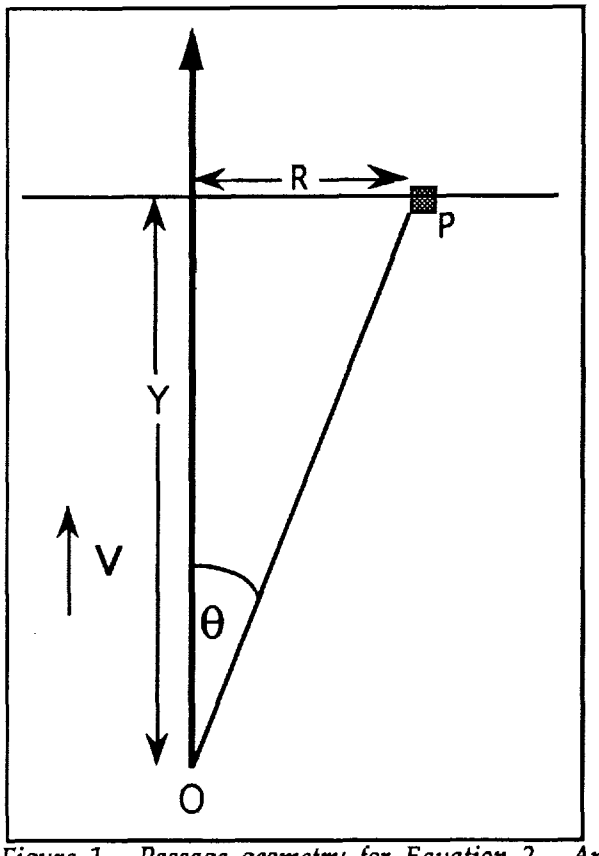

Figure 1. Passage geometry for Equation 2. An observer (O) is moving with velocity (V). A target (P) lies some distance (R) from the track vector, forming angle θ.

Despite the generality of Lee's formulations, empirical studies of human performance have focused almost exclusively on the direct collision, or TTC, situation (Ref. 2 and 3). These studies examined people's intercept (e.g., catching) and avoidance behaviors. However, for many skilled activities, particularly vehicular control, it is also important to judge the temporal range of objects which are not on a direct collision course. In our laboratory, we have examined observers' sensitivity to visually specified TTP information. Our findings suggest that people are adept at making both relative and absolute TTP judgments.

TTP EMPIRICAL STUDIES

We conducted a series of studies in a low-fidelity, fixed-based simulator. Observers were required to make either relative (i.e., which of two targets they would pass first) or absolute judgments (i.e., indicate when a target that was no longer visible would pass them).

Method

The experimental setting is shown in Figure 2. Observers were seated 2.13 m from a 2.44 m X 1.83 m rear-projection screen, creating a horizontal field of view (FOV) of 46°. Viewing was monocular to reduce anomalous depth cues. Displays were generated by a Silicon Graphics Personal IRIS 4D/25TG, with a refresh rate of 60 Hz, and a vertical resolution of 1024 lines. Displays consisted of a cloud of white dots (n=600) distributed in a virtual volume 17.37 m deep. The eyepoint was translated forward at 1.5 m/s. The projected size of the dots did not vary as a function of distance (or change as the observer approached). Thus, there were no object-expansion cues to temporal range.

For the relative TTP judgments, two of the dots were color-coded (green and purple) as targets. The two targets appeared on opposite sides of the heading vector. After viewing durations of 3 or 4 sec, the display was terminated, and observers predicted which of the two targets they would pass first. In the absolute judgment task, only one colored target was visible. It would pass from the observers' FOV after 3 to 5 seconds. The observers estimated when the target would pass their eye-plane by pressing a mouse button. This button press terminated the display.

Target positions were selected such that TTP was fully independent of the time the target was visible on screen, and largely independent of its initial angular projection from the heading vector. In the relative judgment task, the display terminated when the far target was 2 to 4 sec to passage. In the absolute judgment task, the target was between 1 and 3 secsonds from passage when it exited the FOV.

The relative judgement task was conducted with feedback, i.e., observers were informed after each trial whether their response was correct or incorrect. The absolute judgment task was conducted both with and without feedback. When feedback was given, observers were informed by a message on the screen after each trial how early or late their response was (in msec).

Eight observers (four males and four females) participated in both the relative judgment and absolute judgment with feedback tasks. They

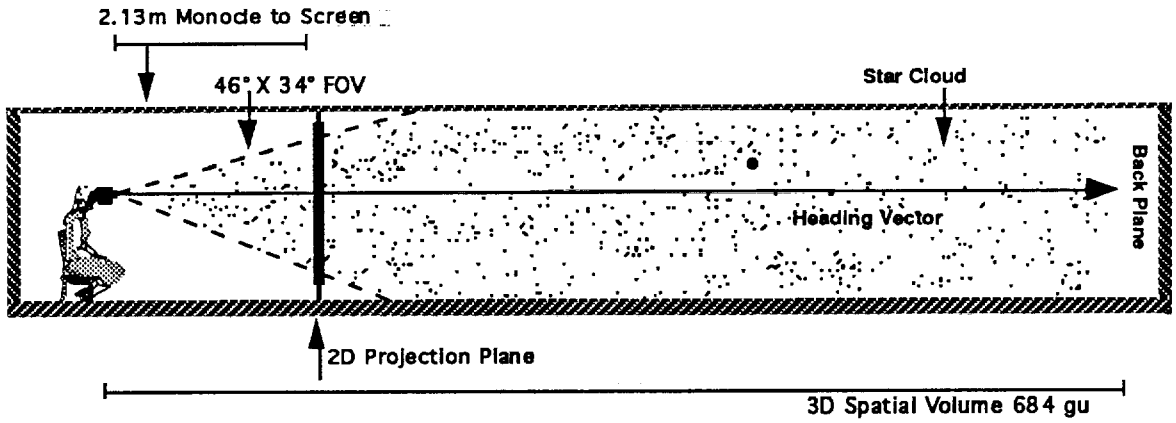

Figure 2. The experimental setting for laboratory experiments. Observers viewed events monocularly with their dominant eye.

ranged in age from 19 to 42 yr; all had normal or corrected to normal vision and were right-eye dominant. Four additional observers (3 males, 1 female) participated in both the feedback version and the no-feedback version absolute judgment task (performing the no-feedback task first). They ranged in age from 24 to 34 yr.

For the relative judgment task, observers completed a total of 160 experimental trials, 80 at the 3-sec duration and 80 at the 4-sec duration. For the absolute judgment task, trials were arranged in blocks of 66 trials. Following initial training trials, observers completed 3 blocks of trials, with 10 min breaks between blocks.

Results

Analyses of the relative judgment data indicated that observers were able to judge above chance level which target they would pass first for all but the shortest (250 msec) temporal separation. The percentages of correct responses averaged across observers are shown in Figure 3. Performance was not affected by whether observers viewed the targets for 3 or 4 seconds. Percent correct differed for the longest temporal difference (1000 msec) only, however this difference was not statistically significant [$F(1,15) = 1.05$, ns].

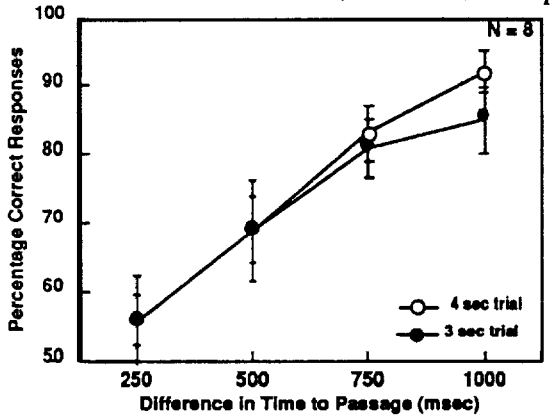

Figure 3. Average percent correct on relative TTP task for the four temporal separation and two display exposure times.

The absolute judgment data were analyzed by performing linear regressions. Judged TTP was regressed against actual TTP. The linear fits (R^2) for the data ranged from 0.55 to 0.85, with a mean of 0.73. The regression slopes for all observers were less than 1 (the mean value was 0.84), indicating a temporal compression (i.e., an additional sec in actual time resulted in less than one sec increase in judged time). The intercepts were all positive (the mean value was about 500 msec). This, coupled with the less-than-unity slopes, indicates that shorter TTPs were overestimated and longer TTPs were underestimated. Across observers, the correlation between constant error and extrapolation time was $r = -0.94$.

For the four observers who participated in both the feedback and no-feedback conditions, the presence of feedback did not significantly impact the linear regression fits, either in terms of slope and intercept, or the goodness of fit.

Discussion

Taken together, the findings from our empirical studies suggest that people are able to make reasonably reliable TTP judgments.

Observers could reliably discriminate differences in TTP of a half sec or more.

Observers' absolute judgments did demonstrate non-veridical temporal scaling (i.e., slopes less than unity and positive intercepts). This bias, however, could either represent a warping of the perceptual space (e.g., a target four sec distant appears to be less than twice as far as a target two sec distant), or result from systematic error in the cognitive extrapolation component of the judgment task. Further research is needed to decompose this bias into its components. Despite this bias, however, observers' judged TTPs were highly correlated with actual TTPs. Further, observers did not require any training or feedback to achieve well-calibrated judgments.

USING TTP TO CONTROL FLIGHT

Optical tau variables thus provide a useful metric for control related activities. Given such temporal metrics, how might a pilot utilize them for vehicular control? We propose that pilots tend to maintain a window of safe maneuverability, which is defined in terms of the handling qualities of the aircraft. For example, consider the geometry shown in Figure 4. For any given eyeheight (i.e., altitude), the forward field can be scaled in terms of eyeheights: the terrain along the 45° declination is one eyeheight distant, a gaze angle of -26.5° corresponds to 2 eyeheights, -18° to 3 eyeheights, and so forth. The time it takes to traverse 1 eyeheight is a function of speed relative to altitude (AGL). If the vehicle is at an altitude of 31 m, a speed of 30 knots will create a flow of 1 eyeheight/sec . If that altitude is doubled, the speed must likewise double to create the same flow rate (or TTP) at a given gaze angle. We suggest that pilots are most comfortable with speed/altitude profiles which allow them to maintain acceptable TTP values at some nominal gaze angle. Acceptable TTP values are defined by the time required to allow the pilot to safely perform necessary flight maneuvers.

In a normal walking gate, people move at about 1 eyeheight/sec. Our sense of subjective speed is geared to this metric. The same objective speed feels faster at lower eyeheights (thus the thrill of low-slung sports cars) and slower at higher ones (thus the boredom of minivans and the early tendency of pilots to taxi B747s too fast). Likewise, as a pilot reduces altitude, the natural tendency will be to reduce speed such that the temporal lead time along a given gaze line is consistent. The flight environment is scaled in a temporal, rather than spatial domain. This temporal scaling is highly relevant for flight control. However, this metric will bias the pilot against maintaining constant speed during altitude change.

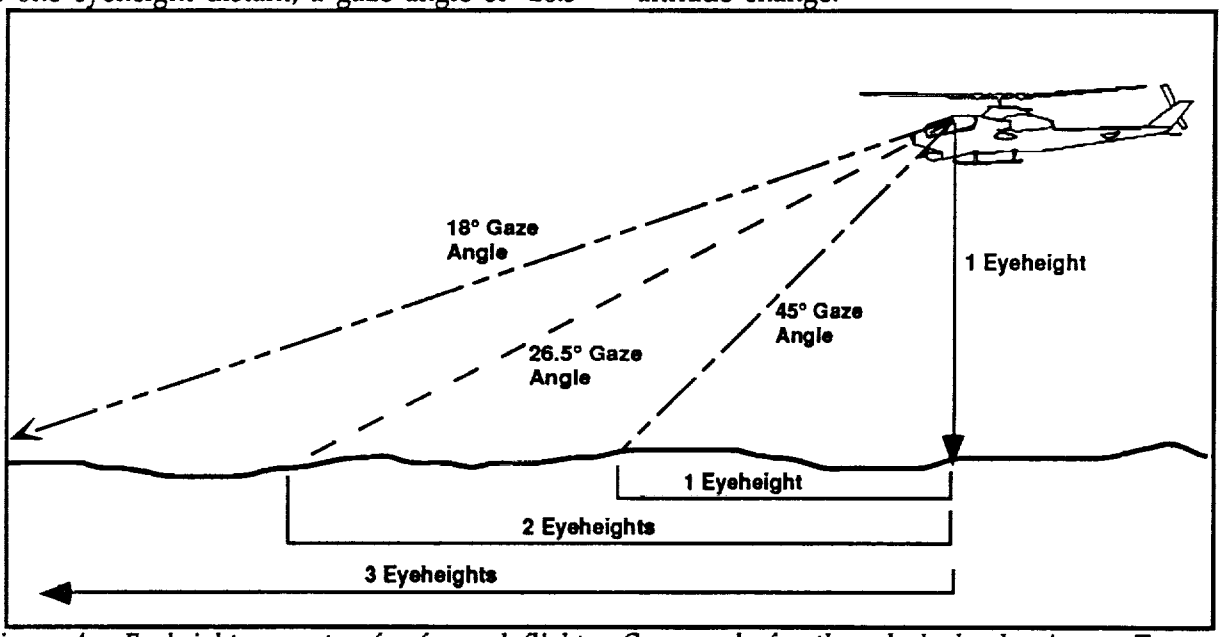

Figure 4. Eyeheight geometry for forward flight. Gaze angle for three look-aheads given. Temporal value of look-aheads determined by velocity in eyeheights/sec.

LIMITATION OF TTP INFORMATION

Given that pilots may utilize optical tau variables to orchestrate control and avoidance maneuvers, it is important to consider limitations and degenerate cases of these variables. As mentioned above, such temporal scaling can result in undesired speed changes during altitude transitions (although a consistent "safety window" is maintained). In addition, there is an interesting degenerative case of TTP that occurs when the observer and a moving target are on a collision course, but the object is not on the observer's track vector. If the observer and object maintain constant velocities, the center of the object maintains a fixed angle to the observer's track vector, as shown in Figure 5.

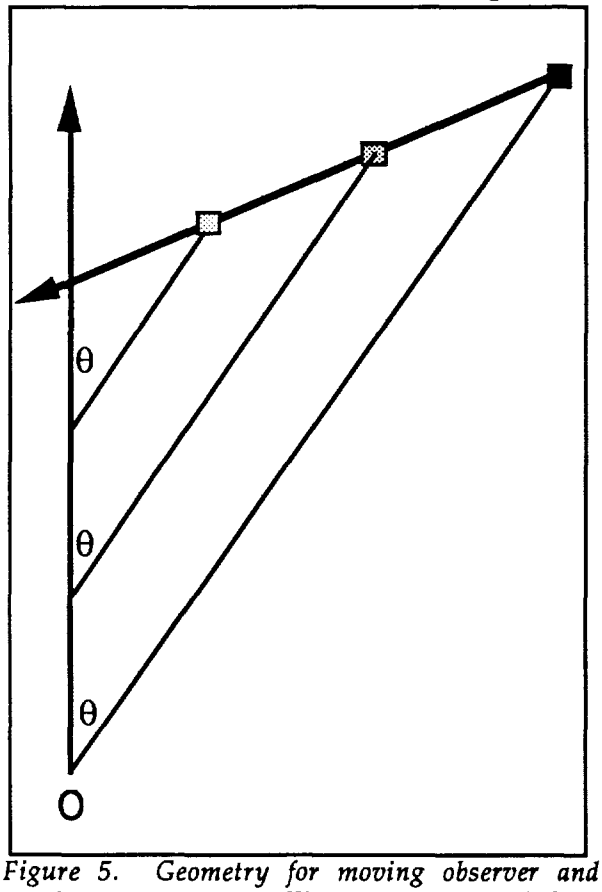

Figure 5. Geometry for moving observer and moving target on collision course. If both maintain a constant velocity and track, θ is constant.

Thus, θ for the centroid of the target is constant (i.e., $\delta\theta/\delta t$ is zero), and $\delta\theta/\delta t$ for all other points is small, reflecting only image expansion. Consider what value of TTP is specified in this condition: TTP = $\theta / \delta\theta/\delta t$, so as $\delta\theta/\delta t$ approaches zero, TTP approaches infinity. Thus, an object on such a collision course can be mistaken for an object at a very large distance, since the TTP information is virtually identical. Image expansion will differentiate these cases, but may not be salient at large distances. Only when image expansion becomes noticeable (or if the observer is cued by some non-motion information, such as familiar size) are the two cases discriminable. Since image expansion may not become salient until the object is temporally proximal, the observer may be required to make a last second correction to avoid collision. Such maneuvers are highly undesirable in flight situations. This examination of the TTP information lends insight into how such mishaps may occur, particularly in visually impoverished (e.g., night flight) environments.

CONCLUDING REMARKS

This "unmoving objects on a collision course" scenario, however, represents a degenerate (albeit interesting) case of TTP information. Most of the time, optical tau variables provide reliable information concerning objects' temporal distance. Moreover, our empirical studies demonstrate that observers possess a robust ability to utilize this information. We propose that these tau cues provide a useful temporal metric for pilots to employ in planning and orchestrating vehicular control. However, the maintenance of such temporal windows result in altitude-related speed changes, which are undesirable in some flight profiles.

REFERENCES

1. Lee, D. N., "A Theory of Visual Control of Braking Based on Information About Time-to-Collision," Perception, Vol. 5, 1976.

2. Tresilian, J. R., "Empirical and Theoretical Issues in the Perception of Time to Contact," Journal of Experimental Psychology: Human Perception and Performance, Vol. 17, 1991.

3. Kaiser, M. K. and Mowafy, L., "Optical Specification of Time-to-Passage: Observers' Sensitivity to Global Tau," Journal of Experimental Psychology, Vol. 19, in press.

Visual Cueing Considerations in Nap-of-the-Earth Helicopter Flight by Head-Slaved Helmet-Mounted Displays[1]

Arthur J. Grunwald[2]
NRC Senior Research Associate
Aerospace Human Factors Research Divisions
NASA Ames Research Center
Moffett Field, California, 94035

Silvia Kohn
Faculty of Aerospace Engineering
Technion, Haifa, Israel

ABSTRACT

The Pilot's ability to derive Control-Oriented Visual Field Information from teleoperated Helmet-Mounted displays in Nap-of-the-Earth flight, is investigated. The visual field with these types of displays, commonly used in Apache and Cobra helicopter night operations, originates from a relatively narrow field-of-view Forward Looking Infrared Radiation Camera, gimbal-mounted at the nose of the aircraft and slaved to the pilot's line-of-sight, in order to obtain a wide-angle field-of-regard. Pilots have encountered considerable difficulties in controlling the aircraft by these devices. Experimental simulator results presented here, indicate that part of these difficulties can be attributed to head/camera slaving system phase lags and errors. In the presence of voluntary head rotation, these slaving system imperfections are shown to impair the Control-Oriented Visual Field Information vital in vehicular control, such as the perception of the anticipated flight path or the vehicle yaw rate. Since, in the presence of slaving system imperfections, the pilot will tend to minimize head rotation, the full wide-angle field-of-regard of the line-of-sight slaved Helmet-Mounted Display, is not always fully utilized.

INTRODUCTION

With head-slaved Helmet-Mounted Displays (HMD's), the image of a forward looking camera, such as an Infrared Radiation or a low-light level camera, mounted on a servo-driven gimbals system at the front of the helicopter, is transferred to a miniature helmet mounted Cathode Ray Tube (CRT). By means of collimating optics and a beam splitter, the image is presented to a single eye so that it appears to be superimposed on the visual field at infinity. The camera motions are slaved to the pilot's Line-of-Sight (LOS), by measuring the pilot's head angles in pitch and yaw, and by imparting this information to the camera servo drives. The LOS slaving system of HMD's allows the field-of-regard of the pilot to be extended well beyond the limits of the narrow field-of-view of the HMD's viewing optics. Thus, just by rotation of the head, the pilot is able to cover a field-of-regard of nearly up to 180 deg horizontally, and 90 deg vertically. In addition, in most cases, the camera is positioned such that its view is not obstructed by the aircraft body. This allows the pilot to view areas which are usually blocked out by the cockpit. This wide-angle coverage is very essential in Nap-of-the-Earth (NOE) flight, both for vehicular control by allowing the pilot the necessary spatial orientation with respect to terrain and obstacles, and for the detection and location of targets or mission threats in military missions, or survivors in rescue missions.

Although the LOS slaved HMD apparently solves the problem of providing a wide-angle coverage for the given narrow field-of-view of the HMD optics, vehicular control with such systems is still very difficult, and demands high pilot proficiency and work load. Part of these difficulties can be attributed the fact that the viewpoint of the camera is displaced with respect to the actual eye position. In the presence of fast vehicle pitch or yaw rotations this might result in misjudged vehicle motions. Furthermore, for a camera mounted in front of the pilot, near objects will appear larger than they actually are.

Additional difficulties arise from the relatively narrow field-of-view of the HMD's viewing optics, resulting from practical limitations on the miniature CRT face-plate dimensions, the dimensions and shape of the beam splitter and its minimal safe distance to the pilot's eye, and the collimating system design. Thus, essential parts of the pilot's peripheral vision are missing, which may result in impaired motion perception.

Considerable difficulties are also encountered in the interpretation of FLIR images, which are basically different from visible light images, usually resulting in misjudged object size and impaired depth perception.

The head-slaved HMD resembles a viewing aperture without optics, attached to the pilot's head, which allows him to frame-in different areas of the outside world by rotation of the head. The HMD one-to-one slaving system and the deliberate choice of a

[1] In part presented earlier at the SPIE/SPSE Symposium on Electronic Imaging: Science and Technology, Feb. 24 - March 1, 1991, San Jose, Ca.

[2] On Sabbatical leave from the Faculty of Aerospace Engineering, Technion, Haifa, Israel.

unity image magnification, attempt to give the pilot the illusion of viewing a natural visual scene through such an aperture. For an ideal slaving system, the viewed image would appear to be part of an inertially stable background. However, slaving system errors will be experienced by the pilot as undesired shifts of the displayed visual field with respect to the true "natural" visual field. The effect of these shifts is two-fold: (1) they will alter the optical flow-field pattern and result in incorrect estimation of the self-motion; and (2) the visually estimated self-motion will be different from the motion estimated by vestibular cues. This might lead to visuo-vestibular conflicts or motion sickness, Oman [1]. In coordinated fixed-wing aircraft flight, the velocity vector will coincide with the vehicle longitudinal axis and the pilot can infer the direction of motion from vehicle-based references, by means of his kinesthetic sense of straight ahead. However, in helicopter flight, the direction of motion can deviate substantially from the vehicle axis. Thus helicopter control in NOE flight, is susceptible in particular to these slaving system imperfections, since the Control-Oriented Information has to be derived entirely from the visual field, and can not rely on vehicle based references.

This paper deals with the basic experiments for understanding the Visual Field Information in HMD's Displays, and investigates how this information is affected by slaving system imperfections. Two types of experiments were carried out: (1) a flight path estimation experiment, in which the pilot had to judge the anticipated vehicle path, while being flown passively in a straight or curved horizontal path over flat textured terrain, and (2) a simulated Nap-of-the-Earth flight experiment, in which the pilot subject had to fly actively through a winding canyon, in the presence of purposefully induced head motions.

VISUAL FLOW FIELD CUES

A detailed geometrical analysis of visual flow field cues in horizontal flight over textured flat terrain, is given in Ref. [2]. In this paper we shall suffice with a brief qualitative description.

The visual flow field resulting from an observer's self-motion, is given by the time derivative of a set of line-of-sight (LOS) vectors extending from the pilot's eye to conspicuous points in the visual field (texture points). The flow field is the pattern traced by the intersection of these LOS vectors with a unity sphere about the observer's head. These traces are commonly referred to as the "streamer" pattern. For straight or constantly curved motion at fixed velocity and altitude above a flat surface, the flow field is constant.

Flow field cues in straight flight

The horizontal situation for straight and level flight is shown in Fig. 1a. The center of gravity of the vehicle moves along a straight path in the direction of the velocity vector $\underline{V}$, while the longitudinal vehicle axis is x_b is rotated with respect to $\underline{V}$ by the crabbing angle β. The camera axis x_h is rotated with respect to the vehicle axis by the angle ψ_h. The corresponding streamer pattern is shown in Fig. 1b. The horizontal and vertical axes in Fig. 1b are the viewing azimuth angle and elevation angle, (the latter is measured positive in upwards direction).

For straight flight the streamer pattern appears to expand from a common focal point on the horizon, point F, see Fig. 1b. This point has often been called the "focus of expansion", Gibson [3-5]. The straight vehicle path is defined by the set of points which do not have an azimuth LOS rate component, see solid line. This is also the streamer that is apparently vertical, i.e. perpendicular to the horizon or to the base of the HMD image frame, for zero vehicle roll angle. The dotted box in Fig. 1a indicates the area of the visual field, viewed by the HMD. The center of this box, H, indicates the camera axis x_h and coincides with the pilot's direction of gaze. The vehicle longitudinal axis x_b is indicated by point C. The head angle ψ_h is the angle between H and C, and the vehicle crabbing angle β is the angle between F and C. In case the crabbing angle β is zero, F and C coincide and the direction of motion is presented to the pilot implicitly by kinesthetic head position cues. However, for arbitrary large angles of β this is not the case, and the direction of motion has to be derived solely from the streamer pattern.

Fig. 1b. indicates that the focal point F is not necessarily located within the HMD field-of-view. In this case, the direction of motion is derived by estimating the point where the streamers line segments, visible within the HMD viewing area, would intersect. It has been shown in Ref. [2] that the detectability of the direction of motion depends on the local expansion, which is defined as the derivative of the streamer direction with respect to the azimuth angle. This local expansion is shown to be proportional to the viewing distance to the texture point, measured along the LOS. It therefore appears, that the direction of motion is most easily perceived in the far visual field, where the local expansion is the largest. However, the streamer pattern can only be perceived when the magnitude of the LOS rates are above a certain threshold. It is shown in Ref. [2] that these LOS rates are inverse proportional to the squared viewing distance. A possible mechanism for estimating the straight vehicle path is to extrapolate the focal point from converging streamer segments, located within an area of the visual field, at the farthest

viewing distance at which the streamer direction can still be detected, and at which the local expansion is the largest. It is clear that when this area is not within the HMD field-of-view, the pilot will have to shift his gaze to a different area of the visual field.

Flow field cues in curved flight

The horizontal situation for steady curved flight over flat terrain is shown in Fig. 2a. The instantaneous velocity vector is $\underline{V}$, and β is again the crabbing angle. However, the actual vehicle path is a circle with radius R, tangential to $\underline{V}$ and with its center at point M. The corresponding streamer pattern is shown in Fig. 2b. This pattern shows a converging, curved set of lines, and a common focal point on the horizon no longer exists. The curved vehicle path is the dashed, central line in the bundle. The vehicle path is defined by the streamer which, for very close viewing ranges, will have a zero azimuth LOS rate component and which tend to be tangential to the velocity vector (solid vertical line). This tangent is again apparently vertical, i.e. perpendicular to the horizon or to the base of the HMD image frame, for zero vehicle roll angle.

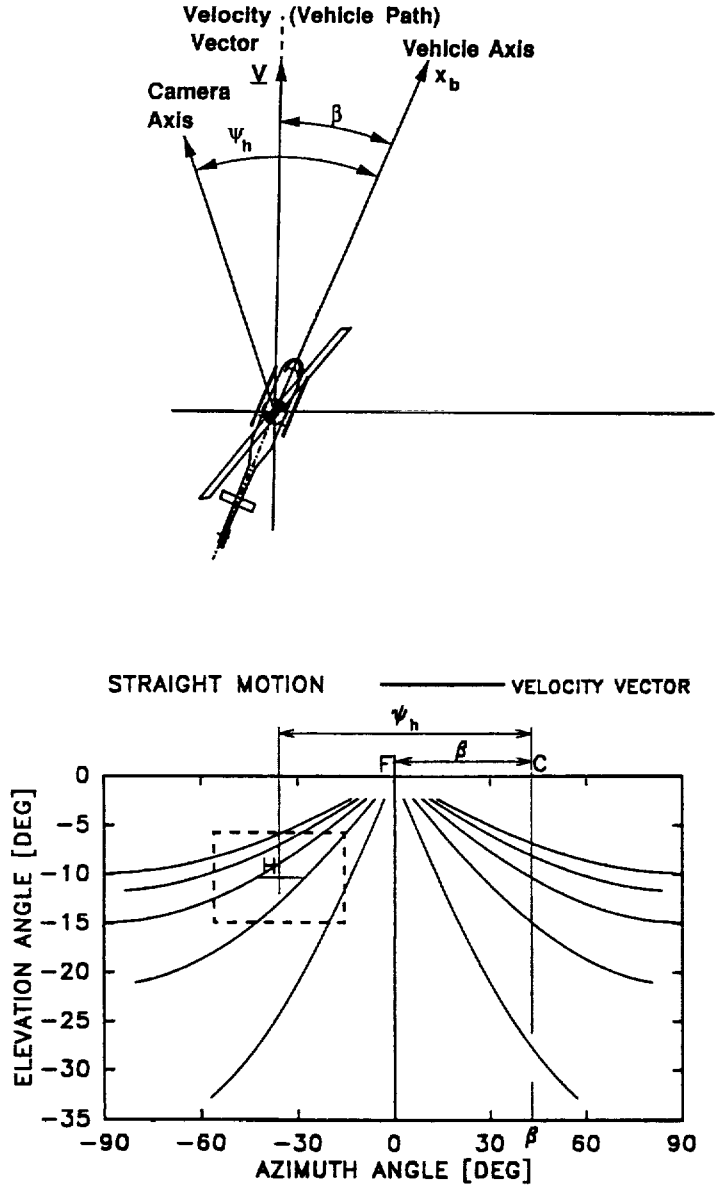

Figure 1. (a) Horizontal Situation for Straight and Level Flight; (b) Streamer Pattern for Straight and Level Flight over Flat Textured Terrain

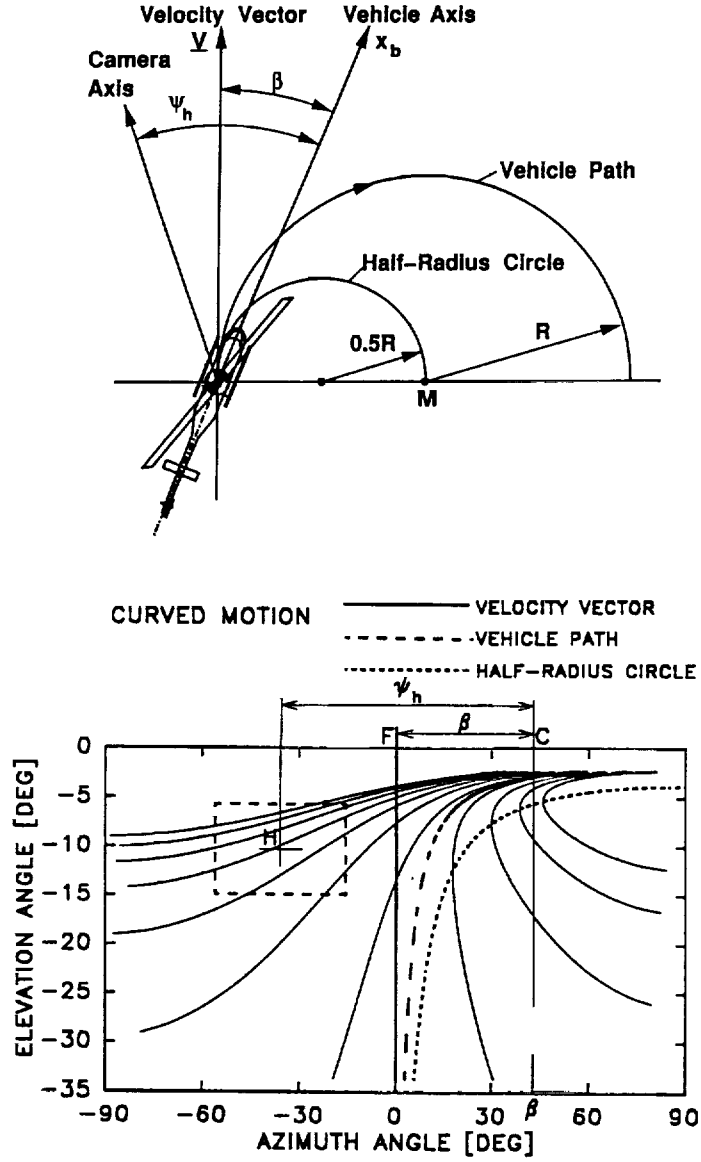

Figure 2. (a) Horizontal Situation for Curved Level Flight; (b) Streamer Pattern for Curved Level Flight over Flat Textured Terrain

It is of interest to consider points in the visual field, which do not have an azimuth LOS rate component. It is shown in Ref. [2] that the locus of these points is formed by the circle, tangential to $\underline{V}$ and with radius 0.5R , hereafter referred to as the "half-radius circle". This locus is shown in Fig. 2b as the dotted line. For viewing distances D<<R, the azimuth angle of a point on the vehicle path is about half way in between the azimuth angle of the velocity vector and of a point on the half-radius circle.

A possible mechanism for estimating a point on the vehicle path, would look for the azimuth angle of the area at viewing distance D, with a zero azimuth LOS rate component, (on the half-radius circle). In addition, the mechanism would estimate the azimuth of the velocity vector by looking, at very close distances, for points with a zero azimuth LOS rate component. It would then estimate the azimuth of a point on the vehicle path at distance D to be half way in between the two angles. A shortcoming of this mechanism is that it will break down when the point on the half-radius circle is outside the field-of-view.

Another possible mechanism would be to look for continuity of motion between points in the visual field. It would select a set of points which belong to a certain section of the streamer, by following the motion of a texture point over a given interval of time. It would then find the correspondence between streamer sections which would add up to the central streamer, i.e. the one of which the azimuth LOS rate component for close viewing distances, is zero, or, alternatively, the streamer which tends to be tangential to the apparent vertical. This would involve viewing near as well as far areas of the visual field.

The dotted box in Fig. 2b. again shows the area of the visual field, viewed by the HMD. Regardless of the mechanism used, active head motions of the pilot will be required, since the estimation of the curved

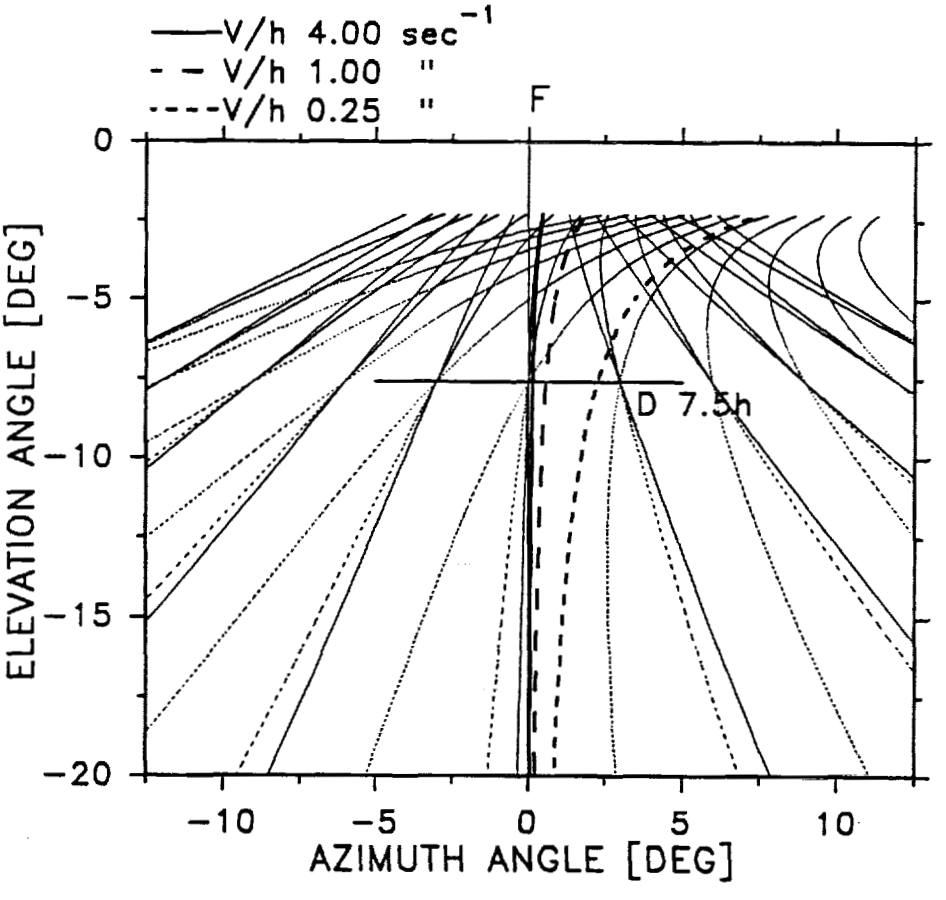

Figure 3: Streamer Pattern "Bending" Effect Resulting From Line-of-Sight Slaving System Lags

vehicle path is based on different areas of the visual field,which involve either points on the half-radius circle or points nearby.

Flow field cues in helmet mounted displays

As mentioned before, for an observer in straight or steady curved level flight, a stationary streamer pattern is obtained. Under natural, unconstrained viewing conditions, the streamer pattern and consequently the ability to estimate the vehicle path, will not be affected by voluntary head rotations. This can be attributed to the visuo-ocular reflex, which will inertially stabilize the eye line-of-sight with respect to the viewed background. In this situation, changes in the pattern only result from changes in self-motion parameters. However, the viewing conditions for LOS slaved HMD's differs from natural unconstrained conditions in two ways: (1) the narrow viewing aperture and (2) slaving system imperfections. Due to the narrow viewing aperture, areas essential for estimating the vehicle path might not be in view. Attempts of the pilot to acquire the information might require quick scans of different areas of the visual field, resulting in rapid head motions. However, due to the frame-of-reference effect caused by the narrow viewing aperture, the observer might experience an apparent yaw motion in opposite direction of the voluntary head rotation, Boff [6]. This illusion is caused by strong edge rate effects of image elements passing the edge of the HMD image frame during rotation. The smaller the reference frame, the stronger the effect.

Slaving system imperfections are detrimental in particular in perceiving self-motion information from the visual field. Random tracking errors, scaling errors, or phase lags will result in undesired shifts of the displayed visual field with respect to the true "natural" visual field. These undesired image shifts will make the viewed visual scene appear to move with respect to an inertially stable background. The negative effects of this apparent motion are twofold: (1) Since, during voluntary head rotation, the eye LOS is stabilized with respect to inertial space, the parasitic image shifts will alter the visual field information. (2) The self-motion estimated from the shifted visual field is in conflict with the vestibular signals. This visuo-vestibular conflict might cause motion sickness or disorientation. The following example demonstrates the effect of parasitic image shifts due to LOS slaving system servo lags, on the visual field information contents.

Consider the LOS slaving system to be a second-order system with an natural frequency of ω_n=94.3 rad/s (15 Hz) and with a damping factor of ζ=0.707. Consider the head yaw rotation to be sinusoidal with amplitude A deg and frequency ω rad/s. It is easily shown that for $\omega << \omega_n$ the image shift rate amplitude s is given by: $s=2\zeta A\omega^2/\omega_n$ deg/s.

For example, for A=10 deg and ω=1.0 rad/s the image shift rate amplitude is s=0.15 deg/s. This parasitic yaw rate will add a constant azimuth component to all LOS vector rates. For an observer in straight motion the parasitic yaw rate will make the expanding pattern appear to "bend" momentarily, just as if the observer were in curved motion. It is clear that the larger the ratio between parasitic yaw rate and LOS rate, the larger the "bending" effect. Therefore the negative effects of servo lags are noticed in particular for low self-motion velocities. Fig. 3 shows examples of this "bending" effect, for A=10 deg and ω=1.0 rad/s, for various velocities. Both the velocity V and the viewing distance D are expressed in units of the height h above the terrain. For V/h ratios of 0.25 s and 4.0 s, the angular errors introduced by the bending effect at viewing distance D=7.5h are 2.26 deg and 0.14 deg, respectively.

EXPERIMENTAL PROGRAM

Experimental setup

The visual scene was generated at a Silicon Graphics IRIS 4D 50/GT work station. The pilot subject was seated in a general aviation simulator cabin, wearing an operational flight helmet, on which a Hughes Aircraft miniature CRT with beam splitter and collimating optics was mounted. The monochromatic image, of aperture 22.8 deg horizontally and 18.4 deg vertically, was presented to the subject's left eye only. The right eye was uncovered, viewing the low-light level cockpit background, normally present in night helicopter missions. No outside view or panel mounted display images were presented. A Polhemus head tracking system was used to measure the angular orientation of the head. The measured yaw, pitch and roll head angles were send to the graphics work station, and used for generating the image corresponding with the subject's line-of-sight. Although the Polhemus was sampling at 30 Hz, the image was updated at about 15 Hz. Thus, the system roughly simulated a line-of-sight slaving system with a bandwidth of 15 Hz. Pilot controls included a two-axis high-precision strain gauge operated side-arm controller with response buttons.

Flight path estimation experiment

Each trial represented the situation of passively being flown over nominally flat terrain at height h, either in a straight or constantly curved, level motion pattern. The terrain consisted of a field of randomly placed poles with constant density and with no visible alignment. The average distance between the poles was 1.17 units of h, and their average height was 0.25h. Both the vehicle velocity vector $\underline{V}$, and the vehicle

longitudinal axis x_b were parallel to the ground plane. The vehicle axis was deviating from the velocity vector V by the crabbing angle β, and the curved path was tangential to $\underline{V}$. In order to conserve computational resources and realize an update rate of 15 Hz, the field was not drawn beyond a viewing distance of D=15h.

The subjects initiated an experimental trial by pressing a response button, after which the visual field became visible from an initially blank screen. For each trial the side slip (crabbing) angle β and/or the path curvature radius R were uncorrelated and chosen randomly. A marker was visible in the visual field at viewing distance D, in the direction of gaze, consisting of a circular base of diameter 0.625 h placed in the ground plane with a vertical pole at its center of height 0.125 h. The marker remained at the center of the HMD image, and the subjects could change the marker azimuth just by turning their head. It should be noted that through appropriate geometrical transformations, the marker was kept at all times perpendicular to the ground plane and at a fixed viewing distance D, regardless of head pitch and roll. The subjects were asked to place the marker on the estimated flight path. They were instructed to do this intuitively, as quickly as possible and to acknowledge their choice by pressing a response button. During the training runs, after each trial, a dotted line was displayed for two additional seconds, indicating the true flight path.

Three types of experiments were conducted: (1) Straight and level flight in the presence of a constant side slip angle β, chosen from a uniformly distributed random set, ranging from -45 to +45 deg. (2) Steady curved and level flight with zero side slip, where the path curvature radius was chosen from a uniformly distributed random set ranging from 15h to 40h and where the curvature could be to the left or to the right with equal probability, and (3) Steady curved and level flight in the presence of side slip, with the curvature chosen as in (2) and with the side slip angle β chosen from an uncorrelated uniformly distributed random set, ranging from -14 to +14 deg.

The relevant parameters investigated were: the velocity-to-height ratio and the viewing distance. Five velocity-to-height ratios were chosen, ranging from 0.25s to 4s. Two viewing distances were chosen, D=7.5h for the far field, and D=3.0h for the near field.

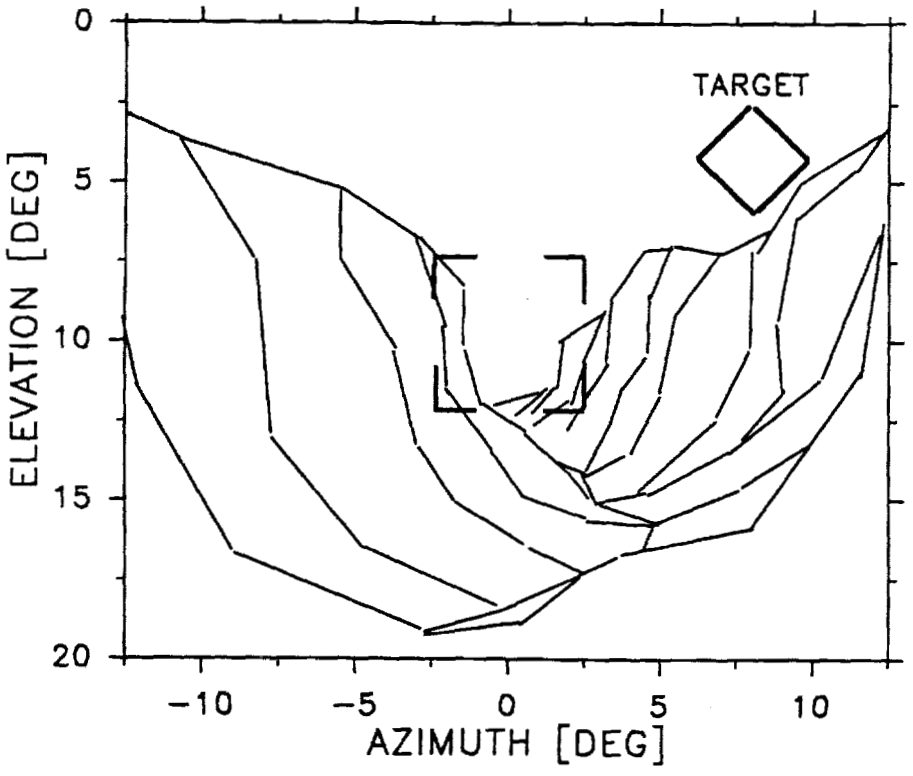

Figure 4: Image of the Randomly Curved Canyon used in the Simulated NOE Flight Experiments

Simulated NOE flight experiment

This experiment simulated the task of actively flying a control-augmented H-19 helicopter through a V-shaped randomly curved canyon, shown in Fig. 4. The horizontal canyon path, and the vertical path profile were generated by passing band-limited white noise processes through a series of shaping filters. The horizontal and vertical path correlation length was about 1500 ft. Two trajectory shapes were considered: a "moderately" curved trajectory with maximum horizontal curvature radii of 500 ft and a strongly curved trajectory with maximum radii of 250 ft. For each run, lasting 180 s, a different random path was generated. The canyon was formed by randomly shaped cross sections spaced 30 ft apart and interconnected by monochrome, solidly drawn polygons of randomly different brightness, simulating a FLIR image. The subjects were instructed to follow the canyon while staying as close as possible to its base without hitting the sides.

Deliberate head rotation was introduced by a secondary task. At random intervals, a diamond-shaped target appeared at a location, fixed with respect to the canyon, see Fig. 4. The target became first visible at a viewing range of 550 ft and disappeared at 300 ft. The subject had to lock his line-of-sight on the target, by bringing it within a 5.7 by 5.7 deg tick mark area in the center of the image. After a successful lock-on, the target and tick marks disappeared. During each run a total of 15 targets were presented. The target locations were chosen such that they involved considerable head rotation, in addition to the rotation needed for following the canyon.

Subject training and experimental procedure

Eight male and one female subject, all of them Technion Aerospace undergraduate students, participated in the experiment. Subject age was between 19 and 24. Subject training for the vehicle path estimation experiments included several one-hour training sessions. After that each subject carried out a series of runs for each one of the three experiments (straight, curved, curved with side slip, in this order). Each series included a number of configurations, each of which was repeated four times and addressed in a random fashion. Each configuration consisted of a set of 20 consecutive trials, each of which was initiated by the subject by pressing a response button. Each trial lasted for about 2-8 seconds, depending on the time needed by the subject to estimate the direction of motion. About 8 one-hour sessions were needed for each subject to finish the experimental program.

Training for the simulated NOE flight experiment required several one hour sessions. Production included simulation runs of 180 s duration, repeated 5 times for each subject and for each configuration. Subject motivation was enhanced by a reward system based on competition.

Experimental measurements

In the flight-path estimation task, for each trial in a set, the error in azimuth angle between the true and estimated location of a point on the flight path at viewing distance D, were recorded, together with the time needed to make the estimate. The upper limit on the estimation time was 8 seconds, after which the run was terminated and marked as a failed run. In addition, the head activity was recorded in terms of the standard deviation of the head yaw angle and yaw angle rate.

For each set of 20 trials, the average and the standard deviation of the estimation error and estimation time, were computed. Since the average of the estimation error was found to be almost zero, i.e. no preference for an error in left or in right direction existed, the standard deviation of the estimation error was adopted as the representative estimation error score of each set. For the estimation time, the average of the set was taken as the representative score.

Performance scores for the NOE flight experiments included the power of the deviation from the bottom of the canyon, standard deviations of head activity, stick activity, vehicle roll and roll rate and the average time needed to lock the line-of-sight on the target.

EXPERIMENTAL RESULTS

Flight path estimation task

Effect of the velocity-to-height ratio:

Figs. 5-8 show the various performance scores as a function of the V/h ratio, for the three motion patterns. For straight motion, (dotted line) the estimation error score strongly decreases with V/h, both for the "far" viewing distance of D/h=7.5h (Fig. 5a) and for the "near" viewing distance of D/h=3.0h (Fig. 5b). In contrast, the downslope of the curves for curved motion and curved motion with side slip, is considerably less. For the near viewing distance the curves are even sloping upwards (Fig 5b). Furthermore, the curves for straight motion for the estimation time and the head yaw rate activity are markedly above the ones for the curved motion patterns, see Figs. 6a,b. This indicates that the subjects probably used a different strategy in the straight motion task. The curves for the head yaw angle and yaw angle rate activity show pronounced and consistent upward slopes, Figs. 7 and 8. This effect can be attributed to the LOS slaving system imperfections, discussed in Section 2.4. The smaller V/h, the stronger the "bending" of the streamer pattern

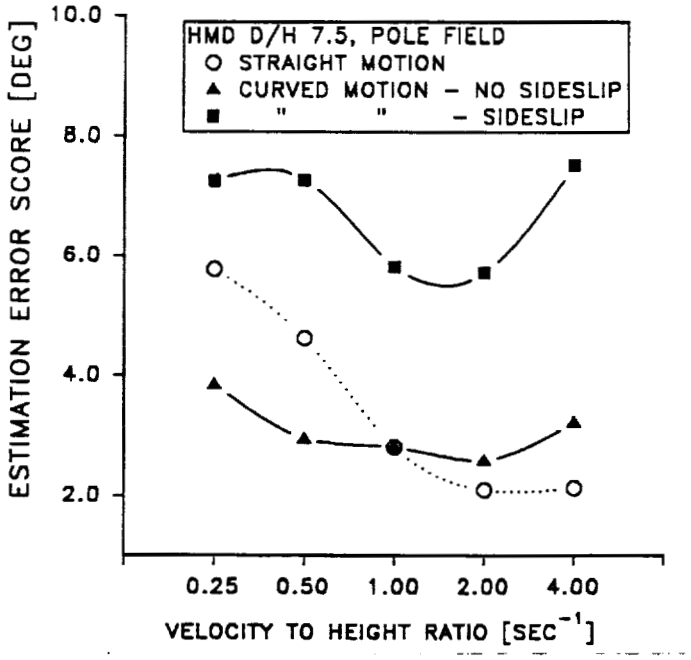

Figure 5a. Estimation Error Score for D=7.5h

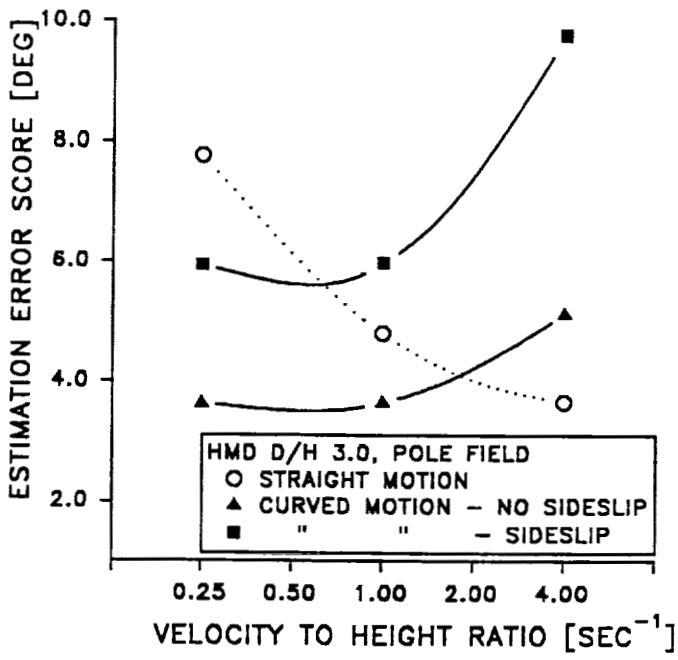

Figure 5b. Estimation Error Score for D=3.0h

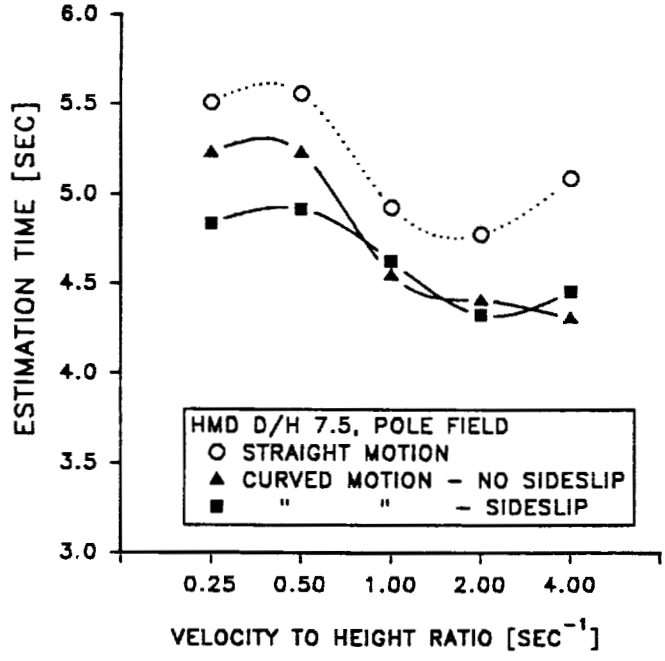

Figure 6a. Estimation Time for D=7.5h

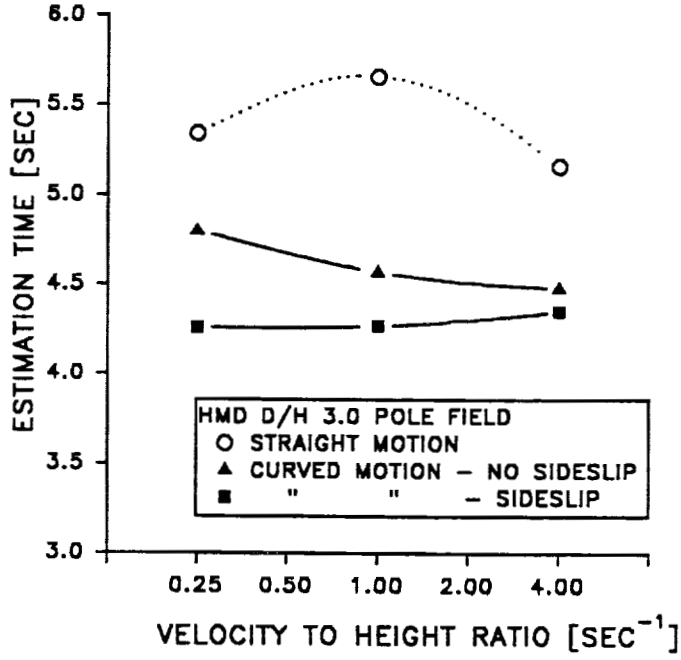

Figure 6b. Estimation Time for D=3.0h

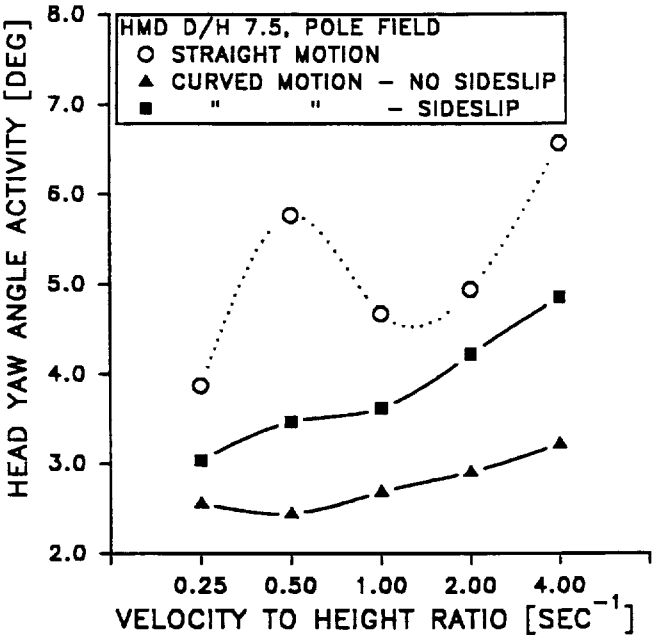

Figure 7a. Head Yaw Angle Activity for D=7.5h

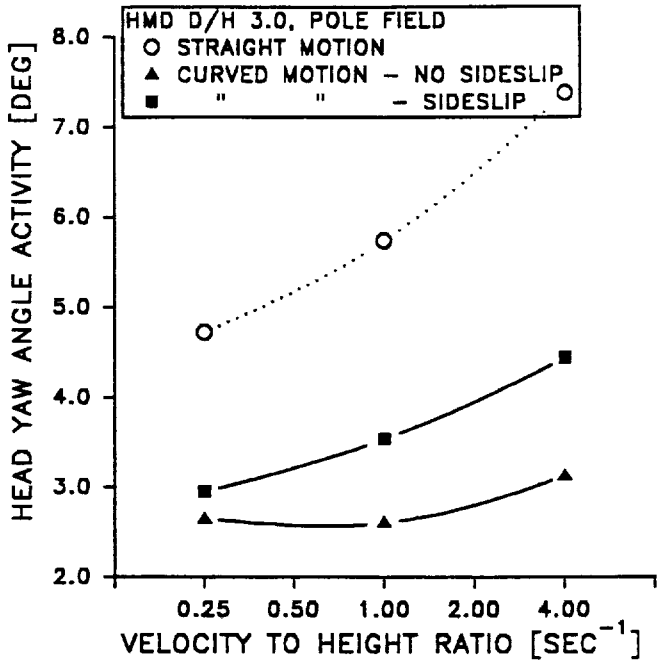

Figure 7b. Head Yaw Angle Activity for D=3.0h

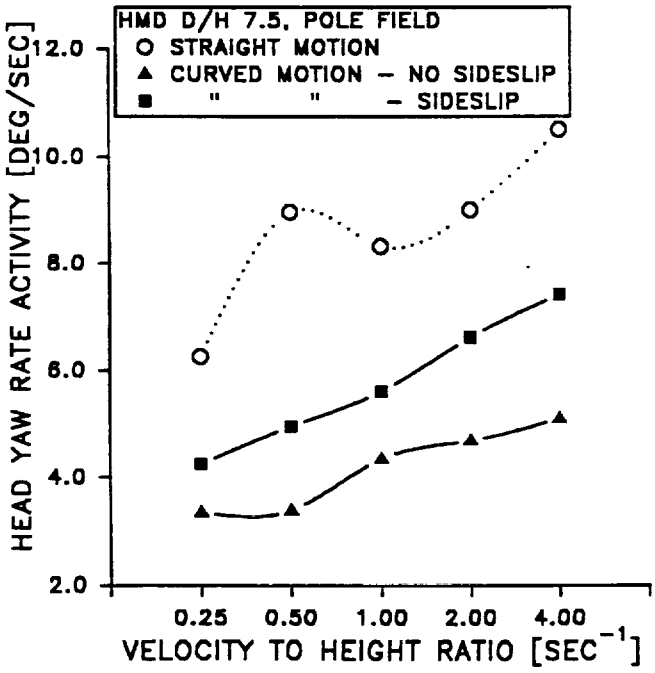

Figure 8a. Head Yaw Rate Activity for D=7.5h

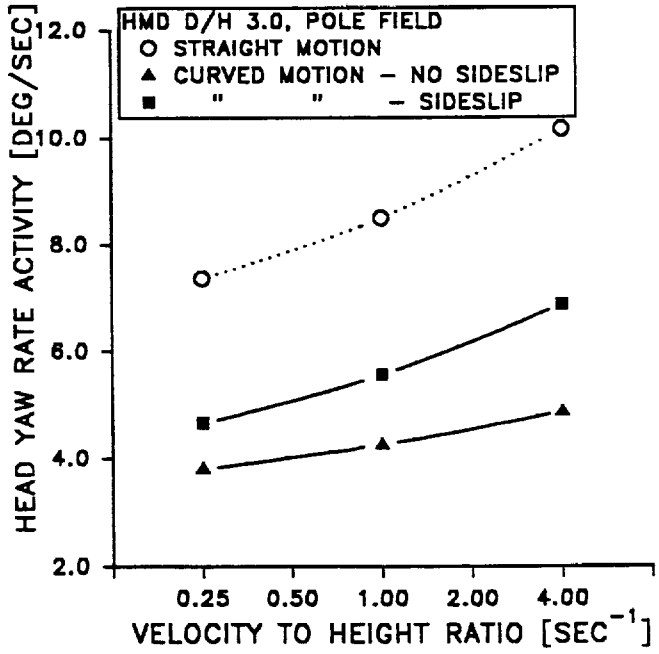

Figure 8b. Head Yaw Rate Activity for D=3.0h

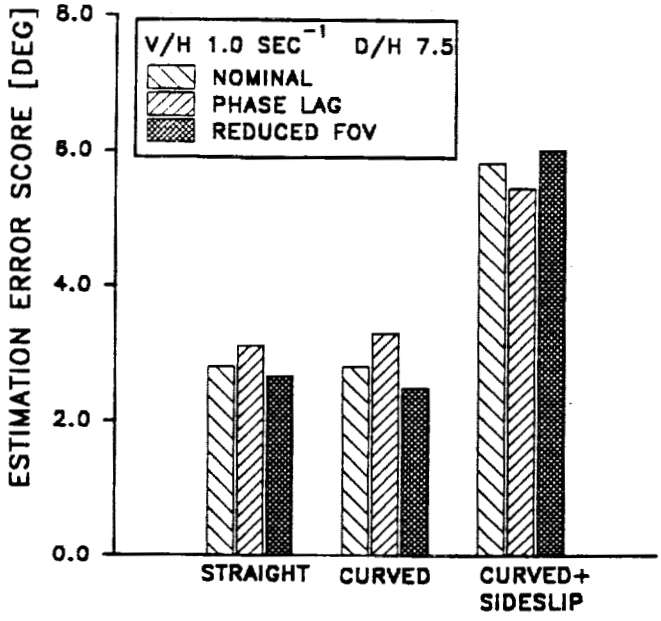

Figure 9a. Effect of Reduced Field-of-View and LOS Slaving Lags on Estimation Error Score

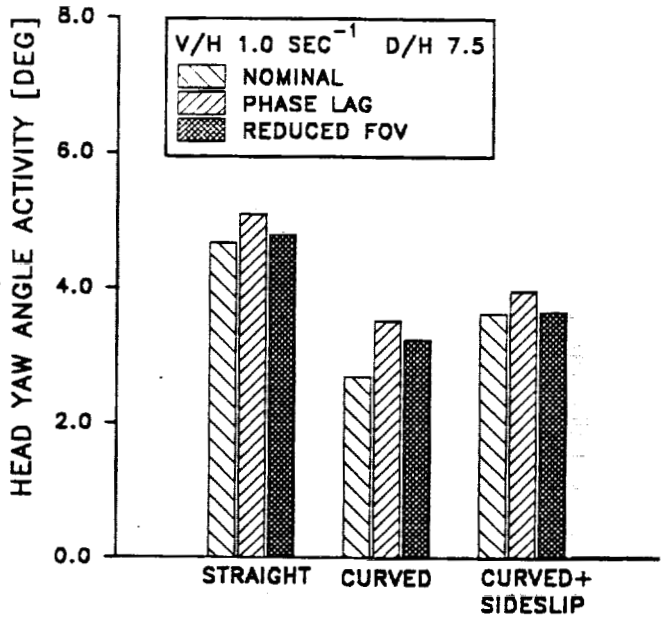

Figure 9c. Effect of Reduced Field-of-View and LOS Slaving Lags on Head Yaw Angle Activity

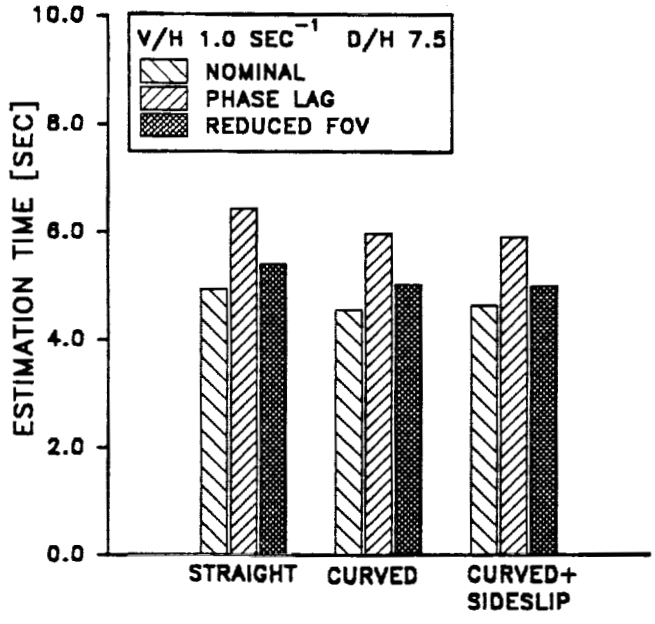

Figure 9b. Effect of Reduced Field-of-View and LOS Slaving Lags on Estimation Time

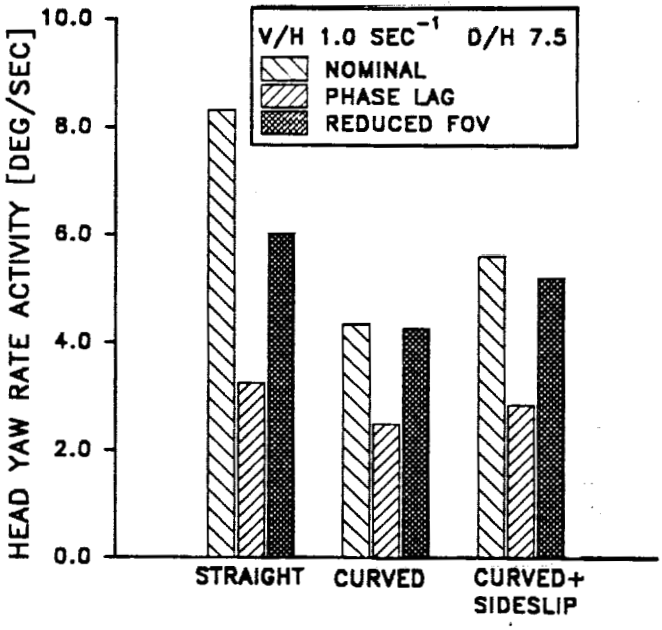

Figure 9d. Effect of Reduced Field-of-View and LOS Slaving Lags on Head Yaw Rate Activity

during head rotation resulting from slaving system lags, and the less accurate the perception of the streamer direction. This is detrimental in particular in the straight motion task, in which the streamer "bending" makes it almost impossible to find the apparent vertical streamer. As a result, for small velocities subjects will minimize their head rotation, estimates will take longer and estimation errors will be larger. This explains the strong downward slope of the estimation error curve for straight motion, as compared to the more flat curves for curved motion, see Fig. 5a.

Strategy differences between straight and curved tasks are apparent when considering that the subjects are expecting a straight expanding motion pattern in the straight task. Thus, bending effects due to slaving system lags will be identified immediately, and estimates are made only at moments at which the head is stationary. The subjects might have employed a "null measurement" method, in which a sequence of correcting steps is made aimed at placing the apparent vertical streamer at the center. In contrast, in the curved task the subjects might have employed a "deflection measurement" method in which the vehicle path is found intuitively, more or less in an open manner, triggered by the amount of streamer "bending" in the field. Consequently, estimation times and head yaw activity are much larger for the straight task.

Effect of side slip on curved motion:

The estimation error score curves for motion with and without side slip have similar characteristics, i.e. for the far viewing distance a minimum at V/h=1.0 s (Fig. 5a), and for the near viewing distance similar up slopes, (Fig.5b). This up slope might be due to motion "blurring" effects, which prevent the subject from making accurate estimates on the streamer pattern direction. However, the error score curve for motion with side slip is on the average about 3 deg above the one for motion without side slip. This was expected, since in the first case, in the process of estimating the vehicle path, the observer has to derive the direction of motion from the near visual field, whereas in the latter case the direction of motion is at zero azimuth. This direction is presented to him implicitly by kinesthetic head position cues. The increased difficulty to estimate the vehicle path in the presence of side slip is also noticed in the higher head yaw angle and yaw angle rate activity, see Figs. 7 and 8.

Effect of the viewing distance:

A comparison of the curves of Figs. 5a and 5b shows that the near viewing distance yields generally larger estimation errors than the far distance. This might result from the smaller local expansion in the near field. The difference is large in particular for high V/h ratios, probably as a result of image blurring. In contrast, the head yaw rate activity shown in Fig. 8a,b for the near and far viewing distance were found to be very similar. It would be expected that the near field, with its higher LOS rates, would allow larger head rotation, since less streamer "bending" will occur. However, the negative effect of the "bending" will be stronger, due to the smaller local expansion. Therefore, the subjects will still minimize their head rotation for low V/h and for the near viewing distance.

Effect of reduced field-of-view:

The results for an HMD field-of-view reduced to 13.7 deg horizontally and 11.0 deg vertically (40% reduction), are shown in Fig. 9. Contrary to what was expected, estimation errors for all three motion patterns were about the same as for the nominal viewing situation, Fig 9a. However, estimation times were slightly higher (by 9%), and head yaw rate activity lower (by 15%), in particular for straight motion, Fig 9b,c. This indicates that although the reduced field-of-view did not affect estimation accuracy, the subjects might have reduced their head yaw rates due to increased edge rate effects. On the other hand, as expected, the reduced field-of-view demanded slightly more headmotions, as seen in the 6.5% increase in head yaw angle activity

Effect of LOS slaving system lags:

A first-order slaving system lag with a time constant of 0.5 s was introduced. Although the phase lag yielded an only 4% higher error score as compared to the nominal viewing situation, the head yaw rate activity was markedly smaller (by 53%) and, consequently, the estimation time higher (by 30%), see Fig. 9. This clearly demonstrates that slaving system phase lags primarily constrain the subject from making fast head motions, they require from him to make more corrections (14% larger head yaw angle activity), and they result in longer estimation times.

Simulated NOE flight task

Results for the NOE flight task are summarized in Table I. For flight without target capture secondary task, the increase in path curvature has its primary effect on the tracking performance (a 65% increase in tracking error score). The increased path curvature is also strongly noticed in the 31% larger head yaw angle rate. Thus, the high-curvature canyon demands more head activity, which, in the presence of inherent LOS slaving system lags, adversely affects tracking performance. As expected, the increased curvature also yields larger control activity and vehicle roll motions.

The effect of adding the target capture secondary task to the vehicular control task is strongly noticed both in the markedly higher tracking error and in the larger head yaw rates (tracking error scores increase by

Table 1. Simulated NOE Flight Experiment

	Without Target Task		With Target Task	
	Low Curvature	High Curvature	Low Curvature	High Curvature
Tracking Error [ft^2]	390.1	643.9	1168.6	1072.5
Head Yaw rate [deg/s]	3.2	4.2	7.4	8.4
Comm. Roll rate [deg/s]	25.7	27.7	27.2	29.1
Comm. Pitch rate [deg/s]	2.6	3.1	3.2	3.7
Vehicle Roll Angle [deg]	7.5	9.4	8.8	10.7
Vehicle Roll Rate [deg/s]	15.6	16.7	16.3	17.5
Target Capture Time [s]	-	-	1.48	1.94
% Missed Targets/Run			6.6	13.0

116% and head yaw rates by 113%). In contrast, control activity and vehicle roll activity increase only slightly. The high correlation between head yaw activity and tracking errors, again demonstrate that head rotation, in excess to the amount needed for the vehicular control task, negatively affects performance. As expected, due to increased main task difficulty, the high-curvature canyon resulted in a 31% higher average target capture time and yielded twice as much missed targets.

Although in this experiment the head rotation is artificially and purposefully induced, similar performance degradation is expected to occur, when the pilot voluntarily moves his head in search of targets or mission threats. Consequently, for HMD's subjected to line-of-sight slaving system lags, the pilot will tend to reduce his head rotation to the minimum required for carrying out the vehicular control task. However, under these conditions, the wide-angle coverage of the line-of-sight slaving system will not be fully utilized and target search performance and spatial orientation will be seriously impaired.

Summary of results

1. The experimental results have clearly shown that line-of-sight slaving system imperfections in HMD's seriously impair the pilot's ability to derive Control-Oriented Information from the visual field. Since, under these conditions, the pilot will tend to minimize head rotations, the wide-angle coverage provided by the slaving system, will not be utilized and search performance and spatial orientation will be impaired.

2. Canyon following performance was found to deteriorate with increased head rotation, either when introduced in a "natural manner" through a higher path curvature, or when induced purposefully by using the target capture secondary task.

3. The vehicle path estimation accuracy and head yaw rate activity generally increase with the V/h ratio. Due to the larger "local expansion" the far viewing distances yield more accurate estimates than close distances. However, due to blurring effects, close distance estimates no longer improve with V/h.

4. The flight path for curved motion is considerably more difficult to estimate than for straight motion, since it relies on the entire streamer pattern rather than on local field estimates. Since in curved flight the near as well as the far field is used, the estimates are less accurate and improve less with increasing V/h ratio.

DISCUSSION

The display system discussed in this paper can be classified as a virtual environment display. Head-mounted displays have become a vital component of virtual environments, which attempt to give the operator the illusion of being physically present in a remotely existing or synthetically generated world. Frequently this objective is achieved by fully immerging the operator in the visual scene by completely blocking out the direct view of the outside world and by presenting the operator with a stereo image of the environment, which is derived either from a remotely located stereo camera pair or computer generated. Although state-of-the-art miniature display technology and computer generated image techniques enable to display images of high quality, detail and authenticity, most system fail to provide the operator with the confidence to move around freely without the fear of stumbling or falling.

The main findings in this paper are valid for this general class of displays as well. While designers of virtual environments are devoting considerable attention to picture contents, quality and detail, the dynamic aspects are often neglected. Detrimental

factors are insufficient update rates, too large time delays due to time-consuming signal communication or highly band limited camera slaving systems. Other factors are inaccurate head position measurements and a lack of rigidity between the display and the head. While these displays may be adequate for a seated person in a near-static environment, in the presence of slow head motions, they often fall short in situations in which self-motion estimation is essential, such as walking, running or controlling a vehicle. Since correct motion estimation from visual cues is only possible when the illusion of an inertially stable background is preserved, deviations induced by system lags or slaving system errors, will result in estimation errors in the self-motion variables. Furthermore, for the person immerged in the environment, the visual cues will be in conflict with the vestibular ones, resulting in disorientation, loss of balance or even motion sickness.

The display, discussed in this paper provides only "partial immersion" since the outside world remains directly visible both to the uncovered eye and to the covered one through the beam-splitter. This arrangement allows the pilot to maintain direct visual contact with the outside world in case of HMD system failures, or for scanning the cockpit instruments. Part of the task difficulty can be attributed to this dichoptic viewing situation, in which the pilot has to switch his attention consciously between the two eyes.

Future research effort should be devoted to exploring ways to eliminate the need for maintaining direct visual contact with the outside world by incorporating all necessary information in a stereoscopic, full immersion display. This might require integrating the present cockpit panel information in the HMD image, and the use of superimposed display symbology, such as a vehicle path trace, a vehicle axis or velocity vector symbol. This superimposed symbology would serve in compensating for the lack of peripheral vision resulting from the narrow HMD field-of-view. Engineering efforts should be devoted primarily to solving the display-to-head rigidity problem, minimizing slaving system errors and enlarging the effective HMD field-of-view.

ACKNOWLEDGEMENTS

This research has been supported by a grant from NASA Ames Research Center, Aerospace Human Factors Research Division, Moffett Field, Ca. 94035, under cooperative agreement No. NAGW-1128. Dr. S. Hart and Dr. D. Foyle of Ames Research Center have been the Scientific monitors for this grant.

REFERENCES

1. Oman, C.M., "Sensory Conflict in Motion Sickness: an Observer Theory Approach," in: Pictorial Communication in Virtual and Real Environments, Eds. Ellis, S.R., Kaiser, M.K. and Grunwald, A.J., Taylor and Francis, 1991.

2. Grunwald, A.J., Kohn, S. and Merhav, S.J., "Visual Field Information in Nap-of-the-Earth Flight by Teleoperated Helmet-Mounted Displays," SPIE/SPSE Symposium on Electronic Imaging: Science and Technology, Feb. 24 - March 1, 1991, San Jose, Ca., Paper No, 1456-17, 1991.

3. Gibson, J.J., "The Perception of the Visual World," Houghton Mifflin, Boston, Mass., 1950.

4. Gibson, J.J., Olum, P. and Rosenblatt, F., "Parallax and Perspective During Aircraft Landings," American Journal of Psychology, Vol.68, 1955, pp.372-385.

5. Gibson, J.J., Visually Controlled Locomotion and Visual Orientation in Animals," British Journal of Psychology, Vol.49, 1958, pp.182-194.

6 Boff, K.R., Kaufman, L. and Thomas, J.P., "Handbook of Perception and Human Performance," Vol. 1, Wiley N.Y., 1986, page 16-18, pages 17-18 to 17-20.

Handling Qualities Effects of Display Latency

David W. King
Technical Specialist
Flying Qualities

Boeing Defense & Space Group, Helicopters Division
Philadelphia, Pennsylvania

Abstract

Display latency is the time delay between aircraft response and the corresponding response of the cockpit displays. Currently, there is no explicit specification for allowable display lags to ensure acceptable aircraft handling qualities in instrument flight conditions. This paper examines the handling qualities effects of display latency between 70 and 400 milliseconds for precision instrument flight tasks of the V-22 Tiltrotor aircraft. Display delay effects on the pilot control loop are analytically predicted through a second order pilot crossover model of the V-22 lateral axis, and handling qualities trends are evaluated through a series of fixed-base piloted simulation tests. The results show that the effects of display latency for flight path tracking tasks are driven by the stability characteristics of the attitude control loop. The data indicate that the loss of control damping due to latency can be simply predicted from knowledge of the aircraft's stability margins, control system lags, and required control bandwidths. Based on the relationship between attitude control damping and handling qualities ratings, latency design guidelines are presented. In addition, this paper presents a design philosophy, supported by simulation data, for using flight director display augmentation to suppress the effects of display latency for delays up to 300 milliseconds.

Notation

AFCS	Automatic Flight Control System
CHPR	Cooper-Harper Pilot Rating
FCSIR	V-22 Flight Control Systm. Interface Rig
ILS	Instrument Landing System
IMC	Instrument Meteorological Conditions
K	Pilot control gain (in/deg)
N_{cw}	Pilot workload metric
N_{perf}	Tracking performance metric
MFD	V-22 cockpit Multi-Function Display
P	Aircraft roll rate (deg/sec)
T_L, T_I	Pilot model lead, lag time constants (sec)
$Y_c(j\omega)$	Aircraft + control system transfer funct.
$Y_p(j\omega)$	Pilot model transfer function
δ	Lateral stick control input (inches)
Φ	Phase of pilot-a/c-display system (deg.)
Φ_m	Phase margin pilot-a/c-disp. systm. (rad)
Φ_{mo}	Phase margin of aircraft system(rad)
σ	Tracking error standard deviation(deg)
$\Delta\gamma$	Localizer tracking error (deg)
$\Delta\Gamma$	Glideslope tracking error (deg)
ΔV	Airspeed tracking error (kts)
ξ	Pilot-a/c-display system damping ratio
ω_c	Pilot crossover frequency (rad/sec)
τ_c	Control system delay (sec)
τ_d	Display delay (sec)
τ_f	Display low-pass filter time constant (sec)
τ_p	Pilot delay (sec)

Presented at Piloting Vertical Flight Aircraft: A Conference on Flying Qualities and Human Factors, San Francisco, California, 1993.

Introduction

The next generation of military rotorcraft are being designed to fulfill an astonishingly wide range of mission objectives. Due to an explosive growth in avionic system technology tasks which were unthinkable ten years ago, including nap-of-the-earth flight in low visibility, are now possible. Crew station designers are challenged to integrate the state-of-the-art technologies to provide the means to accomplish ambitious mission objectives, while also assuring that the performance of "routine" flight tasks is not degraded. Unfortunately, one side effect of complex avionic systems, known as *display latency*, stands as an obstacle to this challenge.

Display latency is defined as "the time delay between sensor detection of aircraft movement and the corresponding indication on the cockpit displays." The advent of the fully integrated all-glass cockpit allows pilots to selectively access a wide range of flight information including aircraft attitude, rates, navigation information, threat and/or target status, aircraft systems information, and engine parameters. Aircraft sensor information is digitally processed in onboard computers and may be accessed by the pilot through selectable cockpit displays, or through head-up/helmet-mounted display systems. However, the processing and

transportation of the flight data takes time. During nighttime or adverse weather conditions the delay of fundamental flight information, such as aircraft attitude and rates, may adversely affect the pilot's ability to control his aircraft. Currently, there is no explicit military specification for display latency and little research data on the subject. Designers of new aircraft are thus faced with the unanswered question of how much latency is acceptable.

This paper evaluates the relationship between display latency and instrument flight handling qualities for the V-22 Tiltrotor aircraft. The three goals of this study were to quantify handling qualities trends (performance, workload, and pilot ratings) from varying levels of display latency, to generate methods to predict aircraft sensitivity to display latency, and to investigate methods to subdue latency effects. Using classical control theory, a second order linear model of the pilot-aircraft-display system was developed to analyze latency effects. Extensive piloted simulation was performed to support the analytical model and gather handling qualities data for different levels of latency. Finally, flight director displays were investigated as a means to augment the pilot control loop and suppress the latency effects.

Background

The V-22 Osprey Tiltrotor is a revolutionary aircraft designed to meet the mission requirements of all four military services. Besides providing basic control functions in multiple flight modes (helicopter - conversion - airplane), the V-22 digital flight control system and fully integrated avionic system provide maneuver limiting, fully coupled flight path tracking, integrated cockpit management, and thrust - power management regulation. Subsequently, the V-22 exhibits a substantial amount of display latency due to the digital processing and transportation of the sensor data as it is passed from an avionics data bus to the Flight Control Computer and the Mission Computer, where it is processed, and then passed to the Display Electronics Unit (DEU) where the symbology is drawn on the cockpit Multi-Function Displays (MFD) as shown in Figure 1. Measurements indicate an average latency of 211 milliseconds (ms) for the V-22 attitude display.

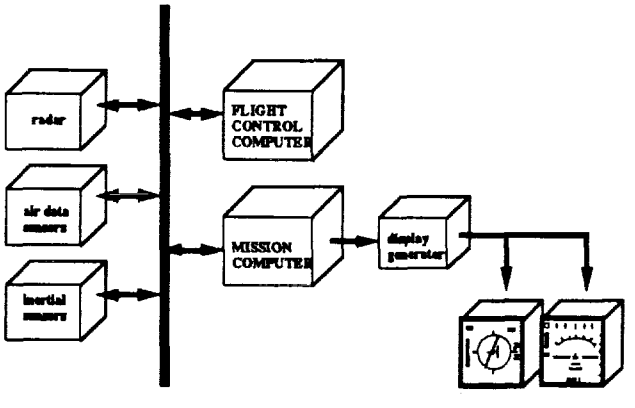

Figure 1. Avionics architecture

It is intuitive to assume that in the absence of any out-the-window visual cues, a quarter-second display delay might be troublesome. For a precision flight task in instrument conditions, the pilot controls his aircraft by closing the loop between the cockpit displays and the aircraft control inputs as shown in Figure 2. The pilot acts as an optimal, adaptive, multi-loop control element by applying control inputs to track a prescribed flight condition indicated on the displays. System delays, such as control system and aircraft lags, have been shown to degrade aircraft handling qualities for tasks requiring high frequency control inputs (Ref. 1). Extensive research (Refs. 2,3) has shown that control system delays in excess of 100 ms are likely to degrade the ease and accuracy at which a pilot can successfully perform demanding visual tasks. Subsequently, control system lags are limited to 100 ms (for level 1 handling qualities) in flying qualities military specifications (Refs. 4,5). However, fundamental differences in pilot technique between visual flight and instrument flight preclude the direct application of control system delay specifications to display delay. Pilots are trained to fly instrument tasks with milder and more deliberate control inputs than corresponding visual tasks. Furthermore, precision instrument tasks often require display augmentation, visual aids, or selectable automatic control modes which are not considered in visual flight task specifications. Unfortunately, most of the previous research on display delays has been limited to simulator delays (Ref. 6) and highly maneuverable fixed-wing aircraft (Ref. 7).

The bottom-line handling qualities criterion for a developmental aircraft such as the V-22 is to provide Level 1 Cooper-Harper pilot ratings. Cooper-Harper pilot ratings (Ref. 8) provide a qualitative assessment of the pilot's ability to successfully perform a given task with a tolerable amount of workload. A Level 1 rating implies the aircraft is "acceptable without improvement." In order to substantiate Level 1 compliance, the aircraft must be flight-tested

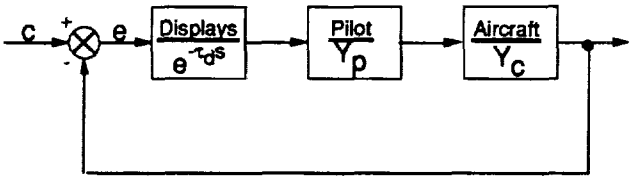

Figure 2. Pilot control loop

throughout its flight envelope including the full range of mission tasks. Subsequent handling qualities ratings depend on several variables including performance requirements, aircraft stability characteristics, flight control system functionality, cockpit displays, crew station format, and pilot proficiency. It is therefore not straightforward to isolate the effects of a single factor such as display latency on handling qualities results during limited flight testing of a developmental aircraft. In order to prevent display latency from unexpectedly handicapping a developmental aircraft late in its flight test program, system designers require either specific latency guidelines or simple techniques to evaluate latency effects.

Evaluation Procedure

Handling qualities engineers often employ analytical models of the pilot-aircraft closed-loop system to predict and analyze the effects of specific aircraft and control system parameters on simple flight task performance. The pilot is modelled as a servo-actuator control element which provides aircraft control inputs to follow a command profile. Various linear pilot models have been developed including single-input/single-output, multiple-input/multiple-output (Ref. 9), optimal control (Ref. 10), and structural models (Ref. 11). One of the simplest and most often used is the classical control theory *pilot crossover model*. The crossover model (Refs. 12,13) states that a sufficiently trained pilot linearly relates a control input to a tracking error such that the open-loop pilot-aircraft system provides the following frequency domain characteristics (Figure 3):

1) Sufficient bandwidth (crossover frequency) for task tracking and disturbance rejection,
2) Adequate stability margins (phase margin > 45 degrees), and
3) An integrator-like response at the crossover frequency.

Use of the crossover model has several advantages including: a) ease of implementation, b) flight task and aircraft characteristics sufficiently define pilot parameters, c) straightforward validation from flight or simulator data, and d) frequency-domain approach easily related to physical system. The primary limitation of the crossover model is that pilot behavior for most flight tasks cannot be accurately described in a fixed, linear, single-input/single-output (SISO) context. However, the display latency problem is well suited to the crossover model. Most instrument tasks are characterized by a control objective to maintain a displayed parameter (i.e. attitude, airspeed, vertical velocity) in a desired position (i.e. level, fixed speed, constant altitude). This results in a relatively simple control loop and describes the pilot's innermost control loop for each input axis. Also, there is less likelihood of "nonlinear" pilot behavior due to external stimuli such as abrupt motion and peripheral visual cues for instrument flight compared to visual flight. Research has shown (Refs. 12,13) that handling qualities ratings are best correlated with the stability characteristics of the inner control loop for the *most difficult control axis*. For the V-22 in helicopter and conversion modes (Ref. 17), the roll axis exhibits the lowest stability margins and will thus be the focus of the analytical study.

Fixed-base piloted simulation was used extensively to evaluate the handling qualities effects of display latency in a controlled environment. Since the reduced visual cue environment of simulators is not an issue for instrument flight, simulation provides a high fidelity platform for handling qualities testing. The display generator of the V-22 simulator at the Boeing Helicopters Flight Simulation Laboratory (Ref. 18) was reconfigured to allow latency to be varied from 70 ms to 400 ms in 33 ms increments. Two flight tasks were simulated in instrument meteorological conditions (IMC) to serve the dual purpose of validating the single-loop crossover model analysis and evaluating latency effects for a high-gain operational task. The first task consisted of single-axis roll attitude tracking where the pilot maneuvered the aircraft to track a commanded bank angle symbol which prescribed moderate rate roll maneuvers. In the second task, the pilot was required to capture and track the final leg of an Instrument Landing System (ILS) approach to a vertical landing at a VTOL pad. Both moderate and high speed approaches were tested with visibility lim-

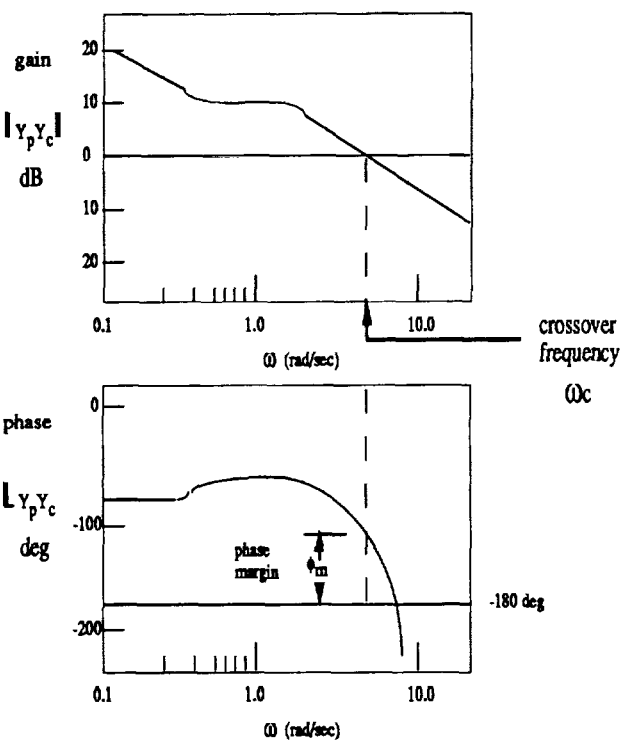

Figure 3. Pilot/aircraft system crossover model

ited to 2500 feet so that the landing pad was not observable until the approach Decision Height (200 feet above ground level) was reached. Moderate levels of turbulence, wind shear, and crosswind were utilized to demand constant pilot control inputs.

Attitude Loop Analysis

Time delay effects on aircraft controllability are best described by the innermost (attitude) control loop. For attitude control, the crossover model relates the pilot control input to the displayed attitude error in the transfer function form:

$$Y_p = K \frac{T_L s + 1}{T_I s + 1} e^{-\tau_p s} \qquad (1)$$

where K is the pilot control gain and T_L, T_I, and τ_p are the pilot lead, lag, and neuromuscular delay time constants, respectively. The neuromuscular delay is defined as "the time required for the pilot to comprehend display information, determine, and physically apply the appropriate input." Included in the pilot delay parameter are fixed and variable components. The fixed component, estimated at around 60 ms - 100 ms (Ref. 12), is due to inherent physiological delays, and the adjustable component is due to the pilot display scan rate and concentration level. The adjustable delay component can be reduced, where necessary, at the expense of increased cognitive workload. The control gain and lead compensation parameters are optimized by the pilot in the same hierarchial fashion as a control system designer tunes a servomechanism. That is, the gain is set for stabilility, then compensation is added to meet bandwidth requirements with the parameters subject to energy constraints. For example, during a high frequency target tracking task the pilot will provide a control gain sufficient to minimize the tracking error while maintaining adequate stability margins. If system delays, or aircraft dynamics, do not allow stable, high frequency control, the pilot will be forced to add lead compensation to perform the task. Lead compensation, which may be perceived as "stick pulsing", significantly increases the pilot control workload. On the other hand, if the task is simply to maintain level flight with only moderate disturbances, the pilot will act to minimize workload in the form of lower control gain, no lead compensation, and a comfortable scan rate.

Simply stated, the pilot-aircraft crossover frequency may be estimated based on control theory given knowledge of the aircraft stability characteristics, system delays, and task control bandwidth requirements. In order to accommodate demanding visual tasks (i.e. shipdeck hovering, in-flight refueling), the V-22 digital flight control system provides high bandwidth control throughout its operational envelope. Figure 4 shows the frequency response of the lateral axis for the augmented V-22 (AFCS on, rate command-

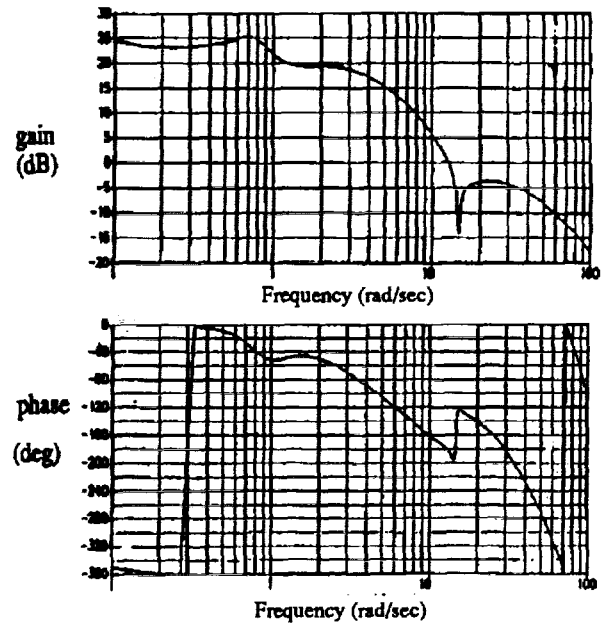

Figure 4. P/δlat (deg/sec/in) frequency response at 120 kts.

attitude hold system) at a 120 knot flight condition. It is seen from the Bode diagram that if the pilot-aircraft-display system contained no time delays, the pilot could maintain integrator response (-20 db/decade gain slope) for control bandwidths up to 6 rad/sec with pure gain compensation and sufficient stability margins. High gain flight tasks, such as precision hover, mandate control bandwidths in the range 1 rad/s < ω_c < 4 rad/s (Refs. 15,16).

The most demanding operational requirements for the V-22 in IMC consist of "flight path tracking tasks" at high speed and low altitude such as terrain following and aggressive approach-to-landings. Flight path tracking may be viewed as an "outer-loop" control function, as shown in Figure 5, where the pilot corrects for low-frequency flight path errors by adjusting commands to the high-frequency attitude control loop. In general, the flight path tracking outer-loop requires a bandwidth one-quarter of the attitude tracking inner loop. Therefore, for limited amounts of delay, the V-22 stability bandwidth (based on phase characteristics) is significantly greater than the required task bandwidth for flight path tracking instrument tasks. This implies that the pilot crossover frequency will be determined by workload factors alone. A general rule-of-thumb in this case (Ref. 16) is that the crossover frequency will equal the maximum of the phase plot such that

$$\omega_c = \omega_{\phi_{max}}.$$

Applying the rule to Figure 4 indicates that for the V-22 lateral axis at 120 knots,

$$\omega_c = 2 \text{ rad/sec.} \qquad (2)$$

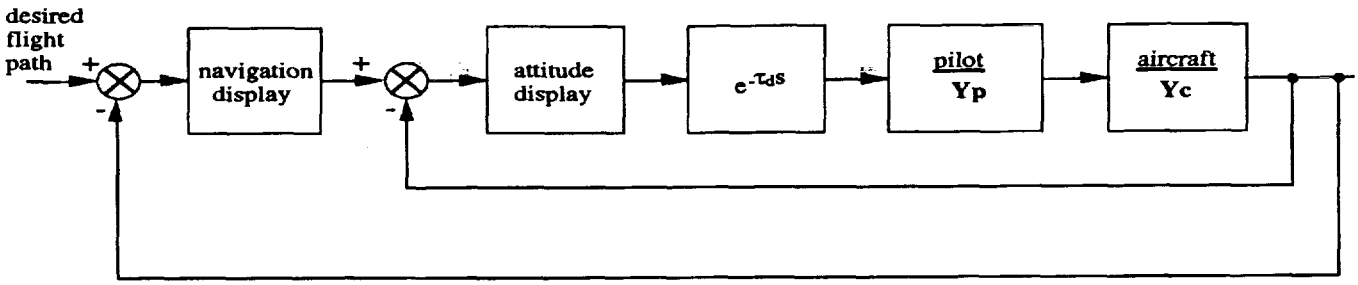

Figure 5. Pilot control structure for flight path tracking

Assuming that the crossover frequency is 2 rad/s for V-22 precision instrument tasks, the crossover model may be used to predict the effects of pilot and display delays. System delays act to linearly reduce the phase of the pilot-aircraft system such that,

$$\Phi = \Phi_o - \omega_c (\tau_p + \tau_d + \tau_c) \qquad (3)$$

where Φ_o is the phase of the aircraft alone and τ_p, τ_d, τ_c are the delay times of the pilot, displays, and control system, respectively. Control system delays for the V-22 have been measured through frequency response testing on the Boeing Helicopters Flight Control System Interface Rig (FCSIR) (Ref. 17) and the data is presented in Table 1. Using the second order system approximation between phase margin and damping ratio, and combining the maximum control system delay of 50 milliseconds with a conservative estimate of the pilot neuromuscular delay of 250 ms (based on simulator time history matches), the system damping ratio is related to the latency such that

$$\xi = \Phi_m \left(\frac{57.3 \text{ deg/rad}}{100 \text{ 1/deg}} \right) \qquad (4)$$
$$= 0.573\,\Phi_{mo} - 0.573\,\omega_c\,(\tau_d + 0.3)$$

where Φ_m is the phase margin of the pilot-aircraft-display system, and Φ_{mo} is the aircraft phase margin (1.92 radians). Figure 6 shows the system damping reduction due to display latency increases between 70 milliseconds and 400 milliseconds. Handling qualities studies (Refs. 17,18) have shown that for phase margins less than 45 degrees, task performance may be limited by overshoot tendencies for abrupt control inputs, and this corresponds to the required aircraft phase margin in the military specifications (Ref. 5). Therefore, it is expected that the pilot will reduce the control gain, or add lead compensation, to continually maintain stability margins over 45 degrees. It is observed from Figure 6 that the pilot is unable to sustain this criterion with pure gain compensation for latencies exceeding 317 milliseconds.

Input	Output	FCSIR delay	SIM delay
longitudinal stick	longitudinal cyclic	50.75 ms	50.0 ms
longitudinal stick	elevator	26.25 ms	50.0 ms
lateral stick	diff. collective pitch	50.75 ms	50.0 ms
lateral stick	flaperon	25.00 ms	50.0 ms
pedals	diff. collective pitch	50.75 ms	50.0 ms
pedals	rudder	34.85 ms	50.0 ms
thrust contrl. lever	collective pitch	50.75 ms	50.0 ms
thrust control lever	engine command (FADEC)	38.75 ms	50.0 ms

Table 1. V-22 control system delays

Piloted Simulation

The V-22 simulator consists of a validated aircraft mathematical model operated real-time on a multi-processor computer with a fixed-base emulation of the V-22 dual-place crew station. Cockpit cues are provided to the pilot through out-the-window scenes produced by an Evans and Sutherland CT-6 computer image generation system, a displacement cyclic controller with a programmable force-feel system, a small-displacement (+/- 2 inches) thrust control lever, and two CRT multi-function displays per pilot station. The simulator has been shown to be a high fidelity representation of the aircraft through time histories and handling qualities evaluations matched to flight test (Ref. 14). Real-time simulation processing is run at a

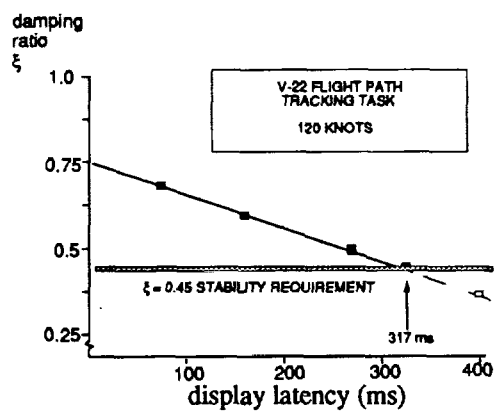

Figure 6. Predicted damping ratio vs. latency

frequency of 20 hertz which yields, on average, a control delay of 50 milliseconds. This falls within 25 ms of the aircraft control delays as shown in Table 1. A high performance Silicon Graphics IRIS-4D/80 CG display generator computer drives the simulator displays interlaced at a frequency of 60 hertz. In order to vary the display latency, a software buffer was inserted in the display generator which held the symbology data in multiples of two display cycles according to an operator selectable index. The inherent display delay, from the mathematical model output until completion of the display generation cycle, was measured at an average of 73 milliseconds. Therefore, the possible display latency test points were 73 ms, 107 ms, 140 ms, etcetera. In order to verify the latency values, measurements were taken prior to each simulation test by sending a discrete signal through the mathematical model and measuring the analog time difference between the model output and display generator optical output.

Attitude tracking task

Display delay effects on the attitude control loop were evaluated with a pilot-in-the-loop through an attitude tracking task simulation. The pilot was asked to track a commanded attitude symbol with the aircraft nose symbol on the displays, as shown in Figure 7, "to the best possible control accuracy." Moderate rate (3 to 5 deg/sec) bank angle captures of 10 degree amplitude were used to drive the command symbol. The commands were interjected in a random manner to prevent "pilot anticipation" from masking the results. Results were obtained with two highly trained V-22 evaluation pilots during a total of 4.6 hours simulation time. The data consisted of both tracking performance and workload measurements which were digitally recorded and statistically processed real-time, combined with qualitative pilot comments. All tests were run at a flight condition of 120 knots airspeed with the nacelles tilted at a 60 degree incidence (where 90 degrees is referenced at helicopter mode). This flight condition was chosen as representative of precision instrument tasks for the V-22.

A straightforward metric, referred to as the 2σ-bound, was used to gauge the attitude tracking accuracy. During each test run, which consisted of bank angle captures in each direction over a one minute test period, the 2σ–bound was calculated by doubling the standard deviation of the bank angle tracking error and adding the mean value. In simple terms, this statistic measures the aircraft dispersion about the commanded attitude. For a normally distributed tracking error, the 2σ–bound represents the absolute value such that the probability of exceeding the bound is approximately 5% at any instant in time.

In a similar manner, a workload metric referred to as the *control workload index* was used to quantify the magnitude of pilot control activity. The control workload index (N_{cw}) was calculated as

$$N_{cw} = \frac{1}{2}\left(\frac{\delta_{rms}}{\delta_{rms\text{-}req}} + \frac{\dot{\delta}_{rms}}{\dot{\delta}_{rms\text{-}req}} \right) \quad (5)$$

where,

δ_{rms} = root-mean-square of lateral stick deflection

$\dot{\delta}_{rms}$ = root-mean-quare of lateral stick rate.

The normalizing parameters represent the minimum required stick activity to track the command as determined from the V-22 autopilot. By combining a measure of stick deflection variance and stick rate variance, the control workload index measures the amount the pilot is forced to move the controls and vary the control frequency. This provides a basis for comparing control activity between test runs.

Figure 8 presents the simulation performance and workload measurements plotted against latency value. The plots indicate the average values from four data runs at each latency value (for each latency test point the pilots were allowed a few training runs prior to data collection). From the workload plot it is clear that the display delay effects can be broken into three regions:

1) $\tau_d < 140$ ms: a no-effect region where the latency does not significantly impact attitude control,
2) 140 ms $< \tau_d <$ 307 ms: a degraded attitude control region where the pilot works harder to maintain desired attitude, and
3) $\tau_d > 307$ ms: a gain reduction region where the pilot is forced to ease control aggressiveness to assure adequate system stability.

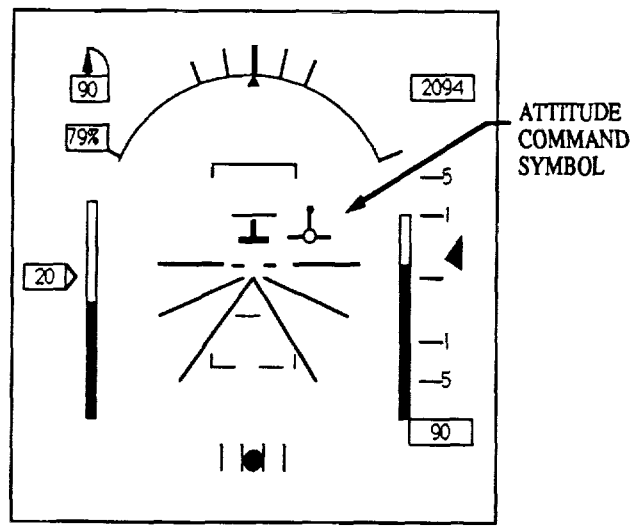

Figure 7. Attitude tracking display

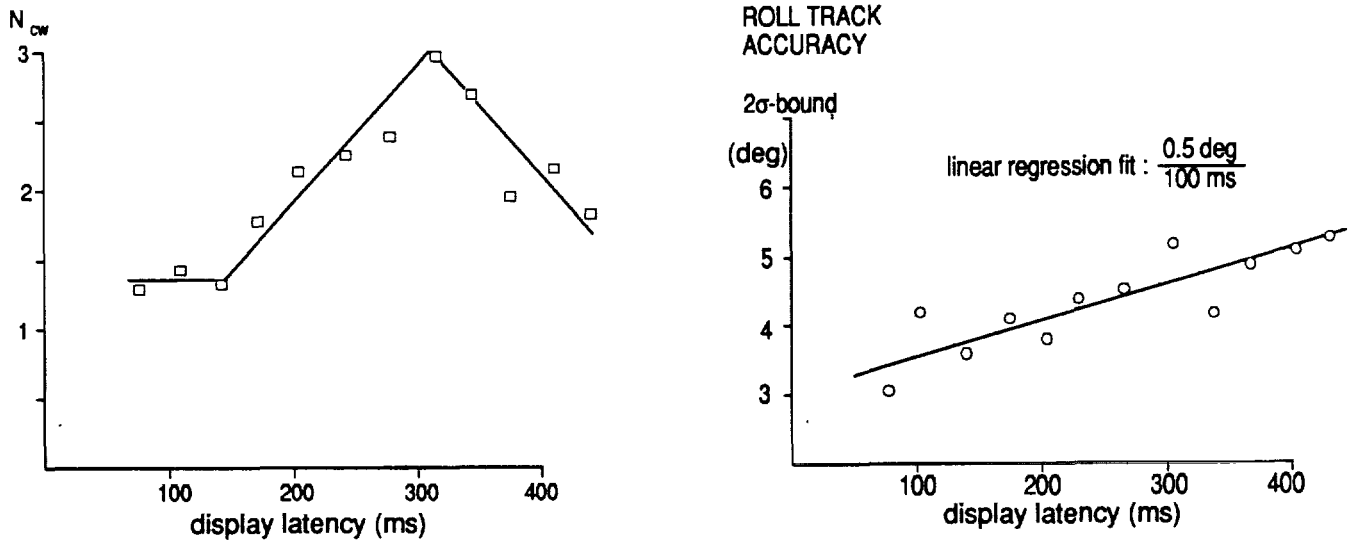

Figure 8. Attitude tracking simulation results

The pilot gain reduction breakpoint corresponds well with the pilot model analysis which predicted that the 45 degree phase margin criterion would not be met for latencies exceeding 317 ms. Sample time histories for one run in each of the three regions are shown in Figure 9 and illustrate the loss of control damping with latency variations. Superimposed on the plots are time histories from the second order analytical model. At the higher latency values, the control oscillations of the simulator data were more prominent than the model predicted and are most likely due to nonlinearities in the pilot compensation.

Accordingly, the tracking performance plot indicates that as the delay increases and stability margins are reduced, tracking difficulty increases. A linear regression fit to the tracking performance data shows a bank angle control degradation of one-half degree for every 100 ms of added latency. Pilot comments indicated that lead compensation was applied for latencies over 240 ms in an attempt to alleviate tendencies to overshoot the commanded attitude.

ILS approach task

The final leg of a low-visibility ILS precision approach was simulated with six different latency values between 70 ms and 400 ms. The task was initialized with an inital offset from the desired glidepath at approximately 2000 feet above ground level, challenging the pilot to acquire the ILS glidepath and track to a decision height of 200 feet. The approaches were flown at airspeeds of 85 knots and 120 knots, and the task was terminated at decision height. Turbulence, wind shear, and crosswind models were implemented in the simulation to induce disturbances. The turbulence consisted of a body-fixed sampling Dryden model with the intensity and scale length parameters set according to "moderate" specifications of MIL-F-8785C (Ref. 4). In addition, a 20 knot wind at a 45 degree azimuth from the approach course was implemented with a "moderate" wind shear profile added per MIL-F-8785C.

The flight displays consisted of the vertical situation display

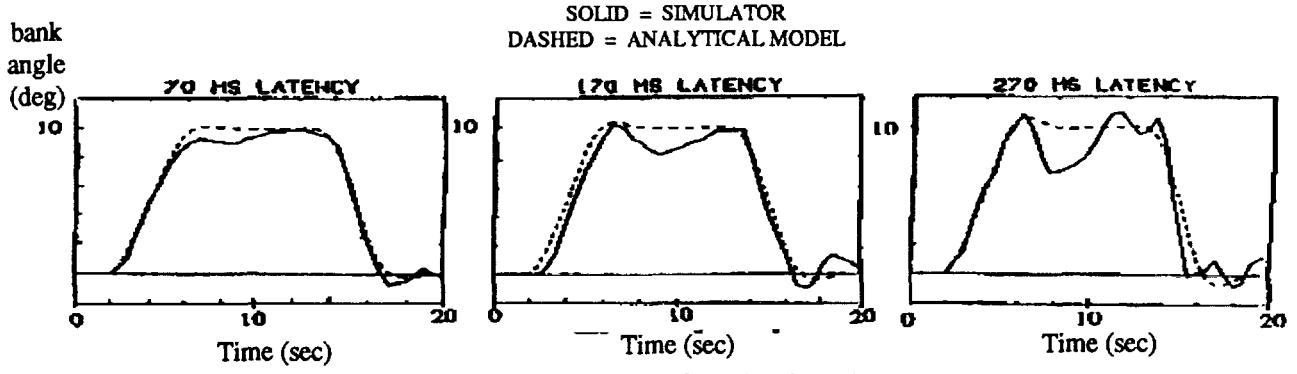

Figure 9. Attitude tracking time histories

of Figure 7 plus a horizontal situation display with the ILS localizer and glideslope deviation indicators as shown in Figure 10. In order to receive pilot handling qualities ratings per the Cooper-Harper scale, performance constraints were issued to the pilot. For "desired" performance the pilot was required to track the glidepath within the following constraints for more than 80% of the approach and be within constraints at decision height: localizer deviation ($\Delta\gamma$) less than +/- 1 degree, glideslope deviation ($\Delta\Gamma$) less than +/- 0.25 degree, and airspeed deviation (ΔV) less than +/- 5 knots. Yaw axis control was not required since the V-22 control system automatically provides trun coordination and heading hold features. "Adequate" performance constraints were set at double the desired constraints. It should be noted that in the V-22 the pilot is required to scan an azimuth of approximately 10 degrees to monitor all necessary ILS flight information on the two displays.

Data was recorded for five highly trained evaluation pilots during simulation spanning over 34 hours. In addition to 126 data runs, more than 200 runs were performed for pilot training purposes. Simulation studies (Refs. 18,19) have shown that biases may result in handling qualities evaluations between alternate configurations due to *cross-training* effects. This means that variations in pilot rating between different configurations may depend on the order in which they are tested. To subdue cross-training effects, latency values were tested in varying sequence and several runs were alloted for training at each test point. For each data run, performance and workload metrics were calculated real-time. The performance metric consisted of the normalized 2σ-bound averaged between the three tracking variables such that

$$N_{perf} = \frac{1}{3}\left(\frac{\Delta V_{2\sigma}}{5\text{ kts}} + \frac{\Delta\gamma_{2\sigma}}{1\text{ deg}} + \frac{\Delta\Gamma_{2\sigma}}{0.25\text{ deg}}\right) \quad (6)$$

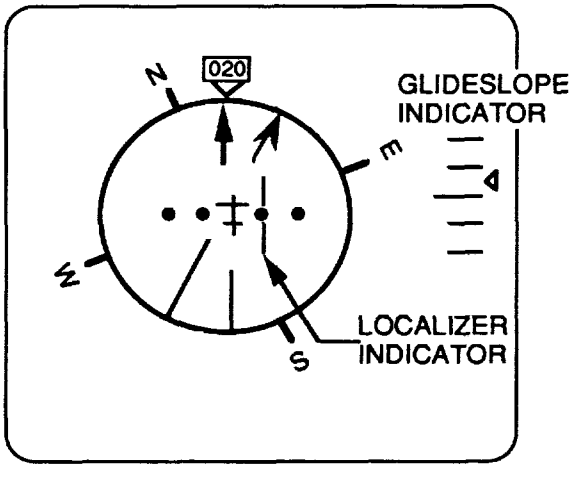

Figure 10. ILS displays

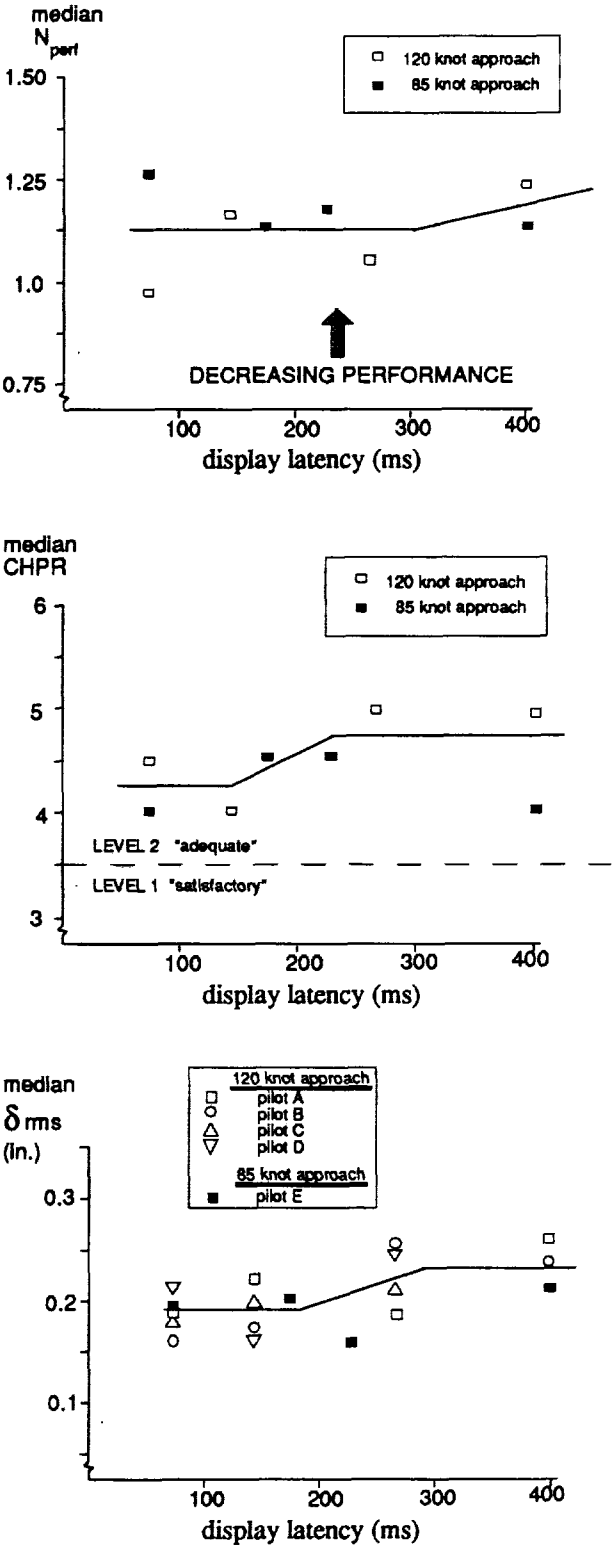

Figure 11. ILS task simulation results

The desired constraint parameters were used as the normalizing factors such that performance indices less than unity indicate that the aircraft was maintained within desired constraints for at least 95% of the run. The root-mean-square of the control deflections from trim were used as the workload metric.

Figure 11 displays the median performance indices, Cooper-Harper pilot ratings (CHPR), and lateral stick workload metric (lateral inputs were by far the most active) versus display latency. Median values, as opposed to averages, were used to eliminate the weighting effect of poor performance data during a few runs when the pilot aborted the approach and prepared for a go-around. The performance plot indicates that, although variations in performance resulted, there were no discernable trends relating tracking performance to latency for test points between 70 ms and 300 ms, and only a slight reduction in tracking accuracy at 400 ms, as indicated by the relatively flat distribution of the median values. This was predicted by the attitude loop analysis which showed that delays up to 300 ms are not sufficient to degrade the performance of the low bandwidth flight path tracking outer loop. However, the pilot ratings and workload plots do indicate a control degradation for latencies between 140 ms and 300 ms which is consistent with the "degraded attitude control region" identified in the attitude tracking task. Comments indicated that the pilots were perceptually unaware of latency changes between configurations, but that they acquired different control techniques due to "slight changes in aircraft response characteristics." The altered control techniques appeared as lateral stick pulsing during small heading changes at the 270 ms and 400 ms latencies which was not required at 70 ms. This was caused by the loss of attitude control damping and resulted in a one-half Cooper-Harper point degradation between 140 and 270 milliseconds.

Corrective Measures

At 211 ms of display latency, the loss of attitude control damping produced a slight degradation (less than 1/2 CHPR point) in V-22 instrument approach handling qualities relative to a minimum latency of 70 ms. Furthermore, the handling qualities ratings for all latency values tested were consistently a level 2 classification which implies that "deficiencies warrant improvement." Pilot comments indicated that workload issues mandated the level 2 ratings, and the workload was increased by a difficulty in assimilating all the necessary flight information and determining the proper input to zero the ILS tracking deviations. It is therefore desirable to 1) suppress the latency-induced attitude damping reduction and 2) reformat the presentation of ILS information to the pilot. These two objectives may be accomplished by the addition of *flight director* displays.

Flight director

Flight director displays provide the pilot with pursuit-type cues to steer the aircraft along a commanded path. The command path is based on the flight path tracking error, such as an ILS deviation, and all control cues are presented to the pilot in a centralized location. Figure 12 shows the V-22 flight director symbology on the vertical situation display which consists of power, roll, and pitch cues. The dynamics of the flight director cues are selected to augment the stability characteristics of the closed-loop pilot-aircraft-display system to provide sufficient tracking performance with only pure gain pilot compensation. Several methodologies to optimize flight director designs are presented in the literature (Refs. 20,21) but do not address the issue of display latency.

Flight director designs can be used to suppress latency effects to only a limited degree. From Equation 3 it is observed that for pure gain pilot compensation and a fixed amount of display latency, the phase margin of the pilot-aircraft-display system can be increased by 1) reducing the pilot delay, 2) adding phase lead at the crossover frequency through display compensation, or 3) decreasing the crossover frequency. The ability of a flight director to reduce the pilot delay is easily recognizable. By using centralized cues, the display scan time will be reduced. And any time spent from pilot cognition (deduction of control input from flight path deviation indicators) will lessen since the flight director processor assumes the responsibility of calculating control inputs from the tracking error. However, benefits gained from adding phase lead or reducing the crossover frequency are mostly counter-productive since a reduction in the crossover frequency, through smaller gains or low-pass filtering, precludes any effect of phase lead. Similarly, adding phase lead in the displays will increase the crossover frequency unless the display gains are reduced. Therefore, with inherent display latency, the potential performance

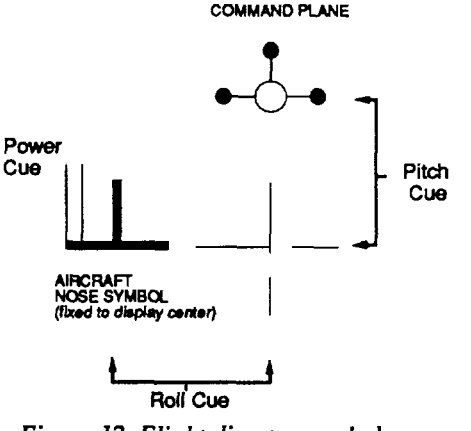

Figure 12. Flight director symbology

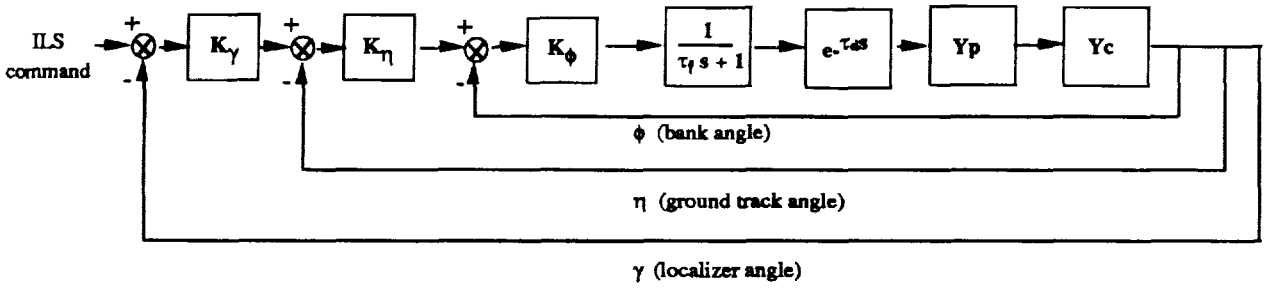

Figure 13. Flight director lateral cue processing

gains of a flight director are limited, but the flight director can improve instrument handling qualities by reducing the pilot delay and forcing the pilot to control at an "acceptable" crossover frequency.

For an ILS task the V-22 flight director lateral cue (Ref. 22) is driven by the localizer deviation shaped by washed-out bank angle and ground track angle feedback signals as shown in Figure 13. The gain ratios between the three feedback loops determine the relationship between the localizer deviation and the commanded lateral stick input. By increasing the gain on the bank angle loop, lead compensation is introduced which increases the crossover frequency of the pilot's attitude control loop. By adjusting the flight director gains, the inner loop crossover frequency can be selected to tradeoff the adverse effects of display latency with the benefits of increased tracking bandwidth. For the V-22 ILS task, the tradeoff can be biased toward subdueing the latency effects since sufficient tracking performance was obtained with raw-data displays.

ILS re-simulated

The ILS approach task was repeated with the V-22 flight director active at a fixed latency value of 300 ms. Initially, several training runs were used to tune the flight director parameters at the fixed latency value. Since the baseline design did not account for large latency values, underdamped control responses were initally observed, and the flight director parameters were adjusted to reduce the system bandwidth. Figure 14 presents the median tracking performance and pilot rating results for six flight director runs with two evaluation pilots superimposed on the results from the raw-data runs. Level 1 pilot ratings, with tracking performance well within performance constraints, were consistently obtained with the flight director active. Furthermore, it was observed that consistency between runs was greatly improved, described by one pilot as "an improvement in damping and predictability with milder control inputs commanded from the flight director." Apparantly, by forcing the pilot to control at a lower crossover frequency, the flight director improved the overall response characteristics of the pilot-aircraft-display system.

Conclusions

It is the general belief in the rotorcraft handling qualities community that display latency degrades an aircraft's instrument flight capabilities, but, up to this point, no requirements on allowable latency have been produced. This paper investigates the handling qualities effects of varying levels of display latency analytically through the pilot crossover

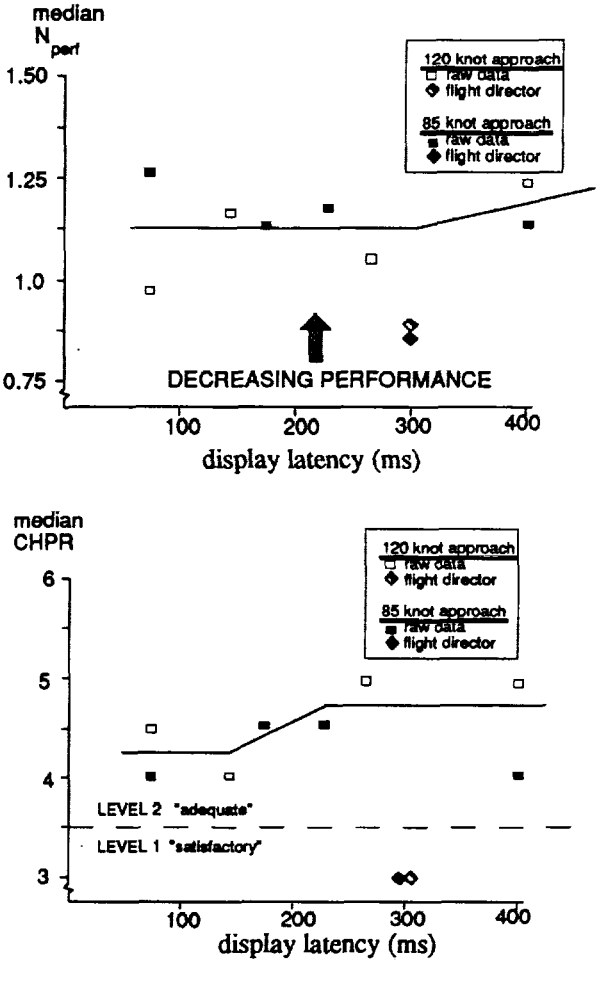

Figure 14. Flight director simulation results

model and experimentally through piloted simulation of the V-22 Tiltrotor aircraft. Latency effects on the lateral axis of the V-22 Tiltrotor aircraft were predicted through a second order crossover model of the attitude control loop, and the effects were tested through piloted simulation of both an attitude tracking task and a precision ILS approach. The results showed that the pilot workload involved in the ILS approach was directly related to a linear reduction in the damping ratio of the roll attitude control loop from 0.60 to 0.45 as latency was increased from 140 ms to 310 ms. The control damping reduction was predicted by the model based on the V-22 frequency response characteristics, control system lags, and instrument task bandwidth requirements. The display latency did not degrade flight path tracking performance, due to its low bandwidth, until the attitude loop phase margins fell below 45 degrees and the pilot was forced to reduce control gain. For an ILS approach task, the results indicated that pilot workload was increased as the attitude control damping was reduced, resulting in pilot rating degradations of 1/2 CHPR between 140 ms and 270 ms of latency.

Flight director displays were then investigated as a means to suppress the increased workload effects of display latency. The results showed that flight director displays improve instrument flight handling qualities by reducing pilot cognitive workload, and they can suppress latency effects by regulating pilot control at an "optimal" crossover frequency.

Based on the results of this study the following conclusions were reached:

1) The handling qualities effects of display latency, in terms of pilot workload and task performance, are driven by the stability characteristics of the pilot's inner control loop.

2) In general, an aircraft's robstness to display latency is proportional to its stability margins, and inversely proportional to the bandwidth required for its instrument flight mission tasks. Based on the test results which showed that damping ratios below 0.6 induce difficulties in precise attitude control, and damping ratios below 0.45 degrade precise flight path control, proposed latency guidelines are presented in Figure 15. The guidelines specify maximum delay values such that the latency will not significantly degrade handling qualities. The maximum delay values (display latency plus control system delay) are shown as a function of the aircraft phase margin and crossover frequency.

3) The benefits of flight director lead compensation ("display quickening" - which increases control bandwidth), often used for high bandwidth instrument tasks, is limited by display latency since latency-induced reductions in control damping are linearly proportional to the crossover frequency.

4) The V-22 exhibited "satisfactory" (level 1) handling qualities for latency values less than 300 ms based on its instrument task requirements and the use of flight director displays. Without flight director displays, an aggressive ILS approach task with moderate disturbances yielded level 2 handling qualities even at a minimum display latency of 70 milliseconds.

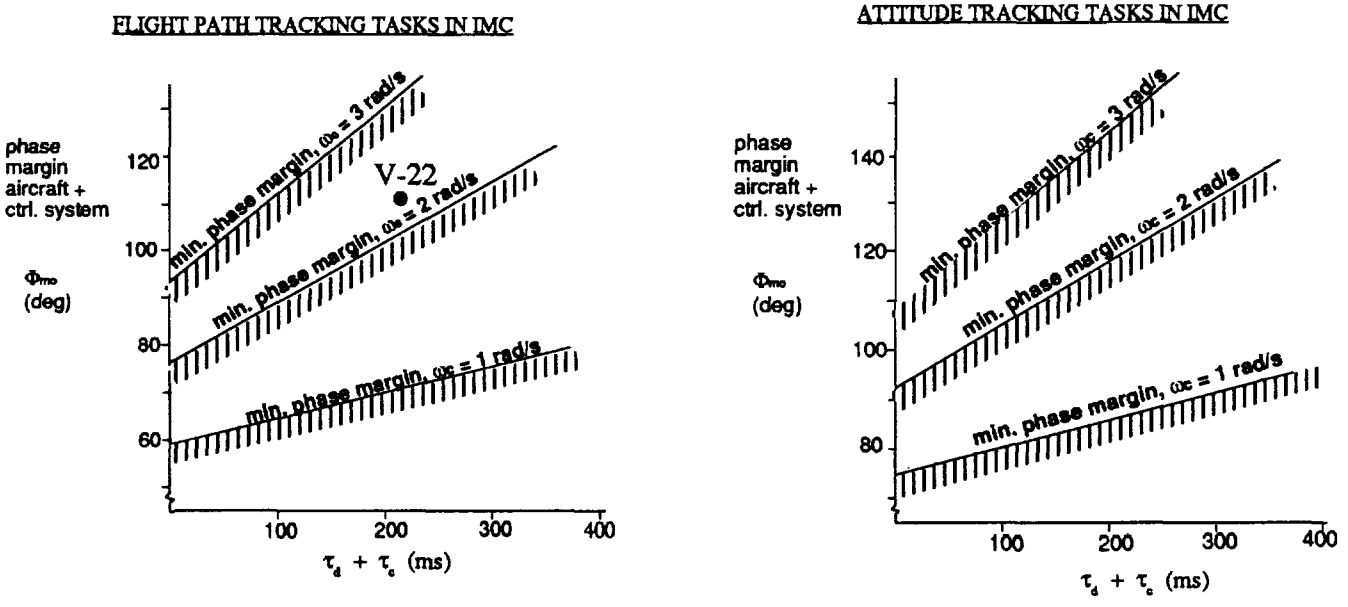

Figure 15. Proposed latency guidelines

References

1. Smith, R.E., and Sarrafian, S.K., "Effect of Time Delay on Flying Qualities: an Update", AIAA Journal of Guidance, Control, and Dynamics, Sept.-Oct., 1986.

2. Hoh, R.H., and Ashkenas, I.L., "Development of VTOL Flying Qualities Criteria for Low Speed and Hover," Systems Technology, Inc., Hawthorne, CA, TR-1116-1, Dec. 1979.

3. Cooper, F.R., Harris, W.T., and Sharkey, V.J., "The Effect of Delay in the Presentation of Visual Information on Pilot Performance," NAVTRAEQIPCEN IH-250, Orlando, FL, Naval Training Equipment Center, 1975.

4. Military Specification: "Flying Qualities of Piloted Airplanes," MIL-F-8785C, 5 Nov. 1980.

5. Military Specification: "Flight Control Systems - Design, Installation, and Test of Piloted Aircraft, General Specification for," MIL-F-9490D, 6 June 1975.

6. Ricard, G.E. , and Puig, J.A., "Delay of Visual Feedback in Aircraft Simulators," NAVTRAIEQUIPCEN TN-56, Orlando, FL, Naval Training Equipment Center, 1976.

7. Bailey, R.E., Knotts, L.E., Horoweitz, S.J., and Malone, H.L., "Effect of Time Delay on Manual Flight Control and Flying Qualities During In-Flight and Ground-Based Simulation," Proceedings of the AIAA Flight Simulation Technologies Conference, 1987.

8. Cooper, G.E., and Harper, R.P., "The Use of Pilot Rating in the Evaluation of Aircraft Handling Qualities," NASA TN D-5153, April 1969.

9. Hess, R.A., "Feedback Control Models," Handbook of Human Factors, edited by G. Salvendy, Wiley, New York, 1987, pp. 663-676.

10. Kleinman, D.L., Baron, S., and Levison, W.H., "An Optimal Control Model of Human Response, Parts I,II," Automatica, Vol. 6, 1970, pp. 357-373.

11. Hess, R.A., "A Theory for Aircraft Handling Qualities Based Upon a Structural Pilot Model, "AIAA Journal of Guidance, Control, and Dynamics, Vol. 12, No. 6, 1989, pp. 792-797.

12. McRuer, D.T., and Jex, H.R., "A Review of Quasilinear Pilot Models," Transactions of Human Factors in Electronics, Vol. HFE-8, No. 3, Sept. 1967, pp. 231-249.

13. McRuer, D.T., and Krendel, E.S., "Mathematical Models of Human Pilot Behavior," AGARDograph No. 188, Jan. 1974.

14. Dabundo, C., White, J., and Joglekar, M., "Flying Qualities Evaluation of the V-22 Tiltrotor," presented at the 47th Annual Forum of the AHS, May 1991.

15. Heffley, R.K., and Bourne, S.N., "Helicopter Handling Requirements Based on Analysis of Flight Maneuvers," presented at the 41st Annual Forum of the AHS, May 1985.

16. Tischler, M.B., Fletcher, J.W., Morris, P.M., and Tucker, G.E., "Flying Qualities Analysis and Flight Evaluation of a Highly Augmented Combat Rotorcraft," AIAA Journal of Guidance, Control, and Dynamics, Vol. 14, No.5, 1991, pp. 954-963.

17. Robinson, C., Dabundo, C., and White, J., "Hardware-in-the-Loop Testing of the V-22 Flight Control System Using Piloted Simulation," presented at the AIAA Flight Simulation Technologies Conference, Aug. 14-16, 1989, Boston, MA.

18. Riccio, G.E., Cress, J.D., and Johnson, W.V., "The Effects of Simulator Delays on the Acquisition of Flight Control Skills: Control of Heading and Altitude," Proceedings of the Human Factors Society - 31st Annual Meeting, 1987.

19. Ricard, G.L., Norman, D.A., and Collyer, S.C., "Compensation for Flight Simulator CGI System Delays," Proceedings of the 9th NTEC/Industry Conference, 1976.

20. Garg, S., and Schmidt, D.K., "Cooperative Synthesis of Control and Display Augmentation," AIAA Journal of Guidance, Navigation, and Control, Vol.12, No. 1, 1989, pp. 54-61.

21. Weir, D.H., Klein, R.H., and McRuer, D.T., "Principles for the Design of Advanced Flight Director Systems Based on the Theory of Manual Control Displays," NASA CR-1748, March 1971.

22. Kilmer, R., "Design Analysis Report for the V-22 Guidance and Flight Director Sybsystem", submitted to Boeing Military Airplane Company by IBM Federal Systems Division - Owego, NY, June 1987.

EFFECTS OF SIMULATOR MOTION AND VISUAL CHARACTERISTICS ON ROTORCRAFT HANDLING QUALITIES EVALUATIONS

David G. Mitchell
Systems Technology, Inc.
Hawthorne, CA 90250

Daniel C. Hart
Aeroflightdynamics Directorate
U.S. Army Aviation and Troop Command
Ames Research Center
Moffett Field, CA 94035

ABSTRACT

The pilot's perceptions of aircraft handling qualities are influenced by a combination of the aircraft dynamics, the task, and the environment under which the evaluation is performed. When the evaluation is performed in a ground-based simulator, the characteristics of the simulation facility also come into play. Two studies were conducted on NASA Ames Research Center's Vertical Motion Simulator to determine the effects of simulator characteristics on perceived handling qualities. Most evaluations were conducted with a baseline set of rotorcraft dynamics, using a simple transfer-function model of an uncoupled helicopter, under different conditions of visual time delays and motion command washout filters. Differences in pilot opinion were found as the visual and motion parameters were changed, reflecting a change in the pilots' perceptions of handling qualities, rather than changes in the aircraft model itself. The results indicate a need for tailoring the motion washout dynamics to suit the task. Visual-delay data are inconclusive but suggest that it may be better to allow some time delay in the visual path to minimize the mismatch between visual and motion, rather than eliminate the visual delay entirely through lead compensation.

INTRODUCTION

Ground-based simulation is an important tool in the assessment of handling qualities for both research and development. The strengths and limitations of simulation are well known and recognized in the handling qualities community. What is not as well documented, however, is the relative impact of various elements in the simulator itself on perceived handling qualities. For example, past studies (Ref. 1) have demonstrated that rate-augmented vehicles that exhibit good handling qualities in flight are much more difficult to control on ground-based simulators (e.g., Fig. 1).

Besides the obvious issues of simulation fidelity and flight/simulation transference (Ref. 2), there are other fundamental issues in simulation design that also impact the use of ground-based simulators for handling qualities research. All of these issues, such as inherent time delays and their compensation (Refs. 3 and 4), simulator sickness (Ref. 5), and the requirements on motion (Refs. 6, 7, 8, and 9), have been investigated in great detail in terms of their impact on human operator response dynamics and assessments of fidelity. Few studies, however, have explored the specific impact of these issues on handling qualities evaluations.

A two-part study was conducted on NASA Ames Research Center's Vertical Motion Simulator (VMS) to evaluate the effects of simulator characteristics on handling qualities. The primary focus of the two piloted simulations was on piloted assessment of the variations — i.e., Cooper-Harper Handling Qualities Ratings (HQRs; Ref. 11) and comments. Evaluations were conducted with several sets of vehicle dynamics, using a simple transfer-function model of an uncoupled helicopter, with Level 1 handling qualities based on Aeronautical Design Standard ADS-33C (Ref. 10). Changes in the simulation environment were made by adding time delays in the visual path and in the overall simulated response, and by changing motion system washout filter dynamics. The pilots were instructed to evaluate each variation in the environment as if it were a new aircraft; therefore, it may be assumed that differences in HQRs were due entirely to the pilots' perceptions of handling qualities, rather than to changes in the aircraft model itself.

The first simulation (Simval I) was an exploratory study of the tradeoffs in the motion and visual elements. A more systematic evaluation of these tradeoffs was conducted

Presented at the American Helicopter Society Conference on Piloting Vertical Flight Aircraft, San Francisco, CA, Jan. 1993.

in the second simulation (Simval II). This paper reports on the overall results and conclusions from both simulations.

FACILITY

Hardware

The VMS is a six-degree-of-freedom simulator with a cab mounted on a Rotorcraft Simulator Motion Generator (RSMG) gimbal (Fig. 2). Translational motion is limited by hard stops at ± 30 ft vertically, ± 20 ft laterally, and ± 4 ft longitudinally. Software trips in the motion system further limited the available range of linear travel from center position to ± 25 ft vertically, ± 18 ft laterally, and ± 2.5 ft longitudinally. The cockpit was representative of a single-pilot helicopter configuration. In the first simulation three horizon-level monitors provided the out-the-window view; the rightmost window included a view of the ground environment near the helicopter as well. In this simulation visual display generation was via a Singer-Link Digital Image Generator (DIG I). In the second simulation, a four-window cab was used with three forward-looking windows and one downward-looking chin window. For this simulation a three-channel CT5A CGI system was used; since only three channels were available for four windows, the leftmost forward display was not used. In both simulations the cockpit head-down instruments were conventional, with the addition of a digital altimeter. No head-up displays were used. Cockpit controls were also conventional, with a center-mounted cyclic, left-hand collective, and pedals. The command signals were displacement for all controllers.

Motion Description

The general structure of the VMS cockpit stick-to-motion response is shown in Figure 3. Control inputs made by the pilot result in aircraft model accelerations, rates, and positions. The motion washout software generates motion commands in the simulator axes reference frame from the aircraft model accelerations. In the motion washout software, first the aircraft accelerations are transformed into simulator axes. Then, each of the six simulator axes accelerations is sent through a washout filter. The washout filter is a linear, constant-coefficient, second-order high-pass filter of the following form:

$$\frac{\text{simulated acceleration}}{\text{model acceleration}} = \frac{K_{wo}\, s^2}{[s^2 + 2\zeta_{wo}\omega_{wo}s + \omega_{wo}^2]}$$

Different sets of motion washout filter gains, damping ratios, and break frequencies were devised and evaluated in the two experiments. These washout filter sets were designed to transmit different forms of acceleration information to the pilots. Details of the washout filter sets are given in the Description of the Experiment section of this paper.

The washed-out commands are sent to the lead compensation software, where phase lead is added to the motion drive commands to compensate for some of the lags in the motion drive hardware. No modifications were made to the lead compensation software.

The motion drive has dynamics associated with the hardware in each axis. The response of the combination of lead compensation and motion hardware constitutes the motion response. If the effective delay of the motion response is large enough, then it will be noticeable to the pilot. The effective delays in each axis of the motion response (feedforward and motion drive hardware dynamics combined) are presented in the next section.

The roll-lateral washout configuration will be explained in more detail as an example of the interplay between the motion system axes. Without compensation, the rotational accelerations of the Vertical Motion Simulator induce a spurious linear acceleration since the rotational axis of the simulator is below the pilot's seat. This effect is compensated by subtracting the induced angular acceleration term from the linear motion command. The correction factor is washed out through the same filter as the rotation that generated the lateral acceleration; it is multiplied by the rotational washout filter and divided by the lateral washout filter before the command is sent to the lateral washout.

In a constant lateral acceleration maneuver, the aircraft linear accelerations are eventually washed-out by the high-pass filter. In this case, the cab is tilted to change the relative orientation of the gravity vector to the cab, simulating the sustained lateral accelerations that are not achievable with finite linear motion. Similar coordination is achieved between the pitch and surge axes.

Time Delays

Delays in the Motion System. During the simulation, the dynamics of the motion response to motion command were quantified by measuring these responses to a cockpit controller input. The inputs, generated by a random number generator, were shaped with a Gaussian distribution over the frequency range of 0.1 to 30 rad/sec and added directly to the cockpit control signal of interest. The result of the Gaussian distribution was that the higher frequency inputs were of smaller magnitude, and no saturation occurred in

the motion hardware. The resulting motion command and motion response to these inputs were recorded, CIFER (Ref. 12) was used to generate frequency responses and the generalized transfer-function fitting program NAVFIT (Ref. 13) was used to identify an effective time delay of the combined feedforward and motion drive dynamics.

The effective delays in each axis of the motion response are presented in Table 1. Recall that the sway and roll axes were necessary to provide rotation about the aircraft center: although the motion washout software generates the correct commands for an aircraft rotation, the sway and roll motion responses were asynchronous (a time difference of 30 to 40 msec existed between the responses). It was found that this difference between the sway and roll axes in the lateral response was noticeable in many of the evaluated configurations.

Delays in the Visual System. The sources of time delay in the stick-to-visual response with the CT5A CGI (used in Simval II) are shown in Figure 4 and identified delays are listed in Table 2. It takes 10 msec for the cockpit stick position signal to get to the host computer, and the host computer updates the model states based upon the stick position and the aircraft rates. The computation time of the model acceleration is T_{cycle}, but the model positions and rates are forward integrated by one cycle so that they are concurrent with the accelerations of the next time frame (when they will be used in the calculation of the next frame's accelerations). The forward integrated positions and rates are sent to the Image Generator (IG); there is a 2 msec transport delay in this transmission. The IG takes 3 internal CGI cycles to display the visual scene, consisting of one cycle for the object manager, one cycle for the geometric processor and the polygon manager, and one cycle for the display processor. The IG then requires 1/2 cycle to prepare the data and 1/4 cycle to draw half of the model response to the stick on the screen. The IG computer cycles at 60 Hz (16.67 msec), resulting in an IG transport delay of 62.5 msec (3.75 cycles). The overall delay of stick-to-visual response is 74.5 msec - T_{comp}, with a standard deviation of 3 msec. The overall stick-to-visual response was varied by adjusting the visual lead compensation, T_{comp} (Ref. 16).

While Simval II used the Evans and Sutherland CT5A CGI as described above, Simval I used a Singer-Link Digital Image Generator (DIG I). There is a small difference in the update rates between these systems resulting in an IG transport delay for the DIG I of 83.3 msec compared to 62.5 msec for the CT5A. The visual variations for the experiments are outlined in the Description of the Experiment section of this paper.

Interactions of Motion and Visual Delays

The dynamics of the tested configurations were characterized in terms of their pitch and roll attitude Bandwidth parameters (Ref. 10), i.e., Bandwidth frequency ω_{BW} and phase delay τ_p. Each of the time-delay sources in the VMS facility outlined above can have a very large effect on the values of these parameters. For ground-based simulation, it is necessary to properly account for three separate response elements, the math model, the visual scene, and the motion system, since the pilot is, to some extent, aware of and operating in response to all of them. In the case of the VMS it is possible for the Bandwidths of these three responses to be quite different for the same configuration. An example of this is shown in Figures 5 and 6.

The frequency-response plot of Figure 5 illustrates the dramatic effects of cascading the individual elements of the simulation onto the ideal math model. The model (shown as solid lines in Figure 5) is the transfer function for an ideal rate-augmented helicopter model with roll damping L_p = -4 rad/sec; p/δ represents the model response to measured control actuator position (i.e., after the A/D and D/D interfaces in Figure 4). As expected, in the absence of time delays this ideal system exhibits a Bandwidth frequency of $\omega_{BW_\phi} = -L_p = 4$ rad/sec, and phase delay $\tau_{p_\phi} = 0$.

The response of the compensated visual display (p_v/δ_{as}) in Figure 5 introduces the 10-msec control position measurement delay for the A/D and D/D (Fig. 4). This delay has no effect on magnitude and only a slight effect on phase angle. Bandwidth frequency is reduced from 4 rad/sec to 3.7 rad/sec, and phase delay increased from zero to 0.01 sec. Turning the visual compensation filter off also does not affect the magnitude curve, but there is further phase lag, with $\omega_{BW_\phi} = 2.4$ rad/sec and $\tau_{p_\phi} = 0.07$ sec.

The motion response of the VMS cab (p_m/δ_{as} in Figure 5) is quite different from the model and visual responses. The combination of washout filter and effective motion time delay contributes low-frequency phase lead and high-frequency phase lag. The low-frequency lead introduced by the motion washout serves to increase the Bandwidth frequency to $\omega_{BW_\phi} = 3.9$ rad/sec, but the motion-system lags increase phase delay to $\tau_{p_\phi} = 0.05$ sec.

Figure 5 serves to illustrate several important points. First, it shows the beneficial effect of the visual compensation filter, since the phase curve of the compensated response is closer to ideal to higher frequencies. Second, the phase distortions and gain reductions introduced by the washout are evident, as the responses of the ideal

math model and cab roll motion are in phase for effectively only a single frequency. Third, Figure 5 shows that in terms of visual-motion synchronization, the uncompensated visual response actually corresponds most closely to the motion response, especially at high frequencies.

The significance of the Bandwidth differences of Figure 5 is illustrated by Figure 6. This figure shows the eight possible measurements of the Bandwidth parameters to describe the responses of Figure 5. The parameters for the ideal model are the most straightforward, especially for position-referenced values of measured roll rate to measured control actuator deflection (p/δ). The visual-display Bandwidth, with compensation on, is referenced back to cockpit control position inputs, ϕ_v/δ_{as}, and hence reflects 10 msec of time delay; with compensation removed the Bandwidth decreases and phase delay increases. The phase delays for motion are about equal to those for the uncompensated visual display, but with increased Bandwidths due to the washouts. Addition of stick force feel dynamics, typical of those used in the two simulations, greatly increases τ_{p_ϕ} and decreases ω_{BW_ϕ} when these values are referenced to force.

DESCRIPTION OF THE EXPERIMENT

Effects of variations in the three major elements of the simulation — the motion and visual systems and math model — were evaluated. Specific variations and the philosophies behind them were as follows.

Motion System

Even though the VMS provides a large range of linear and angular travels, there are still very tight limitations on maneuvering space that necessitate lowered response gains and high washout break frequencies (Ref. 9). The selection of such gains and washouts is a compromise between the desire for realism in motion and the realities of space limitations. Potential criteria for determining washout limits (both gain and break frequency) for linear washouts have been developed (Refs. 14 and 15). These limits generally indicate that for minimum loss of motion fidelity, washout filter break frequencies should be no greater than about 0.3 rad/sec (for a second-order filter with damping ratio of 0.7). Ideally, the values selected reflect the requirements of the particular maneuvers to be flown and the expectations of the pilot.

As Figure 5 indicates, the combined effects of motion washouts and delays results in only a narrow range of frequencies for which the phase angle of the motion response accurately reflects the model response. In addition, the reduced gain in the motion system results in an attenuation in the motion response at all frequencies. This difference between the ideal system and the achieved motion is complex and is a function of frequency. Nonetheless, it is useful to find a simpler metric for judging the fidelity of the motion response. In terms of phase differences, it has been suggested (e.g., Refs. 14 and 17) that a phase distortion of less than about 30 deg corresponds to high motion fidelity. Therefore, in this paper we will consider two parameters to define the model-to-motion differences as shown in Figure 5: 1) the washout gain, or reduction in motion response as compared to full-scale motion; and 2) the frequency range for which the phase distortion (difference in phase angles between model and motion) is 30 deg or less. While these parameters are not as explicit as complete transfer-function plots, they will greatly facilitate the comparison of the different motion washout values evaluated in these simulations.

Baseline Washout Dynamics

The Baseline set of motion washouts used in this experiment was developed for the Simval I simulation by NASA engineers. This Baseline set followed the NASA philosophy of transmitting initial accelerations at the expense of motion/visual/model phasing (Ref. 9). Scaling of the initial response was on the order of 30% to 60% of full scale, with washout break frequencies of 0.2 to 0.7 rad/sec.

The frequency range where the phase distortion of the motion washout filter is less than 30 degrees is plotted versus washout filter gain for the Baseline washouts in Figure 7. The plots were produced by concatenating the identified motion system dynamics with the washout filters. The high-frequency end of this low-phase-distortion range is almost entirely a function of motion dynamics and delays and cannot be increased. At the low-frequency end, the low-distortion range can be improved by reducing washout break frequency. The gain of the washout filter must also be reduced, however; otherwise, saturation of the motion drive occurs in position, rate, or acceleration.

The Baseline motion system represents a typical design for helicopter low-speed handling qualities studies on the VMS. The washout filters were selected conservatively, so that the motion system did not saturate during any of the Simval I tasks. The motion washout filters can be designed independently for each task of a simulation, to take full advantage of the capabilities of the motion system; the gain and phase distortion would be dependent on the task aggressiveness in each of the motion system axes and on the simulator capabilities. This is not always done, however, as

it is a difficult and sometimes time consuming process to perform. The more that is understood about the effects of the motion washout filters on pilot performance and pilot opinion, the better they can be adjusted for handling qualities evaluations.

Modified Washout Dynamics (Simval I). An alternate set of Modified washouts was developed during the Simval I simulation. This set was designed with the specific goal of reducing the phase distortions in motion around the frequencies of pilot closed-loop control (and maximum acceleration sensitivity), 0.5-5 rad/sec. Since this requires a washout break frequency below that of the Baseline washouts, the decreased phase distortion comes at the expense of further attenuated amplitude of motion. The phase-distortion ranges for the Modified washouts are compared with the Baseline set in Figure 7. These washouts emphasized the large-amplitude axes of response of the VMS — pitch, roll, and heave.

Systematic Variations in Washout Dynamics (Simval II). In the second experiment, only two tasks were evaluated, a precision hover and a sidestep, so that the development of the motion washout filters could be studied in greater detail. The precision hover allows for a substantial increase in gains (including one-to-one), due to the relatively small aircraft positions and attitudes generated during the task. Schroeder et al. performed a VMS simulation that successfully utilized gains of one in all six motion system axes (Ref. 18). The Simval II hover task actually consisted of a 6-8 knot translation to hover and a precision hover, and consequently the gains had to be reduced below one-to-one.

The sidestep task is an aggressive task that primarily emphasizes the roll and sway axes, secondarily emphasizing the heave axis. The design of the motion washout filters for the sidestep task addressed the interplay between roll, sway, and heave axes of the simulator; the yaw, surge, and pitch washout filters were not varied among the sidestep configurations.

Three motion washout configurations were designed for the sidestep to investigate the gain attenuation versus phase distortion trade-off. Phase-distortion plots are shown in Figure 8. The washout break frequency for the roll, sway, and heave axes was systematically varied and the gains adjusted so that the pilots did not run into any motion limits while flying the task. The yaw, surge, and pitch washout filters were similar to the Baseline washouts. The roll and sway washouts cannot be designed independently because of the interdependence of the rotational and linear axes of the VMS, mentioned previously. It can be seen in Figure 8 that while variation was made in the roll gain, sway gain remained 0.3 or less for all three Sidestep washout configurations.

Visual System Delays

While the visual compensation filter (Ref. 3) used on simulations on the VMS effectively removes the overall visual delays, it increases the mismatch in phasing between the visual and motion responses: the motion system experiences unavoidable delays due to anti-aliasing filters, mass, inertia, and control limiting effects that cannot be removed entirely. Past studies of time delays in either the visual or motion path, resulting in a visual/motion mismatch, show mixed results. For example, a simulation on the NASA Ames Six-Degree-of-Freedom (S.01) simulator (Ref. 19) suggests that based upon measures of pilot performance, 1) it is better to have the motion response lag visual rather than to intentionally lag the visual just to reduce mismatch, and 2) in terms of pilot high-frequency lead generation, motion compensation is more important than visual compensation. A study of a vertical pursuit tracking task on the NASA Langley Visual/Motion Simulator (Ref. 20) investigated visual/motion mismatch by introducing delays in the visual system. Pilot performance measures of total tracking error and control activity were taken. Slight improvements in performance were found for the case where total visual delay most closely matched the effective delays of the motion system (approximately 97 ms).

Effects of removing the visual delay compensation were evaluated in both simulations. The total visual time delays for both Simval I and II are listed in Table 3.

MATH MODEL

The mathematical model for the rotorcraft was a generic, uncoupled stability-derivative model that has been used for several simulations at Ames (Ref. 21). Changes in dynamic response characteristics are effected by altering the basic aircraft stability and control derivatives; for example, the transfer function for pitch attitude response to longitudinal cyclic for the rate-augmented aircraft was represented by

$$\frac{\theta}{\delta_e} = \frac{M_{\delta_e}}{s^2 - M_q s}$$

TASKS

Simval I

Seven tasks were evaluated in the preliminary simulation. These tasks consisted of precision and aggressive maneuvers at hover and in low-speed flight as defined by Section 4 of ADS-33C (Ref. 10). The precision tasks were a one-minute hover, vertical translation (a surrogate for landing), and pirouette. The aggressive tasks were a bob-up/bob-down, dash/quickstop, and sidestep. A 40-kt lateral slalom task, which has no counterpart in ADS-33C, was included to emphasize a combination of precision and aggressiveness. Desired and adequate performance limits were defined for each task, based as much as possible on ADS-33C limits but adapted when necessary to the specific visual environment of the DIG. Details of the tasks are given in Refs. 22 and 23.

Simval II

The second simulation focused on two tasks, a precision hover and a sidestep. The visual scenes for these tasks were tailored to adhere to recently revised task definitions, and performance limits were consistent with those for the revised tasks.

Because of the emphasis on these two tasks for the systematic study of motion and visual variations, an analysis of the pilots' control activity was performed to verify that the tasks were sufficiently demanding (i.e., exhibited sufficient task bandwidth) to elicit the desired effects in pilot performance and opinion. Figure 9 shows frequency-response plots of an example power-spectral density (PSD) for lateral cyclic activity. These plots show that 70 percent of all input power (corresponding to the pilot's "cut-off frequency," Ref. 24) occurs at 2.4 rad/sec for the hover (Fig. 9a) and 1.1 rad/sec for the sidestep (Fig. 9b). As expected, these frequencies confirm that the hover is a higher-bandwidth task than the sidestep. They also suggest that the pilots will be more sensitive to visual delay variations in the hover (where visual delay introduces high-frequency phase rolloff), and more sensitive to motion delay variations in the sidestep (where the cut-off frequency is very near the low edge of phase distortion as introduced by the washouts, Fig. 8).

PILOTS

Seven pilots, with varying backgrounds and levels of experience, participated in the first simulation. Two pilots had relatively little previous experience in ground-based simulation, and none in the VMS. In Simval II four pilots participated, including two with over 300 hours in the VMS. The other two pilots in Simval II had no previous VMS exposure. Two of the experienced pilots flew in both simulations.

RESULTS

Effects of Task

Motion and task effects were evaluated in Simval I. The seven tasks were evaluated fixed-base and with the Baseline and Modified motion washouts. Figure 10 is a summary plot of the HQRs for the tasks. Average HQRs are depicted by solid symbols that are connected by a solid line for clarity. Each data symbol represents a single rating. There is evidence in Figure 10 of rating differences across the tasks. Generally, the easiest tasks (in terms of best average HQR) were the hover, bobup/bobdown, and dash/quickstop. Since no turbulence, gusts, or winds were simulated, the one-minute precision hover was low-workload as long as the helicopter was reasonably well stabilized before starting the formal maneuver. Pilot comments indicated that the bobup/bobdown was relatively easy because of the decoupled helicopter model, making this almost entirely a single-axis task, while the dash/quickstop was rated well because of the ample forward field-of-view for initiating the maneuver. By contrast, the vertical translation, pirouette, and slalom maneuvers were inherently multi-axis and thus tended to receive higher HQRs, while pilot comments indicate that the poor ratings for the sidestep maneuver are due primarily to the lack of a sideward field-of-view for adequately determining the endpoints of the maneuver.

Effects of Motion Washout Filters

The effects of motion washout filters were investigated in both of the experiments. Simval I was an exploratory study that looked at a variety of tasks for only two motion washout configurations (Fig. 10). Simval II concentrated on understanding washout filter design for two tasks; results for the sidestep task are discussed below.

Simval I. Figure 10 illustrates the importance of motion on pilot opinion: all tasks were Level 2 fixed-base, and average HQRs improved by 1/2 to 2 rating points when motion was introduced. Comparison of the HQRs for the Baseline and Modified washouts in Figure 10 shows a general trend for slightly improved ratings with the Modified set. There are exceptions, however, as the average ratings for the bobup/bobdown and sidestep tasks are slightly worse. The slight improvements for the other tasks suggest that the pilots were either aware of the more consistent motions

provided by the Modified set, or, conversely, that the rapid washouts of the Baseline set mitigated the beneficial effect of the increased initial accelerations provided by the higher gains. It is likely that the answer is a blend of the two, supported by the degraded ratings for the bobup/bobdown (where initial accelerations are an important cue to the pilot) and the sidestep (where the Modified motion washouts overdrove the vertical axis in response to lateral commands).

By their nature, aggressive tasks involve rapid changes of state — i.e., large initial accelerations — compared to the precision tasks. Since the Baseline motion gains transmitted more of the initial acceleration onset cues, it might be expected that this set would be preferred for the aggressive tasks, and this is the case for the bobup/bobdown and sidestep (Figs. 10e and 10g). By contrast, the Modified motion set was designed to provide more accurate phasing of the motion and visual responses, at the cost of reduced gain. Therefore, it is reasonable to expect this system to be preferred for those tasks that involve continuous closed-loop operations, such as the precision tasks, and this is the case as well (Figs. 10a, 10b, and 10c).

Several important factors must be considered in comparing the HQRs for the two motion gain/washout sets: first, the Modified set as developed for Simval I was intended to be exploratory in nature, and it did not take advantage of all axes (see Fig. 7); and second, since the basic aircraft was good to begin with, small changes in average HQR may or may not be significant. Simval I indicated that further testing was required, in a more systematic fashion, as was conducted on Simval II.

Simval II. The pilot ratings for the Sidestep task with the medium bandwidth helicopter dynamics are shown versus the motion washout configuration in Figure 11. As was found in Simval I, there is a substantial improvement in the pilot ratings for all the motion configurations over the fixed-base case (1/2 to 1-1/2 rating points). Of the three configurations developed for the sidestep task, the lowest phase distortion (and lowest gain) configuration, SS1, was preferred by all the pilots, as indicated by the pilot ratings in Figure 11 and the pilot comments outlined below.

Pilot A thought that both the Baseline and the low-phase-distortion, low-gain combination (SS1) were good configurations (HQR = 3). He perceived stronger motion cues in the medium phase distortion case (SS2), "Motion seemed a little strong ... you got bounced around pretty good... [I] could feel the difference between this and the previous configuration (SS1) just by the high level of motion... and that lowered the rating" (HQR = 4.5). The highest gain washouts brought the impression that the simulator was always moving around, and "[the motion response] felt like it was not in sync with the control movements or visual movements" (HQR = 4).

Pilot B was the most sensitive of the pilots to the strong movements of the simulator, preferring the low phase distortion (SS1) configuration over all the others. For example, with SS2, the medium gain configuration, "Every time I made any kind of aggressive rollout, then I was feeling a negative motion cue during the roll out to the hover" (HQR = 5). But for SS1, "I was getting good positive cues, but the negative cues that I felt before weren't present... In most of these cases where you do have a problem, you excite the problem by being more aggressive... [this] system lets me be more aggressive and then attain a tighter performance... this is good" (HQR = 3). It is possible that the pilots were feeling the effect of the mis-coordination between the roll and sway responses, in which the sway motion response to a lateral stick input was delayed by 30-40 msec behind the roll response (Table 1). The roll-axis bandwidth in this case was 4.3 rad/sec, and the effect of the asynchronous responses would have been magnified as the gain of the motion system was increased. These results suggest that the higher gain, higher phase distortion cases are not as robust to changes in pilot technique.

Pilot C's comments indicate that out of the three sidestep washout configurations, SS1 was the best because it was less jerky, easier to control, and required slightly less workload than the others. SS1 was also the only configuration where he noted that the motion system felt like it was in synchronization with what he was seeing and doing.

The low-phase-distortion, low-gain configuration SS1 offered two advantages over the others. The first advantage was that the phase distortion between the visual and motion responses was minimized for the roll, sway, and heave axes, as described earlier (Fig. 8). This was apparent in the pilot comments where they noted that the responses were more in synch and the helicopter was easier to control. The second advantage of the low-phase-distortion, low-gain configuration was that any motion miscues, such as those mentioned above, were diminished by lowering the gains. The pilots were very attuned to these motion miscues, as indicated in their comments.

For this study, the 30 degree phase distortion has been used as a reference by which the motion configurations were compared. The lower end of the low-distortion frequency range of the SS2 configuration is well above 1 rad/sec in all axes, while the SS1 configuration range spans down to almost 0.7 rad/sec (Fig. 8). The PSD of the Sidestep in Figure 9b indicates that the pilot cut-off frequency (the

frequency below which 70 percent of control power is contained) was 1.1 rad/sec. So 70 percent of the control power is below the lower bound of the 30-deg phase-distortion frequency range for SS2, while more control power is contained above the lower bound of the SS1 configuration. It is therefore suggested that pilots preferred the SS1 washout configuration because they perceived lower phase distortion in the frequency range in which they were operating, i.e., below 1.1 rad/sec, even though it had lower motion gains.

Effects of Visual Delays

The baseline visual transport delay of the Vertical Motion Simulator is 63 - 83 msec, depending on the Computer Image Generator, as seen in Table 2. The effect of adding lead to the visual command to compensate for visual delay was investigated in both studies. When comparing the results from the two studies, the baseline visual delay case refers to the uncompensated visual delay for both studies, while the compensated visual case refers to the added visual lead compensation.

Sensitivity to Visual Delays. Before reviewing the pilot ratings for the visual-delay evaluations on the moving-base simulation, it is important to establish that the pilots were sensitive to the relatively small change in visual delay resulting from the addition of the lead compensation. To answer this question, we look at the results of fixed-base evaluations, where the pilots' only cue is visual. Five pilots flew back-to-back evaluations of the compensation on and off for the hover task, fixed base during the two simulations. The HQRs, shown in Figure 12, indicate that there was a preference for the compensated visual case, as expected.

Effects of visual delays were further investigated by calculating the improvement in phase margin at the pilot cut-off frequency (Fig. 9b) for the compensated visual case. For the Simval II high-bandwidth helicopter response, the phase margin at 2.4 rad/sec was increased from 67 to 75 degrees when the visual delay was compensated. This eight-degree increase in the phase margin alone is not enough to explain the improvement in ratings from Level 2 to Level 1. The bandwidth of the stick-to-visual response was greatly improved with the compensated case, from 4.8 rad/sec to 8.9 rad/sec in roll, and from 2.8 rad/sec to 4.0 rad/sec in pitch. So it is assumed that the reduction in pure time delay in the open-loop aircraft response was the major factor in the improved ratings.

Simval I. For this simulation, the baseline visual delay was 83.3 msec (Table 2), and the compensated visual delay was effectively zero; the model and motion responses remain unchanged. These evaluations were made with the Baseline motion washout filters (Fig. 7).

The pilot ratings for two precision tasks from the Simval I simulation, chosen because the same pilots flew both visual delay configurations and because the tasks are similar to the Simval II hover, are shown in Figures 13a and 13b. The results indicate that Pilots Mc and M preferred the visual-delay case over the no-delay case, while the third pilot (Pilot S) was just the opposite.

Comments by pilot S for the baseline visual delay case deal almost exclusively with motion problems, rather than visual. It is not clear whether the adverse comments about motion for these evaluations reflect the change in the motion/visual relationship, or simply Pilot S's dissatisfaction with the motion response.

Pilots M and Mc had relatively little previous exposure to ground based simulation. These pilots generally preferred the baseline visual delay case over the compensated case because of the reduction in the crispness of the response. For pilot M, "The [baseline visual configuration] was the least as far as the crispness goes... This last one is more in tune... It was easier to control." Pilot Mc commented that "[The baseline visual case]..., overall, felt more like flying than any of the others... The motion and visual cues seemed to be the most consistent between my inputs and the aircraft response."

Simval II. For this simulation, the baseline visual delay was 62.5 msec, and the compensated visual delay was effectively zero; the motion dynamics were held constant for the visual delay evaluations, but they were slightly different than the Simval I motion dynamics. These dynamics were used because the Simval II pilots felt that this set of washouts was slightly better than the baseline dynamics. However, the one pilot who flew both simulations gave almost identical ratings for these precision tasks, so the motion system difference does not appear to have affected results.

Pilot ratings for the hover task evaluations of the baseline and compensated visual are shown in Figures 13c and 13d. Two helicopter response configurations are represented here. The pilots rated the high-bandwidth helicopter better than the medium-bandwidth helicopter, but the trends are the same for both sets of dynamics. Pilots B and A, experienced VMS pilots, preferred the compensated visual in both cases, and the novice VMS pilot (Pilot C) preferred the baseline visual.

Pilot B, a veteran VMS pilot who flew both simulations (Pilot S in Simval I), noticed the motion system more with the baseline visual: "The visual system seems to be still correlating with the inputs, however, the motion seems to be giving me some uncorrelated response... causing me to make inputs to correct something that I don't think was wrong." It appears that Pilot B was compelled to pay more attention to the motion response with the baseline visual: "Maintaining the precision took all of my capacity... [the response] was slow when I gave my first input to move over to the hover position." With the compensated visual, however, "I didn't detect any time delay in the visual displays or the motion...the cues seemed very succinct and very in tune with the inputs... I could be as aggressive as I felt necessary... actually it did have spare capacity in this case...even though I was pretty active on the control.... The initial inputs to arrest the translation seem just a hair abrupt... It is a very sharp response, but very predictable."

Pilot B's ratings and comments are backed up by his performance, shown for the hover task with the medium bandwidth helicopter model in Figure 14a. The lateral and longitudinal errors are appreciably reduced with the compensated visual configuration.

Pilot C, the novice VMS pilot, agreed with the novice pilots in Simval I (Pilots M and Mc), but directly contradicted the other two pilots from Simval II. For the baseline case, "The motion I was picking up and the visual scene seemed to be in sync... minimal pilot compensation" (HQR = 3), whereas for the compensated case, "Motion/display cues were worse than the [baseline case]... the visual and motion felt out of phase.... [I] was working a lot harder to control height, and there was a lot of cyclic activity.... [Compared to the baseline, this system was] less sensitive. I thought you changed the control system, it seemed like lower bandwidth" (HQR = 4).

An example of Pilot C's performance for the hover task with the medium bandwidth helicopter model is shown in Figure 14b. Here we can see that, in contrast to Pilot B's performance, Pilot C's longitudinal and lateral errors were reduced in the baseline visual case.

General Conclusions on Visual Delay Effects. While the pilots do not agree on the visual configurations, the results are consistent between the two simulations. A summary of the HQRs from the two simulations is presented in Figure 15.

Based on the HQRs, the experienced VMS pilots prefer the visual compensated. It was seen that these pilots actually get better performance with this configuration, because they use primarily the visual cues for the task. Even Pilot B mentioned, however, that the response for the compensated visual was abrupt; it was this same abruptness that made some of the other pilots dislike the compensated case. It seems that the pilots with experience on the VMS have the ability to filter out the adverse motion responses.

The novice pilots prefer the baseline visual, where the motion and visual responses were most closely matched (Fig. 15). There is some rationale for this, since the high-frequency response of the visual scene with the baseline visual exhibits approximately 63-83 msec of total delay (depending on the CIG), and the VMS cab motion in pitch and roll exhibits 70-90 msec of effective delay due to high-frequency lags. Thus the baseline visual and motion responses are nearly in phase, whereas the implementation of the visual filter actually increases the discordance between visual and motion responses (Fig. 5).

It appears that the most practical solution is to match the motion and visual responses as closely as possible in the frequency range that is being exercised, even though some pilots may be able to achieve better performance with the visual response leading the motion response. With the visual and motion responses in phase, the simulation represents a more realistic helicopter response.

CONCLUSIONS

This two-phase study of the interactions of simulator motion, visual, and response dynamics on rotorcraft handling qualities has both confirmed previous observations and revealed areas deserving of more indepth study. Unlike most previous motion/visual simulation studies, the primary goal of this study was the measurement of these interactions on perceived handling qualities, rather than on objective performance measures.

Motion was necessary to obtain satisfactory handling qualities: none of the tasks received Level 1 average HQRs fixed-base. Improvements in HQRs when motion was added were generally 1/2 to 2 rating points.

Based on average HQRs, motion washouts with low break frequency and low response gain are slightly better than correspondingly high-gain, but high-break-frequency, washouts for the low-speed tasks evaluated. This may be a function of task aggressiveness.

The data suggests that the best handling qualities occur with the lowest motion/model phase distortion, even though this occurs at the cost of a reduction in the motion gain. The results of the motion washout configurations may have

been mitigated by anomalies encountered in the motion system.

Pilots with little or no experience in the VMS or other ground-based simulators expect the visual and motion responses to be synchronized, and they are sensitive to changes in the phasing between the motion and visual responses. As a result, they prefer the situation where the visual response, although delayed, best matches the motion response. On the other hand, experienced VMS pilots were able to improve their performance with the visual delays compensated, apparently because they were able to filter out the mismatched motion responses and use the visual response as their primary cue.

The best solution to problems with visual/motion/model mismatches would be to improve the delays in the motion response, but this has proven to be difficult due to hardware limitations. The most practical solution may be to match the motion and visual responses as closely as possible in the frequency range that is being exercised, even though some pilots may be able to achieve better performance with the visual response leading the motion response. With the visual and motion responses in phase, the simulation represents a more realistic helicopter response.

ACKNOWLEDGEMENTS

The authors wish to thank the pilots, Messrs. Monroe Dearing, Rickey Simmons, and George Tucker of NASA, Freddie Mills, Gerald McVaney, and Tom Reynolds of the U.S. Army, Ron Gerdes of SYRE, Kevin Emerson of the RAF (on assignment with the U.S. Army), and Roger Hoh of Hoh Aeronautics for their efforts in this simulation. Appreciation is also extended to the SYRE simulation personnel and NASA engineers, especially Messrs. Richard E. McFarland and Richard Bray.

REFERENCES

1. Mitchell, D. G., Hoh, R. H., and Morgan, J. M., "Flight Investigation of Helicopter Low-Speed Response Requirements," J. Guidance, Control, and Dynamics, Vol. 12, No. 5, Sept.-Oct. 1989, pp. 623-630.

2. Ferguson, S. W., Clement, W. F., Cleveland, W. B., and Key, D. L., "Assessment of Simulation Fidelity Using Measurements of Piloting Technique in Flight," AHS Paper No. A-84-40-08-4000, May 1984.

3. McFarland, R. E., Transport Delay Compensation for Computer-Generated Imagery Systems, NASA TM 100084, Jan. 1988.

4. Jewell, W. F., Clement, W. F., and Hogue, J. R., "Frequency Response Identification of a Computer-Generated Image Visual Simulator With and Without a Delay Compensation Scheme," AIAA Flight Simulation Technologies Conference, Monterey, CA, Aug. 1987, pp. 71-76.

5. McCauley, M. E., ed., Research Issues in Simulator Sickness: Proceedings of a Workshop, National Academy Press, Washington, DC, 1984.

6. Stapleford, R. L., Peters, R. A., and Alex, F. R., Experiments and a Model for Pilot Dynamics With Visual and Motion Inputs, NASA CR-1325, May 1969.

7. Jex, H. R., Magdaleno, R. E., and Junker, A. M., "Roll Tracking Effects of G-Vector Tilt and Various Types of Motion Washout," Fourteenth Annual Conference on Manual Control, NASA CP-2060, Nov. 1978, pp. 463-502.

8. Jex, H. R., Jewell, W. F., Magdaleno, R. E., and Junker, A. M., "Effects of Various Lateral-Beam-Motion Washouts on Pilot Tracking and Opinion in the 'LAMAR' Simulator," 15th Annual Conference on Manual Control, AFFDL-TR-79-3134, Nov. 1979, pp. 244-266.

9. Bray, R. S., Visual and Motion Cueing in Helicopter Simulation, NASA TM 86818, Sept. 1985.

10. Handling Qualities Requirements for Military Rotorcraft, U.S. Army AVSCOM Aeronautical Design Standard, ADS-33C, Aug. 1989.

11. Cooper, G. E., and Harper, R. P., Jr., The Use of Pilot Ratings in the Evaluation of Aircraft Handling Qualities, NASA TN D-5153, Apr. 1969.

12. Tischler, M. B., and Cauffman, M. G., "Frequency Response Method for Rotorcraft System Identification: Flight Applications to the BO-105 Coupled Rotor/Fuselage Dynamics," J. American Helicopter Society, Vol. 37, No. 3, pp. 3-17, July 1992.

13. Hodgkinson, J., LaManna, W. J., and Heyde, J. L., "Handling Qualities of Aircraft With Stability and Control Augmentation Systems — A Fundamental Approach," Aeron. Journal, Vol. 80, No. 782, Feb. 1976, pp. 75-81.

14. Sinacori, J. B., The Determination of Some Requirements for a Helicopter Flight Research Simulation Facility, NASA CR 152066, Sept. 1977.

15. Jex, H. R., Magdaleno, R. E., and Jewell, W. F., Effects on Target Tracking of Motion Simulator Drive-Logic Filters, AFAMRL-TR-80-134, Oct. 1981.

16. McFarland, R. E., and Bunnell, J. W., "Analyzing Time Delays in a Flight Simulation Environment," AIAA-90-3174, presented at the AIAA Flight Simulation Technologies Conference, Dayton, OH, Sept. 1990.

17. Sinacori, J. B., Stapleford, R. L., Jewell, W. F., and Lehman, J. M., Researcher's Guide to the NASA Ames Flight Simulator for Advanced Aircraft, NASA CR-2875, Aug. 1977.

18. Schroeder, J. A., Watson, D. C., Tischler, M. B., and Eshow, M. M., "Identification and Simulation Evaluation of an AH-64 Helicopter Hover Math Model," AIAA-91-2877, presented at the AIAA Atmospheric Flight Mechanics Conference, New Orleans, LA, Aug. 1991.

19. Shirachi, D. K., and Shirley, R. S., The Effect of a Visual/Motion Display Mismatch in a Single Axis Compensatory Tracking Task,NASA CR2921, Oct. 1977.

20. Miller, G. K., Jr., and Riley, D. R., The Effect of Visual-Motion Time Delays on Pilot Performance in a Simulated Pursuit Tracking Task, NASA TN D-8364, Mar. 1977.

21. Blanken, C. L., Hart, D. C., and Hoh, R. H., "Helicopter Control Response Types for Hover and Low-Speed Near-Earth Tasks in Degraded Visual Conditions," American Helicopter 47th Annual Forum Proceedings, May 1991, pp. 169-193.

22. Mitchell, D. G., Hoh, R. H., Atencio, A., Jr., and Key, D. L., Ground-Based Simulation Evaluation of the Effects of Time Delays and Motion on Rotorcraft Handling Qualities, US Army AVSCOM TR-91-A-010, Jan. 1992.

23. Mitchell, D. G., Hoh, R. H., Atencio, A., Jr., and Key, D. L., "The Use of Ground Based Simulation for Handling Qualities Research: A New Assessment," Piloted Simulation Effectiveness, AGARD-CP-513, Feb. 1992, pp. 23-1 — 23-14.

24. Pausder, H.-J., and Blanken, C. L., "Investigation of the Effects of Bandwidth and Time Delay on Helicopter Roll-Axis Handling Qualities," Paper No. 80, presented at the 18th Annual European Rotorcraft Forum, Avignon, France, Sept. 1992.

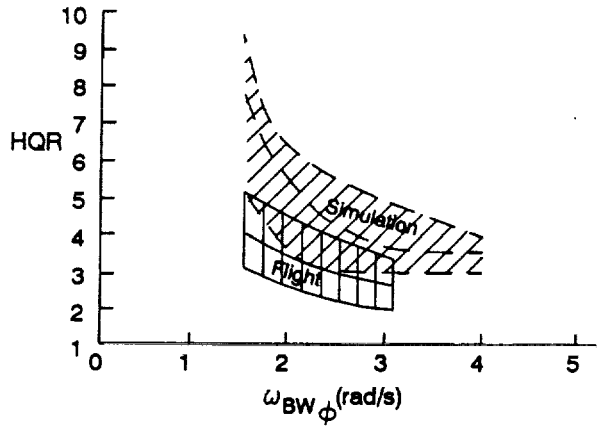

a) ACAH Response-Type

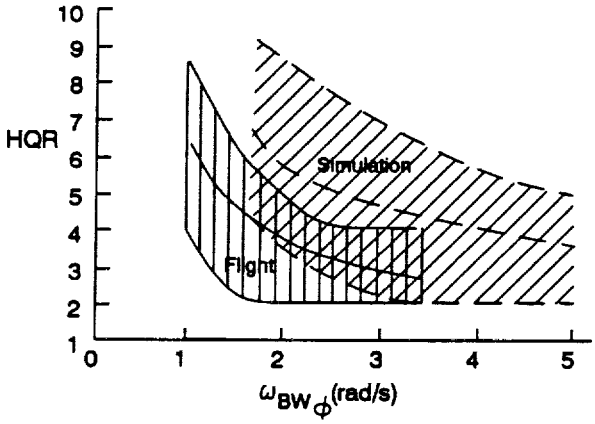

b) RCAH Response-Type

Figure 1. Comparison of HQR Ranges from Simulation and Flight for Landing (Ref. 1)

VMS NOMINAL OPERATIONAL MOTION LIMITS			
AXIS	DISPL	VELOCITY	ACCEL
VERTICAL	±30	16	24
LATERAL	±20	8	16
LONGITUDINAL	±4	4	10
ROLL	±18	40	115
PITCH	±18	40	115
YAW	±24	46	115
ALL NUMBERS, UNITS ft, deg, sec			

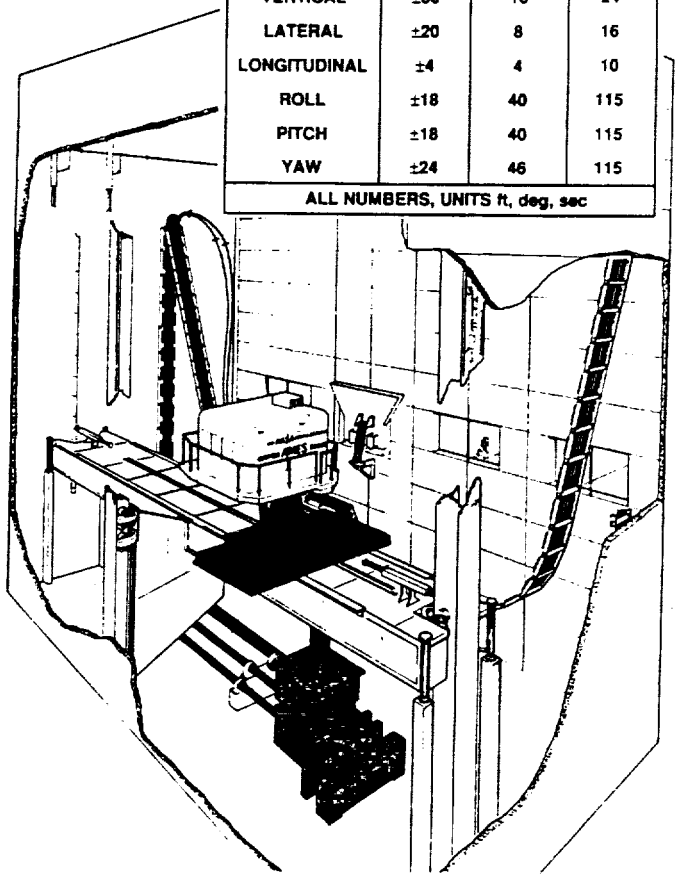

Figure 2. Vertical Motion Simulator

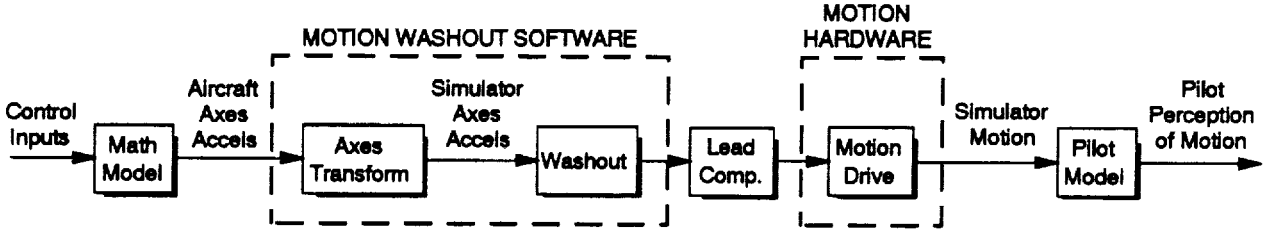

Figure 3. General Structure for the VMS Motion Response

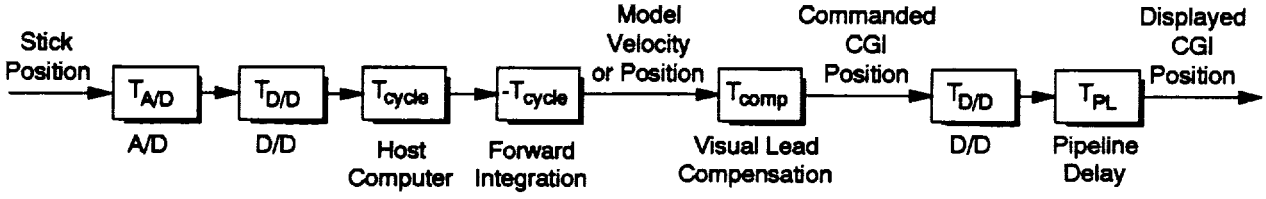

Figure 4. Stick-to-Visual Path Timing Diagram

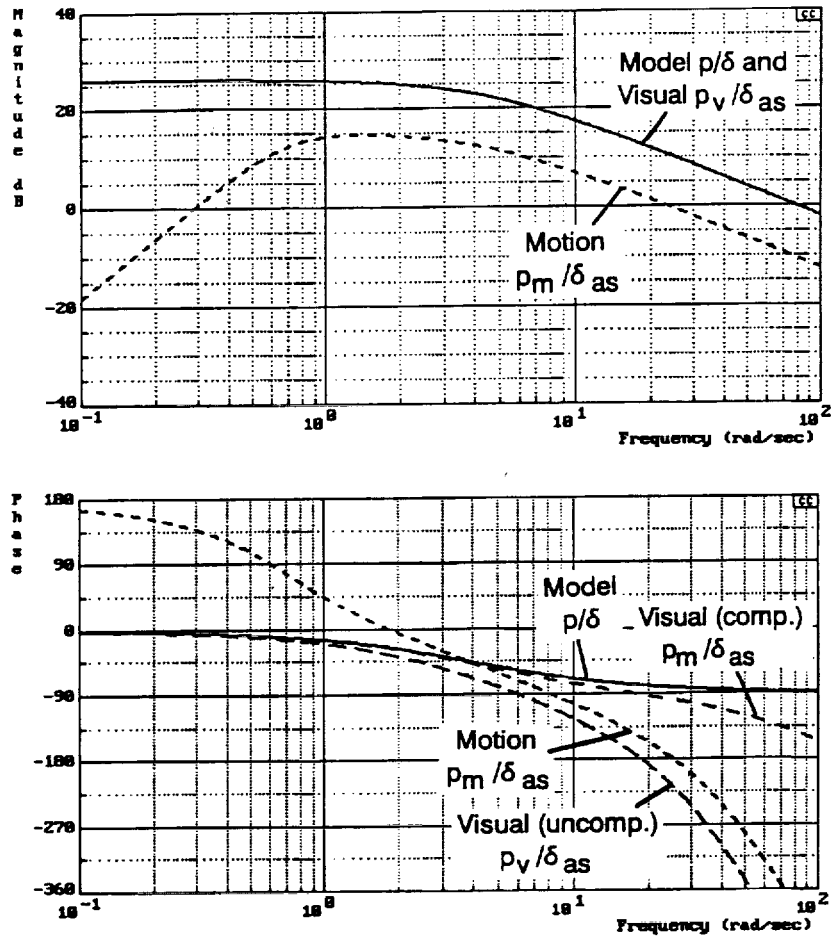

Figure 5. Frequency-Response Comparisons of Roll Rate to Control Input (Inputs are Measured Control Position, δ, and Cockpit Control Actuator Position, δ_{as}; Outputs are Roll Rate for Model, p, Visual Display, p_v, and Motion, p_m)

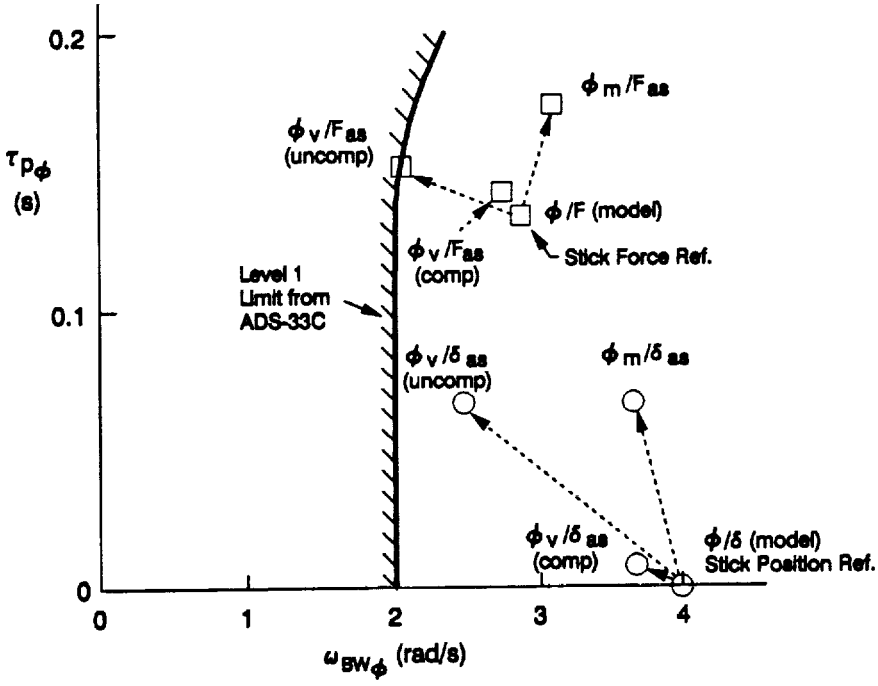

Figure 6. Migration of Bandwidth Parameters as Stick Force/Deflection, Visual, and Motion Effects are Introduced

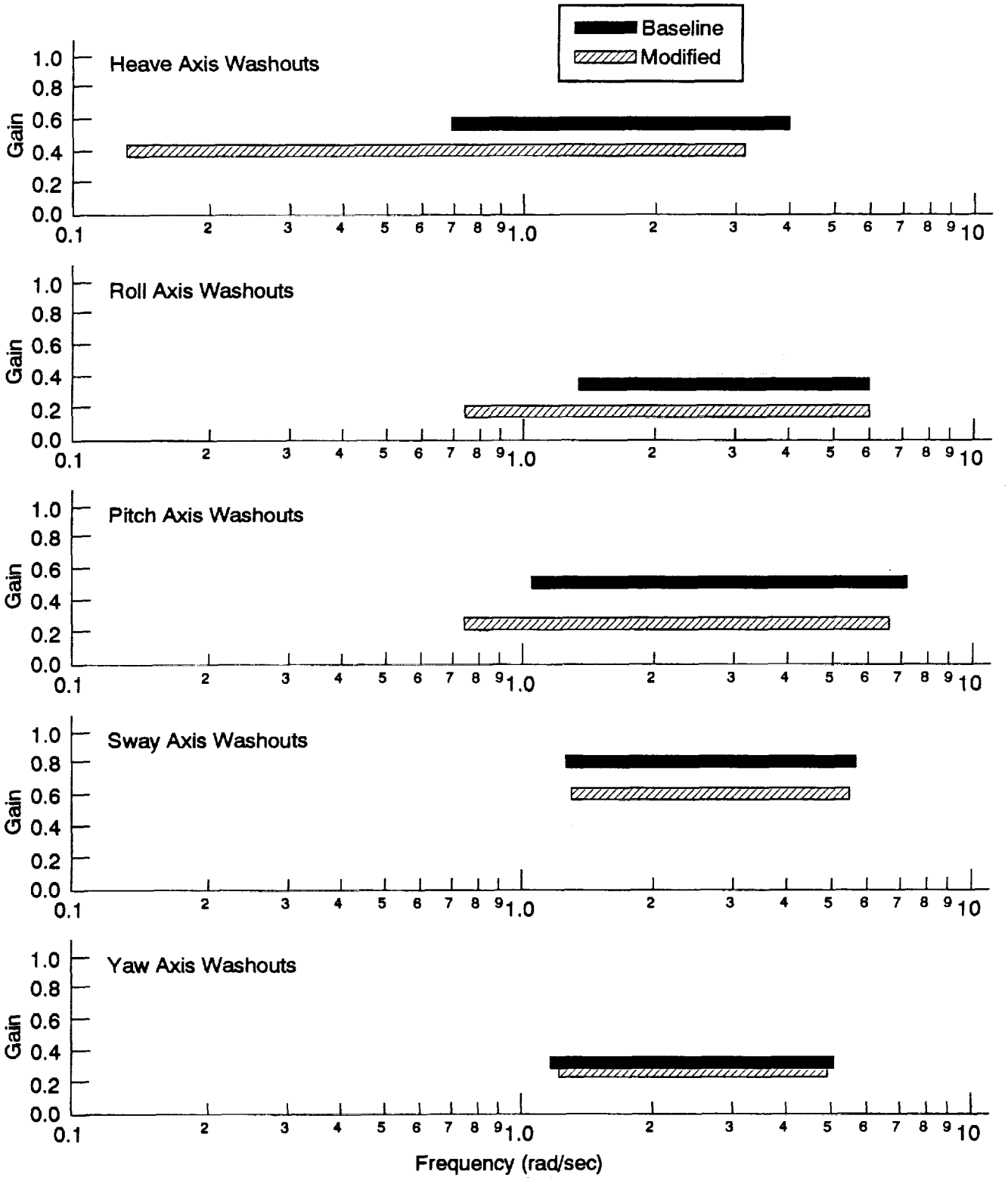

Figure 7. Frequency Range for Less than 30° Motion-to-Model Phase Distortion for Baseline and Modified Washout Configuration

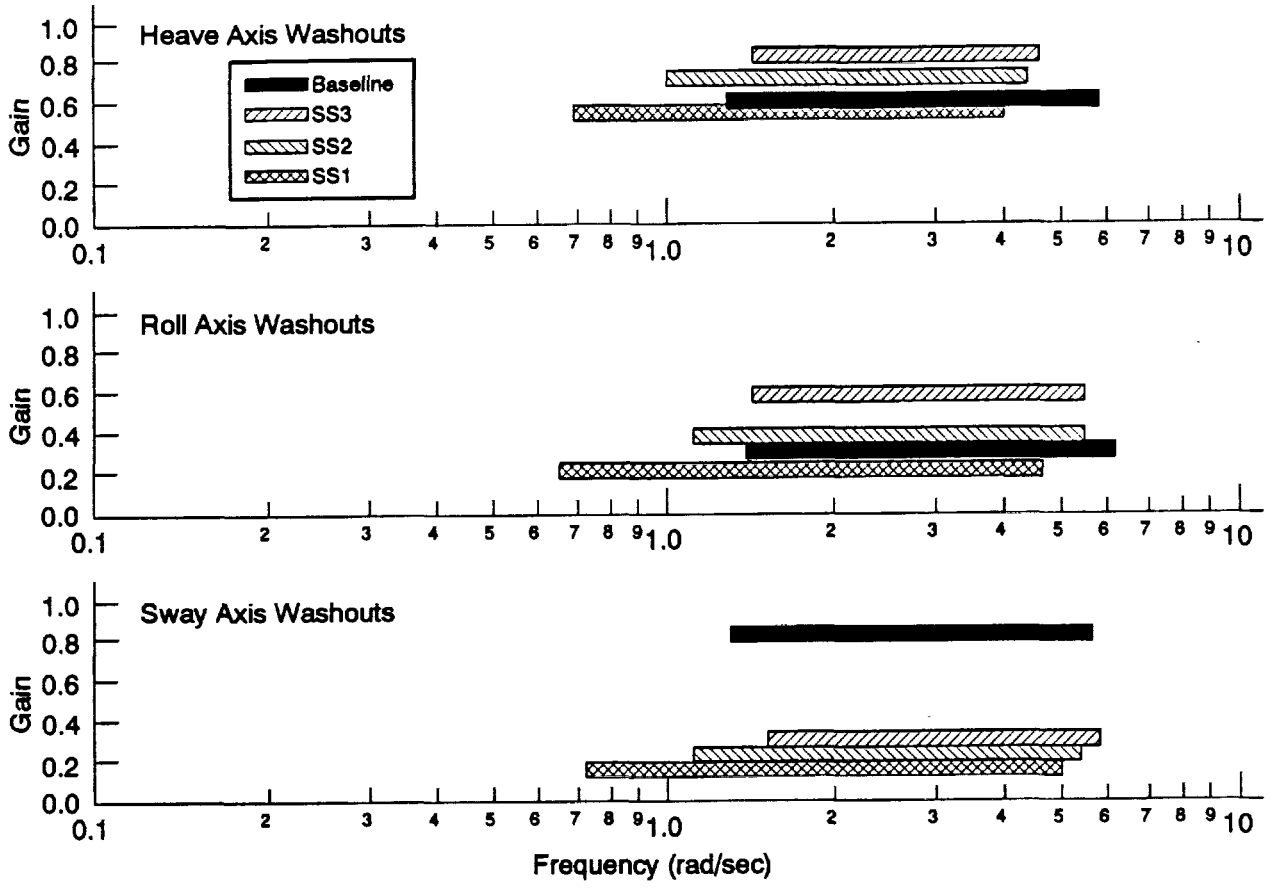

Figure 8. Frequency Range for Less than 30° Motion-to-Model Phase Distortion for Sidestep Washout Configurations

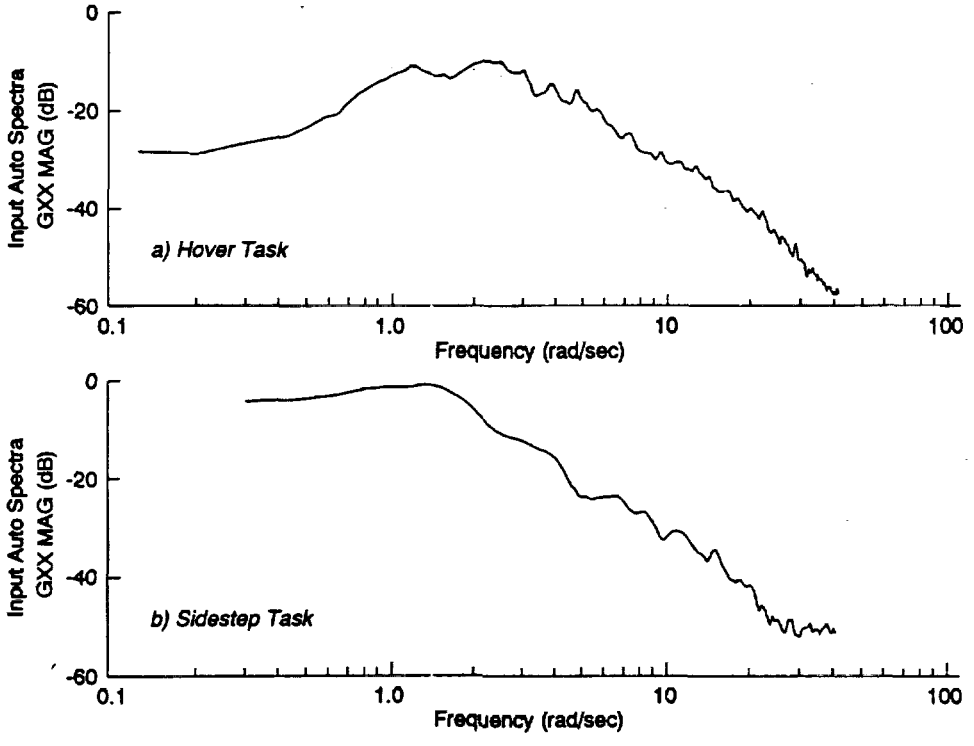

Figure 9. Lateral Stick Frequency Content (Pilot A)

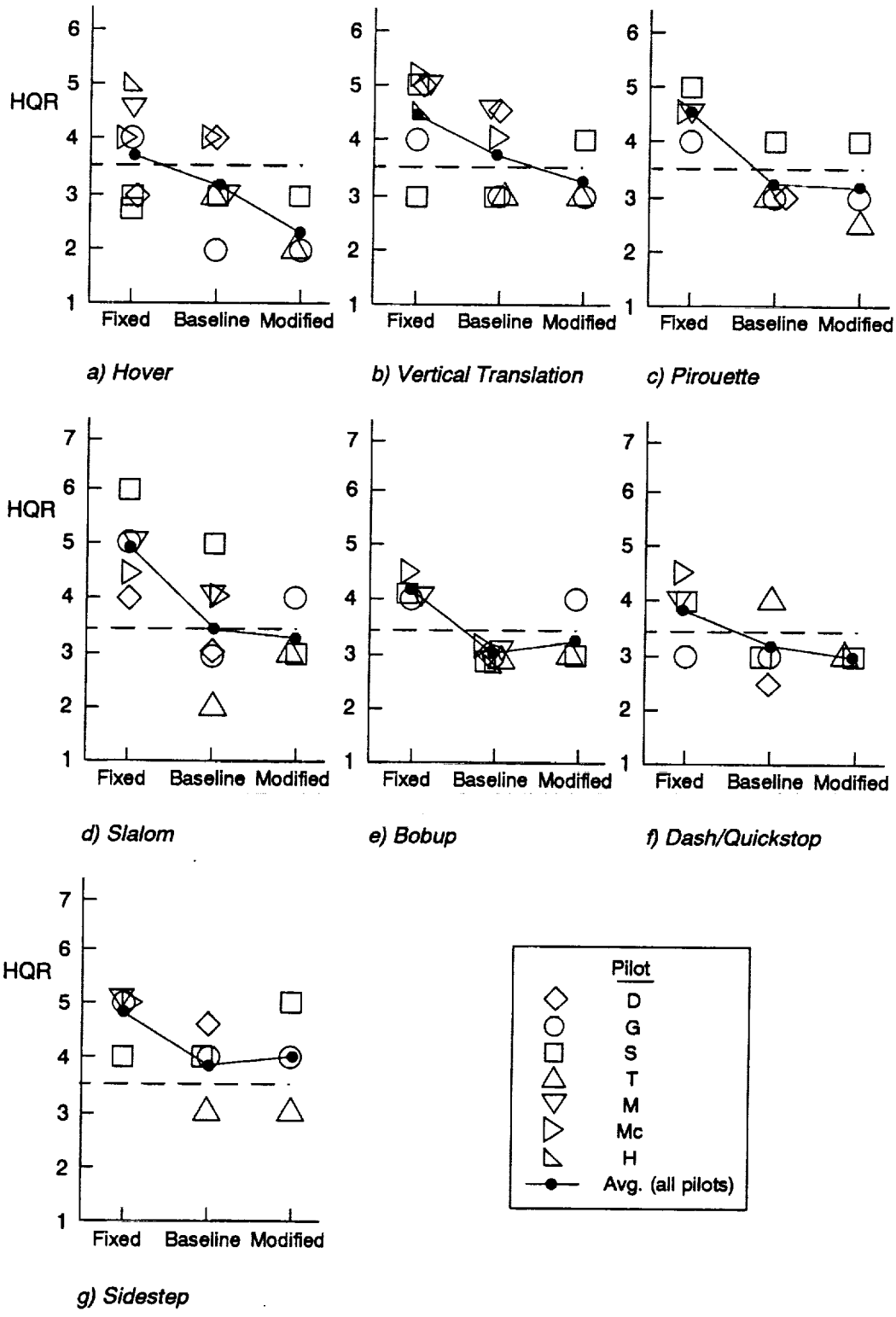

Figure 10. Effects of Task and Motion on HQRs from Simval I
(Baseline Motion, Visual Compensation On)

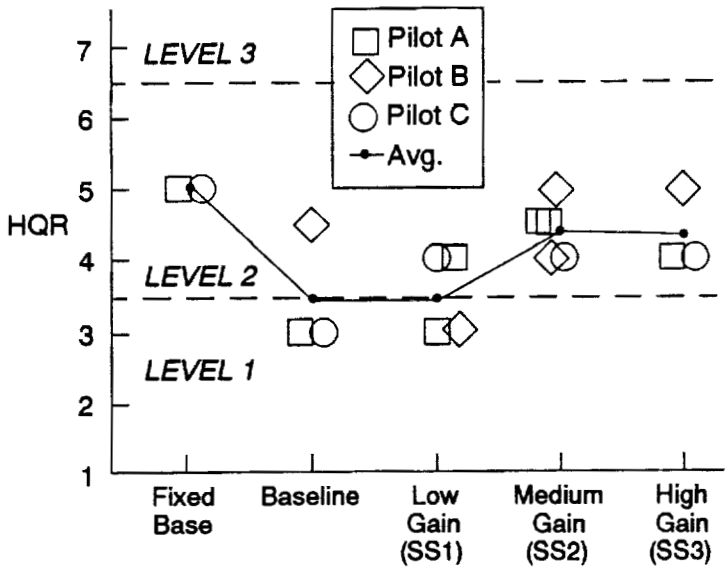

Figure 11. Pilot Ratings for Sidestep, Motion Variations from Simval II (Medium-Bandwidth Helicopter)

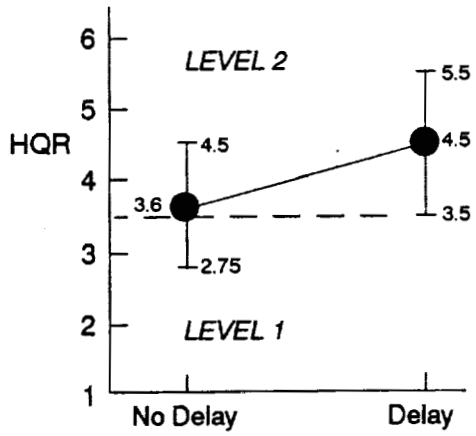

Figure 12. Effects of Visual Time Delay on Average HQR, Fixed Base

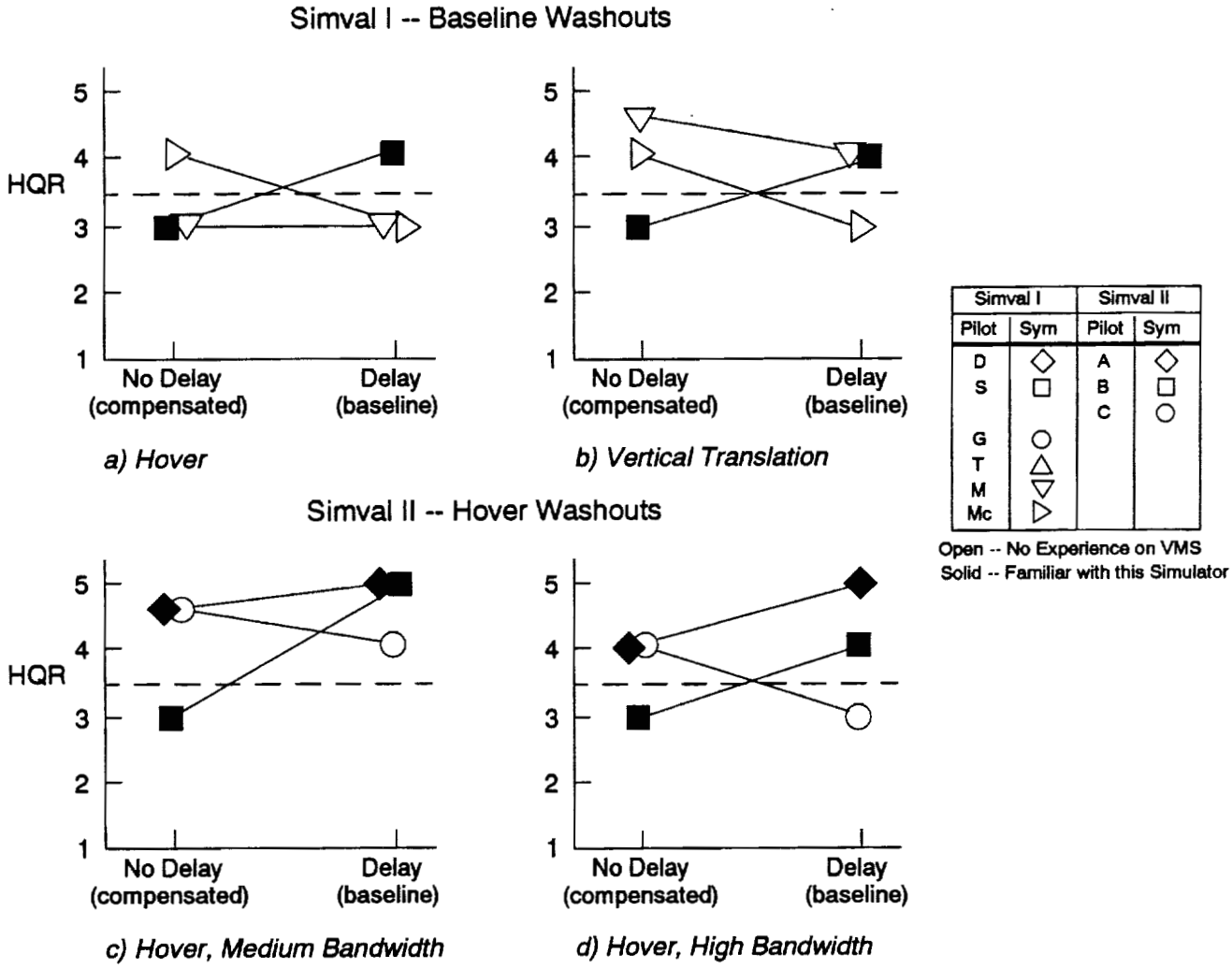

Figure 13. HQRs for Hover Task with Visual Delay Compensation (Moving Base)

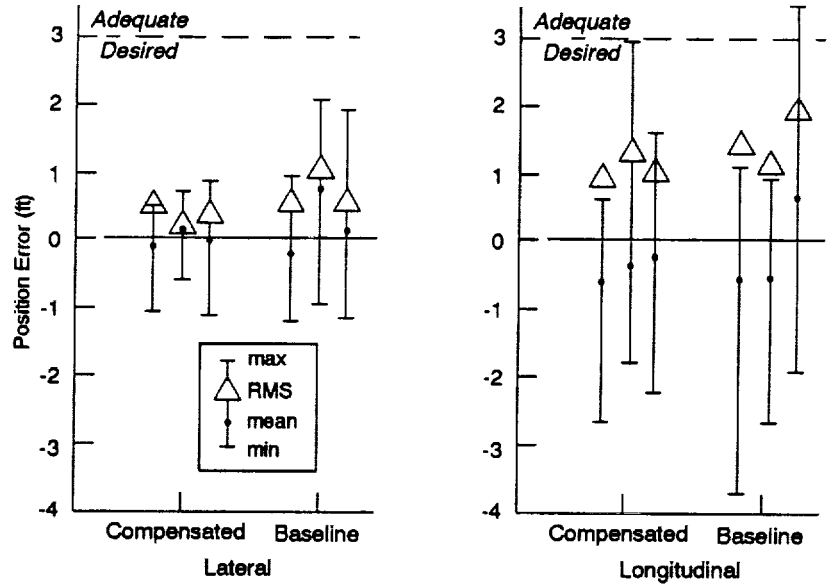

a) Experienced VMS Pilot (pilot B)

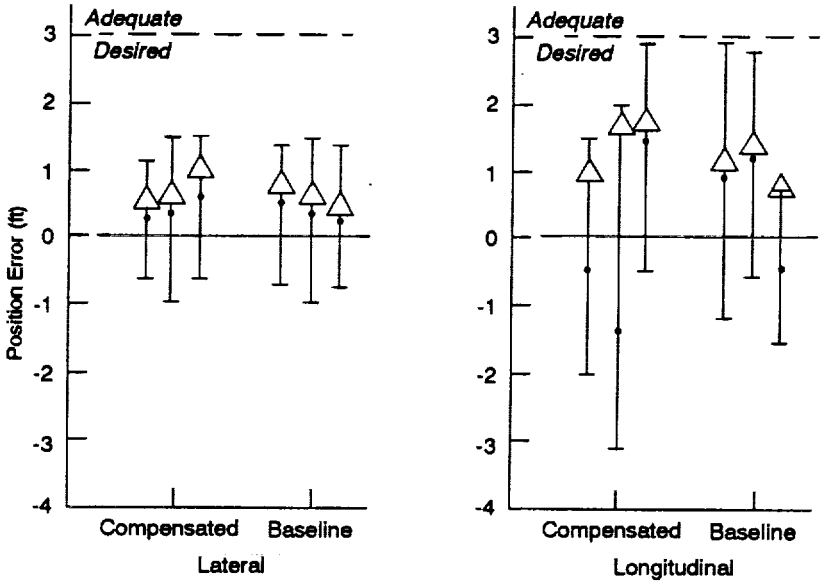

b) Novice VMS Pilot (pilot C)

Figure 14. Hover Performance with Visual Delay Compensation On and Off for Experienced and Novice VMS Pilots (Simval II)

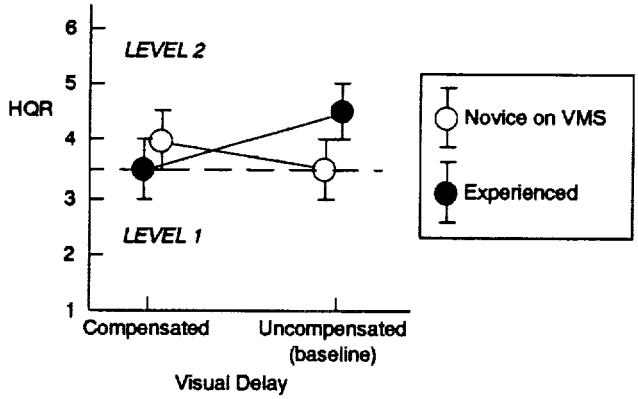

Figure 15. Effect of Visual Delay Compensation on HQRs for Experienced and Novice VMS Pilots

TABLE 1. EFFECTIVE TRANSPORT DELAY OF MOTION SYSTEM (INCLUDING MOTION LEAD COMPENSATION)

Axis	Delay (msec)	
	Simval I	Simval II
Pitch	70	91
Roll	70	88
Yaw	70	157
Surge	170	169
Sway	100	128
Heave	130	168

TABLE 2. SOURCES OF VISUAL TIME DELAY

Source	Delay (msec)	
	Simval I	Simval II
A/D (Stick measurement)	8	8
D/D	2	2
Host Computer (T_{cycle})	20	25
Forward Integration ($-T_{cycle}$)	-20	-25
Visual Lead (T_{comp})	variable	variable
D/D	2	2
Visual Transport Delay	83.3	62.5
Overall	95.3 - T_{comp}	74.5 - T_{comp}

TABLE 3. VALUES OF STICK-TO-VISUAL DELAY EVALUATED

	Simval I	Simval II
COMP ON	12	14.2
COMP OFF	95.3	74.5

N94-13318

Primary Display Latency Criteria Based on Flying Qualities and Performance Data

by
John D. Funk,Jr.*
and
Corin P. Beck
Naval Air Warfare Center
Aircraft Division
Warminster, PA
and
John B Johns*
Army Aeroflightdynamics Directorate
Ames Research Center
Moffet Field, CA

ABSTRACT

With a pilots' increasing use of visual cue augmentation, much requiring extensive pre-processing, there is a need to establish criteria for new avionics/display design. The timeliness and synchronization of the augmented cues is vital to ensure the performance quality required for precision mission task elements (MTEs) where augmented cues are the primary source of information to the pilot. Processing delays incurred while transforming sensor-supplied flight information into visual cues are unavoidable. Relationships between maximum control system delays and associated flying qualities levels are documented in MIL-F-83300 and MIL-F-8785. While cues representing aircraft status may be just as vital to the pilot as prompt control response for operations in instrument meteorological conditions, presently, there are no specification requirements on avionics system latency. To produce data relating avionics system latency to degradations in flying qualities, the Navy conducted two simulation investigations. During the investigations, flying qualities and performance data were recorded as simulated avionics system latency was varied. Correlated results of the investigation indicates that there is a detrimental impact of latency on flying qualities. Analysis of these results and consideration of key factors influencing their application indicate that: (1) Task performance degrades and pilot workload increases as latency is increased. Inconsistency in task performance increases as latency increases. (2) Latency reduces the probability of achieving Level I handling qualities with avionics system latency as low as 70 ms. (3) The data suggest that the achievement of desired performance will be ensured only at display latency values below 120 ms. (4) These data also suggest that avoidance of inadequate performance will be ensured only at display latency values below 150 ms.

INTRODUCTION

This paper documents the results of two piloted simulations conducted to generate data regarding display latency effects on flying qualities. A theoretical foundation is presented first to facilitate discussion. In this introduction, latency, flying qualities and a general closed-loop system are defined. The predictions that provided the impetus for the simulation investigations are presented.

Definition of Latency

Latency associated with a system component can be viewed as a pure time delay between some input or change and the corresponding output. Avionics system latency can be defined as the time delay between aircraft motion and the corresponding indication of that motion on the aircraft displays. Based on this definition, the terms latency, time delay, and delay are considered equivalent and are interchanged throughout this paper.

Definition of Flying Qualities

The acceptability of aircraft dynamics and control characteristics can be quantified in terms of achievable mission task performance and resulting pilot workload. This quantification is typically performed using the Cooper-Harper pilot opinion scale shown in Figure 1.[1] Aircraft flying qualities evaluations and specification development are based on results obtained from the use of this scale tempered with actual task performance data. Military flying qualities specifications typically quantify acceptability in terms of flying qualities levels. Explicit in the definition of these levels is not only pilot workload, but also mission task performance as indicated in Figure 1.

*Member American Helicopter Society

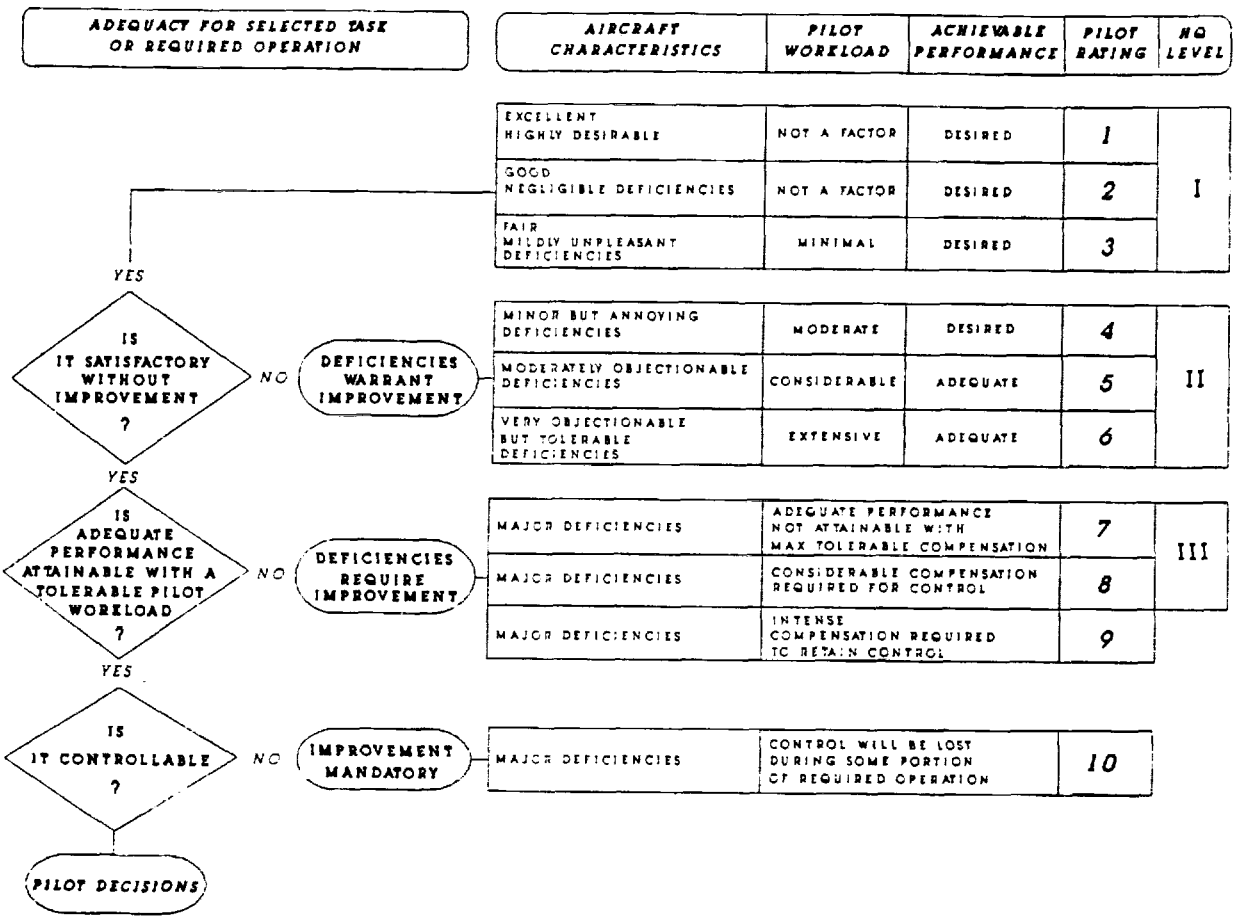

Figure 1. Handling Qualities Rating Scale

MIL-F-83300[2] and MIL-F-8785C[3] have been used to define the flying qualities requirements for many military V/STOL aircraft. These requirements are established with respect to the flying qualities levels as defined above. Most Navy aircraft in normal state conditions are required to exhibit Level I flying qualities. This level of flying qualities is required even during the more demanding tasks intended to be flown and in the more adverse environments expected to be encountered. In general Navy aircraft will be required to perform routine and tactical flight operations satisfactorily (including high-speed terrain following flight and shipboard operations) in adverse weather and combat conditions.[4]

General Latency Effects and Flight Control System (FCS) Latency Specifications

The effect of time delays on flying qualities is common knowledge in the flying qualities community. In summary, data from numerous experiments indicates that time delays reduce closed-loop system stability, thereby increasing pilot workload and degrading task performance. These data further indicate that latency will have an increasingly detrimental effect as task difficulty, aggressiveness and precision requirements are increased.

The data referenced above was generated in experiments designed to identify the effects of FCS latency and has been used to define FCS latency limits. Shown in Table 1, these limits have been associated with handling qualities levels and incorporated into military flying qualities specifications.[2,3]

Table 1. FCS Delay Specifications

Specification	Flying Qualities		Requirement Time Delay
MIL-F-83300	Level	I	≤ 100 ms
MIL-F-8785	Level	I	≤ 100 ms
		II	≤ 200 ms
		III	≤ 250 ms

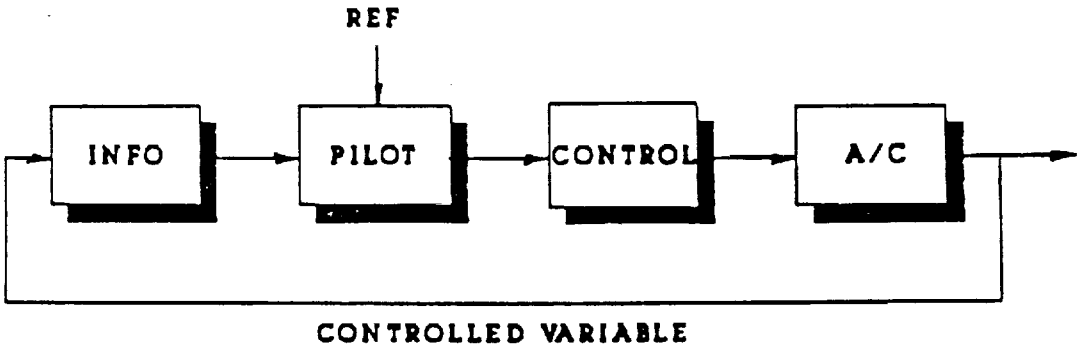

Figure 2. Standard Closed-Loop System

The time delay limits shown are typical of delay limitations associated with high difficulty/high gain/high precision tasks and may appear conservative. However, it should be noted that most experiments used to support these limits have investigated delay effects with delays inserted in only a single axis of control. Delays in all axes, which is more representative of a real system may result in an even more severe degradation than that indicated above. In this sense, the specifications may be liberal.

Definition of a Closed-Loop System

A simplified closed-loop system is illustrated in Figure 2 and includes airframe, control, pilot and information components. A typical loop closure will involve pilot control of an aircraft state or flight parameter. During control, the pilot will attempt to minimize the difference or error between a reference or desired value of the selected state and the actual or perceived value of the selected state. Information on the reference value, controlled parameter and the error between the two will be available to the pilot through outside world visual cues, motion cues and displays. To close the loop, the pilot will apply control proportional to the error.

As an example, consider a precision approach to a ship. The pilot's goal is to track the instrument landing system (ILS) beacon, both vertically (glideslope) and laterally (localizer), with precision sufficient to allow a safe landing. Outer loop control is accomplished with closure around the pilot's reference parameters, glideslope angle, localizer and recovery heading. Inner loop control is accomplished with closure around descent rate, airspeed, and pitch and roll attitude.

Since precise glideslope and localizer error are available only from the displays, the displays can be considered the primary source of information in the above task. This is clearly the case during an approach with degraded visibility, where the displays are the pilot's only reliable source of flight information.[5] Under these circumstances, the pilot would find it difficult, if not impossible, to distinguish between display dynamics, control dynamics and airframe dynamics. The effect of a delay in displayed information could, therefore, be considered equivalent to the effect of an airframe or control delay of the same magnitude.

The most severe delay-induced degradations in flying qualities are expected during high difficulty, high gain, high precision tasks requiring the use of displays as the primary source of flight information. In particular, the concern lies with the performance of manual, high frequency, precision control of aircraft attitude, position and vertical speed in degraded visual conditions (instrument meteorological conditions (IMC), visual meteorological conditions (VMC) with an obscured horizon, and night VMC). Under these circumstances, the head-down displays or helmet-mounted displays would most likely be used to provide the required flight information, either alone or superimposed on a Forward Looking Infra-red (FLIR) image.

FLIGHT SIMULATION INVESTIGATIONS AND RESULTS

Two manned flight simulations, one in an engineering simulator and one in a high fidelity developmental simulator, were conducted to generate data specific to avionics or display system latency effects on aircraft flying qualities. The first, conducted in a basic engineering simulator to generate initial data, simulated avionics system latency which was swept from 47 ms to 447 ms. The second, conducted in a high fidelity developmental simulator to produce high quality data, was conducted with latency values varying from 70 ms to 240 ms.

A precision approach task was selected as the primary task for the simulation. Performance constraints were established based on mission or safety requirements. Adequate performance constraints were based on maximum safe or

acceptable spatial deviations. Desired performance constraints were established as limits reflecting a desired margin of performance or safety beyond adequate performance constraints. The tasks and the corresponding performance constraints are described below.

Unless specified otherwise, "Latency", "Delay", "Display Delay" and are used in short for "Avionics System Latency" in the following text.

Engineering Simulation

Simulation Facility

This investigation utilized a fixed-base engineering research simulator. This simulator employs standard fixed-wing controls: center stick, pedals, and throttle. The computer generated outside-world image is projected onto a single, forward screen. For this investigation, primary flight information was superimposed on the outside-world image in a standard uncluttered format. This format presented glideslope as a fly-to horizontal bar and localizer as a fly-to vertical bar. Range and airspeed data were digitally represented. The symbology is shown in Figure 3.

The aircraft model used was a generic medium weight, medium agility fixed-wing aircraft with level I baseline handling qualities.

Evaluation Task

The primary task consisted of a precision approach on a 3.5 degree glideslope to a ship. Environmental conditions were extremely limited visibility and crosswinds up to 45 kt. Direction and magnitude were selected at random, prior to each evaluation run. The initial conditions were glideslope (GS) and localizer (LOC) offsets of 1 degree and 5 degrees, respectively. These were combined randomly to result in four initial positions: above GS and left of LOC, below GS and right of LOC, etc.. Range at the initial position was 24000 ft. Trim approach speed was 128 kt.

The pilot was instructed to capture GS/LOC prior to reaching a 15,000 ft range and to track GS/LOC to 1,500 ft range within the following performance tolerances:

Desired	Adequate
± 5 kt	± 10 kt
± 1/4 degree GS	± 1/2 degree GS
± 1 degree LOC	± 2 degrees LOC

A given level of performance was to be maintained for at least 80-percent of the approach (between 15,000 and 1,500 ft range) for that level to be considered achievable during evaluation.

A secondary task was used to examine the effect of side task workload on primary task performance. This secondary task consisted of the pilot physically setting and verbally repeating the barometric altitude pressure reference to random values called by the engineer every 3000 ft range (with the last call made at 4000 ft). No degradation in performance was tolerated in this task.

Latency Matrix and Evaluation Technique

Limited by hardware, minimum achievable simulated delays were 57 ms flight controls (from stick displacement to aircraft motion) and 47 ms displays (from aircraft motion to head-up display update). The matrix of delay configurations evaluated is shown in Table 2.

Table 2. Delay Evaluation Matrix

Flight Control Delay (ms)	Display Delay (ms)
57	47
	167
	327
	447
107	47
	167
	327
	447

Two Marine Corps operational test and evaluation pilots performed as evaluation subjects. Each pilot was given between four and eight hours familiarization time. During evaluation, each pilot was given as many runs as necessary to confidently assess achievable task performance and his workload. This technique resulted in as many as eight flights per delay configuration evaluation (single pilot rating). Further, each pilot evaluated each configuration at least twice.

Results

Result are presented in the form of pilot ratings and sample time histories of stick activity and tracking error. Pilot ratings as a function of display delay are shown in Figure 4. Sample longitudinal and lateral stick activity with glideslope and localizer tracking error are shown in Figure 5 and 6, respectively.

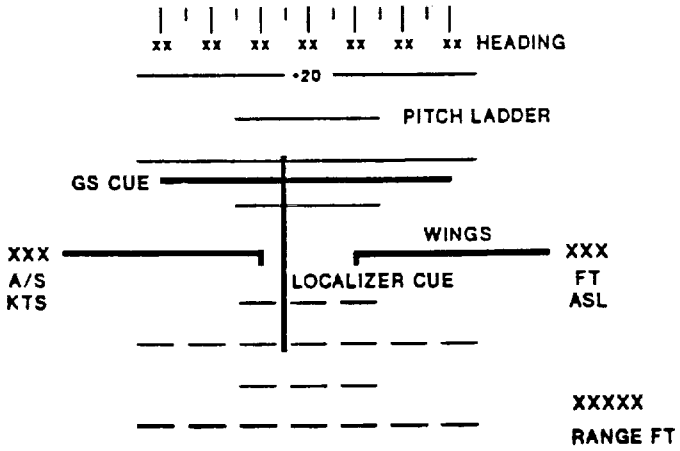

Figure 3. Engineering Simulation Head Up Display for Precision Approach

The engineering simulation study supported the following conclusions:

a. No significant, quantifiable differences in handling qualities were observable between evaluations with 57 and 107 ms control delays. As a result, the data for these control system delay configurations were combined and plotted together.

b. A handling qualities degradation with increasing display delay, although shallow, is observable. This trend, apparent in the pilot rating data, is supported by stick activity and actual tracking performance.

c. A transition from Level I to Level II occurs between 47 and 167 ms display delay for the primary task alone. A transition from desired to adequate performance (HQR 4 to 5) for the primary and secondary task also occurs between 47 and 167 ms.

High Fidelity Simulation

Simulation Facility

The fixed-base simulator used in this investigation employs a representative tilt-rotor cockpit with a multi-window, high-resolution, computer-generated, outside-world image. The simulator mathematical model represents a low to medium agility medium weight tilt rotor aircraft.

Evaluation Task

Again, the evaluation involved the performance of a precision approach task. This task is similar to that of the engineering simulation. The precision approach task was flown at 85 kt (75^{o} i_n) on a 3.5 degree glideslope. Environmental conditions consisted of mild-to-moderate turbulence[3] with a mild (10 kt) windshear (between 1000 and 100 ft AGL) in addition to a moderate (20 kt) crosswind. A ceiling was simulated at 300 ft AGL. A constant altitude, 30 degree ILS intercept profile was flown from the initial conditions. Tracking constraints for evaluation were identical to those used in the engineering simulation, with one exception. The pilots were instructed to place emphasis on the performance and the workload near decision height, 200 AGL, which was the task termination point.

The approach configuration flown was at 120 kt, 60^{o} nacelle angle (i_n) and represented a nominal combat or expedited recovery. Environmental conditions were fixed with mild-to-moderate turbulence, 10 kt windshear, 20 kt crosswind, 200 ft ceiling. As illustrated in Figure 7, initial positions were located at 5.9 nm range with randomly selected offsets of 1 degree in glideslope and 5 degrees in localizer. The initial heading corresponded to the recovery heading with a minor trim adjustment for the crosswind.

The pilot was instructed to maneuver from his initial position to intercept glideslope and localizer by 4.8 nm range and to track glideslope and localizer to decision height (300 ft AGL). For evaluation purposes the task began at initial glideslope and localizer intercept and terminated at decision height.

Tracking constraints were also similar to those used in the engineering simulation, with additional emphasis placed on the last half of the approach. Because of the evolution of these constraints, they are summarized in Table 3. Precision approach flight symbology was mildly cluttered with a vertical bar for localizer, and an arrow indicator for the glideslope and is shown in Figure 8. The above desired, geometric, GS and LOC constraints corresponded to 1/2 of a display tic and 2/3 of a display tic, respectively. Airspeed was indicated with a digital numeric display.

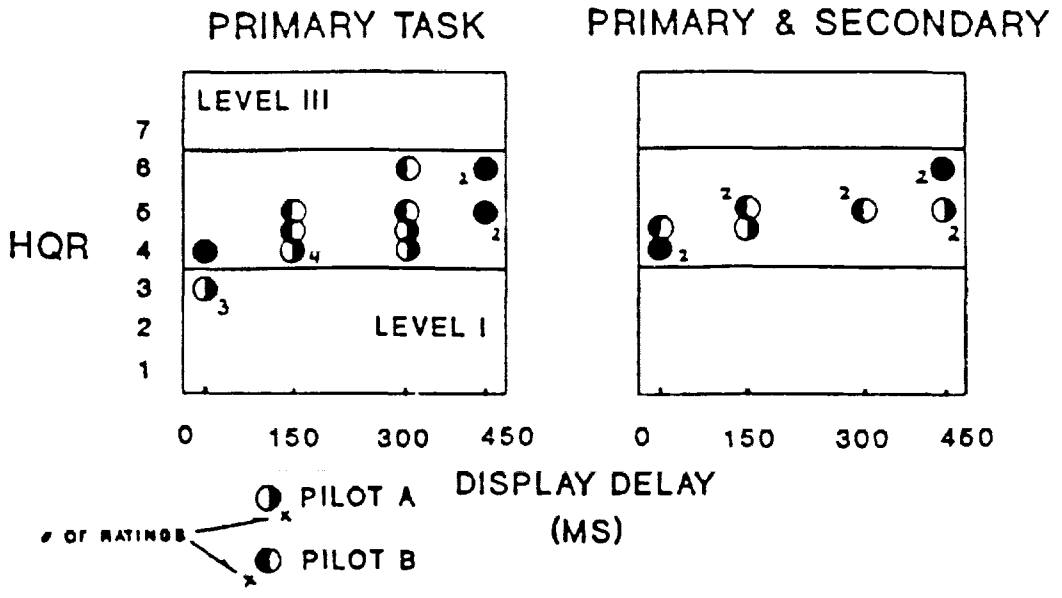

Figure 4. Handling Qulaities as a Function of Display Delay - Engineering Simulation

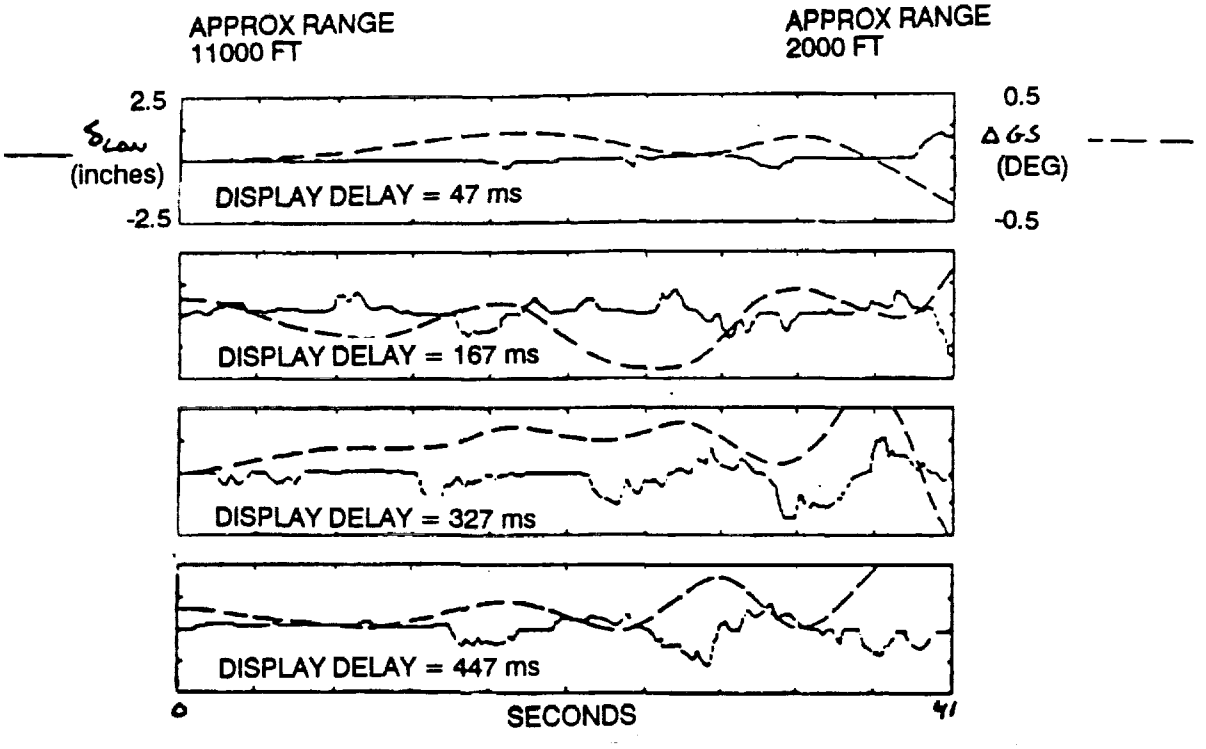

Figure 5. Longitudinal Stick Activity and Glideslope Tracking Error - Engineering Simulation

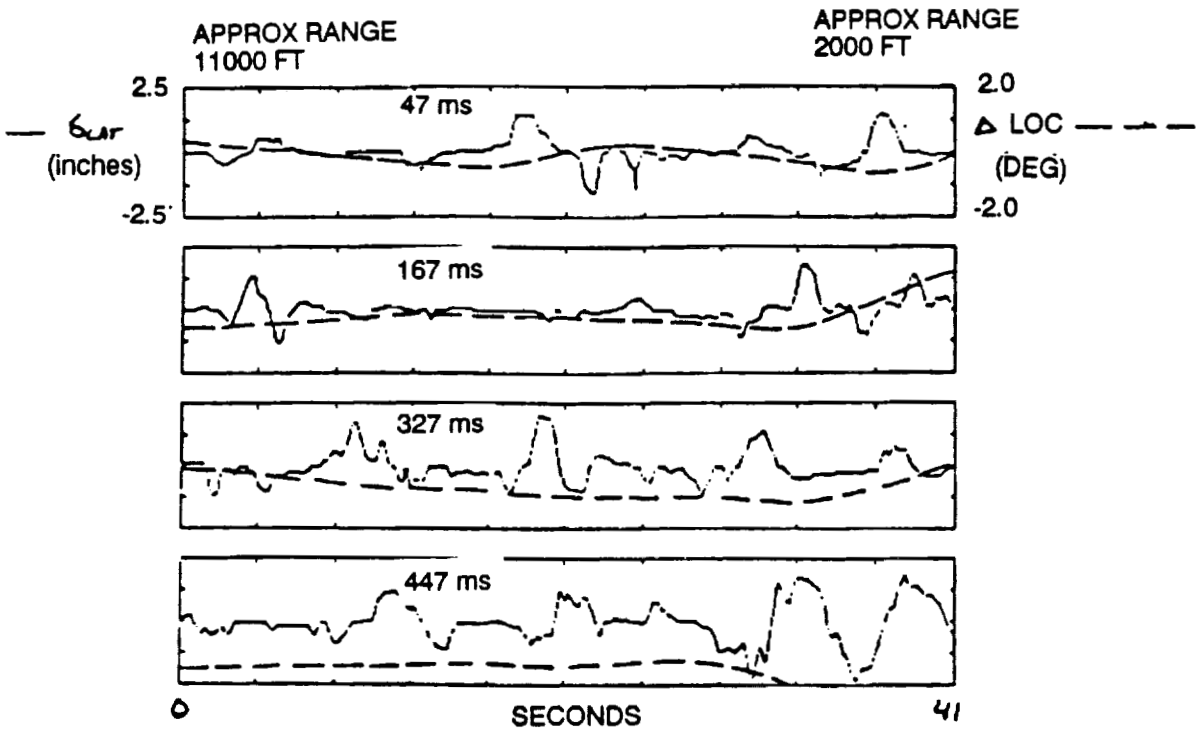

Figure 6. Lateral Stick Activity and Localizer Tracking Error - Engineering Simulation

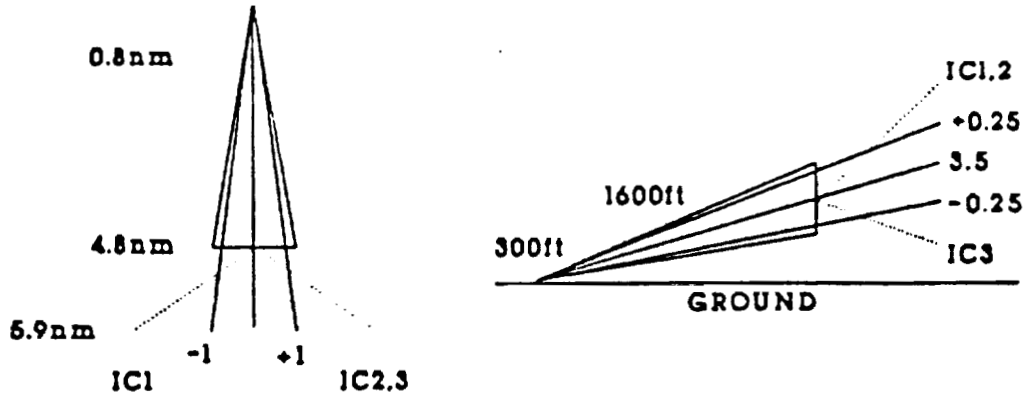

Figure 7. Precision Approach Geometry

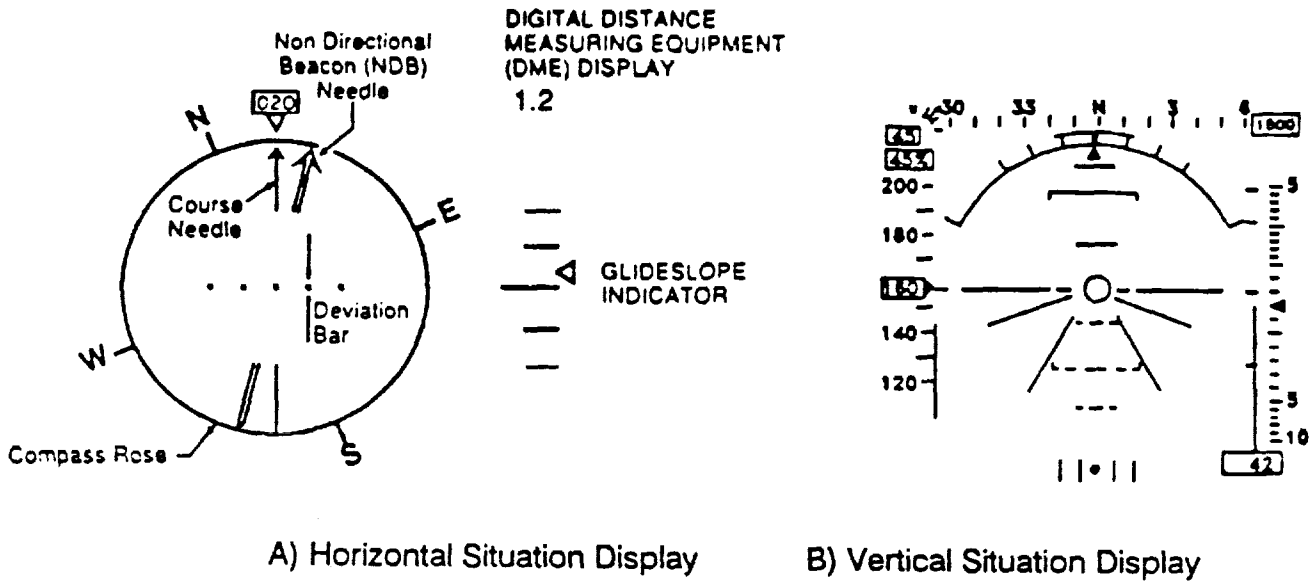

A) Horizontal Situation Display B) Vertical Situation Display

Figure 8. High-Fidelity Simulation Display - Simulated Precision Approach Mode

Table 3. Tracking Constraints

Geometry:	Desired:	± 5 kt A/S ± 1/4 degree GS ± 1 degree LOC
	Adequate:	± 10 kt A/S ± 1/2 degree GS ± 2 degree LOC
Time:	-	maintain given level of performance for at least 80% of task for given level to be considered achievable
	-	exceedance of adequate performance constraints for 5 seconds or more could not be considered desirable
Emphasis:	-	performance and workload during last half of approach (approximately 60 seconds, 1000 ft to 300 ft AGL)
	-	performance and workload at decision height

Latency Matrix, Pilots, Evaluation Technique

i. Latency Matrix - The FCS latency was fixed at 50 ms. Three display latency configurations (73, 179, and 241 ms) were evaluated.

ii. Pilots - Four military test pilots served as evaluation subjects. The pilots and their backgrounds are listed in Table 4.

Table 4. Government Pilot Evaluation Team

PILOT A	2100 HRS HELO (H-53) 250 HRS FW HMX-1 OT+E 1 YR V-22 SIM
PILOT B	1900 HRS HELO (H-1) 1500 HRS FW (T-34) HMX-1 OT+E 4 YRS HQ EVAL EXPERIENCE V-22 SIM
PILOT C	4000 HRS HELO 1000 HRS FW TPS RW INSTRUCTOR 2 YRS
PILOT D	3400 HRS HELO (H-3) 400 HRS FIXED WING TPS/RW V-22 SIM + FLT

iii. Evaluation Technique - Each pilot underwent extensive familiarization prior to evaluations. This familiarization was accomplished with the mini-

mum latency and proceeded as follows. Each pilot took approximately 1 hour of free-flight without turbulence or wind to become familiar with the cockpit and math model. An additional 2 hours was taken by each pilot to fly approximately 20 precision approaches with and without turbulence and wind. During evaluations, the pilots provided an HQR following each run. A complete evaluation consisted of, at least, three runs. When both the pilot and the engineer were satisfied that the delay configuration had been adequately evaluated, the engineer informed the pilot that the delay configuration was to be changed and the next evaluation commenced. The pilot was not informed of the latency value during evaluations. Each pilot performed a minimum of two evaluations per latency configuration.

Results

Among all pilots, 254 approaches were flown during six days of simulation. Results presented here take the form of pilot ratings and tracking performance as a function of display delay. Pilot rating data is shown in Figure 9. Tracking performance, in terms of time outside desired glideslope envelope, weighted time outside desired glideslope envelope, and time outside adequate glideslope envelope, is shown in Figures 10, 11, and 12 respectively.

Localizer tracking and airspeed maintenance performance is not shown for the following reasons:

- with two exceptions in 254 runs, airspeed error was within desired performance constraints for all values of latency evaluated;
- even though lateral-axis workload seemed to increase as latency increased, no trend in localizer tracking error as a function of latency was apparent;
- glideslope tracking performance drove both pilot ratings and comments.

Returning to the glideslope tracking performance data shown in Figures 10, 11, 12, several issues are worth mentioning. First, these data represent the last 60 seconds of the task (from approximately 1000 to 300 ft AGL). Following the time constraints and evaluation emphasis specified, 12 seconds (20% of 60 seconds) can be considered the time constraint associated with desired performance. Any runs with excursions outside of the desired glideslope envelope beyond 12 seconds, during the last 60 seconds of the task, were considered to have, at best, adequate performance. Second, examining time outside of constraints as an isolated performance metric may be misleading if the magnitude of the angular excursion is inversely related to the time of the excursion. To examine this possibility, the time of the excursions were weighted by the corresponding magnitude of the excursions outside of the desired glideslope envelope. These weighted values are plotted in Figure 11. A trend similar to that of the unweighted data exists. This indicates that time outside of constraints may legitimately be used as a measure of performance.

Finally, considering adequate performance (Figure 12) and following the time constraints and evaluation emphasis, 5 seconds can be considered the time constraint associated with adequate performance. With the time constraint defined, specifying that "exceedance of adequate performance constraints for 5 seconds or more could not be considered desired," any excursion beyond 5 seconds could legitimately be classified as either adequate or inadequate. Nearly all excursions outside of the adequate glideslope envelope occurred, however, just prior to decision height. The pilots, observing the emphasis on performance near decision height, typically classified the excursions beyond the adequate glideslope envelope of 5 seconds or more as inadequate.

Examining the results, one general observation can be made:

> A handling qualities degradation with increasing display delay is apparent in both the pilot ratings and tracking performance.

The nature of this degradation and its applicability to defining an acceptable level of latency is discussed in the following section.

DEFINING AN ACCEPTABLE LATENCY LEVEL

When attempting to define a limit on any flying qualities parameter, several criteria may be considered:

- achievement of Level I handling qualities
- achievement of desired performance (note that achievement of desired performance does not mean that Level I handling qualities are achievable; Level II handling qualities (HQR 4) could result if workload is moderate or greater - see Figure 1)
- avoidance of inadequate performance

Regarding these criteria the results will first be considered in isolation. A discussion of the issues affecting the definition of delay limits will be discussed subsequently.

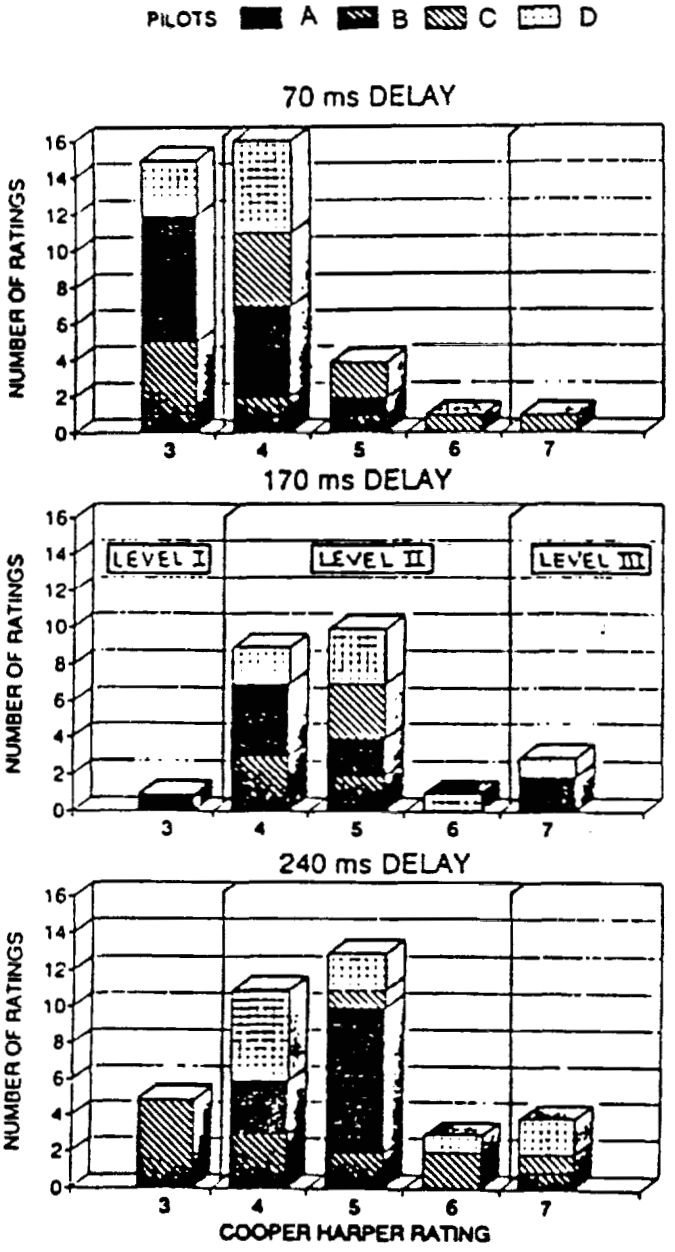

NOTE: The data shown above are the result of two modifications of the raw data. During the evaluation process pilots were permitted to give a rating of 4.5 for either of two reasons: desired performance was achievable with maximum pilot compensation only adequate performance was achievable but with minimal pilot compensation. Ratings of 4.5 with desired performance achievable and 4.5 with adequate performance achievable were redistributed to HQR 4 and 5 respectively. The other modification involved adjustment of ratings to reflect corresponding actual performance. In this case, the minimal possible adjustments were made and only when the original rating clearly was not supported by actual performance. Here, 3, 1, and 8 ratings were adjusted at 70, 170, and 240 ms, respectively. Neither of these modifications altered the true nature of the results.

Figure 9. Handling Qualities Ratings for Precision Approach

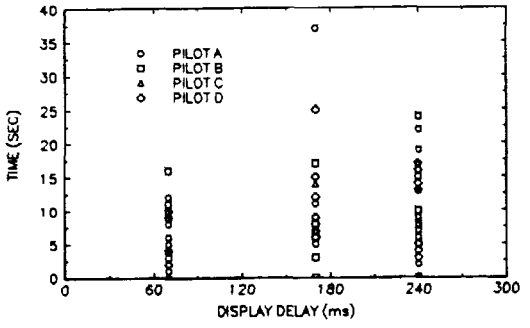

Figure 10. Tracking Performance - Time Outside of Desired Glideslope Envelope

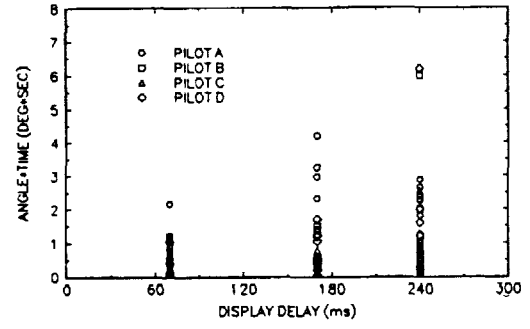

Figure 11. Tracking Performance - Weighted Time Outside of Desired Glideslope Envelope

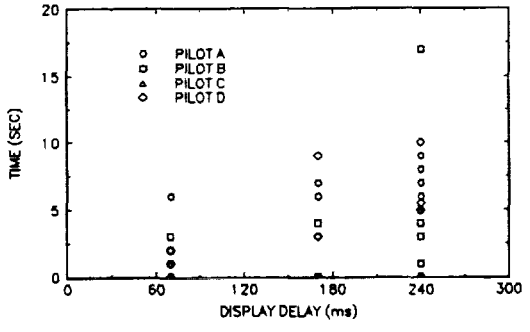

Figure 12. Tracking Performance - Time Outside of Adequate Glideslope Envelope

Achievement of Level I Handling Qualities

In applying the first criterion, pilot rating data (Figure 9) and performance data (Figure 10) must be examined. From Figure 9, it is apparent that, although there is a clear improvement in handling qualities between 170 and 70 ms, consistent Level I handling qualities are still not achievable at 70 ms. Further, from Figure 10, an improvement in tracking performance through a reduction in time outside of constraints is apparent with decreasing latency. A continuation of this trend, although shallow, is reasonable to assume if latency were dropped below 70 ms. It may also be reasonable to assume based on the available data that, as latency is reduced below 70 ms, workload would first incrementally decrease and then level off at some baseline. Taken together, these observations and assumptions lead to the conclusion that reducing latency below 70 ms should result in consistent Level I handling qualities.

Achievement of Desired Performance

Workload is not a consideration when applying this criteria. Tracking performance may therefore be examined directly. For this purpose, time outside of the desired glideslope envelope as a function of latency is shown in Figures 13 A, B, C.

The probability bands in Figure 13 are defined by the worst 10, 20, or 30 percent of the main body of the performance data. Examination of these bands reveals the nature of latency effects on flying qualities. The following observations are made regarding achievement of desired performance.

- As latency increases, an increasing rate of performance degradation is apparent.

- Extrapolating the bands below 70 ms, very little performance benefit is expected with a latency reduction below 70 ms.

- If an increased probability of exceeding overall desired performance constraints is tolerable, then a higher latency is acceptable. As an example, if a 10-percent probability of exceeding desired constraints is tolerable, then a latency of 120 ms is acceptable. If a 20 percent probability of exceeding desired constraints is tolerable, then a latency of 170 ms is acceptable.

However, noting that there are significant occurrences of inadequate performance at 170 and 240 ms (see Figure 9), avoidance of inadequate performance must be considered.

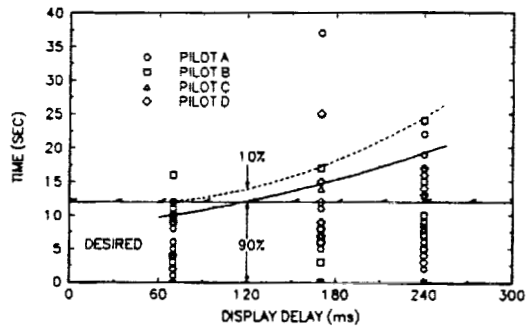

A) 10 percent probability

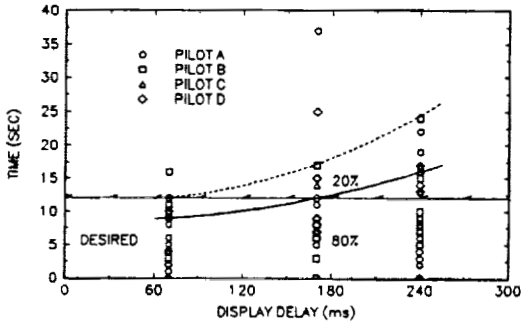

B) 20 percent probability

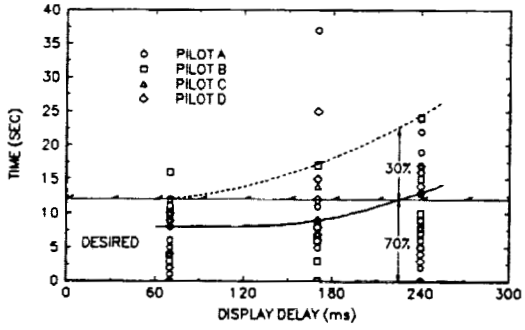

C) 30 percent probability

Figure 13. Probability of Exceeding Desired Performance Envelope for More Than 20 Percent of the Last Half of the Approach

Avoidance of Inadequate Performance

Tracking performance can also be examined directly in this section. Here, however, time outside of adequate glideslope envelope is used in the analysis. As in Figure 13, the probability bands shown in Figures 14 A and B are defined by the worst 10 and 20 percent of the main body of the performance data.

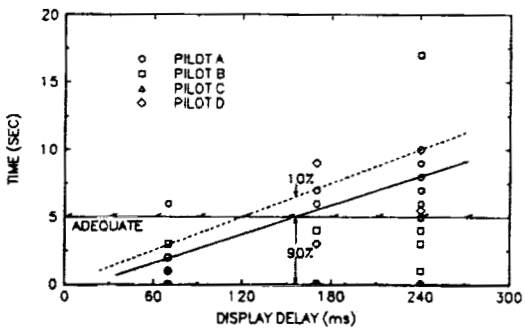

A) 10 Percent Probability

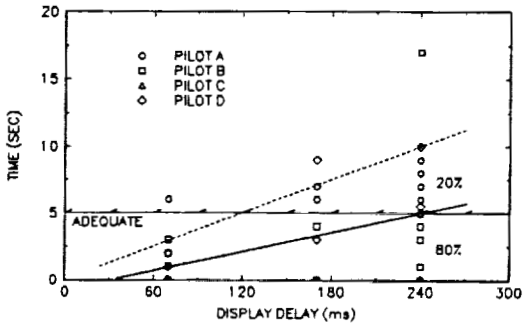

B) 20 Percent Probability

Figure 14. Probability of Exceeding Adequate Performance Envelope for More Than 5 Seconds During the Last Half of the Approach

Examination of these bands provides additional insight into the effects of latency on flying qualities. The following observations can be made regarding the avoidance of inadequate performance:

- A linear degradation in tracking performance and consistency with increased latency is apparent.
- Extrapolating the bands below 70 ms, a substantial performance benefit is expected with a latency reduction below 70 ms. This extrapolation indicates that below 10 to 20 ms no excursions outside of adequate constraints would occur.
- If an increased probability of exceeding overall adequate performance constraints is tolerable, then a higher latency is acceptable. As an example, if a 10-percent probability of exceeding adequate constraints is tolerable, then a latency of 150 ms is acceptable. If a 20-percent probability of exceeding adequate constraints is tolerable, then a latency of 240 ms is acceptable.

ISSUES AFFECTING DEFINITION OF A LATENCY LIMIT

Due to the origin and quantity of data used in the analysis, the following issues must be considered when applying the results of the previous section to definition of a latency limit:

- Data Quality
- Simulation vs. Actual Flight
  - Simulation Fidelity
  - Cues Available to the Pilot
  - Pilot Gain
- Severity of Task/Environment
- Training

Data Quality

The data used in the previous analysis were generated under controlled conditions using accepted flying qualities evaluation techniques. The evaluation pilot population was diverse and representative of the general pilot population. Minor adjustments were made to the pilot rating data to better reflect actual performance; actual performance data were used "as is."

A general qualitative check on both the experiment and data validity can be made by examining the trends in Figures 10, 13, and 14. These trends are what is physically expected from the effects of latency on tracking performance and workload.

Based on the above, the data used in the analysis are considered to be "high quality."

Simulation vs Actual Flight

Motion cues are not available in a fixed-base simulator. As a result, lead information available through actual commanded aircraft acceleration was not available. In the task used in evaluation this is not a factor for several reasons. First, tracking error information is only available to the pilot from the display. Motion cues do not provide any tracking error information. Even though motion cues aid inner-loop control this provides only marginal benefit in a primary visual tracking task[6]. Second, during precision approach in IMC, the displays are the only reliable source of flight information[5]. Anomalous aircraft motion cues, from both the pilot's head orientation and turbulence, force the pilot to rely on display information for an accurate assessment of the flight condition. A detrimental effect, if any, is expected due to the display latency induced mismatch between actual dynamics and display dynamics.

Finally, pilot gain would be higher in flight than in the simulator. Pilots would be less tolerant of tracking errors. This tolerance change would manifest itself through an increase in control activity. In turn, this increase in control activity would accentuate the effects of latency.

Therefore, given the same task, configuration and conditions, tracking performance and workload in flight are expected to be worse than that in the simulator.

Severity of Task and Environment

The precision approach evaluation task used was representative of a nominal combat or expedited recovery in IMC. This task should be able to be performed with Level I handling qualities. Potentially more demanding tasks such as terrain following or target tracking have not been explored.

The wind and turbulent environment can be classified as mild to moderate. Much more severe environments are frequently encountered in the field.

A lower limit than that associated with a nominal precision approach may be required to ensure satisfactory performance of potentially more demanding tasks or nominal tasks in more severe environments.

Training and Pilot Compensation Techniques

Pilots, with sufficient training will develop delay compensation techniques. In compensation, the pilot would reduce his input magnitude and frequency. This technique would not only allow the aircraft and display to respond, but also limit the response magnitude to a controllable level. This technique, by its nature prohibits high frequency precision control, and requires the acceptance of task performance degradations.

Another technique that can be used is lead compensation. This technique involves an initial control overshoot by the pilot to quicken the response followed by a reduced steady state input to limit the response magnitude. As with lead compensation implemented with the avionics or FCS, pilot lead is effective, but only over a given frequency range. Furthermore, this technique, by its nature, requires the pilot to stay in the control loop, with his energy split between two primary control frequencies, one associated with his application of lead (high frequency), and one associated with the fundamental task requirements.

Under normal conditions, pilot compensation can be effective. In emergency conditions or during sudden severe disturbances, the pilot tends to abandon compensation techniques instinctive control. Under these circumstances, the pilot will increase input magnitude and frequency in an attempt to retain control of his aircraft. This, however, accentuates the detrimental effects of latency and only aggravates the control problem. In the extreme, an aircraft with large delays, but readily controllable with appropriate pilot compensation, will become uncontrollable in emergency conditions or during sudden severe disturbances.

Negative training is also an issue. Although the compensation techniques described above can be effective with large delays, they can be detrimental if applied to a system with low delays. If compensation techniques used in IMC are retained in performance of a visual task, a degradation in task performance and increase in workload are expected.

Integrating the above issues, the net impact on the application of the simulation data is minimal. Any latency limit, based on analysis of the previously presented simulation data, is expected to be applicable to an actual production aircraft.

CONCLUSIONS

The results from the Navy simulations correlate well. These studies further indicate that performance and flying qualities degradations can be expected to occur with increasing avionics system latency. Considering the simulation data, several latency limits are suggested.

- 70 ms or below to ensure Level I handling qualities.
- 120 ms or below to ensure desired performance (with a maximum 10-percent probability of exceeding constraints).
- 150 ms or below to ensure the avoidance of inadequate performance (with a maximum 10-percent probability of exceeding adequate performance constraints).

These limits were established from analysis of data generated during simulation where the flight control latency was 50 ms. If actual flight control latency differs significantly from 50 ms, the above limits must be examined from a system latency point of view.

ACKNOWLEDGEMENTS

The authors would like to thank pilots USAF Maj. Joe Bonin, USMC Majs. Kevin Dodge and Doug Isleib, and USA CWO4 Reggie Murrell for participating in the study.

REFERENCES

1. Cooper, G.E. and Harper, R.P., *The Use of Pilot Rating in Evaluation of Aircraft Handling Qualities*, NASA TN D-5153, April 1969.

2. Anon., Military Specification, *Flying Qualities of Piloted V/STOL Aircraft*, MIL-F-83300, 31 Dec 1969.

3. Anon., Military Specification, *Flying Qualities of Piloted Airplanes*, MIL-F-8785C, 5 Nov 1980.

4. Anon., *Joint Services Operational Requirements, Joint Services Vertical Lift Aircraft*, 14 Dec 1982.

5. U.S. Department of Transportation, Federal Aviation Administration, Instrument Flying Handbook, AC 61-27C, 1980.

6. Jex, H.R., et al., *Roll Tracking Effects of G-Vector Tilt and Various Types of Motion Washout*, Fourteenth Annual Conference on Manual Control, NASA Conference Publication 2060, November 1978.

7. Clement, W.F., et al., *Systematic Manual Control Display Design*, 13th AGARD Guidance and Control Panel Symposium, Paris, France, Oct 1971.

Session 5

Aircraft Applications and Development

HUMAN FACTOR IMPLICATIONS OF THE EUROCOPTER AS332L-1 SUPER PUMA COCKPIT

R. RANDALL PADFIELD

Flight Instructor, AS332L
Helikopter Service A/S, Norway

ABSTRACT

The purpose of this paper is to identify and describe some of the human factor problems which can occur in the cockpit of a modern civilian helicopter. After examining specific hardware and software problems in the cockpit design of the Eurocopter (Aerospatiale) AS332L-1 Super Puma, the author proposes several principles that can be used to avoid similar human factors problems in the design of future cockpits. These principles relate to the use and function of warning lights, the design of autopilots in two-pilot aircraft, and the labeling of switches and warning lights, specifically with respect to abbreviations and translations from languages other than English. In the final section of the paper, the author describes current trends in society which he suggests should be taken into consideration when designing future aircraft cockpits.

NOMENCLATURE

ADF	Automatic Direction Finder
ADI	Attitude Deviation Indicator
CDI	Course Direction Indicator
DECCA	Area Navigation System
DME	Distance Measuring Equipment
EFIS	Electronic Flight Info. System
FFCL	Fuel Flow Control Lever
HSI	Heading Situation Indicator
IFR	Instrument Flight Rules
ILS	Instrument Landing System
LORAN	Area Navigation System
MGB	Main Gear Box
NG	Gas Generator Speed
NR	Rotor Speed
T4	Engine Exhaust Gas Temp.
VLF/OMEGA	Area Navigation System
VOR	VHF Omnidirectional Receiver

INTRODUCTION

The Eurocopter (Aerospatiale) AS332L-1 Super Puma is a twin-engine commercial helicopter, primarily designed for passenger transport. It is a derivative of the SA 330 Puma which was developed initially to meet a French Air Force requirement for a medium-sized helicopter able to operate day or night in all weather and in all climates. Although used very little in the United States, the Super Puma is popular in many parts of the world and has been particularly successful in offshore oil market in the North Sea. The AS332L-1 is equipped with Turbomeca Makila 1A1 engines, can carry up to 24 passengers, has a maximum gross weight of 18,960 pounds, and has a maximum cruise speed of 150 knots.

The author flew and instructed in Super Pumas for Helikopter Service A/S of Norway, a North Sea offshore operator, and Trump Air of New Jersey, a FAR Part 135 operator. The information contained in this report comes from over five years and 2000 hours of flying experience in the Super Puma and from over 600 hours of instruction and observation of other experienced professional pilots in a six-axis AS332L-1 Rediffusion simulator owned by Helikopter Service.

It is the author's contention that the optimum cockpit design for any aircraft will not be found by the manufacturer alone. Line pilots and instructors can and should help manufacturers decrease the incidence of human factor errors by providing enlightened feedback about ergonomic problems encountered in the cockpit.

Presented at the Fifteenth European Rotorcraft Forum, Amsterdam, The Netherlands, 1989.

THE SHELL MODEL

The SHELL Model (Fig. 1) is one conceptual model of human factors. In the center of the model, is the human operator, or LIVEWARE. When working with a machine, the operator must contend with SOFTWARE, HARDWARE, the ENVIRONMENT, and other LIVEWARE. A mismatch anywhere in the system causes stress, which decreases efficiency and safety.

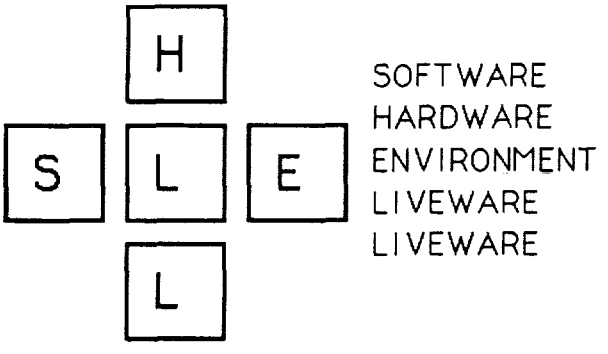

FIGURE 1. The SHELL model of human factors.

HARDWARE relates to the machine itself and, with respect to aircraft, includes such things as controls, displays, warning systems, safety equipment, seat design, and cabin facilities.

SOFTWARE, again in relation to aircraft, includes operating procedures, format of manuals, checklist design, language of information, graphs/tabulation design, and symbology.

ENVIRONMENT includes temperature, noise, vibration, humidity, pressure, light, pollution, and circadian/biorhythmic cycles.

LIVEWARE includes personal relations, crew coordination, discipline, communications, and leadership.[1]

The main concerns of this paper are with the hardware and software portions of the SHELL model. Although there is room for improvement of environmental factors in many aircraft and particularly helicopters, problems with these factors are generally well-known. Liveware factors, i.e. the human-to-human interactions, are usually outside the realm of the designer's influence, although such things as radio and intercom systems, which are also hardware items, have obvious effects on communications. Therefore, both environmental and liveware concerns are outside the scope of this paper.

HARDWARE FACTORS OF THE AS332L-1 COCKPIT

Engine Malfunction Warnings

"OVSPD" warning switch/light. To protect against an engine and rotor overspeed, the fuel control on the Aerospatiale AS332L-1 Super Puma is designed to shut down the engine automatically if the power turbine speed goes too high. Because the main conditions that can cause a power turbine overspeed (high speed shaft or free-wheeling unit failure) happen so quickly, an overspeed warning light (Fig. 2) is provided so that the pilots realize the engine has shut itself down due to an overspeed. This is a good thing to know because one should normally not re-start an engine if this happens.

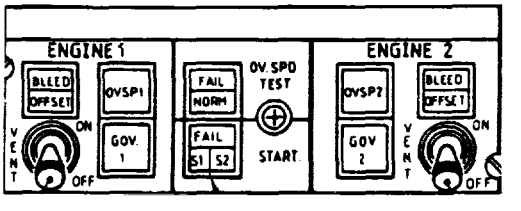

FIGURE 2. "OVSPD" warning switch/light.

A relevant point is that the "OVSPD" light burns steadily when the engine is shut down normally, but the light flashes when the overspeed mechanism shuts the engine down.

This creates a human factors problem. Most pilots have a built-in aversion (although actually it is a conditioned response) to flashing lights in the cockpit. Their immediate gut reaction to a flashing lighted switch is to press the switch to make it stop blinking. A typical example is the master caution light in some aircraft. Another

example is the RACAL Avionics RNAV 1 DECCA system which flashes a warning light that must be depressed when there is a problem. There are certainly many other good examples.

How can a flashing light be a problem? Consider the following scenario. First, one engine fails due to an overspeed. The copilot sees the flashing "OVSPD" light, says nothing, and then, unconsciously, presses the light to stop it flashing. Many companies even specify that the first action during any emergency procedure is to extinguish the master warning light.

A few minutes later, the captain, who up to this point has been concentrating on flying the aircraft, considers trying a restart because he didn't see the overspeed warning light flashing and the light is now steady. The copilot, who cancelled the only indication that would tell them they had an engine overspeed, readily agrees to a restart because he cancelled the light without consciously thinking about it. The engine starts normally, because the broken engine-to-MGB shaft has no effect during the starting sequence, but as the pilots increase power, the unburdened power turbine and its broken shaft spin faster and faster until something else breaks. Although this has never happened in flight, there is one instance of a Super Puma engine being re-started by a mechanic on the ground after the engine had shut down due to an overspeed. The aircraft caught fire and was destroyed.[2]

Three lessons can be learned from this example. First, flashing warning lights should only be used for the most serious of malfunctions. Too many flashing lights in a cockpit defeats their purpose, which is to catch the pilots' attention and alert them to a particular problem.

Second, it should only be possible to extinguish a flashing warning light by taking the proper corrective action and removing the hazard. For example, a flashing fire warning light should only go out when the fire itself has been extinguished.

Third, extreme care must be used when designing a switch to function as both a switch and a warning light. If the light in a switch does more than simply indicate whether an item is off or on, the function of the switch must be easily understood at all times and under all conditions. One should not assume that a task people can do under normal conditions will still be error-free when a panic is on.[3]

"POWER" light. Another engine light that causes problems is the "POWER" light. The "POWER" light is under the direction of the power calculation system which is designed to help the pilots determine which engine is malfunctioning under various conditions. Very basically, the power calculation system examines the Ng (gas generator rpm) readings from both engines and the Nr (rotor rpm) to determine which engine has malfunctioned and why; then it illuminates the "POWER 1" or "POWER 2" light as appropriate.

This is particularly good information to provide the pilot when the automatic fuel control of one engine fails and that engine, although still operating, must be controlled manually. Because the other engine automatically varies its power output in order to maintain Nr within limits, it can be difficult to determine which engine is malfunctioning.

The problem with the "POWER" lights is that they don't illuminate until Nr varies approximately 6-7% above or below the usual in-flight setting of 100-101%. Although these Nr values are neither dangerously high nor low, they are well outside the "usual" Nr values.

Notice the use of the word "usual" and not "normal." After one hundred or so hours in any aircraft, most pilots know what the "usual" values are for pressures, temperatures, rpm, etc. As a result, they become suspicious when they see "unusual" values, even if these values are within the specified "normal" limits. When a helicopter pilot observes an "unusually" high or low Nr, his first reaction is to adjust collective pitch to bring the Nr back to its "usual" normal value.

What happens when an automatic fuel control malfunctions and causes the Nr to vary is that the pilot instinctively adjusts the collective pitch to bring the Nr back to where it belongs. This defeats the intention of the power calculator

system because it cannot illuminate a "POWER" light unless the Nr is above 107% or below 94%. The pilot is left to figure out which engine is malfunctioning by interpreting the Ng and T4 indications; or he can choose to raise or lower the collective until the Nr changes enough to cause the power calculator to illuminate a "POWER" light, an action which many pilots are reluctant to do.

Autopilot System

General. Any pilot who has ever worked with an advanced autopilot knows that the most frequent mistakes made by pilots, even after they know how the system operates, are:

1) pushing the wrong buttons at the right time,
2) pushing the right buttons at the wrong time,
3) pushing the right buttons in the wrong sequence,
4) thinking that an autopilot function is off when it is on, and
5) thinking that an autopilot function is on when it is off.

A primary cause of these errors is the manner by which the autopilot functions are displayed. Usually, the annunciator lights are shown on one central autopilot panel, which is often on the center cockpit console (easy to reach, but out of sight). Sometimes the annunciators are duplicated elsewhere in the cockpit, on the panels in front of the pilots or even on the flight instruments themselves. For example, airspeed hold may be displayed on the airspeed indicator, altitude hold on the barometric or radar altimeter, localizer and glide slope hold on the HSI (Horizontal Situation Indicator) or artificial horizon (ADI).

Of the three methods, indicating autopilot functions on the flight instruments is the best because this is the method the autopilot annunciators will be seen most often by the pilot. The simple reason is that the flight instruments are an integral part of every experienced pilot's cockpit scan. The autopilot annunciator panel on the center console is not a frequent part of most pilots' instrument cross-check.[4]

AS332L-1 autopilot system. The Helikopter Service AS332L-1 Super Pumas are equipped with SFIM 155 duplex autopilot systems, SFIM CDV 85 four-axis couplers, Collins ADI-77 Attitude Direction Indicators, and Astronautics 133640 Horizontal Situation Indicators.[5]

Mixing boxes from different manufacturers may not always be desirable, but due to economic reasons (mixing may be less expensive), operational considerations (one system may not provide all things to all operators), and marketing aspects (compatibility of systems means greater potential sales), mixing systems is not going to go away. As a consequence, designers of the various components have to pay even more attention to human factor problems and, equally important, there must be someone in the loop who is able to examine the resulting system in its entirety.

With respect to the autopilots in Helikopter Service's Super Pumas, when they work as designed, the autopilots are truly impressive. If there is a malfunction, there are, for the most part, sufficient back-ups and warnings for the pilot. In other words, the autopilot hardware, per se, is generally very good.

However, of all the systems in the Super Puma, it is universally agreed in Helikopter Service that the autopilot is the most difficult for pilots to master. Many of the difficulties with the autopilot stem from human factor problems in the design of the system.

Single- or dual-pilot system? The most basic problem with the system is that it can not be fully operated from the left seat. Certain functions, for example coupled ILS and coupled vertical speed, can only be controlled by the pilot in the right seat. The system favors the captain's side of the cockpit to the detriment of the copilot's side.

The reason was Aerospatiale's original intention to obtain single-pilot IFR certification for the Super Puma. This has not been obtained and may never be, but the result is an autopilot system that makes it difficult or impossible to set up, among other things, a coupled ILS approach from the left seat.

Why is this lack of full dual-pilot capability not good? Consider this scenario: The captain becomes incapacitated, the weather at the airport is at minima, and the copilot is young and inexperienced. He needs all the help he can get, but because he can't reach the necessary switches on the right side of the cockpit, he has to fly the ILS uncoupled.

A good general principle to use when designing autopilot and coupler systems is to make all autopilot functions fully controllable from both seats in the cockpit. There should also be one switch, easily accessible to both pilots, that passes autopilot authority from left to right and back again. And there must be a well-defined annunciator prominently located on the front panel (the best place would be right on the artificial horizon) telling the pilots who has the authority.

With respect to single-pilot IFR, the following policy statement from the International Federation of Air Line Pilot Associations (IFALPA) is appropriate:

> "Although IFALPA recognizes that presently single-pilot commercial operations are in widespread use, this type of operation is not acceptable during international public transport flights, including all off-shore flights, because of the reduced level of safety."

Single-pilot IFR capability is great, but it should be available to both captain and copilot alike.

Heading select switch. The Helikopter Service machines have a switch which is used to transfer autopilot authority between the pilot and copilot, however it only controls the heading select function of the system (Fig. 3). Both pilots have a selected heading index, or heading "bug," on their horizontal situation indicator (HSI) which is used to set a desired heading the autopilot coupler should maintain. The heading select switch tells the autopilot which heading index to follow.

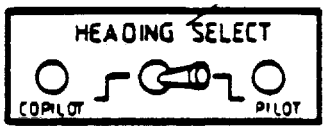

FIGURE 3. Heading select switch.

The idea is simple enough and easy to understand, but the switch and its associated annunciator lights indicating which pilot has heading authority are located on the pedestal console between the pilots, far away from the HSIs and other primary flight instruments. The error, which happens frequently, is that one pilot sets his heading index to the desired heading and, forgetting to check the heading select switch, engages the coupler heading hold. If the switch is still set to the other pilot and his heading index is set at another heading, the autopilot will obviously turn the helicopter to an undesired heading.

This problem could have been avoided by putting the annunciator lights for the heading select switch on the heading indices of the HSIs. When the pilot has heading control, his index is illuminated (or some other way highlighted); when the copilot has heading control, his heading index is highlighted. .

Localizer and glide slope capture modes. The problem with these modes is deceptively small, yet potentially extremely dangerous. The "fix" is probably relatively simple, given the complexities of the rest of the autopilot system.

An Instrument Landing System (ILS) provides precision guidance to a runway while providing very specific obstruction clearances throughout the approach. By regulation and common sense, an aircraft is not allowed to descend on the glide path until it is established on the localizer course.

With the SFIM CDV 85 four-axis coupler, it is possible to arm both the localizer and glide slope modes before being established on either one. This makes sense because the pilots can set up the autopilot before they reach the localizer. What doesn't make sense is that it is possible to capture the glide slope before the localizer is captured, and, in fact, even with the localizer mode unarmed. As a result, the aircraft will descend on the glide slope beam while outside the limits of the localizer, which means that the aircraft could be descending below the minimum altitudes designated for that part of the approach.

Coupler and flight director annunciation. Human factor specialists have often observed that people adapt well to design deficiencies in their working environment. One way Super Puma pilots have adapted to the poor annunciation of the coupler functions is to use the flight director command bars (Fig. 4, #2 & 6) on the ADI as an indication to them that the coupler is on. With the command bars right on the instrument they look at most often, the presence of the bars is not hard to overlook. The pilots simply make it a personal habit to always engage the flight director whenever they engage the coupler.

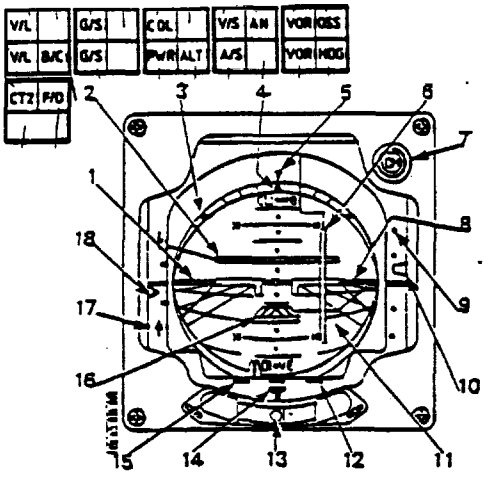

FIGURE 4. Attitude Deviation Indicator

This practice does, however, have one big disadvantage. If the autopilot disengages, due to a malfunction, on purpose, or inadvertently (and it is disengaged inadvertently from time to time), the coupler drops out, but not the flight director. This makes sense because it is useful to have flight direction when the autopilot is out. The problem occurs when the autopilot is switched back on.

It is not difficult to know when the autopilot disengages: one feels the difference in the cyclic at once. The non-flying pilot usually notices the change in the stability of the flight, as well, and if he is alert, he reaches down and re-engages the autopilot within seconds. Both pilots breathe a sigh of relief.

Unfortunately, their problems are not over. For although the autopilot is back on and the flight director command bars are still in view on the ADIs, the coupler is not engaged. The only indication that tells the pilots the green coupler function lights are sending signals to the flight director only and not to the autopilot, is a small, dimly-lit "F/D" light tucked away above the ADIs.

It usually takes some time and perhaps large heading or altitude deviations before the pilots discover that the autopilot coupler functions are not flying the helicopter for them. If this happens during a critical phase of flight, such as during an instrument approach to an oil rig at night, the consequences could be tragic.

"CPL" warning light. Whenever a coupler function fails or is turned off, the "CPL" light on the master annunciator panel and the master "WARN" lights illuminate. Pilots like to have warnings when something fails, but to receive a warning every time something is purposely switched off is counter-productive.

The human factor reason is so obvious that it is difficult to understand how it was overlooked: If a warning light comes on numerous times during every flight,eventually it will be ignored.

The first time a pilot new to the Super Puma switches off a coupler hold function he immediately notices the "CPL" and "WARN" lights illuminating, and, being new to the machine, he logically assumes something has failed. However, by his third or fourth flight, he is already ignoring the "CPL" light or canceling it without thought.

The story about the boy who cried "Wolf!" is a good lesson in human nature which was apparently forgotten when the SFIM designers were working on this part of the CDV 85 four-axis coupler.

Navigation Equipment

NAV-HSI switching panel. Another very confusing part of the Super Puma is the navigation switching panel (FIG. 5). Basically, each pilot has two pointers on the HSI, and he has switches by which he can choose which navigation radios

he wants to monitor. There is also a switch that controls the Course Direction Indicator (CDI) which accepts signals from VOR 1 or VOR 2. However, there is an inflexibility in the system in that the autopilot will accept coupled ILS signals only from VOR 2 and only when the right-seat pilot has selected VOR 2 on his CDI and only when the heading select switch is set to "PILOT." This automatically, restricts the pilots' choices if they want to fly a coupled ILS.

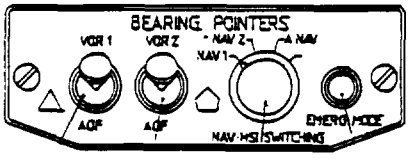

FIGURE 5. NAV-HSI switching panel

The number 1 (green) pointer on both pilots' HSIs takes signals from either VOR 1 or the ADF (or ADF 1 if two are installed). The number 2 (orange) pointer takes signals from VOR 2 and the ADF (or ADF 2 if two are installed).

The confusion occurs because BOTH pointers can indicate either VORs or ADFs and it is common to use both a VOR and an ADF during many VOR and ILS approaches. What can easily happen is that the copilot has the ADF on pointer 1 and the VOR on pointer 2 and the pilot has the opposite indications.

A better system, given the limitations of only two pointers, would be to designate one pointer as the VOR pointer and the other pointer as the ADF pointer, with a switch to reverse these functions in case of a pointer failure. That way both pilots would always know that they have VOR information on the green pointer, for example, and ADF information on the orange pointer. To remove the question of which VOR or ADF is being monitored, the pointers themselves could display a "1" or "2," indicating, respectively, VOR 1 or VOR 2 on the VOR pointer and ADF 1 or ADF 2 on the ADF pointer. The navigation pointers incorporated in many EFIS installations the author has seen are labelled in this manner.

One could monitor two VORs on the same HSI by switching the CDI to one VOR and the VOR pointer to the other. It would not be possible to monitor two ADFs simultaneously on one HSI, but this is a relatively infrequent requirement. (The Helikopter Service Super Pumas are only equipped with one ADF anyway.) If there is a requirement to monitor two ADFs, the pilot could monitor one and the copilot the other, or, as an alternative, either pilot could switch between ADF 1 and ADF 2 every few minutes to check the relative bearings to the NDB stations.

DME selection. It is possible to monitor one of six different DME stations depending on how the switches are set. However, the only indication of which VOR frequency is giving the DME reading is by the position of the switch and a light on the radio itself. The light indicates that the DME is coming from that box (number one or two), but it could be from one of three possible frequencies, one of which may not be displayed, depending on the position of the HOLD switch.

This can and does create so much confusion that Helikopter Service instructors recommend setting the DME function switch to VOR 2 (because this is the only VOR that can be used to fly a coupled ILS approach) and just leaving it there all the time, except in those rare cases when DME information from a second VOR is required. The problem is that there are just too many choices -- too many frequencies from which one can receive DME information. In the heat of an approach or a missed approach, it's easy to forget which DME one is monitoring.

Radio frequency selection. This is a generic problem to many aircraft, not just the Super Puma. Many operators do not have 100% standardized fleets. In fact, there are probably very few operators that have the same radios in all their aircraft. This is obviously a matter of economics that pilots just have to live with.

With most radios, the frequency selected increases when one rotates the knobs clockwise, but on a few the frequencies increase when the knobs are turned counter-clockwise. Some radios allow one to rotate the knob past the highest useable frequency and continue turning to the lowest

frequency on the scale, and vice verse. Others stop at the highest and lowest frequencies, making it necessary to turn the knob back the other way. Most two-tiered knobs (like wedding cakes) work so that the lower, bigger knob adjusts the numbers in the left window (therefore the higher numbers) and the higher, smaller knob adjusts the numbers in the right window (therefore the lower numbers); other radios work just the opposite.

It goes without saying that pilots are going to have trouble tuning frequencies when they have to use different radio sets. This may seem like a relatively small thing, and most of the time it is, but it can be a time-waster. In the worst case a pilot may accidently set the wrong frequency, not have time to check the windows, and miss a critical radio call. Standardizing how frequencies are dialed in will eliminate one area in the cockpit that is prone to mistakes.

Landing Lights

When the search light switch in the Super Puma is pushed down, the search light moves up. When the switch is pushed up, the search light moves down.

This is exactly opposite from the way the moveable search light in the S-61 and Bell 212 work and since all Helikopter Service pilots flew one or both of these helicopters before transitioning to the Super Puma, it's no wonder that this causes difficulty.

Most of the time landing lights are not needed until short final when they need to be positioned quickly and accurately. When the light moves in the opposite direction from what is expected, it's not only irritating, but potentially dangerous as well.

As a rule, moveable landing and search lights should move up when the switch is pushed up and move down when the switch is pushed down.

Intercom Switching

The pilot's and co-pilot's intercom switches are two-position switches, "NORM" and "EMER". In the normal position, the voice-actuated system works, which is an extremely good system to use. The emergency position is there in case the normal power supply to the system is lost. When in "EMER," the pilots have to key the microphone switches on the cyclics or the intercom control panel in order to talk to each other.

The intercom system would be better if the need to switch to "EMER" in case of a normal supply failure were eliminated. In other words, once the pilots discover that the voice-actuated system no longer works, all they have to do is use the cyclic or panel microphone switches.

Trouble-shooting an electrical fire is one emergency when the emergency intercom system is needed. Various electrical suppliers must be switched off, including the normal power supply to the intercom and the autopilot. One pilot must therefore concentrate exclusively on flying while the other pilot is trying to isolate the fire. This is no time for communication difficulties. Requiring both pilots to switch to "EMER" just adds an additional burden and stress factor to the emergency.

SOFTWARE FACTORS OF THE AS332L-1 COCKPIT

General

As noted before, software factors include many items, all of them concerned with information. Often, good, well-designed operating procedures and checklists can make up for design faults in the aircraft. For example, with reference to the flashing "OVSPD" light problem, Helikopter Service has a prominent note in the company Emergency Checklist under "Engine Malfunctions," stating that a failed engine should not be re-started if the "OVSPD" light is flashing.

It is not the intention of this paper to try to examine the flight manual, operating procedures, and all other information sources about the Super Puma, but rather to limit the discussion to the information presented to the pilot in the cockpit. In the author's opinion, the "AS332L-1 Super Puma Instruction Manual" is is very well written. However, there are two main problems with the

manual, which also apply to the cockpit indications. The first is the occasional inconsistency among terms and the second is occasional poor translations from French to English, including abbreviations. These two problems are probably related in many instances.[6]

An example of the first is the use of both "generator" and "alternator" to describe the same thing in the electrical system. Examples of the second type of problems, translations and abbreviations, are discussed below.

"MGB COOL" Warning Light

The Super Puma main gear box has two lubrication pumps, a normal one and an emergency one. Both pumps are essentially the same and both run continuously. The main differences are (1) the main pump delivers a slightly higher pressure, (2) the input to the emergency pump is positioned below the input to main pump, and (3) the emergency pump system bypasses the transmission oil cooler.

If the main pump stops delivering oil, either due to a leak in the system or failure of the pump itself, the emergency pump will continue to supply oil to the main gear box. The emergency pump bypasses the transmission oil cooler because a leak in the system will most likely be in the plumbing to the oil cooler. The emergency pump lubricates everything in the main gear box, but the oil is no longer cooled. As a consequence, one can expect a gradual rise in transmission oil temperature with a failure of the main pump or a leak.

It's obviously important to warn the pilot that this has happened and the "MGB COOL" light (Fig. 6, #6) serves this function. It is triggered by a pressure switch which senses the drop in pressure in the line downstream of the oil cooler.

The theory is very good and the light works in practice, but the language on the light creates confusion. "MGB COOL" does not mean that the MGB is now cool or will become cool. Quite to the contrary, the oil will now become hotter. Nor

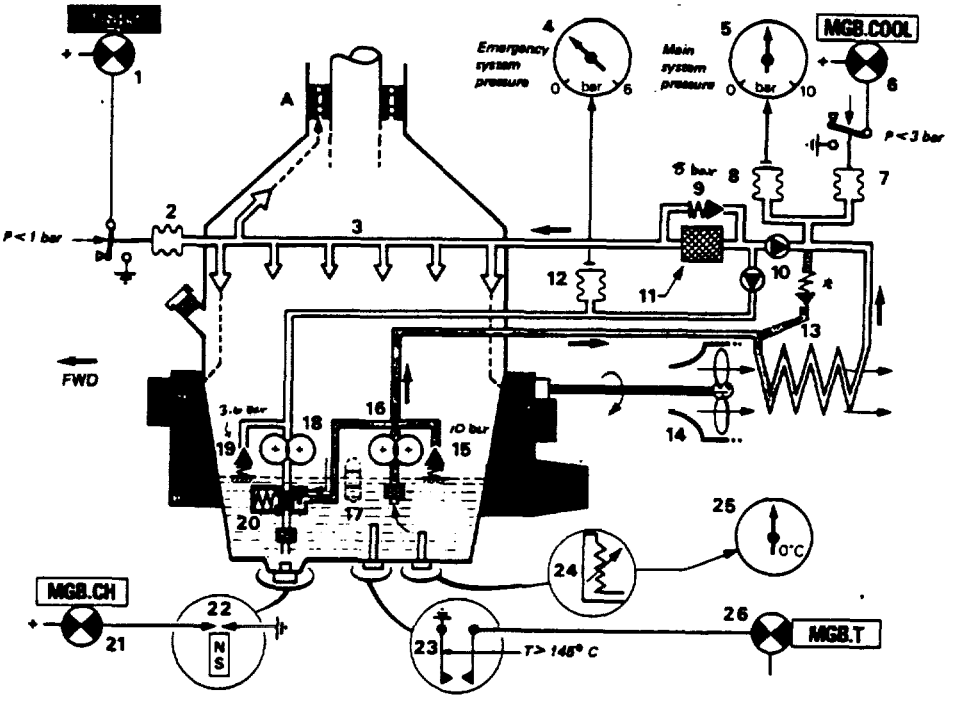

FIGURE 6. Main gear box lubrication system.

does the light mean that the MGB cooler has failed. If the cooler fails, due to a broken drive shaft or shattered fan blades (both of which have happened a number of times), the "MGB COOL" light does not illuminate; what one sees is a rise in MGB temperature and, eventually, a "MGB TEMP" warning light. "MGB COOL" means that the MGB cooler has been bypassed. This is not, however, the most important thing the pilot needs to know at this point, even if he does remember what the light signifies.

The important thing is that the main pump is no longer delivering oil to the system, either because of a failure or a leakage. Therefore, it would seem to make more sense for the light to be labelled so that it better conveys this information, for example, "MGB PUMP." The point is: The wording used on warning lights must be carefully chosen so that the most critical factor of a given malfunction is immediately comprehended.

Hydraulic Panel

The labelling on the hydraulic panel is particularly confusing, even to pilots who have flown the Super Puma for many years (Fig. 7A & 7B). The problem is that the abbreviations are not consistent and this was a result of translating abbreviations from French to English.

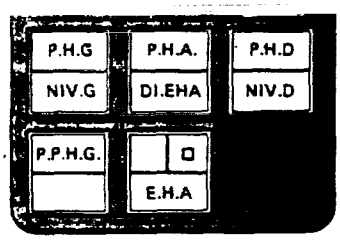

FIGURE 7A. Hydraulic panel with French abbreviations.

The culprits on the English switches are the letters "P" and "H." On some of the switches, the letter "P" stands for "pump" and on other switches it stands for "pressure." On every switch "P" appears, it could logically stand for either "pump" or "pressure."

On some of the switches, the letter "H" stands for "hand" and on others it stands for "hydraulic." On many of the switches, "H" could stand for either "hand" or "hydraulic." On one switch, "H" stands for both "hand" and "hydraulic."

The correct meanings are as follows:

LH.P = LEFT HAND PRESSURE (low)

LH.LEV = LEFT HAND LEVEL (low)

LH.H.MP = LEFT HAND HYDRAULIC MAIN PUMP (failure)

AP.H.P = AUTOPILOT HYDRAULIC PRESSURE (low)

AUX.HP = AUXILIARY HYDRAULIC PRESSURE (low)

AUX.P = AUXILIARY PUMP (failure)

AUX.P = AUXILIARY PUMP (on/off switch)

RH.P = RIGHT HAND PRESSURE (low)

RH.LEV = RIGHT HAND LEVEL (low)

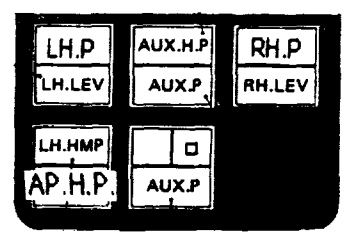

FIGURE 7B. Hydraulic panel with English abbreviations.

It's easy to understand how this creates confusion. Anything that does this, particularly during an emergency, is going to increase the stress level and the chances for mistakes. The lesson is obvious: Make all abbreviations readily understandable and consistent.

"THROT" Light

This light indicates that one or both of the fuel flow control levers (FFCL) is not in the "FLIGHT" position, where they normally should be if they are working normally. It's a useful light with an engine failure and subsequent shut-down because it is the only warning light that remains illuminated after the FFCL has been set in the shut-off position. (The "DIFF NG" and "PRESS 1" or "PRESS 2" lights extinguish when the FFCL is in the shut-off position.)

But why is it called the "THROT" light, and not, for example, the "FFCL" light? The term "throttle" is not used anywhere in the Instruction Manual or the Flight Manual. The proper term is "Fuel Flow Control Lever." The use of the word "throttle" and its abbreviation "THROT" is, perhaps, either a carry-over from the days when most helicopters had reciprocating engines and, therefore, throttles (admittedly, some still do) or perhaps it's just another translation problem from French to English.

The point is: Consistency. Items should always be referred to by the same correct name, both in the flight manual and in the cockpit.

Autopilot Panel

The hardware aspects of the autopilot were discussed previously. The software aspects of the panel are actually quite good, with only a few minor exceptions.

To test the basic autopilot system, one moves the test switch from "TEST" to "RUN," meaning, apparently, that one is "running the test."

On the other hand, to test the collective part of the autopilot (the fourth-axis), one moves the test switch from "NORMAL" to "TEST."

Again, it's a small point, but one that is easily corrected.

"RB. SAFE" and "ROT.BR" Lights

The Super Puma has a two-lever rotor brake system with a rotor brake safe lever and a rotor brake lever. It is possible to move the rotor brake lever to the braking position in flight (which obviously should not be done), but it will do nothing more than cause the "ROT.BR" light to illuminate (Fig. 8). Hydraulic pressure to the rotor brake is obtained only when both levers are pushed forward, a sensible system which just about guarantees that the rotor brake won't be engaged inadvertently at the wrong time.

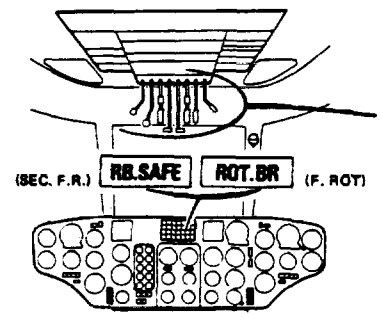

FIGURE 8. "RB. SAFE" AND "ROT.BR" lights

"RB. SAFE" means that the rotor brake safety lever is in the forward position, not, as one may be lead to suspect, that the rotor brake is safe. Actually, one could argue that with the safety lever in the forward position, the rotor brake system is unsafe because, now, if the rotor brake lever is moved forward, braking pressure will be applied to the rotor system. In effect, moving the rotor brake safety lever forward arms the rotor brake system.

So why not label the "RB. SAFE" light "RB ARM?" One could also change the "ROT.BR" light to "RB ON" to make the abbreviation of "rotor brake" consistent.

Heater Distributor Valve Control

The heater has a three-position distributor valve control lever so that the pilots can choose where they want the heat directed. In the forward position, the heat is divided between the cockpit and the autopilot; in the middle position, heat goes to the cockpit, the autopilot, and the cabin; in the aft position, all heat distribution to the aircraft is cut off. The problem with the heater lies in the

fact that the distributor valve control lever has been poorly labelled.

The forward position is labelled "COCKPIT POSTE PILOTE." This looks like a blending of English and French -- it probably means the cockpit will be heated. But it says nothing about the autopilot which is also heated.

The middle position is labelled "O." A person who knows a little French might conclude that "O" is an abbreviation for "ouvert" which means "open." But what is being heated with the switch open? There's no way to determine this from the labelling of the switch. On the other hand, a person who knows no French might think the "O" (oh) is a "0" (zero) and that it means the heater is off or closed.

The aft position is labelled vertically "F C." Again, a French speaker might assume the "F" stands for "fermé" which means "closed" and the "C" might be an English abbreviation for "closed." Then again, both letters could be either French abbreviations or English abbreviations. It's very hard to tell.

This may seem like a small thing again; after all, it's only the heater switch. But it is also confusing, annoying, and totally unnecessary. With only a bit more thought and effort, the lever could have been labelled so that the function of the three positions were obvious.

SPURIOUS WARNINGS

As was mentioned before concerning the "CPL" light illuminating every time a coupler function is switched off, continuous unnecessary warnings eventually are ignored. Complacency with respect to the warning is the result. In some aircraft, pilots have gone so far as to pull circuit breakers for certain specific warning lights because they were so prone to false warnings. MGB chip warning lights are notorious examples.

Sophisticated electronic systems seem to be all too prone to spurious warnings. The numerous landing gear position switches in the Super Puma are particularly sensitive, and if it weren't for the aircraft's emergency electrical and hydraulic extension possibilities, there would be a lot of gear-up landings at Helikopter Service. These switches are not, however, just a problem for the landing gear, but also for all the auxiliary equipment which receive "GROUND" or "FLIGHT" signals from these same switches.

For example, a common problem with the Super Puma is for the area navigation system (be it VLF/OMEGA, DECCA, LORAN, or whatever) to "freeze up" in flight. The solution is to re-cycle the landing gear. The cause is the loss of the "FLIGHT" signal to the area nav system because one of the landing gear has moved out of position far enough to open a switch which should have been closed.

Another related problem concerns the autopilot. Once the author found it impossible to run the autopilot test, even though the switch was moved from "TEST" to "RUN" several times. All the functions worked, but the test just wouldn't run. A mechanic was notified and he immediately realized the problem was a position switch in the nose gear. He grabbed a tow bar, jiggled the nose wheel, and the autopilot test worked as designed.

Incorrect fire warning system tests during start-up are another headache. Mechanics have changed system control cards, wiring harnesses, and fire detectors, but usually the problem is simply moisture. Most of the time the system will test properly after the engines are started and everything is allowed to warm up and dry out.

The point is that pilots quickly loose faith in a warning system if it continually gives false warnings. When a warning system cries "Wolf!" all the time when there is no wolf, the one time there really is a wolf at the door, it may be ignored. The increased use of electronics and computers in helicopters promises numerous advantages for the pilots, but the systems must be constructed so that they are not adversely affected by the environment.

FUTURE CONSIDERATIONS

"New technologies incorporating multiple redundancy and fail-safe concepts are becoming so reliable that, in future years, the proportion of human factor accidents may reach 100 percent simply because the total, irrecoverable failure of machine components of the man-aircraft system will be eliminated."

Dr. Robert B. Lee
Australian Bureau of Air Safety Investigation[7]

"The Space Invader-playing kids of today will be the fighter and bomber pilots of tomorrow."

Ronald Reagan
40th President of the United States

Even though former President Reagan didn't mention helicopter pilots in the above quote, they certainly must be included. What is just as certain is that his prediction is already coming true.

How will this effect human factor problems in the cockpit?

Not more than ten or fifteen years ago, the space and aircraft industries were the epitome of high-tech. In many ways, they still are, but since the advent of inexpensive micro-chips, "smart" machines are now commonplace in most homes. Today, the gap between sophisticated aircraft and sophisticated household machines has narrowed. Entire houses can now be controlled by a central computer. In late 1988, the Electronic Industries Association/ Consumer Electronics Group announced a new wiring standard called the Consumer Electronics Bus which will enable microprocessor-equipped appliances built by one company to communicate with those built by another.[8]

This means that more and more people will use sophisticated electronic and computer-controlled devices on a daily basis. Today, many children learn to operate machines even before they can read.[9] At age four, the author's youngest son knew how to operate the remote controls of a video cassette recorder and television, find and play games on a Macintosh computer, use various cassette players, and heat food in a microwave oven. Operating machines is second nature to him.

Aircraft designers will have a new human factor element to consider. Instead of the automobile, electronic, and other industries mimicking the designs of equipment found in aircraft, the aircraft manufacturers may find themselves copying panel designs from these industries in order to avoid human factor problems in the cockpit. This is not to say that aircraft will loose their place on the cutting edge of technology, but that aircraft designers will have to be more aware of the designs of equipment made by other industries.

For example, affordable, hand-held GPS systems are now available for less than $1000 from a number of manufacturers. It won't be long before a dashboard-mounted GPS becomes a common option in automobiles and trucks. If the GPS receivers pilots find in their aircraft are very dissimilar from these car systems and hand-helds, human factor errors will occur.

In the past, pilots had to contend with transfer of learning problems between their airplanes and their automobiles.[10] These problems will seem minor to the pilots of future generations who will have to contend with transfer of learning problems between their aircraft and their cars, their computers, their home entertainment systems, and numerous other gadgets, appliances, and machines, some of which have yet to be invented.

There will be international "standards" developed and accepted, sometimes by agreements and official decrees, but perhaps more often by the company that is able to sell the most of a particular product first. If a similar machine does not fit the accepted "norm" or the standard that people have become accustomed to, problems will arise.

A human factors problem occurred when Helikopter Service installed a new security system in the main office and hanger. Like the old system, the new one required the use of magnetic-strip identity cards. The old system required one to insert the card in the controller and punch in a four-digit code before the door would open. The new system required that the code be punched in first,

then the card inserted. If the card was inserted first and then the code punched in, as with the old system, a red light blinked indicating something was wrong.

On the first day, hardly anyone could get into the building. Even though instructions had been distributed beforehand, few bothered to read them, assuming wrongly that the new system worked the same way as the old one. Most people thought there was something wrong with their card or their code. The problem was the system itself; the fault was that of the engineer who had not realized that a "standard" for card-and-code door opening systems had already been established at the company.

There may have to be a radical change in the way aircraft are designed. In the past, the machine was foremost. The goal was to make the machine work and if a switch or lever was in an awkward position for the pilot, then he just had to adapt to it. Fortunately, this attitude has changed a great deal since World War II and aircraft designers spend much more attention to ergonomic factors inside the cockpit.

In the future, however, designers will also have to look outside the cockpit, at the numerous other sophisticated machines that are becoming or are already commonplace, when considering human factors problems.

Everything in the cockpit will have to be considered in this light. From the simplest mechanical things, such as the way the seats are adjusted, to the most sophisticated computer-driven systems. Designers will have to stay up-to-date with currently accepted standards in the "outside world." Are computer pull-down menus and "windows" so widespread that they should be considered standards to be used in the cockpit? Should the "QWERTY" keyboard found on typewriters or the keypad used on touch-tone telephones be the standard for aircraft navigation and computer systems? Should the clock be digital or analog, or both? Should the artificial feel in a fly-by-wire control stick have the same "feel" as a Nintendo joystick? These are the kinds of questions that must be constantly and continually asked.

To help answer questions like these, manufacturers must establish, promote, and use an effective feedback system so that ideas and suggestions from line pilots in the field can be obtained on a regular basis.

Every successful company believes it is "the man on the shop floor" who best knows how to do his job and who has the most useful suggestions about how to do it better. Good companies solicit information from every level.

In the author's experience, aviation companies are often very conservative and many even have military-like organizations. Information in military hierarchies goes up and down the chain of command, although it usually flows down a lot easier than it goes up. If the chief pilot or chief of maintenance does not agree with a line pilot's or mechanic's suggestion, the idea stops there and never gets to the manufacturer where it might have been accepted. The only exception is in the case of an accident. Then people are listened to.

A reporting system connecting line pilots directly to manufacturers would be an excellent way to get feedback about present and future cockpits.[11]

CONCLUSIONS

The author readily concedes the subjective nature of this paper. However, given the fact that the very nature of the applied technology of human factors presupposes a degree of subjectivity, the author hopes his departure from the scientific method will not cause his conclusions to be summarily disregarded. In lieu of a feedback system described above, a forum such as this is one of the few ways a line pilot can make his observations and opinions known to people who can make a difference.

1. Flashing warning lights should only be used for the most serious of malfunctions; taking the proper corrective action and removing the hazard, should be the only possible way to extinguish a flashing warning light.

2. Extreme care must be used when designing a switch to function as both a switch and a warning light. One should not assume that a task people can do under normal conditions will still be error-free during an emergency.

3. Autopilot functions should be annunciated on the flight instrument relevant to each particular function.

4. All autopilot functions should be fully controllable from each seat. Single-pilot IFR capability is great, but it should be available to both captain and copilot alike.

5. It should not be possible for the autopilot to capture the glide slope portion of an instrument landing system until the localizer is captured.

6. Warning lights that illuminate every time a minor item, such as an autopilot coupler function, is switched off have a tendency to be ignored by pilots after a few hours of experience in the aircraft.

7. All radio frequency selectors should rotate the same direction: clockwise to increase frequency; counter-clockwise to decrease.

8. Moveable landing or search lights should move up when the switch is moved up and move down when the switch is moved down.

9. The language used on warning lights and switches should be consistent with the wording used in the flight manual, checklists, and other related material; the wording must be carefully chosen so that the most critical factor of a given malfunction is immediately comprehended; abbreviations should be consistent, logical, and easily interpreted; translations to other languages must be very carefully checked for correct meanings.

10. Electronic and computer-based systems must be constructed so they are not adversely affected by the environment.

11. Cockpit designers must look outside the cockpit, at the numerous other sophisticated machines that are becoming or are already commonplace, when considering human factors problems that may occur in the cockpit.

12. Manufacturers should establish, promote, and use an effective feedback system so that ideas and suggestions from professional pilots are obtained on a regular basis.

FINAL THOUGHT

If Dr. Lee's predictions about the proportion of human factor accidents reaching 100% is right, then constant awareness of and attention to human factor problems by everyone involved with the design and operation of aircraft will be the only way to prevent aircraft accidents in the future.

REFERENCES

1 Hawkins, F., Edwards, E., A HUMAN FACTORS AWARENESS COURSE, KLM.

2 Padfield, R., "Man/Aircraft Interface and Aviation Safety," VERTIFLITE, July/August 1988.

3 Warr, P., PSYCHOLOGY AT WORK, Penquin Books, 1987.

4 Padfield, R., "Human Factor Problems of North Sea Helicopters in the 1990's," VERTIFLITE, September/October 1988.

5 FLIGHT MANUAL AS 332 L, Customized Helikopter Service, Aerospatiale, 1984 with later revisions.

6 SUPER PUMA AS332 INSTRUCTION MANUAL, Aerospatiale, Issue 1983.

7 Lee, R., PILOT PERFORMANCE AND FLIGHT SAFETY, Flight Safety Foundation, 1987.

8 Elmer-DeWitt, P., "Boosting Your Home's IQ," TIME Magazine, 23 January 1989.

9 Blake, P., "How Machines Can Defeat People," TIME Magazine, 4 July 1988.

10 Termøhlen,J., Byrdorf,P., GENERAL PILOT INSTRUCTOR COURSE, SAS, 1989.

11 Padfield, R., Learning to Fly Helicopters, TAB Books/McGraw-Hill, PA, 1992.

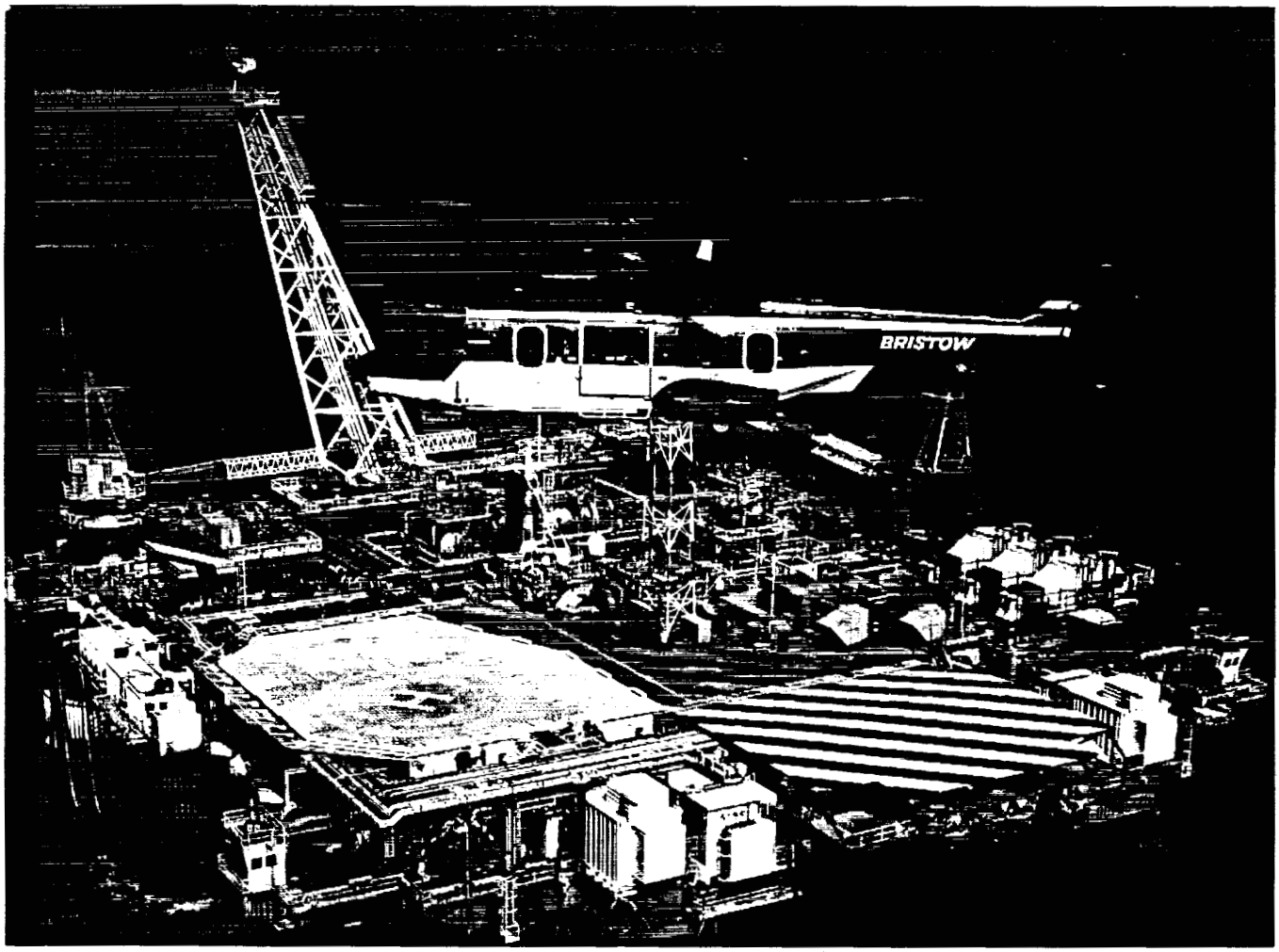

EUROCOPTER AS332L-1 SUPER PUMA

Piloting Considerations for Terminal Area Operations of Civil Tiltwing and Tiltrotor Aircraft

William S. Hindson
Gordon H. Hardy
George E. Tucker
Research Pilots

William A. Decker
Aerospace Engineer

NASA Ames Research Center
Moffett Field, California

ABSTRACT

The existing body of research to investigate airworthiness, performance, handling, and operational requirements for STOL and V/STOL aircraft was reviewed for its applicability to the tiltrotor and tiltwing design concepts. The objective of this study was to help determine the needs for developing civil certification criteria for these aircraft concepts. Piloting tasks that were considered included configuration and thrust vector management, glidepath control, deceleration to hover, and engine failure procedures. Flight control and cockpit display systems that have been found necessary to exploit the low-speed operating characteristics of these aircraft are described, and beneficial future developments are proposed.

NOMENCLATURE

CTOL	Conventional Takeoff and Landing
IMC	Instrument Meteorological Conditions
SAS	Stability Augmentation System
STOL	Short Takeoff and Landing
V	Airspeed
V/STOL	Vertical/Short Takeoff and Landing
γ	Flightpath angle
θ	Pitch angle

INTRODUCTION

After many years of research and testing of numerous and diverse V/STOL concepts, the possibility is now emerging that tiltrotor and tiltwing aircraft might enter civil operations during the next decade (Refs. 1, 2). Indeed, the V-22 Osprey tiltrotor aircraft, a military prototype currently undergoing acceptance testing, is paving the way for possible civil applications.

Presented at *Piloting Vertical Flight Aircraft: A Conference on Flying Qualities and Human Factors*, San Francisco, California, January 1993.

During the past several years, various piloted simulations have been conducted of both of these design concepts (Refs. 3 - 5). The objectives of these simulations have included concept evaluation, detailed systems development, and the investigation of airworthiness and certification issues associated with the operation of these aircraft in instrument meteorological conditions (IMC) in the terminal area.

At the same time, many research efforts conducted over the past three decades have examined the stability and control, handling, and performance requirements for both powered-lift STOL transport-category aircraft and military jet V/STOL aircraft. References 6-11 and their associated bibliographies provide a comprehensive summary of this research. More recently, the introduction of digital flight control technologies has stimulated research in integrated flight/propulsion control for V/STOL aircraft, partly with the objective of providing a consistent control mechanization for the pilot over the high-speed and low-speed flight envelopes where thrust vector orientation differs markedly (Refs. 12, 13). Even though the tiltrotor and tiltwing design concepts received scant mention in the evolution of these V/STOL design requirements, much of this background research is relevant to these aircraft. Consequently, it is one objective of this paper to associate some of the airworthiness and piloting issues for these two aircraft design concepts with some of the general criteria contained in these references.

Considerable research has also been conducted over the past two decades to investigate operational procedures, flight control, and cockpit display systems needed to support terminal area operations by powered-lift STOL, V/STOL, and rotary wing aircraft in IMC. In addition to exploiting the short or vertical landing capabilities of these aircraft, the expectations implicit in this research have been to take advantage of their potential to operate in airspace not easily used by higher speed conventional

aircraft and hence increase the throughput of the air traffic control environment. The low-speed kinematics associated with these operations dominate many of the piloting issues, such as the initial deceleration procedure, the determination of the scheduled glidepath angle, the corresponding selection of the aircraft approach configuration, the attendant safety margins, and the influence of winds and turbulence. Hence, much of this research is also generally applicable to tiltrotor and tiltwing operations (Refs.14-17).

In addition, investigations focusing on IMC terminal area operations specific to the tiltrotor and tiltwing design concepts have been conducted. A large moving-base simulator was used to evaluate three candidate conversion procedures for tiltrotor aircraft executing 6 degree instrument approaches (Ref. 3). A subsequent simulation evaluated various levels of control integration and flight director sophistication during both constant speed and decelerating approaches on glidepaths as steep as 25 degrees (Ref. 4). For the tiltwing concept, flight tests in simulated IMC using a programmable electronic display system for approach guidance were conducted (Refs. 18-20). The research reported in Ref. 21, although conducted in "visual" conditions, represents a recent ground-based simulation of the tiltwing concept that included investigations of decelerating and descending approaches to hover.

This paper seeks to distill from this body of prior research those piloting considerations deemed important in the operation of civil tiltrotor and tiltwing aircraft. In the presentation which follows, the distinguishing characteristics of each design that impact pilot control are discussed briefly. Basic procedural philosophy from transport category CTOL operations is reviewed to establish a desirable guideline for civil V/STOL operations. Next, configuration management issues associated with thrust vectoring and conversion from cruise to powered-lift flight are discussed, including recommendations specific to both tiltrotor and tiltwing concepts. Glidepath tracking considerations are reviewed, including comments concerning the execution of curved, decelerating, and descending approaches. Throughout, there is discussion of flight control and cockpit display systems that must be provided to ease the piloting task. Finally, some of the piloting considerations that would be involved in the event of engine failure during the steep approach (or go-around) are reviewed.

PRINCIPAL FEATURES OF TILTROTOR AND TILTWING

The tiltrotor and tiltwing design concepts have significant differences that have long presented the opportunity for interesting technical discussion (Ref. 22) . Although it is not the objective of this paper to promote the relative merits of each design concept, some of their unique characteristics are worthy of emphasis because they lead to differing piloting considerations for the operation of these vehicles in instrument conditions in the terminal area.

Throughout this paper there is little discussion of basic dynamic response criteria, particularly for the angular degrees-of-freedom that are important for the inner control loops. This is not to de-emphasize the importance of these handling qualities to the pilot, but rather is recognition of their already thorough treatment, exemplified in Refs. 7, 8, 10, and 11. Following the approach taken in Ref. 7, for example, it is assumed that good attitude stabilization is provided so that handling qualities in the pitch axis particularly are not a consideration.

Two aircraft, the XV-15 Tiltrotor (Ref. 23) and the CL-84 Tiltwing (Ref. 24) are used to illustrate the principal features of each concept. The helicopter-like characteristics of the XV-15 (Fig. 1) are embodied in two features, the significantly lower disc loading (Table 1), and the use of longitudinal cyclic pitch. Low disc loading results in good low-speed operating efficiencies, lower noise, lower downwash impingement effects, and good vertical axis damping in hover and during low-speed steep approaches.

The use of cyclic pitch control introduces a rotor flapping degree-of-freedom not usually found in tiltwing designs. Not only does this feature eliminate the need for a separate moment-generating device for pitch control at low airspeeds when the nacelles are rotated, it also alleviates some of the sustained pitch attitude changes that otherwise would be required to orient the thrust vector.

Table 1. Disc loading (lb/ft^2)

Titltwing CL-84-1[a]	Titlrotor XV-15[b]	Helicopter S-76B[b]
41	13	7.7

[a] At design max hover weight

[b] At design gross weight

For the CL-84 Tiltwing (Fig.2), the higher disc loading and the fully immersed wing are mainly responsible for its unique characteristics. Much higher propulsive efficiencies make the tiltwing more suitable for missions that emphasize cruise performance, while at low speed, downwash velocities are high and vertical damping is low. Furthermore, the high drag associated with the fully immersed and tilted wing, and the absence of any propeller

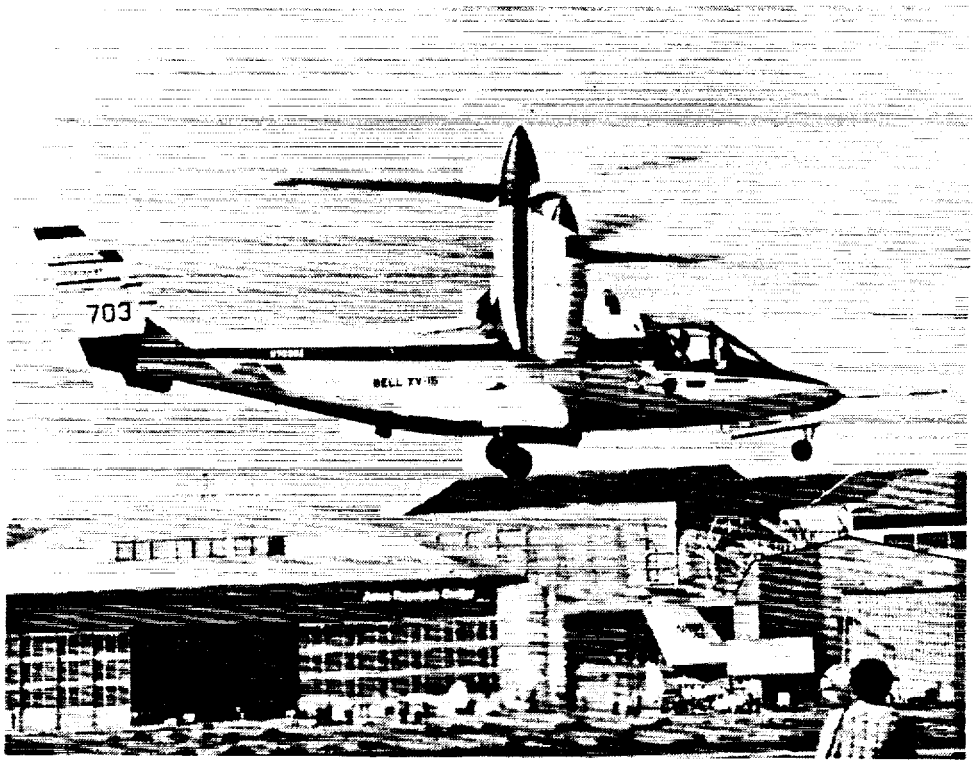

Figure 1. XV-15 Tiltrotor

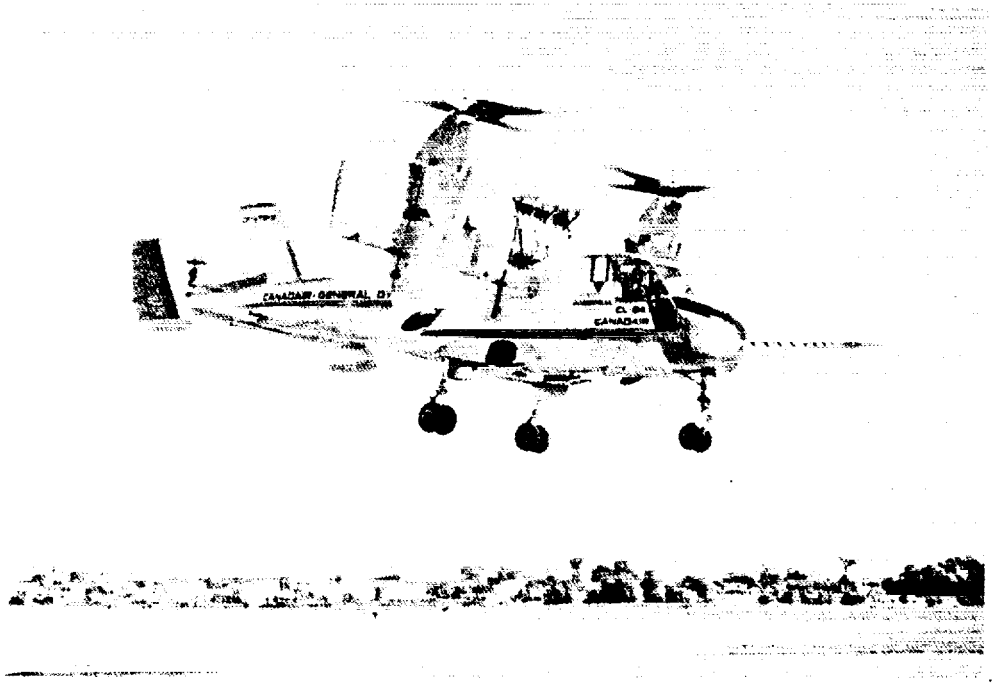

Figure 2. CL-84 Tiltwing

flapping degree of freedom both serve to make pitch attitude an unusually ineffective control at low speed for accomplishing speed or flightpath control. In the tiltwing, an auxiliary effector is used in the absence of propeller cyclic for pitch attitude control at low speed.

One of the major differences in the two designs is reflected in their level flight "conversion corridors", depicted in Fig. 3. Figure 3(a) shows the relatively wide range of airspeeds available to the XV-15 pilot in level flight at nacelle angles above zero (Ref. 23). In contrast, Fig. 3(b) shows that the CL-84 pilot had available only a very narrow range of airspeeds at each intermediate wing angle when constraints on comfortable pitch attitudes are taken into account (Ref. 24). To be discussed subsequently, these characteristics are the source of important procedural, workload, and handling qualities considerations for the pilot in his configuration management of the aircraft during terminal area entry, approach, and landing.

Further information concerning the pilot control requirements during the conversion to powered-lift is revealed in the level-flight power-required curves for the XV-15 and CL-84 shown in Fig. 4 (Refs. 25, 24). The progression of operating points from the frontside of the power-required curve during initial maneuvering, to the minimum drag point (typically) during steep low-speed descent, and then fully onto the backside for deceleration to hover is of significance. Especially for the tiltwing, a large increase in power is required as hover is approached. Associated with this change in operating points for both concepts, and corresponding to the change in orientation of the thrust vector angle from horizontal to vertical, is a change in pilot technique for managing airspeed and flightpath angle. Some of the pilot control and cockpit display issues involved in transitioning from a conventional "frontside" technique to a "backside" control technique during precision instrument approaches are described in Refs. 4, 8, 13, 15, and 26.

The flightpath angle-airspeed (γ-V) trim maps described in Ref. 8 portray best the piloting technique, aircraft performance, and safety margin considerations associated with the low-speed steep approach configurations. The γ-V map for the simulated tiltrotor aircraft of Ref. 4 in the approach configuration with nacelle angle 80 is shown in Fig. 5(a). The vertical slopes of the constant attitude lines indicate that flightpath control about the scheduled 6 degree path, D in Fig. 5(a), can be achieved with minimum crosscoupling into speed using power adjustments alone while maintaining constant attitude. The locally horizontal segments of the constant power lines indicate that airspeed control about the scheduled operating point can be achieved with minimum crosscoupling into flightpath by using attitude adjustments while maintaining constant power. The

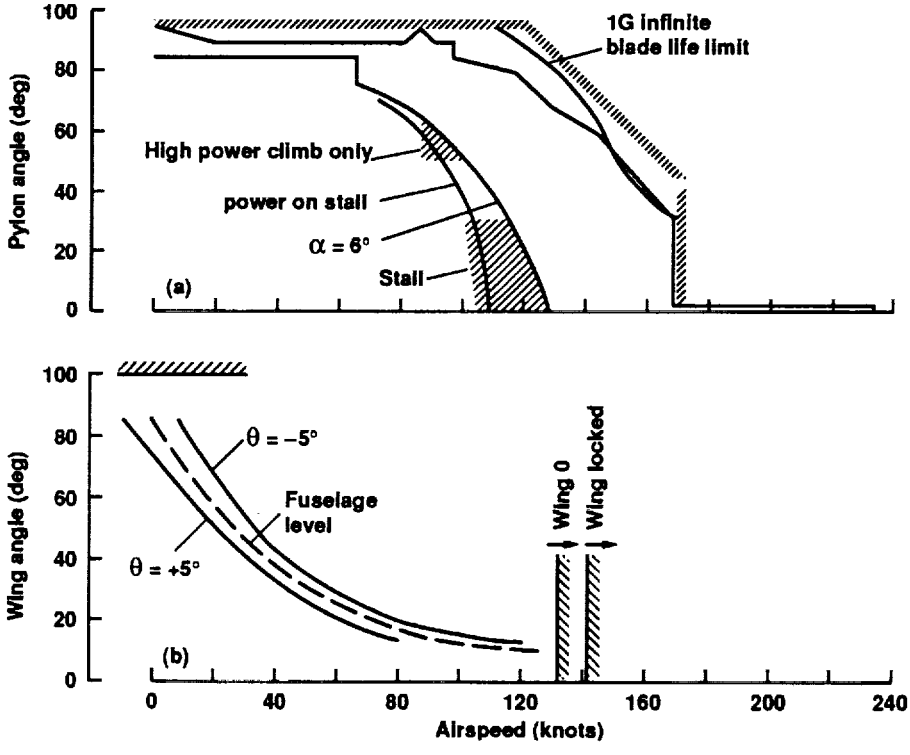

Figure 3. Level-flight conversion corridors. (a) XV-15; (b) CL-84

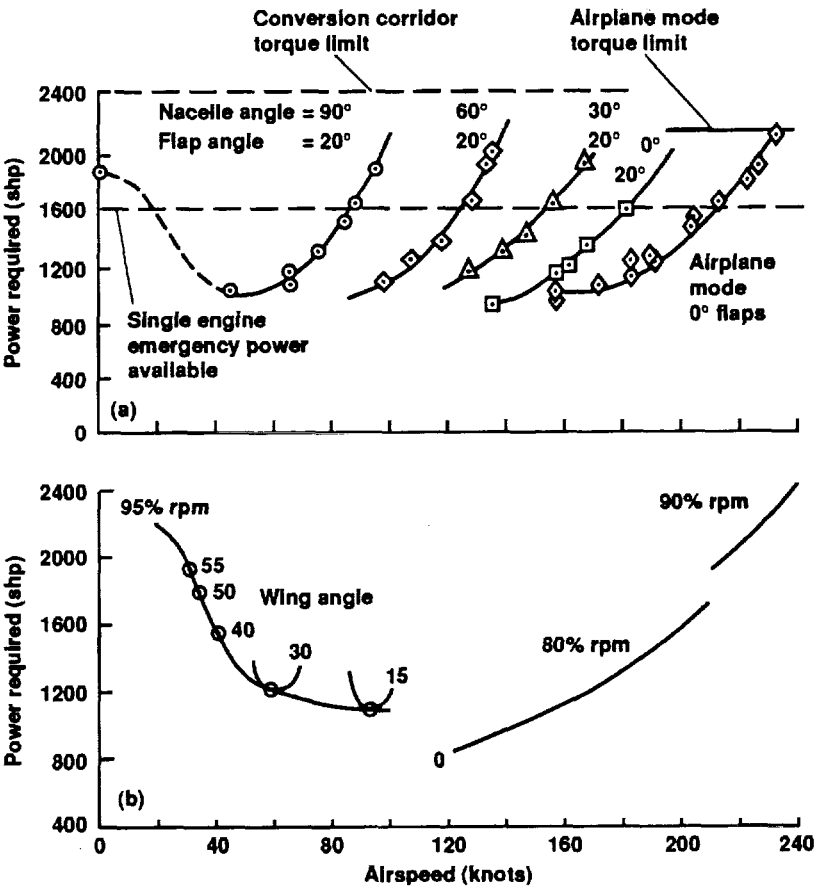

Figure 4. Level-flight power required. (a) XV-15; (b) CL-84

relatively shallow gradient between the constant attitude lines indicates that pitch attitude changes would be moderately effective in controlling airspeed with a sensitivity of about 6 kt/deg. Yet the speed-attitude stability of the tiltrotor is strong enough that the piloting technique of maintaining a specific pitch attitude reference during approach (within 0.5 degrees for example on an expanded-scale attitude indicator) would be effective in maintaining the approach airspeed within a narrow range. A good pitch-attitude-hold stability augmentation system (SAS) would greatly facilitate this aspect of the pilot's control task.

In comparison, the tiltwing is characterized by such excessive speed stability that the use of pitch attitude is considered impractical as a mechanism for speed control because excessively large attitude changes would be required. This consideration becomes of particular concern for civil operations, where pitch attitude usage for both trim and control should be kept within about 5 degrees of fuselage level. Figure 5(b) shows a γ-V map representative of a tiltwing with wing angle 40. Flight-test data from Ref. 24 were used to plot the strikingly steep gradient between the constant attitude lines, only 1.2 kt/deg. Changes in the component of gravity along the aircraft longitudinal body axis brought about by pitching are offset by the large changes in drag that result from only very small speed changes.

Pitch attitude thus cannot be used effectively as an active method for setting or even for regulating airspeed in the tiltwing. Rather, airspeed is so strongly determined by wing angle that pitch attitude should be considered simply as a configuration setting, controlled most effectively by a good attitude-hold SAS. In the final analysis, speed regulation at the intermediate and higher wing angles is of little importance anyway, since it has little influence on aerodynamic safety margins, or on trajectory. Instead, wing angle and power setting strongly dominate these considerations.

Finally, the buffet that is characteristic of the tiltwing in the low-speed descent configuration poses significant design, piloting, and operational considerations, since it presents a significant limitation on feasible descent and deceleration profiles. Figure 6 from Ref. 27, to which

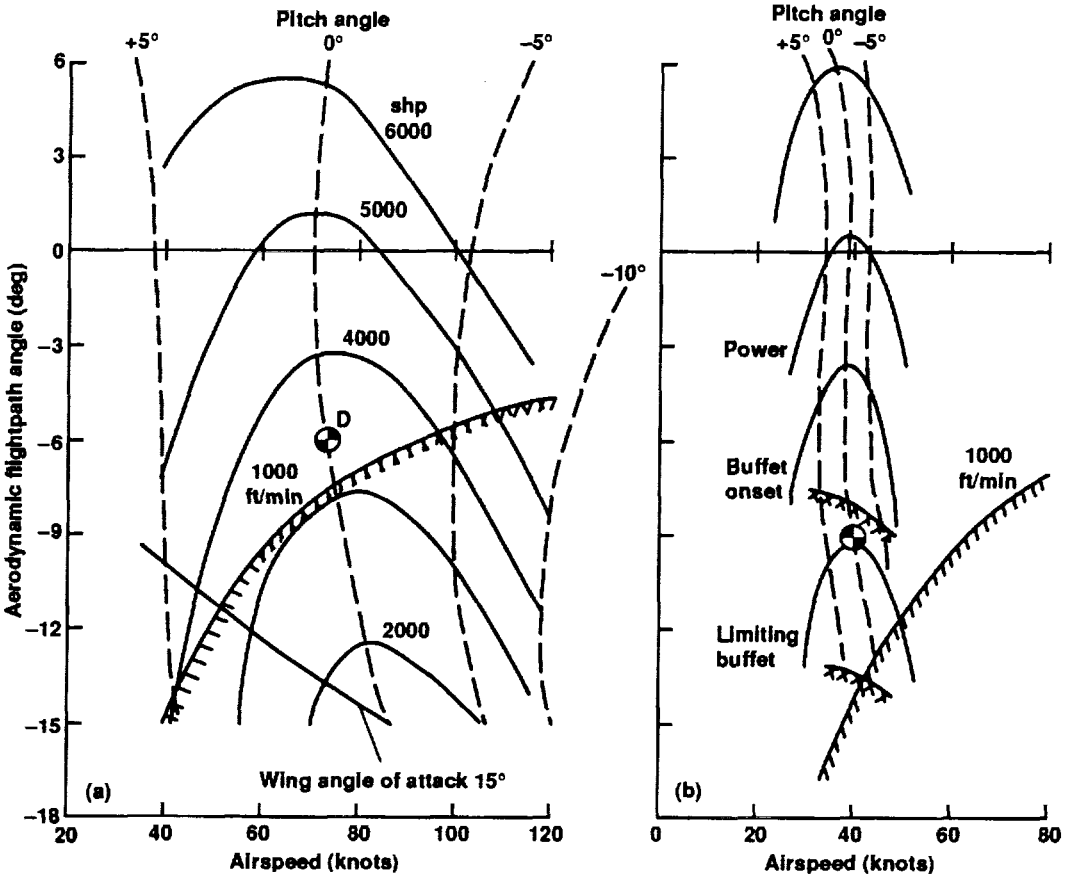

Figure 5. Trim conditions during steep descent. (a) Tiltrotor, nacelle 80 deg; (b) Tiltwing, wing 40 deg

flight-test data provided in Refs. 24 and 28 have been added, depicts the buffet boundaries for the CL-84 prototype and a subsequent model, the CL-84-1 aircraft. The buffet occurs when operating near the maximum lifting conditions for the wing, and is thought to be influenced by the basic wing chord/propeller diameter ratio, the details of the wing leading edge and trailing edge flap schedules, the fuselage incidence angle as reflected by the trim pitch angles used for approach (nosedown attitudes were alleviating), and details in local wing contours and surface condition. The reasons for the differences in the buffet characteristics between the two models were not well understood even by the aerodynamic designers (Ref. 27). Indeed, the published data appear to be somewhat inconsistent, suggesting that efforts were constantly underway to improve the aerodynamics associated with the problem.

Reference 28 describes a buffet encounter in the CL-84-1 in the wing 40 configuration that represented a limiting flight condition: "Although the power was held constant for the next 7 to 8 seconds, the indicated rate of descent did not stabilize and continued to increase (above 850 fpm) until buffeting and nose and wing drop occurred." Relatively small low frequency pitching oscillations frequently preceded nose-drop. Although progressively deeper penetration into buffet represented a significant disruption to the flight condition, recovery of the aircraft was easily effected by adding power.

The significantly different characteristics of these two aircraft designs, and their clear differences from CTOL aircraft argue undeniably for special operating procedures. Yet it is important to recognize that there remain aspects of their operation that can be patterned beneficially on CTOL experience.

CTOL OPERATING GUIDELINES

It might be said that there are at least two fundamental differences between CTOL and V/STOL operations. The first arises from the operating environment. To facilitate the integration of V/STOL aircraft in the confined noise-sensitive route structures of busy terminal areas and to exploit the operating potential of these aircraft, curved and steep flightpaths to vertiports or to designated sections of existing airports will be required. The unusual low-speed kinematics and the correspondingly greater effect of winds at the surface and along the approach path impact both the

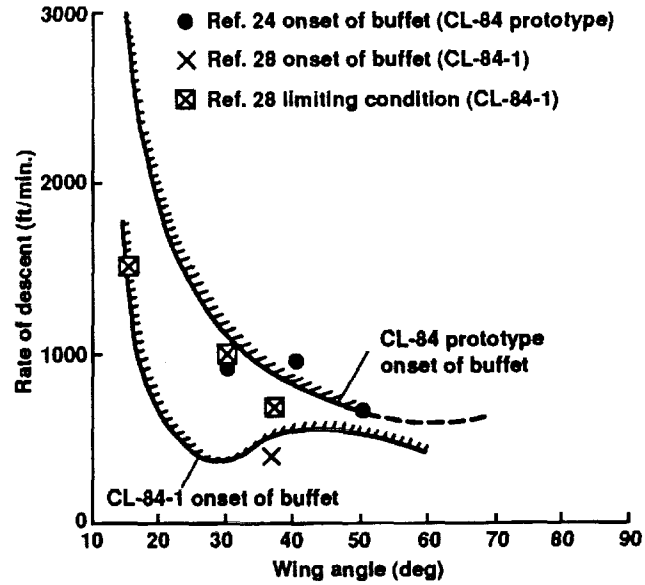

Figure 6. CL-84 Tiltwing buffet boundaries

geometry of terminal area flightpaths and the descent and climb performance of the aircraft in its low-speed high-drag configuration.

The second fundamental difference is associated with the requirement to orient the thrust vector from a general horizontal direction to a vertical direction in order to gain access to the low-speed portion of the flight envelope. This creates unique configuration management and aircraft control problems for the pilot, and for the designer who seeks to alleviate some of the lift, thrust, drag, and pitching moment effects on the pilot's behalf through various sophistications in flight/propulsion control integration.

These differences notwithstanding, there is a clear need and good justification to strive for close similarity with the operational procedures and flight control characteristics that have evolved over decades of operating CTOL aircraft in the civil environment. These procedures and characteristics, broadly reflecting simplicity and conservatism and motivated largely by achieving maximum possible safety, are often substantially different than ones that may be appropriate for the military missions with which V/STOL aircraft typically have been associated. Hence, it may be important to emphasize within the V/STOL community the sometimes differing character of civil operations as civil V/STOL designs are developed. Those operational procedures and flight control considerations that follow CTOL experience and which are relevant to the theme of this paper are discussed below.

1. On arrival in the terminal area, a reasonable maneuvering speed is established that is consistent with air traffic control requirements. This typically involves an initial flap setting and a speed in the vicinity of 200 kt. For V/STOL aircraft, there would also be preparation for initial thrust vectoring (such as wing or pylon unlock).

2. At a well delineated point just prior to beginning descent, the approach configuration is established while in level flight. For a CTOL aircraft, this often involves several progressive flap selections, each accomplished by a single pilot or co-pilot action. Specific guidelines are used to determine when it is appropriate to effect the next configuration change, such as known distance from the final approach fix, approaching glideslope intercept, or crossing the outer marker. Configuration changes are designed or indeed required to be benign to the pilot's control task and to the quality of the passengers' ride. For V/STOL aircraft, these configuration changes would involve thrust vectoring. The final action just prior to beginning descent (such as undercarriage selection) is often one that yields the drag and thrust settings appropriate to the scheduled descent angle.

3. During descent, the pilot is actively manipulating at most two longitudinal controls, one to maintain or adjust the flight reference (usually airspeed) and the other to maintain the flightpath. Prior to landing, there may be at most one more single-action configuration change, such as the selection of final landing flaps. The lateral flightpath is maintained by actively manipulating the same pilot control inceptor used for active control in the longitudinal axis. In normal circumstances pedal control is not required.

4. Should an engine failure occur at any point on the

approach, there is at most one single-action configuration change needed to continue to land, or to achieve a positive climb rate if the pilot elects to go around.

These important guidelines are reflected in the proposed airworthiness standards for civil powered-lift aircraft contained in Ref. 8. The remainder of this paper discusses the terminal area operation of civil tiltrotor and tilwing aircraft in the context of these well-established general procedures.

CONFIGURATION MANAGEMENT DURING INITIAL CONVERSION

Findings from Previous Tests

In V/STOL aircraft, decelerating transitions to hover have typically been more difficult to perform than accelerating departures. Even so, the management of aircraft configuration through conversion from cruise to hover did not emerge as a significant problem area until flight in instrument conditions was investigated (Refs. 18, 29). Reference 20 describes some of the piloting difficulties encountered in the CL-84 tiltwing aircraft during hooded partial conversions from wing 0 to wing 12, and subsequently, through wing 45 to hover. In that aircraft, the wing was tilted using a beep switch mounted on the top of the power lever. At wing 0, the wing-up tilt rate was 2 deg/sec, increasing linearly from wing 0 to wing 45 where it was maintained at 6 deg/sec. (The wing-down tilt rate was 12 deg/sec from wing 100 to wing 45, thereafter the rate decreased linearly to 3 deg/sec at wing 0.) Although these tilt rates at low wing angles seem modest, their nearly direct equivalence with angle of attack changes assured strong lift, drag, and pitching moment interactions. The effects of these interactions were the main causes for the slower wing tilt-rate scheduling. It is significant that these wing tilt-rates were developed for visual conversions conducted close to the ground where visual cues were good.

In simulated instrument conditions, the piloting difficulties encountered when converting from an initial wing 0, 120 kt configuration to the wing 12, 90 kt initial approach configuration consisted of a strong vertical response to initial wing incidence change, together with a strong nose-up pitching moment. The recommended technique for the CL-84 during this initial wing tilting was to reduce the power temporarily and to simultaneously adjust the fuselage attitude to level, a change of about 5 degrees. The CL-84 had a rather weak pitch SAS in this regime, so the pilot had little assistance in resisting the nose-up trim change and in coordinating the required nose-down pitch change. As the conversion progressed beyond wing 35, which corresponded to about 45 kt, the ballooning tendency decreased rapidly and power had to be added progressively. As described in Ref. 20, even though the correct coordination to maintain level flight during conversion was a demanding task, acceptable levels of performance could be achieved in visual conditions. However, when visual cues were limited to only those available from the CL-84 display symbology, the pilot workload became extremely high.

Similar piloting problems, described extensively in Refs. 3 and 29, were encountered during conversions in "visual" and IMC for simulated tiltrotor aircraft. Schedules ranging from full conversion in level flight to full conversion along the glidepath were investigated. It was determined that "instrument operations employing thrust vector conversion are going to have to provide some additional assistance to the pilot to achieve ratings in the 'satisfactory' category". In addition to the use of a three-cue flight director system, consideration was given to the use of discrete nacelle angle detents rather than the incremental nacelle-rate "beep" switch which was located on the power lever. This detent concept was implemented subsequently and evaluated briefly with favorable results (Ref. 4). Not surprisingly, good attitude stabilization was found beneficial in suppressing unwanted pitching upsets arising from aerodynamic crosscoupling effects when first tilting the nacelles.

Indeed, there seems to be little justification in a civil V/STOL design for the pilot to exercise continuous control over the full range of thrust vector angles, as traditionally provided in the past. Instead, there seems to be a good foundation for implementing several discrete, single-action configuration changes, each tailored to the inherent deceleration characteristics of the aircraft and for minimum crosscoupling. This tailoring would include an appropriate wing or nacelle actuation rate, as well as appropriate flap scheduling. If the pitching moments associated with initial vectoring are strong, an interconnect with the moment effector should be considered to absorp them. Alternatively, the authority and off-load features of the pitch-attitude stabilization system should be such that the moments can be contained. Consistent with existing CTOL procedures, it is preferred to implement these configuration changes as discrete selections in level flight, where the operational significance of flightpath disturbances due to configuration changes is minimized.

Tiltrotor

Shown in Fig. 7 is a possible level-flight conversion sequence for the 40,000 pound tiltrotor aircraft simulated in Ref. 4. Associated with the nacelle angle changes is the automatic flap schedule tabulated in the figure. A

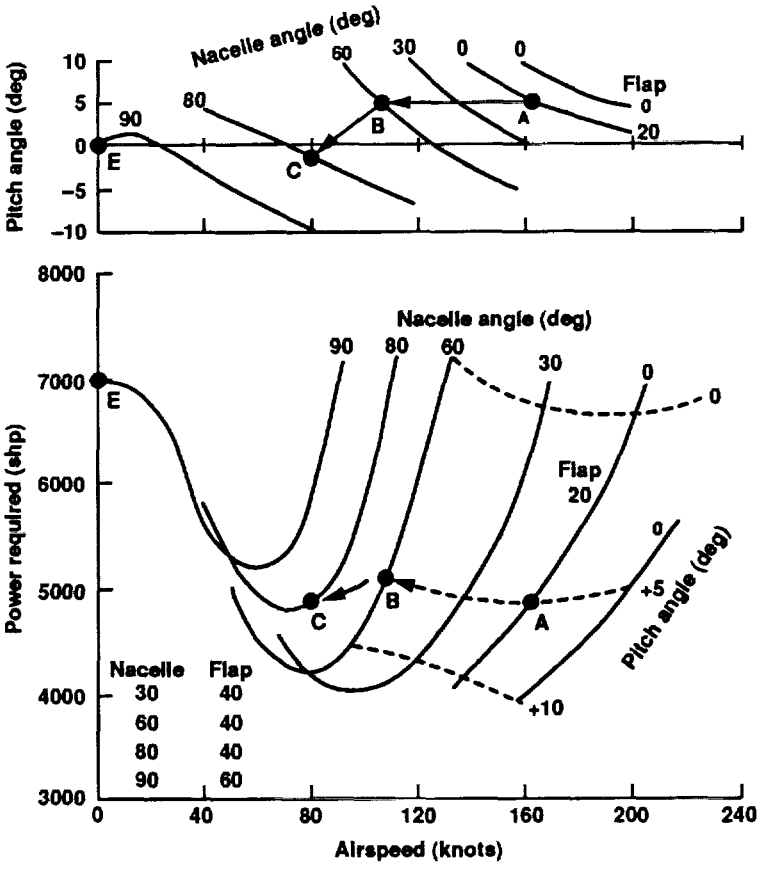

Figure 7. Tiltrotor level-flight trim conditions

manual flap setting of 20 degrees is first selected by the pilot to facilitate initial maneuvering and to reduce the trim pitch angle at lower airspeeds. Point C in Fig. 7 represents the nacelle angle 80 configuration that will be used for descent. Point D in Fig. 5(a) represents the trim conditions on the 6 degree glidepath chosen for this example. To arrive at this approach configuration in level flight with minimal power changes and with the most predictable and repeatable adjustments in pitch attitude, the sequential attainment of points A, B, and C might be recommended. Alternatively, it may be elected to bypass C, and transition directly from B to D upon glideslope intercept. In either case, the management of pitch attitude during this sequence and during the subsequent descent includes regulation about significantly different trim values, emphasizing the importance of pitch axis stability augmentation. In Ref. 4, an attitude-command system with the capability to "beep" the reference attitude to the desired reference value was used. A three-cue flight director was also found necessary to assist the pilot in maintaining the ± 100 ft standard for altitude performance during the level-flight conversion sequence (Ref. 30). The use of attitude-command stability augmentation and flight director guidance is consistent with the findings of Ref. 17, which reviewed many prior investigations of systems requirements for IMC approaches in both helicopters and V/STOL aircraft.

This depiction of the conversion trajectory as a succession of quasi-steady trim conditions is an idealization, since power will still have to be retarded and pitch angle reduced to counter ballooning. Nevertheless, the proposed trajectory represents a useful goal in determining programmed flap and nacelle angles to be achieved in response to each single action configuration change. A final smaller (single-action) configuration change to nacelle angle 90, and a final deceleration would be accomplished late in the approach in order to adjust the trim pitch angle to a range more appropriate for hover and subsequent vertical landing at E.

The data of Fig. 7 were used to plot the conversion corridor shown in Fig. 8, bounded by trim pitch angles deemed in a comfortable range for civil operations. The higher speed portion of the corridor is further limited by torque available at the lower nacelle angles. In the presence of these practical constraints the conversion corridor for the simulated tiltrotor aircraft of Ref. 4 is seen

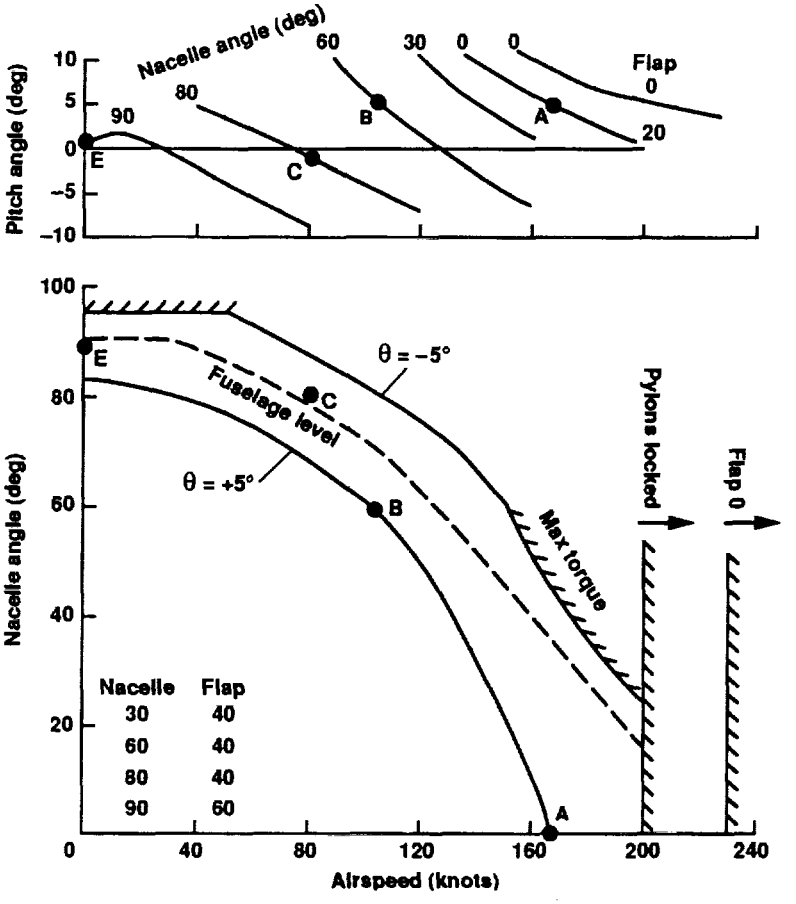

Figure 8. Tiltrotor conversion corridor with attitude limits

to be significantly narrower than first implied by the XV-15 corridor that was presented in Fig. 3(a).

Tiltwing

It should be emphasized that the extreme narrowness of the tiltwing conversion corridor shown in Fig. 3(b) does not imply any difficulty for the pilot in remaining within it. Rather, it reflects an unusually constrained relationship between aircraft configuration and airspeed over which the pilot has little control other than by adjusting wing angle. The utilization of wing angle during the approach and landing, and the influence of this on height control requirements dominate the pilot's task.

For the tiltwing aircraft entering the terminal area, initial procedures would involve a manual flap selection to facilitate maneuvering down to an airspeed in the vicinity of 120 kt, as well as preparation for wing tilting. This would include unlocking the wing, engaging the drive mechanism for the tail-mounted propeller used for low-speed pitch control, and selecting the higher propeller rpm needed for V/STOL operation. For the tiltwing aircraft represented by the conversion characteristics shown in Fig. 3(b), the very strong pitch-heave coupling associated with the first 10-15 degrees of wing angle change, combined with the recommended procedure of simultaneously adjusting fuselage angle to level, both argue strongly for a slowly programmed initial configuration change to about wing 15. Other aerodynamic surfaces such as leading and trailing edges flaps would be scheduled automatically. Selection of this configuration change should be accomplished by a single pilot action, not through the incremental or sustained operation of a wing-tilt rate switch. Control over pitch attitude during this period might be achieved most effectively with an attitude-command system for which the pilot "beeps" the reference attitude down to level. A tailored pitch command implemented within the flight director display would probably be helpful. Additional single-action selections to wing angles 25 and 40, for example, would provide flexibility to the pilot in dealing with strong headwinds during approach while also configuring the aircraft beyond the range where ballooning is most problematic. Although these sequential configuration changes would position the aircraft for the

steep descent portion of the approach, continuous control of higher wing angles must somehow be provided in order to achieve hover.

STEEP DESCENT

Tiltrotor

Having established the desired approach configuration, represented by C in Fig. 7, and just prior to capturing descent guidance, the tiltrotor pilot reduces power and lowers the undercarriage with the objective of arriving at the scheduled descent condition represented by point D in Fig 5(a). Many of the pilot control considerations during the steep low-speed descent are evident from this figure. The 6 degree descent condition selected corresponds to a still air descent rate of 785 fpm, a suitable margin from the maximum value of 1000 fpm recommended in Refs. 6 and 8, and close to the nominal 500 fpm recommended for low-speed aircraft in Ref. 28. The 15 degree angle-of-attack line shown in Fig. 5(a) does not necessarily represent any limiting aerodynamic phenomenom, but in general, any aerodynamic limits along with the minimum and maximum power limits would be represented on this diagram. The nearly vertical constant attitude lines and the locally horizontal segments of the constant power lines at the scheduled operating point reflect little coupling between power and speed as long as attitude is held constant. This permits the pilot to track the glidepath easily using power alone, while simply maintaining a level fuselage angle. A good attitude-retention SAS would facilitate this task, especially in the presence of any transient pitching moments caused by power changes, or by atmospheric turbulence (Ref. 17).

As concluded in Ref. 4, also corroborated by research reviewed in Ref. 17, a three-cue flight director is essential to assuring satisfactory handling qualities and performance during steep approaches, even when conducted at constant speed. Further, the restriction of control in the longitudinal plane to the active manipulation of at most two inceptors, offers the potential identified in Ref. 15 for flying precision curved approach profiles in IMC. As identified in Refs. 15 and 31, the additional aid needed in these circumstances is an adequate means (such as a moving-map electronic display) to assure situational awareness during the approach procedure.

Consistent with other recommendations set forth in Ref. 8 for civil powered-lift operations and easily seen from the γ-V map of Fig. 5(a), (1) there are available at least four degrees of aerodynamic flightpath angle margin above and below the scheduled path with which to accomplish corrections, (2) level flight is easily achievable without any configuration change, and (3) ample safety margins exist surrounding the scheduled operating point to account for gusts and normal tracking errors. In addition, as required by Ref. 8, only two controls are being actively manipulated to track the flightpath and maintain the speed reference.

Tiltwing

As readily seen from the comparitive γ-V trim maps in Fig. 5, the situation during low-speed steep descent is very different for the tiltwing. The useful speed range is dramatically smaller, and the occurrence of buffet even at moderate descent angles severely limits the envelope available. An approach wing angle of 40 degrees and an airspeed of about 40 kt is used as the basis for this discussion, since characteristics of the CL-84 in this configuration are amply described in the literature.

The wing 40 configuration was selected for the CL-84 flight investigations of Refs. 18-20, whose emphasis was on IMC recovery of V/STOL aircraft to small ships. The approach profiles consisted of initial descents on 9 or 12 degree approach paths followed by level decelerations to hover at 100 feet. The wing 40 configuration was chosen as the best overall compromise towards minimizing handling difficulties during final stages of the approach to hover. In strong headwind conditions, a lesser wing angle was used with the objective of maintaining approach groundspeed in the vicinity of 40 kt. Although height rate damping was poor at these low speeds, necessitating display or flight director compensation, the control effectiveness was more consistent and there was less crosscoupling than at lower wing angles. The attitude stabilization system was reasonably effective in assisting the pilot in maintaining the fuselage attitude a few degrees negative during descent, a technique found effective to reduce buffet. However, the crosscoupling from power or wing angle changes to the pitch axis was still considered significant and a source of difficulty (Ref. 20).

The buffet characteristics of the CL-84 were not reported in Refs. 19 and 20 as presenting limitations or causing particular difficulties during the simulated IMC approaches. This implication of relatively benign characteristics is offset by the potential for the much more significant limitations that were described earlier. This characteristic of the tiltwing, barring its complete resolution in future designs, poses the difficulty that the pilot and passengers will likely encounter buffet routinely during descent, if not on the nominal path then during downward corrections to it. Most importantly, it represents a limiting angle-of-attack condition from which protection must be assured.

The methodology developed in Ref. 8 for this type of

limiting flight condition recognizes that angle-of-attack excursions away from the scheduled approach condition are a result of piloting actions such as corrections to glidepath, aircraft or system variabilities such as gust sensitivity or the standards of guidance provided to the pilot, and exposure to vertical gusts. Corrections to glidepath are accommodated by requiring that the scheduled approach path be at least 4 degrees above the prohibited angle-of-attack boundary (which could be drawn on the γ-V map of Fig. 5(b)). The location of the prohibited angle-of-attack boundary is determined by applying the required vertical gust protection, or angle-of-attack margin, to the limiting angle-of-attack (buffet) condition. As seen in the example of Fig. 5(b), there is virtually no angle-of-attack margin available, since the limiting condition is already coincident with the 4 degree maneuvering requirement.

The angle-of-attack margin that is proposed in Ref. 8 provides protection from a 20 kt vertical gust, giving the same level of protection for powered-lift aircraft that is enjoyed by conventional transports. The 30 degree margin (at the 40 kt approach speed) required by this "equivalent safety" standard seems conservative, especially for the tiltwing with its high slipstream velocities. However, it serves to emphasize the improvements that are required in tiltwing buffet characteristics. Equally important, it points to the need to gain operating experience with this class of aircraft to provide a sound basis for the development of sensible airworthiness criteria.

DECELERATION TO HOVER

Operations to designated areas of existing airports might adequately require only short landings from approach conditions like those just described. However, operations to vertiports will require the capability for final deceleration to hover in poor visibility conditions. This final phase was investigated for the tiltrotor during the simulations reported in Ref. 4, and for the tiltwing during the flight-tests reported in Refs. 18-20.

Tiltrotor

Programmed decelerations along the glideslope to a ten foot hover were carried out on 9, 15, and 25 degree descent paths from initial speeds of 55, 35, and 20 kt respectively. The aircraft was first established in the final hover configuration with nacelle angle 90 degrees prior to glideslope intercept, and three-cue flight director guidance was used. The programmed deceleration rate to a 10 ft hover over the pad was 0.025g, or slightly less than 0.5 kt/sec. Breakout altitude was 200 ft, after which the remaining deceleration was accomplished using a combination of flight director guidance and visual references. On the 9 and 15 degree glideslopes, fully satisfactory pilot ratings were obtained for operations in calm air, and borderline satisfactory ratings were achieved in moderate turbulence. (The very steep 25 degree approaches involved high pilot workload, suggesting that such profiles would have to be strongly justified on the basis of vertiport siting requirements to receive continued consideration.) These results are consistent with the CTOL operating guidelines; no final configuration change was required after acquiring the glideslope, and only two longitudinal controls required active manipulation.

A six degree approach initially at 80 kt and nacelle angle at 80 degrees was also investigated. Programmed deceleration was again 0.025g and a 200 ft breakout altitude was used. A fourth flight director cue was incorporated to prompt the pilot when he should begin beeping the nacelle angle to 90 degrees. Satisfactory pilot ratings were achieved, even in moderate turbulence. Similar to the 9 and 12 degree approaches, glideslope tracking performance was approximately 0.2 degree standard deviation. Pilot rating and tracking performance data for the decelerating approaches of Ref. 4 are shown in Fig. 9. Since the power trim data shown in Fig. 7 for the nacelle 80 and 90 configurations indicate only small differences, it can be inferred that the small pitch attitude adjustment associated with selecting nacelle 90 could be accommodated easily within a final single-action selection. This would be comparable to the final flap selection in a CTOL aircraft.

An additional piloting consideration that was identified during the Ref. 4 simulations was the influence of pitch attitude during deceleration on the pilot's field of view. To allow adequate visual reference to the landing zone and vertiport environment, pitch angles within about 5 degrees of level were desired. Although this consideration depends on the particular cockpit environment, it is also considered reasonable for passenger comfort.

Tiltwing

Although piloting considerations in achieving the final hovering configuration are relatively minor for the tiltrotor, they dominate the tiltwing deceleration. In the CL-84, the task in Ref. 20 consisted of beeping the wing from 40 to about 86 degrees while maintaining pitch attitude with the centerstick. Power was slowly increased as wing angle increased, and was modulated to maintain altitude. Despite the pitch SAS that incorporated only a weak pitch attitude term, both power and wing angle changes coupled into the pitch axis, requiring the pilot to intervene to improve attitude-retention performance. The benefits of improved pitch-attitude-hold characteristics in these circumstances were confirmed recently during

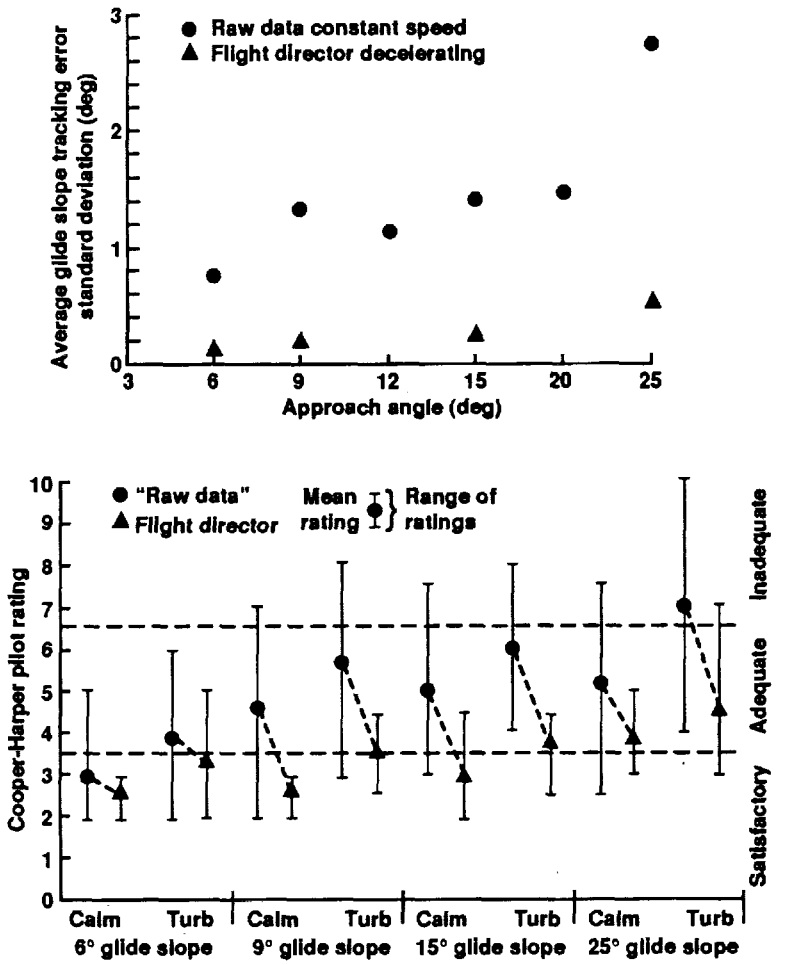

Figure 9. Performance and pilot ratings for steep descents in the simulated Tiltrotor of Ref. 4

investigations conducted in a large moving-base simulator (Ref. 21).

During the CL-84 IMC flight-tests and in the simulation, not only were three longitudinal controls involved in the deceleration, they were also inappropriately available to the pilot. The most traditional and effective control inceptor, the stick, was used only for stabilization, a task that could be accomplished wholly by an automatic system, while the two remaining active controls needed to manage the flightpath were concentrated in one inceptor, the throttle lever. Further, Ref. 32 pointed out the potential confusion in the operation of these power-lever controls in gusty conditions near hover.

Various alternatives have been proposed over the years to resolve these dilemma, such as driving the wing with the longitudinal stick once established in the powered-lift regime. However, the emerging technology of flight/propulsion control integration is perhaps the most effective means for resolution, since it offers the opportunity to optimize not only airframe and propulsion dynamics and aerodynamics, but also the pilot control interface with the vehicle. Various forerunners of this technology have been evaluated both in flight and in piloted simulations (Refs. 13, 33). The concept is illustrated in Fig. 10, taken from Ref. 12. Since it involves modern fly-by-wire architecture, this approach has the added advantage of dispensing with a complex mechanical mixing box and associated control runs.

The piloting difficulties encountered during the IMC decelerations reported in Refs. 19 and 20 were attributed to both control and display factors. Both of the display formats used were exclusively situational in nature, without the incorporation of dynamic compensation in any of the controlled symbology elements. While both display concepts were deemed effective for providing deceleration guidance, both were criticized as deficient in compensating for low vertical damping during approach. Since these early investigations, considerable improvements in display concepts for the shipboard

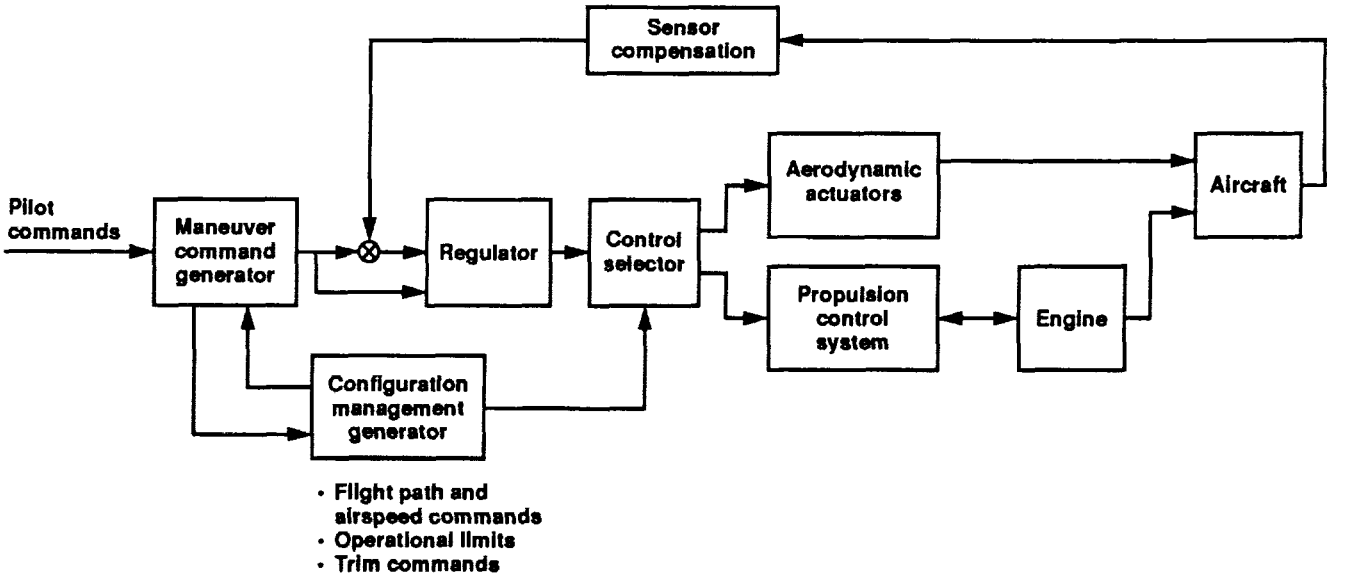

Figure 10. Integrated flight/propulsion control system structure (Ref. 12)

recovery task have been developed (Ref. 34).

The tiltrotor simulations and the tiltwing flight evaluations both confirm the general findings of Ref. 17 that an integrated display format incorporating directly or implicitly groundspeed and range guidance to the hover point is required for decelerating approaches. The display requirements may be reduced if higher levels of control sophistication, such as velocity or acceleration command systems are incorporated. (It is worth pointing out that the very high velocity-damping of the tiltwing results in characteristics that are essentially velocity-command and hold in response to wing tilting.) In any implementation, there is a clear need for symbology drive laws tailored to vehicle dynamics, using methods such as those described in Refs.15, 35, and 36.

Effect of Crosswinds

An important consideration for very low-speed and decelerating approaches is the effect of crosswind. For the pilot it represents perhaps the most significant accommodation that must be made between the air and ground reference frames, requiring the use of an additional control and creating additional display interpretation requirements. Both of these tasks can increase workload substantially in an IMC environment, especially when occurring simultaneously with deceleration.

A variable-stability helicopter was used to evaluate crab versus sideslip during steep decelerating approaches to 25 kt in crosswinds as high as 30 kt (Ref. 37). Only control considerations during simulated IMC were investigated; field-of-view and orientation issues at breakout were not addressed. Under these constraints, crabbed approaches were found satisfactory, as were sideslipped approaches up to a steady-state lateral acceleration level of approximately 0.07g. In the tiltrotor simulation reported in Ref. 4, the pilots evaluated lateral cyclic trim as an alternate means for generating the sideforce required for sideslipped approaches, finding that training in its use and the knowledge of current trim position were important requirements. An important additional control consideration is the availability of adequate authorities in both the yaw and lateral axes for steady-state trim, control, and disturbance-rejection purposes.

The display requirements in crosswind conditions require equally important consideration. Both head-up and head-down implementations are affected by large crab angles. Consistent with the findings of Ref. 17, and based on a review of recent electronic display concepts (eg. Refs. 34, 35), the display feature employed most frequently at very low speed appears to be a horizontal situation format with velocity-vector and landing-pad representation. Other display concepts, such as the flightpath oriented concept evaluated in Ref. 38, together with new head-mounted display technologies warrant further research.

ENGINE FAILURE

Aircraft control, propulsion system management, and aircraft performance are the primary considerations following engine failure. The cross-shafting that is incorporated in both the tiltrotor and tiltwing designs assures that roll and yaw moments are suppressed more

than was typically the case for the powered-lift configurations considered in the development of Ref. 8. Consequently, the tiltrotor or tiltwing pilot, like the helicopter pilot, does not have to deal with lateral-directional control transients and can instead concentrate on the longitudinal control task, particularly propulsion system and flightpath management.

Propulsion system management following engine failure, however, is different than in helicopters and more similar to that required in the powered-lift aircraft considered in Ref. 8. Because of the blade-angle governing system that is typically used on tiltrotor and tiltwing aircraft, the pilot (or an automatic power compensation system) must effectively advance the power-demand lever in order to make available additional power from the remaining engine(s). The reaction time in restoring approach power or in establishing go-around power can be a critical factor in minimizing altitude loss immediately following engine failure. A limited amount of research in this area for powered-lift STOL aircraft has been conducted (Refs. 39-41). One method for assuring that all of the remaining power is easily and immediately available to the pilot without the requirement for an immediate action is with the flight/propulsion control integration concept described in Ref. 12. An integrated flight/propulsion control system with these characteristics was developed and tested in a powered-lift STOL aircraft (Ref. 13). The automatic engine failure compensation feature incorporated in the V-22 Tiltrotor represents a direct approach to solving this problem (Ref. 42).

Tiltrotor and tiltwing aircraft which have been flown to date exhibit engine out performance that is similar to twin-engine helicopters. The operating gross weight is usually such that level flight cannot be sustained below some airspeed in the vicinity of 30 to 40 kt, even at maximum contingency power, or without exceeding transmission limits. As an example, the engine-out climb performance for the simulated tiltrotor aircraft of Ref. 4 is shown in Fig. 11.

If operating at low altitude and at an airspeed lower than about 40 kt at the time of engine failure, the aircraft is committed to land, or if at sufficient altitude, it can be accelerated to a higher airspeed to achieve sustained level flight or climb. In the tiltrotor, the pilot may use either a temporary reduction in pitch attitude or a forward nacelle tilt to achieve, if necessary, the required speed and thence the sustained climb. In the tiltwing, the pilot may have to establish a specific nose-up pitch attitude and the wing angle may have to be reduced simultaneously to achieve the necessary steady climb gradient. Either maneuver is severely challenging for the pilot. As indicated in Fig. 11, the pitch attitudes needed to maximize single-engine climb performance may vary significantly among configurations, pointing to potential benefits that may be gained from specially-programmed engine-out flight director guidance.

Reference 8 includes extensive discussion of both continued approach and go-around for low-speed powered-lift aircraft with one engine inoperative. Performance requirements as well as permitted pilot actions for

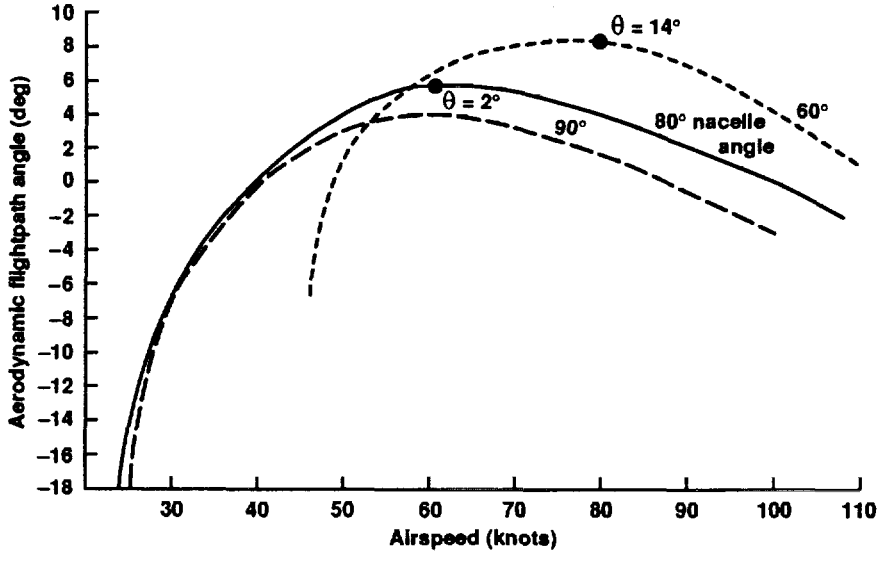

Figure 11. One-engine-inoperative climb performance for the simulated Tiltrotor of Ref. 4

reconfiguration are proposed. Pilot or system delays in initiating the proper go-around action, the environmental conditions, and the obstacle field of the particular landing and take-off zone will all influence critical decision heights and required climb gradients. The recommendations offered in Ref. 8 and the experience to be gained in future V-22 operations can provide important guidelines for developing engine failure criteria for V/STOL aircraft decelerating to hover.

CONCLUSION

Piloting considerations in the operation of tiltrotor and tiltwing aircraft during instrument approach to hover have been discussed on the basis of prior flight-test and simulation investigations, and in the context of general research that has been conducted over the decades on powered-lift aircraft. Operational procedures that have been discussed were patterned on CTOL precepts. Where appropriate, previously developed airworthiness proposals for powered-lift STOL aircraft have been applied to tiltrotor and tilwing V/STOL aircraft. Principal conclusions that can be drawn from this review suggest that (1) single-action discrete configuration changes are preferred that do not require continuous attention from the pilot, (2) attitude stabilization, probably attitude-command in pitch, is desired to reduce workload, and (3) a three-cue flight director are all required to achieve fully satisfactory pilot ratings for the conversion, steep approach, and deceleration. The use of deceleration guidance, including special cuing for setting configurations also appears to be required.

For the tiltwing, there are additional requirements. Low heave damping at the higher wing angles demands compensating dynamics in the flight director or in the vertical axis of the flight control system. The available descent envelope may be limited by airframe buffet. Finally, effective pilot control over wing tilt from initial conversion to hover may require advanced flight/ propulsion control integration.

For both concepts, there is the need to investigate the potential of modern digital flight/propulsion control integration concepts to permit curved, decelerating, and descending approaches in constrained airspace. While the V-22 Tiltrotor is equipped with a redundant digital architecture, the pilot interface with the flight control system remains relatively conventional. At the same time, the thrust and power management systems in the V-22 are highly flexible and represent major advances, but they have not yet been integrated fully with the pilot's controls. These systems provide the means for fully integrated flight/propulsion control, optimizing the mechanization of the pilot's controls and simplifying the pilot's control task. Reductions in pilot workload to be accomplished in this manner can then lead to the benefits long expected from V/STOL aircraft, exploiting time and fuel operating efficiencies, and improving the throughput of the integrated air traffic control system.

REFERENCES

1. Clay, W., Baumgaertner, P., et al., "Civil Tiltrotor Missions and Applications: Summary Final Report," NASA CR 177452, Jul. 1987.

2. Colucci, F., "Tilt-Wing Again." Helicopter World, Vol.10 (2), Apr.-Jun. 1991.

3. Lebacqz, J.V., et al., "Ground-Simulation Investigations of VTOL Airworthiness Criteria for Terminal Area Operations," RAE Conference on Helicopter Simulation, London, Great Britain, May 1990.

4. Decker, W.A., "Piloted Simulator Investigations of a Civil Tilt-Rotor Aircraft on Steep Instrument Approaches," American Helicopter Society 48th Annual Forum, Washington, DC, Jun. 1992.

5. Totah, J.J., "Description of a Tilt Wing Mathematical Model for Piloted Simulation," American Helicopter Society 47th Annual Forum, Phoenix, Arizona, May 1991.

6. Innis, R.C., Holzhauser, C.A., and Quigley, H.C., "Airworthiness Considerations for STOL Aircraft," NASA TN D-5594, Jan. 1970.

7. Franklin, J.A., Innis, R.C., and Hardy, G.H., "Design Criteria for Flightpath and Airspeed Control for the Approach and Landing of STOL Aircraft," NASA TP 1911, Mar. 1982.

8. Hynes, C.S., Scott, B.C., et al., "Progress Toward Development of Civil Airworthiness Criteria for Powered-Lift Aircraft," Report No. FAA-RD-76-100 and NASA TM X-73,124, May 1976.

9. anon., "Interim Airworthiness Criteria for Powered-Lift Transport Category Aircraft." Federal Aviation Administration, Southwest Region Fort Worth, TX, Jul. 1988.

10. anon., "Military Specification: Flying Qualities of Piloted V/STOL Aircraft." MIL-F-83300, Dec. 1970.

11. Franklin, J.A., and Anderson, S.B., "V/STOL Maneuverability and Control," NASA TM 85939, Apr. 1984.

12. Franklin, J.A., Stortz, M.W., and Mihaloew, J.R., "Integrated Flight/Propulsion Control for Supersonic STOVL Aircraft," International Powered-Lift Conference Proceedings, London, England, Aug. 1990.

13. Franklin, J.A., Hynes, C.S., Hardy, G.H., Martin, J.L., and Innis, R.C., "Flight Evaluation of Augmented Controls for Approach and Landing of Powered-Lift Aircraft," *AIAA Journal of Guidance, Control, and Dynamics*, Vol. 9, Sept.-Oct. 1986.

14. Hoh, R.H., Baillie, S.W., Kereliuk, S., and Traybar, J.J., "Determination of Decision Height Windows for Decelerating IMC Approaches in Helicopters," AGARD Conference on Flying Qualities CP-508, Feb. 1991.

15. Hindson, W.S., Hardy, G.H., and Innis, R.C., "Flight-test Evaluation of STOL Control and Flight Director Concepts in a Powered-Lift Aircraft Flying Curved Decelerating Approaches'" NASA TP 1641, Mar. 1981.

16. Lebacqz, J.V., Radford, R.C., and Beilman, J.L., " An Experimental Investigation of Control-Display Requirements for Jet-Lift VTOL Aircraft in the Terminal Area," NADC-760999-60, Jul. 1978.

17. Lebacqz, J.V., "Survey of Helicopter Control/Display Investigations for Instrument Decelerating Approach," NASA TM 78565, 1979.

18. Barrett, J.N., and White, R.G., "The Flight Development of Electronic Displays for V/STOL Approach Guidance," AGARD Symposium on the Guidance and Control of V/STOL Aircraft at Night and in Poor Visibility, CP-148, May 1974.

19. Gold, T., and Walchli, R.M., "Head-Up Display for All-Weather Approach and Landing of Tilt-Wing V/STOL Aircraft." AIAA Paper No. 74-952, AIAA 6th Aircraft Design, Flight Test, and Operations Meeting, Los Angeles, CA, Aug. 1974.

20. Rustin, C.C., "Piloting Aspects of V/STOL Approach Guidance." AGARD Symposium on the Guidance and Control of V/STOL Aircraft at Night and in Poor Visibility, CP-148, May 1974.

21. Birckelbaw, L.G., and Corliss, L.D., "Phase II Simulation Evaluation of the Flying Qualities of Two Tilt-Wing Flap Control Concepts." Paper No. 920988, SAE Aerospace Atlantic Conference, Dayton, OH, Apr. 1992.

22. Prouty, R.W., "What's Best to Tilt: The Rotor or the Wing." Rotor and Wing International, Vol. 24 , No. 6 , Jun. 1990.

23. Dugan, D.C., Erhart, R.G., and Schroers, L.G., "The XV-15 Tilt Rotor Research Aircraft," NASA TM 81244, Sept. 1980.

24. Honaker, J.S., et al., "Tri-Service Evaluation of the Canadair CL-84 Tilt-Wing V/STOL Aircraft," U.S. Army Aviation Materiel Laboratories Technical Report 67-84, Nov. 1967.

25. Churchill, G.B., and Dugan, D.C., "Simulation of the XV-15 Tilt Rotor Research Aircraft," NASA TM 84222, Mar. 1982.

26. Hoh, R.H., Klein, R.H., and Johnson, W.A., "Development of an Integrated Configuration Management /Flight Director System for Piloted STOL Approaches," NASA CR-2883, 1977.

27. Michaelson, O.E., "Application of V/STOL Handling Qualities Criteria to the CL-84 Aircraft," AGARD Conference on Handling Qualities and Performance Criteria for Conventional and V/STOL Aircraft, CP-106, Ottawa, Sept. 1971.

28. Kelly, H.L., Reeder, J.P., and Champine, R.A., "Summary of the Flight-Test Evaluation of the CL-84 Tilt-Wing V/STOL Aircraft," NASA TM X-1914, Mar. 1970.

29. Lebacqz, J.V., and Scott, B.C., "Ground Simulation Investigation of VTOL Airworthiness Criteria for Terminal Area Operations," *AIAA Journal of Guidance, Control and Dynamics*, Vol.8 No.6, 1985.

30. anon., "Airline Transport Pilot and Type Rating, Practical Test Standards for Airplane and Helicopter," FAA-S-8081-5, AVN-130, Aug. 1988.

31. Swenson, H.N., Hamlin, J.R., and Wilson, G.W., "NASA-FAA Helicopter Microwave Landing System Curved Path Flight Test," NASA TM 85933, Feb. 1985.

32. Beck, D., "U.S. Navy Shipboard Trials of the CX-84 Aircraft," SETP European Section 7th Annual Symposium, Munich, FRG., Apr. 1975.

33. Merrick, V.K., "Simulation Evaluation of Two VTOL Control/Display Systems in IMC Approach and

Shipboard Landing," NASA TM 85996, Dec. 1984.

34. Merrick, V.K., Farris, G.F., and Vanags, A.A., "A Head-Up Display for Application to V/STOL Aircraft Approach and Landing," NASA TM 102216, Jan. 1990.

35. Schroeder, J.A., Eshow, M.M., and Hindson, W.S., "An In-Flight Investigation of Symbology Drive Law Improvements to an Operational Attack Helicopter," American Helicopter Society 46th Annual Forum, Washington, D.C., May 1990.

36. Hynes, C.S., Franklin, J.A., Hardy, G.H., Martin, J.L., and Innis, R.C., "Flight Evaluation of Pursuit Displays for Precision Approach of Powered-Lift Aircraft," *AIAA Journal of Guidance, Control, and Dynamics*, Vol.12, No.4, 1989.

37. Baillie, S., Kereliuk, S., and Hoh, R.H., "An Investigation of Lateral Tracking Techniques, Flight Directors, and Automatic Control Coupling on Decelerating IFR Approaches for Rotorcraft," National Research Council of Canada Report No. NAE-AN-55, Oct. 1988.

38. Decker, W.A., Bray. R., Simmons, R.C., and Tucker, G.E., "Evaluation of Two Cockpit Display Concepts for Civil Tiltrotor Instrument Operations on Steep Approaches," Piloting Vertical Flight Aircraft: A Conference on Flying Qualities and Human Factors, San Francisco, CA, Jan. 1993.

39. Nieuwenhuijse, A.W., and Franklin, J.A., "A Simulator Investigation of Engine-Failure Compensation for Powered-Lift STOL Aircraft," NASA TMX 62363, May, 1974.

40. Harris, J.L.,"Flight Experiments Investigating Engine Failure on a Powered-Lift STOL Aircraft During Approach and Landing," The De Havilland Aircraft Company of Canada Ltd. Report No. DHC 79-6, Mar. 1980.

41. Sattler, D.E., Sinclair, M., Kereliuk, S., and Fowler, R.H., "An Investigation of the Recovery from an Engine Failure in a Twin Engine Augmentor Wing Aircraft Using the NAE Airborne Simulator," Canadian Aeronautics and Space Journal, Vol.27, 1st Quarter 1981, p. 26-40.

42. Schaeffer, J., Alwang, R., and Joglekar, M., "V-22 Thrust Power Management Control Law Development," American Helicopter Society 47th Annual Forum, Phoenix, Arizona, May 1991.

DESIGN AND PILOT EVALUATION OF THE RAH-66 COMANCHE CORE AFCS

Donald L. Fogler Jr.
Flight Controls Engineer, Electronic Flight Control Systems
United Technologies Corp., Sikorsky Aircraft Division

James F. Keller
Senior Technical Specialist, Flying Qualities
Boeing Defense and Space Group, Helicopter Division

ABTRACT

This paper addresses the design and pilot evaluation of the Core Automatic Flight Control System (AFCS) for the Reconnaissance / Attack Helicopter (RAH-66) Comanche. During the period from November 1991 through February 1992, the RAH-66 Comanche control laws were evaluated through a structured pilot acceptance test using a motion base simulator. Design requirements, descriptions of the control law design, and handling qualities data collected from ADS-33 maneuvers are presented.

NOMENCLATURE

ADS	Aeronautical Design Standard
AFCS	Automatic Flight Control System
AGL	Above Ground Level
FCS	Flight Control System
FMS	Full Mission Simulator
HMD	Head Mounted Display
HQR	Handling Qualities Rating
LH	Light Helicopter
MFD	Multi-Function Display
NOE	Nap Of the Earth
PFCS	Primary Flight Control System
PMGW	Primary Gross Weight
RAH	Reconnaissance Attack Helicopter
SAS	Stability Augmentation System
VFR	Visual Flight Rules
D(s)	Desired Response
G(s)	Aircraft Dynamics
K_a	Attitude Feedback Gain
K_r	Rate Feedback Gain
$P^{-1}(s)$	Plant Canceller
F_B	Bank Angle

INTRODUCTION

The Comanche is the first helicopter to be procured under the new handling qualities specification ADS-33. Designed to be the next generation scout / attack helicopter, the Comanche incorporates many advanced technology features, including a high equivalent flap hinge offset bearingless main rotor and a FANTAIL$_{TM}$ antitorque system. In order to excel in its intended mission, as well as satisfy ADS-33, the Comanche flight control design is a multimode system that enables the pilot to tailor handling qualities to the varying demands of each mission. The heart of this control law design is the Primary Flight Control System (PFCS) and AFCS which were designed to make the Comanche mission capable in day / Visual Flight Rules (VFR) conditions. From the pilot's point of view, this control law structure is designed to allow the maximum maneuverability and agility of the Comanche to be exercised, and to provide adequate handling qualities in the event of multiple flight control system (FCS) failures. From the control law designer's perspective, it is structured to allow straightforward integration of all selectable modes including navigation and targeting levels of augmentation.

The Comanche flight controls take advantage of many new technologies in addition to its fly-by-wire digital architecture. In order to meet stringent weight and cockpit ergonomic specifications, the primary pilot control for longitudinal, lateral, and directional axes is a small displacement sidestick controller. The sidestick controller also features a limited vertical axis capability when used in conjunction with the Selectable Altitude Hold mode. The Comanche also uses a bi-ocular helmet mounted display (HMD) as its primary instrument display to allow the pilot to keep eyes out of the cockpit at all times. A visual and aural cueing system allows the pilot to maximize use of the flight envelope while not exceeding limits. Fly-by-wire architecture on the system level and use of these cockpit features with respect to piloting requirements permits the control law designer to layout a more flexible and robust design than would otherwise be possible with a mechanical system. At the same time, the design does not sacrifice the utility and safety elements of a sound mechanical design. This paper concentrates on the PFCS and Core AFCS design which was developed to comply with ADS-33 by using all of the preceding elements.

The Comanche Flight controls used in this evaluation were designed in detail based on the flight controls which resulted from preliminary design. Preliminary design was conducted at Sikorsky aircraft during the Demonstration / Validation and Prototype phases of the Comanche program. A formal ADS-33 evaluation of the Comanche Core AFCS will be conducted at the Sikorsky Full Mission Simulator (FMS) in 1993.

MODEL FOLLOWING STRUCTURE

The Comanche flight control system uses explicit model-following to meet the stringent requirements of ADS-33 and the Light Helicopter (LH) System Specification. Model Following control laws consist of a "desired response" and a "plant canceller" depicted in Figure 1. The plant canceller is an inverse first order transfer function used to cancel the inherent on-axis dynamics of the aircraft. The plant canceller is also designed to minimize the AFCS port activity for all modes of operation. The desired response portion of the model following control system is the transfer function of the response which the aircraft will follow if the errors between the model and aircraft are zero. This model following control system uses rate and attitude feedbacks where the feedback gains are Kr and Ka respectively. Refer to reference 1 for more information on explicit model following systems.

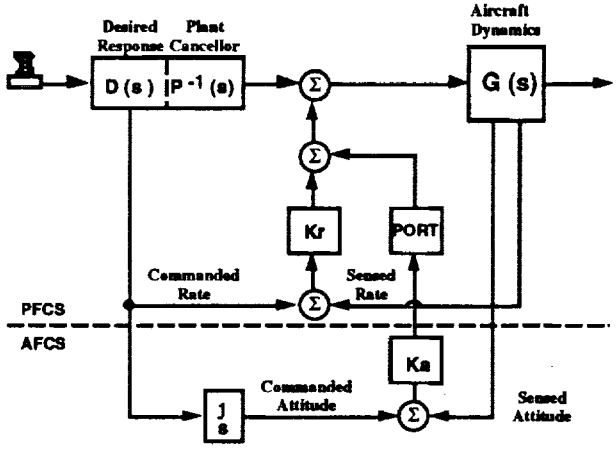

FIGURE 1: DIAGRAM OF A MODEL FOLLOWING SYSTEM

FUNCTIONAL ARCHITECTURE

The pilot is able to select Mission PFCS, Core AFCS, or Velocity Stabilization mode using the AFCS Control Panel located on the cockpit console. Altitude Hold may be selected during Core AFCS operation or during Velocity Stabilization operation. The fourth axis of the sidearm controller commands the vertical axis while Altitude Hold mode is engaged. Mission PFCS mode is the flight critical link between the pilot and aircraft. It may be manually selected or automatically selected following multiple identical failures in the AFCS. This mode of operation is unaugmented except for rate feedback in the directional axis. Core AFCS operation adds rate feedback in pitch and roll, and attitude feedback in pitch, roll, and yaw. Velocity Stabilization provides additional velocity and position referenced augmentation for degraded visual conditions and hands off operation.

The Architecture of Comanche Flight Controls is presented in Figure 2. In general, the pilot inputs are passed through command shaping which generates a high authority, high frequency command path. Rate stabilization and port limited AFCS commands are summed with the PFCS feedforward command and the total trim requirement in each axis to produce a total PFCS command. This command is mapped into a control mixing algorithm then scaled to produce a command used to drive the actuators.

PFCS DESCRIPTION

The forward loop shaping function is designed to provide three basic functions. First, notch filters and other appropriate filters are included to attenuate the effects of biodynamic feedback caused by structural modes. Second, it provides deadzones about the detent of the sidearm controller to overcome mechanical hysteresis and to prevent unintentional cross coupling into other axes. Finally, a nonlinear shaping map is used to desensitize the command near detent. For large inputs, the sensitivity is increased.

The Dynamic Shaping function is a generic architecture which consists of a second order over second order transfer function with variable parameters which define the gain and phase characteristics of the model. For Core and Mission PFCS operation, dynamic shaping is parameterized to provide control quickening. For AFCS operation, dynamic shaping is configured to provide a high frequency command and a rate command typical of the model-following control law architecture.

The primary function of the mode selector is to compute the parameters for the dynamic shaping function. The parameters; desired bandwidth, trim follow-up break frequency, command sensitivity, plant canceller sensitivity, and plant canceller break frequency completely describe the command shaping for all modes of operation. The Mode Selector function works in conjunction with the Dynamic Shaping to provide a smooth transition between the rate command model and the attitude command model. The attitude command model is used during selectable mode operation.

The Trim Follow-up / Transfer function contains two operations. First, Automatic Trim Follow-up is a low frequency network that accommodates unique trim repositioning of the sidearm controller for PFCS operation. It consists of a digital integration of the difference of the demixed actuator position and the PFCS trim requirement. Second, Trim Transfer integrates the trim requirement produced in the AFCS during AFCS operation. All trim is stored in a common location within the system therefore minimizing switching transients associated with disengaging the AFCS.

The Rate Augmentation function computes stability augmentation signals based on sensored rates in the pitch, roll, and yaw axes. In addition, the rate augmentation function includes airspeed scheduled feedback gains and structural mode filters. In degraded modes of operation, the Mission PFCS utilizes only yaw rate feedback and the Core PFCS uses no rate feedback. The use of yaw rate feedback in Mission PFCS greatly improves the directional axis response and was needed to satisfy Mission PFCS design requirements for Level 2 handling qualities in NOE flight.

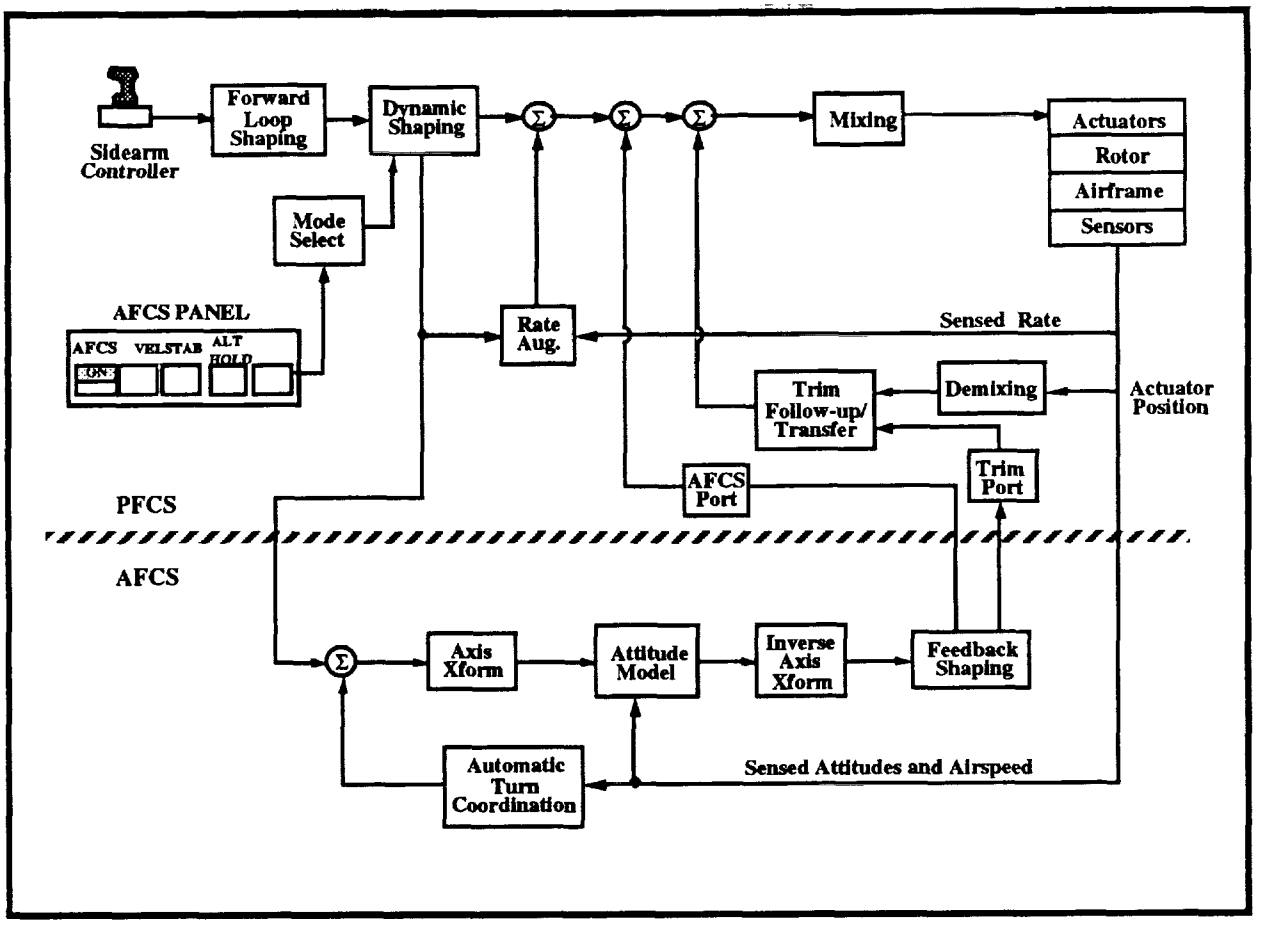

FIGURE 2: ARCHITECTURE OF THE COMANCHE FLIGHT CONTROLS

The AFCS and trim ports were designed to comply with the failure recoverability requirement in ADS-33. The ports are authority and rate limiting devices respectively where low amplitude commands are passed while large commands are limited to a predetermined rate. The purpose of the ports are to permit the pilot to recover from unannunciated AFCS failures. In sizing the ports, consideration is given to AFCS failures and handling qualities of the aircraft. A small port tends to decrease the handling qualities of the aircraft while a large port may not permit recovery from a failure. The port size is set to try and meet both requirements.

The purpose of the mixing function is to decouple the initial response of the aircraft to pilot inputs. Commands from the four axes are row inputs into a four by four matrix multiplication while airspeed scheduled gains are column inputs. The outputs are pitch, roll, yaw, and collective commands that provide an uncoupled response. These commands, which have units of degrees of blade pitch, are processed through an actuator kinematic algorithm to produce three swashplate actuator commands and a Fantail actuator command in units of millimeters. The Demixing algorithm takes the swashplate actuator positions obtained from sensors and performs a matrix multiplication with the inverse of the mixing matrix. This function produces a feedback signal which is used for the trim follow-up function.

CORE AFCS CHARACTERISTICS

Core AFCS mode of the Comanche Control System provides a rate command/attitude hold response-type system at all airspeeds. This response type allows maximum use of the Comanche agility at all speeds. Figure 3 provides a graphical representation of the Core AFCS characteristics versus airspeed for the pitch, roll, and yaw axes.

The pitch axis provides attitude hold whenever the longitudinal axis of the sidearm controller is in detent. At airspeeds below 80 knots airspeed the maximum commanded pitch rate is a constant 60 deg/sec. Above 80 knots airspeed the maximum pitch rate is scheduled with airspeed to provide a nearly constant stick force per 'g' of commanded load factor. Duringaggressive turns at high speed, positive maneuvering stick stability is provided for load factor limiting of 1.5G, roughly equivalent to 30 degrees of bank, requiring the pilot to command aft stick. While for non-aggressive, shallow turns the aircraft remains coordinated requiring no pilot pitch command thus reducing pilot workload.

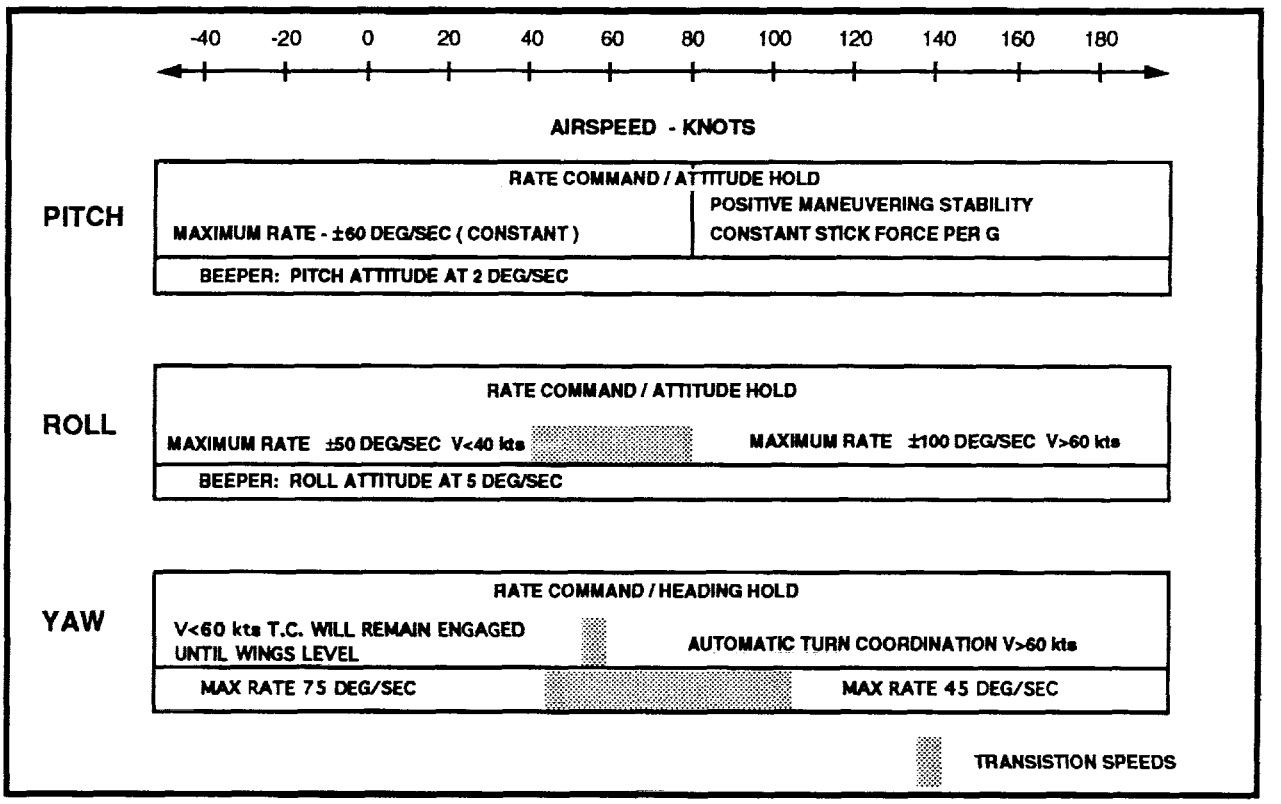

FIGURE 3: CORE AFCS CHARACTERISTICS VERSUS AIRSPEED

The roll axis provides attitude hold at all airspeeds whenever the lateral axis of the sidearm controller is in detent. At airspeeds above 60 knots airspeed the maximum commanded rate is 100 deg/sec. From 60 knots to 40 knots airspeed the commanded maximum roll rate decreases to 50 deg/sec.

The yaw axis provides heading hold at all airspeeds whenever the sidearm controller is in detent and the aircraft is not in a coordinated turn. Above 60 knots airspeed the yaw axis provides automatic turn coordination which allows the pilot to perform turns using only lateral stick inputs. In this configuration the directional axis of the controller commands sideslip.

AFCS OPERATION

The PFCS rate command signal from the Dynamic shaping function is passed to the AFCS where it is summed with other rate commands. Since the total AFCS rate command is in the body reference frame and the attitude sensors are in the earth reference frame, the commanded rates must pass through an axis (Euler) transformation. Comanche uses a standard Yaw-Pitch-Roll rotation sequence Euler angle system. It is important to note that the control laws do not tailor these transformations in any way. The result is a rate command in the earth reference frame. This rate is integrated to produce an attitude command signal in the Attitude Model function of the AFCS. The attitude model command is compared with the sensed attitude to create an attitude error. This attitude error is transformed back into the body reference frame via the Inverse Axis Transformation function.

Attitude Hold in the Longitudinal, Lateral, and Directional axes is accomplished using a proportional plus integral control system. The shaping of the attitude error signal into a proportional plus integral command occurs in the feedback shaping function. The attitude error signal is multiplied by the attitude feedback gain and trim integral gain and outputted to the AFCS port and Trim Port respectively. The integral signal is generated by the PFCS integrator which is located in the Trim Follow-up / Transfer function. The Feedback Shaping function also provides integral hold when the aircraft is in a non-maneuvering state.

The trim transfer algorithm is also resident in the Feedback shaping function. Trim from the AFCS is continuously moved onto the PFCS trim integrator via the trim port allowing the AFCS to have a steady state output value of zero. The performance of the AFCS may be enhanced in part by varying the trim transfer time constant.

The turn coordination function provides automatic turn coordination above 60 knots airspeed. The turn coordination algorithm uses roll angle and airspeed to predict the desired turn rate and then modifies it with lateral acceleration feedback and a roll rate signal to provide ball centered turns. Lateral acceleration feedback is faded out below 40 knots airspeed.

The Turn Coordination function calculates the desired Heading rate for a given bank angle, pitch atti-

tude, and airspeed. This rate is transformed into body axis pitch, roll, and yaw commands and summed with other rate commands in the AFCS.

EVALUATION TESTING

The Comanche AFCS control laws were evaluated in a simulator based pilot acceptance test. The simulator used to conduct the test is a six degree of freedom medium displacement motion base located at the Boeing Defense and Space Group, Helicopter Division facility in Philadelphia, Pennsylvania. The simulator uses a 30 foot diameter fixed dome onto which the simulated visual scene is projected. The computer image generator used to supply the visual is an Evans and Sutherland CT6 system.

The simulated Comanche cockpit features a Lear Astronics 3 axis sidestick controller mounted orthogonally to the seat. The displacement collective stick is configured for the desired range of motion. Friction is used to hold the stick in position and provide force feel.

Flight status symbology is available on the head-down Multi-Function Display (MFD) and the heads-up Kaiser Head Mounted Display. The HMD is the primary instrument which the pilot used for judging task performance during each maneuver. The HMD is displayed to the pilot using the Kaiser Helmet which projects the display over the outside scene. This allows the pilot's eyes to remain outside the cockpit. Figure 4A and 4B show the information presented on the MFD and the HMD.

The gaming areas developed for the piloted evaluation include an acceleration / deceleration area, Pirouette course, Rapid Sidestep course, and a Rapid Bob-up and Bop-down area. All other tasks were performed in the vicinity of the Edwards Air Force Base gaming area of the standard CT6 visual database. In some cases the gaming areas were enriched visually to assist in task performance.

During the formal task evaluation, the test pilot was left as the sole judge of the task performance with respect to the ADS-33 maneuver requirements. No task specific software was written to measure task performance. The pilot was advised any time his performance failed to meet the desired limits following the completion of the maneuver and before the pilot rating was recorded. Typically, a maneuver was repeated until the pilot was familiar with all aspects of the task at which point the Cooper-Harper Handling Qualities Rating Scale was used (refer to reference 2). All tests, except where noted, were conducted at Primary Mission Gross Weight (PMGW), mid Center of Gravity (CG), 2000 ft, and 95 degrees F.

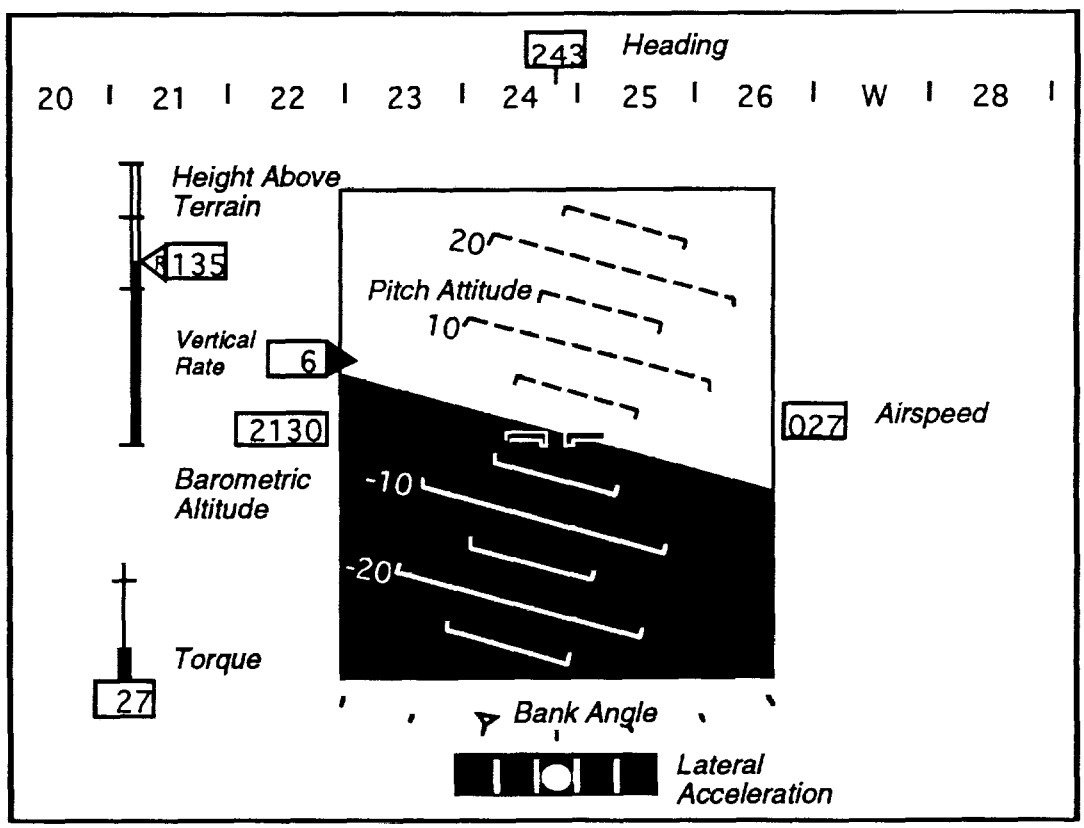

FIGURE 4A: HEAD-DOWN MULTIFUNCTION DISPLAY

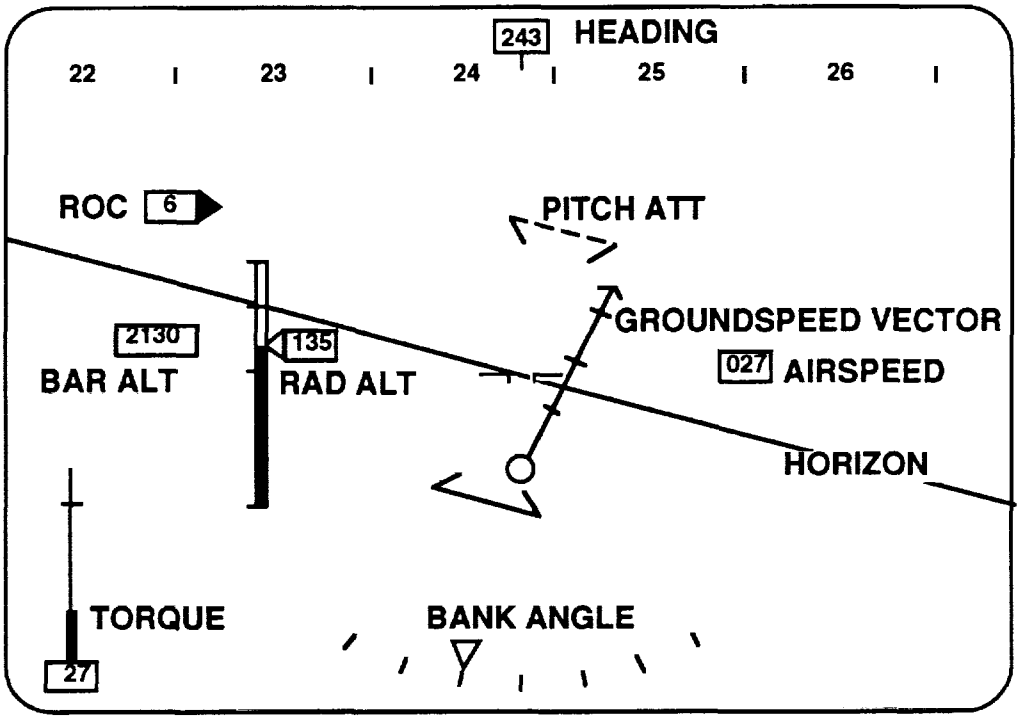

FIGURE 4B: HEAD MOUNTED DISPLAY

ADS-33 MANEUVERS AND TASK PERFORMANCE

A subset of tasks from ADS-33 were selected to provide a good evaluation of the handling qualities of the Comanche Core AFCS. The objective of the Core AFCS is to provide Level 1 handling qualities for mission task elements performed in Usable Cue Environment (UCE) of 1. Conditions having a UCE=1 have the best visual cues attainable. It is important to note that the simulation visuals by themselves reflect a UCE=2. The handling qualities ratings were not expected to be Level 1 overall. The following maneuvers were selected to evaluate the performance of the Core AFCS consistent with aggressive NOE flight; precision hover, pirouette, accel/decel, rapid sidestep, rapid slalom, transient turn, and rapid bob-up and bob-down. The following text lists the maneuver with a brief description about how it is performed followed by a task performance section for that maneuver. Figure 5 summarizes the handling qualities ratings for each task.

Precision Hover - For the Precision Hover maneuver the pilot is required to maintain a precision hover for at least 30 seconds in winds of at least 20 knots from the most critical direction. If a critical direction has not been defined, the hover shall be accomplished with the wind blowing directly from the rear of the rotorcraft. The hover altitude shall be equal to or less than 20 ft. Refer to references 3 for more descriptions of the performance criteria for each maneuver.

Task Performance - Workload for this task with respect to the vertical axis was strongly dependent on the hover altitude. When attempted at 5 feet, there was significant workload to maintain this altitude. However, at 10 feet, the task was much easier, probably due to improved visual cues. The addition of the HMD was found to be significant for altitude and rate of climb cueing. With the HMD, the pilots were typically able to hold ±1 ft altitude. Task rated Level 1 handling qualities, HQR=3.

Pirouette - This maneuver is initiated from a stabilized hover over a point on the circumference of a 100 ft radius circle. The nose of the rotorcraft is pointed at a reference point at the center of the circle while the aircraft is at a hover altitude of approximately 10 ft. The maneuver consists of lateral translation, keeping the nose of the rotorcraft pointed at the center of the circle, and keeping the pilot station over the circumference of the circle. This maneuver is performed in both directions.

Task Performance - The pirouette was demonstrated with level 1 handling qualities, HQR=2.5. The HMD was essential to task performance because the task required constant attention outside the cockpit. With the HMD the pilot was able to align his sight with the critical symbology needed for this maneuver (altitude and rate of climb). If the pilot had to cross check the MFD to verify performance the workload became too great to be considered minimal. Task com-pletion was within the 45 second limit.

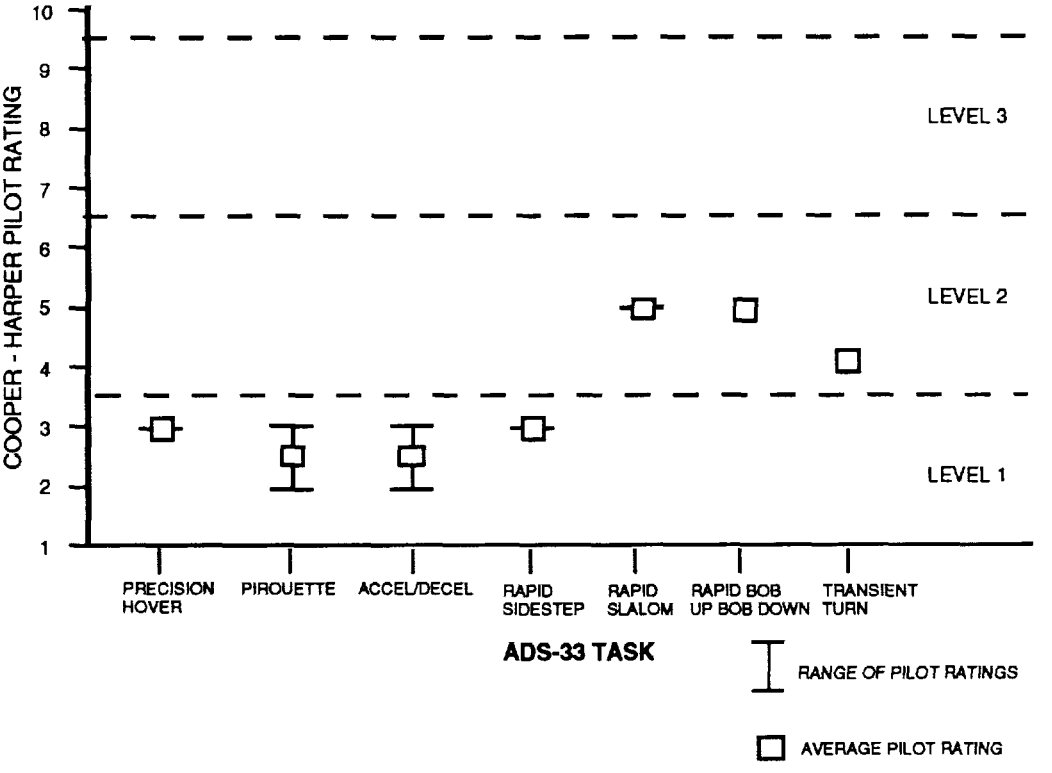

FIGURE 5: CORE AFCS COOPER-HARPER RATINGS VS. ADS-33 TASK

Acceleration and Deceleration - Starting from a stabilized hover, a rapid and aggressive acceleration is initiated up to an airspeed of at least 60 knots. Immediately, a deceleration is initiated and the aircraft is brought to a hover over a defined reference point. A constant altitude is maintained at or below 40 ft.

Task Performance - The altitude and course criteria was met without difficulty. However, the deceleration to a hover was difficult to judge due to the high pitch angle commanded during the flare. During flight test, when visual cues are UCE=1, the flare to hover will not be a problem. The HMD symbology was a valuable source of airspeed and altitude cues. Level 1 handling qualities, HQR=2.5

Rapid Sidestep - This maneuver is started from a stabilized hover, with the rotorcraft oriented 90 degrees to a reference line marked on the ground. A rapid and aggressive lateral translation is initiated with a constant heading up to a speed of between 30 and 45 knots. This speed is maintained for approximately 5 seconds followed by an aggressive lateral deceleration to hover. The maneuver is conducted at a constant altitude at or below 30 ft. The cockpit station is maintained over the reference line. This maneuver is performed in both directions.

Task Performance - This task is easier to perform to the left, since the critical HMD symbology was coincident with the pilot's line of sight. With UCE=1 conditions during flight test the pilot will not be as dependent on the HMD. Performance to the right will likely improve. Heading hold keeps the directional axis out of the pilot's primary workload, so the pilot is able to use the HMD to set lateral airspeed and then not worry about lateral position until the termination phase. Additionally, fore/aft drift was not a factor. Level 1 handling qualities, HQR=3 was achieved.

Rapid Slalom. - This maneuver is initiated in level unaccelerated flight, and in the direction of a line or series of objects on the ground. The aircraft is rapidly displaced 50 feet laterally from the center line using a bank angle of at least 50 degrees. Direction is immediately reversed to displace the aircraft 50 ft on the opposite side of the center line. The aircraft is then returned to the center line as quickly as possible while maintaining a reference altitude below 50 ft. The maneuver is accomplished so that the initial turn is both to the right and to the left.

Task Performance - Even though the pilot was able to complete this maneuver within the specified tolerances, he did not have a strong sense that all tolerances had been met because the task unfolded too rapidly. Since the pilot had to command a bank angle of at least 50 degrees the maneuver lasted less than 10 seconds. Once the maneuver was mastered, performance was relatively repeatable, but the pilot had to consult observers to verify that altitude constraints were met. This inherently is a difficult maneuver due to its short duration and

manual workload. Simulator cueing probably also makes this task more difficult than would be the case in flight test. The task rated level 2 handling qualities, HQR=5.

Rapid Bob-up Bob-down - This maneuver is initiated from a stabilized hover at an altitude of 10 ft. An ascent is performed to clear an obstacle approximately 25 ft high to achieve a line-of-sight with a simulated threat. As soon as the target is stabilized in the sight, a descent is performed to the initial hover position. Total task time is 8 seconds.

Task Performance - This task was judged to exhibit level 2 handling qualities HQR=5 due to the high workload required to maintain position. The HMD used did not incorporate the latest Comanche design with dedicated hover symbology that provides additional cues to hold station.

Transient Turn - Starting at 120 knots and an altitude at or above 100 ft, a 180 degree heading change is made in as little time as possible. Use of yaw control to induce a lateral acceleration in the direction of the turn is acceptable. The maneuver is performed both to the right and to the left.

Task Performance - A combination of roll and yaw commands were used to satisfy this maneuver within its time constraints. It was easier to accomplish to the right since less anti-torque is required. The high bank angle created moderate workload in keeping the aircraft's pitch angle aligned with respect to the horizon. The aircraft handled satisfactorily considering the level of aggressiveness of the maneuver. This task was rated Level 2 handling qualities, HQR=4.

Core AFCS failure recovery was also evaluated using piloted simulation. The simulated failure included a single axis hardover to a control axis. The AFCS Output and Trim Transfer port authorities were set based on providing a system capable of recovery to a trim flight condition following a reasonable failure transient. The initial altitude for this evaluation was 40 ft AGL and the maximum desired body axis rate following the failure was ±10 deg/sec. This was relaxed for lateral axis failures, since lateral transients are more tolerable than longitudinal transients. The following lists the sequence of events following an unannunciated AFCS failure; (1) The AFCS fails and a hardover occurs. (2) Following a 1 second delay, the pilot initiates a recovery and retrims the vehicle. (3) The pilot deselects the AFCS using the button on the AFCS Panel. (4) The pilot must retrim the vehicle as the hardover begins to linearly decay off the AFCS port. (5) Four seconds after the AFCS is deselected, the Mode Select parameters switch to the Mission PFCS values. (6) 12 seconds after deselect the PFCS Rate Augmentation path is linearly faded out. At this point the system is fully in Mission PFCS operation.

It is important to switch the hardover out in steps in order to minimize any secondary transients. The pilot must be able to track the hardover as it is fading out. The rate feedback gain is the primary system element which opposes and minimizes the failure transient. A detailed tabulation of port sizes versus rate feedback gains can be compiled to allow the flight test engineers to simultaneously vary rate feedback and port size as required during flight test to provide the desired stability and control response.

CONCLUSION

The simulator test found most of the maneuvers evaluated to have level 1 handling qualities. The maneuvers rated level 2 handling qualities were the Bob-up/Bob-down, Rapid Slalom, and Transient Turn. Improved HMD symbology now available would help improve all Handling Qualities ratings. The Bob-up/Bob-down maneuver can greatly be improved with the position hold function of the velocity stabilization mode. Position hold will allow the pilot to concentrate on the vertical axis without constantly correcting for lateral and longitudinal drift. The Transient Turn and Rapid Slalom are very aggressive maneuvers which require the pilot to fly within specified tolerances even though workload is expected to be high. These maneuvers may be considered more of performance measuring tasks rather than a handling qualities tasks although the task descriptions do not read as such. While the Comanche is aerodynamically capable of completing this maneuvers, compliance with this mission task element is impractical and possibly undesirable because the aircraft must be taken to the limit of the maneuver capability to meet the criteria.

The simulation results indicate that Level 1 handling qualities ratings should be achievable for virtually all UCE=1 tasks in the real world.

REFERENCES

1. Hilbert, K. B., Lebacqz, J. V., "Flight Investigation of a Multivariable Model-Following Control System for Rotor-craft", AIAA-86-9779, 1986.

2. Cooper, G. and Harper, R., "The Use of Pilot Rating in the Evaluation of Aircraft Handling Qualities", NASA TN D5153, 1969.

3. ADS-33C, "Aeronautical Design Standard, Handling Qualities Requirements For Military Rotorcraft", August, 1989.

DESIGN AND PILOT EVALUATION OF THE RAH-66 COMANCHE SELECTABLE CONTROL MODES

Phillip J. Gold
Senior Engineer Handling Qualities
United Technologies Corporation, Sikorsky Aircraft Division
Stratford, Connecticut

James B. Dryfoos
Technical Specialist Flying Qualities
Boeing Defense & Space Group, Helicopters Division
Philadelphia, Pennsylvania

ABSTRACT

The RAH-66 Comanche helicopter has been designed to possess superior handling qualities over a wide range of flight conditions. The control laws have been tailored to satisfy the requirements of ADS-33C and the Weapon System Specification (WSS). This paper addresses the design of the Comanche Selectable Mode control laws (Velocity Stabilization / Hover Hold and Altitude Hold), which provide the additional stabilization and control augmentation needed when flying in a Degraded Visual Environment (DVE) . An overview of the RAH-66 control laws is presented, including a detailed description of the Selectable Modes design. The primary focus of this paper is the results of piloted evaluation of these control laws in the Boeing motion-base simulator. These tests substantiate the detailed design of the Comanche Selectable Mode control laws. All tested DVE tasks (ADS-33C, sections 4.4 and 4.5) were rated Level 1. Other evaluation tasks confirmed the mission suitability of the control system. These control laws are ready for formal ADS-33C compliance testing in the Sikorsky Full Mission Simulator (FMS).

NOMENCLATURE

AC/AH	Attitude Command/Attitude Hold
AC/VH	Attitude Command/Velocity Hold
AFCS	Automatic Flight Control System
AGL	Above Ground Level
ALTHLD	Altitude Hold
BMR	Bearingless Main Rotor
DEM/VAL	Demonstration/Validation
DVE	Degraded Visual Environment
FOV	Field of View
FMS	Full Mission Simulator
HAC	Helicopter Air Combat
HMD	Helmet Mounted Display
HQR	Handling Qualities Rating
LSTC	Low Speed Turn Coordination
MEP	Mission Equipment Package
NOE	Nap of the Earth
PFCS	Primary Flight Control System
PIO	Pilot Induced Oscillations
PMGW	Primary Mission Gross Weight
RC/AH	Rate Command/Attitude Hold
RFOV	Restricted Field of View
TC	Turn Coordination
UCE	Usable Cue Environment
VCR	Visual Cue Rating
VC/PH	Velocity Command/Position Hold
VELSTAB	Velocity Stabilization
WSS	Weapon System Specification

INTRODUCTION

Control Law Design

The RAH-66 control system consists of a Primary Flight Control System (PFCS) and an Automatic Flight Control System (AFCS). The PFCS and AFCS use explicit model-following control laws to provide both control and stability augmentation. The PFCS is the flight critical portion of the flight control system while the AFCS is the mission critical portion. The AFCS augments the performance of the PFCS in order to meet the requirements of ADS-33C (Reference 1) by providing Level 1 handling qualities for all mission task elements in a Usable Cue Environment (UCE) of 1 or 2 and at least Level 2 handling qualities in a UCE of 3. To provide these capabilities, the AFCS consists of both automatic and manually selected modes which allow the pilot to tailor the control system for the existing flight conditions. These modes provide increasing levels of vehicle augmentation combined with improved control precision to produce superior flight performance and low pilot workload. The Core AFCS is the basic operational mode of the control system and allows the pilot to make full use of the maneuverability / agility of the Comanche.

The Comanche Selectable Modes, Velocity Stabilization (VELSTAB) and Altitude Hold (ALTHLD), can be engaged anywhere in the flight envelope in order to respond to changing flight/visual conditions or when reduced pilot workload is desired. VELSTAB provides air and ground referenced Velocity Hold, Hover Hold with linear Velocity Command, and ground referenced Low Speed Turn Coordination. ALTHLD provides either radar or barometric referenced Altitude Hold with automatic reference switching and Rate of Climb Command. A simplified block diagram of the longitudinal VELSTAB axis and its integration with the PFCS and Core AFCS, is presented in Figure 1. In the PFCS, pilot inputs are passed through appropriate command shaping to generate a high authority, high frequency command path. Rate

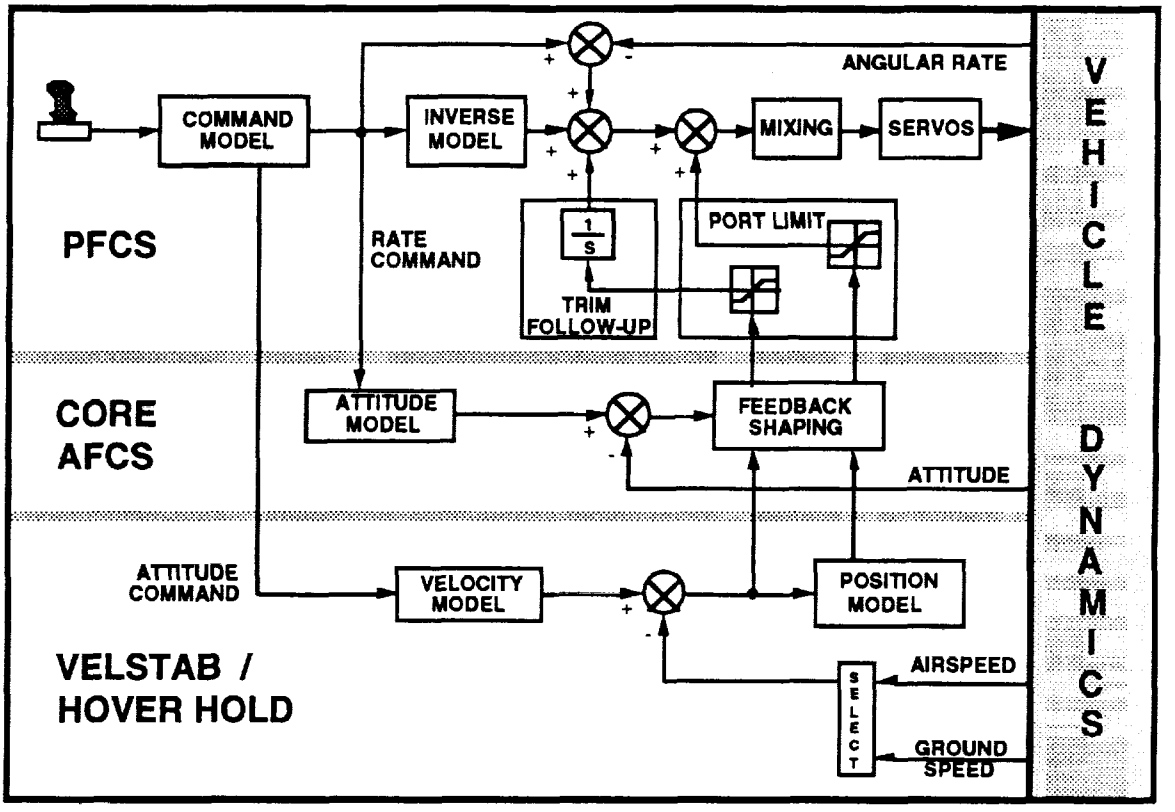

FIGURE 1. COMANCHE LONGITUDINAL CONTROL LAWS

stabilization and port limited AFCS commands are summed with the PFCS feed-forward command and the total trim requirement in each axis to produce a total command vector. The resulting command vector is mapped into actuator position commands through mixing to drive the control surfaces. The AFCS, which includes VELSTAB / Hover Hold, consists of attitude, velocity, and position models and both feed-forward control augmentation and feedback stabilization to the PFCS for model following.

Preliminary design of the Core AFCS and Selectable Modes was conducted at Sikorsky during the LH DEM/VAL contract and as part of the current prototype contract. Following preliminary piloted evaluation in the Sikorsky FMS, the control laws were transferred to the Boeing facility for detailed design and further pilot testing. The "final" detail design has been recently returned to Sikorsky.

PFCS / Core AFCS Operation and Structure

The Comanche PFCS control laws are partitioned into two distinct layers: Core and Mission PFCS. While these control laws use a common structure, they are parameterized differently. Both are degraded modes with respect to the default Core AFCS control laws. The system reverts to the Mission PFCS when the Core AFCS is either deselected or multiple failures occur. The system automatically reverts to its most degraded flight capable mode, Core PFCS, when the sensor requirements of the Mission PFCS are no longer available. The Core PFCS may be characterized as a fixed gain system that does not rely on any feedback sensors. The Mission PFCS features airspeed scheduling of parameters and yaw rate damping. Both sets of control laws feature command shaping that has been designed to be commensurate with the types of tasks envisioned for the respective degraded modes.

The Comanche Core AFCS control laws complement those in the PFCS. The PFCS control law structure is augmented with attitude and heading hold control laws. On each axis, the parameters of the PFCS command shaping are altered to provide the basis for the AFCS model-following control laws. Rate feedback is added to the longitudinal and lateral axes of the PFCS (note, the directional axis already includes rate feedback through the Mission PFCS). Collectively, these control laws execute an explicit model-following rate command / attitude hold (RC/AH) system.

The Core AFCS predominantly executes the attitude hold portion of the overall control law. Full-time attitude stabilization is featured via the model following control structure. Integral hold of commanded attitudes and heading are featured once the aircraft is brought to trimmed state, to enhance disturbance rejection. All steady state attitude errors are washed out of the AFCS and transferred to the PFCS trim follow-up module. In this manner, all trim resides in the PFCS. Since the Comanche is not expected to be constrained with respect to inertial attitude, the attitude errors of the AFCS are

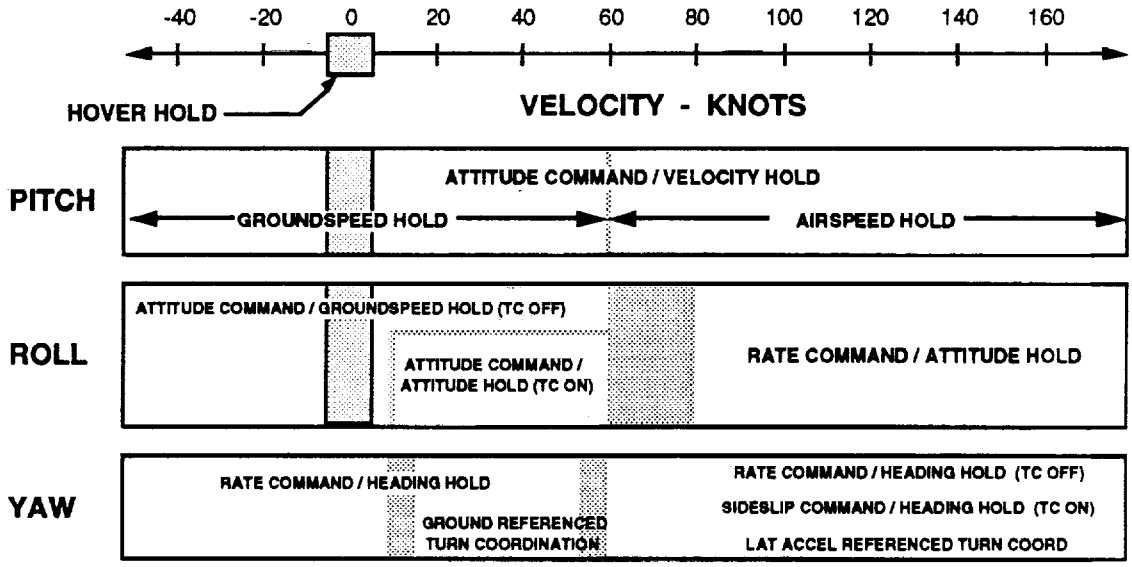

FIGURE 2. VELSTAB CHARACTERISTICS vs VELOCITY

referenced in inertial space. This requires transformation of body referenced rate commands for all sources to the earth axes and subsequent re-referencing of errors back into the body axes, where the controls are referenced.

Automatic turn coordination is enabled above 60 kts. In general, the turn coordination function provides longitudinal, lateral and directional body axis rate commands which minimize lateral acceleration in a turn. These commands not only integrate with the AFCS attitude command control laws, but also provide feed-forward outputs to directly offset PFCS rate feedback not consistent with coordinated turning flight. While the vehicle is in coordinated flight, the directional controller may be used to adjust the coordinated yaw rate, producing an apparent sideslip command control law. A momentary turn coordination release switch (TC Release) is available on the cyclic grip so that the pilot may manually suppress the automatic turn coordination to facilitate mission tasks that are not encompassed by the inhibit logic such as high speed lateral maneuvers.

Velocity Stabilization / Hover Hold

The Velocity Stabilization mode is engaged manually by pressing the VEL/HVR HOLD switch on the AFCS control panel. Figure 2. provides a graphical representation of the VELSTAB characteristics versus groundspeed for the pitch, roll, and yaw axes. The pitch axis response-type is attitude command / velocity hold (AC/VH) at all speeds, except when in the Hover Hold mode where a velocity command / position hold (VC/PH) response is provided. Although not required by ADS-33C, velocity hold was selected (instead of attitude hold) in order to further reduce pilot workload and more easily yield satisfactory (Level 1) handling qualities. Groundspeed is used as the velocity reference at low speeds, while airspeed is used at high speed.

The roll axis response-type is AC/VH at low speeds, except when in the Hover Hold mode (VC/PH) or when in a low speed coordinated turn (attitude command / attitude hold {AC/AH}). The roll response-type automatically changes modes from AC/VH to RC/AH between 60 and 80 kts. This combination of response-types provides the pilot with good tactile cues related to the roll attitude of the aircraft when maneuvering at low speeds while eliminating trim forces on the controller at high speeds when in a steady turn.

Hover Hold is enabled whenever the VELSTAB mode is engaged and Hover Hold engages when groundspeed, pitch and roll rates, longitudinal and lateral linear accelerations, and pitch and roll stick commands are all small. This 'gate' allows the pilot to maneuver through hover without being inadvertently grabbed by hover hold. As previously mentioned, the pitch and roll axis response-types are VC/PH when in the Hover Hold mode. The velocity command response is provided at groundspeeds of less than ±5 kts making it easier for the pilot to precisely position the aircraft in DVE conditions. Auto-moding of the pitch and roll response-types from velocity command to attitude command occurs when the pilot commands a velocity that exceeds the 5 kt threshold or when the pilot applies a large cyclic input. The second criteria allows the pilot to break out of Hover Hold quickly.

Figure 3 presents a more detailed block diagram of the VELSTAB control laws for the pitch axis. The Velocity Command Model calculates the desired longitudinal velocity based on inputs from the PFCS and the core AFCS. The commanded pitch attitude is multiplied by the acceleration due to gravity to get the commanded longitudinal acceleration. The acceleration is integrated to get commanded velocity. The commanded velocity is compared to the reference and the result is the velocity error. The velocity reference is air-

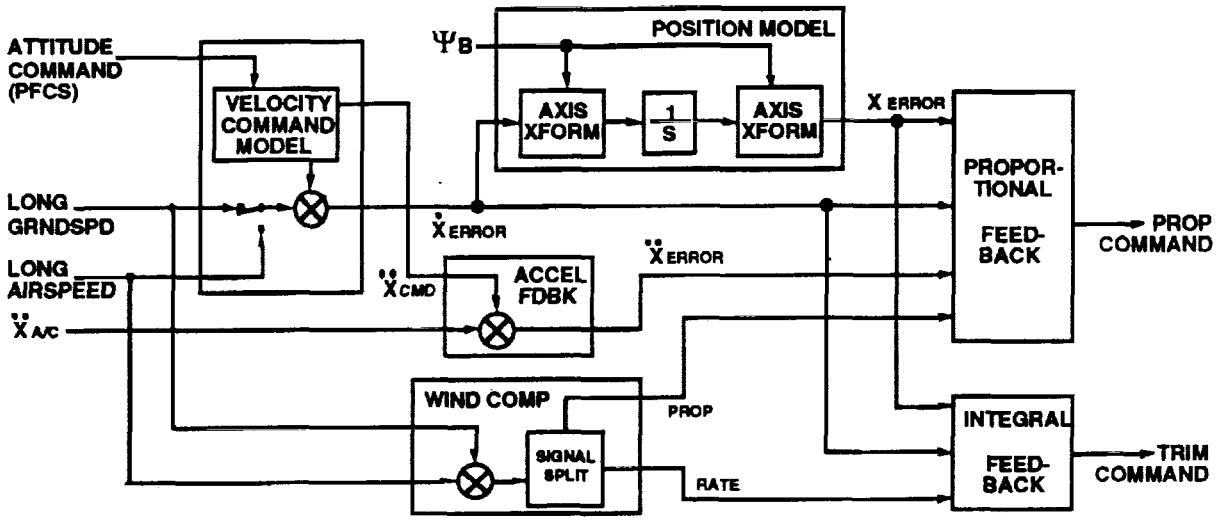

FIGURE 3. VELSTAB BLOCK DIAGRAM

speed when both groundspeed and airspeed exceed 60 kt, otherwise the reference is groundspeed. The Position Model calculates the inertial velocity error from the longitudinal and lateral velocity errors (body referenced) and heading. When position hold is engaged, this velocity error is integrated to yield an inertial position error. The inertial position errors are then converted back to body axis errors. This position error is passed to the VELSTAB Proportional and Integral Feedback Modules described below.

Acceleration Feedback is active when position hold is engaged. The commanded longitudinal acceleration is compared to the actual longitudinal acceleration and the acceleration error is passed to the Proportional Feedback Module described below.

To further enhance low speed operation, Wind Compensation is active when groundspeed is the velocity reference. Airspeed and groundspeed are compared to calculate the wind speed, which is multiplied by a gain to yield a feed-forward trim command. This signal is split into proportional and rate terms and sent to the Proportional and Integral Feedback Modules respectively. This implementation maintains a zero steady-state output.

The Proportional Feedback Module multiplies the acceleration, velocity, and position error signals by gains and sums the result. The wind and VELSTAB shaping compensation (described below) signals are then added and the total signal is passed to the Core AFCS Output Module (see Figure 4).

The Integral Feedback Module selects either the velocity error signal or the position error signal for integral feedback depending on whether position hold is engaged. The wind compensation signal is added to the selected signal and the total is sent to the Core AFCS Trim Transfer Module (see Figure 4).

VELSTAB Shaping Compensation (not shown) is active when in velocity command mode, and is used to cancel a portion of the PFCS commands. The PFCS feed-forward commands are lagged and then passed to the

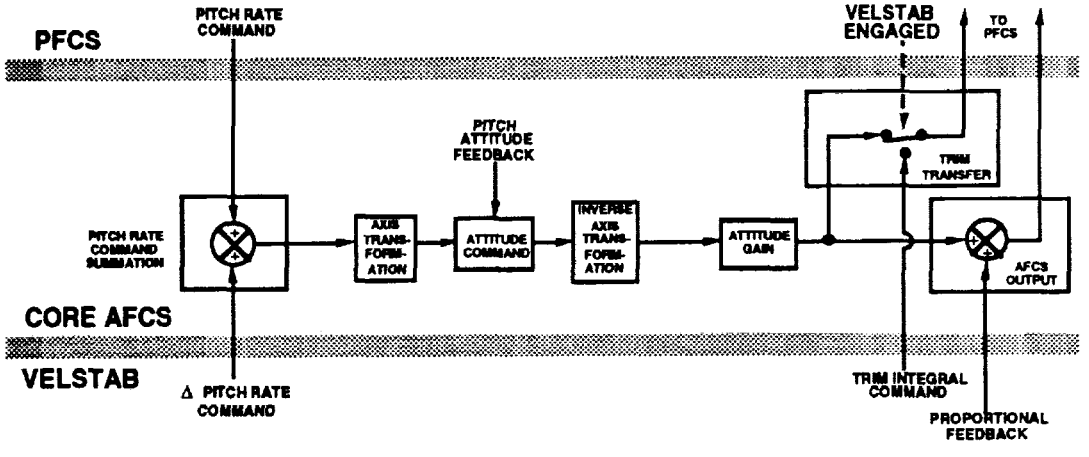

FIGURE 4. VELSTAB INTERFACE TO CORE AFCS

Proportional Feedback Module. The net effect of this module is to yield a washed-out command shaping which is desired when in velocity command mode.

The Attitude Model Command function (not shown) cancels the low frequency trim follow-up contained in the pitch rate command input to the Core AFCS. It also adds a washout to get the appropriate pitch rate transfer function for velocity command mode. The output of this module is sent to the Core AFCS Pitch Rate Command Summation Module (see Figure 4).

Some mode switching of the longitudinal and lateral axes of the PFCS control laws are necessary for implementing VELSTAB. In the longitudinal axis, the Command Model (see Figure 1) parameters are changed to provide attitude command instead of rate command when VELSTAB is selected. In the lateral axis, the Command Model changes from a pure rate command to an airspeed scheduled auto-moding of rate and attitude command at high and low speed respectively when VELSTAB is selected. Moding to rate command is inhibited if VELSTAB is in the groundspeed reference mode (low groundspeed or airspeed).

Low Speed Turn Coordination

When VELSTAB is engaged, the yaw axis control laws provide automatic low speed turn coordination (LSTC), which is enabled above 15 kts groundspeed. This mode provides ground-referenced coordination (i.e. lateral groundspeed is minimized in a turn). The pilot can momentarily interrupt LSTC via the Turn Coordination Release switch. The yaw axis reverts to lateral acceleration referenced turn coordination when not in groundspeed mode (see Figure 2).

In order to provide ground-referenced turn coordination, longitudinal groundspeed and commanded bank angle are used to calculate a feed-forward commanded turn rate. A feedback signal proportional to lateral groundspeed is also calculated. This correction drives the aircraft lateral speed to zero so that the aircraft heading aligns with its ground-track in a turn.

Altitude Hold

The altitude hold mode is engaged manually by pressing the Altitude Hold (ALTHLD) switch on the AFCS control panel. This mode also engages automatically when in VELSTAB and the Hover Hold mode is entered. A simplified block diagram of the collective axis, both PFCS and AFCS, is shown in Figure 5. The Altitude Hold mode allows the pilot to maneuver the Comanche vertically using either the left-hand displacement collective stick or the vertical axis of the right-hand sidearm controller. The normal procedure for using the displacement stick is to press and hold the Trim Release switch prior to moving the control. This switch disengages the ALTHLD logic, disables the sidearm vertical axis, and releases stick trim. This allows the pilot to move the stick freely in order to

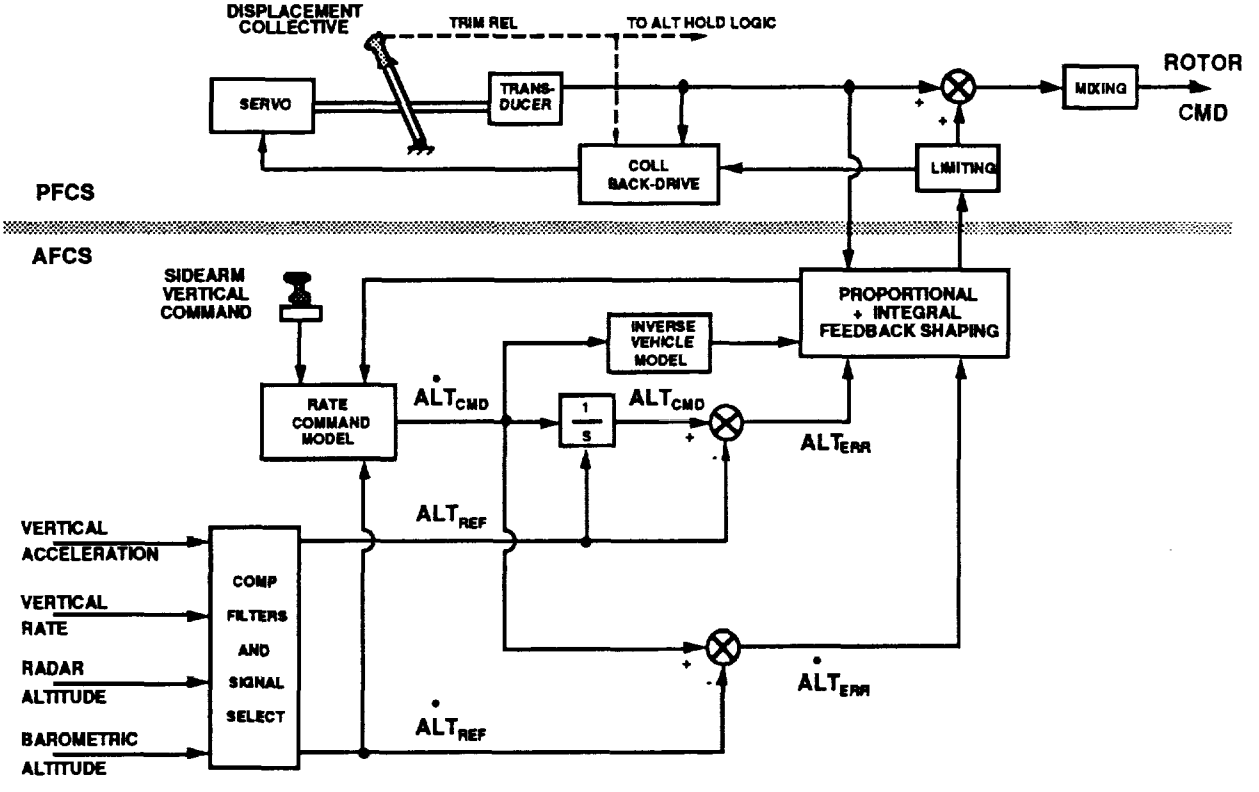

FIGURE 5. COLLECTIVE AXIS BLOCK DIAGRAM

maneuver the aircraft vertically. When the switch is released (trim engaged), the ALTHLD logic smoothly transitions the aircraft to level flight and then holds altitude. If the pilot moves the collective stick against trim without releasing trim, the ALTHLD logic senses this override condition and prevents the collective trim integrator from saturating. When the pilot ceases to override the control, the aircraft returns to its original altitude.

The response of the aircraft to vertical inputs applied to the sidearm controller is controlled by model following control laws similar to those found in the other axes of the control system. The response-type of the control laws is vertical rate command / altitude (height) hold (RC/HH). The maximum commanded vertical rate is ±600 ft/min.

The logic for switching between radar and barometric altitude references is a function of radar altitude, 'radar altitude reliable' logic (from the MEP), or pilot selected reference (from a MEP menu). The altitude reference switches from radar to barometric at 300 feet radar altitude, which coincides with the altitude at which the radar altitude symbology disappears from the HMD. The ALTHLD logic has 25 ft of hysteresis so that the reference won't flip back and forth when the aircraft is flying near this limit. The radar altitude reference is a complementary filtered signal combining the low frequency portion of radar altitude and the high frequency portion of inertial vertical acceleration. The control laws provide a transient-free transition from radar to barometric altitude reference.

PILOT EVALUATION

A simulation experiment was conducted to document pilot acceptance of the detailed design for the RAH-66 Comanche Selectable Mode control laws. The test was conducted in the Boeing Helicopters motion-base simulator. Full specification compliance testing will be subsequently carried out at the Sikorsky Full Mission simulator.

Simulation Facility

The Philadelphia simulation facility uses a 30' diameter fixed dome onto which the simulated visual scene is projected. The two-place simulator cab sits atop a 6 degree-of-freedom motion-base within the dome. The visual scene is corrected for relative motion between the cab and the fixed dome. The scene is projected through 4 light valves onto the dome surface. The computer image generator used to supply the visual is an Evans & Sutherland CT6 system. Note, the CT6 visual databases have been tailored specifically for the tasks simulated in this experiment. The ADS-33 task related gaming areas used for this test included: Accel / Decel, Pirouette, Sidestep, and Bob-up / down.

The Hover, Hover Turn, and Slalom tasks were evaluated in the vicinity of the Edwards AFB gaming area of the standard CT6 visual database. An attempt was made to provide the pilot with sufficient cues in order to ascertain task performance relative to the specified constraints.

The Degraded Visual Environment was simulated by restricting the pilot's field-of-view (FOV) to match the Helmet Mounted Display (HMD) FOV. This was done by placing a black felt mask over the helmet visor with holes placed in front of the HMD optics. A portion of the mask was also removed so that the pilot could view the head-down displays (moving map and pilot instruments). An additional piece of felt was placed between the optical elements to prevent cross-eye inter-visibility. Figure 6 is an illustration of the helmet. The test pilots estimated the field of view to be approximately 55° wide X 34° high which closely matches the Comanche design.

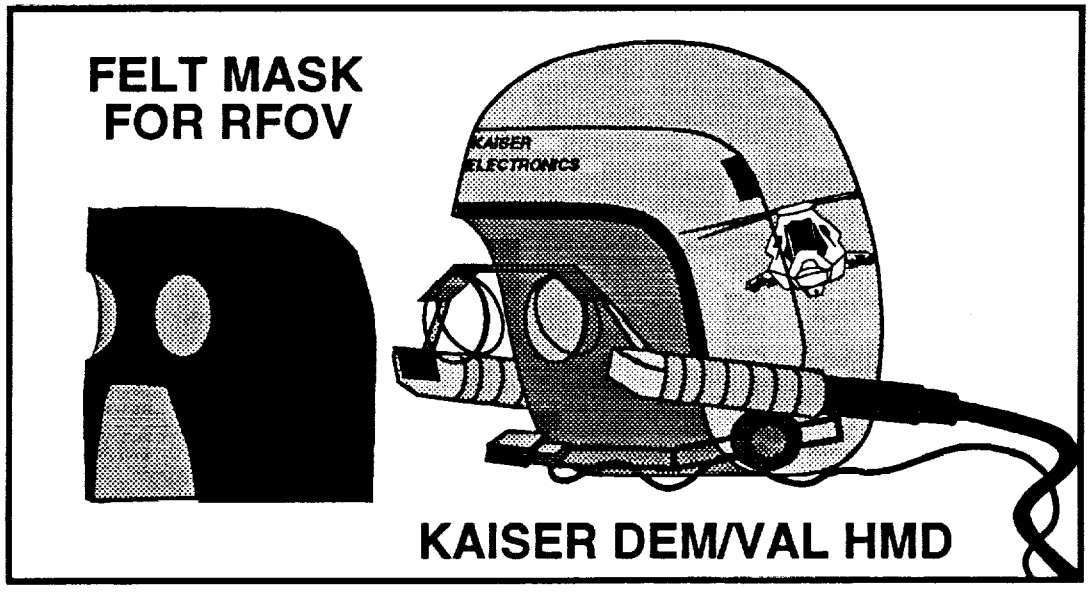

FIGURE 6. KAISER HMD WITH RESTRICTED FIELD OF VIEW

The Kaiser Helmet Mounted Display was used for all of the formal Selectable Modes testing. The HMD was cited as being essential to provide all of the cues necessary for the pilot to view all task constraints in the simulation environment. This was particularly true when the pilot's field-of-view was restricted to simulate the effects of flying with an HMD displayed visual image. With the RFOV, the pilots relied even more heavily on the HMD for cues.

The symbology displayed in the HMD (Figure 7) represented the LH DEM/VAL design. The symbology provides the pilot with the following heads-up information: horizon line, indicated airspeed, ground-speed vector (< 40 kt only) with acceleration cue and Hover Hold engagement cue (circle fills in), barometric altitude, rate of climb, radar altitude (< 300 ft only), pitch and roll attitudes, heading, and lateral acceleration (V > 40 kt only).

Cockpit Layout

The simulated Comanche cockpit featured a Lear Astronics 3 axis sidestick controller mounted next to the seat. The controller pitch, roll, and yaw orientation matches the Comanche design. The controller force characteristics were optimized during the PFCS / Core AFCS simulation testing. A DEM/VAL 4-axis controller, modified to approximate the force and displacement characteristics of the 4-axis controller design, was also available for several tasks.The collective stick was configured for the proper range of motion (6 inches) and was hydraulically backdriven to simulate the RAH-66 displacement collective force characteristics. The backdrive was also used to move the collective stick when the Altitude Hold mode was engaged.

Simulated Flight Conditions

All Selectable Mode evaluation was conducted at the following conditions: primary mission gross weight (PMGW - 10250 lb), mid CG (398.8 in), 2000 ft / 95 °F density altitude. The HMD was used for all tasks and the RFOV was used for formal pilot evaluation of DVE maneuvers.

Simulation Model

The math model representing the RAH-66 aircraft consisted of a classical (Bailey) rotor representation of the BMR, a fan-in-fin model of the FANTAIL™, and a simplified engine model. The control laws are modelled using the same algorithms that will be used in the flight aircraft. The flight control system redundancy was not modelled. Ideal sensors were assumed, i.e. sensor accuracy, dynamics, and filtering were not modeled.

Handling Qualities Assessment

During formal task evaluation, the pilot was the primary judge of task performance with respect to the desired parameters. Typically, this followed a series of familiarization sessions, during which both pilots and engineers scrutinized all aspects of the task performance relative to the specified maneuvers. Pilots did not commence the formal evaluation until they had become familiar with the control laws and the tasks. The Cooper-Harper Handling Qualities Rating Scale (Reference 2) was used to assess handling qualities with respect to the tasks evaluated.

TASK DESCRIPTIONS

The following tasks were evaluated during the simulation experiment. In general, the ADS-33C maneuvers were performed as written. *Any changes to the tasks are indicated in italics.*

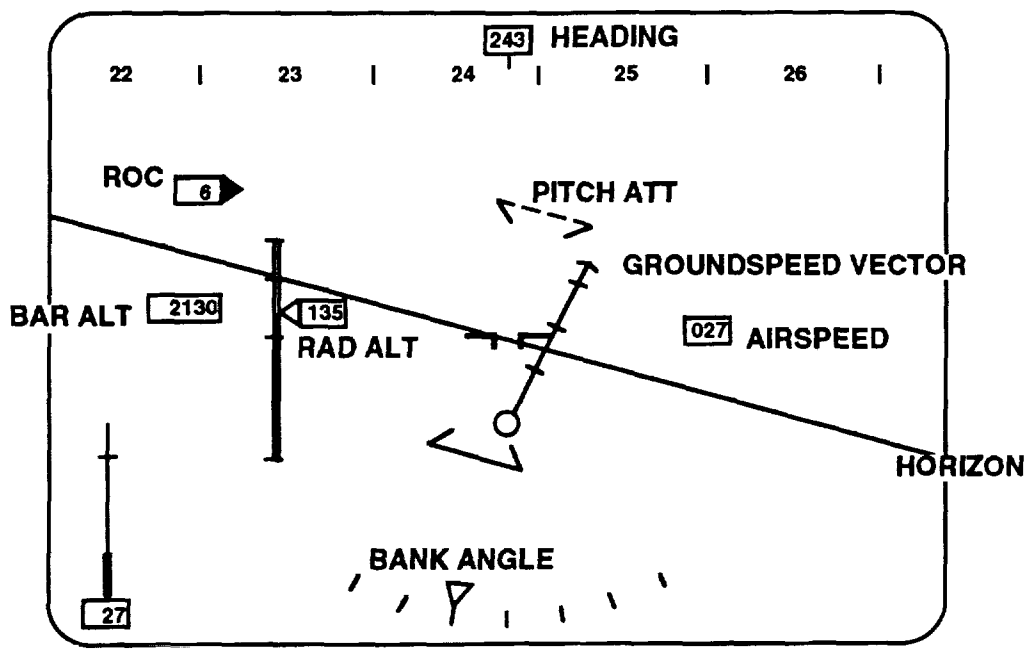

FIGURE 7. HMD SYMBOLOGY

ADS-33C DVE Maneuvers

Since the Comanche Selectable Modes were specifically designed to provide Level 1 Handling Qualities while performing the ADS-33C DVE maneuvers, these tasks were the primary focus of the simulation experiment. The following are only the task descriptions of the maneuvers. A complete description including desired performance is contained in Reference 1.

Hover. (ADS-33C 4.4.1) Maintain a steady hover at an altitude of not more than 6.1 m (20 ft) above the ground. *Starting approximately 50 to 100 ft from the desired hover point, fly to the hover point and establish a stable hover. Approach may be made from any direction. Perform maneuver with both velocity command / position hold (V < 5 kt) and attitude command / velocity hold (5 <V < 10 kt) response-types. Pilot ratings for task shall include acquisition of hover point.*

Hovering Turn. (ADS-33C 4.4.2) From a steady hover at an altitude of not greater than 6.1 m (20 ft), complete a 180 degree turn as rapidly as possible, in both directions.

Pirouette. (ADS-33C 4.4.4) Initiate the maneuver from a stabilized hover over a point on the circumference of a 30.5 m (100 ft) radius circle, marked on the ground, with the nose of the rotorcraft pointed at a reference point at the center of the circle, and at a hover altitude of approximately 3 m (10 ft). Accomplish a lateral translation around the circle, keeping the nose of the rotorcraft pointed at the center of the circle, and the circumference of the circle under the pilot station. Perform the maneuver in both directions.

Acceleration and Deceleration. (ADS-33C 4.5.1) Starting from a hover over a defined point, accelerate to a groundspeed of at least 50 knots, and immediately decelerate to hover over a defined reference point. *Deceleration may be delayed to adapt task to existing accel/decel course.* Maintain a constant altitude at or below 12.1 m (40 ft).

Sidestep. (ADS-33C 4.5.2) Starting from a stabilized hover, with the rotorcraft oriented 90 degrees to a reference line marked on the ground (or a series of objects such as traffic cones, etc.), initiate a lateral translation at approximately constant heading up to a speed of at least 17 kts. Maintain constant speed for approximately 5 sec, followed by a lateral deceleration to hover. The maneuver is to be conducted at a constant altitude at or below 9.1 m (30 ft). Maintain the cockpit station over the reference line. The maneuver shall be performed in both directions.

Bob-up and Bob-down. (ADS-33C 4.5.3) From a stabilized hover at an altitude of 3 m (10 ft), bob-up to clear an obstacle approximately 7.6 m. (25 ft) high to achieve a line-of-sight with a simulated threat. Simulate the attack using a fixed gun-sight. *Turn approximately 5 degrees to acquire the target.* As soon as the target is stabilized in the sight, perform a descent to the initial hover position.

Slalom. (ADS-33C 4.5.4) The maneuver is initiated in level unaccelerated flight, and in the direction of a line or series of objects on the ground. Maneuver rapidly to displace the aircraft 15.2 m (50 ft) laterally from the center-line and immediately reverse direction to displace the aircraft 15.2 m (50 ft) on the opposite side of the center-line. Return to the center-line as quickly as possible. Maintain a reference altitude below 15.2 m (50 ft) AGL. Accomplish the maneuver so that the initial turn is both to the right and to the left.

Other ADS-33C Maneuvers

The following ADS-33C tasks were performed during the Core AFCS evaluation but were judged to require the additional stabilization provided by the Selectable Modes in order to achieve Level 1 ratings.

Hovering Turn. (ADS-33C 4.1.2) From a steady hover at an altitude of not greater than 6.1 m (20 ft), complete a 180 deg turn as rapidly as possible, in both directions, with a wind of at least 20 knots from the most critical direction. If a critical direction has not been defined, the turn shall be completed with the wind blowing directly from the rear of the rotorcraft.

Rapid Bob-up and Bob-down. (ADS-33C 4.2.3) From a stabilized hover at an altitude of 3 m (10 ft), bob-up to clear an obstacle approximately 7.6 m (25 ft) high to achieve a line-of-sight with a simulated threat. Simulate the attack using a fixed gun-sight. *Turn approximately 5 degrees to acquire the target.* As soon as the target is stabilized in the sight, perform a descent to the initial hover position.

Additional Tasks

The following tasks were performed to demonstrate other system requirements, to evaluate critical control law elements, and to substantiate mission suitability.

Turn to Target. (LH BAFO System Specification, section 2.3.2.1.2.4.1 - Reference 3) From OGE and IGE conditions in winds from zero to 45 knots from any direction, yaw 180° over a point. It shall be possible to maintain the axis of turn within a circle whose radius is 1.5 m at zero knots and 3 m at 45 knots over a point. The maximum excursion in vertical position shall be less than ±.61 m at zero and ±1.22 m at 45 knots. Tolerance on heading shall be ±2 degrees. Time allowed to complete maneuver is 4.7 sec.

DVE NOE Mission. Perform a simulated NOE scout mission requiring the pilot to follow a prescribed path designated by waypoints on the HMD and head-down map display. The mission is to be flown in a DVE, with VELSTAB and Altitude Hold engaged.

Performance criteria:

- complete task within a predetermined time
- maintain altitude below 40 ft AGL
- maintain groundspeed at or below 25 kt (except for quick dash across open terrain)
- decelerate to a stabilized hover at each way-point

SIMULATOR TEST RESULTS

This section provides the results of the pilot simulation evaluation of the Selectable Mode control laws. A brief discussion of the degraded visual environment is presented including data from a UCE test. Data is in the form of Cooper-Harper handling qualities pilot ratings and summaries of the pilot comments with respect to each task.

Degraded Visual Environment

Restricted Field-of-View The helmet and method used to provide the restricted field-of-view (RFOV) are shown in Figure 6. The RFOV mask was qualitatively assessed by the pilots and found to be a simple but effective means of modeling the Comanche FLIR/II DVE. The RFOV was considered to be the most important characteristic of the DVE, forcing the pilot to make frequent head motions and eliminating any peripheral vision cues. The RFOV also made the pilots rely more heavily on the data provided by the HMD.

UCE Test During the simulation experiment, a UCE test was conducted in accordance with ADS-33C (except with a single pilot only) to check the simulator DVE with the restricted field-of-view. The purpose of this test is to rate the visual database and displays in terms of how "good", "fair", or "poor" the cues are for performing a subset of the mission tasks. UCE is a new concept to V/STOL HQ specs and is used to determine the required levels of stability and control augmentation needed to achieve desired levels of handling qualities as the mission environment changes.

The test, by spec, is conducted with a Level 1 rate command system. For this experiment, a simplified linear based model, the Helicopter Air Combat (HAC) simulation model with a rate command response-type (as defined by ADS-33C Section 3.2.5) was chosen. The pilot attempted to perform 6 of the ADS-33C DVE maneuvers to the desired levels of performance. The pilot provided visual cue ratings (VCRs) for each task as well as handling qualities ratings (HQRs). Using the procedure described in ADS-33C, the VCRs were used to calculate the Usable Cue Environments (UCEs) for each task. Figure 8 shows the spread of UCEs for the various tasks - UCE = 1 for hover, vertical landing, and accel/decel; UCE = 2 for bob-up; and UCE = 3 for sidestep and pirouette. The average UCE = 2.

Pilot comments and HQRs for each task performed in the UCE test are provided below. Keep in mind these ratings are for a rate command response-type in a DVE and were not done with the Comanche model.

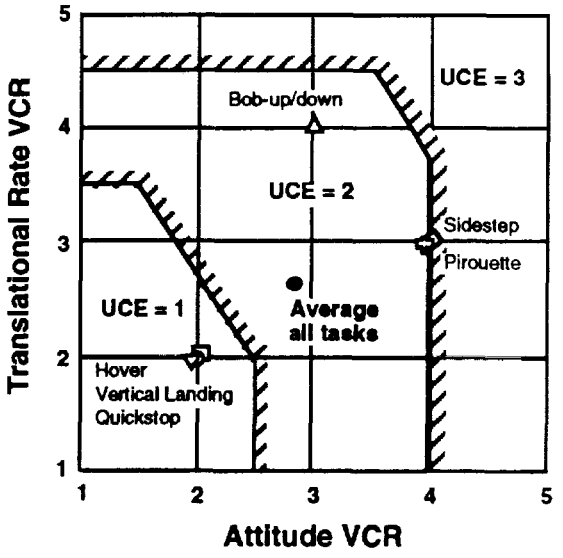

FIGURE 8. SIMULATOR UCE FOR DEGRADED VISUAL ENVIRONMENT

Hover task was rated HQR = 3. Primary source of workload was fore and aft drift which was difficult to detect unless the pilot turned his head to the side and looked downward. The HAC model was setup to trim at 0° pitch and roll attitude which complicated the task since the pilot was familiar with the RAH-66 hover trim attitudes of about +5° and -4° respectively. The HMD radar altitude and vertical speed symbology provided the necessary cues for the vertical axis.

Vertical landing task was also rated HQR = 3 and the comments from the hover task apply.

Bob-up/down was rated HQR = 7. The HQR and VCR ratings were primarily due to inadequate horizontal translation cues. In addition, the version of the HMD symbology used in the Boeing simulator did not provide sufficient velocity / acceleration cues due to a deadband of about ±1 ft/sec in the groundspeed velocity vector.

Sidestep maneuver was rated HQR = 7 (to right slightly easier). This task forced the pilot to turn his head to the side blanking out some of the symbology which is airframe referenced. Pilot could not meet desired performance due to high workload. The pilot commented that altitude hold (available in the Comanche Selectable Modes) would have made the desired performance achievable.

Accel/decel (quick-stop) task was rated HQR = 4. The cues were quite good but high workload degraded rating somewhat. Pilot noted a slight mismatch in the pilot station altitude and symbology, which added to the workload.

Pirouette was rate HQR = 6. High workload and loss of cues when the pilot turned his head to the side contributed to the rating. External vertical cues were

almost nonexistent; the pilot had to rely on his symbology.

The UCE test confirmed that the cue environment of the simulated DVE was indeed UCE 2/3 as expected. The HQRs of the evaluation tasks agree quite well with the ADS-33C predictions for a rate command system in various UCEs.

COMANCHE HQ TEST RESULTS

ADS-33C DVE Task Performance

Summary charts of the Cooper Harper Handling Qualities ratings for the DVE tasks are presented in Figures 9 and 10. The handling qualities of all of the ADS-33C tasks were rated Level 1 on the average by 4 or 5 pilots. All of the DVE maneuvers were evaluated with the pilots wearing the Helmet Mounted Display, with both an unrestricted and restricted-field-of-view. Average pilot ratings were only slightly higher for the maneuvers evaluated with the RFOV. The spread of ratings was noticeably higher.

Several pilot comments were generally true for all of the tasks (exceptions are noted). The Position Hold and Altitude Hold modes, when engaged, alleviated the pilot of virtually all workload in the pitch/roll and collective axes respectively. This made many of the tasks single axis maneuvers. Aircraft responses to control inputs were predictable and well damped, with no objectionable oscillations or overshoots. Pilot compensation, when needed, was due to inadvertent stick cross-coupling, but this compensation was not considered high enough to reduce the HQRs to Level 2. These difficulties appear to be due to the mechanical characteristics of the 3-axis side stick controller, since the force characteristics (low breakout, low force gradient, and high damping) were optimized for multi-axis input control feel with less system stabilization. However, the pilots all commented that they did not want the sidearm controller characteristics changed in any way.

Hover. As described previously, this task was expanded to include the acquisition of the hover position. Only the ratings for the maneuver performed with the VC/PH response are shown on the charts. Making the approach at a higher speed with the AC/VH response and then transitioning to Hover Hold only increased the pilot ratings approximately 1 HQR point (still well within Level 1). The hover task received average HQRs of 1.5 and 1.8 for the non-RFOV and RFOV respectively. All of the pilots commented that in this mode the vehicle response was very predictable and the workload was very low. Some of the pilots had a little difficulty determining if the desired hover position was being acquired to within the desired performance criteria and down graded their ratings slightly.

Hovering Turn. Hovering turn in zero wind received average HQRs of 2.5 and 2.4 for the non-RFOV and RFOV respectively. Several pilots degraded their ratings for the turn to the right because of inadvertent yaw to roll stick cross-coupling. Pilots found the yaw capture to be predictable for the yaw rates required for the DVE task, making the yaw axis

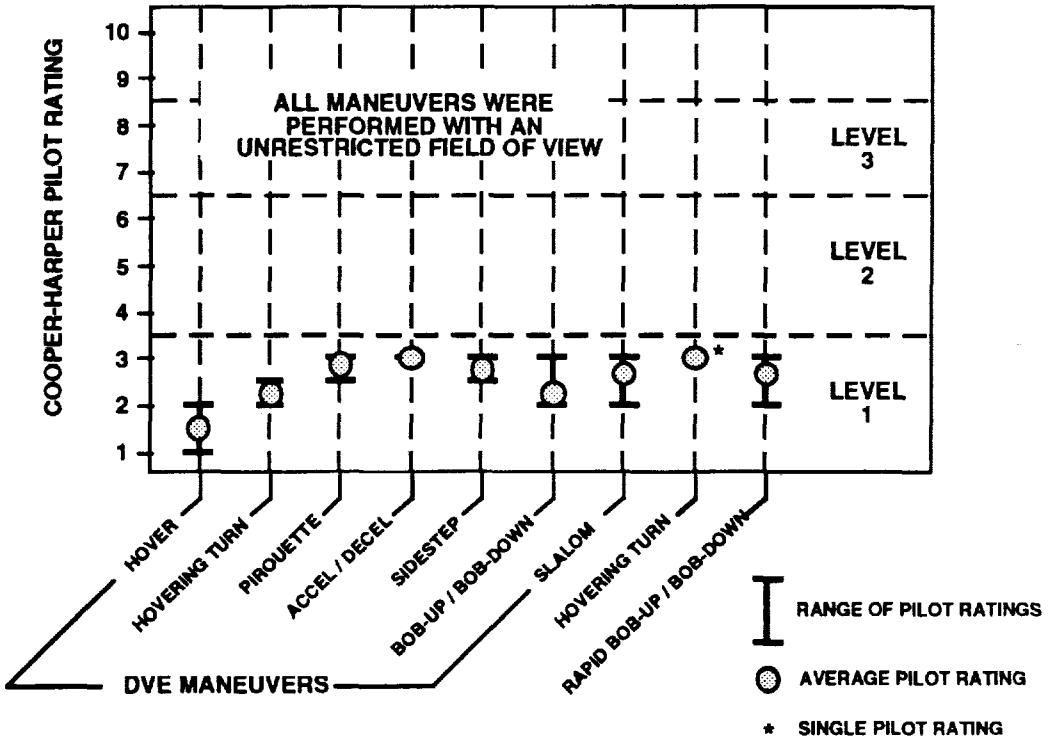

FIGURE 9. PILOT RATINGS OF ADS-33C TASKS - NO RFOV

workload low. Pilots commented that RFOV made it more difficult to pick up the final heading visually.

Pirouette. Pirouette received average HQRs of 2.875 and 3.25 for the non-RFOV and RFOV respectively. In general the pilots were able to perform this maneuver with relative ease (the Army pilot, who has considerable simulator experience, was particularly impressed). During most of the maneuver, the pilots could hold a nearly constant stick force and meet the desired performance. The time constraint for the task was not a problem. Nearly all of the pilots found it more difficult to perform this maneuver to the left although only one pilot split his HQRs (non-RFOV). Possible explanations for this difference include stick cross-coupling and right eye dominance.

Acceleration and Deceleration. Accel / decel received the same average HQRs of 3.0 for both the non-RFOV and RFOV. Most of workload was due to lateral inputs needed to correct the aircraft inherent lateral drift when accelerating and decelerating. Momentary / inadvertent entry into low speed turn coordination when pilot applied lateral inputs didn't effect workload but were disconcerting. The pilots were able to perform the task to the desired levels of performance without using the TC Release Switch (which was difficult to use due to poor grip placement). The pilots also had a little difficulty stopping precisely at the desired point because of the nose high attitudes used during the deceleration portion of the maneuver. This was particularly evident with the RFOV and could have been alleviated with better cues along the sides of the course.

Sidestep. The sidestep received average HQRs of 2.75 and 2.875 for the non-RFOV and RFOV respectively. The pilot ratings were down graded slightly due to cross-coupling of the pilot roll inputs into both the pitch and yaw axes. Several pilots perceived more coupling when applying inputs to the right (pushing on the stick with just their thumb) and split their HQRs. Optimally this would have been a single axis task.

Bob-up and Bob-down. The bob-up / down received the same average HQRs of 2.25 for both the non-RFOV and RFOV. This maneuver was performed with the displacement collective stick. The pilots learned to time the release of the collective trim switch (turning ALTHLD Off and On) to obtain desired altitude performance. Five degree turn to target (*an additional step not required by ADS-33C*) was performed easily. Position hold system kept position errors very small (< ±1.0 ft). Pilots commented that little or no compensation was required to correct for deficiencies. Desired duration of task (15 seconds) allowed the pilots to perform the maneuver smoothly and precisely.

Slalom. The slalom received average HQRs of 2.5 and 2.75 for the non-RFOV and RFOV respectively. The slalom was performed using low speed turn coordination (lateral inputs only). Pilots commented that low speed turn coordination was a major plus in reducing workload for this task. Some pilot ratings were degraded due to the slight tendency to cross-couple right roll into forward pitch inputs. This necessitated occasional pitch

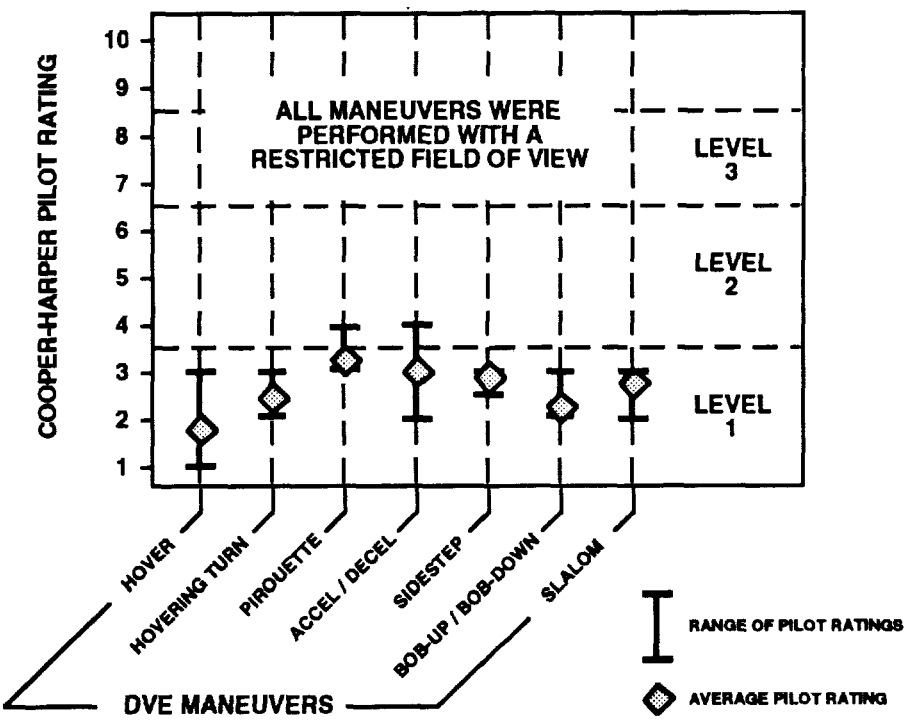

FIGURE 10. PILOT RATINGS OF ADS-33C DVE TASKS WITH RFOV

corrections to maintain airspeed. The pilots found the aggressiveness of the task to be somewhat high for a DVE task , however according to the Army pilot that participated in the test, the 50 ft lateral displacement from the center-line was intended as a minimum; the true intent was 50 - 75 ft (this would have reduced the aggressiveness). One pilot commented that the rating would be down graded if desired performance criteria existed on the recapture of the center-line ground track.

Other ADS-33C Maneuvers
These maneuvers were performed without the RFOV. The pilot ratings for these tasks are shown in Figure 9.

Hovering Turn. (non-DVE) The ADS-33 Precision Hovering Turn task was performed in 20 kt winds without the RFOV and received an HQR of 3 (Level 1). Some saturation of the lateral AFCS port limiter was experienced but the pilot found the resultant transients to be acceptable ("comfortable") and predictable. The pilot (using the visual cues from the hover pad) was required to apply some lateral compensation to meet the desired performance.

Rapid Bob-up and Bob-down. The rapid bob-up / down was performed without the RFOV and received average HQRs of 2.67. The maneuver was made a bit more difficult by the small turn to target when unmasked. The pilots commented that the Position Hold mode made Level 1 ratings achievable. The pilots had to fly the vertical axis manually for the whole maneuver because the Altitude Hold Mode bandwidth was not compatible with the level of vertical aggressiveness needed to perform this task in 8 seconds.

Additional Tasks (not performed with RFOV)
Turn to Target. The system spec turn to target maneuver was performed in both calm air and 45 kt winds; HQRs were not required. Three pilots evaluated this task, but only one pilot performed the task in the final control system configuration. In calm air the pilot was able to meet the system requirements consistently while applying only yaw inputs. Although not required, the pilot rated the maneuver an HQR = 3. The same maneuver in 45 kt winds was significantly more difficult. The AFCS port limits, sized for hardover recoverability, saturated during this maneuver and pilot compensation was required to hold position. Primary workload was in the lateral axis. With limited practice, the pilots could intermittently meet and consistently come close to meeting the specified performance. Table 1 are the last five data runs for a left-hand turn with a 45 kt head-wind. The hardest part of the maneuver was meeting the 4.7 second time limit. Graceful degradation of position hold when port saturation was encountered made the maneuver do-able since necessary pilot compensation was predictable. Attempts to perform this maneuver in the simulator in the Core AFCS mode were not as successful.

Total Time (4.7 sec allowed)	Max Pos. Error (10 ft allowed)	Max Alt. Error (4 ft allowed)
5.0	9	2
4.8	5	2
7.5	12	2
4.6*	9*	2*
5.0	8	2

* meets spec

TABLE 1. TURN TO TARGET TASK RESULTS

DVE NOE Mission. Pilots found the performance of the Selectable Modes to be appropriate for the NOE mission task. No deficiencies were identified. HQRs were not generally provided, but one pilot rated the vertical handling qualities Level 1 with Altitude Hold engaged. The Altitude Hold performance, although not terrain-following in nature (no look-ahead capability), was capable of maintaining satisfactory clearance in most cases. In general, ALTHLD exhibited no undesirable oscillations or drift. Radar altitude would typically return to the desired value after one over/undershoot following a sudden change in ground slope. Occasionally, the pilot had to assist the system (provide lead) when the ground was particularly steep or the aircraft was descending towards upward sloping terrain. Because the Altitude Hold response degraded in a predictable manner with no long term drift or oscillations, the pilot was able to quickly / easily determine when additional compensation was needed.

Groundspeed hold was found to be "very helpful and predictable" and staying out of the loop (not applying compensation) in this axis "works very well." The pilot judged the hover hold system to be "perfect" once established and was able to enter the hover hold gate even with moderate aggression. No changes were recommended.

The low speed turn coordination was of particular benefit in allowing the pilots to precisely fly around trees and other features with just roll inputs. The predictability of the LSTC engagement / disengagement contributed to the precision of the mode. One pilot stated that manual coordination would have been difficult with the RFOV due to a lack of relative motion cues. The RFOV forced the pilot to fly most of the course at 25 kt in order to have sufficient time to visually survey the terrain and chose a flight-path. The course had been designed for 40 kt cruise (without the RFOV). When hovering at each way-point, the pilot had to be less aggressive when doing pedal turns to make sure the tail was clear of obstructions.

CONCLUSIONS

General

Test results provide a high level of confidence that the Comanche Selectable Mode control laws, VELSTAB / Hover Hold and Altitude Hold, will comply with the requirements that flow down from ADS-33C and the Weapons System Specification.

The Selectable Mode control laws are ready for formal ADS-33C compliance testing in the Sikorsky Full Mission Simulator.

The method used to provide the restricted field-of-view was a simple but effective way of modeling the primary characteristics of the Comanche DVE.

The UCE test results combined with the Comanche DVE tests confirm the ADS-33C requirements for increased levels of stability and control augmentation in order to achieve satisfactory handling qualities in a degraded cue environment.

Task Performance

A subset of required maneuvers directly from ADS-33C and the WSS were evaluated. All requirements were met; Level 1 Handling Qualities were achieved for all tested DVE and non-DVE maneuvers, regardless of UCE. The handling qualities of the Comanche Selectable Mode control laws were accepted by the pilots and were judged mission suitable.

Restricting the pilot's field-of-view only slightly degraded the Handling Qualities Ratings of the various DVE tasks. All of the average ratings were Level 1. The RFOV increased pilot workload / head motion and forced the pilots to place more reliance on the HMD symbology for the cues needed to execute the tasks to the desired levels of performance.

Stick cross-coupling was the only source of workload for many of the tasks. However, pilot compensation was never considered high enough to reduce the HQRs to Level 2 and all of the evaluation pilots agreed that the controller characteristics were optimum. A controller with these force characteristics has been flight tested in the Sikorsky Shadow aircraft and found to be satisfactory.

Pilots were not always able to accurately judge quantitative performance for some tasks. Improvements to portions of the database are warranted, however, they were beyond the scope and budget of this test.

REFERENCES

1. ADS-33C, Aeronautical Design Standard, Handling Qualities Requirements For Military Rotorcraft, August, 1989.

2. Cooper, G. and Harper, R., "The Use of Pilot Rating in the Evaluation of Aircraft Handling Qualities", NASA TN D5153, 1969.

3. Light Helicopter Program (LH), System Specification, BAFO Proposal, 2000-315-512-1.

Evaluation of Two Cockpit Display Concepts for Civil Tiltrotor Instrument Operations on Steep Approaches

William A. Decker, Richard S. Bray, Rickey C. Simmons, George E. Tucker
NASA Ames Research Center
Moffett Field, CA

ABSTRACT

A piloted simulation experiment was conducted using the NASA Ames Research Center Vertical Motion Simulator to evaluate two cockpit display formats designed for manual control on steep instrument approaches for a civil transport tiltrotor aircraft. The first display included a four-cue (pitch, roll, power lever position, and nacelle angle movement prompt) flight director. The second display format provided instantaneous flight path angle information together with other symbols for terminal area guidance. Pilots evaluated these display formats for an instrument approach task which required a level flight conversion from airplane-mode flight to helicopter-mode flight while decelerating to the nominal approach airspeed. Pilots tracked glide slopes of 6, 9, 15 and 25 degrees, terminating in a hover for a vertical landing on a 150 feet square vertipad. Approaches were conducted with low visibility and ceilings and with crosswinds and turbulence, with all aircraft systems functioning normally and were carried through to a landing. Desired approach and tracking performance was achieved with generally satisfactory handling qualities using either display format on glide slopes up through 15 degrees. Evaluations with both display formats for a 25 degree glide slope revealed serious problems with glide slope tracking at low airspeeds in crosswinds and the loss of the intended landing spot from the cockpit field of view.

FLIGHT DIRECTOR SYMBOLS

ABAR	Roll command bar displacement
CTAB	Power lever command tab displacement
EBAR	Pitch command bar displacement
K_A	Roll command bar gain
$K_{C\dot{z}}$	Height rate error gain for power lever
K_{Cz}	Altitude error gain for power lever
K_C	Power lever command tab gain
$K_{C\dot{z}}$	Velocity error gain for power lever
K_{DC}	Power lever position washout gain
K_E	Pitch attitude command bar gain
$K_{E\dot{x}}$	Velocity error gain for pitch attitude
$K_{E\dot{z}}$	Height rate error gain for pitch attitude
K_{Ez}	Altitude error gain for pitch attitude
$K_{\dot{y}}$	Lateral velocity error gain for roll attitude
$K_{\dot{\theta}}$	Pitch rate gain for pitch attitude
K_θ	Pitch gain for pitch attitude
$K_{\dot{\phi}}$	Roll rate gain for roll attitude
K_ϕ	Roll attitude gain for roll attitude
K_y	Yaw attitude gain for roll attitude
s	Laplace operator
ϕ	Roll attitude
λ_{Awo}	Lateral command bar washout frequency
λ_{Cwo}	Power lever command tab washout frequency
λ_{Ewo}	Pitch command bar washout frequency
θ	Pitch attitude
τ_A	Lateral stick position washout filter time constant
τ_C	Power lever position washout filter time constant
τ_{CL}	Power lever position lead filter time constant
τ_E	Longitudinal stick position washout filter time constant
ψ_{ac}	Aircraft yaw attitude

Presented at *Piloting Vertical Flight Aircraft: A Conference on Flying Qualities and Human Factors*, San Francisco, California, January, 1993.

INTRODUCTION

Increased air travel using hub-and-spoke airline systems has increased airport air traffic congestion and delays. A feeder airline system based on vertical flight aircraft, principally tiltrotor aircraft, has been proposed as a means of alleviating the conventional, long-haul aircraft runway operations problems (Ref. 1). Such a system would employ vertiports, conveniently located to population and industry centers. Vertiport design must

consider both the land requirements for obstruction clearance (Ref. 2) and community noise impact (Refs. 3-4). Steep terminal operations have been proposed as a possible means of reducing vertiport land requirements and noise impact (Ref. 1).

Government and industry studies seek to define operational and aircraft design requirements for a civil tiltrotor transport and the ground and airway infrastructure required to support it. As part of this effort, a series of piloted simulation experiments was conducted at NASA Ames Research Center to identify handling qualities and flight mechanics influences on terminal operations and cockpit design issues for civil tiltrotor transports (Refs. 5 & 6). Reference 6 describes two experiments. The first experiment utilized "raw data" glide slope and localizer approach guidance and demonstrated the need for improved flight path cuing. The second experiment evaluated two display concepts: a four-cue (pitch, roll, power and nacelle angle) flight director and a flight path vector display. The flight path vector display presented instantaneous aircraft state information and a suggested flight path in the terminal area. It represents an alternate display and guidance technology which should provide the pilot with better situational awareness by graphically presenting information as it might be viewed from the cockpit windshield. This second civil tiltrotor terminal operations simulation experiment provided the initial evaluations of this display concept applied to tiltrotor aircraft. Pilot handling qualities ratings and comments and objective task performance measures for the flight director were reported in Reference 6. This paper expands upon that report and documents similar results using the alternate flight path vector display, thereby providing a comparative assessment of the two display concepts.

This paper presents the design, conduct, and results of the piloted simulator investigation of the two display concepts for the instrument approach task flown to civil transport standards. Recommendations for further development and evaluation are provided.

EXPERIMENT DESIGN

Facility

The experiment was conducted using the NASA Ames Research Center Vertical Motion Simulator (VMS). The VMS features a reconfigurable, interchangeable, cockpit cab mounted on a large motion platform as shown in Figure 1. Maximum vertical acceleration capability is limited to ± 0.67g. Since longitudinal cues are particularly important during tiltrotor conversion operations, the cab was oriented for the longitudinal axis motion along the main beam of the VMS, turning it 90 degrees to that shown in Figure 1. With this cab orientation, the maximum longitudinal acceleration limit is $\pm$ 0.5g. The lateral acceleration capability of the VMS was not used for this experiment. The motion washout logic used in the VMS is described in detail in Reference 7. Table 1 lists the motion gain and filter frequencies used for the low speed operations of the simulation experiment.

The simulator cockpit was configured to provide a basic instrument panel with sufficient instrumentation for tiltrotor instrument approaches (Figure 2). The center panel CRT display presented computer-generated images of either conventional instruments (Figure 3) or a flight path vector display (Figure 4). The conventional instrument display provided a "standard T" layout (the attitude-direction indicator, ADI, above the horizontal situation indicator, HSI, and flanked by airspeed, torque and rotor speed on the left and altitude, climb rate and radar altitude on the right). The flight path vector display provided an abstract representation of cues available in visual flight plus aircraft state data. The functions of the flight path vector display symbology are described later in this paper. For both displays, the nacelle angle was displayed on an analog instrument to the left of the center panel CRT and on a digital display immediately above the CRT. A digital distance measuring equipment (DME) display was located above the altitude indicator and provided the horizontal distance to go to the landing spot.

The experiment used a three-window cockpit view with the external scene provided by an Evans and Sutherland CT-5A Computer Image Generation system. The three windows were arranged horizontally, covering a field of view approximately 140 degrees wide by 34 degrees high as shown in Figure 2. This provided a 17 degree look-down capability. An alternate window arrangement having a right lower "chin" window instead of the left side view was available, but pilots preferred the three-across arrangement. Reasons cited included the desire for mostly level pitch attitude operations of a

commercial transport, a preference for the velocity and position cues provided by the left side window, and the small size and generally poor visual cuing provided in the chin window.

Control inceptors included a center stick, pedals and a power lever with the nacelle beep switch located on its grip (see Fig. 2). The throttle-like power lever geometry was similar to that used in the V-22. As shown in Figure 5, the grip reference point rotated from a position just aft of vertical for minimum power through 24 degrees forward for maximum power, with a total linear motion of four inches. A laterally-oriented thumbwheel on the power lever grip was used to control a lateral translation control mode, described below. The flaps were automated based on schedules of nacelle angle and airspeed. The landing gear was extended throughout the approach evaluation task.

A system of preprogrammed nacelle angle stops was developed to assist the conversion from airplane mode to helicopter mode. The stops were typically provided at 60, 80 and 90 degree nacelle angles. In addition to the tiltrotor continuous movement "beep" controller, pilots could activate a semiautomatic nacelle movement system. Depressing a button on the power lever started the nacelles moving aft at a fixed rate to the next stop. Forward movement of the nacelles, toward airplane mode, was not inhibited by these stops.

Aircraft Model

The aircraft math model was based on the generic tiltrotor simulation model (Ref. 8) and configured as a large transport of 40,000 pounds gross weight. An attitude command-attitude stabilization control system was used for pitch and roll. Yaw axis augmentation featured heading hold at low speeds (below 40 knots) and turn coordination at high speeds (above 80 knots) with linear blending between these modes. The control system was derived from an early design intended for the V-22 (Ref. 9). Table 2 lists approximate aircraft dynamic response characteristics identified using the "CIFER" system identification software described in Reference 10. A torque command and limiting system (TCLS) was employed for the power lever controller (Ref. 11). A lateral translation control mode, LTM (Ref. 9), was implemented to provide nearly pure, wings level, side force in helicopter mode by applying lateral cyclic pitch to both rotors.

The aircraft mathematical model was implemented on a digital simulation computer which cycled at 26 msec. The computational pipeline for the CT-5A produced a new external view image 100 msec after a new aircraft position was supplied by the mathematical model. The cockpit panel center display received update information from the main simulation every other cycle, i.e. every 52 msec. The panel display image had an asynchronous delay of up to 33 msec.

Evaluation Task

The experiment investigated an instrument approach task with evaluation subtasks of: (1) a level flight conversion to approach configuration and airspeed, (2) glide slope tracking, and (3) completion of the landing following breakout. Evaluation atmospheric conditions are listed in table 3. The winds and turbulence were modeled using the "BWIND" routine described in Reference 12. Crosswinds (speed and direction) remained constant to touchdown with no wind shear modeled near the ground. Approach angles of 6, 9, 15 and 25 degrees were investigated. Based on previous flight research experience at NASA Ames (Ref. 13), the nominal glide slope tracking airspeed was adjusted for each approach angle to keep the rate of descent below 1000 feet per minute. Table 4 lists the approach speed and nacelle angle specified for each glide slope.

The nominal approach profile shown in Figure 6 guided flight director command law development. It was briefed to pilots using the flight path vector display as the recommended procedure. Evaluation runs were begun in airplane mode in level flight at 180 knots, 1300 feet altitude above ground level (AGL), 6.5 nm out from the landing spot, and offset from the localizer by 1000 feet. The pilot's first task was to capture and track the localizer as closely as possible. Deceleration and conversion toward helicopter mode began approximately 4 nm out. A pause in the configuration change was recommended at the intermediate configuration of 120 knots and 60 degrees nacelle angle. This allowed the aircraft to stabilize on a trim condition prior to commencing the final nacelle angle change before glide slope intercept. The conversion was continued to 80 knots and 80 degrees nacelle angle. This condition placed the aircraft at the airspeed for minimum level

flight power required in helicopter-mode. It also served as the nominal approach configuration for a 6 degree glide slope. The 6 degree glide slope was intercepted and captured at 2 nm out. For steeper glide slopes, a further level flight deceleration and movement of the nacelles toward the helicopter position took place prior to glide slope intercept and capture. Table 4 lists these nominal approach configurations.

Pilots were required to decelerate to a hover above a minimum-sized, 150 feet square, vertipad (Ref. 2). The flight director command laws were adjusted to terminate the approach in a hover at 10 feet altitude above the landing pad, on glide slope. Pilots completed a vertical landing using visual cues. Following the flight path vector display, a pilot would achieve a hover at 30 feet altitude over the center of the vertipad. The pilot could then complete the vertical landing visually or by using the vertical landing guidance provided by the display.

Flight Director

A flight director which drove command needles on the ADI (Figure 3) was adapted from earlier flight evaluations on the X-22 (Ref. 14) and simulation evaluations of the XV-15 (Refs. 5 and 15). Pitch and roll command bars were displayed on the ADI with "fly to" logic, i.e. a pitch up command would be displayed as an upward deflection of the flight director pitch command bar movement. Similarly, a command to fly to the right would be displayed as a roll command bar displacement to the right. A supplemental scale with an indicator tab for power lever position was placed to the left of the ADI, as shown in Figure 7. During the experiment set-up phase, this tab was selected to drive in a "fly from" fashion, i.e. a command to reduce power was displayed when the moving (rectangular) tab was above the fixed (diamond) center reference. This sensing seemed to better match pilot responses with the power lever motion. An airspeed schedule prompted nacelle angle movements via a "beep nacelle" ("ITVIC" of Ref. 14) command light on the cockpit panel and by an upward pointing triangle above the power command indicator as seen in Figure 7.

Drive laws for the flight director command symbols were adapted from a design for the XV-15 (Ref. 5). They were tailored to the transport tiltrotor model with airspeed-based gain changes. The flight director response was tuned to the aircraft response to provide "K/s" controlled-element (flight director needle) response to pilot input for pitch and roll. Power director tab dynamics approximated "K" response for the height rate control task on the steep approaches. Incremental configuration changes were commanded through the "beep nacelle" symbol and based on a desired airspeed versus nacelle angle schedule. The command law in pitch was:

$$\mathrm{EBAR} = K_{\mathrm{E}}\left[\begin{array}{l} K_{\mathrm{E}\dot{x}}\varepsilon_{\dot{x}} + K_{\theta}\dfrac{s\theta}{s+\lambda_{\mathrm{Ewo}}} + K_{\dot{\theta}}\dot{\theta} \\ +K_{\mathrm{E}\dot{z}}\varepsilon_{\dot{z}} + K_{\mathrm{E}z}\varepsilon_{z} \end{array}\right]\frac{1}{\tau_{\mathrm{E}}s+1}$$

where $\varepsilon_{()}$ represents the difference between the commanded flight profile and the actual path. Similarly, the roll command bar (ABAR) and power lever command tab (CTAB) were driven by:

$$\mathrm{ABAR} = K_{\mathrm{A}}\left[\begin{array}{l} K_{\dot{y}}\varepsilon_{\dot{y}} + K_{\phi}\dfrac{s\phi}{s+\lambda_{\mathrm{Awo}}} \\ +K_{\dot{\phi}}\dot{\phi} + K_{\psi}\psi_{\mathrm{ac}} \end{array}\right]\frac{1}{\tau_{\mathrm{A}}s+1}$$

$$\mathrm{CTAB} = K_{\mathrm{C}}\left[\begin{array}{l} K_{\mathrm{C}\dot{z}}\varepsilon_{\dot{z}} + K_{\mathrm{C}z}\varepsilon_{z} + K_{\mathrm{C}\dot{x}}\varepsilon_{\dot{x}} \\ +K_{\mathrm{Dc}}\delta_{\mathrm{C}}\dfrac{s}{s+\lambda_{\mathrm{Cwo}}} \end{array}\right]\frac{\tau_{\mathrm{CL}}s+1}{\tau_{\mathrm{c}}s+1}$$

Values for the gains, washout frequencies, and time constants of these equations are listed in table 5 for airspeeds of 180 and 80 knots and hover. Note the shift in gains for the height ($K_{\mathrm{E}z}$) and height rate ($K_{\mathrm{E}\dot{z}}$) errors for the pitch (EBAR) and power lever (CTAB) commands as the airspeed moves from airplane mode at 180 knots to helicopter mode in hover. Opposite trend shifts in gains occur for the velocity ($\dot{x}$) gains. This technique is used to command a shift of flight control strategy such that pitch attitude is used to control altitude at high speeds while, in hover and at low airspeeds, altitude is controlled by power lever movements. Referring to the power-required-versus-airspeed curve, the pitch-attitude-for-altitude control technique is known as "front-side" while the latter technique for low speed flight is known as the "back-side" control technique.

Flight director command laws were designed to accomplish the approach task under instrument

meteorological conditions (IMC) based on an approach profile using DME range to the landing spot. This profile required a level flight deceleration and conversion from airplane-mode flight to helicopter-mode flight at the desired approach speed. Conversion and deceleration were accomplished in two segments starting at 3.5 nm out to achieve a condition of 80 degrees nacelle angle at 80 knots by 2 nm from the intended landing spot. This condition represents the level flight minimum power required airspeed and signals a shift of control strategy to use power to control altitude (or glide slope angle) for the approach. The control strategy shift below 80 knots was commanded in the flight director drive laws by changing the gains on altitude and airspeed errors to feed those errors to the appropriate control command bar (pitch command for airspeed and power command for altitude or glide slope). For glide slope angles steeper than 6 degrees, an additional level-flight deceleration (at 0.1 g) was commanded for the pilot to slow the aircraft to the appropriate approach speed (see table 4). Glide slope intercept was commanded at a half degree of flight path angle change per second. Once on glide slope, a gentle deceleration was commanded, based on distance to go, to achieve a hover on glide slope at 10 feet altitude. The deceleration initiation point was adjusted based on the required time to decelerate from the approach speed to achieve the desired hover location. To keep the pitch attitude below 5 degrees nose-up, the deceleration was kept to a very low value, 0.025 g. This allowed the pilot to concentrate on the glide slope tracking task with power adjustments. Upon achieving a stable hover ten feet above the pad, pilots were instructed to complete the landing visually.

Flight Path Vector Display

As an alternative to the compensatory tracking form of the flight director, a flight path vector display format was evaluated. Based on display designs investigated at Ames Research Center for conventional transport (Ref. 16), short takeoff and landing (Ref. 17) and vertical takeoff and landing aircraft (Ref. 18), this flight path vector display sought to apply to tiltrotor aircraft a "situation" display philosophy featuring a flight path vector symbol representing the instantaneous flight path of the aircraft. The movements of earth-frame-related references, which include the guidance elements, reflect the pitch, roll and yaw motions of the aircraft in an "out-the-window" format. The guidance elements are presented as "follow the leader" advisors or "suggesters", which, if closely tracked by the pilot with the flight path symbol, provide precise control of the approach flight path. Abstract "command" indications as seen in a typical flight director display are avoided. Control of the aircraft during reconversion and approach is conducted essentially as in the visual flight mode. Without explicit prompting or command, as with a flight director, the pilot adjusts his control strategy from "front-side" to "back-side" as the reconversion toward helicopter mode progresses.

Aircraft status and guidance selection data are displayed in the upper right and left corners of the display as seen in Figure 4. The flap angle, as driven by the automatic flap system, and average engine torque, commanded and limited by the TCLS are displayed in the upper left corner. The selected altitude and heading and the status of the approach and landing guidance system appear in the upper right corner of the display. Some of these information blocks are deleted from the display function diagrams (Figs. 8-14).

Initial Approach Display — Figure 8 shows the symbols used for initial approach to a terminal area. The panel-mounted display used for this investigation provided a selection of colors to help separate symbols by function e.g. flight path, aircraft status, and guidance or command information. Significant features include a winged flight path symbol with aircraft status information arrayed about it, a horizon line and pitch ladder (omitted from Figure 8), and the aircraft attitude reference provided by a pair of large, subdued, diamonds. As illustrated in Figure 9, airspeed, altitude, longitudinal acceleration (referenced to the airspeed numerals), and either DME distance to a terminal (in airplane mode) or nacelle angle (in tiltrotor mode) are arrayed about the flight path symbol and move with it. Moving the nacelles off the airplane stops changes the flight path array by replacing the DME distance below the flight path symbol with nacelle angle. A bracket about the airspeed numerals is added which moves to represent the relative position (airspeed versus nacelle angle) in the conversion corridor. A longitudinal deceleration command may be displayed relative to the flight path symbol "wing tips" to convey a deceleration profile based on DME distance to the landing spot.

Several guidance command symbols are

available for the initial approach flight phase including a selected heading, specified or target altitude, and the selected approach angle (microwave landing system or equivalent capability assumed). Using these command symbols, the pilot flies the aircraft in such a fashion as to overlay the flight path symbol on the command heading line and the altitude reference as seen in Figure 10. This strategy will bring the aircraft onto the desired flight path.

Glide Slope Capture — When the aircraft enters the localizer capture cone as it approaches the terminal area, the pitch ladder field below the horizon line is replaced by perspective lines representing the ground plane (Fig. 11). The central line of this ground plane represents the extended runway or approach course. In addition, as the aircraft comes within the glide slope capture cone (defined as one third of the selected glide slope angle, e.g., within 2 degrees for a 6 degree glide slope), a "leader" symbol appears which represents an aircraft on the desired track, three seconds ahead of the own aircraft. Figure 11 shows the display view seen as the aircraft approaches the glide slope (from below it). As the aircraft approaches the glide slope from below, the leader symbol will descend until it overlays the glide slope reference line (the dashed horizontal line in Figure 11) at the point of glide slope intercept. A pilot may achieve a smooth glide slope capture by beginning the descent prior to the leader symbol overlaying the selected approach angle. Note that the runway centerline now terminates in a small "goal post" symbol at its lower end, which becomes larger in the display as distance to the landing spot decreases.

Also seen in Figure 11 are the acceleration command symbols which display error from the approach deceleration profile by their position with respect to the flight path symbol. A position above the flight path symbol indicates airspeed too high for the approach profile. The pilot obtains the nominal approach deceleration schedule by nulling the displayed error with respect to the flight path symbol, using power at high speed or pitch attitude at low speed.

Glide Slope Tracking — Pilot strategy on approach is to overlay the own-aircraft flight path vector symbol on the leader symbol to achieve the desired track. Figure 12 shows the display for a condition where the aircraft is above and to the left of the desired course track. The dashed line in this figure, extending from the landing spot "goal posts" through the leader symbol is not displayed but is drawn here to help the reader visualize the desired course track.

Hover and Vertical Landing — A unique hover symbology set is provided near the landing pad. It attempts to provide additional longitudinal position cuing for the landing without resorting to the planform view common to many hover displays. With the addition of a longitudinal "hover position" bracket, the display provides X-Y hover guidance while maintaining its consistent Y-Z plane perspective, similar to that seen outside the cockpit windshield.

Figure 13 shows the aircraft approaching hover over the landing spot. In this figure, the aircraft is on course, at 45 feet and 15 knots, with the nacelles in the pure helicopter position of 90 degrees. Following the leader symbol and nulling the acceleration command symbols will bring the aircraft to a hover at 30 feet altitude over the intended landing spot. At low speeds in the vicinity of the landing spot, the conversion corridor bracket is doubled in size and changed to a white color (as with other terminal guidance symbols such as the goal posts) and now represents the longitudinal position with respect to the intended landing spot.

With the aircraft in a hover within the desired landing zone, a display function switch, located on the center stick grip, may be cycled to provide vertical landing guidance. When activated, the leader symbol drops below the flight path symbol. Reducing power to overlay the flight path symbol on the leader symbol, as seen in Figure 14, will achieve a gentle landing.

Data Collection

Data collection included objective performance measures, such as tracking accuracy, and subjective measures, including Cooper-Harper Handling Qualities Ratings (Ref. 19) and pilot commentary. Figure 15 shows the dichotomous decision tree of the Cooper-Harper Handling Qualities Rating system. Task performance standards were established based on airline transport pilot (ATP) check flight criteria (Ref. 20). Adequate task performance was defined equal to the ATP standards. Desired task performance was defined as half the ATP standards. For the mostly decelerating approach task (little constant speed flight), desired performance

standards included altitude (within fifty feet of the designated altitude in level flight) and guidance error (consistently less than a half "dot" error with no one "dot" exceedances). One "dot" error on the raw data indicators was 1.25 degrees in elevation and 2.5 degrees in azimuth.

Eight evaluation pilots, representing NASA, FAA, the British Civil Aeronautics Authority, Bell Helicopter Textron International, and Boeing Defense and Space Group, Helicopter Division participated in the experiment. Each pilot had both rotary-wing and fixed-wing flight experience. Four also had tiltrotor flight experience. All received familiarization training and task training in the simulator prior to beginning evaluations. Table 6 lists the number of pilots and evaluation runs contributing to handling qualities and performance statistics for each glide slope angle and display format combination.

RESULTS

The experimental results for each of the two display formats (flight director and flight path vector display) are described below for each of the evaluation subtasks of the instrument approach.

Initial Approach and Reconversion Using a Flight Director

During the initial approach phase, the aircraft was reconfigured from airplane mode to helicopter mode and decelerated to the final approach airspeed. The baseline transport tiltrotor configuration of this investigation produced a strong "ballooning" tendency during the initial phase of the reconversion due to early deployment of 40 degree flaps and the increment of rotor thrust aligned with the vertical axis. An alternate flap movement schedule based on both nacelle angle and airspeed and the development of a pilot-initiated, semiautomatic, nacelle movement control provided some workload relief. A large nose-down pitch input was still required, though, to maintain the desired altitude. The flight director helped prompt this movement. It also proved helpful in commanding a steady deceleration and prompting required nacelle movements.

Figure 16 shows handling qualities ratings for level flight reconversions flown in calm or turbulent conditions and ending at the nominal approach speeds for the four glide slopes investigated. Borderline satisfactory handling qualities were achieved for reconversions to airspeeds appropriate to approaches up to 15 degrees. A slight degradation in handling qualities was associated with reconversion and deceleration to the 20 knot airspeed required for the steepest (25 degree) glideslope. Pilot commentary identified workload (particularly in crosswinds and turbulence) during the final deceleration segment, from 80 knots to the approach speed, as the principal reason for degraded ratings.

The flight director commanded a deceleration at 0.1 g for the final deceleration below 80 knots required for approaches at 9, 15 and 25 degrees. This contrasts with the 0.025 g deceleration commanded on the glide slope. For the 6 degree glide slope, the on glide slope deceleration began at 80 knots, overlapping the airspeed range of the final level-flight deceleration used for the steeper glide slopes. Since the 0.025 g deceleration from 80 knots was successful on the 6 degree glideslope, one may infer that a smaller deceleration command might have helped the final level-flight deceleration required for the steeper glide slopes. Based on pilot commentary noting an abrupt nose-up pitch input to accomplish this final level-flight deceleration at 0.1 g, a slower deceleration should be investigated.

Task standards required maintaining less than 50 feet altitude variation during the level flight segment of the approach. The average maximum altitude gain during reconversions using the flight director was 51.6 feet for borderline satisfactory performance as reflected in the pilot ratings. Three of the 164 evaluation runs contributing to this statistic yielded altitude gains in excess of 100 feet, exceeding the tolerance for adequate performance.

Turbulence contributed to altitude control degradation as reflected in the handling qualities ratings for deceleration to the approach speeds for 6, 9 and 15 degree glide slopes. The average altitude gain in calm conditions was 45.2 feet, while the addition of crosswinds and turbulence resulted in a 55.4 feet average altitude gain. In contrast to level-flight decelerations for the other glide slopes where the peak altitude gain occurred early in the conversion, the peak altitude gain for deceleration to 20 knots often occurred in the final level-flight deceleration segment. This altitude peak during the final

level-flight deceleration occurred in both calm and turbulent conditions, reflecting more on the commanded deceleration than the atmospheric conditions.

Glide Slope Tracking Using a Flight Director

Execution of the final approach using only raw angular tracking error instrumentation proved difficult on steep glide slopes in previous investigations (Ref. 6). The flight director was designed to provide additional instrument cuing important for control and tracking at the low airspeeds required for steep approaches. The flight director response and command laws provided cuing appropriate to the "backside-of-the-power-curve" control technique required for the approaches evaluated. It also commanded a deceleration on glide slope to achieve a hover just above the intended landing spot.

Figure 17 shows the handling qualities ratings for the glide slope tracking subtask with the flight director compared to previous results using raw guidance data only. Satisfactory glide slope tracking was achieved with the flight director on approaches up to 15 degrees. Ratings for the 15 degree glide slope were degraded somewhat by the loss of the intended landing spot from the cockpit field of view through much of the approach in clear conditions or after breakout in low visibility conditions. While particular cockpit windshield fields of view vary among aircraft models, this points to an important criteria for developing an approach procedure. The pilot must assure himself of a clear landing spot on final approach whenever atmospheric visibility conditions permit and certainly prior to moving over the landing spot. The 25 degree glide slope ratings reflect both the complete loss of visual contact with the landing spot and the increased workload required to correct for crosswinds and turbulence at the slow (20 knots) approach speed. Ratings for the 25 degree glide slope degrade to include some inadequate (very high workload) ratings in moderate turbulence. The spread of handling qualities ratings was much less with the flight director than with only "raw data guidance," reflecting the consistent performance and implicit workload reduction achieved with a flight director.

Objective task performance measures are consistent with the pilot ratings. Glide slope and localizer tracking errors are typically distributed equally on both sides of the desired path, averaging to a small, meaningless error statistic. Root mean square (rms) of the tracking error is a time-weighted average of the absolute value of the error; hence it is a better measure of tracking accuracy. The rms tracking errors were averaged for all pilots and atmospheric conditions for the four approaches. Figures 18 and 19 show the average rms tracking error for the glide slope and localizer, respectively. Also shown are the ranges of rms tracking error for the evaluation runs. Average tracking errors were less than 0.25 degree for glide slopes up through 15 degrees, with none worse than the "half dot" specified for desired performance. Tracking performance on the 25 degree glide slope averaged about a half degree, within the desired "half dot" criteria. Note that some runs on this glide slope, however, produced elevation tracking errors as large as 2.16 degrees, much worse than the "one dot" error specified for adequate performance. High workload coupled with large tracking errors caused the evaluation pilots to state that the 25 degree approach procedure with manual control using the flight director did not meet certification standards.

Initial Approach and Reconversion Using the Flight Path Vector Display

The flight path vector display provides cuing analogous to visual flight. While guidance for a nominal approach deceleration profile is provided, the pilot may fly a different airspeed profile. This display provides considerably better situational awareness of position during minor deviations when compared to the information provided by the flight director with its structured command approach profile. In contrast to the flight director, the flight path vector display, as evaluated, provides no discrete prompts for configuration changes, relying on the pilot to maintain flight within the nacelle angle-airspeed conversion corridor. In contrast to the flight director, which was largely conventional in presentation, the flight path vector display required considerable training for proper pilot interpretation and response to its symbology and graphical presentation.

Figure 20 shows handling qualities ratings for the reconversion and deceleration to approach airspeed subtask. Four pilots were trained sufficiently with the flight path vector display to contribute to these ratings. The 25 degree approach was rated by only two of the four evaluation pilots, somewhat reducing the statistical validity of the results presented. Satisfactory ratings

were achieved with the flight path vector display for the conversion task. Pilots commented that displacements of the flight path vector symbol with respect to the horizon and the selected altitude symbol were sufficiently compelling to achieve tight altitude tracking performance. Altitude ballooning during configuration change was reduced to half that experienced with the flight director with an average maximum altitude gain of 24.3 feet. Reconversions in calm air produced an average maximum altitude gain of 20 feet while reconversions in turbulence produced an average maximum gain of 26.9 feet. Both altitude statistics were well within the desired tolerance of fifty feet.

Conversion cuing in the form of a sliding bracket around the airspeed numerals on the display was not compelling enough to prompt configuration changes. During a deceleration, as airspeed approached the lower conversion corridor bound at a fixed nacelle angle, the bracket bottom would move close to the bottom of the display's airspeed numerals. This situation should have prompted pilot action--typically a further aft movement of nacelle angle. Instead, pilots flew the approach task by initiating discrete steps in nacelle position at prebriefed DME distances. The semiautomatic nacelle movements, coupled with the modeled tiltrotor's drag characteristics, tended to keep the aircraft in the center of the broad conversion corridor. Thus the potential configuration change cuing provided by the corridor bracket was not used by the pilot, being replaced by the approach profile briefing which suggested configuration changes at specified DME distances. In the final analysis, pilots expressed a preference for discrete cuing (such as that provided by the "beep nacelle" light of the flight director) to prompt the required configuration changes at appropriate positions during the approach.

Glide Slope Tracking with the Flight Path Vector Display

Handling qualities ratings for glide slope tracking using the flight path vector display are shown in Figure 21. The glide slope tracking handling qualities were assessed as satisfactory up through a 15 degree approach in calm air. Handling qualities in crosswinds and turbulence degraded into the adequate range based on reported higher pilot workload at the slower approach speeds. Pilots reported a higher workload associated with all control axes to maintain the desired track. Most pilots commented on the lack of sufficient guidance for power lever positioning, reflecting more on the actual power lever geometry (to be discussed below) than the difficulty of height / flight path control during the approach. As with the flight director, degraded handling qualities ratings on glide slopes of 15 degrees and steeper, reflect the loss of the intended landing spot from the cockpit field of view.

Desired tracking performance was clearly achieved for glide slopes up through 15 degrees as shown by the flight path vector display tracking statistics in Figures 18 and 19. Glide slope and localizer tracking performance similar to that obtained with the flight director was achieved. With one third as many evaluation runs contributing to these tracking statistics, one should not draw too many comparisons between the two displays for the maximum rms error achieved. What is significant about the worst rms tracking errors are that they never exceeded the "half dot" error specified for desired performance. Thus, although the pilot workload increased on steeper glide slopes as reflected in the handling qualities ratings, the tracking performance remained consistently good up through a 15 degree glide slope.

With only two pilots rating the 25 degree approach, the numerical handling qualities rating and tracking error averages are included only for completeness. Pilot commentary associated with the use of the flight path vector display on the 25 degree glide slope amplified similar comments made for shallower glide slopes. Marginally adequate glide slope tracking performance (Fig. 18) and only adequate handling qualities (Fig. 21) were recorded for this glide slope angle. Detailed examination of the tracking performance data show adequate performance, on average, with an extended range from very good in calm conditions to worse than "one dot" tracking in moderate turbulence and crosswinds.

Both pilots reported extensive activity required in all controls axes with cuing insufficient for the large, precise, control inputs desired. In particular, they reported difficulty maintaining airspeed control, citing difficulty attaining precise pitch control as the issue. In contrast to the flight director which provided attitude command for airspeed control at low airspeed, the flight path vector display concentrated the pilot's attention on

the control of flight path. On the 25 degree glide slope, the flight path symbol was displaced well below the display horizon which drew attention away from the pitch attitude references which were expected to remain near the horizon for level attitude. To obtain the desired attitude status, pilots had to scan a larger area of the display while maintaining precise flight path tracking. Within the scope of this evaluation, it was not clear whether this pilot concern for pitch attitude reference was a training, display design, or other flight dynamics and control issue.

Further development and evaluation are warranted for the use of the flight path vector display on steep glide slopes.

Flight Path Vector Display Issues

The flight path vector display was originally developed as a head-up-display (Refs. 16-18) where its angular presentation was conformal with outside visual cues. The pitch axis, in particular, was designed to displace on the display through the same angle as the real world when the display was viewed from the design eye point. This experiment employed the flight path vector format in a panel-mounted display which was expected to represent the display capability of a typical civil transport. As a panel-mounted display, the flight path vector display was no longer constrained to a conformal pitch scale, although conformal scaling was used for the shallower glide slope angles. Flight path status and guidance for the steepest glide slopes was accommodated on the panel mounted display with reduced pitch scaling (typically half of conformal scaling). This had a desensitizing effect on the display for these approaches, perhaps loosening tracking performance. Conversely, reduced scaling may be the technique needed to desensitize the flight path vector display for the shallower glide slopes which most pilots reported as too sensitive in response leading to higher workload. Further tuning of this display's sensitivity is warranted.

Displacement of the flight path vector symbol below the horizon was another aspect of the display affecting handling qualities ratings and comments on all approaches. Figure 12 provides an illustration of the display in use for glide slope tracking. Attention was focused primarily on the flight path vector symbol and the attempt to overlay it on the "leader" symbol. Steeper glide slope angles displaced the flight path symbol further below the horizon and pitch reference. Pilots had to develop new scan patterns to pick up the pitch reference which was normally close to zero (the horizon line) for the approach task.

Reduced awareness of the heading situation was an issue when the flight path vector symbol was displaced well below the horizon on steep glide slopes. With the heading tape overlaying the horizon and pilot attention focused on the flight path symbol, well below, pilots lost awareness of the heading situation. Pilots who reacted to the effect of crosswinds at low airspeed with a large crab angle required a large heading change upon breakout to locate the landing spot. Likewise, pilots who used sideslip to compensate for crosswinds required constant attention to both desired heading and flight path control. Both control strategies required awareness of heading which was well separated in the display from the flight path symbol. The desired heading was displayed with a large tick mark on the heading tape, but it was not easily identified.

All pilots noted the relatively long training time required to achieve a satisfactory skill level with the flight path vector display, especially relative to the more conventional presentation format of the flight director. Even after ten to fifteen hours of experience with the display flying a familiar task (approach and landing), pilots were discovering additional ways to use the display. This experience parallels that for previous uses of the flight path vector display philosophy on head-up displays (Ref. 16). Although some structured training with the display was conducted, a more structured training and familiarization program should be developed.

A strong feature of this display format was its consistent Y-Z plane presentation, to include the low airspeed portion of the envelope. The landing pad longitudinal position bracket alongside the airspeed numerals was easily interpreted for longitudinal position. The goal posts in the immediate area of the landing zone provided lateral position cuing. Most pilots commented favorably on the display's cuing for final hover position and let-down. Pilots noted, however, that use of the display for hover position was often driven by difficulties in transitioning between the display and outside visual cues. In addition, pilots noted for the final let-down using

the display that the flight path vector symbol gave them instant feedback on power lever movements as they controlled height. The flight path vector symbol drive laws did not provide this height response cuing at speeds above those associated with hover.

Power Lever Geometry

Concern for wrong-way movement of the power lever during critical flight phases was frequently expressed by most pilots throughout this experiment. Its combination of shaft rotation and grip orientation (shown in Figure 5) provided the sense of a helicopter collective control at high power settings. Neither its throw length (4 inches) nor the fact that it rotated, much as an airplane throttle quadrant, were questioned; rather, it was the sensation of collective-like movement (up-down) but with opposite sense that provoked the concern expressed in pilot comments. The flight director provided a direct indication of power lever movement relative to a desired setting thus helping compensate for the power lever geometry and sensing. The flight path vector display had no such direct indication of power lever position, similar to flight with visual references. The lack of power lever position indication and consequent concern for improper power lever movement were frequently cited as increasing pilot workload with the flight path vector display. Development and evaluation of alternative power control inceptors is warranted for the approach and landing task.

CONCLUSIONS

A piloted simulation experiment conducted on the NASA Ames Research Center Vertical Motion Simulator investigated the use of two types of cockpit displays to help guide and control instrument approaches on steep glide slopes for a civil transport tiltrotor. The experiment was conducted with all aircraft systems functioning normally, full engine power available (no one engine inoperative evaluations), and with an attitude command control mode (pitch and roll, plus heading hold at low speeds). All approaches were carried through breakout to a vertical landing (no missed approaches). Environmental conditions included either clear or restricted visibility and either calm air or crosswinds with turbulence. Based on the results of 550 simulated approaches flown by eight evaluation pilots, the following conclusions may be drawn:

1. Pilots attained desired performance with both display formats on approaches up through 15 degrees. Generally satisfactory handling qualities were reported in calm conditions for these approaches. Crosswinds and turbulence degraded the handling qualities such that only adequate handling qualities were reported on a 15 degree glide slope.

2. Approaches on a 25 degree glide slope resulted in degraded performance and handling qualities with either display format. Pilot workload was strongly affected by crosswinds and turbulence, the large variations in power lever position required for height control at low airspeed to maintain glide slope tracking, and the loss of the landing spot from the cockpit field of view during visual flight segments of the approach.

3. The four-cue (pitch, roll, power and nacelle angle) flight director was quickly learned and easily interpreted. Pilots commented favorably on its configuration change (nacelle angle movement) prompts and the power lever cuing. The power lever cuing helped overcome a power lever geometry which was not well suited to the task and often was referred to during the final landing phase, even when hover longitudinal and lateral positioning was done with outside visual references.

4. The flight path vector display provided a Y-Z plane format, similar to an out-the-window view, for presentation of aircraft state, status (including torque and configuration settings) and guidance information for a variety of glide slope angles. Pilots achieved more precise altitude control during level flight conversions using this display. Pilots achieved precise glide slope tracking at the expense of higher workload than that experienced with the flight director. The flight path vector display provided flight status information in a format useful to operation in a variety of situations and warrants further development and evaluation.

REFERENCES

[1] Thompson, P., et al, "Civil Tiltrotor Missions and Applications, Phase II: The Commercial Passenger Market, Summary Final Report." NASA CR 177576, Feb. 1991.

[2] anon., "Advisory Circular: Vertiport Design Guide." FAA AC No: 150/5390-3, Jan. 1991.

[3] Advisory Circular 150/520-2, "Noise Assessment Guidelines for New Heliports," Dec. 1983.

[4] Federal Aviation Regulations Part 36 "Noise Standards: Aircraft Type and Airworthiness Certification," Amendment 36-14, Federal Aviation Administration, Washington, DC, Dec. 1988.

[5] Lebacqz, J.V., et al, "Ground-Simulation Investigations of VTOL Airworthiness Criteria for Terminal Area Operations." RAE Conference on Helicopter Simulation, London, Great Britain, May 1990.

[6] Decker, W.A., "Piloted Simulator Investigations of a Civil Tilt-Rotor Aircraft on Steep Instrument Approaches." AHS 48th Annual Forum, Washington DC, June 1992.

[7] Bray, R.S., "Visual and Motion Cuing in Helicopter Simulation." NASA TM-86818, Sept. 1985.

[8] Ferguson, S.W., "A Mathematical Model for Real Time Flight Simulation of a Generic Tilt-Rotor Aircraft." NASA CR-166536, Oct. 1983.

[9] Goldstein, K.W. and Dooley, L.W., "V-22 Control Law Development." 42nd Annual Forum of the American Helicopter Society, Washington, DC, June 1986.

[10] Tischler, M.B. and Cauffman, M.G., "Frequency-Response Method for Rotorcraft System Identification With Applications to the BO-105 Helicopter." 46th Annual Forum of the American Helicopter Society, Washington, DC, May 1990.

[11] Kimball, D.F., "Recent Tilt Rotor Flight Control Law Innovations." Journal of the American Helicopter Society, July 1987.

[12] Sinacori, J.B., et al, "Researchers Guide to the NASA Ames Flight Simulator for Advanced Aircraft (FSAA)." NASA CR-2875, 1977.

[13] Scott, B.C., et al, "Progress Toward Development of Civil Airworthiness Criteria for Powered-Lift Aircraft." FAA-RD-76-100, May 1976.

[14] Lebacqz, J.V. and Aiken, E.W., "A Flight Investigation of Control, Display, and Guidance Requirements for Decelerating Descending VTOL Instrument Transitions Using the X-22A Variable Stability Aircraft, Volume 1: Technical Discussion and Results." CALSPAN Report No. AK-5336-F-1 (Volume 1), Sept. 1975.

[15] Lebacqz, J.V. and Scott, B.C., "Ground Simulation Investigation of VTOL Airworthiness Criteria for Terminal Area Operations." AIAA Journal of Guidance, Control, and Dynamics, Vol. 8, (6), 1985.

[16] Bray, R.S., "A Head-Up Display Format for Application to Transport Aircraft Approach and Landing." NASA TM 81199, 1980.

[17] Hynes, C.S., et al, "Flight Evaluation of Pursuit Displays for Precision Approach of Powered-Lift Aircraft." AIAA Journal of Guidance, Control, and Dynamics, Vol. 12, (4), 1989.

[18] Merrick, V.K., Farris, G.G., and Vanags, A.A., "A Head Up Display for Application to V/STOL Aircraft Approach and Landing." NASA TM-102216, 1990.

[19] Cooper, G.W. and Harper, R.P., "The Use of Pilot Rating in the Evaluation of Aircraft Handling Qualities." NASA TN D-5153, 1969.

[20] anon., "Airline Transport Pilot and Type Rating, Practical Test Standards for Airplane and Helicopter." FAA-S-8081-5, AVN-130, Aug. 1988

TABLE 1. Vertical Motion Simulator Motion Drive Characteristics

Motion Axis	Gain	Filter Break Frequency (rad/sec)
Roll	0.5	0.25
Pitch	0.5	0.7
Yaw	0.5	0.5
Longitudinal	0.6	0.7
Lateral	0.0	1.0
Vertical	0.8	0.25
Pitch-tilt	0.7	6.0
Roll-tilt	0.7	3.0

TABLE 3: Evaluation Task Atmospheric Conditions

a. Winds

Wind Condition	Crosswind (knots)	Turbulence (feet per second, root mean square)
Calm	—	—
Light	5	1.5
Moderate	10	4.5

b. Visibility

Ceiling (feet)	Visual Range (feet)
Clear	unlimited
200	2000
100	1000

TABLE 2. Reduced-order Aircraft Response Dynamic Model Characteristics.

a. Pitch response to longitudinal stick:

$$\frac{\theta}{\delta_{LNG}} = \frac{Ke^{-\tau s}}{\left[s^2 + 2\zeta\omega s + \omega^2\right]}$$

	Airspeed (knots) / Nacelle Angle (degrees)		
Parameters	Hover / 90	80 / 80	180 / 0
K, deg/in	22.4	20.0	23.0
τ, sec	0.0096	0.0	0.0043
ζ, ND	1.0	1.16	1.58
ω, rad/sec	1.27	1.36	1.30

b. Heave (height rate) response to power lever:

$$\frac{\dot{h}}{\delta_{THT}} = \frac{Ke^{-\tau s}}{(s+a)}$$

	Airspeed (knots) / Nacelle Angle (degrees)		
Parameter	Hover / 90	80 / 80	180 / 0
K, ft/sec/in	9.23	16.3	N/A
τ, sec	0.041	0.052	
a, rad/sec	0.33	0.35	

TABLE 4: Nominal Approach Conditions.

Glide Slope (degrees)	Airspeed (knots)	Nacelle Angle (degrees)
6	80	80
9	55	85
15	35	90
25	20	90

TABLE 5. Flight director gains.

	Hover	80 knots	180 knots
EBAR			
K_E, in/in	1.0	1.0	0.5
$K_{E\dot{z}}$, in/ft/sec	-0.0140	-0.0093	0
K_θ, in/rad	-3.50	-3.50	-3.50
λ_{Ewo}, 1/sec	0.1	0.1	0.1
$K_{\dot{\theta}}$, in/rad/sec	-1.40	-0.70	-0.70
$K_{E\dot{z}}$, in/ft/sec	0	0	-0.0150
K_{Ez}, in/ft	0	0	-0.0070
τ_E, sec	0.1	0.1	0.1
ABAR			
K_A, in/in	1.00	1.00	0.25
$K_{\dot{y}}$,in/ft/sec	0.055	0.055	0.055
K_ϕ, in/rad	-2.00	-2.00	-2.00
λ_{Awo}, 1/sec	0	0	0
$K_{\dot{\phi}}$, in/rad/sec	-0.60	-0.60	-0.60
K_ψ, in/rad	0	0	0
τ_A, sec	0.1	0.1	0.1
CTAB			
K_C, in/in	3.0	1.0	1.0
$K_{C\dot{z}}$, in/ft/sec	-0.010	-0.0250	0
K_{Cz}, in/ft	-0.015	-0.0070	0
$K_{C\dot{x}}$, in/ft/sec	0	0	0
K_{DC}, in/in	-0.30	-0.14	0
λ_{Cwo}, 1/sec	0.2	0.4	0.4
τ_{CL}, sec	0	0	0
τ_C, sec	0.1	0.1	0.1

TABLE 6. Evaluation runs and pilots.

	Glide Slope Angle (degrees)			
	6	9	15	25
Flight Director				
pilots	8	8	8	6
evaluation runs	46	44	42	31
Flight Path Vector Display				
pilots	4	3	4	2
evaluation runs	23	16	15	11

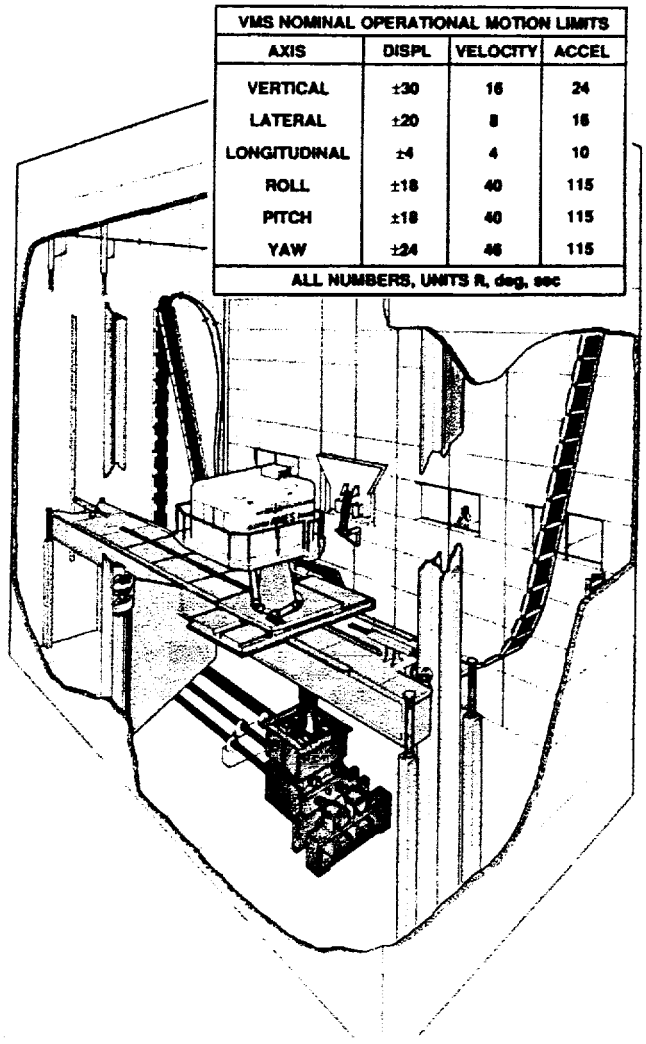

Figure 1. Vertical Motion Simulator. Cab was oriented along the beam for large longitudinal acceleration for tiltrotor simulation.

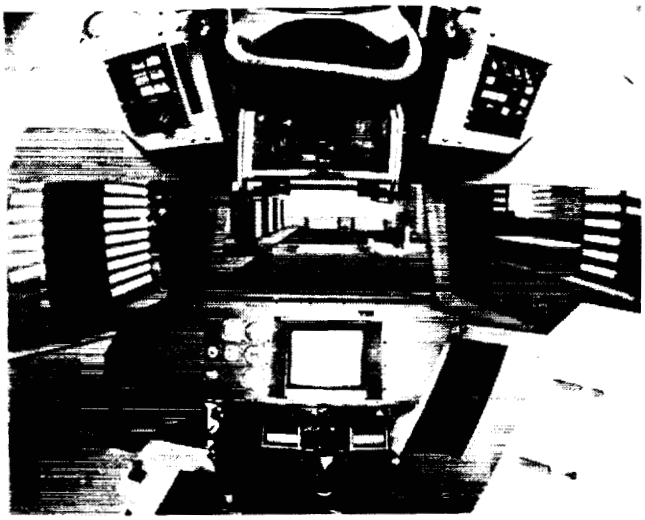

Figure 2. Cockpit interior. Visual scene portrays approach to urban vertiport.

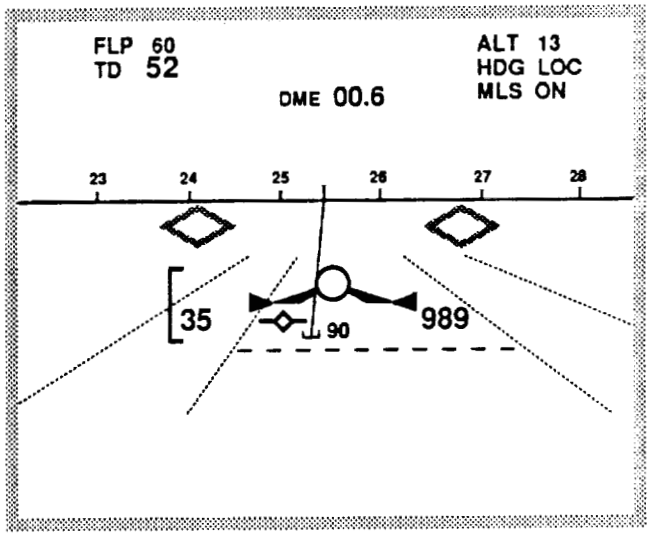

Figure 4. Diagram of flight path vector display for cockpit center panel CRT.

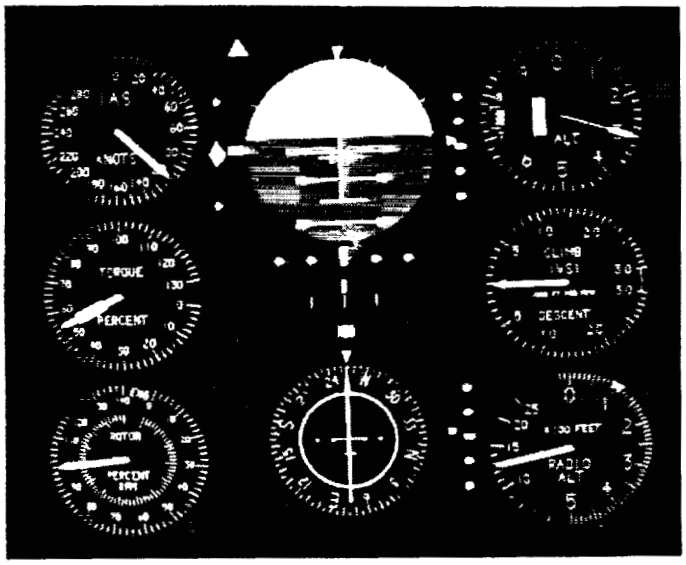

Figure 3. Central cockpit panel display with conventional instrument format.

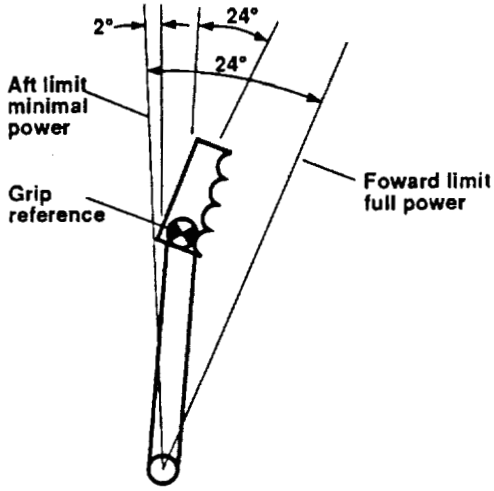

Figure 5. Power lever geometry.

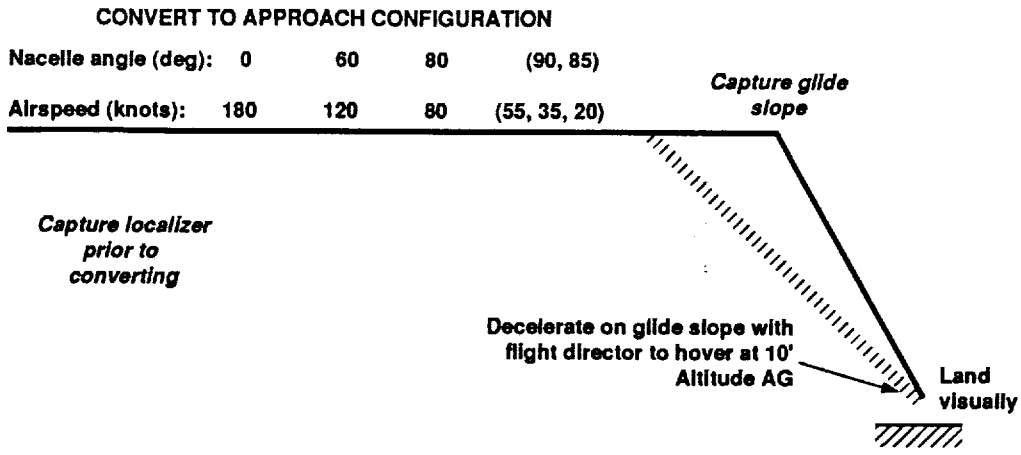

Figure 6. Approach profile.

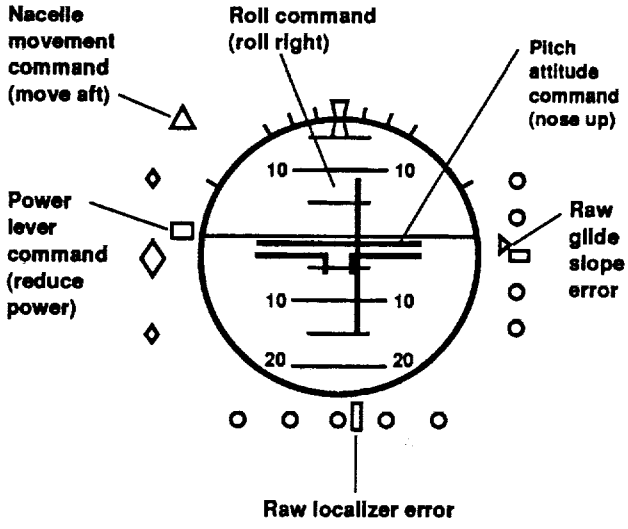

Figure 7. Flight director command symbols arrayed about the attitude direction indicator (ADI).

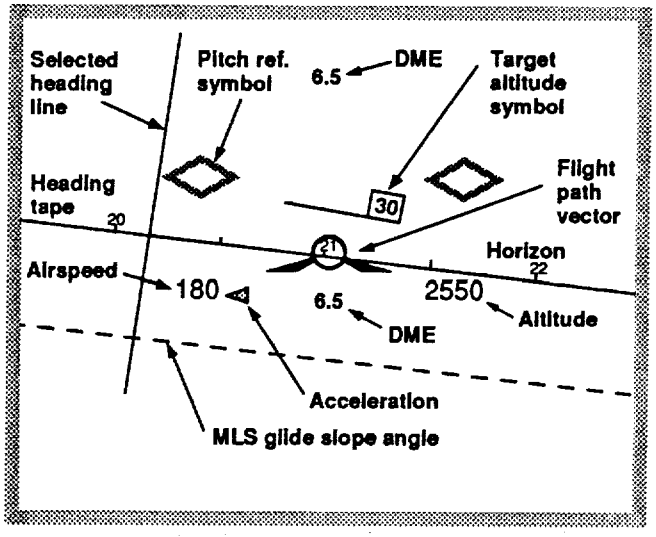

Figure 8. Flight path vector display for the initial approach.

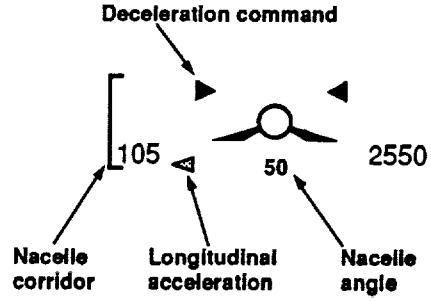

Figure 9. Flight path array elements

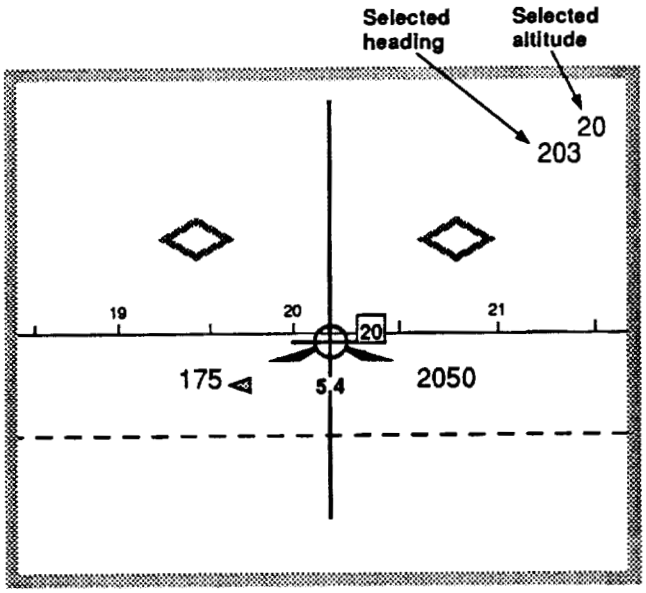

Figure 10. Flight path vector display showing flight on selected heading and approaching selected altitude. At the selected altitude (2000 feet), the selected altitude command bar will overlay the horizon. The aircraft is decelerating through 175 knots and is 5.4 nm from the DME reference point.

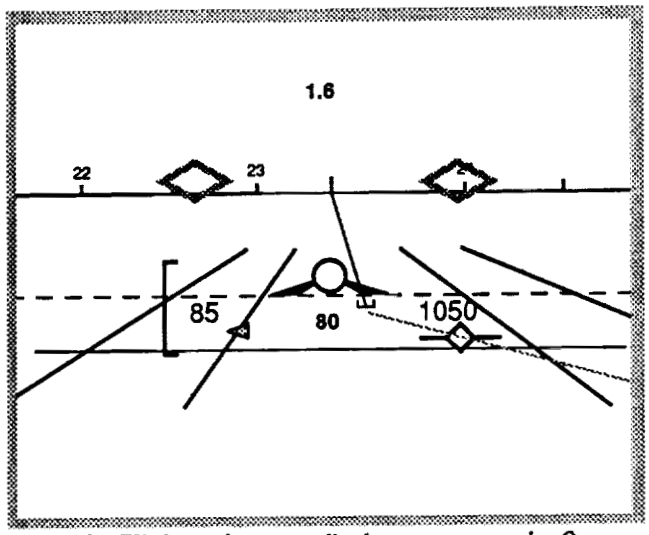

Figure 12. Flight path vector display on approach. Own aircraft is above and to the left of the desired glide slope.

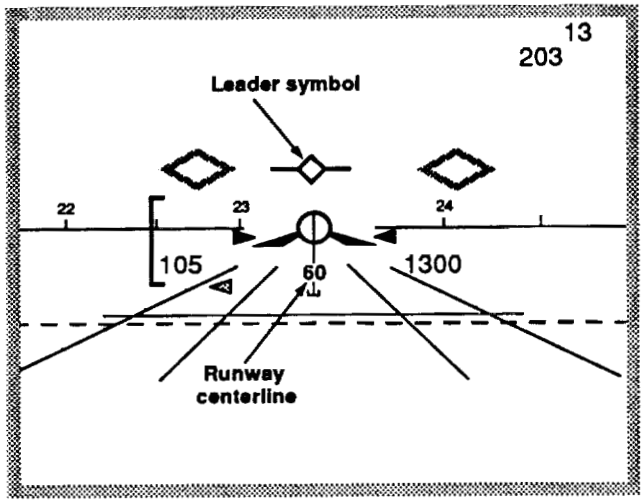

Figure 11. Flight path vector display approaching glide slope intercept (from below).

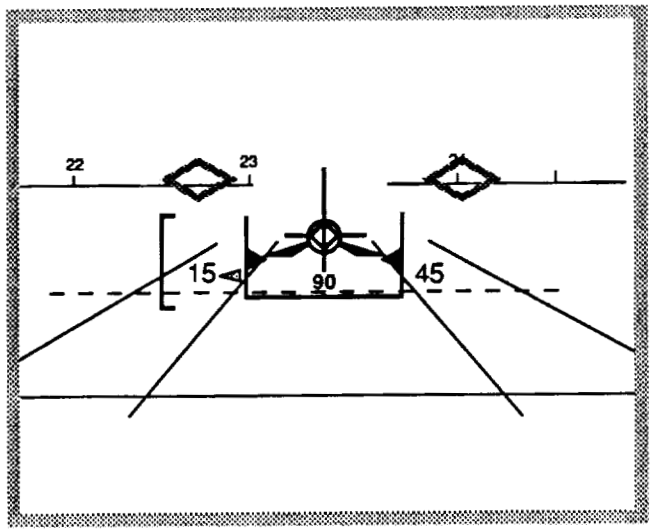

Figure 13. Flight path vector display on final approach to a vertipad.

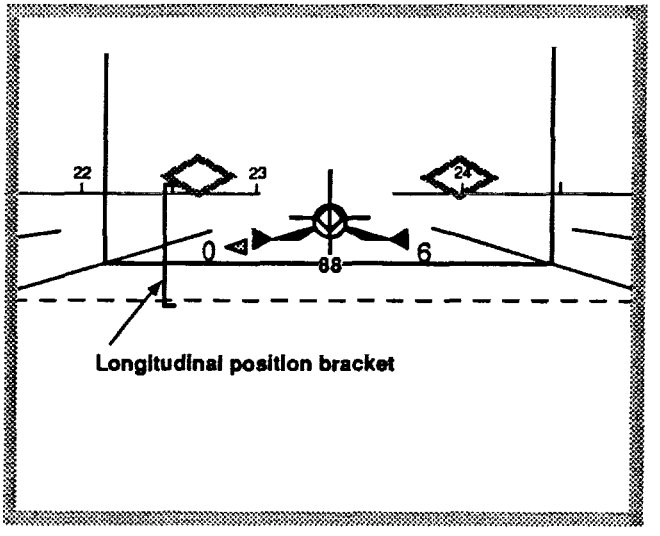

Figure 14. Flight path vector display showing vertical landing guidance.

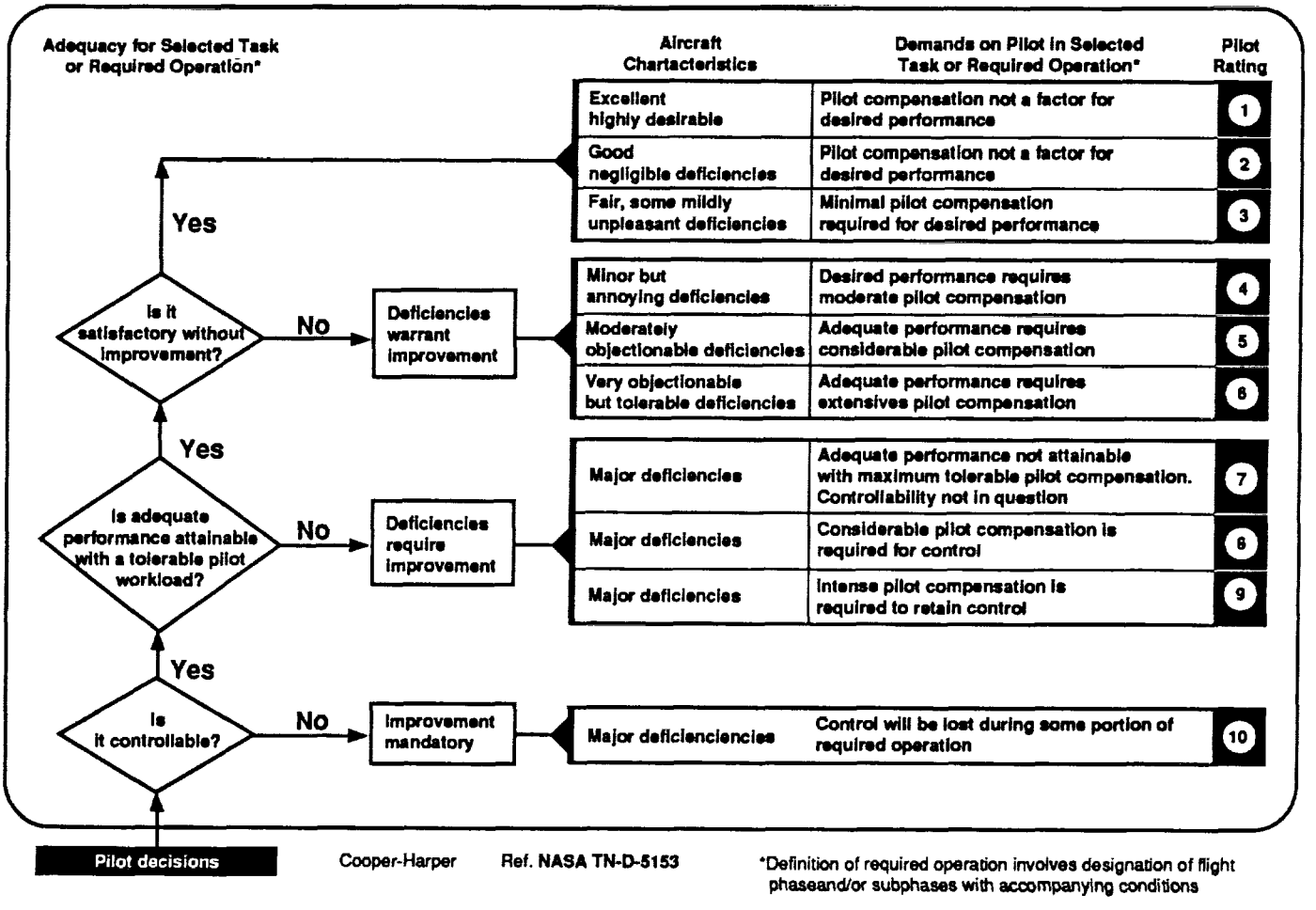

Figure 15. Dichotomous decision tree for Cooper-Harper Handling Qualities Ratings from NASA TND-5153 (ref. 18).

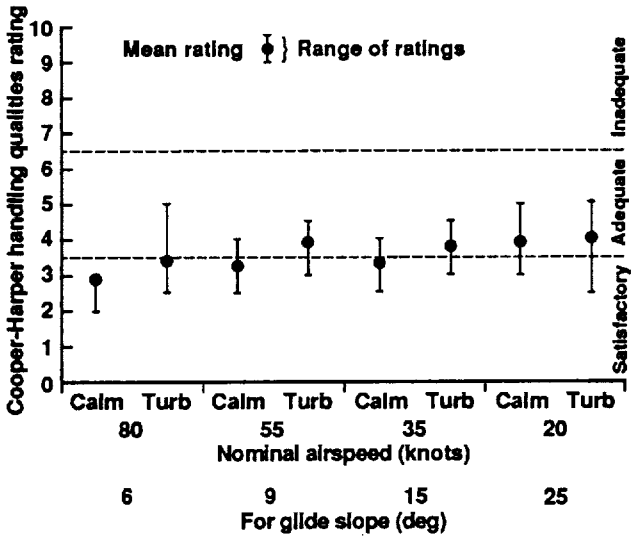

Figure 16. Level flight conversion handling qualities ratings using the flight director.

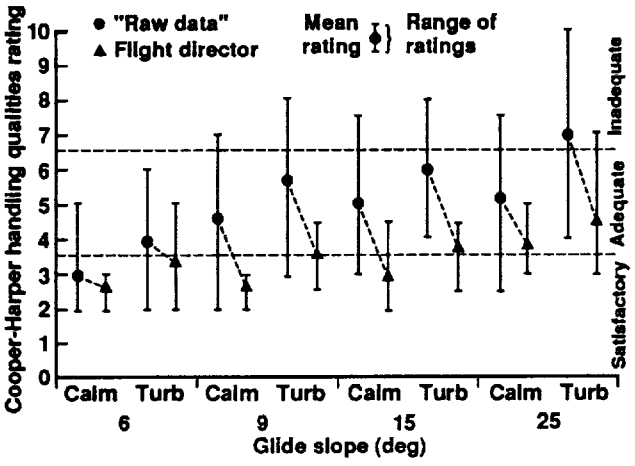

Figure 17. Handling qualities ratings for glide slope tracking using the flight director.

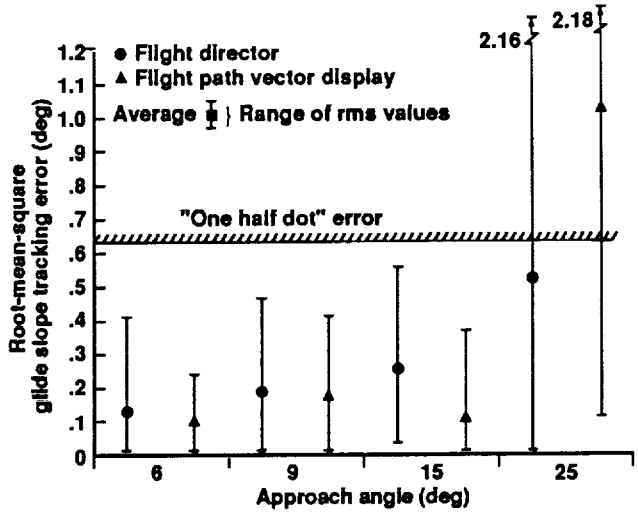

Figure 18. Glide slope elevation tracking root mean square error.

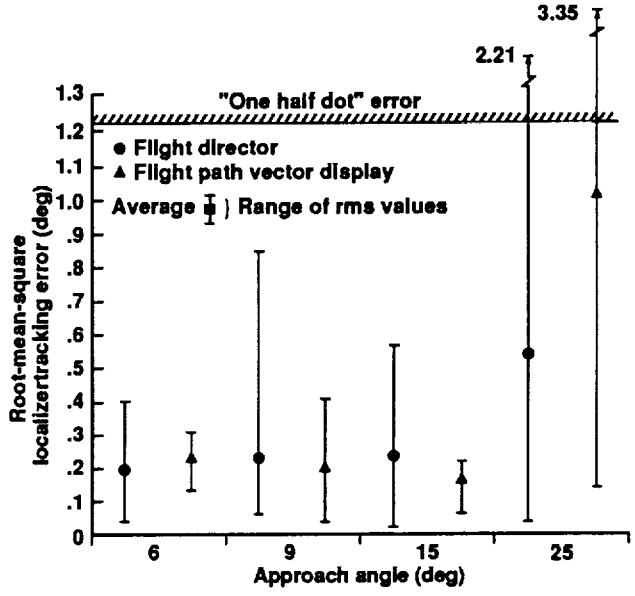

Figure 19. Localizer tracking root mean square error.

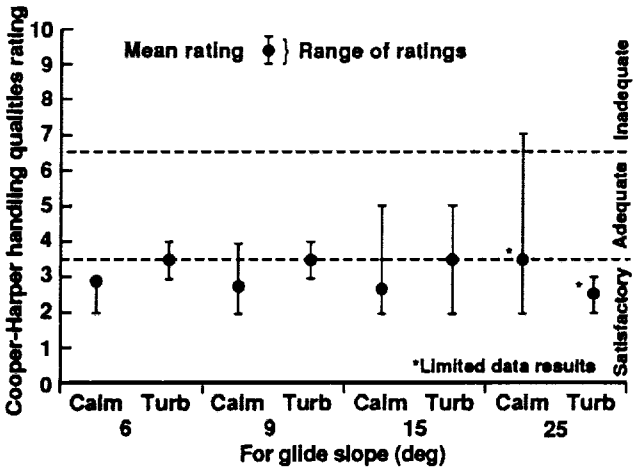

Figure 20. Level flight conversion handling qualities ratings using the flight path vector display.

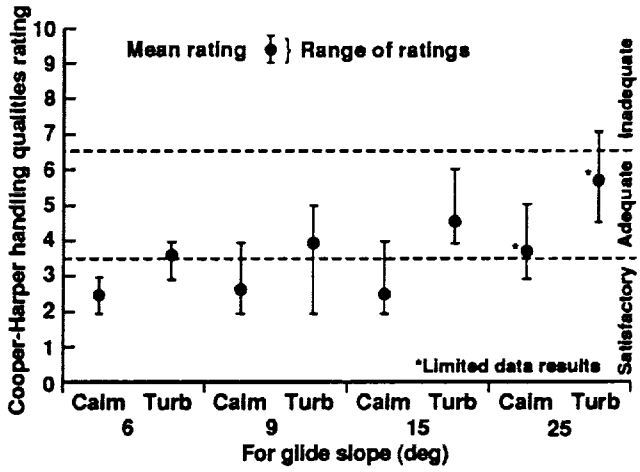

Figure 21. Glide slope tracking task handling qualities ratings using the flight path vector display.

FLIGHT TESTING AND FREQUENCY DOMAIN ANALYSIS FOR ROTORCRAFT HANDLING QUALITIES CHARACTERISTICS

MAJ Johnnie A. Ham
Charles K. Gardner
Airworthiness Qualification Test Directorate (Edwards AFB, CA)
US Army Aviation Technical Test Center
Ft Rucker, Alabama

Mark B. Tischler
Aeroflightdynamics Directorate
U.S. Army ATCOM
Ames Research Center
Moffett Field, California

Abstract

A demonstration of frequency domain flight testing techniques and analyses was performed on a U.S. Army OH-58D helicopter in support of the OH-58D Airworthiness and Flight Characteristics Evaluation and the Army's development and ongoing review of Aeronautical Design Standard 33C, Handling Qualities Requirements for Military Rotorcraft. Hover and forward flight (60 knots) tests were conducted in 1 flight hour by Army experimental test pilots. Further processing of the hover data generated a complete database of velocity, angular rate, and acceleration frequency responses to control inputs. A joint effort was then undertaken by the Airworthiness Qualification Test Directorate (AQTD) and the US Army Aeroflightdynamics Directorate (AFDD) to derive handling qualities information from the frequency response database. A significant amount of information could be extracted from the frequency domain database using a variety of approaches. This report documents numerous results that have been obtained from the simple frequency domain tests; in many areas, these results provide more insight into the aircraft dynamics that affect handling qualities than do traditional flight tests. The handling qualities results include ADS-33C bandwidth and phase delay calculations, vibration spectral determinations, transfer function models to examine single axis results, and a six degree of freedom fully coupled state space model. The ability of this model to accurately predict aircraft responses was verified using data from pulse inputs. This report also documents the frequency-sweep flight test technique and data analysis used to support the tests.

Presented at the American Helicopter Society's Specialists' Meeting, "Piloting Vertical Flight Aircraft, A Conference on Flying Qualities and Human Factors," San Francisco, CA, January 1993 .

Introduction

Background

Quantifying the "handling qualities" of rotorcraft has been a difficult task for the flight test community to accomplish. In its truest form, an aircraft's handling qualities are comprised of a set of metrics that measure objectively, the ease with which a pilot can perform a specified task. In the past, one method used by the testing community has been to measure specified static and dynamic characteristics, such as trim control positions and forces, stick characteristics, and aircraft responses to disturbances. There has been an attempt to measure selected stability and control derivatives individually through separate tests (in essence, a rough method of system identification). As an example, the character of speed stability (M_u, the pitching moment generated due to longitudinal velocity perturbations), has been measured by relating the longitudinal cyclic position to changes in airspeed from a trim condition, as shown in the following quasi-static equation:

$$M_u = - M_{\delta_{long}} (d\delta_{long} / du)$$

If forward cyclic is required for increasing velocity from trim, there is positive longitudinal static stability, which is considered "good." This provides information on the character of the speed stability, but not its magnitude, since there is no direct measurement of pitching moment due to longitudinal cyclic. It also becomes an invalid test for sophisticated modern control systems, such as a sidearm controller that commands acceleration, but holds velocity. A plot of stick position versus airspeed for this system would show neutral static stability, when in fact the aircraft may possess strong speed stability.

The demands of the next generation of rotorcraft require a closer than ever link between flight control

system design and aircraft handling qualities. This requirement, coupled with the presence of powerful computing systems and sophisticated software and tools, allows us to carefully characterize the aircraft dynamics that affect its handling qualities. The analysis tools presented in this paper allow for the accurate determination of the aircraft frequency responses, which can then be approximated with transfer function and stability and control derivative models to yield quantitative descriptions of the aircraft behavior. The analyses for this paper were conducted using a frequency domain based approach, which first requires generation of the flight test frequency domain database. Once the database has been generated, numerous applications can be derived from the data, as shown in figure 1.

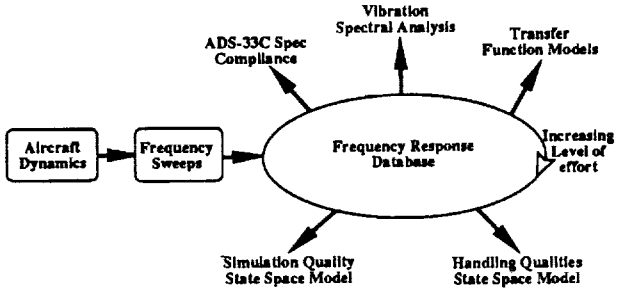

Fig. 1 Diagram of the applications

attach the blade to the yoke. Control inputs to the rotors are provided through an irreversible hydraulic system with a limited-authority stability and control augmentation system. The helicopter can be armed with a .50 caliber machine gun, 2.75" folding-fin aerial rockets, heat-seeking air-to-air Stinger missiles, and laser-guided HELLFIRE missiles. A sight mounted above the rotor hub houses a laser rangefinder and target designator, and both infrared and television sensors that provide images to the crew. The helicopter has a maximum gross weight of 5500 pounds in the armed configuration and 4500 pounds in the unarmed configuration. A sideview of the OH-58D helicopter is shown in Figure 2, and additional physical characteristics of the helicopter are listed in Table 1.

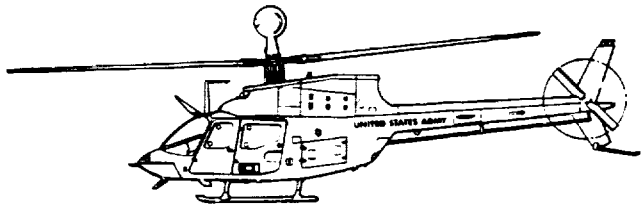

Figure 2. OH-58D Sideview

Coverage of the Paper

This paper presents a detailed flight test example of the application of these methods to the OH-58D. The goal of the system identification was to characterize the aircraft handling qualities with simple models rather than to create very high fidelity models that may be needed for detailed simulation validation. The simple models provide significant insight into the aircraft's dynamic behavior in the piloted frequency range, using significantly less flight test time than traditional tests. The paper discusses testing requirements, instrumentation, data processing, and interpretation, and shows its usefulness as a tool in testing new and modified aircraft.

Table 1 OH-58D Physical Characteristics

Maximum gross weights:	
unarmed	**4500 lb**
armed	**5500 lb**
Main rotor:	
number of blades	**4**
diameter	**35.0 ft**
chord	**13.0 in**
tip speed	**725 ft/s**
effective hinge offset	**2.9%**
Tail rotor:	
number of blades	**2**
diameter	**5.42 ft**
chord	**5.3 in**

Description of the Test Aircraft

The test aircraft was a production OH-58D helicopter. This aircraft is a two-place, single-main-rotor helicopter powered by an Allison 250-C30R engine rated at 650 shaft horsepower. The engine drives a 4-bladed, soft in-plane composite main rotor and a two-bladed teetering tail rotor. The main rotor is outfitted with elastomeric lead-lag dampers and pitch-change bearings; flapping occurs through bending of the blade and the yoke to which the blades are attached, as well as through movement allowed by the elastomeric fittings which

The OH-58D helicopter is used primarily in the scout mission, where it acquires, tracks and designates targets for AH-64A attack helicopters. The mission includes battlefield management, which entails a range of battle coordination tasks including artillery, air defense, and Air Force ground attack integration, as well as maneuver unit control. In an armed configuration, the helicopter can perform light attack missions by providing air-to-air and air-to-ground fire.

Tests for this paper were conducted at approximately 4800 pounds with weapon pylons and empty ejector racks on the helicopter. The aircraft had a pulse-code-modulation instrumentation system onboard which recorded measurements on magnetic tape and also transmitted these measurements to a ground monitoring station. The instrumentation system included an extensive array of sensors, although measurements for this paper were all provided by angular attitude and rate gyros, linear accelerometers, and potentiometers that indicated cockpit control positions. Further details of the test aircraft are provided in reference 1.

Flight Test Technique

Instrumentation

The results of frequency domain analyses are strongly influenced by the characteristics of the aircraft instrumentation system. And although useful data can be gathered with an instrumentation set-up not intended for frequency domain tests (as were the data for this paper), a properly designed instrumentation package can greatly improve results. This section describes innstrumentation considerations for frequency domain testing.

Measurements typically required for handling qualities analyses consist of angular rates and attitudes, linear velocities and accelerations, and control positions. The accelerometers should be located as close to the center of gravity as possible, and their positions with respect to the cg should be accurately known. This information is used to correct the acceleration measurements to the cg--a step that is necessary to determine meaningful aircraft accelerations. Control positions can be measured at the pilot's stick or at the actuator outputs. Frequency responses derived from pilot stick measurements represent the closed-loop aircraft dynamics (aircraft dynamics as modified by the stability and control augmentation system), whereas frequency responses derived from actuator output measurements represent the open-loop or bare-airframe dynamics.

One consideration with all the measurements is that the range of the measurement is not so large that the resolution is unacceptably large. With an 8-bit data system, for example, the resolution of a roll attitude gyro with a range of $\pm$180 degrees is 1.4 degrees--probably not acceptable for analyses of small-amplitude aircraft motions.

Aircraft instrumentation systems usually employ analog anti-aliasing filters. Because their properties are often not well-defined, these filters can unacceptably distort the data. To minimize such effects, similar filters should be used on all the measurements. This ensures, most importantly, that time delays introduced by the filters affect all measurements alike (time delays greatly influence the frequency response phase curves derived from the data). The cutoff frequency of the filters should not be less than about five times the highest frequency of interest. This guarantees that the data is modified only by the low-frequency end of the filter pass band, where filter phase distortions are small. Additional filtering with well-defined digital filters can be performed after the data is recorded. The data sample rate must be at least twice the filter cutoff frequency; a sample rate five times the filter cutoff frequency is preferable to avoid aliasing effects. Obviously, a common sample rate among all measurements is desirable, although not necessary.

A final issue is the time skew between measurements inherent in a data system that samples measurements sequentially. These time skews are usually small (10 ms is typical). Nevertheless, a data system structured to sample handling qualities measurements in the shortest time interval possible minimizes time skews between channels.

Measurements taken on the OH-58D and used for this paper consisted of aircraft attitudes, angular rates, linear accelerations, and control positions. Longitudinal, lateral, and vertical accelerometers were located under the pilot's seat, and an additional vertical accelerometer was positioned near the center of gravity. Control positions were measured at the pilot's stick.

The aircraft instrumentation system was not intended to gather data for frequency response analyses. For example, the accelerometers were not located at the cg, and the position of the cg was not accurately known. Different analog filters and sample rates (from 75 to 450 Hz) were used on different measurements. And linear velocities were not measured. Data processing to account for some of the shortcomings of the data required considerable effort: data were filtered and decimated or expanded to create a common sample rate, linear accelerations were referred to the estimated cg position, and linear velocity time derivatives were reconstructed from the other measurements. And although these corrections ultimately yielded a useful database, better results could have been obtained with less effort if the instrumentation setup had followed the simple rules-of-thumb described above.

Test Inputs

The set of test inputs needed for this type of analysis consists of pilot induced frequency sweeps, and doublets or pulses. The sweeps are used to generate the frequency response database, and the doublets and pulses are used for time domain verification of resulting models. The basic pilot technique used in the frequency sweep is to produce a sinusoidal input about a reference trim condition, beginning at very low frequency and progressively increasing the frequency of inputs.

Generally, a frequency range of 0.1 Hz (10 sec period) to 2 Hz is adequate for handling qualities analyses. The frequency sweeps in these tests were conducted using small amplitude inputs starting with a period of about 16 seconds and progressing to a desired frequency of 2-3 Hz. Input and response data should be recorded over at least a 90-second period (minimum to maximum frequency). A minimum of two (ideally three) frequency sweeps per axis should be recorded for data reduction. Maintaining the trim condition for each axis throughout each maneuver is essential to eliminate errors. Control input size should be as small as possible with the pilot perceiving continuous control movement, but large enough to get an airframe response at low and mid frequencies (generally +/- 1/2 inch control deflection is a maximum). Intermittent, uncorrelated off-axis inputs are allowable as required to counter large excursions due to control coupling effects. An example of a lateral axis frequency sweep is presented in Figure 3.

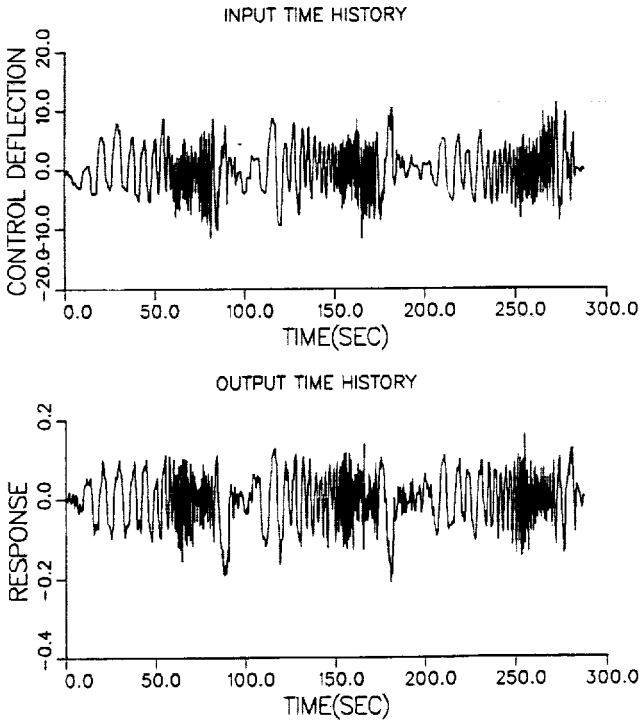

Fig. 3 Lateral stick frequency sweep, hover

Safety Considerations

Although the technique is straightforward, experience with frequency response testing during the AH-64A and OH-58D tests emphasizes the need to carefully plan the frequency sweep tests. Tests conducted with frequency sweeps revealed the potential for damage caused by structural resonances. Some of these are documented by AQTD in reference 2. Unexpected structural resonances which were not identified during structural demonstrations or during operational flying have been encountered during frequency sweep tests. The lesson is frequency response testing should be approached cautiously.

There are some methods that can be used to minimize the risks from frequency response testing. One is to limit the range of the frequency sweep to a pre-determined value. Guidance from Tischler (Ref. 3) suggests testing a frequency range from 1/2 the bandwidth frequency to $2\omega_{180}$. Unfortunately, no bandwidth data is available prior to conducting testing. Therefore, the tester must make an educated guess at the neutral stability frequency. Ideally, one would like to start at a very low frequency, and build up to a frequency high enough to make the bandwidth and phase delay computations. The low frequency range is the most difficult to acquire data with adequate coherence, due to the small control inputs required to minimize translation during the low frequency portion of the sweep. To reduce the risk of damage and save flight test time, it is suggested that one sweep be performed in each axis to more closely identify the range of frequencies actually required to accurately determine the bandwidth. An initial limit of 1.5 Hz should be used. Once a more accurate estimation of the bandwidth has been attained, the frequency sweep can be repeated over a more restricted (or expanded, if needed) frequency range. The object of this method is to avoid the higher frequencies, thus reducing the likelihood of driving other aircraft components into a damaging resonance. The technique will also reduce the number of asymmetrical and off-axis inputs required by the pilot to restrict translations started during the low frequency portions. Another method that will help minimize risk is to restrict the input magnitude. The size of the input should be kept to a minimum, which will reduce cyclic loads imposed upon the airframe.

Training the pilot and the engineer is another important ingredient to a successful frequency sweep test. The input magnitude and frequency ranges must be thoroughly understood prior to flight. The pilot has a tendency to increase the magnitude of the inputs at higher frequencies, to compensate for a reduction in aircraft response. Using a fixture may help to relieve this tendency, but so will adequate ground training. The pilot should be coached by the engineer both for input timing and input magnitude. This pilot-engineer interface should be practiced on the ground. Realtime monitoring of the stick inputs is valuable for this task. Once the engineer determines that the inputs have met this frequency, he should make the "knock-it-off" call to the pilot. At frequencies above 1 Hz, it is difficult for the pilot to accurately estimate the input frequency. Experience has shown that pilots are capable of generating input frequencies in the range of 5-6 Hz (30-40 rad/sec) which may excite rotor modes. As a general rule, it appears that handling qualities frequency tests can be terminated at 2 Hz, and sufficient information will be available for

handling qualities analyses. A combination of establishing a pre-determined cutoff frequency, realtime input monitoring, limiting the magnitude of the inputs, and pilot-engineer ground training makes the test technique safe and efficient.

Generation of the Frequency Response Database

General

Generation of the frequency response database is the starting point for any of the analyses shown in figure 1. The overall goal is to extract a complete set of nonparametric input-to-output (pilot control-to-vehicle response) frequency responses that fully characterize the behavior of the helicopter.

CIFER Overview

The US Army/NASA and Sterling Software have jointly developed an integrated software facility (CIFER) for system identification based on a comprehensive frequency-response approach that is uniquely suited to the difficult rotorcraft problem. This program provides a set of utilities that reduce the frequency sweep time histories into high quality multi-input/multi-output frequency responses. A full description of the CIFER software is provided in reference 4. Essentially, three steps are used to generate the frequency response database. The first step is to produce the single-input/single-output (SISO) frequency response from the time histories using an advanced Fast Fourier Transform. An example of the autospectrum and Bode plots generated from this step are presented in Figure 4 for the roll axis. The input autospectrum shows good excitation up to 21 rad/sec (3.3 Hz).

The second step is to condition the responses to account for the effect of secondary inputs. These conditioned multi-input/single-output (MISO) responses are the same as the SISO frequency responses that would have been obtained had no correlated controls been present during the frequency sweep of a single control. A further detailed description of this conditioning process is presented in reference 6. Figure 5 shows how results are affected by the presence of secondary inputs, especially for off-axis identification.

Step three is to combine multiple window lengths into a composite response. A further detailed description of this composite process is presented in reference 4. The overall result of these three steps (CIFER programs -FRESPID, MISOSA, and COMPOSITE) is the rapid identification of a set of broadband frequency responses for all input/output pairs for which there is dynamic excitation. This set of composite conditioned frequency responses and associated coherence functions forms the core of the frequency response database. An example of the final response is shown in Figure 6.

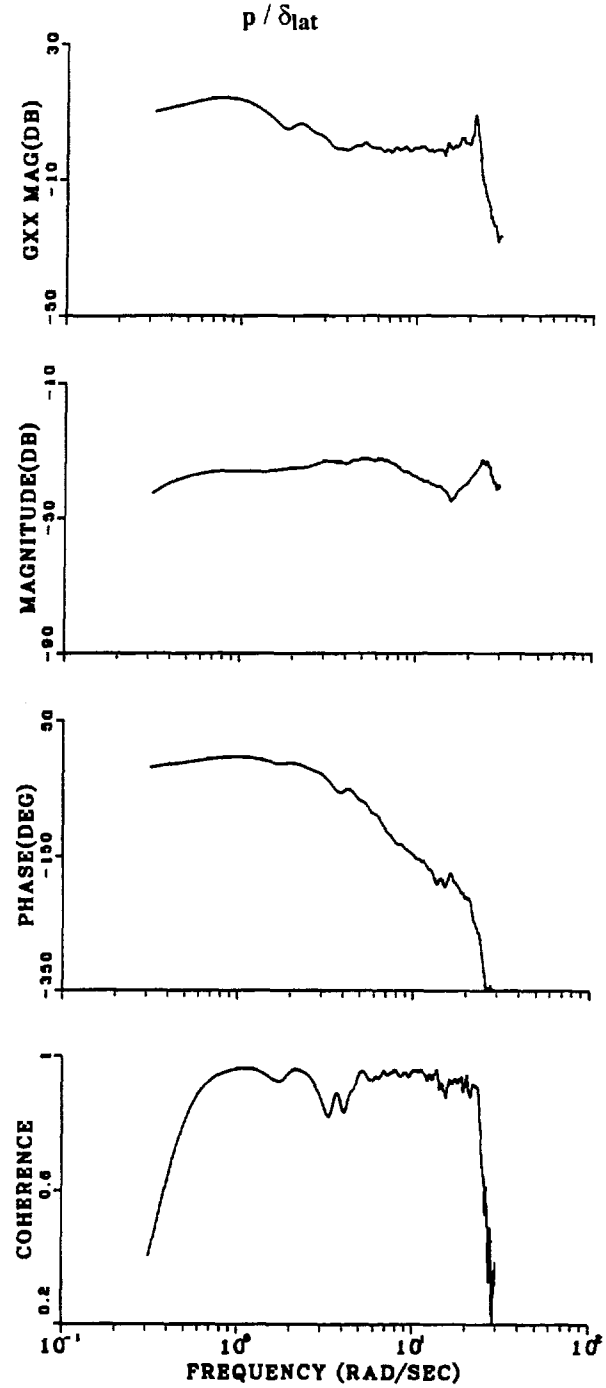

Fig. 4 Roll axis SISO frequency response

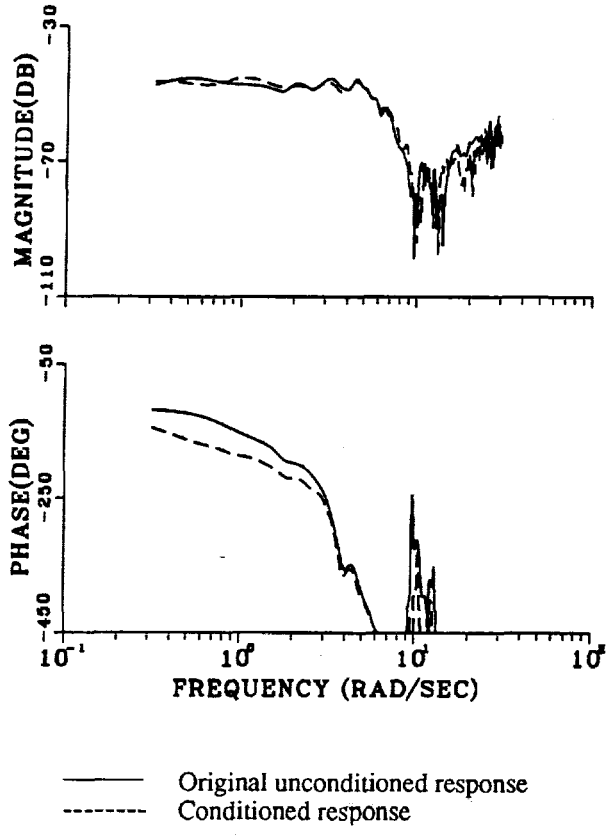

Fig. 5 Conditioned response, q/δlat

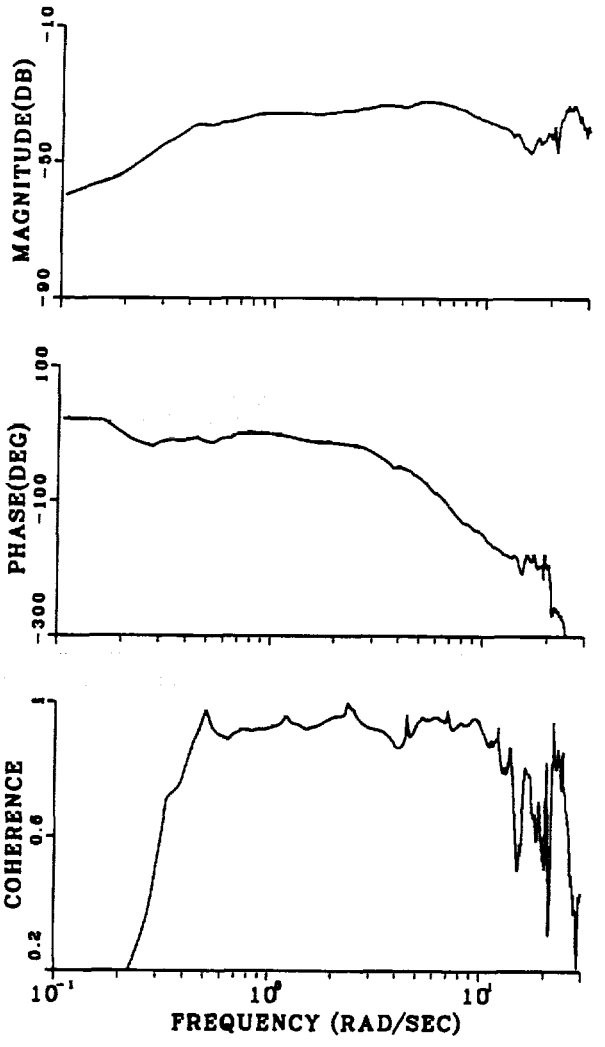

Fig. 6 Final composite response, p/δlat

Applications

ADS33C Specification Compliance

The requirements for response to small amplitude inputs are specified in ADS-33C (Ref. 8) using two frequency domain parameters, bandwidth and phase delay. The bandwidth parameter is the end to end, pilot control input to airframe angular response closed loop frequency that assures at least a 6 db gain margin, and a 45 degree phase margin from the neutral stability frequency. Essentially, it is a measure of the "quickness" with which the aircraft can respond to an input. Since any input can be modeled as a series of sine (or cosine) waves of differing frequencies and magnitudes, using Fourier analysis, the bandwidth defines the highest input frequency that results in a usable response both in magnitude and phase. The criterion in ADS-33C is based on the premise that ... the maximum frequency that a pure gain pilot can achieve, without threatening stability, is a valid figure-of-merit ... (Ref. 9). An aircraft with a high bandwidth would nearly mirror the input, and would be described as sharp, quick, crisp, or agile. A low bandwidth aircraft would be more sluggish, with a smooth response. Typical high gain tasks that would be most affected by bandwidth include slope landings, precision hover over a moving platform, air-to-air and air-to-ground target tracking, and running landings.

The phase delay parameter is effectively a measure of the steepness of the slope of the phase plot at the point where the output lags the input by 180 degrees (neutral stability). As the pilot increases his gain in a task, he approaches the frequency where the aircraft responds out of phase with the input. The natural pilot reaction is to apply a "mental lead filter" to compensate for this phase

shift. The success of this technique depends in large part on the predictability of the response. If the phase slope near the -180 degrees point is shallow, minor control deviations in the vicinity of this frequency will not change the phase shift significantly resulting in predictability. However, if the slope is too steep, minor changes in frequency will cause major changes in the phase shift, causing the "mental lead filter" to be less effective, or less predictable. An aircraft with a large phase delay is prone to Pilot Induced Oscillations, or PIOs. Phase delay is calculated based on either a two point fit, or a least-squares fit of the phase data between the neutral stability frequency and the phase at twice the neutral stability frequency. This assumes of course, that reliable data is available in this region, which may be a source of potential problems.

The bandwidth and phase delay are measured from a frequency response plot of the angular attitude response to cockpit controller deflection or force. CIFER applies the simple 1/s correction to the angular rate frequency responses to obtain the attitude to stick deflection frequency response. Phase margin and gain margin bandwidths are directly calculated, and the phase delay is calculated using either a two point fit, or a least squares fit algorithm, as shown in Figure 7. The least squares fit in CIFER uses an exponential coherence weighting function to place more emphasis on the higher quality spectral data present in the frequency response.

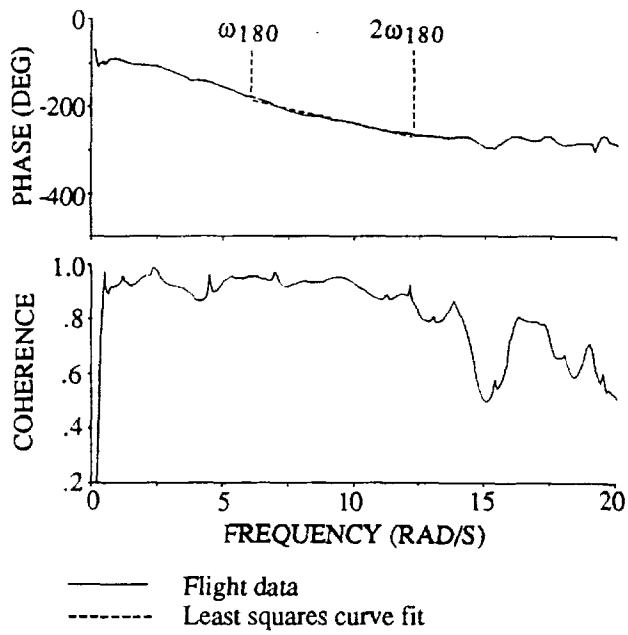

Fig. 7 ADS-33C phase delay calculation with least squares fit (p/dlat)

The resulting bandwidth and phase delay are then plotted against specification boundaries detailed in ADS-33C for Levels 1, 2, and 3. As an example, the roll axis results plotted in Figure 8 predict Level 2 handling qualities in the hover roll axis using the ADS-33C small amplitude criteria for the Target Acquisition and Tracking Mission Task Elements (MTEs). A review of earlier evaluations indicate that the aircraft possesses generally Level 2 handling qualities (Ref. 10). Right and left slope landings, a very high gain task, were rated HQRS 4 and 5 (Level 2) in the lateral axis. A pilot induced oscillation (PIO) in roll was documented at a hover in these two evaluations. The PIO disappeared when the pilot gained experience in the aircraft. A PIO significantly degrades handling qualities, and has been related to gain margin limited systems. Target Acquisition and Tracking MTEs were not performed during these tests. As can be seen, the predicted handling qualities trends from the frequency response criteria do compare with the actual handling qualities obtained in flight test.

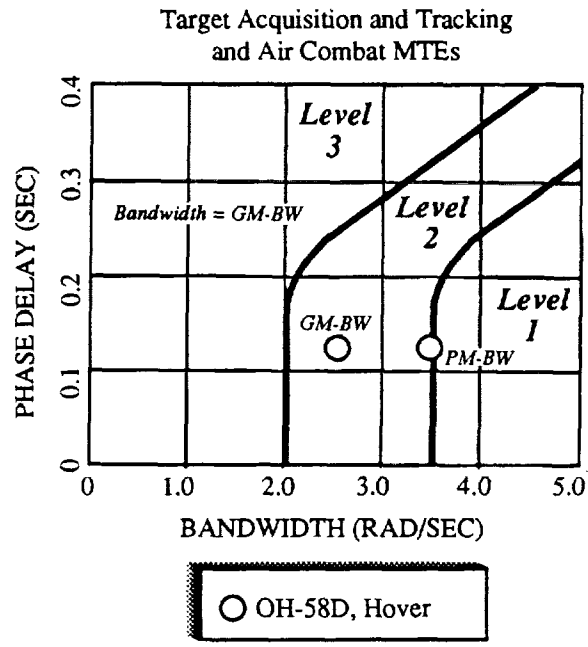

Fig. 8 ADS-33C Small amplitude roll criteria

Spectral Analysis of Helicopter Vibration

Helicopter vibration levels are routinely measured in flight test programs to determine compliance with specifications and to document in-flight vibration characteristics. The analysis associated with determining vibration levels is virtually identical to that of generating frequency responses; the CIFER software is therefore capable of performing all the functions required for a

vibration analysis. This section presents the results of such a vibration analysis for the OH-58D helicopter.

A vertical accelerometer was mounted under the pilot's seat on the test aircraft to measure vibration levels experienced by the pilot. The distribution of vertical vibration level with frequency is indicated by the power spectral density of the vertical acceleration time history. Between two frequencies, the area under this curve is proportional to the mean square value of vertical acceleration in this frequency range. Figure 9 shows the power spectral density of the pilot's seat vertical acceleration for the OH-58D in a hover. The data used to generate this plot was taken from the trim portions of several maneuvers. Vibration peaks are evident at frequencies corresponding to 1/rev, 2/rev, 4/rev, and 8/rev. Vertical vibration levels at each of these frequencies were determined by the CIFER software by calculating the area under each peak. The total vibration level was also calculated by integrating under the curve from 5 to 60 Hz. The results are presented in Table 2.

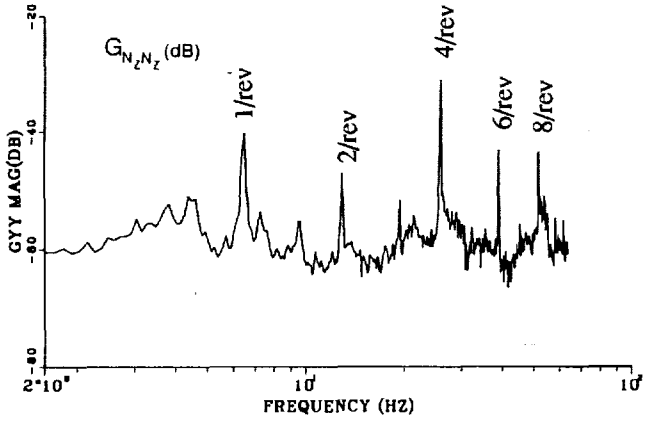

Fig. 9 Power spectral density, vertical vibration

Table 2. OH-58D Vertical Vibration Levels in a Hover

Vibration Mode	Frequency (Hz)	RMS of Vertical Acceleration (g's)
1/rev	6.5	.006
2/rev	13.1	.003
4/rev	26.1	.018
8/rev	52.2	.006
Total	5 to 60	.032

The peak amplitude of the acceleration is typically two to three times the root-mean-square value of the vertical acceleration. The maximum vibratory acceleration the pilot feels at the 4/rev frequency, for example, is therefore about 0.045 g's. The military handling qualities specification MIL-H-8501A requires vibrations levels lower than .15 g's for frequencies less than 32 Hz.

Transfer Function Modeling

Transfer-function modeling is a rapid and useful tool for characterizing the helicopter responses when the *overall* input-to-output behavior is of concern, rather than a complete physical representation based on the force and moment equations. In CIFER, transfer-functions are extracted directly by minimizing the magnitude and phase errors between the identified frequency-responses and the model. CIFER adjusts the transfer-function model parameters until a best fit is achieved. These transfer-function models are often referred to as "equivalent system" representations since they characterize the dominant dynamics in terms of simple "equivalent" first and second order responses. Examples of the applicability of transfer-function models are:

- flight mechanics studies - determination of key rotor parameters, and coupled rotor/fuselage modes

- handling-qualities analysis - comparison of equivalent system parameters such as short period damping and frequency, and time delay with the handling-qualities data base

- flight control system design model - classical design and analysis techniques such as Bode and Root Locus are based on the transfer-function descriptions of the on-axis angular responses to control inputs

- structural and rotor elasticity - damping and frequency of rotor lead-lag and airframe structure modes

Detailed examples of these applications are found in reference 11 for the BO-105, Puma, and AH-64A helicopters. In the following sections, the OH-58D data base is exercised to yield transfer-function models for the flight mechanics and handling-qualities applications.

Roll Response Modeling

An equivalent system model of the roll rate response to lateral stick input of Figure 6 was desired for flight mechanics analysis purposes. The frequency range of interest was selected as 1-16 rad/sec, which encompasses the dominant coupled fuselage/rotor flapping response. At present we choose to cut off the fit at 16 rad/sec to exclude the lead-lag dynamics prominent for higher frequencies as seen in Figure 6.

Two models of the roll-response were evaluated. In the simplest model, the response dynamics are characterized as first-order leading to the "quasi-steady" formulation in which the rotor and residual (mechanical and other higher-order) dynamics are represented by a pure time delay (τ_{lat}), and the coupled fuselage/rotor

dynamics are represented by the roll gain ($L_{\delta lat}$), and the first order roll damping (L_p):

$$\frac{p}{\delta_{lat}} = \frac{L_{\delta_{lat}} \; e^{-\tau_{lat}s}}{s - L_p} \qquad (1)$$

The parameters obtained for this model are listed in Table 3 and result in the rather poor frequency-response fit shown in Figure 10. The large cost function (CF=126) indicates that the model does not satisfactorily characterize the response. Also, the parameters in the table are very sensitive to the exact fitting range of the fit, a further indication of the inadequacy of the quasi-steady formulation for this helicopter. The same limitations for the quasi-steady model were found for the BO-105 (Ref. 11).

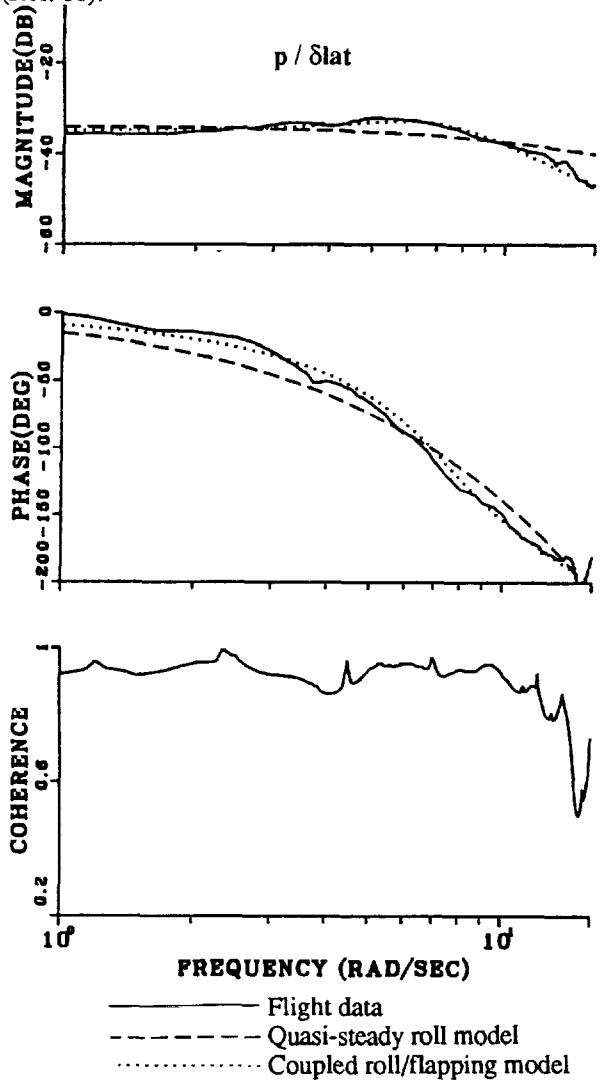

Fig. 10 Equivalent system model of p/δlat

As discussed by Heffley (Ref. 12), the roll response in the frequency range of interest is essentially second-order, owing to the coupling of the rotor regressive flapping and fuselage roll modes. A simple model involving the rotor flap inverse time-constant ($1/\tau_f$), the total flapping stiffness (L_{b1s}), the lateral stick gearing ($K_{\delta lat}$), and the residual time delay (τ_{lat}):

$$\frac{p}{\delta_{lat}} = \frac{K_{\delta_{lat}} \; e^{-\tau_{lat}s}}{s^2 + (1/\tau_f)s + L_{b1s}} \qquad (2)$$

The resulting model listed in Table 3 matches the frequency-response data quite well (cost function =21) as seen in Figure 10. Also the model parameters are not sensitive to the exact fitting range. The high level of rotor fuselage coupling is evident from reference to the second order poles [ζ=0.42 and ω_n=7.4], clearly showing why the quasi-steady approximation is not appropriate for this response.

Heffley (Ref. 12) tabulates the rotor parameters of eqn 2 for a broad range of helicopters. The report lists an OH-58 "D" model which includes the mast mounted sight (MMS), but the data of reference 13 used in Heffley's analysis excludes the MMS. The main differences are do the change in inertias and center of gravity (cg) associated with the MMS for the "D" model. In hover, the inflow effects on the flapping time constant are significant, and can be accounted for by making a correction to the Lock number γ as described by Harding (Ref. 14). Applying this correction to the OH-58D reduces the Lock number from the theoretical value of γ=7.06 to an effective value of γ_{eff} =5.33. The resulting rotor flap time constant prediction based on Heffley's analysis is τ_f=0.131 sec, which is quite close to the identified value of τ_f=0.155 sec. The flapping stiffness for the OH-58D is determined by Heffley from simulation data as L_{b1s}=47.7, which is also quite close to the identified value. The small identified residual time delay (τ_{lat}=0.051 sec) reflects the sensor filtering, hydraulic actuator and linkage dynamics between the stick measurement and the swashplate motion, and additional unmodeled rotor dynamics (e.g., lead-lag motion).

The maximum achievable roll rate can be assessed from the steady state response per unit input and the full throw control authority by noting from reference 12 that the roll rate response is to stick inputs is highly linear:

$$p_{max} = \left(\frac{p}{\delta_{lat}}\right)_{ss} (\delta_{lat})_{max} \qquad (3)$$

$$= \frac{K_{\delta_{lat}}}{L_{bls}}(\delta_{lat})_{max}$$
$$= (0.01785 \text{ rad / sec / \%})(\pm 50\%)$$
$$= 0.875 \text{ rad / sec}$$
$$= \pm 50 \text{deg / sec}$$

which meets ADS-33 Level 1 roll rate requirements for limited and aggressive maneuvering.

A final parameter of interest is the effective first-order inverse time-constant $1/T_{eff}$, where:

$$T_{eff} = \frac{2\zeta}{\omega_n} = 0.1163 \text{ sec} \quad (4)$$

so

$$1 / T_{eff} = 8.6 \text{ rad / sec} \quad (5)$$

As expected, this value is comparable with the first-order quasi-steady model parameter (L_p) shown in Table 3, and indicates a rather rapid roll rate command response for the OH-58D. A somewhat lower simulation value of $1/T_{eff}$=6.25 rad/sec is obtained based on Heffley's rotor parameters.

Table 3 Transfer Function Models for p/δ_{lat}

Model Structure	Transfer Function	Cost
Quasi-steady	$\frac{p}{\delta_{lat}} = \frac{0.184\ e^{-0.155s}}{s + 9.27}$	125.6
Coupled body/ rotor flapping	$\frac{p}{\delta_{lat}} = \frac{0.988\ e^{-0.051s}}{s^2 + (1/0.155)s + 55.35}$	21.4

Heave Axis Modeling

Transfer function modeling was also used to investigate the helicopter vertical speed response due to collective control inputs. Previous work has shown that inflow dynamics significantly affect the vertical response in hovering flight, and are primarily responsible for determining the pilot's perception of the aircraft's "crispness" during vertical maneuvers (Ref. 15). Figure 11 (solid line) shows the frequency response of the vertical acceleration due to collective control; the increasing magnitude with frequency is caused by inflow effects. The physical mechanism that creates this peak in the magnitude plot is the dynamic response of the inflow velocity. Because the air has mass, the inflow velocity does not assume a new steady value instantaneously after an abrupt collective pitch change. This dynamic lag of the inflow velocity influences the angle of attack of the rotor blades such that the blades experience their largest angle of attack immediately after an abrupt collective pitch increase, and a decreasing angle of attack as the inflow velocity increases. The result is a large rotor thrust spike after a rapid collective pitch change, which causes the high-frequency peak in the magnitude plot. This phenomenon is also responsible for much of the vertical acceleration cues the pilot feels while making abrupt collective inputs in a hover, and is therefore necessary to include in simulation models to capture the "crispness" of the actual helicopter.

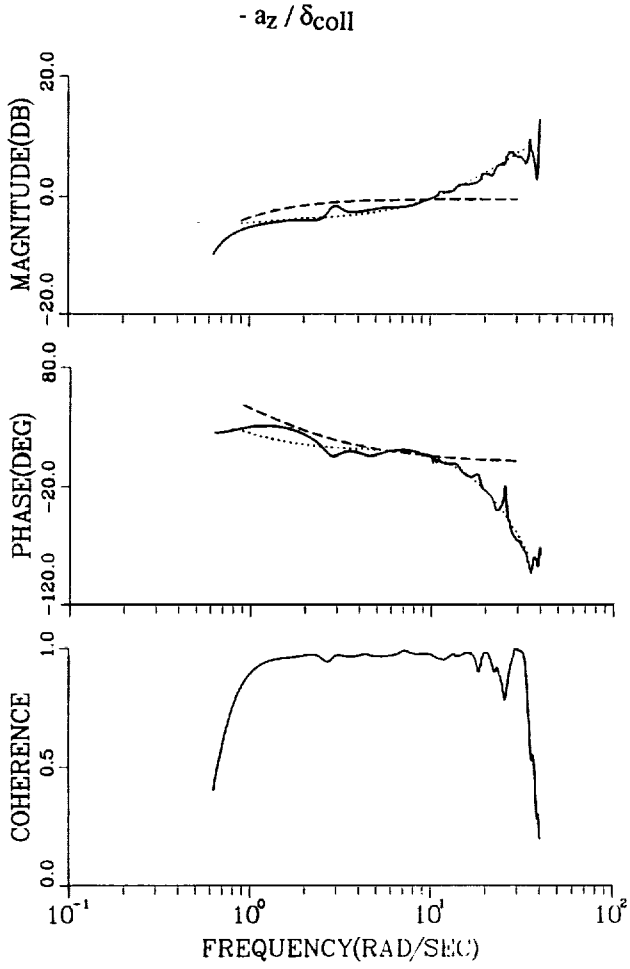

Fig. 11 Heave Axis Response

Two transfer function models were used to approximate the vertical axis response to collective stick.

The first model is a first-order description of vertical velocity to collective which neglects inflow dynamics:

$$\frac{a_z}{\delta_{coll}} = s\,\frac{Z_{\delta_{coll}}}{(s-Z_w)} \qquad (6)$$

Figure 11 (dashed line) illustrates that this model fits the vertical frequency response poorly. In particular, the model cannot follow the increasing magnitude with frequency that the frequency response exhibits.

The second model includes terms to model the inflow. The influence of dynamic inflow is approximated in the transfer function through the addition of a zero and a time delay to the first-order model of vertical velocity to collective stick :

$$\frac{a_z}{\delta_{coll}} = s\,\frac{Z_{\delta_{coll}}(s-Z_L)e^{-\tau_{coll}s}}{(s-Z_w)} \qquad (7)$$

where the coefficient values are Z_w = -.413, $Z_{\delta coll}$ = -0.071, Z_L = -9.25, and τ_{coll} = .0785. Figure 11 compares this transfer function to the actual frequency response and to the first model. The match is significantly better than that of the model which neglects inflow dynamics, illustrating the importance of including these effects in handling qualities models.

Single-input-single-output transfer function modeling, as illustrated in the preceding two examples, can reveal a great deal about the behavior of the helicopter. Quite often the physical mechanisms influencing the helicopter behavior are evident in this simple analysis--a benefit more complicated modeling approaches usually cannot offer. This makes transfer function modeling ideal for many common flight test and handling qualities analyses not considered here. For example, the effects of changing the external configuration of an aircraft, either by the addition of new components (antennae, wing stores, etc.) or modification of existing parts, are often assessed in flight test. Low-order transfer function models can quickly reveal and quantify aircraft behavior changes, most simply in terms of damping ratios and natural frequencies obtained from the transfer function coefficients.

Handling Qualities Model Identification

State-space modeling provides a comprehensive characterization of the coupled helicopter dynamics in terms of linear differential equations of motion. The coefficients of these equations are the fundamental force and moment perturbation (stability and control) derivatives of classical aircraft flight mechanics. State-space models are useful for control system design, simulation model fidelity assessment and improvement, comparison of wind tunnel and flight characteristics, and multi-input/multi-output (MIMO) handling-qualities analysis. CIFER identifies state-space models of general structure and of high-order by simultaneously fitting the entire frequency-frequency data base.

The goal of the state-space modeling effort in this paper is to characterize the MIMO rotor-flapping/body dynamics of the OH-58D helicopter. The frequency range of concern is for pilot-in-the loop handling qualities (0.5-15 rad/sec), as assumed by Heffley (Ref. 12). The larger goal is to develop a general approach for identification of rotorcraft handling-qualities models that can be routinely applied to future test programs. Such a model must be sufficient to capture the important dynamic modes and key coupling, without being overly complex and thus requiring an unacceptable level of labor or computer effort for the analysis.

Model Structure

A key aspect in the identification of a state-space model is the choice of model structure. Model structure refers to the form and order of the differential equations to be identified by CIFER. The earlier transfer-function modeling results described earlier show the angular responses of the OH-58D helicopter are dominated by the 2nd-order coupled fuselage/regressive-rotor dynamics. This modeling approach is generalized in the state-space formulation by expressing the lateral and longitudinal regressive flapping responses as first order differential equations. This approach follows Heffley's "primary analysis model" for handling-qualities analysis (Ref. 12) and is developed further into the "hybrid model" formulation of reference 4. The decoupled lateral regressive-flapping response (b_{1s}) is expressed as:

$$\tau_f \dot{b}_{1s} = -b_{1s} - \tau_f p + K_{b1s}\,\delta_{lat}(t-\tau_{\delta_{lat}}) \qquad (8)$$

where τ_f is the rotor flap time constant as in eqn (2) and K_{b1s} is the stick gain.

The rotor is coupled to the fuselage through rotor flapping springs L_{b1s} and Y_{b1s}

$$\dot{p} = L_{b1s}\,b_{1s} + L_q q + L_r r + L_u u + \ldots + L_{\delta_{lon}}\delta_{lon} + L_{\delta_{ped}}\delta_{ped} + L_{\delta_{col}}\delta_{col} \qquad (9)$$

$$\dot{v} = Y_{b1s}\,b_{1s} + Y_p p + Y_q q + Y_r r + Y_u u + \ldots + Y_{\delta_{lon}}\delta_{lon} + Y_{\delta_{ped}}\delta_{ped} + Y_{\delta_{col}}\delta_{col} \qquad (10)$$

where it is important to remember that L_p, M_q, $L_{\delta lat}$, $M_{\delta lon}$, $Y_{\delta lat}$, and $X_{\delta lon}$ are omitted since their effects are associated with the steady-state rotor flapping response. The Y_p term is retained to correct for errors in

the assumption of the vertical cg location. The same form of the equations is used for the decoupled longitudinal regressive flapping (a1s), pitch rate (q), and axial velocity (u) responses. The rotor flapping time constant (τ_f) is constrained to be equal in the pitch and roll equations, as predicted by theory for hovering flight. Harding (Ref. 14) adopts a coupled rotor flapping formulation and eliminates the quasi-steady coupling derivatives, which was found to produce a slightly less accurate model in the current study.

The model was further simplified by assuming a diagonal form of the force-speed derivatives and force-control derivatives; i.e.,

$$X_v = X_w = Y_u = Y_w = Z_u = Z_v = 0 \qquad (11)$$

$$X_{\delta lat} = X_{\delta ped} = X_{\delta col} = Y_{\delta lon} = Y_{\delta col} = Z_{\delta lat} = Z_{\delta lon} = Z_{\delta ped} = 0 \qquad (12)$$

The low frequency speed derivatives Xu and Yv were fixed at their OH-58D simulation values (Ref. 13), because their effects are not significant to the dynamic response in the frequency range of interest and could therefore not be identified. The vertical response is essentially decoupled from the other degrees-of-freedom and is modeled as in eqn (7) to include the heave damping Zw, the inflow lead Z_L, the control derivative $Z_{\delta col}$ and a time delay $\tau c1$. Finally, time delays were included as a time shift on each of the angular controls. In the vertical axis, a second time delay $\tau c2$ was applied to the angular response to collective (r/δcol) which accounts for the torque response time constant (about 0.25 sec). More sophisticated models can be developed that include the complete engine/rpm engine dynamics (Ref. 15), and the coupled flap-inflow dynamics (Ref. 14).

Model Identification Using CIFER

The hybrid model structure discussed above was identified using CIFER. After convergence was achieved with the initial fully populated model, an accuracy analysis was completed to determine which parameters are insensitive or highly correlated and should be removed from the model (Ref. 4).These unimportant derivatives are sequentially eliminated and the model is reconverged and re-analyzed for accuracy at each step. The final model parameters are listed in Table 4 together with their Insensitivities and Cramer-Rao bounds. Target Insensitivities and Cramer-Rao bounds are for the most part within their target limits (10% and 20% respectively), indicating that a good final model structure has now been achieved. A comparison of the frequency domain model results with selected flight test results is presented in Figure 12, which shows excellent agreement, including the off-axes responses.

The entire system identification and analysis procedure using CIFER required about 3 man-weeks of effort. All calculations were completed on a VAX 8650 computer.

The model parameters of Table 4 convey important flight mechanics characteristics of the OH-58D helicopter. The rotor flapping spring ($L_{b_{1s}}$) is within 4% of the simple roll-response transfer function result of eqn (2). The rotor flapping time constant (τ_f), which for the state-space model is based on both pitch and roll responses, is 15% larger than the previous roll-response transfer-function result. These results show overall that the addition of the coupling effects and lower-frequency quasi-steady parameters do not substantially alter the dominant 2nd order roll/flapping behavior predicted by simple transfer function methods.

The identified pitch and roll spring constants should be (physically) related to the inertia ratios:

$$L_{b_{1s}} / M_{a_{1s}} = 53.06 / 22.05 = 2.406 = I_{yy} / I_{xx} \qquad (13)$$

Bivens (Ref. 13) provides inertias for the OH-58D simulation model: $I_{yy} / I_{xx} = 2939.9 / 1208.4 = 2.43$ which is amazingly close to the identified value. The identified yaw damping is also quite close to the simulation value. The identified heave damping value (Z_w) is nearly the same as the earlier transfer-function fit result of eqn (7), and very close to the simulation value of $Z_w = -0.32$. The inflow zero is identified as $Z_L = -8.6$ rad/sec, which is also very close to the transfer function results in eqn (7).

The level of pitch-roll coupling is appreciated by comparison of the control and response coupling derivatives with the on-axis derivatives. The roll due-to-pitch response ratio is:

$$\frac{|L_q|}{|(L_p)_{eff}|} = \frac{|L_q|}{|1/(\tau_f L_{b_{1s}})|} = \frac{2.16}{9.61} = 0.23 \qquad (14)$$

while the pitch due-to-roll response coupling ratio is 0.26.

The coupling ratio for longitudinal control input is:

$$\frac{|L_{\delta_{lon}}|}{|(L_{\delta_{lat}})_{eff}|} = \frac{|L_{\delta_{lon}}|}{|(L_{b_{1s}} K_{b_{1s}})|} = \frac{0.030}{0.166} = 0.18 \qquad (15)$$

and 0.26 similarly for the lateral control input. These results indicate a pitch-roll interaxis coupling of about 25%, which is about half of that of the BO-105 (Ref. 4),

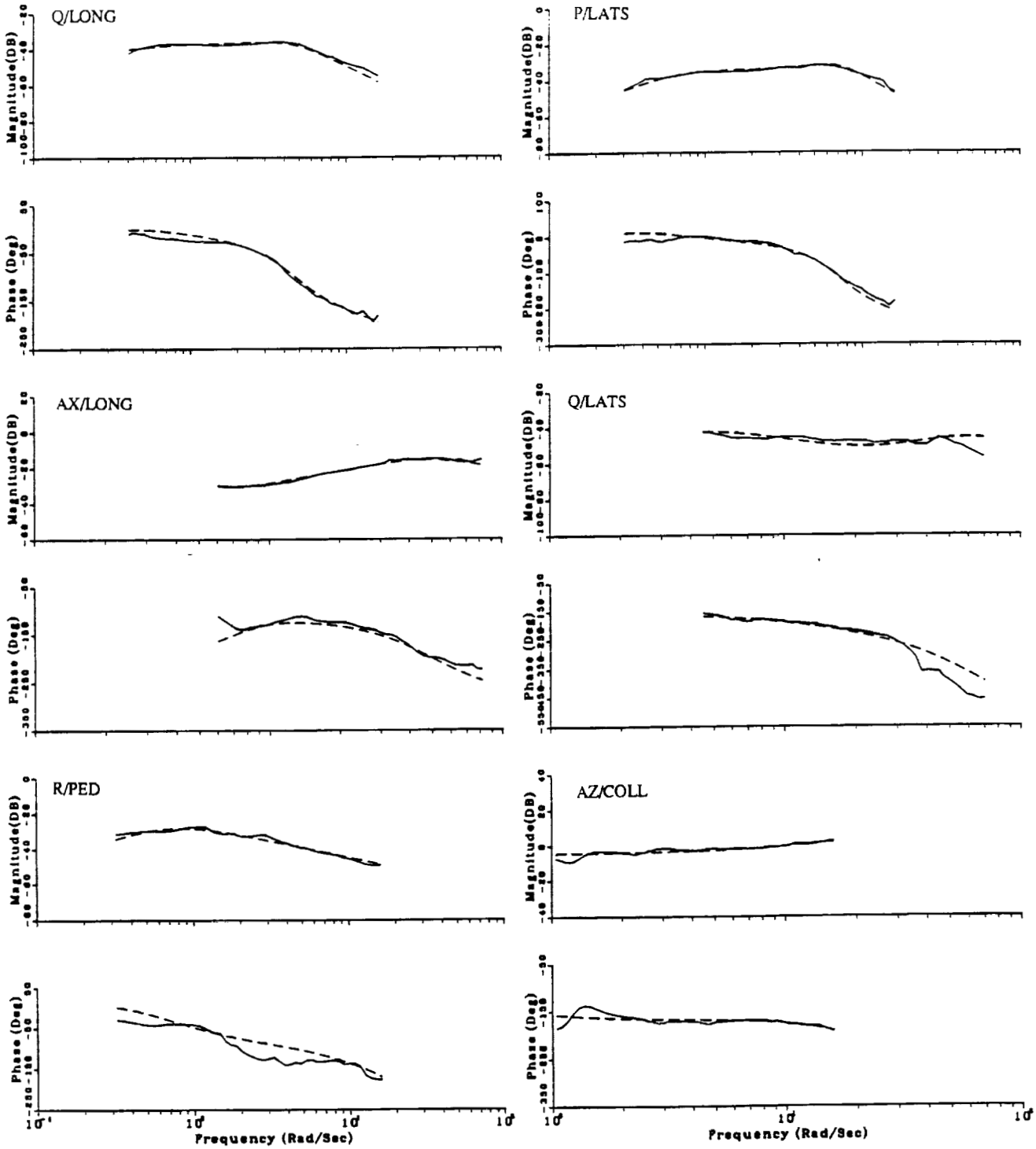

——— Flight data
------- Identified model including flapping and vertical inflow

Figure 12 Model Results

C-6

	Identified model		
Derivative	Param Value	C.R. (%)	Insens.(%)
X_u	-0.01440 †	.....	.....
X_v	0.000 +	.....	.....
X_w	0.000 +	.....	.....
X_p	4.751	13.03	4.149
X_q	0.000 +	.....	.....
X_r	0.000 +	.....	.....
G	32.17 †	.....	.....
X_{als}	-55.53	6.696	1.984
Y_u	0.000 +	.....	.....
Y_v	-0.03300 †	.....	.....
Y_w	0.000 +	.....	.....
Y_p	1.569	18.03	6.575
Y_q	0.000 +	.....	.....
Y_r	3.535	10.58	0.7944
G	32.17 †	.....	.....
Y_{bls}	127.8	4.412	0.7742
Z_u	0.000 +	.....	.....
Z_v	0.000 +	.....	.....
Z_w	-0.3980	34.04	13.98
Z_p	0.000 +	.....	.....
Z_q	0.000 +	.....	.....
Z_r	0.000 +	.....	.....
L_u	0.000 +	.....	.....
L_v	0.01636	20.75	3.744
L_w	0.000 +	.....	.....
L_p	0.000 +	.....	.....
L_q	-2.159	11.37	1.687
L_r	1.049	11.24	0.9681
L_{bls}	53.06	4.350	0.6191
M_u	-9.662E-03	20.66	5.398
M_v	0.03279	11.86	2.498
M_w	0.000 +	.....	.....
M_p	-1.032	9.622	1.604
M_q	0.000 +	.....	.....
M_r	0.000 +	.....	.....
M_{als}	22.05	5.208	1.185
N_u	0.000 +	.....	.....
N_v	0.03547	15.89	3.144
N_w	-0.3780	32.45	11.60
N_p	-0.6021	16.10	4.212
N_q	1.906	10.31	3.087
N_r	-0.5644	13.51	3.394
K_{in1}	1.000 †	.....	.....
K_{in2}	1.000 †	.....	.....
T_1	-0.1806 *	.....	.....
T_3	-0.1806 *	.....	.....
Z_L	**-8.60**	**14.6**	**2.3**

	Identified Model		
Derivative	Param Value	C.R. (%)	Insens.(%)
X_{lon}	0.000 +	.....	.....
X_{lat}	0.000 +	.....	.....
X_{ped}	0.000 +	.....	.....
X_{col}	0.000 +	.....	.....
Y_{lon}	-0.1480	4.248	0.9466
Y_{lat}	0.000 +	.....	.....
Y_{ped}	-0.1191	5.096	2.073
Y_{col}	0.000 +	.....	.....
Z_{lon}	0.000 +	.....	.....
Z_{lat}	0.000 +	.....	.....
Z_{ped}	0.000 +	.....	.....
Z_{col}	-0.07450	10.72	1.868
L_{lon}	-0.03062	5.902	1.463
L_{lat}	0.000 +	.....	.....
L_{ped}	0.01420	6.542	2.928
L_{col}	0.000 +	.....	.....
M_{lon}	0.000 +	.....	.....
M_{lat}	0.01290	15.32	2.648
M_{ped}	0.000 +	.....	.....
M_{col}	0.000 +	.....	.....
N_{lon}	-7.613E-03	21.71	8.117
N_{lat}	0.01823	9.564	2.754
N_{ped}	0.05702	5.314	2.004
N_{col}	0.03830	5.080	2.376
K_{als}	2.227E-03	6.157	1.059
K_{bls}	3.123E-03	5.023	0.8559
τ_{c1}	0.08110	10.53	3.661
τ_{c2}	0.2660	4.191	1.729
τ_{long}	0.03646	15.67	6.197
τ_{lats}	0.05956	9.163	3.632
τ_{ped}	0.09027	5.346	2.518

	Identified Model		
Derivative	Param Value	C.R. (%)	Insens.(%)
T_{aur}	0.1806	4.228	0.5924
T_2	0.1806 *	.....	.....

+ Eliminated during model structure determination
† Fixed value in model
* Fixed derivative tied to a free derivative

Table 4 Model Results - OH58D Stability and Control Derivatives

but which is still quite significant from a handling-qualities point of view.

The longitudinal and lateral moment derivatives (M_u and L_v) have small values, but are negative in sign -- opposite from first principles result. This problem reflects poor low frequency identification (e.g., for frequencies less than 0.5 rad/sec in the roll response of Figure 6) and suggests that these parameters may better be determined from the static calculation, given in the introduction, using the identified effective control moment derivatives of equations 14 and 15.

Finally, the eigenvalues of the model listed in Table 5 give the coupled natural modes of the OH-58D. The roll/flapping response [ζ=0.407, ω_n=7.17] matches the transfer-function result of eqn (2) as expected. The pitch/rotor-flap response is also coupled but at a lower frequency [ζ=0.550, ω_n=4.64], but at a lower frequency due to the higher pitch inertia.

Table 5 OH-58D Hover Eigenvalues

Mode	Real	Imag	ω rad/sec	ζ
Long Phugoid	**0.242**	**0.0**		
Long Phugoid	**-0.269**	**0.0**		
Lat velocity	**0.433**	**0.0**		
Yaw/sway	**-0.578**	**0.349**	**0.675**	**0.856**
Heave Mode	**-0.398**	**0.0**		
Roll/flapping	**-2.916**	**6.550**	**7.17**	**0.407**
Pitch/flapping	**-2.554**	**3.877**	**4.64**	**0.550**

Model Verification in the Time-Domain

Comparison of the pulse responses for the identified hybrid model and the flight data are shown in Figure 13 for lateral stick and pedal inputs. Similar accuracy is achieved for longitudinal and collective inputs. The results show that key characteristics of the on- and off-axis responses are very well predicted, and the model is quite acceptable for handling-qualities characterization purposes.

Full Simulation Quality Identification

The last, most complex application of the frequency domain database is the identification of a state space model that could be used for detailed analyses, with fidelity equivalent to a complete nonlinear model. The utility of such an identification includes simulation validation, piloted simulation, and detailed flight control design. Several researchers have documented the effectiveness of the frequency domain identification approach on the BO-105 (Ref. 4), the AH-64A (Refs. 14 and 15), and the UH-60A helicopters (Ref. 16). The data required from flight test is essentially the same, except that more attention is placed on the test inputs to maximize data quality. An extended frequency range is usually needed to obtain information at higher frequencies where rotor dynamic effects become more prominent. Detailed angular and kinematic consistency analysis, measurement error modeling, state reconstruction, detection of bad data, calibration of control rigging, all need to be examined to ensure high quality frequency response data that has a high degree of confidence (Ref. 11). Further data that would improve results could include rotor measurements such as flapping and lead/lag angles. Additional states are usually added to account for higher order rotor and inflow dynamics, as well as engine and stick dynamics. Obviously, the level of effort increases from 3-4 manweeks to 3-4 manmonths, as well as the amount of time necessary to plan and conduct the flight test program needed to obtain the data. The payoffs, however can be significant, resulting from the high fidelity simulation quality models that are generated from this process.

CONCLUSIONS

This paper has described the variety of handling qualities related information that can be derived from the frequency domain database generated from the relatively simple frequency sweep flight test technique. In many cases, substantially more information is available than the results produced from claasical flight test techniques, which demonstrates the unique power of the frequency based approach over the classical time domain approaches. Resaerch needs to continue in this area to determine further applications of the information available from the frequency doamin database. Some particular conclusions from this study are:

Non-parametric models are easily obtained from frequency sweep flight tests, and provide useful handling qualities information.

Simple parametric models are useful for characterizing the dominant vehicle characteristics using a few number of parameters.

An example of a simple parametric model of the OH-58D illustrates that frequency domain identification can reliably be used to support handling qualities studies.

Simple 1st order rigid body models are inadequate for even simple handling qualities models. A coupled fuselage/regressive flapping model must be used to characterize the vehicle response.

RECOMMENDATIONS:

A technical note should be written for H-Q frequency domain testing.

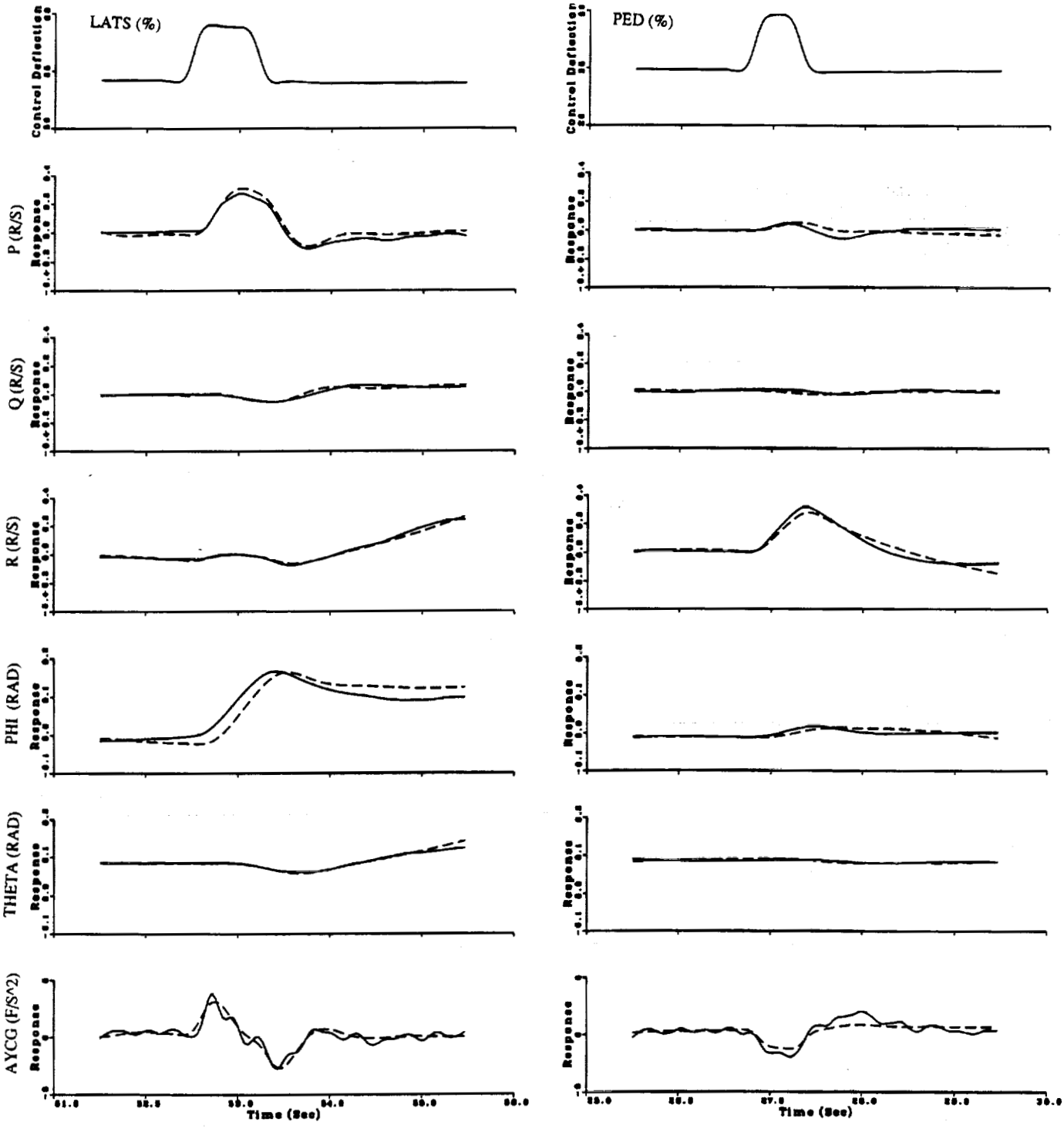

——— Flight data
------- Identified model including flapping and vertical inflow

Fig. 13 Time-domain verification of model

Incorporate procedure in future airworthiness testing of new and modified aircraft.

Store FR database for future use and make available a compatible format for wide dissemination and further research.

ACKNOWLEDGMENTS

The authors gratefully acknowledge the support, comments and contributions of David Key, AFDD; and Mavis Cauffman, Sterling Federal Systems.

REFERENCES

[1]Brown, J.D., Stormer. W.H., Hopkins, G.J., and Nagata, J.L., "Airworthiness and Flight Characteristics Evaluation of the OH-58D Helicopter," USAAEFA Project No. 83-27-1, October 1990.

[2]Ham, J.A., and Butler, C.P., "Flight Testing the Handling Qualities requirements of ADS-33C - Lessons Learned at ATTC," American Helicopter Society 47th Annual Forum, May 1991.

[3]Tischler, M.B., et al., "Demonstration of Frequency-Sweep Testing Technique Using a Bell 214-ST Helicopter," NASA TM 89422, April 1987.

[4]Tischler, M.B., Cauffman, M.G., "Frequency-Response Method for Rotorcraft System Identification: Flight Applications to BO-105 Coupled Rotor/Fuselage Dynamics," Journal of the American Helicopter Society, Vol 37, No 3, pgs 3-17, July 1992.

[5]Tischler, M.B., Leung, J.G.M., and Dugan, D.C., "Frequency Domain Identification of XV-15 Tilt Rotor Aircraft Dynamics in Hovering Flight," AHS J. Vol.30(2), pp 38-48, April 1985.

[6]Otnes, R.K., and Enochsen, L., *Applied Time Series Analysis*, John Wiley and Sons, Inc., New York, 1978, pp. 363-412.

[7]Carter, C.G., et al, "Estimation of the Magnitude-Squared Coherence Function Via Overlapped Fast Fourier Transform Processing," IEEE Transaction on Audio and Electroacoustics, Vol. AU-21, (4), Aug 1973, pp. 337-344

[8]Aeronautical Design Standard, "Handling Qualities Requirements for Military Rotorcraft," AVSCOM, ADS-33C, August 1989.

[9]Hoh, R.H., et al, "Background Information and User's Guide for Handling Qualities Requirements for Military Rotorcraft," Technical Report No. 89-A-008, AVSCOM, December 1989.

[10]Ham, J.A., , "Frequency Domain Flight Testing and Analysis of an OH-58D Helicopter," AHS J. Vol.37(4), pp 16-24, October 1992.

[11]"Rotorcraft System Identification," AGARD AR 280, Sept. 1991.

[12]Heffley, R.K., Bourne, S.M., Curtiss, H.C., Jr., Hindson, W.S., Hess, R.A., "Study of Helicopter Roll Control Effectiveness Criteria, NASA CR 177404, April 1986.

[13]Bivens, C.C., Guercio, J.G., "A Simulation Investigation of Scout/Attack helicopter Directional Control Requirements for Hover and Low-Speed Tasks, NASA TM 86755, March 1987.

[14]Harding, J.W., "Frequency-Domain Identification of Coupled Rotor/Body Models of an Advanced Attack Helicopter," AHS 48th Annual Forum, Washington, D.C., June 1992.

[15]Schroeder, Tischler, Watson, Eshow, "Identification and Simulation Evaluation of an AH-64 Helicopter Hover Math Model" , AIAA Atmospheric Flight Mechanics Conference, Aug 12-14, 1991, New Orleans, Louisiana.

[16]Ballin, M.G., Dalang-Sectretan, M.A., "Validation of the Dynamic Response of a Blade-Element UH-60 Simulation Model in Hovering Flight," American Helicopter Society 46th Annual Forum, May 1990.

PRELIMINARY DESIGN FEATURES OF THE RASCAL—A NASA/ARMY ROTORCRAFT IN-FLIGHT SIMULATOR

Edwin W. Aiken* and Robert A. Jacobsen**
NASA Ames Research Center
Moffett Field, California

Michelle M. Eshow†
U.S. Army Aeroflightdynamics Directorate
Moffett Field, California

William S. Hindson‡ and Douglas H. Doane§
NASA Ames Research Center
Moffett Field, California

Abstract

Salient design features of a new NASA/Army research rotorcraft—the Rotorcraft-Aircrew Systems Concepts Airborne Laboratory (RASCAL)—are described. Using a UH-60A Black Hawk helicopter as a baseline vehicle, the RASCAL will be a flying laboratory capable of supporting the research requirements of major NASA and Army guidance, control, and display research programs. The paper describes the research facility requirements of these programs together with other critical constraints on the design of the research system, including safety-of-flight. Research program schedules demand a phased development approach, wherein specific research capability milestones are met and flight research projects are flown throughout the complete development cycle of the RASCAL. This development approach is summarized, and selected features of the research system are described. The research system includes a full-authority, programmable, fault-tolerant/fail-safe, fly-by-wire flight control system and a real-time obstacle detection and avoidance system which will generate low-altitude guidance commands to the pilot on a wide field-of-view, color helmet-mounted display.

*Chief, Flight Dynamics and Controls Branch. Member AIAA.
**RASCAL Project Manager, Aircraft Systems Branch. Member AIAA.
†Aerospace Engineer, Flight Control Branch. Member AIAA.
‡Research Pilot, Aircraft Operations Branch.
§Aerospace Engineer, Guidance and Navigation Branch.

This paper was originally presented at the AIAA/AHS Flight Simulation Technologies Conference, Aug 24-26, 1992, Hilton Head Island, SC.

Introduction

The preface to the proceedings from an International Symposium on "In-Flight Simulation for the 90's" held in Braunschweig, Germany, in July 1991 contains the following assessment of flight simulation:

> Within the aerospace community, flight simulation has become virtually synonymous with the reproduction of the cockpit flight environment in a ground-based simulation facility. As this discipline has matured and assimilated the advances in digital processor and electronic imaging technologies, ground-based flight simulation has found its legitimate role in pilot-in-the-loop applications, both as a research and development tool and as a training aid. Nevertheless, ground-based flight simulation does have limitations related to the incomplete – and sometimes conflicting – nature of visual and motion cues which are presented to the pilot. As a result, in-flight simulation has played a unique role in aerospace research, development, and test pilot training by providing the proper environment and immersing the pilot in a real flight situation.

For rotorcraft, in-flight simulation is becoming increasingly important as fly-by-wire flight control technology is exploited and as autonomous systems are developed to relieve pilot workload, particularly during nap-of-the-Earth flight. In addition, the fidelity of aerodynamic modeling for rotorcraft is far from maturity, with the result that important handling and performance phenomena such as rotor wake interactions cannot be adequately simulated on the ground. This paper describes

the planned development and preliminary design features of a modern rotorcraft in-flight simulation facility—the Rotorcraft-Aircrew Systems Concepts Airborne Laboratory (RASCAL)—heavily influenced by the requirements of major NASA and Army rotorcraft guidance, control, and display research and development (R&D) programs at the Ames Research Center, Moffett Field, California.

As described in Ref. 1, the Army/Sikorsky UH-60A Black Hawk helicopter (Fig. 1) was determined to be the most appropriate available baseline vehicle for RASCAL development. In October of 1989, a UH-60A, originally used as the Army's Advanced Digital-Optical control System (ADOCS) demonstrator aircraft, was loaned to NASA-Ames Research Center by the U.S. Army, and the development of the RASCAL research facility was initiated.

The paper begins with a statement of the objective of the RASCAL development, including an overview of the research programs which will utilize its capabilities. These research requirements and other critical design constraints, including flight safety, are then summarized. The approach to be taken in the development of the RASCAL, which is also driven by the requirements of the flight research elements of the programs it will support, is then described. Finally, selected design features of the RASCAL Research Flight Control System are presented.

Project Objective and Research Requirements

The objective of the RASCAL facility development project is the design, development, integration, and testing of an airborne laboratory capable of supporting the flight research requirements of several major NASA and Army guidance, control, and display R&D programs. These programs are described in Ref. 1 and include the following:

1. Superaugmented Concepts for Agile Maneuvering Performance (SCAMP): Analysis, ground simulation, and flight research to investigate methods for the enhancement of rotorcraft maneuverability and agility through the application of advanced flight-control concepts

2. Automated Nap-of-the-Earth Flight (ANOE): Analysis, ground simulation, and flight research to develop low-altitude guidance algorithms and pilot's display laws for rotorcraft terrain-following/terrain-avoidance and obstacle avoidance

3. Rotorcraft Agility and Pilotage Improvement Demonstration (RAPID): In-flight validation and demonstration of ground simulation-derived solutions to selected Army-identified "technology barriers" to the development of next generation/future systems.

Fig. 1 Rotorcraft-Aircrew Systems Concepts Airborne Laboratory (RASCAL).

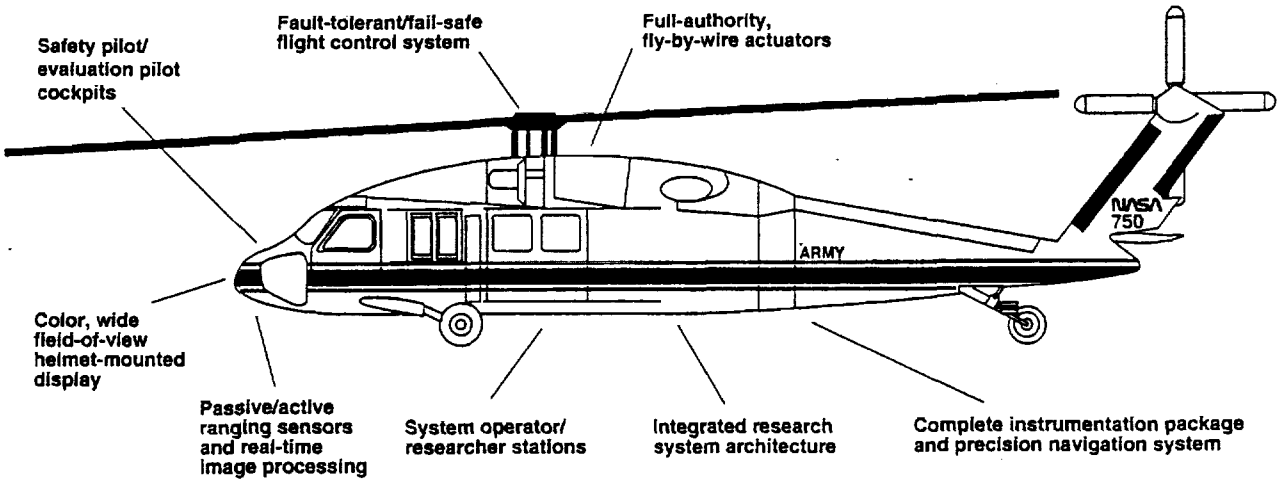

Fig. 2 RASCAL research system components.

To support the requirements of these R&D programs, the RASCAL research system will include the following (Fig. 2):

1. A high quality instrumentation, signal conditioning, and data acquisition system including rigid body, rotor state, and propulsion system sensors, suitable for both experimental data and flight control applications

2. A programmable, fly-by-wire research flight control system including high-performance actuators; a flight control computer, programmable in a higher-order language, with a hardware/software architecture necessary for the throughput and speed requirements of the various SCAMP control concepts; and a high-speed data bus with sufficient capacity for the anticipated bus traffic

3. The capability to evaluate both conventional controllers, using an artificial force-feel system, and integrated, multi-axis side-stick controllers

4. An in-flight researcher interface with the system for monitoring the experiments and for effecting configuration changes to allow productive use of the available flight time

5. An on-board precision navigation system suitable for low-altitude flight

6. Appropriate passive (e.g., TV or FLIR) and active (e.g., radar or laser) sensors for image-based guidance and navigation including obstacle detection/avoidance

7. On-board computational capability for real-time image processing, vehicle motion estimation, guidance algorithm generation, and pilot's display generation

8. Terrain data base storage for low-altitude navigation with no image sensor-aiding

9. A flexible, programmable pilot's display system including a panel-mounted display suitable for a digital map and a color, wide field-of-view, helmet-mounted presentation of flight status and command information and sensor-based imagery

10. A capability for the integration of autonomous guidance commands with the research flight control system

RASCAL Research System Design Requirements

An in-house preliminary design of the RASCAL research system was conducted during the summer and fall of 1991. The efforts of the preliminary design team included the establishment of prioritized design requirements for the research system. The top six of these requirements, in priority order, are:

1. Flight Safety: The RASCAL research system shall not degrade the flight safety reliability of the baseline Black Hawk helicopter.

2. Performance: The RASCAL research system shall have the capability to implement SCAMP high-bandwidth flight control laws, which include the use of rotor state feedback, and a real-time image processing,

guidance, and display system suitable for the ANOE program. The capability of the research flight control system shall be limited only by the performance of the basic UH-60A flight control system.

3. Research Flight Envelope: The RASCAL allowable research flight envelope shall be the Black Hawk flight envelope. No expansion of that flight envelope is required. Aggressive maneuvering while using the research system shall be conducted at altitude, clear of terrain and obstacles. Aggressiveness may be limited near the terrain and obstacles.

4. Cost Constraints: The RASCAL research system design must be compatible with the available funding from NASA, Army, and Federal Aviation Administration (FAA) sources.

5. Research Productivity: The RASCAL research system shall be designed with a high mission reliability and with the capability of obtaining a maximum number of research data points per flight hour.

6. Schedule Constraints: The RASCAL research system shall be developed in a manner that allows specific SCAMP, ANOE, and RAPID flight research experiments to be flown at intervals throughout the overall facility development period.

The milestones for RASCAL facility capability dictated by the requirements of the SCAMP, ANOE, and RAPID flight research experiments schedule are indicated in Fig. 3. These experiments are summarized as follows:

SCAMP and RAPID

Rigid-Body Modeling. Data acquisition to support the development and validation of rigid-body models suitable for use in SCAMP control law development

Baseline Maneuverability/Agility Measures. Development of relevant measures of rotorcraft maneuverability and agility and measurement of the maneuverability and agility characteristics of the basic Black Hawk

Rotor-state Modeling. Rotor state data acquisition to support the extension of the SCAMP rotorcraft models to include rotor system dynamics

Rigid-Body Flight Control Systems (FCS). Flight implementation and evaluation of SCAMP control laws involving the feedback and control of rigid-body states

Rotor-State Feedback FCS. Flight implementation and evaluation of SCAMP control laws which include the feedback and control of rotor states

ANOE

Passive Ranging Validation. Acquisition of airborne video imagery data from stereo TV cameras for off-line validation of range estimation algorithms

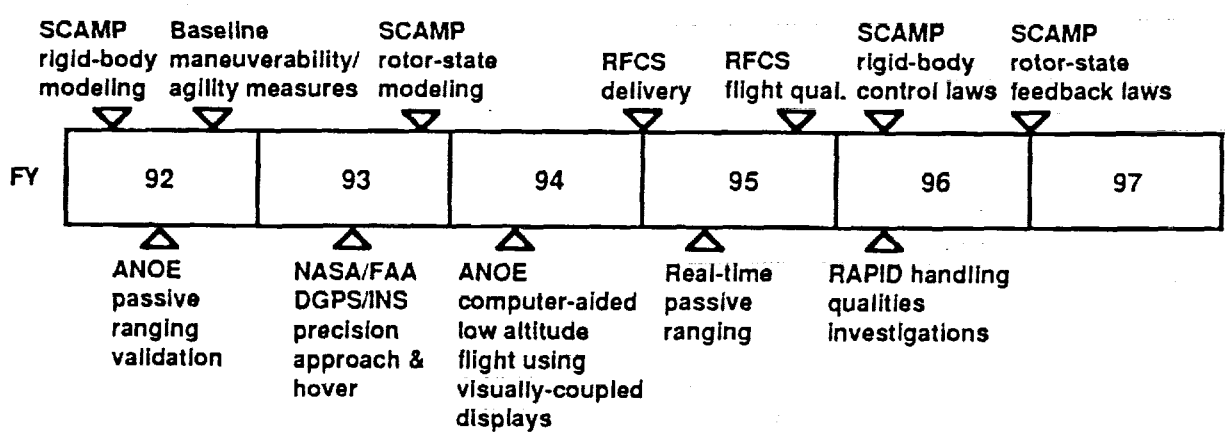

Fig. 3 RASCAL research facility capability milestones.

Differential Global Positioning System (DGPS)/ Inertial Navigation System (INS) Precision Approach and Hover. In-flight evaluations of the suitability of a DGPS/INS for helicopter terminal area operations under Instrument Meteorological Conditions

Computer-Aided Low-Altitude Flight Using Visually Coupled Displays. Flight evaluations of low-altitude guidance algorithms and the presentation of fused guidance symbology and sensor imagery on a color, wide field-of-view helmet-mounted display

Real-Time Passive Ranging. Flight evaluations and demonstrations of pilot aids for low-altitude flight including real-time obstacle detection and avoidance systems employing TV and FLIR sensors

The facility capability milestones established by the requirements of these experiments demand a phased approach to the development of the overall research capability of the RASCAL.

RASCAL Research System Development Program

Research program requirements dictate that RASCAL flight test programs be conducted at several stages throughout the development of the RASCAL as a research facility. The research system that is to be installed on the RASCAL must meet the research objectives of these programs in a timely manner. A phased development program has been defined to provide a system that can support research activities at several stages as the system is developed. The functional capability that is implemented at any phase of the development program to meet the immediate research goals is maintained and adds to the overall facility capability. This additive approach results in a system that, upon completion, will have more integrated capability than any of the individual research programs presently require. Future research programs will have the full integrated capability available for the conduct of flight test programs.

A critical element of this approach to the development of the RASCAL is that the system development risks must be minimized. This constraint requires that the facility be developed using state-of-the-art, but proven, technology. Care will be taken to severely limit technology development requirements in specifying the RASCAL Research System.

The research programmatic milestones identified for the RASCAL and presented in Fig. 3 have been grouped into four development phases as indicated in Fig. 4. Each of these four phases results in the accomplishment of specific, reportable research goals. The system requirements for each of the phases is presented below.

Phase 1. Measurement and documentation of the basic UH-60A dynamics and controls characteristics are to be accomplished, thereby providing a baseline against which future improvements in maneuverability and agility can be judged. Acquisition of stereo video data for post-flight processing will be accomplished, allowing the validation of passive ranging algorithms.

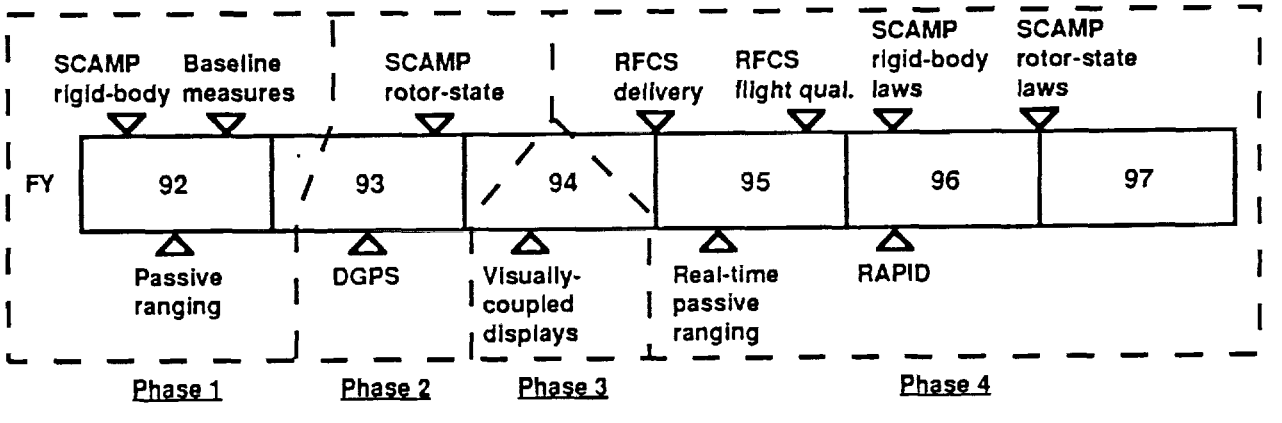

Fig. 4 RASCAL facility development phases.

Phase 2. The additional capability of acquiring and documenting rotor state measurements will complete the UH-60A baseline identification. Differential Global Positioning System (DGPS) position measurement capability will allow the development of guidance/display laws for precision approach and hover.

Phase 3. A wide-field-of-view, color, helmet-mounted display will add the capability to provide enhanced guidance information to the pilot, allowing the development of display laws to assist in the ability to conduct missions in an NOE environment.

Phase 4. A full-authority, fly-by-wire research flight control system will allow development and demonstration of control laws that more fully utilize the maneuverability and agility capabilities of the UH-60A. Real-time processing of the stereo video data on board the RASCAL will allow the presentation of obstacle ranging information and sensor/computer-aided guidance commands to the pilot.

System architectures have been established for each of the phases of the RASCAL development program that allow the additional capabilities to add to the overall system capability. The specific research requirements of each phase are met by this approach while the facility capability is always increased. This approach will be beneficial as new research programs are defined and the full capability of the RASCAL can be utilized.

Phase 1

The architecture for the RASCAL Phase 1 Research System is shown in Fig. 5. The central element of the research system for Phase 1 is the data acquisition computer, which uses an Intel 80486 processor. Analog sensors provide control position and a limited set of body state measurements. A Litton LN-93 Inertial Navigation Unit (INU) is installed to measure body attitudes and angular rates, and linear velocities and accelerations. Communication between the INU and the data acquisition computer is provided by a Mil-Std-1553B bus. A GEC Marconi HADS Air Data Computer that had been installed on the aircraft previously has been incorporated to provide low airspeed and local flow angle information.

A pair of high resolution video cameras is mounted on the nose of the RASCAL to provide data for the post-flight validation of passive ranging algorithms. The video data are time-correlated with the aircraft state data and processed post-flight. Provisions are incorporated to replace the video cameras with a FLIR installation. An experimenter's station is installed in the cabin allowing convenient control of the video and data systems.

Phase 2

Additional components added to the Phase 1 RASCAL system architecture will allow the research goals of Phase 2 to be accomplished. The resulting architecture is shown in Fig. 6. The basic data acquisition capability installed for Phase 1 will remain, with additional sensors installed to provide rotor state information. A guidance/navigation computer will be added to perform the guidance and navigation law computations. To provide guidance information to the pilot, a panel-mounted display will be installed and driven by the guidance/navigation computer. A DGPS that communicates directly with the guidance/navigation computer through a digital bus will be included. An uplink data stream from a ground-based GPS is required to provide the differential corrections to the airborne unit.

A research system operator's station will be implemented in the forward area of the RASCAL cabin for control of the research system. An experiment support/observer's station will be installed in the aft cabin to accommodate a second researcher or to provide for an observer during flight test operations.

Phase 3

The most significant addition to the RASCAL research system architecture to accommodate the low-altitude guidance research goals for Phase 3 will be the addition of a wide-field-of-view, multi-color helmet-mounted display system as shown in Fig. 7. Included will be the helmet, incorporating the display capability, a programmable display generator and a head tracker system. A second Mil-Std-1553B bus is anticipated to provide the data communications required to process guidance and navigation laws and to pass that information to the helmet. Additionally, that information must be recorded by the data acquisition system for post-flight processing.

Provisions for the acquisition of additional data regarding propulsion system performance will be added during this phase. Truth data for evaluation of the guidance system performance will be provided by uplinking data from the laser tracking system that Ames operates at its Crows Landing flight test facility.

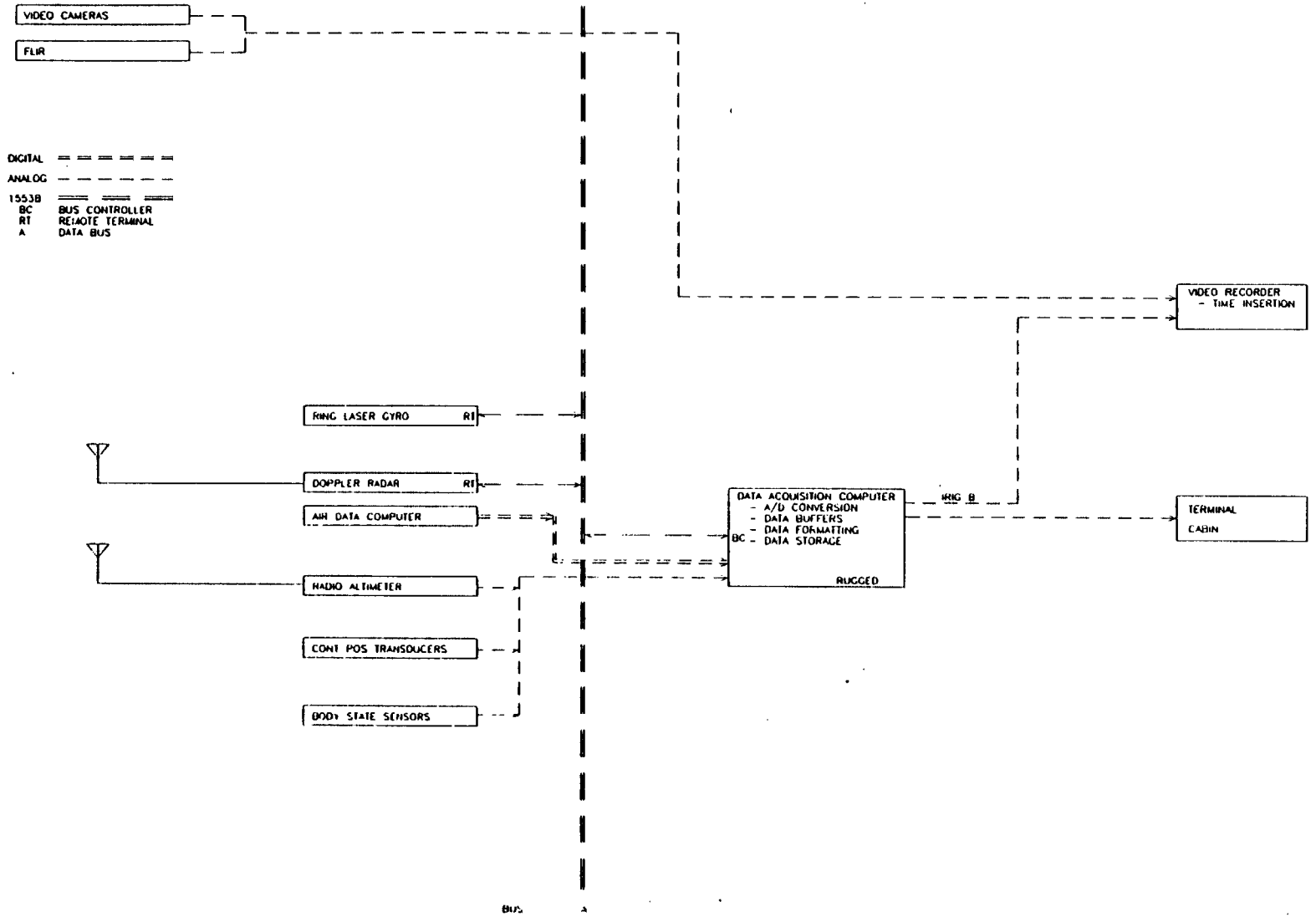

Fig. 5 RASCAL Phase 1 architecture.

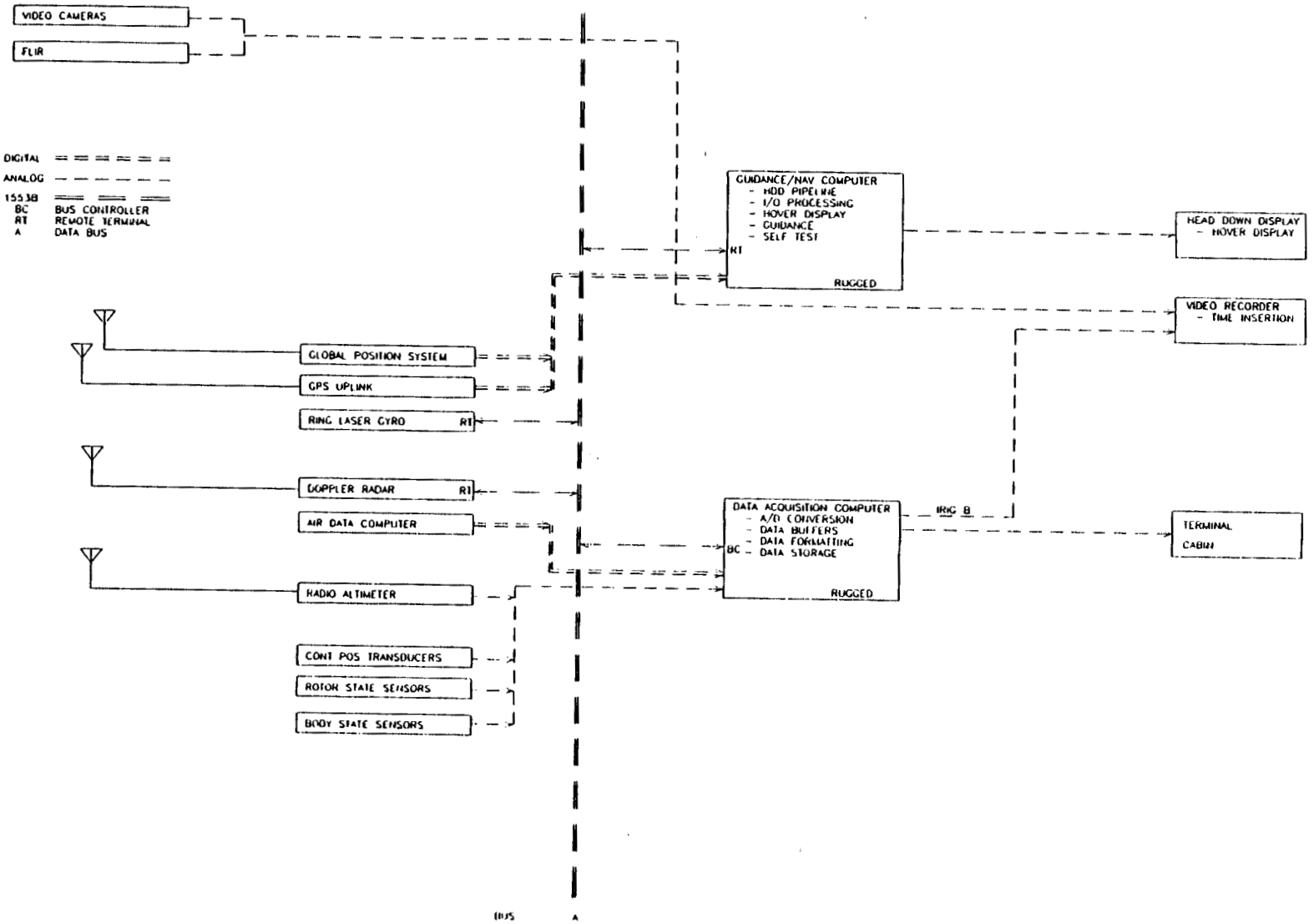

Fig. 6 RASCAL Phase 2 architecture.

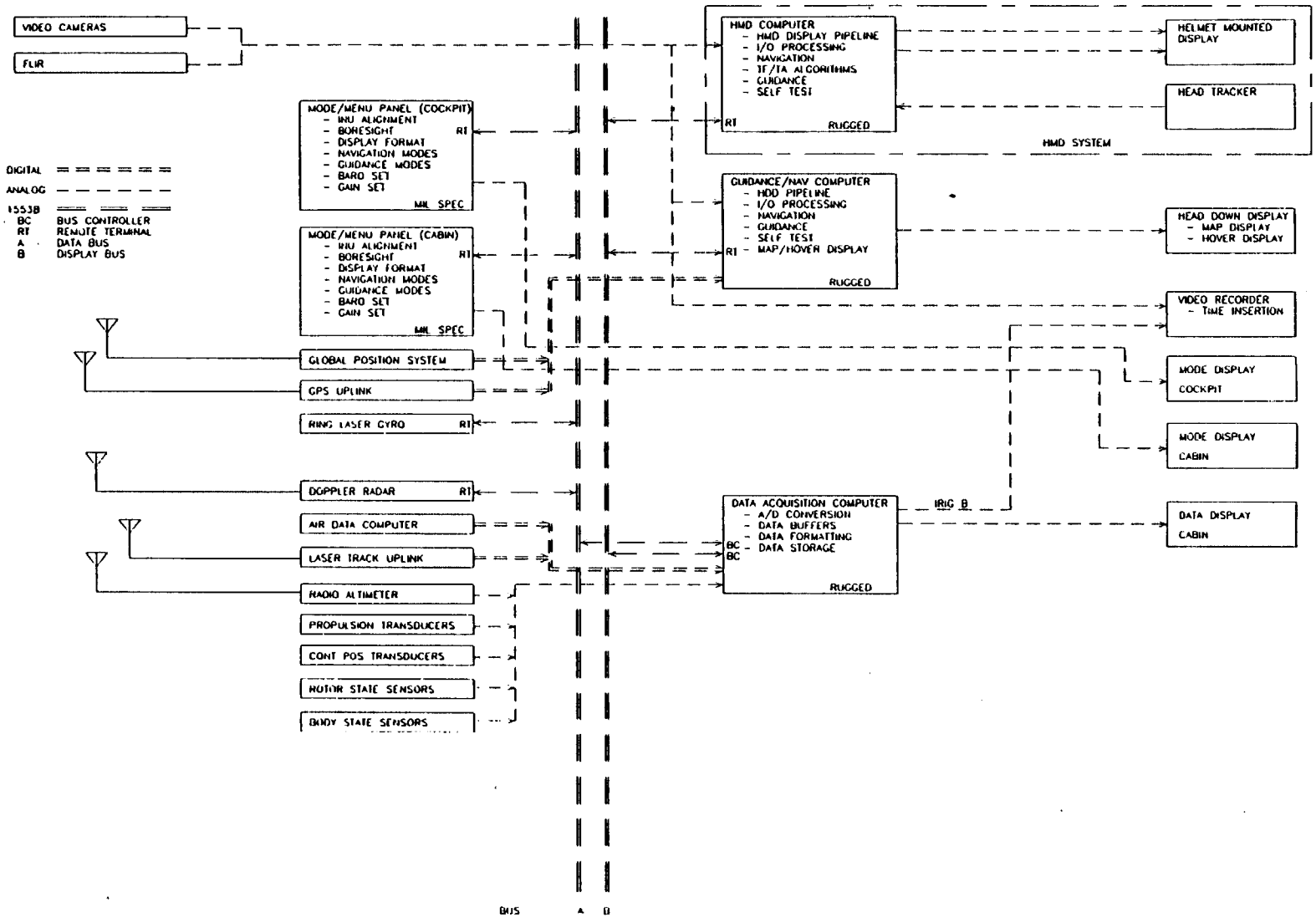

Fig. 7 RASCAL Phase 3 architecture.

The research system will be, by this phase of development, sufficiently complex to require the incorporation of mode control capability. The mode-menu panels will be used by the evaluation pilot to select guidance and display modes and by the researcher/system operator to centrally control and monitor the research system components and to vary experiment parameters during the flight test. Control/display units will be installed in the cockpit and at the research operator's station to provide this interaction with the research system, which will be accomplished using the Mil-Std-1553B bus.

Phase 4

Two major system installations will be added to the research system to accomplish the research goals for Phase 4. The completion of this phase defines the final system architecture as shown in Fig. 8.

The first of these major installations is a real-time image processor for the passive video ranging system. This unit will process the video signals to extract ranging information and provide it to the guidance/navigation computer. Obstacle avoidance information generated by the guidance/navigation computer will be displayed to the pilot. A high-speed digital bus will be used to communicate the information among the image processor, the guidance/navigation computer, and the helmet-mounted display system.

The second major addition to the RASCAL research system in Phase 4 is the fly-by-wire research flight control system (RFCS). This installation provides the RASCAL with its full in-flight simulator capability. An "evaluation pilot's" station will be implemented by mechanically disconnecting the controls at the right crew station and installing new controls that electrically signal the RFCS. The RFCS will be a full-authority flight control system incorporating the functional components shown in the lower right section of Fig. 8; it is described in the next section.

On-board data analysis capability will be provided by the data analysis computer, which will be capable of real-time data display and post-run data analysis for use by the on-board researcher. A rearrangement of the Mil-Std-1553B buses may be required to accommodate the increased data flow requirements. Telemetry capability will be provided to allow the acquired data to be displayed and recorded on the ground at Ames' flight test facilities.

During Phases 3 and 4, a ground development facility will be built up to support the on-board systems development. A combination of actual and emulated flight hardware will be employed to support hardware flight qualification and subsystems integration and software validation and verification. Inclusion of a simplified fixed-base simulation capability will allow pilot-in-the-loop testing and will support experiment development and pre-flight training activities.

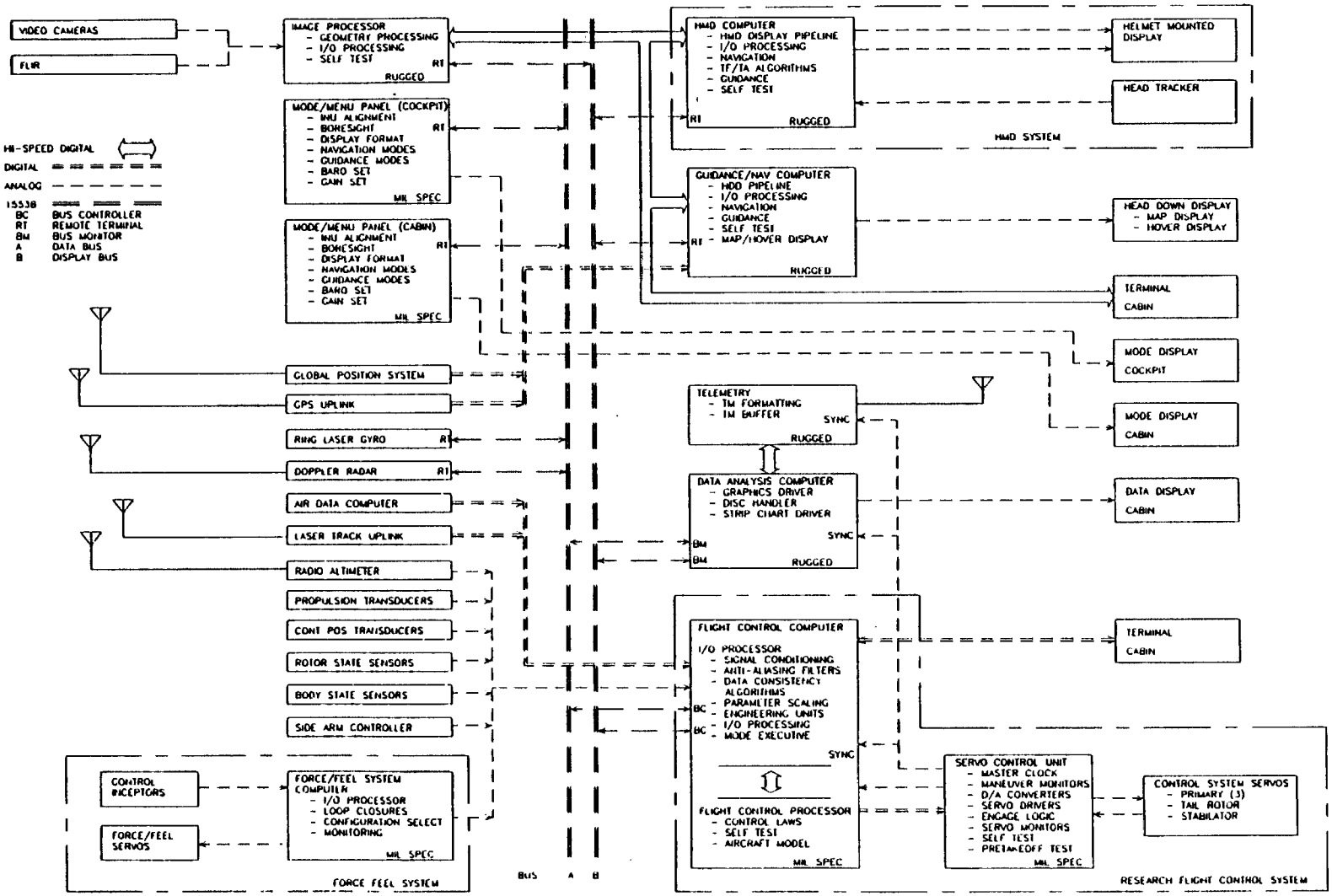

Fig. 8 RASCAL Phase 4 architecture.

Research Flight Control System Requirements and Design Features

The RASCAL RFCS comprises those elements of the research system necessary to achieve full-authority, fly-by-wire flight control by the evaluation pilot. The elements include control inceptors, sensors, a flight control computer, a servo control unit, and research servo-actuators, as illustrated in Fig. 9. Because it is the largest single RASCAL subsystem and because of its flight critical nature, special attention is given in this section to describing the RFCS flight safety issues, performance requirements, and component functional requirements.

Safety and Reliability Requirements

The basic design philosophy of the RFCS is fail-safe. On detection of a system fault, the RFCS reverts to a disengaged condition allowing the safety pilot to resume control of the aircraft using the existing mechanical flight control system of the UH-60A. Preferably, the fault is recognized and the RFCS disengaged without any significant control transient,characteristics that are often described as fail-soft or fail-passive. The research flight envelope, especially the allowable aggressiveness near the ground or obstacles, is directly impacted by the expected magnitude of these fault recognition and system disengagement transients.

Most system faults that do not pose an immediate or severe threat to the aircraft can be recognized and acted upon by the safety pilot who is directly and continuously monitoring the action of the basic UH-60A pilot controls. However, the faults that would result in a hardover control transient must be detected very quickly by automatic monitors. Furthermore, control transients associated with detection and isolation of these faults must be small enough to permit the safety pilot to safely regain control even when operating near the ground or among obstacles. Consequently, the most stringent requirement for RFCS system flight-safety reliability is focused on two essential functions:

1. The ability to disengage when required, whether initiated by the automatic safety monitoring system, the safety pilot, or the evaluation pilot

2. The immediate detection, typically within 100 msec, of component failures or software errors that would otherwise lead to unacceptably large and rapid control transients

The performance and response time requirements for these automatic monitors have been established in piloted simulations. The reliability of these safety-critical functions must be such that the probability that they will fail to operate as designed is extremely remote, less than one in 10^7 flight hours. The quantitative basis of this requirement lies in an assumed 1000 flight-hour operating life of RASCAL, to which standard protection from potentially catastrophic failures has been applied.

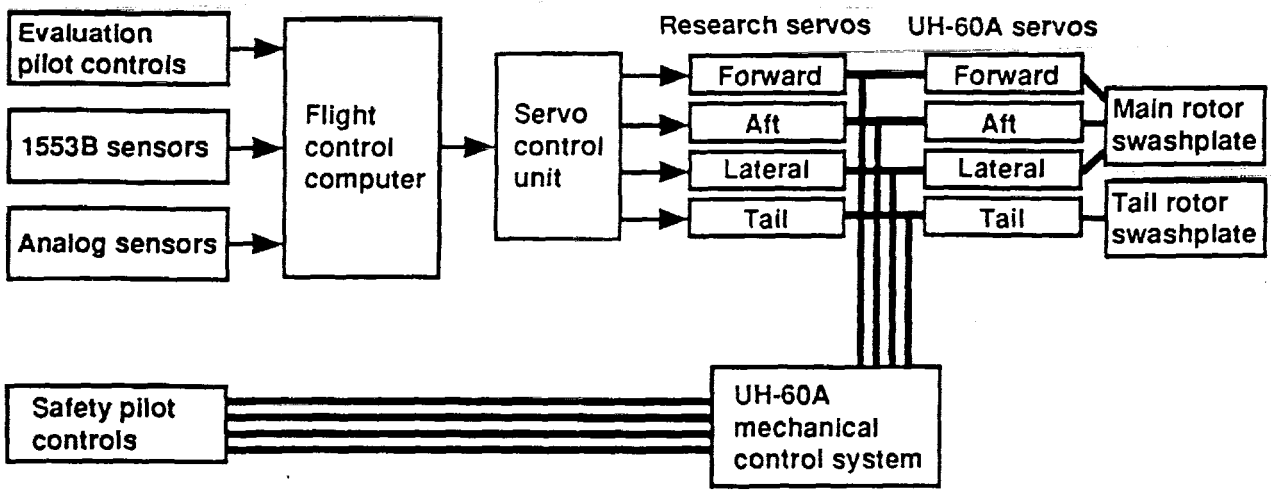

Fig. 9 RFCS components and aircraft interface.

For system disengagement, this level of reliability can be achieved with state-of-the-art components and techniques that will assure that the RFCS servos can be hydraulically bypassed. Force-override features such as shear pins may also be included for added safety. Detection of component failures associated with the actuation loop itself is similarly straightforward, with good assurance that detection and isolation will be fast enough to result in insignificant control transients. Nevertheless, achieving these functions to the level of reliability that is required will undoubtedly entail some level of redundancy of hydraulic system components and servo control hardware.

Achieving high reliability in the passive detection and isolation of hardover commands that may be generated within the RFCS is a more difficult problem, particularly as it is intended that the aircraft be flown aggressively through the fly-by-wire system so that large command signals may be the norm. Component redundancy with cross-channel comparison could be used to quickly detect system hardware faults. However, this method of fault detection increases system complexity and is subject to nuisance trips, especially if only two channels are employed. It is essential that an appropriate balance be struck between system complexity in the form of dual or triplex systems and the impact of nuisance trips and system maintainability on research productivity.

To provide protection from software errors using a redundant design approach, independent software specifications and implementations would be required. Although software is the most frequent source of control system transients in a research facility of this type, the prospect of generating wholly dissimilar software or implementing cumbersome validation and verification procedures is distinctly unattractive.

A preferred approach to fault detection is to monitor the character of the command signals to the RFCS servos, with the objective of identifying commands of unacceptable magnitude, regardless of their source. This has been the general technique employed for this type of research facility in the past, for example, in the CH-47B variable stability helicopter.[2] In practice, it may be more effective to detect these large commands by examining the character of the error signal within the actuator loop itself. This approach has the advantage of diminishing the requirement for component and software redundancy, but it has less potential to provide as effective transient suppression. This relatively simple approach permits location of these monitors in a dedicated, protected, and hence more reliable area of the RFCS, removed from ever-changing research software. However, without additional intelligence, this monitor concept is unable to differentiate between large commands generated intentionally by the evaluation pilot and actual system faults. Hence it is susceptible to nuisance trips that would result from aggressive maneuvering. In addition, whatever the design details of the fault detection monitors, redundant implementations may be required to achieve the necessary functional reliability.

In light of these considerations, a question remains whether the maneuvering flight envelope achievable with the fail/safe RFCS/aircraft system is consistent with the research program requirements. The SCAMP objective of developing and evaluating control laws designed using advanced methodologies can be met with aggressive maneuvering away from obstacles or the ground and with reduced aggressiveness near obstacles. The RAPID program embodies a more traditional in-flight simulation role and in addition is intimately tied to the ADS-33C handling qualities specification.[3] Section 4 of ADS-33C requires very aggressive maneuvering at low altitudes to demonstrate specification compliance, for example, an acceleration/deceleration with pitch attitudes in excess of 30 degrees performed at altitudes of 50 ft above ground level or lower. It is desired to achieve these maneuver objectives with the RASCAL RFCS. However, it is not yet clear whether the fail/safe architecture, which is highly desirable from a cost, complexity, and research productivity standpoint, will permit very aggressive maneuvering near terrain and obstacles.

System Performance Requirements

To meet the high-bandwidth flight control performance goals of the SCAMP and RAPID programs, it is well understood that the RFCS design must minimize the delay contributed by each component versus a total time delay budget and the nonlinearities introduced into the control path by rate limits and hysteresis.

The time delay budget was arrived at using, as a baseline, the ADOCS case study performed by Tischler[4] and the RASCAL preliminary design study described in Ref. 5. The Ref. 4 study found that the ADOCS forward loop equivalent delays from pilot input to aircraft response was over 240 msec. This delay was thought to be the source of the handling qualities shortcomings that became apparent in the vehicle during high-precision, high-gain pilot tasks.[4] The goal for the RASCAL budget was to reduce the total delay by 50% to roughly 120 msec, which is below the critical point of handling qualities degradation according to fixed-wing experiments.[6] Further reduction is not feasible because a significant

portion of the delay arises from the UH-60A main rotor and primary servo-actuators, which will not be modified.

Table 1 shows the component breakdown of forward loop equivalent delays for the pitch axis for ADOCS (from Ref. 4) and the goal for RASCAL for centerstick and sidestick configurations. The major areas of improvement for RASCAL are a reduction in the computation frame to 10 msec and improved research servo performance leading to an approximation of 10 msec of delay. This equates to a second-order servo response natural frequency of 22 Hz.

Table 1 Comparison of ADOCS and RASCAL component equivalent delays. pitch axis

Element	ADOCS delay, ms	RASCAL goal, ms
Main rotor	66	66
UH-60A primary servos	24	24
Research servos	26	10
Zero-order hold	17	5
Computations	22	5
Stick sampling skew	17	5
Total delay, centerstick	n/a	115
Sidestick notch filter	40	30
Sidestick biodynamic filter	32	10
Total delay, sidestick	244	155

Regarding nonlinearities, SCAMP control laws will require the maximum amount of precision attainable with the UH-60A. Concern about the impact of hysteresis in the UH-60A control linkages led to requiring that the research servos be mounted at the input to the UH-60A primary servos, rather than near the safety pilot. This is especially crucial for the tail rotor servo, which will be mounted in the vertical tail at the UH-60A tail servo input linkage to avoid the compliance of the tail rotor cable and lost motion in the mechanical linkages. It is recognized that these locations cause the hysteresis to be present in the safety pilot's backdriven controls; however, piloted simulation studies have indicated that this loss of precision is not a critical factor.

The major source of nonlinearity remaining is the rate limit of the servos. The UH-60A primary servos have a rate limit of 100%/sec which, due to the linkage gains and mechanical mixing box, lead to higher and nonuniform rate limits of the cockpit controls. There is no advantage to driving the servos beyond their rate limit, so the research servos will have the same rate capability. The maximum sine wave input amplitude that a servo will respond to linearly is equal to the servo maximum rate divided by the input frequency. For example, at the 1/rev frequency of 27 rad/sec, the servos can respond linearly to inputs of up to ±3.7%. At the pilot controls, this corresponds to between ±0.3 and ±1.3 inches depending on the control axis. The SCAMP control designs have considered this limitation. To date the rate limit does not appear to be a major impediment during aggressive maneuvering even with rotor state feedback.

Component Functional and Performance Requirements

This section describes the requirements of the components of the RFCS (Fig. 9) that derive from the safety and performance considerations just described. Depending on the design selected to meet the fail/safe requirements and associated reliability goals, the system architecture may incorporate redundancy of some or all components. However, because the redundancy and redundancy management features are not yet well defined for the RFCS, they are not addressed in this paper.

Sensors. The primary sensors for the RFCS are indicated in Fig. 8. Of particular interest is that, as part of the SCAMP program, a major effort will be undertaken to measure rotor states. Current plans call for use of rotary variable differential transformers (RVDTs) at the blade roots to sense blade flap, lag, and pitch. Optical methods of sensing these angles are also being investigated. In addition, it is planned to mount pairs of linear accelerometers on each blade to obtain duplicate measures of flap, lag, and pitch and possibly their rates using the state estimation methods described in Ref. 7. These signals will be transmitted or routed through slip rings for processing in the on-board computers.

Controls. The first set of pilot controllers will likely consist of a multi-axis sidestick controller on the evaluation pilot's right with a collective lever on the left. Optional spring-loaded pedals will likely be included. Ultimately, it is planned to have in addition a conventional centerstick, pedals, and collective driven by a fully programmable force-feel system.

Flight Control Computer. The flight control computer (FCC) will contain signal conditioning, bus control, signal processing, and control laws. The internal architecture of the FCC has not yet been determined, especially with regard to the number of processors

required. However, it is a requirement that the FCC as a whole be able to perform extensive analog and digital signal processing as described below. Apart from input/output processing, it is estimated that the processor(s) used for the control law computations will need to a have 32-bit, floating point architecture and be capable of 16 million instructions per second (MIPS) or 6 million floating point operations per second (MFLOPS). The FCC will have a large memory requirement, on the order of 4 Mbytes, to accommodate future growth and to permit loading several sets of control law applications code from different experiments to allow maximum flight test flexibility.

The FCC will communicate with the other subsystems via Mil-Std-1553B data buses (Fig. 8). Those systems include the 1553B-based sensors, the cockpit and cabin mode-menu computers, the guidance and navigation system, and the data acquisition and analysis system. The number and arrangement of buses required for these interactions are being determined based on estimates of projected loading, traded off against hardware and software requirements and compatibility with the phased research system development.

There is a requirement for extensive analog input into the FCC to accommodate the analog sensors. Many of the signals will be used for flight control, while others will be converted to 1553B format and sent on to the data analysis computer or telemetry system for recording. All the analog signals will be anti-alias filtered at a single frequency. A digital processor will then be used as required for lower-frequency filtering of both the analog and 1553B-based sensor signals using low-pass or notch filters. The advantage of this approach is to permit flexibility in changing filter complexity and characteristics while retaining a single hardware configuration. It is expected that for control applications the highest frequency of interest is at 2/rev, or 8.6 Hz, while for parameter identification activities higher frequencies will be desired.

A real-time operating system or real-time executive will be employed for program execution. A high-order language will be used for control law and signal processing applications. Depending on software tools that are available, the language will be either C or Ada. A commercial, workstation-based, software development environment will likely be employed, with appropriate cross-compilers and a complete window-oriented symbolic debugging capability. The real-time shell, including software to drive all of the input/output devices, will be developed such that new signal processing and control law modules can be easily integrated. The project teams will develop the signal processing and control law applications software using a structured design approach similar to that used for the Ames V/STOL Systems Research Aircraft (VSRA) program.[8]

Servo Control Unit. The servo control unit (SCU) will receive, process, and monitor control commands from the FCC. It will contain servo loop closure electronics, control engagement and disengagement of the RFCS, and provide fault detection and isolation logic. These SCU functions are considered flight-safety critical and must meet the 10^{-7} failures/flight hour reliability requirement discussed above.

The SCU will receive servo position commands from the FCC that will be appropriately processed and will become the commands to the RFCS servos' electrohydraulic valves. The servo loops will be analog, and linear variable differential transformers (LVDTs) will be used for the servo ram position feedback. Each element of the servo loop will be monitored; for example, by using the actual ram position versus one predicted by a low-order model. In addition, the servo motions will be monitored for "reasonableness" to assure that the SCU has not received a hardover or slowover command from an upstream component such as the FCC. The requirements for these command monitors have been established in piloted simulations that defined the maximum servo motion that can be tolerated before the monitor disengages the RFCS. The monitor thresholds will have some selectability to account for different flight environments and task aggressiveness levels.

When any of these monitors detects a failure, the RFCS will be disengaged by bypassing and depressurizing the RFCS servos. The bypass functions may be redundant if necessary to assure proper disengagement. Disengagement will also be effected via failure discretes to the SCU from all upstream monitors, for example the FCC watchdog timer. Finally, both the safety and evaluation pilots will be able to command disengagement via switches mounted on their controls. Unique aural tones will accompany RFCS engagement and disengagement.

Research Servos. As discussed previously, the research servos will be mounted at the inputs to each of the UH-60A primary swashplate and tail rotor servos and will provide full-authority control of those servos. Their performance will be consistent with the 10 msec time delay and 100%/sec rate limit discussed above. The servos will be electrically signaled hydraulic actuators mounted in parallel with the UH-60A mechanical flight control system so that their motions are reflected, via movement of the mechanical linkages, back to the safety

pilot's cockpit controls. The detail designs of the research servos' hydraulic and mechanical interfaces to the UH-60A will be modeled on those used successfully for ADOCS.[9] At the same time, lessons learned in the ADOCS program will be used to improve the design for RASCAL. For example, the RASCAL servo rams will be balanced or semi-balanced to provide the same response in both directions.

Concluding Remarks

Since the first in-flight simulator was developed in 1947 at what was to become NASA Ames Research Center, these devices have been successfully applied to all aspects of the aircraft development process. The RASCAL represents the latest in a series of helicopter in-flight simulators that began in the late 1950s with the Princeton University variable stability HUP-1, used as a research tool to generate roll and yaw handling qualities requirements. The RASCAL is being developed as much more than a handling qualities research tool and will be capable of supporting major NASA, Army, and FAA research programs in integrated guidance, control, and display systems for rotorcraft. A fundamental requirement for these programs is that both ground- and in-flight simulation be applied in a complementary fashion to ensure the completeness and accuracy of the results.

References

[1]Aiken, E. W., Hindson, W. S., Lebacqz, J. V., Denery, D. G., and Eshow, M. M., "Rotorcraft In-Flight Simulation at NASA Ames Research Center: A Review of the 80's and Plans for the 90's," International Symposium on In-Flight Simulation for the 90's, Braunschweig, Germany, July 1-3, 1991 (NASA TM-103873, Aug. 1991).

[2]Kelly, J. R. et al., "Description of the VTOL Approach and Landing Technology (VALT) CH-47 Research System," NASA TP-1436, Aug. 1979.

[3]*Handling Qualities Requirements for Military Rotorcraft*, U.S. Army AVSCOM Aeronautical Design Standard ADS-33C, St. Louis, MO, Aug. 1989.

[4]Tischler, M. B., "Assessment of Digital Flight Control Technology for Advanced Combat Rotorcraft," *Journal of the American Helicopter Society*, Vol. 34, No. 4, 1989.

[5]Deazley, W. R., "UH-60 RASCAL Variable Stability System Configuration Study," Calspan Final Report No. 7738-3, Feb. 1991.

[6]Smith, R. E. and Sarrafan, S. K., "Effect of Time Delay on Flying Qualities: An Update," *Journal of Guidance, Control, and Dynamics*, Vol. 9, No. 5, 1986.

[7]McKillip, R. A., Jr., "Kinematic Observers for Active Control of Helicopter Rotor Vibration," Paper No. 65, Twelfth European Rotorcraft Forum, Gramisch-Partenkirchen, Germany, Sept. 1986.

[8]Foster, J. D., Moralez III, E., Franklin, J. A., and Schroeder, J. A., "Integrated Control and Display Research for Transition and Vertical Flight on the NASA V/STOL Research Aircraft (VSRA)," NASA TM-100029, Oct. 1987.

[9]Dones, F. D., and Glusman, S. I. et al., "Advanced Digital/Optical Control System Final Technical Report, Volume 2 - Systems Engineering," AATD Report No. D358-10055-2, Applied Aviation Technology Directorate/Boeing Helicopters, Dec. 1989.

List of Attendees

LIST OF ATTENDEES

Theodore B. Aldrith
Sikorsky Aircraft
Sikorsky Aircraft
6900 Main St.
Stratford, CT
06601-1381
(203) 386-5834

Anthony D. Andre
West. Aero. Lab
MS 262-3
NASA Ames Research Center
Moffett Field, CA
94035-1000
(415) 604-3665

Harold Andrews
Starmark Corp.
3800 No. Fairfax Dr. #102
Arlington, VA
22203-1703
(703) 528-1552

Adolph Atencio
U.S. Army AFDD
U.S. Army Aeroflightdynamics Directorate
MS 210-7
NASA-Ames Research Center
Moffett Field, CA
94035-1000
(415) 604-6863

Stuart Atkins
Piasecki Aircraft Corp.
Piasecki Aircraft Corp.
West End of Second Street
Essington, PA
19029
(215) 521-5700

Stewart W. Baillie
NRC Flight Res. Lab.
National Research Council Flight Research Laboratory
Uplands Bldg. U-61
Ottawa, Ontario
KEY-0R6
Canada
(613) 998-3790

Dwight L. Balough
Flight Experiments Branch
MS 237-5
NASA Ames Research Center
Moffett Field, CA
94035-1000
(415) 604-3152

Lourdes G. Birckelbaw
STOVL/Powered-Lift Tech. Br.
MS 237-3
NASA Ames Research Center
Moffett Field, CA
94035-1000
(415) 604-5592

Bob Blake
Sikorsky Aircraft Div., UTC
Sikorsky Aircraft
120 Winter Club Court
P.B.G, FL
33410
(407) 775-5298

Chris Blanken
U.S. Army AFDD
U.S. Army Aeroflightdynamics Directorate
MS 210-7
NASA-Ames Research Center
Moffett Field, CA
94035-1000
(415) 604-5836

Joseph J. Bonin
AFOTEC/TFM
AFOTEC/TFM
8500 Gibson Blvd. SE
Kirtland AFB, NM
87112
(505) 846-5344

Paul F. Borchers
Flight Dynamics and Controls Br.
MS 211-2
NASA Ames Research Center
Moffett Field, CA
94035-1000
(415) 604-6115

Prof. Roy Bradley
Univ. of Glasgow
University of Glasgow
The University
Glasgow, G128QQ
U.K.
041 339 8855 (x8070)

R. James Breiding
Naval Training Systems Center
Naval Training Systems Center
12350 Research Parkway
Orlando, FL
32826-3224
(407) 380-4723

LCDR Christopher D. Brown
USNTPS
USNTPS
522 Lake Drive
Lexington Park, MD
20653-000
(301) 863-4411

Robert Buckanin
U.S. Army AATD
Flight Controls Team Center
U.S. Army ATCOM - AATD
Bldg 401
Ft. Eustis, VA
23604
(804) 878-4101

A. N. Cappetta
Naval Air Dev. Cent.
Air Vehicle and Crew Systems Technology Department
Naval Air Development Center
Warminster, PA
18974-5000
(215) 441-7047

Dean Carico
NAWC
Naval Air Warfare Center
Patuxent River, MD
20670
(301) 826-1382

Roberto Celi
Univ. of Maryland
Dept. of Aerospace Eng.
University of Maryland
College Park, MD
20742
celi@eng.umd.edu
(301) 405-1132

Charles A. Chalk
Calspan Corp.
Calspan Corp.
PO Box 400
Buffalo, NY
14225
(716) 631-6708

Dr. Robert T. N. Chen
Flight Dynamics and Controls Br.
MS 211-2
NASA Ames Research Center
Moffett Field, CA
94035-1000
(415) 604-5008

Monique Chetelat
SYRE Inc.
SYRE Inc.
P.O. Box 81
Moffett Field, CA
94035
(415) 604-3245

Benny K. Cheung
Flight Experiments Branch
MS 237-5
NASA Ames Research Center
Moffett Field, CA
94035-1000
(415) 604-5432

Bill W. Chung
Flight Dynamics and Controls Br.
MS 211-2
NASA Ames Research Center
Moffett Field, CA
94035-1000
(415) 604-6002

John W. Clark
NAWC
Naval Air Warfare Center
PO Box 5152
Warminster, PA
18974
(215) 441-2165

Clayton R. Coler
Rotorcraft Human Factors Research Branch
MS 262-3
NASA Ames Research Center
Moffett Field, CA
94035-1000
(415) 604-5716

Richard A. Coppenbarger
Guid and Nav. Br.
MS 210-9
NASA Ames Research Center
Moffett Field, CA
94035-1000
(415) 604-5433

Lloyd D. Corliss
Military Technology Office
NASA Ames Research Center
Moffett Field, CA
95035-1000
(415) 604-6269

H. C. Curtiss, Jr.
Princeton Univ.
Engineering Quad, Room D-224
Princeton University
Princeton, NJ
"08544"
(609) 258-5149

Dr. Joseph De Maio
U.S. Army AFDD
Crew Station Research and Development Branch
MS 243-4
NASA Ames Research Center
Moffett Field, CA
94035-1000
(415) 604-6974

William A. Decker
Flight Dyn. and Cont. Br.
Flight Dynamics and Controls Branch
MS 211-2
NASA Ames Research Center
Moffett Field, CA
94035-1000
(415) 604-5362

James Dryfoos
Boeing Helicopters
Boeing Helicopters
PO Box 16858, MS P32-31
Philadelphia, PA
19142-0858
(215) 591-7305

Maj. Mike Duva
NAVAIRSYSCOM, U.S.M.C.
NAVAIRSYSCOM
PMA205-2I
Washington, D.C.
20361
(703) 692-2641 x3015

Ronald DuVal
Advanced Rotorcraft Technology
Advanced Rotorcraft Technology
1685 Plymouth Street
Mountain View, CA
94022
(415) 968-1464

Shawn Engelland
Flight Dynamics and Controls Br.
MS 211-2
NASA Ames Research Center
Moffett Field, CA
94035-1000
(415) 604-5271

Dorothy L. Englehardt
NAVAIR
NAVAIR
Washington, DC
20361-1205
(703) 692-2641

Michelle Eshow
U.S. Army AFDD
U.S. Army Aeroflightdynamics Directorate
MS 211-2
NASA Ames Research Center
Moffett Field, CA
94035-1000
(415) 604-5272

Donald L. Folger
Sikorsky, UTC
S336A1
United Technologies, Sikorsky Aircraft
6900 Main Street
Stratford, CT
06601-1381
(203) 386-7449

Dr. James A. Franklin
Flight Dyn. and Cont. Br.
Flight Dynamics and Controls Branch
MS 211-2
NASA Ames Research Center
Moffett Field, CA
94035-1000
(415) 604-6004

Ron Friedman
Boeing Helicopters
Boeing Helicopters
PO Box 16858
Philadelphia, PA
19142-0858
(215) 591-6167

John D. Funk
Naval Air Warfare Cent.
Aircraft Division
Naval Air Warfare Center
Warminster, PA
18974-5000
(215) 441-3463

R. Thomas Galloway
Naval Training Systems Center
Naval Training Systems Center
12350 Research Parkway
Orlando, FL
32826-3224
(407) 380-4648

Charles K. Gardner
U.S. Army
U.S. Army
STEAT-AQ-TC
Edwards AFB, CA
93525
(805) 277-4023

Philip J. Gold
Sikorsky Aircraft Div., UTC
MS 336A
Sikorsky Aircraft Div., UTC
6900 Main St.
Stratford, CT
06601-1381
(203) 386-3208

David L. Green
Starmark Corp.
Starmark Corp.
1745 Jefferson Davis Highway, Suite 507
Arlington, VA
22202
(703) 413-0250

Dr. Arthur J. Grunwald
West. Aero. Labs
MS 262-2
NASA Ames Research Center
Moffett Field, CA
94035-1000
(415) 604-0104

Thomas F. Gruzleski
CAE-Link
CAE-Link
PO Box 1237
Binghamton, NY
13902-1237
(607) 721-4251

J. Hagen
NTPS
National Test Pilot School
Box 658
Mojave, CA
93501
(805) 824-2977

Maj. Johnnie Ham
U.S. Army AQTD
Airworthiness Qualification Test Directorate
Bldg. 1820
Edwards AFB, CA
93523-5000
(805) 940-8940

Daniel C. Hart
U.S. Army AFDD
U.S. Army Aeroflightdynamics Directorate
MS 210-7
NASA-Ames Research Center
Moffett Field, CA
94035-1000
(415) 604-3485

Sandra G. Hart
Rotorcraft Hum. Fac. Res. Br.
MS 262-3
NASA Ames Research Center
Moffett Field, CA
94035-1000
(415) 604-6072

Loran A. Haworth
U.S. Army AFDD
MS 243-3
NASA Ames Research Center
Moffet Field, CA
94035-1000
(415) 604-6944

Robert K. Heffley
Robert Heffley Engineering
Robert Heffley Engineering
349 First Street
Los Altos, CA
94022
(415) 949-1747

William S. Hindson
Flight Operations Br.
Flight Operations Branch
MS 211-3
NASA Ames Research Center
Moffett Field, CA
94035-1000
(415) 604-1106

Roger H. Hoh
Hoh Aeronautics, Inc.
Hoh Aeronatics, Inc.
2075 Palos Verdes Drive North #217
Lomita, CA
90717
(310) 325-7255

Patrick J. Hollifield
Bell Helicopter Textron Inc.
Bell Helicopter Textron Inc.
PO Box 482
Fort Worth, TX
76101
(817) 280-2288

Steven W. Hong
United Tech. Res. Cent.
MS 85
United Technologies Research Center
East Hartford, CT
"06108"
(203) 727-7068

Thomas L. House
U.S. Army ATCOM
U.S. Army Aviation and Troop Command
4300 Goodfellow Blvd.
St. Louis, MO
63132
(314) 263-1012

J. Howitt
U.K. Defence Res. Agcy.
31 Whitley Rd.
Shortstown, Bedford
MK42 OXA
U.K.
023-422-5368

James J. Howlett
Sikorsky Aircraft Div., UTC
MS 336A
Sikorsky Aircraft Div., UTC
Main Street
Stratford, CT
06601-1381
(203) 386-6010

Carla D. Ingram
SYRE Inc.
SYRE Inc.
P.O. Box 81
Moffett Field, CA
94035
(415) 604-5381

Laura Iseler
Flight Dynamics and Controls Br.
MS 211-2
NASA Ames Research Center
Moffett Field, CA
94035-1000
(415) 604-6196

Kenneth G. Jay
British Embassy
British Embassy
3100 Massachusetts Ave.
Washington, DC
20008
(202) 898-4640

John B. Johns
U.S. Army AFDD
MS 215-1
NASA Ames Research Center
Moffett Field, CA
94035-1000
(415) 604-6214

Walter W. Johnson
Rotorcraft Human Factors Br.
Rotorcraft Human Factors Branch
MS 262-3
NASA Ames Research Center
Moffett Field, CA
94035-1000
(415) 604-3667

Mary K. Kaiser
Rotorcraft Human Factors Br.
Rotorcraft Human Factors Branch
MS 262-3
NASA Ames Research Center
Moffett Field, CA
94035-1000
(415) 604-4448

Andrew W. Kerr
U.S. Army AFDD
U.S. Army AFDD
MS 215-1
NASA Ames Research Center
Moffett Field, CA
94035-1000
(415) 604-5837

David L. Key
U.S. Army AFDD
U.S. Army Aeroflightdynamics Directorate
MS 210-7
NASA Ames Research Center
Moffett Field, CA
94035-1000
(415) 604-5839

Lee Khinoo
Veda Inc.
Veda Inc.
300 Exploration
Lexington Park, MD
20653
(301) 826-4411

Dr. Fredrick D. Kim
Flight Dynamics and Controls Br.
MS 211-2
NASA Ames Research Center
Moffett Field, CA
94035-1000
(415) 604-5272

Dwayne F. Kimball
Ishida Aerospace Res., Inc.
Ishida Aerospace Research, Inc.
Alliance Airport
2301 Horizon Drive
Fort Worth, TX
76177
(817) 837-8000 x229

David W. King
Boeing Helicopters
Boeing Defense and Space Group: Helicopter Div.
PO Box 16858
Philadelphia, PA
19142-0858
(215) 591-2257

Rene Knorr
Eurocopter Deutschland GmbH
Eurocopter Deutschland GmbH
Postfach 80 11 40 D-8000
Munchen, 80
Germany
089-6000-6575

Masaki Komoda
Tokyo Met. Inst. of Tech.
Tokyo Metropolitan Institute of Technology
6-6 Asahigaoka, Hino
Tokyo, Japan 191

William E. Larsen
FAA
MS 210-2
NASA Ames Research Center
Moffett Field, CA
94035-1000
(415) 604-6380

Dr. Victor J. Lebacqz
Flight Human Factors Br.
Flight Human Factors Branch
MS 262-4
NASA Ames Research Center
Moffett Field, CA
94035-1000
(415) 604-5792

Sikorsky Library
United Technologies Res Ctr
Attn: Library Acquisitions
411 Silver Lane
East Hartford, CT
6108

Tom MacDonald
Boeing Helicopters
Boeing Helicopters
MS P20-38
PO Box 16858
Philadelphia, PA
19142-0858
(215) 591-5204

John A. Macrino
U.S. Army AATD
U.S. Army AATD
Ft. Eustis, VA
23604
(804) 878-2122

M. Hossein Mansur
U.S. Army AFDD
MS 211-2
NASA Ames Research Center
Moffett Field, CA
94035-1000
(415) 604-6037

Bob Marshall
no address information

Walter E. McNeill
Flight Dyn and Contr. Br.
MS 211-2
NASA Ames Research Center
Moffett Field, CA
94035-1000
(415) 604-5362

Robert V. Miller
USNTPS
U.S. Naval Test Pilot School
NAS
Patuxent River, MD
20653
(301)826-4411

David G. Mitchell
System Technologies Inc.
Systems Technology Inc.
13766 S. Hawthorne Blvd.
Hawthorne, CA
90250-7083
(310) 679-2281

Manoj Mittal
Georgia Tech.
Georgia Tech Research Facility, Cobb County
7220 Richardson Rd, Bldg. 2 Trailer
Smyrna, GA
30080
(404) 528-7110

Maj. V. D. Mize
Naval Training Systems Center
Naval Training Systems Center
12350 Research Parkway
Orlando, FL
32826-3224
(407) 380-4219

J. Murray Morgan
NRC Flight Res. Lab.
National Research Council Flight Research Laboratory
Uplands Bldg. U-61
Ottawa, Ontario
KEY-0R6
Canada
(613) 998-3180

Michael W. Mosher
USNTPS
U.S. Naval Test Pilot School
4350 Jimmy Carter Blvd.
Norcross, GA
30093-0000
(301) 863-4411

CW4 Craig R. Nixon
U.S. Army AQTD
U.S. Army AQTD
75 North Flightline Rd.
Edwards AFB, CA
93524-6100
(805) 277-4992

Randall L. Oser
Naval Training Systems Center
Naval Training Systems Center
12350 Research Parkway
Orlando, FL
32826-3224
(407) 380-4818

Dean Owen
Univ. of Canterbury
Department of Psychology
University of Canterbury
Christchurch
New Zealand
(03) 667-001, FAX (03) 642-181

Gareth D. Padfield
Defence Res. Agency
Defence Research Agency
Flight Systems Dept.
Bedford
MK41 6AE
U.K.
0234-225-370

Heinz-Jurgen Pausder
DLR Inst. Fuer Flugmechanik
DLR Inst. Fuer Flugmechanik
Buchhorstblick 13
3302 Cremlingen
Germany
email: FK17%DLRBMBS.BITNET@VM.GO.DLR.DE
(531) 395-2694

Frederick O. Porter
NAWCAD
NAWCAD
Patuxent River, MD
20650
(301) 826-1335

Ian Postlethwaite
Leicester Univ.
Control Systems Research, Dept. of Engineering
Leicester University
Leicester, LE1 7RH
U.K.
(301) 826-1335

Raymond W. Prouty
Consultant
4334 Deerpark Court
Westlake Village, CA
91361
(818) 889-8955

Leigthon Kf. Quon
SYRE Inc.
SYRE Inc.
P.O. Box 81
Moffett Field, CA
94035
(415) 604-3891

J. J. Rabeni
Reflectone Inc.
Reflectone
4908 Tampa West Blvd.
P.O. Box 15000
Tampa, FL
33684-5000
(813) 885-7481

Thomas L. Reynolds
U.S. Army AFDD
MS 211-3
NASA Ames Research Center
Moffett Field, CA
94035-1000
(415) 604-5101

David (Tom) Ruttledge
McDonnell Douglas Hel. Co.
McDonnell Douglas Helicopter Co.
MS 530/B346
5000 E. McDowell Rd.
Mesa, AZ
85205
(602) 891-2272

Richard A. Schott
USMC
USMC
HMT-204
MCAS New River
Jacksonville, NC
28460
(919) 451-6422

Jeffery A. Schroeder
Flight Dyn. and Contr. Br.
Flight Dynamics and Controls Branch
MS 211-2
NASA Ames Research Center
Moffett Field, CA
94035-1000
(415) 604-4037

LCDR Timothy Sestak
Naval Air Warfare Center
Naval Air Warfare Center
Aircraft Division
PO Box 51 52
Warminster, PA
18974-0591
(215) 441-1047

Rickey C. Simmons
Flight Operations Branch
MS 211-3
NASA Ames Research Center
Moffett Field, CA
94035-1000
(415) 604-3130

Donovan Spurgeon
NAVAIR
NAVAIR PMA-205M
COMNAVAIRSYSCOM
Washington, DC
20361
(703) 692-2641 x 3002

Dr. Wendell B. Stephens
U.S. Army Aeroflightdynamics Dir.
MS 243-3
NASA Ames Research Center
Moffett Field, CA
94035-1000
(415) 604-5794

Michael W. Stortz
Flight Operations Branch
MS 211-3
NASA Ames Research Center
Moffett Field, CA
94035-1000
(415) 604-3131

Karen Studebaker
Rotorcraft Technology Br.
MS 237-5
NASA Ames Research Center
Moffett Field, CA
94035-1000
(415) 604-5469

Selwyn Sturisky
Georgia Tech
School of Aerospace Engineering
Geogia Tech.
Atlanta, GA
30332-0150
(404) 894-2995

Shoichi Sugiyama
Ishida Aerospace Res., Inc.
Ishida Aerospace Research, Inc.
Alliance Airport
2301 Horizon Drive
Fort Worth, TX
76177
(817) 837-8000

Armin Taghizad
ONERA-DED
ONERA
21 Avenue de la Division Leclerc
B.P. 72 92322 Chatillon Cedex
France
32.16.4-46.73.40.40

Dr. Marc D. Takahashi
U.S. Army AFDD
MS 211-2
NASA Ames Research Center
Moffett Field, CA
94035-1000
(415) 604-5271

Nigel Talbot
CAA
CAA
Aviation House, South Area
Gatwick Airport
Gatwick, Surrey
RH6 OYR
UK
44293 573107

Peter D. Talbot
Rotorcraft Technology Branch
MS 237-5
NASA Ames Research Center
Moffett Field, CA
94035-1000
(415) 604-5108

Robert Tam
SYRE Inc.
SYRE Inc.
P.O. Box 81
Moffett Field, CA
94035
(415) 604-5000 (22433)

Dr. Douglas G. Thomson
Univ. of Glasgow
University of Glasgow
The University
Glasgow, G128QQ
U.K.
041 339 8855 (x4334)

Dr. Mark B. Tischler
U.S. Army AFDD
MS 211-2
NASA Ames Research Center
Moffett Field, CA
94035-1000
(415) 604-5563

Joseph J. Totah
Rotorcraft Technology Branch
MS 237-5
NASA Ames Research Center
Moffett Field, CA
94035-1000
(415) 604-4126

D. J. Walker
Leicester Univ.
Control Systems Research, Dept. of Engineering
Leicester University
Leicester, LE1 7RH
U.K.
0533-522529

Don Welch
Bell Helicopter Textron
MS 1302
Bell Helicopter Textron
PO Box 482
Fort Worth, TX
76101
(817) 280-3608

Matthew S. Whalley
U.S. Army AFDD
U.S. Army Aeroflightdynamics Directorate
MS 210-7
NASA-Ames Research Center
Moffett Field, CA
94035-1000
(415) 604-3505

Gregory P. Wright
Sikorsky Aircraft Div., UTC
MS 336A
Sikorsky Aircraft Div., UTC
Main Street
Stratford, CT
06601-6010
(203) 386-6010

Richard E. Zelenka
Aircraft Guidance and Navigation Branch
MS 210-9
NASA Ames Research Center
Moffett Field, CA
94035
(415) 604-5433

REPORT DOCUMENTATION PAGE

Form Approved
OMB No. 0704-0188

1. AGENCY USE ONLY *(Leave blank)*	2. REPORT DATE	3. REPORT TYPE AND DATES COVERED
	July 1993	Conference Publication

4. TITLE AND SUBTITLE
Piloting Vertical Flight Aircraft
A Conference on Flying Qualities and Human Factors

5. FUNDING NUMBERS
505-59-52

6. AUTHOR(S)
Christopher L. Blanken and Matthew S. Whalley

7. PERFORMING ORGANIZATION NAME(S) AND ADDRESS(ES)
Aeroflightdynamics Directorate
U.S. Army Aviation and Troop Command
Ames Research Center
Moffett Field, CA 94035-1000

8. PERFORMING ORGANIZATION REPORT NUMBER
A-93074

9. SPONSORING/MONITORING AGENCY NAME(S) AND ADDRESS(ES)
Ames Research Center
Moffett Field, CA 94035-1000 and
American Helicopter Society
217 N. Washington St., Alexandria, VA 22314

10. SPONSORING/MONITORING AGENCY REPORT NUMBER
NASA CP-3220

11. SUPPLEMENTARY NOTES
Point of Contact: Christopher L. Blanken, Ames Research Center, MS 210-7, Moffett Field, CA 94035-1000
(415) 604-5836

12a. DISTRIBUTION/AVAILABILITY STATEMENT
Unclassified — Unlimited
Subject Category 08

12b. DISTRIBUTION CODE

13. ABSTRACT *(Maximum 200 words)*

This document contains papers from a specialists' meeting entitled "Piloting Vertical Flight Aircraft: A Conference on Flying Qualities and Human Factors." The conference was co-sponsored by the American Helicopter Society—San Francisco Bay Chapter, and the NASA Ames Research Center. It was held January 20–22, 1993 at the Sheraton Hotel Fisherman's Wharf, San Francisco, California.

Vertical flight aircraft, including helicopters and a variety of Vertical Takeoff and Landing (VTOL) concepts, place unique requirements on human perception, control, and performance for the conduct of their design missions. The intent of this conference was to examine, for these vehicles, advances in: (1) design of flight control systems for ADS-33C standards; (2) assessment of human factors influences of cockpit displays and operational procedures; (3) development of VTOL design and operational criteria; and (4) development of theoretical methods or models for predicting pilot–vehicle performance and mission suitability. Recognizing that human capabilities and limitations form an integral aspect of the operations for these classes of vehicles, a secondary goal of the conference was to provide an initial venue for enhanced interaction between human factors and handling qualities specialists.

14. SUBJECT TERMS	15. NUMBER OF PAGES
Helicopter, Rotorcraft, Stability and control, Flying qualities, Human factors, Handling qualities	502
	16. PRICE CODE A22

17. SECURITY CLASSIFICATION OF REPORT	18. SECURITY CLASSIFICATION OF THIS PAGE	19. SECURITY CLASSIFICATION OF ABSTRACT	20. LIMITATION OF ABSTRACT
Unclassified	Unclassified		